LEABHARLANN CHOLÁISTE NA TRÍONÓIDE, BAILE ÁTHA CLIATH | TRINITY COLLEGE LIBRARY DUBLIN
Ollscoil Átha Cliath | The University of Dublin

Terms and Conditions of Use of Digitised Theses from Trinity College Library Dublin

Copyright statement

All material supplied by Trinity College Library is protected by copyright (under the Copyright and Related Rights Act, 2000 as amended) and other relevant Intellectual Property Rights. By accessing and using a Digitised Thesis from Trinity College Library you acknowledge that all Intellectual Property Rights in any Works supplied are the sole and exclusive property of the copyright and/or other IPR holder. Specific copyright holders may not be explicitly identified. Use of materials from other sources within a thesis should not be construed as a claim over them.

A non-exclusive, non-transferable licence is hereby granted to those using or reproducing, in whole or in part, the material for valid purposes, providing the copyright owners are acknowledged using the normal conventions. Where specific permission to use material is required, this is identified and such permission must be sought from the copyright holder or agency cited.

Liability statement

By using a Digitised Thesis, I accept that Trinity College Dublin bears no legal responsibility for the accuracy, legality or comprehensiveness of materials contained within the thesis, and that Trinity College Dublin accepts no liability for indirect, consequential, or incidental, damages or losses arising from use of the thesis for whatever reason. Information located in a thesis may be subject to specific use constraints, details of which may not be explicitly described. It is the responsibility of potential and actual users to be aware of such constraints and to abide by them. By making use of material from a digitised thesis, you accept these copyright and disclaimer provisions. Where it is brought to the attention of Trinity College Library that there may be a breach of copyright or other restraint, it is the policy to withdraw or take down access to a thesis while the issue is being resolved.

Access Agreement

By using a Digitised Thesis from Trinity College Library you are bound by the following Terms & Conditions. Please read them carefully.

I have read and I understand the following statement: All material supplied via a Digitised Thesis from Trinity College Library is protected by copyright and other intellectual property rights, and duplication or sale of all or part of any of a thesis is not permitted, except that material may be duplicated by you for your research use or for educational purposes in electronic or print form providing the copyright owners are acknowledged using the normal conventions. You must obtain permission for any other use. Electronic or print copies may not be offered, whether for sale or otherwise to anyone. This copy has been supplied on the understanding that it is copyright material and that no quotation from the thesis may be published without proper acknowledgement.

TERTIARY DYKES IN NORTHWEST IRELAND: FIELD OCCURRENCE, EMPLACEMENT MECHANISMS, HOST ROCK DEFORMATION, AND POST-EMPLACEMENT STRAIN AND DENUDATION

by

Stuart D. Bennett

Submitted to the University of Dublin, Trinity College, for the degree of Doctor of Philosophy

November 2005

TRINITY COLLEGE
10 NOV 2006
LIBRARY DUBLIN
THESIS
7989

Declaration

This thesis is entirely my own work, except where otherwise stated. It has not previously been submitted to this or any other university. All references are duly acknowledged.

The library of Trinity College may lend or copy this thesis upon request.

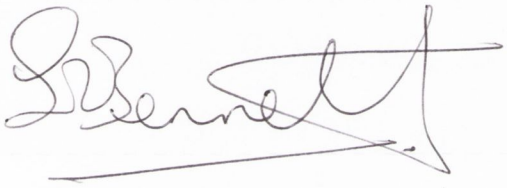

Stuart D. Bennett

To my family

Summary

This work provides insight into the Tertiary tectonic and stress history of northwest Ireland. It focuses on igneous dykes, as these are the only rocks of Tertiary age in the region. The work also looks at the fundamental processes of dyke emplacement and host rock deformation.

Three groups of dykes, the West Connacht systems, and the Killala and Donegal-Kingscourt swarms, are studied. By analysing the forms of the dykes and their relationships with the host rock structure, it is shown that the dykes largely exploited pre-existing structures in the oldest host rocks, but propagated hydraulic fractures in segmented en échelon arrays in the relatively young Carboniferous host rock. It is shown that the West Connacht systems were emplaced under NW-SE extension, the Killala swarm under N-S extension, and the Donegal-Kingscourt swarm under NE-SW extension. It is envisaged that the E-W trend of the Killala swarm is representative of a swing in the crustal stresses, influenced by the proximity of the Brendan centre and its apparent large-scale radial dyke arrangement. Large intra-swarm range in dyke orientation, and the tendency for dykes to open orthogonal to strike, implies that the difference in magnitude between the horizontal principal stresses was not great during the Palaeocene at the time of emplacement.

The dykes caused deformation of the host rock as they were emplaced. In the host rock bridge zones between overlapping en échelon dyke segments, structures are classified whose style and orientation can be used to infer the three-dimensional geometry of segmentation. A model of deformation of the bridge by flexural slip during segment dilation accounts for many of the structures described. Elsewhere in the host rock, deformation is manifest mainly as dyke-parallel fractures, many of which have accommodated shear. Close to the dykes, structures are related to hydraulic fracturing that took place as the dyke tip propagated. Away from the dykes the cause of the fracturing is not known. However, the *extent* of host rock deformation away from the dykes is dependent on dyke width. It is suggested that the thermal input from the dyke into the host rock caused the host rock to fracture, and controlled the extent of the fracture zones; the wider the dyke the greater the thermal input.

Analysis of Tertiary dykes that are faulted shows that N-S directed compression in a strike-slip stress regime affected northwest Ireland not long after dyke emplacement. This is compatible with the general understanding that northwest Europe has been locked in compression since opening of the northeast Atlantic at the start of the Eocene. However, it is shown that, to infer a dyke as being faulted, the fault offset must be exposed. This allows elimination of the possibility that the fault was a pre-existing structure reactivated as a transform between two intruding offset dyke segments.

Lastly, dykes have fission track ages and (U-Th)/He ages that are within error of their emplacement age of about 60 Ma. This indicates that the Tertiary thermal history of northwest Ireland is beyond to resolution of these two thermochronological techniques. Thus, denudation in northwest Ireland appears to have been less than around 1.4 km since the dykes were emplaced, and may even have been as little as a few hundred metres.

Acknowledgements

Adrian Phillips supervised me before sadly passing away on November 1st 2003. I thank Adrian for the enthusiasm, support and friendship he gave me over the time I knew him. I also thank Adrian's wife, Rosamond, for all her encouragement. Adrian is sadly missed.

Ian Sanders supervised me after Adrian's passing. I am indebted to Ian for his help and encouragement during my final year in Trinity.

Thanks to Phillips Petroleum for funding this project, and to Philip Allen for his contribution to the fission track study presented here. I am grateful to Andrew Carter of University College, London, and Kerry Gallagher of Imperial College, London, for their help regarding fission track analysis, especially Andy who ran the samples. Thanks also to Steve Bergman of Southern Methodist University, Texas, for allowing me to present his unpublished Ar-Ar age data, and to Zoe Shipton for advice on structural aspects of this project.

Many thanks go to the staff in the Geology Department, Trinity College. I am very grateful to John Graham for his support over the years, especially his tormenting whilst writing up! Thanks to George for his enthusiasm towards my work, and to Mike Philcox for his interest. Thanks also to Patrick and Geoff for all their help. I owe a lot to the technical staff, Neil, Declan, Frank and Maura who all deserve special thanks for being available to help regardless of their workload. Also, a very big thank you to Mags for her assistance and advice over the years.

Special thanks go to my friend Michael Cunningham. I am very grateful for all the support, time and encouragement he has given me over the last few years. Also, a big merci to my pal FX who served as the perfect guinea pig for many a hot curry! Thanks to Rory for making me the brunt of countless jokes, and to Gerry, the best joker of them all! Thank you to Aileen for discussions on structure, and to Mira for remote support via the web. Also, I am grateful to Robbie for producing the finest beer this side of the English breweries. Thanks to Neil for some great golf outings, and a big thank you to Jeff and Delwyn for dinners of the highest order that kept me well fed whilst I was writing up.

This being a field-based project, I have great memories of time spent across in northwest Ireland. A heartfelt thank you goes to Pat and Sue Hegarty in Easkey, who helped make a five-month field season fly by. Thanks also to Mary for the blood, sweat and tears sacrificed in Donegal for a few measly 25 kg rock samples!

Thank you to Cristina, Jamie and Becky for some great times over the years. I also am grateful to Eoghan for encouraging chats, and to Brian for being such a good running partner! Thanks to my officemates Jane and Ben for being good company in the final throws of writing up, to Ann Marie and Catherine for their support and encouragement, to Aoife for feeding me at the end, and to Steve for frequent sound advice. Much thanks goes to all my other college colleagues, past and present, many of whom are good friends. Thanks to Kay, Ric, Brian MacSharry, David Jordan, Niamh, David Hardy, Eddy, and Eloise for some memorable times.

A very special thank you now goes to Dolly, who is the best landlady, housemate and friend

anyone could wish for, and I truly appreciate all the support and friendship she has given me during my time in Dublin.

Lastly, I thank my parents for their unwavering support and faith in me. They have always been there to help, and for this I am truly grateful.

Contents

Summary

Acknowledgements

Chapter 1 Introduction

1.1 Aims of the thesis 1
1.2 Ireland in the Palaeozoic 1
1.3 The Mesozoic history of Ireland and surrounding area 2
1.4 The Tertiary period 2
1.4.1 The North Atlantic Igneous Province and mantle plume 2
1.4.2 Crustal stresses during the Palaeocene 4
1.4.3 Tectonics after the onset of northeast Atlantic sea floor spreading 5
1.4.4 Uplift and denudation during the Tertiary 6

Chapter 2 The emplacement of Tertiary dykes in northwest Ireland

2.1 Introduction 8
2.2 Dyke intrusion theory 8
2.2.1 Basic theory 8
2.2.2 En échelon segmented dykes 9
2.2.3 Dyke emplacement into fractured rock 10
2.3 The West Connacht systems 12
2.3.1 Previous work 12
2.3.2 Dyke orientations and relationships with host rock structure across the West Connacht systems 13
2.3.3 Dyke forms 14
2.3.4 Dyke widths and the distribution of dykes within the systems 15
2.3.5 Dyke opening directions, the direction of extension, and implications for the tectonic setting at the time of dyke emplacement 16
2.3.6 Summary model for emplacement of the West Connacht systems 17
2.4 The Killala swarm 18
2.4.1 Previous work 18
2.4.2 Variation in dyke orientation across the Killala swarm 19
2.4.3 Host rock structure 20
2.4.4 Dykes in Precambrian host rock – dyke forms and relationships with host rock structure 21
2.4.4.1 Interpretation 22

2.4.5 Dykes in Carboniferous host rock – en échelon forms and relationships with host rock structure 22
2.4.5.1 A proposal for dyke emplacement under hybrid extension and shear 25
2.4.5.2 A generalised model for the intrusion of en échelon dykes into Carboniferous host rock 25
2.4.6 Relationships between geometric parameters of en échelon dykes in Carboniferous host rock 26
2.4.7 Dyke width and crustal extension 27
2.4.8 Dyke opening directions, the direction of extension, and implications for the tectonic setting at the time of dyke emplacement 28
2.4.9 Summary model for emplacement of the Killala swarm 29
2.5 The Donegal-Kingscourt Swarm 30
2.5.1 Previous work 30
2.5.2 Dykes emplaced into Carboniferous host rock 32
2.5.2.1 The Blind Rock dyke and associated intrusions 32
2.5.2.2 Carn quarry 33
2.5.2.3 St. John's Point peninsula 35
2.5.2.4 Dyke opening directions and the direction of extension 35
2.5.3 Dykes emplaced into Dalradian host rock 35
2.5.4 Dykes emplaced into granite host rock 36
2.5.4.1 Fracture structure of the Rosses and Thorr granites 36
2.5.4.2 Dyke forms and relationships with the granite host rock structure 36
2.5.4.3 Dyke opening directions, the direction of extension, and implications for the tectonic setting at the time of dyke emplacement 37
2.5.5 Summary model for emplacement of the Donegal-Kingscourt swarm 38
2.6 A model for dyke emplacement in western Ireland 38
2.7 Conclusions 39

Chapter 3 Host rock deformation resulting from dyke emplacement

3.1 Introduction 41
3.2 Background 41
3.3 The extent of host rock deformation caused by dyke emplacement 42
3.3.1 Dyke locations and rationale 43
3.3.2 Methods 43
3.3.3 Results 45
3.3.4 Preliminary remarks 47
3.4 Structures in the host rock related to dyke emplacement: examples from Killala Bay 47
3.4.1 Structures associated with dyke segmentation 48

3.4.1.1 Interpretation of deformation related to segment overlap and application to further examples of dykes 49
3.4.2 Structures within (and related to) the dyke-associated fracture zone 52
3.4.2.1 Closely spaced dyke-parallel fracturing (fracture cleavage) 52
3.4.2.2 Shear structures 53
3.4.2.3 Veins at high angle to the dyke 54
3.4.3 Structures within the dykes 55
3.4.4 Structural maps of host rock shear fracturing within the dyke-associated fracture zone 55
3.4.5 Timing of deformation in relation to dyke intrusion 56
3.4.6 Mechanisms behind the formation of fracture cleavage and shear structures in the dyke-associated fracture zone, and implication for the stress regime during dyke emplacement 57
3.5 Integrating all dyke-associated deformation in the host rock 59
3.5.1 Comparing the extent of shear fracturing with that of all dyke-associated deformation in the host rock 59
3.5.2 Thermal stress as a possible cause of dyke-parallel fractures in the host rock 60
3.5.2.1 Heat flow modelling - methods 60
3.5.2.2 Heat flow modelling – results 62
3.5.2.3 Discussion of mechanisms for fracture formation in the host rock by thermal means 63
3.6 Conclusions 64

Chapter 4 The stress regime in northwest Ireland after dyke emplacement

4.1 Introduction 66
4.2 The Tertiary stress regime of Ireland and surrounding areas 66
4.2.1 Tectonics associated with the North Atlantic Igneous Province 67
4.2.2 Post-magmatism tectonics 67
4.3 Examples of segmented dykes that exploit existing faults to facilitate transform offsets 71
4.3.1 The Rosses, northwest Co. Donegal 71
4.3.2 Firkeel Bay, Beara Peninsula, Co. Cork 72
4.4 Dykes where the cause of offset is uncertain 74
4.4.1 Corvock Granite, south Co. Mayo 74
4.4.2 Bloody Foreland east, northwest Co. Donegal 75
4.5 Tertiary palaeostress of onshore Ireland: dykes displaced by post-emplacement faulting 76
4.5.1 Downpatrick Head west, north Co. Mayo 76
4.5.2 St John's Point peninsula, Co. Donegal 77
4.5.2.1 Description of structures 78

4.5.2.2 Palaeostress analysis and interpretation 79
4.5.2.3 Validity of analysis and overall model for the faulting 81
4.5.3 Localities around Lower Lough Erne, Co. Fermanagh 81
4.5.3.1 Classification of the surfaces that contain slip 82
4.5.3.2 Kinematics 83
4.5.3.3 Cross-cutting relationships 84
4.5.3.4 Minerals forming the slickenfibres 84
4.5.3.5 Factors controlling the slip vector 85
4.5.3.6 Palaeostress analysis 86
4.5.4 Carn quarry, Co. Fermanagh 88
4.5.4.1 Description of dyke internal structure and faulting 88
4.5.4.2 Faulting 91
4.5.4.3 Interpretation of structures and overall model for intrusion and deformation 92
4.6 Compatibility of palaeostress analysis with the established tectonic framework for the Tertiary 94
4.7 Conclusions 95

Chapter 5 Tertiary denudation across northwest Ireland, using fission track analysis and (U-Th)/He dating

5.1 Introduction 96
5.2 Fission track analysis 96
5.2.1 Fission track age 96
5.2.2 Fission track annealing 97
5.2.3 Thermal history reconstruction 97
5.2.4 Uncertainties – low temperature annealing and compositional effects 98
5.3 (U-Th)/He dating 98
5.3.1 (U-Th)/He age 98
5.3.2 Thermal sensitivity 99
5.3.3 Grain size effects 99
5.3.4 Mineral inclusions 100
5.3.5 Thermal history reconstruction 100
5.3.6 Compositional and other effects 101
5.4 Fission track and (U-Th)/He age-elevation/depth relationships 101
5.5 Previous studies in Ireland 101
5.6 Rationale behind this study 102
5.7 Sampling 104
5.8 Preparation and analysis 106
5.9 Results 108
5.9.1 Fission track results 108

5.9.2 (U-Th)/He results 109
5.9.3 Microprobe analyses 110
5.9.4 Age-elevation relationships 110
5.10 Interpretation of fission track and (U-Th)/He results 111
5.11 Quantifying Tertiary denudation across west and northwest Ireland 113
5.12 Conclusions 114

Chapter 6 Summary of conclusions 115

References 119-136

Tables

Figures

Appendices

List of Tables

Table 3.1 The dyke-associated fracture zones
Table 5.1 Sample locations for fission track and (U-Th)/He dating
Table 5.2 Fission track analytical data
Table 5.3 Binned fission track length data
Table 5.4 (U-Th)/He analytical data

List of Figures

Chapter 1

Figure 1.1 Geological map of Ireland
Figure 1.2 Basins around Britain and Ireland
Figure 1.3 Migration of extension axes through the Mesozoic
Figure 1.4 The North Atlantic Igneous Province
Figure 1.5 The British Tertiary Igneous Province
Figure 1.6 Timescale for the North Atlantic Igneous Province
Figure 1.7 Denudation and inversion around Britain and Ireland

Chapter 2

Figure 2.1 Dyke propagation

Figure 2.2 Dyke en échelon segmentation
Figure 2.3 The development of an en échelon segmented dyke
Figure 2.4 Relationships between stress ratio and fracture orientation for dykes following pre-existing fractures
Figure 2.5 Location map for the West Connacht systems
Figure 2.6 West Connacht systems: dyke segment orientations
Figure 2.7 West Connacht systems: en échelon dyke forms
Figure 2.8 West Connacht systems: dyke opening directions
Figure 2.9 Location map for the Killala swarm
Figure 2.10 Killala swarm: dyke orientation across the swarm
Figure 2.11 Killala swarm: dyke orientation in different host rock lithologies
Figure 2.12 Killala swarm: host rock structure plotted
Figure 2.13 Killala swarm: photographs of Precambrian host rock structure
Figure 2.14 Killala swarm: photographs of Carboniferous host rock structure
Figure 2.15 Killala swarm: dyke forms in Precambrian host rock
Figure 2.16 Killala swarm: relationships between the dykes and Carboniferous host rock structure
Figure 2.17 Killala swarm: en échelon dyke forms in Carboniferous host rock
Figure 2.18 Mohr circles for hybrid extension/shear fractures
Figure 2.19 Killala swarm: en échelon dyke geometrics plots
Figure 2.20 Killala swarm: dyke widths plotted
Figure 2.21 Killala swarm: crustal extension
Figure 2.22 Killala swarm: dyke opening directions
Figure 2.23 Location map for the Donegal-Kingscourt swarm
Figure 2.24 Donegal-Kingscourt swarm: dyke orientations in Carboniferous host rock
Figure 2.25 Donegal-Kingscourt swarm: en échelon dyke forms in Carboniferous host rock
Figure 2.26 Donegal-Kingscourt swarm: plan of Carn quarry with dyke
Figure 2.27 Donegal-Kingscourt swarm: dyke orientations in Dalradian host rock
Figure 2.28 Donegal-Kingscourt swarm: dyke forms in Dalradian host rock
Figure 2.29 Donegal-Kingscourt swarm: dyke orientations in granite host rock
Figure 2.30 Donegal-Kingscourt swarm: background fracture orientations in granite host rock
Figure 2.31 Donegal-Kingscourt swarm: dyke orientations and forms compared with background fracture orientations in granite host rock
Figure 2.32 Donegal-Kingscourt swarm: dyke opening directions plotted
Figure 2.33 Regional model for Tertiary dyke intrusion

Chapter 3

Figure 3.1 Location maps of dykes where fracture frequency profiles were taken
Figure 3.2 Fracture frequency profile schematic
Figure 3.3 Subtraction of the background frequency from the dyke-associated fracture zone
Figure 3.4 Fracture frequency profiles

Figure 3.5 Fracture frequency profile form comparison
Figure 3.6 Plot of maximum fracture frequency in the host rock against dyke half-width
Figure 3.7 Plot of dyke half-width against width of the dyke-associated fracture zone
Figure 3.8 Classification of limestone by average background fracture frequency for narrow dykes
Figure 3.9 Schematic showing the locations of structures in the host rock margins of dykes
Figure 3.10 Deformation within the host rock bridges of en échelon dykes
Figure 3.11 Deformation outside the host rock bridges of en échelon dykes
Figure 3.12 Overlapping fracture tip interaction for en échelon dykes, and local stress reorientation
Figure 3.13 Conjugate high angle fractures in the host rock bridge zone
Figure 3.14 Model for recognising the oblique propagation of a segmented dyke
Figure 3.15 Schematic showing mechanisms for deformation of the host rock bridge by flexural slip
Figure 3.16 A dyke with a dilation differential, and associated structures
Figure 3.17 Photographs and diagrams of structures in the host rock
Figure 3.18 Photographs and diagrams of structures in the dykes
Figure 3.19 Structural maps of different dykes showing host rock shear deformation
Figure 3.20 Compilation stereographic projection of host rock shear data
Figure 3.21 Histogram of shear displacements
Figure 3.22 Relationship between dyke width and width of the shear zone in the host rock
Figure 3.23 The timing of host rock deformation in relation to dyke emplacement: example 1
Figure 3.24 The timing of host rock deformation in relation to dyke emplacement: example 2
Figure 3.25 Mechanism for shear by failure along en échelon arrays
Figure 3.26 A comparison between the extents of the dyke-associated fracture zones and shear zones in the host rock for a number of dykes
Figure 3.27 Classification of fracture types within the dyke-associated fracture zone
Figure 3.28 Thermal modelling results: a comparison between the width of the dyke-associated fracture zone and the thermal influence of the dyke
Figure 3.29 The modelled total thermal decay of a dyke

Chapter 4

Figure 4.1 Compilation of Tertiary palaeostresses for Ireland and surrounding area
Figure 4.2 Location map
Figure 4.3 Dyke transform offset on The Rosses, Co. Donegal
Figure 4.4 Dyke transform offset at Firkeel Bay, Co. Cork
Figure 4.5 Dyke offset in the Corvock granite, Co. Mayo
Figure 4.6 Dyke offsets east of Bloody Foreland, Co. Donegal
Figure 4.7 Model for *Andersonian* fracturing
Figure 4.8 Faulted dyke west of Downpatrick Head, Co. Mayo
Figure 4.9 Faulted dyke on St. John's Point peninsula
Figure 4.10 St. John's Point peninsula: stereographic projections of fault data
Figure 4.11 St. John's Point peninsula: fault model

Figure 4.12 Location map for Doonan, Drogan and Drumskew quarries, and the A46 road cutting
Figure 4.13 Fermanagh quarries: stereographic projections of all data and view of a quarry face
Figure 4.14 Fermanagh quarries: schematic representation of the structures
Figure 4.15 Fermanagh quarries: stereographic projections of data from Doonan quarry
Figure 4.16 Fermanagh quarries: stereographic projections of data from Drogan and Drumskew quarries, and the A46 road cutting
Figure 4.17 Fermanagh quarries: X-ray diffraction traces for mineralisation associated with slip
Figure 4.18 Fermanagh quarries: the control on the slip vector by columnar jointing
Figure 4.19 Mohr circles for reactivation of existing fractures
Figure 4.20 Failure criteria for various coefficients of static friction on existing planes
Figure 4.21 Fermanagh quarries: schematic representations of reactivation slip within the dykes
Figure 4.22 Carn quarry: local geology
Figure 4.23 Plan of Carn quarry
Figure 4.24 Carn quarry: dyke segments 1 and 2, northwest end of dyke exposure
Figure 4.25 Carn quarry: photographs and sketches from dyke segments 1 and 2, northwest end of dyke exposure
Figure 4.26 Carn quarry: dyke segments 2 and 3, southeast end of dyke exposure
Figure 4.27 Carn quarry: photographs and sketches from dyke segments 2 and 3, southeast end of dyke exposure
Figure 4.28 Carn quarry: photograph mosaic of flower structure in ramp marginal face
Figure 4.29 Carn quarry: faults plotted, and derivation of displacement
Figure 4.30 Carn quarry: photographs and sketches of faults
Figure 4.31 Comparison of Tertiary palaeostresses derived from this study with previous palaeostress trajectories for Ireland and surrounding area

Chapter 5

Figure 5.1 Palaeotemperature maps for Ireland at 65 Ma using two different fission track annealing models
Figure 5.2 A schematic cross-section of three sampling scenarios with respect to the partial annealing zone (fission track) and the partial retention zone (helium)
Figure 5.3 Sample locations
Figure 5.4 Plots of fission track age against mean track length for the margin samples
Figure 5.5 Plots of fission track age against mean track length for the control samples
Figure 5.6 Fission track age-elevation profiles
Figure 5.7 Fission track and (U-Th)/He ages for the margin samples, plotted in comparison with published radiometric dates

List of Appendices

Appendix 1	Published ages for the North Atlantic Igneous Province
Appendix 2	Field sheets
Appendix 3	Basic data for the West Connacht systems
Appendix 4	Basic data for the Killala swarm
Appendix 5	Killala swarm: host rock structure
Appendix 6	Killala swarm: en échelon dyke array orientations and segmentation geometrics
Appendix 7	Killala swarm: derivation of crustal extension
Appendix 8	Basic data for the Donegal-Kingscourt swarm
Appendix 9	Donegal-Kingscourt swarm: background fracture orientations in the Rosses and Thorr granites
Appendix 10	Dyke-parallel fracture frequency in the host rock: all fracture count data
Appendix 11	Dyke-parallel fracture frequency in the host rock: fracture orientation
Appendix 12	Dyke-parallel fracture frequency in the host rock: binned fracture data
Appendix 13	Dyke-parallel fracture frequency in the host rock: re-binned data for the plotting of individual profiles
Appendix 14	Host rock bridge deformation associated with dykes K141 and K135i/ii of the Killala swarm
Appendix 15	Shear structures from the host rock margins of dykes in the Killala swarm
Appendix 16	Code for the 'Schmidt Plot' thermal modelling program
Appendix 17	Results for the thermal modelling of dyke cooling
Appendix 18	Conjugate vein orientation data from the system CI dyke offset in the Corvock granite
Appendix 19	Structural data from faulted dyke, K85, west of Downpatrick Head
Appendix 20	Structural data from faulted dyke, DK18a, St. John's Point peninsula
Appendix 21	Structural data from Doonan, Drogan and Drumskew quarries, and the A46 road cutting
Appendix 22	X-ray diffraction traces from Doonan, Drogan and Drumskew quarries, and the A46 road cutting
Appendix 23	Structural data from Carn quarry
Appendix 24	Apatite fission track data from Allen *et al.* (2002) (Tertiary Uplift of Ireland Project)
Appendix 25	Apatite fission track single grain ages
Appendix 26	Apatite fission track length data
Appendix 27	The reproducibility of (U-Th)/He ages for the Durango apatite
Appendix 28	Apatite microprobe data for the control samples

Chapter 1 *Introduction*

1.1 Aims of the thesis

The aims of this thesis are two-fold. The first aim is to understand the Tertiary tectonic and stress history of northwest Ireland. During this period Ireland was affected by igneous activity of the North Atlantic Igneous Province (NAIP), generally believed to be related to a mantle plume, and was also situated close to where the northeast Atlantic Ocean was opening. To the south of Ireland the Alpine collisional front was developing. Igneous dykes and occasional sills and plugs, part of the NAIP, are the only rocks of Tertiary age that occur in northwest Ireland. Thus, the second aim of the thesis is to study, and provide insight into, some of the fundamental processes of dyke emplacement and host rock deformation. This part of the thesis has wider implications. The thesis is split into four chapters that inter-relate to address these aims.

Each chapter is self-contained, so this opening chapter sets the scene for the rest of the thesis by introducing the geology of Ireland and Ireland's position in the tectonic development of the northeast Atlantic region since the Mesozoic.

1.2 Ireland in the Palaeozoic

Most of Ireland is comprised of Palaeozoic and older rocks at the surface (Figure 1.1). Apart from this, Mesozoic and Tertiary rocks occur in the northeast of the country, and Tertiary intrusives occur sporadically in the northwest and extreme southwest of the country. During the Palaeozoic era, three major tectonic events occurred that have had influence in shaping the geology of Ireland that we see today. During the Ordovician period, the Grampian orogeny caused intense deformation of the Precambrian Dalradian rocks, evidently in response to an island arc colliding with the continental block on the north side of the Iapetus Ocean as it was closing (Phillips 2001b and references therein). This was followed by the Caledonian orogeny (Phillips 2001a and references therein), which marked the complete closure of the Iapetus Ocean in late Silurian to early Devonian times. The northwest and southeast parts of the country were juxtaposed along a NE-SW line (the Iapetus Suture) that crosses the Irish midlands. The majority of the Caledonian granites were then emplaced (see Figure 1.1). Caledonian structures are of fundamental importance in Irish geology, manifest in the many NE-SW faults that cross the country. It is rocks affected by, and associated with, the Grampian and Caledonian orogenies that form most of the high ground around the periphery of Ireland. There then followed a period of rifting, during which earlier Caledonian structures were reactivated, and much of Ireland was beneath sea level. The extensive Carboniferous limestones were deposited, which now form the relatively flat Irish midlands (Sevastopulo 2001 and references therein). Around the end of the Carboniferous period the third major tectonic event, the Variscan orogeny (Graham 2001 and references therein), occurred and the super-continent Pangaea was formed. The orogenic front was to

the south of Ireland, but the effects of the collision caused widespread deformation of Devonian and Carboniferous sediments that had been deposited after the Caledonian orogeny. In the south of the country, where Variscan deformation was most intense, the E-W Variscan signature is preserved in the structural grain (Figure 1.1). To the north, Variscan deformation effects generally consist of gentle folding, faulting, fracturing and veining.

1.3 The Mesozoic history of Ireland and surrounding area

During the Mesozoic, Ireland and surrounding areas were subjected to extensional forces that caused widespread rifting and progressive marine incursions (e.g. Doré *et al.* 1999; Roberts *et al.* 1999). Basins around Britain and Ireland formed (Figure 1.2), commonly by reactivation of older Caledonian and Variscan structures (e.g. Clayton *et al.* 1986; Shannon 1991; Dobson & Whittington 1992; McCaffrey & McCann 1992; Naylor *et al.* 1993; Tate 1993; Anderson *et al.* 1995; Coward 1995; Musgrove & Mitchener 1996; Dancer *et al.* 1999; Tate *et al.* 1999). Ireland is thought to have largely remained above sea level during most of the Mesozoic (Naylor 1992), except for the northeast of the country where the Ulster Basin, controlled partly by reactivation of the Caledonian Tow Valley fault, cumulated sediment (McCaffrey & McCann 1992; Anderson *et al.* 1995) (Figure 1.1). Around Britain and Ireland, from the Jurassic into the Cretaceous, the axes of rifting migrated westwards (Figure 1.3) towards where the northeast Atlantic Ocean would eventually open. The axes also rotated in orientation from N-S to NW-SE (Doré *et al.* 1999; Roberts *et al.* 1999). For example, basins west and northwest of Ireland underwent major rifting and subsidence during the Cretaceous (e.g. Dancer *et al.* 1999). The Rockall Trough underwent major crustal thinning (O'Reilly *et al.* 1995) that was the probable cause of late Cretaceous volcanic activity in the area (Upton 1988; Musgrove & Mitchener 1996). Rifting in the Rockall Trough is thought to have ceased towards the end of the Cretaceous as sea floor spreading, that had been taking place in the central Atlantic since the mid-Jurassic (Doré 1992), propagated north and then northwest towards the Labrador Sea (Roberts *et al.* 1999). During the late Cretaceous, the Irish landmass probably had a thin cover of chalk (Doré 1992; Naylor 1992). Chalk preserved in northeast Ireland, in an outlier in the southwest of the country (Evans & Clayton 1998) and also offshore (e.g. Naylor 1992), lends credence to this argument. Also by this time, Alpine plate collision had commenced to the south (Ziegler 1989). Inversion began to take place in Mesozoic basins around the British Isles (e.g. Roberts 1989; Ziegler 1989; Jones *et al.* 1999). However, Alpine tectonic activity temporarily abated at the end of the Cretaceous (Dewey & Windley 1988). By the start of the Palaeocene (~65 Ma), sea floor spreading had penetrated into the Labrador Sea (Chalmers *et al.* 1993) and the North Atlantic Igneous Province (NAIP) began to develop, possibly aided by the cessation of tectonic activity in the south (Ziegler 1989).

1.4 The Tertiary period

1.4.1 The North Atlantic Igneous Province and mantle plume

The start of the Tertiary saw the widespread extrusion of basaltic lavas in northeast Ireland, and also

the emplacement of dykes across the northwest of the country (the focus of this study) and in the far southwest (Figure 1.1). Igneous activity was part of the NAIP which, during the Palaeocene from around 62.5 Ma, developed over an area 2000 km in diameter, encompassing Greenland, the Vøring Plateau, the Faeroes, the Faeroe-Shetland Basin, the Rockall Plateau and northwest Scotland (White 1988) (Figure 1.4). The province comprises flood basalt lava fields, sediment-sill complexes, dyke swarms and central or shield type volcano complexes. The British Tertiary Igneous Province (BTIP) occupies an area within the NAIP (e.g. Mussett *et al.* 1988), and incorporates the volcanism of northeast Ireland (Figure 1.5).

After the global sea level maximum at the end of the Cretaceous (Haq *et al.* 1987), lavas were extruded across the NAIP subaerially, or initially into shallow marine conditions before syn-magmatic uplift caused subsequent subaerial eruption (Saunders *et al.* 1997). The igneous activity and apparent associated uplift is widely believed to have resulted from the influence of a mantle plume, probably that lying beneath Iceland at the present day (e.g. Bott 1988; Cope 1994; Lawver & Müller 1994; Chalmers *et al.* 1995; Nadin *et al.* 1997; White & Lovell 1997; Clift *et al.* 1998; Jones *et al.* 2002). A presumed Cretaceous chalk cover was stripped from Britain and Ireland, and most of the Irish Sea as a result of this uplift (Naylor 1992). In contrast, non-volcanic margins of the Atlantic Ocean to the south subsided by 2 km or more at this time (White 1988).

Figure 1.6 is a compilation timescale for igneous activity of the NAIP. (See also Appendix 1.) Major magmatism across the NAIP took place in two phases (Saunders *et al.* 1997). The first phase occurred from 62 to 58 Ma and consisted of major continent-based magmatism, basalt lavas and associated intrusive rocks, over eastern Canada, west and east Greenland and the British Isles. This phase preceded continental break-up between Greenland and northwest Europe but coincided with sea floor spreading in the Labrador Sea. The second phase of igneous activity coincided with break-up and plate separation between Greenland and northwest Europe around the start of the Eocene (56 to 53.5 Ma), and saw the formation of widespread seaward-dipping reflector sequences (Saunders *et al.* 1997) (Figure 1.4). In Ireland, igneous activity is largely confined to the first magmatic phase (Figure 1.6), the most obvious exception being the Mourne granites, which mainly belong to the second phase of magmatism (e.g. Thompson *et al.* 1987). Anomalously young ages for the West Connacht and Kerry systems are probably due to argon loss (Mitchell & Mohr 1986).

The position of the mantle plume, and its form, is not well constrained. The distribution of picritic magmatism, and the timing of its extrusion, is not consistent with a single stem plume model (Chalmers *et al.* 1995). Picrite should be local to the plume stem and therefore extrude early on. This is not the case in the NAIP, as picrites are distributed across the province. It could be that a single plume head maintained an anomalously high temperature beneath the crust over the extent of the NAIP, and the position of magmatism was controlled by lithospheric weakness simply where the magma could be channelled through the crust, regardless of the stem position (Chalmers *et al.* 1995). Indeed, crustal weakness has been suggested as a means for allowing the formation of the Hebridean igneous centres in the BTIP (Speight *et al.* 1982; Emeleus 1983) (Figure 1.5). Alternatively, a multiple plume model with plumes beneath both west and east Greenland, and northwest Britain is

possible (Chalmers *et al.* 1995), as is an initial chaotic series of transient plume pulses, which then evolved into the more stable Iceland plume (Nadin *et al.* 1997).

1.4.2 Crustal stresses during the Palaeocene

Along the northwest European margin during the Palaeocene, there was apparent opposition between the crustal stresses; those that facilitated dyke emplacement, and those that were ultimately responsible for the opening of the northeast Atlantic. Northwest-southeast extension had acted since Cretaceous times (Doré *et al.* 1999), but was seemingly much reduced in the basins during the Palaeocene (Tate 1993; Corfield *et al.* 1999; Roberts *et al.* 1999). The dominant extension switched to NE-SW, being associated with the largely NW-SE dyke swarms of the BTIP, including northeast Ireland (England 1988) (Figure 1.5). Conversely, along the east Greenland margin, dykes are orientated ENE-WSW to NE-SW (Figure 1.4), i.e. parallel to and in stress-accordance with rifting in the northeast Atlantic. It has been suggested that deep-seated magma upwellings controlled the location of the Scottish dyke swarms (Speight *et al.* 1982), the most intense swarms being located in basinal areas where the crust is relatively thin (Emeleus 1983). The swarms' central complexes occur at the intersection with major Caledonian NE-SW structures. For example, Rhum is associated with the Great Glen fault (Speight *et al.* 1982). In the south of the BTIP, the Lundy igneous centre in the Bristol Channel lies on the seaward extension of the NW-SE Sticklepath-Lustleigh fault (Brooks 1973). There are a number of models that account for the NE-SW extension direction. Brooks (1973) suggested that NE-SW extension in the BTIP was caused by frictional drag in the same direction at the base of the upper crust by a NW-SE orientated plume head. Alternatively, the two extension directions implied by the BTIP and Greenland dyke swarms might be explained if they were both part of a rift-rift-rift triple junction caused by the doming effect above the mantle plume (Geoffroy *et al.* 1994).

The *type* of stress regime that caused the NE-SW extension east of the proto-Atlantic rift has been suggested in the Faeroe Islands to have been dominantly strike-slip (Geoffroy *et al.* 1994), but in northeast Ireland dominantly extensional (Geoffroy *et al.* 1996). Speight *et al.* (1982) have suggested that the Scottish dyke swarms were emplaced under weak dextral transtension. Across the Scottish part of the BTIP, NW-SE trending syn-volcanic normal faults cut early basalts so can therefore be related to Palaeocene NE-SW extension (England 1988) in an extensional stress regime.

Alpine compressional forces were renewed in the mid-Palaeocene, causing further inversion around the British Isles (e.g. Johnson *et al.* 1999), but had reduced again by the Palaeocene-Eocene boundary, coinciding with onset of sea floor spreading in the northeast Atlantic (Ziegler 1989).

The crustal stresses that operated during the Palaeocene to facilitate dyke emplacement across northwest Ireland are the focus of Chapter 2 of this study. The Donegal-Kingscourt swarm (e.g. Pitcher & Berger 1972) is parallel to the general NW-SE trend of dykes in the BTIP. However, the Killala swarm (e.g. Mohr 1987) and the West Connacht systems (e.g. Mohr 1982) adopt anomalous E-W and NE-SW trends respectively (Figure 1.1 and Figure 1.5). Chapter 2 investigates the mechanisms of dyke emplacement, derives the directions of extension that were associated with

intrusion, and discusses how the intrusions fit into the overall picture of the NAIP.

Following on from Chapter 2, Chapter 3 looks in detail at host rock deformation resulting from dyke emplacement, with emphasis on dykes of the Killala swarm. The study provides new insights into the fundamental processes that operate during intrusion of dykes.

1.4.3 Tectonics after the onset of northeast Atlantic sea floor spreading

With the onset of plate separation at the start of the Eocene, and as sea floor spreading developed and the thermal anomaly decayed, the area uplifted by the Iceland plume did not subside. The continued raised elevation has been attributed to magmatic underplating (Brodie & White 1994; Shannon *et al.* 1995; White & Lovell 1997). Horizontal plate stresses at the rift changed from NW-SE extension to southeast-directed compression along the margins of the opening northeast Atlantic, consistent with ridge-push forces (Doré *et al.* 1999). Inversion structures have been mapped along the northwest Atlantic margin (Roberts 1989; Doré & Lundin 1996; Boldreel & Anderson 1998) and are generally manifest either as elongate domes of gentle deformation or as inverted normal faults. The structures range in age between late Eocene and late Miocene (Doré *et al.* 1999).

In addition to ridge-push forces, Alpine compression from the south continued through the Tertiary (Ziegler 1989), and is generally believed to have caused widespread inversion between the Eocene and Miocene in the southern England and Irish Sea region (e.g. Plint 1982; Roberts 1989; Turner 1997; Jones 1999a; Blundell 2002). Also linked to this inversion, dextral displacements occurred along NW-SE faults, e.g. the Sticklepath-Lustleigh fault (e.g. Dearman 1963), and sinistral displacements took place along NE-SW faults (e.g. Turner 1997). In the west, between the Porcupine Basin and Bay of Biscay, Eocene inversion structures have been related to the Pyrenean orogeny (Masson & Parson 1983; Roberts 1989). Alpine compressional tectonic activity continued intermittently into the Pliocene and possibly into the Pleistocene (Ziegler 1989).

The emergent pattern of intraplate stresses for the Tertiary is therefore one of ridge-push deformation in the area of the northeast Atlantic margin, and to the southeast, inversion associated with Alpine compressional forces.

In Ireland after the cessation of igneous activity, Tertiary tectonics are manifest most clearly in the fault-controlled Lough Neagh Basin that formed during the Oligocene (Figure 1.1), and also along the Tow Valley fault where lacustrine basins formed from sinistral strike-slip movement along the fault, also during the Oligocene. (It is also worth mentioning that high-resolution aeromagnetic data, recently acquired by the Geological Survey of Northern Ireland, show dykes to be sinistrally offset along an extension of the Tow Valley fault in Co. Fermanagh.) Lough Neagh has been compared to similar basins that formed around the same time along the Sticklepath-Lustleigh fault to the east (e.g. Wilkinson *et al.* 1980). In addition to this large-scale evidence for tectonics, Geoffroy *et al.* (1996) have carried out small-scale structural mapping in northeast Ireland. Generally though, elucidating Tertiary tectonic activity in Ireland is difficult since, apart from a few occurrences of non-marine Tertiary sediments that predominantly fill karst features across the country (as shown in Figure 1.1), Ireland is devoid of a Tertiary sedimentary rock record. Study has therefore focussed on other

techniques. Evidence has been presented by studying geomorphology, deformation in older rocks, and fission track ages (Dewey & McKerrow 1963; Dewey 2000; Badley 2001; Pasquali 2002; Solla Hach 2002; Cunningham *et al.* 2003; Cunningham *et al.* 2004), but much of this remains questionable. Chapter 4 of this study investigates evidence for Tertiary tectonic activity in northwest Ireland by the mapping of structures that affect Tertiary dykes. These structures are indisputably Tertiary in age and should allow the elucidation of stress systems that were in operation after dyke emplacement.

1.4.4 Uplift and denudation during the Tertiary

Tertiary uplift and denudation was widespread across Britain and Ireland after the region was permanently uplifted at the start of the Tertiary. It also affected Scandinavia and Greenland at different times and to varying extents. For the British Isles, early estimates of up to 3 to 4 km of denudation in the Irish Sea and northwest England region from apatite fission track analysis (Green 1986; Lewis *et al.* 1992) are now believed to be too high. The same is the case for fission track estimates from eastern England made by Bray *et al.* (1992). It has been recognised that elevated heat flow led to high geothermal gradients at the time. Denudation values of between 0.7 and 1.6 km for the Irish Sea and Lake District region are now thought to be more realistic (Green *et al.* 2002). In support, thermal subsidence modelling gives a value of 1 to 2.6 km of Tertiary denudation for the East Irish Sea Basin (Rowley & White 1998), and sonic velocity modelling gives Tertiary denudation to be less than 1.5 km for the same basin (Ware & Turner 2002). For Ireland, Tertiary denudation is estimated from apatite fission track analysis at between 1.2 and 1.5 km (Allen *et al.* 2002). This is supported by other such studies in Ireland (e.g. McCulloch 1993; Green *et al.* 2000). Widespread Tertiary structural inversion (described in the previous section) produced uplift and erosion. However, Hillis (1995) and Menpes & Hillis (1995) observed that denudation during the Tertiary was not just centred on areas that underwent structural inversion. This is shown in Figure 1.7, which uses denudation data from Jones *et al.* (2002). Hillis (1995) concludes that an average of 1 km denudation took place around Britain in such structurally uninverted areas.

Tertiary uplift is generally believed to have occurred in two phases (e.g. Lewis *et al.* 1992; Japsen 1997; Green *et al.* 2002; Hall & Bishop 2002; Rohrman *et al.* 2002). The first phase dominated the Palaeogene and is attributed to a combination of effects of the proto-Iceland plume and inversion from Alpine tectonics, although the exact nature of the interplay between these two factors is unresolved (as alluded to above) (Green *et al.* 2002). The second, Neogene, phase of exhumation is now widely recognised to have occurred across the British Isles (e.g. Japsen 1997), much of Scandinavia (e.g. Huuse 2002), and in Greenland (Chalmers 2000). In parts of Scandinavia it is the main or only uplift event that occurred in the Tertiary (Japsen 1997; Japsen & Bidstrup 1999; Chalmers 2000; Lidmar-Bergström & Näslund 2002). Towards the Atlantic margin, in the Hebridean basins the main exhumation is mid to late Tertiary (Green *et al.* 1999).

The cause of the Neogene uplift is controversial. Compressional forces, e.g. from ridge-push, cannot explain uplift of the whole north Atlantic region (Japsen & Chalmers 2000), although in

southern England Alpine compressional tectonics is believed to be the cause (Jones 1999b). In southern Norway, Huuse (2002) states that late Tertiary climatic deterioration and eustatic sea level fall was enough to induce accelerated denudation, whereas Nielsen *et al.* (2002) and Stuevold & Eldholm (1996) attribute Neogene uplift and denudation to mantle plume/convection processes, followed by glacial erosion.

Chapter 5 of this study attempts to quantify the amount of denudation that has taken place across northwest Ireland during the Tertiary period. It is apparent from the distribution of deposits dated as Tertiary associated with karstification (Drew & Jones 2000) (see Figure 1.1), that Ireland was above sea level during this time. Previous studies have used the apatite fission track method, the limitations of which will be discussed. For this work, a new apatite fission track study is combined with apatite (U-Th)/He dating, which has sensitivity to lower temperatures, to more confidently quantify Tertiary rock removal for the Tertiary across this region.

The conclusions of the thesis are summarised in Chapter 6.

Chapter 2 *The emplacement of Tertiary dykes in northwest Ireland*

2.1 Introduction

Three sets of Tertiary dykes cut northwest Ireland. These dykes, the Donegal-Kingscourt swarm (e.g. Pitcher & Berger 1972), the Kilalla swarm (e.g. Mohr 1987) and the West Connacht systems (e.g. Mohr 1982), are part of the first phase of the North Atlantic Igneous Province that developed immediately prior to the opening of the northeast Atlantic around 55 Ma (e.g. Mussett *et al.* 1988; Saunders *et al.* 1997) (Figure 1.4). The dykes were emplaced contemporaneously with the development of the Antrim lavas and British Tertiary Igneous Province as a whole (e.g. Mussett *et al.* 1988). The NW-SE trending Donegal-Kingscourt swarm follows the trend of other swarms in the British Tertiary Igneous Province, but the E-W Killala swarm and NE-SW West Connacht systems have anomalous trends in the regional context (Figure 1.5). The dykes were first mapped at the end of the 19th Century. The maps from this time proved invaluable in this study and are listed in Appendix 2.

To date, the dykes of northwest Ireland have not been studied in detail from a structural perspective. This chapter aims to use basic observations of dyke form, and the dykes' relationships with the host rock structure, to investigate emplacement mechanisms and to quantify the directions of palaeostress acting at the time of intrusion. After firstly reviewing the mechanics of dyke intrusion (Section 2.2), the chapter is split into three main sections addressing the three swarms/systems. Section 2.3 looks at the West Connacht systems, Section 2.4 the Killala swarm, and Section 2.5 is a study of the Donegal-Kingscourt swarm. Lastly, a model is presented that attempts to reconcile the emplacement of each of the dyke swarms in terms of Palaeocene crustal stresses.

2.2 Dyke intrusion theory

2.2.1 Basic theory

Igneous dykes are essentially fluid-filled cracks, and as such their propagation characteristics can be explained using fracture mechanical theory (e.g. Pollard 1987).

Dykes either propagate their own hydraulic fractures (Delaney & Pollard 1981; Delaney 1986; Rogers 1987; Lister & Kerr 1991), or occupy existing weaknesses in the host rock (Currie & Ferguson 1970; Baer & Beyth 1990; Jolly & Sanderson 1995). In both cases, the tensile stress at the dyke tip must be greater than the resistance to opening across the potential dyke plane (Anderson 1938; Pollard 1987). This stress is generated by magma pressure and the *driving stress* at the dyke tip.

To propagate a new hydraulic fracture, the dyke tip must exert a greater tensile stress than the strength of the host rock. A series of parallel fractures will form and will open in the direction that requires the least work. Typically, one of these fractures will be invaded by magma to form the dyke.

Therefore, since the host rock will be at its strongest parallel to the direction of remote maximum compressive stress in the horizontal plane (S_H), the direction of opening of the fractures will be orthogonal to this direction, i.e. parallel to the remote least compressive stress direction (σ_3). A dyke propagating its own fractures, therefore, will align parallel to S_H and orthogonal to σ_3 (Anderson 1951; Pollard 1987) (Figure 2.1a). Thus palaeostress trajectories can be inferred by analysing dyke orientation (e.g. Odé 1957; Smith 1987; England 1988).

In highly fractured host rock, it may take less work for a dyke to dilate an existing fracture than propagate a new one. An existing fracture will be used if the magma pressure, which acts orthogonal to the dyke wall, is greater than the oppositional resolved normal component of remote compressive stress on that wall, which itself is less than the tensile strength of the rock for new fracture formation (e.g. Delaney 1986) (Figure 2.1b). However, unlike where a dyke propagates its own hydraulic fractures, any dilated pre-existing fractures that are not orthogonal to σ_3 will show an *oblique* opening, i.e. a combination of extension and shear across the fracture (Figure 2.1b). A fracture that aligns parallel to σ_3 will not be dilated, but may act as a transform between two dilating parts of a dyke. Therefore, the opening direction of dykes exploiting pre-existing fractures can be simplistically considered to align parallel to σ_3 (e.g. Baer & Beyth 1990). In reality though, opening might be oblique to σ_3 depending on the tectonic setting of dyke emplacement (see below) (Jolly & Sanderson 1995).

In this study, dykes are generally seen only in the horizontal plane. Therefore, the dimensions of *length* and *width* are used as shown in Figure 2.1. Dyke width as described here is usually termed dyke *thickness* in the literature when dyke emplacement is studied numerically and considered in three dimensions.

2.2.2 En échelon segmented dykes

The concept of a *segmented* dyke has been alluded to above, in that a dyke can consist of portions, or segments, that do not form a continuous plane. In this thesis, the term dyke *segment* is also used as a general term for portions of dykes that are delineated by changes in strike. It will be apparent from the context in which the term is used as to the applicable situation. Dyke segments might be separated across an existing host rock structure, as shown in Figure 2.1b, or might form without the use of earlier structures. In the latter case, segments can occupy the same plane and appear like a string of boudins in cross-section (Pollard *et al.* 1975; Nicholson 1985), or, much more commonly, they can be segmented in en échelon form (Currie & Ferguson 1970; Escher *et al.* 1976; Delaney & Pollard 1981; Nicholson & Pollard 1985; Hoek 1991).

Traditionally, en échelon fracture sets were assumed to represent shear zones (e.g. Hancock 1972), and this theory was extended to dyke intrusion by Escher (1976). It is now accepted, however, that another mechanism for their formation involves mode I (i.e. extensional) fractures (Beach 1975; Pollard *et al.* 1982; Segall & Pollard 1983; Nicholson & Pollard 1985; Gudmundsson 1987; Mandl 1987; Rothery 1988; Olson & Pollard 1991). (Figure 2.2 defines the three fundamental fracture modes, I, II and III in relation to a propagating dyke tip.) The commonly described mechanism

relating to dyke intrusion involves the break-up of a mode I fracture into a series of en échelon fractures (Pollard *et al.* 1982; Pollard 1987; Hoek 1991) (Figure 2.2). This occurs due to a slight rotation of the extension direction, causing the parent fracture tip to undergo mixed-mode I-III stress that causes break-up into segments. Each segment forms perpendicular to the rotated extension direction, and the array direction is parallel to the parent fracture. En échelon dykes are therefore associated with the propagation of hydraulic fractures that facilitate intrusion. They also indicate the direction of magma transport, i.e. along the length of segments from the parent fracture source.

Segments of an en échelon fracture/dyke array do not propagate laterally indefinitely. This is borne out by the fact that each segment usually only partially overlaps its adjacent segments. The local stress field around the tip of one mode I fracture alters the equivalent stress field around the tip of the adjacent fracture (and vice versa) resulting in the impeding, and ultimately prevention, of further tip propagation (e.g. Pollard *et al.* 1982). This is discussed in more detail in Chapter 3. The en échelon array is therefore preserved as the dyke propagates.

Figure 2.3a shows the development of an en échelon dyke array. Propagation paths where segments overlap can be either curved or straight (e.g. Pollard *et al.* 1982; Nicholson & Pollard 1985), following the same theory as that for an array of unfilled extensional fractures (e.g. Segall & Pollard 1983; Olson & Pollard 1991; Acocella *et al.* 2000). Straight propagation paths are thought to be formed over curved ones if there is a large compression parallel to the propagating fractures (Figure 2.3b), a strong planar fabric exists in the host rock to 'guide' fracture propagation, or high magma pressure and driving stress (Nicholson & Pollard 1985; Olson & Pollard 1989; Renshaw & Pollard 1994). Magma pressure dilates the segments and, in doing so, causes rotation of the host rock *bridges*. Further dilation causes the bridges to fail, and so the segments coalesce. The tips of the initial en échelon segments are preserved as *horns* in the walls of the dyke where the bridges have not been completely lost. The dyke wall *steps* in accordance with the geometry of the original en échelon array.

2.2.3 Dyke emplacement into fractured rock

Existing fractures in the host rock must be suitably orientated to be invaded by magma. This orientation depends on a balance between host rock tensile strength, magma pressure, and the relative magnitudes of the remote principal stresses (Delaney 1986; Jolly & Sanderson 1995, 1997). If the remote differential stress is low (S_H and σ_3 are similar in magnitude) there will be less variation in the normal component of compressive stress acting on fractures ranging in orientation, meaning a given magma pressure will dilate a greater range of fracture orientations.

Delaney *et al.* (1986) define the stress ratio, R, which, by considering the angle (90 - θ) between σ_3 and the normal to the fracture to be dilated (θ is therefore the angle between S_H and the normal to the fracture), relates S_H, σ_3 and the magma pressure, P_m (Figure 2.4a):

$$R = \frac{(P_m - S_H) + (P_m - \sigma_3)}{S_H - \sigma_3}.$$

(Instead of σ_3 Delaney *et al.* (1986) use the term S_h, which means the least compressive stress in the horizontal plane.)

Delaney *et al.* (1986) graphically relate R to the angle, (90 - θ). This is shown in Figure 2.4b. Four fields are defined on the graph. When $R < -1$, P_m is less than σ_3 and therefore will be insufficient to dilate fractures of *any* orientation. When $R > 1$, P_m is greater than S_H and will therefore dilate *any* vertical fracture. There are two fields defined when $-1 < R < 1$. Above the curve defined by the above equation, P_m is sufficiently high to dilate suitably orientated fractures. Below the curve, suitably orientated fractures are absent, but P_m might be sufficiently high for the dyke to propagate a new fracture.

The stress ratio, R, varies with tectonic setting, or less specifically, varies depending on the magnitude of the differential stress. In tectonically inactive regions, there is little difference between the horizontal principal stresses and dykes may dilate fractures of any orientation ($R > 1$), whereas in tectonically *active* regions, dyke orientation gives a better indication of the principal stress directions ($-1 < R < 1$). Here, the direction of maximum compressive stress is relatively large and dyke orientation will be confined close to parallel to this stress.

Obviously, high magma pressure will also increase the value of R, for a given value of differential stress. Jolly & Sanderson (1995) conclude that dykes within the Mull swarm, northwest Scotland, intruded under a range of R values depending on their proximity to the Mull centre. Close to the centre where magma pressure was higher (and thus R values were higher), dykes show a relatively large range in orientation. This is compared to dykes that adopt a narrower range in trend (lower R values) at greater distance from the centre.

Jolly & Sanderson (1995) take further the theory of Delaney *et al.* (1986) by noting that when magma invades pre-existing fractures the opening direction should vary with dyke strike for certain tectonic (or differential stress) settings. They define the opening direction as the angle, μ, of opening relative to the dyke wall (rather than relative to north as it is defined in this study), and derive the relationship,

$$\tan\mu = \frac{\sin 2\theta}{R - \cos 2\theta}.$$

This is represented graphically in Figure 2.4c. When the stress ratio, R, tends towards infinity (i.e. the difference between the principal stresses is small, and any orientation of fracture will dilate), the opening direction is normal to the dyke walls (Figure 2.4c and d). When $R = 1$ ($P_m = S_H$), $\mu = 90 - \theta$, and the dykes open parallel to σ_3. Where $-1 < R < 1$, those fractures that are orientated favourably to dilate will show opening directions that are *dependent on the orientation of the fracture*. When $R = -1$ ($P_m = \sigma_3$), only fractures that are normal to σ_3 can dilate and will only open parallel to σ_3.

A major aim of this chapter is to understand the variation in palaeostress that acted at the time of intrusion around the start of the Tertiary across northwest Ireland. As alluded to above, palaeostress can be inferred by the observation of dyke orientations and measurement of opening directions. However, it is also apparent that the mechanisms for intrusion should also be established to

understand what, if any, control crustal anisotropies/heterogeneities had on dyke emplacement. Observation and measurement of dyke forms allows these aims to be addressed.

2.3 The West Connacht systems

Figure 2.5 shows the study area for the West Connacht systems, the regional geology, and the locations of intrusions referred to in the text. The dyke numbers refer to Appendix 3, in which grid references and raw data for all plots can be sourced.

2.3.1 Previous work

The West Connacht systems trend NE-SW to ENE-WSW across Connemara (Co. Galway) and south Co. Mayo. As well as dykes, a number of sills and plugs associate with the systems. The term *system* is used instead of *swarm* as the dykes are relatively wide and are few in number (Mohr 1982). The host rocks are Caledonian granite, in the form of the Omey and Corvock granites, Dalradian metasediments, Lower Palaeozoic clastics, and Carboniferous sediments in the northeast.

Mohr (1982) describes five systems, IBF, CI, CO, CM, and TD based on spatial relationships of outcrops and geochemical affinities (Figure 2.5). The largest of these systems, CI, trends for 50 km and swings in strike at the northeast end, running sub-parallel to host rock strike immediately south of Croagh Patrick. It appears to terminate further northeast in a series of sills intruding Carboniferous rocks. Here, the intrusions are close to the boundary where the Carboniferous cover lies atop the Dalradian basement. System CM has intermittent exposure for 35 km. The Síofra gabbro, a circular plug (Mohr 1991), lies along strike to the northeast from system CM, and also from a splay off system CI (Mohr 2000). Systems CO and TD are dubious due to lack of outcrop. System CO is based on the positioning of the Doon Hill plug and the Dromchogaidh sill (Mohr *et al.* 1984). The sill, however, might instead associate with system CM (Mohr 1982). In addition, an intrusion near Clifden, of unknown form (Mohr 1992), lies between systems CM and CO, not appearing to be spatially linked with either. System IBF, solely consisting of dykes, is confined to Inishbofin and has an east-northeast trend.

The age of the West Connacht systems is fairly well established as Palaeocene ((Macintyre *et al.* 1975; Mohr *et al.* 1984; Thompson 1986; Mussett *et al.* 1988)). A number of anomalously young ages were obtained in a K-Ar study, but are probably the result of argon loss (Mitchell & Mohr 1986).

Discounting apparent anomalously young ages, intra-system dates show some agreement. Two ages for system CI, a K-Ar age of 57.3 ± 1.1 Ma (Mitchell & Mohr 1986) and an Ar-Ar age of 58.1 ± 0.3 Ma (Steve Bergman *pers. comm.*), are in agreement. However, for system CM, ages of 60.1 ± 1 Ma (K-Ar) (Macintyre *et al.* 1975) for the Doon Hill plug and 55 ± 2 Ma (Ar-Ar) (Mohr *et al.* 1984) for the Dromchogaidh sill are not within error of each other (see Figure 1.6).

Fission track ages from the host rock immediately adjacent to system CI (Chapter 5 of this study) are around 59 Ma, in agreement with the most reliable radiometric ages.

Thin-section and micro-probe analyses show that the majority of intrusions are alkaline,

undersaturated, analcime-olivine dolerites. However, as with the Killala swarm (see later), they also have a MORB (mid-ocean ridge basalt) signature of low K_2O (Mohr 1982). Exceptions include the Síofra gabbro and a minor sill next to the Dromchogaidh sill that are saturated sub-alkaline dolerites (Mohr *et al.* 1984; Mohr 1991).

The magma source for the West Connacht systems is believed to be the Brendan centre, offshore to the southwest. The systems lie along a line that intersects the centre (Riddihough & Max 1976; Mohr 1982) and that then continues southwest to similarly orientated dykes, the Slyne fissures, which were emplaced into the northern part of the Porcupine Basin, also during the Palaeocene (Tate 1993) (Figure 1.5). The Brendan centre is, in addition, thought to have sourced the NNW-SSE Kerry systems of southwest Ireland, implying it produced a radial arrangement of intrusions during its development (Mohr 1982; Tate 1993).

According to Mohr (1982), width variation along the strike of systems CI and CM can be explained by post-emplacement differential denudation along the strike of the dykes. Here, Mohr (1982) uses the model of Dewey & McKerrow (1963) for late Tertiary differential uplift of the Connemara region. The central sectors of the two systems, which are the widest sectors, would correspond to an approximate intrusion depth of 750 m, with narrower dyke widths to the southwest corresponding to shallower intrusion depths (Mohr 1982). This model of uplift, however, has recently been somewhat discredited by Worthington *et al.* (2003).

The emplacement mechanisms/styles of the West Connacht systems have not been studied in much detail. At the southwest end of the swarm, dykes are described as exploiting fractures in the Omey granite, and also the E-W foliation in Dalradian host rock (Cobbing 1961). According to Cobbing (1961), this implies crustal tension was weak on intrusion, as the dykes do not appear to have propagated their own hydraulic fractures. This statement is somewhat enigmatic. Mohr (1982) describes the dykes further northeast as being unaffected by older structures, excepting the strike swing of system CI south of Croagh Patrick and host rock structures that occasionally cause the systems to bend or jump abruptly. Vertical offsets of the Dromchogaidh sill are interpreted as having resulted from syn-intrusion buoyancy adjustments accommodated by faults (Mohr *et al.* 1984).

In the sections below, orientation data is presented for dykes of the West Connacht systems, and dyke forms and opening directions are described. A general model for emplacement is then presented.

2.3.2 Dyke orientations and relationships with host rock structure across the West Connacht systems

Figure 2.6 shows dyke orientation across the West Connacht systems. The orientation data is displayed for different areas, with each area being confined to a single system and a single general host rock type as defined. There is a lot of variation in dyke segment orientation across the region. In the majority of areas where the host rock is Dalradian, dyke emplacement was influenced by the metamorphic grain, which generally strikes WNW-ESE and dips to the north between 50° and 70°. For example, the narrow dykes WC8, WC15 and WC16 were all emplaced along the Dalradian fabric,

and as a result are not vertical, but dip around 60°NNE. Dyke WC1 (system CM) was also emplaced along the host rock grain, but possibly then becomes dyke WC2, which cuts orthogonal to the grain. The dykes of system IBF on Inishbofin almost exclusively follow the metamorphic fabric, which here has a ENE-WSW trend. The one area where the Dalradian fabric does *not* appear to have exerted influence during dyke emplacement is on the Renvyle peninsula. Here, the dyke segments of system CI show a dominant NE-SW trend. However, the main dyke, WC25/28, of the system is relatively wide when compared to other dykes that have been emplaced parallel to the metamorphic fabric, apart from system IBF where dykes of substantial width exploit the host rock grain. The area of Dalradian host rock that contains dykes WC7 to WC17 shows a relatively broad range of dyke segment orientations. It is probable that other host rock structures control dyke orientation here.

In the Omey granite, dykes (associated with system CI) show quite a broad range of orientations, as described by Cobbing (1961). This appears to be typical of dykes emplaced into granite (e.g. dykes of the Donegal-Kingscourt swarm described in later sections). However, where system CI cuts the Corvock granite near its northeast end, dyke orientation is a consistent NE-SW, although here the dyke is much wider at >12 m.

The host rock type that yields dykes with the greatest consistency in orientation are the Lower Palaeozoic sediments. Systems CI and CM are at their widest here, north and immediately south of Killary Harbour. The trend of system CI is dominantly NE-SW, whereas system CM adopts a more ENE-WSW trend. Northeast of the Corvock granite, system CI takes a relatively variable path, compared with its path to the southwest at the mouth of Killary Harbour. Pre-existing structures in the host rock may, therefore, have had more of an influence on dyke intrusion at the northeast end of system CI. Indeed (Mohr 1982) reaches the same conclusion, noting the swing in strike of the dyke behind Croagh Patrick.

It is interesting to compare the range of dyke segment orientations within the microdiorite that outcrops at the top of the mountain Benchoona, with orientations in the surrounding Lower Palaeozoic sediments. There is a greater range in the former, with apparently more discrete populations of preferred orientations. This likely indicates increased heterogeneity in the igneous host rock. Indeed, the broad range of dyke orientations within the microdiorite implies that the dyke exploited pre-existing fractures on intrusion.

2.3.3 Dyke forms

Where dykes follow the metamorphic grain of the host rock, they typically periodically jog across foliation planes. This gives the dykes an overall trend that is slightly oblique to the host rock fabric (e.g. dyke WC8). Occasionally, they show segmented forms between host rock fabric planes, but never is an en échelon array seen.

The few dykes in granite show mostly straight forms. The narrow dyke, WC3, however, has an angularly zig-zagging form, much like that seen for dykes of the Donegal-Kingscourt swarm intruded into granite (see later sections).

It has been described above how system CI shows consistent NE-SW orientation in Dalradian host

rock where it cuts the Renvyle peninsula. That is, the dykes do not exploit the Dalradian fabric. Figure 2.7 shows how the dykes here show segmented en échelon geometry. This is the only place where such geometry is seen. Dyke WC25a consistently right-steps along its strike where exposed on the coast. Steps can be seen to exploit the host rock fabric, and in one place a horn is a remnant of the original segment array that now makes up the dyke margin. At the northeast end of the exposure, at the overburden, the dyke terminates abruptly, the geometry of which indicates that this must be a segmentation of the dyke. A right-stepping form is implied, consistent with the smaller scale jogs already described. Due to the proximity of the overburden, the adjacent segment is not seen, but must occur to the southeast. Dyke WC24 outcrops to the southeast as a narrow, tapering (to the southwest), dyke. The reconstruction in Figure 2.7 incorporates this dyke with dyke WC25 as part of a right-stepping en échelon intrusion cutting Tully mountain. To the northeast, dyke WC28 (the along-strike equivalent of dyke WC25) outcrops in right-stepping configuration, as does dyke WC17 to the southwest. Towards the northwest end of the Renvyle peninsula, dyke WC26a shows a right-stepping configuration (viewed from the cliff top), but is inaccessible.

The strikes of the dykes that cut the Renvyle peninsula are therefore consistent in their orientation with a right-stepping segment array, in that they are aligned anticlockwise of the array direction. This form of intrusion is in agreement with the relatively narrow distribution of dyke strikes shown in Figure 2.6 for the peninsula. Consistent en échelon geometry would also suggest that the dykes propagated their own hydraulic fractures on intrusion (see Section 2.2.2 above). Indeed, in Chapter 3 it is shown how closely spaced fractures concentrated at the margins of dykes WC25 and WC32a (along strike to the northeast) were probably, at least in part, created by hydraulic fracturing as the dykes were emplaced. System CI cutting the Renvyle peninsula is therefore probably a good indicator of the palaeostress direction that acted to cause intrusion (as discussed below).

2.3.4 Dyke widths and the distribution of dykes within the systems

Dyke width varies considerably within the West Connacht systems. At its southwest end, the dyke that describes system CM (dykes WC1 and WC2) is around 3 m wide. Cutting through Benchoona, near the northeast end of the system, the dyke (WC9) reaches a width in excess of 9 m, before becoming narrower again on the banks of Killary Harbour where the dyke (WC 30) is 5.6 m wide.

On Inishbofin, system IBF appears to consist of two main dykes that are exposed, dykes WC39 to WC42 and WC43/WC44. Dykes WC39 to WC42 show an initial widening, followed by a progressive narrowing from west to east (from 12 m at dyke WC40 to 2 to 3 m at dyke WC42a). (It is apparent throughout this study that on the scale of metres, or even kilometres, along strike, the amount of extension that a accommodated by dykes remains remarkably constant. This can often be verified by summing the widths of a number of dykes that are parallel at points along their strike, and finding that this width remains the same despite the widening and corresponding narrowing of the element intrusions.) The amount of narrowing that has taken place between dyke WC40 and dyke WC42d is roughly balanced by the width of the second main dyke, WC43. At the eastern end of the system a dyke is probably situated offshore to the north, given that dyke WC42d is so narrow. Similarly, dyke

WC43 probably continues west, i.e. to the north of dyke WC41. These inferences would maintain the total amount of extension (which is possibly represented by dyke WC40 at around 12 m) of the system from east to west.

System CI shows a gradual widening from southwest to northeast along its strike of around 50 km. South of Killary Harbour, the system does not just consist of one dyke, but often a main dyke that generally has a NE-SW strike, and narrow 'subsidiary' dykes that commonly follow the Dalradian metamorphic fabric. At the southeast end the summed widths of dykes WC4 and WC5 is in the order of 9 to 10 m, although this might be an overestimate of the total system width if widening of one dyke has accommodated an unseen narrowing of the other. Cutting through Tully mountain, the system width is probably around 7.5 to 8 m, given by the summed widths of dykes WC25a and WC26a. An inferred narrowing of dyke WC26 across the Renvyle peninsula (to become dyke WC27), probably accounts for the corresponding widening of dyke WC25 to the northeast, although the width of dyke WC28 (the along-strike equivalent of dyke WC 25) cannot be accurately ascertained.

It must be stated that dykes might exist that have not been mapped due to poor exposure, thus bringing into question some of the interpretation above. There are a number of beaches around the Renvyle peninsula where dykes may pass undetected.

North of Killary Harbour, system CI appears to have substantially gained in width, and consists of just the one dyke, which continues to widen from 12 m (dyke WC 32a) to 15 m (dyke WC33). It is unclear as to whether the dyke widens further to the northeast, but in the Corvock granite the dyke (WC35d) is still >13 m wide. It is suggested (Mohr 1982) that system CI terminates as the series of sills in Carboniferous host rock east of Clew Bay, as shown in Figure 2.5.

Mohr (1982) postulates that the widening of system CI northwestwards on the north side of Killary Harbour is due to the fact that outcrop here is sampling relatively deep parts of the system (as explained in Section 2.3.1 above). Mohr (1982) invokes 100 m of post-emplacement dip-slip displacement on the fault believed to run along Killary Harbour. This is based on the uplift model of Dewey & McKerrow (1963)), which has actually been somewhat discredited by Worthington *et al.* (2003). In addition, it is extremely rare to find that a Tertiary dyke has been faulted (see Chapter 4). It may therefore be that the widening of system CI is simply accommodating a corresponding narrowing of a dyke elsewhere. The dyke of system CM, with its apparent narrowing northeast of Benchoona (described above), is a candidate for such an intrusion. Alternatively, a dyke might exist offshore that pinches out before intersecting the coast northwest of Mweelrea mountain. This idea can be applied over the total outcrop extent of systems CI and CM. At the southwest end of the exposed systems, the summed width of systems CI and CM is probably around 13 m. This is close to the maximum width of around 15 m attained by system CI to the northeast, at which point system CM appears to have terminated, seemingly having not propagated past the Síofra gabbro (Figure 2.5).

2.3.5 Dyke opening directions, the direction of extension, and implications for the tectonic setting at the time of dyke emplacement

Figure 2.8 shows opening directions (see also Figure 2.1) for some of the dykes in the West Connacht

systems. Opening directions are all roughly orthogonal to the strike of the dykes, leading to great variation in the direction of dyke opening.

It has been suggested above that much of the variation in dyke strike across the West Connacht systems is due to emplacement into the metamorphic fabric of the Dalradian host rock and pre-existing fractures within granite and the Benchoona microdiorite. Given this, and the range of orientations and opening directions displayed by the dykes, the theory of Delaney & Pollard (1986) and Jolly & Sanderson (1995) (as detailed in Section 2.2.3 above and Figure 2.4), for dykes emplaced along pre-existing structures, can be used to infer the tectonic setting at the time of dyke intrusion.

There is just a 10° window, between 160° and 170°, in which no dykes are found to outcrop. That is, almost every possible orientation of dyke exists within the systems. Given this, and the implication by Figure 2.8 that horizontal opening directions are generally perpendicular to a wide range of dyke strikes, it can be inferred that the stress ratio, R (as defined by Delaney & Pollard (1986)), was greater than +1 at the time of intrusion (Figure 2.4d). The implication here, however, is that *all* orientations of fractures can be dilated by the magma. Given this, the magnitude of σ_3 (least horizontal compressive stress) was tending towards S_H (maximum horizontal compressive stress), i.e. the differential stresses were low at the time of dyke emplacement. This could indicate that the tectonic setting was relatively inactive when the dykes intruded. Alternatively, or in addition, the magma pressure may have been high, sufficiently so as to cause dilation of a wide range of fracture orientations. However, the fact that the dyke systems as a whole trend NE-SW at approximately 060° is an indication of NW-SE directed extension (or least compressive stress). In support of this, system CI cuts the Renvyle peninsula as a NE-SW en échelon array (as described previously in Section 2.3.3) with an average segment strike of 032°, and therefore an extension direction of 122°.

2.3.6 Summary model for emplacement of the West Connacht systems

It appears that the West Connacht systems were emplaced under NW-SE directed extension during the Palaeocene. Dyke emplacement took place by a combination of intrusion along pre-existing structures and hydraulic fracture of the host rock. The extension was probably relatively weak, i.e. the difference between the horizontal principal stresses was not great, but was still enough to control the overall NE-SW trend of the intrusives. The palaeostress direction for dyke emplacement is probably most directly reflected by the en échelon arrays of system CI where it crosses the Renvyle peninsula.

The apparent northeast termination of System CI as a series of sills in Carboniferous host rock, close to where it lies atop the Dalradian basement, is an interesting feature of the system. It is suggested that these sills could have facilitated the change from likely variable orientation of the dykes in the basement, to a more uniform orientation of intrusion in the Carboniferous cover that has since been stripped away. Such sills would be expected to occur at, or close to, the basement/cover interface.

The suggestion that the West Connacht systems are related to the Brendan centre (see Section 2.3.1 above) as part of a radial relationship with the Kerry systems and the Slyne fissures seems likely.

This is discussed at the end of the chapter.

2.4 The Killala swarm

2.4.1 Previous work

Figure 2.9 shows the study area for the Killala swarm, the regional geology, and the locations of intrusions referred to in the text. The dyke numbers refer to Appendix 4, in which grid references and raw data for all plots (unless otherwise stated) can be sourced.

The Killala swarm trends E-W through the northern areas of counties Sligo and Mayo, across Killala Bay, roughly following the trend of the north Co. Mayo coastline. In the east the swarm intrudes Carboniferous sediments, and in the west basement comprising Dalradian rocks of Precambrian age and older metasediments and gneisses of the Inishkea and Annagh Divisions respectively (Figure 2.9). The Carboniferous is the cover sequence and sits unconformably on top of the Precambrian basement. The swarm extent is delineated in the north by the E-W coastline and an isolated dyke on the west-facing coast of Donegal Bay. Excepting this dyke, the swarm appears to reach an easternmost extent at Aughris Head. In the south the swarm extent is delineated by outcrops on the west side of the Belmullet peninsula, and also by sporadic inland exposures. Inland exposures to the southeast are possibly part of the Killala swarm and appear to curve towards the NW-SE trend of the Donegal-Kingscourt swarm (Figure 1.1). Mohr (1987) divides the swarm into three left-stepping sub-swarms, delineated by zones of low dyke density.

The swarm shows two phases of intrusion (Preston 1965). The earliest intrusions outcrop in Killala Bay and are centred on the Killala gabbro. The gabbro, on the west side of the bay, is a 5 km long by 400 m wide funnel-shaped dyke-like body of parallel trend to the dykes (Preston 1979) (Figure 2.9). On the east side of the bay, the Inishcrone gabbro, and several wide multiple dykes with broad metamorphic aureoles, are believed to be the along-strike equivalent of the Killala gabbro (Preston 1965). At Inishcrone, the gabbro is wedge-shaped (Emeleus & Preston 1969), comprising a narrow sill fed from a dyke beneath its northern margin (Mohr 1987). To the west, a 9 m wide dyke at Belderg may be the along-strike extension of the gabbro (Mohr 1987).

The second intrusion phase forms the majority of the swarm and is manifest as multiple and single phase (flash injection) dykes. Some of the latter cut the Killala gabbro (Preston 1965; Emeleus & Preston 1969).

A K-Ar age of 52.8 ± 4.1 Ma for the Inishcrone gabbro is not in agreement with a K-Ar age of 58.2 ± 1.1 Ma (Macintyre *et al.* 1975) for a dyke cutting the Killala gabbro, given the relative ages described above. A more recent Ar-Ar age of 58 ± 1 Ma for the Killala gabbro (Thompson 1986) would seem, therefore, more accurate. However, a 63.1 ± 1.1 Ma Ar-Ar age for an unspecified dyke at Inishcrone (Steve Bergman *pers. comm.*) may mean the swarm was emplaced even earlier (see Figure 1.6).

An apatite fission track age of 56 ± 5.4 Ma from the Mullaghmore Sandstone Formation in the metamorphic aureole of the Killala gabbro (McCulloch 1993) roughly supports the Ar-Ar ages.

Fission track ages from the host rock immediately adjacent to dykes at the western end of the swarm are around 59 Ma (Chapter 5 of this study), and further support the radiometric ages for the swarm.

Chemically, the dykes of the Killala swarm are undersaturated analcime-olivine dolerites, similar to the Kerry and West Connacht systems. However, the low K_2O levels are more characteristic of mid-ocean ridge basalts (MORB) than of alkali basalts. They thus appear quite distinct from the sub-alkaline olivine tholeiites of northeast Ireland and the Donegal-Kingscourt swarm (Mohr 1987).

Basic physical parameters, emplacement mechanisms and styles of intrusion have been described for some dykes in the Killala Bay area (Mohr 1987; Joesten & Van Horn 1999). These dykes opened in pure extension (Mohr 1987), in a series of en échelon segments indicating vertical magma ascent. They intruded parallel to a regional joint set and are associated with zones of dyke-parallel closely spaced joints in the host rock indicating that hydraulic fracturing took place. Dykes show offset contacts to the left or the right where en échelon segments became coalesced (Joesten & Van Horn 1999). Mohr (1987) observes a common tendency for dykes to left-step along strike and, with the apparent left-stepping sub-swarms, suggests a weak dextral shear regime active during emplacement.

The western parts of the swarm, where dykes intrude structurally more complex host rock, are unstudied.

On a regional scale, the anomalous trend of the Killala swarm could be considered intermediate between the NE-SW trend of the West Connacht systems and the NW-SE trend of the Donegal-Kingscourt swarm. However, there are geochemical differences when comparing the Killala and Donegal-Kingscourt swarms. In addition, the West Connacht and Kerry systems are thought to derive from the offshore Brendan centre (Figure 1.5), and it is difficult to spatially associate the Killala swarm with this offshore intrusion (Mitchell & Mohr 1987).

The sections below firstly introduce the variation in dyke orientation across the swarm, before describing and relating host rock structure to dyke forms and emplacement. Then, various observations/parameters are described with a view to deriving an overall model of intrusion for the Killala swarm.

2.4.2 Variation in dyke orientation across the Killala swarm

Figure 2.10 shows dyke segment strike for areas across the Killala swarm. It is immediately apparent that there is a much wider range of orientations displayed within the Precambrian host rock in the west. In the east, the E-W trend of the swarm is more clearly represented in Carboniferous host rock by individual dyke orientations. Overall, the overwhelming majority of dykes display an E-W strike. The above observations are highlighted in Figure 2.11, which also shows that dyke dip shows a wider range in the older host rock when compared to the mainly sub-vertical inclination of dykes emplaced into Carboniferous host rock.

Of interest to note in Figure 2.10 is the abundance of NE-SW dykes in the far west of the swarm, together with the wide range of orientations shown by dykes K42 to K65, particularly the NW-SE peak. Centrally within the swarm, for both Precambrian and Carboniferous host rock, the majority trend is WNW-ESE rather than E-W. There are no outcrops showing dykes crossing the boundary

between Precambrian basement and Carboniferous cover. Lastly, dyke orientations are anomalous in the vicinity of the Killala gabbro in Carboniferous host rock, the majority of dyke segments trending NW-SE.

2.4.3 Host rock structure

The host rock of the Killala swarm can be split into two main groups. In the east, Carboniferous limestone and sandstone, and in the west, Precambrian Dalradian metasediments and the older Inishkea and Annagh Divisions of schist and gneiss respectively.

Figure 2.12 plots host rock structure (see Appendix 5 for raw data). The Precambrian host rock invariably has a pervasive metamorphic fabric. It can be seen that this fabric shows regional variation in orientation. Strike is generally either WNW-ESE or ENE-WSW. The exception is a zone southeast of Erris Head that shows a NNE-SSW strike. The fabric is generally inclined from the horizontal and often dips steeply (Figure 2.13a).

This study does not attempt to quantify in detail brittle structure within the Precambrian host rock, but rather describes a few general observations made in the vicinity of the Tertiary dykes. Many faults are mapped along the coast, the majority having a trend close to N-S. In exception, there is a dominance of NW-SE and NE-SW faults along the northwest-facing coast of the Belmullet peninsula. In addition, a NE-SW fracture set exists across the peninsula. This is particularly apparent on the west side where the structures are exposed cutting the cliffs (Figure 2.13b).

In many places along the coast there is a fracture set that strikes between 115° and 130°, dipping steeply. Also noted is a roughly N-S, steeply dipping, fracture set that pervades the coast north of Pollatomish and the N-S peninsula across the bay to the north (Figure 2.13c).

The age relationships between the brittle structures described is unknown.

Structure within the Carboniferous host rock is a lot simpler than within the Precambrian host rock (Figure 2.12). Strata are orientated sub-horizontally in the main, and there are just three main groups of structures, distinct in their orientations, which are pervasive throughout the area. These groups can then be further split if there are both veins and unfilled fractures of the same orientation with a group. Firstly, steeply-dipping structures occur that are sub-parallel to the dykes and most commonly strike between 095° and 100°. Secondly, there are structures that occupy a high angle in strike with respect to the dykes. They are most commonly orientated between 160° and 170° and also dip steeply. Thirdly, steeply dipping fractures orientated NE-SW pervade most areas. The first two groups of structures adopt a sub-parallel orientation to structures observed to the south in The Burren, Co. Claire, described by Gillespie *et al.* (2001).

In the case of the dyke-parallel and high angle structures, they are mostly manifest as fractures, but in some areas of limestone host rock they occur as veins (labels of 'mineralisation' in Figure 2.12) as well as fractures. As fractures, they appear not to have accommodated any shear and occur over a variety of length scales. In the case of the dyke-parallel fractures, their frequency of occurrence within individual beds is dependent on the host rock lithology and bed thickness, with thickly bedded limestone and sandstone typically having the lowest fracture frequency. This relationship between

bed thickness and fracture spacing is commonly seen in sedimentary successions (e.g. Ladeira & Price 1981). It follows then that fractures do not propagate up sequence very far. In addition, dyke-parallel fractures often show a change in strike by a few degrees crossing from bed to bed. Again, this is common in sedimentary sequences where propagating fractures are reorientated and may break down at bedding planes (e.g. Helgeson & Aydin 1991; Cooke & Underwood 2001). The dyke-parallel fractures are therefore not continuous through-section. As veins, the dyke-parallel structures are typically extensional and continuous over only a few tens of centimeters along strike, and are generally restricted to individual beds. In contrast, the high angle fractures appear to be much more pervasive through-section, and occur over larger length scales across the platform. As veins, they often show shear kinematics, e.g. pull-apart arrays. There are apparent conjugate relations between sinistral and dextral shears that strike at the two extremes of the strike range shown by this group of structures.

Age relationships between the dyke-parallel and high angle structures are shown in Figure 2.14. Generally, where mineralisation is absent, either one of the structure types abuts against the other, as shown in Figure 2.14a. This indicates that the structures are at least in part coeval in their formation. Where mineralisation occurs, however, dyke-parallel veins are consistently offset by high angle shear structures (Figure 2.14b and c) showing that the latter are the younger structures.

The NE-SW fractures show less clear age relations with the other two sets of structures. They might be the youngest structures given that they are not seen to abut against the dyke-parallel or high angle structures, tending to just cut straight through.

Gillespie *et al.* (2001) and Odling *et al.* (1999) suggest that N-S veins, i.e. sub-parallel to the high angle veins described here, in The Burren were formed by Variscan tectonics. Gillespie *et al.* (2001) state that E-W unfilled fractures from the same area probably formed much later and are likely related to uplift and unloading. The same may therefore be true of the E-W fractures described here in the Killala Bay region.

2.4.4 Dykes in Precambrian host rock – dyke forms and relationships with host rock structure

The dykes show a wide variety of forms and orientations within the Precambrian host rock in the west of the swarm. This appears to be afforded by the relative structural complexity of the older host rock.

Many of the dykes emplaced into Dalradian host rock follow exactly, or roughly, the metamorphic fabric (Figure 2.15a). Examples include dykes K47, K49, K65, K13 and K41. Given that the host rock fabric strike is close to E-W in many places (Figure 2.12), such dykes retain a strike sub-parallel to the overall E-W trend of the swarm. Some dykes exploit only partially the host rock metamorphic fabric, being also emplaced along fractures (apparently pre-existing) of different orientation. This is shown in Figure 2.15b for dyke K40. Occasionally a dyke is emplaced along a fault. Dyke K4 is one such dyke, as shown in Figure 2.15c. Other such dykes are K42 and K46.

A few dykes take the form of en échelon segmented arrays. The two best examples of this are shown in Figure 2.15d and e (dykes K27 and K10 respectively); but note the different trends of E-W

and NE-SW respectively for the two dykes. In both cases the metamorphic fabric is oblique to the dykes. These dykes therefore do not appear to exploit the metamorphic grain of the host rock (the exception being the bending horns of dyke K27). However, in Chapter 3 it is shown that a dyke sub-parallel fracture set exists in the host rock in the vicinity of dyke K27. Also, it is noted that in the vicinity of dyke K10, NE-SW pervasive fractures cut the Precambrian host rock, as described in Section 2.4.3 above and shown in Figure 2.13b.

As well as en échelon segmentation in the sub-horizontal plane, dyke K17 (Figure 2.15f) shows that segmentation also occurs in the sub-vertical plane, although obviously this is rarely seen.

2.4.4.1 Interpretation

It is interpreted that pre-existing structure in the Precambrian host rock at the western end of the Killala swarm influenced dyke emplacement and commonly exerted control on dyke orientation. The metamorphic fabric is the most common such structure. En échelon dykes such as dyke K27 (Figure 2.15d) probably propagated their own hydraulic fractures on intrusion but may still have been influenced to a degree by sub-parallel fractures in the host rock. The frequent occurrence of NE-SW orientated dykes at the extreme west of the swarm is interesting, especially since dykes K10 and K11/12 display quite consistent right-stepping en échelon geometry. These dykes could be invading at depth the major NE-SW fractures seen in this area (Figure 2.13b), but at the current outcrop level such orientated fractures may have terminated. This may have caused the dykes to break down into segmented forms as they continued to propagate upwards. Indeed, dykes K10, K11 and K12 might all be part of the same NE-SW intrusion. Alternatively, the abundance of NE-SW orientated dykes might be reflecting a rotation in the principal stress directions at the western end of the Killala swarm (see later Section 2.4.8).

2.4.5 Dykes in Carboniferous host rock – en échelon forms and relationships with host rock structure

Most dykes emplaced into Carboniferous host rock occupy a roughly E-W trend, with relatively little deviation from this orientation. The majority of the dykes display an en échelon segmented form of intrusion.

The age relationships between the dykes and Carboniferous host rock structures described above in Section 2.4.3 can, in some cases, be readily identified. The NE-SW fracture set is often seen dilated by the dykes, by which the intrusion opening direction can be measured (Figure 2.16a). In addition, dykes sometimes jog along these fractures. When this occurs, the distance over which the dyke occupies the NE-SW strike is usually only a few centimetres. An exception, however, is dyke K180, which appears to have exploited a NE-SW fracture over a few metres, linking two E-W dyke segments (Figure 2.16b). The NE-SW fracture set is therefore older than the dykes.

The high angle (NNW-SSE) structures, when manifest as veins, are also always cut by the intrusions (Figure 2.16c) and thus are older than the dykes. Similar structures have been seen further

south and have been given a Variscan age (Gillespie *et al.* 2001) (see Section 2.4.3 above). As unfilled fractures, it is difficult to ascertain whether the structures are older or younger than the dykes.

The regionally pervasive E-W fracture/vein set is problematic in terms of its age relations with the dykes, given that it is sub-parallel to the intrusions. It has been established above that, as veins, the E-W structures are older than the high angle veins, which themselves are older than the dykes. However, as unfilled fractures, it is not possible to say if the E-W structures are older than the dykes. It has been established above in Section 2.4.3 that the high angle and E-W unfilled fractures are at least in part coeval in their formation, but whether they formed before or after dyke emplacement is not known. There may have not, therefore, been a fracture set sub-parallel to the dykes in the host rock as the dykes intruded. Indeed, the suggestion by Gillespie *et al.* (2001) that E-W fractures in the Burren, Co. Clare, formed relatively recently due to unloading (see Section 2.4.3) would imply this to be the case.

The question is therefore asked as to if the dykes *appear* to have utilised E-W fractures when they were emplaced. Indeed, in some cases, dykes do appear to strike exactly parallel to nearby host rock fractures where the latter are particularly pervasive horizontally across bed surfaces. This is shown in Figure 2.16d for dyke K153. Such dykes typically follow very straight paths on the outcrop scale of a few metres, and show a dearth of jogs that would indicate en échelon segmentation. Conversely, some dykes indisputably propagated their own fractures on intrusion and bear no relation to any E-W structures (see Figure 2.16e showing dyke K128ii, and dyke K175 a few metres from where it terminates in the platform). Figure 2.16f shows dykes K123i and K123ii, whose forms are preserved in different stages of array development. Interestingly, these two dykes have opposing stepping geometries and are separated in strike by an angle of 20°, with the former intersecting the margin of the latter.

A cliff section that exposes dyke K155a shows the E-W fracture set in relation to the dyke in vertical profile. This is shown in Figure 2.16g. In the platform at the base of the cliff the dyke follows a straight path and exactly parallels pervasive widely spaced fractures in the limestone host rock. It can be seen in cliff section, however, that E-W host rock fractures are generally *not* stratigraphically continuous up-section for more than a few beds or few tens of centimetres. Despite this, the dyke cuts up through the section with no deviations from a straight (south-dipping) path. In the inset part of Figure 2.16g, closely spaced fractures parallel the dyke immediately adjacent to the intrusion and for a short distance away from it. The vertically discontinuous E-W fracture set does not, however, parallel the dip of the dyke; rather, these fractures are sub-vertical. It would seem, therefore, that whilst in the platform the dyke may be following an older fracture, in vertical section the dyke has largely propagated its own hydraulic fracture on intrusion. The dyke might have dilated pre-existing fractures if they existed and if it encountered them during its ascent. Indeed, Chapter 3 presents strong evidence for hydraulic fracture of the host rock during dyke emplacement, from the mapping of extensive zones of host rock fracturing. Also, the orientation of the E-W fracture set can change by a few degrees from one bed to the next. A dyke would not be able to exploit two such sets of fractures without some injection along the separating bedding plane; this is rarely seen.

Figure 2.17 shows en échelon dyke forms within Carboniferous (and the Tertiary Killala gabbro) host rock. Also shown is the orientation of E-W fractures in the host rock measured at various points along the coastal sections. Comparing the orientation of these fractures with that of nearby dykes, it seems that, on the regional scale, there is a sub-parallelism between fractures and dykes. This is especially evident north of Ballycastle and north of Inishcrone in Figure 2.17.

Most of the dykes shown in Figure 2.17 have consistent en échelon geometry, i.e. the dykes consistently either left-step or right-step. Where the host rock platform is less seawardly extensive, many dykes show just one or two jogs/segmentations along their strike, making it impossible to identify a consistent geometry should it exist. Conversely, some dykes mapped do not show consistent stepping geometry along their strike. They might show a series of left-steps followed by some right-steps (one such dyke is K157a), or an array might consist of a seemingly random mix of left and right steps. Dykes K169 to K171 show the latter style of arrangement, where the host rock is the Mullaghmore Sandstone Formation. To the east and west of this headland limestone is the dominant host rock and appears to yield dykes with consistent stepping geometries, as shown in Figure 2.17.

It is interesting to note in Figure 2.17 that there is a dominance of right-stepping en échelon dykes over those that left-step. This is especially the case west of Killala Bay. The mean array orientation of right-stepping forms is 104° and that of left-stepping dykes is 089° (see Appendix 6). (This is contrary to the statement of Mohr (1987) that the dykes have a tendency to *left*-step along strike.) Overlapping segments in an array show both curved (e.g. dykes K85 and K181) and straight (e.g. dykes K157a and K176) propagation paths (Figure 2.17 and Figure 2.3). This is described by many authors for fractures and/or dykes (e.g. Delaney & Pollard 1981; Nicholson & Pollard 1985; Rogers 1987; Olson & Pollard 1989; Thomas 1993; Acocella *et al.* 2000). The same is the case for horns that extend from a left or right step in a dyke whose segments have coalesced. It seems that many, if not the majority, of horns maintain an in-plane path with respect to the dyke, e.g. dyke K117 of Figure 2.17; that is, they do not curve. The formation of straight overlapping structures in an en échelon array is thought to result from there being high magma pressure or driving stress, or either a relatively high remote compressive stress parallel to the fractures at the time of formation (Figure 2.3b) or a pre-existing weakness in the host rock parallel to the fractures that would 'guide' the fractures in their propagation (Olson & Pollard 1989; Renshaw & Pollard 1994). The possibility that a relatively large horizontal compressive stress acted parallel to the dykes is discussed below and might have been the case. However, it seems more likely that either magma pressure was high enough to reduce the effect of segment tip interaction, and thus cause overlapping segments to be straight, or dyke-parallel fractures in the host rock influenced the path of overlapping dyke segments. A pre-existing fracture set could have been influential if it existed, but closely spaced hydraulic fractures propagating ahead of the dyke tip (as shown in Figure 2.1) would have more readily provided the necessary dyke-parallel weakness in the host rock to facilitate the straight propagation of overlapping segments. It is shown in Chapter 3 that closely spaced hydraulic fractures were indeed produced associated with dyke tip propagation. Delaney & Pollard (1981) reach a similar conclusion to explain the straight overlapping

paths of segments of the Ship Rock dyke, New Mexico.

2.4.5.1 A proposal for dyke emplacement under hybrid extension and shear

It was noted in the previous section that dykes K123i and K123ii have opposing stepping geometries and subtend an angle of 20° with each other, with the former intersecting the latter (Figure 2.16f and Figure 2.17). Dykes K128i and K128ii share a similar relationship, with an angle of 14° between the two dykes. Current opinion regarding en échelon segmented fractures/dykes is that they are extensional structures and did not form under shear (as described in Section 2.2.2 above), i.e. they are different in their genesis from the classic en échelon shear arrays. It is suggested here that the two pairs of dykes mentioned above might actually represent conjugate pairs of dykes, where the left-stepping dykes formed with an element of dextral shear, and the right-stepping dykes formed with an element of sinistral shear. Given this, the dykes would represent hybrid extension/shear fractures. The formation of such structures is explained in Figure 2.18. En échelon dykes are interpreted as representing conjugate shears by Escher *et al.* (1976). The angles of 20° and 14° between the dykes in each pair would therefore be the dihedral angles. These angles are low, which would be expected for hybrid structures. For such structures to form, a sufficiently high pressure parallel to the dykes combines with the tensile stress (Davis & Reynolds 1996), which, in this case, would be caused by hydraulic fracturing as the dyke propagated upwards. The concept of there being a relatively large dyke-parallel remote horizontal compressive stress, enough to cause hybrid fracture formation, is also addressed in Chapter 3 when discussing the formation of shear fracturing in the host rock margins of dykes east of Killala Bay. Figure 3.24 shows dyke K157b (also shown in Figure 2.17), which has clearly exploited a left-stepping fracture array that formed during emplacement. The fracture array is interpreted as representing dextral shear by analogy with identical structures that are seen to have accommodated shear in the host rock margins of other dykes. It therefore seems possible that emplacement of some dykes occurred into fracture arrays that formed under an element of shear.

2.4.5.2 A generalised model for the intrusion of en échelon dykes into Carboniferous host rock

The observation made in Section 2.4.5 above (and shown in Figure 2.17) that the average strikes of left-stepping and right-stepping dykes are 15° apart is not to say that they are being interpreted as having been emplaced under hybrid extension/shear. Rather, a more generalised interpretation, based on the breakdown of extensional parent dykes at depth (as described in Section 2.2.2 and Figure 2.2), is proposed.

If an E-W fracture set existed in the host rock when the dykes were emplaced, it did not play a significant role in controlling intrusion. The facts that the dyke-parallel fractures in the host rock change orientation and frequency through the section, and that they are stratigraphically discontinuous, means that their influence must have been minimal. The predominance of en échelon dyke forms (and associated host rock fracturing as described in Chapter 3) shows that hydraulic fracture ahead of the dyke tip was the dominant mechanism of dyke propagation. Lithological variation across bedding planes through-section meant that the advancing dyke tip encountered host

rock of differing mechanical properties. This would have led to variation in the orientations of the principal stresses at the dyke tips, thus leading to breakdown of the dykes into segments, as described by Baer & Beyth (1990). This is commonly seen for joints in sedimentary sequences (as described above) (e.g. Helgeson & Aydin 1991).

The widespread occurrence of en échelon dykes seen in the sub-horizontal platform implies that at least a component of the direction of dyke propagation was upwards. (However, in Chapter 3 evidence is presented for oblique propagation of some dykes through the crust, i.e. with a horizontal component to the direction of propagation.)

2.4.6 Relationships between geometric parameters of en échelon dykes in Carboniferous host rock

The geometry of en échelon dykes, fractures and faults has been studied at various scales in terms of simple measurable parameters (e.g. Delaney & Pollard 1981; Segall & Pollard 1983; Acocella *et al.* 2000; Weinberger *et al.* 2000). These parameters include segment overlap, offset and length (Figure 2.19). It has been suggested that these dimensions are proportional over a broad range of scales for extensional fractures, normal faults and strike-slip faults with similar constants of proportionality (Aydin & Nur 1982; Acocella *et al.* 2000). This suggests a uniform mechanism controls the interaction process for all these structure types (Acocella *et al.* 2000).

The three parameters listed above were measured for a range of dykes in the Killala swarm emplaced into Carboniferous host rock (and also dyke DK15ii of the Donegal-Kingscourt swarm). Dykes used are either an array of separate or coalesced segments. (It is noted that the extent of the platform over which the dykes are exposed in the Killala Bay area restricts the scale of segmentation over which the data can be collected; high-resolution aerial photographs might be useful to increase the scale at which these parameters can be measured.) The data is plotted in Figure 2.19, and the raw data (with a list of the dykes used) is displayed in Appendix 6. Comparisons are made directly with the same parameters for segmented dykes re-plotted from Delaney & Pollard (1981), and for normal faults, extensional fractures and ridge spreading centres from Acocella *et al.* (2000).

It is suggested by Acocella *et al.* (2000) that data for normal and extensional faults, and ocean spreading centres lies on the same power law regression line. The exponent of 0.87 (Figure 2.19) indicates that the amount by which the overlap increases for a given increase in offset decreases slightly with offset (an exponent of 1 would yield a linear relationship). A power law regression fitted to data from dykes of Delaney & Pollard (1981) gives a reasonable fit and shows that the amount by which the overlap increases for a given increase in offset *increases* markedly with offset. A power law regression applied to the data from this study appears to give a good fit, since the majority of points lie close to the line of best fit. The relationship is almost linear, with an exponent of 0.99. The data lie close to the line of Acocella *et al.* (2000) and its projection, but are removed from the data of Delaney & Pollard (1981). The few points that occur at the large value end of the line describing the data from this study lie substantially off the line, giving larger values of overlap than predicted by the fitted regression. This implies that the calculated goodness of fit might be misleading. The inset

clarifies this, showing the apparent sudden increase in segment overlap with offsets in excess of 1.5 m. Below this value of offset, the relationship is obviously close to linear, with quite tightly clustered points. A power law regression with an exponent of 0.93 still gives a better fit than a linear regression for this range. It could be, however, that the apparent deviation (from predicted values of the regression) in segment overlap for large segment offsets, are part of a natural scatter in the data, which may be influenced by factors such as host rock lithology, the presence of a pre-existing sub-parallel fracture set etc. Alternatively, it is accepted that there may be a degree of error in the data, since some of the data are derived from reconstructions of the segmentation forms (as shown in Figure 2.17). The point that is the most deviated from the regression line is derived from dyke K158. This segmentation is described in Chapter 3 (Figure 3.11a), with the majority of the overlap actually being comprised of a curving fracture that was *not* dilated by magma. None of the other data points are derived from such a style of segmentation. If this data point is discarded then the other points that lie off the regression line look more like natural scatter. It is suggested that this might be the case. It is thus considered that the data *do* conform to a power law relationship, and looks likely to represent an extension of the same regression derived from the data presented by Acocella *et al.* (2000) in Figure 2.19a.

Figure 2.19b and Figure 2.19c plot offset and overlap respectively against the total length of overlapping segments for dykes (from this study) and data from Acocella *et al.* (2000). Both the datasets from this study conform to almost linear relationships, with power law regressions giving slightly better fits than linear regressions. The regression lines show good conformity with those for extensional fractures, normal faults and ocean spreading centres of Acocella *et al.* (2000).

It would also be interesting to measure dyke thickness/overlap ratios for the dykes studied here. This would quantify strain in the host rock bridge in terms of the angle through which a bridge is typically rotated as segments overlap and dyke segments dilate.

From the data presented here, it appears that dykes conform to the same basic mechanism of segmentation as normal faults, extensional fractures and ocean spreading centres. This is not surprising, since dykes are essentially fluid-filled extensional fractures, and might be thought of as vastly scaled-down segmented ocean spreading centres. As mode I fracture arrays, dykes preserve especially well these geometrics described, which tend to be destroyed by segmented normal faults that develop under mode III shear (Treagus & Lisle 1997). The data further highlights the apparent scale-independence of basic geometric relationships between segmented structures.

2.4.7 Dyke width and crustal extension

Figure 2.20 plots dyke width for the Killala swarm. For both Carboniferous and Precambrian host rock types dyke widths most commonly lie in the range 0.5 m to 1 m. The distributions show a power law form for dyke width greater than 0.5 m. Below this frequency drops off and power law conformity is lost. This change in the distribution is not a function of a lack of outcrop, since exposure is almost fully continuous on the east side of Killala Bay. Similar distributions in dyke width are described by Jolly & Sanderson (1995) for the Tertiary Mull swarm, northwest Scotland.

The major difference between the distributions for the two host rock types is the higher probability

of finding dykes less than 0.5 m wide in Carboniferous host rock, whilst there are proportionally a greater number of dykes wider than 1 m in Precambrian host rock. This is reflected in the higher mean dyke width of 1.72 m for Precambrian host rock, versus 1.38 m for Carboniferous host rock. An overall mean dyke width of 1.52 m is obtained for the Killala swarm, which includes those dykes emplaced into the Tertiary Killala gabbro. These values are within the range of average dyke widths, 1.06 m to 4.27 m, for component 'sub-swarms' within the Mull swarm (Jolly & Sanderson 1995).

The east side of Killala Bay allows the amount of crustal extension to be derived that accommodated emplacement of the Killala swarm (Figure 2.21). An almost uninterrupted 9 km of platform section runs orthogonal to the dykes. The dykes' opening directions are orthogonal to strike, given their en échelon form (see Section 2.4.8 below). Extension in the horizontal plane was therefore simply calculated by converting the summed dyke width (individual dyke widths summed) to a percentage of the distance between Inishcrone and Lenadoon Point. The few places where the section is missing (cobbled beaches) (see Figure 2.21) are not included in the calculation (Appendix 7 lists the distances used and the dyke widths). A value of 1.45% crustal extension is obtained. This is low in comparison with the value of between 2% and 20% obtained for the Mull swarm by Jolly & Sanderson (1995).

2.4.8 Dyke opening directions, the direction of extension, and implications for the tectonic setting at the time of dyke emplacement

Figure 2.22 shows opening directions (see also Figure 2.1) for dykes of the Killala swarm. They are all roughly orthogonal to the strike of the dykes, regardless of the host rock and the style of intrusion. For the en échelon dykes in Carboniferous host rock, this is to be expected since each segment is supposedly an extensional fracture (see Section 2.2.2). The orientation of these dykes should, therefore, yield the extension direction that acted to cause intrusion. The dykes and their constituent segments show some variation in strike (Figure 2.10, Figure 2.17 and Figure 2.22), but have a strong unimodal distribution yielding an average segment strike of 096°. This is discounting any parts of the dykes that exploit NE-SW fractures in the host rock. Also discounted are dykes K104i/ii and K105 of anomalous orientation immediately south of the Killala gabbro, whose average strike is 130°. An average extension direction of 006° is therefore obtained, with an apparent localised swing to 040° immediately south of the Killala gabbro.

Given the propensity for dyke emplacement into pre-existing structures in the west of the swarm, the theory of Delaney & Pollard (1986) and Jolly & Sanderson (1995) (as detailed in Section 2.2.3 above and Figure 2.4) can be used to infer the tectonic setting at the time of dyke intrusion. In this, it is approximated that the dykes are vertical.

All possible orientations of dykes exist in the western portion of the Killala swarm (Figure 2.10). Given this, and the implication by Figure 2.22 that horizontal opening directions are generally perpendicular to dyke strike, it can be inferred that the stress ratio, R (as defined by Delaney & Pollard (1986)), was probably greater than +1 at the time of intrusion (Figure 2.4d), i.e. *all* orientations of fractures were able to be dilated under extension by the magma. Given this, the

magnitude of σ_3 (least horizontal compressive stress) was tending towards S_H (maximum horizontal compressive stress), i.e. the differential stresses were low at the time of dyke emplacement, with neither stress dominating over the other. This implies that the tectonic setting was relatively inactive. In addition, it might be that magma pressure was high, enough to dilate the large range of fractures seen.

The extension direction derived above (006°) for the eastern end of the swarm presumably acted over the whole of the swarm, but was sufficiently weak (and/or magma pressure was sufficiently high enough) to allow the range in dyke orientations seen in the west where the intrusions exploit pre-existing weaknesses in the host rock. It is unlikely that differences in the magnitude of the principal stresses between the east (cover host rock) and west (basement host rock) ends of the swarm led to the observed variation in dyke trend.

The relative abundance of NE-SW orientated dykes at the extreme west end of the swarm might represent a localised rotation of the extension direction that acted during intrusion to NW-SE (as suggested in Section 2.4.4.1 above).

2.4.9 Summary model for emplacement of the Killala swarm

It is apparent that the Killala swarm was emplaced under N-S directed extension during the Palaeocene. Dyke emplacement took place mainly by intrusion along pre-existing structures in the west of the swarm, and hydraulic fracture of the host rock in the east. It appears that the differential stresses in the crust at the time of intrusion were not great, but were still enough to control the overall E-W trend of the swarm. The extension direction (a value of 006° is obtained) for dyke emplacement is most clearly preserved by the en échelon dykes emplaced into Carboniferous host rock in the east.

It is suggested that some dykes in Carboniferous host rock may have been emplaced under hybrid extension/shear. This is not really an accepted mechanism for en échelon dyke emplacement, but the possibility of there being a conjugate arrangement between some dykes raises it as a possible mechanism for dyke intrusion.

A swing to NW-SE extension may have occurred at the very western end of the swarm as exposed, as evidenced by a relative abundance of NE-SW dykes. Another apparent localised rotation in the extension direction, to NE-SW, caused emplacement of anomalously orientated dykes immediately south of the Killala gabbro. The exact role that the gabbro played in emplacement of the swarm is unclear, apart from the belief that its formation was part of a first intrusion phase (see Section 2.4.1). However, it appears to have locally affected the principal stress directions for dyke emplacement. Similarly, Jolly & Sanderson (1995) describe a broad range of dyke orientations close to the Mull centre, a direct result of higher magma pressures close to the intrusion that fed the dykes.

Dykes are not seen crossing the interface between Carboniferous cover and Dalradian basement. However, it is envisaged that dykes of variable orientation passing through the basement would have quickly reorientated to an E-W orientation within the cover. Dykes would have twisted by breaking down into segments, and may also have adopted a sub-horizontal attitude at or close to the interface. A similar idea was put forward in Section 2.3.6 to explain the series of sills belonging to system CI in

the West Connacht Systems.

Fitting the Killala swarm into the broader scale setting is discussed in at the end of the chapter.

2.5 The Donegal-Kingscourt Swarm

2.5.1 Previous work

Figure 2.23 shows the study area for the Donegal-Kingscourt swarm, the regional geology, and the locations of intrusions referred to in the text. The dyke numbers refer to Appendix 8, in which grid references and raw data for all plots (unless otherwise stated) can be sourced.

The Donegal-Kingscourt swarm traverses the north of Ireland intruding Devonian and Carboniferous sedimentary basins, Precambrian basement (Dalradian) and Caledonian granite (Figure 1.5). The locus of intrusion for the swarm runs from the northwest coast of Co. Donegal, southeast to the igneous centres of Mourne, Carlingford and Slieve Gullion before cutting the shores in the area around Dundalk Bay and Carlingford, Co. Louth (e.g. Emeleus & Preston 1969; Pitcher & Berger 1972). The southernmost intrusions sub-crop in the Navan mines, Co. Cavan. Along strike to the southeast, aeromagnetic imaging coupled with outcrop identifies the swarm extension on Anglesey and in North Wales (Evans *et al.* 1973; Bevins *et al.* 1996). In the northwest, the swarm may be related offshore to the Rockall igneous centre, and continues into the English midlands to the southeast (e.g. Macintyre *et al.* 1975).

In northwest Ireland, all intrusions in the swarm are dykes except for two igneous plugs close to Donegal town, and the Garrison sill southwest of Lower Lough Erne (Figure 2.23). The majority of intrusions are tholeiitic olivine-dolerites in composition (Pitcher & Berger 1972). Mostly, the dykes are flash injections, i.e. they consist of one phase of intrusion (Preston 1965). However, some of the wide dykes, confined to the sedimentary basins of the Donegal and Omagh synclines (e.g. the Doraville dyke (Preston 1967b), the Blackslee dyke (Wilson 1964) and the Blind Rock dyke (Preston 1967a)), are multiple dykes and are thought to have been feeders. The Doraville dyke is the largest such intrusion, being 60 to 90 m wide and quarried at Doonan and Drogan quarries, Co. Fermanagh. Along strike to the northwest, the igneous plug, Doonan Rocks, has the same geochemistry as the Doraville dyke suggesting a genetic relationship between the two intrusions. These 'feeder dykes' are similar in geochemistry to the vertically differentiated Tertiary plateau basalts of northeast Ireland (Lyle 1980).

In contrast, acidic dykes dated as Tertiary outcrop in northwest Co. Donegal (Whitten 1954), and intrude the Barnesmore granite in the south of the county (Walker & Leedal 1954). In the Barnesmore area, pitchstone and felsite occur in multiple intrusions with dolerite but are confined to a NW-SE zone, possibly indicating a Tertiary granite body at depth (Walker & Leedal 1954). In addition, an unusually high Bouguer anomaly, the 'Dromore dense body', may indicate a buried basic igneous body (Readman *et al.* 1997) in line between the Barnesmore dyke suite and the Tertiary centres of Slieve Gullion, Mourne and Carlingford to the southeast (e.g. Preston 1965; Macintyre *et al.* 1975).

The Donegal-Kingscourt swarm has been dated by both the K-Ar method (Macintyre *et al.* 1975; Johnston & Rundle 1993) and the Ar-Ar method (Steve Bergman *pers. comm.*), and intruded mainly during the first phase of NAIP development, as described by Saunders (1997). However, there are a number of exceptions. An old K-Ar age of 69 Ma for the Doraville dyke (Johnston & Rundle 1993) is complimented by a host rock aureole fission track age of 73 Ma (Allen *et al.* 2002), but is in conflict with a relatively young Ar-Ar age of 55 Ma (Steve Bergman *pers. comm.*) for the same dyke. Also, a very young Ar-Ar age of 43 Ma exists for a dyke near Inver in southern Co. Donegal (Kirstein & Timmerman 2000) (see Figure 1.6). This particular dyke contains mantle xenoliths, so may have a different origin than the majority of dykes in the Donegal-Kingscourt swarm.

If Rb-Sr ages of 57 and 54 Ma for the offshore Rockall igneous centre (Hawkes *et al.* 1975) are accurate, doubt might be cast on the proposed relationship (Preston 1967b) between Rockall and the Donegal-Kingscourt swarm.

Chapter 5 of this study supports the established age of the swarm with new fission track ages that average 59 Ma.

Geomorphological evidence suggests that current outcrop levels may represent an intrusion depth of 1000 m or less, i.e. shallow levels of intrusion (Pitcher & Berger 1972). The fission track study presented in Chapter 5 independently suggests a shallow level of intrusion for dykes in northwest Co. Donegal. It is possible that feeder dykes and associated plugs in counties Fermanagh and Donegal fed early Tertiary extrusive volcanism in northwest Ireland (Preston 1967a, b; Pitcher & Berger 1972).

The intrusion style and mechanism for emplacement of dykes in the Donegal-Kingscourt swarm has been generally described. Across northwest Ireland the swarm appears to consist of fewer, wider fissures in the Devonian/Carboniferous sedimentary basins, and of numerous narrower dykes in the Caledonian granites of Co. Donegal (Walker & Leedal 1954; Preston 1967b). There is an apparent scarcity of dykes in the Dalradian metamorphic basement (Pitcher & Berger 1972), although this is probably due to poor exposure (Walker & Leedal 1954).

According to the mapped geology, major Caledonian NE-SW faults appear to cause the termination of some dykes. Crustal slices delineated by these faults appear to have independently extended in a NE-SW direction to facilitate intrusion (Preston 1965). For example, the Blind Rock dyke fails to outcrop at Inver Bay in the northwest and on the opposite shore of Donegal Bay to the southeast. It may terminate to the northwest forming the dolerite plug near Inver, and to the southeast there is alignment with the multiple dykes of Magho mountain, including the Blackslee dyke (Figure 2.23). Alternatively, the dyke may be contained between the Mountcharles and Laghy faults to the northwest and southeast respectively (Preston 1967a). Interestingly however, high-resolution aeromagnetic data, recently acquired over Co. Fermanagh by the Geological Survey of Northern Ireland, shows dykes offset by ~2 km in a sinistral sense across the Tempo-Sixmilecross fault. This structure is possibly a continuation of the Tow Valley fault, itself associated with Oligocene sinistral strike-slip movement and the formation of the Ballymoney pull-apart basins (see Chapter 4).

On a local scale, Walker & Leedal (1954) state that emplaced into the Barnesmore granite most dykes are unrelated to pre-existing fractures. Pitcher & Berger (1972), however, state that all dykes of

the Donegal-Kingscourt swarm follow pre-existing fractures, and they note how some dykes strike NE-SW along the Gweebarra fault for some of their length.

Regionally, the overall trend of the swarm is parallel to the Scottish swarms of the British Tertiary Igneous Province, i.e. orthogonal to the early Tertiary northeast Atlantic rift axis. This anomalous orientation may be a result of stress polarisation from a mantle plume derived radial extensional stress regime. In other words, the NW-SE extensional stress component was relieved by rifting of the Atlantic, leaving orthogonal extension that became manifest in the dyke swarms (Macintyre *et al.* 1975).

In the following sections dyke forms are described from the different host rock types, and are related to host rock structure where possible. An overall model of intrusion is then described.

2.5.2 Dykes emplaced into Carboniferous host rock

Dykes recorded within Carboniferous host rock come from a mix of inland, quarry and coastal exposures. Figure 2.24 shows that the vast majority of dyke segments are orientated NW-SE. Apart from this there is a small N-S peak. There is a large angular range between 020° and 110° that does not contain any dyke segments. Dips are generally steep with many dykes being only a few degrees from vertical.

Three areas/localities are described below. Firstly, the area in the vicinity of the Blind Rock dyke (dyke DK17) is described, where a number of dykes are exposed in the wave-cut platform of the Bundoran Shale Formation. Secondly, a dyke is described (dyke DK9) cutting the Ballyshannon Limestone Formation at Carn quarry. Thirdly, a dyke of anomalous N-S orientation is highlighted cutting the St. John's Point peninsula.

2.5.2.1 The Blind Rock dyke and associated intrusions

The Blind Rock dyke (Preston 1967a) and associated intrusions are exposed in the wave-cut platform of the Bundoran Shale Formation (Figure 2.23) west of Donegal town. The host rock dips up to 13°NW, but mostly is nearer to flat-lying. As is the case for the Carboniferous host rock of the Killala swarm, there is an E-W fracture set that strikes at around 100°. There are also occasional fractures that strike NE-SW. Lastly, a fracture set that strikes between ~125° and ~145° is pervasive through the host rock.

Figure 2.25 shows the dyke forms that outcrop in the platform. Dyke DK14 shows a stepping morphology (mostly left-stepping), indicating that it probably originated as an en échelon array of dyke segments (Figure 2.3). En échelon form is shown by dykes DK15i/ii, where it is apparent that two separate dykes have been emplaced in very close proximity. There is no consistency in stepping direction of the dykes. Note that dyke DK15ii progressively thins along strike to the southeast. This might correspond to balance the progressive thickening of dyke DK16 in the same direction. There are a couple of N-S orientated segments as part of dyke DK15, the southeast one of which is seen to have opened obliquely.

The outline of the Blind Rock dyke (dyke DK17) is taken from Preston (1967a). A number of horns appear to indicate that a right-stepping en échelon arrangement of segments existed before major dilation took place.

It is noted that the average strike of 129° for the NW-SE dyke segments is at the lower end of the NW-SE fracture set described above.

En échelon dykes of identical form in the Killala swarm are believed to have been emplaced by hydraulic fracturing of the host rock. The same process for emplacement is therefore invoked here.

2.5.2.2 Carn quarry

A dyke cuts the Ballyshannon Limestone Formation within (the working) Carn quarry, near Ederny, Co. Fermanagh. In addition, two other (disused) quarries west of Carn quarry both have dykes cutting their faces.

Dyke outcrop distribution within Carn quarry and host rock fracture structure

The quarry plan shown in Figure 2.26 was accurately constructed using a combination of bearing triangulation and handheld GPS measurements. The full height/depth of the quarry, ~15 m, is manifest in the northernmost face. A second level along the southern margin of the quarry has split the back face into two sections of roughly equal height. The dyke is exposed on the two working levels of the quarry, and also midway up a ramp linking the levels (Figure 2.26). The outcrops of dyke all have NW-SE strikes in accordance with the regional trend of the Donegal-Kingscourt swarm. The host rock, the Ballyshannon Limestone Formation, is quite thickly bedded (typically 5 to 40 cm) in most parts with occasional shale interbeds that act as markers. Several faults are confined to an area southwest of the dyke; these will be discussed in Chapter 4.

At the northwestern side of the quarry, two dykes intersect the quarry face at A (Figure 2.26). The face slopes around 50° to the south before becoming sub-vertical upslope. The eastern dyke widens from 1.9 m to ~ 3.5 m at the highest accessible point upslope, and the western dyke narrows from 3.1 m at the base of the face, to having almost pinched out at the top (Figure 2.26, inset 1). The eastern dyke is also exposed in plan in the quarry floor a few metres southeast along its strike, but is much narrower, thinning to 80 cm before being lost beneath rubble.

To the southeast, a dyke intersects the bottom working level, north-facing face of the quarry at B. The dyke narrows up-scarp to 2.8 m from between 4 and 5 m at the base (Figure 2.26, inset 2). An accurate width measurement at the base is difficult to ascertain, as part of the dyke crumbles very easily, its scree obscuring the margin. At the intersection with the southernmost face of the quarry at C on the top working level, a dyke is 2.8 m wide. The dyke shows no narrowing up-scarp to the quarry top.

Along the ramp linking the two levels, dyke is thinly accreted in patches to the northeast-facing wall. Midway up the ramp at D a dyke outcrops in section, is 1.8 m wide, and shows no evidence of narrowing in the section, which is around 2.5 m in vertical extent. Along strike to the southeast, a dyke outcrops, 2.1 m wide, with no narrowing in vertical section.

All the dykes described dip steeply to the northeast.

There are two obvious fracture sets pervasive within the quarry. Firstly a sub-vertical set strikes just south of E-W. These fractures control the orientation of the main quarry faces. Secondly, there is a NW-SE sub-vertical set that strikes roughly parallel to the dykes.

Interpretation of dyke geometry

The key to understanding the dyke geometry is the observation that the dykes narrow in a number of the outcrops in both the horizontal and vertical planes. This implies that the dykes may be part of a single segmented system. Possibilities as to the form of the segmentation can be tested assuming that, at a given elevation, the overall extension is equal to the summed widths of adjacent dyke segments, and that this extension will not vary greatly along strike and in height given the scale of the quarry. This is, indeed, shown to be the case in Figure 2.26, where, for the segmentation reconstruction, the extension at three positions in the quarry is around 5 m.

At A, en échelon segmentation is inferred in the vertical plane by the upslope thickening of the western dyke (segment 1) versus the thinning of the eastern dyke (segment 2) (Figure 2.26, inset 1). In addition, the thinning of segment 1 to the southeast implies a corresponding thickening of segment 2 in the same direction. Therefore, segment 2 is inferred to traverse the bottom working level as the sole dyke segment.

Intersection of segment 2 is inferred to take place at B given the closeness in width between the dyke here and the summed width at A. The presence of dyke accreted to the ramp scarp between B and D indicates that the ramp margin is in fact the southwestern margin of a third segment. The narrowing up-face of segment 2 at B is assumed to mirror what would be a corresponding thickening of segment 3 (Figure 2.26, inset 2). On the top working level, the loss of width of segment 2 compared to its outcrop in the bottom working level is balanced by the width of segment 3 at E to give a total width of around 5 m (although these summed widths are not directly adjacent to each other).

The proposed apparent narrowing, in plan, of segment 3 to the northwest is due to the combination of the segment's proposed narrowing down-section (Figure 2.26, inset 2) and the lowering of the ramp in elevation towards B.

In addition, the apparent swing, in plan, of segment 3 towards segment 2 near the base of the ramp is controlled by the drop in elevation of the ramp, and must therefore represent a *true* swing in vertical section. The apparent swing is not controlled by a combination of the dip of the dyke and the elevation drop, as the dyke dips to the northeast.

Such a swing would be expected, a result of the mixed-mode I-II stress intensity that is induced where dyke segments overlap (see Section 2.2 and Chapter 3).

In summary, the dyke outcrops are interpreted to belong to a single segmented dyke. Segmentation occurs with components in both the vertical and horizontal planes at the northwestern face (segments 1 and 2), and it occurs in the vertical plane between segments 2 and 3 to the southeast. Consistent with this model, values of total extension at three positions of equal elevation in the quarry are

roughly equal at around 5 m. En échelon dyke segmentation is consistent elsewhere with emplacement by hydraulic fracturing of the host rock. This may have been the case here. However, in Chapter 4 it is shown that this dyke was emplaced along a fault that was active at the time of emplacement. So, this model for intrusion does not necessarily hold here (see Chapter 4).

2.5.2.3 St. John's Point peninsula

Half way down the west side of St. John's Point peninsula a narrow dyke, around 30 cm wide, strikes roughly N-S. The dyke cuts the coast again to the north having widened considerably to 1 m. Its orientation is anomalous compared to other dykes intruding Carboniferous host rock, as described above. The dyke is faulted in at least two places (see Chapter 4). A left-step that appears to have originated from en échelon segmentation shows that the dyke opened under extension. The dyke is faulted and is studied in more detail in Chapter 4.

2.5.2.4 Dyke opening directions and the direction of extension

It has been established from the locations in the previous two sections that dykes were emplaced into Carboniferous host rock in en échelon style. The concept of an en échelon intrusion invokes individual segments of an en échelon array as extensional fractures forming orthogonal to the direction of extension, which is preserved in the opening direction. A mean segment strike of 131° is derived, which gives a mean opening direction of 041°. This value discounts the small N-S peak seen in Figure 2.24, as this includes those segments shown in Figure 2.25 for dyke DK15i that opened obliquely, as described in Section 2.5.2.1 above. The N-S peak also includes dyke DK18, described in the previous section. This dyke occupies an anomalous N-S strike but still opened in an extensional manner. A mean 'anomalous' opening direction of 097° is obtained for dyke DK18.

These opening directions are therefore used to infer the extension direction (or direction of least compression), σ_3, which caused the emplacement of the Donegal-Kingscourt dykes into Carboniferous host rock. Since segments of en échelon dykes form orthogonal to the extension direction, a mean extension direction of 041° is obtained. Dyke DK18 might represent a local swing in the stress to an E-W trend.

2.5.3 Dykes emplaced into Dalradian host rock

The vast majority of dykes emplaced into Dalradian host rock are inland outcrops and do not, therefore, readily yield their forms. Dyke DK73 is the only intrusion that can be seen to exploit the metamorphic fabric of the host rock, at around 170°. Figure 2.27 shows that the vast majority of the dyke segments are orientated NW-SE. In addition, there are small N-S and E-W peaks. There are several angular ranges that do not contain any dyke segments, the largest of which is 020° to 040°. Dips are generally steep with many dyke segments being only a few degrees off vertical.

Two dyke pairs are shown reconstructed from isolated outcrops in Figure 2. 28 (dykes DK26i/ii and DK30i/ii). The dykes show a range in strike. The reconstructions are based on the observed

changes in dyke width along strike, using the theory that overall width between the two dykes in the dyke pair does not change. Note that the reconstructions appear to represent large-scale en échelon segmentations. Opening directions were not obtained for dykes emplaced into Dalradian host rock due to the lack of exposure.

The range in strike shown by these dykes in places suggests that host rock structure influenced dyke orientation to some extent.

2.5.4 Dykes emplaced into granite host rock

Most of the dykes recorded emplaced into granite are from within the Rosses and Thorr granites in northwest Co. Donegal. Here, good coastal exposures allow accurate recording of the dyke forms. Some dykes are also recorded from the Barnesmore granite. Figure 2.29 shows that there is a wide range of orientations of dykes that are emplaced into granite, with the majority occupying a strike between N-S and E-W. Apart from this there is a NNE-SSW peak. The angular range 050° to 080° does not contain any dyke segments. Dips are generally steep with many dykes being only a few degrees off vertical.

Below, dykes from the Rosses and Thorr granites are described and their orientations compared with the fracture structure of the granite.

2.5.4.1 Fracture structure of the Rosses and Thorr granites

At various points along the coast south of Bloody Foreland (Figure 2.23), in the vicinity of Tertiary dykes, fracture orientation measurements were made in the granite host rock. Fifty counts were made at each location of all fracture orientations in a small area (Appendix 9). The results are shown in Figure 2.30. There are distinct preferred fracture orientations at all locations. NNE-SSW to NE-SW peaks of varying magnitude are universal. In the north around Bloody Foreland there is a distinct NNW-SSE fracture trend. Also here, there is an E-W fracture set that largely does not exist south of Bloody Foreland. Northwest-southeast peaks at locations south of Bloody Foreland appear to swing anticlockwise and possibly become the E-W peaks in the north referred to above. All fractures dip steeply within a few degrees of vertical.

2.5.4.2 Dyke forms and relationships with the granite host rock structure

Figure 2.31 compares dyke segment strikes with the local host rock fracture strikes, as described above. It is typical for dykes to follow a trend with many abrupt changes in strike. The histograms show that there is a distinct correlation between the orientation of fractures and that of the dykes. This is most striking in the two summed histograms for the areas around Bloody Foreland and midway down the coastal section to the south. Fracture data was summed for these areas since it was deemed that their component localities shared common modal fracture orientations.

The histograms for the individual locations show that the changes in fracture strike over the region (as mentioned above) correspond with changes in the modal dyke segment strikes. There are a few

exceptions; these being dykes that have a NW-SE strike, i.e. parallel to the regional strike of the swarm. In addition, the high dip angles of the dykes (Figure 2.29) are comparable with those of the host rock fractures (Figure 2.30).

Figure 2.31 also shows the dyke forms, and that it is typical for dykes to follow a trend with many abrupt changes in strike. This is characteristic of dykes that are emplaced along pre-existing fractures, as shown in Figure 2.1. Just two dykes, DK44 and DK64, show en échelon segmentations, these dykes having a NW-SE trend. Dyke DK54 consistently steps to the right and may have originated as an en échelon array. There is no E-W fracture set identified in the vicinity of this dyke (Figure 2.30), so it seems likely that an en échelon propagation of hydraulic fractures may have taken place in its formation.

It is apparent therefore that, for the majority of dykes, the pre-existing fracture structure of the granite has been exploited for the passage of magma.

2.5.4.3 Dyke opening directions, the direction of extension, and implications for the tectonic setting at the time of dyke emplacement

Opening directions in the horizontal plane were readily measured (as shown in Figure 2.1) for many of the dykes within the Rosses and Thorr granites where the dykes make an angular change in strike. Figure 2.32a shows that, as would be expected, opening directions cover the angular range across which no dyke segments have been recorded. The mean opening direction is 047°.

Figure 2.32b shows that there does not appear to be any trend in the variation in opening direction with distance around the coast.

Figure 2.32c shows, interestingly, that there appears to be a variation in opening direction with average strike of the dykes. This is only a crude relationship though, as indicated by the low value (0.49) of correlation coefficient.

Using the theory of Delaney & Pollard (1986) and Jolly & Sanderson (1995) (as detailed in Section 2.2.3 above and Figure 2.4), suggestions can be made as to the tectonic setting at the time of dyke intrusion. The wide range in strike of the dyke segments emplaced into the Rosses and Thorr granites (there is just a 30° window between 050° and 080° where no dykes are found) (Figure 2.32a), and the relatively consistent opening direction, would suggest that the stress ratio, R (as defined by Delaney & Pollard (1986)), was about +1 at the time of intrusion (Figure 2.4d). This disregards the apparent dependence of opening direction on the average strike of the dykes, since its form is not what would be predicted by the theory of Jolly & Sanderson (1995). This theory would define some form of parabolic curve with its apex (the point at which opening is extensional with no shear component) centred on the strike that is orthogonal to the direction of extension. It is noted though that there is scatter in the data shown in Figure 2.32c. If there is indeed a true relationship of the required form between dyke strike and opening direction, then this would suggest that $-1 < R < 1$ at the time of emplacement.

Given the evidence described and the ambiguity regarding any relationship between dyke strike and opening direction, it is suggested that the R was around +1 at the time of dyke intrusion into the

granite. Such a value of R is indicative of a tectonic setting that is neither particularly active nor completely inactive (Delaney 1986), and suggests that the difference between the horizontal principal stresses was small, i.e. differential stresses were small.

The mean opening direction of 047° can be approximated as the extension direction for these dykes emplaced into granite. This compares well with the mean extension direction of 041° obtained for dykes in Carboniferous host rock to the southeast (see Section 2.5.2.4 above).

2.5.5 Summary model for emplacement of the Donegal-Kingscourt swarm

Evidence suggests that the Donegal-Kingscourt swarm was emplaced under NE-SW directed extension during the Palaeocene. Dyke emplacement took place by hydraulic fracturing of Carboniferous sedimentary host rock. Where the host rock is granite, at the northwest end of the swarm as exposed, the dykes exploited pre-existing fractures. The magnitude of the least compressive stress (extension direction) was probably relatively weak, i.e. the difference between the horizontal principal stresses was not great, but still produced the overall NW-SE trend of the swarm. An extension direction of 044° is obtained by averaging the two values derived from dykes within Carboniferous and granite host rocks.

The suggestion that dykes of the Donegal-Kingscourt swarm are fewer and wider in the Carboniferous and Devonian sedimentary basins, and narrower and more frequently occurring when in granite (see Section 2.5.1 above), is difficult to verify as being true from this study. From the dykes studied, the widths of dykes in granite are not noticeably different from the widths of dykes in Carboniferous host rock (see Appendix 8). However, the overall distribution of mapped dykes (see Figure 2.23) certainly seems to indicate that the host rock at least had control on dyke *spacing*. The extension direction derived from this study shows that major NE-SW Caledonian structures were aligned perfectly to act as transform faults to facilitate dyke segmentation and the extension of discrete crustal blocks (as described in Section 2.5.1 above).

It is noted that the western edge of the Donegal-Kingscourt swarm appears to veer away from a NW-SE trend towards a WNW-ESE trend in sub-parallel alignment with the Killala swarm (Figure 1.1). This is discussed below.

2.6 A model for dyke emplacement in western Ireland

The Donegal-Kingscourt swarm conforms to the regional NW-SE trend of dykes in the British Tertiary Igneous Province (BTIP). However, the Killala swarm is anomalous in its E-W trend. The West Connacht systems are again anomalous, but have been related to the offshore Brendan centre to explain their trend, and are believed to be part of a three-element radial dyke arrangement, with the Kerry systems and the Slyne fissures (Figure 1.5). If the model for a radial dyke arrangement away from the Brendan centre is correct, then such an arrangement is on a scale greater than any other radial dyke pattern seen in the BTIP.

It is apparent from Figure 1.1 that dykes of the Donegal-Kingscourt swarm swing in strike towards

the trend of the Killala swarm. This would suggest that the orientation of the Killala swarm is a response to a stress reorientation from NE-SW extension to N-S extension, and that the dykes formed coevally. This is shown in Figure 2.33. Indeed, there is no evidence from published ages to suggest that the two swarms are of different age (see Figure 1.6 and Chapter 5). It is suggested that the scale of the stress regime associated with the Brendan centre might have caused deflection of the regional NE-SW extensional stresses acting at the time (Figure 2.33). Again, published ages for the West Connacht systems are in line with the other two swarms. It is envisaged that the radial arrangement of dykes associated with the Brendan centre is analogous to a triple-junction. Given this, the Killala swarm was emplaced due to an interplay between NW-SE extension associated with the Brendan centre and the regional NE-SW extension direction of the BTIP. The observation has been made that there is a propensity for dykes at the western end of the Killala swarm to strike NE-SW. At this point, the dykes are closer to the Brendan centre than other dykes in the Killala swarm, and are roughly equidistant from, and lying between, the Brendan centre and dykes of the Donegal-Kingscourt swarm. It is possible that the orientation of these dykes is a function of the suggested influence of the Brendan centre. The fact that there are geochemical differences between the dykes of northwest Ireland does not necessarily contradict the model outlined above. It is suggested that different magma sources were feeding dykes that were being emplaced under a regionally varying stress regime.

2.7 Conclusions

This chapter has described the emplacement of early Tertiary dykes in northwest Ireland, and derived the palaeostress directions that acted at the time of intrusion.

Dykes were emplaced either by exploiting pre-existing structures, or in en échelon form propagating their own hydraulic fractures. Generally speaking, dykes that intruded pre-Carboniferous host rock were influenced to a much greater extent by the host rock structural grain. In granite, dykes generally follow the pre-existing fracture pattern, e.g. the Donegal-Kingscourt swarm, and regional variation in the fracture pattern is mirrored by variation in dyke orientation. In Dalradian host rock, dyke emplacement was often along the metamorphic fabric. Dykes emplaced into Carboniferous host rock almost exclusively show en échelon styles of intrusion. The basic geometric relationships of these dykes conform to those of extensional fractures at a much larger scale and even ocean spreading centres. The dykes were emplaced by hydraulic fracture of the host rock. Differences in host rock lithology and bed thickness are likely to have caused breakdown of the extensional fractures into en échelon arrays. It is suggested that some en échelon dykes in the Killala swarm show conjugate relations and may have propagated under hybrid extension/shear with horizontal compression in the direction of the dykes. This leads to the possibility that the stress regime at the time of intrusion was, for at least part, strike-slip, i.e. with the maximum principal compressive stress in the horizontal plane.

The interface between basement and cover in the host rock may have caused local intrusion of sills, as seen at the northeast end of the West Connacht systems. It is envisaged that these sills would have facilitated adjustment in orientation of dykes of variable trend rising through pre-existing structures in

the basement, as they adopted the much narrower range in orientation seen in the Carboniferous cover host rock.

In each of the Donegal-Kingscourt and Killala swarms and the West Connacht systems, the dykes show a wide range of orientations, although the overall trend of the dykes is NW-SE, E-W and NE-SW respectively. These trends reflect the extension directions that operated in the Palaeocene to accommodate dyke intrusion. For the West Connacht systems, the trend of the systems indicates an extension direction of ~150°. The mid section of system CI, however, which is emplaced in en échelon form, implies an extension direction of ~122°. The extension direction for the Killala swarm, derived from the en échelon dykes within Carboniferous host rock, is 006° with a swing to NE-SW extension in the vicinity of, and probably related to, the Killala gabbro. Crustal extension that accommodated the Killala swarm is 1.45%. The Donegal-Kingscourt swarm shows consistency in derived extension directions of 041° from dykes in Carboniferous host rock, and 047° from averaging the opening directions of dykes in granite.

The opening directions of dykes that exploit pre-existing fractures in the Killala swarm and the West Connacht systems are generally orthogonal to dyke strike. This extensional opening, and the wide range in orientation of the dykes, implies that differential stresses in the crust were low in northwest Ireland during the early Tertiary. This might indicate a relatively inactive tectonic setting. In addition, magma pressures may have been high, sufficiently so as to cause dilation of fractures over a range of orientations. Surely the *interplay* between crustal stresses and magma pressures was crucial in controlling the range in dyke orientation observed. The only dykes that do not show extensional opening directions are those emplaced into granite in northwest Co. Donegal. This might reflect a greater difference between the principal stresses acting during the Palaeocene in this part of Ireland.

On reflection, therefore, the most important factor for reliably establishing the regional extension direction for the dykes across northwest Ireland (apart from looking at the geometry of the swarm as a whole on the largest scale) is that a number of dykes across an area show en échelon geometry. For example, taking the Killala swarm, without studying the dykes in Carboniferous host rock it would be difficult to ascertain the extension direction given the large range in dyke orientation, and extensional openings, in the west of the swarm. Oblique openings that preserve the extension direction are only seen in northwest Co. Donegal in granite host rock.

On a regional scale, the apparent anomalous trend of the Killala swarm might be explained by a deflection in the crustal stresses caused by emplacement of the Brendan centre and its associated radial dyke systems. In this sense, the Killala swarm represents an intermediate (or transition) stress direction in a regional swing from NE-SW extension to the NW-SE extension associated with the northeast side of the Brendan centre.

Chapter 3 *Host rock deformation resulting from dyke emplacement*

3.1 Introduction

Dykes emplaced by hydraulic fracture of the host rock typically create a zone of fracturing, i.e. 'damage' by inelastic deformation, at and ahead of the dyke tip, parallel to the plane of intrusion, (e.g. Anderson 1951; Andrews & Emeleus 1975; Delaney 1986; Pollard 1987; Rogers 1987; Rubin 1993; Mériaux *et al.* 1999). Dykes emplaced along pre-existing fractures would not be expected to create such deformation in the host rock (Delaney 1986). The mechanism that causes fracturing ahead of the dyke tip, and the factors that control the extent of fracturing, are not well understood (Delaney & Pollard 1981; Delaney 1986; Lister & Kerr 1991; Rubin 1993; Mériaux *et al.* 1999).

This chapter aims to provide new insight into what is a complicated problem, by studying Tertiary dykes from northwest Ireland. The chapter is split into three main parts. The first part (3.3) defines the extent of dyke-associated deformation in the host rock for a range of host rock lithologies and dykes of differing emplacement styles. Deformation is studied both associated with dykes that appear to have been emplaced by hydraulic fracture of the host rock in classic en échelon style, and with dykes that apparently have exploited pre-existing fractures on intrusion. Secondly, in Section 3.4 structures are described and classified from the host rock deformation zones in the margins of dykes in the Killala Bay area and, where possible, their temporal relationship with dyke intrusion is established. Thirdly, in Section 3.5 all the results are discussed and interpreted as far as possible to derive a model for the cause of host rock deformation related to dyke emplacement. A largely disregarded mechanism for fracture of the host rock is then suggested to be of major importance during dyke emplacement.

3.2 Background

The mechanisms that cause fracturing ahead of a dyke tip as the dyke propagates, and the factors that control the extent of fracturing, are not well understood (Delaney & Pollard 1981; Delaney 1986; Rubin 1993; Mériaux *et al.* 1999). In addition, dyke propagation can cause faulting and folding of the host rock strata (Pollard *et al.* 1975; Rubin 1993). Rubin (1993) highlights the problems and paradoxes with using Linear Elastic Fracture Mechanics (LEFM) to explain the formation and observed extent of dyke-parallel fractures in the host rock. Field observations suggest that dyke-parallel fractures can extend several tens of metres from the dyke margin into the host rock (Delaney 1986), invoking large scale 'process zones' that propagate ahead of the dyke tip. This, however, is in contrast to the much smaller millimetre-scale process zones produced in laboratory rock fracture experiments, explained by LEFM (Pollard 1987; Rubin 1993). It would therefore appear that increased energy for fracture occurs at high confining pressure, as evidenced by the extent of dyke-

parallel fracture zones in the field (Rubin 1993). Indeed, Rubin (1993) concludes that at high confining pressures greater than the cohesive strength of the rock, i.e. at normal dyke emplacement depths, LEFM does not apply and the near-tip stress field of a propagating crack is determined by the crack size and the loading configuration. Delaney *et al.* (1986) conclude that differences in magma driving stress, host rock tensile strength, regional stress, and emplacement depth are all factors that contribute to the different sizes of observed zones of dyke-parallel fractures. They say that thermal stresses caused by heating of the host rock are unlikely to extend far enough to explain the extent of fracturing. However, Delaney & Pollard (1981) conclude that fracturing of the host rock results from a combination of thermal stresses, stresses due to cooling and contracting of the dyke, and tensile stresses at the dyke tip.

The most important factor, according to Delaney *et al.* (1986) in controlling the extent of fracturing in the host rock, is the dyke length. Large dyke lengths that propagated with the largest driving pressures might produce fracturing several hundred metres from the dyke. However, Rubin (1993) invokes pore pressure acting within a cavity created ahead of the dyke tip as being the dominant controlling factor over the near-tip stress field of a propagating dyke. This pressure depends on the influx of magmatic volatiles and/or host rock pore fluids into the cavity and, if sufficiently large, will create much greater tensile stresses off the dyke plane than seen in the cavity, enough to cause fracturing of the host rock.

A major part of this chapter is the study of host rock deformation associated with en échelon dyke segmentation. Little work has been published that documents field examples of the types of structures that occur in this setting (Kattenhorn & Watkeys 1995; Weinberger *et al.* 2000), although the theory of how extensional fractures in en échelon arrays interact, and the resultant stress perturbations that occur, is well known (e.g. Pollard *et al.* 1982; Pollard & Segall 1987).

The generation of dyke-parallel fractures and deformation in the host rock is obviously a process that is complicated and depends on a range of factors. The observations made in this chapter are from field examples of dykes where host rock deformation is apparent. It is beyond the scope of this work to reconcile every feature seen with the theory described above. However, basic trends and observations of processes not previously described allow insight into the mechanisms behind host rock deformation resulting from dyke emplacement.

3.3 The extent of host rock deformation caused by dyke emplacement

Figure 3.1 shows the locations of all dykes discussed in this section and whose host rock fracture frequency was counted. Numbering of the dykes is the same as in Chapter 2, and basic data for the dykes can be sourced in Appendix 3 (for dykes of the West Connacht systems), Appendix 4 (for dykes of the Killala swarm), and Appendix 8 (for dykes of the Donegal-Kingscourt swarm).

This section attempts to define the *total* extent of emplacement-related deformation in the host rock by simply counting dyke-parallel fractures away from the margins of dykes in the host rock.

3.3.1 Dyke locations and rationale

Most of the fracture data was collected from dykes with continuous exposure of host-rock away from one, or preferably both, margins. Coastal exposures were therefore used in the main. Dykes intruding a range of host rock lithologies were investigated, but in most cases the host rock was Carboniferous limestone due to the excellent platform exposures (Figure 3.1). In addition, dykes of different widths were sampled, some of which have been interpreted previously as feeder dykes (Preston 1967a). Data therefore come from the three swarms/systems across the region. Table 3.1 lists the dykes studied.

3.3.2 Methods

Data collection, preparation and plotting

Data was collected with a view to creating graphical representations of the frequency of fractures in the host rock orientated parallel or sub-parallel to the dyke as a function of distance from the dyke margin. These graphical representations are here termed *fracture frequency profiles*. In the vast majority of cases, the fracture counts were made remote from any en échelon segmentation zones, so as not to include structures relating to dyke segment interaction (as described later). Every fracture visible to the eye in outcrop that intersected the profile was counted, regardless of spacing. All types of fractures were included, including any shear structures. No quantitative attempt was made to distinguish between fractures in terms of length. Also, where applicable, stratigraphic (vertical) continuity of fractures was mostly impossible to determine due to the platform nature of the host rock exposure and the lack of vertical section.

It has been shown in Chapter 2 that in many places regional joints/fractures sub-parallel to dyke orientation exist in the host rock, whose age is not known in relation to the dykes. This is most clearly displayed in the Killala Bay region. Fracture counting was stopped when it was deemed in the field that numbers were representative of this 'background frequency'.

Figure 3.2 shows schematically the spatial relationship between the closely spaced fractures typically found adjacent to a dyke, and the background fracture set.

For a few dykes, close to the margins, water/weed-filled channels obscured the host rock, precluding the collection of fracture data.

In general, fractures were counted on both sides of dykes. For dykes emplaced into Carboniferous sediments and Caledonian granite, the host rock was generally flat-lying. However, Dalradian metasedimentary host rock was less flat and remnant bedding and the metamorphic fabric was generally steeply dipping.

In Carboniferous host rock where several dykes were relatively closely spaced, fractures were counted in a continuous profile with no break in data between dykes. In most cases it was possible to confine data collection to a single bed either side of a dyke, but when making a multi-dyke profile this was not always possible. Collecting data from the same lithology on either side of a given dyke was deemed important due to the possibility that lithological variation and/or bed thickness would affect the way the host rock behaves mechanically. Some control could therefore be maintained over this

variable in subsequent analysis of the data.

Two methods were used for collecting the data. Counts were made either by recording the spacing between each fracture, or by recording the number of fractures in distance 'bins'. Raw fracture count data is listed Appendix 10. A collection of individual fracture spacings is the best form in which to have the data, but to study a large number of dykes this method was deemed too time consuming. So, most data was collected over distance bins. Bins were chosen to increase in size as the fracture spacing increased away from the dykes. Generally, bin size at the dyke margins was in the order of 10 to 20 cm. As fracture spacing increased appreciably 50 cm bins were used, followed by 1 m bins distally in the profile. If, close to the dyke margin, fracture spacing increased markedly over a shorter distance than the bin size, the bin size was reduced temporally to reflect this change. In addition, at random points in most profiles, the dyke sub-parallel fracture strike was measured (as shown in Figure 3.2) (see Appendix 11).

For plotting of the fracture frequency profiles, the raw data for all dykes was re-binned to a uniform bin size to allow ease of comparison between dykes. A bin size of 25 cm was chosen for each dyke (see Appendix 12). This was deemed narrow enough to reflect the change in fracture frequency close to the dyke margins, and broad enough to show the low fracture frequencies away from the dykes.

Defining the background fracture frequency

The background fracture frequency was quantified for all host rock apart from granite. (In granite, the frequency of fractures remote from the dykes showed less uniformity than for the other host rocks; hence it was difficult to define an average frequency.)

To define the background frequency a sample interval of 5 m was used on each side of a given dyke, further out from the furthest apparent discernable affect of the dyke, as shown schematically in Figure 3.2. This gave a total sampling distance of 10 m away from each dyke.

In a few cases, for Carboniferous host rock, where beds of noticeably different lithology were sampled either side of a dyke, two background frequency values were obtained, one for each lithology sampled over 5 m each. This was to allow for the fact that the two frequency values might be different.

Where the plotted fracture frequency profiles were short, a distance less than 5 m was used to measure the background frequency. This, however, is not ideal.

Defining the width of the dyke-associated fracture zones

Dyke-associated fracture zones are defined as extending from the dyke margin to a point where the fracture frequency drops to the background frequency. In some cases, however, it was not easy to tell from the fracture frequency profiles just where the influence of the dyke ended. For some dykes, subtraction of the average background fracture frequency from the whole data for a given dyke made delineation of the dyke-associated fractures easier. This is shown in Figure 3.3. For dykes whose host rock showed a very uneven background fracture frequency, subtraction of the average did not really help. The method was not applied to dykes intruding granite for this reason. For these dykes

and for others where ambiguity remained, the edge of the dyke-associated fracture zone was generally chosen to be the midpoint of this 'uncertainty zone'. In other words, for these dykes it was unclear as to the exact position of the edge of the dyke-associated fracture zone.

Extracting the dyke-associated fracture frequency profiles for comparison

The data was then prepared so as to be able to compare the form of the dyke-associated fracture frequency profiles for different dykes. The cumulative data for individual fracture spacing (see Appendix 10) was simply cut as close as possible to the interpreted width of the dyke-associated fracture zones. These data are tabulated in Appendix 13. For each extracted dataset, the distance, i.e. the width of the fracture frequency profile, was then re-binned to fifteen bins. This number was chosen to be the best compromise between faithfully representing the form of the profiles and not resulting in many bins showing zero fracture counts. The background fracture frequency was then subtracted from the profiles. This was carried out by calculating the number of fractures to be subtracted from each bin in the newly binned data, and then subtracting this number. The remaining profile thus contains only those fractures associated with the dyke.

3.3.3 Results

Description of fracture frequency profiles

Figure 3.4 shows all the fracture frequency profiles. The profiles have been grouped based on their host rock lithology: limestone; sandstone, quartzite and psammite (i.e. quartz dominated); and granite. The term 'limestone' is used in a generic sense, comprising a range of lithologies from thickly bedded hummocky limestone to relatively thinly bedded limestone with higher organic content. Most of the profiles relate to single dykes, but five 'multi-dyke' profiles were taken across dykes in the Killala swarm. Figure 3.5 compares the forms of individual dyke-associated fracture profiles, with the background frequency removed as described above.

For all dykes, there is an increase in the number of dyke-parallel fractures towards the dyke margin. In general, between the dyke margin and the interpreted edge of the dyke-associated fracture zone, the profiles follow a curvature akin to that of a power law. It is also apparent that the three widest dykes, K127, DK17a, and WC33a, are associated with the widest dyke-associated fracture zones.

For limestone host rock, the curvature of the profiles is generally smoother and more regular than for quartz-dominated host rock, the latter showing a more uneven curvature away from the margins of dykes. For most dykes, the highest fracture frequency occurs at the dyke margin. However, for some dykes there is a relative reduction in fracture frequency at the dyke margin. This occurs more so with dykes emplaced into quartz-dominated host rock. In the cases of K117 and K127, emplaced into limestone, a major reduction in fracture frequency corresponds with a wide baked zone where the host rock has completely re-crystallised and is bleached white as a result.

In most cases, there is a background fracture frequency remote from the dykes, evident in the profiles (Figure 3.4). The most obvious exception is DK17a, the Blind Rock dyke, where the limit of

the dyke-associated fracture zone can be pinpointed with confidence, as there are no dyke-parallel fractures existing in the host rock beyond this point.

It is apparent from Figure 3.4 and Figure 3.5 that the maximum fracture frequency is generally higher for limestone and granite host rock than it is for quartz-dominated host rock. Given this, and the similarity in profile shape between the different host rock lithologies, quartz-dominated host rock appears to be relatively resistant to fracturing related to dyke emplacement. In general, the fractures counted were unfilled, except for some associated with wider dykes in limestone host rock where mineralisation has occurred along fractures close to the dyke (see later sections).

Relationships between dyke width and the dyke-associated fracture zone

Figure 3.6 plots the maximum fracture frequency against dyke width for the different host rocks. There is a hint that, for quartz-dominated host rock, wider dykes might be associated with relatively high maximum fracture frequencies.

For limestone host rock, it is apparent in the field that lithological variation exerts some control over the background fracture frequency (compare in Figure 3.4 the overlap in profiles between dykes K111 and K112, and the two profiles, x and y, for dyke K116ii). For example, thickly bedded hummocky limestone generally tends to show a lower background fracture frequency than more thinly bedded tabular limestone often with apparent higher mud content. These observations of a relationship between fracture spacing and bed thickness and the 'strength' of the rock (the higher mud content producing a weaker rock) are well known (e.g. Ladeira & Price 1981; Davis & Reynolds 1996). It is probable that bed thickness has more control on fracture spacing than lithology alone. Therefore, the variation in background fracture frequency may be a crude indication of host rocks' general susceptibility to fracture. Given this, in Figure 3.6 limestone has been classified in terms of its derived background fracture frequency. There does not appear to be any relationship between the maximum fracture frequency and the dyke width for limestone host rock classified in this way.

Figure 3.7 plots the interpreted width of the dyke-associated fracture zones against the widths of their respective dykes. For all host rock lithologies there is a linear relationship between dyke width and the width of the dyke-associated fracture zone. The trend line is pinned by the widest dykes, which clearly associate with the widest fracture zones. For relatively narrow dykes, less than ~1.5 m wide, the association is less clear.

Three of the wide dykes that help to define the relationship, dykes DK17a, K117 and K127, are multiple intrusions. Dyke DK17a, the Blind Rock dyke, has been described as a feeder dyke by Preston (1967a). These dykes have wide baked margins (Table 3.1) indicating that magma flowed for a relatively long period of time through the dykes. They are also believed to be multiple intrusions (see later).

Looking at the different host rock types individually (Figure 3.7), the linear relationship is relatively strong for the few dykes emplaced into granite, and the trend line appears to be steep. For quartz-dominated host rock the trend line is shallower.

For dykes emplaced into limestone, the slope of the trend line is similar to that of quartz-dominated

host rock. For narrow dykes alone though, a linear relationship cannot really be distinguished. It has been suggested above that host rock type may influence the extent to which it fractures due to dyke emplacement. Figure 3.8 classifies limestone host rock in terms of background fracture frequency (using the same classification shown in Figure 3.6) for the narrow dykes, and shows that there are two zones where two of the classes cluster. (There are points belonging to these classes, however, that do not fall into these zones.) Perhaps, if these zones are to be taken as roughly linear, there is an offset along the x-axis of the higher background fracture frequency points. This would imply that, for a given dyke width, dykes emplaced into host rock with a higher background fracture frequency tend to produce a wider dyke-associated fracture zone, due to an increased susceptibility of such host rock to fracture. Therefore, the lack of definable relationship between dyke width and width of dyke-associated fracture zone for narrow dykes intruded into limestone, may result from the range of host rock lithologies and their differing susceptibility to fracturing.

3.3.4 Preliminary remarks

In simplistic terms, for dykes that propagate hydraulic fractures on intrusion, the dyke-parallel fracture zone propagated ahead of the dyke tip will not increase in extent once the dyke tip has propagated on and dilation ensues towards the final width of the dyke. In fact, once the dyke is dilating the magma pressure will exert compressional forces to keep the fracture open (Delaney & Pollard 1981). All else being equal between dykes emplaced under the same stress regime and into relatively uniform host rock lithology, there should surely not occur large differences in the extent of the hydraulic fracture zones between intrusions. If all the fractures in the dyke-associated fracture zones identified here were hydraulically formed on initial emplacement, then why does there appear to be this relationship (as shown in Figure 3.7) between the width of the dyke and the width of the dyke-associated fracture zone?

3.4 Structures in the host rock related to dyke emplacement: examples from Killala Bay

The host rock of dykes on the east side of Killala Bay yields many structures that relate to dyke emplacement. Mineralisation close to the dyke margins, and the abundance of fossils and pre-intrusion veins acting as displacement markers, allow the structures to be classified into two main groups (Figure 3.9). The first group contains structures that form part of, or are associated with, the dyke-associated fracture zone, as defined in the previous section. The second group of structures appears to be exclusively associated with dyke segmentation, not affecting the host rock remote from segmentation zones. All these structures are described below. Given the platform nature of the outcrop, structures are almost exclusively observed in plan view. It is therefore often impossible to obtain dip information for a structure. If shear has been accommodated along a structure, only the horizontal component of shear is indicated in outcrop.

3.4.1 Structures associated with dyke segmentation

A distinctive style of fracturing occurs in the host rock associated with the overlap of two en échelon dyke segments. Narrow dykes, whose segments are typically relatively closely spaced, say within a few tens of centimeters, generally show characteristic deformation within and around the host rock bridge. Wider dykes, whose overlapping segments tend to be more widely spaced, may not show as much deformation within the bridge zone, but characteristic structures are usually still present locally in the host rock.

Broadly speaking, deformation within the bridge zone consists of two main fracture groups, dyke sub-parallel fractures and fractures that subtend a high angle to the dyke segment strike (Figure 3.10). (Note, the term 'dyke-parallel' is used loosely and includes those fractures within the bridge that have been rotated by dilation of the dyke segments.) The high angle fractures often show a degree of curvature, commonly terminate against the dyke-parallel fractures, and are orientated roughly orthogonal to the line that would join the tips of the dyke segments in a given en échelon pair. They also often show a range in orientation within the host rock bridge and sometimes appear to have formed in conjugate pairs (Figure 3.10a). The closely spaced fracturing, introduced above in Section 3.3.3 to be typical of limestone host rock against the dyke margin, is normally diminished in segmentation zones, giving way to more widely spaced dyke-parallel fractures, as shown in Figure 3.10.

This host rock bridge fracturing is usually accompanied by mineralisation, i.e. calcite-filled veins, and shear. Left-stepping dykes are associated with dyke-parallel sinistral shear (Figure 3.10b), and right-stepping dykes, dextral shear (Figure 3.10c). Shear is generally accommodated along dyke-parallel fractures, and offsets, generally of around a few millimeters, are indicated by pull-aparts along the plane of shear. Alternatively, the high angle fractures might have opened and been filled with calcite (Figure 3.10c), or occasionally magma (Figure 3.10d), under the imposed shear. Shear structures of opposing sense sometimes occur sub-parallel to the high angle fractures.

Shear structures also often extend from the tips of en échelon segments. The shear sense is the same as would be expected to occur within the bridge zone for the given dyke geometry. Figure 3.10b shows dyke-parallel fractures that opened under the imposed shear, extending from the tip of the southern dyke segment.

Figure 3.11 shows two dykes whose overlapping segments are relatively widely spaced, and whose bridge zones are apparently devoid of any high angle fracturing and shear structures. Instead, shear fracturing extends from the segment tips and is therefore localized ahead of the tips. Figure 3.11a shows dextral shear structures extending from the southern dyke segment of a right-stepping dyke; the structures strike in towards the southern segment. In this case, pull-aparts are opened *between* dyke-parallel fractures. Figure 3.11b shows a left-stepping dyke whose northern segment shows a curved propagation path in the zone of overlap. Intense sinistral shearing has taken place outside of the host rock bridge along dyke sub-parallel fractures, and several dyke tip injections terminate in what appear to be sinistral pull-apart structures.

In addition to the structures described above, shear structures between en échelon segments occur

that relate to how rapidly the amount of extension changes as a segment terminates. In Figure 3.10b and Figure 3.11a, the abrupt termination of dyke segments in blunt ends has resulted in what are interpreted as transform structures extending from the point at which the dilation differential exists. In the case of Figure 3.11a, the sinistral transform extends into the marginal zone of the opposing dyke segment. Intrusion had therefore begun before the stage of dilation took place that formed the blunt end to the southern segment. Similar structures have been described by Kattenhorn & Watkeys (1995) to propagate from blunt dyke segment ends.

3.4.1.1 Interpretation of deformation related to segment overlap and application to further examples of dykes

The structures described above are interpreted separately from structures in the dyke-associated fracture zone and other structures in the host rock margin, due to their apparent exclusive association with the segmentation zones (as shown in Figure 3.9).

Individual segments of an en échelon dyke are expected to orientate orthogonal to the regional extension direction (e.g. Delaney & Pollard 1981) (Figure 2.2). In Chapter 2 it has been shown that the en échelon dykes being described here are consistent with this model in that, generally speaking, individual segments opened under extension in the horizontal plane. Each dyke is therefore a series of mode I fractures whose tips propagate laterally (as the dyke as a whole propagates upwards) to eventually overlap with adjacent fractures/segments. It is well established that mechanical interaction between two mode I fractures propagating towards each other impedes further advance of the crack tips due to local modification of the regional stress field (Delaney & Pollard 1981; Pollard *et al.* 1982; Nicholson & Pollard 1985; Pollard & Segall 1987; Olson & Pollard 1989; Thomas 1993; Acocella *et al.* 2000). This is explained in Figure 3.12. Mode II shear stress is induced when the cracks 'see each other', causing the cracks firstly to bend away, and then to bend in towards each other (Figure 3.12a). In doing so the fractures are trying to maintain an orientation orthogonal to the (modified) extension direction around the host rock bridge zone (Figure 3.12b). Where crack propagation remains straight, however, this is thought to be a result of either a relatively high remote compressive stress acting parallel to the cracks (Figure 2.3b) that negates the effect of the induced mode II stress, or a pre-existing weakness in the host rock parallel to the cracks that 'guides' crack propagation (Olson & Pollard 1989; Renshaw & Pollard 1994). Alternatively, in the case of dykes, high magma pressure might cause the overlapping segments' tips to maintain a straight path. Indeed, both curved and straight forms are seen for dykes in this study. (This is shown in Chapter 2, e.g. Figure 2.17, where it is suggested that high magma pressure and/or closely spaced fractures propagating ahead of the dyke might have guided the oft-seen straight propagation of overlapping segments.) It is suggested that the reduction of closely spaced fractures in the host rock bridge zone might be due to the formation of extensional fractures being inhibited as the two dyke segments mechanically interact. After fracture/dyke propagation ceases in the overlap zone the segments will continue to dilate. The dilation differential along a tapering segment will cause rotation of the host rock bridge. This must further stress the bridge, which will ultimately fail given sufficient dilation of the segments (Figure

3.12a). There are therefore *two* obvious sources of stress that will affect the host rock bridge. They are, firstly, segment interaction and, secondly, dilation differentials and bridge rotation. Both of these are considered in the interpretation below.

The shear structures associated with segment tip propagation (e.g. Figure 3.11) are interpreted as a result of mode II stress induced by segment interaction. Shear structures that extend from the dyke tips and bend in towards the adjacent segment fit the accepted model and the predicted stress trajectories shown in Figure 3.12b. The sense of shear on dyke-parallel fractures *within* the host rock bridge is consistent with the predicted stress trajectories for the two (left-step and right-step) overlap geometries. It is possible that these structures originated as extensional fractures that were created ahead of the dyke segments before they overlapped, and were then reactivated under the imposed mode II shear. This is consistent with the observation that the high angle fractures often abut against the dyke-parallel structures, thus implying that the latter are older. In further support of this, considering Figure 3.10d, high angle fractures are seen to extend from dyke-parallel fractures, having the appearance of 'tail structures' that typically form when an existing fracture is loaded with mode II shear (e.g. Price & Cosgrove 1990 p. 148; Cruikshank & Aydin 1994). In this sense they are behaving in the same way as the dyke segments when they are loaded with mode II shear.

Regarding the high angle fractures, the strike component of their orientation in the host rock bridge zones is in agreement with the stress trajectories shown in Figure 3.12b, assuming the fractures to be extensional, sub-vertical structures. The curvature of the fractures that is often seen (Figure 3.10) might relate to the variation in the stress trajectories within the bridge zone.

It has been noted, however, that the high angle fractures can occur in apparent conjugate arrangement (Figure 3.10a). If this interpretation is correct then at least some of these structures are not extensional fractures, but formed with at least a component of shear. Figure 3.13 shows dyke K141, with high angle fractures in apparent conjugate relationship that are manifest exclusively within a block of host rock that has been uplifted and tilted within the bridge zone. In two places magma has injected along the fractures. (Appendix 14 contains the data plotted.) The cross-section across the southern dyke segment indicates that it is thinning downwards (in addition to eastwards, as shown in the plan), and the tilt therefore appears to be a result of host rock bridge rotation in the vertical plane. This implies that segmentation is occurring with components in both the horizontal *and* vertical planes. The acute and obtuse bisecting lines of the conjugate pairs are plotted and are assumed to indicate the maximum and minimum stress directions. They are inclined from the horizontal, and become further inclined if the tilted block is rotated back to horizontal. If the structures are assumed to be a response to a derivative of the stress trajectory arrangement described in Figure 3.12b, then the inclination of the conjugate bisecting lines supports the observation that segmentation took place in both the horizontal and vertical planes. This is shown schematically in Figure 3.14. If segmentation was purely in the horizontal plane then fractures would be expected to be vertical and the bisecting lines to be contained within the horizontal plane. The fact that the rock appears to have reacted to stress by shear fracture (the dihedral angles indicate this, averaging 47°), rather than tensile fracture (as is implied should be the case in Figure 3.12b), would indicate a

relatively high compressive stress in the directions orthogonal to the extension direction (see Figure 2.18). Magma pressure might have provided this, as the segments struggled to dilate in the overlap zone. Evidence suggests, therefore, that the propagation of dyke K141 was inclined through the crust.

So far the discussion has attempted to explain the structures seen in terms of the stress trajectories resulting from overlapping segment interaction. However, as described above, the stresses induced in the host rock bridge by dilation differentials (as the segments taper), and its rotation, are envisaged to also have an effect. These stresses will dominate in the bridge after dyke segments have ceased to propagate any further in overlap.

Therefore, an alternative explanation for the slip accommodated along dyke-parallel fractures in the bridge zone (e.g. Figure 3.10b and c) is that it occurred as flexural slip during bridge rotation. This is shown schematically in Figure 3.15a. The high angle fractures can be considered as tail structures to these shear planes. Those occasional high angle fractures within the bridge that show the opposite sense of shear to that seen on dyke-parallel fractures for a given dyke geometry (as shown in Figure 3.10b & c) may also be related to bridge rotation in that they are a flexural slip response to the dilation differential as the segment tapers (Figure 3.15b). In this sense they form in the same way that transform shears are a response to blunt ended segments (as shown in Figure 3.11a and described previously).

A model of flexural slip accounting for structures within the bridge zone is perhaps the most obvious explanation for this deformation.

Figure 3.16 shows a pair of dyke segments (dyke K135i/ii), the southern of which widens to the east whilst the northern segment narrows and pinches out. The change in width of the southern segment is considerably greater than that of the northern segment over an equal distance along strike. Between the two dyke segments where the rate of change of width is the greatest for the southern segment, there is extensive fracturing of the high angle type described previously. There are also a number of shear structures. The high angle fractures are inclined, having an average dip of 36°, and occasionally accommodate dextral slip. Magma has injected along the fractures in a similar manner to that shown in Figure 3.10d. The injections take a left-stepping segmented form. Sinistral and dextral shears appear to be related to each other in their genesis by their apparent association with the magma injections. The acute angle bisecting lines of what appear to be conjugate pairs of these shears plot reasonably close to lying within the planes of nearby dyke segments, suggesting that stresses ahead of the injection segment tips might have produced these conjugate fracture sets, which have low dihedral angles (see Section 3.4 below). Alternatively, the sinistral shears, which are mostly dyke sub-parallel, are consistent with the overall form of the dyke having a left-stepping arrangement, and with the host rock between the segments being effectively the host rock bridge (as described above for more 'orthodox' segmented forms). It has been noted above that high angle structures in the bridge might result from shear stresses induced by dilation differentials (as shown schematically in Figure 3.15b). It is suggested then that for this particular dyke, the array of magma injections intruded under dextral shear that resulted from the dilation differential created by the extra widening of the southern segment. In addition, the inclination of the high angle fractures is interpreted in the

same way as for dyke K141 above, i.e. that segmentation of dyke K135i/ii was taking place in both the horizontal *and* vertical planes and that dyke propagation was oblique through the crust (Figure 3.14).

3.4.2 Structures within (and related to) the dyke-associated fracture zone

Structures that occur in the host rock margins of the dykes as part of the dyke-associated fracture zone, i.e. dyke sub-parallel structures, fall into three categories: firstly, closely spaced fracturing (first mentioned in Section 3.3.3) that exists against the dyke margin; secondly, shear structures of high dip angle that subtend a low angle to the dyke trend and often form in conjugate sets with low dihedral angles; and thirdly, other fractures beyond the zone of shear structures and fracture cleavage, but where fracture frequency is still higher than that of the background.

In addition to dyke sub-parallel structures, there commonly exist, immediately adjacent to the dykes, veins that trend at a high angle (sub-orthogonal) to the dyke. These structures are obviously not included as part of the dyke-associated fracture zone but show clear relations with the dyke-parallel fractures.

Below the structures are described and their cross-cutting relations discussed.

3.4.2.1 Closely spaced dyke-parallel fracturing (fracture cleavage)

This is the closely spaced fracturing previously described that is typically found in limestone host rock adjacent to the dyke margins. From here onwards it shall be termed *fracture cleavage,* as in outcrop it bears resemblance to structures described by Foster & Hudleston (1986), and a general term is required when considering its various manifestations, described below. The use of this term will also be addressed later (Section 3.4.6) when considering the mechanisms behind the formation of the structures to be described below.

Spacing of the fracture cleavage is fractions of a millimetre at its lowest, up to a few centimetres, and increases away from the dyke, as has been documented earlier, in Section 3.3. It occurs typically in a zone up to a few tens of centimeters wide parallel to, and against, the dyke margin (Figure 3.17a). Qualitatively, it seems that narrow dykes are associated with relatively narrow zones (distance measured orthogonal to dyke margin) of fracturing, and vice versa. In outcrop the fracture cleavage is often, but not always, obviously mineralised, appearing as hair-width veins. Where not obviously mineralised in outcrop, the fracturing commonly looks like a cleavage, due to its narrow spacing. Indeed, fossils sometimes flatten against fracture cleavage planes indicating that pressure solution has taken place (Figure 3.17b). Thin-section analysis of the host rock from the margins of several dykes, reveals that the fracture cleavage comprises planes across which both extension *and* compression has taken place. The fracture cleavage can exist solely as mineralised extensional fractures (Figure 3.17c). However, it can also be manifest in the same sample as both extensional fractures and stylolites across which shortening has obviously taken place (Figure 3.17d). Stylolites may themselves be mineralised (Figure 3.17e), mineralisation having apparently taken place *after* pressure solution. In addition, an individual plane may change along strike from a stylolite to an apparent

extensional fracture, via a guise that shows progressive mineralisation of the stylolite form (Figure 3.17f).

It seems, therefore, that the fracture cleavage formed and evolved under a mix of extensional and compressional stresses. At some stage there occurred relaxation of compression, as evidenced by the mineralisation of stylolites.

Fracture length is in the order of millimetres to a few centimetres. For example, Figure 3.17e shows the extent of one of the fracture cleavage structures as being around 4 mm.

There is generally a lack of fracture cleavage in the host rock bridges of segment overlap zones, as has been noted above in Section 3.4.1. The dyke-parallel structures that dominate here tend to be more widely spaced.

3.4.2.2 Shear structures

Shear structures occur within the host rock margins of many of the dykes in the Killala Bay east region. They are easily mapped due to oft-accompanying mineralisation and the abundance of fossils and pre-existing veins (as described in Chapter 2) that act as markers for the shear. The structures usually subtend a small angle with the margin of the dyke, dip steeply, often with the dip of the dyke, and are commonly present in conjugate pairs of low dihedral angle.

The structures can be split into two main groups depending on whether or not their forms are influenced by the fracture cleavage.

The relationships between shear structures and fracture cleavage

Individual 'fractures' within the fracture cleavage are commonly mineralised in an en échelon configuration (Figure 3.17g). These arrays have often accommodated shear where individual fractures have become 'pulled apart' and linked by ramps to produce a through-going structure (Figure 3.17h). Alternatively, a 'shear zone' may have formed, in which rotation of the fracture cleavage pull-aparts occurs (Figure 3.17i).

It is noted, however, that en échelon geometries of discontinuous fractures that have accommodated shear do not necessarily *initiate* due to shear stresses (Olson & Pollard 1991). This is discussed further below.

The second way in which the fracture cleavage controls shear structure geometry is by individual fractures accommodating slip and being separated by pull-aparts (Figure 3.17j). The termination of such structures involves a reduction in the spacing (in the direction of the dyke's strike) of the pull-aparts, thus causing the structure to adopt a high angle trend with respect to the dyke (Figure 3.17k). This has the form of a tail structure that is typical for the termination of shear structures, or fractures in general that are loaded with mode II shear (as described above in Section 3.4.1.1 for structures within the host rock bridge) (e.g. Price & Cosgrove 1990 p. 148; Cruikshank & Aydin 1994).

In general, the length of shear structures influenced by the fracture cleavage depends on whether or not the structures failed in shear. Those that have accommodated shear may extend in the host rock for up to several tens of metres. Portions of such structures, however, may appear as discrete planes

of shear.

In the cases described above, it is apparent that the shear structures formed later than, or coevally with, the fracture cleavage, and shear geometry is controlled by the fracture cleavage. Conversely, it is also common to see that the orientation of the fracture cleavage was influenced in its formation by an imposed shear. In places, fracture cleavage is seen to swing into a given shear plane, abutting against it in pinnate geometry (Figure 3.17l). It is clear, therefore, that in these cases the shear plane is the influential structure, controlling the orientation of the fracture cleavage, and that the formation of fracture cleavage and the occurrence of shear were coeval.

Shear structures without the influence of fracture cleavage

Fracture cleavage is not extensively developed in the margins of some dykes e.g. dykes K147 and K148. It appears that some limestone lithologies are more resistant to this deformation. Shear structures may still, however, occur close to the dyke margins, often forming conjugate sets (Figure 3.17m), not always reactivating pre-existing structures. The structures tend to be discrete shear planes with occasional pull-aparts (Figure 3.17n) and other associations such as pinnate fractures.

It has been suggested in Chapter 2 that there is generally a dyke sub-parallel fracture set in the Carboniferous host rock that existed prior to intrusion of the Killala swarm. In the margins of some dykes, pervasive dyke-parallel fractures, that may therefore be older than the intrusion, have accommodated shear. As such, these older structures have been reactivated by imposed shear forces (Figure 3.17o). They tend not to have conjugate partners.

Occasionally, shear is seen to have taken place along the dyke margin (Figure 3.17p and q). In these (rare) cases shear has therefore taken place *after* solidification of at least the marginal zone of the dyke.

3.4.2.3 Veins at high angle to the dyke

Veins at high angle to the dyke margin typically extend from the dyke margin, at a high angle to the dyke strike, for up to several tens of centimetres into the host rock. They generally dip steeply to sub-vertical. The veins are often segmented by offsets across the fracture cleavage (Figure 3.17r). The sections of fracture across which the offsets occur are often also mineralised, and vein segments sometimes split in two across the fracture cleavage. Therefore, the offsets are transforms and are not a result of shear or pressure solution across individual fractures of the fracture cleavage. This is shown clearly in Figure 3.17s.

The sense of offset of the high angle veins across the fracture cleavage is usually consistent along an individual vein (Figure 3.17r). This means that the veins as a whole tend to trend at high angle, but not orthogonal, to the dyke. They resemble shear terminations, similar to the structures shown in Figure 3.17k, interpreted above in Section 3.4.2.2. This is clearly the case along the margin of dyke K155b, where there is association of left-stepping high angle veins with dextral shear (Figure 3.17t). In further support, within the host rock adjacent to dyke K117 there occurred coeval mineralisation of shear pull-aparts and high angle veins, as shown in Figure 3.17u. Conversely however, one example

is known where a high angle vein appears to have been offset by a shear structure under shear (Figure 3.17v).

Occasionally, the high angle veins extend *into* the dyke along dyke-perpendicular cooling joints or other sub-parallel fractures. This is shown in Figure 3.17t, and is described in the next section, indicating that at least some high angle veins, and probably therefore shear structures, did form after dyke emplacement and solidification.

3.4.3 Structures *within* the dykes

High angle veins have already been described above in Section 3.4.2.3 that run from the host rock into the dyke (or vice versa). In addition, some dykes are mineralised along margin-*parallel* fractures. Dyke K117, a multiple intrusion, shows relatively high amounts of mineralisation in the host rock and the dyke. Figure 3.18a shows that margin-parallel veins are, in this case, younger than a high angle vein that runs from the dyke into the host rock.

Shear structures are also occasionally seen within dykes. Within dyke K178, again a multiple intrusion, there are a number of what appear to be conjugate shears with low dihedral angle (Figure 3.18b). These occur in the central part of the dyke. As with shears in the host rock, they occur at low angle to the dyke margin. Furthermore, dyke K113, exposed as a wall protruding from the host rock platform, shows evidence of internal shear close to its margin (Figure 3.18c). Groove marks that are contained within a dyke-parallel cooling joint plane pitch around 10° from the horizontal and show up to a few millimetres relief. They are interpreted as having resulted from shear along the cooling joint plane whilst the dyke was still ductile during cooling.

3.4.4 Structural maps of host rock shear fracturing within the dyke-associated fracture zone

Figure 3.19 presents eight dykes whose host rock shear fracturing (as described in Section 3.4.2.2 above) has been mapped. Appendix 15 contains the raw data. The dykes are all emplaced into limestone, except for dyke K146i (not depicted in map form) whose host rock is the Mullaghmore Sandstone Formation. Four of the dykes described (K117, K134, K137 and K178) show a clear stepping geometry; the others do not. Dyke K118i is mapped as having been emplaced in segmented association with dyke K118ii immediately to the north. The dilations of both dykes balance along strike. However, there is no deformation between these dyke 'segments' of the type associated with segment overlap, as described above in Section 3.4.1. This could be due to the relatively large separation between the two dykes.

For each dyke, stereographic projections show the shear plane orientations in relation to the dyke orientation. Not all shears shown on the maps, however, are plotted. The purpose of the plots is to represent the shears from within the dyke-associated fracture zone (see Figure 3.9). Therefore, those shears (marked with an asterisk) extending from horns where the dykes step are excluded from the plots due to their association with segment overlap zones (as described previously in Section 3.4.1).

Also excluded from the plots are major fractures that appear to be reactivated structures (as shown in Figure 3.17n) and part of the regional background dyke sub-parallel fracture set. For example, dextral shears on the south side of dyke K178, parallel to the dyke margin, are examples of such structures.

The stereographic projections show that, where the dip is known, the shears are inclined at a high angle, similar to the dykes. Given this, the shears for which the dip is unknown are likely to also have similarly steep inclinations. These structures are plotted as vertical.

The shears strike at a low angle to the dykes. The vast majority of sinistral shears are orientated clockwise of the dykes, and most of the dextral shears anticlockwise of the dykes. This is shown strikingly in Figure 3.20 where data from all the dykes are plotted with respect to an E-W dyke plane. The mean angle subtended by a sinistral shear to its dyke margin is 8.9°, and the mean angle subtended by a dextral shear to its dyke margin is 9.0° (these values being derived from an average of all orientations of sinistral and dextral shears respectively over all dykes). Figure 3.21 shows that the majority of shear displacements are less than five millimetres.

Many of the shears occur in apparent conjugate arrangement, as described in Section 3.4.2.2 above. The average dihedral angle for conjugate pairs for each dyke ranges from 9° (dyke K117) to 21° (dyke K118i). The average over all dykes is 17°. The acute angle bisecting lines for the conjugate pairs are plotted in Figure 3.19. For the majority of dykes they plot on, or very close to, the great circle that represents the dyke plane. This is shown clearly in Figure 3.20. This is also demonstrated on the map of dyke K147 whose undulating trend follows a path that would bisect the acute angle between the many host rock conjugate shear pairs.

Dyke K147 shows an approximately equal number of sinistral and dextral shears in its host rock margins, as does the right-stepping dyke, K118i. In contrast, the other two right-stepping dykes, K134 and K178, are associated with predominantly dextral shear, and the one left-stepping dyke, K137, is associated with mostly sinistral shear structures. It is noted that, for the stepping dykes that are associated with a certain shear sense, this shear is the same as that which would be associated with segment overlap for their respective stepping geometries.

The lateral extent of shear deformation (shear zone width) can be defined from the maps in Figure 3.19. This is plotted in Figure 3.22 against dyke width. There is a hint of a relationship between the width of the dyke and the width of its associated zone of fracturing, i.e. wider dykes being associated with wider zones of shear fracturing.

3.4.5 Timing of deformation in relation to dyke intrusion

It has already been established (in Section 3.4.1) that deformation of the host rock associated with overlapping dyke segments took place *during* emplacement. It has also been established (in Sections 3.4.2 and 3.4.3), from structures affecting the dykes themselves that some deformation occurred *after* the cooling of some dykes.

Evidence for the timing of the majority of host rock deformation in relation to dyke emplacement, most of which forms part of the dyke-associated fracture zone, comes from a number of observations from two key dykes. Figure 3.23 shows dyke K132ii. There is a typical series of low dihedral angle

conjugate shears in the host rock (Figure 3.23a), of the form shown in Figure 3.17h. In close proximity, ahead of the termination of the easternmost dyke segment, there is a zone of fracture cleavage that shows clear association with dextral shear (Figure 3.23b). Magma has filled dextral pull-aparts and extensional fractures. Also, high angle veins to the fracture cleavage transform across fractures and have the appearance of dextral shear termination structures, as described previously.

Immediately to the south, a pervasive dextral shear structure extends west for almost 50 m. In three places it shows clear association with dyke intrusion. Figure 3.23c shows magma injection into tension gashes associated with the shear. Further west it is apparent that a displacement of 70 cm has occurred between two phases of magma injection (Figure 3.23d). This is evidenced by dyke that is undeformed being juxtaposed against deformed and brecciated dyke along the shear plane. Figure 3.23e shows further that magma injection continued to occur after displacement, by the entrainment of host rock breccia fragments within the (undeformed) dyke.

The second dyke of interest is dyke K157b. The dyke shows a series of steps, mostly to the left, along its exposed length (Figure 3.24). Running parallel to the northern margin is a dextral (left-stepping) array of mineralised fracture cleavage (like that shown in Figure 3.17g), which is injected by magma near the eastern end. In addition, at one of the jogs in the dyke, the margin shows clear exploitation by the magma of fracture cleavage in left-stepping geometry.

It is clear therefore that, for the development of these dykes, magma injection occurred coevally with the formation of shear structures and the fracture cleavage. This is supported by the previous observations from the host rock margins of other dykes (Section 3.4.2) that indicate coeval formation of shears and fracture cleavage. The fact that, occasionally, some host rock shear structures affect the dykes (shear along dyke margins and high angle shear termination veins), and shears have been recorded exclusively confined to a dyke, indicates that their formation spans the emplacement process from the time of initial magma injection to post-cooling.

It is also a possibility that the fracture cleavage underwent a multi-stage development under extensional and compressive stresses (as well as shear stress), as has been mentioned in Section 3.4.2.1 previously. How these stages relate temporally to magma emplacement is unclear from field relations (see discussion in Section 3.4.6 below).

3.4.6 Mechanisms behind the formation of fracture cleavage and shear structures in the dyke-associated fracture zone, and implication for the stress regime during dyke emplacement

The term 'fracture cleavage' has been used throughout the previous sections as an umbrella term incorporating all closely spaced dyke-parallel structures in the host rock margins of the dykes, some of which have been reactivated and mineralised to form arrays that have failed in shear. Foster & Hudleston (1986) describe fracture cleavage in troctolite that is remarkably similar to that described in this study in terms of spacing, fracture length etc. Fracture cleavage is believed to form from hydraulic fracturing (Price & Hancock 1972). It is therefore appropriate that the term is used here given its apparent formation as the dykes were emplaced. The fact that some of the structures making

up the fracture cleavage are stylolites, some of which appear to have been 'relaxed' and mineralised (Figure 3.17d to f), is obviously in contradiction to the above. It is envisioned though that after creation of tensile fractures ahead of the propagating dykes tip, the host rock will be under compression close to the dyke margin from magma pressure acting to keep the dyke walls apart. It also stands to reason that thermal stresses, as the host rock is heated will reverse the stress from one of tension to a state of compression as the rock tries to expand. This is relevant for Section 3.5 below.

Shear structures have not before been described as occurring extensively in the host rock margins of dykes (apart from the minor shears associated with en échelon segmentation in Weinberger *et al.* (2000). Dyke-parallel fractures have been described from the field and their formation has been simulated (Delaney & Pollard 1981; Delaney 1986; Rogers 1987; Rubin 1993; Mériaux *et al.* 1999). Many of the shear structures described here have mineralised and pulled apart the fracture cleavage in en échelon arrays (Figure 3.17g and h). These structures, however, may not have *initiated* under shear. As Olson & Pollard (1991) describe, mechanical interaction between overlapping extensional fractures can produce fracture arrays with en échelon geometry (e.g. Figure 3.17g) that then are structural boundaries oblique to the principal stress axes, and as a result fail in shear. This process of development is shown schematically in Figure 3.25. Dunn *et al.* (1973) and Wong *et al.* (1982) describe similar structures to that seen in this study, where through-going shear fractures are formed by a complex process involving the coalescence of small-scale extensional fractures. Where the shears have slightly pulled apart the fracture cleavage, the dyke-parallel orientation of the fracture cleavage 'segments' controls the array/shear orientation, keeping the angles low that the shears subtend with the margins of the dykes. Any shears occurring in conjugate pairs presumably *did* form initially under shear. Such pairs that are manifest as en échelon mineralisation of the fracture cleavage therefore show low dihedral angles. Low dihedral angles, however, are still maintained when shear orientation is *not* being controlled by the fracture cleavage (as shown in Figure 3.17m). Shears that propagated for long distances, and that alternated between exploiting the fracture cleavage and propagating a single shear plane, e.g. shears adjacent to dyke K134 (Figure 3.19), are also interpreted as having initiated in shear.

The presence of extensive shear fracturing in the host rock is significant in that it could be giving indication as to the magnitude of the compressive stress parallel the dykes. That is, the dyke-parallel stress was large enough to prevent the exclusive formation of tensile fractures as the dyke propagated. The low dihedral angle of conjugate sets (even those where the fracture cleavage is not controlling the shear orientation) implies that the shears are of hybrid mixed-mode I-II type (Davis & Reynolds 1996 p. 232) (see Figure 2.18). If the stresses that acted in the plane of the dyke, i.e. orthogonal to the direction of tensile stress at the dyke tip, were equal in all directions at the time of intrusion, then conjugate sets of shears could have formed in all such orientations where the acute angle bisecting lines are contained in the plane of the dyke. This is not the case in Figure 3.20, which shows that most bisecting lines are sub-horizontal. (It is noted, however, that the platform nature of the exposure would have biased data collection if conjugate sets exist whose bisecting lines are vertical. These shears would appear parallel to the dykes with the shear direction sub-vertical into the outcrop, i.e.

undetectable.) Therefore, it follows that the compressive stress in the horizontal plane appears to have been greater than the lithostatic load in the vertical plane at the time of intrusion. The compressive stress required to induce hybrid shear fracturing is between three and five times the tensile strength of the rock (Davis & Reynolds 1996 p. 230), which in the case of limestone (of estimated tensile strength 6.9 MPa based on Jaeger & Cook (1979 p. 190)) would be between 20.7 MPa and 34.5 MPa. The lithostatic load at the time of dyke emplacement is calculated to have been in the order of 21.5 MPa, given a density for limestone of 2150 kgm^{-3} (Turcotte & Schubert 2002) and an overburden of 1 km (see Chapter 5). This itself is within the range of compressive stress required to initiate mixed-mode shear fracturing, as described. However, this lithostatic load equates to a horizontal compressive stress, or confining pressure, of only 6.2 MPa using the equation,

$$\sigma_h = \left(\frac{\nu}{1-\nu}\right)\sigma_v$$

where σ_h is the horizontal confining pressure and σ_v is the vertically acting lithostatic load. Therefore, to increase this value to that required to produce shear failure in the host rock, and to be greater than the lithostatic load (as implied by the conjugate bisecting line orientations), a differential stress in the order of 15 MPa is invoked to have existed at the time of dyke intrusion.

3.5 Integrating all dyke-associated deformation in the host rock

3.5.1 Comparing the extent of shear fracturing with that of all dyke-associated deformation in the host rock

Figure 3.26 compares the extent of dyke-associated fracturing (defined in Section 3.3) with the extent of shear structures (defined in Section 3.4) for dykes where information about both exists. For all the dykes shown, the extent of the dyke-associated fracture zone, i.e. all dyke sub-parallel fractures associated with dyke emplacement remote from segmentation zones, is greater than the extent of the shear structures away from the dykes. For some dykes, e.g. K117, K155b and K178, the difference between the two extents is large.

For dyke K117, it is possible in the field to identify two types of fractures in the dyke-associated fracture zone (Figure 3.27). 'Type 1' fractures are mostly extensional, discontinuous over a few millimetres to centimetres, mineralised, and often stand in positive relief from the platform. The group incorporates the fracture cleavage, as described in Section 3.4.2.1 previously, and any shear structures encountered. 'Type 2' fractures are more pervasive, being typically several metres long and they also increase in frequency towards the dyke margin. They are easily distinguished from the type 1 fractures.

The type 2 fractures extend much further from the dyke into the host rock compared with the type 1 fractures, and extend the whole width of the dyke-associated fracture zone, running distally into the background fracture frequency. The extent of the type 1 fractures in the margin of dyke K117 roughly coincides with the extent of the shear structures (Figure 3.27).

Given the evidence presented in Section 3.4 that the shear structures (and fracture cleavage) in the host rock were at least in part formed by hydraulic fracture as the dyke propagated, it is possible then that the mapped extent of shear structures is also the extent of hydraulic fracturing for dyke K117. So, given the coincidence of the extents of shear fracturing and type 1 fractures, the extent of the latter might also be considered as delineating the width of host rock deformation by hydraulic fracture. This would leave the possibility that type 2 fractures, in the distal portions of the dyke-associated fracture zone of dyke K117, formed by some other means.

The point has been made in Section 3.3, that the linear relationship seen between dyke width and the width of the dyke-associated fracture zone in the host rock, is difficult to reconcile if the dyke-associated fracture zone is considered to have formed exclusively by hydraulic fracture as the dyke tip propagated (see Section 3.3.4). Thus, it seems plausible that dyke-parallel fractures in the host rock formed by some other means. The fact that, in Figure 3.26, dyke-associated fracturing consistently extends further into the host rock than fracturing that can at least in part be attributed to hydraulic fracture is also in support of this.

3.5.2 Thermal stress as a possible cause of dyke-parallel fractures in the host rock

The dyke-associated fracture frequency profiles bear similarity to the theoretical thermal profile away from a cooling sheet intrusion (Delaney 1987; Joesten & Van Horn 1999; Turcotte & Schubert 2002 p. 166), as well as adopting an apparent power law form (as described in Section 3.3.3 above). It has been shown that wide dykes produce the widest fracture zones in the host rock (Figure 3.7). Wide dykes obviously input more heat into the host rock compared to narrow dykes. This is evidenced by dykes K117 and K127, having wide baked margins (see Figure 3.19 for dyke K117) where the limestone host rock has been completely recrystallised.

Below, the idea is put forward that the thermal input into the host rock by a cooling dyke might be related to the extent of host rock fracturing. It has been suggested that thermal stresses might play a part in fracture of the host rock (Delaney & Pollard 1981; Delaney 1986), although Delaney *et al.* (1986) conclude that the *extent* of fracturing cannot be explained by just heating the host rock.

Several dykes that show a range in width are modelled for their cooling to ascertain the extent to which the host rock was heated away from the dyke margins.

3.5.2.1 Heat flow modelling - methods

The *Schmidt Plot*, a computer simulation of a numerical model of one-dimensional conductive heat flow (Schmidt 1924; Carslaw & Jaeger 1959), predicts temperature change through time in the host rock adjacent to cooling dykes of differing widths. The Schmidt Plot was originally created in Microsoft QBasic by David Doff of the Department of Geology, Trinity College, but was subsequently rewritten in VBA (Visual Basic for Applications) within Microsoft Excel by Michael Cunningham for McCaughan (2002)). The author has subsequently modified the program to fix bugs and to increase functionality. The code is given in Appendix 16. Running the program in Excel allows the data to be output to a spreadsheet and plotted directly.

The Schmidt Plot is a very simple model. It assumes heat loss in just one direction orthogonal to the plane of the intrusion, by conduction only. Thermal properties are assumed to be the same for both dyke and host rock, and to be independent of temperature. Also, latent heat of crystallisation is ignored. These are all reasonable assumptions to make when looking at heat loss from relatively narrow dykes in the Earth's upper crust (Delaney & Pollard 1982; Delaney 1987). However, it is acknowledged that latent heat of crystallisation may have delayed cooling of the widest dykes (K127, DK17a and WC33a) in this study (Delaney 1987). It is also noted that cooling of the dykes by fluid convection in the host rock might have taken place, especially given the mineralisation described in the previous sections for dykes in limestone host rock.

Dykes chosen to be modelled were those lying close to the trend-line that describes the relationship shown in Figure 3.7 between dyke width and width of the dyke-associated fracture zones. The modelling was carried out for dykes only in limestone host rock, to try and maintain consistency in the thermal properties. The objective was to compare, for a range of dyke widths, the form of the fracture frequency profile with the form of the modelled thermal profile of maximum temperature attained by the host rock, and also the width of the dyke-associated fracture zone with the extent of the thermal effect felt by the host rock due to cooling of the dyke. Dykes K114, K117, K127, K178 and DK17a were modelled. For each dyke, the two values of dyke-associated fracture zone width (either side of the dyke) were averaged to create one value per intrusion. The exception is dyke DK17a (the Blind Rock dyke), which yielded only one profile from the only accessible side of the intrusion.

The Schmidt Plot model requires the input of a set of physical parameters before the model is run (see the screen-shot in Appendix 16). These are discussed below.

Thermal diffusivity, κ, controls the rate of heat dissipation through the rock and is related to the thermal conductivity, k, the density, ρ, and the heat capacity, C, of the material by $\kappa = k/\rho C$. Since the Schmidt Plot model assumes the same thermal properties for both the dyke and its host rock, an averaged value for κ was used between that of basalt and limestone. An averaged value of 8.32×10^{-7} m^2s^{-1} was used, based on average values of 5.34×10^{-7} for basalt and 11.30×10^{-7} for limestone. These values are from Schön (1996).

A *magma temperature* of 1200°C was used based on Delaney & Pollard (1982) for basalts emplaced at high crustal levels.

An ambient *host rock temperature* of 60°C was used. This value was chosen as a maximum temperature for the early Tertiary when the dykes intruded, based on fission track analysis and (U-Th)/He dating results described in Chapter 5. In reality though, the maximum ambient temperature was probably lower at around 40°C (see Chapter 5).

Magma flow is the duration of time over which magma is allowed to flow in the dyke. This would be only a few hours for narrow dykes, but obviously longer for the wider intrusions (Delaney & Pollard 1981, 1982). Varying the magma flow duration does not actually affect the output for the dykes being modelled here; this is a result of the way the program was designed. The program effectively assumes emplacement of a tabular, stagnant magma body, which immediately begins to

cool.

The dyke width is entered as the *half-width* since the model output is a thermal history for one side of the dyke.

The *run time* is the time over which the model is set to run. This value needs to be large enough to allow the dyke to cool and the host rock to dissipate heat. The *number of time increments* controls the resolution of the output in time.

The parameters, *number of distance increments within dyke* and *number of distance increments in profile*, are linked to the dyke width to control the *profile length from dyke centre.* Control can therefore be had over the profile length. (This flexibility has been built into the program by the author.)

Modelling multiple intrusions

Generally, the wide dykes studied (dykes DK17a (the Blind Rock dyke), WC33a, K117 and K127) are multiple intrusions (Preston 1967a; Mohr 1987; Joesten & Van Horn 1999), and therefore accommodated magma flow for relatively long periods of time (e.g. see Figure 3.26 for dykes K117 and K178). These dykes show internal margins delineating successive intrusion phases.

The Schmidt Plot model, for the dykes being modelled here, effectively assumes that the magma did not flow for any period of time (as described above). Although this keeps the model simple, it does not take into account the longer flow duration for wider, and possibly multiple, dykes. Relatively long magma flow durations in wider dykes of a single intrusion phase, or wide sections that represent a single intrusion phase in a multiple dyke, means that the host rock will have been held at the maximum contact temperature (roughly equal to half of the sum of the magma and host rock temperatures (Carslaw & Jaeger 1959)) for longer relative to narrow intrusions.

For the purposes of this modelling, the lack of control over the flow duration was not deemed to be important when considering the low thermal conductivity of rock and the much smaller timescale for magma flow compared with that for the cooling of the intrusion. Indeed Joesten & Van Horn (1999), when comparing contact metamorphic mineral grades as maximum temperature indicators for dykes K117 and K127 with independently modelled thermal profiles, found similarity between the two without the need to invoke a period of magma flow.

A multiple intrusion will also have had a more complicated cooling history than a narrow 'flash-injection' dyke, with successive magma surges likely perturbing the thermal profile in the host rock, depending on the time interval between surges. This is, again, beyond the resolution of the model. So, for the wider dykes here, the modelling simply assumes instantaneous emplacement of the full intrusion width.

3.5.2.2 Heat flow modelling – results

The results of the thermal modelling are shown in Figure 3.28 (and are listed in Appendix 17). The similarity in form between the modelled profiles of maximum temperature attained by the host rock and the fracture frequency profiles is apparent (although it is noted that, given the evidence described

above, much of the fracturing, especially close to the dyke margin, is likely a result of hydraulic forces as the dyke intruded). The thermal profiles are cut distally from the dykes at the point where the maximum temperature attained by the host rock becomes less than 150°C. This cutoff point happens to coincide reasonably well for each dyke with the extent of the dyke-associated fracture zone, and is shown in the central plot. The trend of increasing fracture zone extent with dyke width is roughly parallel and coincident with the line showing a maximum attained host rock temperature of 150°C. This corresponds to a temperature differential of 90°C above the ambient temperature of 60°C as defined.

It seems possible therefore, from the results described, that thermal effects could be responsible for the variation, with dyke width, of the maximum extents of the dyke-associated fracture zones. If this is indeed what Figure 3.28 is indicating, then the controlling factor might be a maximum attained temperature above ambient, during cooling of the dyke.

3.5.2.3 Discussion of mechanisms for fracture formation in the host rock by thermal means

The heating and cooling of rock induces thermal stress causing it to expand and contract respectively. In confined rock, only a small increase (or decrease) in temperature is required to induce a large stress in the order of kilo or mega Pascal (Turcotte & Schubert 2002 p. 172). Wide dykes will cause more protracted and laterally extensive heating, and then cooling, of the host rock compared to narrow dykes. Therefore, the associated thermal stresses will also reach further into the host rock. In addition, a wide dyke will itself undergo a relatively large contractional strain, as its heat is lost to the host rock. It therefore seems intuitive that thermal stresses in the cooling dyke and host rock system are capable of inducing fracturing in the host rock and possibly even controlling the lateral extent of this deformation.

In the discussion below, it is assumed that, apart from lithostatic stress, during cooling of the dyke thermal stresses were the dominant forces acting within the dyke and host rock.

A temperature drop in the order of around 100°C is all that is required to prevent further magma flow within a dyke (Delaney & Pollard 1982). So, very quickly after emplacement the dyke acts as a solid unit, cooling from around 1000°C. Figure 3.29 shows this (modelled) cooling through time. As the dyke cools, the host rock heats up, making it want to expand. The drop in temperature of the dyke will be accompanied by a reduction in its width, a result of thermal contraction. When this occurs, this will effectively be seen by the host rock as a lack of confinement along the dyke margin, and should allow the release of horizontal elastic energy from the host rock, i.e. the host rock will expand into the space created by contraction of the dyke. The elastic energy released will be a combination of lithostatic stress and thermal stress. If the expansion overcomes the strength of the host rock, then fractures might form parallel to the dyke. A process similar to this might be what Delaney & Pollard (1981) mean when they speculate that fractures might form in the host rock due to "cooling and contraction of the dyke".

Whilst it is simple to think of the host rock expanding in this way, it is acknowledged that the host rock experiences a much more complicated thermal history than the dyke as the intrusion cools. All

portions of the dyke are cooling, and therefore contracting, after emplacement. This produces tensile fractures in the dyke. However, as the dyke cools, heating *and* cooling (and therefore expansion and contraction) of the host rock will be taking place at different times and at different distances from the dyke. This is shown in Figure 3.29. For example, for dyke K117 in the time interval between 2 and 4 years after emplacement, at distances greater than 9 m from the dyke margin the host rock is being heated, and at closer distances to the dyke the host rock is cooling (Figure 3.29). This presents a second way in which fractures might form in the host rock, i.e. from contractional forces during cooling, analogous to cooling joints in the dyke.

To some degree, the forces from simultaneous expansion and contraction of the host rock, as the dyke cools, will balance; however, before the system has completely cooled back to ambient, the net thermal effect in the host rock will always be one of expansion.

In summary, mechanisms that might create tensile stresses enough to fracture the host rock are:

Unconfined thermal expansion of the host rock into space derived from contraction of the dyke. This is combined with a release in stored elastic energy from the lithostatic load in the same direction, i.e. orthogonal to the dyke.

Thermal contraction in a direction orthogonal to the dyke, analogous to cooling joints in a dyke.

3.6 Conclusions

This chapter provides insight into the emplacement of en échelon dykes and the mechanisms of host rock deformation.

Emplacement of the Killala swarm dykes caused deformation of the host rock, manifest mainly as dyke-parallel fractures. The extent of this deformation appears to be dependent on dyke width. Structures close to the dyke can be related to hydraulic fracture that took place as the dykes were emplaced. Fractures distal from the dyke may have formed by some other means. It is suggested here that thermal stresses caused fracturing of the host rock and controlled the extent to which fracturing took place in the host rock away from the dykes.

Hydraulic fracturing can, broadly speaking, be split into two types: fracturing associated with dyke segment overlap, and fracturing remote from overlap zones.

Deformation of the host rock in the vicinity of dyke segmentation is controlled by mode II shear that is induced as segments overlap, and then also by the stresses induced as the host rock bridge rotates during segment dilation. Left-stepping segmentations are characterised by sinistral shear and right-stepping segmentations are characterised by dextral shear. The sense of shear induced is in agreement with accepted theoretical models of stress trajectories in the vicinity of overlapping fractures, i.e. the development of a mixed-mode I-II stress intensity. However, when dyke segments stop propagating in overlap, stresses caused by rotation of the host rock bridge and the dilation differential as segments taper take over from the earlier stress regime related to segment overlap. The host rock bridge appears to respond by flexural slip. Features such as blunt ends to segments are accommodated by transforms at high angle to segment strike.

The same structures associated with dyke segmentation occur over a range of scales, from centimetre-scale to tens of metres. Detailed mapping of the orientation of these structures can help define the three-dimensional geometry of en échelon segmentation, with just a horizontal cut through the dyke in wave-cut platform. Given this, it is suggested that propagation of the Killala swarm was, at least in part, oblique through the crust, i.e. not purely either upwards or in a horizontal direction.

Hydraulic fracturing *remote* from segment overlap, but still close to the dyke, is manifest as a combination of coevally forming tensile fractures parallel to the dyke, and shear fractures that subtend small angles to the dyke. Conjugate relations between the shears, with acute angle bisecting lines lying in the plane of the dyke, are consistent with their formation as the dyke propagated. The very low dihedral angles suggest that the shears are mixed-mode I-II hybrid structures, thus implying that the differential stress in the plane of the dyke at the time of intrusion in the early Tertiary was sufficiently great to prevent the exclusive formation of tensile fractures. The orientation of the conjugate bisecting lines appears to suggest that the horizontal differential stress in the plane of the dyke was greater than the lithostatic load. A deviatoric stress may have existed parallel to the dykes at the time of intrusion.

The identification, in some cases, of shear structures that post-date at least the early stages of dyke emplacement, indicates that stresses were protracted over and beyond the time for emplacement and solidification.

It cannot be proved that fractures in the distal portions of the dyke-associated fracture zones formed by hydraulic means. The indication from the dykes studied that the extent of dyke-associated fracturing in the host rock is dependent on dyke width, suggests that fractures, at least distally from the dyke, formed by a different mechanism. Given that wide dykes input a greater amount of thermal energy into the host rock, it is suggested that thermal stress is an additional cause of fracturing adjacent to dykes and might control the *extent* to which fracturing takes place away from dykes. Evidence suggests that the thermal regime in the host rock induced both extensional and compressional stresses, seen in compression and relaxation structures. It is envisaged that fractures might form close to the dyke margin as the host rock expands into space created by contraction of the dyke as it cools. In addition, fractures could form due to thermal contraction of the host rock. Indeed, from thermal modelling, an increase in temperature of the host rock in the order of 90°C above ambient is identified as being possibly the threshold temperature, above which the host rock must be cooled from, for fractures to form in the distal portions of the dyke-associated fracture zone.

In summary, it is concluded that host rock deformation associated with dyke intrusion is complicated! Detailed mapping and understanding the origin of different structures gives insight into dyke emplacement and geometry. Attributing fracture of the host rock solely to hydraulic means as a dyke intrudes is probably not correct. Whilst hydraulic fractures are the first fractures to form in the host rock, as the dyke dilates and then cools thermal stresses probably dominate, and might be sufficiently great to cause further fracturing and even control the extent to which dyke-associated deformation is seen in the host rock.

Chapter 4 *The stress regime in northwest Ireland after dyke emplacement*

4.1 Introduction

The history of Tertiary deformation in northwest Ireland is not well understood. In the Atlantic basins offshore to the west of Ireland, Tertiary sediments are faulted and folded, allowing post-depositional stress regimes to be defined for the Tertiary (e.g. Boldreel & Anderson 1998; Doré *et al.* 1999; Solla Hach 2002). Onshore however, Tertiary rocks in northwest Ireland are exclusively igneous intrusive, belonging to the North Atlantic Igneous Province. Elucidating the Tertiary stress regime in this part of Ireland is therefore difficult. It has previously been attempted by geomorphological studies, the use of river profiles relating to mapped faults, and comparisons with offshore stress systems (Dewey 2000; Solla Hach 2002).

This chapter aims to derive the Tertiary stress regime from the mapping of structures that affect the early Tertiary dykes of northwest Ireland. Such studies have been carried out in northeast Ireland and the Faeroes on the extensive lava flows (Geoffroy *et al.* 1994, 1996). In northwest Ireland, however, there are no lavas providing large areas over which structures can be mapped, so igneous chronologies do not exist. Consequently, it is difficult to find structures that affect Tertiary intrusions. There are a few alleged examples (Mohr 1982; Mohr *et al.* 1984; Dewey 2000; Mohr 2000), where displacement is usually inferred from an 'offset' of the intrusion across the structure. In no case, however, is a fault seen to have physically displaced an intrusion in outcrop. It has been shown in Chapter 2 and Chapter 3 that offsets/steps and en échelon segmentation of dykes is commonplace across the region and relates to emplacement. Therefore, when a potential post-intrusion fault offset is found, the possibility that the offset is an intrusional jog has to be eliminated.

This chapter has four main sections. The first section (4.2) gives an overview of previous work on Tertiary stress regimes that affected Ireland and surrounding areas. The second section (4.3) describes examples of dykes that have previously been mapped as faulted, but where the offset in each case can actually be shown to be a syn-emplacement transform that facilitated intrusion. The third section (4.4) describes examples of offset dykes where ambiguity still remains as to whether faulting of the intrusion has actually taken place. The fourth section (4.5) of the chapter describes examples where dykes are unambiguously faulted. These examples allow palaeostress analysis to be carried out, and the resulting stress trajectories are compared with those defined by previous work onshore and offshore Ireland.

4.2 The Tertiary stress regime of Ireland and surrounding areas

A variety of tectonic processes acted during the Tertiary across the northeast Atlantic region. Ireland was just a small part of the overall picture and may have been subjected to crustal stresses that were

not necessarily regional in extent. The description below reflects this.

Tectonic stresses can be considered in two contexts: firstly, tectonics associated with early Tertiary magmatism and the opening of the northeast Atlantic; secondly, post-magmatism tectonics, i.e. acting during the majority of the Tertiary.

Refer to Figure 4.1 for the review below.

4.2.1 Tectonics associated with the North Atlantic Igneous Province

Ireland and its surrounding area underwent uplift around the time of the Cretaceous-Tertiary boundary. Regional doming due to the Iceland plume is the favoured explanation for this uplift (e.g. White 1988; Nadin *et al.* 1997; White & Lovell 1997; Clift *et al.* 1998). For example, northeast Ireland was uplifted subaerially to expose the latest Cretaceous chalk and cause its karstification, before extrusion of the Palaeocene basalts. The Tertiary igneous rocks of Ireland, therefore, can give some insight into the tectonics and crustal stresses that affected Ireland at the start of the Tertiary.

Geoffroy *et al.* (1996) analysed brittle tectonism of the Antrim basalts and the igneous complexes of Mourne, Carlingford and Slieve Gullion in northeast Ireland (Figure 4.1, time period 1). They found that, during the Palaeocene, syn-magmatic NE-SW to ENE-WSW extension operated in alternating extensional (dominant) and strike-slip (subordinate) stress regimes. There is also evidence for a compressional stress regime playing a minor role. These results are in partial agreement with the results of Kerr (1987), who showed that ENE-WSW extension, in an extensional regime, existed during the Palaeocene. Such fluctuation between extensional, strike-slip and compressional stress regimes is not believed, however, to be regionally significant in terms of evolving tectonics (Geoffroy *et al.* 1996). From a similar study in the Faeroes, Geoffroy *et al.* (1994) suggested that NE-SW extension resulted exclusively from a strike-slip stress regime.

This orientation of extension is in agreement with the NW-SE to NNW-SSE orientated Palaeocene dykes of the British Tertiary Igneous Province as a whole, and has been described in Chapter 2 for dykes of the Donegal-Kingscourt swarm in northwest Ireland.

4.2.2 Post-magmatism tectonics

By late Palaeocene to late Eocene times magmatism had all but ceased onshore Ireland. In northeast Ireland Geoffroy *et al.* (1996) found evidence for NNE-SSW to NE-SW directed compression at about this time (Figure 4.1, time period 2). It acted predominantly in a strike-slip regime, but also showed fluctuation with a subordinate compressional stress regime. Geoffroy *et al.* (1994) found evidence for the same stress regime in the Faeroes. The cause may have been northeast-directed Labrador Sea ridge-push forces immediately prior to break-up of the northeast Atlantic. Also, there may have been a contribution of compression from subduction north of Iberia during the Pyrenean orogeny (Geoffroy *et al.* 1994, 1996). Kerr (1987) describes the same NNE-SSW compression, but dates it as mid-Miocene relating to Alpine compression during Helvetic thrusting.

After break-up, which occurred at the start of the Eocene around 55 Ma, NW-SE extension along

the plate margin ceased and ridge-push forces began to act (Doré *et al.* 1999) (Figure 4.1, time period 3). Inversion structures along the Atlantic margin and into the Bay of Biscay formed during the Eocene through to the Miocene and, depending on their location and orientation, have been attributed to plate reorganisation in the Atlantic (Doré & Lundin 1996; Boldreel & Anderson 1998; Doré *et al.* 1999) and/or the Pyrenean orogeny that was taking place to the south (Masson & Parson 1983; Roberts 1989). In the English Channel Eocene inversion took place, but this was probably related to Alpine compressional forces (Plint 1982).

Dewey (2000) states that Ireland was under NW-SE compression during the Tertiary after the break-up of the northeast Atlantic, a result of ridge-push from the north and Alpine forces from the south.

According to Geoffroy *et al.* (1996), an extensional stress regime of WNW-ESE to NW-SE directed extension, which clearly post-dates the previous strike-slip regime (NE-SW compression), existed in northeast Ireland during the Oligocene and continued for some time after (Figure 4.1, time period 4). Geoffroy *et al.* (1996) note correspondence in time with syn-depositional fault activity along reactivated NE-SW structures (e.g. the Caledonian Tow Valley fault controlling the Ballymoney deposits) and NNW-SSE structures, and graben subsidence in the Lough Neagh Basin (Griffith *et al.* 1987), known to contain Oligocene sediments (Wilkinson *et al.* 1980). Geoffroy *et al.* (1996) attribute this extension to opening of the northeast Atlantic. Normal displacements of the basalts (700 feet) across the Tow Valley fault (Wilson & Robbie 1966), and displacements across a number of other NE-SW Caledonian faults in the BTIP (England 1988), coincide with this stress regime of WNW-ESE extension.

Parnell *et al.* (1989) suggest that the WNW-ESE extension produced sinistral transtensional pull-apart basins along the Tow Valley fault at Ballymoney, into which sediments were deposited. This direction of extension, however, seems wrongly orientated to produce such movement along a NE-SW fault! In addition, sinistral displacement also implies a strike-slip stress regime, rather than the extensional regime Geoffroy *et al.* (1996) invoke to have produced basin subsidence in the Lough Neagh region. Ziegler (1989) relates the subsidence of the Lough Neagh Basin and movement along the Tow Valley fault to sinistral wrench faulting caused by Alpine inversion during the Oligocene.

An exciting development is that new high resolution aeromagnetic data, acquired over Co. Fermanagh by the Geological Survey of Northern Ireland, shows dykes offset by ~2 km in a sinistral sense across the Tempo-Sixmilecross fault. This structure is possibly a continuation of the Tow Valley fault to the northeast. The displacement would seem, therefore, to be Oligocene in age. North-south compression is compatible with this displacement.

Offshore in the Norwegian area of the northeast Atlantic, a NW-SE extension phase that was active in the Oligocene and Miocene has also been identified. A second phase of plate reorganisation is thought to have caused this (Doré *et al.* 1999).

During the Eocene and Oligocene, a number of faults are documented to have been active in the Irish Sea region. The NW-SE Lustleigh-Sticklepath fault, possibly after an initial sinistral reactivation (Holloway & Chadwick 1986), moved in a dextral sense, forming pull-apart basins along

its length (e.g. the Bovey Tracy Basin) containing Eocene to Oligocene lacustrine sediments similar to that of Lough Neagh (Dearman 1963; Bristow & Hughes 1971; Holloway & Chadwick 1986) (Figure 4.1, time period 4). Dextral reactivation is compatible with the recognised WNW-ESE extension. Other parallel faults also moved in a dextral sense on the Cornish peninsula, and NE-SW structures accommodated sinistral displacement in conjugate fashion (Dearman 1963). Similarly, in Ireland the NW-SE Newry fault offsets both the Slieve Gullion and Carlingford igneous centres in a dextral sense, the timing of displacement being inferred from the activity along the Lustleigh-Sticklepath fault described above. In addition, it is thought that the St. George's and Bala faults were reactivated in a sinistral sense in the Eocene (Turner 1997), and Bevins *et al.* (1996) describe two 1.5 km sinistral offsets of Palaeogene dykes across the NE-SW Menai Straits fault zone. In compatibility with the faulting, inversion structures in the Bristol Channel and the Celtic Sea are also believed to be Oligocene in age (Roberts 1989).

The strike-slip faulting and inversion structures described above for the Irish Sea region are generally believed to have resulted from roughly N-S compression that occurred throughout the Alpine Foreland during the late Palaeogene to early Neogene (e.g. Ziegler 1989; Turner 1997).

In Ireland, Oligocene deformation is the youngest that has been identified with any certainty from the Tertiary rock record (Parnell *et al.* 1989; Geoffroy *et al.* 1996). Other attempts to elucidate Tertiary stresses have come from geomorphological studies and structural mapping of pre-Tertiary rocks.

In southeast Ireland, Cunningham *et al.* (2004) use geomorphology and structural mapping within the Caledonian Leinster granite to derive NW-SE directed compression that swung to NNW-SSE compression in a strike-slip stress regime around Oligocene times. The swing to the latter orientation is believed to have facilitated dextral reactivation of the Codling fault, the along-strike equivalent of the Newry fault (Jenner 1981), as well as causing sinistral reactivation of NE-SW faults (Figure 4.1, time period 4).

Cunningham *et al.* (2004) suggest that these stresses could have produced the Lough Neagh and associated basins in northeast Ireland, and attributes the compression to ridge-push forces. However, the invoked NE-SW to ENE-WSW directed extension, is orientated differently from the Oligocene WNW-ESE extension that Geoffroy *et al.* (1996) and Parnell *et al.* (1989) suggest formed the Lough Neagh Basin. Also, as described previously, Geoffroy *et al.* (1996) infer the stress regime at the time in northeast Ireland as being extensional, not strike-slip.

During the Neogene, uplift and erosion was widespread across the northeast Atlantic margin (Japsen & Chalmers 2000). Analysis of a profile of apatite fission track data across the Leinster granite batholith indicates possible Neogene vertical displacements along NW-SE faults (Cunningham *et al.* 2003). In addition, Cunningham *et al.* (2004) invoke Neogene block faulting as possibly controlling the N-S plateau arrangement of the east side of the Leinster granite batholith.

It is not known if tectonics played a dominant role in widespread Neogene uplift, but the amount of shortening of just 1 to 2% from ridge-push related inversion structures active into the Neogene suggests that it did not (Doré *et al.* 1999). In southern Britain, however, Alpine compression appears

to have made a contribution to uplift (e.g. Jones 1999a). Mantle dynamics may have played a part in Scandinavia (Rohrman *et al.* 2002), and the widespread glaciation of the Pleistocene was certainly responsible for a large amount of rock removal (Japsen & Bidstrup 1999; Lidmar-Bergström *et al.* 2000).

In other areas of Ireland, fault activity is suggested to have occurred during the Tertiary. In western Ireland, using a reconstructed sub-Carboniferous surface, Tertiary normal displacements in the order of hundreds of metres have been postulated on a few faults, e.g. the E-W Clew Bay fault (Dewey & McKerrow 1963; Dewey 2000; Badley 2001). Similarly, the sea cliffs of Achill Island may have resulted from Tertiary reactivation of the Achill Head fault (Dewey 2000). This faulting, originally interpreted as Miocene or Pliocene in age (Dewey & McKerrow 1963), is currently interpreted by Dewey (2000) as having occurred in the late Eocene to early Oligocene, a result of rift-shoulder uplift. Conversely, Worthington *et al.* (2003) somewhat discredits the model of Dewey & McKerrow (1963) by presenting strong evidence to suggest that the sub-Carboniferous surface was faulted at the end of the Carboniferous.

Mohr (1982) proposes a normal offset of ~100 m of a Tertiary dyke across a splay of the Killary Harbour fault based on a change in dyke width across the fault. Mohr *et al.* (1984) originally attributed NW-SE faulting of the Droimchogaidh sill to adjustments coeval with movement along the Errif fault, as described by Dewey & McKerrow (1963). Subsequently though, Mohr (2000) has attributed faulting of the sill to syn-intrusion crustal adjustments resulting from the shallow level of intrusion.

In northwest Ireland, Solla Hach (2002) has identified faults that possibly were active during the Tertiary by observing bedrock and elevation discordance and the presence of drainage anomalies such as river knick-points. Most of the faults, e.g. the Bangor fault, trend NE-SW following the regional Caledonian trend, and have postulated normal reactivated displacements. The exact timing of fault movement within the Tertiary is unknown. For example, Solla Hach (2002) identifies a possible normal displacement on the northwest-bounding fault of the Ox mountains. In addition, the Tertiary Garrison sill is mapped as being cut by several NW-SE faults.

In the Irish midlands, using evidence from gravity and depth to bedrock, Pasquali (2002) suggests that NE-SW fault reactivation may have controlled Tertiary river channels. In addition, Dewey (2000) invokes movement along unspecified faults, downthrowing to the north, to explain the mainly southerly dip of the Carboniferous succession in the midlands.

In the south of Ireland, Taylor (2002) describes various drainage anomalies of the type that have been attributed to Tertiary faulting by Solla Hach (2002) and Dewey & McKerrow (1963), but concludes that landforms in the south of Ireland are a result of drainage superimposition, differential erosion and the strike of the Variscan crustal grain, rather than being caused by Tertiary faulting.

There is, therefore, evidence to suggest that Ireland was subjected to active tectonic stresses during at least part of the Tertiary. However, it appears that the existing models are somewhat in conflict with each other over the details and causes of the observed, or inferred, deformation. The following sections include examples from northwest Ireland of Tertiary dykes that show evidence of post-

emplacement strain. Firstly though, examples are described showing how dykes can exploit pre-existing tectonic structures, leading to the wrong interpretation that they have been faulted.

4.3 Examples of segmented dykes that exploit existing faults to facilitate transform offsets

4.3.1 The Rosses, northwest Co. Donegal

This dyke (dyke DK33, Figure 2.23, Appendix 8) is part of the Donegal-Kingscourt swarm, and is a WNW-ESE, ~6 m wide, dyke that intrudes the Caledonian Rosses granite (Figure 4.2).

It has been established in Chapter 2 that joints in the granite controlled the range of dyke orientations in the area. This particular dyke is offset by 22 m to the right across a fault (Figure 4.3), and was interpreted when first mapped (Appendix 2) as being displaced by the fault.

Examination of Figure 4.3 shows how the northerly segment (segment 1) abuts very abruptly against the fault. The cooling joints, however, by swinging to align perpendicular to the fault, indicate that the magma cooled against the fault plane and the dyke at no stage continued un-deflected across the fault.

At the blunt terminal end of segment 1 a cooling joint face contains groove marks that pitch 11° to the southeast. Similar structures are described by Rickwood (1990), and probably indicate slip between cooled blocks of dyke. In this case, shallowly plunging shear stresses acted on the plane. Given the demonstrable cooling of the magma against the fault, these shear stresses were probably imparted by magma flow within the dyke interior against early cooled magma close to the margin of the dyke.

It appears, therefore, that the fault plane was a surface to which magma was accreted during intrusion.

In addition, along the blunt termination of segment 1 against the fault, a series of dyke injections into granite, on a centimetre scale, describe a sinistral tension gash array (Figure 4.3, photo inset). This indicates that sinistral shear acted on the end of segment 1 parallel to the fault.

Segment 2 swings in strike away from the overlap zone before beginning a strike-swing in towards the overlap zone, and in doing so injects a number of anastomosing horns into the granite that clearly propagate their own fractures. Similarly, there is a strike swing away from the overlap zone of segment 1 before it meets the fault.

Crack tips that approach each other and that are non-co-planar, i.e. offset, will bend away from the other immediately before overlap commences, then bend inwards as overlap occurs. This is due to a mixed-mode I-II stress intensity that develops. In the case of right-stepping fractures, as would be the case here, the mode II stress component is firstly sinistral causing bending away of the cracks, followed by dextral causing bending inwards (e.g. Nicholson & Pollard 1985) (see Chapter 2).

Therefore, the dyke swings seen here are consistent with those expected when dyke segmentation occurs.

The horns associated with dyke segment 2 anastomose, and appear, therefore, to have propagated

their own fractures on intrusion. They are a remnant of the early stages of intrusion.

A dyke offshoot emanates from segment 1 and crosses the tidal zone, appearing to abut against the fault. The presence of this offshoot, and the accompanying closely spaced joints (presumed to have formed contemporaneously), is typical of the type of response shown by overlapping dyke segments (see Chapter 3). The offshoot is probably a response to dextral mixed-mode I-II stress, either being effectively a large tension gash, comparable to similar structures described in Chapter 3, or being simply the expected bending in of segment 2 into the overlap zone.

All the evidence described above points towards the fault being a structure that facilitated segmented intrusion by sinistral strike-slip transform movement along the fault. The fault was not dilated as it was unfavourably orientated compared with the mode I dilation vectors of the two dyke segments.

When intruding against a relatively freely slipping surface, a dyke will typically form a blunt segment end, as that seen by segment 1. The fracture toughness of the host rock is decreased, and as the surface slips freely the stress intensity factor reduces to zero and the dyke fails to propagate through the surface (Baer & Beyth 1990; Kattenhorn & Watkeys 1995).

Much of the evidence described above is in the tidal zone and is periodically covered with sand drifts. It is therefore understandable that the dyke was originally mapped as having been faulted.

4.3.2 Firkeel Bay, Beara Peninsula, Co. Cork

This locality is not in northwest Ireland, but is an excellent example of an intrusional transform offset across a pre-existing fault. The dyke is also described by Taylor (2002).

At grid reference 053116 040827 on the east side of Firkeel Bay on the Beara Peninsula (Figure 4.2), a Tertiary dyke intruding Devonian Old Red Sandstone, part of the Kerry systems (Morris 1974), is offset to the left across a fault (Figure 4.4).

Figure 4.4 shows a map of the dyke. The fault displays sinistral kinematics (independent of the dyke offset) across a 'fault zone' gully, and displays a fault gouge in cliff section. The sense of dyke offset, therefore, is in agreement with the fault kinematics. This led Pracht (1994) to interpret the dyke as being faulted in a sinistral sense after emplacement.

The overall form of the dyke, which consists of three segments, shows a left-stepping geometry. South of the fault, a left-step with preserved horns would have derived from the en échelon segmentation of what is now segment 3 (see Figure 2.3). Likewise, to the north of the fault, segment 1 (in the west) narrows as segment 2 widens, thus maintaining overall dyke width.

Segments two and three appear to have propagated in an en échelon left-stepping configuration, consistent with the rest of the dyke, and produced an apparent sinistral offset across the fault, with segment blunt ends, like that described in Section 4.3.1 above.

The orientation of the fault is sub-parallel to the opening direction of the two dyke segments. So, dilation of the fault, which, if otherwise seen, would allow the inference of a syn-emplacement transform jog, would not be expected to have occurred. This is indeed the case, except for a lens of

dyke rock that exists within the fault zone. Its shape suggests that it was either forcibly intruded into the fault zone, or may have intruded into a pull-apart created by transform slip along the fault. Its coherent concentric cooling joint structure shows that it has not been deformed post-cooling.

The slightly differing strike of segments 2 and 3 either side of the fault can most easily be explained by their genesis as separate segments. Also, the slight swinging of segment 3 into the fault (whilst maintaining its cooling joint structure), which widens the segment by ~0.5 m more than the width of segment 2, would seem to preclude physical linkage of segments 2 and 3 at any time in the past.

In addition, there are differences in vesiculation style between segments 2 and 3 across the fault. The former shows more distinct alternations between vesiculated and non-vesiculated dolerite. This implies that they were emplaced as two distinct segments.

The only evidence that acts against the theory of a transform offset is the fact that segment 2 shows no evidence from cooling joint orientation to suggest that it cooled against the fault surface. It is possible, however, that erosion to produce the gully removed the end of the segment.

Most of the evidence listed above, therefore, points towards the offset being a transform jog. However, there is extensive slickenside/slickenfibre development on the terminal face of segment 3 against the fault, where it is exposed in vertical section. This indicates that the blunt end of segment 3 underwent deformation at some stage.

On the lower two thirds of the face the dyke is nodular on a centimetre scale with many nodule faces showing evidence of slip. On individual faces slickensides often show a multitude of slip directions, and on some faces mineral fibre growths of varying orientation are superimposed implying discrete phases of slip in different directions. The upper third of the face resembles 'normal' dyke rock, with large blocks defined by cooling joints. Slip occurs on surfaces up to 1 m from the fault on the western face of the segment 3 outcrop, which exposes a section of the dyke 10 cm from the margin.

The majority of planes accommodating slip are orientated either roughly ENE-WSW or NNW-SSE, implying that slip has taken place along dyke-parallel and dyke-perpendicular cooling joints. The data may be biased, however, by the ENE-WSW and NNW-SSE orientations of the outcrop faces from which the data was taken. Slip-sense is generally not discernable from a total of sixty shears recorded (Taylor 2002).

The lack of consistency in kinematics and slip orientation of the deformation that affects the end of segment 3 would seem to preclude a simple post-emplacement displacement of the dyke as a cause of these structures. Given this and the majority of evidence, which points towards the offset being a transform step, the deformation that affects segment 3 is interpreted as having occurred during emplacement. The rapid drop in fracture toughness of the host rock at the fault could have caused the advancing tip of segment 3 to dilate rapidly along the fault wall (Baer & Beyth 1990), facilitating the rapid accretion of magma onto the fault wall. The continuing magma pressure, acting from behind, might then have deformed this early-accreted magma on the fault wall, at the blunt end of segment 3. In addition, if the fault plane contained water, its interaction with magma could have induced

volatility at the magma front causing chilling and *in situ* break-up of the chilled margin resulting in the visible deformation.

The example described here at Firkeel Bay is not quite as clear-cut as the dyke described above on The Rosses, but nevertheless provides strong evidence that intrusion was facilitated by transform movement on an existing fault, rather than the fault having displaced the dyke after emplacement.

4.4 Dykes where the cause of offset is uncertain

Two localities are described below where dykes are offset across faults, but the origin of the offset remains uncertain.

4.4.1 Corvock Granite, south Co. Mayo

System CI (Mohr 1982), the main intrusive system in the Tertiary West Connacht dyke systems, can be traced NE-SW in the order of 50 km from Aughrus Point in the southwest, to terminate as a series of sills east of Clew Bay in the northeast (Figure 2.5). South of Croagh Patrick, towards the northeastern end of the system, the dyke, around 12 m wide, dipping steeply northwest, cuts the Caledonian Corvock granite (dyke WC35, Figure 2.5, Appendix 3). The granite itself is intruded into the Ordovician Derrymore Formation (locally sandstone) (Figure 4.2 & Figure 4.5a). A NNW-SSE fault, one of many of this trend in the area, cuts the granite and its host rock, and is manifest as a topographic depression. This fault facilitates a left-stepping 320 m offset of the dyke at grid reference 087415 276555 on the northeasterly flank of Tangincartoor mountain (Stanton 1960) (Figure 4.5a).

There appears to be no strike swing or thinning of the dyke on approaching the fault from either side. No exposure exists along the fault plane, only on the flanks of the fault-controlled depression. Thus, it is not clear whether the offset is either a syn-emplacement transform offset, or whether it is due to post-emplacement reactivation of the fault. The strike of the dyke relative to that of the fault suggests that, if the offset is emplacement-derived, it is likely to be a transform offset, since the dilation vector is parallel to the fault. As the dyke is sub-vertical, any reactivation is likely to have been strike-slip (sinistral), since a very large dip-slip displacement would be required to give an apparent displacement of the magnitude seen.

Re-mapping of the fault using handheld GPS indicates that the fault dips west, apparent from the fault and topography intersection trace. Assuming a sloping granite contact surface that tapers upwards, the displacement on the fault appears to be, at least in part, normal dip-slip. The fault plane is calculated as dipping at approximately 30°.

On either side of the fault, in the granite and to a lesser extent in the Derrymore Formation, quartz mineralisation occurs as conjugate vein arrays (Figure 4.5b). They are clearly spatially associated with the fault. In some cases conjugate pairs show shear offsets of one shear in the pair. Other examples are seen where 'offsets' are not consistent with the expected sense of shear. Such examples are interpreted as pinnate conjugate fractures. Quartz growth is syntaxial, and therefore does not record any shear on the fractures. The question arises, therefore, as to the possibility that the

deformation is compatible with sinistral displacement of the dyke along the fault.

Stereographic projections shown in Figure 4.5a show axes of σ_1 (maximum compressive stress) and σ_3 (minimum compressive stress) (see Appendix 18 for all data). They are calculated as being bisectors of the acute and obtuse angles respectively between conjugate vein pairs. There is local variation along the fault but overall σ_3 is orientated sub-horizontal E-W whilst σ_1 ranges from being sub-horizontal to inclined, up to 72°, plunging, on average, north or south (Figure 4.5c). The derived σ_3 stress axes are orientated approximately in accordance with a normal displacement on the fault. However, the orientation σ_1 would be expected to have a higher plunge, nearer the vertical, for compatibility with normal displacement.

Neither are the derived stress axes compatible with a sinistral reactivation movement on the fault. If anything, the average N-S orientation of σ_1 (Figure 4.5c) would be expected to give dextral reactivation along the NNW-SSE fault.

In summary, it is difficult to reconcile the stress analysis for the veining with sinistral displacement of the dyke along the fault. The deformation is more likely to be associated with the genesis of the fault. Also, such extensive quartz veining seems unlikely to have occurred during the Tertiary, when the rocks may only have been at a depth of a few hundred metres (see Chapter 5). A Caledonian age for the deformation is much more likely.

The question as to the origin of the dyke offset cannot, therefore, be resolved with total confidence. A transform offset, however, seems the most likely answer. Indeed, Chapter 2 has shown that emplacement of this sector of system CI was controlled to a relatively high degree by the host rock structure. This is part depicted in the circuitous path that the dyke takes to the northeast of the fault (Figure 4.5a). In two places the dyke takes an angular bend that produces an offset almost as large as that seen at this locality.

4.4.2 Bloody Foreland east, northwest Co. Donegal

This dyke (dyke DK72, Figure 2.23, Appendix 8) (Figure 4.2) lies east of Bloody Foreland and is part of the Donegal-Kingscourt swarm. The dyke has an overall WNW-ESE trend and outcrops in the tidal zone (Figure 4.6). It was emplaced into the Upper Falcarragh Pelite Formation. The dyke shows two large left-stepping offsets of around 25 and 65 m. Weed and rubble cover obscures all outcrop in the vicinity of the eastern offset and most of that around the western offset.

Figure 4.6 shows that there is no thinning or obvious strike swing of dyke segments 1 and 2 approaching the eastern offset. Segment 3, however, swings inwards on approaching the western offset.

For both offsets, along strike of the lines that link the dyke segment ends, faults cut the host rock in the cliff section. They are fault 'zones' as opposed to discrete planes, and show ductile deformation containing sigmoidal clasts.

The left-stepping swing taken by segment 3 aligns the dyke parallel to a polished fault surface that is presumably part of the fault seen cutting the cliff section to the southwest. The dyke then appears to be truncated by the structure, with outcrop ending abruptly in alignment with the fault surface.

As discussed with the previous examples in this chapter, the coincidence of a dyke offset and a fault does not mean that displacement along the fault caused the offset. In this particular case, given that segment 3 swings in towards the fault, it would seem that the structure exerted some control during emplacement of the dyke. The corresponding swing in dyke-perpendicular and dyke-parallel cooling joints as the dyke swings makes it unclear in deducing whether or not magma has cooled against the fault where the dyke and fault appear to intersect. However, a bending of the dyke margins in opposite directions into the fault appears to widen the dyke against the fault. This is an indicator that the structure was controlling intrusion of the dyke.

Along the exposed steeply dipping end plane of segment 3, where it continues along strike of the fault surface, there are no kinematic indicators that would suggest the plane accommodated post-emplacement slip. However, digging at the northernmost end beneath the weed and rubble, the dyke is fragmented into blocks 2 to 4 cm across, with individual block faces having accommodated slip. Slickenfibres appear to pitch steeply (around 60 to 80°), mainly northeast, indicating a majority of dip-slip movement. The appearance of the slip surfaces and blocky nature of the dolerite resembles that seen at the Firkeel Bay dyke (see Section 4.3.2 above), where the structures are interpreted as resulting from syn-emplacement shear accommodated within the chilled dyke margin due to a continuing of magma flow behind, within the dyke.

If, however, the slickenfibres resulted from post-emplacement displacement of the dyke along the western fault, given a slip vector plunging 70°NE, then 58 m of normal dip-slip movement is required to give the observed apparent sinistral displacement. Using the same slip vector, 165 m of dip-slip movement is required for the eastern fault. Such magnitudes seem unlikely given the few, relatively small, Tertiary displacements mapped elsewhere (see later sections). In addition, faulting that occurred during the Tertiary would be expected to have been brittle in nature, not ductile as seen in the cliff section (although brittle reactivation of a previously ductile structure could have taken place).

In summary, it appears that the western offset, between segments 2 and 3, is most likely a syn-emplacement transform. Whilst it is impossible to comment independently on the eastern offset due to lack of exposure, by analogy it is also likely to be an emplacement feature.

4.5 Tertiary palaeostress of onshore Ireland: dykes displaced by post-emplacement faulting

Described below are dykes that have been unambiguously faulted. For each locality, description and analysis of the structures and kinematics is then followed by palaeostress analysis.

Analysis is carried out using the *Andersonian* model of fracturing (Anderson 1951) (Figure 4.7).

4.5.1 Downpatrick Head west, north Co. Mayo

Several E-W Tertiary dykes cut the west side of the Downpatrick Head peninsula, north Co. Mayo, intruding the Carboniferous Minnaun Sandstone Formation (see Chapter 2). One of the dykes (Figure 4.2) (dyke K85, Figure 2.9, Appendix 4) is cut by two strike-slip faults in apparent conjugate

arrangement. This is shown in Figure 4.8.

The dyke is faulted near the eastern (inland) end of its exposure (Figure 4.8a). Two shears, one sinistral and the other dextral, displace the dyke by 6.5 cm and 21 cm respectively. The shears are in conjugate arrangement. They are sub-vertical, having orientations 159/86SW and 024/86NW. They cross to the south of the dyke but are only traceable small distances to the north and south of the dyke in the host rock.

The strikes of the two faults appear to be refracted slightly by the dyke. Associated with the dextral fault, a splay envelops a zone in which sinistral flexural slip along cooling joints has facilitated clockwise rotation of blocks within the zone. The pitch of slickenfibres between blocks is shallow at 6°.

Palaeostress analysis

The faults are plotted on a stereographic projection in Figure 4.8b. (See Appendix 19 for all data.) The fault planes' orientations are the 'non-refracted' values, taken from the host rock. The method of deriving the principal stresses uses the geometry shown in Figure 4.7. The values obtained for the principal stress directions are:

σ_1 = 182/1; σ_3 = 092/4; (σ_2 = 272/86).

The dihedral angle is 45°. This is reasonably close to the oft-quoted 60°.

The orientation of the plane containing σ_1 and σ_3 is sub-horizontal, and almost contains the slip vector from the plane of flexural slip (Figure 4.8b). The slip vector from the plane of flexural slip, and the pole to the same plane, are close to being within the σ_1-σ_3 plane derived from the conjugate faults. This shows compatibility between all the structures within the one stress regime. The fact that, in reality, the slip vector and the pole lie just *outside* the σ_1-σ_3 plane is probably a result of the progressive rotation that took place during shear along the main dextral fault.

The bedding of the Carboniferous host rock bears the orientation 158/5SW. Such slight tilting is typical in the area and probably derives from Variscan deformation that is much more prevalent in the south of the country.

On the east side of Kilcummin Head, 10 km directly east, there is extensive folding and thrusting of the upper few metres of strata in cliff section, caused by northward-directed glacial drag. No such processes, however, are observed here. It is likely, therefore, that the area has undergone no tilting during the Tertiary, and no orientation corrections to the data are needed.

In summary, N-S compression in a strike-slip stress regime caused faulting of the dyke.

4.5.2 St John's Point peninsula, Co. Donegal

A dyke of roughly N-S trend and presumed Tertiary age (dyke DK18, Figure 2.23, Appendix 8) outcrops on the west side of St John's Point peninsula, Co. Donegal (Figure 4.2). It dips steeply east and is emplaced into the Carboniferous Ballyshannon Limestone Formation. The dyke outcrops twice

on the peninsula. In the north, the dyke is 1 m wide. To the south, it intersects the coast on the west side of the peninsula and is around 30 cm wide. It does not cut the east coast of the peninsula along its projected strike and must, therefore, have pinched out.

It is the southernmost outcrop that is the focus of this study. Here, a number of faults affect the dyke (Figure 4.9). Below, these structures are described, and palaeostress analysis is carried out. All structural data is listed in Appendix 20.

4.5.2.1 Description of structures

Based on apparent kinematic style, the faults are split into two groups, A and B. Figure 4.9a shows the dyke and its relationship with the structures. Figure 4.9b shows the structures plotted in stereographic projections.

Fault group A

Fault group A contains faults F1 and F2 and a number of associated structures. The kinematics can be deduced from stepping slickenfibres and dilational kinks on the fault planes, as well as observing the larger scale offsets affecting the dyke.

F1 is the only fault actually seen to displace the dyke, doing so by 1.5 m in the sub-horizontal plane of the host rock platform. There is sinistral displacement with a reverse component. The orientation of the slip vector (pitching 21°W on the slip plane) indicates that strike-slip movement is predominant over dip-slip. F2 is sub-parallel to F1, has almost identical kinematics, and is assumed to displace the dyke beneath the overburden.

Associated with F1 are shears that are pinnate to the fault (shears F1a, F1b and the F1c group), subtending angles of between 28° and 75° to the fault. They show both sinistral and dextral kinematics and contain slip fibres that pitch between 5° and 8° to the north, indicating a small component of dip-slip motion. Shears F1a and F1b are major, through-going, structures in comparison with the F1c group of shears. A small fold also occurs that appears to be a 'drag' structure associated with the F1 fault displacement.

F1 and F2 are projected to intersect beneath rubble to the west. A structure that continues west from here (marked by a down-step in the wave-cut platform) appears to align with F2, but cannot be followed along strike with much confidence. A dextral en échelon vein network in kinematic opposition to F1 and F2 (Figure 4.9, inset 1) appears to coincide with the structure. This vein is interpreted as an old structure, i.e. pre-Tertiary, due to its similarity in form to veins that cut Carboniferous limestone elsewhere in the region (see Chapter 2).

A joint profile measured away from the west dyke margin (Figure 4.9, inset 2) shows an increase in frequency of dyke sub-parallel fractures towards the margin. This is consistent with the dyke having propagated its own hydraulic fractures during intrusion, and is commonplace where Tertiary dykes intrude Carboniferous limestone (Chapter 3). Between F1 and F2, most of these fractures are dilated and mineralised with calcite. Crystals are seen to cover the fracture surfaces where they form the outcrop face in cliff section, having grown orthogonal to the surfaces.

The fault kinematics described above are consistent with the observed sinistral 1.5 m offset of the dyke.

Fault group B

To the north of faults F1 and F2, a number of faults offset bedding in the cliff section (Figure 4.9, inset 3). They show a normal dip-slip component of movement. Fault F3 is the dominant fault in this group, showing fault drag in section, and is slightly oblique to the general strike of the other, minor, faults in the group.

The dip-slip component of displacement across the faults is only a few centimetres, apart from F3, which must have accommodated more slip, as indicated by the fault drag.

The opposing dips of the faults in section gives the impression of conjugate normal faults (Figure 4.9, inset 3). However, their strikes imply there might also be a component of strike-slip movement, following Figure 4.7. The minor faults appear to be in synthetic and antithetic arrangement with respect to fault F3, assuming the faults where formed at the same time.

The only slip vector information obtained for the group B faults is from a small patch of slickenfibres on the F3 fault plane. The pitch is steeper (45°SW) than that seen on F1 and F2 (45°W as opposed to 25°W and 21°W respectively). The sense of slip cannot be determined.

The projection of F3 where it meets the dyke is obscured by rubble, but an apparent sinistral displacement exists (~2 m) of similar magnitude to that across fault F1.

4.5.2.2 Palaeostress analysis and interpretation

The kinematics of fault F1, and by comparison fault F2, are clear, offsetting the dyke in a sinistral-reverse sense. In addition, these faults produced other structures. The dilated fractures striking sub-parallel to the dyke, between faults F1 and F2, are interpreted as having been caught in a shear couple between the two faults. For this, sinistral slip on the structures facilitated dilation of joints whose strike is less than 90° clockwise of the faults.

Secondly, the pinnate shears associated with F1, as described above, are interpreted as riedel and anti-riedel style shears (see Figure 4.7b), and, as such, are consistent in their sense of slip with the main fault displacement (Figure 4.9). When plotted in stereographic projection, the shears are close to intersecting at the same point with the main fault, F1. This point would represent the intermediate stress (σ_2) direction. It is noted, however, that only shear F1c conforms strictly, in terms of the angle subtended to the fault plane, with this model. The other shears do not conform exactly to the classic 15° (for riedel shears) and 75° (for anti-riedel shears) ideal.

For fault group B, the kinematics, at first glance, appear to be different from those of the group A faults. One of the minor faults is interpreted as acting as conjugate partner for the three others. Given this, the average dihedral angle between the conjugate pairs is high, at 82°.

Since the dyke is not actually seen to be displaced by fault F3, the question arises as to whether the offset of the dyke across the fault is due to fault slip, or the result of a syn-emplacement transform offset across the fault.

Palaeostress directions can be derived that treat all of the faults as primary structures that responded individually to regional stress (as in Figure 4.7a). It is a simplistic approach that might not be strictly correct, but is a starting point. The stereographic projections in Figure 4.10 show the principal stress axes derived.

For faults F1 and F2, the orientation of σ_1 is assumed to be 45° from the main plane of shear, as shown in Figure 4.7b. The directions of maximum compressive stress (σ_1) derived for the faults are of similar orientation, being 052/14 for F1 and 028/5 for F2 (Figure 4.10a). The azimuth is therefore roughly NE-SW. The minimum compressive stress direction (σ_3) is, consequently, also inclined with respect to the horizontal. Similarly, the intermediate compressive stress (σ_2) is not contained within the vertical plane.

It is expected that, at relatively shallow depths, the regional principal stresses will be contained in the horizontal and vertical planes (Figure 4.7a). These stress orientations should then be manifest in the slip vectors. Clearly, the principal stress orientations derived for faults F1 and F2 do not conform rigidly to this model.

Palaeostress directions for the group B faults are plotted in Figure 4.10b. As mentioned above, an apparent conjugate relationship exists between the minor faults immediately to the north of fault F3, with a high dihedral angle of 82°. Using these pairs, σ_1 orientations are obtained. For fault F3, the measured slip vector, which pitches 45°SW, is used to derive a plane in which σ_1 and σ_2 are contained. This plane passes through the values of σ_1 derived for the minor faults, and thus F3 appears to be in rough agreement in terms of palaeostress with its accompanying structures, accepting an angle between σ_1 and the F3 fault plane of ~22°.

The analysis for fault group B indicates that σ_3 is contained within the horizontal plane, but the intermediate and maximum compressive stresses are both inclined with respect to the horizontal and vertical planes.

Given this simplistic approach to palaeostress reconstruction, and even ignoring the fact that the principal stress axes are not contained in the horizontal and vertical planes, clearly, the stress axes obtained for the two fault groups are orientated differently, with the σ_1 and σ_3 axes interchanged. Therefore, the stress regimes that produced the two fault groups appear to have been different. The palaeostress regime derived for fault group B could not have produced a sinistral displacement of the dyke across fault F3. Thus, the displacement of the dyke across this fault (F3) is most likely to be a transform offset.

It is possible, however, that fault F3 was reactivated by the stress regime that caused the group A faulting. The fault is of a similar orientation to the faults F1 and F2 and the slickenfibres preserved on the plane of F3 may have resulted from reactivation, of what was previously a majority normal fault, in a sinistral-reverse sense.

It therefore seems that fault group B was formed *before* the dyke was emplaced. The dyke then intruded, during the early Tertiary, and may have made a left-stepping transform offset across fault F3. Alternatively, the intruding dyke was unaffected by F3, which was then subsequently reactivated under the stress regime that produced faults F1 and F2 that displaced the dyke in two places.

4.5.2.3 Validity of analysis and overall model for the faulting

Analyses for both groups of faults show that the principal stress axes do not conform to the general model of containment within the horizontal and vertical planes at relatively shallow crustal depths.

One way to explain the orientation of the derived principal stress axes is by inferring rotation of the faults since their formation. An obvious source of rotation is that which caused the strata to dip 10°SSW. Simply 'un-rotating' the derived stress axes by this amount does not, however, bring them into the vertical and horizontal planes. In any case, the tilting of the strata likely occurred prior to the Tertiary, and is possibly a signature of Variscan deformation, as explained in Section 4.5.1 above.

Alternatively, regional principal stresses can be locally deflected by physical boundaries within the crust. One such heterogeneity can be a change in lithology. Lithological change is seen at this locality, where fault F3 juxtaposes limestone interbedded with shale against sandstone.

Perhaps a more realistic explanation as to the orientation of the derived stress axes is that the faults are actually associated with larger structures, and the stress directions are controlled by this 'parent' structure. That is, the palaeostresses derived are *local* stresses as opposed to faithfully representing the regional principal stresses.

Given the oblique-slip kinematics of fault group A, it is possible that the structures are part of a positive flower structure associated with a larger strike-slip fault. This is shown in Figure 4.11, where the larger structure is inferred to be a NE-SW sinistral fault. Such a structure would form from N-S directed compression and is in agreement with palaeostress directions obtained from other localities of this chapter.

4.5.3 Localities around Lower Lough Erne, Co. Fermanagh

A number of dykes belonging to the Donegal-Kingscourt swarm intrude the Carboniferous and Devonian sedimentary rocks of Co. Fermanagh in the vicinity of Lower Lough Erne (see Chapter 2 and Figure 4.2). There are isolated exposures in river sections, fields and road cuttings, and also more extensive outcrops in quarries. This section describes three localities where dykes show extensive evidence of post-emplacement slip within their internal structure.

The Doraville dyke (dyke DK5, Figure 2.23, Appendix 8), a 60 to 90 m wide multiple intrusion, intrudes the Ballinamallard Formation of the Devonian Old Red Sandstone on the east side of Lower Lough Erne (Preston 1967b) (Figure 4.12a). The dyke is exposed and worked in Drogan and Doonan quarries. Both quarries span the majority of the dyke width and are completely contained within the dyke.

At a road cutting, adjacent to the A46 on the west side of Lower Lough Erne, the Cullen Hill dyke (dyke DK2, Figure 2.23, Appendix 8) outcrops in a section around 50 m in length (Figure 4.12b).

Lastly, in a disused quarry at Drumskew, near the southern tip of the lough, a dyke (dyke DK1, Figure 2.23, Appendix 8), 19 m wide, intruding the Ballyshannon Limestone Formation, cuts the northern and southern faces of the quarry (Figure 4.12c). This exposes two sections of the dyke,

approximately 150 m apart.

At all locations, slip, indicated by extensive mineral slickenfibre growth, has occurred along fractures within the dykes. The majority of data and description was collected from Drogan and Doonan quarries, given the extent of the dyke and, therefore, the exposure.

In the following sections, the fractures that accommodate slip, the structures, and the kinematics are described and classified, and palaeostress analysis is carried out.

4.5.3.1 Classification of the surfaces that contain slip

At all locations, two sets of roughly mutually perpendicular slip surfaces are defined, striking NW-SE and NE-SW (Figure 4.13a) (Appendix 21 contains all fracture orientation data).

For example, in Drogan quarry average strikes are 054° and 147°, and in Doonan quarry average strikes are 048° and 146° for the two sets. Two fractures recorded from Drumskew quarry appear anomalous, having N-S strikes. Angles of dip are also generally high, with fractures in Doonan quarry averaging a dip of 78°, and in Drogan quarry, 76°.

Given the NW-SE trend for the dykes, the fractures have strikes that are orientated parallel to the two expected main cooling joint sets, i.e. of dyke-parallel and dyke-perpendicular orientation. The fractures will, therefore, be treated as such.

In Drogan and Doonan quarries, the dyke-parallel (NW-SE) fractures are generally major, through-going, structures that control large areas of the quarry faces along the length of the quarries. The greater range of strikes in Doonan quarry, compared to Drogan, may represent variation in the strike of the dyke along the length of Doonan quarry. Indeed, the more WNW-ESE striking fractures do concentrate in the northwest end of Doonan quarry.

The majority dip of dyke-parallel fractures in Drogan and Doonan quarries is to the northeast. This probably represents the dip of the dyke. Conversely, the northwesterly dip of the dyke in Drumskew quarry appears not to be reflected in most of the dyke-parallel fractures, which dip southwest, although the dataset is relatively small. For Doonan quarry, most of the few southwest-dipping fractures derive from the northwest end of the quarry, and may reflect a local change in dip of the dyke. This could be linked with the proposed strike swing of the dyke, mentioned above.

The dyke-perpendicular fracture sets in both Drogan and Doonan quarries dip, in approximately equal numbers, northwest and southeast. They also show a wider angular range of dip than is seen for the dyke-parallel fracture set (Figure 4.13a).

In outcrop, these fractures appear to fall into two general groups (Figure 4.13b). Firstly, major structures cut dyke-parallel faces, extending from the base to the top of the quarry. They often change dip up-face, but usually remain sub-vertical. They also often bifurcate and anastomose, being bridged by fractures with a shallow angle of dip. Secondly, minor structures occur that are less pervasive up the face. It is these structures that contribute to the range in dips seen for the dyke-perpendicular fractures in Figure 4.13a.

In the main, the faces in both Drogan and Doonan quarries show a predominance of major, over minor, dyke-perpendicular fractures.

The minor dyke-perpendicular structures are interpreted as being part of a columnar jointing pattern. Columns would have formed orthogonal to the surface of cooling, i.e. the dyke margin. Where columnar jointing is developed, however, it is often quite crude. Such underdevelopment is normally seen in a dyke, since magma flow would prevent the stable cooling needed to form well developed columnar jointing. This might be even more prevalent in a multiple intrusion like the Doraville dyke.

The two main fracture populations seen in all four locations, dyke-parallel and dyke-perpendicular, appear, therefore, to be cooling joint sets. Surfaces that lie well outside the mean for a given set, e.g. a NNE-SSW fracture in Drogan quarry and the N-S fractures from face 1 of Drumskew quarry may be fractures that formed subsequent to cooling. Alternatively, they may just be cooling joints that are out of the 'normal' alignment.

4.5.3.2 Kinematics

Figure 4.14 shows the style of the slip structures and their relationships with the quarry faces and joint distributions in Drogan and Doonan quarries. Stepping slickenfibre growth indicates the sense of slip on flat areas of fracture faces and in dilational kinks.

Stereographic projections in Figure 4.15 and Figure 4.16 show the slip surface data for all locations. (The data are those shown in Figure 4.13a, modified to include the slip vectors.) In the quarries, data were collected from individual faces and are plotted as such.

In the vast majority of cases, at all localities, NE-SW (dyke-perpendicular) cooling joints have consistently accommodated sinistral slip, and NW-SE (dyke-parallel) cooling joints, dextral slip. This is regardless of the dip direction of the planes.

There are just a few anomalies. Firstly, a dyke-parallel surface accommodates sinistral slip within face 1 in Doonan quarry. In addition, similarly orientated fractures within face 1 in Drogan quarry have undergone pure extension, indicated by fibrous mineral growth perpendicular to the joint plane. Lastly, in Drumskew quarry, one dyke-parallel fracture, out of the six where slip-sense is discernable, accommodates sinistral slip, and two out of seven dyke-perpendicular fractures accommodate dextral slip (note, the two N-S fractures from face 1 are included in this number).

There is also a general consistency in the orientation of the slip vectors across all locations.

In Doonan and Drogan quarries (Figure 4.15 and Figure 4.16), the vast majority of dyke-perpendicular fractures contain slip vectors that plunge southwest. In Doonan quarry, the modal slip vector plunge range is 0 to 14° with the majority in this range plunging 0 to 10°, i.e. close to horizontal. Similarly, in Drogan quarry the mean plunge is 12°, with a modal range of 0 to 14°. The road cut exposure (Figure 4.16) also conforms to this trend.

In Drumskew quarry, a small majority of the dyke-perpendicular fractures (4 out of 7) contain slip vectors that plunge at low angles towards the southwest (this includes the two N-S fractures). The mean plunge for all such orientated fractures is 19°.

Dyke-parallel fractures also show similar consistency in their slip vectors. In Doonan quarry, slip vectors mostly plunge northwest. The mean slip vector plunge of 19° is higher than that seen for the

dyke-perpendicular fractures, but is not representative of the modal average, which is 0 to 14°. A few high plunge angles, up to 65°, bias the mean away from the mode. In Drumskew quarry, slip vectors plunge to the northwest and southeast in equal numbers, with a mean plunge of 8°.

It has been established that the fracture structure of the dyke is that of two roughly mutually perpendicular cooling joint sets. It is clear then that the cooling joint structure of the Doraville dyke (Drogan and Doonan quarries) has been extensively reactivated throughout the intrusion. This has also occurred within the dyke cutting Drumskew quarry, and appears also to be the case for the Cullen Hill dyke at the A46 road cutting.

For the quarry localities, reactivation is pervasive throughout the dykes. In the case of Drogan and Doonan quarries, the maximum width of the two quarries, around 50 m, is probably close to the total width of the dyke given the topographic drop on either side of the ridge that contains the quarries. Slip has occurred in all areas of these quarries, from the more marginal faces to the centre of the dyke. Given that the Doraville dyke is a multiple intrusion, displacements should not, therefore, be attributed to stresses applied to early cooled phases of intrusion by subsequent pulses of magma. Displacements probably occurred at some time after the whole dyke had cooled.

4.5.3.3 Cross-cutting relationships

The relative timing of reactivation of the two fracture sets is unclear. It is possible to infer cross-cutting relationships between the two displaced joint sets from the stepping form of the dyke-parallel faces (Figure 4.14). Along the length of the quarries it appears that reactivated dyke-parallel joints are often 'offset', across the reactivated dyke-perpendicular joints. In some instances, however, the latter appear to abut against the former, so there exists opposing cross-cutting relations.

This inconsistency suggests that both fracture sets accommodated slip at the same time. Conversely, such stepping of the faces could just be a function of quarry blasting.

4.5.3.4 Minerals forming the slickenfibres

Samples were taken of the mineralisation from different faces within Doonan and Drogan quarries (from faces showing sinistral and dextral kinematics), and also from Drumskew quarry and the A46 road cutting. X-ray diffraction (XRD) analysis was carried out on bulk cavity mounts for each sample.

(The X-ray generator used was a Phillips PW1720 with a Phillips PW1050/25 diffractometer, and a Phillips PW3313/20 Cu k-alpha anode tube that was run with standard conditions of 40 kV and 20 mA. A soller slit and a 1° divergence slit were used on the incident x-ray beam, and an anti-scatter slit followed by a 0.25° receiving slit were used on the diffracted beam, in front of the AMR detector. The detector controller was a Hilton Brooks. Analyses were run from 0 to 35° (2θ) at a step size of 0.02 $^{o}s^{-1}$.)

The same minerals occur throughout the sample range but in differing combinations depending on the sample. The results for a sample from Drgoan quarry are shown in Figure 4.17; the rest of the results are shown Appendix 22. The zeolite thomsonite occurs in each sample, as does an expandable

clay whose peak consistently shifted to the left after glycolation. Calcite occurs in all but one sample, and the zeolite analcime and the clay mineral fluorapophyllite (a variety of apophyllite) also occur. It is noted that there are some peaks that were not assigned to a particular mineral.

The range of minerals identified defines well the type of assemblage present. Zeolites are a group of minerals that are often found within basic lava piles and high-level intrusives, typically infilling vesicles. They result from low grade (low temperature, low pressure) metamorphic reactions, a result of fluid flow that has occurred soon after lava/magma cooling, but while there is still heat in the system. Zeolites are typically associated with calcite, and also clay minerals (including apophyllite found here) that have formed from breakdown of other minerals due to the fluid flow (Deer *et al.* 1992).

Zeolites have been described in detail from the Antrim basalt lavas of northeast Ireland, where Walker (1960) observed that thomsonite is characteristic of the upper parts of the Antrim basalt succession, whilst analcime is found at the next level down where higher fluid temperatures would have existed. (Demant *et al.* 1998) describes a zeolite and clay mineral assemblage that contains thomsonite from a borehole off Greenland, concluding that its formation took place at temperatures no greater than 170°C.

It is probable, therefore, that the mineral assemblage associated with slip within the dykes resulted from fluid flow that probably took place soon after dyke solidification, but before the dykes had lost all heat to the surrounding host rock. This could be further investigated, and the timing quantified, using the Schmidt Plot thermal model, as described in Chapter 3.

4.5.3.5 Factors controlling the slip vector

Overall, the vast majority of slip vectors contained within the dyke-perpendicular fractures plunge southwest. In a number of cases in both Drogan and Doonan quarries, where columnar jointing is developed, slip fibre pitches on minor dyke-perpendicular fractures exactly parallel the plunge of the column that the fractures form. This is shown schematically in Figure 4.18. It was established above that, from cooling joint orientations, the Doraville dyke dips northeast in the main. A dip of 81° is obtained for the dyke by averaging northeasterly dipping dyke-parallel fracture planes. Such an orientated body of magma would be expected to produce a columnar structure plunging around 9° to the southwest. Indeed, this is seen in face 2 of Drogan quarry and in face 4 of Doonan Quarry.

So, a modal plunge range of 0 to 14° southwest for slip vectors reactivating dyke-perpendicular fractures implies that the columnar joint structure of the dyke is, at least in part, controlling the orientation of the slip vectors. For the minor dyke-perpendicular structures at least, it appears that individual columns slipped past each other, thus implying there was a partitioning of control of the slip vector between the acting external stress regime and the internal columnar structure of the dyke.

There is only one recorded anomaly, in Drogan quarry, where a column plunges 14° southwest and the slickenfibres on one of its faces plunge 8° to the northeast.

The major dyke-perpendicular structures, whilst not forming columns, seem to have accommodated slip in sympathy with the minor 'columnar' structures.

This theory does not account, however, for the dominance of a northwest plunge for the dyke-parallel joints that do not form any of the bounding sides of the columns, but dominate most quarry faces. Also, the relatively rare mineralisation recorded on dyke-perpendicular joints with a low angle of dip suggests that movement by 'column control' is not the dominant means of slip.

4.5.3.6 Palaeostress analysis

It is apparent from the preceding sections that cooling joints were reactivated and accommodated slip, post-emplacement, throughout the interior of the dykes at the localities described. For palaeostress analysis on reactivated planes, there is a necessity that the orientation of the reactivated surfaces and their slip vectors meet certain requirements.

Orientation requirements for reactivated fracture planes

The method used in this study, described below, is that of Sibson (1985; 1990). Figure 4.19 shows, using the Mohr circle construction, the stress criteria required for reactivation of a pre-existing surface, as opposed to propagation of a new fracture. The angle between an existing plane and the maximum principal stress, σ_1, is θ. An existing surface will accommodate slip in favour of a new fracture forming if the existing plane is orientated within a preferred range in θ with respect to the maximum principal stress, σ_1. This angular range will depend on the stress ratio, $R = \sigma_1/\sigma_3$, and the coefficient of static friction, μ_s, of the plane. Above some value of θ, planes will become unfavourably orientated for reactivation, and will eventually become severely misorientated meaning that slip will only occur if fluid pressures, P_f, are high (see Figure 4.19 and Figure 4.20 for a full explanation).

For a reactivated plane, assuming a value for μ_s and R, an angular range can be predicted to contain the maximum and minimum principal stresses (σ_1 and σ_3 respectively). Note that this stress analysis requires that the intermediate principal stress, σ_2, be contained within the fault plane, so the reactivated plane and its slip vector must satisfy certain orientation requirements depending on the stress regime of reactivation.

Brittle faults forming in accordance with the Coulomb criterion for shear failure typically form conjugate sets near to the surface of the Earth (Anderson 1951). The ground surface acts to maintain one of the principal stress axes as vertical. Given this, one of the reactivation stress axes must also be assumed to be vertical.

So, for reactivation stress analysis to be applicable, for inclined planes the slip vector must be dip-slip (σ_2 is horizontal), and for vertical planes the slip vector must be strike-slip (σ_2 is vertical) (Figure 4.21a). (See also Figure 4.7 showing the geometries and relationships between the principal stresses, fault planes, slip vectors and normals to the fault planes.)

If the above requirements are not met then σ_2 cannot be constrained to lie within the plane of reactivation. In such a situation of oblique-slip reactivation, the direction of maximum shear stress, i.e. the slip vector, is not constrained by representing the intersection between the reactivation plane and the σ_1/σ_3 plane, but rather may lie at any orientation being a function of the relative values of the

three principal stresses (Bott 1959).

For the Doraville dyke, data from Drogan and Doonan quarries show that the slip surfaces mostly have high angles of dip, and the slip vectors plunge at low angles. This is also largely the case for Drumskew quarry, and is seen for the one plane recorded at the A46 road cutting. If the planes are approximated as vertical and the slip vectors as horizontal, palaeostress analysis can be carried out for reactivation as shown in Figure 4.21a. This is reactivation of vertical planes in a strike-slip stress regime. Implicit in this assumption is that σ_1 and σ_3 lie in the horizontal plane.

For the data here, all slip probably occurred as a result of the same stress event. For multiple planes of differing strike but with the same sense of slip, e.g. dyke-perpendicular fractures showing sinistral slip, the angular ranges in σ_1 for all the planes must overlap to give a common range for σ_1 to satisfy slip on all those planes. If there is no such common range, the initial assumed values of μ_s and R must be redressed until slip is satisfied on all planes. In addition to this, the principal stress axes must lie in the angular range between the two planes closest in strike to each other with opposing slip (Figure 4.21b).

Palaeostress analysis results

An analysis of palaeostress is carried out below for data collected from the Doraville dyke (Doonan and Drogan quarries). The data for Drumskew quarry is not quite as consistent in its kinematics, so is not included.

Figure 4.21c plots the angular ranges in dyke-parallel and dyke-perpendicular fractures that accommodate dextral and sinistral slip respectively. The principal stress axes for reactivation lie between these ranges save for a 2° zone (166 to 168°) in which dyke-perpendicular planes would be predicted to accommodate dextral slip, which is not the case.

The acute angle between 348° and 016° (or 168° and 196°) contains σ_1 and that between 078° and 111° (or 258° and 291°) contains σ_3, to potentially satisfy slip on all planes as observed. The end of each range in sinistral and dextral slip planes that is closest to the σ_1 range (i.e. the lowest strikes for sinistral slip planes and the highest strikes for dextral slip planes) is favourably orientated for reactivation (for normal values of the stress ratio, R, and the coefficient of static friction, μ_s), being just 28° from the closest possible σ_1 direction (see Figure 4.20). However, the opposite ends of the angular ranges in slip planes are large angles away from the closest possible σ_1 direction, 62° and 85° for sinistral and dextral planes respectively. The greatest possible angles between σ_1 and the slip planes, as defined by Figure 4.21c, are 90° and 85° for sinistral and dextral slip planes respectively. Therefore, sinistral slip planes that are orientated at relatively high angles of strike, and dextral slip planes that are orientated at relatively low angles of strike, are severely misorientated for reactivation (as shown in Figure 4.20) for any possible value of σ_1 given normal values R and μ_s. Either μ_s was low and/or P_f (fluid pressure) was high to have facilitated slip on these planes. It is not possible that an increased value of R alone could have caused slip on such misaligned planes (Figure 4.20). The presence of such extensive mineralisation in the quarries indicates that fluids were in abundance, so P_f could have been high, thus facilitating slip. It is also likely that the control on slip asserted by the

cooling joint structure of the dyke (as described in Section 4.5.3.5 above) caused slip to occur on a wider range of planes.

Finally, it is noted and acknowledged that the structures mapped here might actually be a response to cooling of the dykes. It is envisioned that as the dykes cooled individual blocks of dyke delineated by cooling joints might have cooled differentially (and therefore contracted differentially) with respect to surrounding blocks. This might have caused slip to occur between blocks along the cooling fractures. However, it is suggested that such 'jostling' of blocks of dyke would not have produced the consistency of slip-sense observed here.

The conclusion drawn is that N-S compression caused the extensive slip mapped. This stress acted soon after dyke emplacement, given the zeolite mineralogy associated with slip. The change in stress field must have been rapid after intrusion of the dyke, switching from NE-SW extension to N-S directed compression.

4.5.4 Carn quarry, Co. Fermanagh

A dyke (dyke DK9, Figure 2.23, Appendix 8) cuts the Ballyshannon Limestone Formation within (the working) Carn quarry, near Ederny, Co. Fermanagh (see Figure 4.2 and Figure 4.22). It has been shown in Chapter 2 that this dyke was intruded in en échelon form, as is predominantly the case across the region with dykes that were emplaced into Carboniferous sedimentary host rock.

As well as this, the dyke comprises two distinct 'types' within much of its outcrop in the quarry. In parts, the dyke shows high degrees of strain associated with faulting along its margin. Below, the deformation is described and the implications for the remote stresses acting at the time are discussed. Figure 4.23 shows a plan of the quarry. Appendix 23 lists all data referred to.

4.5.4.1 Description of dyke internal structure and faulting

Segments 1 and 2, northwest end of quarry

Figure 4.24 is a structural map of this area of the quarry (refer back to Figure 4.23 for location within quarry). Figure 4.25 is a series of photographs and sketches depicting some of the features described.

The internal structure of parts of both dyke segments differs from the usual uniformity, where a dyke is divided internally by sets of cooling joints that generally run parallel and perpendicular to the dyke margins.

At the southwest margin of segment 1, a zone ~60 cm wide occurs where the dyke is severely dissected by calcite veins. This is in contrast to the majority of the dyke, which has regular form. Veining of the dyke is more intense towards the margin. The zone appears to be continuous up-slope, and veins run along the typical cooling joint trends and also oblique ones (Figure 4.25a). There is no evidence of shear in the veining itself, but some dyke fragments have sub-vitreous surfaces that contain slickensides. Most of the dyke broken by the veining has altered to a green colour compared to the rest of the dyke. There does not appear to be a discrete boundary between the 'veined' part and the 'regular' part of the dyke, rather the veining becomes less intense into the dyke. At the northeast

margin of segment 1, the dyke is altered and rotten in a narrow zone of a few centimetres, but does not appear to be veined like the opposite margin.

Segment 2 shows similarities in its internal structure, except the veined zone occurs in the centre of the dyke, appearing to narrow up-section. Regular dyke exists either side, but does contain a number of dyke-parallel veins. There is a sharp boundary between the veined and regular zones (Figure 4.25b). A narrow marginal zone (20 cm wide) forms the northeast margin of segment 2, where the dyke is green and rotten.

Both segments 1 and 2 consist of fine-grained dolerite.

Similar veining is also seen in a dyke (dyke DK11) outcropping in the entrance to the westernmost quarry (Figure 4.22, number 2). This dyke, exposed in a topographic mound, is similarly trending, and is at least 4 to 5 m wide. A 3 m wide zone, on the southwest side of the outcrop, is intensely split by veins up to 3 cm wide (Figure 4.25c). Mostly, the veins run sub-parallel to the trend of the dyke, but several cut through the dyke orthogonal to its trend. There does not appear to be any shear associated with this veining. The dyke is mapped as having been emplaced along a fault (Figure 4.22).

The northeast margin of segment 1 has accommodated dextral slip, with a small component of dip-slip movement. This is seen on the limestone scarp that is the dyke margin (shears 1 and 2, Figure 4.24), and also in a window of exposure on the quarry floor (Figure 4.25d), where the segment has narrowed. Here, on the quarry floor, the northeast marginal 5 cm of the dyke is green and more altered/rotten than the rest of the dyke exposed, similar to that described back, northwest, along strike in the scarp section (see above). Extensional veining permeates the dyke, as indicated by fibrous mineral growth (Figure 4.25d).

Between the two dyke segments, a vertical sinistral shear plane (shear 3, Figure 4.24) forms part of the quarry face scarp.

Between the tapering segment 1 and the inferred path of segment 2 there are a number of dyke-parallel fractures exposed in plan and section (shears 4 and 5, Figure 4.24). Associated with these fractures are dextral pull-apart structures that are dyke-filled and show ~20 to 30 cm shear displacement in their opening (inset, Figure 4.24).

To the west of segment 2, fault F1 has a throw of 1.7 m and shows dextral-normal kinematics (Figure 4.23).

It is not possible to deduce any throw of strata across the dyke segments due to lack of clean host rock exposure between the segments.

Segments 2 and 3, southeast end of quarry

Figure 4.26 is a series of structural maps of the area (refer back to Figure 4.23 for locations within the quarry). Figure 4.27 is a series of photographs and sketches depicting some of the features described.

Where dyke segments 2 and 3 intersect the lower and upper quarry faces, part of the internal structure of the dyke differs from the 'regular' structure normally seen within a dyke. A marginal zone exists (Figure 4.26, dark green colour) that is rotten and crumbles away from the outcrop. In

segment 2, this 'irregular' zone occupies the northeast margin (Figure 4.27a and b), and in segment 3 the southwest margin (Figure 4.27c). The irregular zone narrows up-scarp where segment 2 cuts the quarry face on the quarry floor. Within segment 3, the zone is relatively wide, affecting more than half the dyke width, and is accreted along the ramp marginal wall.

These irregular zones consist of fragments of dyke that are typically lens-shaped and have a sub-vitreous lustre to their surfaces. The faces of the 'lenses' usually contain slickensides, but whose lineation orientation is variable (see data plotted in Figure 4.26). It is common to see curvature of slickensides on these faces and abrupt changes in lineation orientation on an individual face.

There is some variability within the irregular zones. 'Irregularity' becomes most intense at the dyke margin where the dyke takes on a foliated character, being clearly sheared in a dextral sense (Figure 4.27c, and d). In the irregular zones, blocks of regular dyke occasionally occur (e.g. Figure 4.27c), but still have slickensided glassy faces. The boundary between regular and irregular zones shows some gradation in places, where recognisable cooling joints are developed to a degree in the irregular zone. Sub-horizontal slickensides often occur on such joints. Where segment 3 outcrops on the ramp, however, the regular-irregular boundary is sharp (Figure 4.27c).

The regular zones of dyke are dolerite. The lenses from the irregular zones, however, are much more finely crystalline.

It is clear that the irregular zone within segment 3 has, at least in part, been deformed by shear (see above). This deformation is ductile in nature. Indeed, dextral shear (with a subordinate normal component) has taken place along the southwest margin of segment 3, evidenced by extensive slickenfibre mineral growth on the host rock marginal wall (Figure 4.27c). In addition, brittle structures with similar kinematics occur in the host rock close to the margin of segment 2 (e.g. Figure 4.27b).

Within the dyke itself, along the regular-irregular zone boundary of segments 2 and 3, dextral slip has taken place with small amounts of normal or reverse components.

The vast majority of the shear structures are located around the northeast margin of segment 2 and the southwest margin of segment 3. They are obviously linked to the irregular zones within the dyke. In both segments the regular part of the dyke has a normal cooling joint structure up to the dyke margin, seemingly having not undergone any deformation.

Along the host rock marginal wall of segment 3, the pitch of slickenfibres is, in the main, around 5°SE. However, shear 3 (Figure 4.26), situated approximately 15 m along the ramp from the quarry floor, shows dextral-normal kinematics but with a curved slip lineation that becomes steeper to the northwest. Also, between shear 3 and the base of the ramp there are a number of cross-cutting structures in the host rock, many of which show curved slickenfibres at steep pitches (see shears 2, 9 and 10 plotted in Figure 4.26). Curvature has resulted from fault-block rotation during slip. Figure 4.28 is a view of the shear planes facing the ramp marginal wall, and cross-sections are shown in Figure 4.26. For example, shear 9 shows dextral-normal to dextral-reverse slip and, at least at the base of the scarp, is the margin of segment 3. Shears 10 and 11 are reverse with only a small dextral component of slip, and dip to the south, contrary to the majority northerly dip of the structures

described.

In addition, displacement of what appear to be scissor faults, cutting shear 9, decreases to zero to the northwest, just outside the bounds of Figure 4.28.

Dyke of irregular form is accreted to the ramp marginal wall all along the base and in places towards the top of the scarp.

There is a throw of marker horizons in the host rock of ~1.5 m and ~1.1 m across segment 2 where it cuts the quarry floor and upper level faces respectively (Figure 4.27a, b). It is not possible to measure any throw across segment 3. A step in the margins of segment 2 at the quarry floor face indicates that opening of the dyke in cross-section was close to horizontal with a slight possible downthrow to the northeast (Figure 4.27a).

4.5.4.2 Faulting

Several faults, southwest of the dyke, cut the quarry faces on both levels (Figure 4.23). The faults show either a true or apparent downthrow to the northeast, the majority component of slip being strike-slip, as evidenced by slickenfibres and pull-apart structures. The faults generally strike at a greater angle than the dyke segments. Faults F1, F3 and F4i/ii are single plane structures, whilst F2 and F4iii are zones of sub-parallel planes across which displacement has taken place, accommodated by all or some of the planes in various amounts.

Figure 4.29 shows the faults plotted in stereographic projection form. Sense of slip is not determinable in the majority of cases, but in three out of four cases where it can be inferred, it is dextral with a small normal component.

Fault F1 is a single plane showing dextral-normal kinematics and downthrows strata 1.7 m to the northeast (Figure 4.30a).

Fault F2 consists of sub-parallel planes in a zone 60 cm wide with a net 27 cm downthrow to the northeast. Sinistral slip is recorded on a plane at F2i, combined with a small reverse component that causes upthrow of the northeastern side (Figure 4.30b). This is contradicted by dextral slip recorded at F2ii.

Fault F3 is a single plane with a downthrow of 11 cm northeast, with the slip lineations indicating mainly strike-slip displacement. Associated with the fault plane of F3ii are pinnate fractures in the downthrown block (Figure 4.30c). The orientations of these fractures were not measured, so their intersection with the quarry face, which appears to indicate the fault as normal, may be misleading.

Fault F4 facilitated the emplacement of a narrow dyke along part of its exposed length. At its northwest end, F4i is a single plane with dextral-normal kinematics and 35 cm throw (Figure 4.30d). F4ii has a throw of 65 cm and is intruded by a dyke 35 cm wide that appears to be segmented (Figure 4.30e). The dyke is altered in a similar way to that described above for segments 1 and 2 at the northern face of the quarry

Sense of slip at F4ii and F4iii cannot be determined in outcrop from the slip lineation, but polished sections reveal at least one phase of dextral transtensional opening at the dyke margin, and a phase of normal extensional opening in one of the minor veins cutting the southwest portion of the intrusion

(Figure 4.30e).

Fault F4iii coincides with a zone of sub-parallel fracturing (Figure 4.30f). Three dyke segments have been emplaced into the zone, their cumulative width of ~21 cm being less than the dyke width at F4ii. A marker horizon is thrown ~50 cm down to the northeast across the fault zone. Slickensides preserved on the dyke margin show mainly strike-slip movement, but a gentle plunge to the southeast indicates also an element of dip-slip. It may be speculated that there is an increase in fracture frequency compared with that to the northeast but, conversely, there appear to be more obvious fracture clusters to the southwest of the zone.

Since displacement appears predominantly strike-slip, and strata dips gently southeast, the throw of each northeastern block is only an *apparent* downthrow. Estimates of true displacement are given in Appendix 23, based on the geometry described in Figure 4.29. Values range between 0.12 m and 12.04 m. A displacement of 4 m is calculated for fault F1. This is the least ambiguous value calculated due to the large differential between the displacement vector pitch and the strata dip, and the knowledge that dextral slip has occurred.

The amount of dextral displacement that occurred along the margin of segment 2 is estimated at almost 13 m, using a strata dip of 10°, and an average slip lineation plunge of 15°SE using the throw of a marker bed across the dyke.

4.5.4.3 Interpretation of structures and overall model for intrusion and deformation

It has been established that the main dyke comprises three segments and was emplaced in en échelon style. Segmentation appears to have taken place in both the horizontal and vertical planes.

The irregular zones of segments 2 and 3 are interpreted as having been deformed by movement along two faults, one being along the northeast margin of segment 2 and the other along the southwest margin of segment 3. Shear in the host rock caused brittle deformation. In the dyke, the irregular zone is fragmented and indicates ductile deformation, whilst brittle shear has occurred between the individual fragments. Therefore, deformation in the dyke appears to be brittle-ductile in nature.

In general, the kinematics are in harmony between the dyke and the host rock. They show mostly dextral shear with a small dip-slip (normal) component.

The 'fault zone' at the base of the ramp near the postulated northwest end of segment 3, however, is anomalous in its kinematics (Figure 4.26). The close proximity of the two segment margin faults at this point, and the nature of the deformation, i.e. mainly reverse shear structures with rotational movement, suggests that this zone is a positive flower structure. Fault block rotation is common in flower structures, where, on a given fault plane, a transition from strike-slip to oblique-slip occurs along strike. The dextral-normal slip that occurs at the southeast edge of the flower structure appears to represent the transition between dextral slip with only a minor normal component, and the varying oblique slip of the flower structure.

Dextral movement has occurred along the whole of the margin of both segments 2 and 3, and has not just been transferred from one to the other across the flower structure. Therefore, it appears that the flower structure is a response to a constrictional bend in segment 3 as it swings in towards the

margin of segment 2.

The fact that deformation was ductile within the dyke segments is significant in suggesting an age for the deformation. The part of the dyke that was deformed must have been hot as faulting occurred. Slip, therefore, probably took place during or immediately after emplacement. In addition, the fact that the regular zones are largely unaffected by deformation suggests that these parts of segments 2 and 3 intruded at a different time and that there occurred two stages of intrusion. Only close to the zone boundary with the dyke segments did the faulting have any effect within the regular zone, indicated by slip along some cooling joint planes. The sharp transition from regular to irregular within segment 2, and the presence of dextral shear indicators on the internal margin of the regular zones within both segments 2 and 3, indicates that the regular zone was emplaced and cooled before subsequent intrusion and deformation took place. In contrast, there is an apparent gradation in places between the regular and irregular zones, which is interpreted as being a gradation in deformation. Either deformation was not as pervasive through the second intrusion phase to reach the earlier cooled regular margin, or there was not long enough of a gap in time to allow the first intrusion phase to cool before subsequent magma injection and accompanying deformation took place.

Where segments 1 and 2 intersect the northern quarry face, both segments contain zones that are heavily mineralised. The abundance of calcite veins sub-parallel to the dyke-parallel and dyke-perpendicular cooling joint trends within the dyke indicates that fluids were present after the dyke cooled with hydraulic pressures high enough to dilate joints of all orientations. Given the deformation described to the southeast, the narrow zones of rotten altered dyke at the northeast margins of both segments and the increase in intensity of veining and break-up at the southwest margin of segment 1 could be a result of similar fault activity. Indeed, dextral shear clearly took place along the northeast margin of segment 1. Similarly in support, dextral-normal slip occurred along dyke-parallel joints between segments 1 and 2 on the quarry floor. This occurred whilst emplacement was taking place, given the presence of dyke filled pull-aparts.

These structures are, therefore, kinematically compatible with the deformation of segments 2 and 3 to the southeast.

The kinematics of the E-W sinistral shear between dyke segments 1 and 2 probably result from block rotation in reaction to a dextral shear couple set up between the two dyke segments.

It is unclear as to the number of intrusion phases associated with segments 1 and 2. There may have been more than one phase of intrusion given the internal variation described within the dyke segments. In segment 2, the fact that the central veined zone narrows up-scarp might indicate that it represents a separate, possibly later, intrusion phase compared to the rest of the segment.

The several faults that cut the quarry to the southwest of the dyke show kinematics that are generally consistent with each other and with the faults along the dyke margin. Fault F4 appears to develop along strike from a single plane in the northwest to a multi-plane fault zone in the southeast. It has been shown that the dyke segments emplaced along the fault at F4ii and F4iii pre-date at least part of the displacement. Veins that cut the dyke show consistent kinematics with dextral displacement at F4i and with the other faults. The similarity in kinematics along fault F4 compared

with the other structures mapped, and the association between dyke and fault, implies that this narrow dyke was emplaced in a similar manner as that described for the main dyke to the northeast; that is, emplacement into a dextral fault.

All the structures described in the quarry, therefore, appear to be in kinematic agreement with each other. It is interpreted that all the faults formed at the same time, with predominantly dextral displacement (with a small normal component) being accompanied by intrusion of the main dyke, in the northeast, and the narrow dyke into fault F4 in the southwest. The dyke was intruded in en échelon form, presumably at least in part controlled by the fault along the northeastern margin of segment 2 and southwestern margin of segment 3. The faults are sub-parallel to other faults mapped in the area (Figure 4.22). Indeed, a dyke is interpreted as having been emplaced parallel to a fault in the westernmost of the quarries shown in Figure 4.22 (shown in Figure 4.25c and described in Section 4.5.4.1 above). The orientation of the dyke and faults and the dextral slip described implies that N-S directed compression acted at the time of their formation. The relatively small amount of normal dip-slip displacement might be explained in a similar way to that affecting the dyke described above (Section 4.5.2) on St. John's Point peninsula. That is, the faults might relate to a larger dextral strike-slip structure, their orientation being slightly clockwise of this structure causing the faults to undergo a small extensional component of stress. Lastly, it is noted that there remains a question over the compatibility of the stress regimes that appear to have been acting during dyke emplacement, i.e. NE-SW extension as indicated by dyke form and orientation, and N-S directed compression as shown by the fault kinematics.

4.6 Compatibility of palaeostress analysis with the established tectonic framework for the Tertiary

Figure 4.31 shows the horizontal stress trajectories derived from the localities described above in comparison with published palaeostress estimates for Ireland and the surrounding areas. All the localities indicate that approximately N-S directed compression acted at some time after dyke emplacement, except Carn quarry, which shows evidence for syn-emplacement stress of this orientation. If the slip along cooling joint planes in Doonan quarry and associated localities is derived from tectonic stress and is not a function of dyke cooling, then the widespread occurrence of zeolites as slip direction indicators suggests that joint reactivation took place soon after dyke emplacement. It is suggested then that N-S compression existing in Ireland soon after dyke emplacement. This is in reasonable agreement with the stress regime that Geoffroy *et al.* (1996) invoke for the late Palaeocene, which they relate to Pyrenean tectonics. It also conforms to the stress required to cause the observed displacement of dykes as resolved from the new aeromagnetic data from Co. Fermanagh and surrounding area, collected by the Geological Survey of Northern Ireland. Opinion is that northwest Europe was subjected to compression after break-up in the northeast Atlantic at the start of the Eocene, a result of ridge-push and Alpine forces (e.g. Ziegler 1989) (see 0). This is supported by the data presented here.

4.7 Conclusions

For a dyke to be considered as faulted, the fault plane really needs to be seen, and kinematic indicators identified, that will unequivocally prove that movement on the fault displaced the dyke. Otherwise, it is likely that the dyke will be wrongly labelled when an alleged fault displacement is actually a transform offset or syn-emplacement jog. Features to look for that will help to classify the offset as a transform rather than faulted include: cooling joints in the dyke that align orthogonal and parallel to the wall of the structure across which the dyke is 'displaced'; the offset segments bending in towards each other on approaching the structure; horns projecting from the dyke segments on approaching the structure, indicating imminent segmentation; any change in width of the dyke segments as they approach the structure; injection into the plane of the structure; and structures in the host rock typically found in the vicinity of overlapping/interacting dyke segments, as described in Chapter 3. When outcrop in the vicinity of the offset is poor it is impossible to classify the offset.

Faulted Tertiary dykes are extremely rare in northwest Ireland. Three dykes have been identified that are unambiguously faulted, two post-intrusion and the other syn-intrusion. From each, a N-S direction of compression in a strike-slip stress regime is derived. A fourth set of examples has been described where intra-dyke displacements along cooling joints again indicate N-S compression. Evidence suggests that this stress acted soon after dyke emplacement in the early Tertiary. The stress is consistent with the general compressional stress state thought to have been affecting the northwest European margin since break-up in the northeast Atlantic around the start of the Eocene.

Chapter 5 *Tertiary denudation across northwest Ireland, using fission track analysis and (U-Th)/He dating*

5.1 Introduction

Using fission track analysis and (U-Th)/He dating, this chapter attempts to quantify the amount of denudation that has taken place since the early Tertiary across west and northwest Ireland.

The magnitude of Tertiary denudation across the northwest European margin has been of interest in recent years, as denudation provided a sediment source throughout the Tertiary for the hydrocarbon-bearing basins offshore to the west (e.g. Doré & Jensen 1996; Green *et al.* 1997; Japsen & Chalmers 2000) (see 0). Regional-scale uplift, probably related to the Iceland plume, occurred around the Cretaceous-Tertiary boundary. As the northeast Atlantic widened and the plume effects became distant, Ireland and Britain remained above sea level, probably as a result of magmatic underplating (e.g. White 1988; Brodie & White 1994; Cope 1994; Saunders *et al.* 1997; Jones *et al.* 2002).

Quantifying the amount of Tertiary denudation across Ireland has been the subject of some investigation, mainly using the fission track technique (e.g. McCulloch 1993; Green *et al.* 2000; Allen *et al.* 2002). This study addresses a two-fold problem with the validity of previous denudation estimates for Tertiary Ireland from fission track analysis. Firstly, for most Irish rock types, fission track data is marred by a pre-Tertiary thermal history spanning a relatively large time interval, which can reduce confidence in the modelled Tertiary thermal history. Secondly, the low temperature sensitivity of the fission track technique may not actually be low enough to reliably quantify denudation.

To address these problems, firstly, sampling was carried out adjacent to early Tertiary dykes. Heating on intrusion would 'reset' the fission track and (U-Th)/He thermochronological clocks, thus eliminating any unwanted pre-Tertiary thermal signature locked in the sample. Secondly, in addition to fission track analysis, (U-Th)/He dating was used for its ability to resolve lower temperature thermal history information. This technique has not previously been used in Ireland.

5.2 Fission track analysis

Fission track analysis is a low temperature thermochronometer. That is, it aids reconstruction of low temperature thermal histories.

5.2.1 Fission track age

The spontaneous fission of U^{238} causes emission of charged heavy particles (two atoms) that produce damage trails in crystals. Apatite and zircon are the two most common minerals with sufficient

amounts of U^{238} for the trails to be detectable and useful. These damage trails, or *fission tracks*, are visible under a high-powered microscope in a polished grain after it has been etched in acid. Given the known rate of fission decay for U^{238} ($\lambda_f = 8.46 \times 10^{-17}\ a^{-1}$), a measurement of the concentration of U^{238}, combined with a count of the number of tracks per unit area (a parent-daughter ratio), can be equated to an age for the crystal; this is the *fission track age*. This 'age', however, does not represent the time elapsed since the crystal formed (see below). Typically, twenty single grain ages are combined to give either the *mean, pooled, or central age* for the whole sample based on a Poissonian distribution (Gallagher *et al.* 1998). The central age, of Galbraith & Laslett (1993), is a weighted modal age and is the generally the preferred method. It deals more effectively with single grain ages that lie outside a Poissonian distribution (Gallagher *et al.* 1998).

5.2.2 Fission track annealing

Fission tracks are not stable above a certain temperature, dependent on the mineral, and shorten, or *anneal*, as a result (Gleadow & Duddy 1981). Complete annealing occurs at sufficiently high temperature, above which tracks no longer accumulate with time since they are destroyed as soon as they form. A temperature range therefore exists in which tracks partially anneal; this is known as the *partial annealing zone*, or PAZ . Therefore, as well as counting the number of tracks (for derivation of fission track age), individual track lengths are measured. A *mean track length* (MTL) with standard deviation is derived per sample, and track length distribution is usually represented in histogram form with 1 μm bins.

Derivation of a fission track age relies on counting the number of tracks intersecting a two-dimensional surface. If annealing has occurred, the probability of tracks intersecting the count surface is reduced, and this yields a younger fission track age. Therefore, residence of a sample within the PAZ will reduce the fission track age (Gallagher *et al.* 1998).

The PAZ for apatite exists between approximately 60°C and 110°C, compared with 200°C and 350°C for zircon (Gleadow & Duddy 1981). Apatite is therefore almost exclusively used for fission track analysis due to its sensitivity as a low temperature thermochronometer. This study uses fission track analysis of apatite, and all the following description refers to the apatite system. The most suitable rock to yield apatite is granite, but sandstone can contain detrital apatite and metamorphic rocks will often also yield apatite.

5.2.3 Thermal history reconstruction

The kinetics of fission track annealing are understood to a large degree (e.g. Laslett *et al.* 1987; Green *et al.* 1993), so the measurement of track *length* and track length *distribution* allows a thermal history to be modelled for the rock, where individual heating and cooling events are inferred (e.g. Lewis *et al.* 1992; Green *et al.* 1995; Gallagher & Brown 1997; Green *et al.* 2000). This can then lead to denudation estimates using a value for the geothermal gradient at the time (Allen *et al.* 2002). Allen *et al.* (2002) used a thermal history modelling software package, MonteTrax, developed by Kerry

Gallagher of Imperial College, London, and based on Gallagher (1995). Obviously, any time the sample has been at higher temperatures than 110°C (the base of the PAZ) all track lengths will have been reduced to zero, so a derived thermal history spans the time since the rock was last above this threshold temperature. The most commonly used annealing model is that of Laslett *et al.* (1987), based on the Durango apatite from Mexico.

Modelled thermal histories will usually apply to shallow crustal depths. Given a geothermal gradient of 30°C km^{-1}, this gives a depth to the base of the PAZ of ~3 km, assuming a surface temperature of around 20°C. The top of the PAZ coincides with a depth of ~1.3 km. Similarly, a geothermal gradient of 20°C km^{-1} and an average surface temperature of 10°C corresponds with a depth of ~5 km to the base, and ~2.5 km to the top, of the PAZ. Samples that have resided between these depths will yield information in their track length distribution allowing a modelled thermal history to be produced. The track length distribution will typically be complicated especially when multiple heating and cooling events have occurred and samples have been in and out of the PAZ. Correspondingly, the MTL will be reduced, indicating some annealing has taken place. Samples that have never been as deep as the PAZ (<60°C), e.g. deriving from shallow level intrusions, will yield a track length distribution that is unimodal with a high (unannealed) MTL. Such samples may have been slightly buried and exhumed several times, but this will not be resolved in the thermal history given the insensitivity of the fission track technique to temperatures less than 60°C.

5.2.4 Uncertainties – low temperature annealing and compositional effects

Below 60°C it is generally assumed in apatite annealing models that no track shortening occurs. However, small scale annealing is known to occur at near surface temperatures over geological timescales (Green 1988), which can lead to overestimates of denudation. In addition, apatite composition affects annealing rate, with Cl-apatite being more resistant to annealing than F-apatite (Gleadow & Duddy 1981; Laslett & Galbraith 1996). The Durango apatite is a Cl-apatite, so the commonly used annealing model of Laslett *et al.* (1987) may underestimate annealing when used to create thermal histories for more fluorine-rich apatites. This dependence on composition actually blurs the boundaries of the PAZ, so the limits of 60°C and 110°C are only approximate.

5.3 (U-Th)/He dating

Like fission track analysis, the (U-Th)/He technique is a low temperature thermochronometer. (U-Th)/He dating compliments fission track analysis, in that it has a slightly lower temperature sensitivity window for thermal history reconstruction (e.g. House *et al.* 1997; Wolf *et al.* 1997).

5.3.1 (U-Th)/He age

Helium is produced within apatite grains as a result of alpha decay from uranium and thorium. The concentrations of the four isotopes, ^{4}He, ^{238}U, ^{235}U and ^{232}Th, are measured in order to derive the helium age of a sample (Wolf *et al.* 1996). In the absence of other factors (one of which is

temperature, as alluded to above), this should indicate the time over which helium has accumulated in the apatite crystal. However, a number of factors need to be considered when interpreting a measured age. These are described below.

5.3.2 Thermal sensitivity

All helium is lost over geological timescales at temperature as low as 75°C. Progressive, or partial, loss of helium takes place between 40 to 45°C and 90°C (Wolf *et al.* 1998; Farley 2000). This is based on laboratory diffusion measurements and borehole data, which are both in general agreement with each other (House *et al.* 1999). The liberation of helium is much like the annealing of fission tracks. The temperature range over which helium is lost is known as the Partial Retention Zone, or PRZ. The PRZ, taken to be between 40/45°C and 75°C, is therefore analogous to the PAZ of the fission track technique. The closure temperature of 75°C for the system is based on an uplift rate of 10°C km^{-1} (Wolf *et al.* 1996). A helium age must therefore be interpreted bearing in mind that helium *loss*, as well as production, probably took place during a cooling episode. However, if a sample rises very rapidly through the PRZ from the closure temperature (75°C), such that there is no appreciable diffusive loss of helium, then the helium age will record the time at which the sample passed through the closure temperature.

5.3.3 Grain size effects

Grain size correction

Alpha particles (helium nuclei) produced by the decay of uranium and thorium isotopes typically travel around 20 μm in apatite, and may therefore escape from the apatite grain resulting in loss of radiogenic helium. This distance is known as the *alpha-stopping distance.* For grains less than a few hundred microns in minimum dimension, alpha-ejection is significant and helium ages are underestimated. To address this, a correction factor (F_T) was derived by Farley *et al.* (1996), and is applied to the raw helium age to yield a corrected age.

$$F_T = 1 - \frac{3S}{4R} + \frac{S^3}{16R^3}$$

R is the grain radius and S is the alpha-stopping distance of 19 to 20 μm (Farley *et al.* 1996). It follows that

$$\text{Corrected Age} = \frac{\text{Measured Age}}{F_T}.$$

Meaningful helium ages therefore either require large crystals or correction. F_T correction is only carried out on helium ages whose samples have cooled rapidly through the closure temperature (see below).

The effect of grain size on diffusion systematics

Helium diffusivity scales with the inverse square of the grain size. So, larger crystals retain a greater fraction of radiogenic helium than small crystals. Firstly, this affects the closure temperature of apatite, with variation of around 5°C for grain radii of 50 to 150 μm (Farley 2000). In addition, and most importantly, helium ages must vary not only with thermal history but also with crystal size (Reiners & Farley 2001). For apatite crystals that have spent time cooling through the PRZ, enough time to cause appreciable helium diffusion, larger grains will yield older helium ages than smaller ones for the same thermal history.

5.3.4 Mineral inclusions

Apatite crystals picked for (U-Th)/He dating should not contain inclusions of other minerals, e.g. zircon, that would themselves produce radiogenic helium. The use of such grains produces anomalously old helium ages. When deducing the uranium and thorium concentrations, mineral inclusions, particularly zircon, typically do not dissolve in the hydrochloric acid used to dissolve the apatite. Therefore, old ages are obtained due to the helium from the inclusions (but not the uranium and thorium) being counted in the analysis. As such, this excess helium is known as 'parentless' helium.

5.3.5 Thermal history reconstruction

Helium ages are only independently useful if it can be shown that cooling was rapid through the closure temperature, as described above. Helium ages are meaningless by themselves if a sample cooled slowly through the PRZ, since there is no way of knowing how much helium has diffused from the crystal. This is in contrast to the fission track technique where a track length distribution records the thermal history within the PAZ. Therefore, helium ages should be interpreted in conjunction with fission track data for the same sample. A helium age should not be older than a fission track age, given the lower closure temperature of the helium system. An older helium age indicates excess helium in the system that was probably derived from mineral inclusions not seen during the grain picking process (see Section 5.3.4 above). The track length distribution can be used to indicate if the sample is likely to have suffered diffusional loss of helium within the PRZ. If it is deemed that helium loss has occurred then the helium age can be modelled with the fission track data given understanding of the relationships between helium diffusion, temperature and grain size.

Kerry Gallagher (Imperial College, London) has adapted his fission track thermal history modelling software, MonteTrax, to model helium ages with fission track data, using the diffusion systematics of Farley (2000). Helium ages can be predicted given a specified thermal history derived from modelling fission track data from the same sample. Then, the observed (actual) helium age is used as a constraint in the fission track modelling process to derive a second thermal history for the sample. If the predicted helium age is in agreement with the observed age, and the two thermal histories are the same, then the helium age has added nothing to the thermal history modelling.

However, if the helium ages and thermal histories disagree with each other, then use of the helium age in modelling of the fission track data has yielded a more likely thermal history than that derived from using just fission track data.

When modelling helium ages, the raw (uncorrected) ages are used since F_T correction does not account for the varying rates of helium production and loss as a sample cools through the PRZ.

5.3.6 Compositional and other effects

Studies suggest that the composition of apatite does not affect the sensitivity of the helium closure temperature (Wolf *et al.* 1996; House *et al.* 1999), and that there is only weak anisotropy in helium diffusion through apatite (Farley 2000). This is in contrast to the effect of chlorine on fission track annealing kinetics (see Section 5.2.4 above). However, Farley (2000) draws attention to the possibility that crystal defects and/or radiation damage sites may impede helium mobility.

5.4 Fission track and (U-Th)/He age-elevation/depth relationships

Apatite fission track and (U-Th)/He studies are generally carried out by sampling over a range of depths, from a well or borehole, or over a range of elevations in areas of high relief. With the fission track technique, such sampling is often carried out with a view to deriving a geothermal gradient (e.g. Bray *et al.* 1992; Green *et al.* 1999; Green *et al.* 2001). If modelled thermal histories of such samples indicate that they all experienced their maximum temperature at the same time, a linear regression of temperature against depth defines the geothermal gradient at this time. This is either a *palaeo*geothermal gradient, or could be the current geothermal gradient if the samples are believed to be at their maximum temperatures at the present day.

Areas that have experienced relatively recent rapid uplift and denudation may show, given sufficient relief, an age-elevation relationship between samples (e.g. Gallagher *et al.* 1995; House *et al.* 1997; Wolf *et al.* 1997; Reiners *et al.* 2002; Cunningham *et al.* 2003). Samples that were deep before the onset of uplift will have either been in the PAZ/PRZ or at even higher temperatures, and will have correspondingly young fission track and helium ages; these samples may be collected from a valley bottom. Samples that were at shallow depths before uplift, residing at lower temperatures, will have older ages; these samples may be collected from a mountain top. Such age-elevation relationships can be used to infer uplift rate if there is enough relief to expose the deepest part of the age-elevation profile.

5.5 Previous studies in Ireland

Regional-scale uplift occurred around the Cretaceous-Tertiary boundary across northwest Europe (e.g. Saunders *et al.* 1997; Jones *et al.* 2002). Throughout the Tertiary, Ireland was being denuded (Allen *et al.* 2002). Indicative of this, there are no Tertiary marine deposits onshore, and non-marine deposits are scattered across the country ranging in age between Eocene and Miocene. In addition,

extensive karstification exists in the limestone lowlands and remnants of Tertiary weathering are widespread (Coxon & Coxon 1997; Drew & Jones 2000; Coxon 2001b). The subsequent glaciations then stripped most of Ireland of its weathered mantle and modified the landscape to its present form (Coxon 2001a).

Allen *et al.* (2002) have quantified the amount of Tertiary denudation across Ireland using the fission track technique. They observed that some areas apparently underwent more denudation than others, and Cunningham *et al.* (2003) suggested that fault movement facilitated such differential denudation in southeast Ireland. Other fission track studies (Keeley *et al.* 1993; McCulloch 1993, 1994; Green *et al.* 2000; Solla Hach 2002) all agree that samples underwent progressive cooling during this time.

Allen *et al.* (2002) use two annealing models (built into MonteTrax) to estimate denudation. The first is that of Laslett *et al.* (1987), and the second an unpublished annealing model by Kerry Gallagher which modifies the Laslett *et al.* (1987) model, attempting to correct for low-temperature annealing out of the PAZ. The modified model does not change the annealing kinetics of that of Laslett *et al.* (1987). They quote an average denudation of between 1.2 km (using Gallagher's model) and 1.5 km (using the model of Laslett *et al.*) for Ireland during the Tertiary, using a palaeogeothermal gradient of 22°C km^{-1}. According to Green *et al.* (1999), there is no evidence to suggest that the northwest Atlantic margin experienced an elevated geothermal gradient at the start of the Tertiary due to igneous activity of the North Atlantic Igneous Province.

The (U-Th)/He technique has not previously been used in Ireland.

5.6 Rationale behind this study

Figure 5.1 shows contoured modelled palaeotemperature at the start of the Tertiary (65 Ma) for the whole of Ireland and the west/northwest region of interest. The data (unpublished in this form) was used by Allen *et al.* (2002) to create denudation maps. (Appendix 24 contains individual sample data and modelled palaeotemperatures.) Sample density is non-uniform across the country, so the fine detail of apparent temperature variations produced by the nearest neighbour contouring method should not be taken as fact.

As expected, the Laslett *et al.* (1987) annealing model (Figure 5.1a) predicts higher palaeotemperatures (a mean of 66°C) compared to those predicted by Gallagher's model (a mean of 51°C) (Figure 5.1b). In the northwest, which has relatively good sample coverage, counties Galway and Mayo generally show cooler predicted palaeotemperatures than do the more northerly counties of Leitrim, Fermanagh and Donegal. For example, a comparison of Connemara with northwest Co. Donegal in Figure 5.1a shows palaeotemperatures may have varied by up to 30°C which, when converted to depth, would correspond to a value in excess of 1 km.

In summary, from thermal history modelling, samples are predicted to have been at ambient temperatures close to 60°C at the start of the Tertiary, and therefore close to the top of the PAZ, be it above or below this threshold temperature.

Whilst the modified annealing model of Gallagher attempts to correct for low temperature annealing, which is otherwise ignored by the Laslett *et al.* (1987) model, neither of the models address the problem of varying apatite chemistry, which can affect how readily fission tracks anneal (see chemical composition changing the annealing characteristics of apatite (see Section 5.2.4 above). Modelled thermal histories may therefore differ between samples whose actual thermal histories are the same, potentially negating the variations in palaeotemperature described above.

Compounding the effects of the uncertainties already described, many Irish samples appear to contain thermal histories dating back to the upper Palaeozoic (Green *et al.* 2000; Allen *et al.* 2002). It therefore becomes increasingly difficult to attach confidence to the modelled timing of the last portion of such samples' thermal histories, all of which may have occurred outside the PAZ if the sample, say, resided at shallow depths during the Mesozoic. Ideally, to study the Tertiary thermal history of Ireland using thermochronology, samples should not contain any pre-Tertiary thermal signature.

Samples taken from Tertiary intrusives obviously conform to this criterion, but are, in the vast majority across the west/northwest region, basic in composition, and would not be expected to yield apatite in useful amounts. However, samples taken from the host rock baked zones of Tertiary intrusions could be useful. One such sample, from close to the Killala gabbro, Co. Mayo, gives a fission track age of 56 ± 5.4 Ma (McCulloch 1993). Another such sample, from close to the Doraville dyke, Co. Fermanagh, gives an age of 73 ± 12 Ma (Allen *et al.* 2002). Both these ages are within error of published radiometric ages for the intrusions (Thompson 1986; Johnston & Rundle 1993). The ages, together with long mean track lengths, indicate that, firstly the fission track ages were reset to zero on intrusion and, secondly no annealing took place subsequently to reduce the age or mean track length.

This study uses such 'thermal history resetting' by early Tertiary dykes. It uses not only the fission track technique, but also (U-Th)/He dating whose dates should reflect the complete liberation of He on intrusion. The sensitivity of the (U-Th)/He technique to slightly lower temperature thermal histories may help constrain with greater confidence the magnitude of Tertiary denudation in west/northwest Ireland. In reality, most Tertiary intrusions in the region have emplacement dates of around 60 Ma (e.g. Macintyre *et al.* 1975) (see Figure 1.6), so results will actually apply to approximately the last 60 Ma.

In simplistic terms, ages might fall into one of three categories (Figure 5.2). If ambient temperatures at the time of intrusion were, say, 80°C (Figure 5.2a (i)), then both the fission track and helium ages should be younger than the age of the dyke, since partial annealing and liberation of He would continue after resetting for the time the sample remained in the PAZ and PRZ. This should also be reflected in a reduced MTL. A sample that was at 30°C on intrusion (Figure 5.2a (ii)) should show fission track and helium ages corresponding to the age of the intrusion, since the sample will have cooled from outside the PAZ and PRZ after resetting. Thirdly, a sample that was at an ambient temperature of around 50°C when resetting occurred (Figure 5.2a (iii)) should show a fission track age corresponding to the age of the dyke, but a slightly reduced helium age reflecting time spent exiting the PRZ after intrusion.

In this simplistic model, if the land surface was initially horizontal when intrusion took place then collection of samples over a range of elevations in the current topography might yield a range of ages. Ideally, borehole samples would give a greater depth range than is afforded by topographic relief in Ireland. However, the necessity of sampling next to an intrusion precludes the use of boreholes.

Estimates of denudation may then be made after application of a suitable geothermal gradient, and will apply to the time period since intrusion, i.e. the Tertiary.

5.7 Sampling

Sample sites were chosen mainly where granite is the host rock, to maximise the potential for sufficient apatite yields. Dykes were chosen to be as wide as possible and to have clear margin exposure. Wide dykes of a single intrusion phase heated the host rock for longer. Wide *multiple* dykes would have also caused prolonged host rock heating, but at successively lower temperatures as each injection phase occurred, presumably centrally within the dyke. In addition, sampling was carried out at a range of elevations to investigate possible age-elevation relationships.

From earlier study of Tertiary dykes across the region (see previous chapters), potential sampling sites were identified. The best exposures exist on the coast, where dyke contacts are invariably accessible. However, whilst inland exposures of dykes are plentiful, especially in mountainous areas, it is rare to find dyke margins exposed, since they often form the locus of channels, streams, etc. The majority of samples, therefore, were collected from the coast at sea level. In addition to sampling from dyke margins, control samples were included, away from the heating effects of the dykes, for fission track and (U-Th)/He dating.

Figure 5.3 shows the sample locations. The sampled areas are west Connemara, northwest Co. Mayo, and south and northwest Co. Donegal. Handheld GPS was used, allowing accurate placement of inland samples.

Samples taken at elevation are confined to the Derryveagh mountains of northwest Co. Donegal and one sample from the Blue Stack mountains in the south of the county. These samples come from dykes that have not been described in the previous chapters. Elevations were obtained from 10 m resolution digital elevation models, compiled from Ordnance Survey of Ireland 1:50000 digital contour data.

Table 5.1 accompanies Figure 5.3 in listing the samples used in this study.

The samples are described below. Refer to Appendix 2 for an index of all the maps used to locate the intrusions, and also to Figure 2.5, Figure 2.9 and Figure 2.23.

Samples M1 to M3

Samples M1, M2 and M3 are from western Connemara, associated with the West Connacht systems of Mohr (1982). M1 was collected at sea level adjacent to a 4 m wide dyke (dyke WC4ib of Figure 2.5) that appears, by proximity, to be associated with the main NE-SW dyke system, CI. The dyke (and a narrower dyke a few metres to the south) trends west towards the southwest end of system CI

through the Caledonian Omey granite.

Samples M2 and M3 are both from the margin of system CI. M2 comes from the north side of Ballynakill Harbour, at sea level, where the dyke (dyke WC25a of Figure 2.5) cuts the south side of Tully mountain. The dyke here is 4.5 m wide and the host rock is psammite, part of the Dalradian Lakes Marble Formation. Sample M3, slightly elevated, is located where the dyke (dyke WC32a of Figure 2.5) cuts the coast north of the mouth of Killary Harbour. The dyke is approximately 12 m wide and looks to be a multiple intrusion of two phases, the first producing a dyke around 7 m wide, the second extending the width to around 12 m. The host rock is sandstone of the Ordovician Mweelrea Formation.

Samples C1i, C1ii and C1iii

Sample C1i was selected as a control for sample M1, and was taken from the Omey granite from the sample set (sample CL1) used by Allen *et al.* (2002) (see Appendix 24).

Samples C1ii and C1iii come from the Galway granite to the southeast, and are also from the sample set (samples GG12 and GG13 respectively) used by Allen *et al.* (2002) (see Appendix 24). They do not act as a control for any of the margin samples.

Fission track data, therefore, already existed for these samples.

Samples M4 and M5

Samples M4 and M5 are associated with the western end of the Killala swarm. Sample M4 was taken from the margin of a 3 m wide dyke (dyke K2 of Figure 2.9) cutting gneiss of the Annagh Division. M5 comes from the margin of a dyke 4.3 m wide (dyke K62 of Figure 2.9) cutting psammite of the Dalradian Broad Haven Formation. Both samples were collected at sea level.

Sample C2

Sample C2 was taken as a control for nearby samples M4 and M5 from gneiss of the Annagh Division.

Sample M6

Sample M6 was collected from the Blue Stack mountains adjacent to a 5 to 8 m wide dyke, part of the Donegal-Kingscourt swarm, at 530 m elevation. The host rock is the Caledonian Barnesmore granite. Unfortunately, this sample did not yield apatite.

Samples M7 to M9

Samples, M7, M8 and M9 associated with the Donegal-Kingscourt swarm, were collected at sea level adjacent to dykes of widths 3.1 m (dyke DK32 of Figure 2.23), 6 m (dyke DK33 of Figure 2.23) and 4 m (dyke DK40 of Figure 2.23) respectively on the northwest Co. Donegal coast. The host rock is the Caledonian Thorr granite.

Samples C3 and C4

Samples C3 and C4, from the Thorr granite, act as controls for samples M6 to M8.

Samples M10 and M11

Both samples M10 and M11 were taken inland in the Derryveagh mountains, Co. Donegal. Comprised of the Caledonian Main Donegal granite, the mountains are cut by many dykes of the Donegal-Kingscourt swarm, and reach an elevation of 652 m above sea level at the summit of Dooish. Other peaks are typically between 450 m and 550 m in elevation. Sample M10 was collected adjacent to a 7 to 8 m wide dyke in the northwest-facing back slope of the Poison Glen. At 340 m elevation, the sample location lies 1.5 km northwest of the Gweebarra fault. Sample M11 comes from the margin of a 5 m wide dyke at 260 m elevation, 400 m southeast of the Gweebarra fault. Although dykes outcrop at higher elevations in the area, a dearth of host rock exposure at dyke margins precluded sample collection.

Samples C5 to C9

Samples C5 to C9 were collected as controls for samples M10 and M11 at a range of elevations in the Main Donegal granite. C5 was taken at 360 m elevation 4 km west of Slieve Snacht. C6 was taken at 665 m from the top of Slieve Snacht. Samples C7 and C8 were taken from the flank and summit of Dooish at 355 m and 640 m respectively. All the above sample locations are on the north side of the Gweebarra fault. Sample C9, to the south of the fault, was taken at 265 m elevation.

Care was taken to ensure that these samples' locations were not close to any Tertiary dykes. The closest known dyke is situated approximately 100 m from sample C6, cutting the summit of Slieve Snacht.

5.8 Preparation and analysis

Initially, some margin samples were thin-sectioned in the Department of Geology, Trinity College to check for the presence of apatite. Mostly, this was carried out with the non-granitic host rock because of uncertainty of apatite yields. Cathode luminescence was used to identify apatite, as it glows a distinctive bright yellow-green and is easily spotted.

All margin samples were crushed using a jaw crusher, sieved to a 500 μm size fraction, washed and dried in the Department of Geology, Trinity College. Heavy liquid and magnetic separation was carried out at Birkbeck College, London by Andrew Carter. All control samples were crushed and separated at Birkbeck College by Andrew Carter.

Fission track and (U-Th)/He analyses were carried out and/or coordinated by Andrew Carter at Birkbeck College, London.

Fission track

Spontaneous fission tracks were revealed by the etching of polished apatite grain mounts with 5N HNO_3 at 20 ± 1°C for 20 s. Mounts were irradiated in the thermal facility at the Hifar reactor at Lucas Heights, Australia (cadmium ratio (thermal/epithermal + fast neutrons) > 200), using the external detector method and 0.5 for the $4\pi/2\pi$ geometry correction factor. Dosimeter glass CN-5 was used to measure neutron fluence. Muscovite mica external detectors were etched after irradiation using 48% HF at 20 ± 1°C for 35 minutes. Observation and measurement of induced fission track density and length was conducted under transmitted light using a Zeiss axioplan microscope with a total dry magnification of x1250. Reflected light was used as a tool for discriminating individual tracks. Only crystals with prismatic sections parallel to the c-crystallographic axis were analysed. Horizontal confined fission track lengths were measured using a digitising tablet calibrated before each analysis against a stage micrometer. Ages were determined using the zeta calibration method ($\xi_{CN\text{-}5} = 338 \pm 4$) and IUGS recommended age standards (Hurford 1990). All data are reported as the central age (modal age weighted for different precisions of individual crystals) together with the percentage age dispersion, or relative error (R.E.%) (Galbraith & Laslett 1993).

$P(\chi^2)$ indicates if the single grain age distribution for a sample has a Poissonian form. A value less than 5% constitutes a 'failure' of the χ^2 test, indicating non-Poissonian distribution and probable multiple grain populations. In this case a relatively high value for R.E.% results.

For a more detailed explanation of analytical terms see the Glossary in Appendix 25. Table 5.2 and Table 5.3 show fission track analytical data. Appendix 25 and Appendix 26 contain individual grain and raw track length data respectively for all samples.

(U-Th)/He

Apatite grains were carefully hand picked to avoid mineral and fluid inclusions. Only granite contained apatite suitable for analysis. Each selected grain was photographed, dimensions recorded for later alpha ejection correction, and loaded into platinum microtubes for helium outgassing and (U-Th) determination. Samples were outgassed using an induction furnace at temperatures of 950°C. The abundance of ^4He was measured relative to a 99.9% pure ^3He spike in a Pfeiffer Prisma 200 quadrupole mass spectrometer. Reproducibility of the ^3He spike is determined from daily measurements against an accurately known ^4He standard. Within-run spike:standard ratio variation is <0.06% (standard:spike ratio variation 0.13% daily, n = 3-4). All samples were subjected to re-extract cycles to monitor for mineral/fluid inclusions. Quantification of (U-Th) was performed on a Micromass Isoprobe multicollector ICPMS using spiked solutions of the dissolved apatite, using 2% HNO_3 / 0.1% HF. Repeated analysis of the California Institute of Technology (CIT) laboratory Durango apatite standard reproducibility, based on 39 analyses, gives an age of 31.3 ± 1.2 Ma (2σ). This error of the mean (3.7%), combined with the (U-Th) and He analytical uncertainties is used throughout the study as a measure of the total uncertainty in sample age.

Table 5.4 shows (U-Th)/He analytical data for all samples.

Microprobe analysis

Microprobe analyses were carried out by Andrew Carter to ascertain the chemistry of the apatite from the background samples, specifically to check the chlorine levels (see Section 5.2.4 above). A 15 KeV beam (5 to 20 μm in diameter) was used with 20 nA of current. The beam was defocused to prevent fluorine and chlorine migration. An average of three spots per grain were taken. NaCl was used as a standard.

5.9 Results

5.9.1 Fission track results

Results are detailed in Table 5.2 and Table 5.3. All errors are quoted at ± 2σ.

The margin samples range in central age between 54.3 ± 9.2 and 61.9 ± 6.0 Ma, and six of the ten samples range between 58 and 60 Ma. All ages lie within error of each other. Mean track length (MTL) values are also confined to a small range between 14.12 ± 0.16 and 14.72 ± 0.42 μm, and all the track length distributions are unimodal (Figure 5.4). The two relative outliers in MTL, M5 and M10, with values of 14.72 ± 0.42 and 14.66 ± 0.20 μm respectively are not spatially related on the scale of this study, the former deriving from northwest Co. Mayo and the latter from northwest Co. Donegal. Sample M2 has a relatively young fission track age of 54.3 ± 9.2 Ma but still overlaps in error with the older ages. M1 and M3, close to M2 and associated with the same dyke system, do not show a similar trend towards younger ages.

Figure 5.5 shows data plotted for the control samples. Fission track ages of the control samples are all much older than those of the margin samples, and are in line with previous fission track studies (e.g. Allen *et al.* 2002) (Figure 5.5a). Track length distributions appear to be unimodal, with the possible exception of sample C5, and four of the eight samples (C2, C4, C7 and C8) show almost identical distributions. In northwest Co. Donegal (samples C3 to C9), fission track ages are in excess of 200 Ma, except for sample C7 at 176.7 ± 18.8 Ma. Mean track lengths are generally around 13 μm, except C5 and C9 with lower values of 12.69 ± 0.30 and 12.60 ± 0.28 μm respectively. These values contrast with published data from this part of Ireland, (see Allen *et al.* 2002), which show younger ages (175 to 200 Ma) and shorter mean track lengths (around 12.25 μm) (Figure 5.5b and Appendix 24). They are also older than the mean values from published data for the whole of the country of 169 Ma, and 12.52 μm for age and MTL respectively (Figure 5.5a).

From northwest Co. Mayo, sample C2 has an old fission track age (203.8 ± 16.8 Ma) and high MTL (13.24 ± 0.28 μm), comparable with the northwest Co. Donegal samples. Most of the closest published samples, which lie to the southeast in the Ox mountains, have younger fission track ages between 150 and 170 Ma, and mean track lengths range between 12.49 and 13.31 μm (Figure 5.5b and Appendix 24).

Samples C1i, C1ii and C1iii (CL1, GG12 and GG13 respectively of Allen *et al.* (2002) from western Connemara have younger fission track ages of 146 ± 10 Ma, 141 ± 8 Ma and 128 ± 10 Ma respectively, and are in line with other samples from the Connemara and south Co. Mayo area (Figure

5.5b).

The control samples, therefore, give relatively old ages and mean track lengths, as discussed above. Other regions showing old fission track ages are the Slieve Bloom mountains in the midlands and the Party mountains in south Co. Mayo. Northeast Ireland, however, has the oldest fission track ages, some being in excess of 300 Ma.

For most of the margin and control samples, $P(\chi^2)$ values (Table 5.2) indicate that samples yielded apatite from single populations in age. Exceptions are samples M1, M8, M11, C2, C8 and C9, which have values of $P(\chi^2)$ <5%. Of these exceptions, all but C2 are samples from granite so should be expected, therefore, to yield a single population of grain ages given that apatite is not 'inherited', and assuming that the apatite has a uniform composition in terms of Cl content.

The shapes of the single grain age histograms show that the margin samples (Figure 5.4) have tighter distributions than the control samples (Figure 5.5a). A failure of the χ^2 test for a sample generally correlates well with an apparent multi-modal histogram distribution, e.g. sample C2. However, samples that statistically indicate a single grain age population do not necessarily imply this in histogram form, e.g. sample C6. This results from the histogram not taking into account errors on the individual grain ages (see Appendix 25) and therefore not being as statistically rigorous.

5.9.2 (U-Th)/He results

Results are detailed in Table 5.4. Since only granite apatite was suitable for (U-Th)/He dating, data come from Connemara, and from northwest Co. Donegal. All replicate ages are shown. FT correction was applied to all raw ages using the equations described above Section 5.3.3. An alpha-stopping distance of 19.7 μm was used (after Farley *et al.* (1996)). Errors for the corrected ages are ± 6% (2σ), based on the reproducibility of ages for the Durango apatite (Andrew Carter *pers. comm.*, and shown in Appendix 27).

Mean ages have been calculated for samples whose replicate ages are deemed to be in reasonable agreement with each other (see below for discussion), and are derived by simply taking the mean of the replicate ages for each sample. Errors of the mean age are reported at one standard deviation (in Table 5.4) as standard errors, by dividing the standard deviation of the replicate ages by (n-1), where n is the number of replicate analyses performed. In the case where only two replicates were analysed, the error is given as half of the age difference. This is the method used by Clark (2005). Where the standard error is reported at two standard deviations, the same method is applied. Ages rejected are those that are, for the control samples, substantially older than the fission track age, and, for the margin samples, those that are anomalously older than the dykes (assuming resetting took place when the dykes were emplaced). See below for further discussion. Rejected ages are assumed to be due to excess helium.

The margin samples show quite good consistency between replicates (Table 5.4). Mean helium ages have been calculated for three of the six samples. Mean ages of 66 ± 1.0 Ma and 68 ± 3.8 Ma were calculated for samples M8 and M11, but each contained one poorly replicating age, which was not included in the mean. Samples M1, M9 and M10 did not replicate well, probably due to excess

helium in the system. Sample M7 yielded the closest replicating ages and yielded a mean age of 59.9 ± 2.2 Ma.

The control samples do not show the same consistency in replicate helium ages as the margin samples (Table 5.4). Mean ages have been calculated for five of the nine samples. For sample C1i, the age of C1ia was not included in the mean. The ages are consistently older than those of the margin samples. Mean helium ages from Connemara, Co. Galway are within error of each other at 85.3 ± 15.6 Ma and 89.6 ± 14.0 Ma. Mean helium ages from northwest Co. Donegal are 171.9 ± 20.4 Ma, 181.7 ± 1.6 Ma and 239.8 ± 17.4 Ma. Ages are therefore consistently older for the Co. Donegal samples. Those ages in Table 5.4 that are indicated to contain excess helium are discussed below in Section 5.10.

5.9.3 Microprobe analyses

All control samples from northwest Co. Donegal, samples C3 to C9, were analysed. The results are listed in Appendix 28 and show that chlorine is below detection levels (value of zero or negative) in all samples, except sample C6 where chlorine is just detectable.

5.9.4 Age-elevation relationships

It has been discussed above in Section 5.4 how fission track age and/or (U-Th)/He age might show a relationship with elevation, with older ages coming from higher elevations. For the whole of Ireland there appears to be no relationship between fission track age and elevation above sea level (Figure 5.6a) using published data (see Section 5.5 for references). This is perhaps not surprising given the diverse geology across the country, and the likelihood that different parts of the country have undergone different thermal histories.

A large amount (relatively) of fission track data exists in the literature for the region of interest in this study. Figure 5.6b shows that, as for the country as a whole, there is no obvious relationship between fission track age and elevation.

For this study, sampling was carried out at a range of elevations for both margin and control samples. Elevation profiles in Figure 5.6c show the relief sampled in northwest Co. Donegal. The margin samples were collected over 340 m relief and the control samples over 665 m (Table 5.4). It is apparent that the margin samples show no relationship between fission track age and elevation above sea level, even just considering samples from Co. Donegal collected in relatively close proximity to each other. The control samples, on the other hand, hint at a trend when viewed all together for the region. Apart from coastal samples C3 and C4, fission track age shows a crude increase with elevation from C1i to C6. In the Derryveagh mountains, samples C5, C7 and C9, at around 350 m elevation, have younger fission track ages than samples C6 and C8, at around 650 m. The old ages of Samples C3 and C4, however, are an exception to this apparent trend.

For the helium ages, margin samples M7 and M8 were collected at sea level only 2 km apart, and sample M11 was collected from the Derryveagh mountains at 260 m elevation (Table 5.4). The ages

of M8 (66.0 ± 1.0 Ma) and M11 (68.0 ± 3.8 Ma) overlap in error, suggesting that helium age does not increase with elevation, although sample M7 does give a younger age at the coast.

The two oldest mean ages for the control samples come from the Derryveagh mountains, although the older age of the two (sample C8) does not come from the highest elevation, and samples C3 (coastal) and C6 (elevated at 665 m) are actually within error of each other. In addition, the validity of the helium age for sample C8 is questionable; this is discussed below. In Connemara, ages for samples C1i and C1ii are within error of each other, despite a difference in elevation of 145 m between the two samples.

The helium ages therefore do not yield with confidence any age-elevation relationships. More data is needed to test and substantiate the tentative trends described above.

Age-elevation relationships are difficult to pick out of the fission track and (U-Th)/He data from this study. This is not surprising given the relatively little amount of relief available and the paucity of data. In southeast Ireland, Cunningham *et al.* (2003) identify age-elevation relationships in the Caledonian Leinster granite, but the relief is greater at around 900 m. They suggest that this is evidence for rapid exhumation of the PAZ during the Tertiary in this part of Ireland, related to widespread uplift and denudation of the Irish Sea area. Also, Green *et al.* (2000) show a fission track age-elevation relationship over 2 km, from borehole data mostly from northwest Ireland.

5.10 Interpretation of fission track and (U-Th)/He results

All the fission track ages for the margin samples are very close to published radiometric ages for the same intrusions, or different intrusions of the same dyke swarm (Figure 5.7). For the dykes of the Donegal-Kingscourt and Killala swarms, the margin samples lie within error of most of the established K-Ar and Ar-Ar ages for their respective swarms. Samples M1, M2 and M3, associated with the West Connacht system CI, show the most deviation, but M1 and M2 still lie within error of the radiometric ages.

This, and the much older ages of the control samples, indicates that the margin samples were 'reset' (for the fission track system) on intrusion as expected, i.e. fission track ages were reduced to zero at this time. In addition, the long mean track lengths (>14 μm) and unimodal length distributions described above show that no annealing took place after resetting. The samples therefore cooled rapidly through the closure temperature and through the PAZ. This is consistent with the samples not having resided within the PAZ subsequent to dyke emplacement in the early Tertiary. Given this, the fission track ages represent the ages of the intrusions. Therefore, it is interpreted that after dyke emplacement (~60 Ma), the samples cooled through the uppermost crust from an ambient temperature of less than 60°C.

The conclusion that the fission track ages from the margin samples represent the age of the intrusions is a nice consequence of the study, as this provides further ages for Tertiary intrusives in northwest Ireland in areas where no dates currently exist, i.e. the western end of the Killala swarm and the northwestern extent of the Donegal-Kingscourt swarm.

Helium ages need to be interpreted in conjunction with fission track ages to ascertain if the sample is likely to have undergone diffusional loss of helium since passing through the closure temperature (as explained previously in Section 5.3.5). Given that the fission track length data for the margin samples indicates rapid cooling to 60°C, and therefore possibly to even lower temperatures, it is appropriate to use the corrected helium ages for interpreting the margin samples. The corrected replicate ages, and associated errors, that make up the means are generally within error of the fission track ages (see Table 5.4). A helium age of 66.9 ± 8.0 for replicate M1b is taken as a good age for sample M1, and sample M7 shows corrected helium ages and a fission track age that agree almost exactly. The helium ages are therefore interpreted as also having been reset by dyke intrusion. The agreement between fission track and helium ages for the margin samples implies that the helium ages also represent the age of the intrusions. That is, the samples cooled rapidly through the closure temperature (70 to 75°C) of the helium system and have not spent any appreciable length of time in the PRZ since dyke emplacement, ~60 Ma. The ambient temperature at the time of dyke emplacement was, it seems, no greater than around 40°C.

This, therefore, invokes situation (ii) of Figure 5.2 for the margin samples; that is, the samples were above (in depth terms) both the PAZ and PRZ at ~60 Ma when the dykes intruded. Given the lack of any apparent helium age-elevation relationship (although there is not much data available!), the current topographic relief (~650 m), if generated since dyke emplacement, is not enough to have exhumed the early Tertiary PRZ at the coast. This scenario would imply that rock now forming the tops of the Derryveagh mountains was actually cooler than 40°C at the time of dyke emplacement. Alternatively, the current landscape might be a relict from the early Tertiary, in which case the samples would have maintained the same level as each other in the crust throughout the Tertiary.

The control samples yield older fission track ages and have shorter mean track lengths than the margin samples, as described previously. Sample C1i has a fission track age of 146 ± 10 Ma, compared with a mean corrected helium age of 85.3 ± 15.6 Ma. The MTL of 12.98 μm, with a standard deviation of 1.57 μm, is consistent with non-rapid cooling from the closure temperature, i.e. time spent in the PAZ. Alternatively, some recent reheating took place to reduce the MTL. This, and the fact that the helium age is younger than the fission track age, implies that helium loss has taken place. This sample, therefore, needs to be modeled in conjunction with the fission track data (as explained in Section 5.3.5 previously) to derive a thermal history.

The same conclusions can be drawn for samples C1ii, C3 and C6. With sample C6, the proportionally small disparity between the corrected age and the fission track age suggests that not much helium has been lost to diffusion, and the sample has been residing at shallow crustal levels for a long time.

The slightly older corrected helium ages for sample C8 (mean of 239.8 ± 17.4 Ma) compared to the fission track age (227 ± 18 Ma) suggest that there may have been excess helium to falsify the age, but the apparent good replication suggests that modelling this sample might be worthwhile. Again, a slightly reduced MTL indicates long-term residence at low temperatures or recent reheating.

Samples C1iii, C4 and C5 all show helium ages that are older than the fission track ages, so

therefore contained excess helium and are not useful. Sample C7 is also of no use due to poor replication and excess helium in replicate C7a.

Thus, samples C1i, C1ii, C3, C6 and C8 should all be modelled with the fission track data to constrain the thermal histories of the samples. The fact that chlorine levels in the control samples are generally undetectable (as described previously in Section 5.9.3) should be borne in mind when choosing the annealing model to use when modelling the data, since Cl-apatite is known to be more resistant to annealing than F-apatite. The modelling program, MonteTrax (of Gallagher), has some flexibility where apatite composition is concerned.

The observation made in Section 5.9 that fission track and helium ages of the control samples are consistently older from Co. Donegal than they are from Connemara (for example, compare sample C1i with sample C6 (Figure 5.3 and Table 5.4)), probably indicates a longer period of time spent at the highest crustal levels by Donegal samples. Indeed, this observation also holds true for published fission track data (see Figure 5.5b). The interpretation, from the margin samples, that the ambient temperature at the time of dyke emplacement was no greater than around 40°C, implies that helium was accruing throughout the Tertiary with no diffusional loss. Therefore, the observed difference in the ages between the two areas is likely to be a relict of the pre-Tertiary thermal history of the samples, probably due to differences in burial during the Mesozoic. It is acknowledged, however, that the mean track lengths are not necessarily longer for the Co. Donegal samples, compared with the Connemara samples, as might be expected from this interpretation (see Figure 5.5a). Also, it is noted that around five million years elapsed between the start of the Tertiary period and dyke emplacement. A substantial amount of denudation is likely to have taken place during this time, related to uplift thought to have been caused by the proto-Iceland plume.

5.11 Quantifying Tertiary denudation across west and northwest Ireland

Quantifying the amount of rock removal during the Tertiary across the west and northwest Ireland region is the major aim of this study. Using a novel sampling strategy and attaining (U-Th)/He ages, an attempt has been made to address the limitations of previous studies (see previous sections). It is stated that any absolute estimates of denudation, based on interpretation of the results attained (Section 5.10 above), are limited in their credibility by uncertainties (discussed above) in the (U-Th)/He data; the fission track results are sound.

In Section 5.10 it is been suggested that the ambient temperature was no greater than around 40°C when the dykes were emplaced ~60 Ma. This temperature range can be converted to a value for denudation over the last 60 Myr, given that the samples are now at the surface. To do this a geothermal gradient must be applied. It would seem logical to assume that the geothermal gradient was high in the early Tertiary, due to the igneous activity of the North Atlantic Igneous Province (NAIP). Importantly however, Green *et al.* (1999) deduced that the geothermal gradient was *not* elevated along the northwest Atlantic margin at this time.

Allen *et al.* (2002) used a value of 22°C km^{-1} for the Tertiary geothermal gradient, to quantify denudation. This value is used here, and an average surface temperature of 10°C is also assumed.

Given these values, a maximum of 1.4 km of denudation is estimated to have taken place in the last 60 Myr across northwest Ireland. Obviously, if the geothermal gradient is reduced, denudation will increase. Similarly, if the average surface temperature was higher than 10°C during the Tertiary, the value for denudation derived here is an overestimate. Indeed, Ireland was likely subjected to a warm, temperate, wet, or sub-tropical environment for much of the Tertiary (Coxon 2001b; Coxon 2001a). The value of 1.4 km lies between the two estimates made by Allen *et al.* (2002) of 1.5 km and 1.2 km based on two different fission track annealing models (see Section 5.5 above). It is also in agreement with the conclusion of Green *et al.* (2000) that rock removal was at least 1 km over the Tertiary, vitrinite reflectance data from the Lough Neagh Group indicating burial to a depth of less than 1 km during the Tertiary (Parnell *et al.* 1989), and the Ballydeenlea Cretaceous chalk outlier in southwest Ireland, which indicates between 1 km and 1.5 km removal of latest Cretaceous and possibly Tertiary rocks (Evans & Clayton 1998). The value is also in agreement with studies of Great Britain, and the Irish Sea area (e.g. Green *et al.* 2002).

The suggestion in Section 5.10 that the samples at elevation might have been at ambient temperatures appreciably less than 40°C in the early Tertiary, implies that the actual amount of rock removed could be somewhere between just a few hundred metres and a kilometre. In support of this, karst-fill deposits across Ireland as old as Oligocene in age (Drew & Jones 2000 and references therein) (see Figure 1.1), suggest that there has been very little denudation, at least in some areas of Ireland, since the mid-Tertiary.

5.12 Conclusions

A value of 1.4 km is obtained as a maximum value for Tertiary denudation across northwest Ireland. The results are in agreement with previous studies, but the nature of the sampling strategy and the use of the (U-Th)/He technique here allows more confidence to be placed in the new estimate. This maximum value is consistent with previous denudation estimates for Great Britain and the Irish Sea region. In reality, however, it is likely that northwest Ireland did *not* undergo as much denudation as these regions during the Tertiary, as the actual value might be a lot less than 1.4 km.

A further outcome of the study is the dating of several intrusions (to an average of 59 Ma) in parts of the Killala swarm and Donegal-Kingscourt swarm that were previously undated.

Chapter 6 *Summary of conclusions*

There were two main aims to this thesis. The first aim was to better understand the Tertiary tectonic/stress history of northwest Ireland. The second aim, as alluded to in the title, was to study mechanisms of dyke emplacement and host rock deformation.

Each of the four results chapters is self-contained, and distinct conclusions have been drawn in each after discussion. Therefore, this final chapter is simply a list of the main conclusions drawn in each chapter.

The emplacement of Tertiary dykes in northwest Ireland

- Tertiary dykes were emplaced across the northwest Ireland region either by exploitation of pre-existing structures, or in en échelon form arising from the propagation of hydraulic fractures, or by a combination of the two.
- Dykes that intruded pre-Carboniferous host rock (basement) were influenced to a much greater extent by the host rock structural grain. Dykes therefore show a wide range of orientations in the older host rocks. In granite, dykes generally follow the pre-existing fracture pattern, and variation in the fracture pattern is mirrored by variation in dyke orientation. In Dalradian host rock, dyke emplacement is frequently along the metamorphic fabric.
- The interface between basement and cover in the host rock may have caused local intrusion of sills. These sills would have facilitated adjustment in orientation of dykes of variable trend rising through pre-existing structures in the basement, as they adopted the much narrower range in orientation in the cover host rock indicative of propagation by hydraulic fracturing.
- Dykes emplaced into Carboniferous host rock show, almost exclusively, en échelon segmented styles of intrusion. The basic geometric relationships of these dykes conform to those of extensional fractures at a much larger scale and even up to the scale of ocean spreading centres.
- En échelon dykes of the Killala swarm were emplaced by hydraulic fracturing and possible local exploitation of pre-existing fractures. Differences in host rock lithology and bed thickness caused breakdown of the extensional fractures into en échelon arrays.
- Some en échelon dykes in the Killala swarm show apparent conjugate relations and may have propagated under hybrid extension/shear with horizontal compression in the direction of the dykes. The stress regime at the time of intrusion might have therefore been, for at least part, strike-slip.
- The overall trends of the Donegal-Kingscourt and Killala swarms, and the West Connacht systems, are NW-SE, E-W and NE-SW respectively. These trends reflect the extension directions that operated in the Palaeocene to accommodate dyke intrusion.

- For the West Connacht systems, the overall trend indicates an extension direction of ~150°. The mid section of system CI, however, emplaced in en échelon form, implies an extension direction of ~122°.
- The extension direction for the Killala swarm, derived from the en échelon dykes in Carboniferous host rock, is 006° with a swing to NE-SW extension in the vicinity of the Killala gabbro. The Killala gabbro, therefore, appears to have locally influenced crustal stresses. Crustal extension that accommodated the Killala swarm is 1.45%.
- The Donegal-Kingscourt swarm shows consistency in independently derived extension directions of 041°, from dykes in Carboniferous host rock, and 047° from averaging the opening directions of dykes in granite.
- The opening directions of dykes that exploit pre-existing fractures in the Killala swarm and the West Connacht systems are generally orthogonal to dyke strike. This implies that either magma pressures were high and/or the tectonic regime at the time of dyke emplacement during the early Tertiary was not particularly active, i.e. the difference in magnitude between the horizontal principal stresses was not large. Surely the *interplay* between crustal stresses and magma pressures was crucial in controlling the range in dyke orientation observed across the region.
- The most important factor for reliably establishing the regional extension direction for the dykes across northwest Ireland (apart from looking at the geometry of the swarm as a whole on the largest scale) is that a number of dykes across an area show en échelon geometry. The best example of this is the eastern end of the Killala swarm.
- On the regional scale, the apparent anomalous trend of the Killala swarm might be explained by a deflection in the crustal stresses caused by emplacement of the Brendan centre and its associated radial dyke systems. The Killala swarm would therefore represent an intermediary stress direction in a regional swing from NE-SW extension to the NW-SE extension associated with the northeast side of the Brendan centre.

Host rock deformation resulting from dyke emplacement

- Emplacement of dyke across northwest Ireland caused deformation of the host rock, manifest mainly as dyke-parallel fractures.
- The extent of the host rock deformation away from the dykes is dependent on dyke width.
- Structures close to the dyke can be related to hydraulic fracture that took place as the dykes were emplaced. Fractures distal from the dyke may have formed by some other means.
- Hydraulic fracturing can, broadly speaking, be split into two types: fracturing associated with dyke segment overlap, and fracturing remote from overlap zones.
- Deformation of the host rock in the vicinity of dyke segmentation is controlled by mode II shear that is induced as segments overlap, and then also by the stresses induced as the host rock bridge rotates during segment dilation. Left-stepping segmentations are characterised by sinistral shear

and right-stepping segmentations are characterised by dextral shear. The sense of shear induced is in agreement with theoretical models of stress trajectories in the vicinity of overlapping fractures, and can also be explained by a deformation model of flexural slip of the host rock bridge as it rotates due to segment dilation. In fact, all deformation observed *within* the host rock bridge may be a response to dyke segment dilation.

- However, when dyke segments stop propagating in overlap, stresses caused by rotation of the host rock bridge and the dilation differential as segments taper take over from the earlier stress regime related to segment overlap. The host rock bridge appears to respond by flexural slip. In fact, all deformation observed *within* the host rock bridge may be a response to segment dilation.
- The same structures associated with dyke segmentation occur over a range of scales, from centimetre-scale to tens of metres. Detailed mapping of the orientation of these structures can help to define the three-dimensional geometry of en échelon segmentation, with just a horizontal cut through the dyke. Propagation of the Killala swarm was, at least in part, oblique through the crust.
- Hydraulic fracturing *remote* from segment overlap is manifest as a combination of coevally forming tensile fractures parallel to the dyke, and shear fractures that subtend small angles to the dyke. Conjugate relations between the shears, with acute angle bisecting lines lying in the plane of the dyke, are consistent with their formation as the dyke propagated. The very low dihedral angles of conjugate pairs suggest that the shears are mixed-mode I-II hybrid structures. The presence of hybrid extension/shear structures implies that stresses in the plane of the dyke at the time of intrusion were great enough to prevent the exclusive formation of tensile fractures. Given, this model, the general sub-horizontal orientation of the conjugate bisecting lines implies that horizontal stress was greater than the lithostatic load. Thus, a sub-horizontal differential stress is invoked to have acted parallel to the dykes at the time of intrusion.
- It cannot be proved that fractures in the distal portions of the dyke-associated fracture zones formed by hydraulic means. The indication that the extent of dyke-associated fracturing in the host rock is dependent on dyke width suggests that fractures, at least distally from the dyke, formed by a different mechanism.
- Thermal stress is a possible additional cause of fracturing in the host rock adjacent to dykes, and might control the *extent* to which fracturing takes place away from dykes. Fractures might form close to the dyke margin as the host rock expands into space created by contraction of the dyke as it cools. Fractures might also form from thermal contraction of the host rock. Thermal modelling shows that an increase in temperature of the host rock in the order of 90° above ambient is possibly a threshold temperature, above which the host rock must be cooled from, for fractures to form in the distal portions of the dyke-associated fracture zone.
- Host rock deformation associated with dyke intrusion is extremely complicated. Attributing fracture of the host rock solely to hydraulic means as a dyke intrudes is probably not correct.

The stress regime in northwest Ireland *after* dyke emplacement

- Tertiary dykes that are faulted are rare in northwest Ireland. For a dyke to be considered as faulted, the fault plane needs to be seen, and kinematic indicators identified, to prove that movement on the fault displaced the dyke. It is much more likely that the 'displacement' is a transform offset or syn-emplacement jog.
- N-S compression in a strike-slip stress regime is derived from three dykes that are unambiguously faulted, and a fourth set of dykes that show intra-dyke deformation.
- Evidence suggests that this stress acted soon after dyke emplacement in the early Tertiary. It is consistent with the compressional stress state thought to have been affecting the northwest European margin since break-up in the northeast Atlantic at the start of the Eocene.

Tertiary denudation across northwest Ireland

- A maximum of 1.4 km of denudation occurred across northwest Ireland after Palaeocene dyke emplacement (based on the stated assumptions). The actual value might be a lot less than 1.4 km.
- This result is more secure than those from previous fission track studies, given the sampling strategy adopted and the use of the (U-Th)/He technique for the first time in Ireland.
- In addition, several dykes have yielded intrusion ages that average 59 Ma in parts of the Killala and Donegal-Kingscourt swarms that were previously undated.

References

ACOCELLA, V., GUDMUNDSSON, A. & FUNICIELLO, R. 2000. Interaction and linkage of extensional fractures and normal faults: examples from the rift zone of Iceland. *Journal of Structural Geology,* **22**, 1233-1246.

ALLEN, P.A., BENNETT, S.D., CUNNINGHAM, M.J.M., CARTER, A., GALLAGHER, K., LAZZARETTI, E., GALEWSKY, J., DENSMORE, A.L., PHILLIPS, W.E.A., NAYLOR, D. & SOLLA HACH, C. 2002. The post-Variscan thermal and denudational history of Ireland. *In*: DORÉ, A.G., CARTWRIGHT, J.A., STOKER, M.S., TURNER, J.P. & WHITE, N. (eds) *Exhumation of the North Atlantic Margin: Timing, Mechanisms and Implications for Petroleum Exploration.* Geological Society, London, Special Publications, **196**, 371-399.

ANDERSON, E.M. 1938. The dynamics of sheet intrusion. *Proceedings of the Royal Society of Edinburgh,* **58**, 242-251.

ANDERSON, E.M. 1951. *The dynamics of faulting and dyke formation with application to Britain.* Oliver and Boyd Ltd., Edinburgh.

ANDERSON, T.B., PARNELL, J. & RUFFELL, A.H. 1995. Influence of basement on the geometry of Permo-Triassic basins in the northwest British Isles. *In*: BOLDY, S.A.R. (ed.) *Permian and Triassic Rifting in Northwest Europe.* Geological Society, London, Special Publications, **91**, 103-122.

ANDREWS, J.R. & EMELEUS, C.H. 1975. Structural aspects of kimberlite dyke and sheet intrusion in south-west Greenland. *Physics and Chemistry of the Earth,* **9**, 43-50.

AYDIN, A. & NUR, A. 1982. Evolution of pull-apart basins and their scale independence. *Tectonics,* **1**, 91-105.

BADLEY, M.E. 2001. Late Tertiary faulting, footwall uplift and topography in western Ireland. *In*: SHANNON, P.M., HAUGHTON, P.D.W. & CORCORAN, D.V. (eds) *The Petroleum Exploration of Ireland's Offshore Basins*, **188**, 201-207.

BAER, G. & BEYTH, M. 1990. A mechanism of dyke segmentation in fractured host rock. *In*: PARKER, A.J., RICKWOOD, P.C. & TUCKER, D.H. (eds) *Mafic Dykes and Emplacement Mechanisms.* A.A. Balkema Publishers, Rotterdam, 3-11.

BEACH, A. 1975. The geometry of en échelon vein arrays. *Tectonophysics,* **28**, 245-263.

BEVINS, R.E., HORÁK, J.M., EVANS, A.D. & MORGAN, R. 1996. Palaeogene dyke swarm, NW Wales: evidence for Cenozoic sinistral fault movement. *Journal of the Geological Society, London,* **153**, 177-180.

BLUNDELL, D.J. 2002. Cenozoic inversion and uplift of southern Britain. *In*: DORÉ, A.G., CARTWRIGHT, J.A., STOKER, M.S., TURNER, J.P. & WHITE, N. (eds) *Exhumation of the North Atlantic Margin: Timing, Mechanisms and Implications for Petroleum Exploration.* Geological Society, London, Special Publications, **196**, 85-101.

BOLDREEL, L.O. & ANDERSON, M.S. 1998. Tertiary compressional structures on the Faeroe-Rockall Plateau in relation to northeast Atlantic ridge-push and Alpine foreland stresses. *Tectonophysics,* **300**, 13-28.

BOTT, M.H.P. 1959. The mechanics of oblique-slip faulting. *Geological Magazine,* **96**, 109-117.

BOTT, M.H.P. 1988. A new look at the causes and consequences of the Icelandic hot-spot. *In*: MORTON, A.C. & PARSON, L.M. (eds) *Early Tertiary Volcanism and the Opening of the NE Atlantic*. Geological Society, London, Special Publications, **39**, 15-23.

BRAY, R.J., GREEN, P.F. & DUDDY, I.R. 1992. Thermal history reconstruction using apatite fission track analysis and vitrinite reflectance: a case study from the UK East Midlands and Southern North Sea. *In*: HARDMAN, R.F. (ed.) *Exploration Britain: Geological Insights for the Next Decade*. Geological Society, London, Special Publications, **67**, 3-25.

BRISTOW, C.M. & HUGHES, D.E. 1971. A Tertiary thrust fault on the southern margin of the Bovey Basin. *Geological Magazine,* **108**, 61-68.

BRODIE, J. & WHITE, N. 1994. Sedimentary basin inversion caused by igneous underplating: Northwest European continental shelf. *Geology,* **22**, 147-150.

BROOKS, M. 1973. Some aspects of the Palaeogene evolution of western Britain in the context of an underlying mantle hot spot. *Journal of Geology,* **81**, 81-88.

BYERLEE, J.D. 1978. Friction of rocks. *Pure and Applied Geophysics,* **116**, 615-626.

CARSLAW, H.S. & JAEGER, J.C. 1959. *Conduction of Heat in Solids*. Oxford University Press.

CHALMERS, J.A. 2000. Offshore evidence for Neogene uplift in central West Greenland. *Global and Planetary Change,* **24**, 311-318.

CHALMERS, J.A., LARSEN, L.M. & PEDERSEN, A.K. 1995. Widespread Palaeocene volcanism around the northern North Atlantic and Labrador Sea: evidence for a large, hot, early plume head. *Journal of the Geological Society, London,* **152**, 965-969.

CHALMERS, J.A., PULVERTAFT, T.C.R., CHRISTIANSEN, F.G., LARSEN, H.C. & OTTERSEN, T.G. 1993. The southern west Greenland continental margin: rifting history, basin development and petroleum potential. *In*: PARKER, J.R. (ed.) *Petroleum Geology of Northwest Europe: Proceedings of the 4th Conference*. Geological Society, London, 915-931.

CHAMBERS, L.M. & PRINGLE, M.S. 2001. Age and duration of activity at the Isle of Mull Tertiary igneous centre, Scotland, and confirmation of the existence of subchrons during Anomaly 26r. *Earth and Planetary Science Letters,* **193**, 333-345.

CLARK, M.K. 2005. Late Cenozoic uplift of southeastern Tibet. *Geology,* **33**, 525-528.

CLAYTON, G., SEVASTOPULO, G.D. & SLEEMAN, A.G. 1986. Carboniferous (Dinantian and Silesian) and Permo-Triassic rocks in South County Wexford, Ireland. *Geological Journal,* **21**, 366-374.

CLIFT, P.D., CARTER, A. & HURFORD, A.J. 1998. The erosional and uplift history of NE Atlantic passive margins: constraints on a passing plume. *Journal of the Geological Society, London,* **155**, 787-800.

COBBING, E.J. 1961. A note on some olivine-dolerite dykes in Connemara. *Irish Naturalists' Journal,* **13**, 249-253.

COOKE, M.L. & UNDERWOOD, C.A. 2001. Fracture termination and step-over at bedding interfaces due to frictional slip and interface opening. *Journal of Structural Geology,* **23**, 223-238.

COPE, J.C.W. 1994. A latest Cretaceous hotspot and the southeasterly tilt of Britain. *Journal of the Geological Society, London,* **151**, 905-908.

CORFIELD, S., MURPHY, N. & PARKER, S. 1999. The structural and stratigraphic framework of the Irish Rockall Trough. *In*: FLEET, A.J. & BOLDY, S.A.R. (eds) *Petroleum Geology of Northwest Europe: Proceedings of the 5th Conference*. Geological Society, London, 407-420.

COWARD, M.P. 1995. Structural and tectonic setting of the Permo-Triassic basins of northwest Europe. *In*: BOLDY, S.A.R. (ed.) *Permian and Triassic rifting in Northwest Europe*. Geological Society, London, Special Publications, **91**, 7-39.

COXON, P. 2001a. Cenozoic: Tertiary and Quaternary (until 10,000 years before present). *In*: HOLLAND, C.H. (ed.) *The Geology of Ireland*. Dunedin Academic Press, Edinburgh.

COXON, P. 2001b. Understanding Irish landscape evolution: pollen assemblages from Neogene and Pleistocene palaeosurfaces in western Ireland. *Irish Journal of Earth Sciences,* **101**, 85-97.

COXON, P. & COXON, C. 1997. A pre-Pliocene or Pliocene land surface in County Galway, Ireland. *In*: WIDDOWSON, M. (ed.) *Palaeosurfaces: Recognition, Reconstruction and Palaeoenvironmental Interpretation*. Geological Society, London, Special Publications, **120**, 37-55.

CRUIKSHANK, K.M. & AYDIN, A. 1994. Role of fracture localisation in arch formation, Arches National Park, Utah. *Geological Society of America Bulletin,* **106**, 879-891.

CUNNINGHAM, M.J.M., DENSMORE, A.L., ALLEN, P.A., PHILLIPS, W.E.A., BENNETT, S.D., GALLAGHER, K. & CARTER, A. 2003. Evidence for post-early Eocene tectonic activity in southeastern Ireland. *Geological Magazine,* **140**, 101-118.

CUNNINGHAM, M.J.M., PHILLIPS, W.E.A. & DENSMORE, A.L. 2004. Evidence for Cenozoic tectonic deformation in southeast Ireland and near offshore. *Tectonics,* **23**, 1-17.

CURRIE, K.L. & FERGUSON, J. 1970. The mechanism of intrusion of lamprophyre dykes indicated by 'offsetting' of dykes. *Tectonophysics,* **9**, 525-535.

DAGLEY, P. & MUSSETT, A.E. 1986. Palaeomagnetism and radiometric dating of the British Tertiary Igneous Province: Muck and Eigg. *Geophysical Journal of the Royal Astronomical Society,* **85**, 221-242.

DANCER, P.N., ALGAR, S.T. & WILSON, I.R. 1999. Structural evolution of the Slyne Trough. *In*: FLEET, A.J. & BOLDY, S.A.R. (eds) *Petroleum Geology of Northwest Europe: Proceedings of the 5th Conference*. Geological Society, London, 445-453.

DAVIS, G.H. & REYNOLDS, S.J. 1996. *Structural Geology of Rocks and Regions*. John Wiley & Sons, Toronto.

DEARMAN, W.R. 1963. Wrench-faulting in Cornwall and south Devon. *Proceedings of the Geological Association,* **74**, 265-284.

DEER, W.A., HOWIE, R.A. & ZUSSMAN, J. 1992. *An Introduction to the Rock Forming Minerals*. John Wiley & Sons, New York.

DELANEY, P.T. 1986. Field relations between dykes and joints: emplacement processes and palaeostress analysis. *Journal of Geophysical Research,* **91** (B5), 4920-4938.

DELANEY, P.T. 1987. Heat transfer during emplacement and cooling of mafic dykes. *In*: HALLS, H.C. & FAHRIG, W.F. (eds) *Mafic Dyke Swarms*. Geological Association of Canada Special Paper, **34**, 31-46.

DELANEY, P.T. & POLLARD, D.D. 1981. Deformation of host rocks and flow of magma during growth of minette dykes and breccia-bearing intrusions near Ship Rock, New Mexico. *U. S. Geological Survey Professional Paper 1202*, 61 p.

DELANEY, P.T. & POLLARD, D.D. 1982. Solidification of basaltic magma during flow in a dyke. *American Journal of Science,* **282**, 856-885.

DEMANT, A., MÜNCH, P., ROMEUF, N. & MORATA, D. 1998. Distribution and chemistry of secondary minerals (zeolites and clay minerals) from hole 917A, southeast Greenland margin. *In*: SAUNDERS, A.D., LARSEN, H.C. & WISE, S.W. (eds). Proceedings of the Ocean Drilling Program, Scientific Results, **152**, 417-424.

DEWEY, J.F. 2000. Cenozoic tectonics of western Ireland. *Proceedings of the Geologists' Association,* **111**, 291-306.

DEWEY, J.F. & MCKERROW, W.S. 1963. An outline of the geomorphology of Murrisk and north-west Galway. *Geological Magazine,* **100**, 260-275.

DEWEY, J.F. & WINDLEY, B.F. 1988. Palaeocene-Oligocene tectonics of NW Europe. *In*: MORTON, A.C. & PARSON, L.M. (eds) *Early Tertiary Volcanism and the Opening of the NE Atlantic*. Geological Society, London, Special Publications, **39**, 25-31.

DICKEN, A.P. 1981. Isotope geochemistry of Tertiary igneous rocks from the Isle of Skye, NW Scotland. *Journal of Petrology,* **22**, 155-189.

DICKEN, A.P. & JONES, N.W. 1983. Isotopic evidence for the age and origin of pitchstones and felsites, Isle of Eigg, NW Scotland. *Journal of the Geological Society, London,* **140**, 691-700.

DICKEN, A.P., MOORBATH, S. & WELKE, H.J. 1981. Isotope, trace element and major element geochemistry of Tertiary igneous rocks, Isle of Arran, Scotland. *Transactions of the Royal Society of Edinburgh,* **72**, 159-170.

DOBSON, M.R. & WHITTINGTON, R.J. 1992. Aspects of the geology of the Malin Sea area. *In*: PARNELL, J. (ed.) *Basins on the Atlantic Seaboard: Petroleum Geology, Sedimentology and Basin Evolution*. Geological Society, London, Special Publications, **62**, 291-311.

DORÉ, A.G. 1992. Synoptic palaeogeography of the Northeast Atlantic seaway: late Permian to Cretaceous. *In*: PARNELL, J. (ed.) *Basins on the Atlantic Seaboard: Petroleum Geology, Sedimentology and Basin Evolution*. Geological Society, London, Special Publications, **62**, 421-446.

DORÉ, A.G. & JENSEN, L.N. 1996. The impact of late Cenozoic uplift and erosion on hydrocarbon exploration: offshore Norway and some other uplifted basins. *Global and Planetary Change,* **12**, 415-436.

DORÉ, A.G. & LUNDIN, E.R. 1996. Cenozoic compressional structures on the northeast Atlantic margin: nature, origin and potential significance for hydrocarbon exploration. *Petroleum Geoscience,* **2**, 299-311.

DORÉ, A.G., LUNDIN, E.R., JENSEN, L.N., BIRKELAND, Ø., ELIASSEN, P.E. & FICHLER, C. 1999. Principal tectonic events in the evolution of the northwest European Atlantic margin. *In*: FLEET, A.J. & BOLDY, S.A.R. (eds) *Petroleum Geology of Northwest Europe: Proceedings of the 5th Conference*. Geological Society, London, 41-61.

DREW, D.P. & JONES, G.L.I. 2000. Post-Carboniferous pre-Quaternary karstification in Ireland. *Proceedings of the Geologists' Association,* **111**, 345-353.

DUNN, D.E., LAFOUNTAIN, L.J. & JACKSON, R.E. 1973. Porosity dependence and mechanism of brittle fracture in sandstones. *Journal of Geophysical Research,* **78**, 2403-2417.

EMELEUS, C.H. 1983. Tertiary igneous activity. *In*: CRAIG, G.Y. (ed.) *Geology of Scotland.* Scottish Academic Press, Edinburgh.

EMELEUS, C.H. & PRESTON, J. 1969. *Field Excursion Guide to the Tertiary Volcanic Rocks of Ireland.* Doorman and Sons, Belfast.

ENGLAND, R.W. 1988. The early Tertiary stress regime in NW Britain: evidence from the patterns of volcanic activity. *In*: MORTON, A.C. & PARSON, L.M. (eds) *Early Tertiary Volcanism and the Opening of the NE Atlantic.* Geological Society, London, Special Publications, **39**, 381-389.

ESCHER, A., JACK, S. & WATTERSON, J. 1976. Tectonics of the North Atlantic Proterozoic dyke swarm. *Philosophical Transactions of the Royal Society of London - Series A,* **280**, 529-539.

EVANS, A. & CLAYTON, G. 1998. The geological history of the Ballydeenlea Chalk Breccia, County Kerry, Ireland. *Marine and Petroleum Geology,* **15**, 299-307.

EVANS, A.L., FITCH, F.J. & MILLER, J.A. 1973. Potassium-argon age determinations on some British Tertiary igneous rocks. *Journal of the Geological Society, London,* **129**, 419-443.

FARLEY, K.A. 2000. Helium diffusion from apatite: general behaviour as illustrated by Durango fluorapatite. *Journal of Geophysical Research,* **105** (B2), 2903-2914.

FARLEY, K.A., WOLF, R.A. & SILVER, L.T. 1996. The effects of long alpha-stopping distances on (U-Th)/He ages. *Geochimica et Cosmochimica Acta,* **60**, 4223-4229.

FITCH, F.J., HEARD, G.L. & MILLER, J.A. 1988. Basaltic magmatism of late Cretaceous and Palaeogene age recorded in wells NNE of the Shetlands. *In*: MORTON, A.C. & PARSON, L.M. (eds) *Early Tertiary Volcanism and the Opening of the NE Atlantic.* Geological Society, London, Special Publications, **39**, 253-262.

FITCH, F.J. & HURFORD, A.J. 1977. Fission track dating of the Tardree Rhyolite, Co. Antrim. *Proceedings of the Geologists' Association,* **88**, 267-274.

FOSTER, M.E. & HUDLESTON, P.J. 1986. "Fracture cleavage" in the Duluth Complex, northeastern Minnesota. *Geological Society of America Bulletin,* **97**, 85-96.

FREEDMAN, S. 2000. Stone veneer-faced precast concrete panels. *PCI Journal,* **45** (4), 72-99.

GALBRAITH, R.F. & LASLETT, G.M. 1993. Statistical models for mixed fission track ages. *Nuclear Tracks and Radiation Measurements,* **21**, 459-470.

GALLAGHER, K. 1995. Evolving temperature histories from apatite fission-track data. *Earth and Planetary Science Letters,* **136**, 421-435.

GALLAGHER, K. & BROWN, R. 1997. The onshore record of passive margin evolution. *Journal of the Geological Society, London,* **154**, 451-457.

GALLAGHER, K., BROWN, R. & JOHNSON, C. 1998. Fission track analysis and its application to geological problems. *Annual Reviews, Earth and Planetary Science Letters*, 519-572.

GALLAGHER, K., HAWKESWORTH, C.J. & MANTOVANI, M.S.M. 1995. Denudation, fission track analysis and the long-term evolution of passive margin topography: application to the southeast Brazilian margin. *Journal of South American Earth Sciences,* **8**, 65-77.

GAMBLE, J.A., WYSOCZANSKI, R.J. & MEIGHAN, I.G. 1999. Constraints on the age of the British Tertiary Volcanic Province from ion microprobe U-Pb (SHRIMP) ages for acid igneous rocks from NE Ireland. *Journal of the Geological Society, London,* **156**, 291-299.

GEOFFROY, L., BERGERAT, F. & ANGELIER, J. 1994. Tectonic evolution of the Greenland-Scotland ridge during the Palaeogene: new constraints. *Geology,* **22**, 653-656.

GEOFFROY, L., BERGERAT, F. & ANGELIER, J. 1996. Brittle tectonism in relation to the Palaeogene evolution of the Thulean/NE Atlantic domain: a study in Ulster. *Geological Journal,* **31**, 259-269.

GIBSON, D., LUX, D.R. & MEIGHAN, I.G. 1995. New 40Ar/39Ar ages for the Mourne Mountains Granites, north-east Ireland. *Irish Journal of Earth Sciences,* **14**, 25-35.

GIBSON, D., MCCORMICK, A.G., MEIGHAN, I.G. & HALLIDAY, A.N. 1987. The British Tertiary Igneous Province: young Rb-Sr ages for the Mourne Mountains granites. *Scottish Journal of Geology,* **23**, 221-225.

GILLESPIE, P.A., WALSH, J.J., WATTERSON, J., BONSON, C.G. & MANZOCCHI, T. 2001. Scaling relationships of joint and vein arrays from The Burren, Co. Clare, Ireland. *Journal of Structural Geology,* **23**, 183-201.

GLEADOW, A.J.W. & DUDDY, I.R. 1981. A natural long term annealing experiment for apatite. *Nuclear Tracks,* **5**, 169-174.

GRAHAM, J.R. 1996. Dinantian river systems and coastal zone sedimentation in northwest Ireland. *In*: STROGEN, P., SOMERVILLE, I.D. & JONES, G.L. (eds) *Recent Advances in Lower Carboniferous Geology*. Geological Society, London, Special Publications, **107**, 183-206.

GRAHAM, J.R. 2001. Variscan structures. *In*: HOLLAND, C.H. (ed.) *The Geology of Ireland*. Dunedin Academic Press, Edinburgh.

GREEN, P.F. 1986. On the thermo-tectonic evolution of northern England: evidence from fission track analysis. *Geological Magazine,* **123**, 493-506.

GREEN, P.F. 1988. The relationship between track shortening and fission track age reduction in apatite: combined influences of inherent instability, annealing anisotropy, length bias and system calibration. *Earth and Planetary Science Letters,* **89**, 335-352.

GREEN, P.F., DUDDY, I.R. & BRAY, R.J. 1995. Applications of Thermal History Reconstruction in inverted basins. *In*: BUCHANAN, J.G. & BUCHANAN, P.G. (eds) *Basin Inversion*. Geological Society, London, Special Publications, **88**, 149-165.

GREEN, P.F., DUDDY, I.R. & BRAY, R.J. 1997. Variation in thermal history styles around the Irish Sea and adjacent areas: implications for hydrocarbon occurrence and tectonic evolution. *In*: MEADOWS, N.S., TRUEBLOOD, S.P., HARDMAN, M. & COWAN, G. (eds) *Petroleum Geology of the Irish Sea and Adjacent Areas*. Geological Society, London, Special Publications, **124**, 73-93.

GREEN, P.F., DUDDY, I.R., BRAY, R.J., DUNCAN, W.I. & CORCORAN, D.V. 2001. The influence of thermal history on hydrocarbon prospectivity in the Central Irish Sea Basin. *In*: SHANNON, P.M., HAUGHTON, P.D.W. & CORCORAN, D.V. (eds) *The Petroleum Exploration of Ireland's Offshore Basins*. Geological Society, London, Special Publications, **188**, 171-188.

GREEN, P.F., DUDDY, I.R., HEGARTY, K., A., BRAY, R.J., SEVASTOPULO, G.D., CLAYTON, G. & JOHNSTON, D. 2000. The post-Carboniferous evolution of Ireland: evidence from Thermal History Reconstruction. *Proceedings of the Geologists' Association,* **111**, 307-320.

GREEN, P.F., DUDDY, I.R. & HEGARTY, K.A. 2002. Quantifying exhumation from apatite fission-track analysis and vitrinite reflectance data: precision, accuracy and latest results from the Atlantic margin of NW Europe. *In*: DORÉ, A.G., CARTWRIGHT, J.A., STOKER, M.S., TURNER, J.P. & WHITE, N. (eds) *Exhumation of the North Atlantic Margin: Timing, Mechanisms and Implications for Petroleum Exploration*. Geological Society, London, Special Publications, **196**, 331-354.

GREEN, P.F., DUDDY, I.R., HEGARTY, K.A. & BRAY, R.J. 1999. Early Tertiary heat flow along the UK Atlantic margin and adjacent areas. *In*: FLEET, A.J. & BOLDY, S.A.R. (eds) *Petroleum Geology of Northwest Europe: Proceedings of the 5th Conference*. Geological Society, London, 349-357.

GREEN, P.F., LASLETT, G.M. & DUDDY, I.R. 1993. Mechanisms and kinetics of apatite fission track annealing - discussion. *American Mineralogist,* **78**, 441-445.

GRIFFITH, A.E., LEGG, I.C. & MITCHELL, W.I. 1987. Mineral Resources. *In*: BUCHANAN, R.H. & WALKER, B.M. (eds) *Province, City and People : Belfast and its region*. Greystone Books, Belfast, 43-58.

GUDMUNDSSON, A. 1987. Tectonics of the Thingvellir fissure swarm, SW Iceland. *Journal of Structural Geology,* **9**, 61-69.

HALL, A. & BISHOP, P. 2002. Scotland's denudational history: an integrated view of erosion and sedimentation at an uplifted passive margin. *In*: DORÉ, A.G., CARTWRIGHT, J.A., STOKER, M.S., TURNER, J.P. & WHITE, N. (eds) *Exhumation of the North Atlantic Margin: Timing, Mechanisms and Implications for Petroleum Exploration*. Geological Society, London, Special Publications, **196**, 271-290.

HAMILTON, M.A., PEARSON, D.G., THOMPSON, R.N., KELLEY, S.P. & EMELEUS, C.H. 1998. Rapid eruption of Skye lavas inferred from precise U-Pb and Ar-Ar dating of the Rhum and Cullin plutonic complexes. *Nature,* **394**, 260-263.

HANCOCK, P.L. 1972. The analysis of en échelon veins. *Geological Magazine,* **109**, 269-276.

HANSEN, H., REX, D.C., GUISE, P.G. & BROOKS, C.K. 1995. 40Ar/39Ar ages on early Tertiary basalts from the Scoresby Sund area, East Greenland. *Newsletters on Stratigraphy,* **32**, 103-116.

HAQ, B.U., HARDENBOL, J. & VAIL, P.R. 1987. Chronology of fluctuating sea-levels since the Triassic. *Science,* **235**, 1156-1167.

HAWKES, J.R., MERRIMAN, R.J., HARDING, R.R. & DARBYSHIRE, D.P.F. 1975. Rockall Island: new geological, petrological, chemical and Rb-Sr age data. *In*: HARRISON, R.K. (ed.) Expeditions to Rockall 1971-72. *Report of the Institute of Geological Sciences*, **75/1**, 11-51.

HELGESON, D.E. & AYDIN, A. 1991. Characteristics of joint propagation across interfaces in sedimentary rocks. *Journal of Structural Geology,* **13**, 897-911.

HILLIS, R.R. 1995. Regional Tertiary exhumation in and around the United Knigdom. *In*: BUCHANAN, J.G. & BUCHANAN, P.G. (eds) *Basin Inversion*. Geological Society, London, Special Publications, **88**, 167-190.

HIRSCHMANN, M.M., RENNE, P.R. & MCBIRNEY, A.R. 1997. 40Ar/39Ar dating of the Skaergaard intrusion. *Earth and Planetary Science Letters,* **146**, 645-658.

HITCHEN, K. & RITCHIE, J.D. 1987. Geological review of the West Shetland area. *In*: BROOKS, J. & GLENNIE, K. (eds) *Petroleum Geology of North West Europe*. Graham & Trotman, London.

HITCHEN, K. & RITCHIE, J.D. 1993. New K-Ar ages, and a provisional chronology, for the offshore part of the British Tertiary Igneous Province. *Scottish Journal of Geology,* **29**, 73-85.

HOEK, J.D. 1991. A classification of dyke-fracture geometry with examples from Precambrian dyke swarms in the Vestfold Hills, Antarctica. *Geologische Rundschau,* **80**, 233-248.

HOLLOWAY, S. & CHADWICK, R.A. 1986. The Sticklepath-Lustleigh fault zone: Tertiary sinistral reactivation of a Variscan dextral strike-slip fault. *Journal of the Geological Society, London,* **142**, 447-452.

HORNE, R.R. & MACINTYRE, R.M. 1975. Apparent age and significance of Tertiary dykes in the Dingle Peninsula, SW Ireland. *Scientific Proceedings of the Royal Dublin Society,* **5**, 293-299.

HOUSE, M.A., FARLEY, K.A. & KOHN, B.P. 1999. An empirical test of helium diffusion in apatite: borehole data from the Otway basin, Australia. *Earth and Planetary Science Letters,* **170**, 463-474.

HOUSE, M.A., WERNICKE, B.P., FARLEY, K.A. & DUMITRU, T.A. 1997. Cenozoic thermal evolution of the central Sierra Nevada, California, from (U-Th)/He thermochronometry. *Earth and Planetary Science Letters,* **151**, 167-179.

HURFORD, A.J. 1990. Standardisation of fission track dating calibration: recommendation by the Fission Track Working Group of the I.U.G.S. Subcommission on Geochronology. *Chemical Geology,* **80**, 171-178.

HUUSE, M. 2002. Cenozoic uplift and denudation of southern Norway: insights from the North Sea Basin. *In*: DORÉ, A.G., CARTWRIGHT, J.A., STOKER, M.S., TURNER, J.P. & WHITE, N. (eds) *Exhumation of the North Atlantic Margin: Timing, Mechanisms and Implications for Petroleum Exploration.* Geological Society, London, Special Publications, **196**.

I.G.S. 1981. *Annual report for 1980 and 1981*. Institute of Geological Sciences, HMSO, London.

JAEGER, J.C. & COOK, N.G.W. 1979. *Fundamentals of Rock Mechanics*. Chapman and Hall, London.

JAPSEN, P. 1997. Regional Neogene exhumation of Britain and the western North Sea. *Journal of the Geological Society, London,* **154**, 239-247.

JAPSEN, P. & BIDSTRUP, T. 1999. Quantification of late Cenozoic erosion in Denmark based on sonic data and basin modelling. *Bulletin of the Geological Society, Denmark,* **46**, 79-99.

JAPSEN, P. & CHALMERS, J.A. 2000. Neogene uplift and tectonics around the North Atlantic: overview. *Global and Planetary Change,* **24**, 165-173.

JENNER, J.K. 1981. The structure and stratigraphy of the Kish Bank Basin. *In*: ILLING, L.V. & HOBSON, G.D. (eds) *Petroleum Geology of the Continental Shelf of North-West Europe*. Institute of Petroleum, London, 426-431.

JOESTEN, R. & VAN HORN, S.R. 1999. Numerical modelling of calcite coarsening in the aureoles of en échelon dykes: analysis of the kinetic control of isograd geometry in contact metamorphism. *In*: JAMTVEIT, B. & MEAKIN, P. (eds) *Growth, Dissolution and Pattern Formation in Geosystems*. Kluwer Academic Publishers, Dordrecht, 109-141.

JOHNSON, H., QUINN, M.F., BULAT, J. & LONG, D. 1999. 'Laramide' events: Mid North Sea High (UK Quadrants 38 & 39). *In*: FLEET, A.J. & BOLDY, S.A.R. (eds) *Petroleum Geology of Northwest Europe: Proceedings of the 5th Conference*. Geological Society, London, 171-178.

JOHNSTON, T.P. & RUNDLE, C.C. 1993. K-Ar results from dolerite intrusions in County Fermanagh, Northern Ireland: evidence for late Cretaceous igneous activity? *Irish Journal of Earth Sciences,* **12**, 65-74.

JOLLY, R.J.H. & SANDERSON, D.J. 1995. Variation in the form and distribution of dykes in the Mull Swarm, Scotland. *Journal of Structural Geology,* **17**, 1543-1557.

JOLLY, R.J.H. & SANDERSON, D.J. 1997. A Mohr circle construction for the opening of a pre-existing fracture. *Journal of Structural Geology,* **19**, 887-892.

JONES, D.K.C. 1999a. Evolving models of the Tertiary evolutionary geomorphology of southern England, with special reference to the Chalklands. *In*: SMITH, B.J., WHALLEY, W.B. & WARKE, P.A. (eds) *Uplift, Erosion and Stability: Perspectives on Long-term Landscape Development*. Geological Society, London, Special Publications, **162**, 1-23.

JONES, D.K.C. 1999b. On the uplift and denudation of the Weald. *In*: SMITH, B.J., WHALLEY, W.B. & WARKE, P.A. (eds) *Uplift, Erosion and Stability: Perspectives on Long-term Landscape Development*. Geological Society, London, Special Publications, **162**, 25-43.

JONES, G., RORISON, P., FROST, R., KNIPE, R. & COLLERAN, J. 1999. Tectono-stratigraphic development of the southern part of UKCS Quadrant 15 (eastern Witch Ground Graben): implications for the Mesozoic-Tertiary evolution of the Central North Sea Basin. *In*: FLEET, A.J. & BOLDY, S.A.R. (eds) *Petroleum Geology of Northwest Europe: Proceedings of the 5th Conference*. Geological Society, London, 133-151.

JONES, S.M., WHITE, N., CLARKE, B.J., ROWLEY, E. & GALLAGHER, K. 2002. Present and past influence of the Iceland Plume on sedimentation. *In*: DORÉ, A.G., CARTWRIGHT, J.A., STOKER, M.S., TURNER, J.P. & WHITE, N. (eds) *Exhumation of the North Atlantic Margin: Timing, Mechanisms and Implications for Petroleum Exploration*. Geological Society, London, Special Publications, **196**, 13-25.

KATTENHORN, S.A. & WATKEYS, M.K. 1995. Blunt-ended dyke segments. *Journal of Structural Geology,* **17**, 1535-1542.

KEELEY, M.L., LEWIS, C.L.E., SEVASTOPULO, G.D., CLAYTON, G. & BLACKMORE, R. 1993. Apatite fission track data from southeast Ireland: implications for post-Variscan burial history. *Geological Magazine,* **130**, 171-176.

KENT, P.E. 1975. The tectonic development of Great Britain and the surrounding seas. *In*: WOODLAND, A.W. (ed.) *Petroleum and the Continental Shelf of Northwest Europe*. Applied Science Publishers.

KERR, I. 1987. *Basement/cover structural relationships in the north Antrim area, Ireland*. PhD thesis, Queen's University, Belfast.

KIRSTEIN, L.A. & TIMMERMAN, M.J. 2000. Evidence of the proto-Icelandic plume in northwestern Ireland at 42 Ma from helium isotopes. *Journal of the Geological Society, London,* **157**, 923-927.

LACHENBRUCH, A.H. & MCGARR, A. 1990. Stress and heat flow. *In*: WALLACE, R.E. (ed.) *The San Andreas Fault System, California*. U. S. Geological Survey Professional Paper 1515, 261-277.

LADEIRA, F.L. & PRICE, N.J. 1981. Relationship between fracture spacing and bed thickness. *Journal of Structural Geology,* **3**, 179-183.

LASLETT, G.M. & GALBRAITH, R.F. 1996. Statistical modelling of thermal annealing of fission tracks in apatite. *Geochimica et Cosmochimica Acta,* **60**, 5117-5131.

LASLETT, G.M., GREEN, P.F., DUDDY, I.R. & GLEADOW, A.J.W. 1987. Thermal annealing of fission tracks in apatite, 2: a quantitative analysis. *Chemical Geology,* **65**, 1-13.

LAWVER, L.A. & MÜLLER, R.D. 1994. Iceland hotspot track. *Geology,* **22**, 311-314.

LEWIS, C.L.E., GREEN, P.F., CARTER, A. & HURFORD, A.J. 1992. Elevated late Cretaceous to early Tertiary palaeotemperatures throughout northwest England: three kilometres of Tertiary erosion? *Earth and Planetary Science Letters,* **112**, 131-145.

LIDMAR-BERGSTRÖM, K. & NÄSLUND, J.O. 2002. Landforms and uplift in Scandinavia. *In*: DORÉ, A.G., CARTWRIGHT, J.A., STOKER, M.S., TURNER, J.P. & WHITE, N. (eds) *Exhumation of the North Atlantic Margin: Timing, Mechanisms and Implications for Petroleum Exploration*. Geological Society, London, Special Publications, **196**, 103-116.

LIDMAR-BERGSTRÖM, K., OLLIER, C.D. & SULEBAK, J.R. 2000. Landforms and uplift history of southern Norway. *Global and Planetary Change,* **24**, 211-231.

LISTER, J.R. & KERR, R.C. 1991. Fluid-mechanical models of crack propagation and their application to magma transport in dykes. *Journal of Geophysical Research,* **96** (B6), 10049-10077.

LYLE, P. 1980. A petrological and geochemical study of the Tertiary basaltic rocks of northeast Ireland. *Journal of Earth Sciences, Royal Dublin Society,* **2**, 137-152.

MACINTYRE, R.M. & HAMILTON, P.J. 1984. Isotopic geochemistry of the lavas from Sites 553 and 555. *Initial Reports of the Deep Sea Drilling Project,* **81**, 775-781.

MACINTYRE, R.M., MCMENAMIN, T. & PRESTON, J. 1975. K-Ar results from Western Ireland and their bearing on the timing and siting of Thulean magmatism. *Scottish Journal of Geology,* **11**, 227-249.

MANDL, G. 1987. Discontinuous fault zones. *Journal of Structural Geology,* **9**, 105-110.

MASSON, D.G. & PARSON, L.M. 1983. Eocene deformation on the continental margin SW of the British Isles. *Journal of the Geological Society, London,* **140**, 913-920.

MCCAFFREY, R.J. & MCCANN, N. 1992. Post-Permian basin history of northeast Ireland. *In*: PARNELL, J. (ed.) *Basins on the Atlantic Seaboard: Petroleum Geology, Sedimentology and Basin Evolution*. Geological Society, London, Special Publications, **62**, 277-290.

MCCAUGHAN, G.A. 2002. *Recognition of abnormal thermal histories of Jurassic source rocks from integrated analyses of vitrinite reflectance and organic matter colour/fluorescence*. PhD thesis, University of Dublin, Trinity College.

MCCULLOCH, A.A. 1993. Apatite fission track results from Ireland and the Porcupine basin and their significance for the evolution of the North Atlantic. *Marine and Petroleum Geology,* **10**, 572-590.

McCULLOCH, A.A. 1994. Low temperature thermal history of eastern Ireland: effects of fluid flow. *Marine and Petroleum Geology,* **11**, 389-399.

MEIGHAN, I.G., McCORMICK, A.G., GIBSON, D., GAMBLE, J.A. & GRAHAM, I.J. 1988. Rb-Sr isotopic determinations and the timing of Tertiary central complex magmatism in NE Ireland. *In*: MORTON, A.C. & PARSON, L.M. (eds) *Early Tertiary Volcanism and the Opening of the NE Atlantic*. Geological Society, London, Special Publications, **39**, 349-360.

MENPES, R.J. & HILLIS, R. 1995. Quantification of Tertiary exhumation from sonic velocity data, Celtic Sea/South-Western Approaches. *In*: BUCHANAN, J.G. & BUCHANAN, P.G. (eds) *Basin Inversion*. Geological Society, London, Special Publications, **88**, 191-207.

MÉRIAUX, C., LISTER, J.R., LYAKHOVSKY, V. & AGNON, A. 1999. Dyke propagation with distributed damage of the host rock. *Earth and Planetary Science Letters,* **165**, 177-185.

MITCHELL, J.G., JONES, E.J.W. & JONES, G.T. 1976. The composition and age of basalts dredged from the Blackstones igneous centre, western Scotland. *Geological Magazine,* **113**, 525-533.

MITCHELL, J.G. & MOHR, P. 1986. K-Ar systematics in Tertiary dolerites from west Connacht, Ireland. *Scottish Journal of Geology,* **22**, 225-240.

MITCHELL, J.G. & MOHR, P. 1987. Carboniferous dykes of West Connacht, Ireland. *Transactions of the Royal Society of Edinburgh,* **78**, 133-151.

MITCHELL, J.G. & REEN, K.P. 1973. Potassium-argon ages from the Tertiary Ring Complexes of the Ardnamurchan Peninsula, Western Scotland. *Geological Magazine,* **110**, 331-340.

MOHR, P. 1982. Tertiary dolerite intrusions of west-central Ireland. *Proceedings of the Royal Irish Academy,* **82B**, 53-82.

MOHR, P. 1987. The Cill Ala dyke swarm, counties Sligo and Mayo: physical parameters. *Irish Naturalists' Journal,* **22**, 326-334.

MOHR, P. 1991. The Síofra Gabbro, West Connacht, Ireland. *Scottish Journal of Geology,* **27**, 127-133.

MOHR, P. 1992. A Palaeocene dolerite intrusion newly discovered from Loch Ana, Clifden, Connemara. *Irish Naturalists' Journal,* **24**, 21-23.

MOHR, P. 2000. Late Palaeozoic and Palaeocene magmatic intrusion levels in West Connacht and inferences for palaeotopography. *Proceedings of the Geologists' Association,* **111**, 337-343.

MOHR, P., MUSSETT, A.E. & KENNAN, P.S. 1984. The Droimchogaidh sill, Connacht, Ireland. *Geological Journal,* **19**, 1-21.

MORRIS, P. 1974. A Tertiary dyke system in South-West Ireland. *Proceedings of the Royal Irish Academy,* **74**, 179-184.

MORTON, A.C., DIXON, J.E., FITTON, J.G., MACINTYRE, R.M., SMYTHE, D.K. & TAYLOR, P.N. 1988. Early Tertiary volcanic rocks in Well 163/6-1A, Rockall Trough. *In*: MORTON, A.C. & PARSON, L.M. (eds) *Early Tertiary Volcanism and the Opening of the NE Atlantic*. Geological Society, London, Special Publications, **39**, 293-308.

MORTON, A.C., HITCHEN, K., RITCHIE, J.D., HINE, N.M., WHITEHOUSE, M. & CARTER, S.G. 1995. Late Cretaceous basalts from Rosemary Bank, Northern Rockall Trough. *Journal of the Geological Society, London,* **152**, 947-952.

MUSGROVE, F.W. & MITCHENER, B. 1996. Analysis of the pre-Tertiary rifting history of the Rockall Trough. *Petroleum Geoscience,* **2**, 353-360.

MUSSETT, A.E. 1984. Time and duration of Tertiary igneous activity of Rhum and adjacent areas. *Scottish Journal of Geology,* **20**, 273-279.

MUSSETT, A.E. 1986. 40Ar-39Ar step-heating ages of the Tertiary igneous rocks of Mull, Scotland. *Journal of the Geological Society, London,* **143**, 887-896.

MUSSETT, A.E., DAGLEY, P., HODGSON, B. & SKELHORN, R.R. 1987. Palaeomagnetism and age of the quartz-porphyry intrusions, Isle of Arran. *Scottish Journal of Geology,* **23**, 9-22.

MUSSETT, A.E., DAGLEY, P. & SKELHORN, R.R. 1988. Time and duration of activity in the British Tertiary Igneous Province. *In*: MORTON, A.C. & PARSON, L.M. (eds) *Early Tertiary Volcanism and the Opening of the Northeast Atlantic*. Geological Society, London, Special Publications, **39**, 337-348.

NADIN, P.A., KUSZNIR, N.J. & CHEADLE, M.J. 1997. Early Tertiary plume uplift of the North Sea and Faeroe-Shetland Basins. *Earth and Planetary Science Letters,* **148**, 109-127.

NAYLOR, D. 1992. The post-Variscan history of Ireland. *In*: PARNELL, J. (ed.) *Basins on the Atlantic Seaboard: Petroleum Geology, Sedimentology and Basin Evolution*. Geological Society, London, Special Publications, **62**, 255-275.

NAYLOR, D., HAUGHEY, N., CLAYTON, G. & GRAHAM, J.R. 1993. The Kish Bank Basin, offshore Ireland. *In*: PARKER, J.R. (ed.) *Petroleum Geology of Northwest Europe: Proceedings of the 4th Conference*. Geological Society, London, 845-855.

NICHOLSON, R. 1985. The intrusion and deformation of Tertiary minor sheet intrusions, west Suardal, Isle of Skye, Scotland. *Geological Journal,* **20**, 53-72.

NICHOLSON, R. & POLLARD, D.D. 1985. Dilation and linkage of échelon cracks. *Journal of Structural Geology,* **7**, 583-590.

NIELSEN, S.B., PAULSEN, G.E., HANSEN, D.L., GEMMER, L., CLAUSEN, O.R., JACOBSEN, B.H., BALLING, N., HUUSE, M. & GALLAGHER, K. 2002. Palaeocene initiation of Cenozoic uplift in Norway. *In*: DORÉ, A.G., CARTWRIGHT, J.A., STOKER, M.S., TURNER, J.P. & WHITE, N. (eds) *Exhumation of the North Atlantic Margin: Timing, Mechanisms and Implications for Petroleum Exploration*. Geological Society, London, Special Publications, **196**, 45-65.

NOBLE, R.H., MACINTYRE, R.M. & BROWN, P.E. 1988. Age constraints on Atlantic evolution: timing of magmatic activity along the E Greenland continental margin. *In*: MORTON, A.C. & PARSON, L.M. (eds) *Early Tertiary Volcanism and the Opening of the NE Atlantic*. Geological Society, London, Special Publications, 201-204.

ODÉ, H. 1957. Mechanical analysis of the dyke pattern of the Spanish Peaks area, Colorado. *Geological Society of America Bulletin,* **68**, 567-576.

ODLING, N.E., GILLESPIE, P., BOURGINE, B., CASTAING, C., CHILÉS, J.-P., CHRISTENSEN, N.P., FILLION, E., GENTER, A., OLSON, C., THRANE, L., TRICE, R., AARSETH, E., WALSH, J.J. & WATTERSON, J. 1999. Variations in fracture system geometry and their implications for fluid flow in fractured hydrocarbon reservoirs. *Petroleum Geoscience,* **5**, 373-384.

OLSON, J.E. & POLLARD, D.D. 1989. Inferring palaeostress from natural fracture patterns: A new method. *Geology,* **17**, 345-348.

OLSON, J.E. & POLLARD, D.D. 1991. The initiation and growth of en échelon veins. *Journal of Structural Geology,* **13**, 595-608.

O'REILLY, B.M., HAUSER, F., JACOB, A.W.B., SHANNON, P.M., MAKRIS, J. & VOGT, U. 1995. The Erris and eastern Rockall Troughs: structural and sedimentological developoment. *In*: CROKER, P.F. & SHANNON, P.M. (eds) *The Petroleum Geology of Ireland's Offshore Basins*. Geological Society, London, Special Publications, **93**, 413-421.

PARNELL, J., SHUKLA, B. & MEIGHAN, I.G. 1989. The lignite and associated sediments of the Tertiary Lough Neagh Basin. *Irish Journal of Earth Sciences,* **10**, 67-88.

PASQUALI, R. 2002. *Onshore sediment transport routes to the Porcupine Basin during the Tertiary*. MSc thesis, University of Dublin, Trinity College.

PEARSON, D.G., EMELEUS, C.H. & KELLEY, S.P. 1996. Precise 40Ar/39Ar age for the initiation of Palaeogene volcanism in the Inner Hebrides and its regional significance. *Journal of the Geological Society, London,* **153**, 815-818.

PHILLIPS, W.E.A. 2001a. Caledonian deformation. *In*: HOLLAND, C.H. (ed.) *The Geology of Ireland*. Dunedin Academic Press, Edinburgh.

PHILLIPS, W.E.A. 2001b. The Grampian orogeny. *In*: HOLLAND, C.H. (ed.) *The Geology of Ireland*. Dunedin Academic Press, Edinburgh.

PITCHER, W.S. & BERGER, A.R. 1972. The Tertiary dyke swarm: the crust under tension. *In*: DE SITTER, L.U. (ed.) *The Geology of Donegal: a Study of Granite Emplacement and Unroofing*. John Wiley & Sons, Chichester, 373-375.

PLINT, A.G. 1982. Eocene sedimentation and tectonics in the Hampshire Basin. *Journal of the Geological Society, London,* **139**, 249-254.

POLLARD, D.D. 1987. Elementary fracture mechanics applied to the structural interpretation of dykes. *In*: HALLS, H.C. & FAHRIG, W.F. (eds) *Mafic Dyke Swarms*. Geological Association of Canada Special Paper, **34**, 5-24.

POLLARD, D.D., MULLER, O.H. & DOCKSTADER, D.R. 1975. The form and growth of fingered sheet intrusions. *Geological Society of America Bulletin,* **86**, 351-363.

POLLARD, D.D. & SEGALL, P. 1987. Theoretical displacements and stresses near fractures in rock: with applications to faults, joints, veins, dykes, and solution surfaces. *In*: ATKINSON, B.K. (ed.) *Fracture Mechanics of Rock*. Academic Press, London, 555-568.

POLLARD, D.D., SEGALL, P. & DELANEY, P.T. 1982. Formation and Interpretation of dilatant échelon cracks. *Geological Society of America Bulletin,* **93**, 1291-1303.

PRACHT, M. 1994. *The Geology of the Beara Peninsula, Ireland*, National University of Ireland.

PRESTON, J. 1965. Tertiary feeder dykes in the west of Ireland. *Proceedings of the Geological Society,* **1626**, 149-150.

PRESTON, J. 1967a. The Blind Rock dyke, County Donegal. *Irish Naturalists' Journal,* **15**, 286-293.

PRESTON, J. 1967b. A Tertiary feeder dyke in County Fermanagh, Northern Ireland. *Scientific Proceedings of the Royal Dublin Society, Series A,* **3**, 1-16.

PRESTON, J. 1979. Tertiary igneous activity. *In*: HOLLAND, C.H. (ed.) *A Geology of Ireland*. Scottish Academic Press, Edinburgh.

PRICE, N.J. & COSGROVE, J.W. 1990. *Analysis of Geological Structures*. Cambridge University Press.

PRICE, N.J. & HANCOCK, P.L. 1972. Development of fracture cleavage and kindred structures. *International Geological Congress, 24th, Montreal, Section 3*, 584-592.

READMAN, P.W., O'REILLY, B.M. & MURPHY, T. 1997. Gravity gradients and upper-crustal tectonic fabrics, Ireland. *Journal of the Geological Society, London,* **154**, 817-828.

REINERS, P.W., EHLERS, T.A., GARVER, J.I., MITCHELL, S.G., MONTGOMERY, D.R., VANCE, J.A. & NICOLESCU, S. 2002. Late Miocene exhumation and uplift of the Washington Cascade Range. *Geology,* **30**, 767-770.

REINERS, P.W. & FARLEY, K.A. 2001. Influence of crystal size on apatite (U-Th)/He thermochronometry: an example from the Bighorn mountains, Wyoming. *Earth and Planetary Science Letters,* **188**, 413-420.

RENSHAW, C.E. & POLLARD, D.D. 1994. Are large differential stresses required for straight fracture propagation paths? *Journal of Structural Geology,* **16**, 817-822.

RICKWOOD, P.C. 1990. The anatomy of a dyke and the determination of propagation and magma flow directions. *In*: PARKER, A.J., RICKWOOD, P.C. & TUCKER, D.H. (eds) *Mafic Dykes and Emplacement Mechanisms*. A.A. Balkema Publishers, Rotterdam, 81-100.

RIDDIHOUGH, R.P. & MAX, M.D. 1976. A geological framework for the continental margin to the west of Ireland. *Geological Journal,* **11**, 109-120.

RITCHIE, J.D., GATLIFF, R.W. & RICHARDS, P.C. 1999. Early Tertiary magmatism in the offshore NW UK margin and surrounds. *In*: FLEET, A.J. & BOLDY, S.A.R. (eds) *Petroleum Geology of Northwest Europe: Proceedings of the 5th Conference*. Geological Society, London, 573-584.

ROBERTS, D.G. 1989. Basin inversion in and around the British Isles. *In*: COOPER, M.A. & WILLIAMS, G.D. (eds) *Inversion Tectonics*. Geological Society, London, Special Publications, **44**, 131-150.

ROBERTS, D.G., THOMPSON, M., MITCHENER, B., HOSSACK, J., CARMICHAEL, S. & BJØRNSETH, H.-M. 1999. Palaeozoic to Tertiary rift and basin dynamics: mid-Norway to the Bay of Biscay - a new context for hydrocarbon prospectivity in the deep water frontier. *In*: FLEET, A.J. & BOLDY, S.A.R. (eds) *Petroleum Geology of Northwest Europe: Proceedings of the 5th Conference*. Geological Society, London, 7-40.

ROGERS, R.D. 1987. Fracture propagation associated with dyke emplacement at the Skaergaard intrusion, East Greenland. *Journal of Structural Geology,* **9**, 71-86.

ROHRMAN, M., VAN DER BEEK, P.A., VAN DER HILST, R.D. & REEMST, P. 2002. Timing and mechanisms of North Atlantic Cenozoic uplift: evidence for mantle upwelling. *In*: DORÉ, A.G., CARTWRIGHT, J.A., STOKER, M.S., TURNER, J.P. & WHITE, N. (eds) *Exhumation of the North Atlantic Margin: Timing, Mechanisms and Implications for Petroleum Exploration*. Geological Society, London, Special Publications, **196**, 27-43.

ROTHERY, E. 1988. En échelon vein array development in extension and shear. *Journal of Structural Geology,* **10**, 63-71.

ROWLEY, E. & WHITE, N. 1998. Inverse modelling of extension and denudation in the East Irish Sea and surrounding areas. *Earth and Planetary Science Letters,* **161**, 57-71.

RUBIN, A.M. 1993. Tensile fracture of rock at high confining pressure: implications for dyke propagation. *Journal of Geophysical Research,* **98** (B9), 15919-15935.

SAUNDERS, A.D., FITTON, J.G., KERR, A.C., NORRY, M.J. & KENT, R.W. 1997. The North Atlantic Igneous Province. *In*: MAHONEY, J.J. & COFFIN, M.F. (eds) *Large igneous provinces; continental, oceanic, and planetary flood volcanism*. Geophysical Monograph, **100**. American Geophysical Union, Washington DC, 45-93.

SCHMIDT, E. 1924. *Föppl's Festschrift*. Springer.

SCHÖN, J.H. 1996. *Physical Properties of Rocks: Fundamentals and Principles of Petrophysics, Seismic Exploration*. Pergamon, Oxford.

SEGALL, P. & POLLARD, D.D. 1983. Joint formation in granitic rock of the Sierra Nevada. *Geological Society of America Bulletin,* **94**, 563-575.

SEVASTOPULO, G.D. 2001. Carboniferous (Silesian). *In*: HOLLAND, C.H. (ed.) *The Geology of Ireland*. Dunedin Academic Press, Edinburgh.

SHANNON, P.M. 1991. The development of Irish offshore sedimentary basins. *Journal of the Geological Society, London,* **148**, 191-196.

SHANNON, P.M., JACOB, A.W.B., MAKRIS, J., O'REILLY, B.M., HAUSER, F. & VOGT, U. 1995. Basin development and petroleum prospectivity of the Rockall and Hatton region. *In*: CROKER, P.F. & SHANNON, P.M. (eds) *The Petroleum Geology of Ireland's Offshore Basins*. Geological Society, London, Special Publications, **93**, 435-457.

SIBSON, R.H. 1985. A note on fault reactivation. *Journal of Structural Geology,* **7**, 751-754.

SIBSON, R.H. 1990. Conditions for fault-valve behaviour. *In*: KNIPE, R.J. & RUTTER, E.H. (eds) *Deformation Mechanisms, Rheology and Tectonics*, **54**, 15-28.

SINTON, C.W. & DUNCAN, R.A. 1998. 40Ar-39Ar ages of lavas from the southeast Greenland margin, ODP Leg 152, and the Rockall Plateau, DSDP Leg 81. *In*: SAUNDERS, A.D., LARSEN, H.C. & WISE, S.W. (eds). Proceedings of the Ocean Drilling Program, Scientific Results, **152**, 387-402.

SINTON, C.W., HITCHEN, K. & DUNCAN, R.A. 1998. 40Ar-39Ar geochronology of silicic and basic volcanic rocks on the margins of the North Atlantic. *Geological Magazine,* **135**, 161-170.

SMITH, R.P. 1987. Dyke emplacement at Spanish Peaks, Colorado. *In*: HALLS, H.C. & FAHRIG, W.F. (eds) *Mafic Dyke Swarms*. Geological Association of Canada Special Paper, **34**, 47-54.

SOLLA HACH, C. 2002. *Cenozoic flexural uplift in northwestern Ireland and sedimentation in the northeastern Irish Rockall Basin*. PhD thesis, University of Dublin, Trinity College.

SPEIGHT, J.M., SKELHORN, R.R., SLOAN, T. & KNAAP, R.J. 1982. The dyke swarms of Scotland. *In*: SUTHERLAND, D.S. (ed.) *Igneous Rocks of the British Isles*. John Wiley & Sons, Chichester.

STANTON, W.I. 1960. The Lower Palaeozoic rocks of southwest Murrisk, Ireland. *Quarterly Journal of the Geological Society,* **116**, 269-291.

STOKER, M.S., MORTON, A.C., EVANS, D., HUGHES, M.J., HARLAND, R. & GRAHAM, D.K. 1988. Early Tertiary basalts and tuffaceous sandstones from the Hebrides Shelf and the Wyville-Thomson Ridge. *In*: MORTON, A.C. & PARSON, L.M. (eds) *Early Tertiary Volcanism and the Opening of the NE Atlantic*. Geological Society, London, Special Publications, **39**, 271-282.

STOREY, M., DUNCAN, R.A., PEDERSEN, A.K., LARSEN, L.M. & LARSEN, H.C. 1998. 40Ar/39Ar geochronology of the West Greenland Tertiary volcanic province. *Earth and Planetary Science Letters,* **160**, 569-586.

STUEVOLD, L.M. & ELDHOLM, O. 1996. Cenozoic uplift of Fennoscandia inferred from a study of the mid-Norwegian margin. *Global and Planetary Change,* **12**, 359-386.

TATE, M.P. 1993. Structural framework and tectono-stratigraphic evolution of the Porcupine Seabight Basin offshore western Ireland. *Marine and Petroleum Geology,* **10**, 95-123.

TATE, M.P. & DOBSON, M.R. 1988. Syn- and post-rift igneous activity in the Porcupine Seabight Basin and adjacent continental margin W of Ireland. *In*: MORTON, A.C. & PARSON, L.M. (eds) *Early Tertiary Volcanism and the Opening of the NE Atlantic*. Geological Society, London, Special Publications, **39**, 309-334.

TATE, M.P., DODD, C.D. & GRANT, N.T. 1999. The Northeast Rockall Basin and its significance in the evolution of the Rockall-Faeroes/East Greenland rift system. *In*: FLEET, A.J. & BOLDY, S.A.R. (eds) *Petroleum Geology of Northwest Europe: Proceedings of the 5th Conference*. Geological Society, London, 391-406.

TAYLOR, S.L. 2002. *Palaeogeomorphology and neotectonics in southwest Ireland*. MSc thesis, University of Dublin, Trinity College.

TEGNER, C., DUNCAN, R.A., BERNSTEIN, S., BROOKS, C.K., BIRD, D.K. & STOREY, M. 1998. 40Ar-39Ar geochronology of Tertiary mafic intrusions along the East Greenland rifted margin: Relation to flood basalts and the Iceland hotspot track. *Earth and Planetary Science Letters,* **156**, 75-88.

THOMAS, A.L. 1993. The geometry of échelon fractures in rock: implications from laboratory and numerical experiments. *Journal of Structural Geology,* **15**, 323-334.

THOMPSON, P. 1986. *Dating of the British Tertiary Igneous Province in Ireland by the 40Ar-39Ar stepwise degassing method*. PhD thesis, University of Liverpool.

THOMPSON, P., MUSSETT, A.E. & DAGLEY, P. 1987. Revised 40Ar-39Ar age for granites of the Mourne Mountains, Ireland. *Scottish Journal of Geology,* **23**, 215-220.

THOMPSON, P., WATT, S. & DURRANI, S.A. 1984. Concordant fission track and 40Ar-39Ar age determination for the Interbasaltic Formation of Northern Ireland. *Geophysical Journal of the Royal Astronomical Society,* **77**, 326 (abst.).

TREAGUS, S.H. & LISLE, R.J. 1997. Do principal surfaces of stress and strain always exist? *Journal of Structural Geology,* **19**, 997-1010.

TURCOTTE, D.L. & SCHUBERT, G. 2002. *Geodynamics*. Cambridge Universtiy Press.

TURNER, J.P. 1997. Strike-slip fault reactivation in the Cardigan Bay basin. *Journal of the Geological Society, London,* **154**, 5-8.

UPTON, B.G.J. 1988. History of Tertiary igneous activity in the N Atlantic borderlands. *In*: MORTON, A.C. & PARSON, L.M. (eds) *Early Tertiary Volcanism and the Opening of the NE Atlantic*. Geological Society, London, Special Publications, **39**, 429-453.

UPTON, B.G.J., EMELEUS, C.H., REX, D.C. & THIRLWALL, M.F. 1995. Early Tertiary magmatism in NE Greenland. *Journal of the Geological Society, London,* **152**, 959-964.

WAAGSTEIN, R. 1988. Structure, composition and age of the Faroe basalt plateau. *In*: MORTON, A.C. & PARSON, L.M. (eds) *Early Tertiary Volcanism and the Opening of the NE Atlantic*. Geological Society, London, Special Publications, **39**, 225-238.

WAAGSTEIN, R., GUISE, P. & REX, D. 2002. 39Ar/40Ar whole-rock dating of zeolite facies metamorphosed flood basalts; the upper Palaeocene basalts of the Faroe Islands, NE Atlantic. *In*: JOLLEY, D.W. & BELL, B.R. (eds) *The North Atlantic Igneous Province: Stratigraphy, Tectonic, Volcanic and Magmatic Processes*. Geological Society, London, Special Publications, **197**, 219-252.

WALKER, G.P.L. 1960. The amygdale minerals in the Tertiary lavas of Ireland III. Regional distribution. *Mineralogical Magazine,* **32**, 503-527.

WALKER, G.P.L. & LEEDAL, G.P. 1954. The Barnesmore granite complex, County Donegal. *Scientific Proceedings of the Royal Dublin Society, Series A,* **26**, 207-243.

WALSH, J.N., BECKINSALE, R.D., SKELHORN, R.R. & THORPE, R.S. 1979. Geochemistry and petrogenesis of Tertiary granitic rocks from the island of Mull, northwest Scotland. *Contributions to Mineralogy and Petrology,* **71**, 99-116.

WARE, P.D. & TURNER, J.P. 2002. Sonic velocity analysis of the Tertiary denudation of the Irish Sea basin. *In*: DORÉ, A.G., CARTWRIGHT, J.A., STOKER, M.S., TURNER, J.P. & WHITE, N. (eds) *Exhumation of the North Atlantic Margin: Timing, Mechanisms and Implications for Petroleum Exploration*. Geological Society, London, Special Publications, **196**, 355-370.

WEINBERGER, R., LYAKHOVSKY, V., BAER, G. & AGNON, A. 2000. Damage zones around en échelon dyke segments in porous sandstone. *Journal of Geophysical Research,* **105** (B2), 3115-3133.

WHITE, N. & LOVELL, B. 1997. Measuring the pulse of a plume with the sedimentary record. *Nature,* **387**, 888-891.

WHITE, R.S. 1988. A hot-spot model for early Tertiary volcanism in the North Atlantic. *In*: MORTON, A.C. & PARSON, L.M. (eds) *Early Tertiary Volcanism and the Opening of the NE Atlantic*. Geological Society, London, Special Publications, **39**, 3-13.

WHITTEN, E.H.T. 1954. Two Arfvedsonitic rhyolite intrusions from Cloghaneely, Co. Donegal. *Mineralogical Magazine,* **30**, 393-399.

WILKINSON, G.C., BAZLEY, R.A.B. & BOULTER, M.C. 1980. The geology and palynology of the Oligocene Lough Neagh Clays, Northern Ireland. *Journal of the Geological Society, London,* **137**, 65-75.

WILSON, H.E. & ROBBIE, J.A. 1966. *Geology of the country around Ballycastle*. Memoir of the Geological Survey of Northern Ireland, HMSO, London.

WILSON, R.L. 1964. The Tertiary dykes of Magho Mountain, County Fermanagh. *Irish Naturalists' Journal,* **14**, 254-257.

WOLF, R.A., FARLEY, K.A. & KASS, D.M. 1998. Modeling of the temperature sensitivity of the apatite (U-Th)/He thermochronometer. *Chemical Geology,* **148**, 105-114.

WOLF, R.A., FARLEY, K.A. & SILVER, L.T. 1996. Helium diffusion and low-temperature thermochronometry of apatite. *Geochimica et Cosmochimica Acta,* **60**, 4231-4240.

WOLF, R.A., FARLEY, K.A. & SILVER, L.T. 1997. Assessment of (U-Th)/He thermochronology: The low-temperature history of the San Jacinto mountains, California. *Geology,* **25**, 65-68.

WONG, T.F. 1982. Micromechanics of faulting in the Westerly granite. *International Journal of Rock Mechanics and Mining Sciences and Geomechanics Abstracts,* **19**, 49-64.

WORTHINGTON, R., WALSH, J. & SHANNON, P.M. 2003. Carboniferous normal faulting in the west of Ireland: a neglected phenomenon. *In*: SANDERS, I. (ed.) *Abstracts of the 46th Annual Irish Geological Research Meeting*, **21**, 165.

ZIEGLER, P.A. 1989. Geodynamic model for Alpine intra-plate compressional deformation in Western and Central Europe. *In*: COOPER, M.A. (ed.) *Inversion Tectonics*. Geological Society, London, Special Publications, **44**, 63-85.

TABLES

Dyke no.	Easting	Northing	Dyke width (m)	Host rock lithology	Baked margin width (m)	Background fracture frequency (m^{-1})	Profile side	DAFZ width (m)	Number of fractures in DAFZ
Killala swarm									
K23	070849	340894	0.93	SCH		1.00	s	4.5	37
K27	074201	337445	1.3	QT		6.76	n/a	n/d	n/a
K32	074728	337466	1.13	PS		1.00	s	6.75	130
							n	8.75	107
K84	111237	340740	3.5	S		n/d	s	n/d	n/a*
						2.20	n	12.25	>120
K90c	119972	337413	5.1	S		n/d	s	5.25	n/a*
						2.00	n	6.25	168
K92	120465	338124	0.8	S		0.72	s	4	21
							n	n/d	n/a**
K93	120482	338154	0.9	S		0.80	s	4	62
							n	4.25	97
K94	120547	338212	0.2	S		0.60	s	2	14
							n	2	23
K111	128596	330414	1	L		6.50	n/a	n/d	n/a
K112	128595	330455	4	L	0.7	5.20	s	2.2	>196
						2.20	n	6.75	243
K113	128571	330530	1.6	L	0.15	2.40	s	1.75	170
							n	1.75	73
K114	128566	330558	1	L	0.2	1.44	s	2.5	101
							n	2.5	107
K115	128476	330762	0.4	L		2.90	n/a	n/d	n/a
K116i	128482	330812	0.15	L		1.50	n/a	n/d	n/a
K116ii	128482	330820	0.6	L	0.1	1.50	s	0.25	37
							n	1	43
K116ii						0.00	n	4.25	174
K117	128516	331106	4.5	L	1	1.40	s	10.5	200
					2.5		n	18.5	272
K118i	128517	331245	2.2	L		5.76	s	4.25	179
							n	4	241
K118ii	128525	331264	0.4	L	0.05	5.68	s	1.25	63
							n	4.25	201
K119	128536	331279	1.2	L	0.1	5.52	s	3.25	146
							n	4	150
K126	128967	331941	1	L	0.05	2.90	s	1.75	149
							n	2	161
K127	128996	332048	9	L	7-8	5.40	s	33	>596
						4.80	n	23	418
K132i	129745	333335	1.1	L		4.88	s	3.65	>207
							n	3.2	>193
K132ii	129745	333339	0**	L		4.88	s	2.25	179
							n	1.5	12
K134	129780	333400	1.7	L		3.12	s	4	240
							n	3.75	290
K136	130279	334520	1.28	L		2.52	s	1.5	217
							n	2	224
K138	130 637	335177	0.81	L		4.60	s	2.75	73
							n	4	68
K147	131594	338052	0.32	L		4.44	s	2.25	36
							n	1.75	23
K148	131581	338062	0.62	L		3.75	s	0.25	38
							n	0.75	45
K155b	142850	335819	0.6	L		4.16	s	4.25	183
							n	6.25	152
K157a	142958	335959	0.75	L		8.76	s	6.5	140
							n	4.5	118
K176	146990	334410	2.5	L		3.78	s	1.95	>177
							n	1.95	>141
K178	147066	334567	2.5	L		4.12	s	7.25	187
							n	7	273
K180	148418	335177	0.92	L		3.30	s	1.25	92
							n	0.75	61
West Connacht systems									
WC25a	065434	261419	4.5	PS		3.20	se	n/d	n/a
							nw	9.5	135
WC25c	065658	261539	6	QT		1.40	se	12.15	>206
							nw	22.15	>268
WC33a	075901	267513	12	S		3.00	se	49.7	>3321
Donegal-Kingscourt swarm									
DK14	185144	375062	1.85	L		1.60	ne	11.75	343
							sw	12.25	336
DK17a	184924	374493	25	L	??	0.00	sw	56.25	634
DK33a	177228	421330	6.2	G		n/a	n	3.5	266
DK42	180100	429730	2.7	G		n/a	s	2	75
DK44	180238	430275	1.3	G		n/a	s	1	80
							n	0.5	38
DK54	181922	434674	1.6	G		n/a	s	1.5	197
							n	1.25	191
DK65	183856	434153	0.71	G		n/a	s	0.5	82
DK65			0.66				w	1	97

Table 3.1. Summary data. DAFZ = 'dyke-associated fracture zone'. n/d = not distinguishable, i.e. when profile is too short to define the width of the DAFZ, or the dyke-associated fracture count is too small relative to the background fracture frequency. *Profile too short to define the background frequency and hence the number of fractures in the DAFZ. **These fracture frequency profiles are influenced by a dyke segment tip that does not cut the plane of the profile.

Sample no.	Grid reference		Technique used	Host rock		Elevation above sea level (m)	Sample relationship to dykes		
	Easting	Northing		Lithology	Age		Maximum sample distance from dyke (m)	Dyke width (m)	Nearest mapped dyke (m)
M1	055571	256654	FT&He	granite	Caledonian	0	0.4	4	
M2	065434	261419	FT	psammite	Precambrian	0	0.4	4	
M3	075901	267513	FT	sandstone	Ordovician	25	1	12	
M4	065968	332704	FT	granitic gneiss	Precambrian	0	0.3	3	
M5	079967	340561	FT	psammite	Precambrian	0	0.2	4.3	
M6	198183	391403	no apatite	granite	Caledonian	535	0.2	5 to 8	
M7	174426	421094	FT&He	granite	Caledonian	0	0.15	3.1	
M8	177228	421330	FT&He	granite	Caledonian	0	0.2	6	
M9	180074	429687	FT&He	granite	Caledonian	0	0.26	4	
M10	195378	416496	FT&He	granite	Caledonian	340	0.4	7 to 8	
M11	196290	414738	FT&He	granite	Caledonian	260	0.2	5	
C1i	056890	257770	FT&He	granite	Caledonian	20			?
C1ii	101740	228360	FT&He	granite	Caledonian	165			n/a
C1iii	109360	222060	FT&He	granite	Caledonian	0			n/a
C2	065166	330993	FT	granitic gneiss	Precambrian	0			800
C3	174243	420422	FT&He	granite	Caledonian	0			500
C4	179459	426028	FT&He	granite	Caledonian	0			900
C5	188313	414496	FT&He	granite	Caledonian	360			2000
C6	192286	414782	FT&He	granite	Caledonian	665			100
C7	197857	421559	FT&He	granite	Caledonian	360			400
C8	198166	420991	FT&He	granite	Caledonian	640			400
C9	194883	413480	FT&He	granite	Caledonian	265			700

Table 5.1. Sample locations and general information. For sample numbers, prefix 'M' indicates margin sample and prefix 'C' indicates control sample. Samples C1i, C1ii and C1iii are samples CL1, GG12 and GG13 respectively from Allen *et al.* (2002).

Sample no.	No. of crystals	Dosimeter		Spontaneous		Induced		Age dispersion		Fission track central age (Ma)
		ρ_d	N_d	ρ_s	N_s	ρ_i	N_i	$P(\chi^2)$	R.E.%	
M1	25	1.098	6089	0.342	483	1.082	1528	<1	23.6	59.9±8.6
M2	18	1.098	6089	0.235	188	0.801	642	74.3	3.8	54.3±9.2
M3	16	1.098	6089	0.988	623	2.946	1858	83.1	<0.1	61.9±6.0
M4	20	1.098	6089	0.469	735	1.447	2265	82.4	<0.1	59.9±5.4
M5	20	1.098	6089	0.423	351	1.356	1124	85.7	<0.1	57.7±7.2
M7	20	1.264	7010	0.597	782	2.162	2832	36.5	3.3	58.7±5.0
M8	20	1.098	6089	0.842	927	2.533	2787	<1	19.0	59.3±7.2
M9	21	1.098	6089	0.373	658	1.219	2149	92.8	<0.1	56.6±5.2
M10	22	1.098	6089	0.543	828	1.704	2601	18.2	10.0	58.6±5.6
M11	20	1.098	6089	0.757	1753	2.337	5410	<1	14.9	59.9±5.4
C1i*										146±10
C1ii*										141±8
C1iii*										128±10
C2	20	1.264	7010	1.010	2561	1.041	2641	<1	12.2	203.8±16.8
C3	20	1.264	7010	2.079	2317	1.758	1959	54.4	1.1	247.8±16.4
C4	20	1.264	7010	1.707	2894	1.411	2391	36.1	1.3	253.5±15.4
C5	20	1.264	7010	2.389	3636	2.5	3805	3.2	7.9	201.7±13.0
C6	20	1.264	7010	1.014	2431	0.859	2060	8.1	8.7	247.4±18.8
C7	15	1.264	7010	1.067	791	1.28	949	16.5	6.0	176.7±18.8
C8	20	1.264	7010	1.549	3500	1.456	3290	<1	11.5	226.9±17.2
C9	20	1.264	7010	2.597	3412	2.471	3247	2.6	8.5	220.1±15.0

Table 5.2. Fission track analytical data. Track densities ($\rho_{d,s,i}$) are (x10^6 tracks cm^{-2}). Uncertainties are ± 2σ. *Samples C1i, C1ii and C1iii are CL1, GG12 and GG13 respectively from Allen *et al.* (2002).

Sample no.	Number of tracks in μm intervals															Mean track length (μm)	Standard deviation (μm)	No. of tracks
	4	5	6	7	8	9	10	11	12	13	14	15	16	17	18			
M1	0	0	0	0	0	0	0	0	2	6	21	25	15	2	1	14.24±0.26	1.05	72
M2	0	0	0	0	0	0	0	0	0	1	7	8	3	2	0	14.31±0.46	1.04	21
M3	0	0	0	0	0	0	0	0	0	6	23	27	11	0	0	14.15±0.22	0.88	67
M4	0	0	0	0	0	0	0	0	0	1	9	11	4	0	0	14.20±0.30	0.76	25
M5	0	0	0	0	0	0	0	0	0	1	5	10	8	1	0	14.72±0.42	1.05	25
M7	0	0	0	0	0	0	0	0	1	4	24	39	17	4	0	14.40±0.20	0.91	89
M8	0	0	0	0	0	0	0	0	2	4	13	22	5	0	0	14.10±0.28	0.93	46
M9	0	0	0	0	0	0	0	0	0	4	8	9	5	1	0	14.17±0.36	0.93	27
M10	0	0	0	0	0	0	0	0	0	6	23	34	27	9	1	14.66±0.20	1.03	100
M11	0	0	0	0	0	0	0	0	1	7	34	41	17	0	0	14.12±0.16	0.83	100
C1i*																12.98±0.22	1.57	
C1ii*																13.11±0.20	1.37	
C1iii*																12.82±0.26	1.85	
C2	0	0	0	0	0	0	2	6	9	21	31	18	12	1	0	13.24±0.28	1.43	100
C3	0	0	0	0	0	0	0	5	20	30	20	17	6	2	0	12.98±0.26	1.34	100
C4	0	0	0	0	0	1	2	5	14	27	31	15	7	0	0	13.01±0.28	1.40	102
C5	0	0	0	0	0	1	1	14	16	23	25	10	10	0	0	12.69±0.30	1.50	100
C6	0	0	0	0	0	0	2	9	9	30	26	16	8	1	0	13.08±0.28	1.35	101
C7	0	0	0	0	1	1	2	6	8	24	30	17	9	2	0	13.10±0.32	1.56	100
C8	0	0	0	0	0	0	2	5	9	26	34	21	7	1	0	13.21±0.26	1.34	105
C9	0	0	0	0	0	0	4	9	19	28	23	16	2	0	0	12.60±0.28	1.40	101

Table 5.3. Binned fission track length data. Each track length interval covers the range n – 1 to n, where n is the interval heading. Uncertainties are ± 2σ. *Samples C1i, C1ii and C1iii are CL1, GG12 and GG13 respectively from Allen *et al.* (2002).

Table 5.4. (U-Th)/He results. EH = excess helium; PR = poor replication. The shaded corrected helium ages were used to produce the means (see text for explanation). *The corrected age for sample M1b is used as a good age for sample M1.

Sample replicate	^{4}He (ncc)	HB (ncc)	^{4}He-HB (ncc)	%SD in Q ±	^{4}He (atoms)	absolute ±	^{238}U (ng)	+/- (%)	^{232}Th (ng)	+/- (%)	Uncorrected He age (Ma)	±2σ (Ma)	Grain radius (μm)	Grain length (μm)	F_T correction factor	F_T corrected He age (Ma)	±6% (2σ) (Ma)	Mean age (Ma)	Standard error (2σ) (Ma)	Fission track age (2σ) (Ma)
M1a	0.859	0.041	0.818	0.288	2.20E+10	6.33E+07	0.0744	0.072	0.182	0.99	59.8	0.6	43	225	0.66	90.3	5.1			60±8
M1b	1.417	0.028	1.389	0.567	3.73E+10	2.12E+08	0.152	0.015	0.367	0.224	50.0	0.58	58	174	0.75	66.9*	4.0*			60±8
M7a	2.332	0.023	2.309	0.345	6.20E+10	2.14E+08	0.2455	0.011	0.757	0.258	46.5	0.34	70	271	0.79	58.8	3.5	59.9	2.2	59±6
M7b	1.354	0.023	1.331	0.345	3.58E+10	1.23E+08	0.1765	0.009	0.426	0.196	41.3	0.3	45	162	0.68	61.0	3.5			59±6
M8a	3.414	0.017	3.397	0.21	9.13E+10	1.92E+08	0.4623	0.019	0.674	0.47	47.3	0.2	54	236	0.73	64.8	3.8	66.0	1.0	59±8
M8b	2.9	0.016	2.884	0.335	7.75E+10	2.60E+08	0.3762	0.016	0.605	0.36	48.0	0.4	52	207	0.72	66.7	3.9			59±8
M8c	2.406	0.018	2.388	0.327	6.42E+10	2.10E+08	0.2665	0.053	0.442	0.56	55.6	0.4	45	117	0.68	82.1	4.9			59±8
M8d	2.344	0.019	2.325	0.358	6.25E+10	2.24E+08	0.291	0.023	0.617	0.6	45.8	0.4	47	167	0.69	66.4	3.9			59±8
M9a	2.003	0.014	1.989	0.165	5.34E+10	8.82E+07	0.2039	0.042	0.308	0.68	62.1	0.4	44	172	0.67	92.7	5.3	EH/PR		57±6
M9b	1.858	0.014	1.844	0.027	4.95E+10	1.39E+07	0.1147	0.057	0.149	0.64	106.1	0.4	51	143	0.71	148.6	8.8			57±6
M10a	4.134	0.12	4.014	0.658	1.08E+11	7.10E+08	0.5009	0.04	0.158	1.005	65.4	0.8	65	193	0.77	84.4	5.0	EH/PR		59±6
M10b	2.242	0.043	2.199	0.318	5.91E+10	1.88E+08	0.2131	0.025	0.069	0.677	83.4	0.6	51	135	0.71	116.8	6.9			59±6
M10c	0.849	0.038	0.811	0.128	2.18E+10	2.79E+07	0.1463	0.032	0.046	0.432	45.4	0.2	36	165	0.60	75.7	4.2			59±6
M11a	10.993	0.013	10.98	0.37	2.95E+11	1.09E+09	1.8089	0.018	0.098	0.56	52.8	0.4	67	263	0.78	67.6	4.0	68.0	3.8	60±6
M11b	10.504	0.059	10.445	1.351	2.81E+11	3.79E+09	1.4587	0.022	0.07	0.6	62.3	1.8	46	243	0.68	91.1	5.1			60±6
M11c	2.066	0.014	2.052	0.096	5.51E+10	5.29E+07	0.3384	0.01	0.044	0.177	51.7	0.1	98	241	0.85	60.8	3.7			60±6
M11d	11.94	0.111	11.829	0.026	3.18E+11	8.26E+07	1.7685	0.024	0.088	0.682	58.2	0.04	67	196	0.78	74.5	4.5			60±6
M11e	8.622	0.017	8.605	0.186	2.31E+11	4.30E+08	1.3095	0.026	0.077	0.879	57.1	0.22	84	322	0.82	69.2	4.1			60±6
C1ia	1.759	0.058	1.701	0.336	4.57E+10	1.54E+08	0.1525	0.03	0.275	0.52	113.0	1.2	74	213	0.80	141.0	8.5	85.3	15.6	146±10
C1ib	9.472	0.024	9.448	0.336	2.54E+11	8.53E+08	1.0962	0.033	0.77	0.74	64.4	0.4	87	241	0.83	77.5	4.7			146±10
C1ic	1.759	0.058	1.701	0.336	4.57E+10	1.54E+08	0.1525	0.03	0.275	0.515	67.4	0.6	53	150	0.72	93.0	5.5			146±10
C1iia	2.801	0.027	2.774	0.107	7.45E+10	7.98E+07	0.215	0.91	0.515	0.6	67.8	0.6	59	231	0.75	90.2	5.3	89.6	14.0	141±8
C1iib	8.457	0.015	8.442	0.189	2.27E+11	4.29E+08	0.571	0.71	1.348	0.66	78.1	0.78	60	208	0.76	103.2	6.0			141±8
C1iic	1.859	0.036	1.823	0.254	4.90E+10	1.24E+08	0.176	1.24	0.4	1.24	55.4	1.04	55	173	0.73	75.4	4.5			141±8
C1iii	3.481	0.022	3.273	0.623	8.79E+10	5.48E+08	0.009	1.57	0.675	1.09	107.6		69	354	0.79	136.7	8.0	EH		128±10
C3a	21.614	0.023	21.591	0.345	5.80E+11	2.00E+09	0.9361	0.014	0.443	0.264	179.5	1.26	93	247	0.84	213.3	12.8	171.9	20.4	248±16
C3b	2.874	0.022	2.852	0.303	7.66E+10	2.32E+08	0.1981	0.018	0.335	0.25	88.6	0.56	35	171	0.59	150.4	8.3			248±16
C3c	2.362	0.022	2.34	0.303	6.29E+10	1.91E+08	0.1348	0.02	0.375	0.122	89.5	0.56	37	206	0.61	146.7	8.1			248±16
C3d	4.316	0.029	4.287	0.591	1.15E+11	6.81E+08	0.171	0.97	0.419	0.84	130.1	2.26	55	183	0.73	177.1	10.4			248±16
C4	9.486	0.023	9.463	0.102	2.54E+11	2.59E+08	0.1995	0.013	0.463	0.345	259.5	0.86	94	230	0.84	307.7	18.5	EH/PR		254±16

Continued over page.

Table 5.4 continued.

Sample replicate	^{4}He (ncc)	HB (ncc)	^{4}He-HB (ncc)	%SD in Q ±	^{4}He (atoms)	absolute ±	^{238}U (ng)	+/- (%)	^{232}Th (ng)	+/- (%)	Uncorrected He age (Ma)	±2σ (Ma)	Grain radius (μm)	Grain length (μm)	F_T correction factor	F_T corrected He age (Ma)	±6% (2σ) (Ma)	Mean age (Ma)	Standard error (2σ) (Ma)	Fission track age (2σ) (Ma)
C5a	4.548	0.029	4.519	0.591	1.21E+11	7.18E+08	0.1336	0.019	0.045	0..13	269.2	3.26	86	271	0.83	324.7	19.5	EH/PR		202±14
C5b	4.1	0.028	4.072	0.214	1.09E+11	2.34E+08	0.1779	0.014	0.051	0.261	185.8	0.82	50	143	0.71	262.3	15.5	EH/PR		202±14
C6a	1.606	0.028	1.578	1.289	4.24E+10	5.47E+08	0.0929	0.034	0.034	0.224	136	3.56	59	151	0.75	180.9	10.9	181.7	1.6	247±18
C6b	1.21	0.028	1.182	1.289	3.18E+10	4.09E+08	0.0697	0.026	0.016	0.242	140.1	3.66	63	178	0.77	182.6	10.9			247±18
C7a	1.41	0.043	1.367	0.591	3.67E+10	2.17E+08	0.073	1.17	0.04	3.59	135.4	8.6	43	184	0.66	204.4	11.6	EH/PR		177±18
C7b	0.441	0.032	0.409	0.69	1.10E+10	7.58E+07	0.038	1.15	0.441	0.032	23.7	0.32	50	151	0.71	33.4	2.0	PR		177±18
C8a	5.249	0.045	5.204	0.295	1.40E+11	4.13E+08	0.263	0.183	0.086	0.4779	189.7	1.1	62	230	0.76	248.4	14.6	239.8	17.4	227±18
C8b	11.744	0.043	11.701	0.295	3.14E+11	9.27E+08	0.565	0.025	0.185	0.4018	193.7	1	91	287	0.84	231.1	14.0			227±18

FIGURES

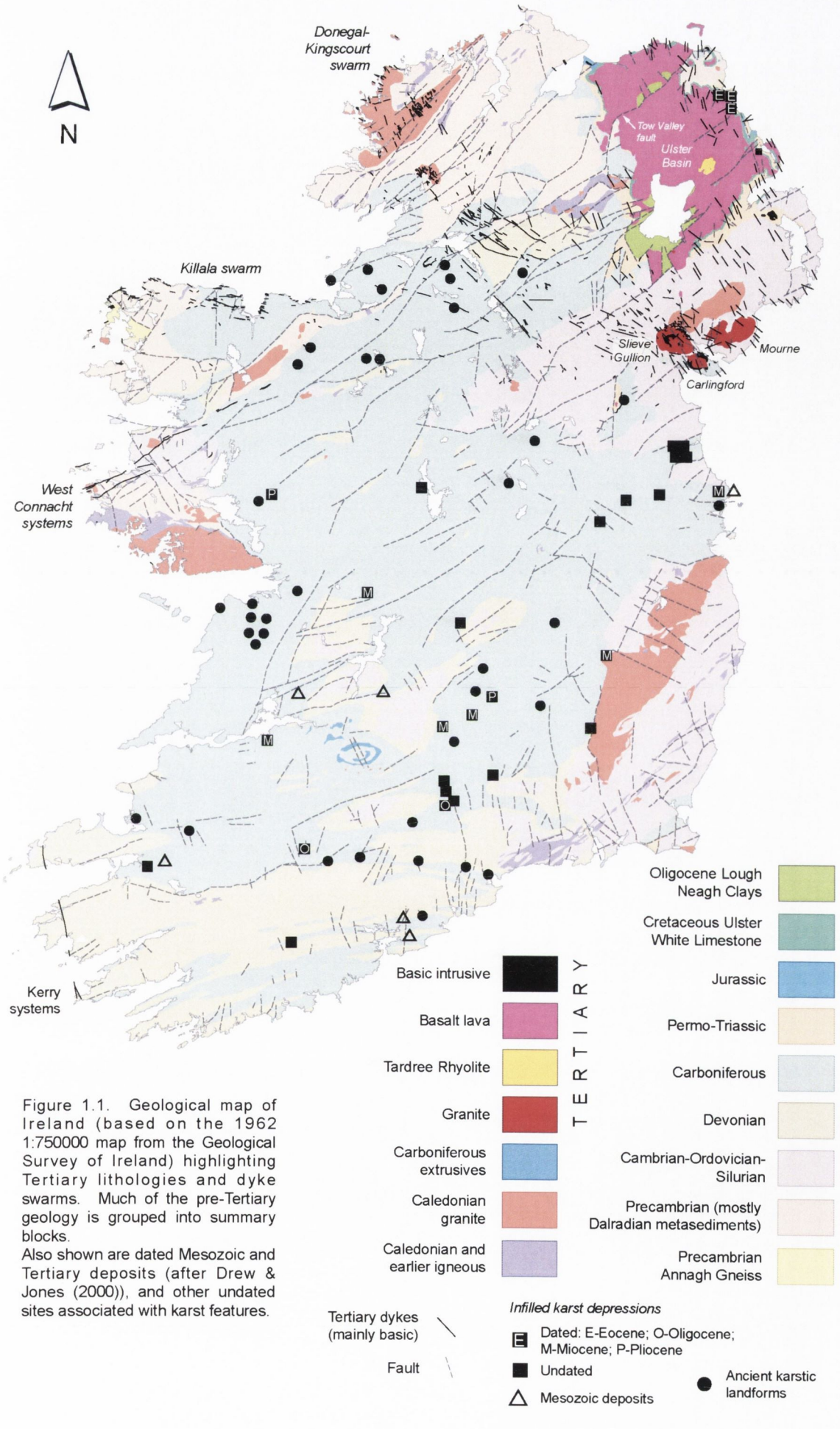

Figure 1.1. Geological map of Ireland (based on the 1962 1:750000 map from the Geological Survey of Ireland) highlighting Tertiary lithologies and dyke swarms. Much of the pre-Tertiary geology is grouped into summary blocks.
Also shown are dated Mesozoic and Tertiary deposits (after Drew & Jones (2000)), and other undated sites associated with karst features.

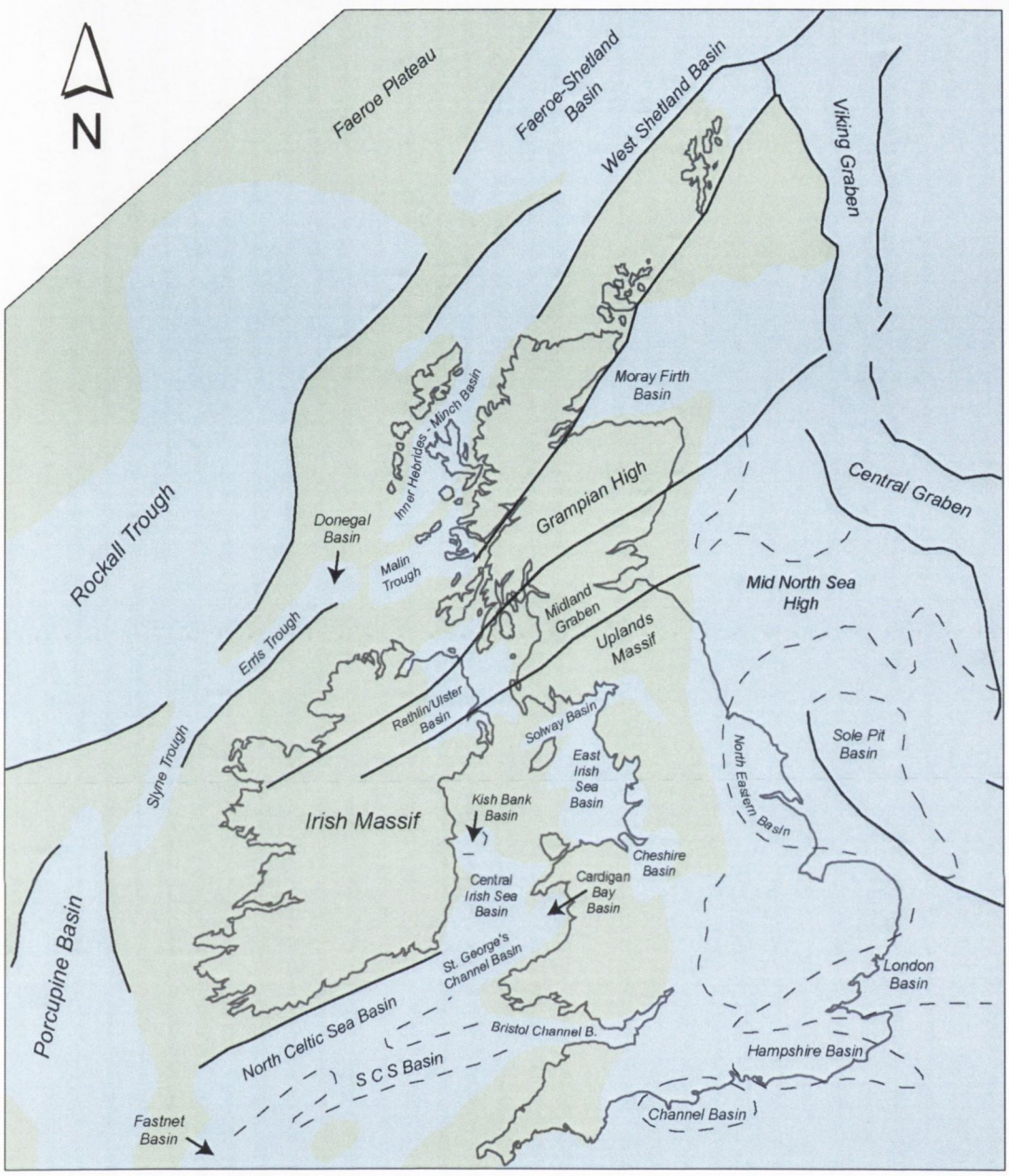

Areas of Mesozoic-Tertiary subsidence

Precambrian and Palaeozoic highs

Basin bounds

Major faults

Figure 1.2. Mesozoic-Tertiary structural units in the British Isles region (modified after Zeigler (1989); Kent (1975); Allen *et al.* (2002)).

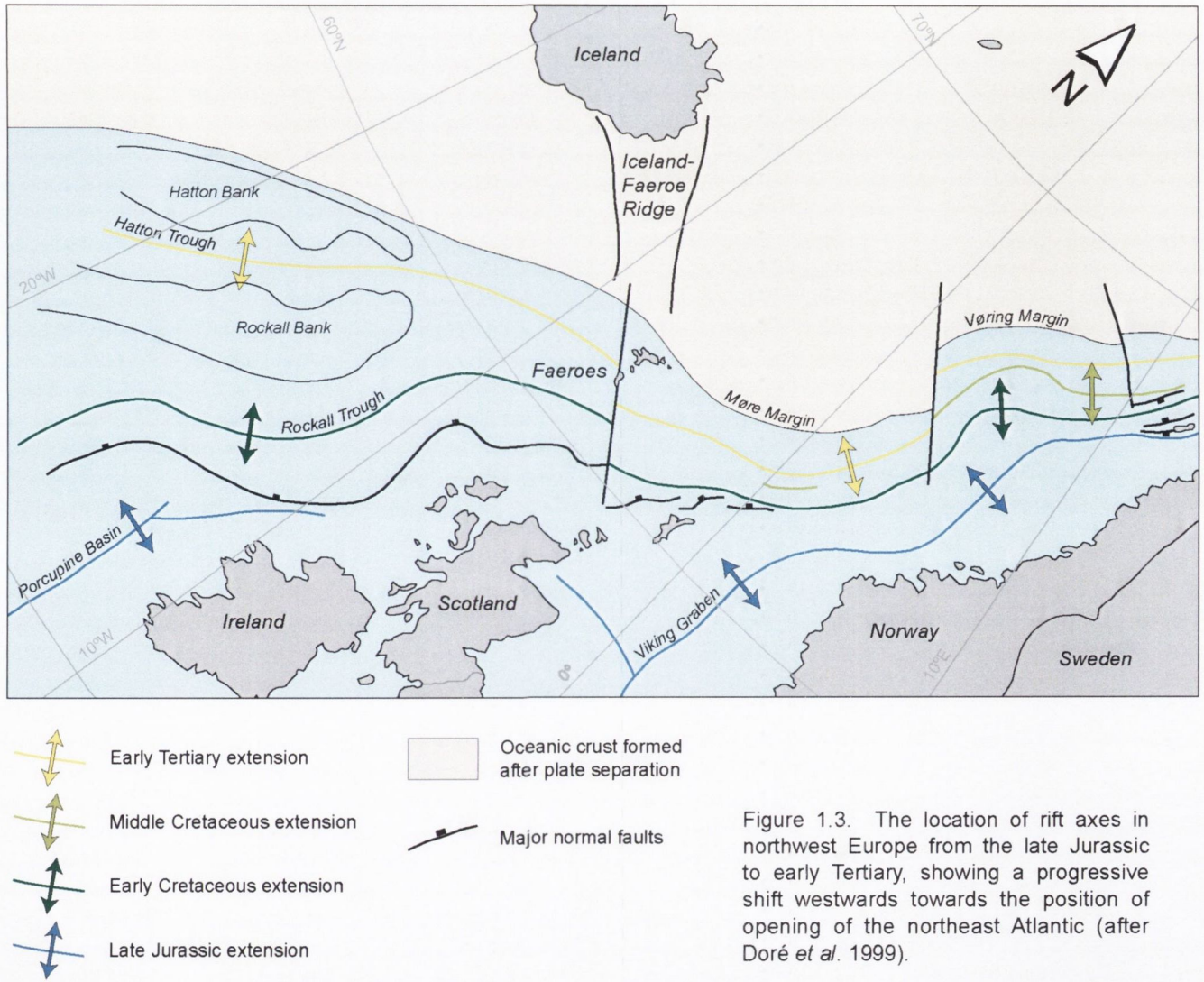

Figure 1.3. The location of rift axes in northwest Europe from the late Jurassic to early Tertiary, showing a progressive shift westwards towards the position of opening of the northeast Atlantic (after Doré *et al*. 1999).

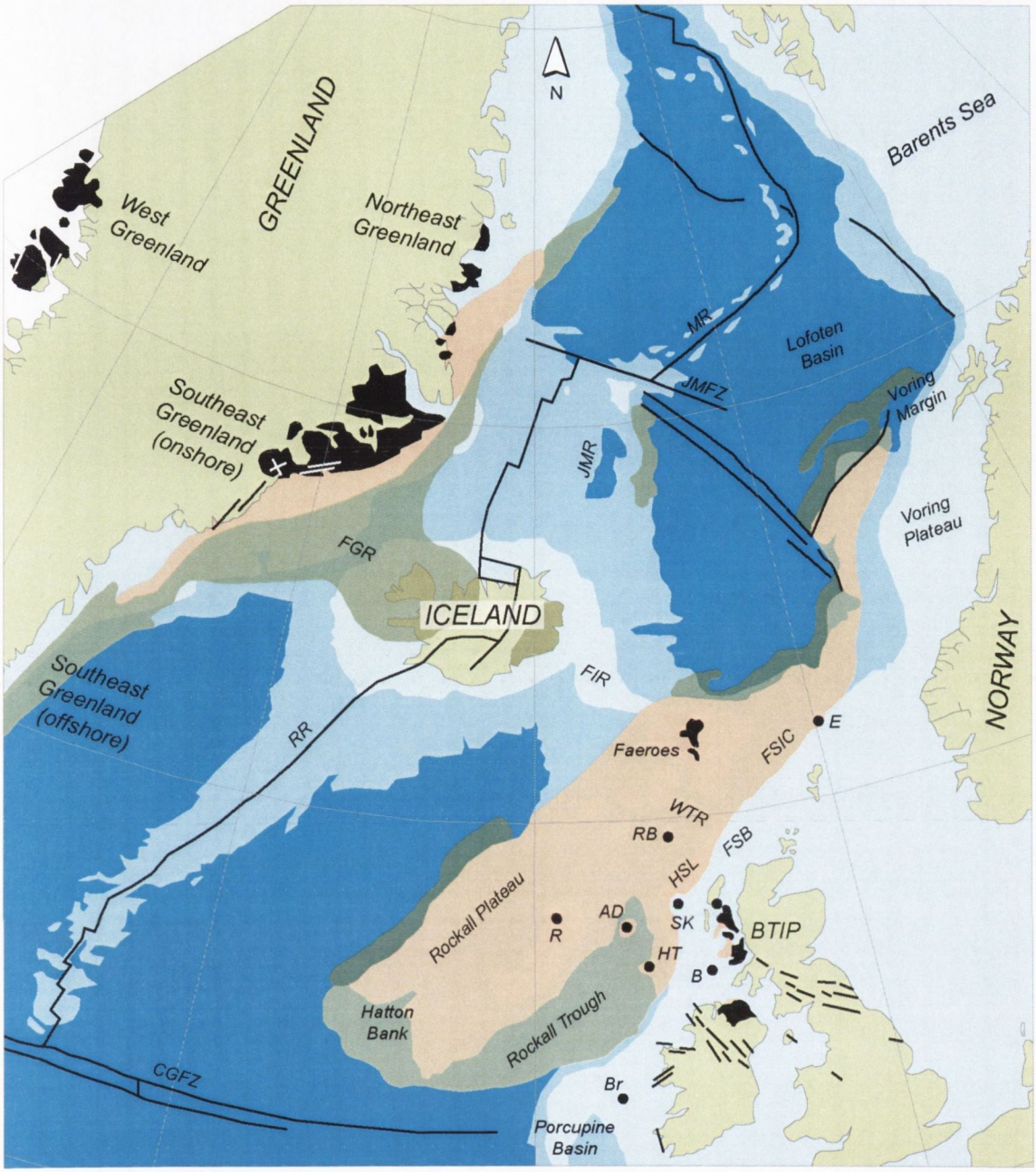

AD Anton Dohrn
B Blackstones
Br Brendan
BTIP British Tertiary Igneous Province
CGFZ Charlie-Gibbs Fracture Zone
E Erland
FGR Faeroe-Greenland Ridge
FIR Faeroe-Iceland Ridge
FSB Faeroe-Shetland Basin
FSIC Faeroe-Shetland Intrusive Complex
HSL Hebridean Shelf Lavas
HT Hebridean Terrace
JMR Jan Mayen Ridge
JMFZ Jan Mayen Fracture Zone
MR Mohns Ridge
R Rockall
RB Rosemary Bank
RR Reykjanes Ridge
WTR Wyville-Thomson Ridge

Figure 1.4. Map of the North Atlantic Igneous Province, showing the location of the British Tertiary Igneous Province and associated offshore complexes. Modified from Saunders *et al.* (1997), with detail from Mussett *et al.* (1988), Storey *et al.* (1998), and Gill *et al.* (1988).

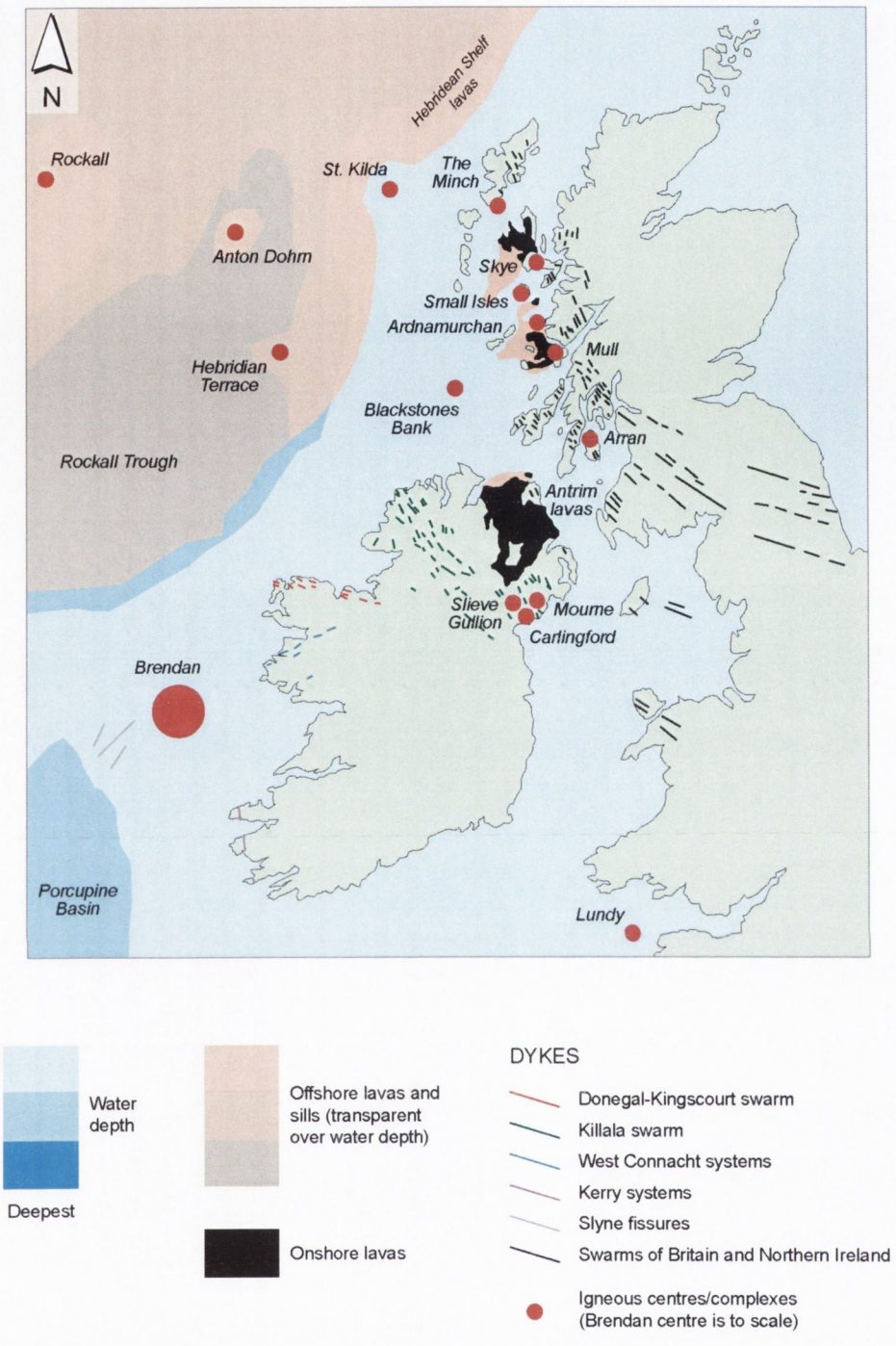

Figure 1.5. Map showing the distribution of Tertiary igneous activity across the British Tertiary Igneous Province and Ireland. Also shown are some of the main offshore igneous centres/complexes. Compiled from Saunders *et al.* (1997), Mussett *et al.* (1988) and Tate (1993).

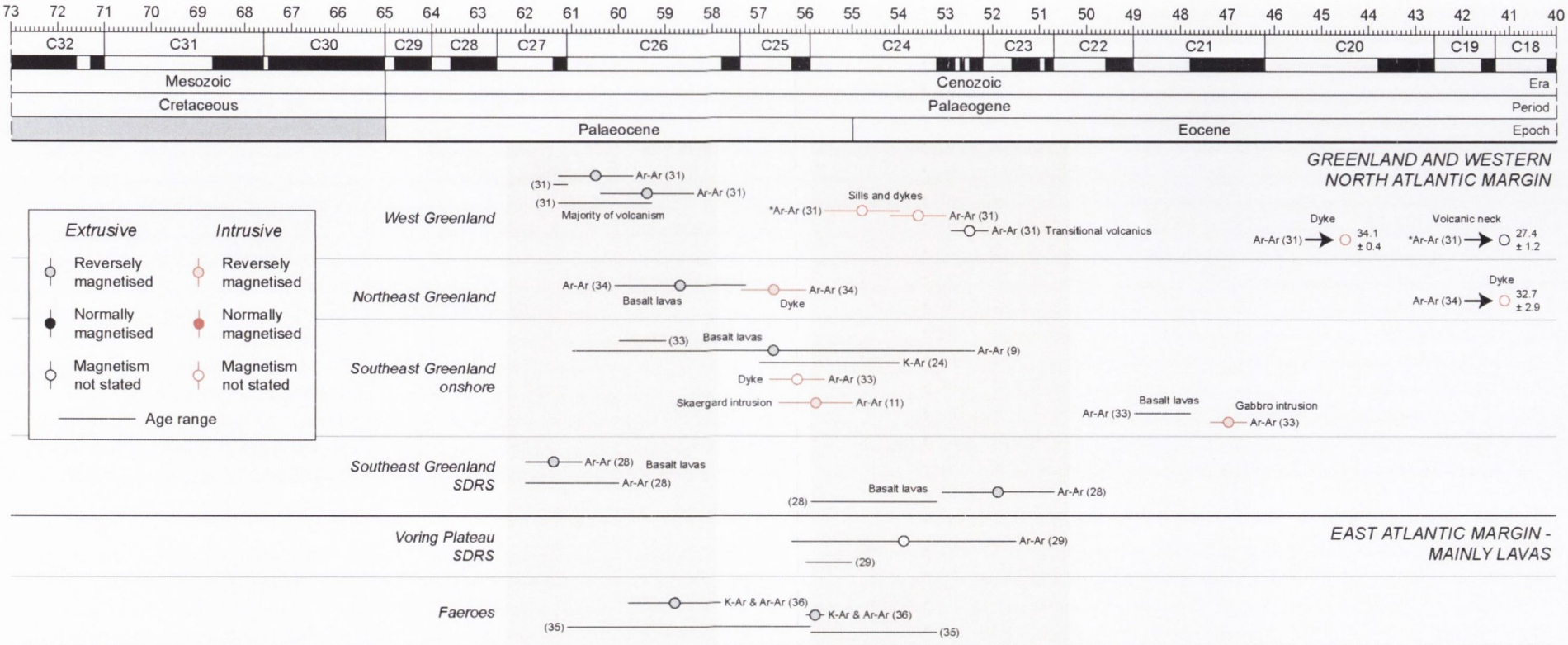

Figure 1.6. A timescale (using the magnetic timescale of Berggren (1995)) for the North Atlantic Igneous Province based primarily on the most reliable published radiometric dates. Irish igneous activity is shown towards the end of the compilation. Shaded areas represent the two main phases of igneous activity in the North Atlantic Igneous Province, as suggested by Saunders *et al.* (1997). Dates on the far left and right sides plot off the scale, so are labelled with their respective ages. The order in which radiometric ages within each area are listed indicates, in most cases, the relative ages from cross-cutting relationships. For the exceptions, dates are placed in chronological order. All errors (represented by the bars) are to 2σ, or marked '?' when the number of standard deviations is unkown. Ages are labelled with their dating method.

The numbers in brackets refer to the source references as follows (sources for Irish ages are listed separately below):

1 - Chambers & Pringle (2001); 2 - Dagley & Mussett (1986); 3 - Dancer *et al.* (1999); 4 - Dicken (1981); 5 - Dicken & Jones (1983); 6 - Dicken *et al.* (1981); 7 - Fitch *et al.* (1988); 8 - Hamilton *et al.* (1998); 9 - Hansen *et al.* (1995); 10 - Hawkes *et al.* (1975); 11 - Hirschmann *et al.* (1997); 12 - Hitchen & Ritchie (1987); 13 - Hitchen & Ritchie (1993); 14 - I.G.S. (1981); 15 - Macintyre & Hamilton (1984); 16 - Mitchell *et al.* (1976); 17 - Mitchell & Reen (1973); 18 - Morton *et al.* (1988); 19 - Morton *et al.* (1995); 20 - Mussett (1984); 21 - Mussett (1986);22 - Mussett *et al.* (1987); 23 - Mussett *et al.* (1988); 24 - Noble *et al.* (1988); 25 - Pearson *et al.* (1996); 26 - Ritchie *et al.* (1999); 27 - Saunders *et al.* (1997); 28 - Sinton & Duncan (1998); 29 - Sinton *et al.* (1998); 30 - Stoker *et al.* (1988); 31 - Storey *et al.* (1998); 32 - Tate & Dobson (1988); 33 - Tegner *et al.* (1998); 34 - Upton *et al.* (1995); 35 - Waagstein (1988); 36 - Waagstein *et al.* (2002); 37 - Walsh *et al.* (1979).

Refer to Appendix 1 for a list of the radiometiric ages.

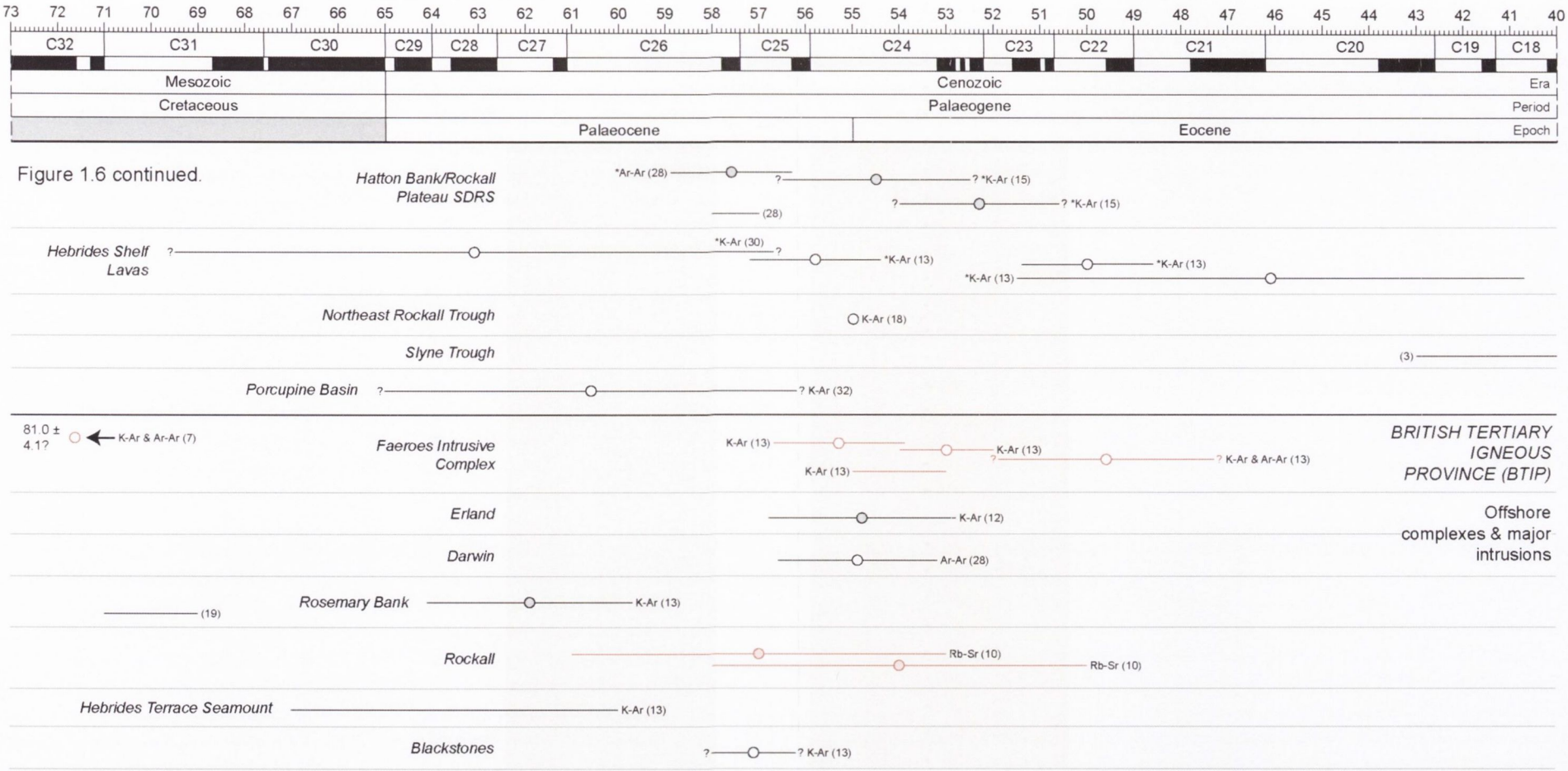

Figure 1.6 continued.

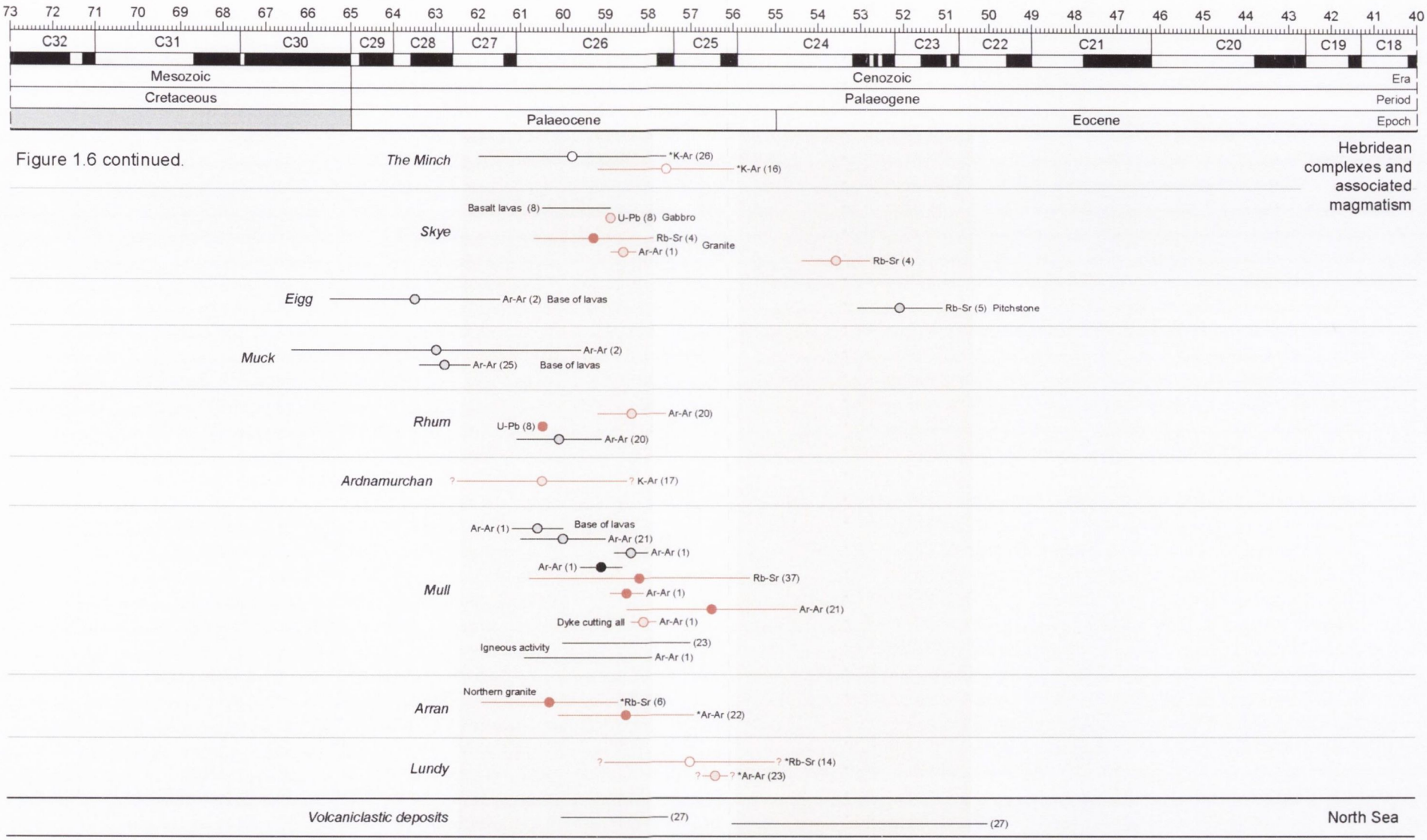

Figure 1.6 continued.

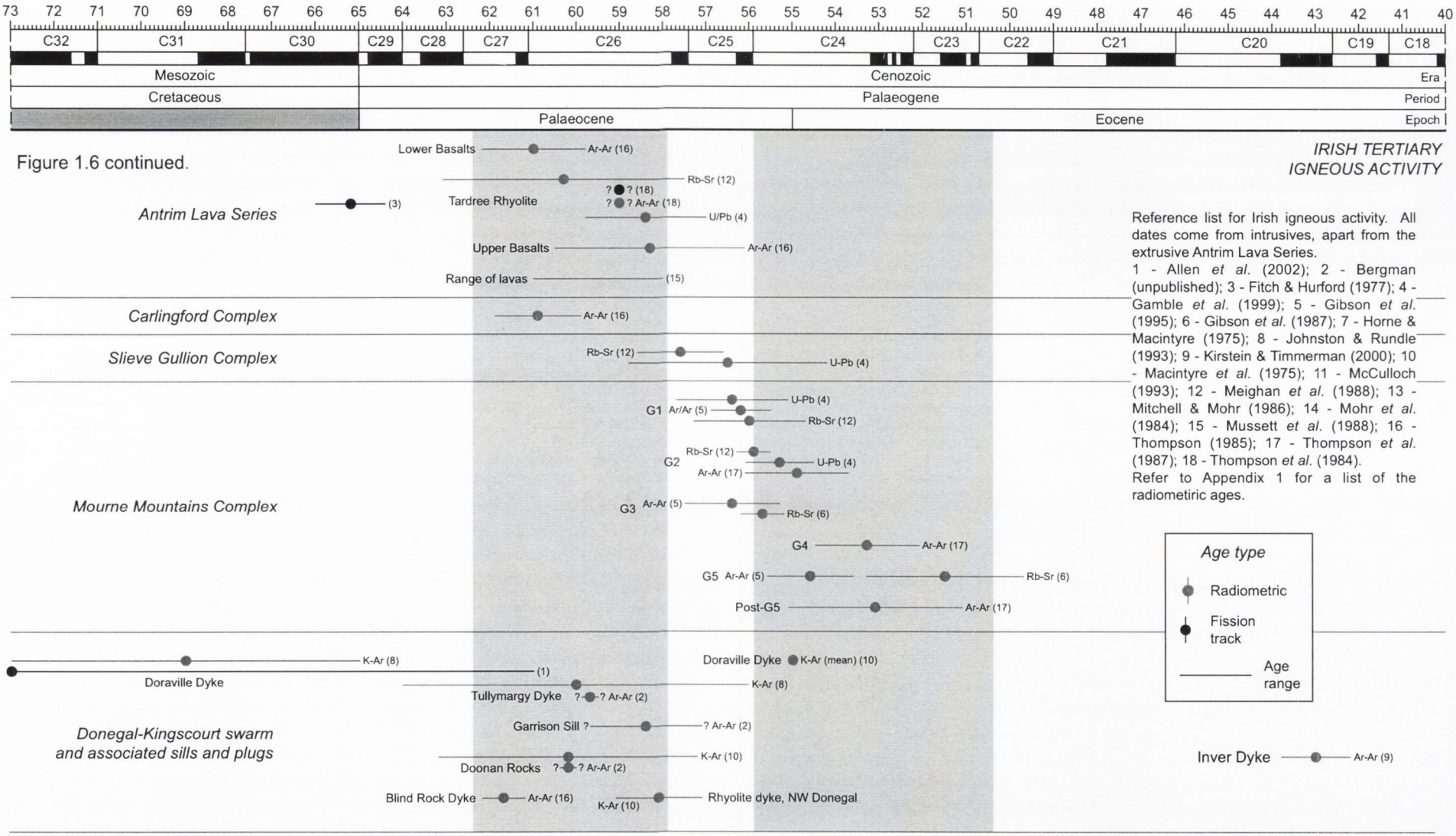

Figure 1.6 continued.

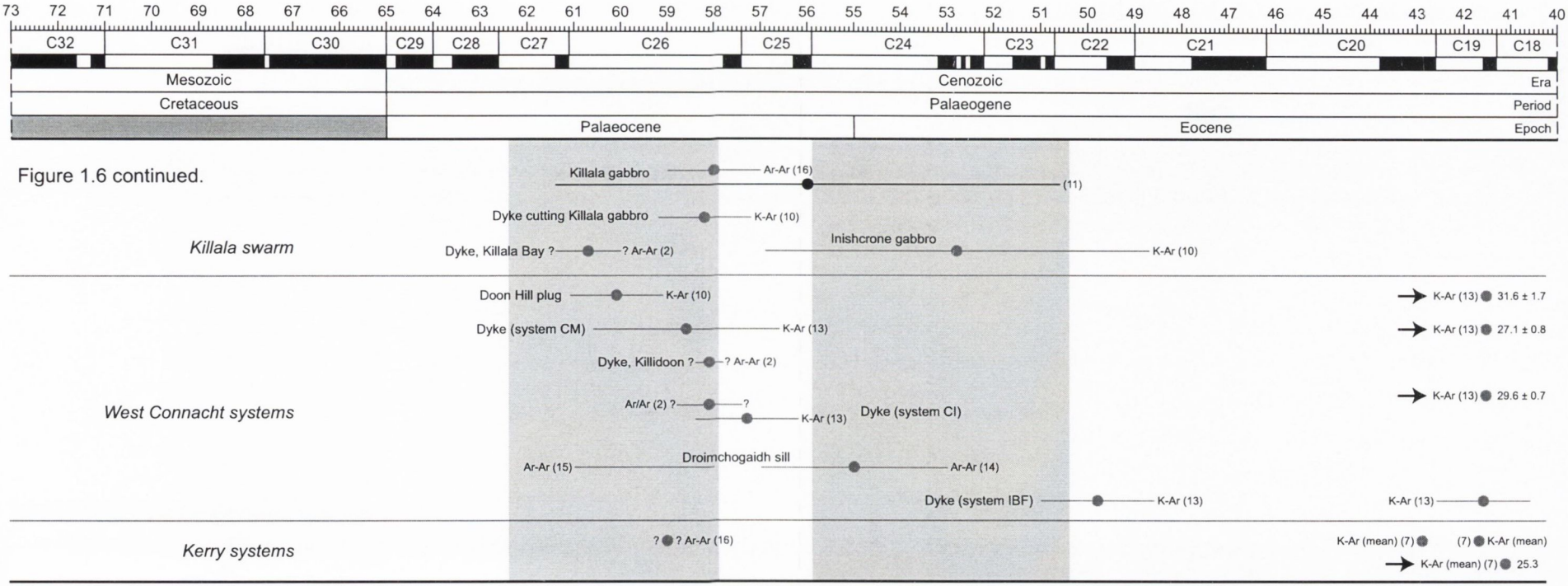

Figure 1.6 continued.

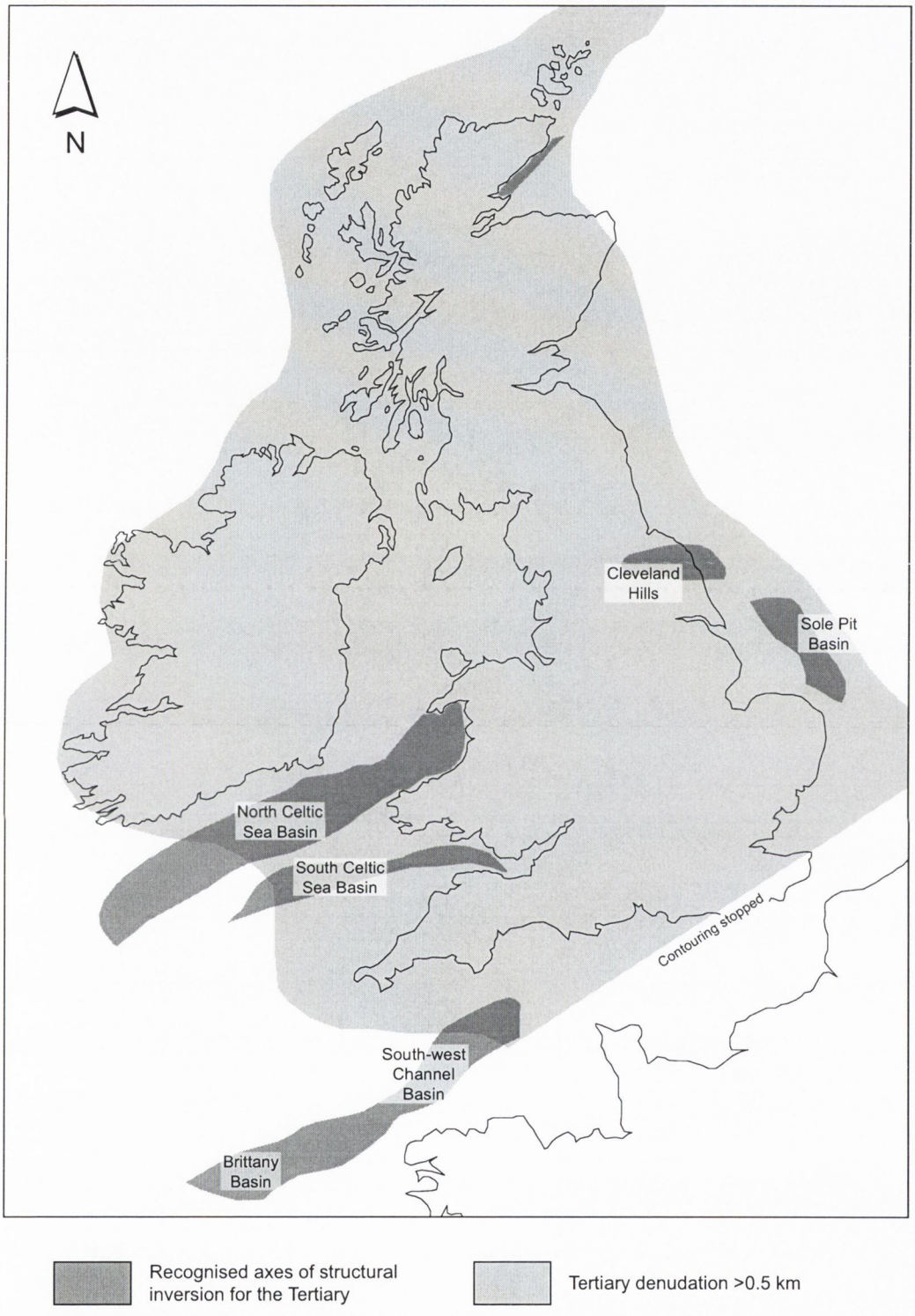

Figure 1.7. Map showing areas of structural inversion around Britain for the Tertiary period (from Hillis (1995)), compared with an estimate of the extent of Tertiary denudation for Britain and Ireland based on modelled subsidence histories and fission track data (from Jones *et al.* (2002)). Denudation is the maximum estimated value of Jones *et al.* (2002).

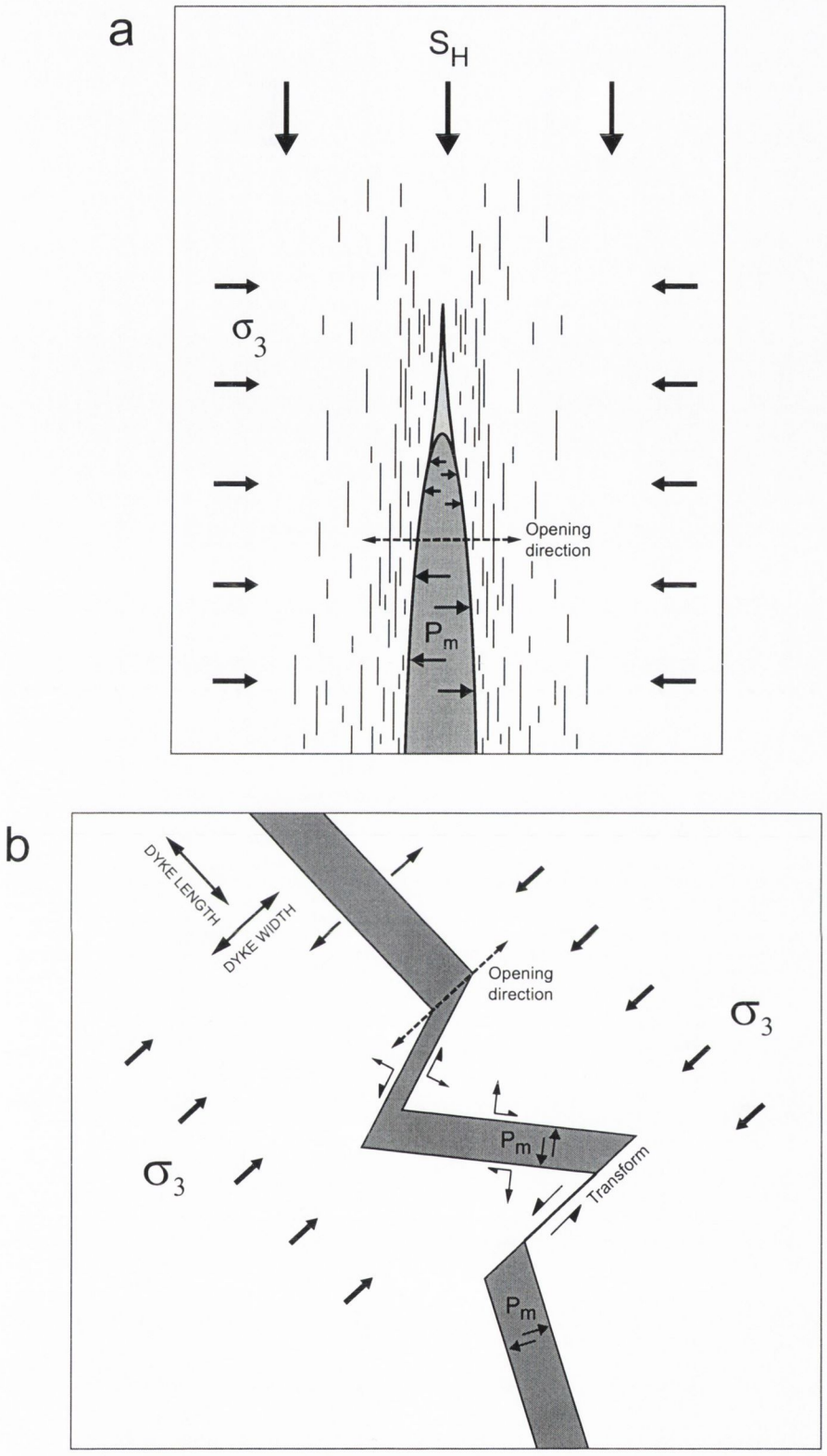

Figure 2.1. The propagation mechanisms of dykes (plan views).
a) The dyke propagates its own hydraulic fractures. Opening direction is parallel to the least compressive stress, σ_3. The dyke plane is parallel to the maximum compressive stress, S_H, in the horizontal plane (modified from Pollard (1987)). See text for full explanation.
b) The dyke exploits pre-existing fractures rather than propagating its own hydraulic fractures. Fractures open under a combination of extension and shear depending on their orientation relative to σ_3.
Opening directions are measured in the field by identifying points on both margins of the dyke that would fit together if the dyke were to close back up. A direction bearing (0 to 180°) between the two points is the opening direction. This can usually only be measured in the horizontal plane for dykes in this study.

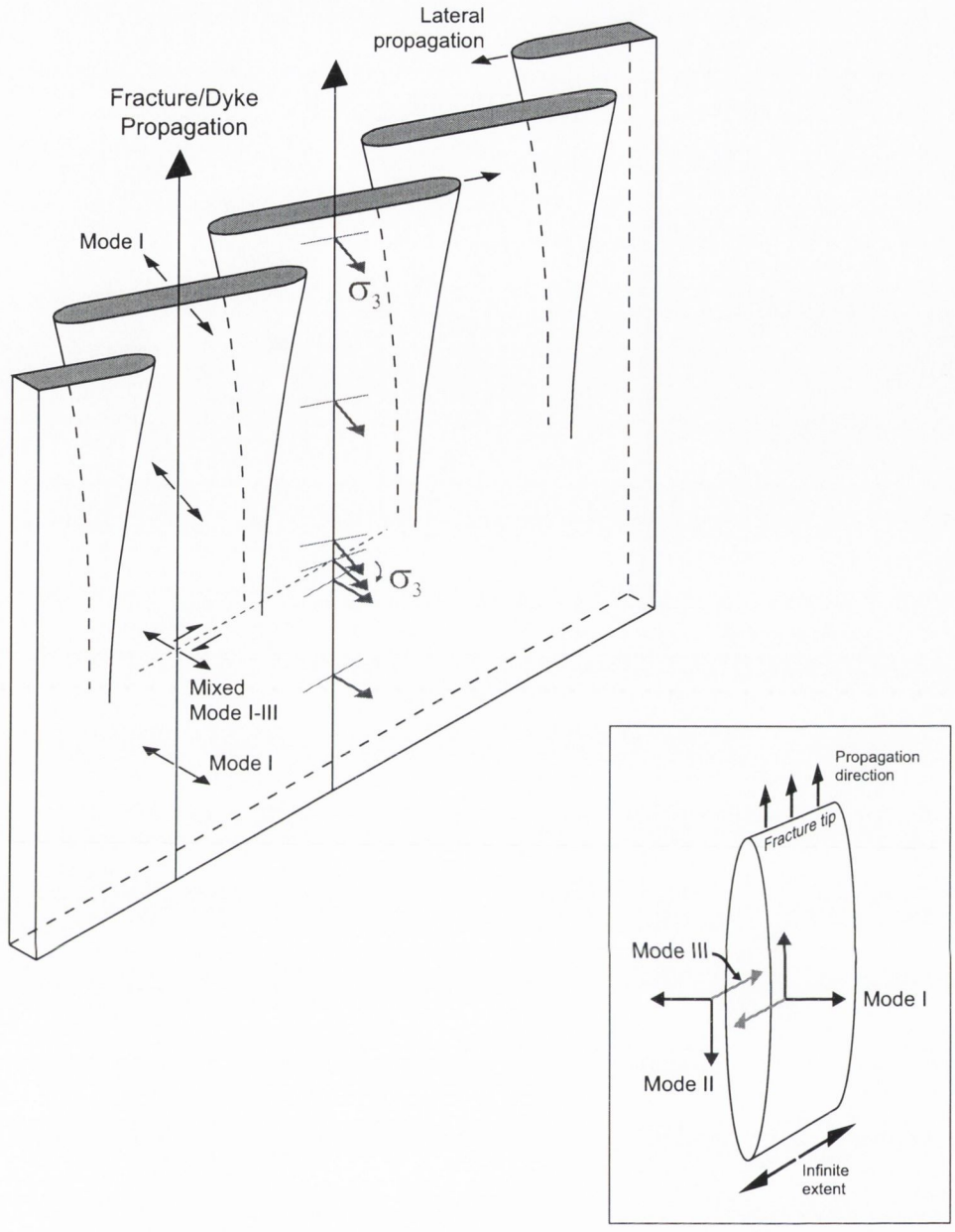

Figure 2.2. Mechanism for the en échelon segmentation of a dyke. The extension direction, σ_3, rotates out of perpendicular alignment with its mode I parent fracture. A mixed mode I-III stress at the propagating fracture tip causes breakdown into en échelon segments (modified from Delaney & Pollard (1981)).
The inset shows the three modes of stress intensities for a propagating fracture. Mode I is extensional and modes II and III are shear stresses. Modes II and III are defined relative to the line of the propagating fracuture tip.

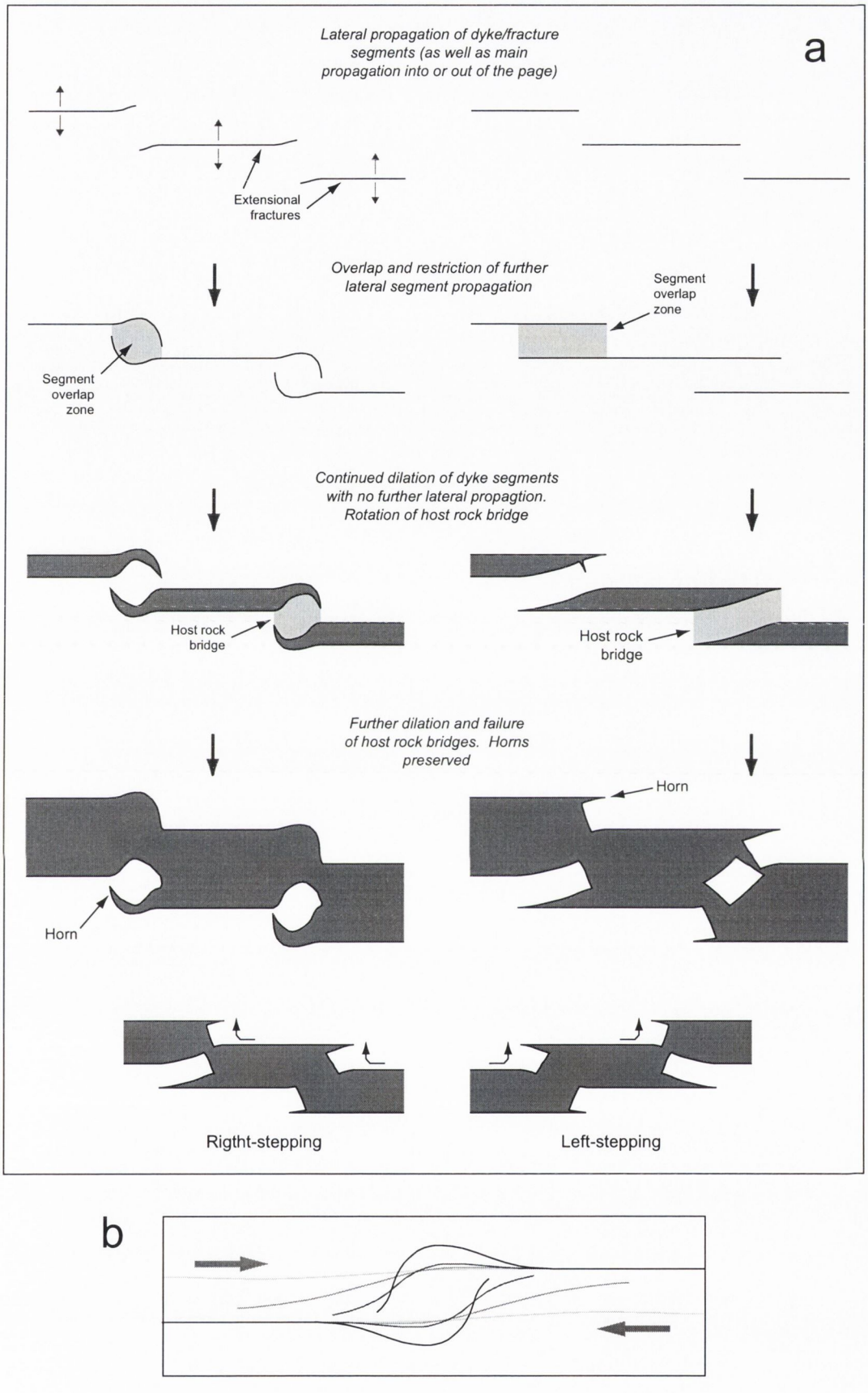

Figure 2.3. Stages in the development of en échelon dykes.
a) Extensional fractures propagate due to tensile stress at the dyke tip. Where segments overlap, fracture propagation can either be straight or curved, as indicated by the two sequences. Eventually, segments coalesce to form a stepping dyke. (Modified from Nicholson & Pollard (1985).)
b) The supression of curvature of overlapping fracture segments due to a high compressive stress parallel to the fractures (after Olson & Pollard (1989)). Fractures in black form under low compressive stress; those in grey form under high compressive stress.

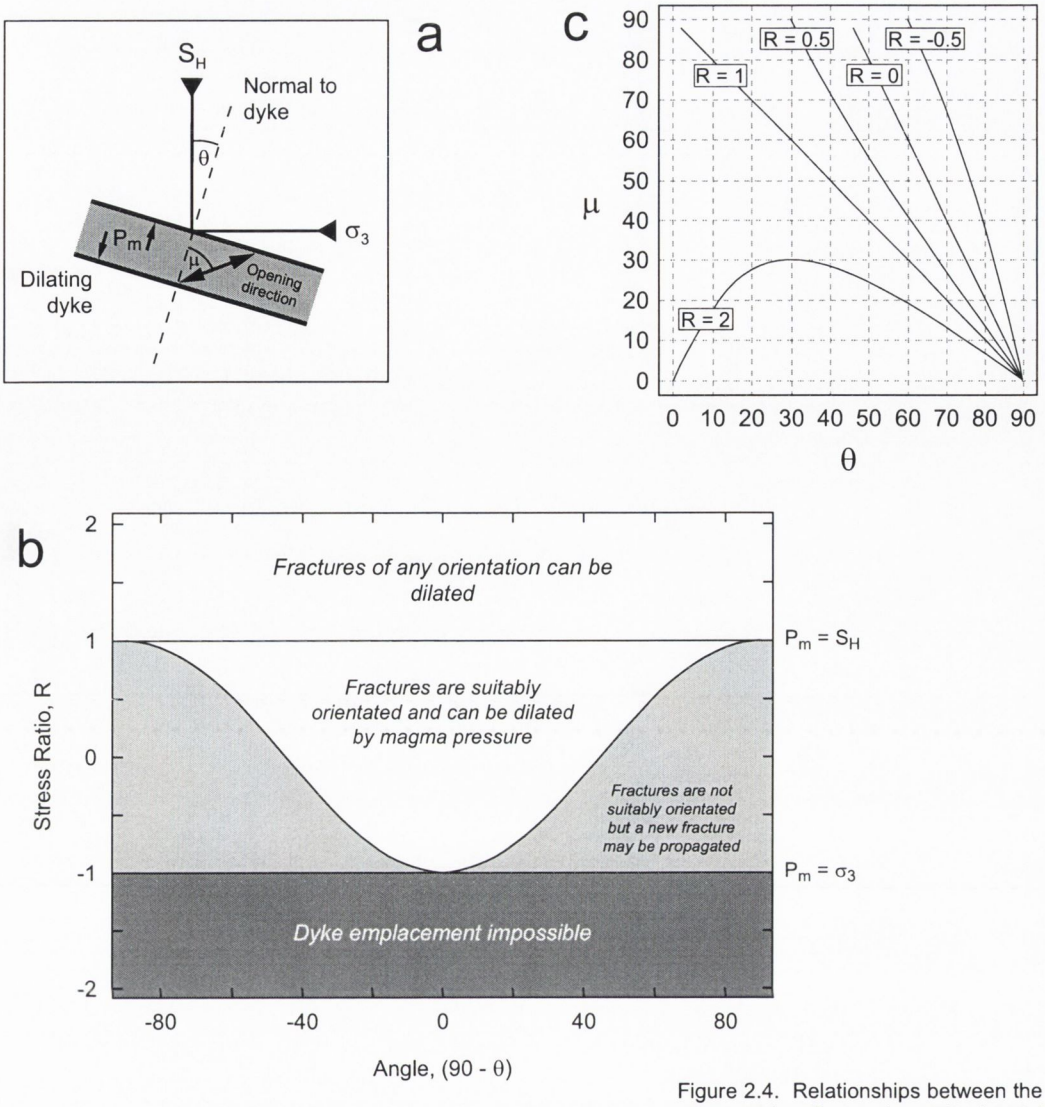

Figure 2.4. Relationships between the stress ratio, R, maximum horizontal compressive stress, S_H, the minimum horizontal compressive stress, σ_3, magma pressure, P_m, dyke orientation (defined by θ), and dyke opening direction (defined by μ) (modified after Delaney *et al.* (1986) and Jolly & Sanderson (1995)).

a) The notation used.

b) Plot of R against (90 - θ) showing the condtions under which fractures may open.

c) Plot of μ against θ defining how the opening direction of a dyke varies with respect to σ_3 for different values of R.

d) The variation in dyke form as R varies, for dykes exploiting pre-existing fractures. The dashed lines indicate opening directions of the dykes. R = -1: only fractures normal to σ_3 will dilate. R = 0: a greater range of fractures will dilate (±45°) with opening directions that are oblique to σ_3. R = 1: all fractures will dilate but with opening directions that are parallel to σ_3. R >> 1: all fracture orientations are able to dilate in all opening directions; tending towards the situation where $S_H = \sigma_3$.

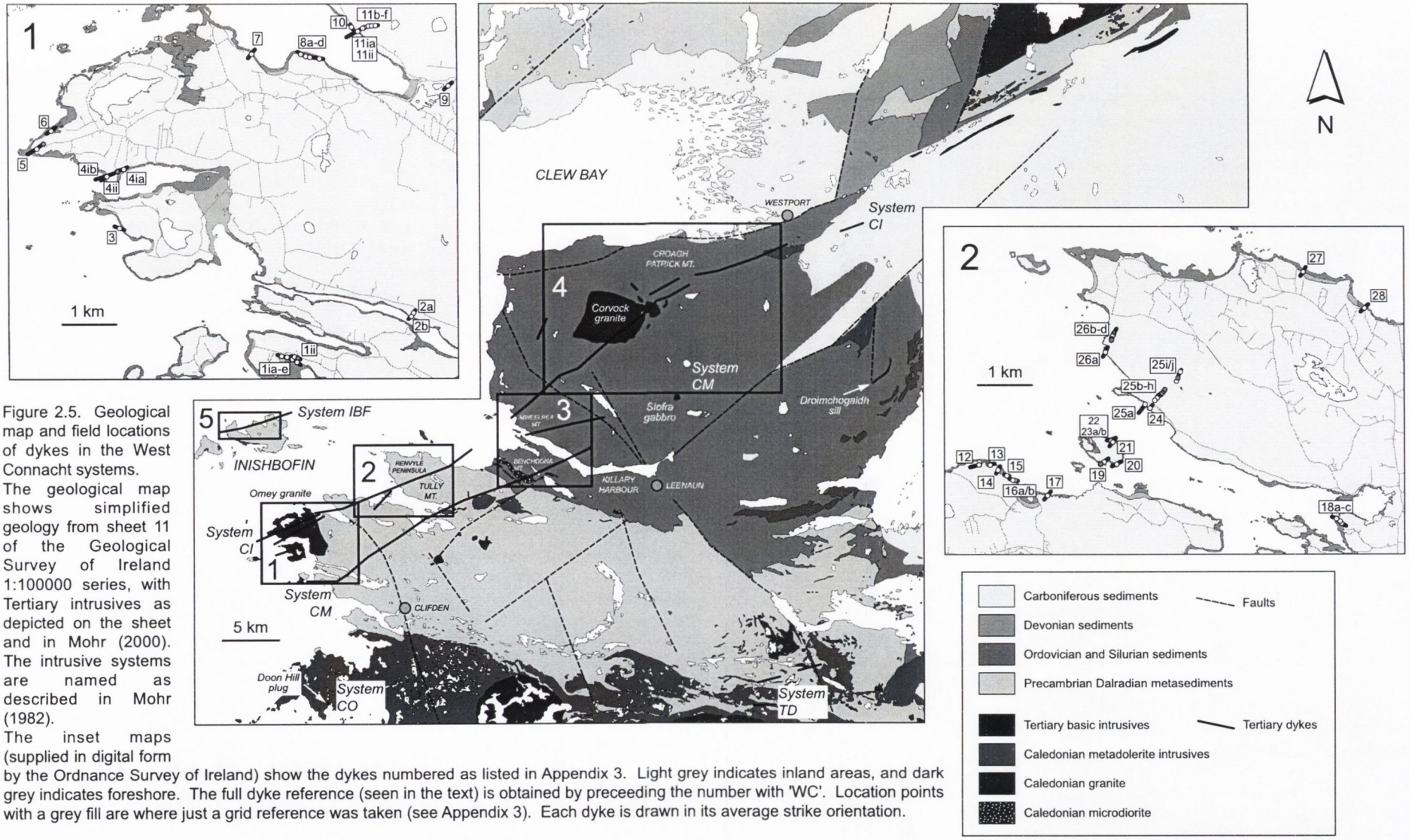

Figure 2.5. Geological map and field locations of dykes in the West Connacht systems.

The geological map shows simplified geology from sheet 11 of the Geological Survey of Ireland 1:100000 series, with Tertiary intrusives as depicted on the sheet and in Mohr (2000). The intrusive systems are named as described in Mohr (1982).

The inset maps (supplied in digital form by the Ordnance Survey of Ireland) show the dykes numbered as listed in Appendix 3. Light grey indicates inland areas, and dark grey indicates foreshore. The full dyke reference (seen in the text) is obtained by preceeding the number with 'WC'. Location points with a grey fill are where just a grid reference was taken (see Appendix 3). Each dyke is drawn in its average strike orientation.

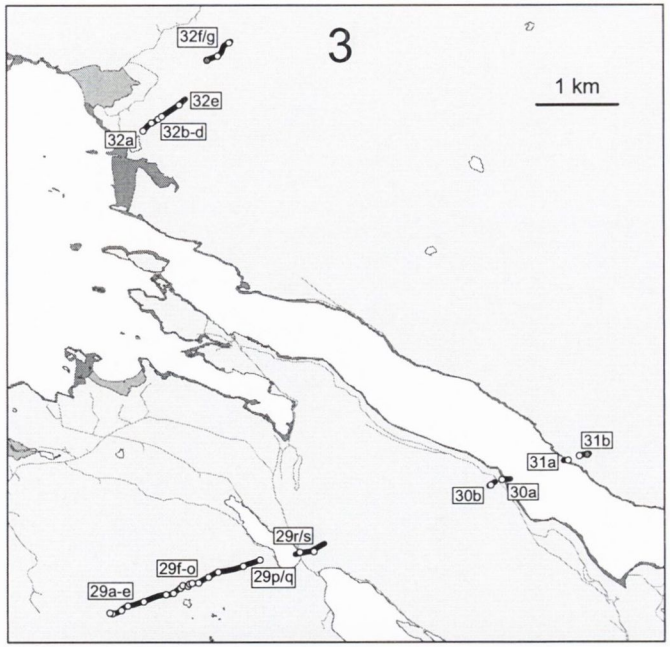

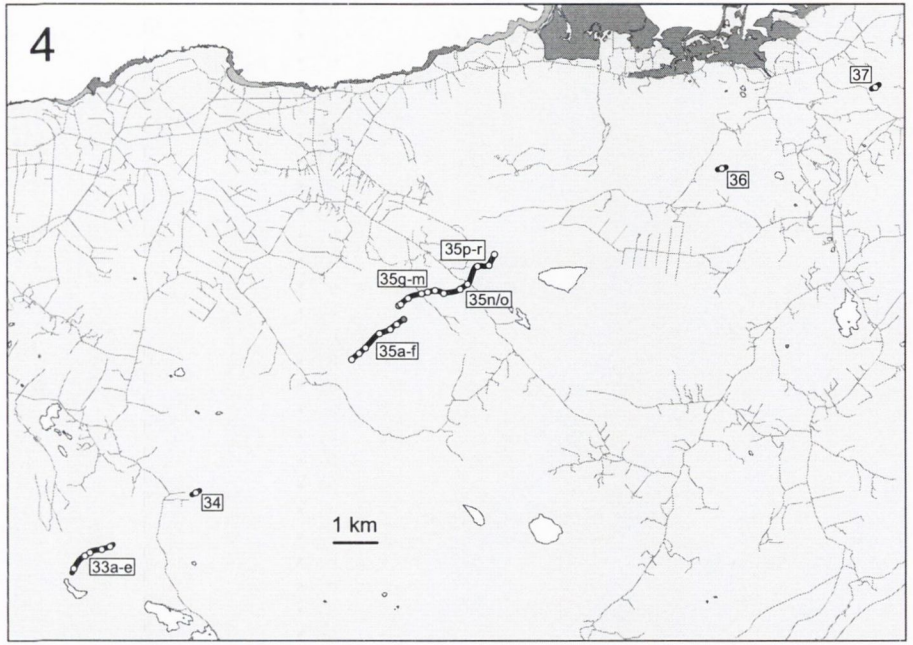

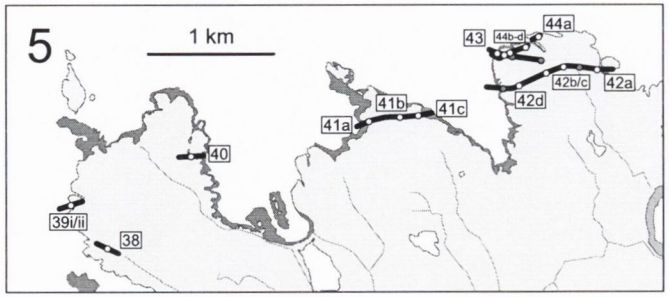



Figure 2.5 continued.

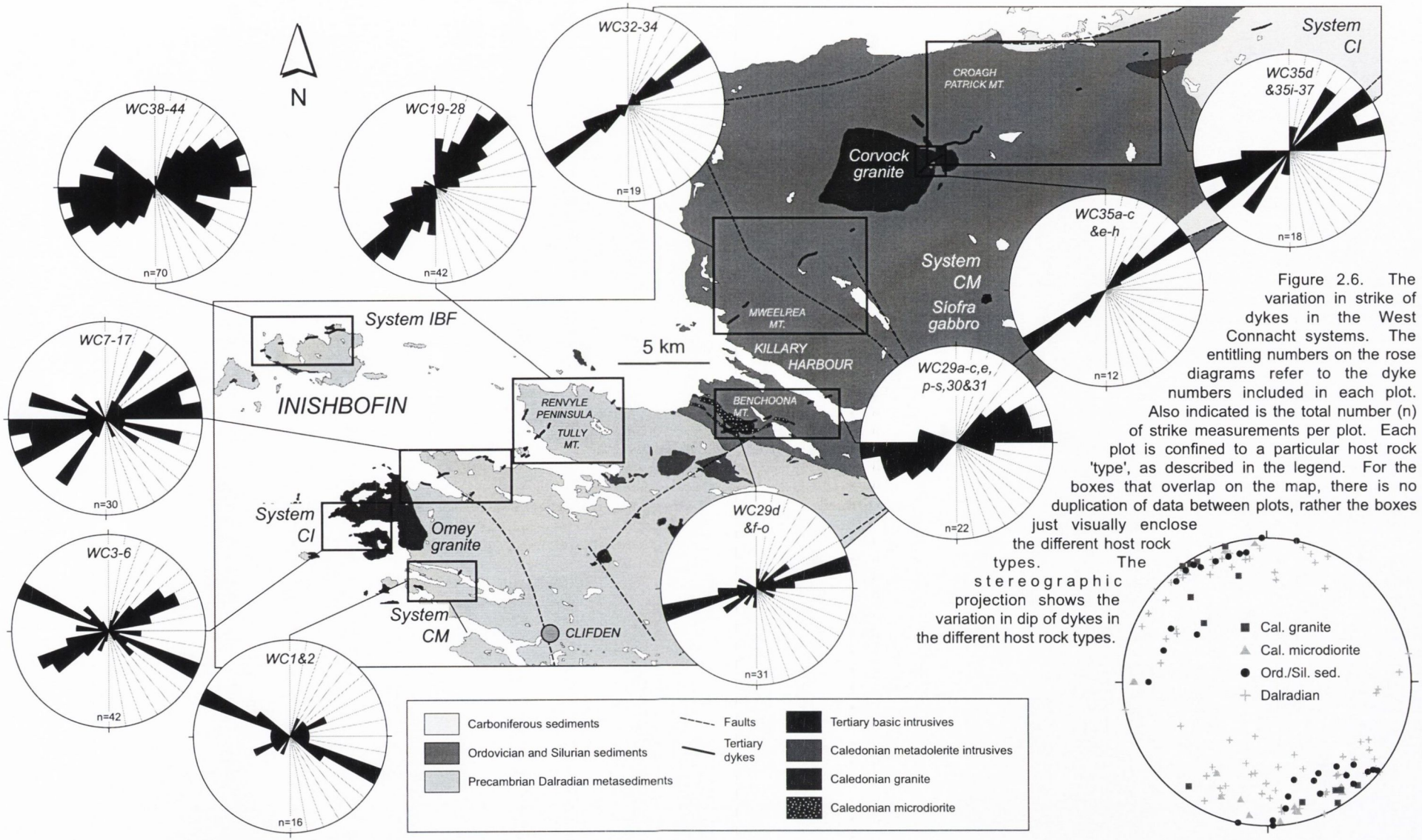

Figure 2.6. The variation in strike of dykes in the West Connacht systems. The entitling numbers on the rose diagrams refer to the dyke numbers included in each plot. Also indicated is the total number (n) of strike measurements per plot. Each plot is confined to a particular host rock 'type', as described in the legend. For the boxes that overlap on the map, there is no duplication of data between plots, rather the boxes just visually enclose the different host rock types. The stereographic projection shows the variation in dip of dykes in the different host rock types.

Figure 2.7. En échelon dyke forms of system CI cutting the Renvyle peninsula. The outlines of reconstructed parts of the dykes are dashed and the fills are light grey. Note that dyke WC28 has a dextral magma-filled pull-apart array associated with the right-step, consistent with host rock bridge deformation described in Chapter 3.

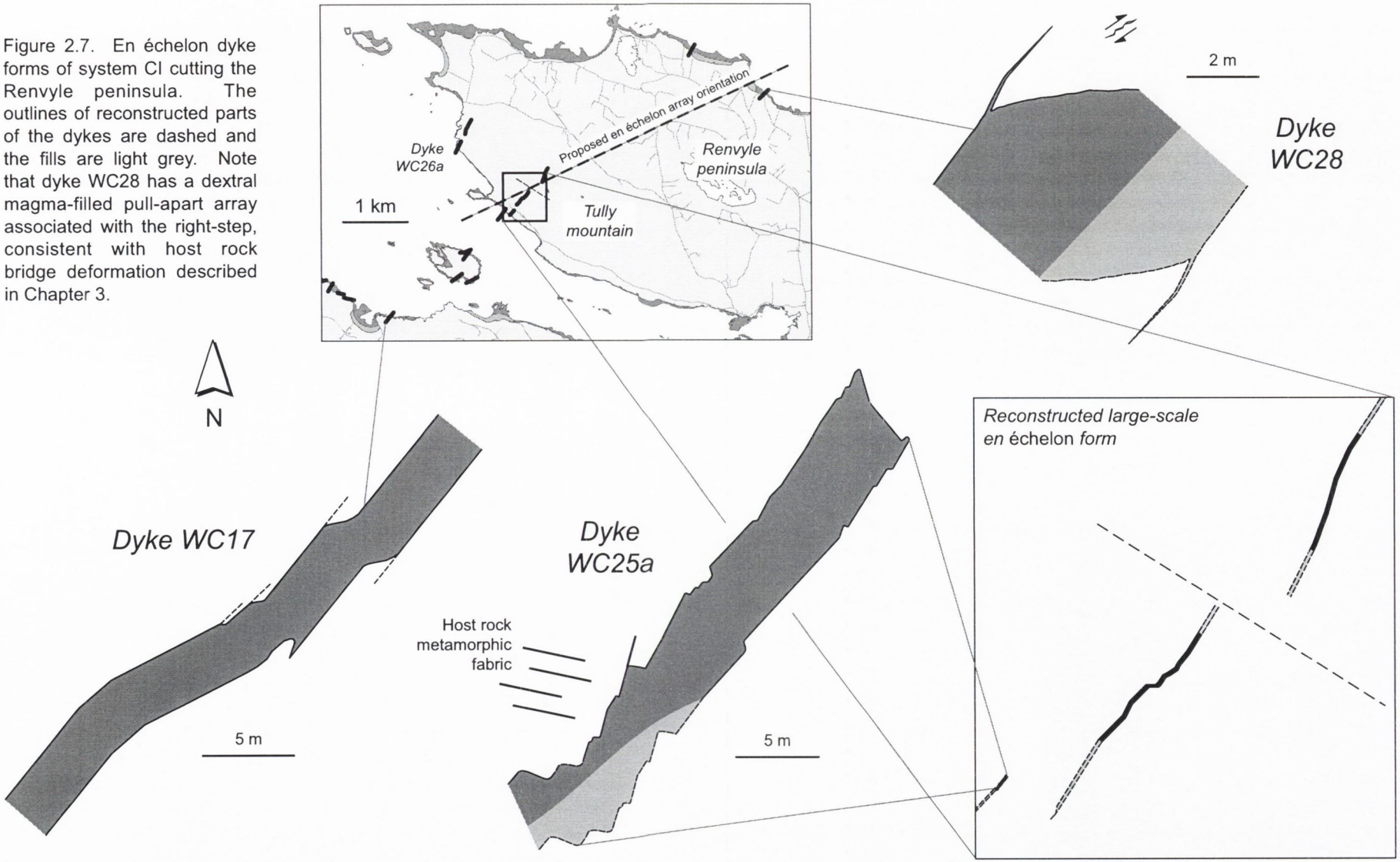

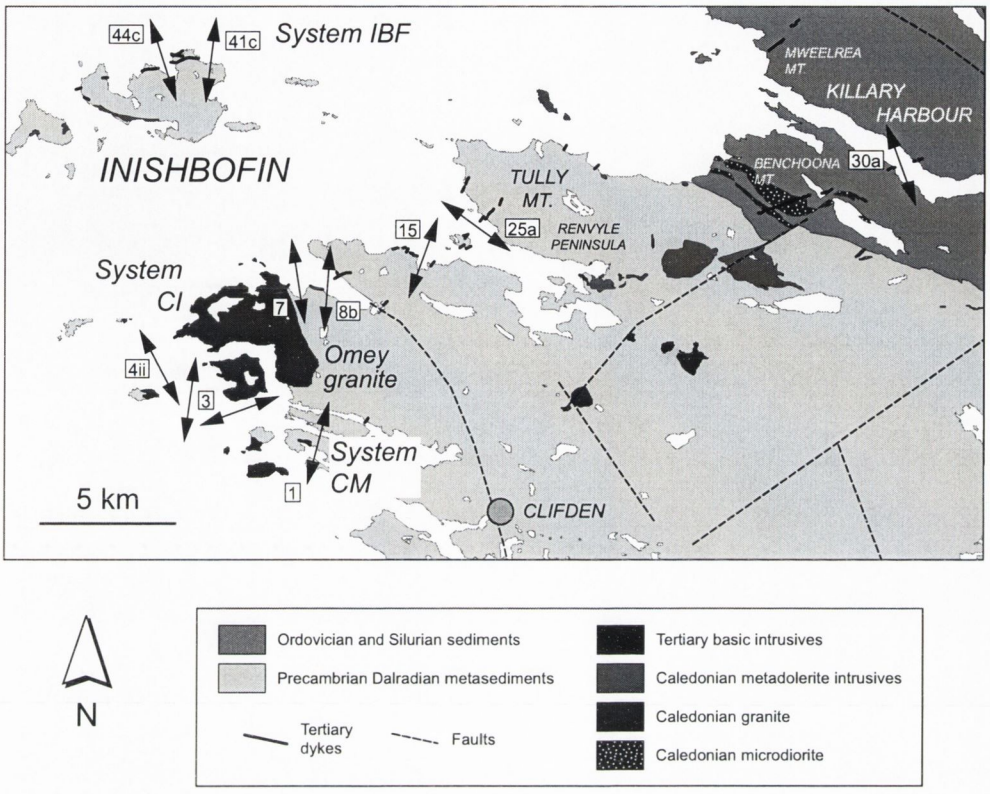

Figure 2.8. Opening directions in the horizontal plane for dykes in the West Connacht systems (dyke numbers are as in Figure 2.5 and are preceeded with 'WC').

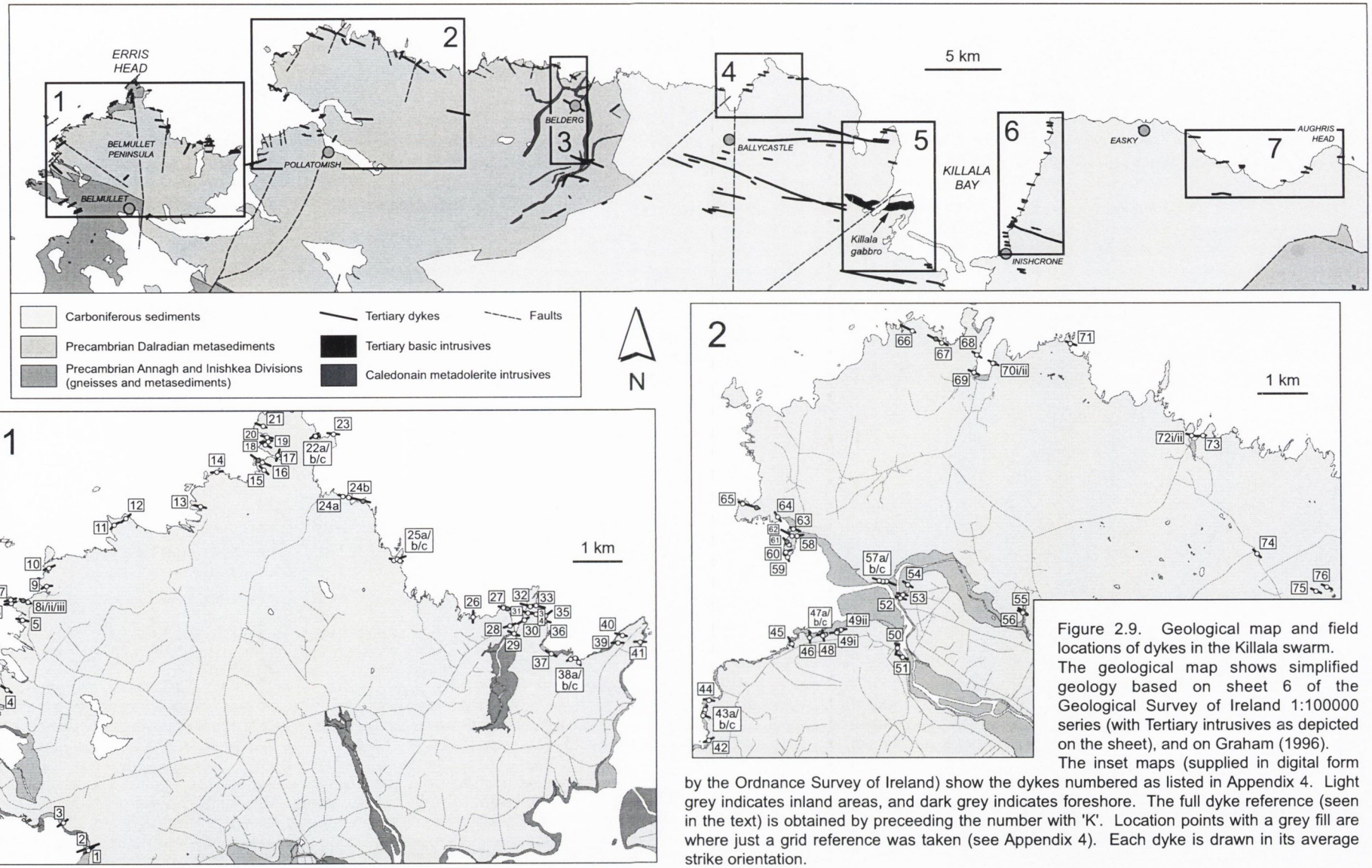

Figure 2.9. Geological map and field locations of dykes in the Killala swarm. The geological map shows simplified geology based on sheet 6 of the Geological Survey of Ireland 1:100000 series (with Tertiary intrusives as depicted on the sheet), and on Graham (1996). The inset maps (supplied in digital form by the Ordnance Survey of Ireland) show the dykes numbered as listed in Appendix 4. Light grey indicates inland areas, and dark grey indicates foreshore. The full dyke reference (seen in the text) is obtained by preceeding the number with 'K'. Location points with a grey fill are where just a grid reference was taken (see Appendix 4). Each dyke is drawn in its average strike orientation.

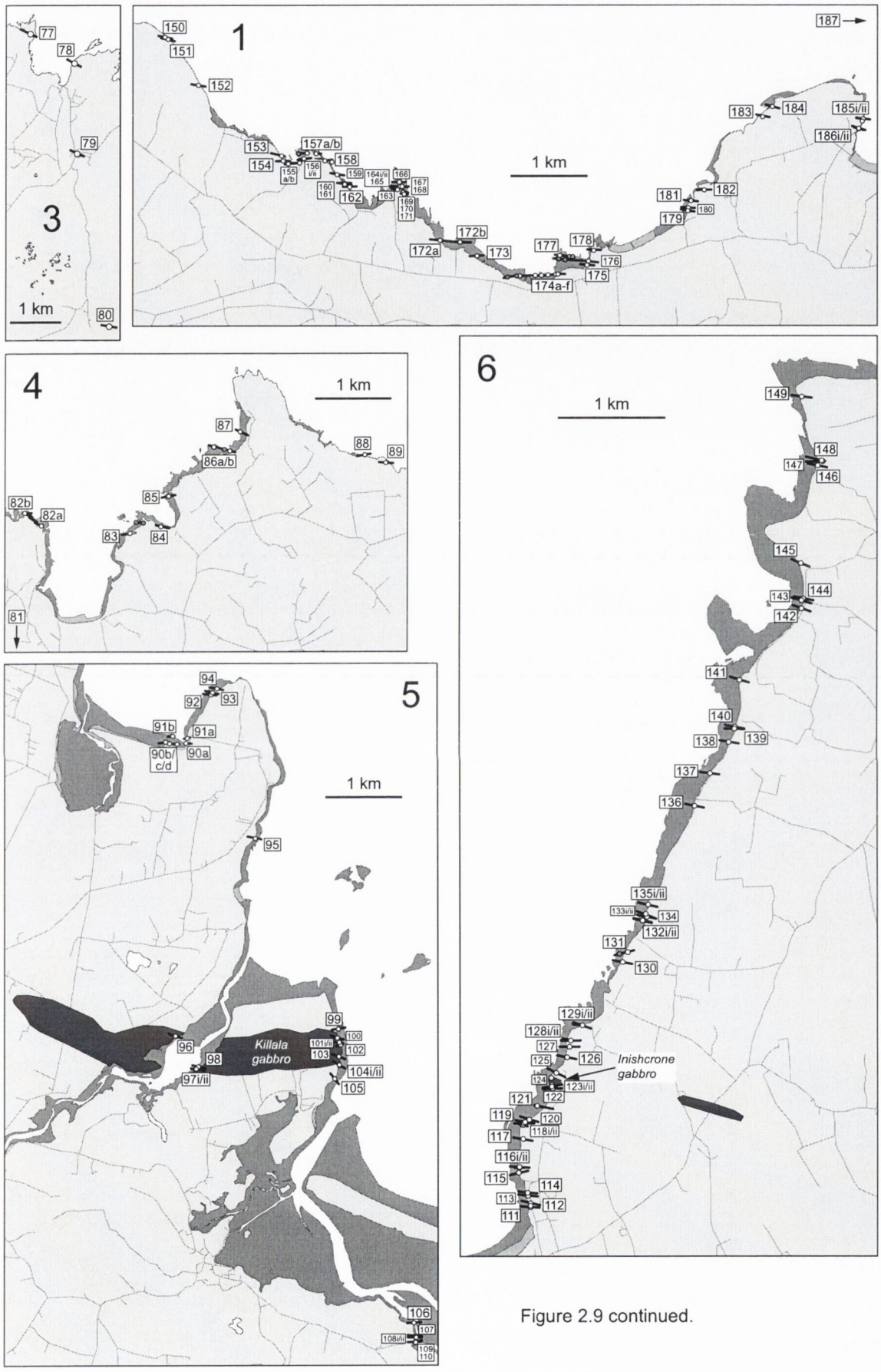

Figure 2.9 continued.

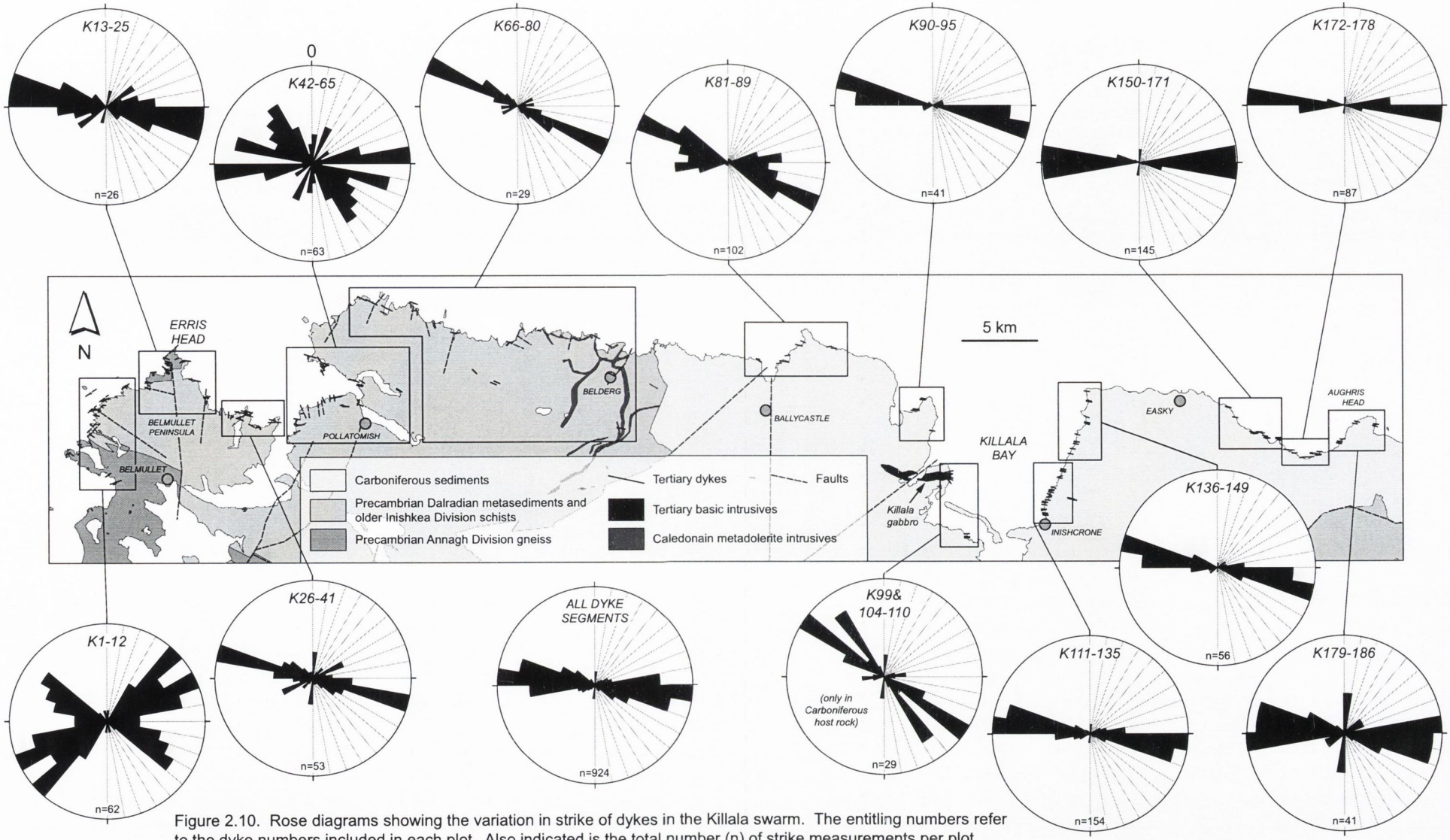

Figure 2.10. Rose diagrams showing the variation in strike of dykes in the Killala swarm. The entitling numbers refer to the dyke numbers included in each plot. Also indicated is the total number (n) of strike measurements per plot.

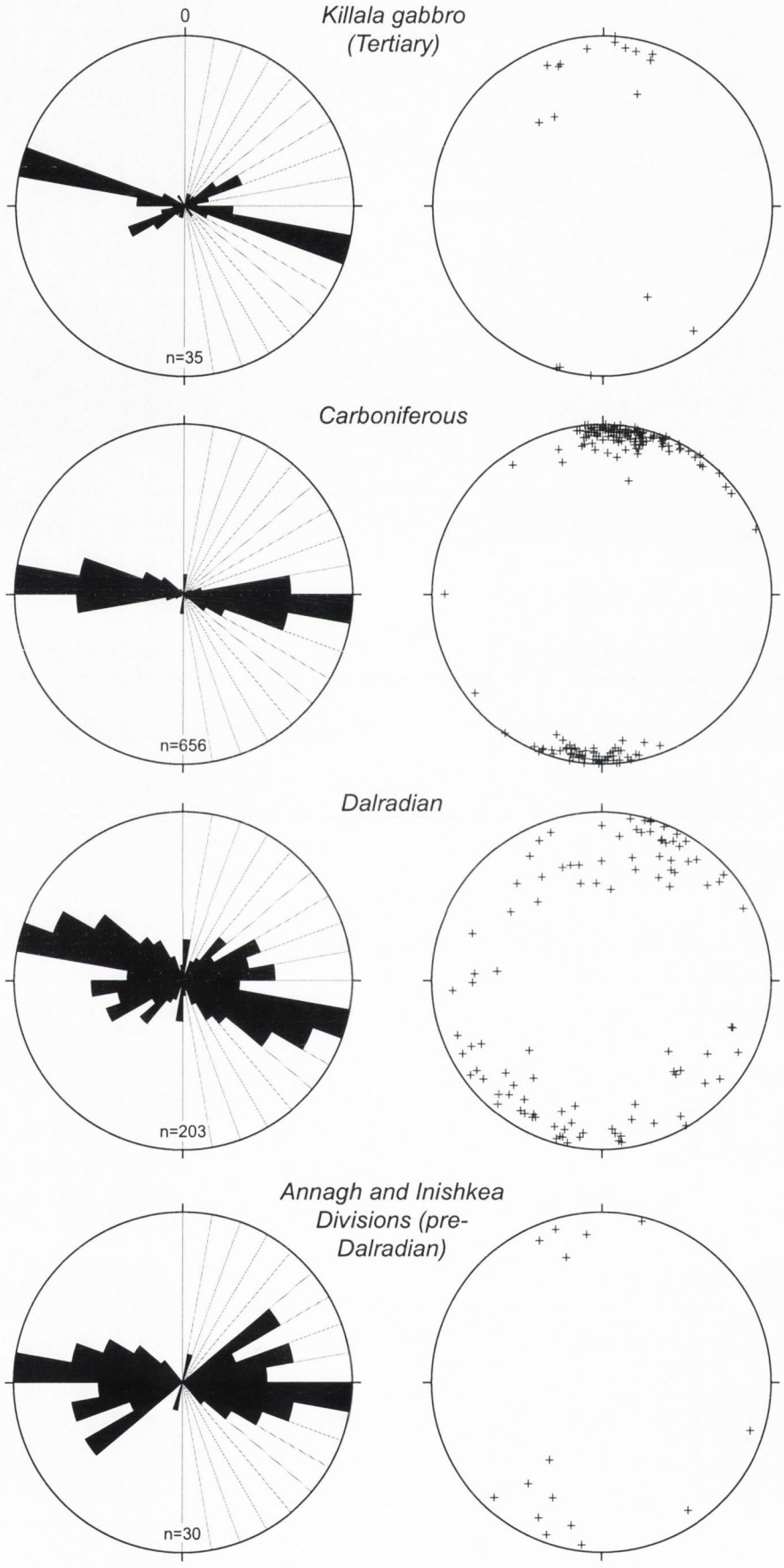

Figure 2.11. Plots showing the range in orientation of dykes belonging to the Killala swarm for the different host rock types. The rose diagrams show the range in strike ('n' is the total number of strike measurements per plot), and the stereographic projections show the range in dip as well as strike.

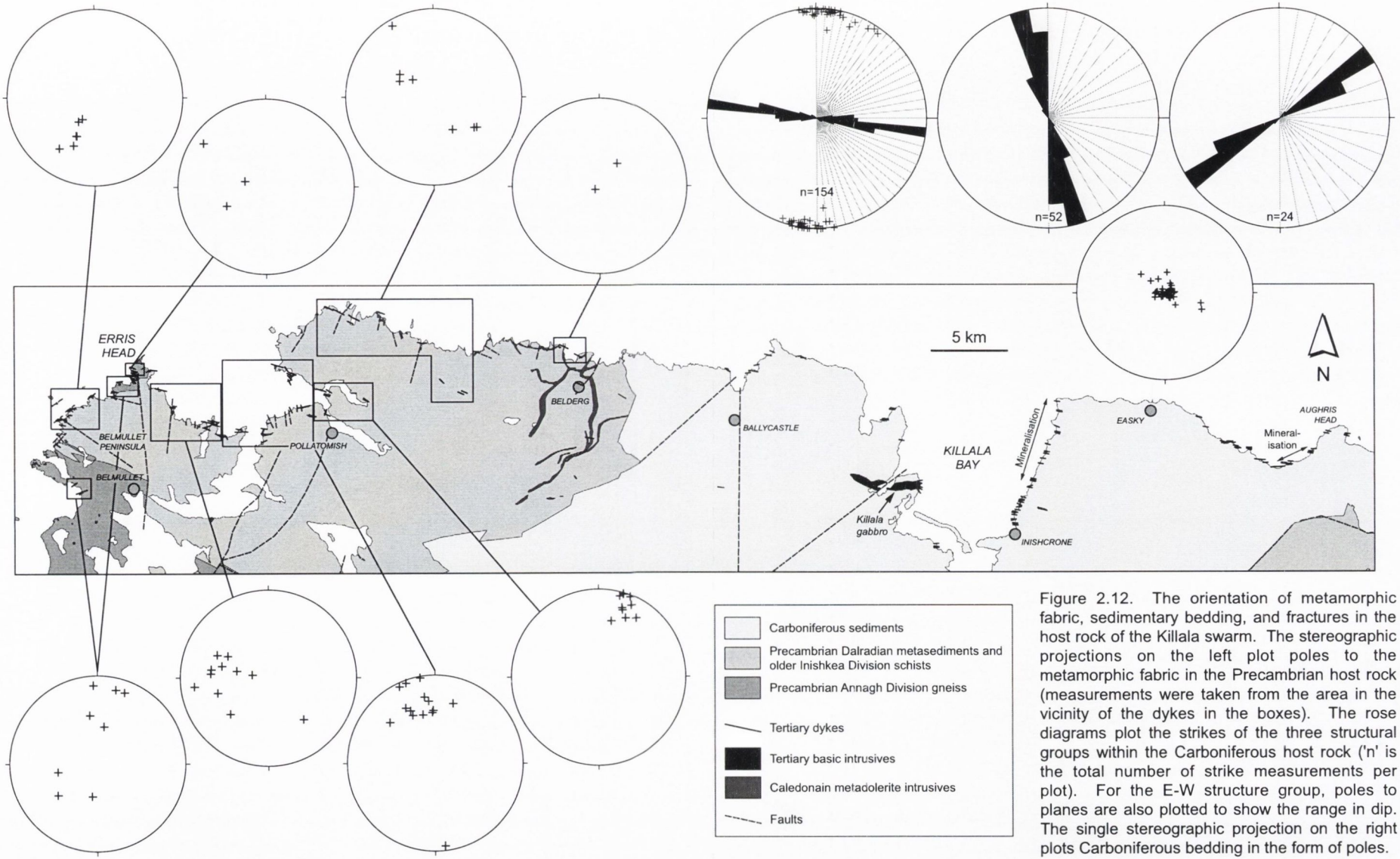

Figure 2.12. The orientation of metamorphic fabric, sedimentary bedding, and fractures in the host rock of the Killala swarm. The stereographic projections on the left plot poles to the metamorphic fabric in the Precambrian host rock (measurements were taken from the area in the vicinity of the dykes in the boxes). The rose diagrams plot the strikes of the three structural groups within the Carboniferous host rock ('n' is the total number of strike measurements per plot). For the E-W structure group, poles to planes are also plotted to show the range in dip. The single stereographic projection on the right plots Carboniferous bedding in the form of poles.

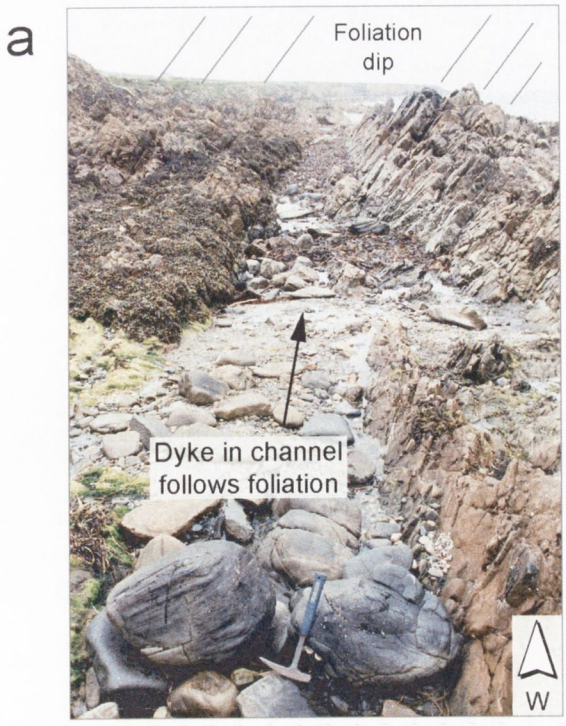

Figure 2.13. Photographs showing structure within the Dalradian and older host rock from the western part of the Killala swarm.
a) Dalradian foliation strikes E-W and dips south. The channel is occupied by a Tertiary dyke (K49).
b) NE-SW major fractures in Dalradian host rock, southwest of dyke K11. The cliffs are around 50 m in height.
c) N-S to NNW-SSE steeply dipping fractures in Dalradian host rock between dykes K45 and K46. The field of view from east to west in the mid-ground is around 10 m.

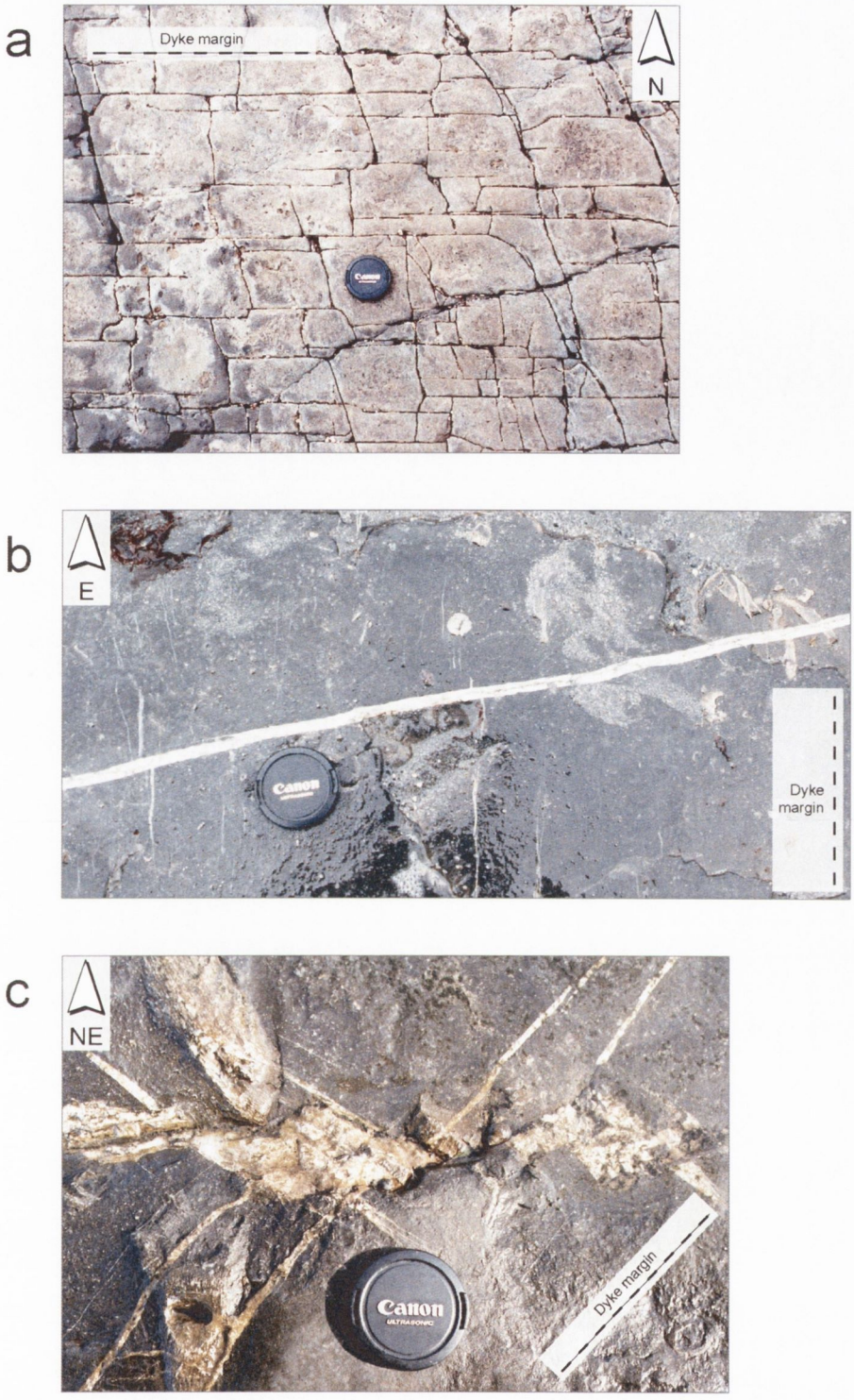

Figure 2.14. Plan views of structures within Carboniferous host rock of the Killala swarm.

a) The relationship between dyke sub-parallel and high angle fractures in limestone north of dyke K87. Both fracture sets show abutting relationships with each other.

b) A sinistral offset of dyke sub-parallel veins across a (thicker) high angle vein (strike 162°) in the vicinity of dyke K147.

c) A dextral offset of dyke sub-parallel veins across a dextral pull-apart array (strike 148°) south of dyke K136.

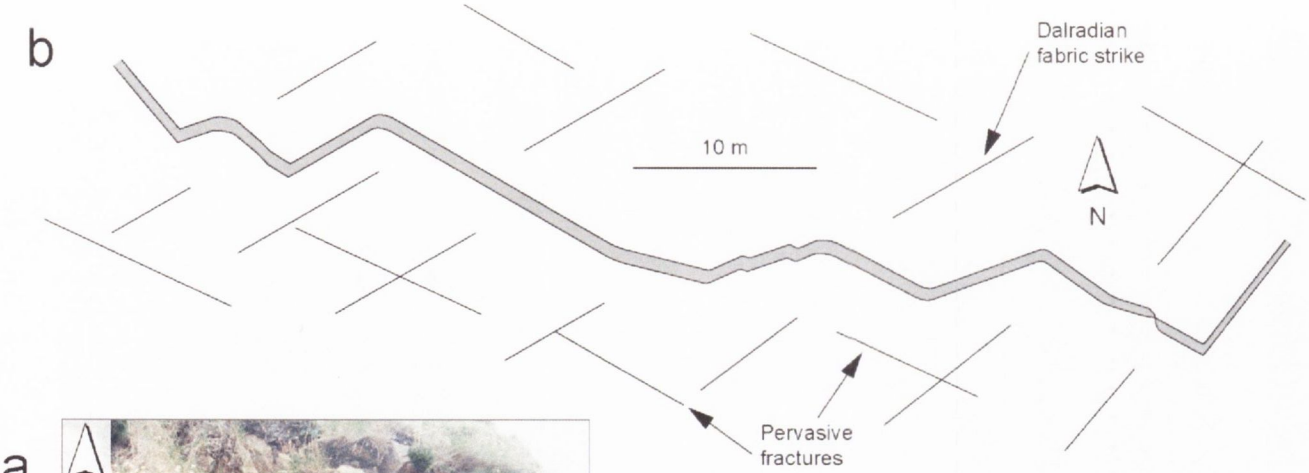

Figure 2.15. Dyke forms within Dalradian and older host rock from the western part of the Killala swarm.
a) Cross-section of dyke K47b following the Dalradian fabric.
b) Plan view of dyke K40 exploiting the Dalradian fabric and a pervasive NE-SW fracture set
c) Cross-section of dyke K4 exploiting a fault of relatively shallow dip to the northeast.



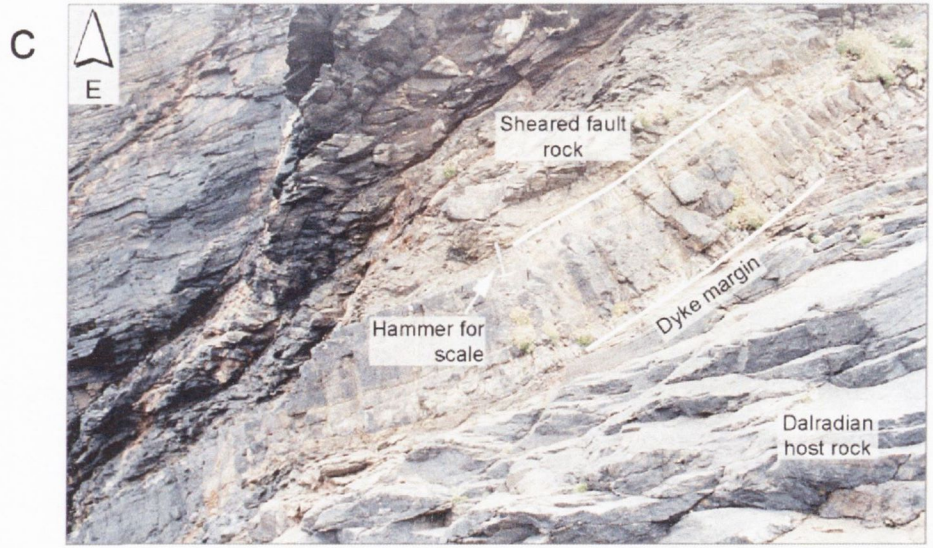

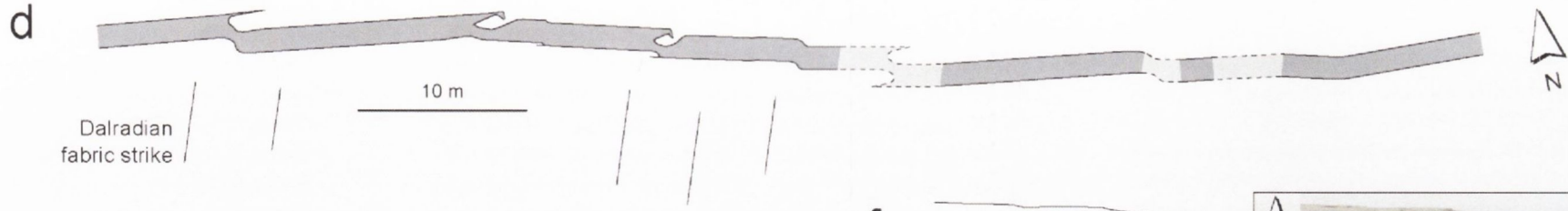

Figure 2.15 continued.
d) Plan view of dyke K27, consisting of a number of right-stepping en échelon segments (dashed lines and lighter fill is where the dyke is inferred).
e) Plan view of dyke K10, consisting of a number of right-stepping en échelon segments.
f) Cliff section showing dyke K17 consisting of two en échelon segments in vertical section, and also showing jogs along the foliation of the Annagh Division host rock. The height of the cliff is around 70 m.

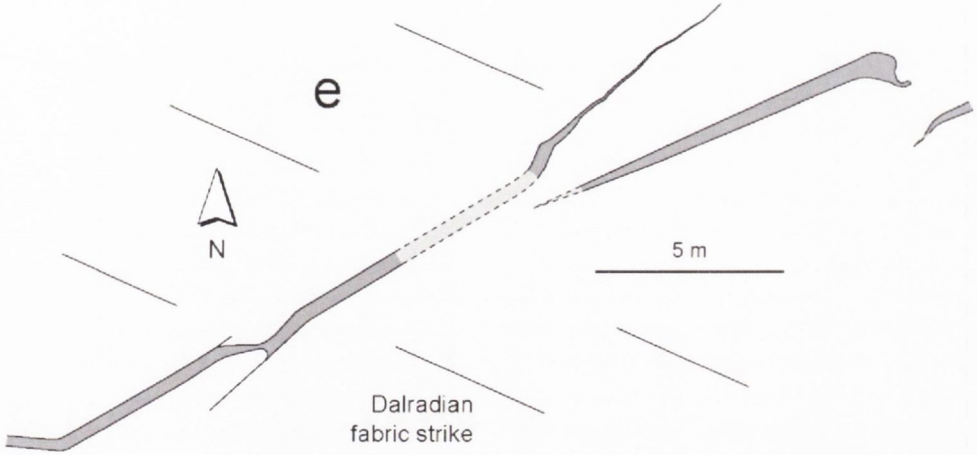

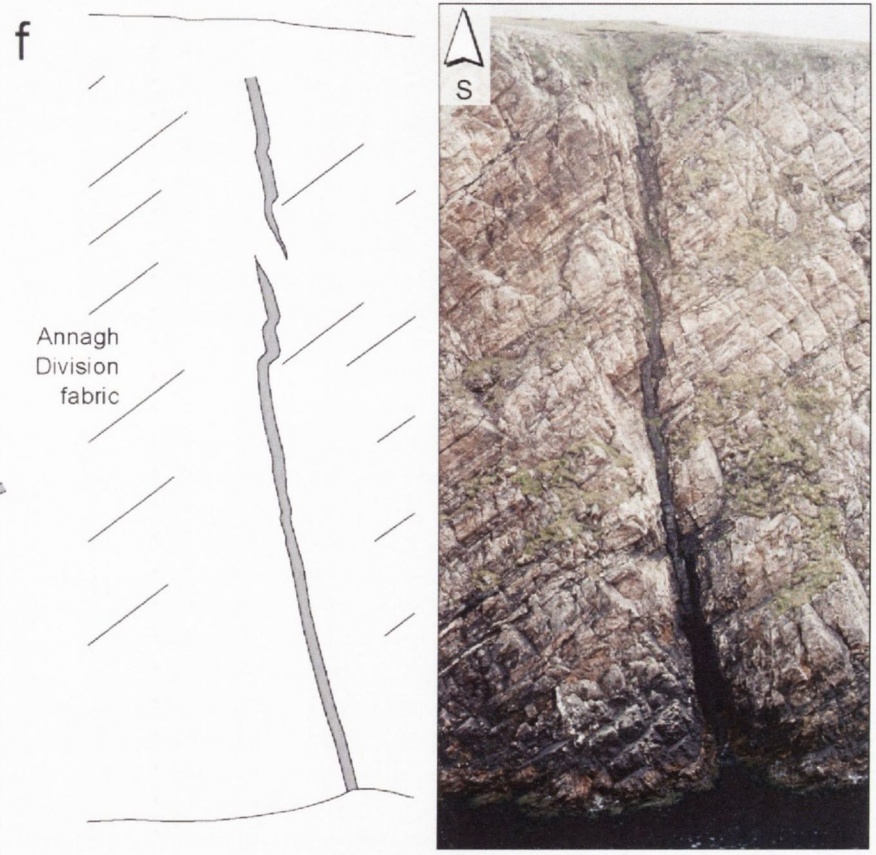

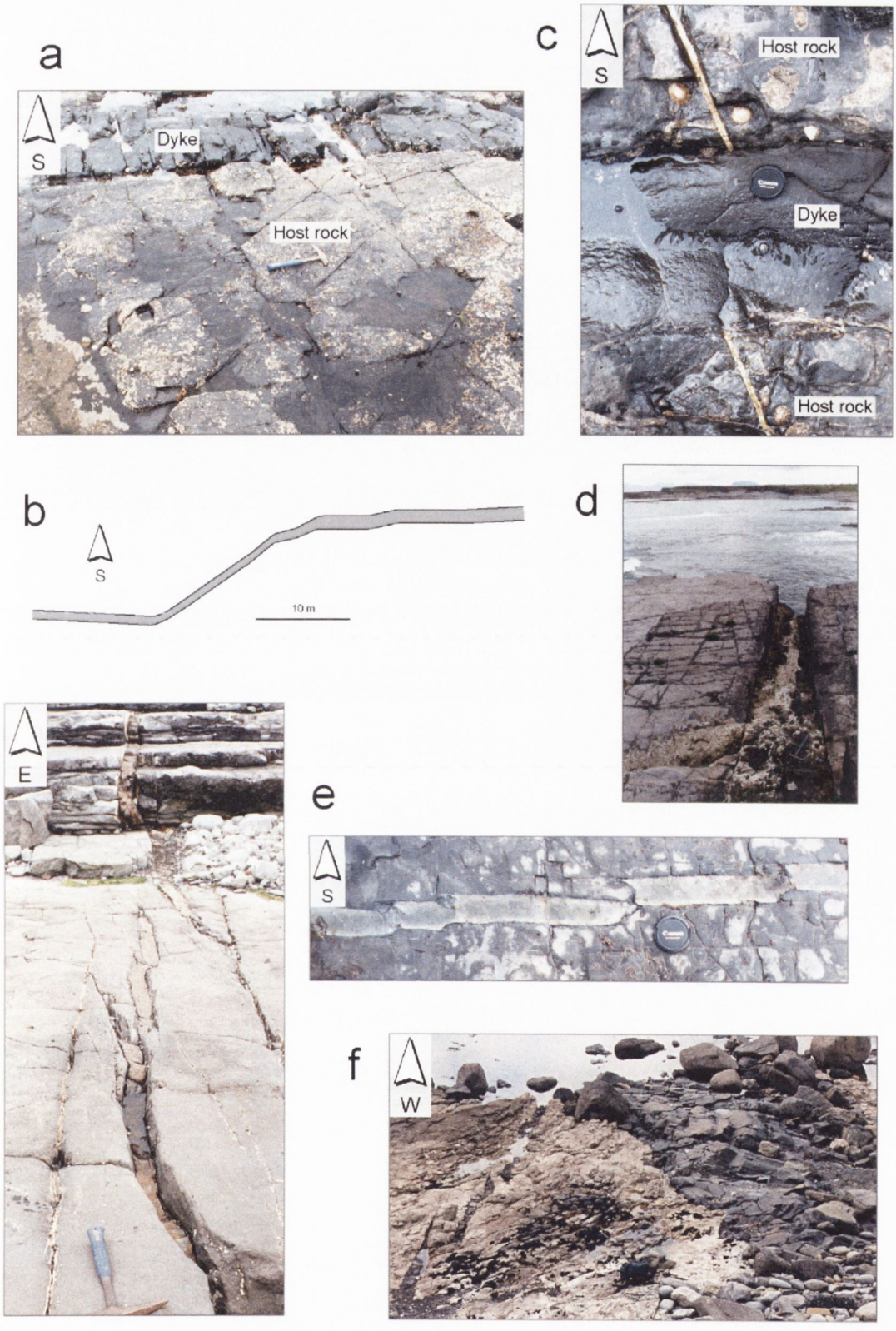

Figure 2.16. The relationships between the dykes and pre-existing structures in Carboniferous host rock.
a) NE-SW fractures abutting against the margin of dyke K119.
b) Plan view of dyke K180 showing the apparent expoitation of a NE-SW fracture.
c) Plan view of dyke K143 offsetting a high angle vein.
d) Dyke K153 appearing to follow the pre-existing dyke-parallel fracture set in the host rock.
e) En échelon forms of dykes K128ii (left, oblique plan view) and K175 (right, plan view).
f) Oblique plan view of dykes K123i (left side - narrow right-stepping en échelon array) and K123ii (right side - wide dyke with a left-stepping south margin (not very clear in the photograph)) in an apparent conjugate relationship within highly baked limestone host rock, just south of the Inishcrone gabbro (dyke K124).

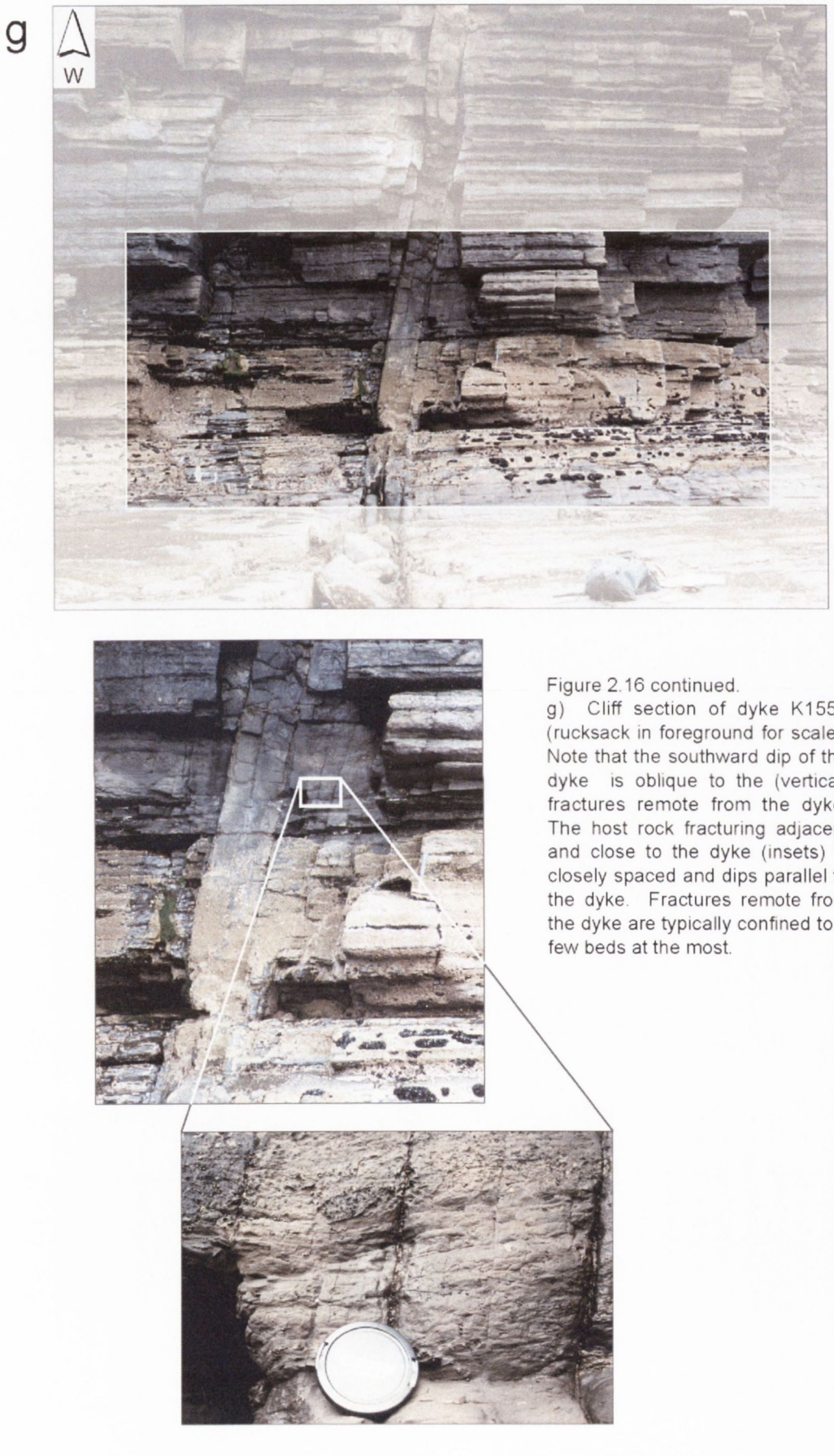

Figure 2.16 continued.
g) Cliff section of dyke K155a (rucksack in foreground for scale). Note that the southward dip of the dyke is oblique to the (vertical) fractures remote from the dyke. The host rock fracturing adjacent and close to the dyke (insets) is closely spaced and dips parallel to the dyke. Fractures remote from the dyke are typically confined to a few beds at the most.

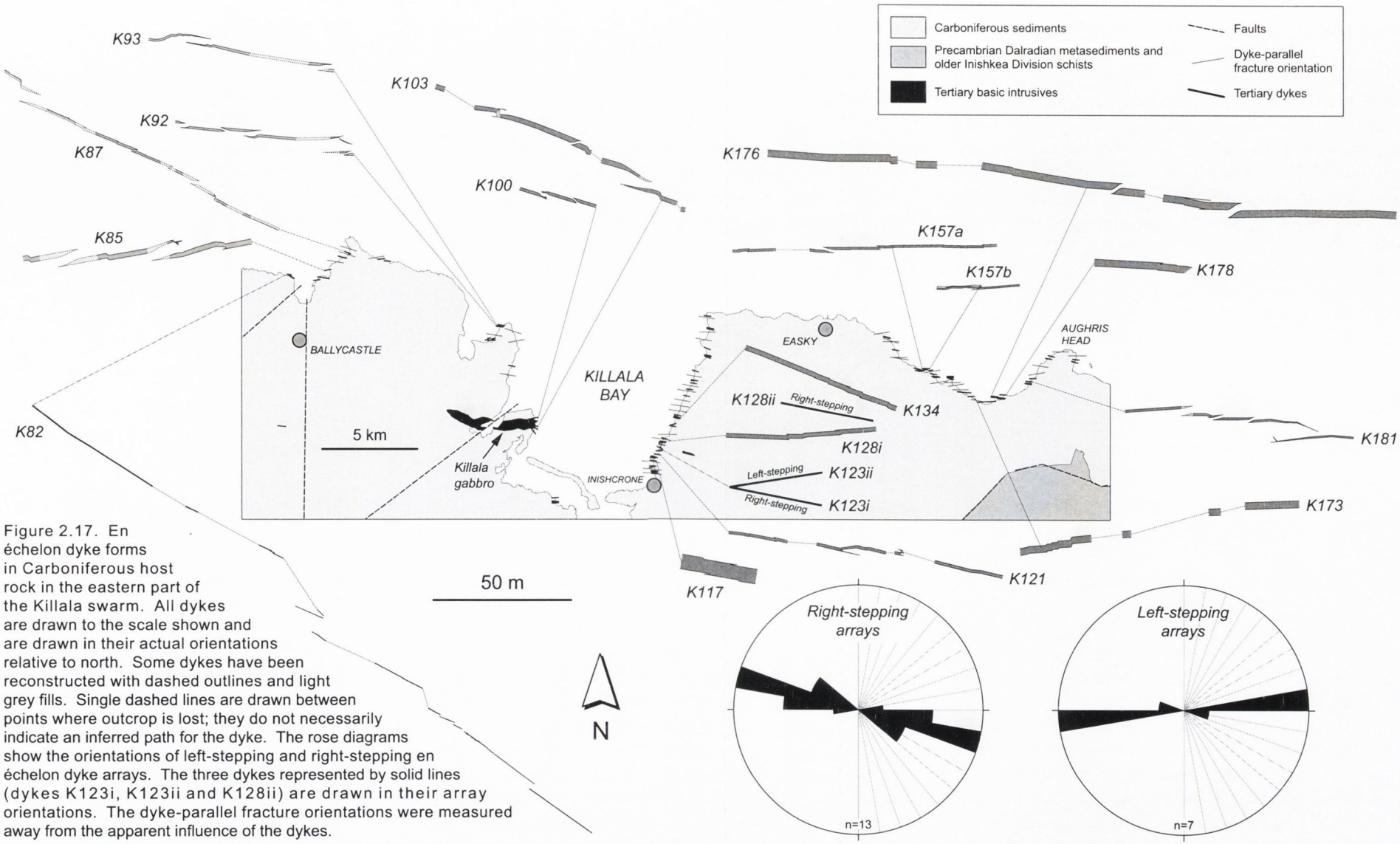

Figure 2.17. En échelon dyke forms in Carboniferous host rock in the eastern part of the Killala swarm. All dykes are drawn to the scale shown and are drawn in their actual orientations relative to north. Some dykes have been reconstructed with dashed outlines and light grey fills. Single dashed lines are drawn between points where outcrop is lost; they do not necessarily indicate an inferred path for the dyke. The rose diagrams show the orientations of left-stepping and right-stepping en échelon dyke arrays. The three dykes represented by solid lines (dykes K123i, K123ii and K128ii) are drawn in their array orientations. The dyke-parallel fracture orientations were measured away from the apparent influence of the dykes.

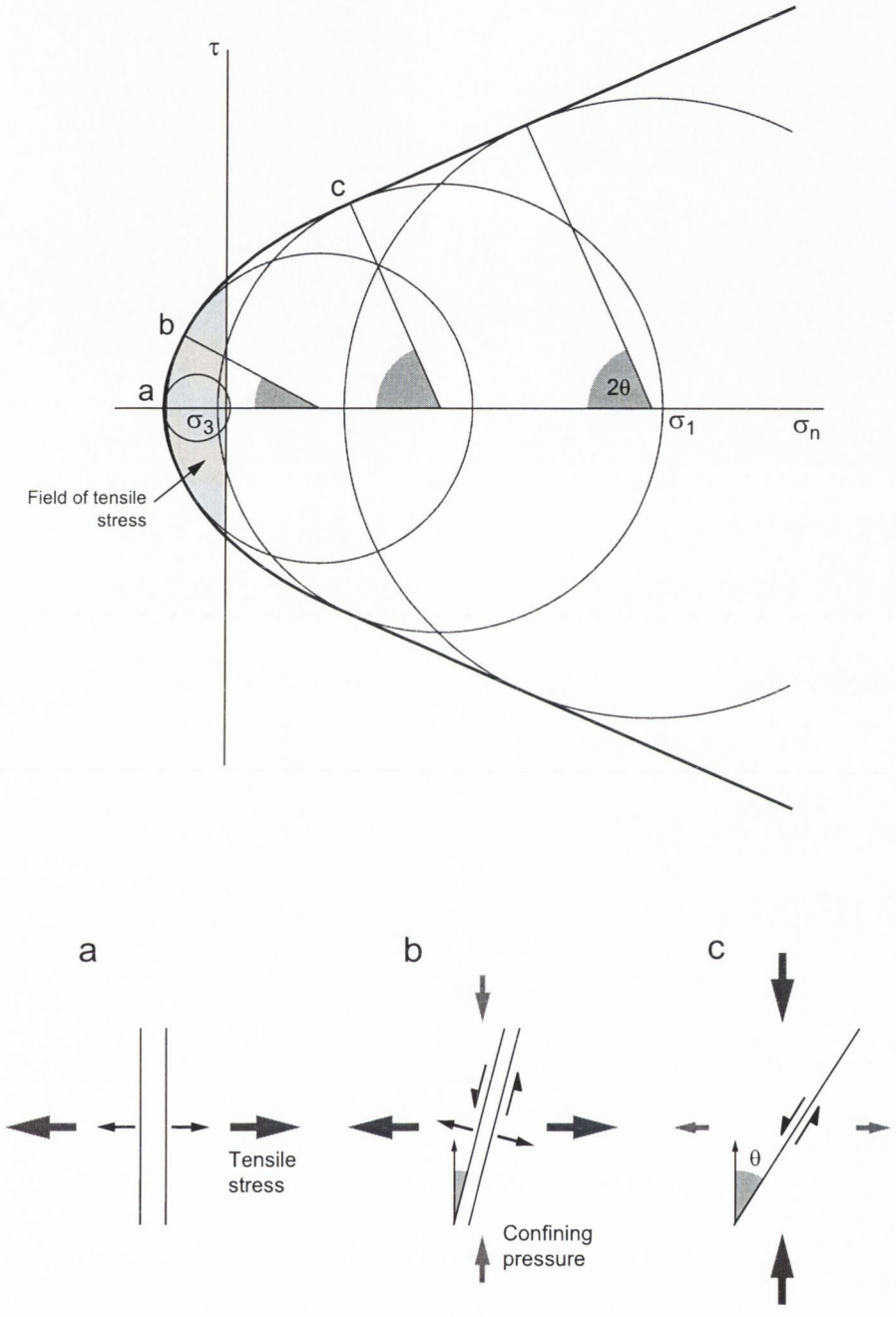

Figure 2.18. Mohr circles showing how hybrid extension/shear fractures develop (modified from Price & Cosgrove (1990)). The curved portion of the Mohr envelope (the Griffith law of failure) controls hybrid fracture geometry, dictating the angle, θ, between the hybrid shear and the principal stresses.
a) θ = 0°. Tensile stress causes the development of extensional (mode I) fractures. A confining pressure can exist but it must be less than or equal to 3*T* (*T* is the tensile strength of the rock).
b) θ = <~30°. Tensile stress with a confining pressure. The fracture opens in a combination of extension (mode I) and shear (mode II). The confining pressure is between 3*T* and 5*T*.
c) θ = ~30°. A large confining pressure dominates, since the least principal stress is just tensile or approaching a compressional state. The Coulomb law of failure is applied and shear (mode II) fractures are formed. This remains the case as the Mohr circle continues to shift to the right, moving further away from the tensile field and the zone for hybrid fracture.

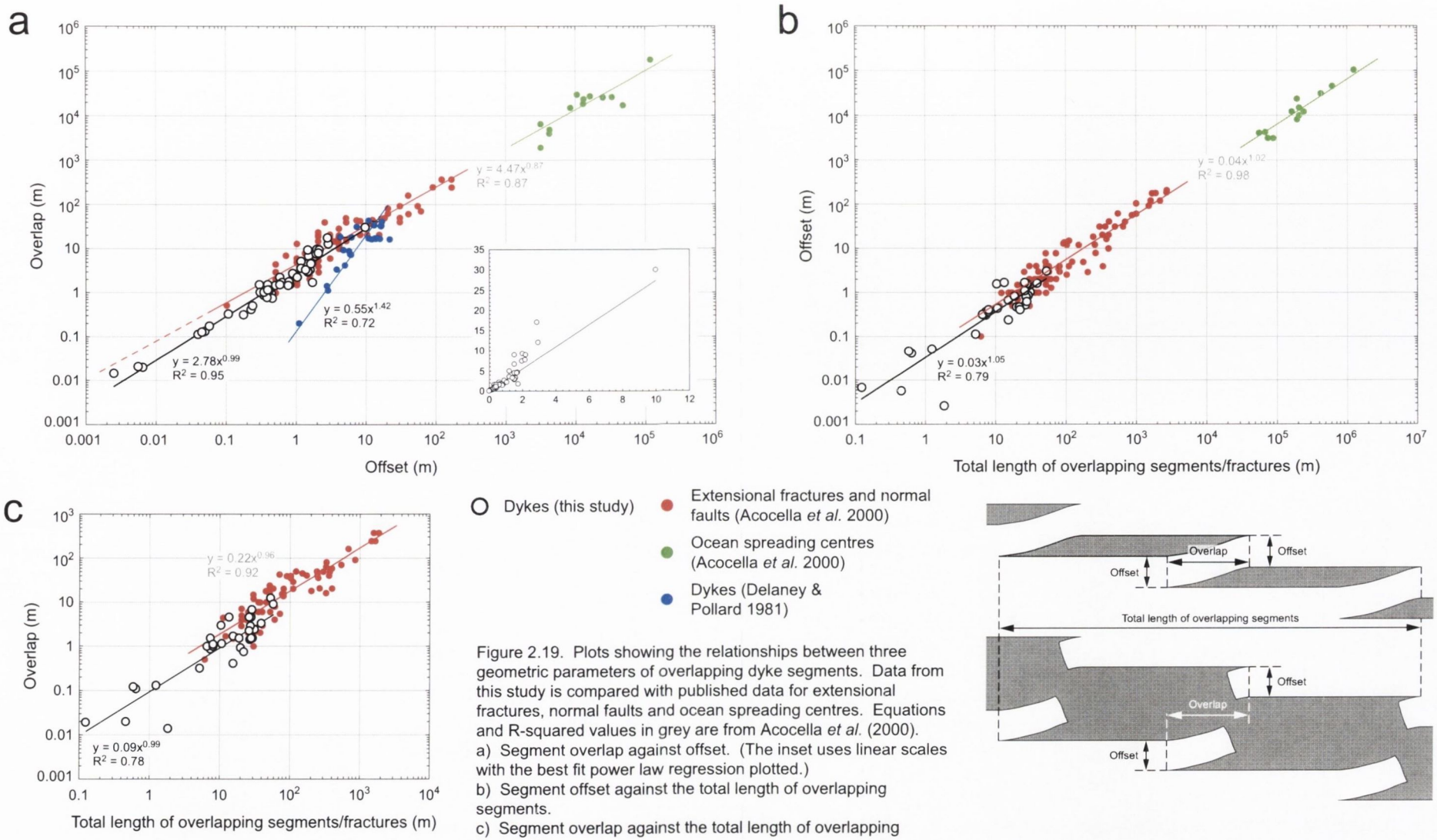

Figure 2.19. Plots showing the relationships between three geometric parameters of overlapping dyke segments. Data from this study is compared with published data for extensional fractures, normal faults and ocean spreading centres. Equations and R-squared values in grey are from Acocella *et al.* (2000).
a) Segment overlap against offset. (The inset uses linear scales with the best fit power law regression plotted.)
b) Segment offset against the total length of overlapping segments.
c) Segment overlap against the total length of overlapping segments.

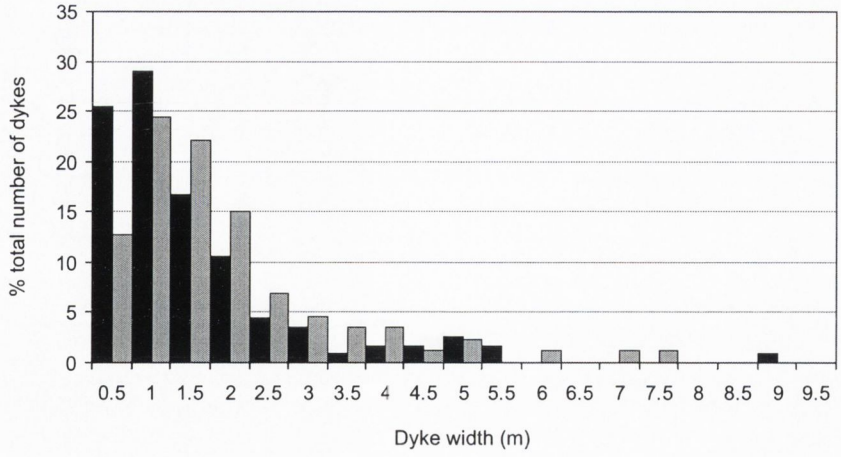

Figure 2.20. Dyke widths for the Killala swarm. The plot compares the distributions of widths for dykes emplaced into Precambrian basement (grey) and Carboniferous (black) host rock.

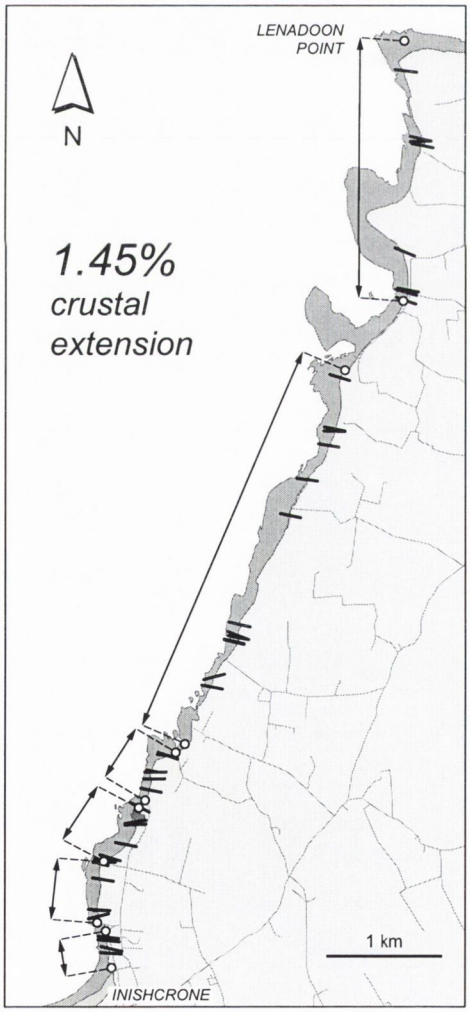

Figure 2.21. Map showing the coastal sections used (indicated by the extent of the arrows) to derive the amount of crustal extension that took place during emplacement of the Killala swarm.

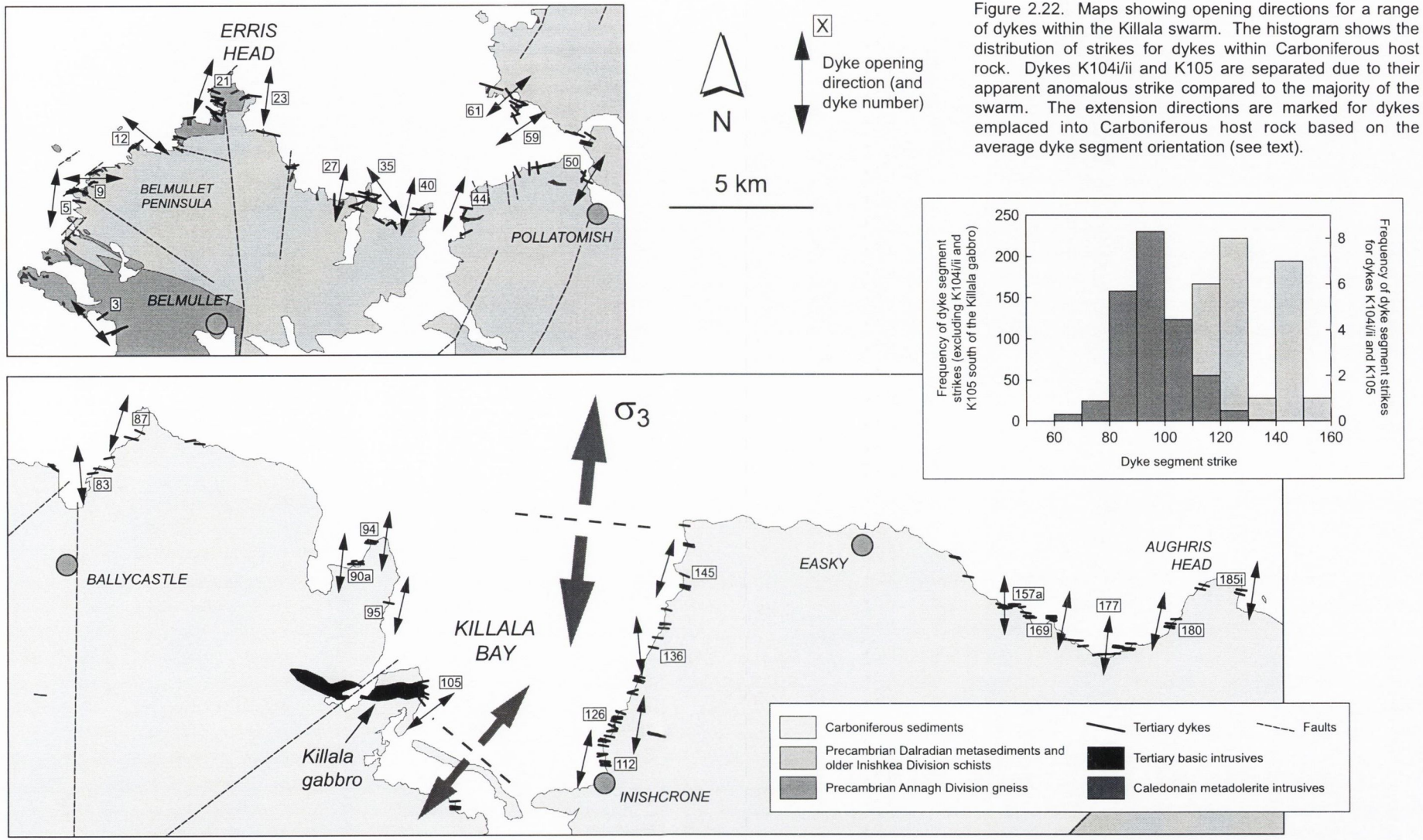

Figure 2.22. Maps showing opening directions for a range of dykes within the Killala swarm. The histogram shows the distribution of strikes for dykes within Carboniferous host rock. Dykes K104i/ii and K105 are separated due to their apparent anomalous strike compared to the majority of the swarm. The extension directions are marked for dykes emplaced into Carboniferous host rock based on the average dyke segment orientation (see text).

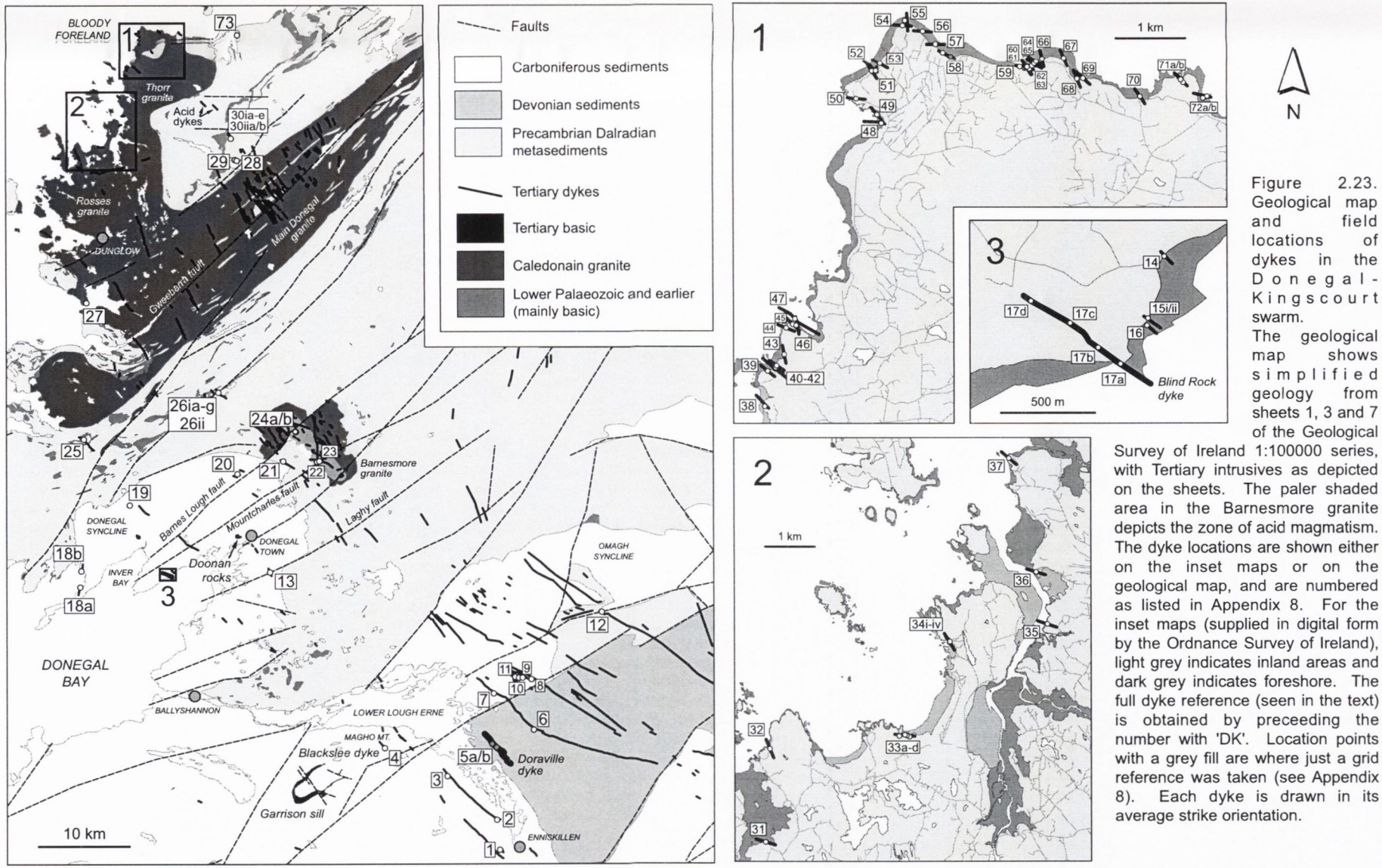

Figure 2.23. Geological map and field locations of dykes in the Donegal-Kingscourt swarm.

The geological map shows simplified geology from sheets 1, 3 and 7 of the Geological Survey of Ireland 1:100000 series, with Tertiary intrusives as depicted on the sheets. The paler shaded area in the Barnesmore granite depicts the zone of acid magmatism. The dyke locations are shown either on the inset maps or on the geological map, and are numbered as listed in Appendix 8. For the inset maps (supplied in digital form by the Ordnance Survey of Ireland), light grey indicates inland areas and dark grey indicates foreshore. The full dyke reference (seen in the text) is obtained by preceeding the number with 'DK'. Location points with a grey fill are where just a grid reference was taken (see Appendix 8). Each dyke is drawn in its average strike orientation.

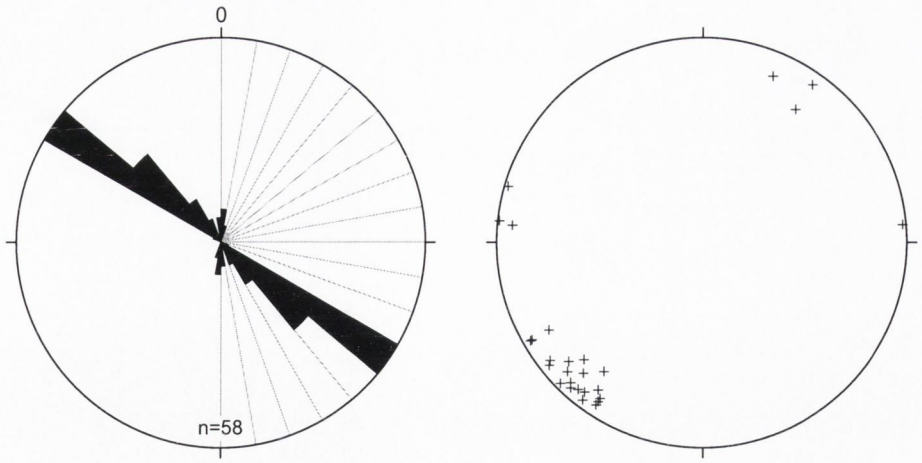

Figure 2.24. Plots showing the range in orientation of dykes in Carboniferous host rock belonging to the Donegal-Kingscourt swarm. The rose diagram shows the range in strike, and the stereographic projection shows (as poles) the range in *dip* as well as strike.

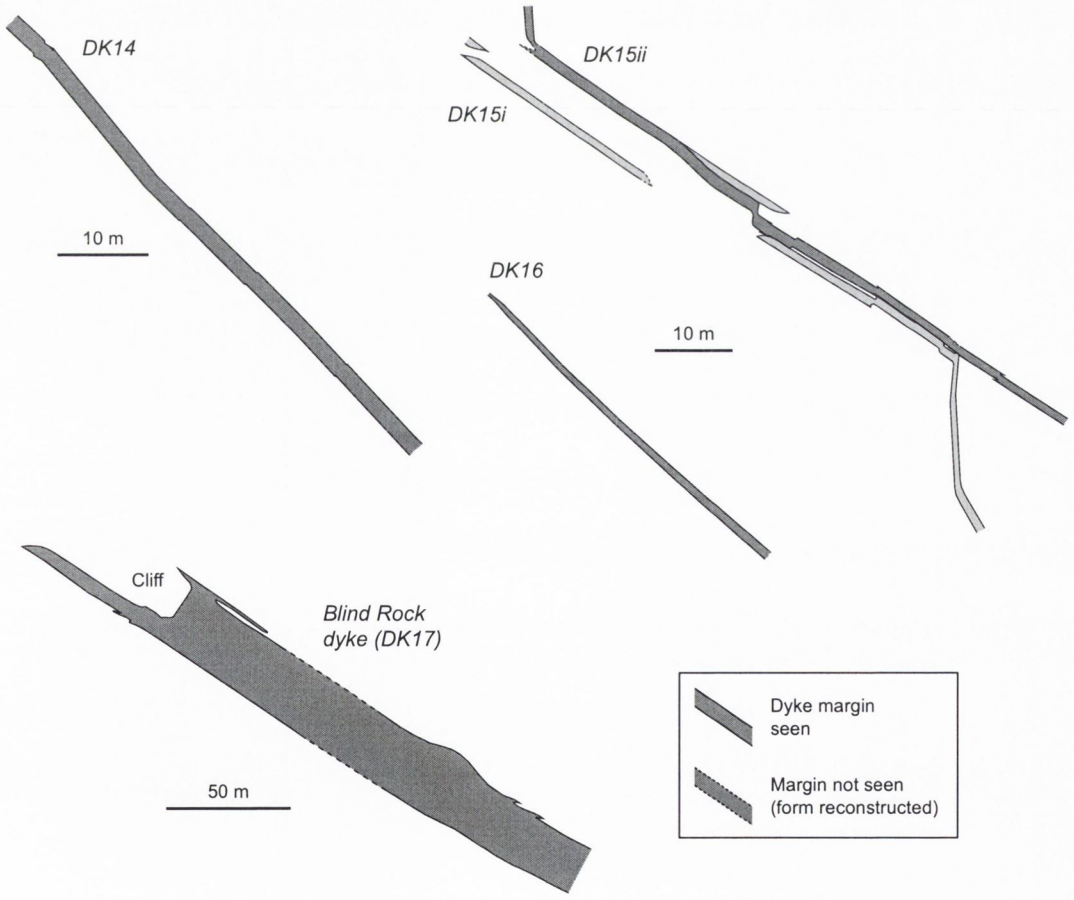

Figure 2.25. Scale diagrams of the Blind Rock and nearby dykes intruding the Carboniferous Bundoran Shale Formation. The outline of the Blind Rock dyke is modified from Preston (1967a). Note, the dykes are drawn at different scales.

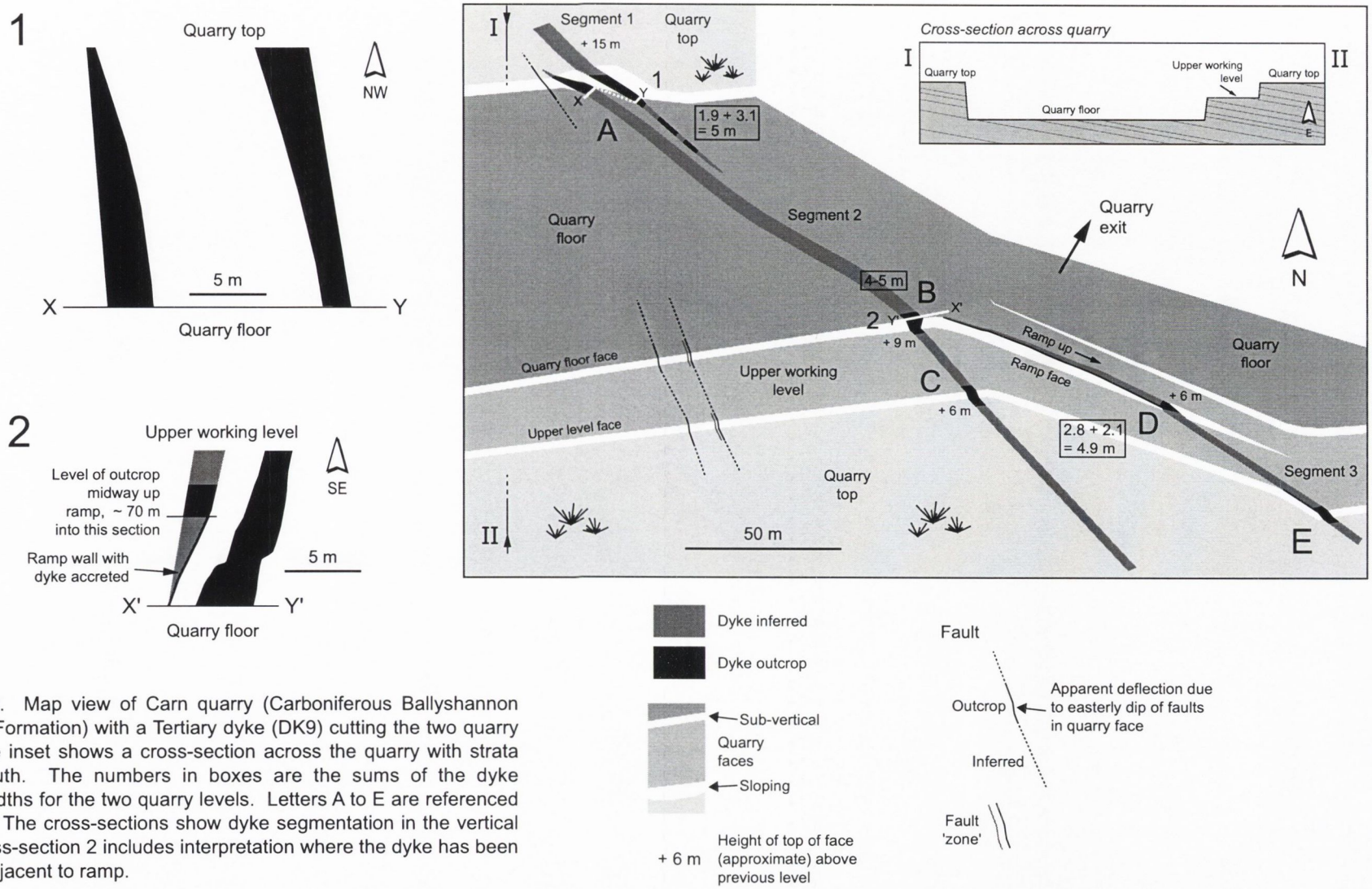

Figure 2.26. Map view of Carn quarry (Carboniferous Ballyshannon Limestone Formation) with a Tertiary dyke (DK9) cutting the two quarry levels. The inset shows a cross-section across the quarry with strata dipping south. The numbers in boxes are the sums of the dyke segment widths for the two quarry levels. Letters A to E are referenced in the text. The cross-sections show dyke segmentation in the vertical plane. Cross-section 2 includes interpretation where the dyke has been removed adjacent to ramp.

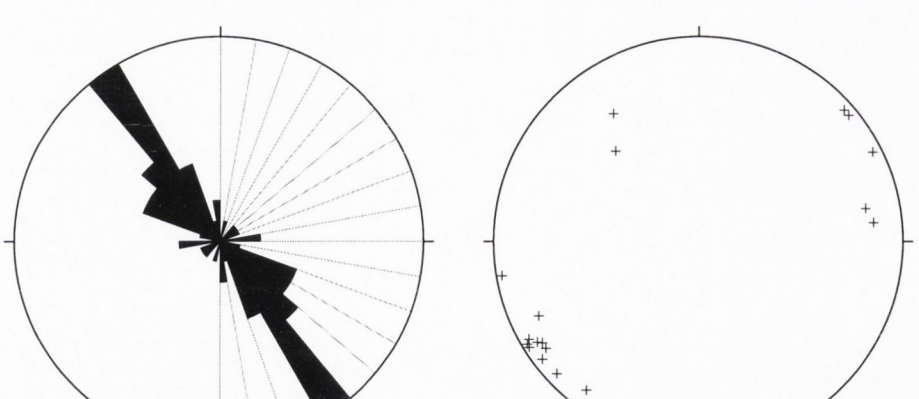

Figure 2.27. Plots showing the range in orientation of dykes in Dalradian host rock belonging to the Donegal-Kingscourt swarm. The rose diagram shows the range in strike, and the stereographic projection shows (as poles) the range in *dip* as well as strike.

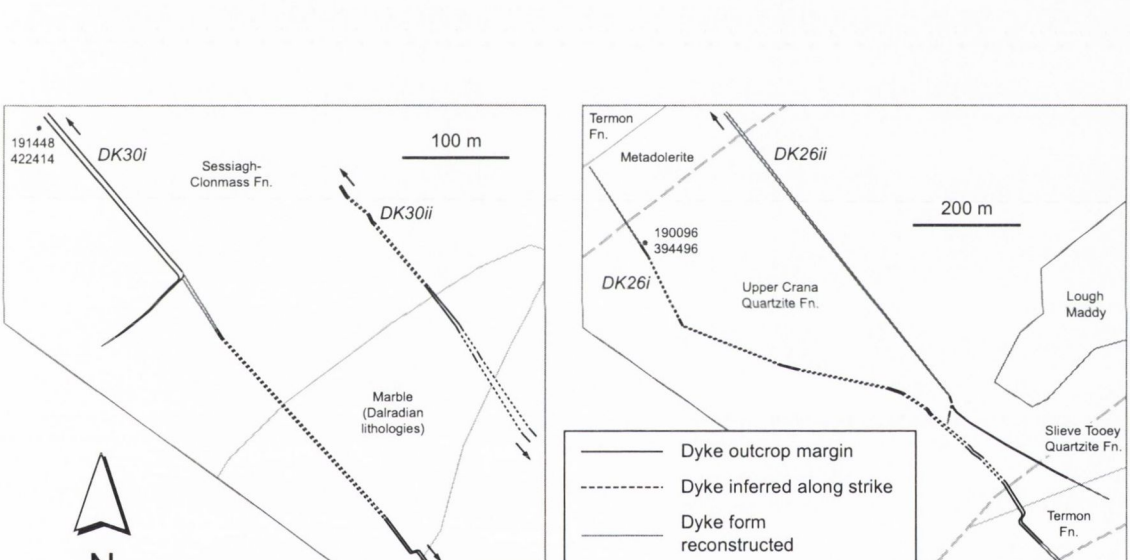

Figure 2.28. Tertiary dykes intruding Dalradian host rock (formations are indicated), mapped from sporadic outcrop. Dyke form reconstructed from outcrop distribution. Grid references are given for a point at each dyke.

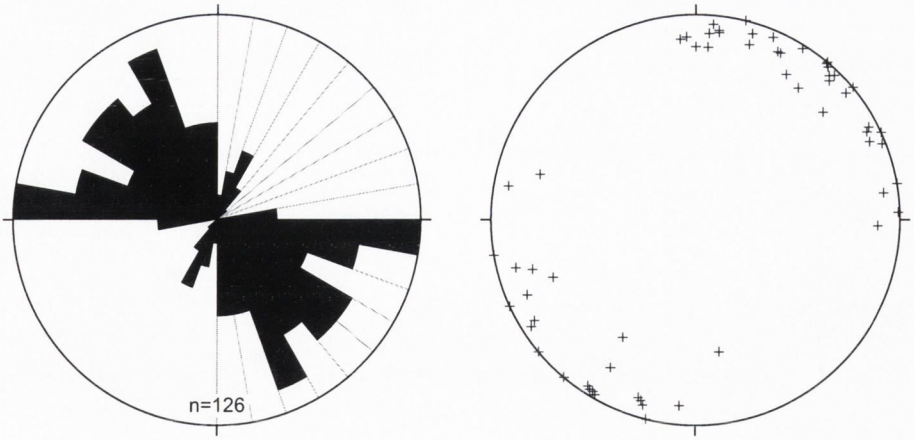

Figure 2.29. Plots showing the range in orientation of dykes in granite host rock belonging to the Donegal-Kingscourt swarm. The rose diagram shows the range in strike, and the stereographic projection shows (as poles) the range in *dip* as well as strike.

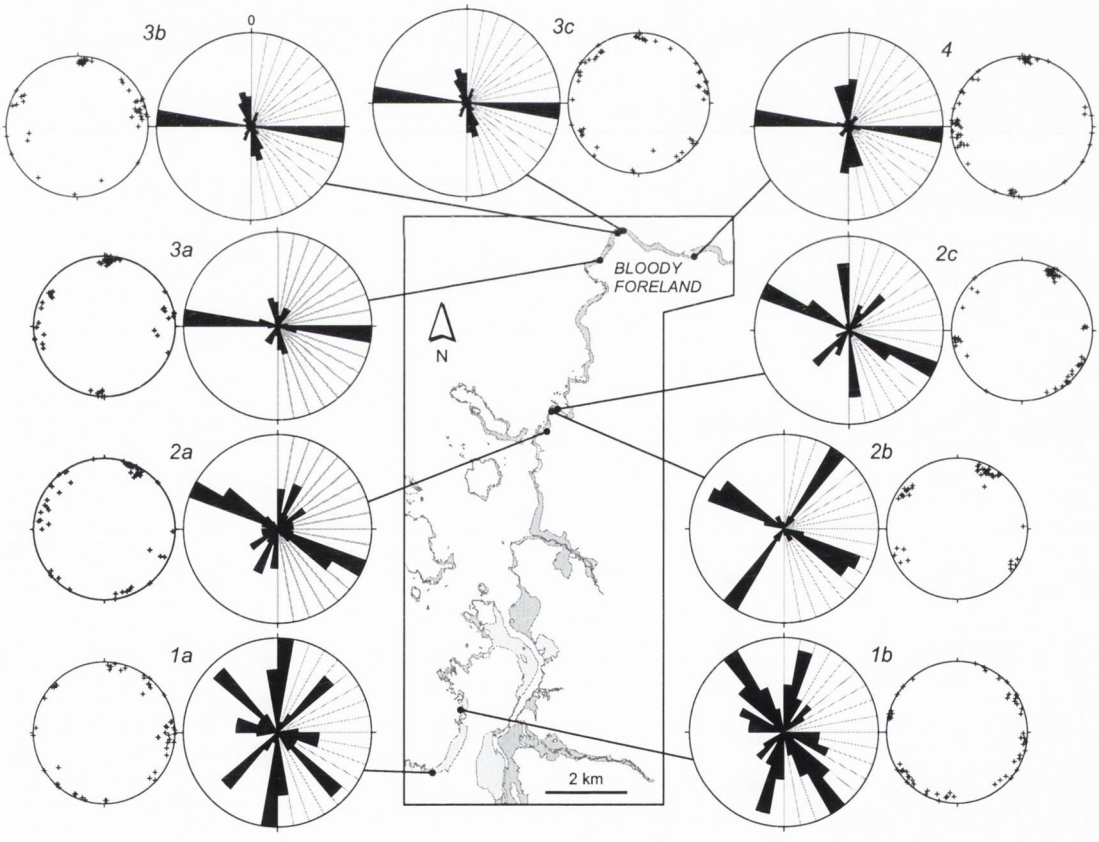

Figure 2.30. Fracture orientations in the Rosses and Thorr granites, northwest Co. Donegal. Rose diagrams show the strikes of fifty fractures recorded at each locality. The stereographic projections show the full orientations as poles to planes.

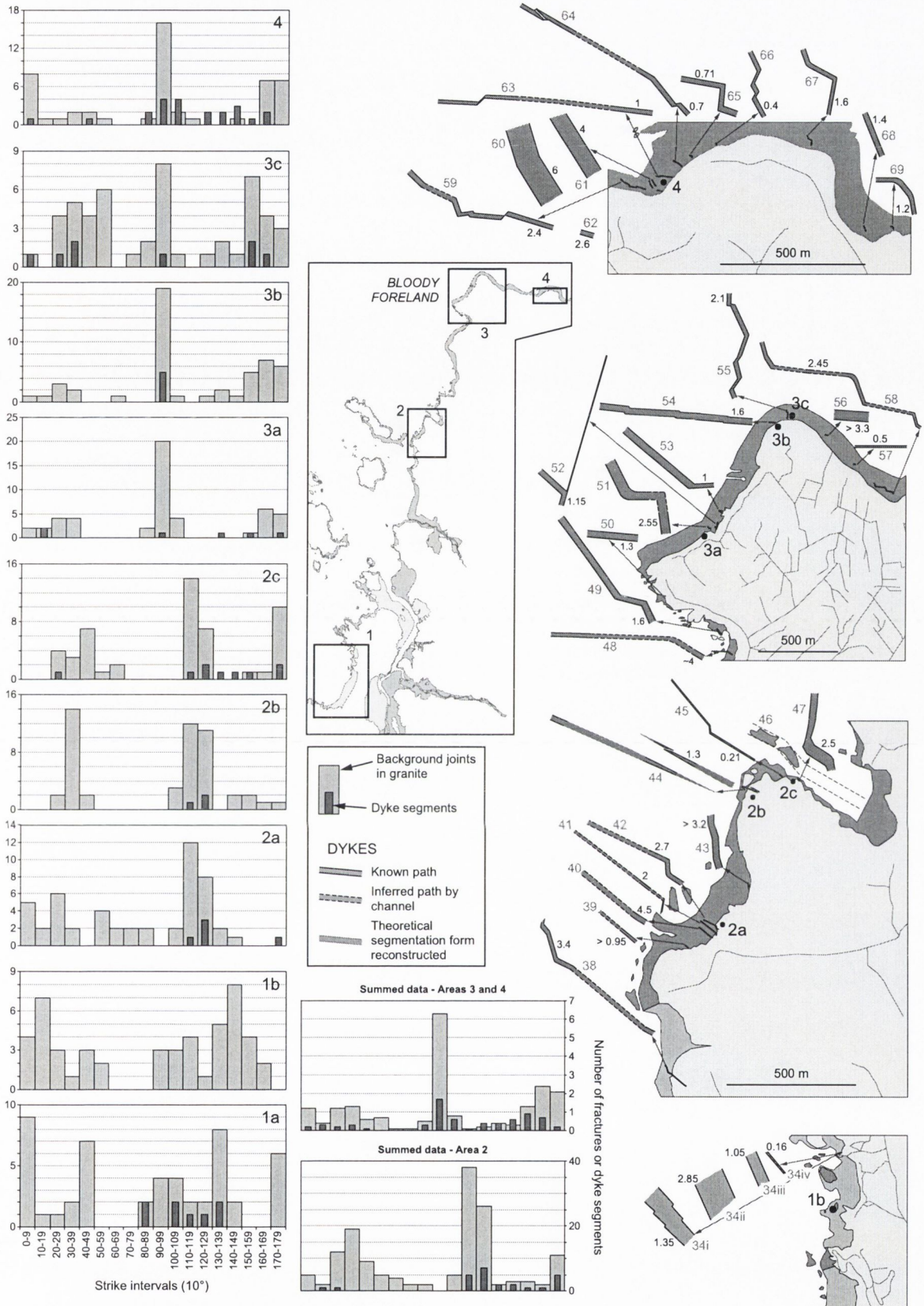

Figure 2.31. A comparison of fracture orientation data with the orientation of dykes (Donegal-Kingscourt swarm) that intrude the Thorr and Rosses granites, northwest Co. Donegal. Areas 1-4 are defined where fracture data was collected and most of the dykes in the area outcrop. Each dyke is drawn to scale but dykes are represented at different scales with widths in metres indicated next to, and corresponding with, individual dyke segments. The dykes are numbered as detailed in Appendix 8 (preceed each number with 'DK'). Positions of fracture orientation data collection (see Figure 2.30) are marked and labelled corresponding with their respective histograms.

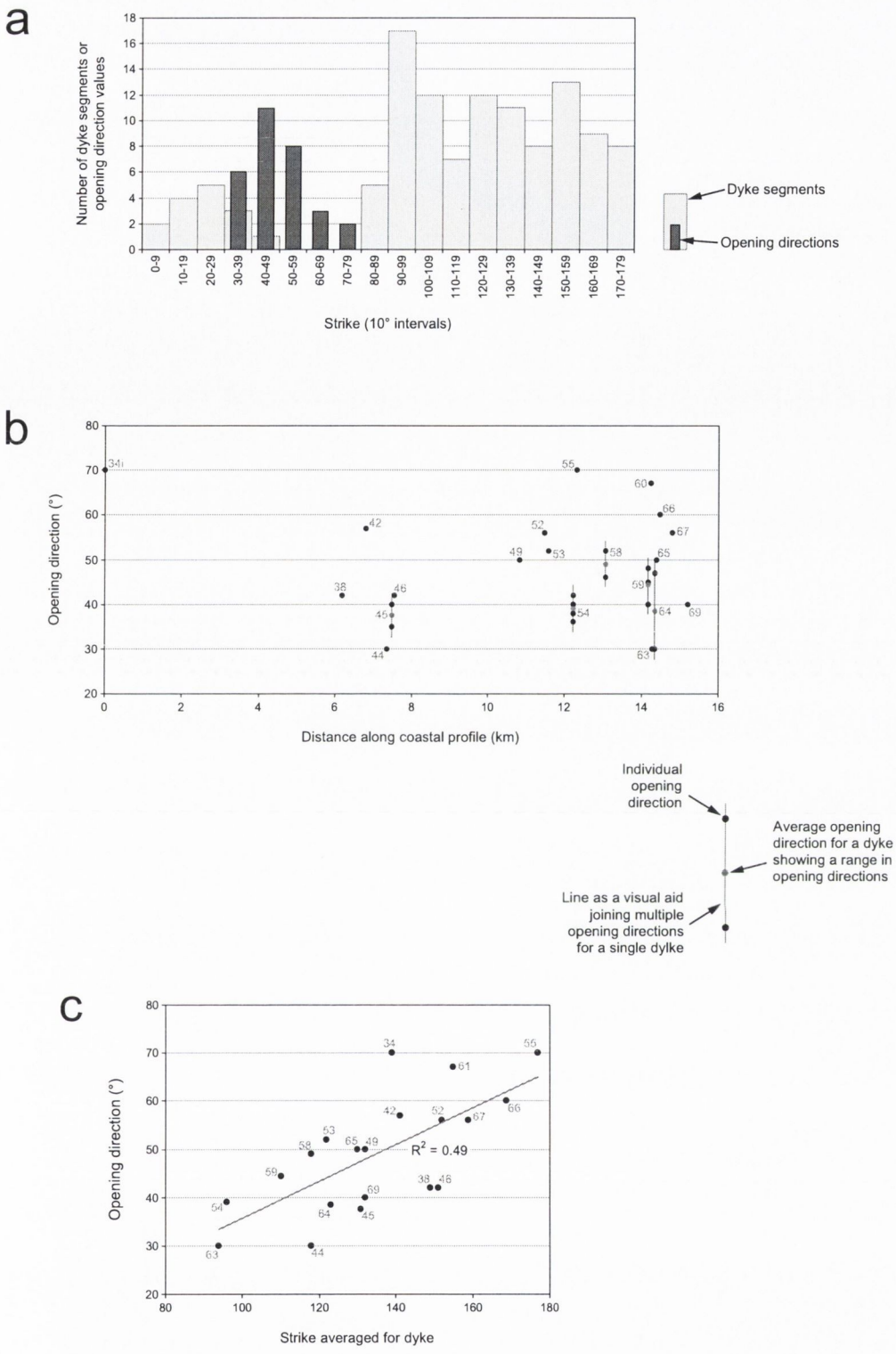

Figure 2.32. Graphs showing opening directions of dykes intruding the Rosses and Thorr granites, northwest Co. Donegal, and relationships with location along the coast and average dyke orientation. Opening directions are relative to north.

a) A comparison between opening direction for all dykes, where deducible, and the strike of all dyke segments from dykes intruding granite along the northwest Co. Donegal coast (as shown in Figure 2.31).

b) A plot to investigate any relationships between opening direction and geographical location. The coastal profile runs around the coast, from south to north to east, incorporating individual numbered dykes where opening directions have been measured.

c) A plot of opening direction against average strike for dykes intruding granite along the northwest Co. Donegal coast. Average strike is derived by drawing a line from one end of the exposure to the other and measuring its orientation.

Figure 2.33. A proposed stress model for the emplacement of dykes across western Ireland during the Palaeocene. The Brendan centre is believed to have sourced a radial arrangement of dykes and caused a deflection of the regionally acting NE-SW directed extension. This deflection is manifest in the orientation of the Killala swarm. The arrows show the inferred directions of extension that caused dyke emplacement.

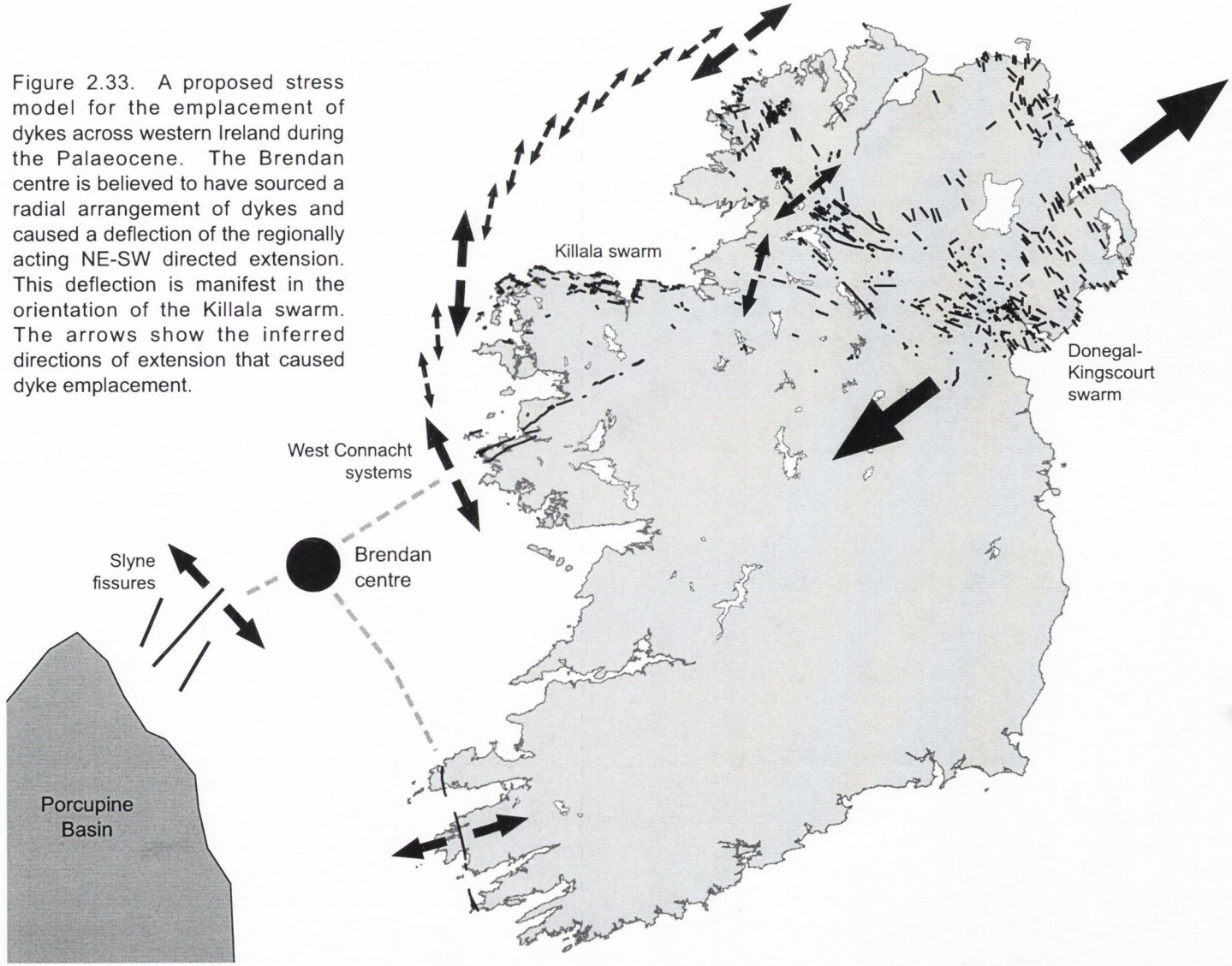

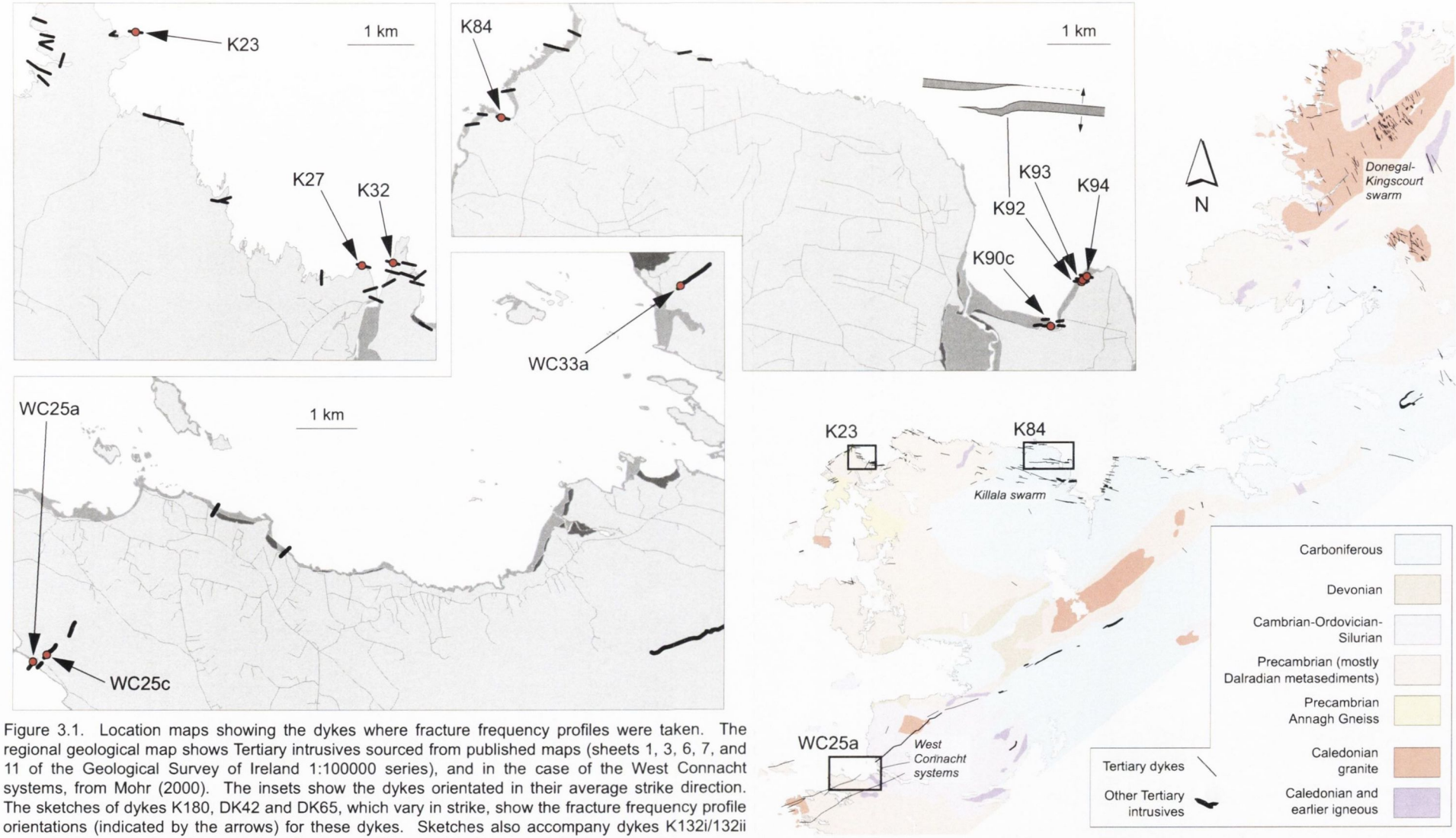

Figure 3.1. Location maps showing the dykes where fracture frequency profiles were taken. The regional geological map shows Tertiary intrusives sourced from published maps (sheets 1, 3, 6, 7, and 11 of the Geological Survey of Ireland 1:100000 series), and in the case of the West Connacht systems, from Mohr (2000). The insets show the dykes orientated in their average strike direction. The sketches of dykes K180, DK42 and DK65, which vary in strike, show the fracture frequency profile orientations (indicated by the arrows) for these dykes. Sketches also accompany dykes K132i/132ii and K92, where fracture frequency profiles are positioned ahead of one of the segments close to en échelon segmentation of the dykes.

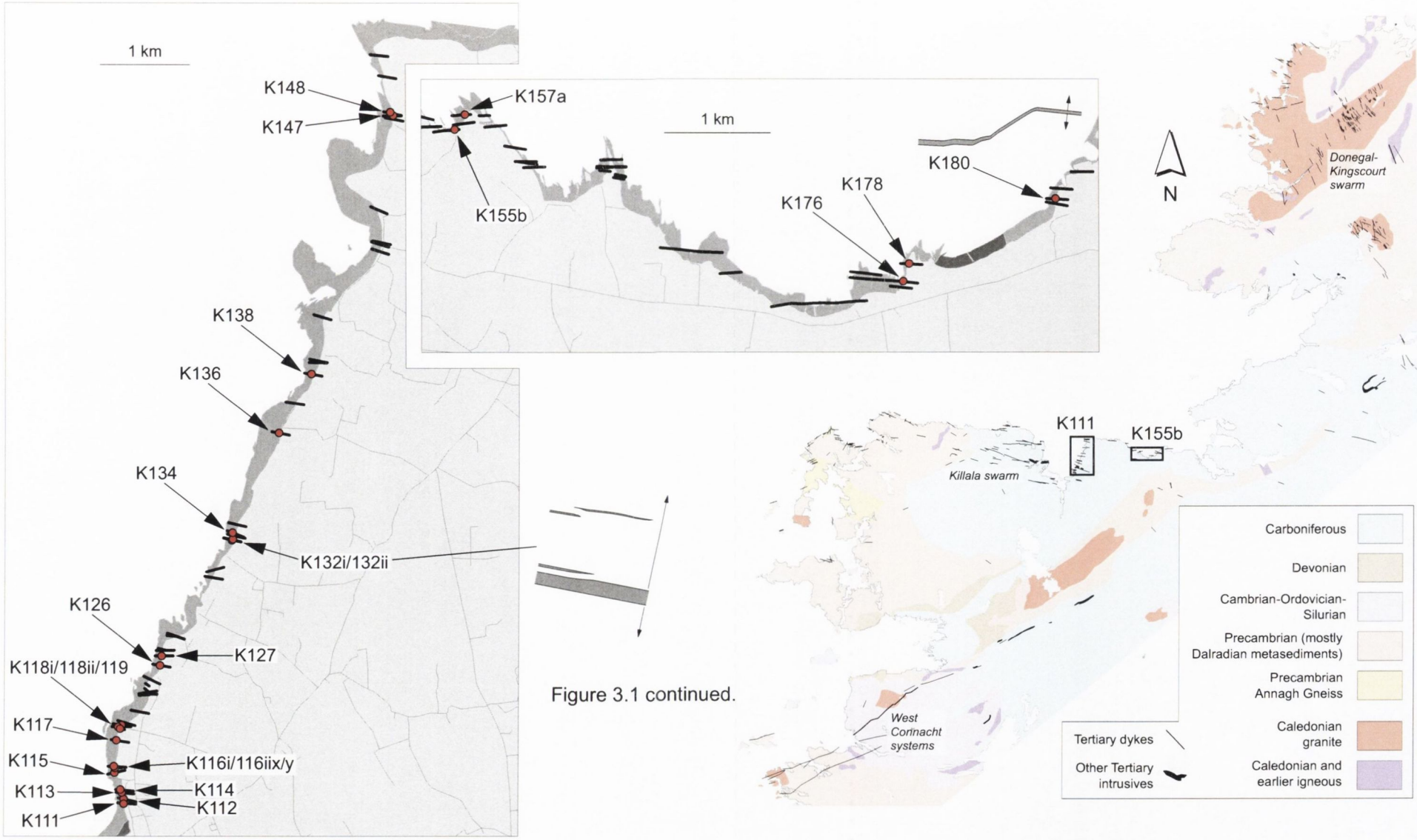

Figure 3.1 continued.

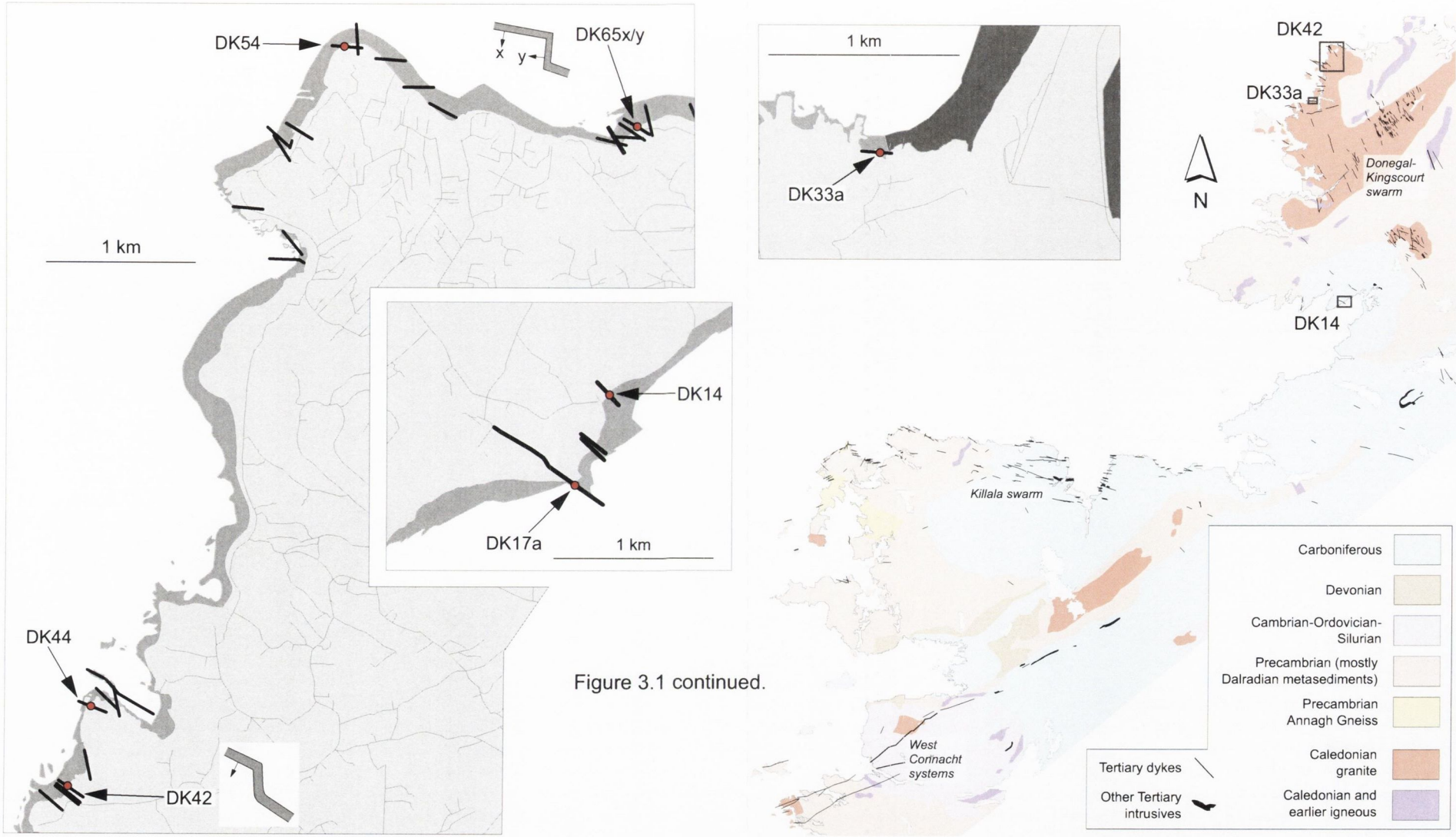

Figure 3.1 continued.

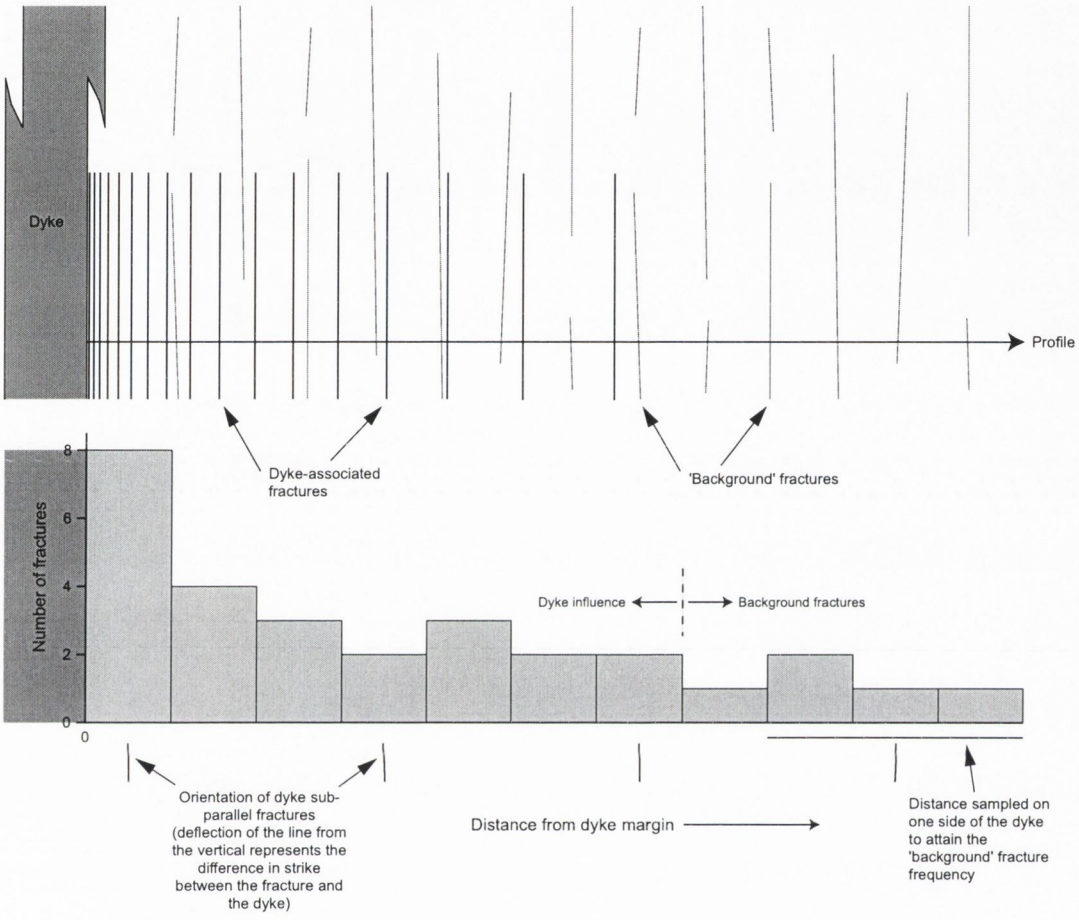

Figure 3.2. Schematic illustration in plan view (top) of the relationship between dyke-associated fractures and the background fracture frequency. The histogram below is a synthetic 'fracture frequency profile' running into the 'background frequency' at the distal end. Also shown on the profile are the strikes of fractures, and an example of the distance sampled over which the background fracture frequency can be attained.

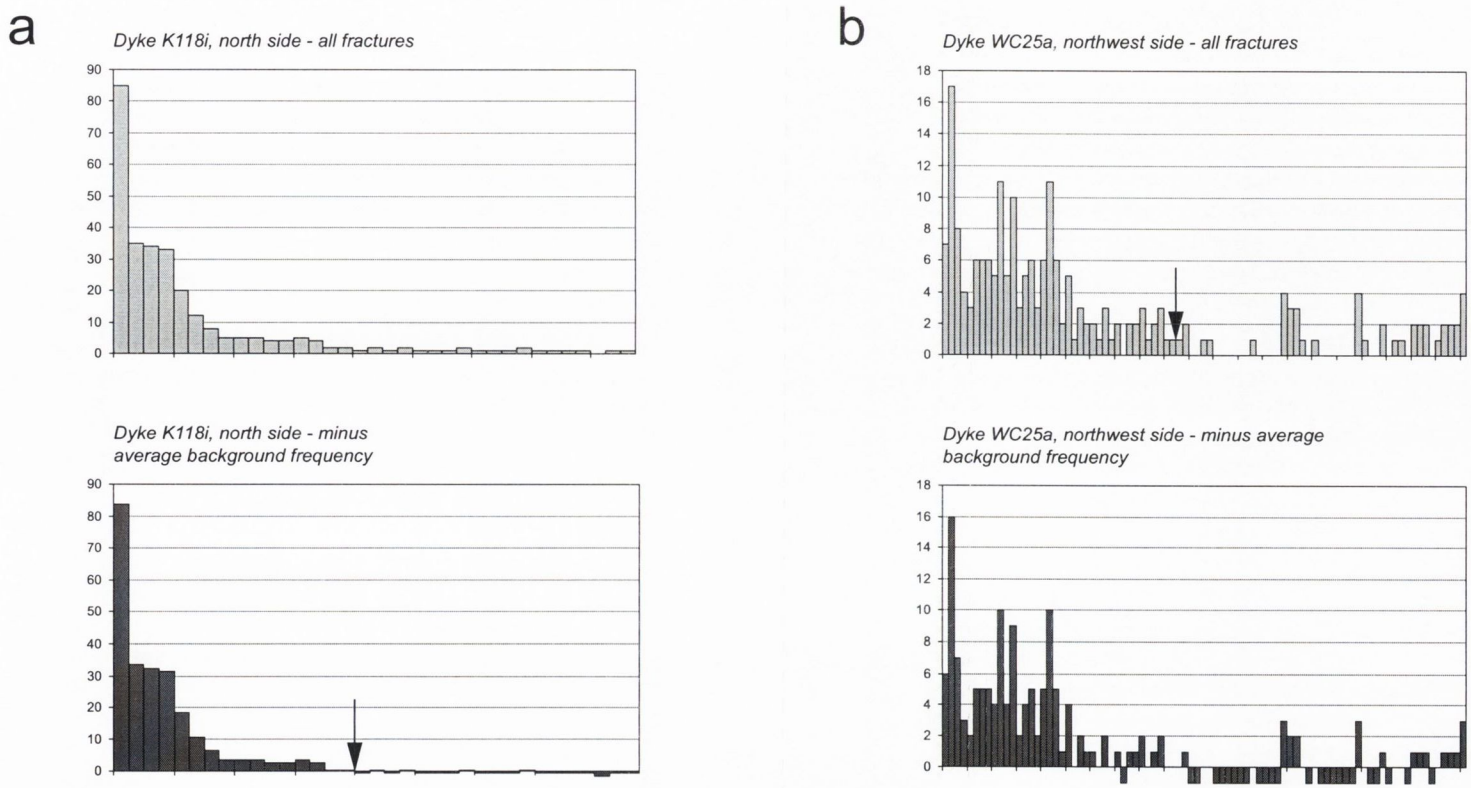

Figure 3.3. Fracture frequency plots showing the effect of subtracting the average background fracture frequency from the whole data to help delineate the edge of the dyke-associated fracture zone. Arrows indicate the interpreted edge of this zone.

a) A relatively uniform background fracture frequency almost disppears when the average is subtracted from the whole data, leaving the dyke-associated fracture zone well defined.

b) A highly variable background fracture frequency when subtracted from the whole data does not really help to identify the edge of the dyke-associated fracture zone.

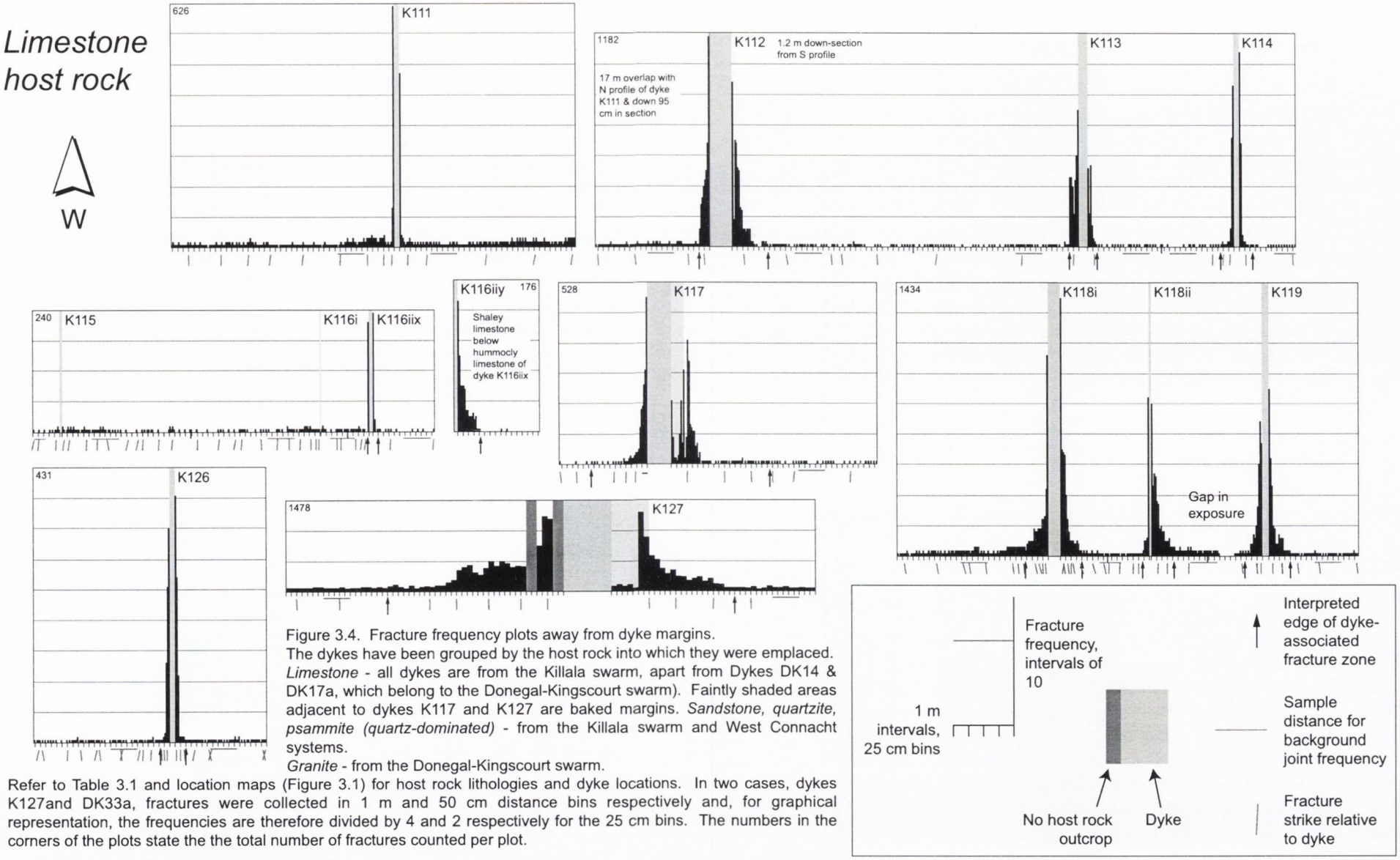

Figure 3.4. Fracture frequency plots away from dyke margins.
The dykes have been grouped by the host rock into which they were emplaced. *Limestone* - all dykes are from the Killala swarm, apart from Dykes DK14 & DK17a, which belong to the Donegal-Kingscourt swarm). Faintly shaded areas adjacent to dykes K117 and K127 are baked margins. *Sandstone, quartzite, psammite (quartz-dominated)* - from the Killala swarm and West Connacht systems.
Granite - from the Donegal-Kingscourt swarm.
Refer to Table 3.1 and location maps (Figure 3.1) for host rock lithologies and dyke locations. In two cases, dykes K127and DK33a, fractures were collected in 1 m and 50 cm distance bins respectively and, for graphical representation, the frequencies are therefore divided by 4 and 2 respectively for the 25 cm bins. The numbers in the corners of the plots state the the total number of fractures counted per plot.

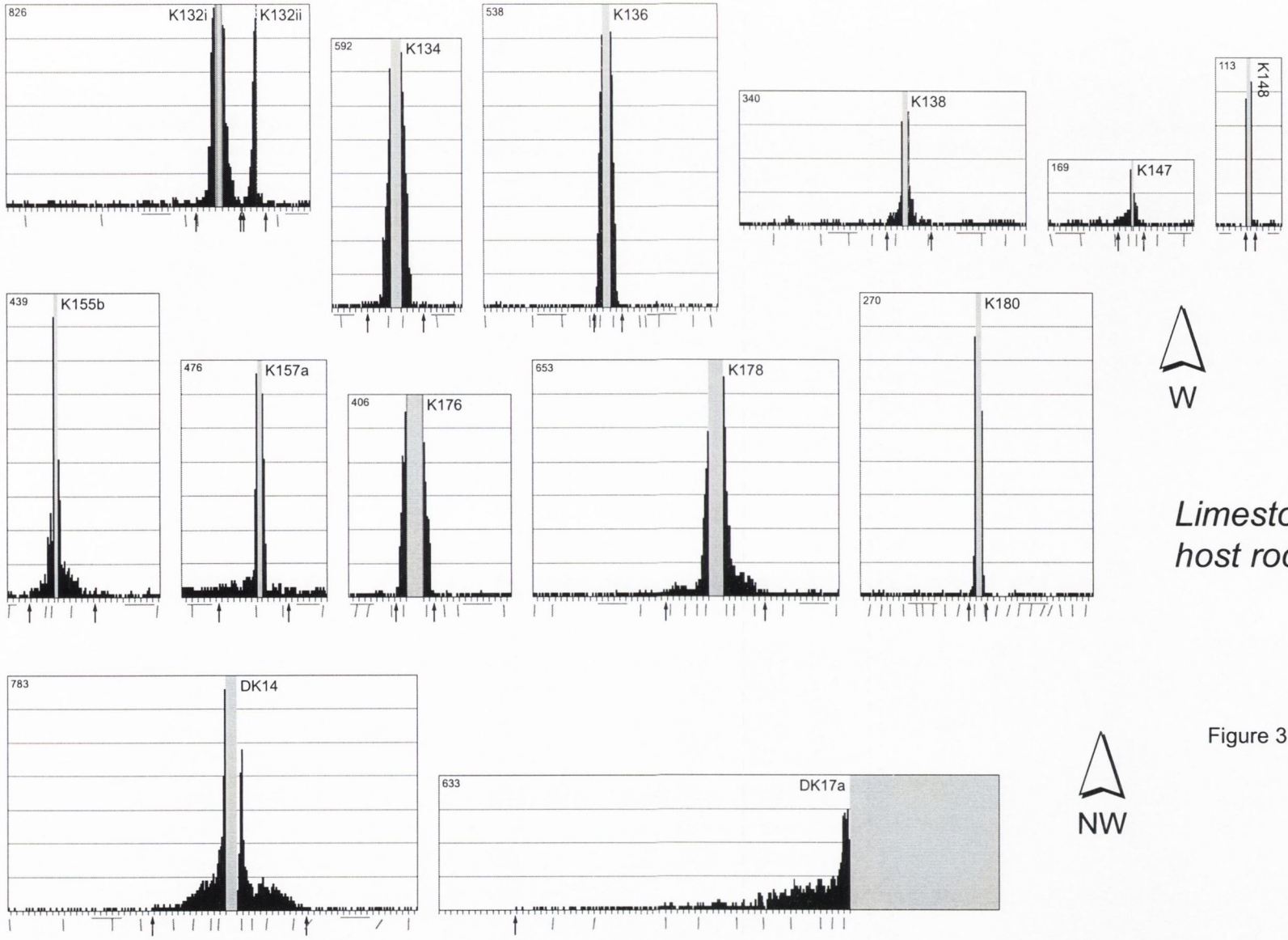

Figure 3.4 continued.

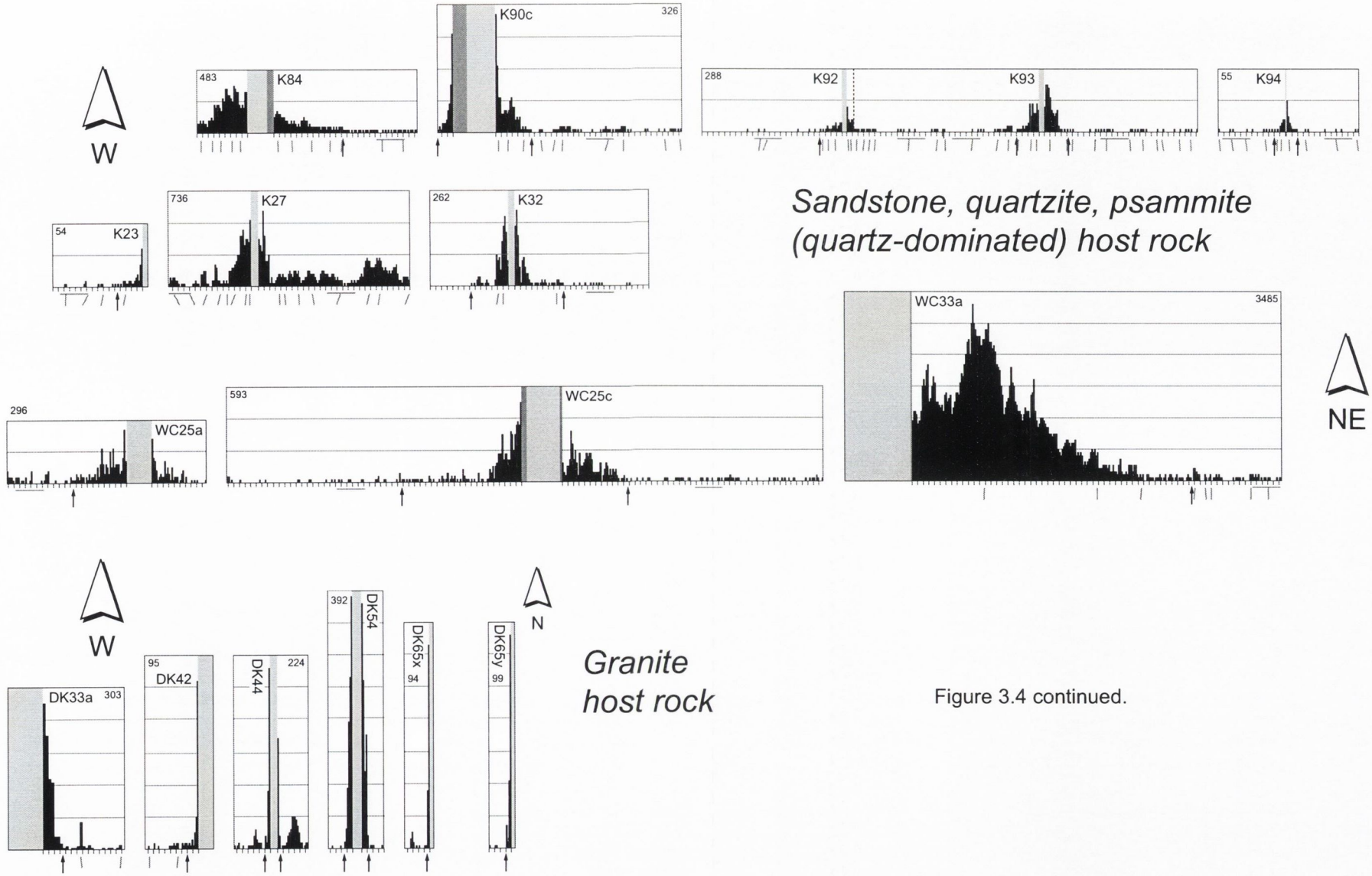

Figure 3.4 continued.

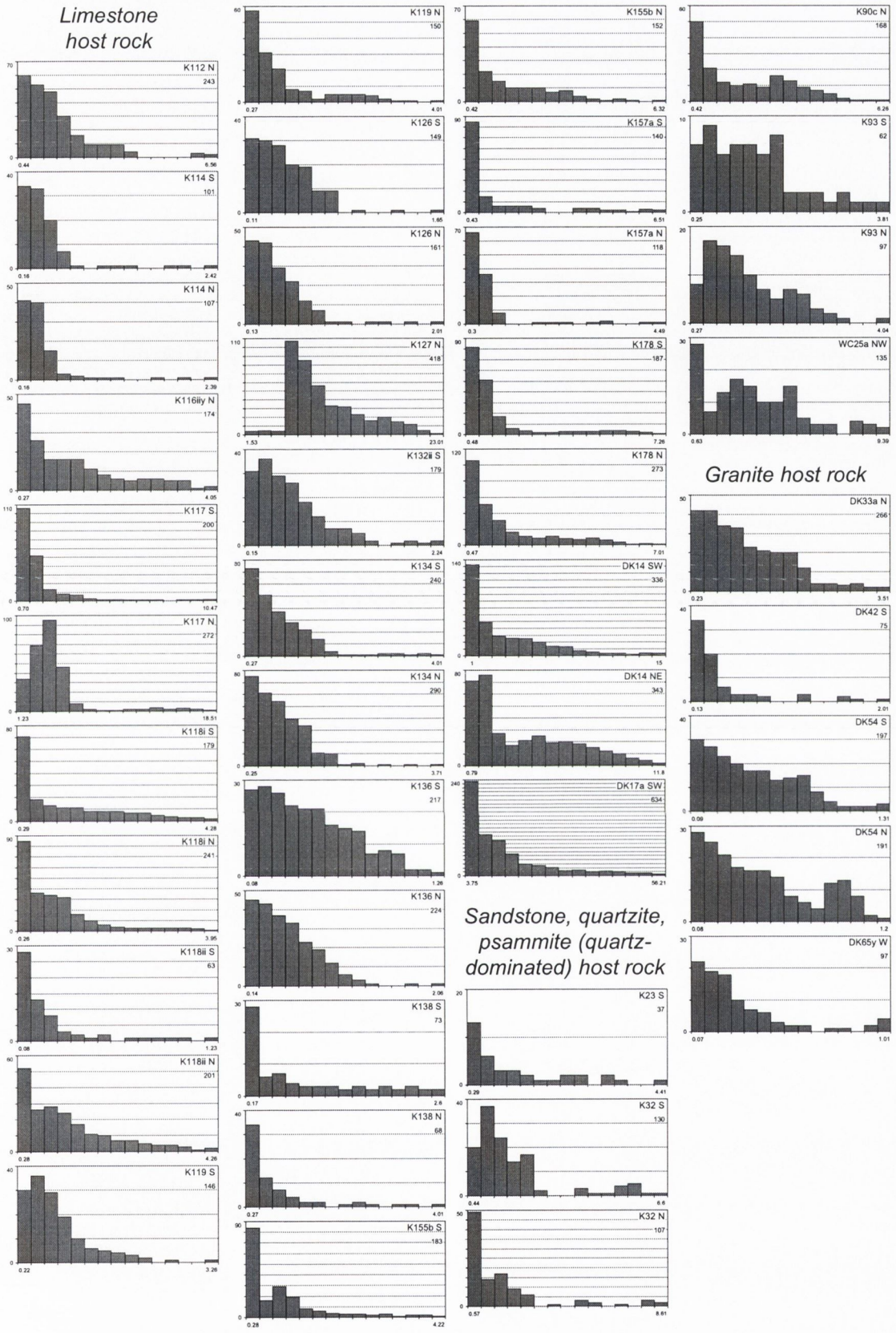

Figure 3.5. Fracture frequency profiles of dyke-associated fractures, extracted from the whole data for each dyke, as described in the text. Not included are those dykes where the dyke-associated fracture zone could not be delineated, or those profiles with gaps in the fracture counts.

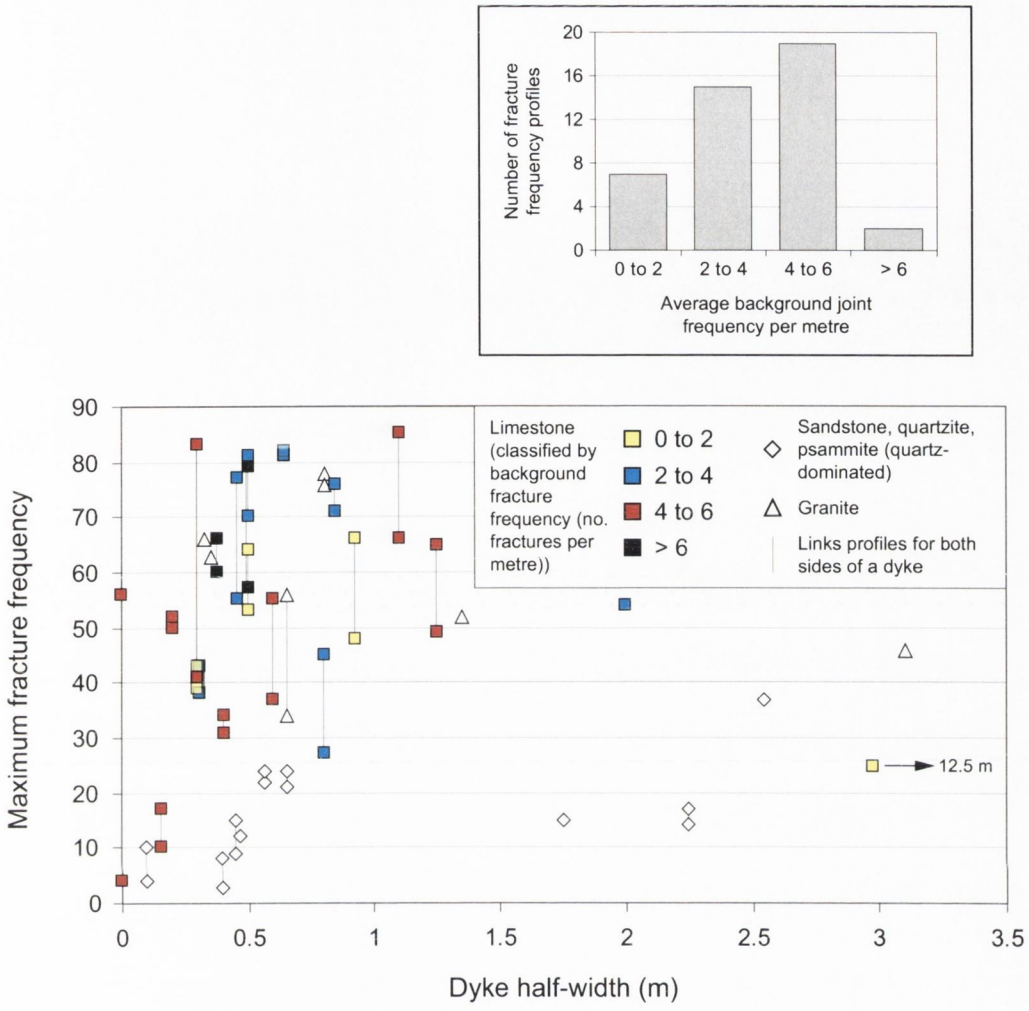

Figure 3.6. Plot of maximum fracture frequency for each side of a given dyke against the half-width of that dyke (main plot). For limestone host rock, each point is classified in terms of the background fracture frequency determined for the host rock. Not included are dykes with no fracture data at the margins where the maximum frequency is likely to occur. Also, dykes K117 and K127 are not included, as they have a reduced fracture frequency coinciding with a strong baked margin.
The inset plot shows the distribution of the background fracture frequencies.

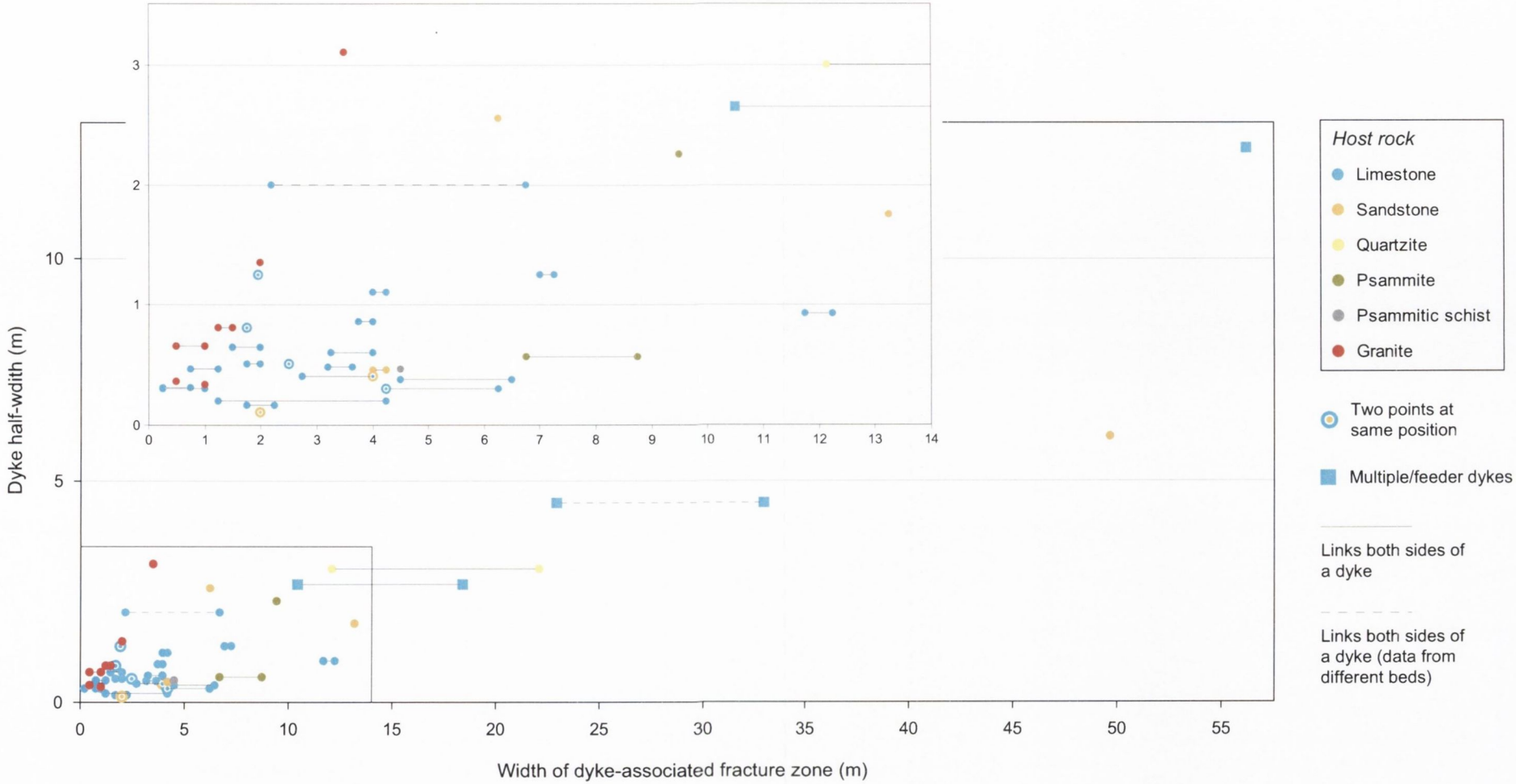

Figure 3.7. Plots showing the relationship between dyke width and the width of dyke-associated fracture zones for all dykes.

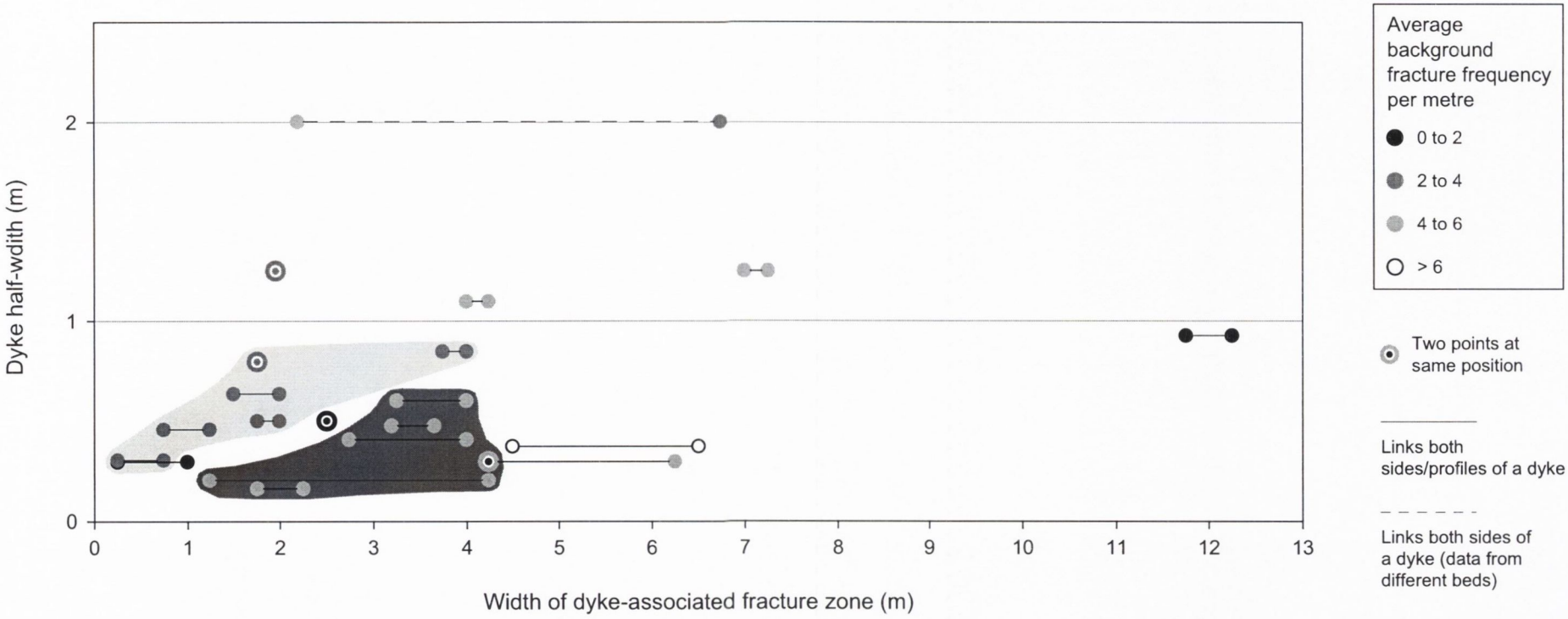

Figure 3.8. Plot showing relationships between dyke width and width of dyke-associated fracture zone for limestone host rock. The host rock is classified in terms of the background fracture frequency. The shaded areas highlight the apparent clustering of the 2 to 4 and 4 to 6 classes of background fracture frequency.

Figure 3.9. Schematic plan view of a segmented dyke showing the two main groups of structures mapped (shaded areas) relating to the emplacement of the dyke, and their spatial relations with the fracture-frequency profiles described previously.

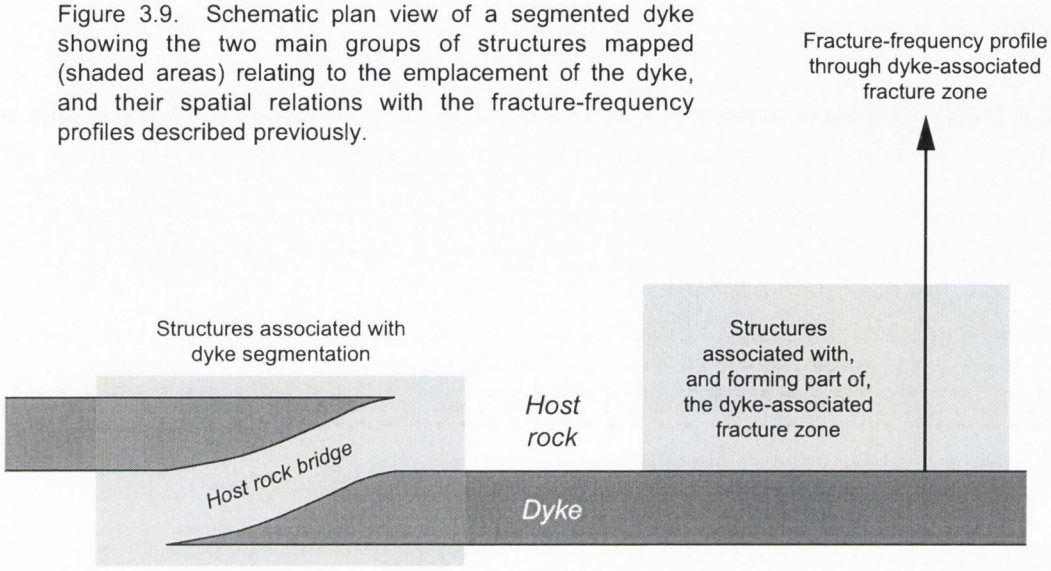

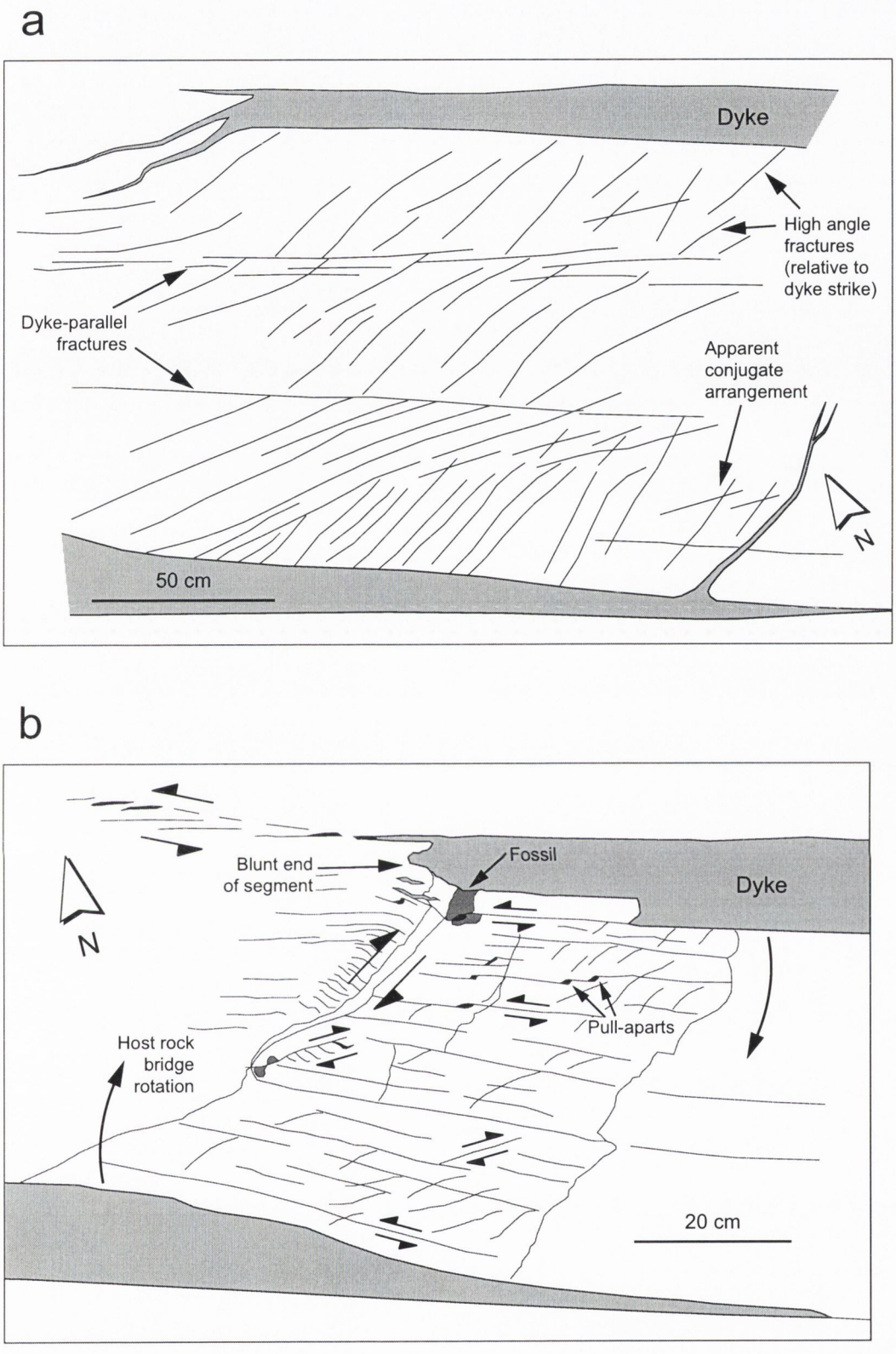

Figure 3.10. Plan views showing deformation of the host rock bridge zone relating to the overlap of en échelon dyke segments.
a) The two main orientations of fractures commonly seen in bridge zones; dyke-parallel and high angle to the dyke strike (dyke K145).
b) A left-stepping segmentation (dyke K132ii) with associated sinistral shear in the bridge zone. Note also the dextral transform shear relating to dilation of the blunt end of the northern segment.

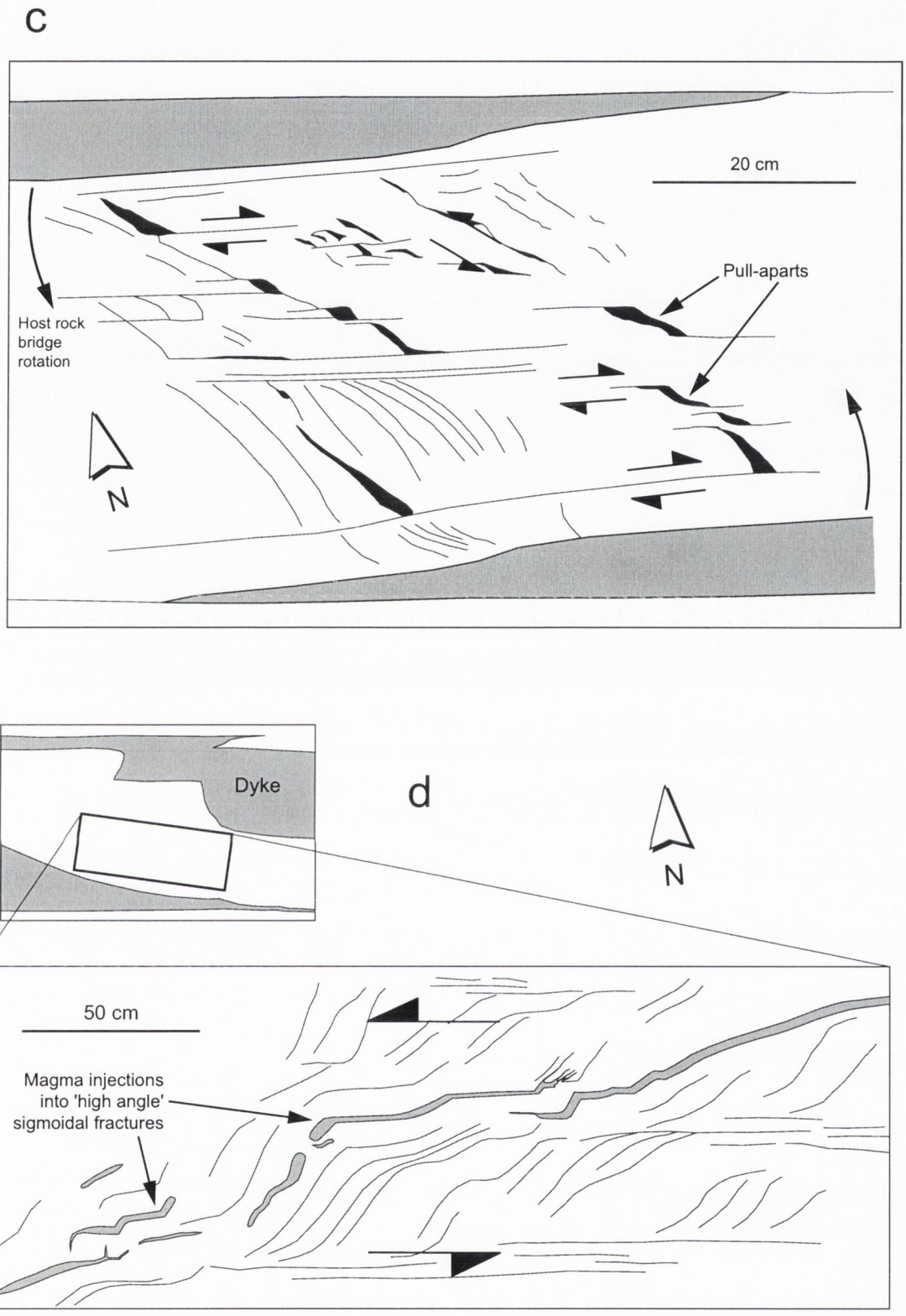

Figure 3.10 continued.
c) A right-stepping segmentation (dyke K132ii) with associated dextral shear in the brige zone.
d) Magma has injected along high angle fractures in the host rock bridge of a left-stepping dyke (dyke K113).

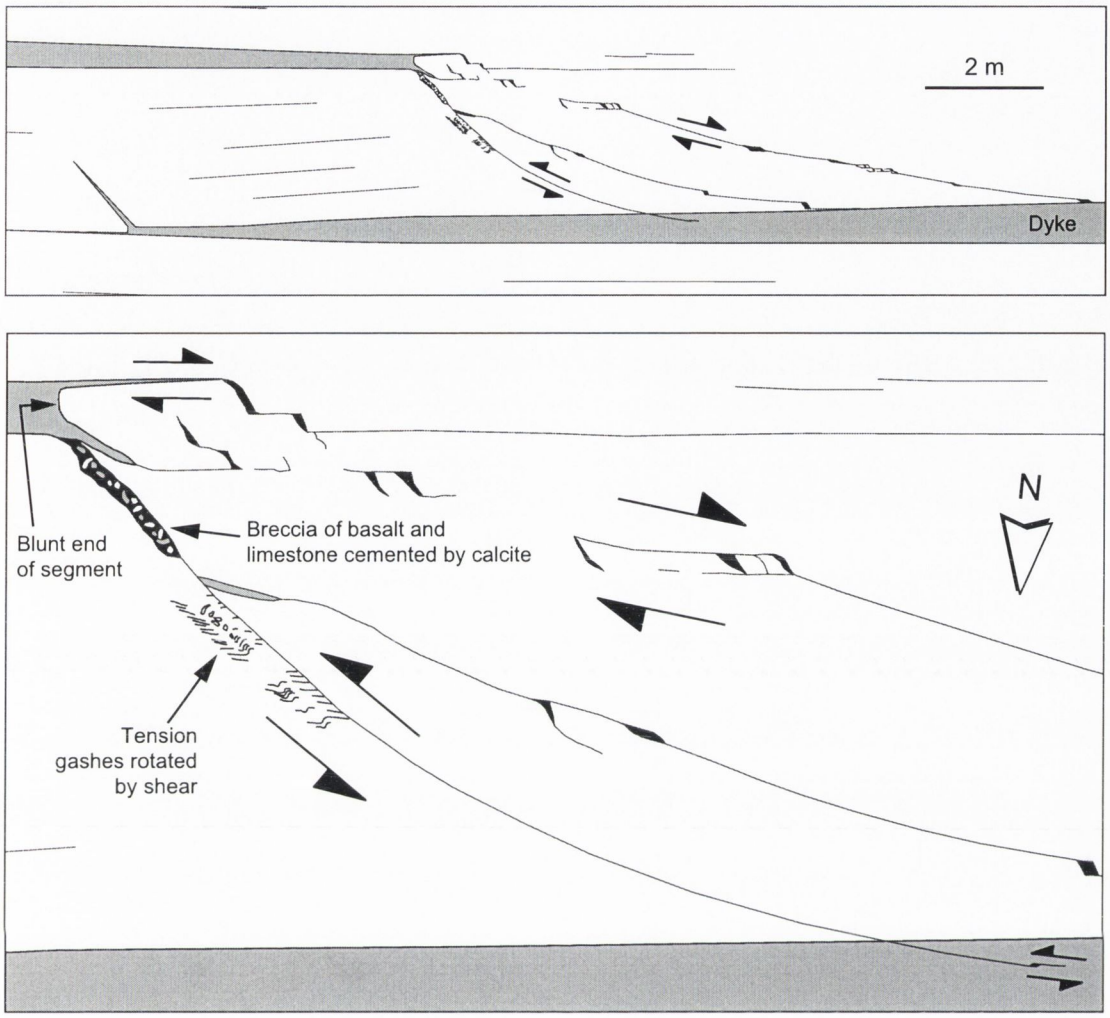

Figure 3.11a. Deformation outside of the host rock bridge related to dyke segment overlap. A right-stepping segmentation (Dyke K158) with associated dextral shear structures extending from the southern segment. Note also the sinistral transform shear relating to dilation of the blunt end of the southern segment.

Figure 3.11b. Deformation outside of the host rock bridge related to dyke segment overlap. A left-stepping segmentation (Dyke K137) with associated sinistral shear extending from, and associated with the bending of, the northern segment. The dyke infills sinistral shear structures and pull-aparts, and shears displace pre-intrusion veins by up to a few centimetres.

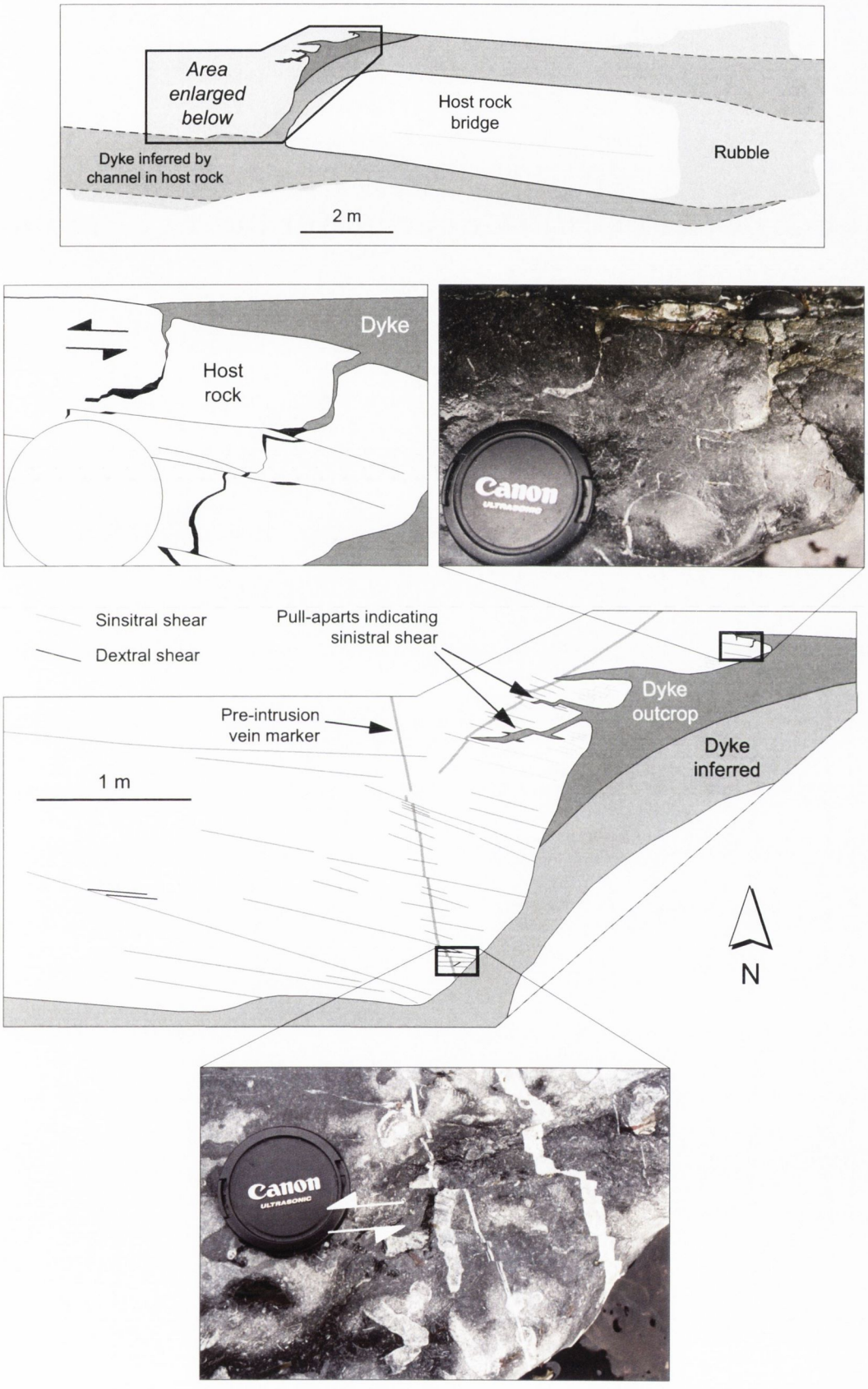

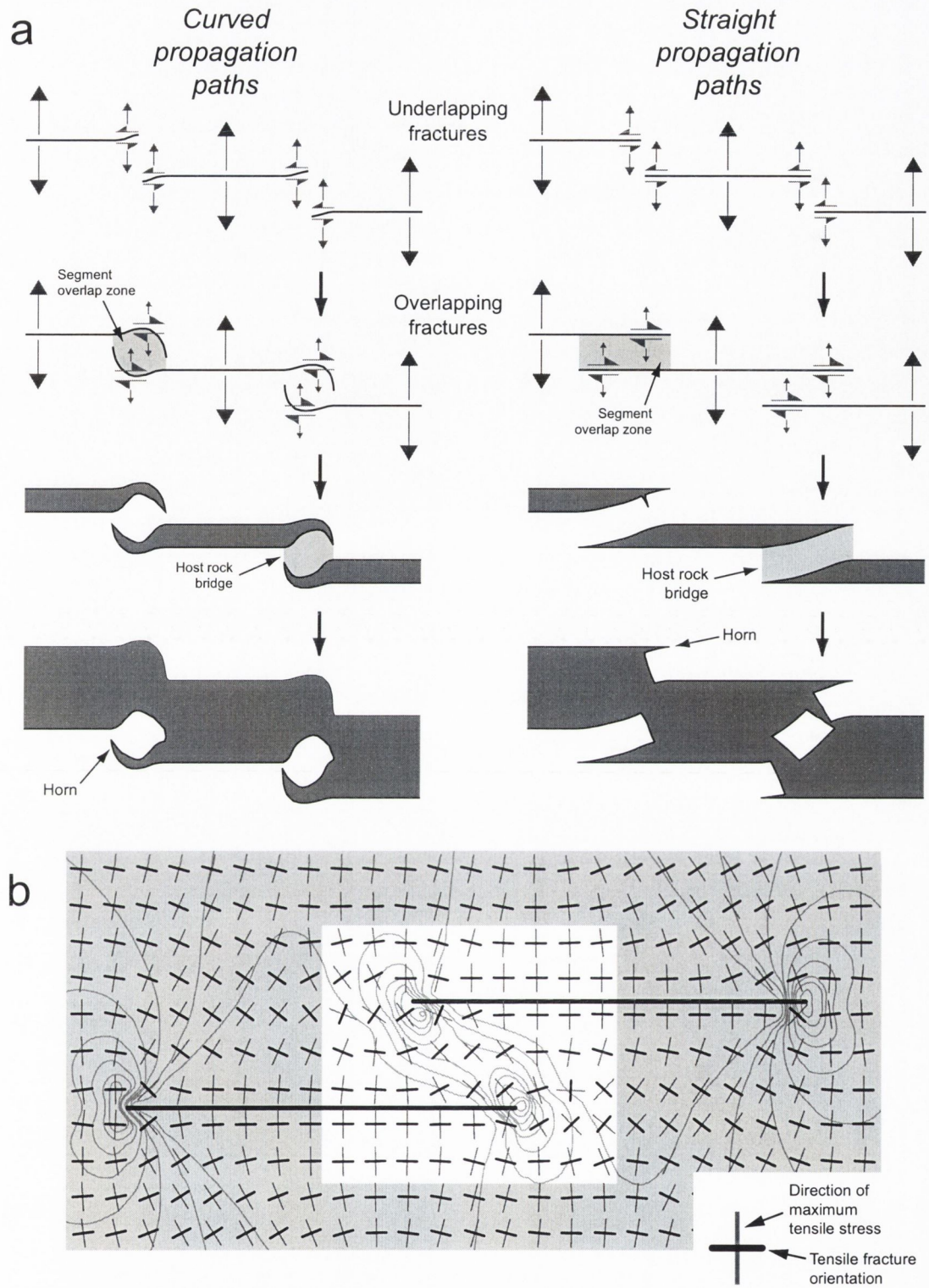

Figure 3.12. Propagation and segment stress interaction of en échelon fractures/dykes.
a) The multi-stage development of a right-stepping en échelon dyke. The first two stages are shown as interacting fractures rather than dyke segments; for dykes some dilation will take place during these stages. On approaching each other there is interaction of the stresses induced locally by each of the two adjacent mode I fractures/segments. A mode II stress is induced when there is still some underlap between the segments, thus creating a mixed mode I/II stress intensity. This generally causes the segments' paths to diverge. As segments begin to overlap, the shear sense of the mode II stress is reversed and its magnitude increases with respect to the mode I stress component. This then causes the fractures/segments to rapidly bend in towards each other. There are a number of reasons why the propagation paths of fractures/dykes may remain straight during interaction; these are explained in the text. Further fracture propagation ceases, and dilation causes bridge rotation. Eventually the bridges fail and the segments coalesce. Note, shear senses are reversed for left-stepping dykes.
b) Maximum principal stress (tensile) in the vicinity of two left-stepping fractures subjected to tensile stress. The contour interval is 10% of the maximum stress, which occurs at the fracture tips (modified from Cruikshank & Aydin (1994)).

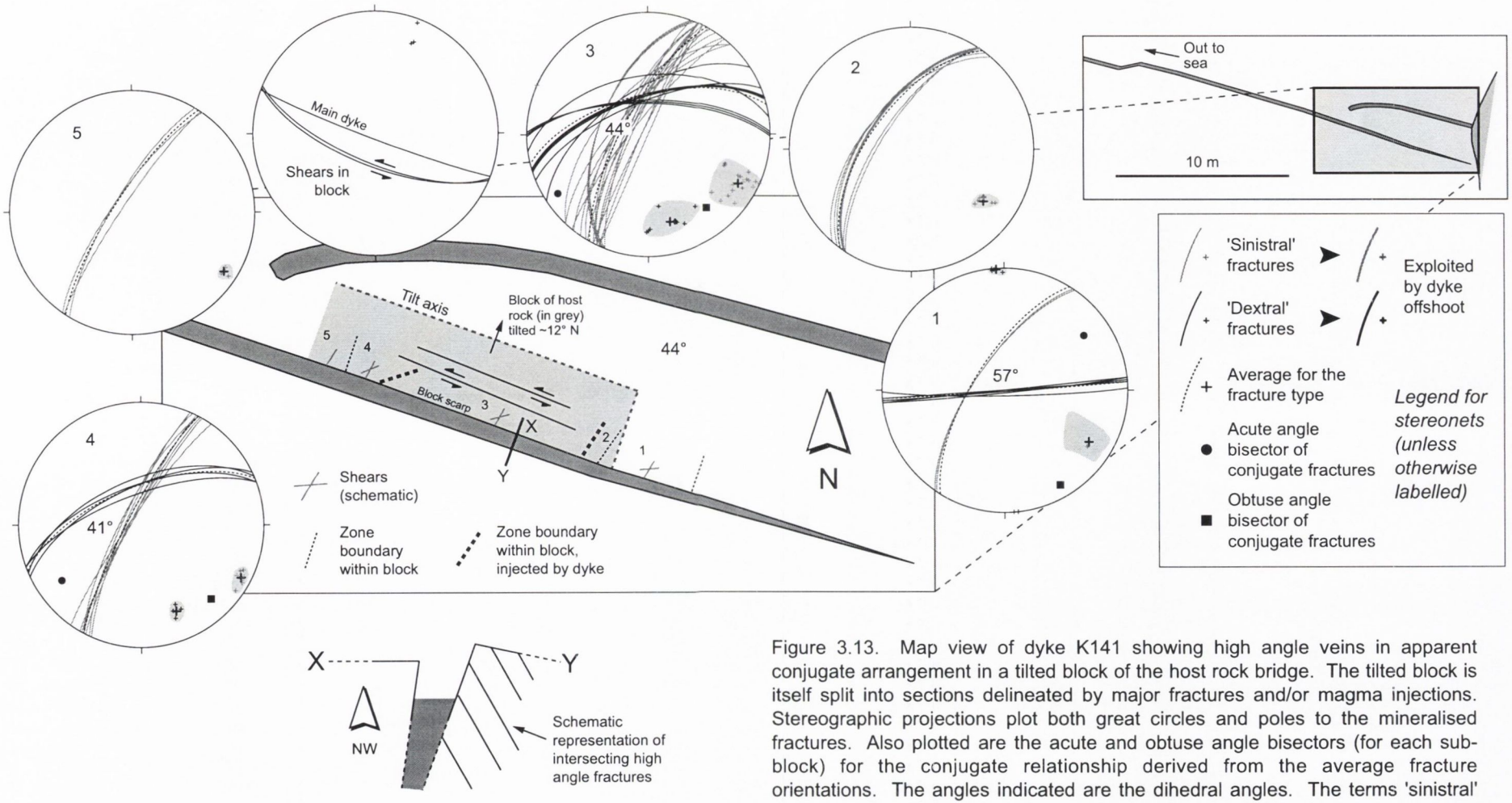

Figure 3.13. Map view of dyke K141 showing high angle veins in apparent conjugate arrangement in a tilted block of the host rock bridge. The tilted block is itself split into sections delineated by major fractures and/or magma injections. Stereographic projections plot both great circles and poles to the mineralised fractures. Also plotted are the acute and obtuse angle bisectors (for each sub-block) for the conjugate relationship derived from the average fracture orientations. The angles indicated are the dihedral angles. The terms 'sinistral' and 'dextral' are used loosely to define the two groups of fractures as they would be expected to fail in shear given the apparent conjugate relations.

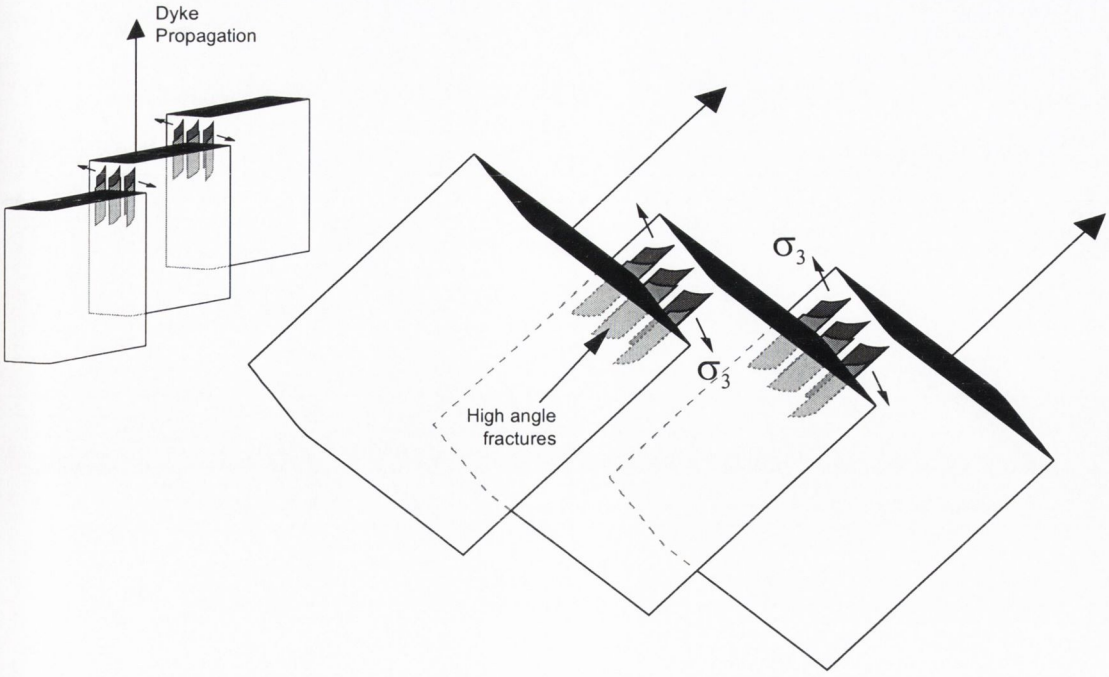

Figure 3.14. A schematic representation of the interpretation of inclined high angle fractures in the host bridge of segmented dykes. The high angle fractures form in response to the rotation of stress trajectories within the host rock bridge, as indicated. Segments propagating upwards will create vertical fractures. Segments propating obliquely through the crust show components of segmentation in both the horizontal and vertical planes, and produce inclined fractures.

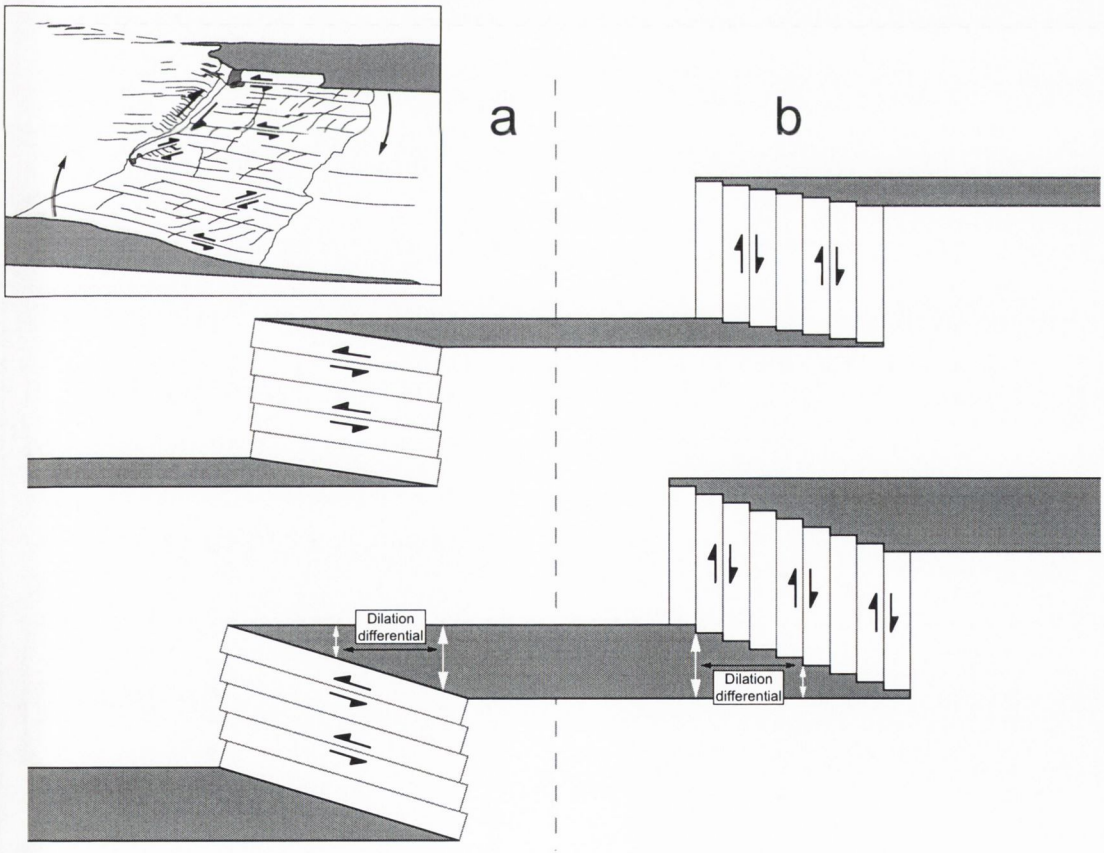

Figure 3.15. A schematic representation of a left-stepping dyke showing how rotation of the host rock bridge might be accommodated by flexural slip type displacements. The inset provides a field example for comparison.
a) Slip occurs along dyke-parallel fractures.
b) Slip occurs along fractures at high angle to the segment strike. For simplicity, these fractures have been drawn as orthogonal to the dyke, but are seen in outcrop at a lower angle to the dyke, as shown in the inset.

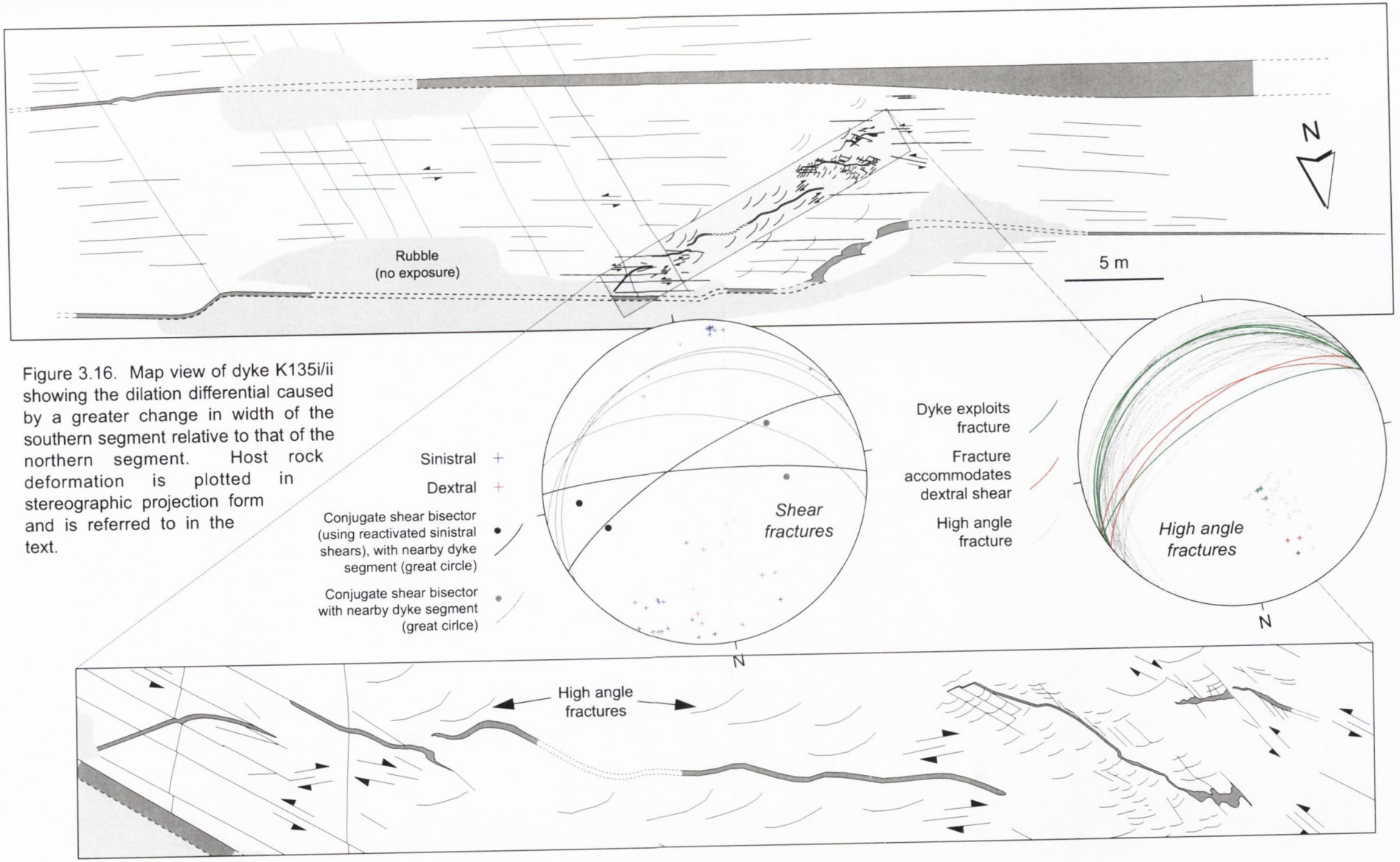

Figure 3.16. Map view of dyke K135i/ii showing the dilation differential caused by a greater change in width of the southern segment relative to that of the northern segment. Host rock deformation is plotted in stereographic projection form and is referred to in the text.

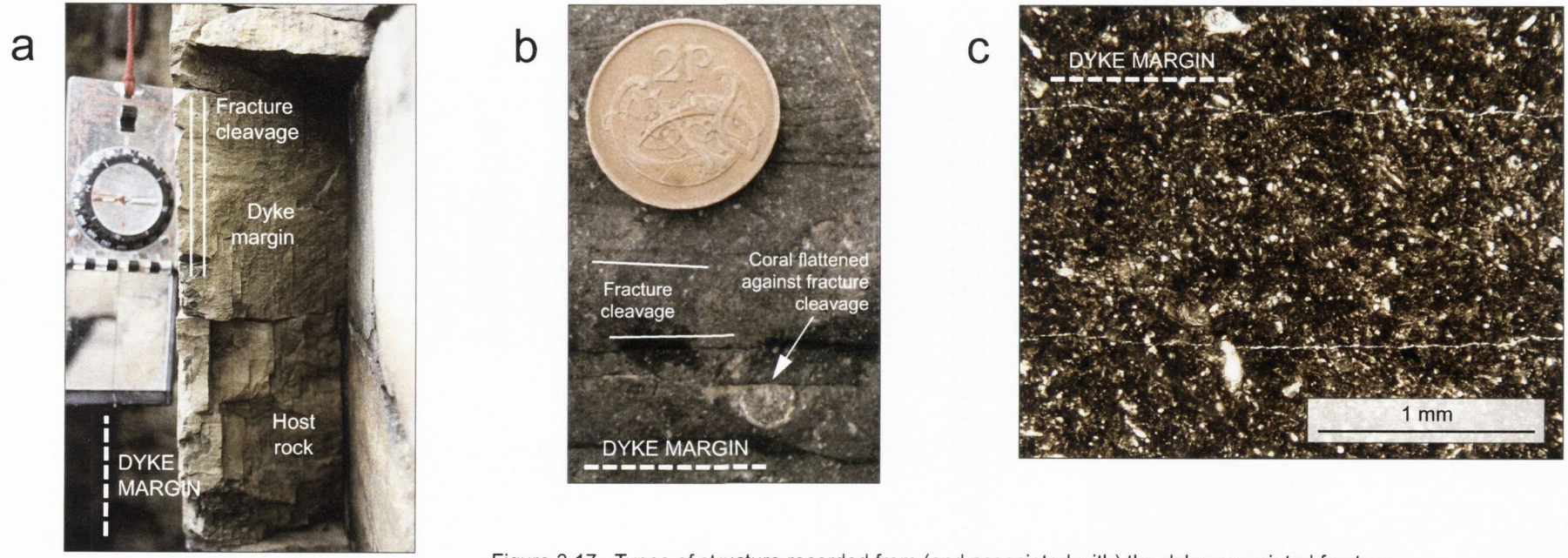

Figure 3.17. Types of structure recorded from (and associated with) the dyke-associated fracture zones in the host rock.

a) Section view of fracture cleavage immediately adjacent to the margin of dyke K155a.

b) Plan view of apparent pressure solution of a coral against a fracture cleavage plane (dyke K132ii).

c) Photomicrograph (plan view) of fracture cleavage in limestone host rock (two fractures running left to right), manifest as mineralised extensional fractures (dyke K180).

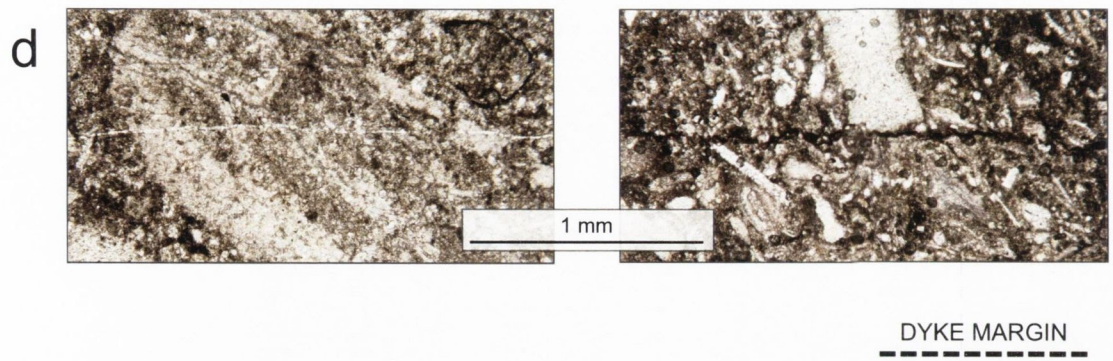

Figure 3.17 continued.
d) Photomicrographs (plan views) of fracture cleavage from the same sample, occurring as both extensional fractures and stylolites (dyke K140).
e) Photomicrograph (plan view) of fracture cleavage manifest as a stylolite that has later been mineralised (dyke K178).
f) Photomicrograph (plan view) showing one fracture cleavage plane changing form along strike from a stylolite (left) to an apparent extensional mineral-infilled fracture (right) (dyke K178). A transitional form exists (middle) in which the stylolite is mineralised.

g



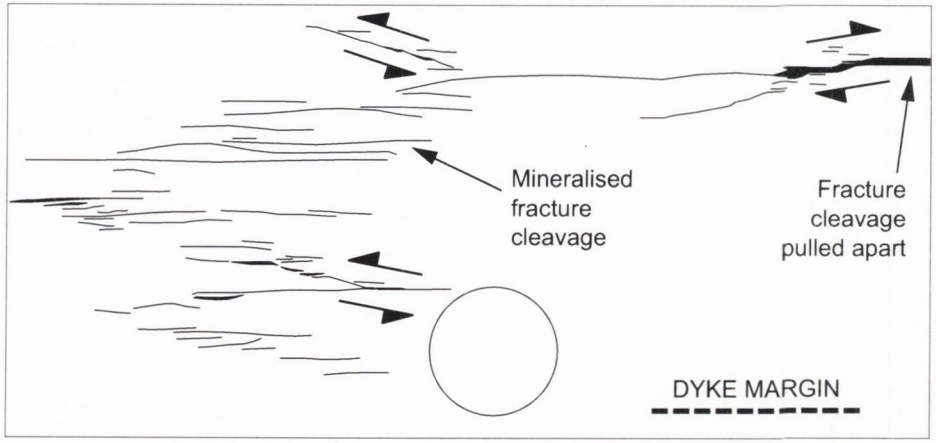

h

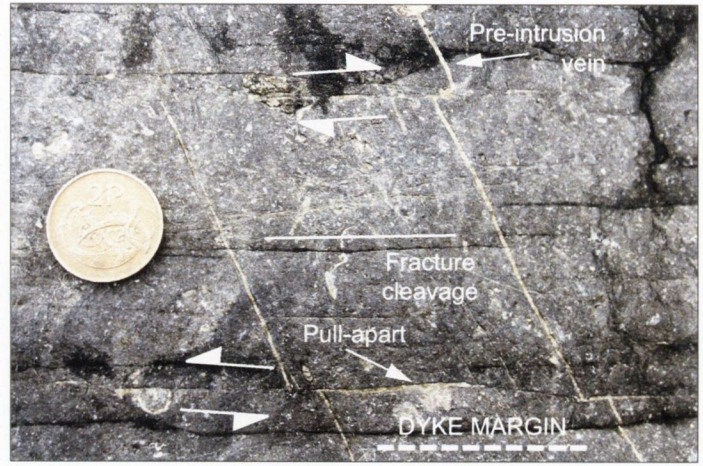

i

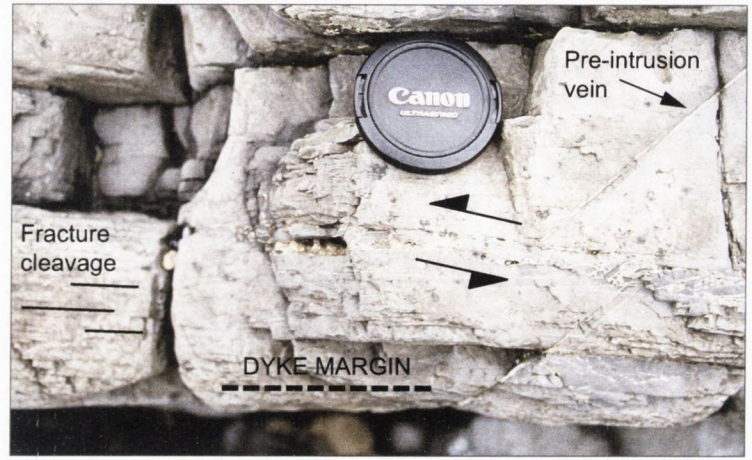

Figure 3.17 continued.
g) Plan view of fracture cleavage mineralised in en échelon geometry (dyke K178).
h) Plan view of low dihedral angle conjugate shear structures with fracture cleavage pulled apart and linked by oblique ramps (dyke K132ii).
i) Plan view of a sinistral shear structure with fracture cleavage pulled apart and rotated (dyke K178).

j

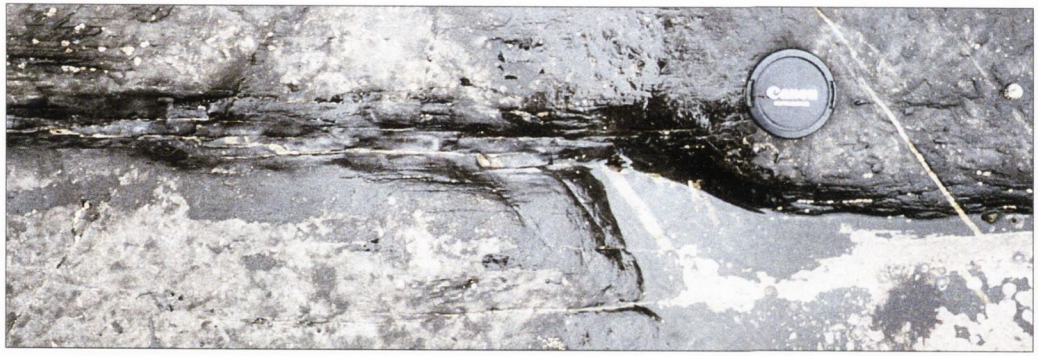

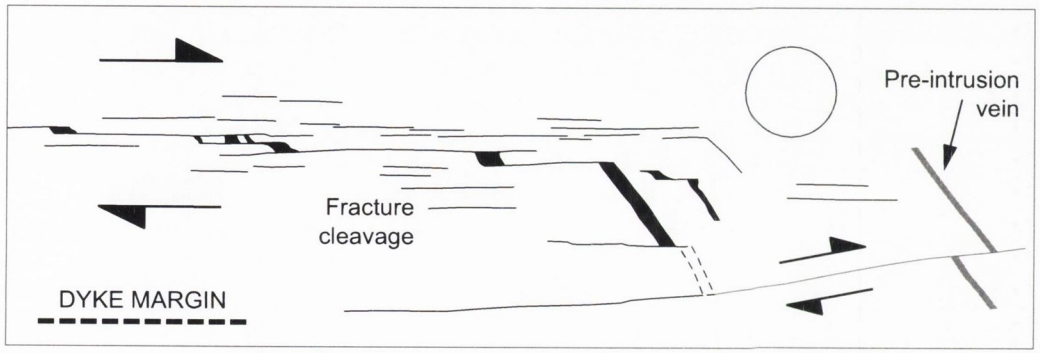

k

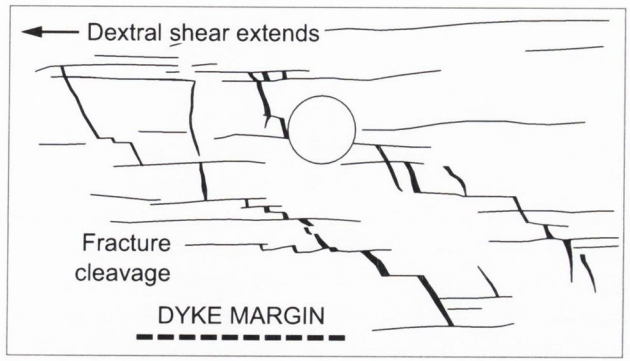

Figure 3.17 continued.
j) Plan view of a dextral shear structure using fracture cleavage to accommodate shear (dyke K134).
k) Plan view showing the termination of a dextral shear structure such as that shown above (dyke K134).
l) Plan view of a dextral shear structure showing rotation of the fracture cleavage into pinnate geometry with the shear plane (dyke K178). Above the shear plane the fracture cleavage parallels the plane of shear; below, it parallels the dyke.

l



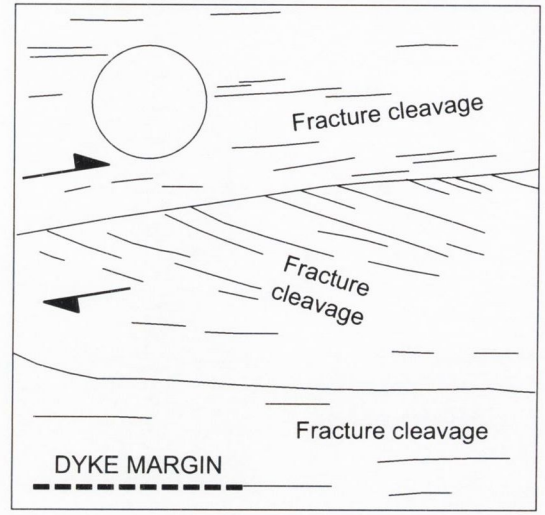

m

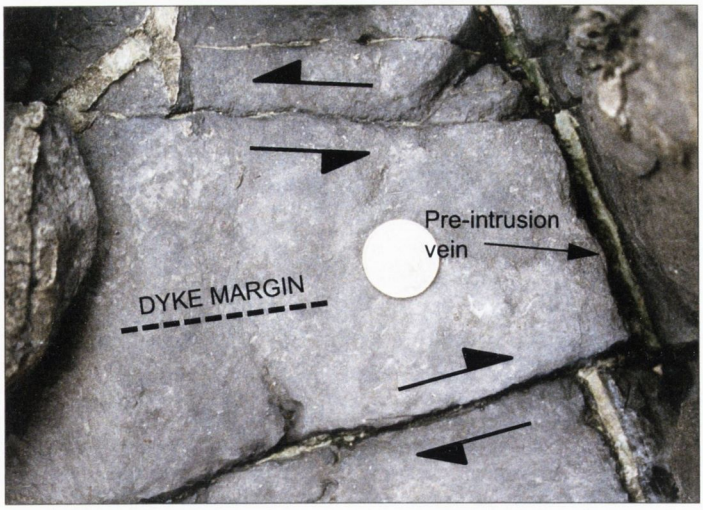

n



o

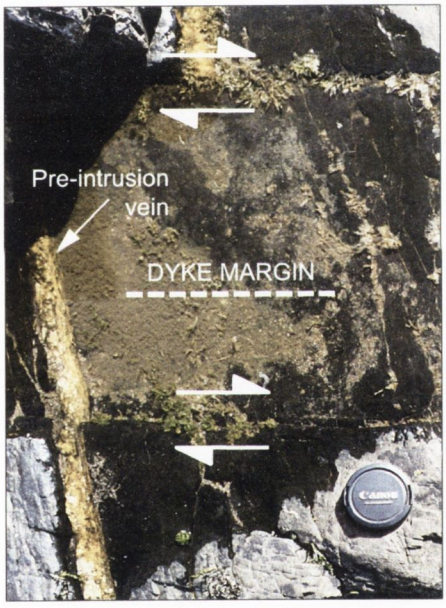

Figure 3.17 continued.
m) Plan view of a pair of low dihedral angle conjugate shears (dyke K147).
n) Plan view of a dextral pull-apart structure (dyke K147).
o) Plan view of dextral slip along major (possibly reactivated) dyke-parallel fractures (dyke K178).
p) Plan view of dextral shear along the margin of dyke K155b.

p

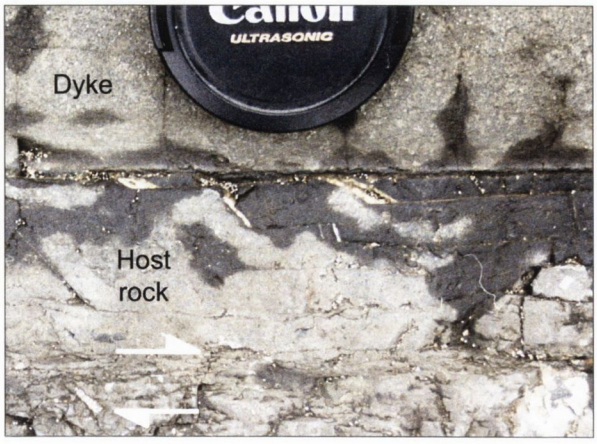

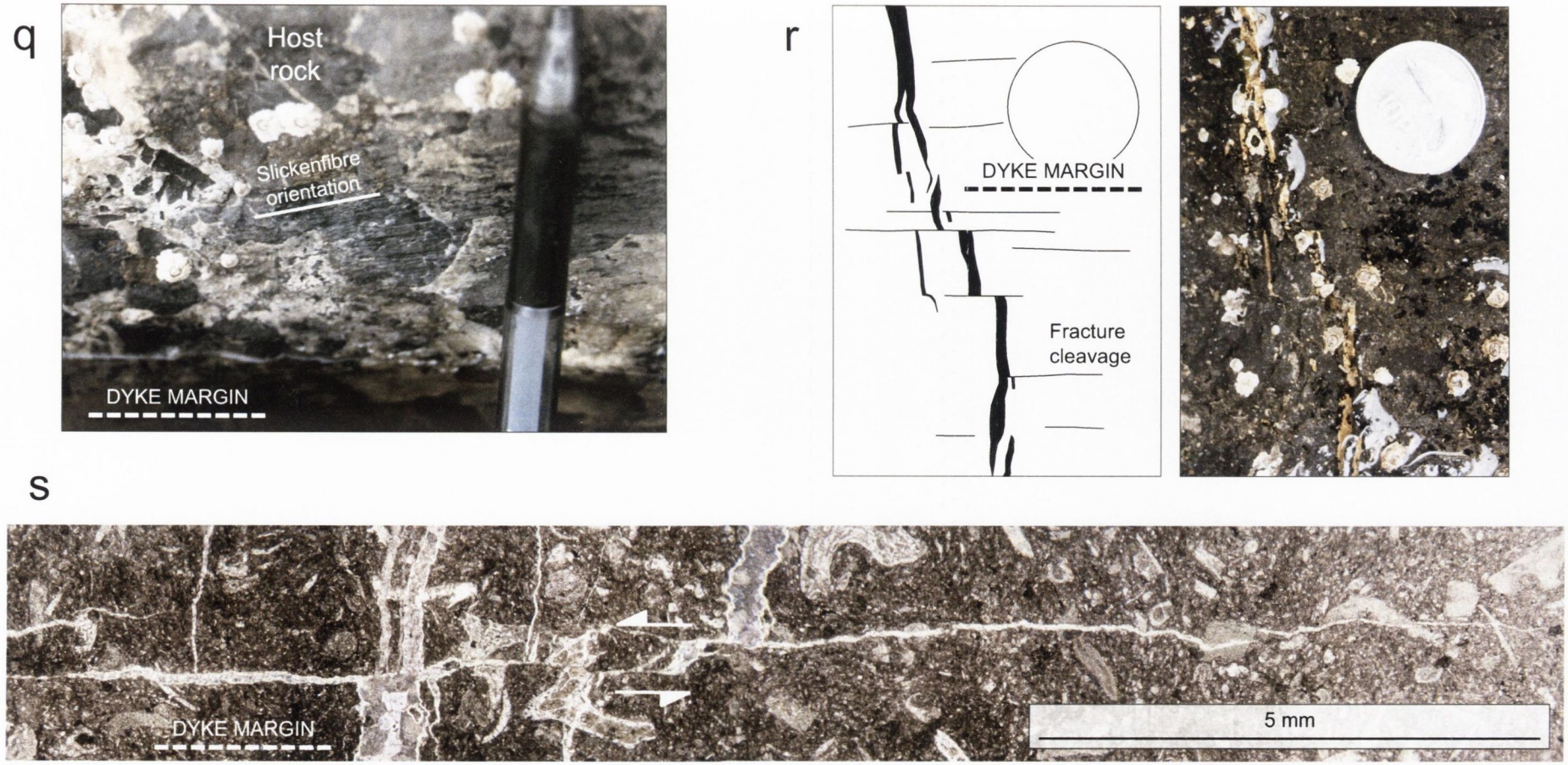

Figure 3.17 continued.
q) Cross-section view of shallow plunging slickenfibres on the host rock margin of dyke K111. Slip is predominantly dextral strike-slip along the dyke margin. Note also the general mineralisation and host rock brecciation.
r) Plan view of a high angle (to dyke margin) vein showing a consistent left-stepping geometry across the fracture cleavage (dyke K117).
s) Photomicrograph (plan view) showing transform offsets of high angle veins (bottom to top) across fracture cleavage (left to right) in the host rock margin of dyke K117. Note the sinstral shear induced on the transform portion of the fracture cleavage.

t

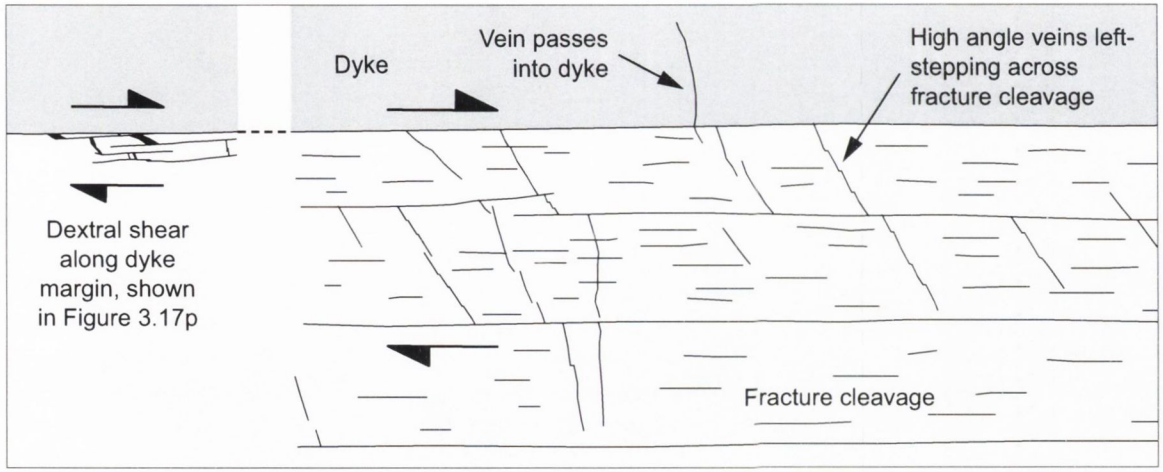

v

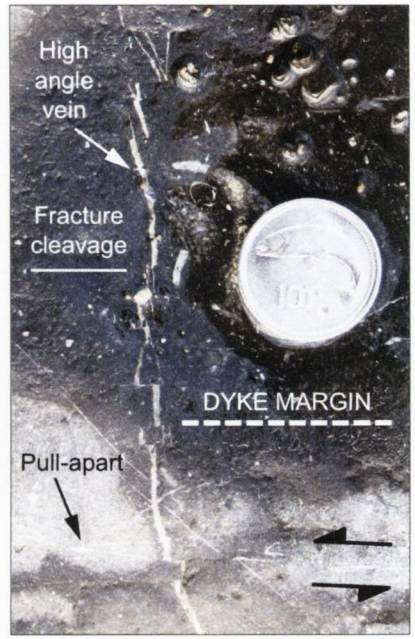

u

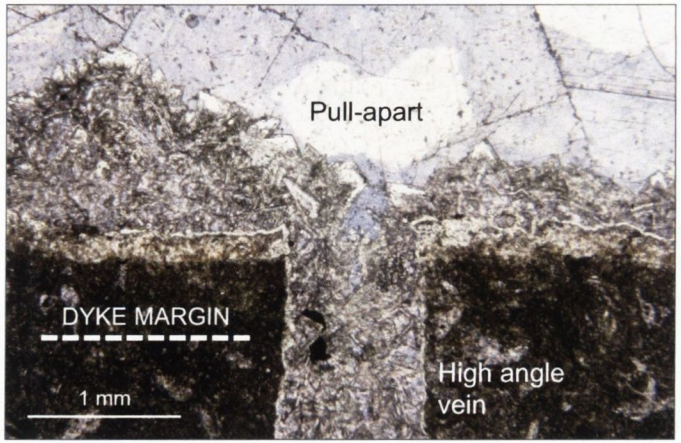

Figure 3.17 continued.
t) Plan view of high angle veins associated with dextral shear along the margin of dyke K155b.
u) Photomicrograph (plan view) showing coeval mineralisation of a shear pull-apart and a high angle vein in the host rock adjacent to dyke K117.
v) Plan view of a high angle vein showing an apparent sinistral shear offset across the fracture cleavage, accompanied by mainly transform offsets (dyke K117).

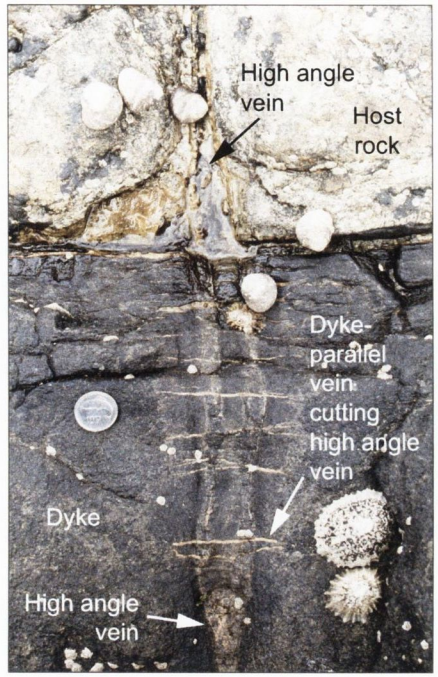

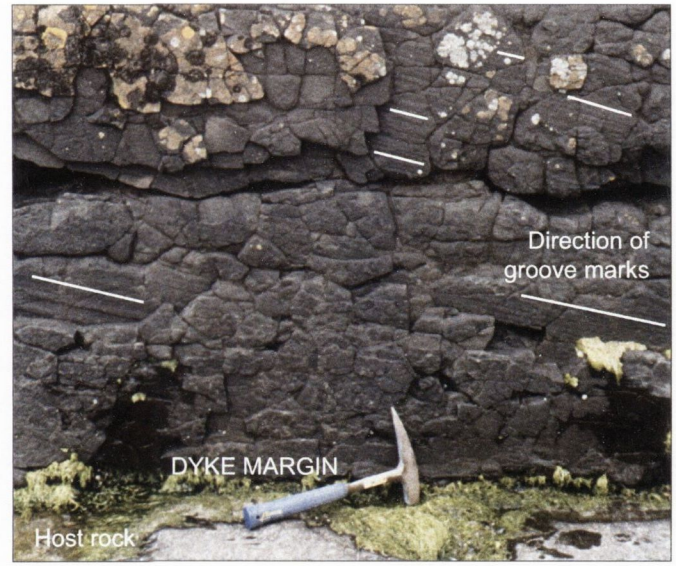

Figure 3.18. Examples of structures within dykes.
a) Plan view of a high angle vein cuts dyke K117 and the host rock. Within the dyke the vein is cut by dyke-parallel veins.
b) Plan view of shear structures within dyke K178, as interpreted, in conjugate arrangement and subtending a low angle to the dyke margin.
c) A view looking at the margin of dyke K113 forming a wall protruding from the platform. Groove marks are contained witihin a dyke-parallel cooling joint plane close to the margin.

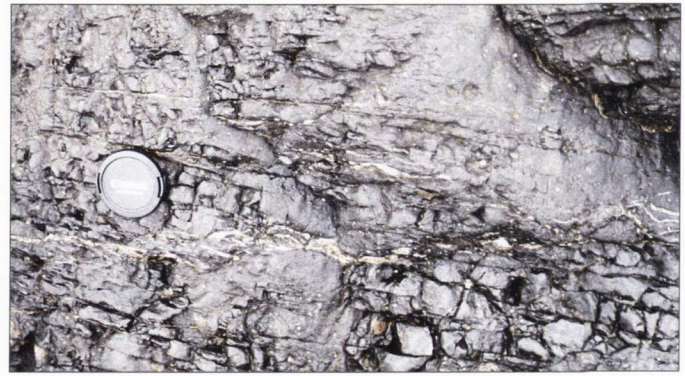

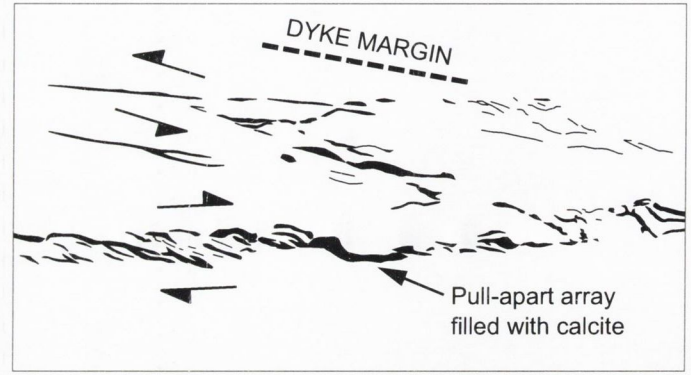

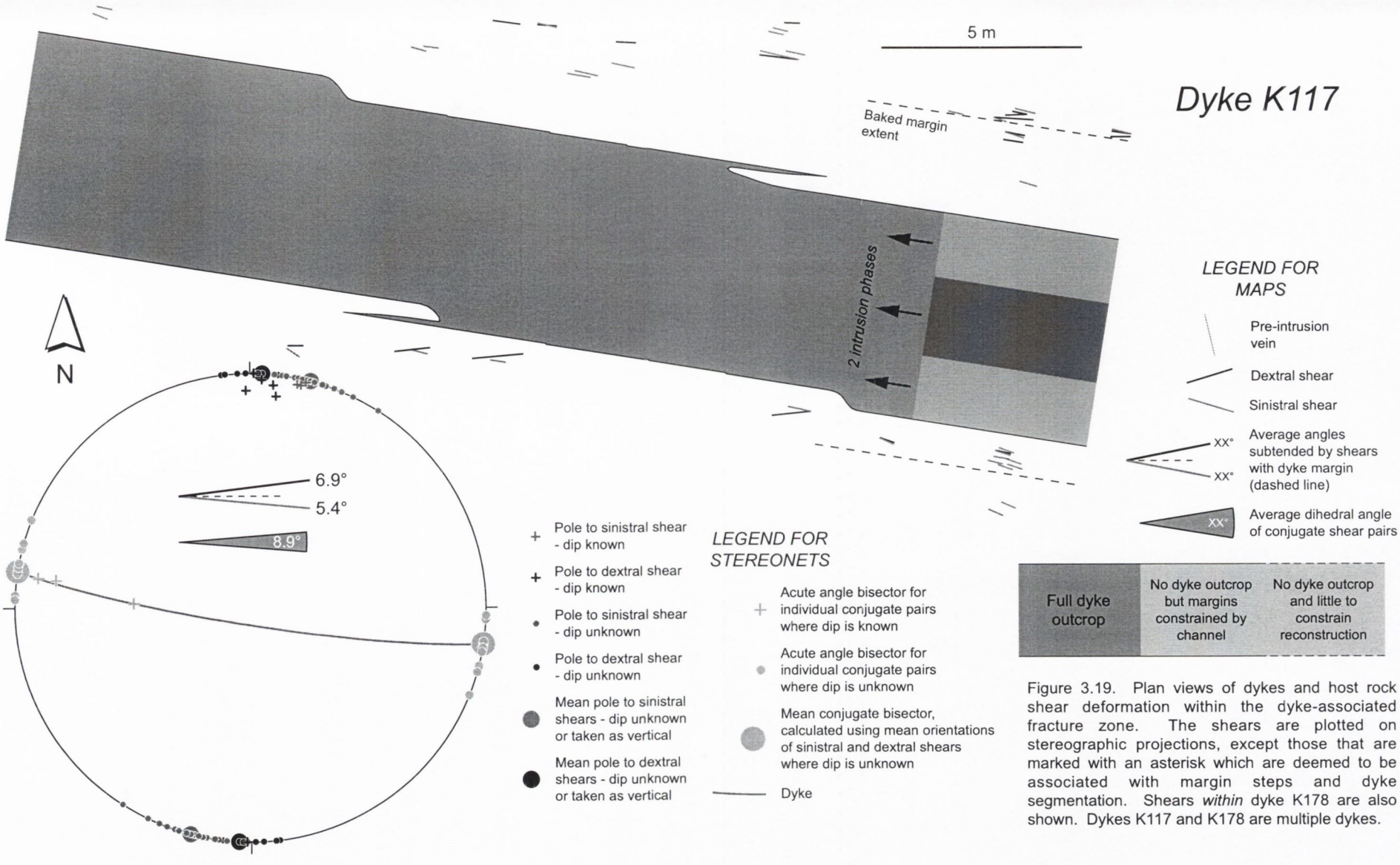

Figure 3.19. Plan views of dykes and host rock shear deformation within the dyke-associated fracture zone. The shears are plotted on stereographic projections, except those that are marked with an asterisk which are deemed to be associated with margin steps and dyke segmentation. Shears *within* dyke K178 are also shown. Dykes K117 and K178 are multiple dykes.

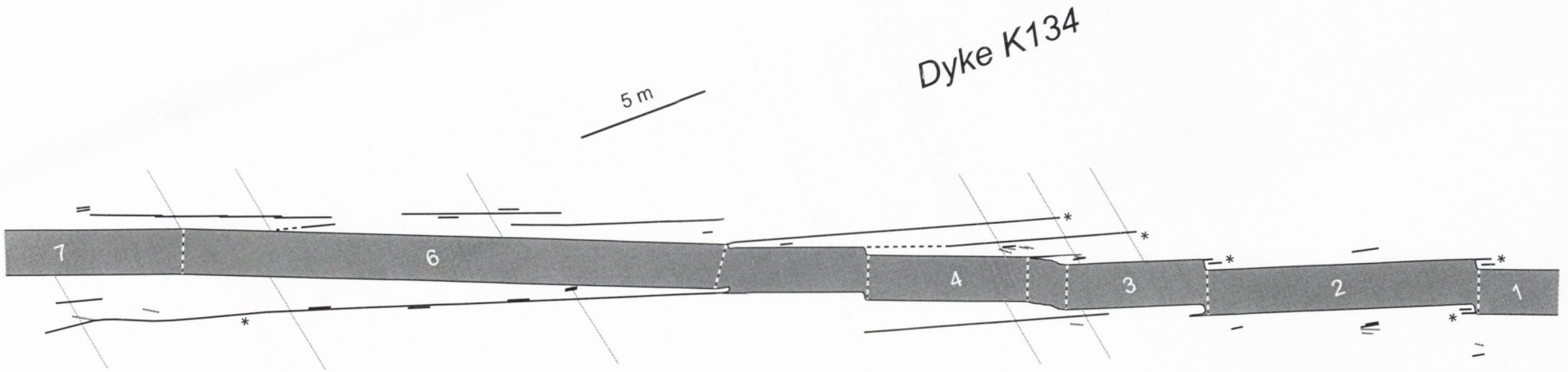

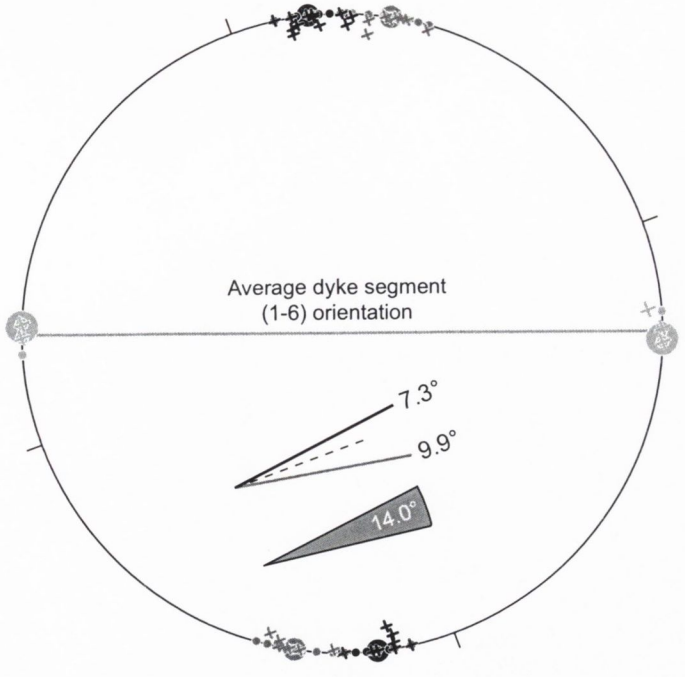



Figure 3.19 continued.

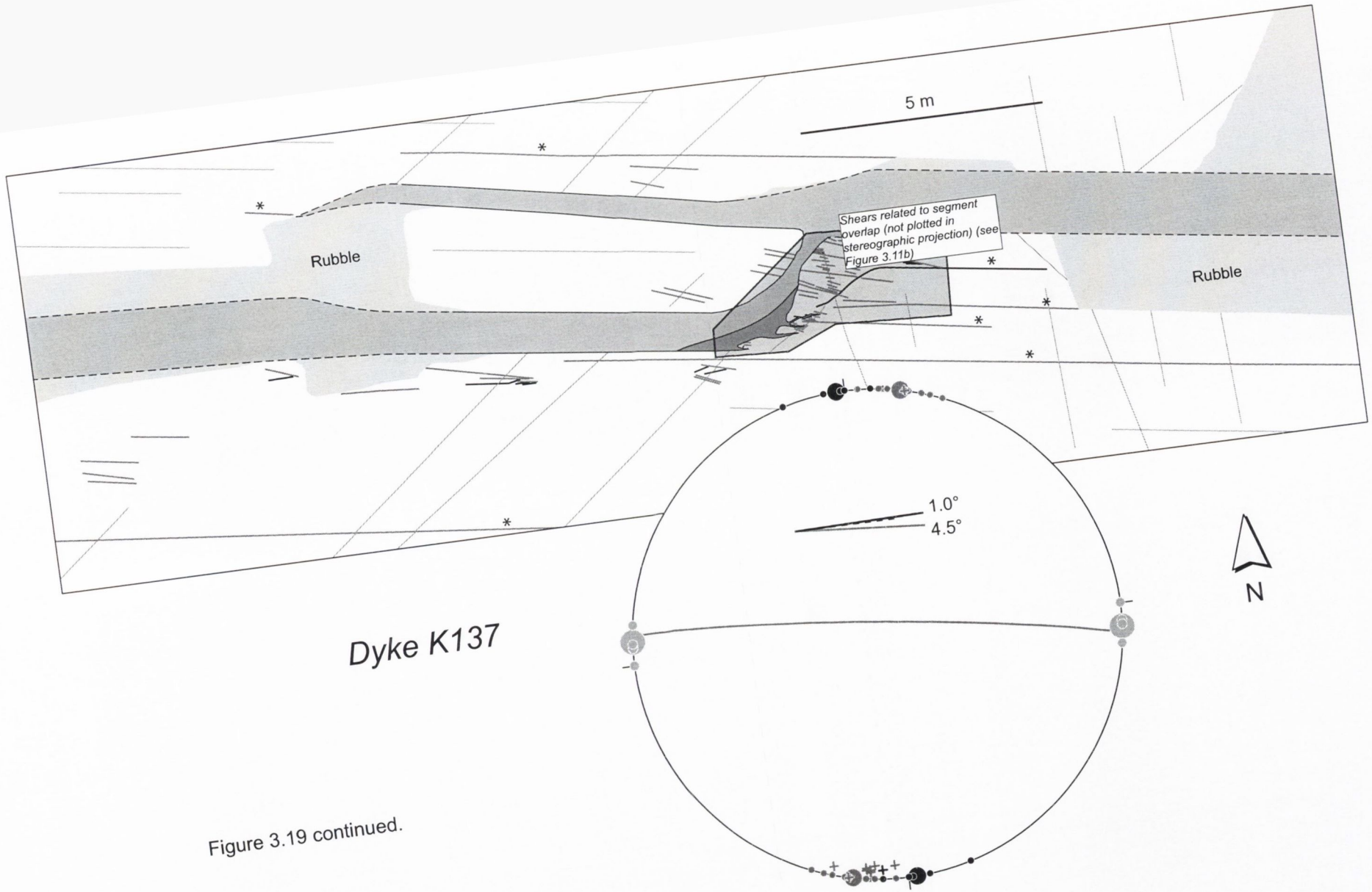

Figure 3.19 continued.

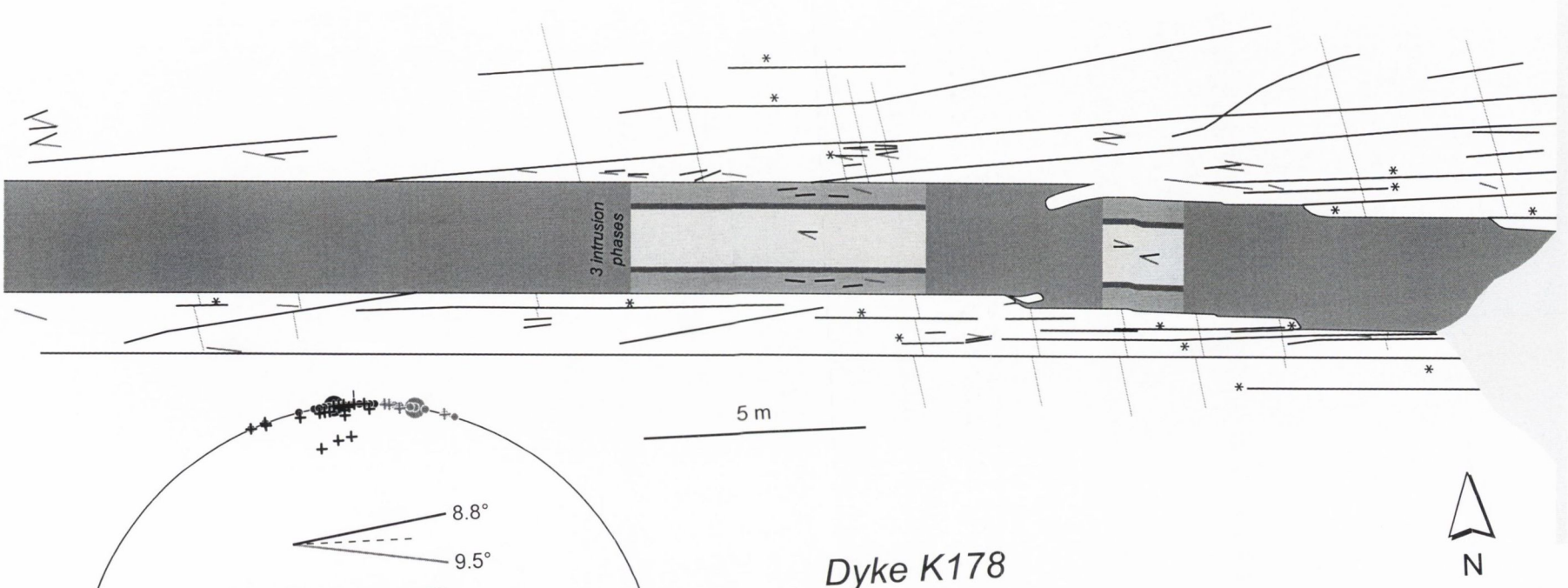

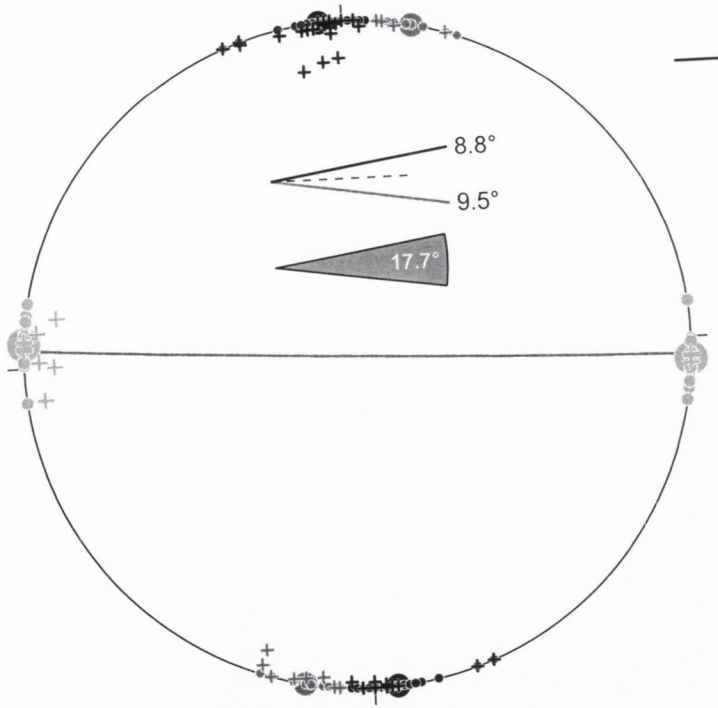

Dyke K178

Figure 3.19 continued.

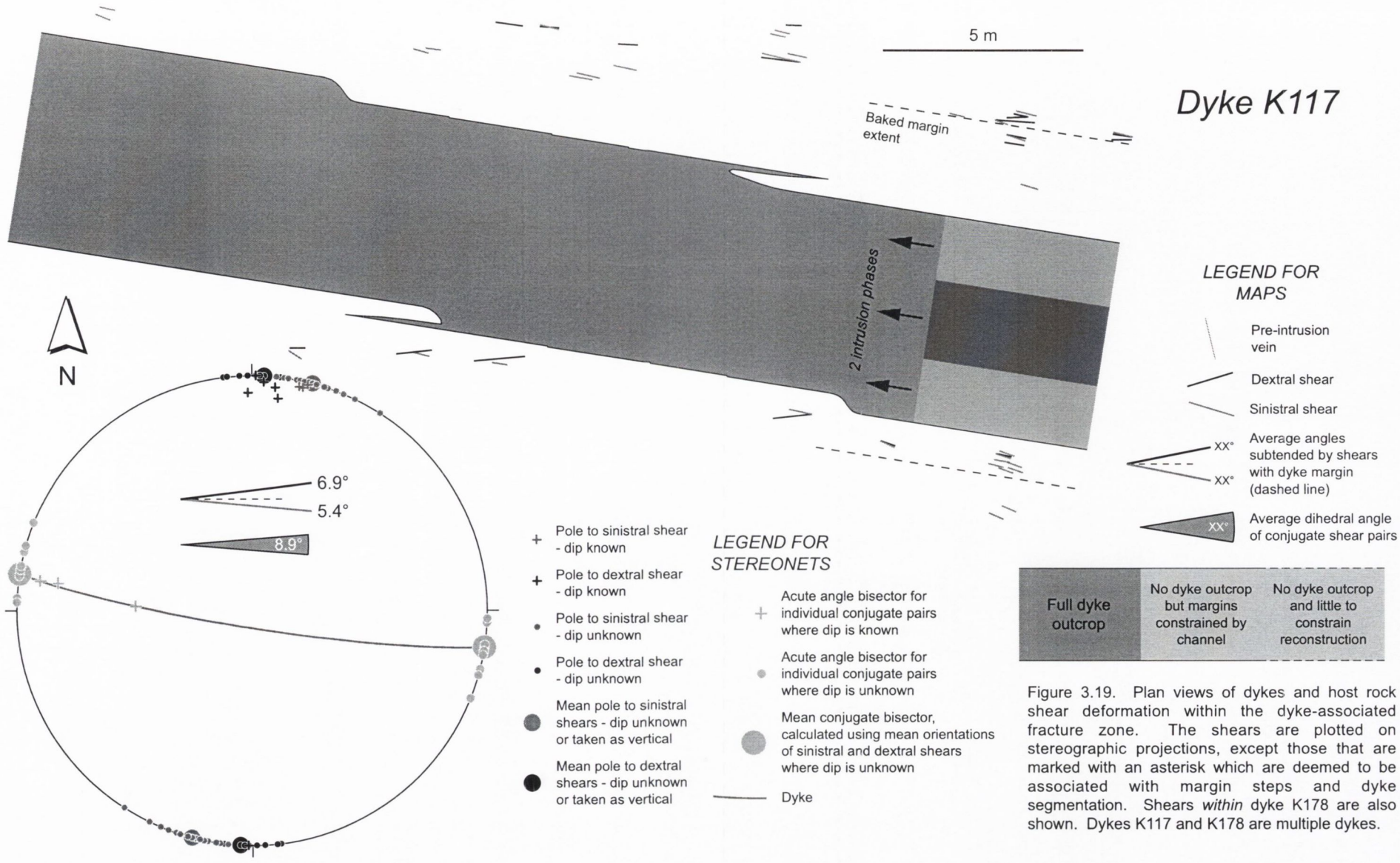

Figure 3.19. Plan views of dykes and host rock shear deformation within the dyke-associated fracture zone. The shears are plotted on stereographic projections, except those that are marked with an asterisk which are deemed to be associated with margin steps and dyke segmentation. Shears *within* dyke K178 are also shown. Dykes K117 and K178 are multiple dykes.

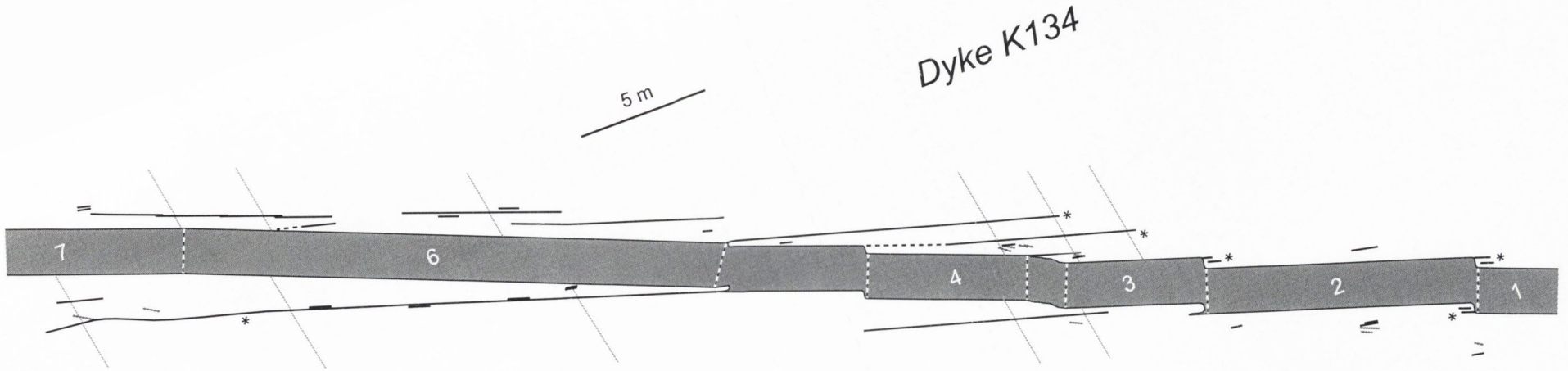

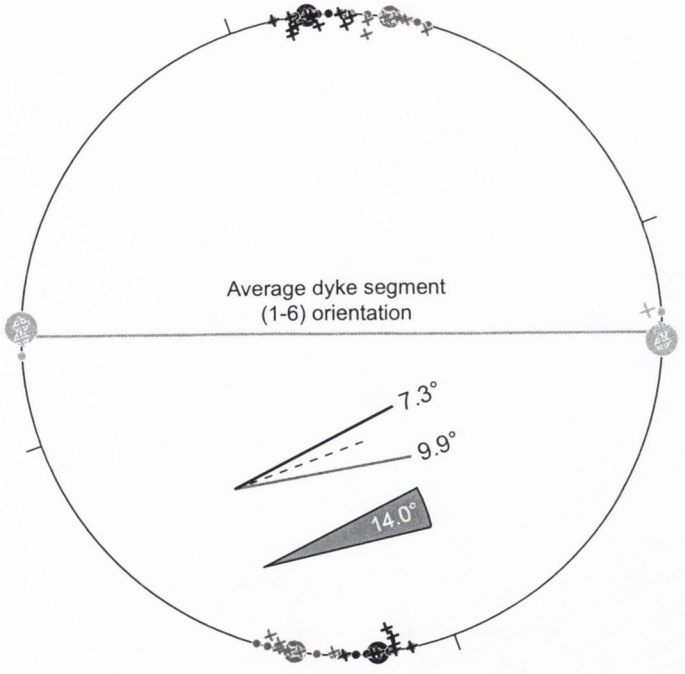



Figure 3.19 continued.

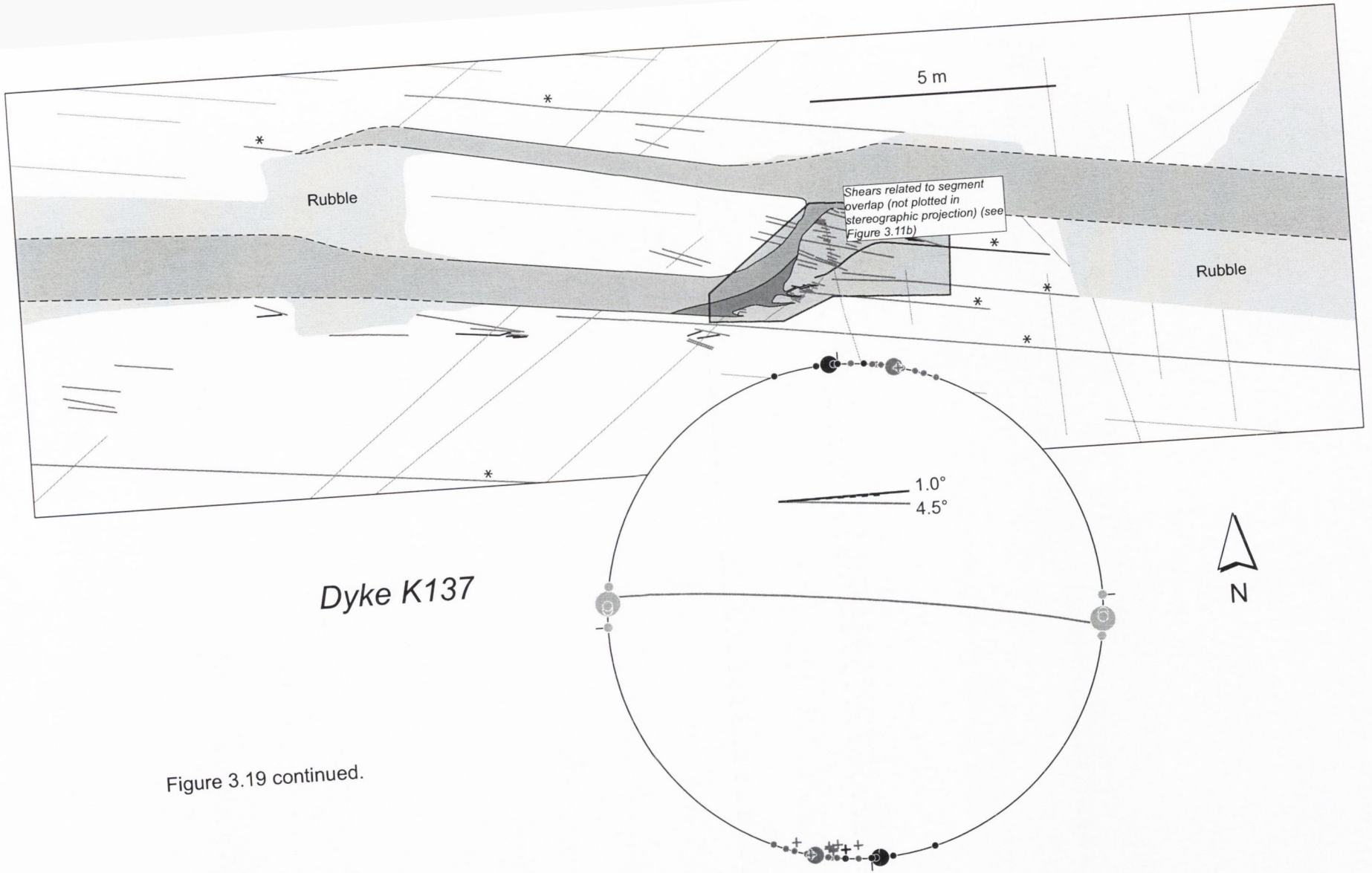

Figure 3.19 continued.

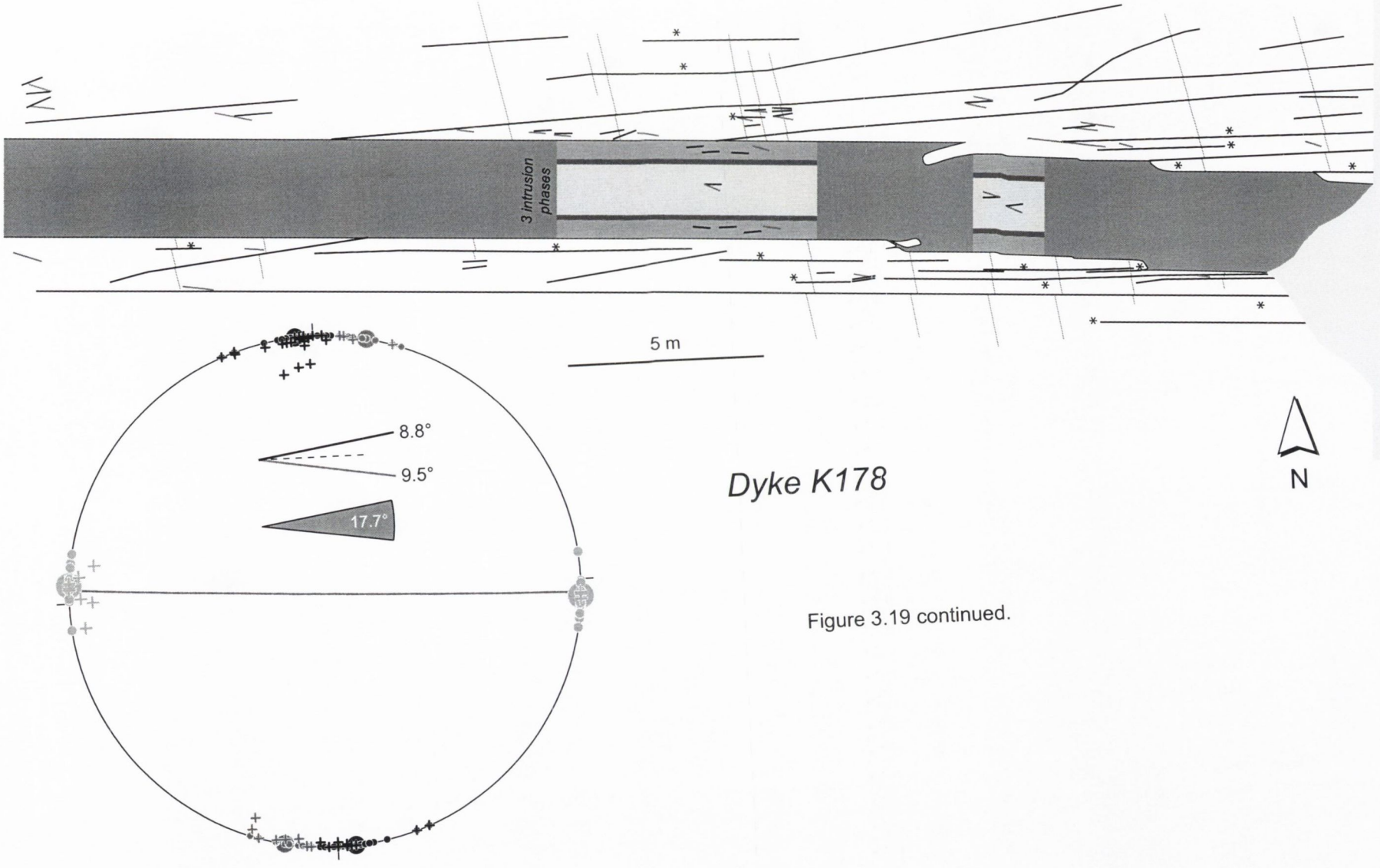

Figure 3.19 continued.

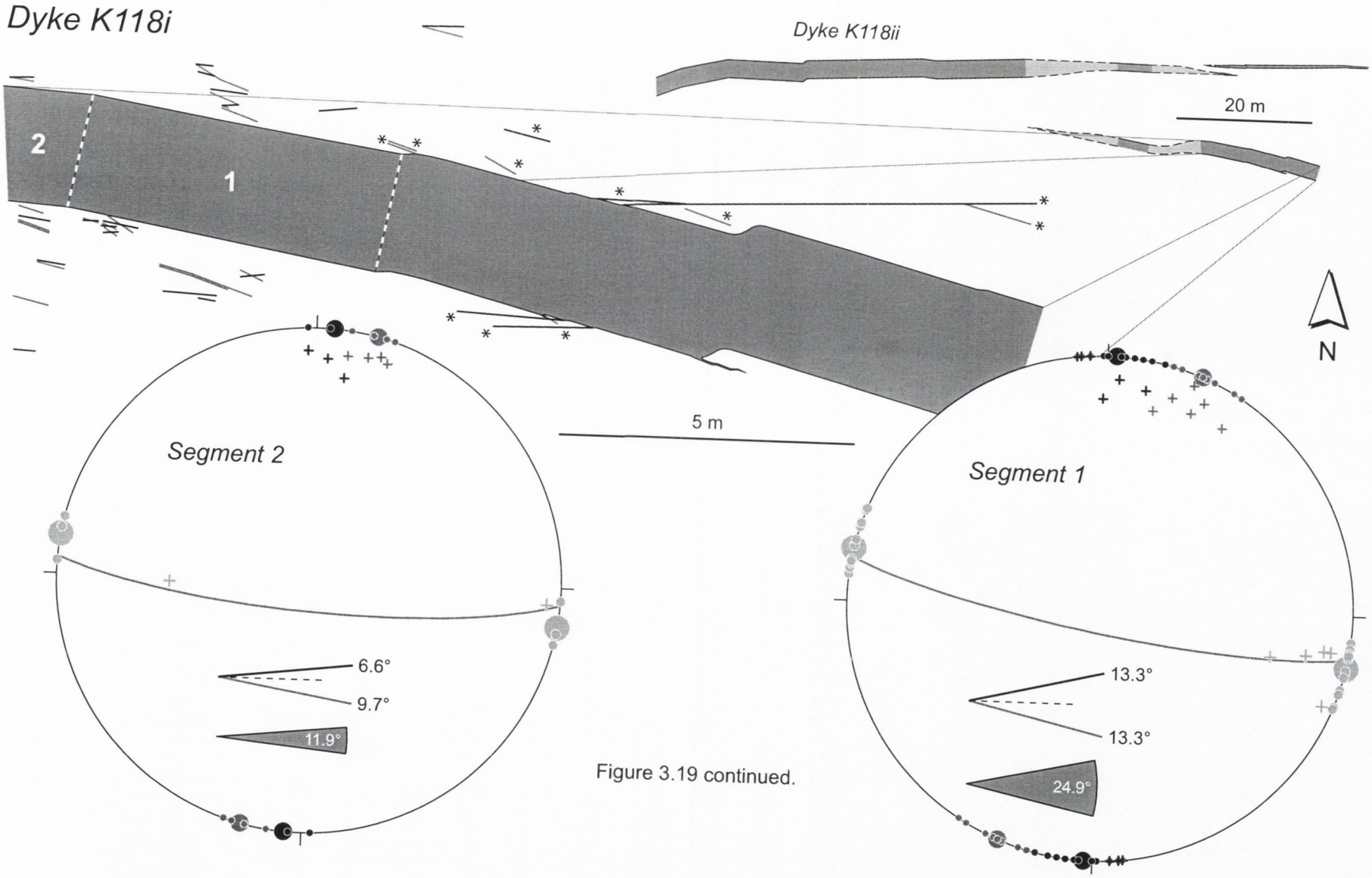

Figure 3.19 continued.

Figure 3.19 continued.

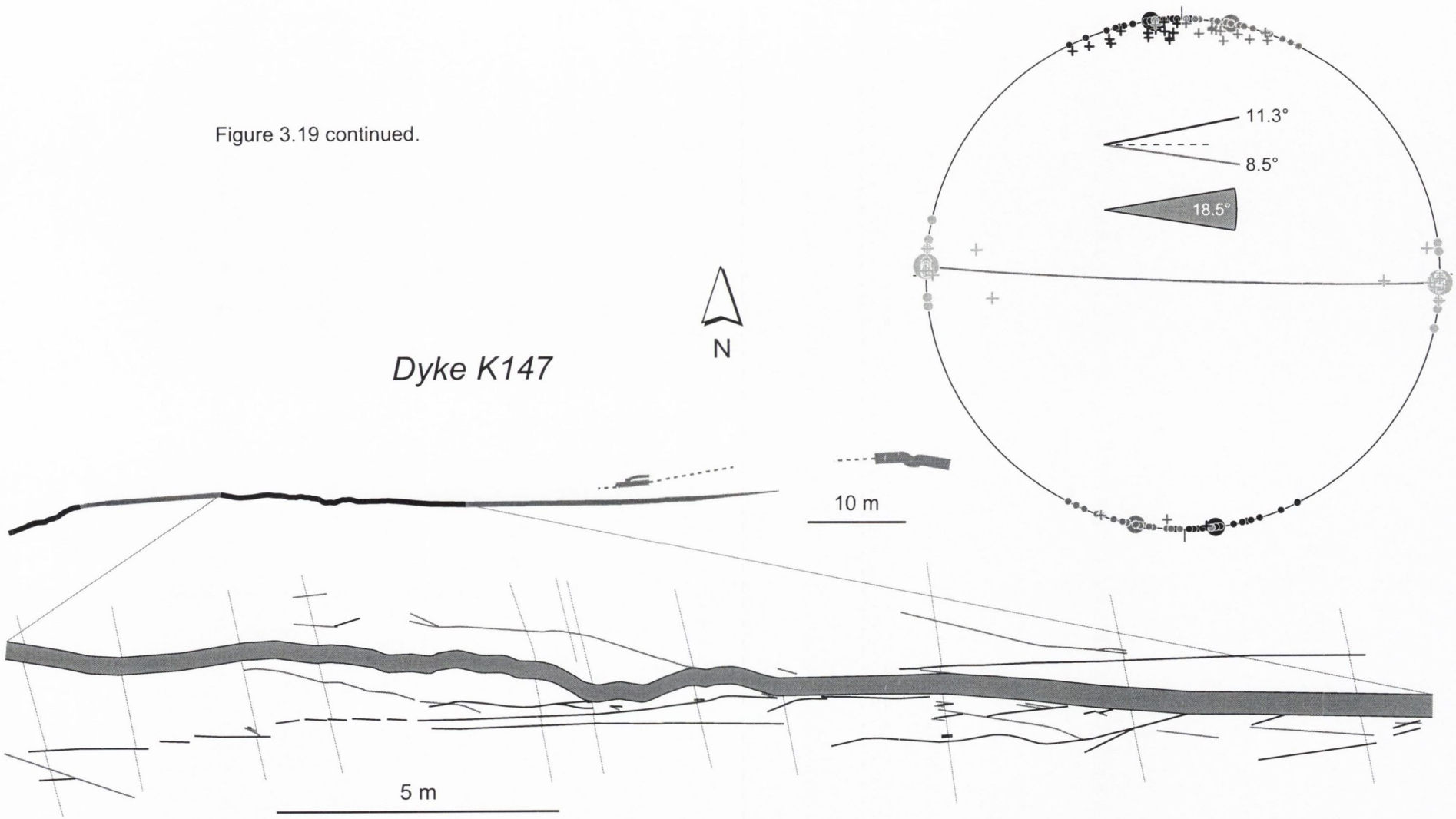

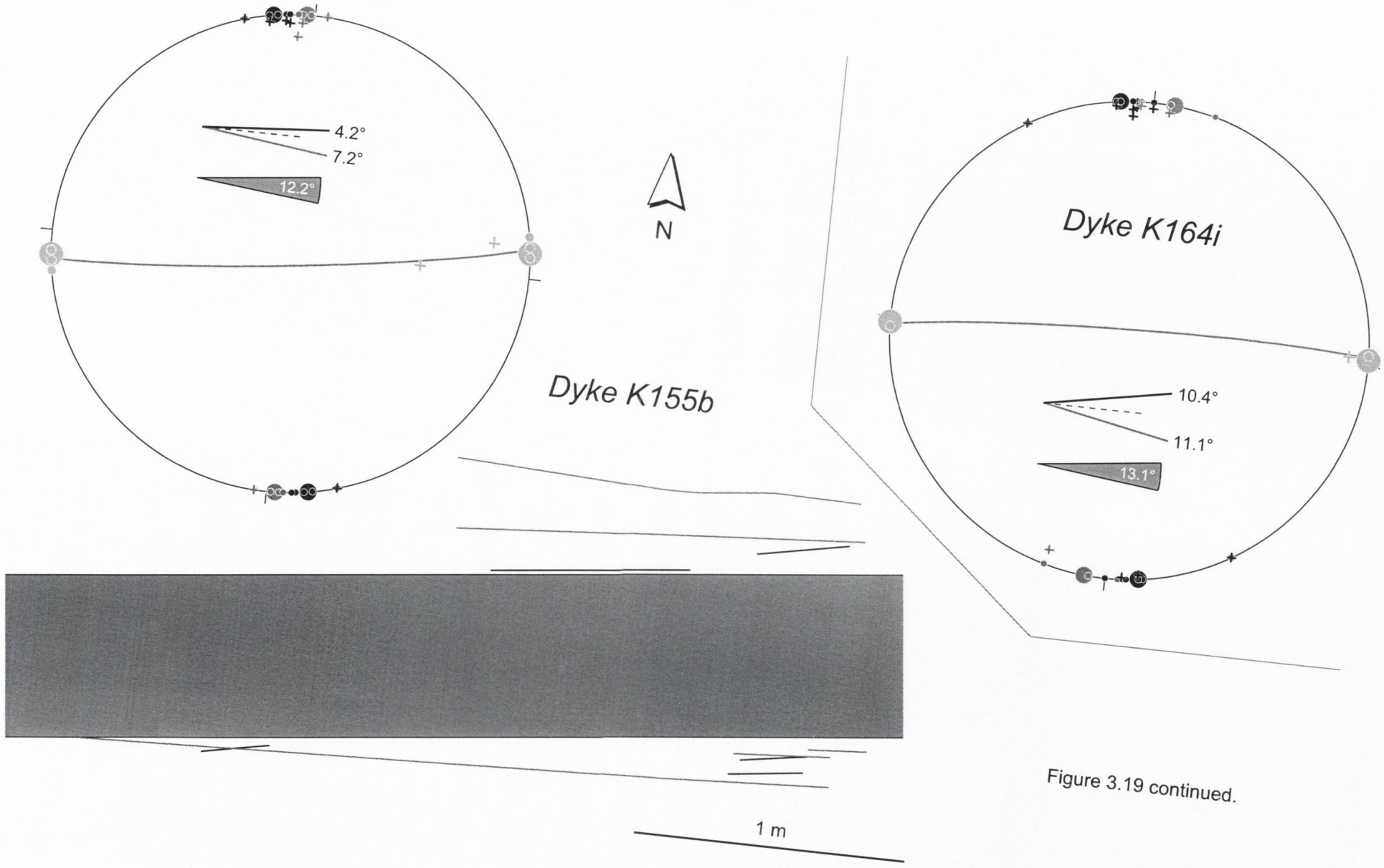

Figure 3.19 continued.

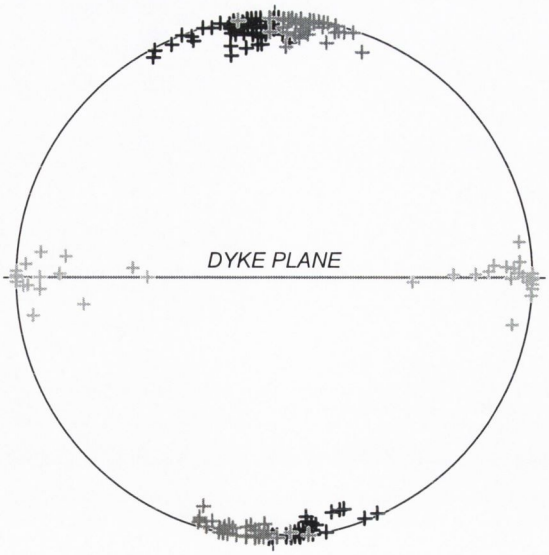

Figure 3.20. Stereographic projection showing all shear data (apart from those marked *) from the dykes in Figure 3.19. The data for each dyke has been rotated to align with respect to an E-W vertical dyke plane. The symbols are as described in Figure 3.19.

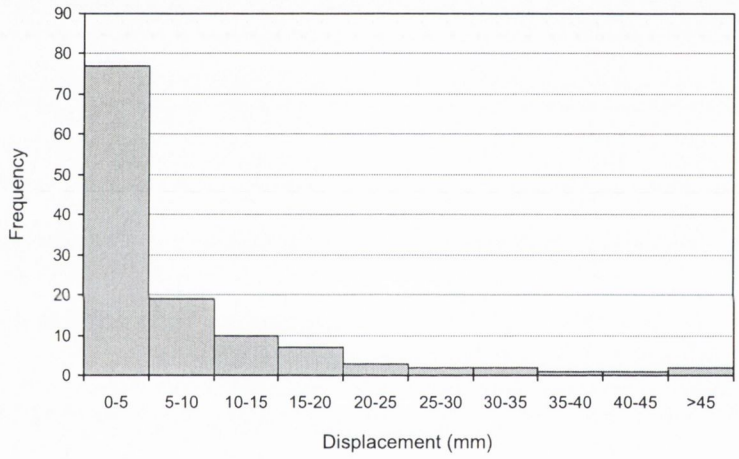

Figure 3.21. Frequency distribution of displacements along host rock shear fractures in the margins of the dykes shown in Figure 3.19 (except those shears marked *). Note, displacements were not recorded for all shears.

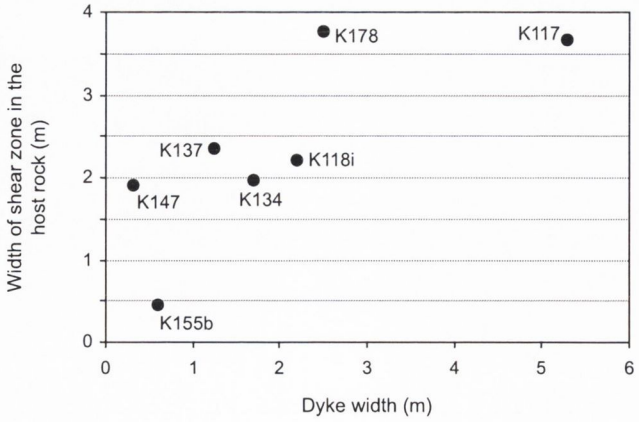

Figure 3.22. A plot of the width of zones where shear occurs in the host rock against dyke width. Values for the extent away of the shear structures away from the dykes were obtained from Figure 3.19.

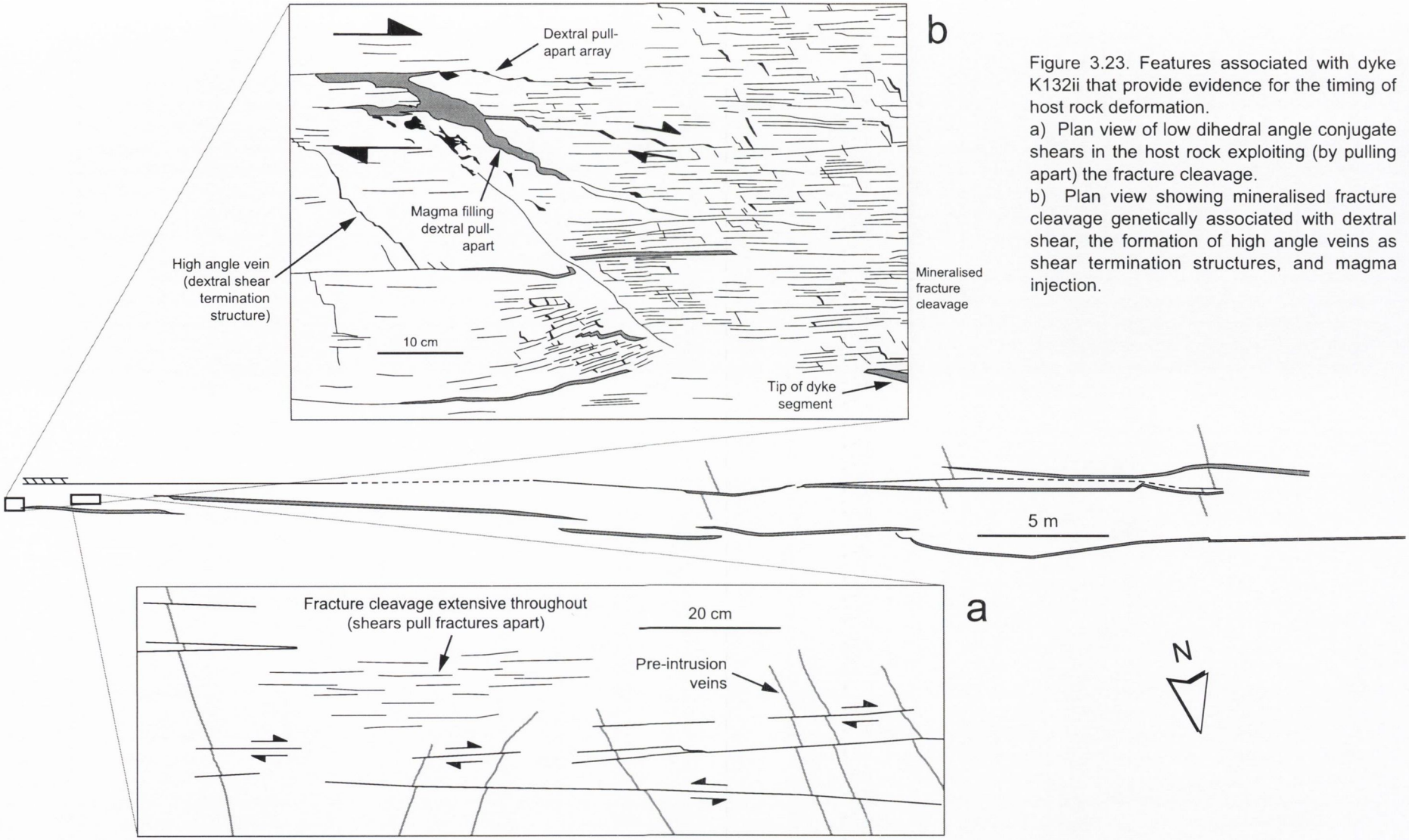

Figure 3.23. Features associated with dyke K132ii that provide evidence for the timing of host rock deformation.
a) Plan view of low dihedral angle conjugate shears in the host rock exploiting (by pulling apart) the fracture cleavage.
b) Plan view showing mineralised fracture cleavage genetically associated with dextral shear, the formation of high angle veins as shear termination structures, and magma injection.

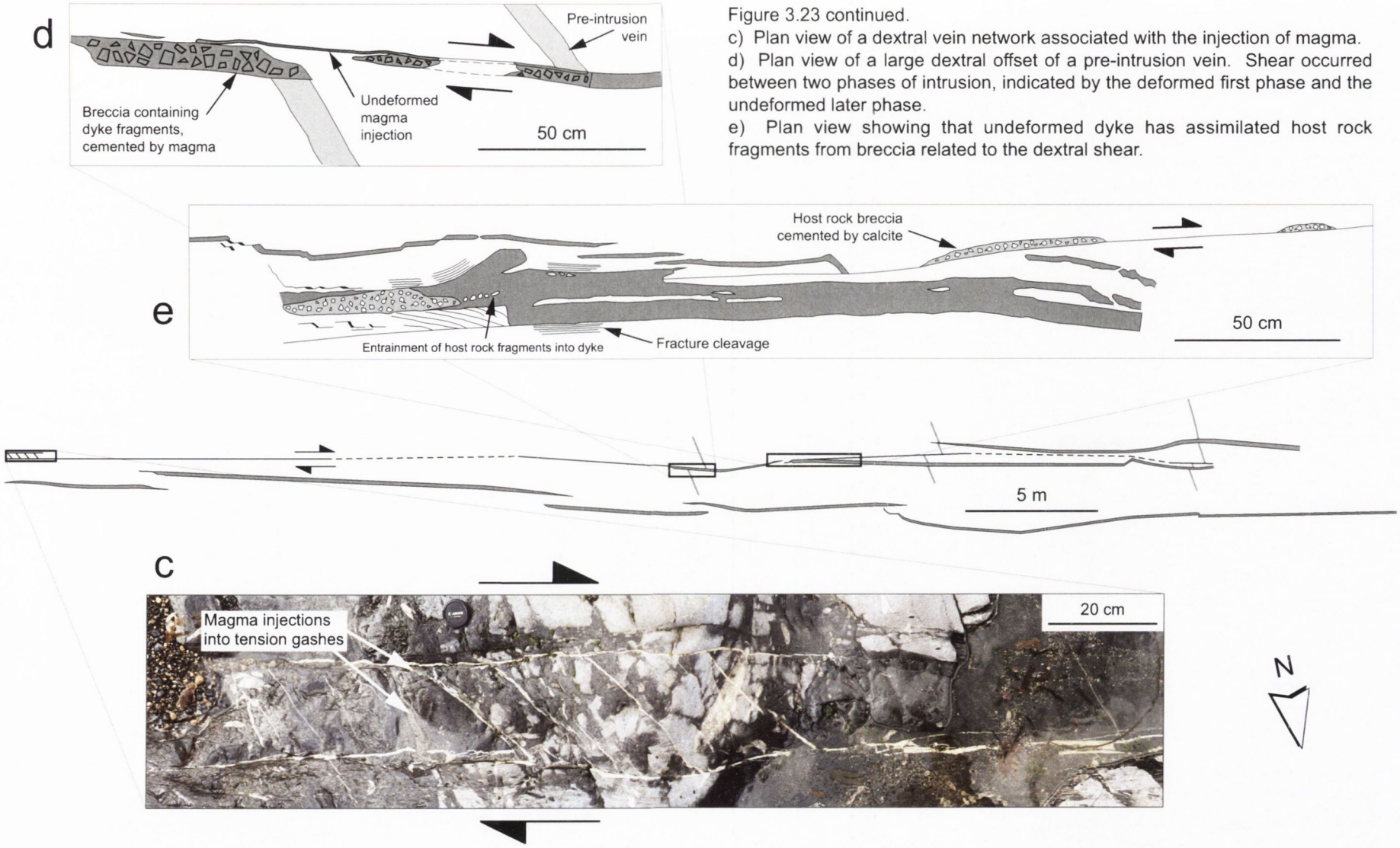

Figure 3.23 continued.
c) Plan view of a dextral vein network associated with the injection of magma.
d) Plan view of a large dextral offset of a pre-intrusion vein. Shear occurred between two phases of intrusion, indicated by the deformed first phase and the undeformed later phase.
e) Plan view showing that undeformed dyke has assimilated host rock fragments from breccia related to the dextral shear.

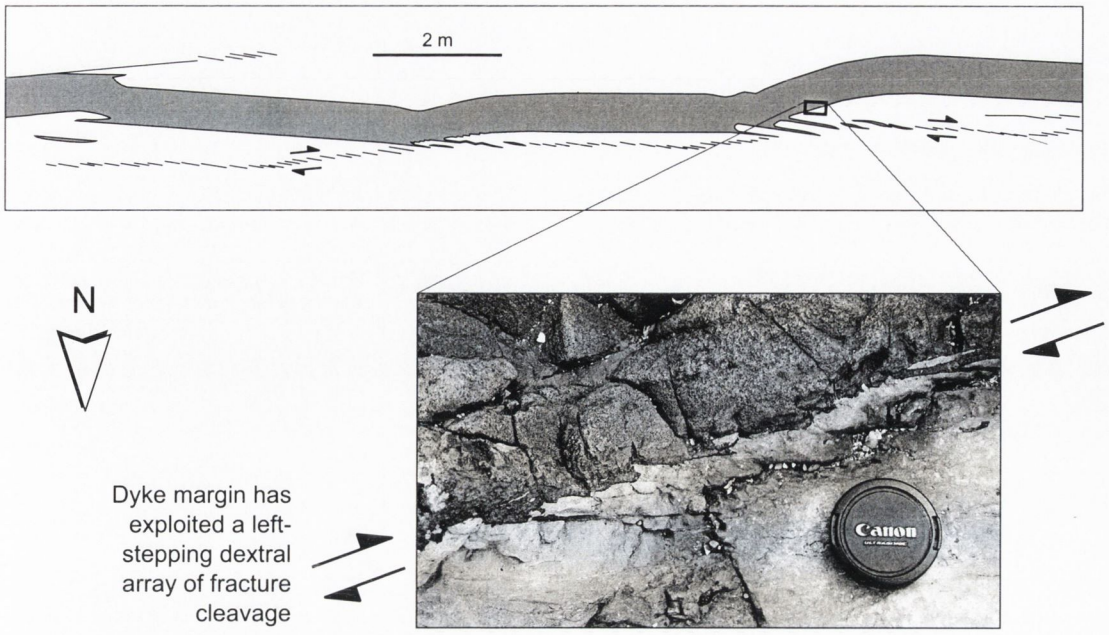

Figure 3.24. Features associated with dyke K157b that provide evidence for the timing of host rock deformation. An extensive dextral fracture cleavage pull-apart array comprises dyke segments in two places. At these points the dyke margin is seen to have exploited similar fracture cleavage arrays.

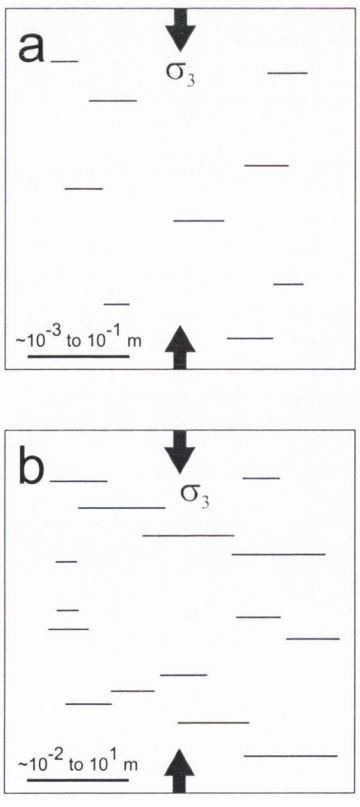

Figure 3.25. Growth sequence for the development of an en échelon array of extensional fractures that then fails in shear (from Olson & Pollard (1991)).
a) Micro-cracks align prependicular to the least compressive principal stress.
b) Fractures propagate laterally and interact if closely enough spaced. This favours the development of en échelon arrays.
c) Subsequent stressing with a compression in the plane of the fractures causes the arrays to fail in shear, as they present structural barriers to the principal stress.

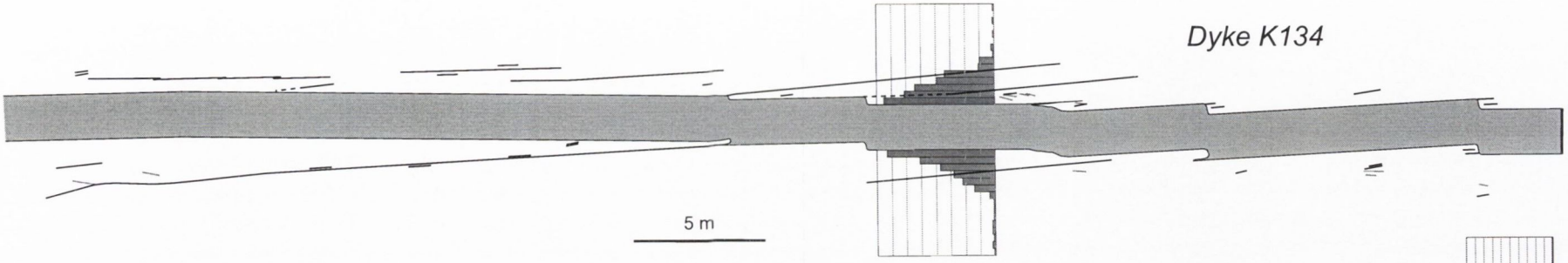

Figure 3.26. Plan views showing dyke-associated fracture frequency profiles compared with the extent of shear deformation associated with dyke emplacement. The dykes have been rotated to fit on the page, so the north direction is only approximate.
Dykes K16 and K32 are multiple intrusions.
The thick black lines show where the dykes are lost beneath the overburden (or, in the case of dyke K24, into the cliff section). Otherwise, the dykes strike out to sea.

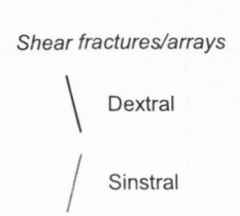



Intrusion phases
Phase 1: dyke-parallel joints closely spaced at the margin, becoming more widely spaced into the dyke; extensive mineralisation along these joints near the margin.
Phase 2: large blocks separated by cooling joints; according to Mohr (1987), has a chilled margin against the first phase.

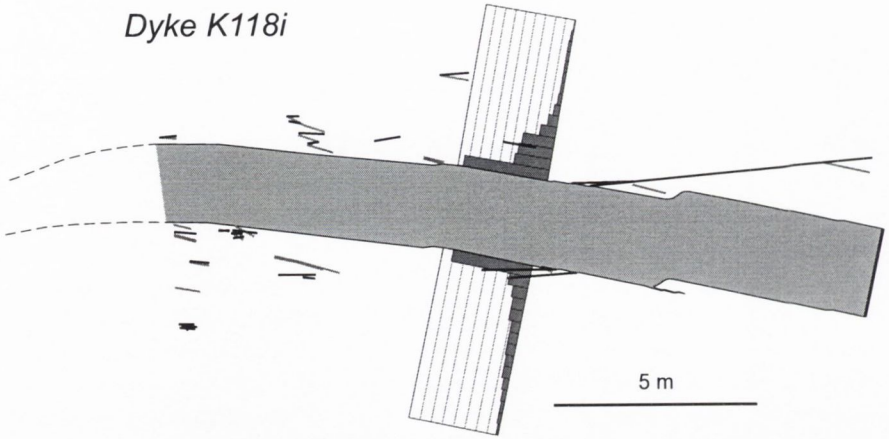

Figure 3.26 continued.

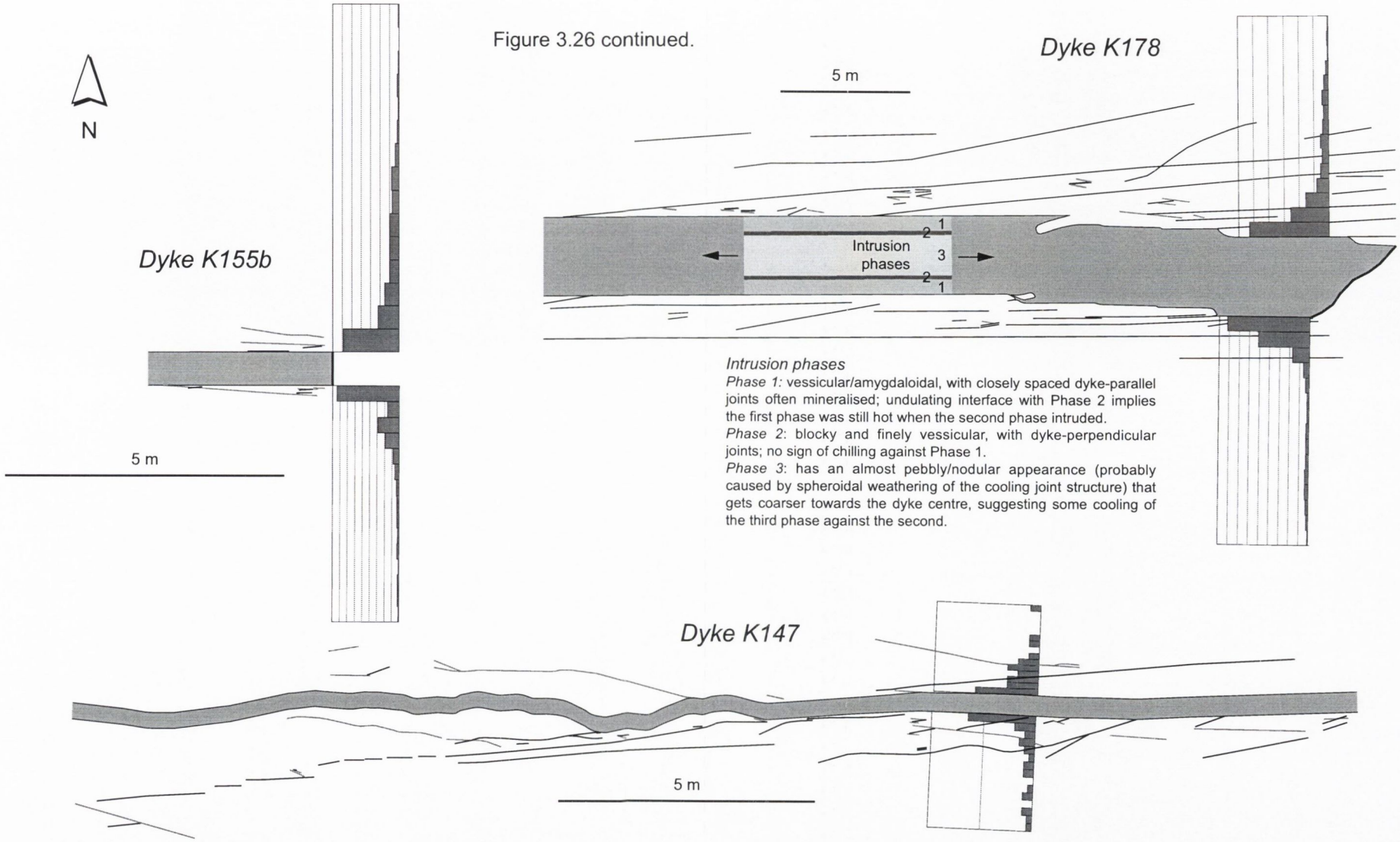

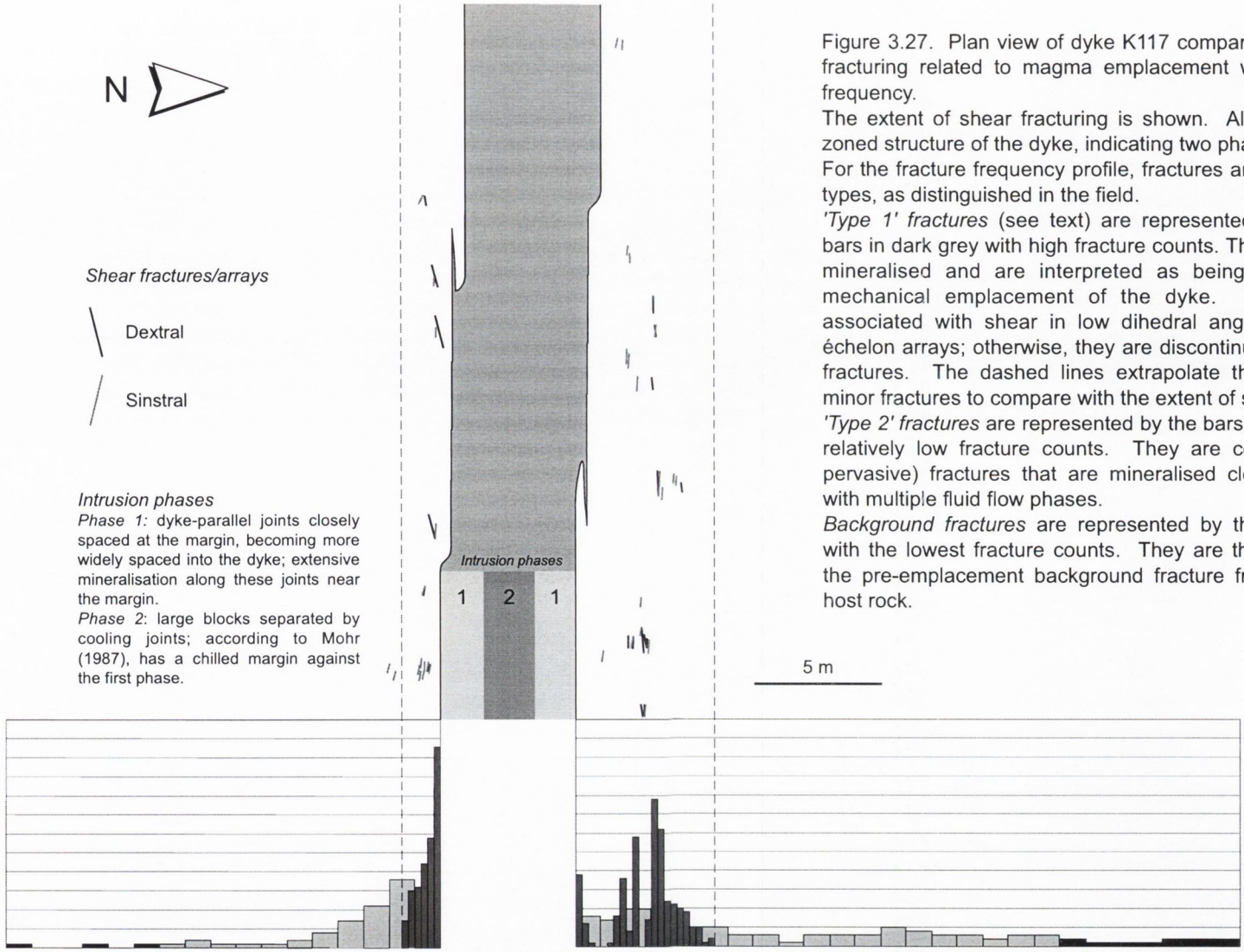

Figure 3.27. Plan view of dyke K117 comparing the extent of fracturing related to magma emplacement with the fracture frequency.

The extent of shear fracturing is shown. Also shown is the zoned structure of the dyke, indicating two phases of intrusion. For the fracture frequency profile, fractures are split into three types, as distinguished in the field.

'Type 1' fractures (see text) are represented by the narrow bars in dark grey with high fracture counts. They are generally mineralised and are interpreted as being related to the mechanical emplacement of the dyke. They are often associated with shear in low dihedral angle conjugate en échelon arrays; otherwise, they are discontinuous extensional fractures. The dashed lines extrapolate the extent of the minor fractures to compare with the extent of shear fracturing.

'Type 2' fractures are represented by the bars in light grey with relatively low fracture counts. They are continuous (more pervasive) fractures that are mineralised close to the dyke with multiple fluid flow phases.

Background fractures are represented by the bars in black with the lowest fracture counts. They are the interpreted as the pre-emplacement background fracture frequency for the host rock.

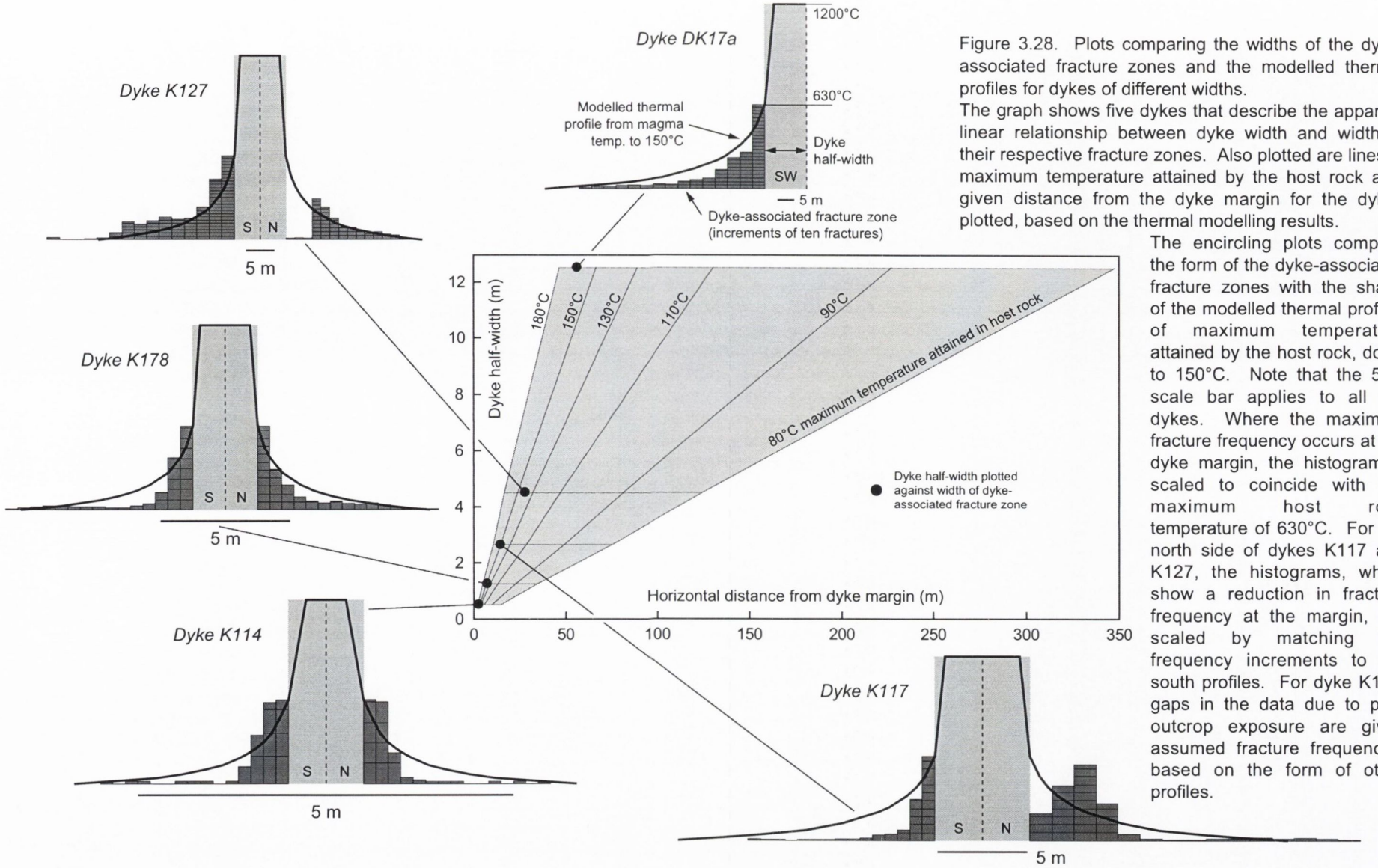

Figure 3.28. Plots comparing the widths of the dyke-associated fracture zones and the modelled thermal profiles for dykes of different widths.

The graph shows five dykes that describe the apparent linear relationship between dyke width and width of their respective fracture zones. Also plotted are lines of maximum temperature attained by the host rock at a given distance from the dyke margin for the dykes plotted, based on the thermal modelling results.

The encircling plots compare the form of the dyke-associated fracture zones with the shape of the modelled thermal profiles of maximum temperature attained by the host rock, down to 150°C. Note that the 5 m scale bar applies to all the dykes. Where the maximum fracture frequency occurs at the dyke margin, the histogram is scaled to coincide with the maximum host rock temperature of 630°C. For the north side of dykes K117 and K127, the histograms, which show a reduction in fracture frequency at the margin, are scaled by matching the frequency increments to the south profiles. For dyke K127, gaps in the data due to poor outcrop exposure are given assumed fracture frequencies based on the form of other profiles.

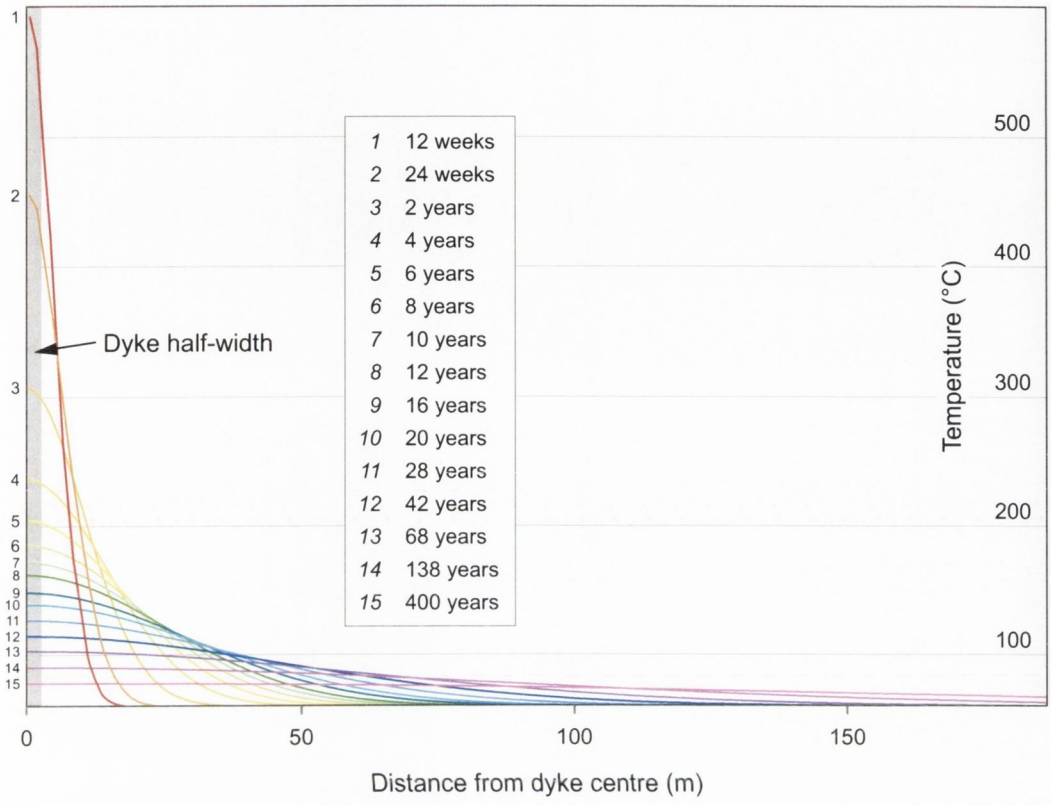

Figure 3.29. Modelled thermal profiles for the cooling of dyke K117, 12 weeks after emplacement.

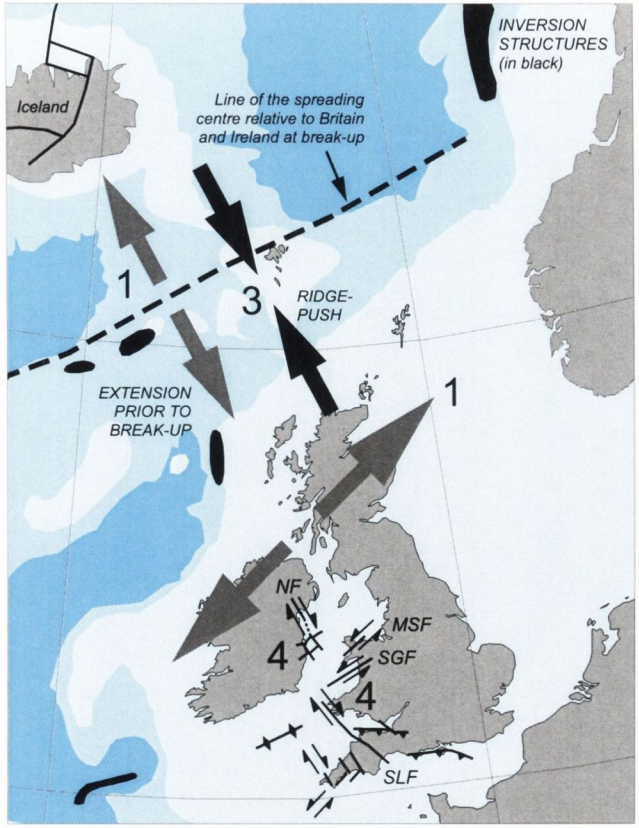

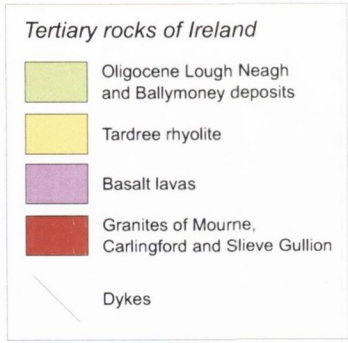

Figure 4.1. A compilation of published stress systems for Ireland and surrounding area during the Tertiary (see text for explanation of the references). Numbers refer to the ages of the stress regimes.

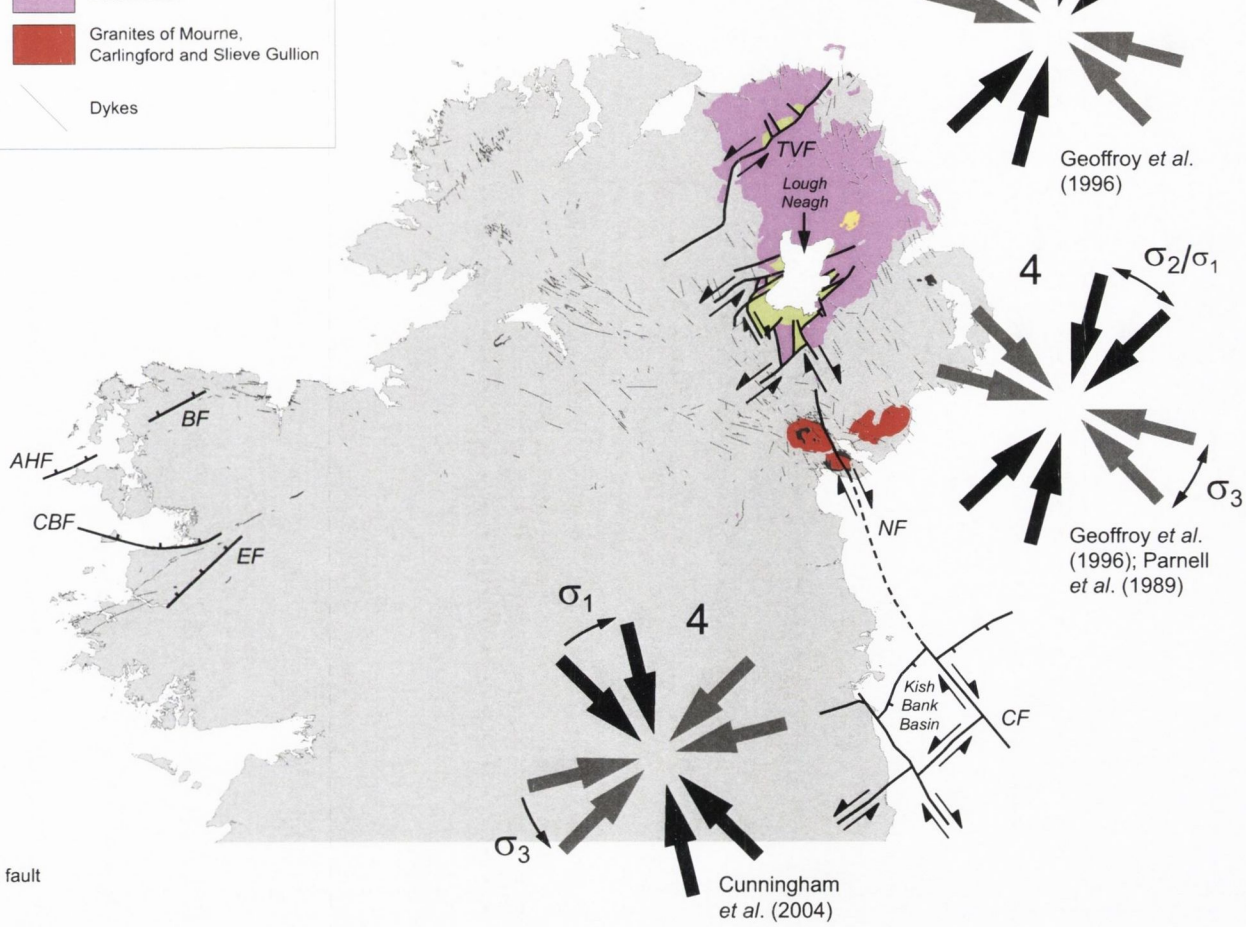

1 Palaeocene

2 Late Palaeocene to late Eocene

3 Post break-up (Eocene onwards) causing inversion structures

4 Oligocene: strike-slip regime (Cunningham *et al.* (2004); Parnell *et al.* (1989)); extensional regime (Geoffroy *et al.* (1996))

AHF Achill Head fault
BF Bangor fault
CF Codling fault
CBF Clew Bay fault
EF Errif fault
MSF Menai Straits fault
NF Newry fault
SGF St. George's fault
SLF Sticklepath-Lustleigh fault
TVF Tow Valley fault

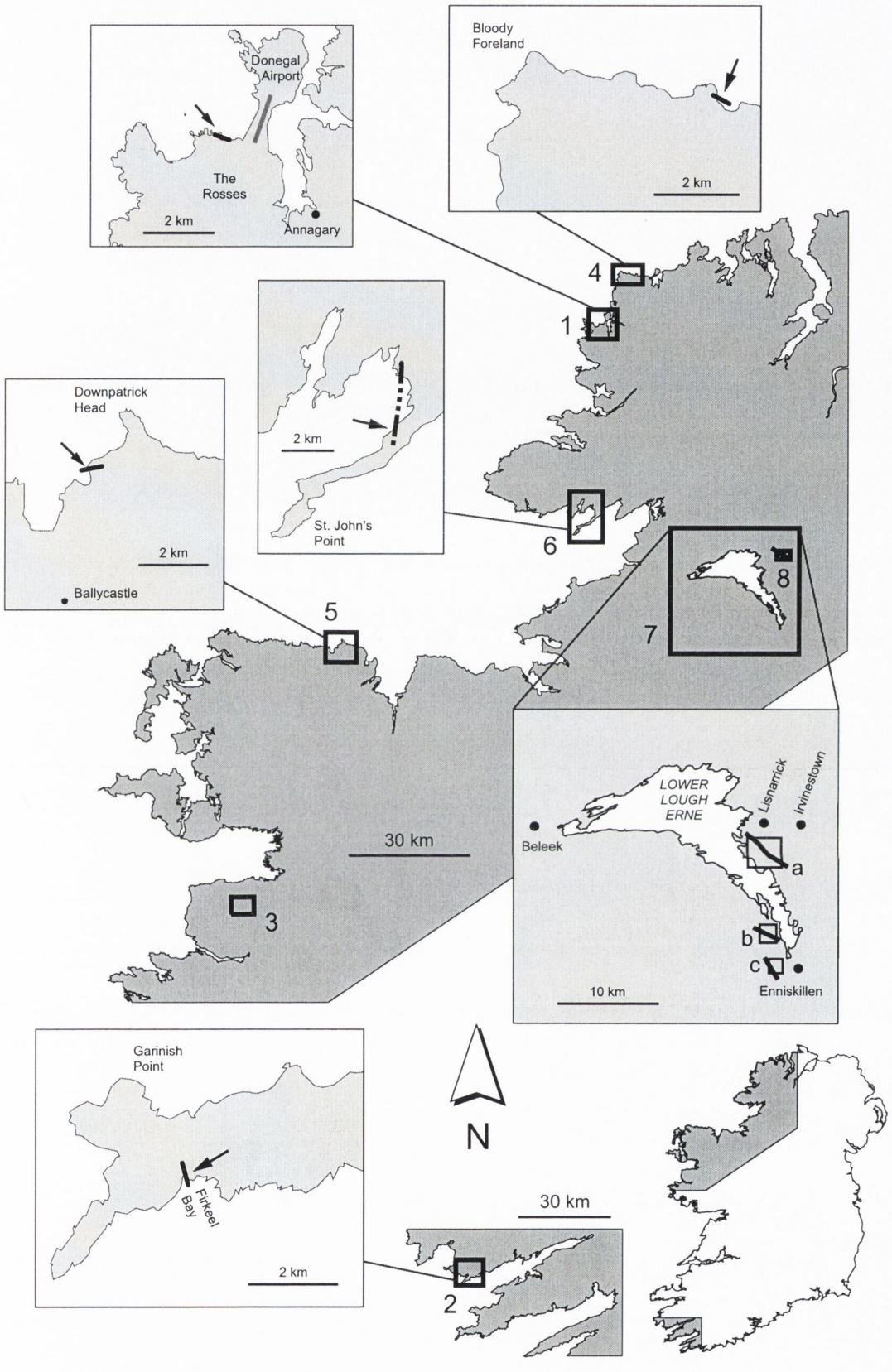

Figure 4.2. Locations described in Chapter 4, listed below (ordered as they appear in the text). Dykes are shown in black lines.

1 - The Rosses, Co. Donegal. 2 - Firkeel Bay, Co. Cork. 3 - Corvock granite, Co. Mayo. 4 - Bloody Foreland east , Co. Donegal. 5 - Downpatrick Head west, Co. Mayo. 6 - St. John's Point peninsula, Co. Donegal. 7 - Localities around Lower Lough Erne, Co. Fermanagh: (a) Drogan and Doonan quarries; (b) A46 road-cutting; (c) Drumskew quarry. 8 - Carn quarry, Co.Fermanagh.

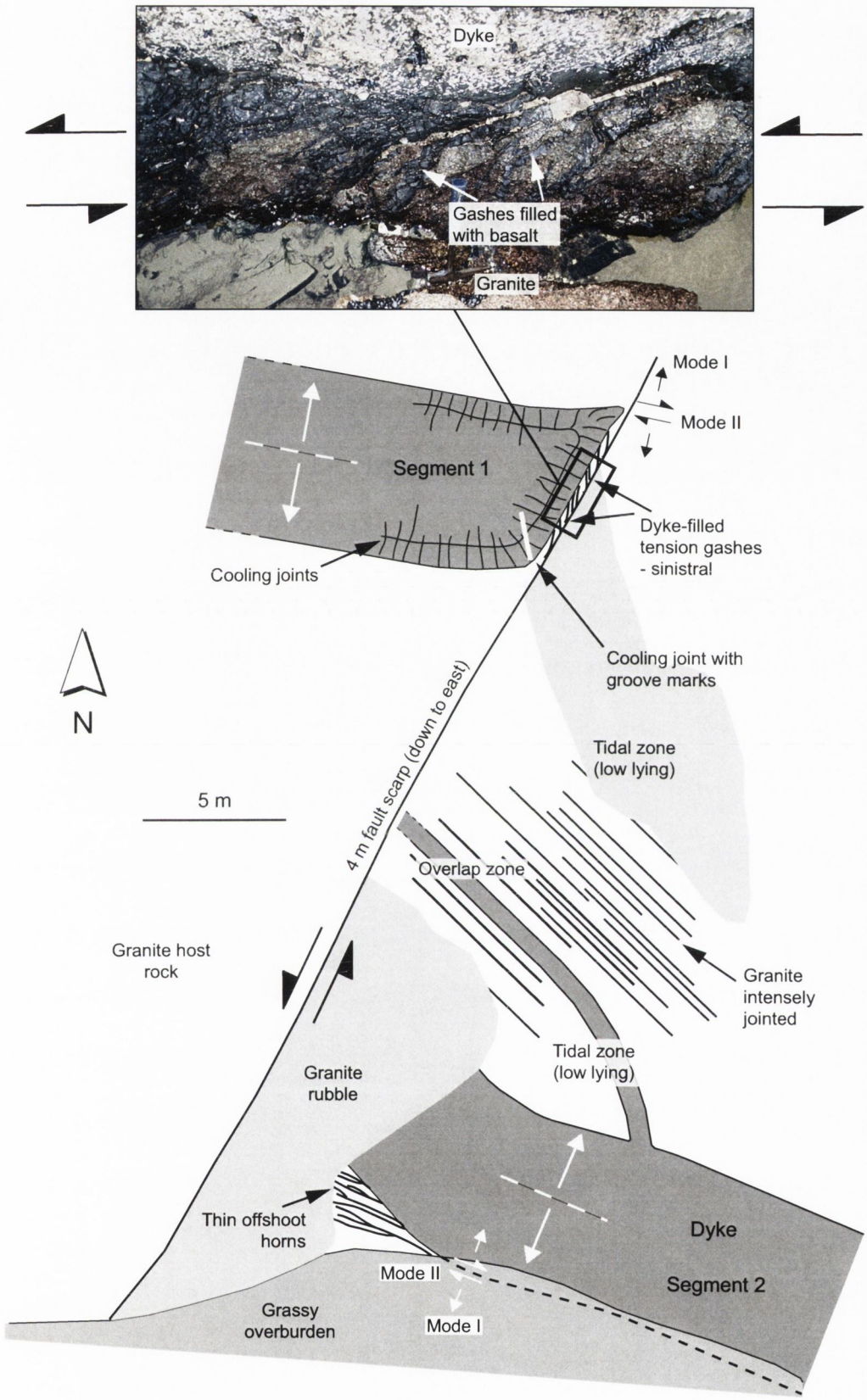

Figure 4.3. Plan view showing a right-stepping transform jog of a Tertiary dyke (dyke DK33) across a fault, on the north coast of The Rosses, Co. Donegal.
The transform shear sense is shown by large arrows on the fault. White arrows show the dilation vector of the dyke segments. Stress intensity components, modes I and II, are also shown.

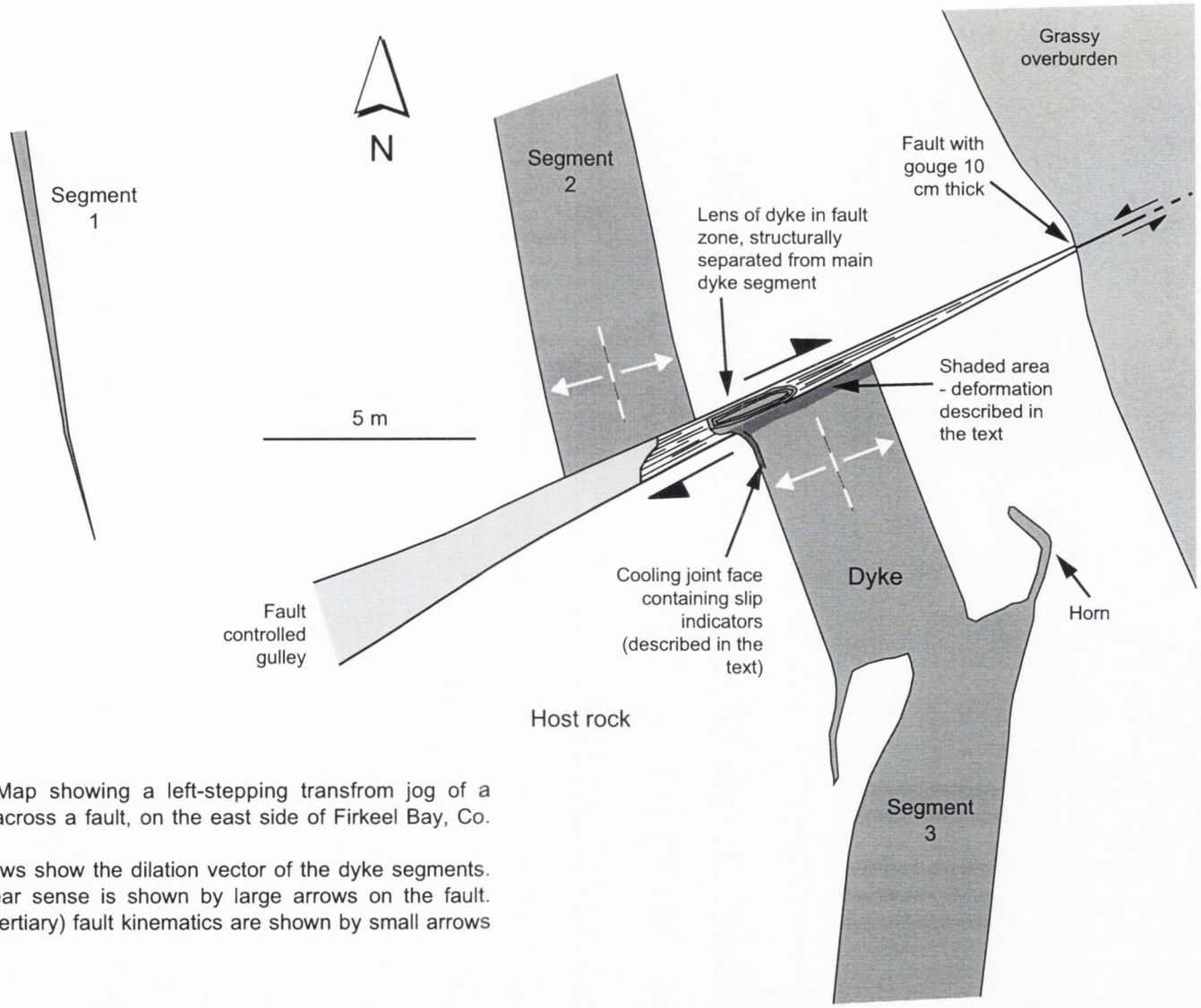

Figure 4.4. Map showing a left-stepping transfrom jog of a Tertiary dyke across a fault, on the east side of Firkeel Bay, Co. Cork.
The white arrows show the dilation vector of the dyke segments. Transform shear sense is shown by large arrows on the fault. Original (pre-Tertiary) fault kinematics are shown by small arrows on the fault.

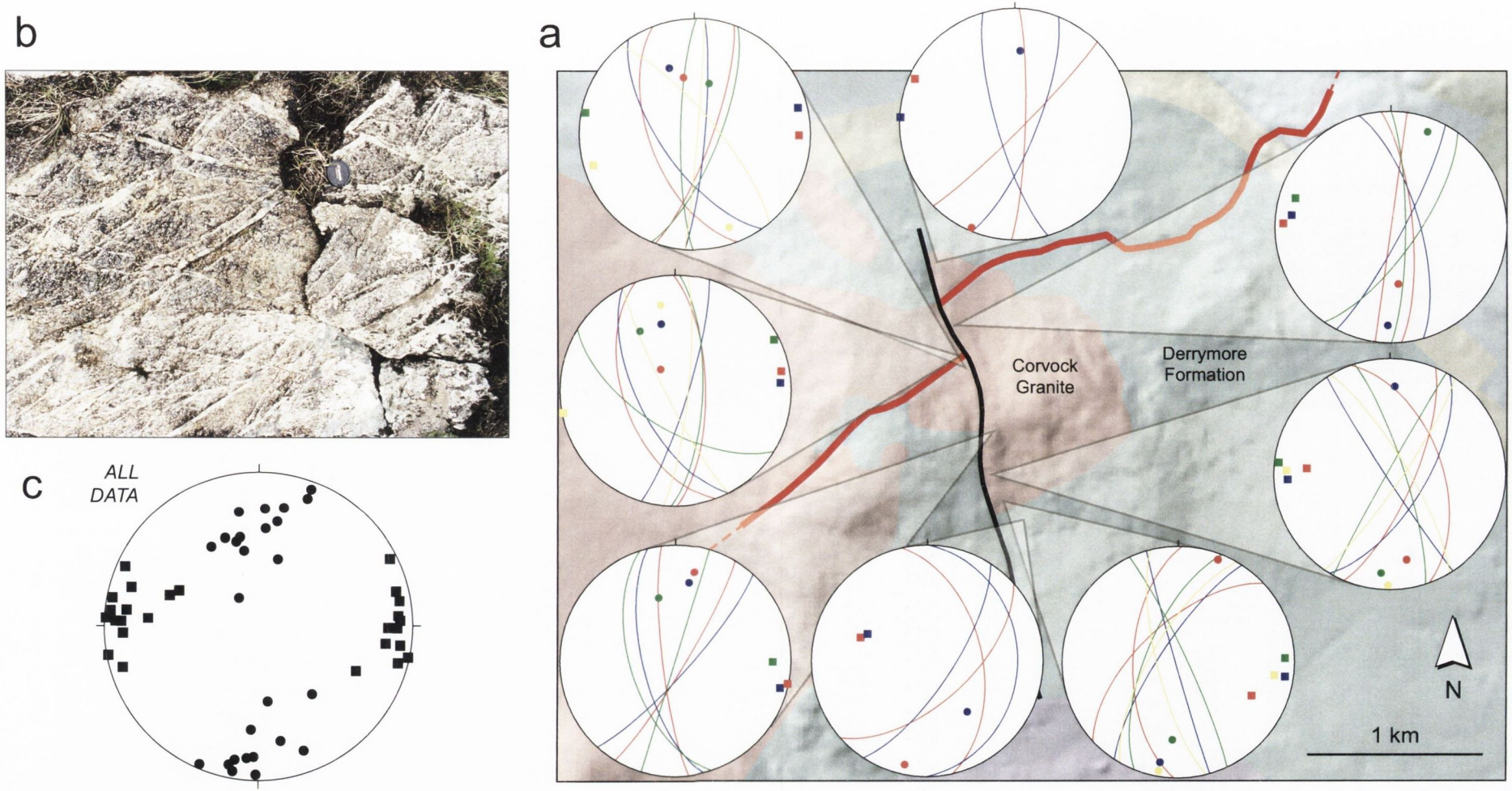

Figure 4.5. Left-stepping offset of the main system CI dyke (dyke WC35) intruding the Corvock granite, Co. Mayo.
a) Map view showing the dyke (in red) offset across the fault (in black). Host rock geology is shown draped over topography with illumination from the northwest. Stereographic projections show data from different sites adjacent to the fault. For each stereonet, each colour indicates a conjugate pair of quartz veins and associated stress axes, σ_1 as circles, and σ_3 as squares.
b) Photograph showing typical conjugate quartz veins in the granite (lens cap for scale).
c) Compilation stereonet for all stress axis data.

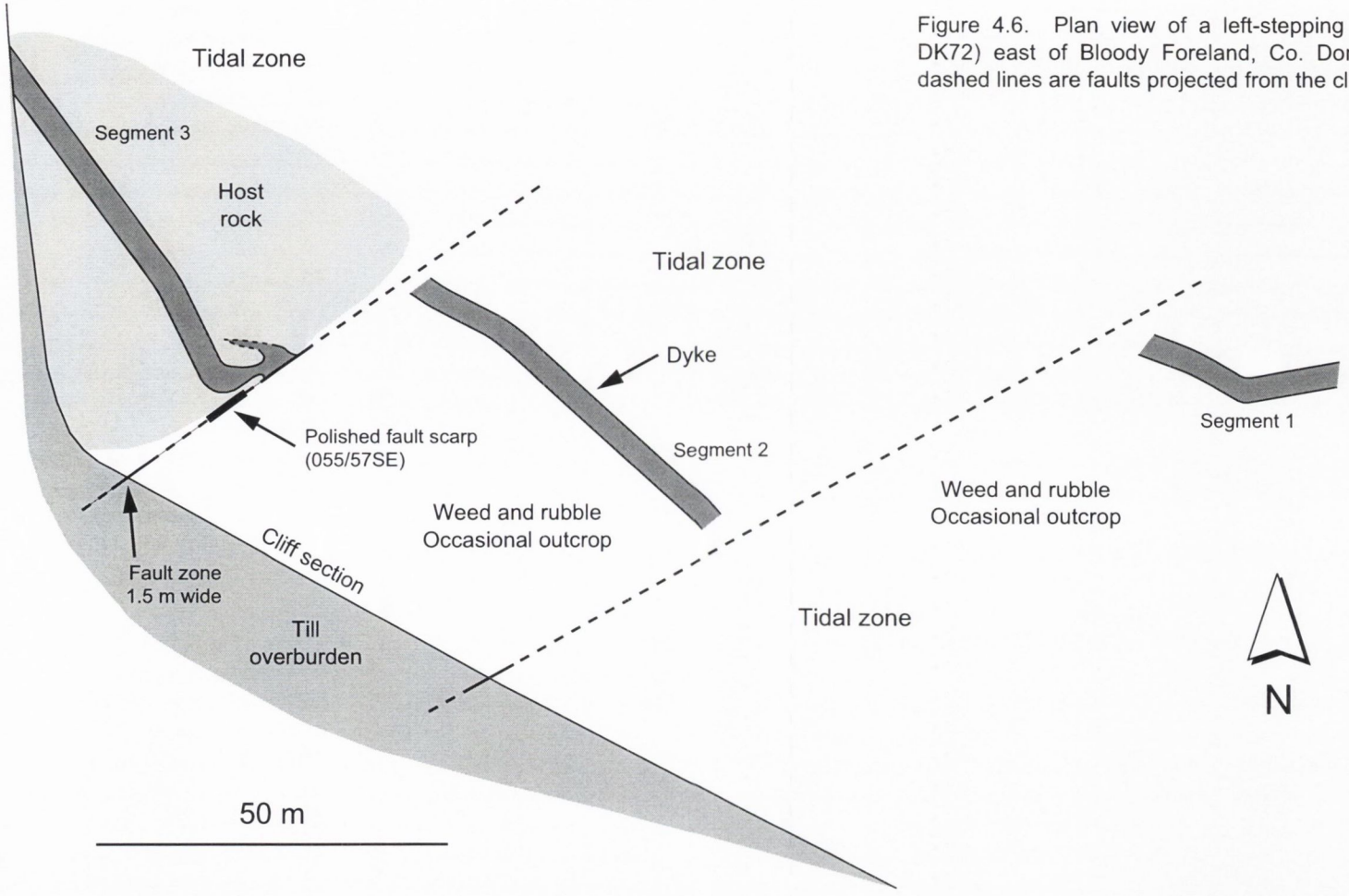

Figure 4.6. Plan view of a left-stepping dyke (dyke DK72) east of Bloody Foreland, Co. Donegal. The dashed lines are faults projected from the cliff section.

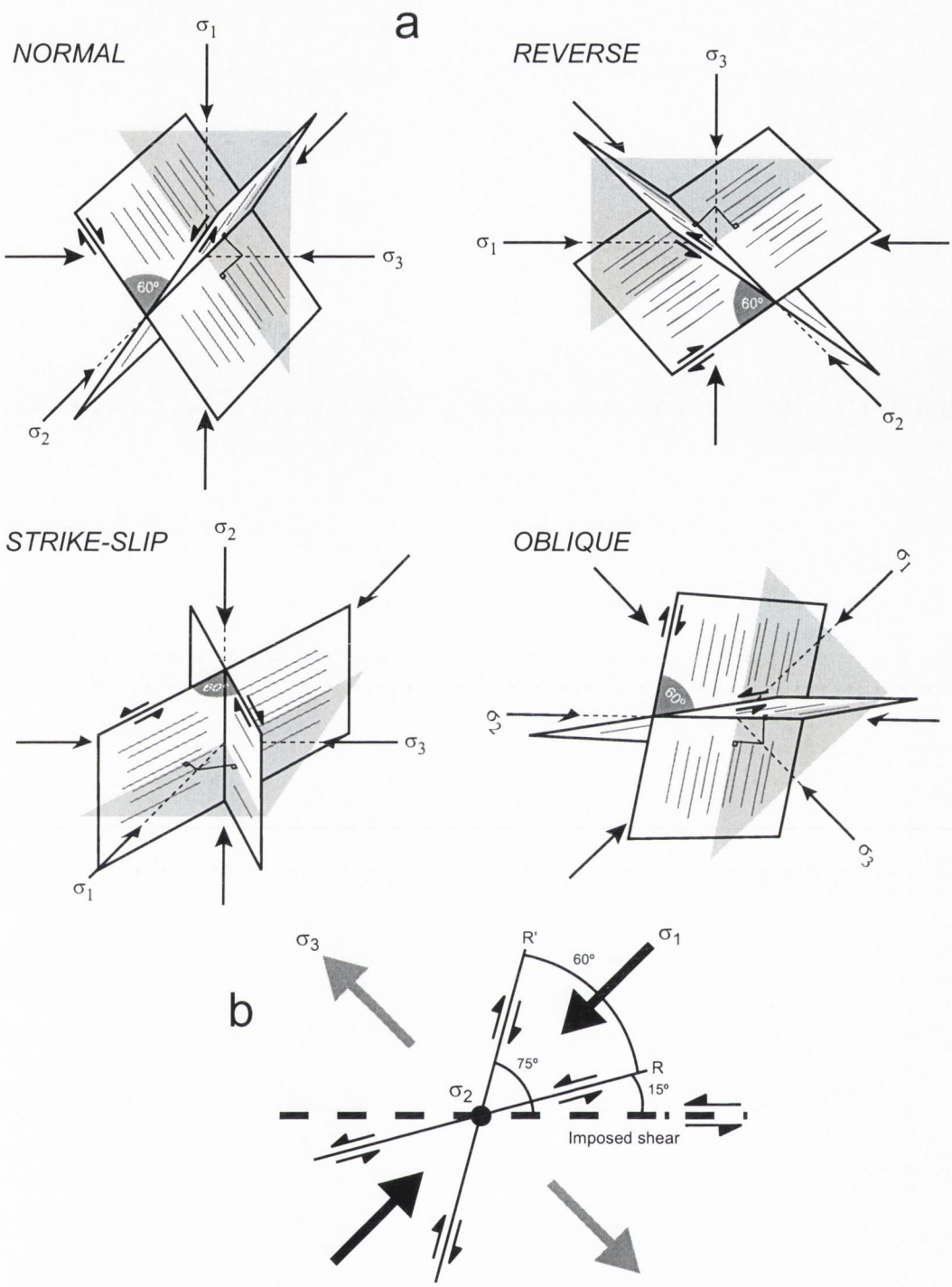

Figure 4.7. Models used for simple palaeostress reconstruction.

a) *Andersonian* faulting producing conjugate fault pairs. The air/ground interface is treated as a plane of zero shear stress. Since the principal stress directions are also of zero shear stress, the surface of the earth must contain two of the three stress directions. The third principal stress direction, therefore, is vertical. This, combined with the Coulomb law of failure, allows only strike-slip and dip-slip (thrust and normal) faults to form at or near the surface of the earth.

The grey lines on the fault planes are the slip vectors (e.g. represented by slickensides).

The maximum principal stress (σ_1) and minimum principal stress (σ_3) bisect the acute (dihedral) and obtuse angles respectively between the faults in a conjugate pair. The intermediate principal stress (σ_2) lies within the fault planes of a conjugate pair, being the of intersection of the two planes. The dihedral angle is indicated in grey.

The slip vector, σ_1, σ_3, and poles to the fault planes all lie in the same plane (plane indicated in semi-transparent grey).

b) The angular relationship of Riedel and anti-Riedel shears with the plane of maximum shear and the principal stress axes.

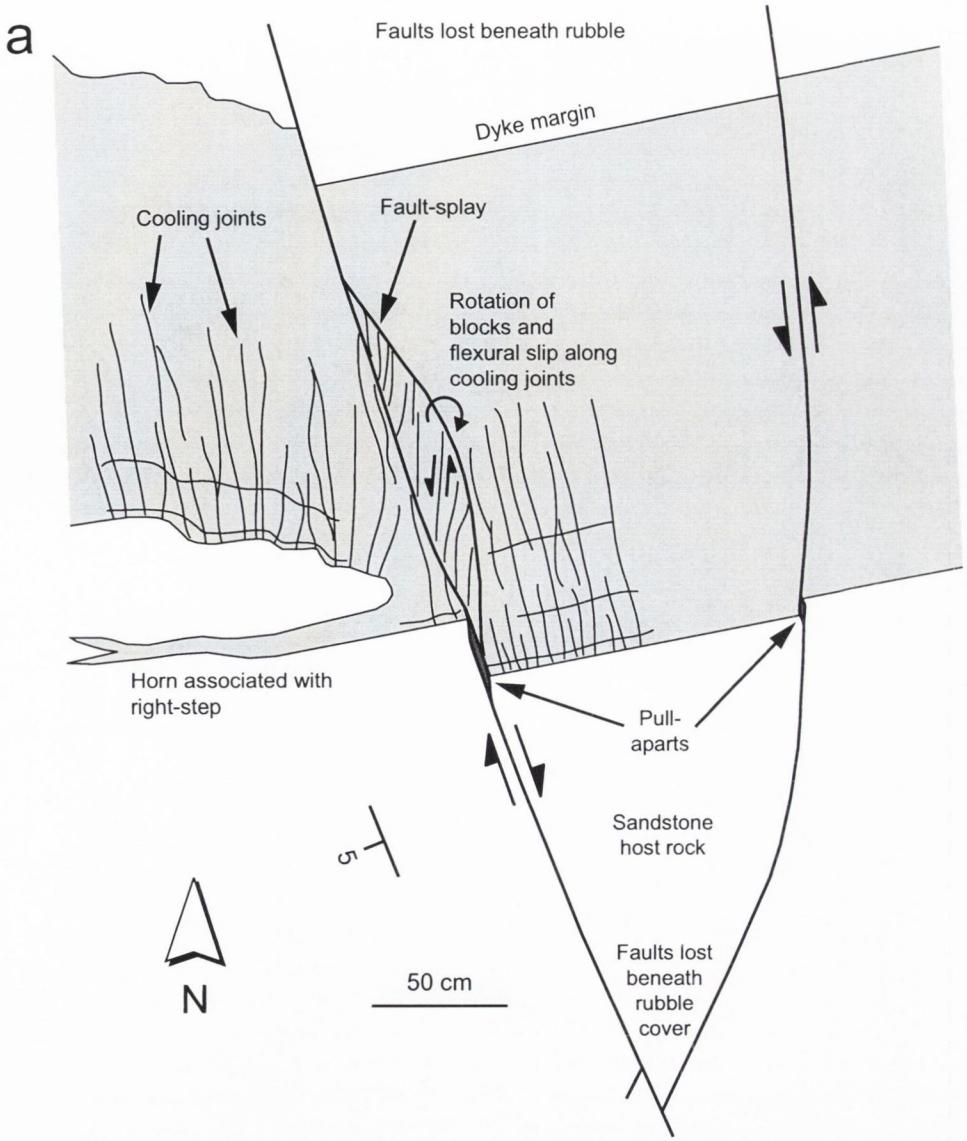

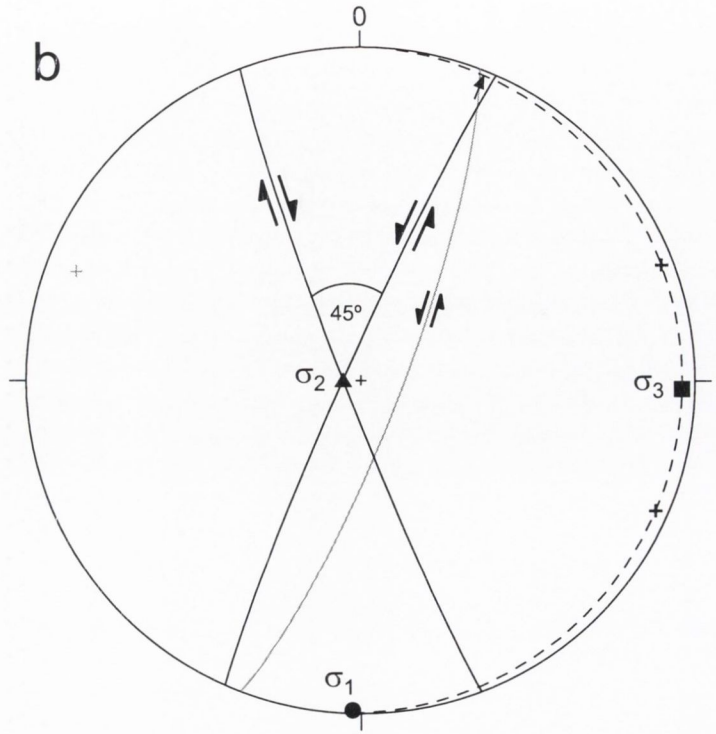

Figure 4.8. A faulted Tertiary dyke (dyke K85), west of Downpatrick Head.

a) Plan view showing conjugate shear faults cutting the dyke. The dyke right-steps at west edge of sketch.

b) Stereographic projection showing conjugate shears (black great circles) cutting the dyke. The principal stress directions are plotted. A rotated cooling joint (in grey) is also plotted, with the slip vector indicated by an arrow (pointing in the direction of hanging wall movement).

The dashed great circle (containing σ_1 and σ_3, and the poles to the faults) approximately contains the slip vector from the rotated cooling joint.

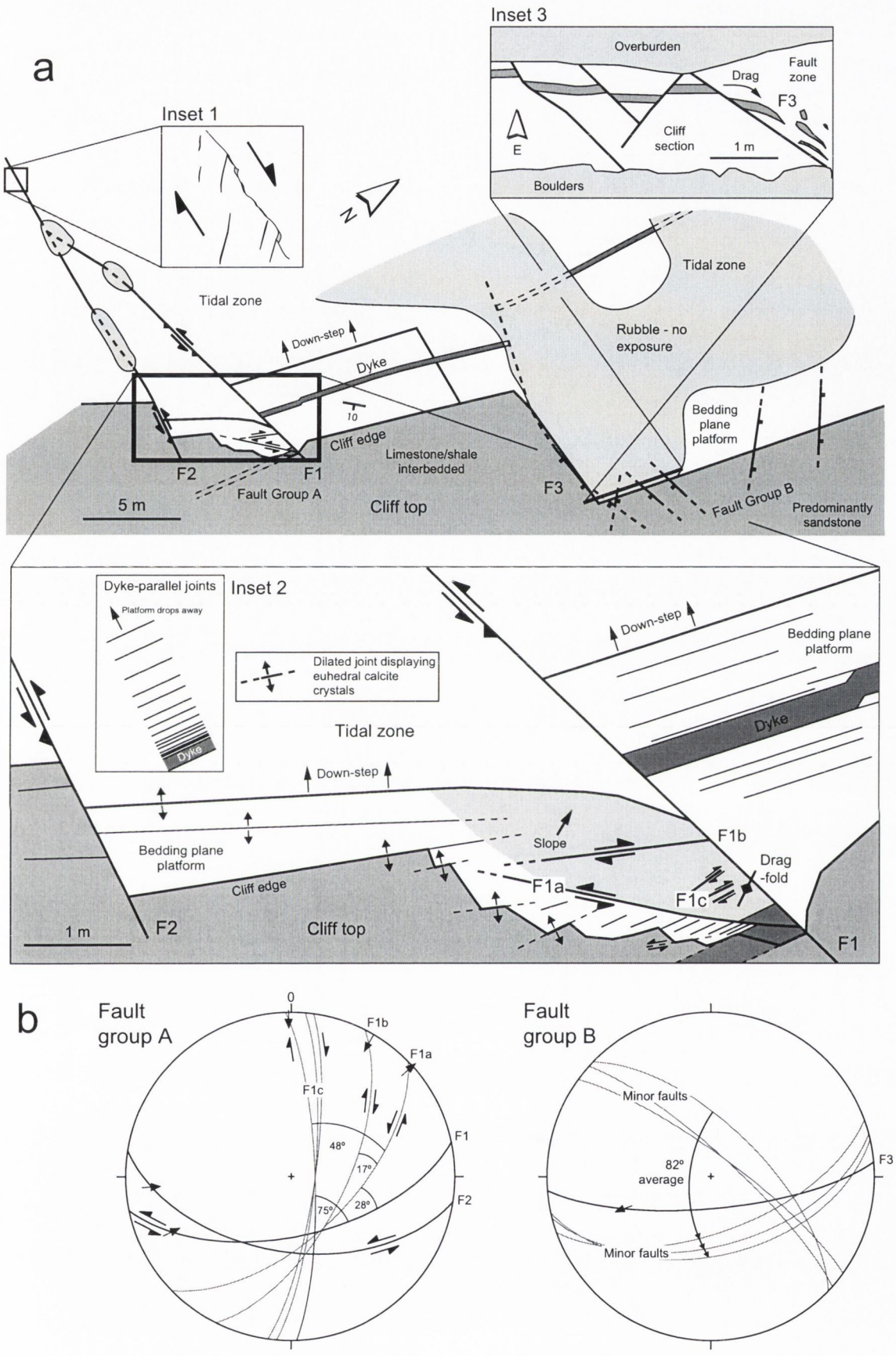

Figure 4.9. A faulted Tertiary dyke (dyke DK18a) cutting St John's Point peninsula, south Co. Donegal.
a) Plan views of the area where the dyke is faulted. For fault group B, the downthrow tick indicates the dip-slip component visible in cliff-section (inset 3).
b) Stereographic projections showing the structures associated with the two fault groups, A and B. Slip vectors are indicated by arrows that point in the direction of hanging wall movement.

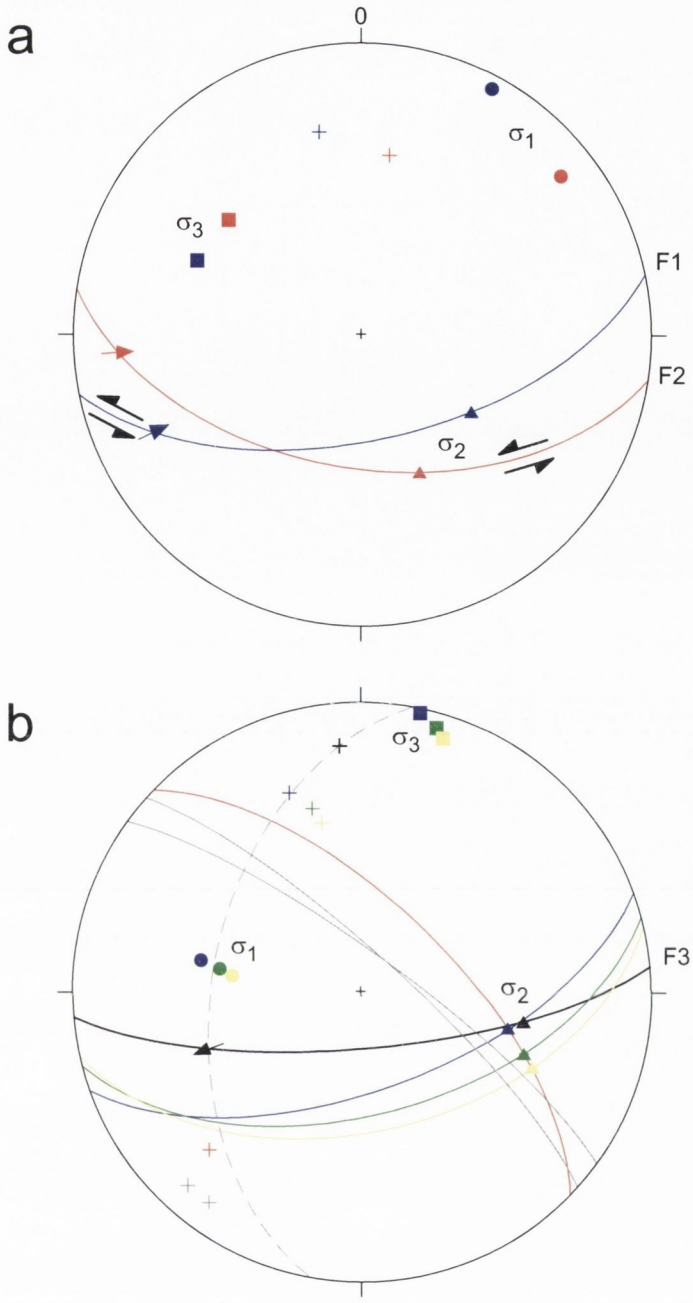

Figure 4.10. Kinematics and derived axes of palaeostress for the faults affecting the St. John's Point peninsula dyke (dyke DK18). All related symbols correspond in colour with their respective faults. Faults are shown as great circles and their poles as crosses. Slickenfibre lineations (slip vectors) are shown as arrows pointing in the direction of hanging wall movement. The strike-slip component of fault displacement is indicated by arrows.

a) Fault group A. Principal stress axis directions were deduced with σ_1 and σ_3 plotted 45° and 135° respectively from the fault plane.

b) Fault group B. The fault shown in red appears antithetic to fault F3 but acts as the main fault with respect to the faults depicted in blue, green and yellow, which show synthetic arrangement with F3. The minor faults further along section to the north (antithetic to F3) are shown in grey. The dashed line is the plane that contains the slip vector and pole to fault F3, and would also contain the principal stress axes for F3 (see text for discussion).

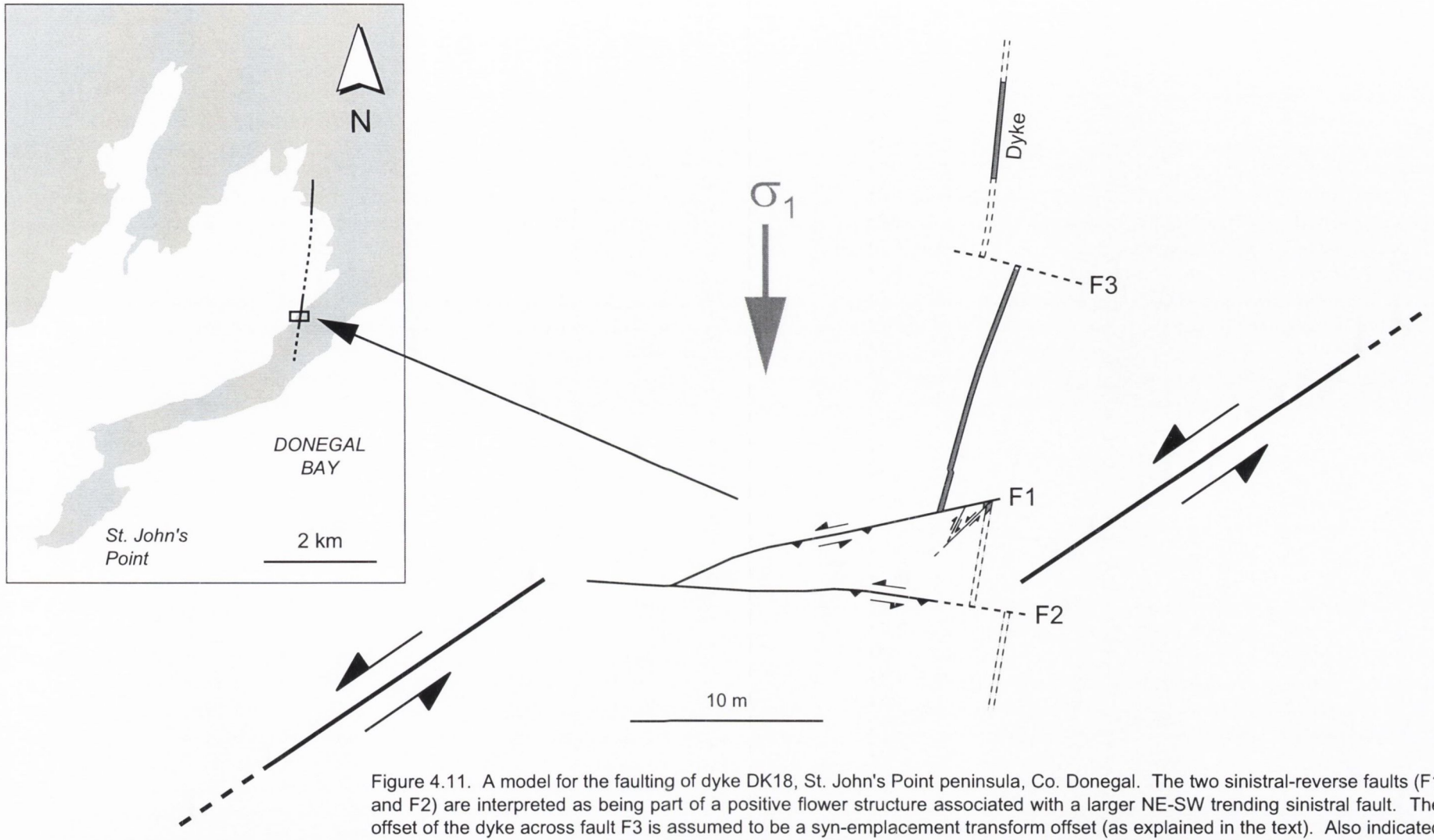

Figure 4.11. A model for the faulting of dyke DK18, St. John's Point peninsula, Co. Donegal. The two sinistral-reverse faults (F1 and F2) are interpreted as being part of a positive flower structure associated with a larger NE-SW trending sinistral fault. The offset of the dyke across fault F3 is assumed to be a syn-emplacement transform offset (as explained in the text). Also indicated is the inferred direction of maximum principal stress, σ_1.

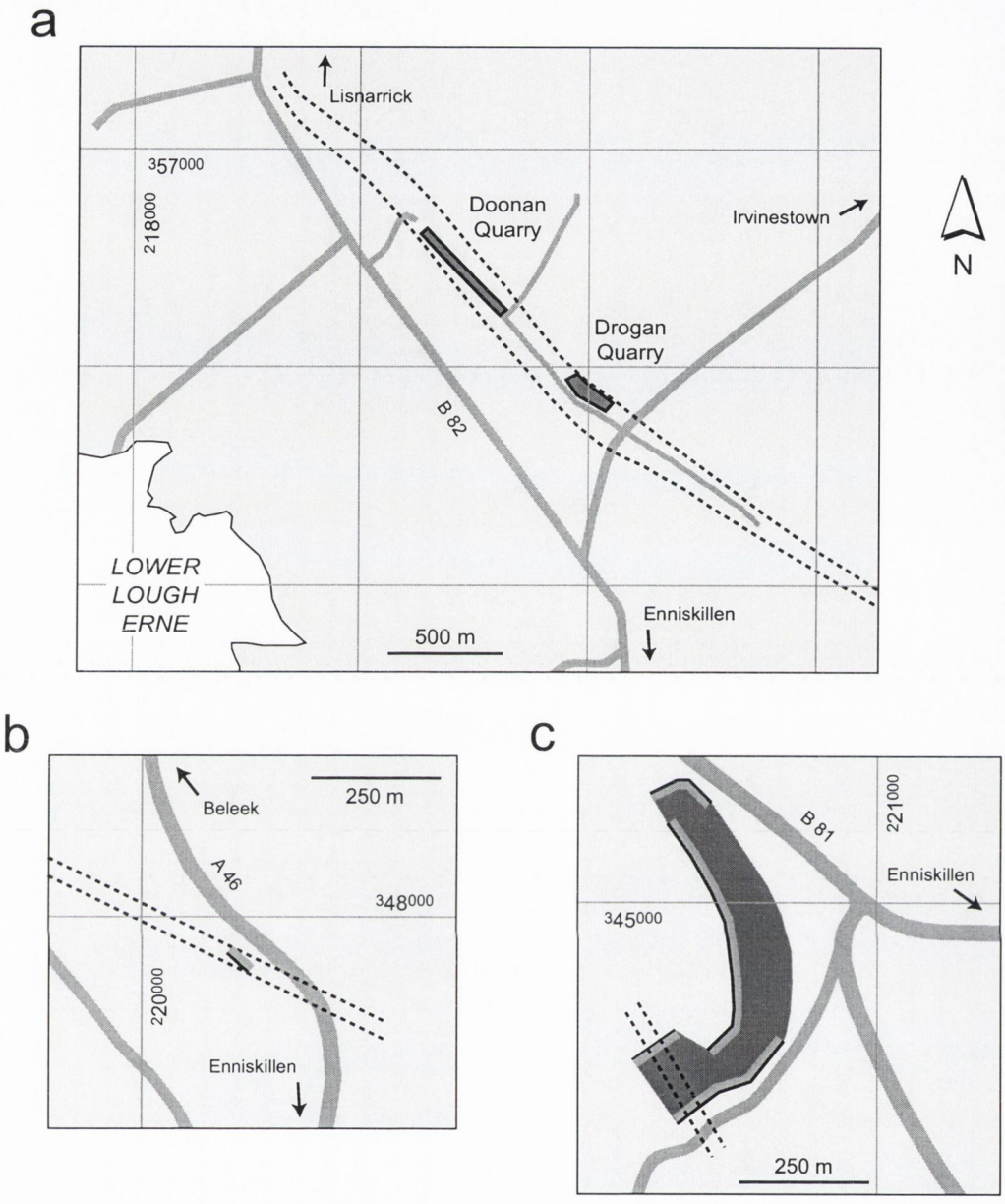

Figure 4.12. Road maps showing dyke localities around Lower Lough Erne, Co. Fermanagh.
a) Drogan and Doonan quarries - Doraville dyke (dyke DK5).
b) A46 Road cut - Cullen Hill dyke (dyke DK2).
c) Drumskew quarry (dyke DK1).

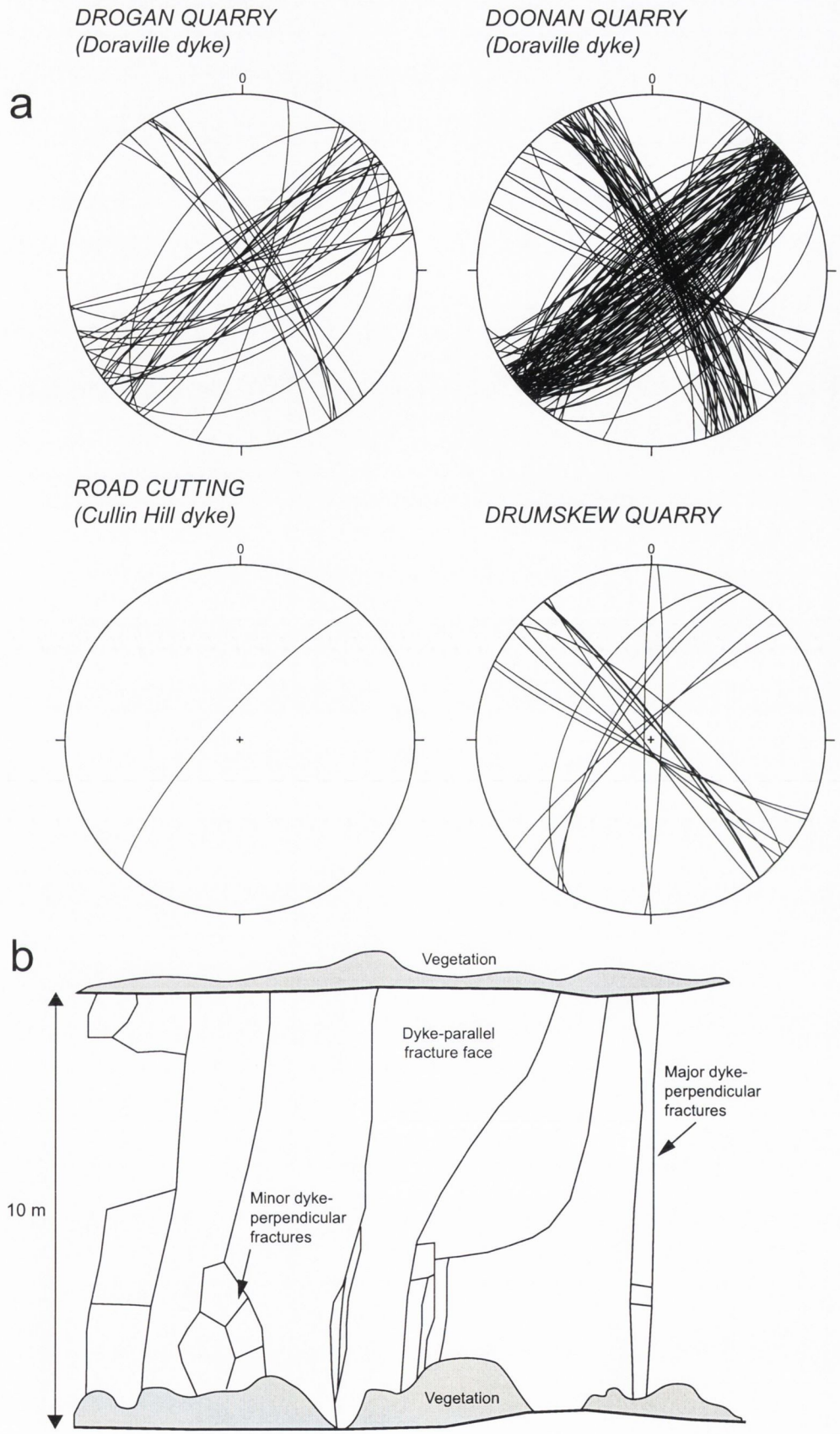

Figure 4.13. a) Stereographic projections showing the orientation of planes that contain slip, recorded from Doonan, Drogan and Drumskew quarries, and the A46 road cutting. For Drumskew quarry, the dyke is marked as a thicker plane.
b) A semi-schematic cross-section from Doonan quarry, facing a dyke-parallel fracture, showing the intersection of dyke-perpendicular fractures and their classification as 'major' and 'minor' structures.

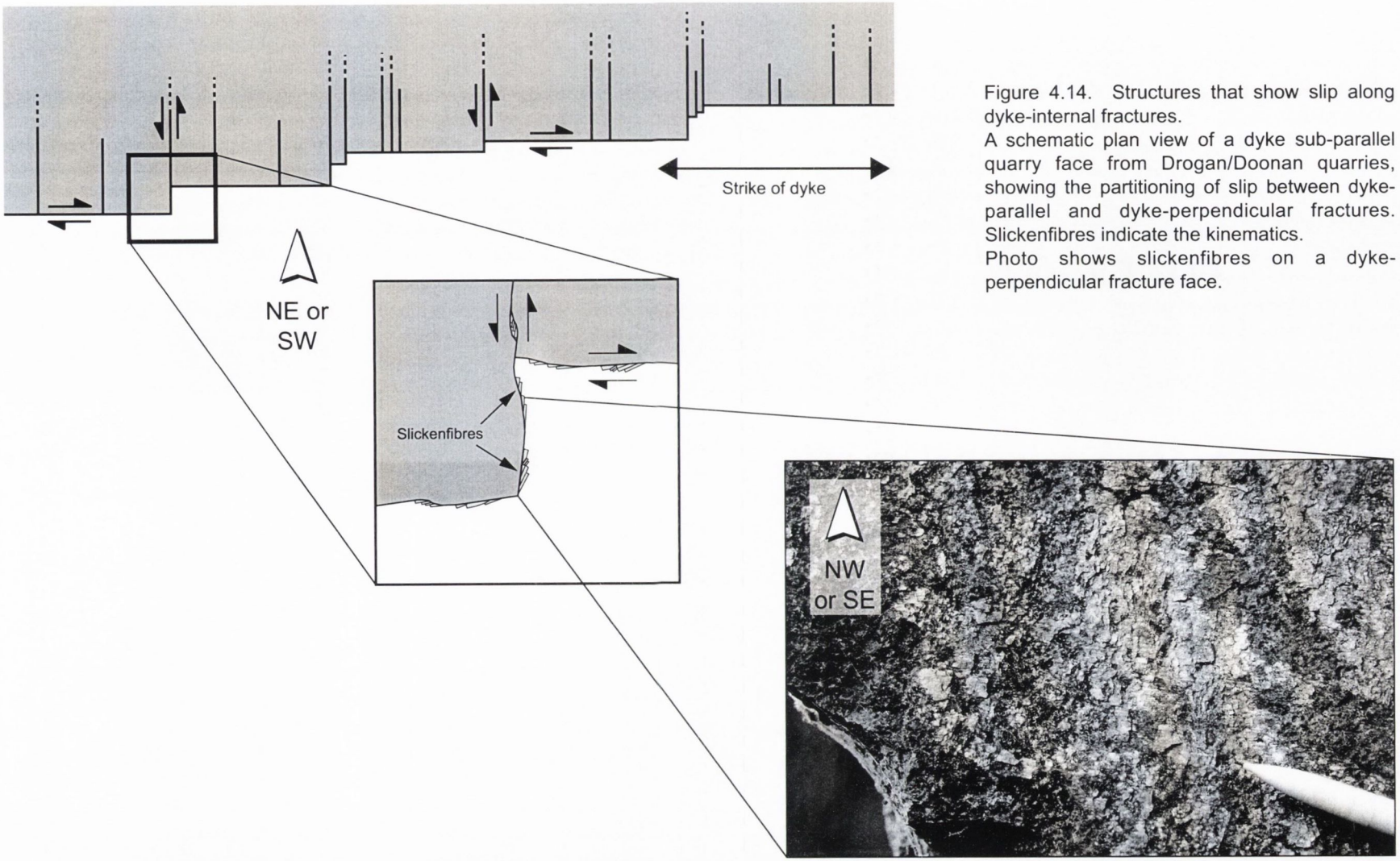

Figure 4.14. Structures that show slip along dyke-internal fractures.
A schematic plan view of a dyke sub-parallel quarry face from Drogan/Doonan quarries, showing the partitioning of slip between dyke-parallel and dyke-perpendicular fractures. Slickenfibres indicate the kinematics.
Photo shows slickenfibres on a dyke-perpendicular fracture face.

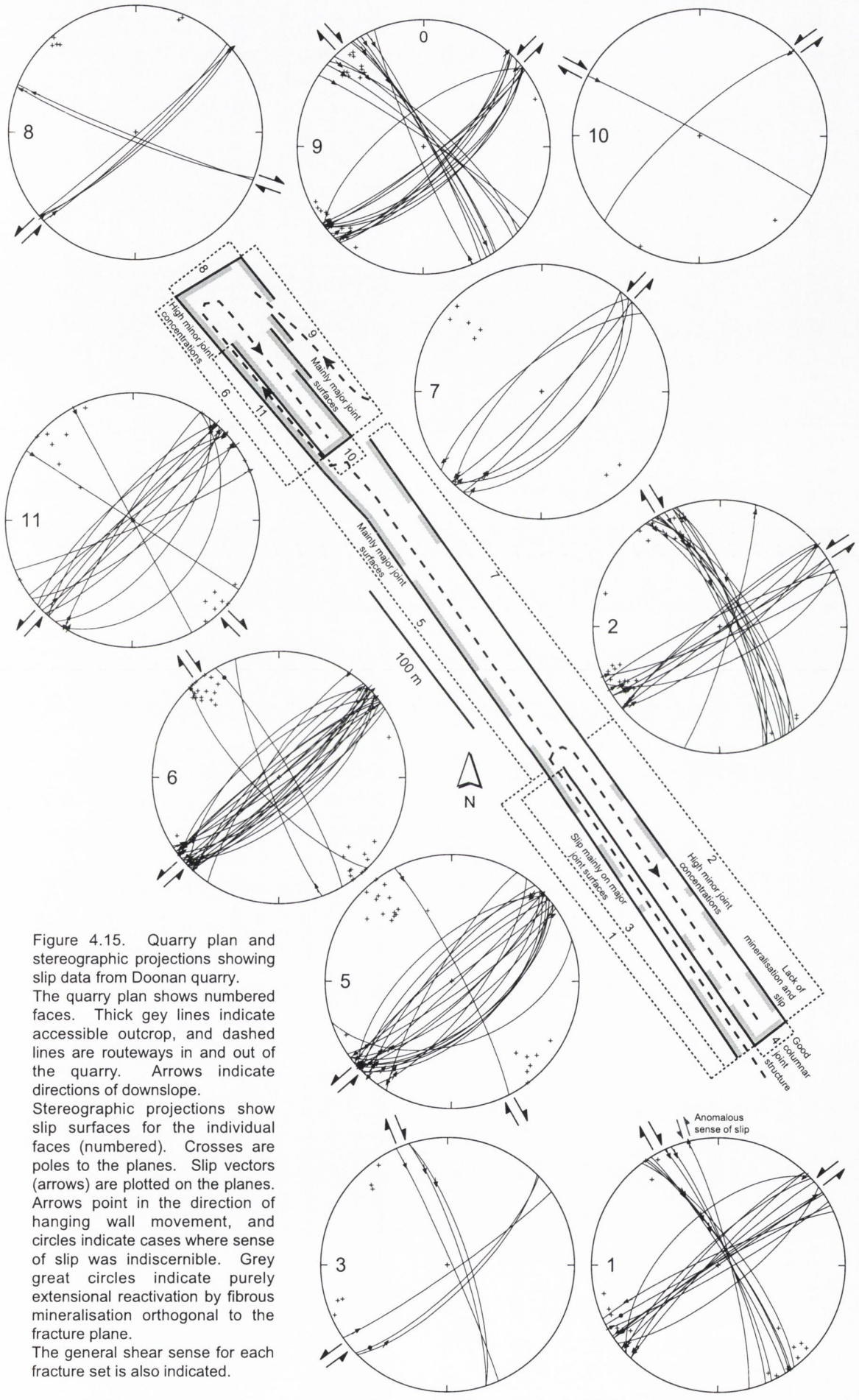

Figure 4.15. Quarry plan and stereographic projections showing slip data from Doonan quarry.

The quarry plan shows numbered faces. Thick gey lines indicate accessible outcrop, and dashed lines are routeways in and out of the quarry. Arrows indicate directions of downslope.

Stereographic projections show slip surfaces for the individual faces (numbered). Crosses are poles to the planes. Slip vectors (arrows) are plotted on the planes. Arrows point in the direction of hanging wall movement, and circles indicate cases where sense of slip was indiscernible. Grey great circles indicate purely extensional reactivation by fibrous mineralisation orthogonal to the fracture plane.

The general shear sense for each fracture set is also indicated.

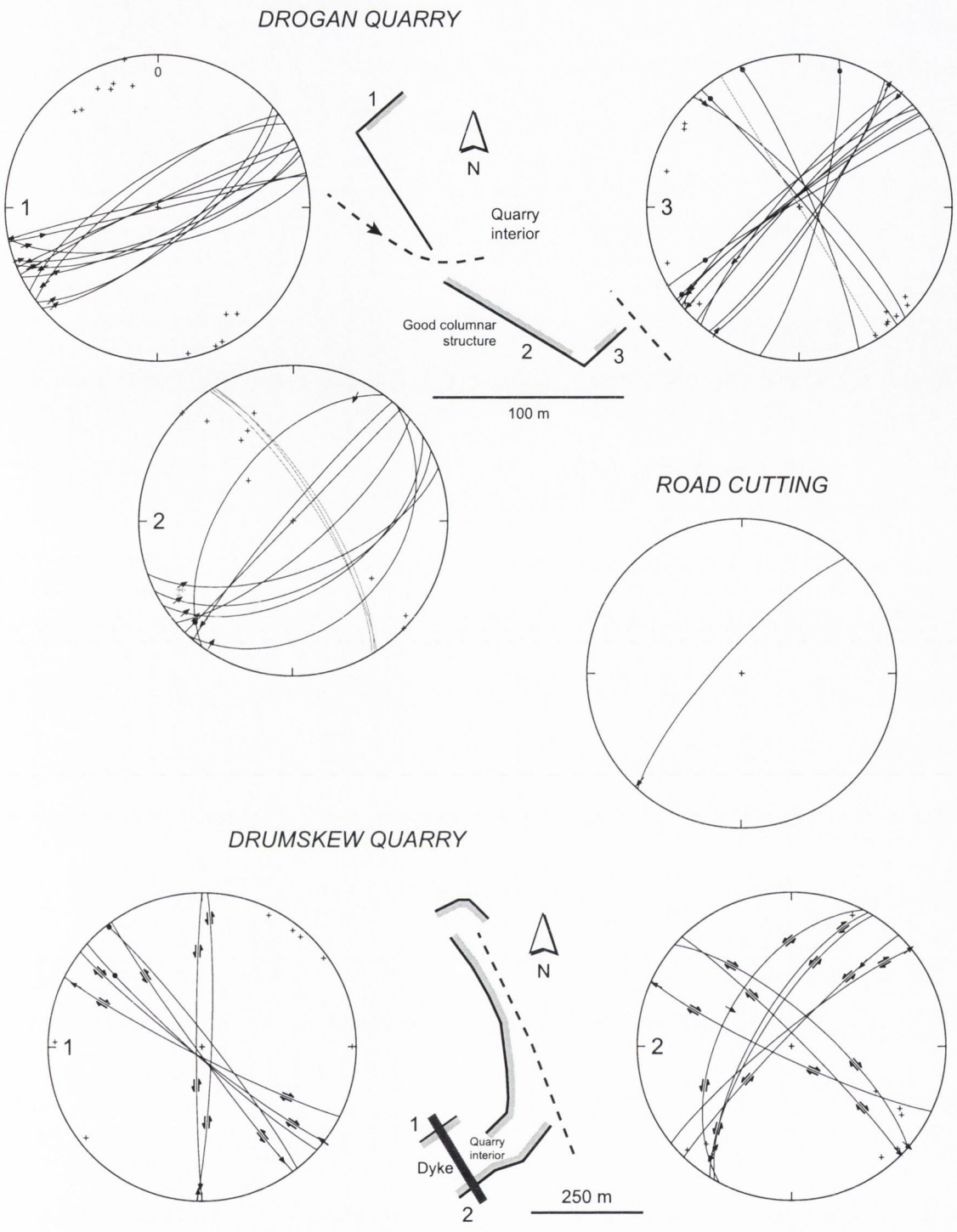

Figure 4.16. Quarry plans and stereographic projections showing slip data from Drogan and Drumskew quarries. Quarry plans show numbered faces. Thick gey lines indicate accessible outcrop and dashed lines are routeways in and out of the quarries. Arrows indicate directions of downslope. Slip data for the A46 road cutting is also included.

The stereographic projections show slip surfaces for individual faces (numbered). Crosses are poles to the planes. Slip vectors (arrows) are plotted on the planes. Arrows point in direction of hanging wall movement, and circles indicate cases where the sense of slip was indiscernible. Grey great circles indicate purely extensional reactivation by fibrous mineralisation orthogonal to the fracture plane.

The general shear sense for each fracture set is also indicated.

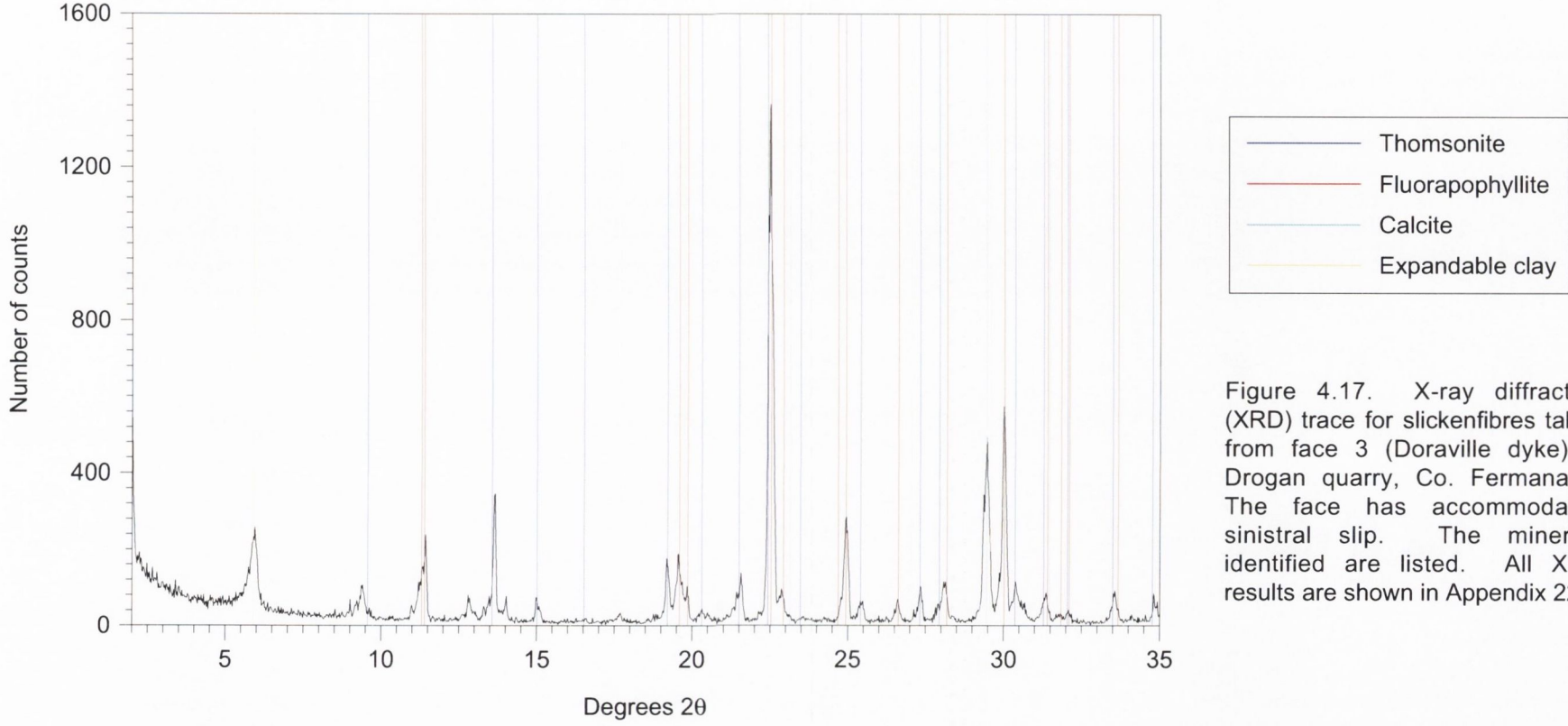

Figure 4.17. X-ray diffraction (XRD) trace for slickenfibres taken from face 3 (Doraville dyke) in Drogan quarry, Co. Fermanagh. The face has accommodated sinistral slip. The minerals identified are listed. All XRD results are shown in Appendix 22.

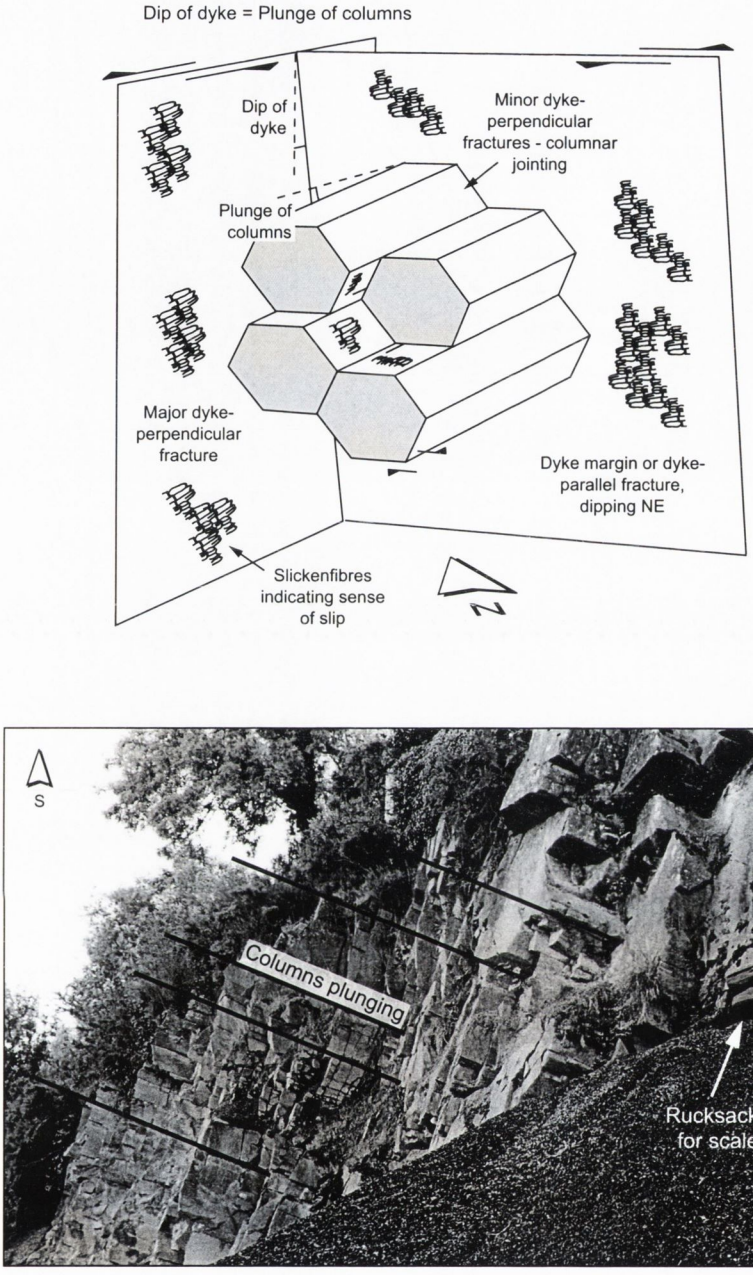

Figure 4.18. Reactivation of the cooling joint structure in Drogan and Doonan quarries.
A schematic sketch (top) shows the control on the slip vector by the plunge of the columns.
The photograph is from Drogan quarry, showing crudely developed columnar jointing, with columns plunging to the southwest.

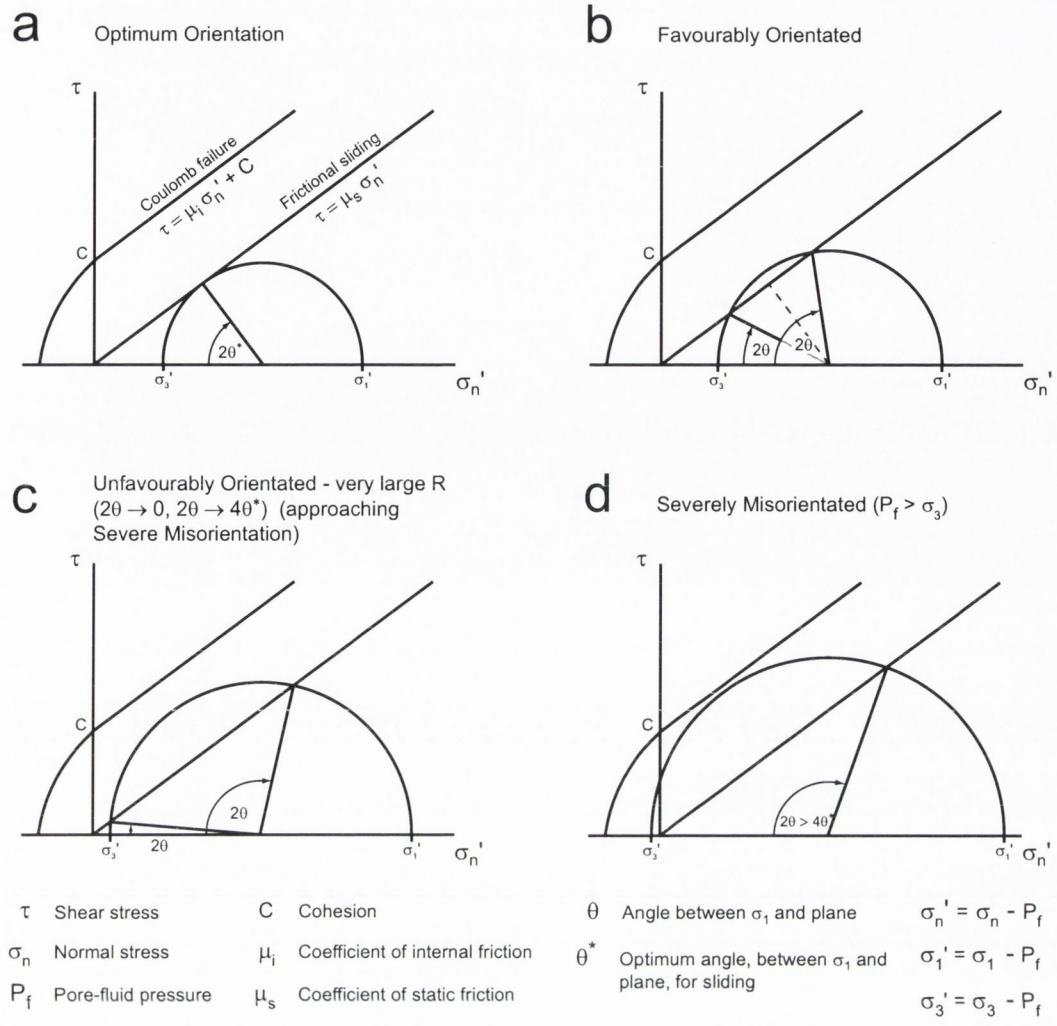

Figure 4.19. Modified from Sibson (1985). Mohr circle construction comparing stress criteria for reactivation by frictional sliding of an existing plane versus propagation of a new fracture under the Coulomb fracture criterion.

The coefficient of internal friction, μ_i, for forming a new fracture can be assumed roughly equal to the coefficient of sliding friction, μ_s, for movement on an existing surface (Sibson 1985). A value of 0.75 is used as an average over a number of rock types at intermediate pressures (Byerlee 1978). Therefore, rock cohesion, C, controls the relative positions of the Coulomb and frictional failure envelopes, and the optimum angle for reactivation, θ^*, between σ_1 and the plane. This is the angle at which movement occurs given the lowest possible stress ratio, $R = R^* = \sigma_1/\sigma_3$, and is the same as that for formation of a new fracture under the Coulomb criterion, i.e. ~ 30°.

a) Given that reactivation is assumed to take place on a cohesionless surface (C = 0), an existing plane orientated at θ^* requires a value of R^* to cause movement as frictional sliding that is much lower than would be required to create a new fracture. Therefore, reactivation of an existing weakness is preferable to propagation of a new fracture.

b) An increase in R will increase the range of θ over which reactivation can take place, overcoming the friction of the fault plane. This is indicated by the points of intersection between the Mohr circle and the frictional failure envelope. For realistic values of R in the Earth, planes falling in the angular range where reactivation can take place are deemed to be favourably orientated for reactivation.

c) Planes that are orientated such that large values of R are required to cause slip are deemed to be unfavourably orientated.

It is apparent from the geometry of the Mohr diagram that, before propagation of a new fracture occurs, very large values of R must be achieved to cause frictional sliding on planes that are non-optimally orientated by a large degree either side of θ^*. The fault then becomes frictionally locked up, as unrealistic values of R are required to cause movement.

d) The only way the plane can slip at high angles of θ is if σ_3 becomes tensile due to the action of pore-fluid pressure (P_f) i.e. σ_3' becomes negative.

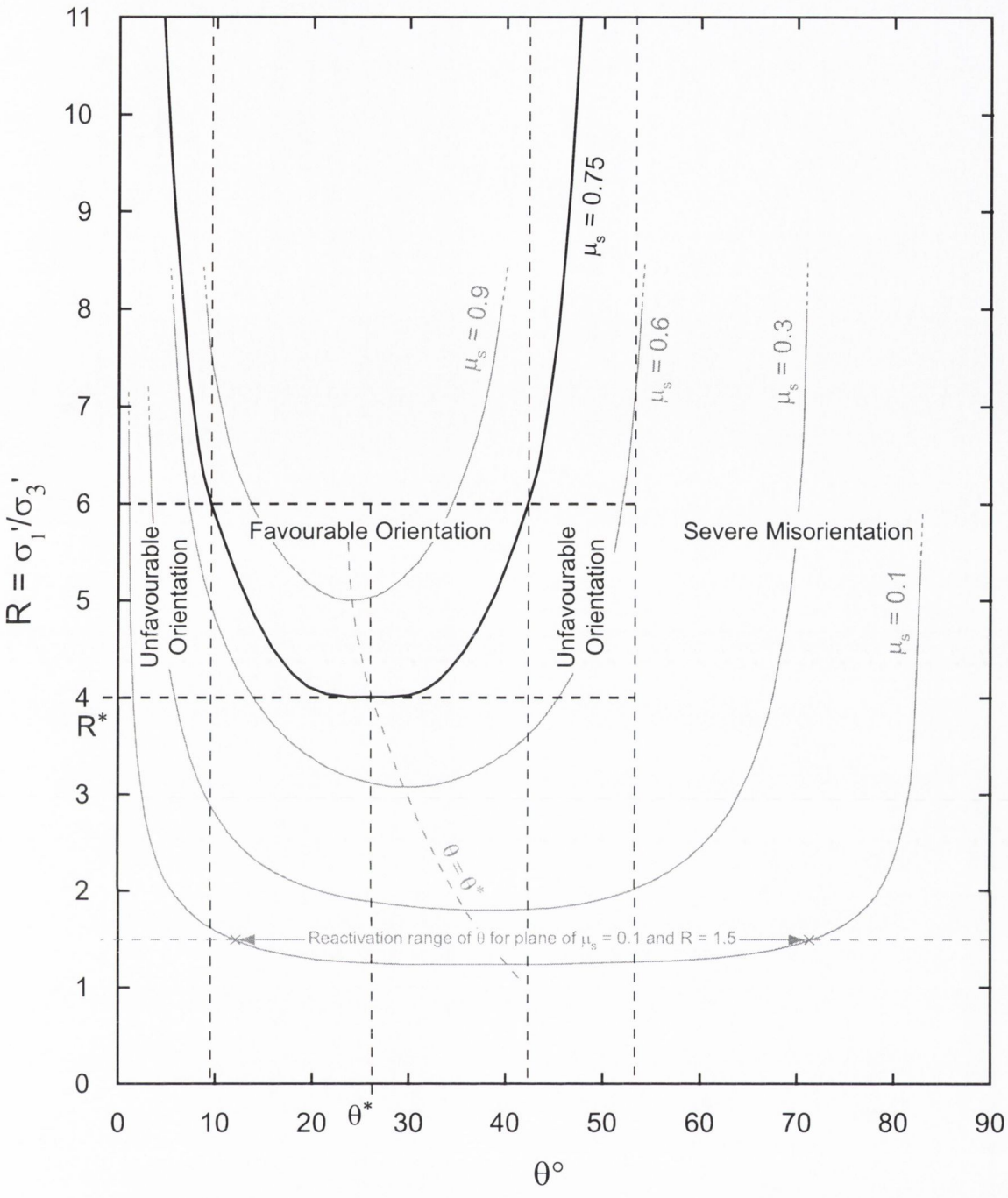

Figure 4.20. Modified from Sibson (1990) and Lachenbruch & McGarr (1990). Failure criteria for various coefficients of static friction, μ_s (see Figure 4.19 for symbol definitions). Black text and solid and dashed lines relate to $\mu_s = 0.75$. Grey text and lines relate to varying μ_s. Since the coefficient of frictional sliding controls the gradient of the envelope (Figure 4.19), a change in μ_s alters the reactivation response of a given orientation of plane. Slip will occur on a existing plane at the range of θ defined by the points of intersection between a horizontal line defined by R and the curve defined by μ_s. As μ_s decreases, R^* decreases and θ^* increases, and vice versa.

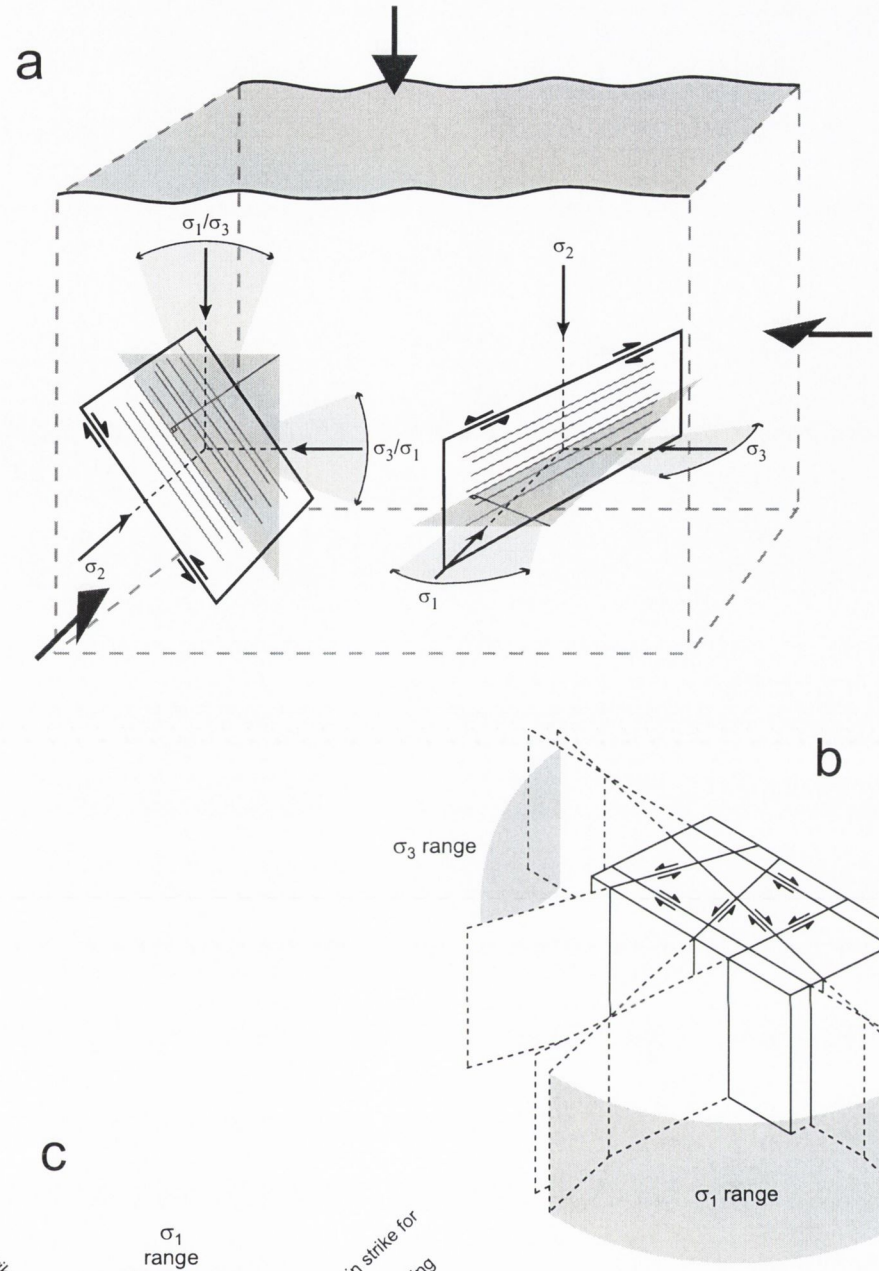

Figure 4.21. Fracture reactivation.
a) The relationship between plane orientation and the stress field of reactivation.
Left - inclined plane in a normal/reverse stress regime.
Right - vertical plane in a strike-slip stress regime.
b) Schematic diagram relating to the Doraville dyke, illustrating the angular range of viable principal stress axis orientations given the illustrated range of reactivated fracture strikes.
c) Actual ranges in strike of the fractures accommodating shear within the Doraville dyke (Doonan and Drogan quarries). Also shown are the corresponding ranges in the principal stress directions.

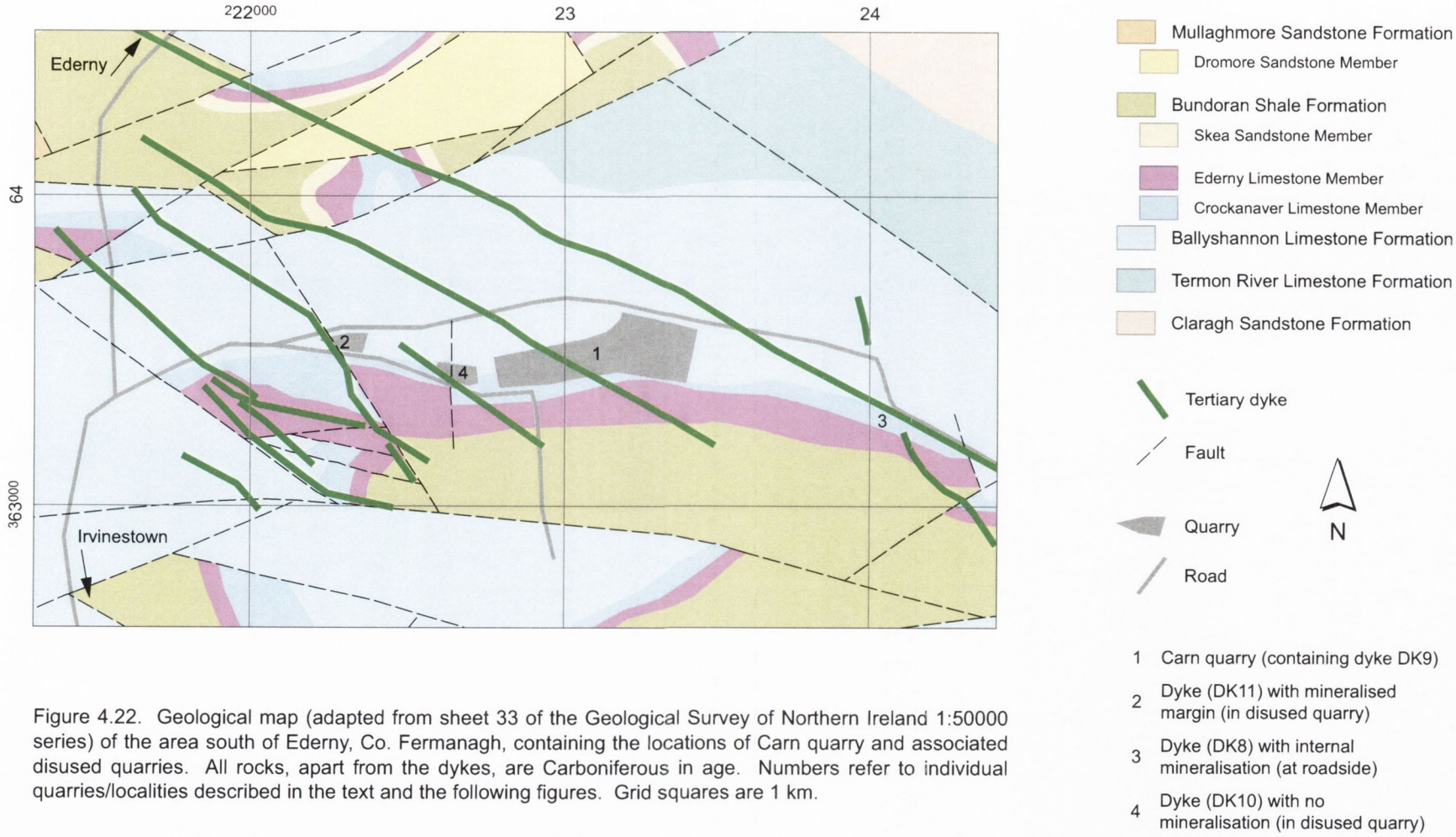

Figure 4.22. Geological map (adapted from sheet 33 of the Geological Survey of Northern Ireland 1:50000 series) of the area south of Ederny, Co. Fermanagh, containing the locations of Carn quarry and associated disused quarries. All rocks, apart from the dykes, are Carboniferous in age. Numbers refer to individual quarries/localities described in the text and the following figures. Grid squares are 1 km.

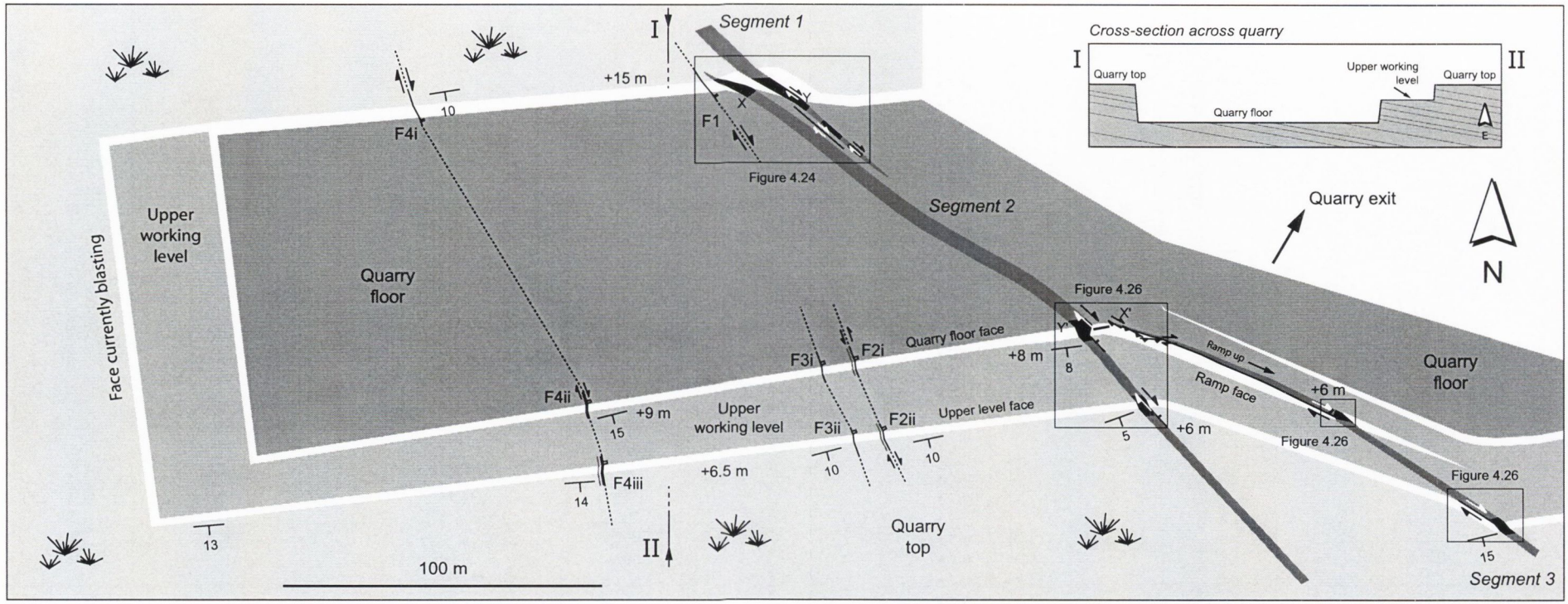

Dyke inferred

Dyke outcrop

Sub-vertical Quarry faces

Sloping

+ 6 m — Height of top of face (approximate) above previous level

Faults (F1-4)

Outcrop — 'Apparent' downthrown side indicated

Inferred — 'True' downthrown side indicated (Normal)

Apparent deflection due to easterly dip of faults in quarry face

Fault 'zone' of multiple sub-parallel planes

Figure 4.23. Map view of Carn quarry (Carboniferous Ballyshannon Limestone Formation) with a Tertiary dyke (dyke DK9) cutting the two quarry levels.
The fault and dyke margin displacement kinematics are indicated (see diagram to the left). Boxes refer to figures showing detailed structural data from the main outcrop areas.
Faults are shown as single planes, but may be a 'zone' of multiple sub-parallel planes (see text and following figures). Kinematics are derived from slickenfibre growth and pull-apart structures. Where full fault kinematics are known, this allows the true downthrown side to be indicated across the fault plane or overall across the fault zone. The 'apparent' downthrown side is indicated where the slip lineation is seen but slip-sense is unkown. In such cases, the inclination of the strata and the predominance of strike-slip over dip-slip displacement creates the apparent downthrow.

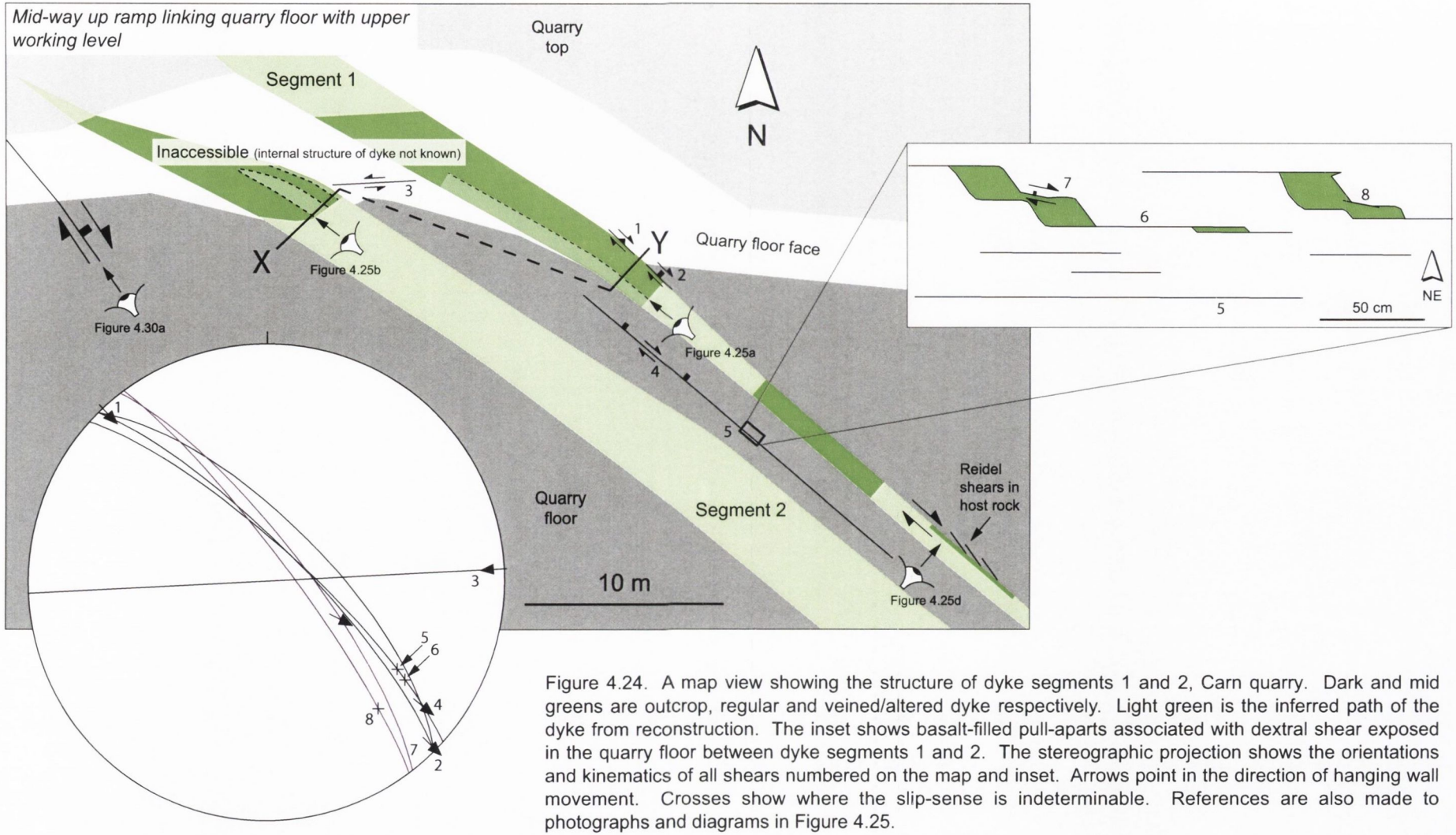

Figure 4.24. A map view showing the structure of dyke segments 1 and 2, Carn quarry. Dark and mid greens are outcrop, regular and veined/altered dyke respectively. Light green is the inferred path of the dyke from reconstruction. The inset shows basalt-filled pull-aparts associated with dextral shear exposed in the quarry floor between dyke segments 1 and 2. The stereographic projection shows the orientations and kinematics of all shears numbered on the map and inset. Arrows point in the direction of hanging wall movement. Crosses show where the slip-sense is indeterminable. References are also made to photographs and diagrams in Figure 4.25.

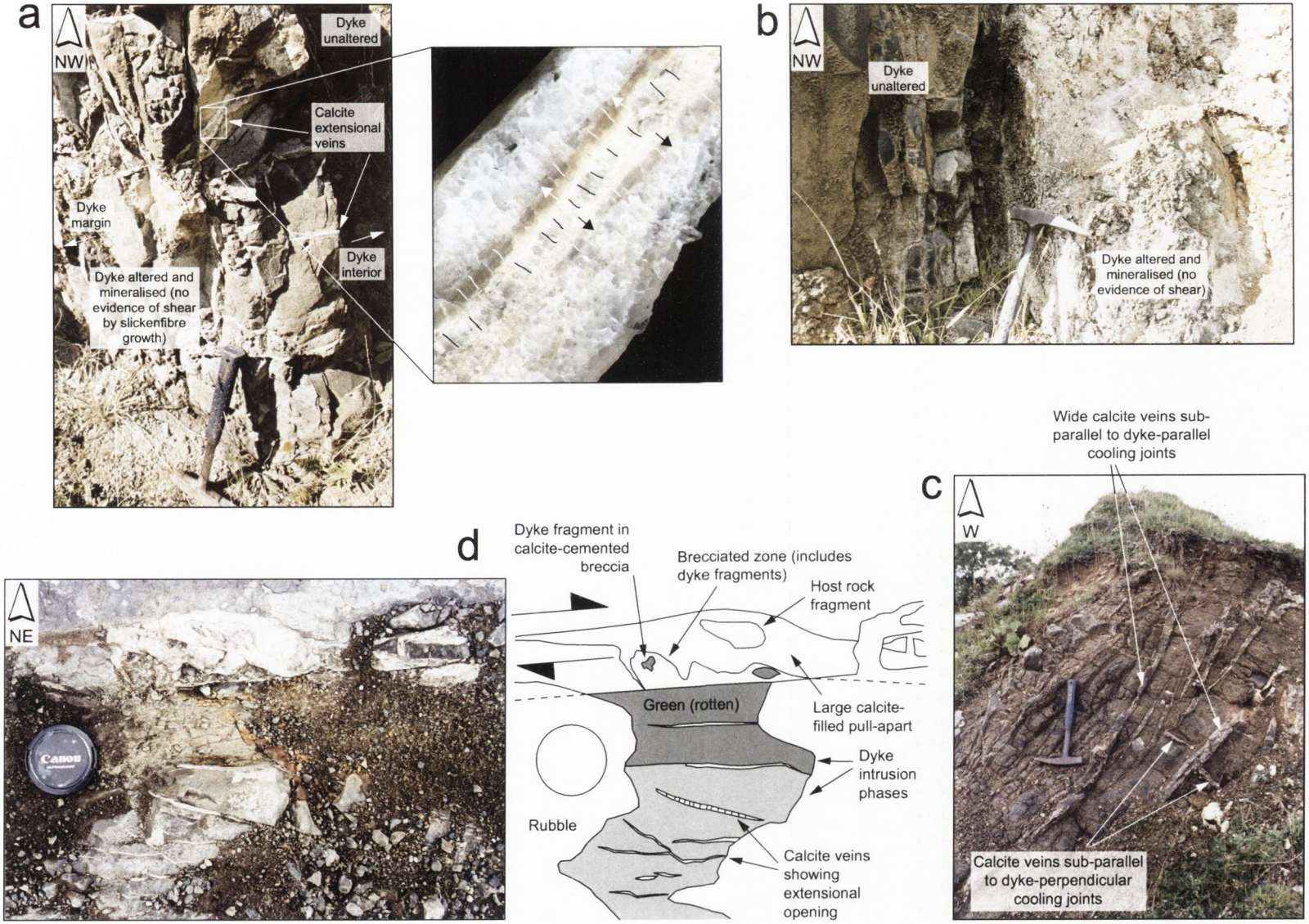

Figure 4.25. Features associated with dyke segments 1 and 2 at the northern face of Carn quarry (see Figure 4.24 for locations).
a) The transition between regular and veined zones within segment 1. The inset shows that the veining is extensional. The lines drawn show crystal edges, so the arrows, therefore, show crystal growth direction.
b) The sharp transition between regular and veined (highly altered) zones within segment 2.
c) Dyke (DK11) in the entrance to one of the disused quarries west of Carn quarry, showing extensive extensional calcite veining throughout the outcrop.
d) Segment 1 in the quarry floor (near projected segment tip), showing two phases of intrusion and dextral shear along the margin.

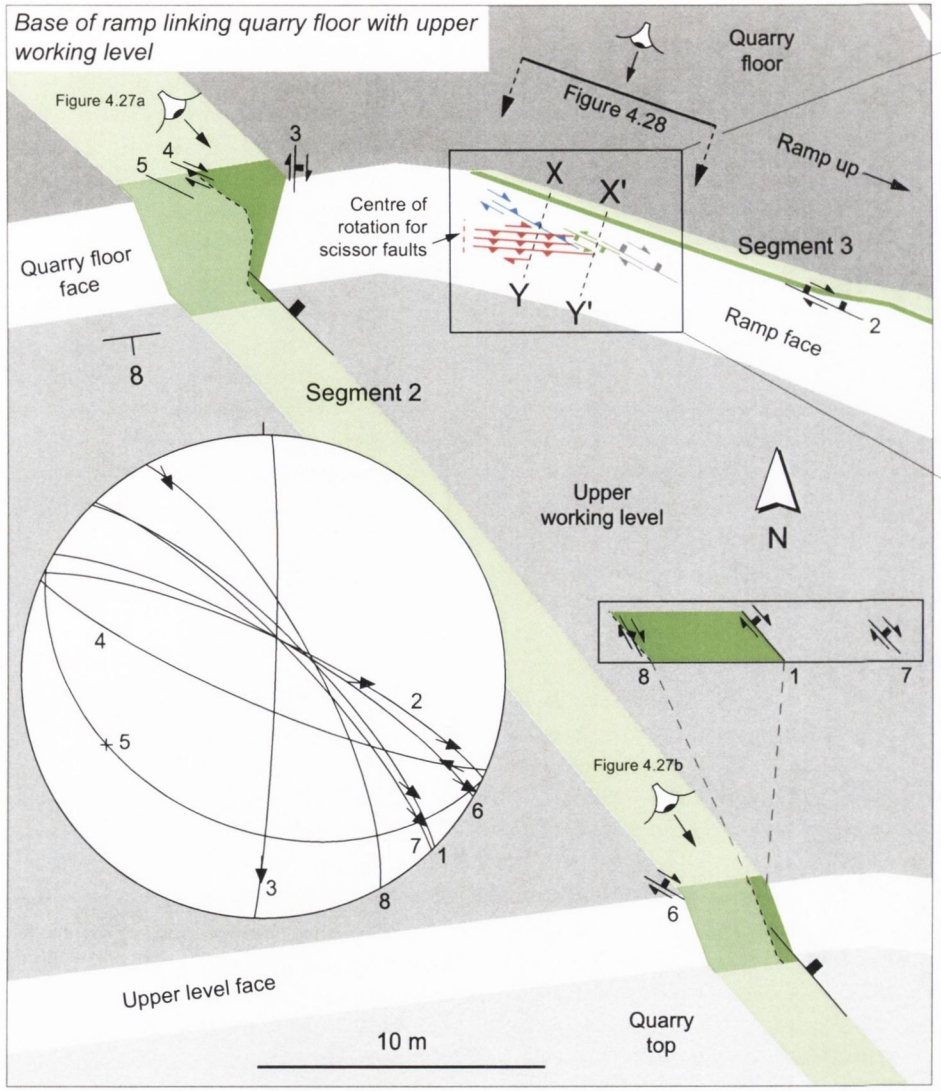

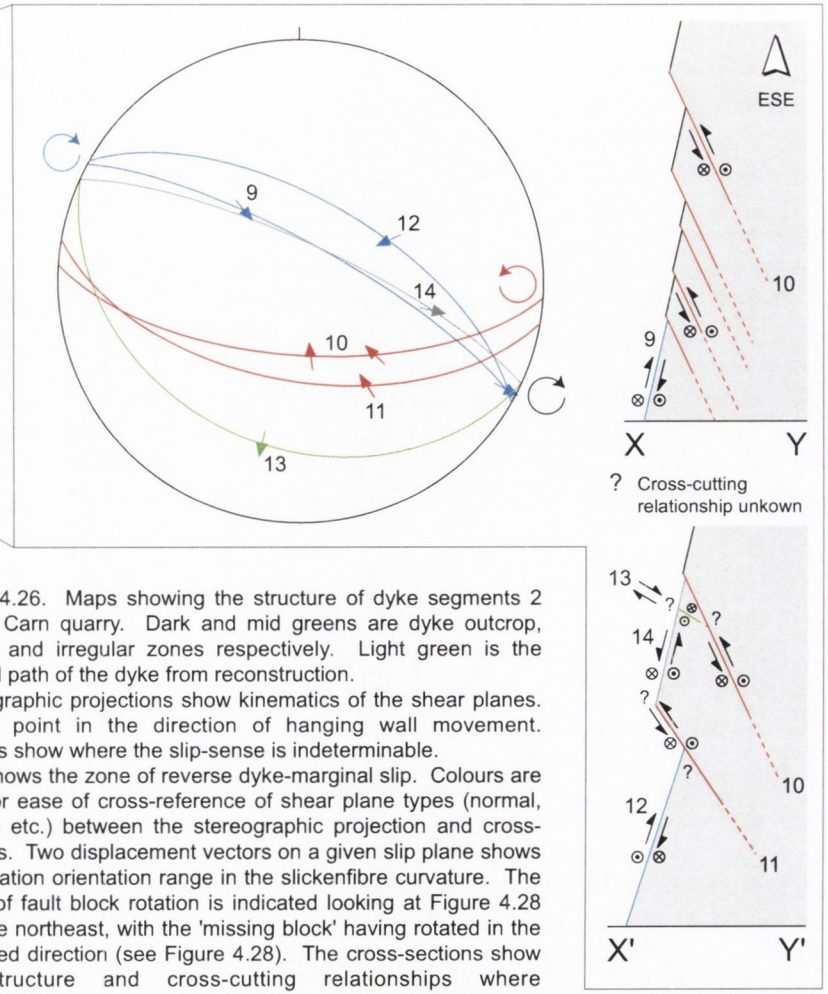

Figure 4.26. Maps showing the structure of dyke segments 2 and 3, Carn quarry. Dark and mid greens are dyke outcrop, regular and irregular zones respectively. Light green is the inferred path of the dyke from reconstruction.
Stereographic projections show kinematics of the shear planes. Arrows point in the direction of hanging wall movement. Crosses show where the slip-sense is indeterminable.
Inset shows the zone of reverse dyke-marginal slip. Colours are used for ease of cross-reference of shear plane types (normal, reverse etc.) between the stereographic projection and cross-sections. Two displacement vectors on a given slip plane shows the lineation orientation range in the slickenfibre curvature. The sense of fault block rotation is indicated looking at Figure 4.28 from the northeast, with the 'missing block' having rotated in the indictated direction (see Figure 4.28). The cross-sections show the structure and cross-cutting relationships where determinable.
References are also made to photographs and diagrams in Figure 4.27.

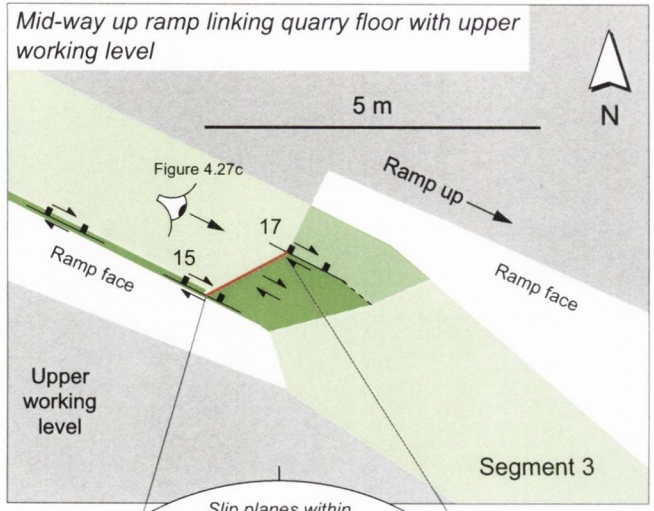

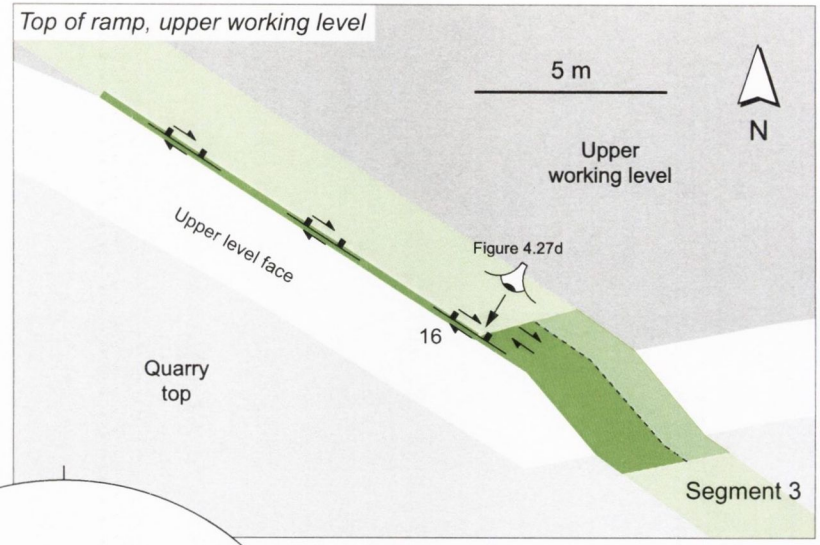

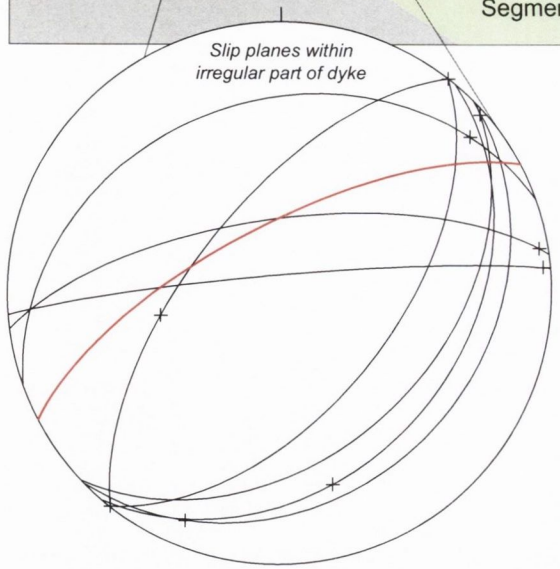

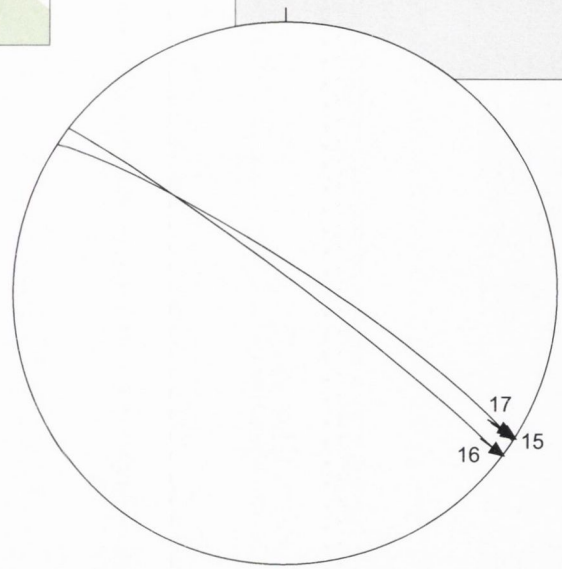

Figure 4.26 continued.

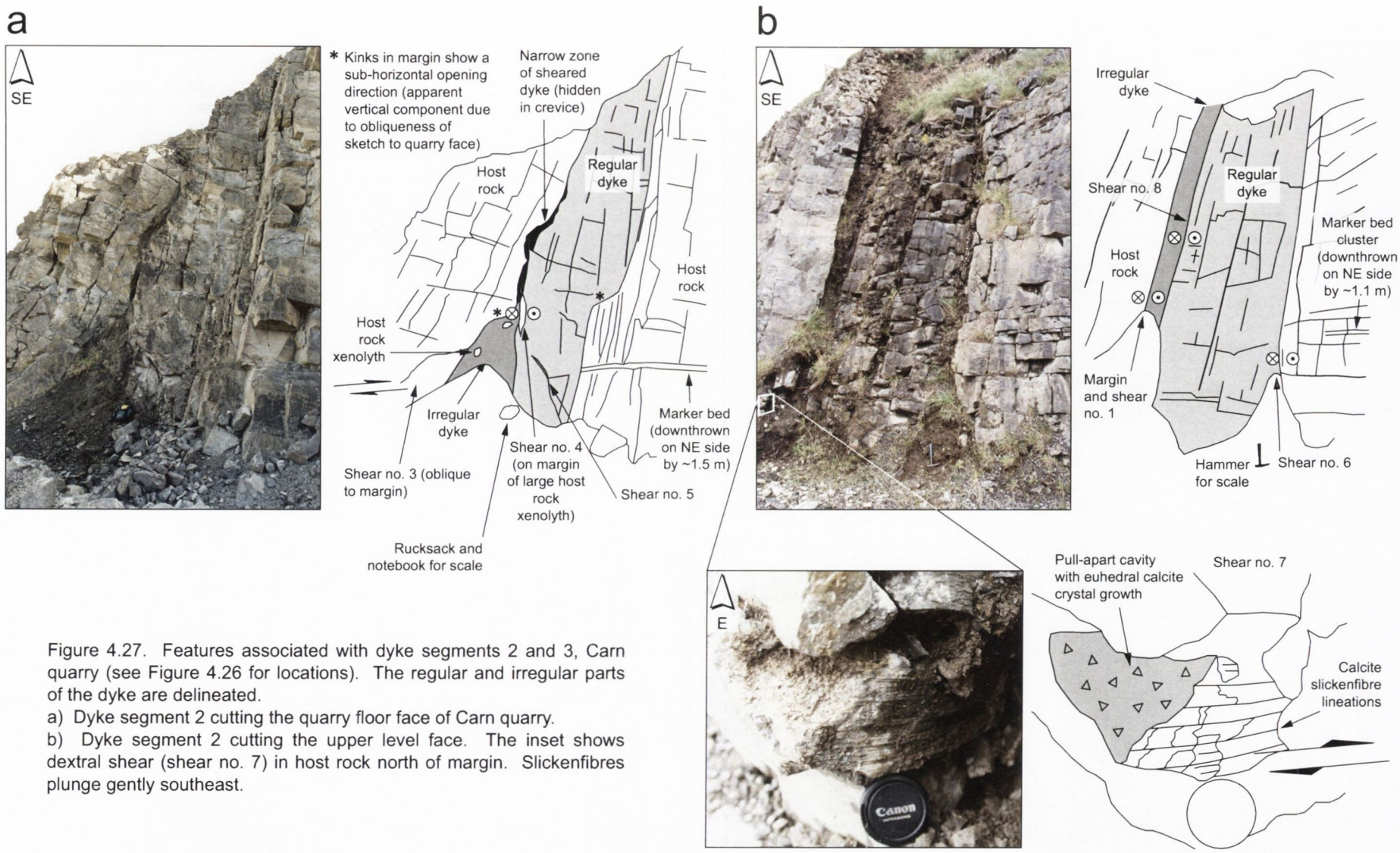

Figure 4.27. Features associated with dyke segments 2 and 3, Carn quarry (see Figure 4.26 for locations). The regular and irregular parts of the dyke are delineated.

a) Dyke segment 2 cutting the quarry floor face of Carn quarry.

b) Dyke segment 2 cutting the upper level face. The inset shows dextral shear (shear no. 7) in host rock north of margin. Slickenfibres plunge gently southeast.

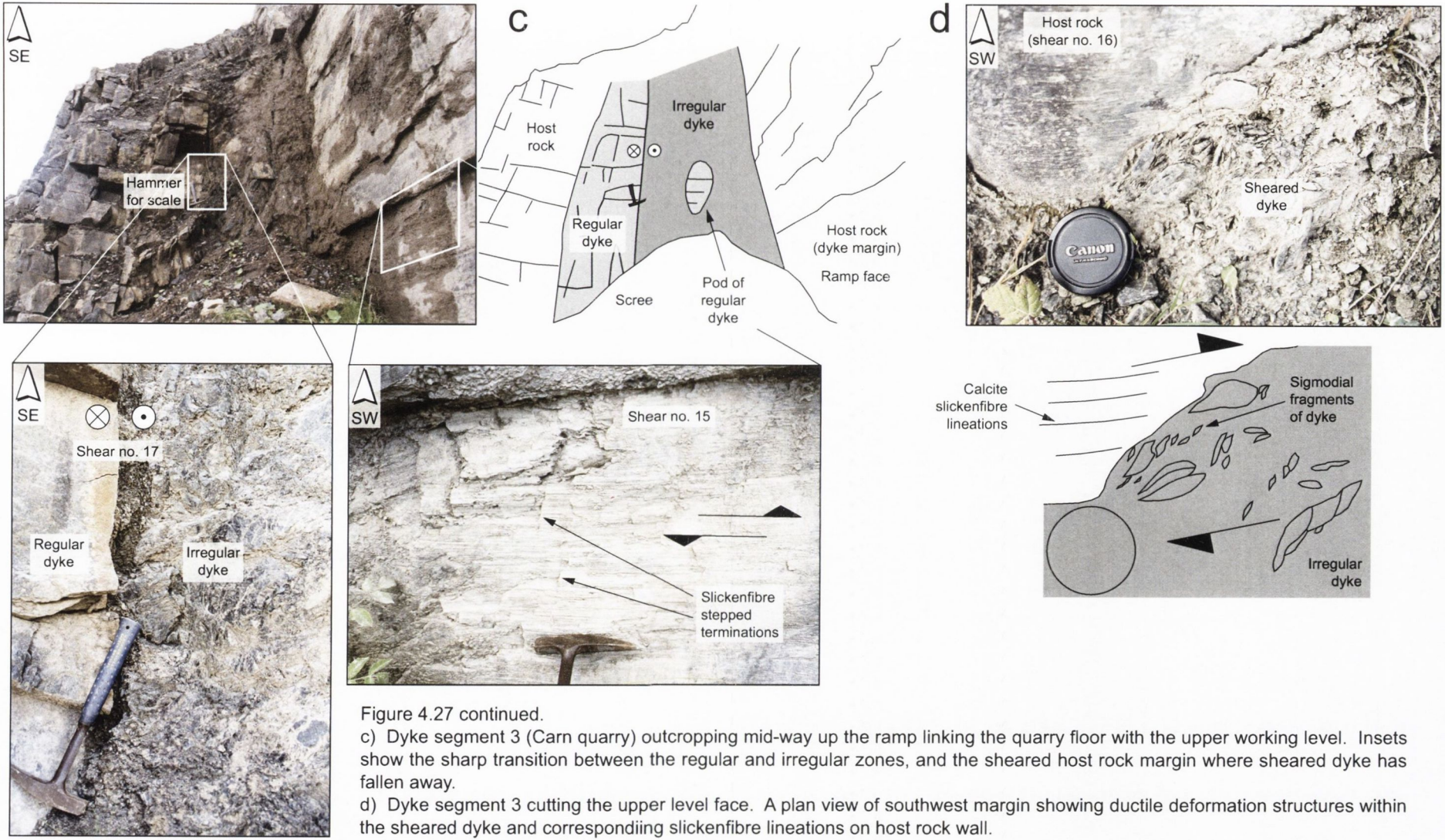

Figure 4.27 continued.

c) Dyke segment 3 (Carn quarry) outcropping mid-way up the ramp linking the quarry floor with the upper working level. Insets show the sharp transition between the regular and irregular zones, and the sheared host rock margin where sheared dyke has fallen away.

d) Dyke segment 3 cutting the upper level face. A plan view of southwest margin showing ductile deformation structures within the sheared dyke and correspondiing slickenfibre lineations on host rock wall.

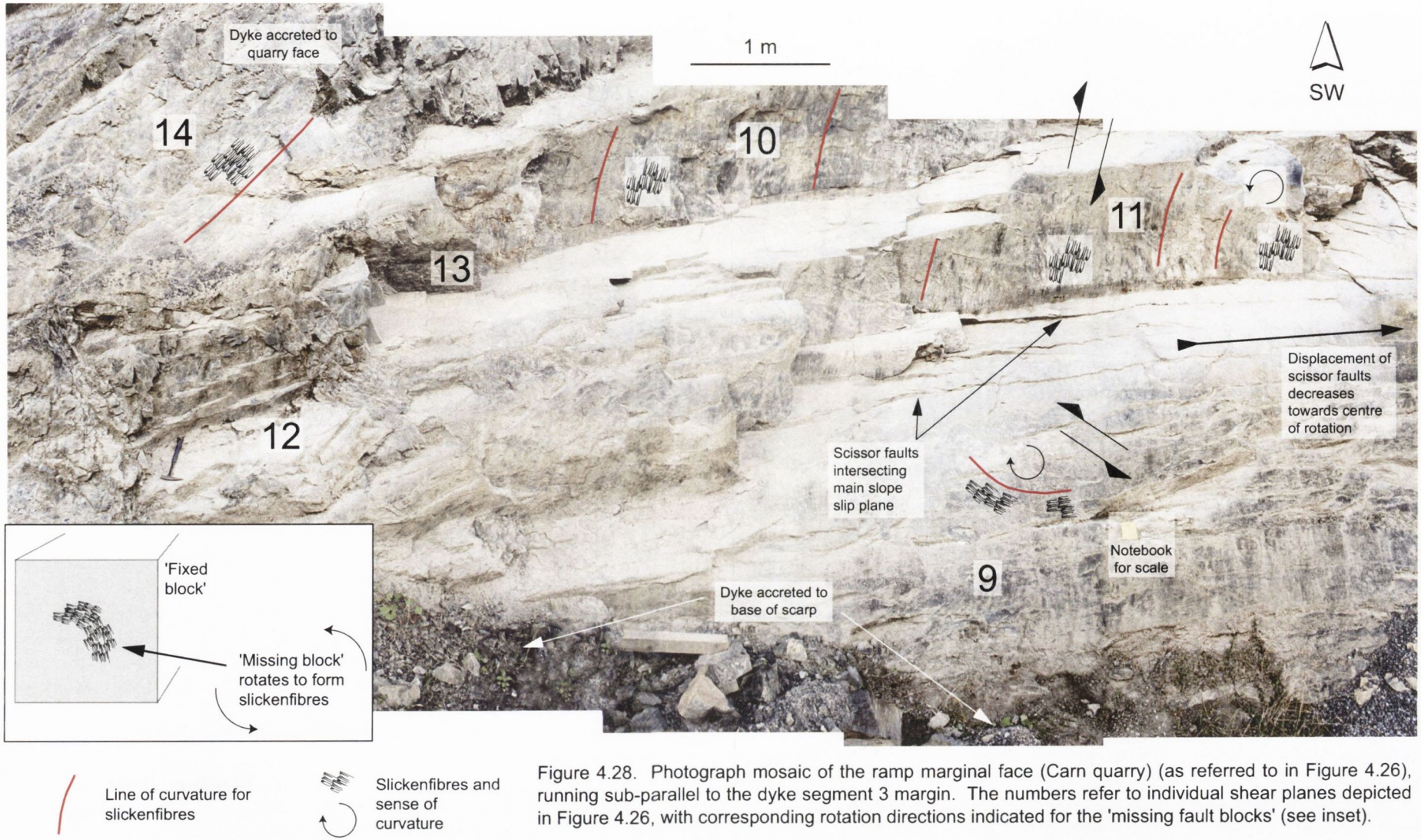

Figure 4.28. Photograph mosaic of the ramp marginal face (Carn quarry) (as referred to in Figure 4.26), running sub-parallel to the dyke segment 3 margin. The numbers refer to individual shear planes depicted in Figure 4.26, with corresponding rotation directions indicated for the 'missing fault blocks' (see inset).

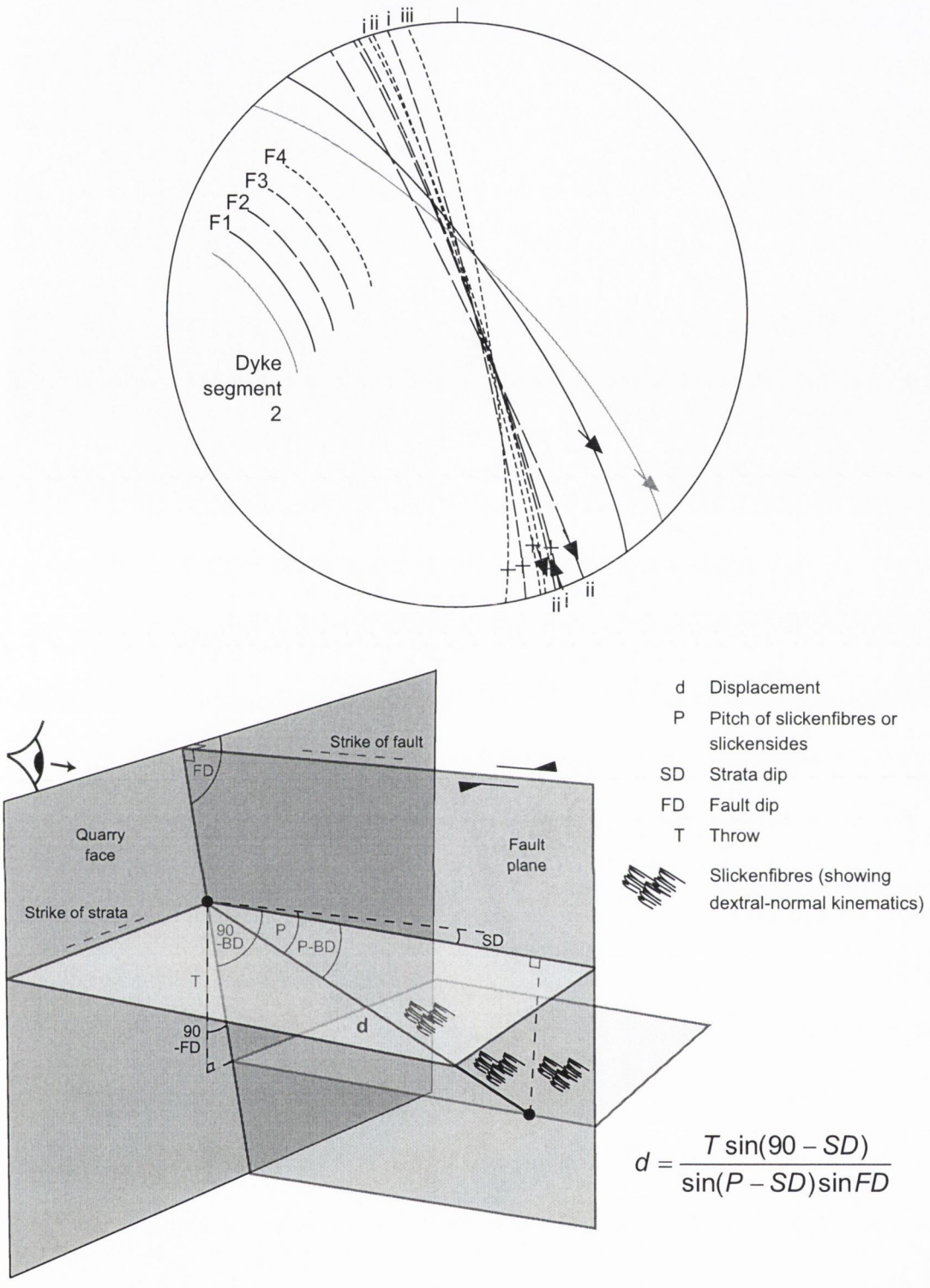

Figure 4.29. Fault data from Carn quarry.
The stereographic projection shows the faults and lineations with kinematics where known. Arrows point in the direction of hanging wall movement, and crosses indicate where the slip-sense is unknown. Also shown is dyke segment 2, plotted with an average slip lineation derived from shear planes where it intersects the upper level face.
The schematic diagram shows the trigonometric theory in deriving estimates of fault displacement. This assumes the plane of the quarry face contains the strata strike and is also perpendicular to fault plane. Where kinematics are unknown they are assumed dextral-normal in accordance with data from the quarry as a whole. Non-applicability of the model occurs when pitch appears to be less than strata dip or when kinematics are known to include a sinistral component of slip.

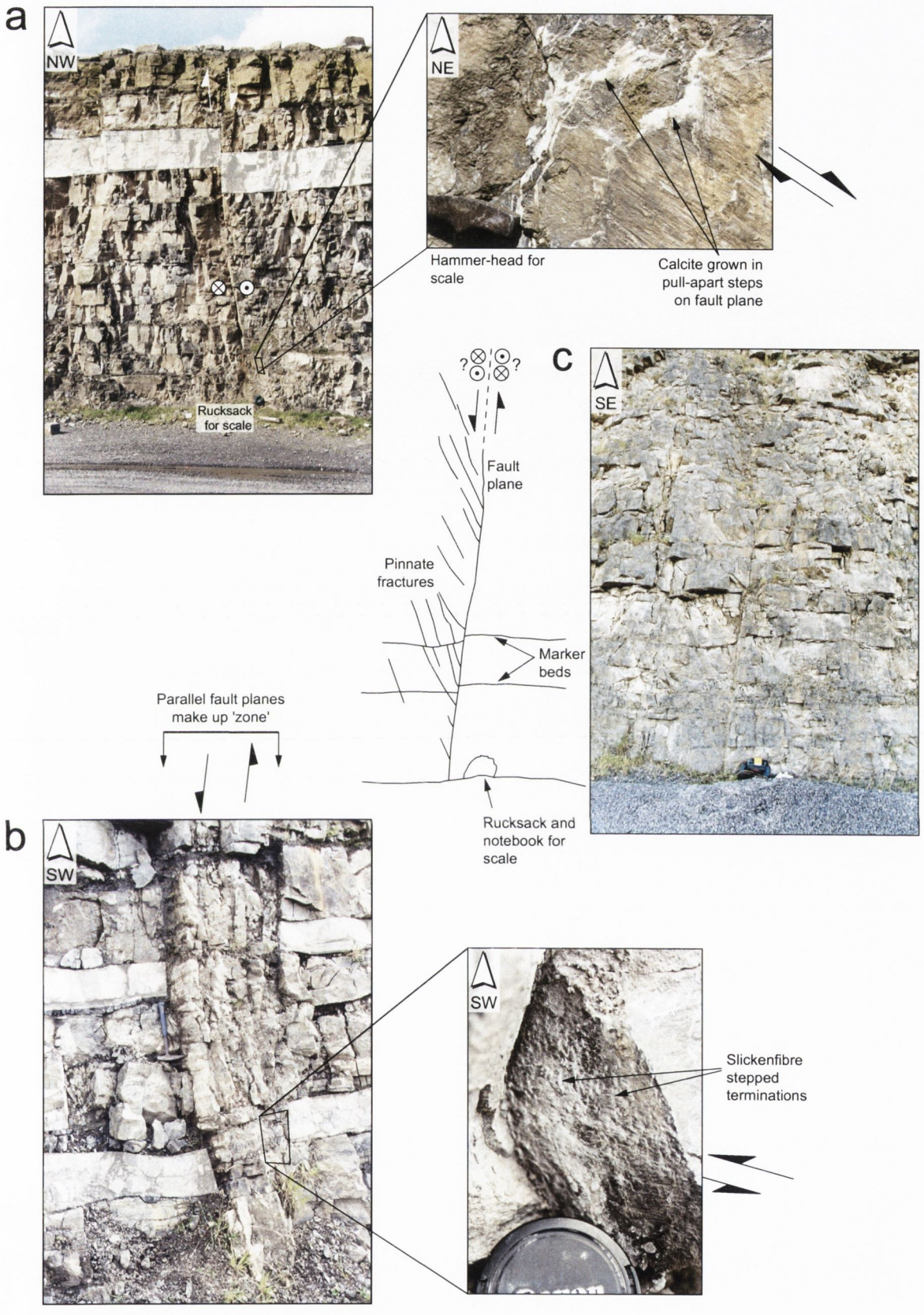

Figure 4.30. Photographs showing the range of forms for faults in Carn quarry.
a) Fault F1 showing dextral-normal oblique slip.
b) Fault F2i comprising a sub-vertical zone of sub-parallel planes, one of which shows sinistral strike-slip kinematics.
c) Fault F3ii comprising a single plane with associated pinnate fractures in the hanging wall.

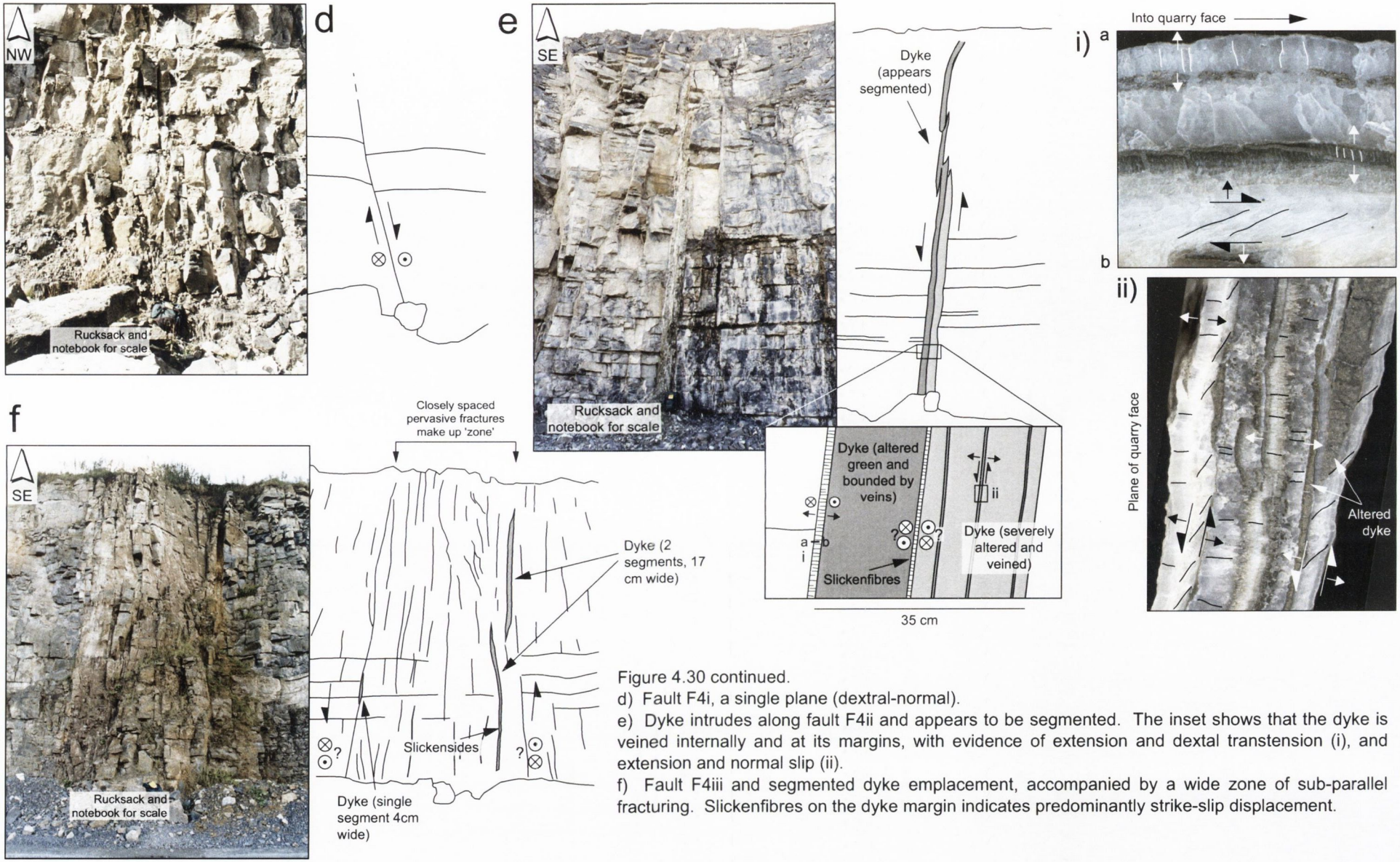

Figure 4.30 continued.

d) Fault F4i, a single plane (dextral-normal).

e) Dyke intrudes along fault F4ii and appears to be segmented. The inset shows that the dyke is veined internally and at its margins, with evidence of extension and dextal transtension (i), and extension and normal slip (ii).

f) Fault F4iii and segmented dyke emplacement, accompanied by a wide zone of sub-parallel fracturing. Slickenfibres on the dyke margin indicates predominantly strike-slip displacement.

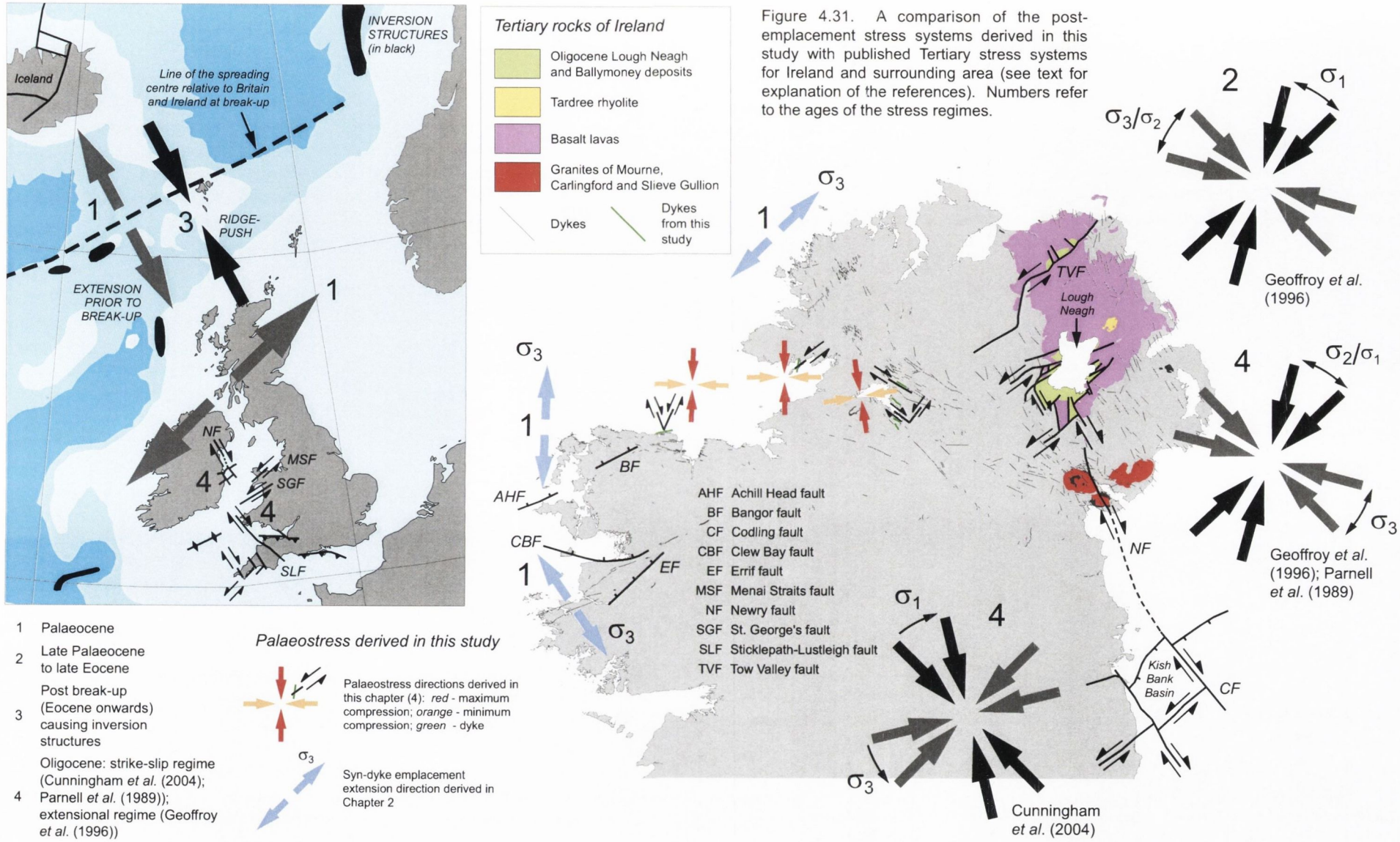

Figure 4.31. A comparison of the post-emplacement stress systems derived in this study with published Tertiary stress systems for Ireland and surrounding area (see text for explanation of the references). Numbers refer to the ages of the stress regimes.

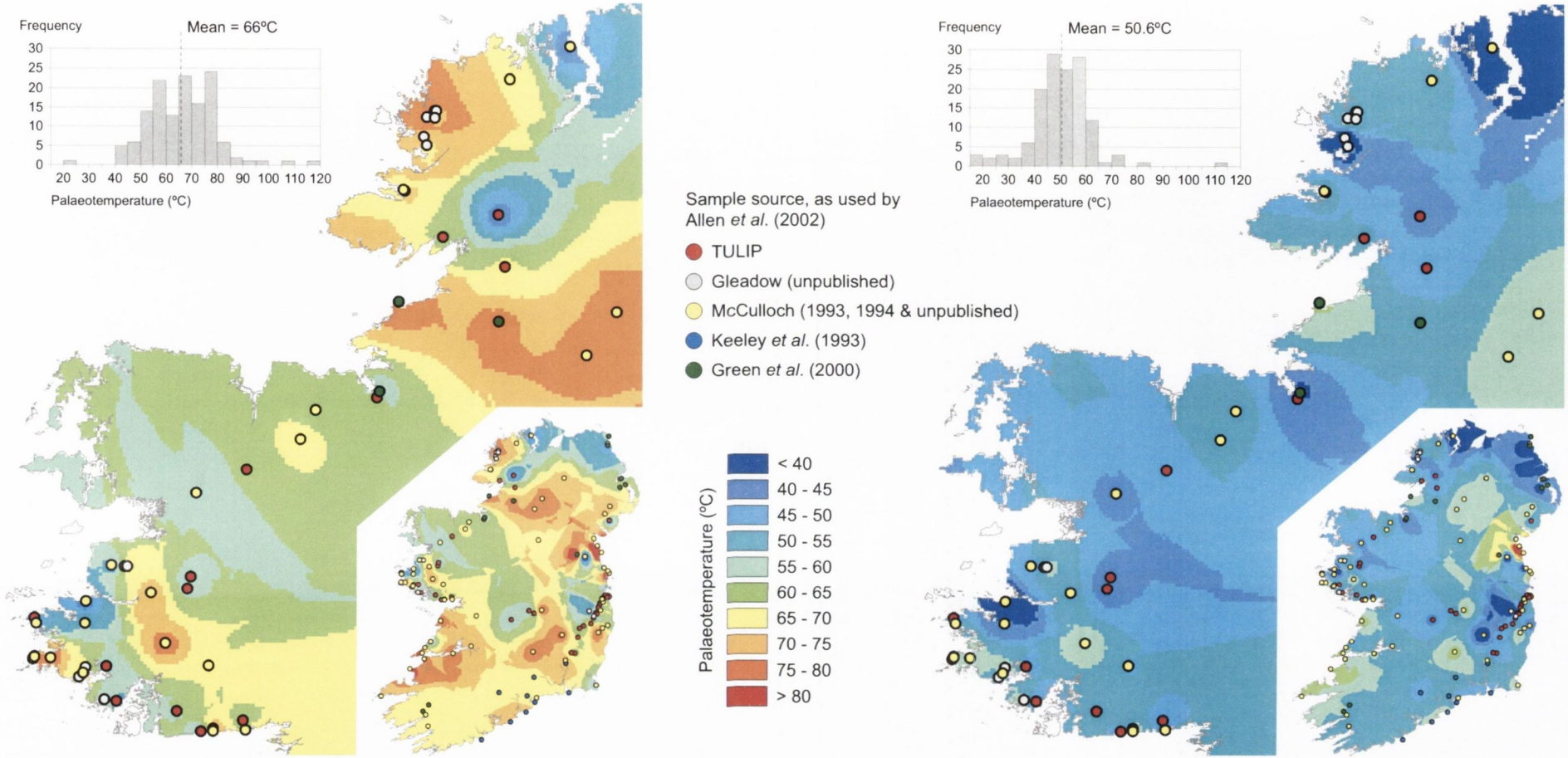

Figure 5.1. Maps showing contoured modelled palaeotemperature at 65 Ma for Ireland and west/northwest region. Each sample point contributes a single modelled palaeotemperature. The modelling uses the two fission track annealing models described in the text. Samples and modelled results are those used to create the denudation maps in Allen *et al.* (2002).

a) Laslett *et al.* (1987) annealing model.

b) Gallagher (unpublished) annealing model.

The contouring was carried out using the IDW nearest neighbour method, with 5 neighbours and a power of 2. The maps are gridded at 1 km cell size.

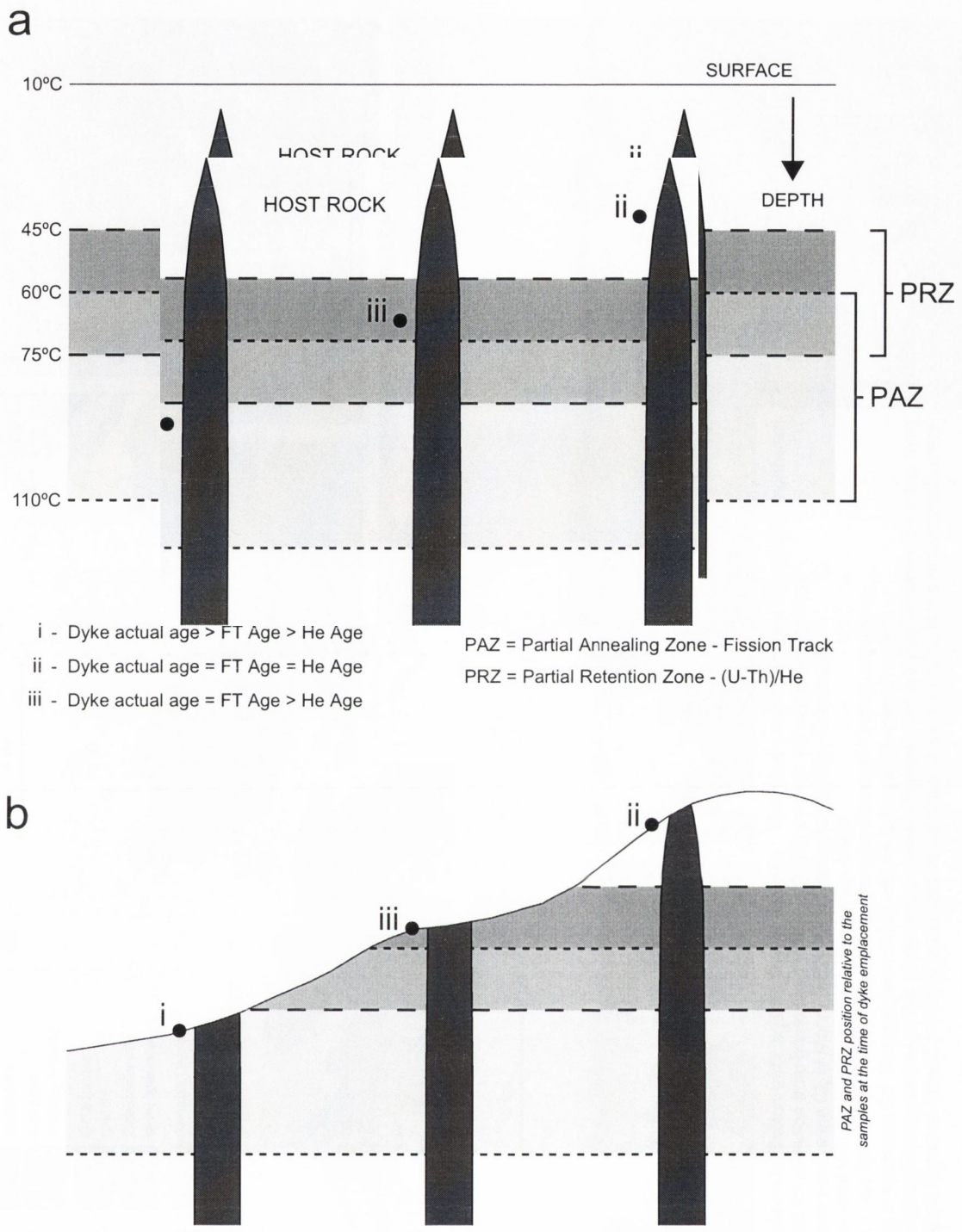

Figure 5.2. A hypothetical schematic cross-sectional representation of three surface sampling scenarios. Variation in fission track and He ages depends on the samples' proximity to the PAZ and PRZ at the time of intrusion.

a) Dykes are emplaced and 'reset' the samples.

i) Sample was at a high ambient temperature at the time of resetting, and rose through the PAZ and PRZ during cooling to the surface.

ii) Sample was at a low ambient temperature at the time of resetting and was not affected by either the PAZ or PRZ during cooling to the surface.

iii) Sample was at a temperature after resetting such that it was affected by only the PRZ during cooling to the surface.

b) Differential denudation brings the samples to the surface, yielding older ages at higher elevations for the two techniques. The positions, at the time of dyke emplacement, of the PAZ and PRZ are indicated relative to the samples.

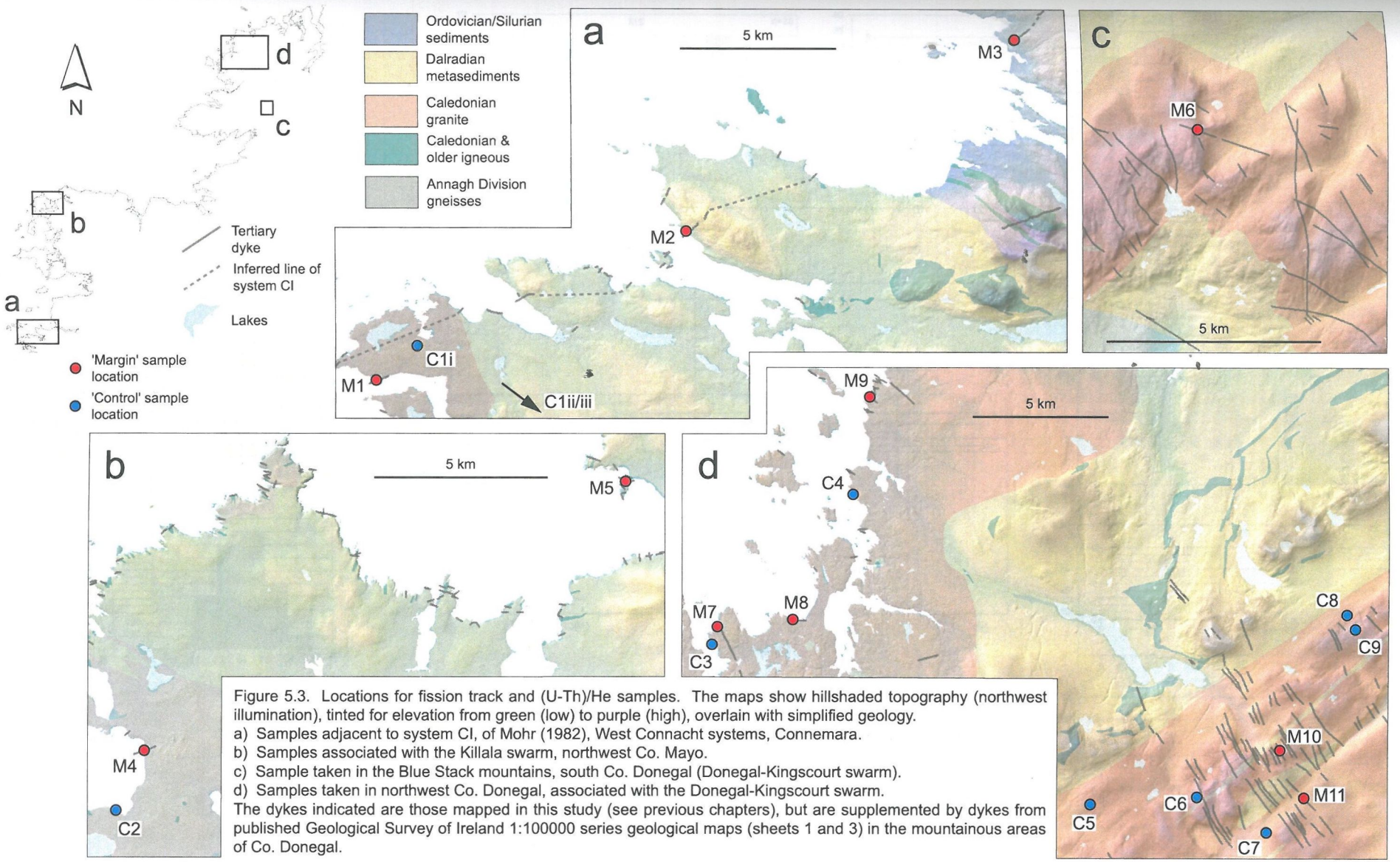

Figure 5.3. Locations for fission track and (U-Th)/He samples. The maps show hillshaded topography (northwest illumination), tinted for elevation from green (low) to purple (high), overlain with simplified geology.
a) Samples adjacent to system CI, of Mohr (1982), West Connacht systems, Connemara.
b) Samples associated with the Killala swarm, northwest Co. Mayo.
c) Sample taken in the Blue Stack mountains, south Co. Donegal (Donegal-Kingscourt swarm).
d) Samples taken in northwest Co. Donegal, associated with the Donegal-Kingscourt swarm.
The dykes indicated are those mapped in this study (see previous chapters), but are supplemented by dykes from published Geological Survey of Ireland 1:100000 series geological maps (sheets 1 and 3) in the mountainous areas of Co. Donegal.

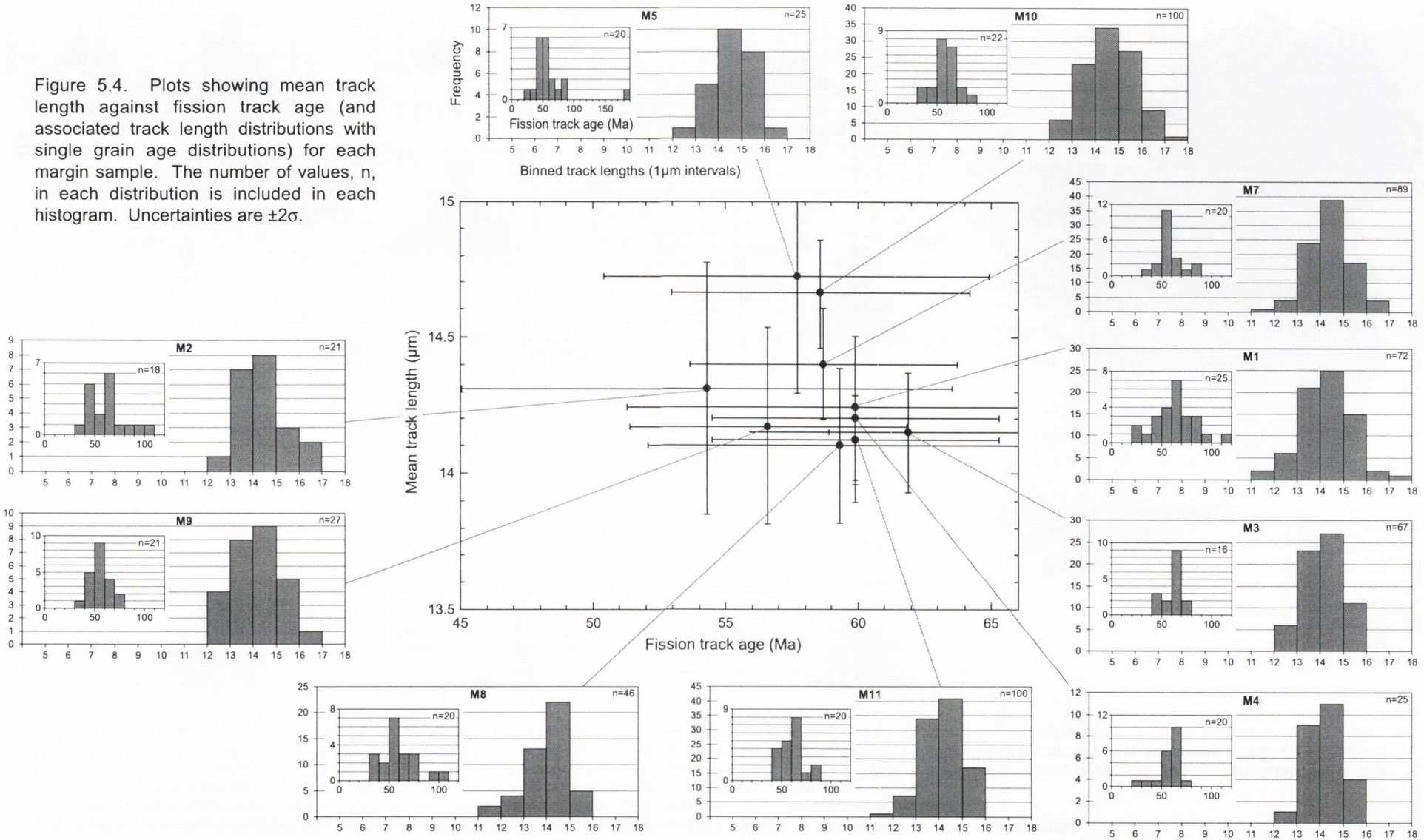

Figure 5.4. Plots showing mean track length against fission track age (and associated track length distributions with single grain age distributions) for each margin sample. The number of values, n, in each distribution is included in each histogram. Uncertainties are ±2σ.

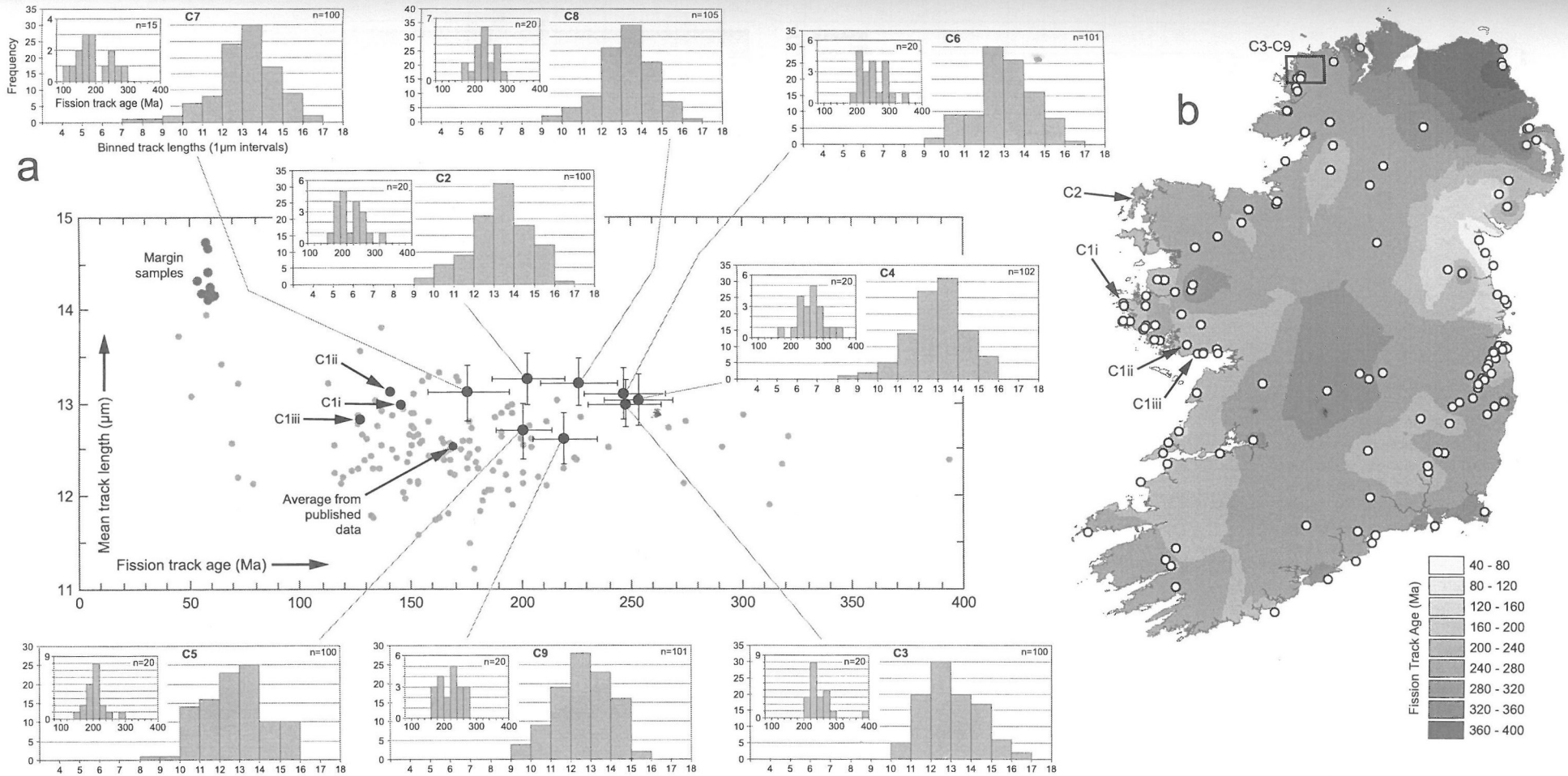

Figure 5.5. Plots showing fission track age and mean track length (MTL) for the control samples in comparison with the margin samples and published data.
a) Plot showing MTL against fission track age (and associated track length distributions with single grain age distributions) for each control sample except C1a and C1b (samples C1i, C1ii and C1iii are CL1, GG12 and GG13 of Allen *et al.* (2002) and are labelled separately). The number of values, n, in each distribution is included in each histogram. The margin samples are plotted for comparison, as is published fission track data for Ireland (light grey circles) used in Allen *et al.* (2002). Uncertainties are ±2σ.
b) A contoured map of fission track age for published data, as used in Allen *et al.* (2002). Indicated are the control sample locations.
The contouring was carried out using the IDW nearest neighbour method, with 5 neighbours and a power of 2. The map is gridded at 1 km cell size.

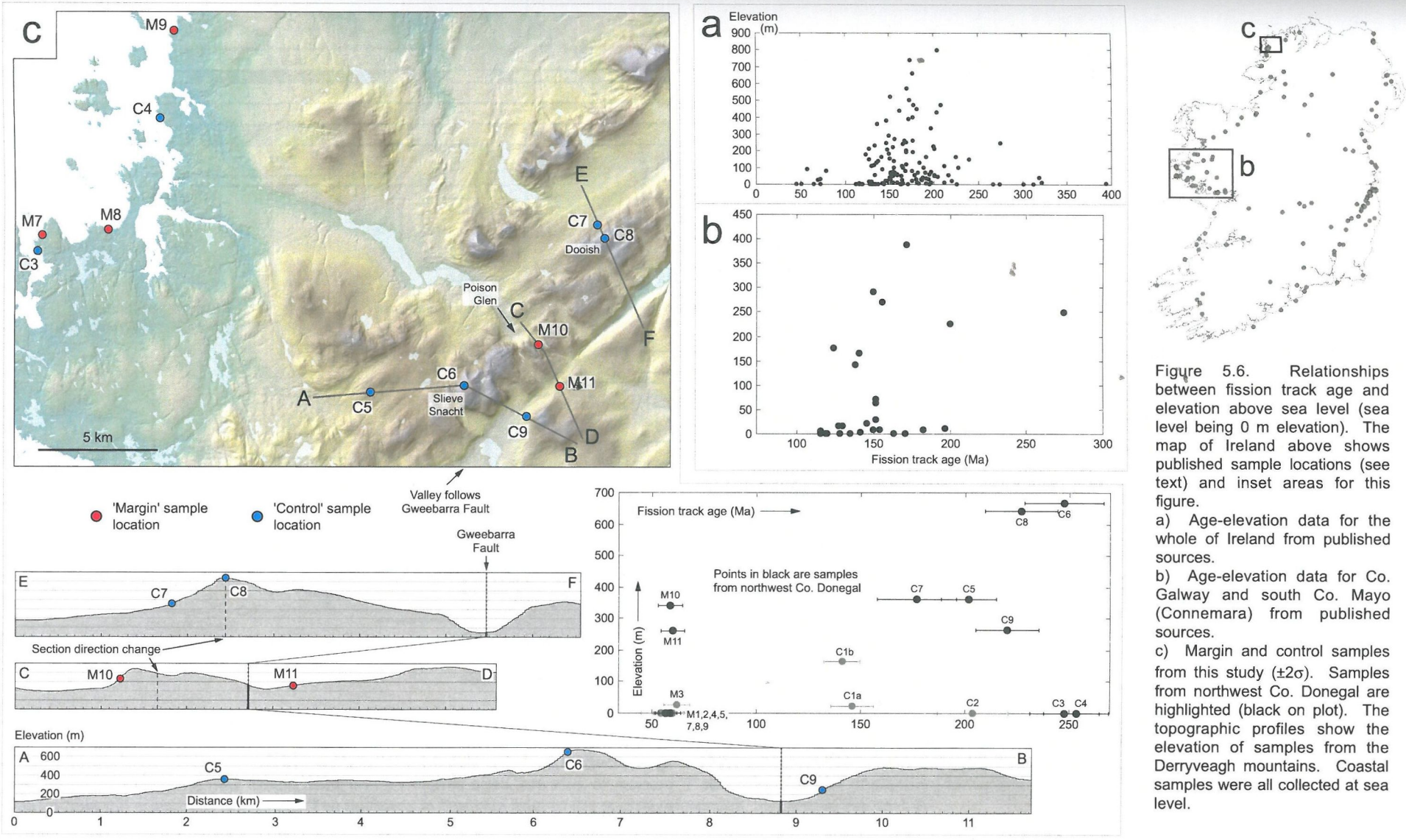

Figure 5.6. Relationships between fission track age and elevation above sea level (sea level being 0 m elevation). The map of Ireland above shows published sample locations (see text) and inset areas for this figure.

a) Age-elevation data for the whole of Ireland from published sources.

b) Age-elevation data for Co. Galway and south Co. Mayo (Connemara) from published sources.

c) Margin and control samples from this study (±2σ). Samples from northwest Co. Donegal are highlighted (black on plot). The topographic profiles show the elevation of samples from the Derryveagh mountains. Coastal samples were all collected at sea level.

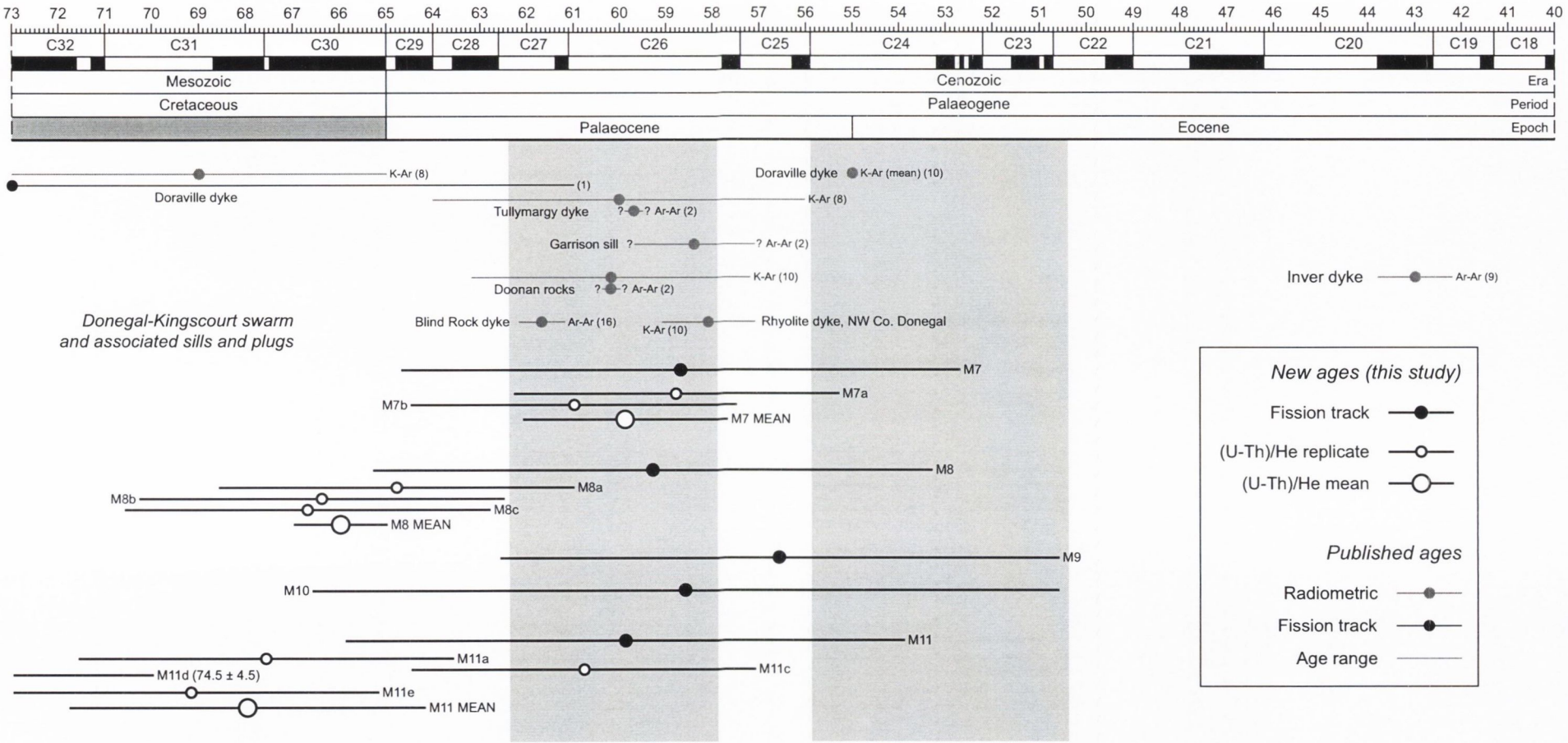

Figure 5.7. Fission-track and (U-Th)/He ages from this study plotted in comparison with all other published ages for Tertiary intrusives across northwest Ireland. All dates come from intrusives. The shaded areas represent the two main phases of igneous activity in the North Atlantic Igneous Province, as suggested by Saunders *et al.* (1997). Dates on the far right side plot off the scale, so are labelled with their respective ages. Most published dates are radiometric and are labelled with their dating method. All errors, including the new fission track and (U-Th)/He ages, are ±2σ, or marked '?' when the number of standard deviations is unknown. For some dates, a mean age is given from the respective reference. The numbers in brackets refer to the source references, as given in Figure 1.6.

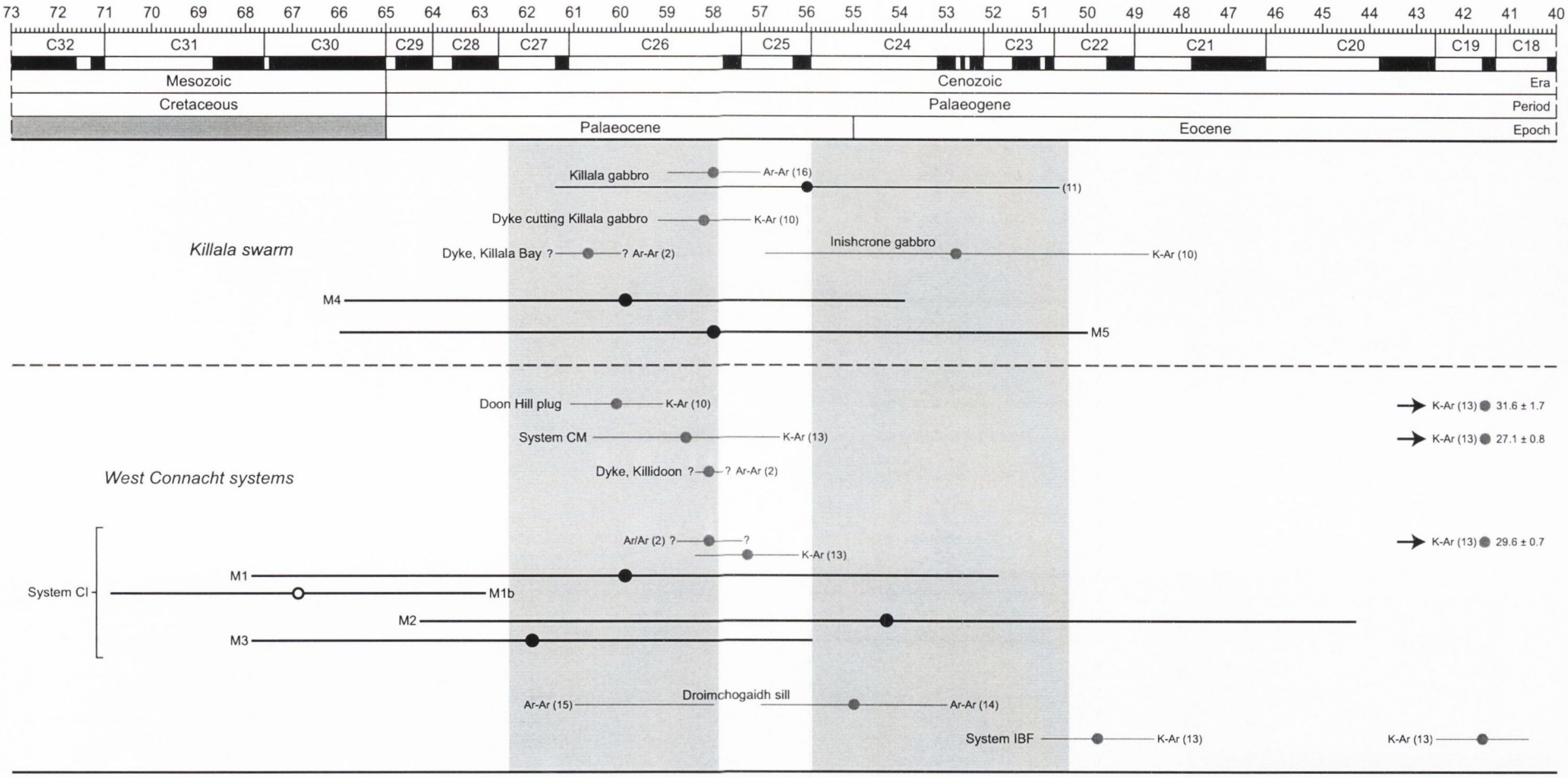

Figure 5.7 continued.

APPENDICES

Appendix 1 Ages for the North Atlantic Igneous Province

Radiometric ages for the North Atlantic Igneous Province.
[a] Denotes where the relative age is unknown compared with those listed above and below.
[b] Indicates where the error is unknown to be quoted at 1σ or 2σ.

Radiometric age (Myr) or age given by magnetic correlation for the different areas	Radiometric technique used (FT = fission track age)	Reference (number as referred to in Figure 1.6 and Figure 5.7)	Magnetic polarity	Comments
West Greenland				
60.5 ± 0.8	Ar-Ar	Storey *et al.* (1998) (31)	reverse	Vaigat & L. & M. Maligât Form. (basalt)
Range C27n	inference	Storey *et al.* (1998) (31)	normal	Base of lavas (L. Vaigat Form.) (basalt)
59.4 ± 1.0	Ar-Ar	Storey et al. (1998) (31)	reverse	U. Maligât Form. (basalt)
Range 61.3-59.3	Ar-Ar	Storey et al. (1998) (31)	normal & reverse	Majority of volcanism
54.8 ± 0.8[a]	Ar-Ar	Storey et al. (1998) (31)	?	Sill & dyke system (Nuussuaq)
53.6 ± 0.6	Ar-Ar	Storey et al. (1998) (31)	?	N-S to NNW-SSE basalt dyke - swarm cuts all lavas (Disko)
52.5 ± 0.4	Ar-Ar	Storey et al. (1998) (31)	?	Tuff from transitional volcanics (Nuussuaq)
34.1 ± 0.4	Ar-Ar	Storey et al. (1998) (31)	?	Lamprophyre dyke - swarm cuts all volcanics (Ubekendt Ejland)
27.4 ± 1.2[a]	Ar-Ar	Storey et al. (1998) (31)	?	Volcanic neck (W of Disko)
Northeast Greenland (Hold With Hope area)				
58.7 ± 1.4	Ar-Ar	Upton *et al.* (1995) (34)	reverse	Base of L. Plateau Lava Series (basalt)
56.7 ± 0.7	Ar-Ar	Upton et al. (1995) (34)	reverse	Dolerite dyke (NE-SW), post U. Plateau Lava Series (basalt)
32.7 ± 2.9	Ar-Ar	Upton *et al.* (1995) (34)	?	Late dolerite intrusion
Southeast Greenland (Scoresby Sund & Kangerdlugssuaq area)				
Range 60-59	inference	Tegner *et al.* (1998) (33)	reverse	L. basalts
56.7 ± 4.3	Ar-Ar	Hansen *et al.* (1995) (9)	reverse	Plateau basalts (Tegner *et al.* 1998) / Main Series (Noble *et al.* 1988)
Range 57-54	K-Ar	Noble *et al.* (1988) (24)	normal & reverse	Plateau basalts (Tegner *et al.* 1998) / Main Series (Noble *et al.* 1988)
56.2 ± 0.6	Ar-Ar	Tegner *et al.* (1998) (33)	?	Dolerite dyke (NE/SW)
55.8 ± 0.8	Ar-Ar	Hirschmann *et al.* (1997) (11)	reverse	Skaergaard Intrusion; others of similar age (Tegner *et al.* 1998)
Range C21r	Ar-Ar	Tegner et al. (1998) (33)	reverse	Igtertiva basalts
47.0 ± 0.4	Ar-Ar	Tegner et al. (1998) (33)	reverse	Igtutarajik gabbro; others of similar age (Tegner *et al.* 1998)
Southeast Greenland SDRS				
61.4 ± 0.6	Ar-Ar	Sinton & Duncan (1998) (28)	reverse	M. Series lavas (dacite)
Range 62-60	Ar-Ar	Sinton & Duncan (1998) (28)	reverse	L. & M. Series lavas (mainly basalt)
51.9 ± 1.2	Ar-Ar	Sinton & Duncan (1998) (28)	reverse	U. Series lavas or a sill (basalt)
Range C24r	inference	Sinton & Duncan (1998) (28)	reverse	Possible lavas
Voring Plateau SDRS				
53.9 ± 2.4	Ar-Ar	Sinton *et al.* (1998) (29)	?	Tuff near bottom of lava pile (mainly basalt)
Range 56-55	inference	Sinton et al. (1998) (29)	normal & reverse	Based on lowest point drilled in lavas
Faeroes (Faeroe Plateau Lava Group)				
58.8 ± 1.0	K-Ar, Ar-Ar	Waagstein *et al.* (2002) (36)	reverse	L. Series, base of drilled
55.8 ± 0.2	K-Ar, Ar-Ar	Waagstein et al. (2002) (36)	reverse	L. Series, top
Range early C26r to early C24r	inference	Waagstein (1988) (35)	normal & reverse	L. Series (basalt)
Range C24r	inference	Waagstein (1988) (35)	normal & reverse	M. & U. Series (basalt)
Hatton Bank/Rockall Plateau SDRS				
57.6 ± 1.3[a]	Ar-Ar	Sinton & Duncan (1998) (28)	reverse	Basalt flow (upper part)
54.5 ± 2.0[ab]	K-Ar	Macintyre & Hamilton (1984) (15)	reverse	Basalt flow (upper part)
52.3 ± 1.7[ab]	K-Ar	Macintyre & Hamilton (1984) (15)	reverse	Basalt flow (upper part)
Range 57-58	inference	Sinton & Duncan (1998) (28)	normal & reverse	Similarities to conjugate margin basalts
Hebrides Shelf Lavas				
63.1 ± 6.4[ab]	K-Ar	Stoker *et al.* (1988) (30)	?	Basalt flow
55.8 ± 1.4[a]	K-Ar	Hitchen & Ritchie (1993) (13)	?	Basalt flow
50.0 ± 1.4[a]	K-Ar	Hitchen & Ritchie (1993) (13)	?	Basalt flow
46.1 ± 5.4[a]	K-Ar	Hitchen & Ritchie (1993) (13)	?	Basalt flow
Northeast Rockall Trough				
55	K-Ar	Morton *et al.* (1988) (18)	?	Basalts above dacites
Slyne Trough				
40-43	inference	Dancer *et al.* (1999) (3)	?	Basalt lavas
Porcupine Basin				
60.6 ± 4.4[b]	K-Ar	Tate & Dobson (1988) (32)	?	Basalt sill
Faeroes-Shetland Intrusive Complex				
81 ± 4.1[b]	K-Ar, Ar-Ar	Fitch *et al.* (1988) (7)	?	Lower sill
55.3 ± 1.4	K-Ar	Hitchen & Ritchie (1993) (13)	?	Gabbro/dolerite sill
53.0 ± 1.0	K-Ar	Hitchen & Ritchie (1993) (13)	?	Gabbro/dolerite sill
49.6 ± 2.3[b]	K-Ar, Ar-Ar	Fitch et al. (1988) (7)	?	Hornfels in sill contact
Range 55-53	K-Ar	Hitchen & Ritchie (1993) (13)	?	Main activity
Erland				
54.8 ± 2.0	K-Ar	Hitchen & Ritchie (1987) (12)	reverse	Dacite (beneath basalt)
Darwin				
54.9 ± 1.7	Ar-Ar	Sinton *et al.* (1998) (28)	?	Dacite (beneath basalt)
Rosemary Bank				
61.9 ± 2.2	K-Ar	Hitchen & Ritchie (1993) (13)	reverse	Basalt - minimum age
Range 69-71	inference	Morton *et al.* (1995) (19)	reverse	Basalt
Rockall				
57 ± 4.0	Rb-Sr	Hawkes *et al.* (1975) (10)	reverse	Granite
54 ± 4.0	Rb-Sr	Hawkes et al. (1975) (10)	reverse	Granite
Hebrides Terrace seamount				
Range 67-60	K-Ar	Ritchie *et al.* (1999) (26)	reverse	Basalt
Blackstones				
57.1 ± 0.9[b]	K-Ar	Mitchell *et al.* (1976) (16)	?	Basalt dredged
The Minch				
59.8 ± 2.2[a]	K-Ar	Hitchen & Ritchie (1993) (13)	?	Basalt clast in conglomerate
57.6 ± 1.6[a]	K-Ar	Hitchen & Ritchie (1993) (13)	?	Dolerite intrusion
Skye				
Range 58.9-60.5	inference	Hamilton *et al.* (1998) (8)	reverse	Basalt lavas
58.9 ± 0.1	U-Pb	Hamilton et al. (1998) (8)	reverse	Cullin gabbro
59.3 ± 1.4	Rb-Sr	Dicken (1981) (4)	normal	Late granite in the Cullins
58.6 ± 0.3	Ar-Ar	Chambers & Pringle (2001) (1)	reverse	Granite in Western Red Hills
53.5 ± 0.8	Rb-Sr	Dicken (1981) (4)	reverse	Eastern Red Hills
Eigg				
63.5 ± 2.0	Ar-Ar	Dagley & Mussett (1986) (2)	reverse	Base of lavas
52.1 ± 1.0	Rb-Sr	Dicken & Jones (1983) (5)	reverse	Pitchstone
Muck				

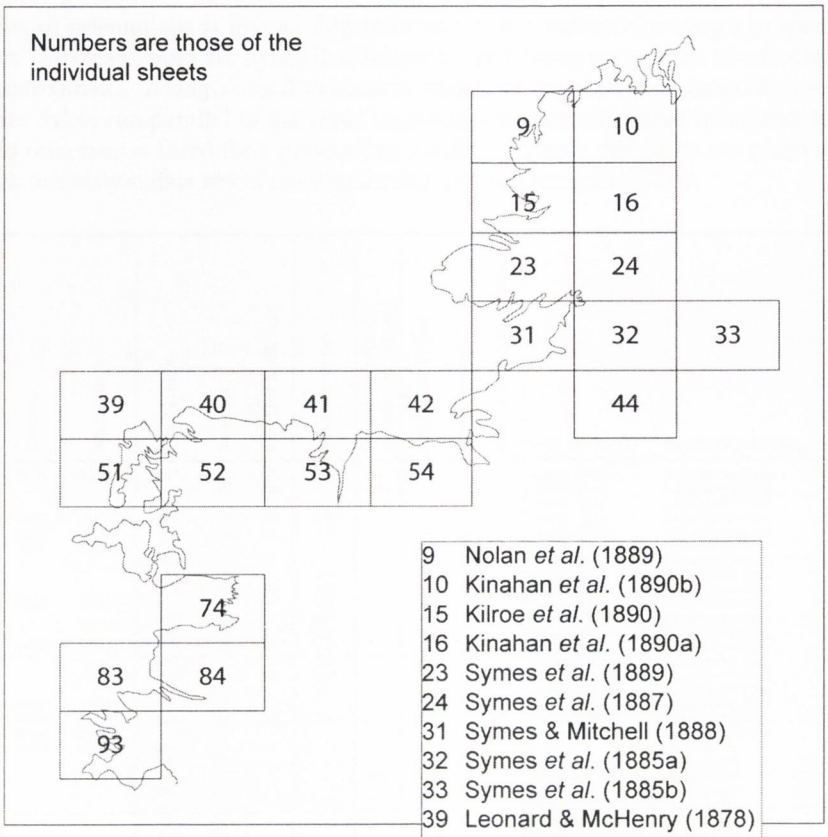

9 Nolan *et al.* (1889)
10 Kinahan *et al.* (1890b)
15 Kilroe *et al.* (1890)
16 Kinahan *et al.* (1890a)
23 Symes *et al.* (1889)
24 Symes *et al.* (1887)
31 Symes & Mitchell (1888)
32 Symes *et al.* (1885a)
33 Symes *et al.* (1885b)
39 Leonard & McHenry (1878)
40 Traill & Leonard (1877)
41 Symes (1877)
42 Symes & Hardman (1883)
44 Wilkinson & Symes (1884)
51 Symes *et al.* (1878)
52 Symes *et al.* (1879)
53 Symes (1876)
54 Symes & Kilroe (1878)
74 Symes & Wilkinson (1870)
83 Kinahan *et al.* (1874a)
84 Kinahan *et al.* (1874b)
93 Kinahan *et al.* (1876)

16a	62977	260022	105	49	NE	0.45						Precamb. (Dal.)	Bennabeola Quartzite Form.
16b	63013	260017	103	32	NE	0.70						Precamb. (Dal.)	Bennabeola Quartzite Form.
17	63620	259730	039	79	SE			098	50	NE		Precamb. (Dal.)	Bennabeola Quartzite Form.
			066	82	SE							Precamb. (Dal.)	Bennabeola Quartzite Form.
			039	90		3.2						Precamb. (Dal.)	Bennabeola Quartzite Form.
			039	90								Precamb. (Dal.)	Bennabeola Quartzite Form.
18a	69072	259209	122	65	SW	0.8		120	79	NE		Precamb. (Dal.)	Ben Levy Grit Form.
18b	69042	259251	169	90		>1.6		033	60	NW		Precamb. (Dal.)	Ben Levy Grit Form.
18c	68979	259298	103			>2		003	75	NW		Precamb. (Dal.)	Ben Levy Grit Form.
			094									Precamb. (Dal.)	Ben Levy Grit Form.
			123	40	NE							Precamb. (Dal.)	Ben Levy Grit Form.
19	64669	260357	030	84	SE	4.3		110	52	NE		Precamb. (Dal.)	Undifferentiated schists
			115									Precamb. (Dal.)	Undifferentiated schists
			063									Precamb. (Dal.)	Undifferentiated schists
			050									Precamb. (Dal.)	Undifferentiated schists
			073									Precamb. (Dal.)	Undifferentiated schists
			026									Precamb. (Dal.)	Undifferentiated schists
			063									Precamb. (Dal.)	Undifferentiated schists
19	64607	260316										Precamb. (Dal.)	Undifferentiated schists
20	64905	260311	064	76	NW	1.3						Precamb. (Dal.)	Undifferentiated schists
21	64830	260713	039	86	NW	1.5						Precamb. (Dal.)	Undifferentiated schists
			034	74	NW							Precamb. (Dal.)	Undifferentiated schists
22	64800	260740	176	81	SW	0.2		125	55	NE		Precamb. (Dal.)	Undifferentiated schists
			070	45	NW							Precamb. (Dal.)	Undifferentiated schists
23a	64794	260748	068	55	NW			125	50	NE		Precamb. (Dal.)	Undifferentiated schists
23b	64778	260750	083	50	NW	0.13						Precamb. (Dal.)	Undifferentiated schists
24	65522	261350	043	83	NW	0.27						Precamb. (Dal.)	Lakes Marble Form.
25a	65434	261419	036	81	NW	4.5	126					Precamb. (Dal.)	Lakes Marble Form.
25b	65614	261494	042									Precamb. (Dal.)	Streamstown Schist Form.
25c	65658	261539	024	84	SE							Precamb. (Dal.)	Streamstown Schist Form.
			040									Precamb. (Dal.)	Streamstown Schist Form.
25	65671	261562										Precamb. (Dal.)	Bennabeola Quartzite Form.
25d	65686	261578	040									Precamb. (Dal.)	Bennabeola Quartzite Form.
			050									Precamb. (Dal.)	Bennabeola Quartzite Form.
25e	65690	261583	047									Precamb. (Dal.)	Bennabeola Quartzite Form.
25f	65710	261597	098	54	NE	6						Precamb. (Dal.)	Bennabeola Quartzite Form.
			049									Precamb. (Dal.)	Bennabeola Quartzite Form.
25g	65725	261601	053									Precamb. (Dal.)	Bennabeola Quartzite Form.
25h	65736	261613	050	73	NW	>3.5						Precamb. (Dal.)	Bennabeola Quartzite Form.
25i	65758	261632	045									Precamb. (Dal.)	Bennabeola Quartzite Form.
25	65781	261657										Precamb. (Dal.)	Bennabeola Quartzite Form.
25	65800	261696						116	70	NE		Precamb. (Dal.)	Bennabeola Quartzite Form.
25j	66019	261852	023	65	SE	>4						Precamb. (Dal.)	Bennabeola Quartzite Form.
25	66044	261914										Precamb. (Dal.)	Bennabeola Quartzite Form.
25k	66087	262032	040			>5-6		130	85	NE		Precamb. (Dal.)	Bennabeola Quartzite Form.
			028	60	SE							Precamb. (Dal.)	Bennabeola Quartzite Form.
26a	64701	262394	014			~3.25						Precamb. (Dal.)	Streamstown Schist Form.
			014									Precamb. (Dal.)	Streamstown Schist Form.
26	64814	262621										Precamb. (Dal.)	Streamstown Schist Form.
26b	64819	262644	009			>2						Precamb. (Dal.)	Streamstown Schist Form.
26c	64829	262689	010	64	SE	>3						Precamb. (Dal.)	Streamstown Schist Form.
26	64850	262711						118	76	NE		Precamb. (Dal.)	Streamstown Schist Form.
26d	64856	262736	030	62	SE							Precamb. (Dal.)	Streamstown Schist Form.
27	68375	263899	006	65	NW	0.2						Precamb. (Dal.)	Ben Levy Grit Form.
			030	70	NW							Precamb. (Dal.)	Ben Levy Grit Form.
			004	66	NW							Precamb. (Dal.)	Ben Levy Grit Form.
			004									Precamb. (Dal.)	Ben Levy Grit Form.
28	69510	263211	082			>4		130	55	NE		Precamb. (Dal.)	Ben Levy Grit Form.
			039									Precamb. (Dal.)	Ben Levy Grit Form.
			053	70	NW							Precamb. (Dal.)	Ben Levy Grit Form.
29a	75478	261572	102	90		5-6						Siliurian	Lettergesh Form.
29b	75510	261561	093									Siliurian	Lettergesh Form.
			087									Siliurian	Lettergesh Form.
			065	75	NW							Siliurian	Lettergesh Form.
29c	75615	261601	044	72	NW	>5.5		132	48	NE		Siliurian	Lettergesh Form.
			057									Siliurian	Lettergesh Form.
29d	75698	261654	078	78	NW							Caledonian	Microgranite / microdiorite
29e	75894	261709	072			9-9.5						Siliurian	Lettergesh Form.
29f	76167	261796	090	81	N	>7.8						Caledonian	Microgranite / microdiorite
29g	76257	261813	076									Caledonian	Microgranite / microdiorite
			054	83	SE							Caledonian	Microgranite / microdiorite
			084									Caledonian	Microgranite / microdiorite
			055	78	NW							Caledonian	Microgranite / microdiorite
29h	76342	261876	*055*			5						Caledonian	Microgranite / microdiorite
29i	76372	261906	098	83	NE							Caledonian	Microgranite / microdiorite
29j	76433	261898	085	87	NW							Caledonian	Microgranite / microdiorite
29k	76455	261927	*160*									Caledonian	Microgranite / microdiorite
			050	82	NW	4.7						Caledonian	Microgranite / microdiorite
29l	76487	261934	077	82	NW							Caledonian	Microgranite / microdiorite
			085	86	SE							Caledonian	Microgranite / microdiorite
			056	82	NW							Caledonian	Microgranite / microdiorite
29m	76563	261939	048			>4.5						Caledonian	Microgranite / microdiorite
			010									Caledonian	Microgranite / microdiorite
			078	81	NW							Caledonian	Microgranite / microdiorite
			079									Caledonian	Microgranite / microdiorite
			076									Caledonian	Microgranite / microdiorite
			070									Caledonian	Microgranite / microdiorite
29n	76690	262009	063			>5						Caledonian	Microgranite / microdiorite
			037									Caledonian	Microgranite / microdiorite
			090	82	S							Caledonian	Microgranite / microdiorite
			060									Caledonian	Microgranite / microdiorite
			103	73	NE							Caledonian	Microgranite / microdiorite
29o	76807	262073	072	85	SE							Caledonian	Microgranite / microdiorite
			080									Caledonian	Microgranite / microdiorite
			075									Caledonian	Microgranite / microdiorite
			095									Caledonian	Microgranite / microdiorite
			072									Caledonian	Microgranite / microdiorite
			112	75	NE							Caledonian	Microgranite / microdiorite
			119	62	NE							Caledonian	Microgranite / microdiorite
			034									Caledonian	Microgranite / microdiorite
29p	77115	262143	060	81	SE							Siliurian	Lettergesh Form.
			040	85	NW							Siliurian	Lettergesh Form.
			051									Siliurian	Lettergesh Form.
			088	90								Siliurian	Lettergesh Form.
			076									Siliurian	Lettergesh Form.
			070									Siliurian	Lettergesh Form.
			060									Siliurian	Lettergesh Form.
			107									Siliurian	Lettergesh Form.
			093									Siliurian	Lettergesh Form.
			075									Siliurian	Lettergesh Form.
29q	77317	262217	055			>3.5						Siliurian	Lettergesh Form.
29r	77807	262311	082	78	NW			108	66	NE		Siliurian	Lettergesh Form.
29s	77984	262320	064			>3.5						Siliurian	Lettergesh Form.
30a	80300	263211	088	86	NW	5.6	160	002	67	SE		Siliurian	Salrock Form.
30b	80160	263144	058	85	SE	>4						Siliurian	Salrock Form.
31a	81119	263443	081	80	SE	>3.5		96	57	NE		Ordovician	Mweelrea Form.
31b	81255	263496	*046*									Ordovician	Mweelrea Form.
31	81355	263514										Ordovician	Mweelrea Form.
32a	75901	267513	048	83	SE	12						Ordovician	Mweelrea Form.
32b	76004	267612	054	85	SE	>9.5						Ordovician	Mweelrea Form.
			053			>11						Ordovician	Mweelrea Form.
32c	76083	267660	050			>11.7		45	25	SE		Ordovician	Mweelrea Form.
			044									Ordovician	Mweelrea Form.
32d	76127	267692	055									Ordovician	Mweelrea Form.
			067									Ordovician	Mweelrea Form.
32e	76341	267837	039	88	NW	>10						Ordovician	Mweelrea Form.
			050	82	NW							Ordovician	Mweelrea Form.
32	76687	268388										Ordovician	Glenummera Form.
32f	76815	268436	060			>14.5						Ordovician	Glenummera Form.
			084									Ordovician	Glenummera Form.
			073	80	SE							Ordovician	Glenummera Form.
32g	76955	268605	057			15						Ordovician	Glenummera Form.

33a	79744	270748	029	65	SE						Ordovician	Sheeffry Form.
33b	80001	271053	057								Ordovician	Sheeffry Form.
33c	80122	271129	042	83	NW			107	85	SW	Ordovician	Sheeffry Form.
33d	80397	271208	067	80	SE	>14.5					Ordovician	Sheeffry Form.
33e	80594	271265	054								Ordovician	Sheeffry Form.
34	82592	272524	**061**	62	NW	>11		100	47	SW	Ordovician	Sheeffry Form.
35a	86211	275625	048	68	SE						Caledonian	Corvock granite
			060	87	NW						Caledonian	Corvock granite
35b	86383	275758	056	80	NW	>12.5					Caledonian	Corvock granite
			052								Caledonian	Corvock granite
35c	86533	275894	043								Caledonian	Corvock granite
			037								Caledonian	Corvock granite
35d	86857	276221	050	82	NW	>13					Ordovician	Derrymore Form.
			078								Ordovician	Derrymore Form.
			069								Ordovician	Derrymore Form.
			060								Ordovician	Derrymore Form.
35e	87102	276322	052								Caledonian	Corvock granite
			045								Caledonian	Corvock granite
35f	87254	276440	057								Caledonian	Corvock granite
			039								Caledonian	Corvock granite
35	87415	276555									Caledonian	Corvock granite
35g	87308	276875	052			>12					Caledonian	Corvock granite
35h	87358	276915	058	78	NW	>10.5					Caledonian	Corvock granite
35i	87523	277054	051	65	NW						Ordovician	Derrymore Form.
35j	87832	277159	087								Ordovician	Derrymore Form.
35k	87972	277201	065	65	NW	>11					Ordovician	Derrymore Form.
35l	88153	277236	080	70	NW	>11					Ordovician	Derrymore Form.
35m	88350	277174	090	71	N						Ordovician	Derrymore Form.
35n	88731	277267	037			>5					Ordovician	Derrymore Form.
35o	88901	277383	050	74	NW	>6		114	57	NE	Ordovician	Derrymore Form.
35p	89131	277797	078	80	SE						Siliurian	Bouris Form.
35q	89393	277813	034	49	SE						Siliurian	Bouris Form.
35r	89526	278067	017	64	SE			103	60	NE	Siliurian	Bouris Form.
			034	49	SE						Siliurian	Bouris Form.
36	94773	280070	075	60	NW	>4		088	18	NW	Siliurian	Lough Nacorra Form.
37	98314	281955	070								Siliurian	Bouris Form.
			050								Siliurian	Bouris Form.
38	50809	265679	*115*			~1		115			Precamb. (Dal.)	Cornamona Marble Form.
39i	50511	266034	112	78	SW	7.9					Precamb. (Dal.)	Ben Levy Grit Form.
			064								Precamb. (Dal.)	Ben Levy Grit Form.
			040								Precamb. (Dal.)	Ben Levy Grit Form.
			038			7.1					Precamb. (Dal.)	Ben Levy Grit Form.
			073								Precamb. (Dal.)	Ben Levy Grit Form.
			121								Precamb. (Dal.)	Ben Levy Grit Form.
			074								Precamb. (Dal.)	Ben Levy Grit Form.
			055								Precamb. (Dal.)	Ben Levy Grit Form.
			097								Precamb. (Dal.)	Ben Levy Grit Form.
			080								Precamb. (Dal.)	Ben Levy Grit Form.
			100								Precamb. (Dal.)	Ben Levy Grit Form.
			070								Precamb. (Dal.)	Ben Levy Grit Form.
			056								Precamb. (Dal.)	Ben Levy Grit Form.
			042								Precamb. (Dal.)	Ben Levy Grit Form.
			054			7.3					Precamb. (Dal.)	Ben Levy Grit Form.
39ii	50511	266034	060	80	SE	2.15		122			Precamb. (Dal.)	Ben Levy Grit Form.
			036								Precamb. (Dal.)	Ben Levy Grit Form.
			068								Precamb. (Dal.)	Ben Levy Grit Form.
			138								Precamb. (Dal.)	Ben Levy Grit Form.
			053								Precamb. (Dal.)	Ben Levy Grit Form.
			088			2.6					Precamb. (Dal.)	Ben Levy Grit Form.
			080								Precamb. (Dal.)	Ben Levy Grit Form.
			064								Precamb. (Dal.)	Ben Levy Grit Form.
			100								Precamb. (Dal.)	Ben Levy Grit Form.
			093								Precamb. (Dal.)	Ben Levy Grit Form.
			100	55	NE						Precamb. (Dal.)	Ben Levy Grit Form.
			065			2.1					Precamb. (Dal.)	Ben Levy Grit Form.
			125								Precamb. (Dal.)	Ben Levy Grit Form.
40	51492	266433	086	65	NW	12		089	59	NW	Precamb. (Dal.)	Ben Levy Grit Form.
41a	52943	266716	084	80	NW	9		080			Precamb. (Dal.)	Ben Levy Grit Form.
			033	66	NW						Precamb. (Dal.)	Ben Levy Grit Form.
			062	76	NW						Precamb. (Dal.)	Ben Levy Grit Form.
			076	80	NW						Precamb. (Dal.)	Ben Levy Grit Form.
			077					103			Precamb. (Dal.)	Ben Levy Grit Form.
41b	53197	266751	077			8.7					Precamb. (Dal.)	Ben Levy Grit Form.
			083	80	NW						Precamb. (Dal.)	Ben Levy Grit Form.
			090								Precamb. (Dal.)	Ben Levy Grit Form.
			110								Precamb. (Dal.)	Ben Levy Grit Form.
41c	53347	266763	084	77	NW	8	007	089	79	NW	Precamb. (Dal.)	Ben Levy Grit Form.
			042	70	NW						Precamb. (Dal.)	Ben Levy Grit Form.
			082								Precamb. (Dal.)	Ben Levy Grit Form.
			110								Precamb. (Dal.)	Ben Levy Grit Form.
42a	54811	267137	091	60	NE	2-3		089	58	NW	Precamb. (Dal.)	Ben Levy Grit Form.
42	54665	267157									Precamb. (Dal.)	Ben Levy Grit Form.
42b	54534	267160	074			>2.8		110	66	NE	Precamb. (Dal.)	Ben Levy Grit Form.
			072					093	70	NE	Precamb. (Dal.)	Ben Levy Grit Form.
42c	54394	267109	092			7.1					Precamb. (Dal.)	Ben Levy Grit Form.
			109	83	SW						Precamb. (Dal.)	Ben Levy Grit Form.
			060					130	73	NE	Precamb. (Dal.)	Ben Levy Grit Form.
			051	82	SE						Precamb. (Dal.)	Ben Levy Grit Form.
			057								Precamb. (Dal.)	Ben Levy Grit Form.
42d	54172	267008	063			8					Precamb. (Dal.)	Ben Levy Grit Form.
			086					105			Precamb. (Dal.)	Ben Levy Grit Form.
			095								Precamb. (Dal.)	Ben Levy Grit Form.
42	54042	266983									Precamb. (Dal.)	Ben Levy Grit Form.
43	53994	267270	112	74	NE	2.75		112	54	NE	Precamb. (Dal.)	Ben Levy Grit Form.
			096								Precamb. (Dal.)	Ben Levy Grit Form.
			116								Precamb. (Dal.)	Ben Levy Grit Form.
			118								Precamb. (Dal.)	Ben Levy Grit Form.
			094	65	SW	2.95		120	65	NE	Precamb. (Dal.)	Ben Levy Grit Form.
43	54116	267243									Precamb. (Dal.)	Ben Levy Grit Form.
43	54351	267211									Precamb. (Dal.)	Ben Levy Grit Form.
44a	54330	267405	063	77	NW	1.5		121	70	NE	Precamb. (Dal.)	Ben Levy Grit Form.
			020								Precamb. (Dal.)	Ben Levy Grit Form.
			026								Precamb. (Dal.)	Ben Levy Grit Form.
44b	54225	267320	054	70	NW	0.85					Precamb. (Dal.)	Ben Levy Grit Form.
			120	62	NE			120			Precamb. (Dal.)	Ben Levy Grit Form.
			040								Precamb. (Dal.)	Ben Levy Grit Form.
			120								Precamb. (Dal.)	Ben Levy Grit Form.
			040								Precamb. (Dal.)	Ben Levy Grit Form.
			120								Precamb. (Dal.)	Ben Levy Grit Form.
			075	55	SE						Precamb. (Dal.)	Ben Levy Grit Form.
			060								Precamb. (Dal.)	Ben Levy Grit Form.
44c	54097	267274	**090**				162				Precamb. (Dal.)	Ben Levy Grit Form.
			025								Precamb. (Dal.)	Ben Levy Grit Form.
			065			0.45					Precamb. (Dal.)	Ben Levy Grit Form.
44d	54050	267255	**050**			0.12					Precamb. (Dal.)	Ben Levy Grit Form.
			065			0.32					Precamb. (Dal.)	Ben Levy Grit Form.
			030								Precamb. (Dal.)	Ben Levy Grit Form.
			120					120			Precamb. (Dal.)	Ben Levy Grit Form.

Data for dykes of the Killala swarm. Dyke numbers are listed from the west end of the swarm (the west side of the Belmullet peninsula), eastwards (see Figure 2.9). Dykes split into Xi, Xii etc. are situated in close proximity to each other and may be part of the same intrusion. Dykes listed as Xa, Xb etc. are different points along the same intrusion where the dyke outcrops over a relatively large distance. In some cases only a grid reference is listed for a point along a dyke. Dyke orientations apply to whole dykes, or segments of dykes when a list of orientations is given. Dip information was derived for only a proportion of the total number of dykes. Strikes in bold are dykes that follow an undulating path of the given orientation. Strikes in italics are approximate. Along coastal exposures (i.e. the vast majority of dykes) strikes of segments are generally listed in the direction out to sea. Dyke widths are given in two columns. The first column lists all widths as measured in the field for the dyke segment to which the width value lies opposite in the table. Values in bold are where the dyke is not changing width along strike, and these values are averaged to give the dyke width (indicated in the second column). Values in italics are those widths that do not represent the true width of the dyke, e.g. a tapering segment. The second column fro width lists the final widths (one value per dyke) of the dykes derived from the averaged values, or where just one value was obtained for a dyke. Not included are any of the widths of, e.g. tapering segments, shown in italics in the first width column. Dyke width in the second column is indicated in the same row as the grid reference for each dyke. Opening directions are given in the horizontal plane, and also sometimes in the 90ical plane where exposure allowed. 'Ext.' refers to an extensional opening, i.e. no element of strike-slip (horizontal plane) or dip-slip (90ical plane). 90ical plane openings are listed with reference to a particular side of the dyke having moved up or down with respect to the opposing side. Where marked in bold, these values of opening directions are displayed in Figure 2.21. Host rock orientation data refers to either bedding or metamorphic fabric. The 'comments' column gives general information on host rock fracture orientations and whether the dyke follows a pre-existing fabric, structure etc.

Dyke Number	Easting	Northing	Dyke Strike	Dyke Dip	Dyke Dip Direction	Dyke Width (m)	Final Dyke Width (m)	Opening Direction (Horizontal Plane)	Opening Direction (90ical Plane)	Baked Margin Width (m)	Host Rock Strike	Host Rock Dip	Host Rock Dip Direction	Host Rock Age	Host Rock Detail	Comments on Relationship between Dykes and Host Rock Structure
1	065988	332666	**052**	83	NW	1.00	1.00				141	48	NE	Precamb. (pre-Dal.)	Annagh Division	no distinct dyke// set
			075											Precamb. (pre-Dal.)	Annagh Division	
			052											Precamb. (pre-Dal.)	Annagh Division	
			061	80	SE									Precamb. (pre-Dal.)	Annagh Division	
2	065968	332704	073	83	SE	3.02	3.02				168	38	NE	Precamb. (pre-Dal.)	Annagh Division	
			086											Precamb. (pre-Dal.)	Annagh Division	
			070											Precamb. (pre-Dal.)	Annagh Division	
3	065495	333214	**055**				0.80	**140**			099	31	NE	Precamb. (pre-Dal.)	Annagh Division	
			066	80	SE	**0.80**								Precamb. (pre-Dal.)	Annagh Division	
			050											Precamb. (pre-Dal.)	Annagh Division	
			050			**0.8**								Precamb. (pre-Dal.)	Annagh Division	
			060											Precamb. (pre-Dal.)	Annagh Division	
4	064391	335848	124	46	NE	1.04	1.04				120	30	NE	Precamb. (pre-Dal.)	Inishkea Division	intrudes fault sub// to foliation
5	064701	337227	113	80	SW	**0.38**	0.38	**007**			124	27	NE	Precamb. (Dal.)	Doonamo Form.	
			097											Precamb. (Dal.)	Doonamo Form.	
			093			**0.38**								Precamb. (Dal.)	Doonamo Form.	
			074											Precamb. (Dal.)	Doonamo Form.	
			115											Precamb. (Dal.)	Doonamo Form.	
6	064474	337562	**071**	80	SE	1	1				116	40	NE	Precamb. (Dal.)	Doonamo Form.	dyke exploits 060, 100 jts
			100											Precamb. (Dal.)	Doonamo Form.	
			070											Precamb. (Dal.)	Doonamo Form.	
			060											Precamb. (Dal.)	Doonamo Form.	
			080											Precamb. (Dal.)	Doonamo Form.	
7	064468	337629	075	65	NW		1.28				115	40	NE	Precamb. (Dal.)	Doonamo Form.	
			050											Precamb. (Dal.)	Doonamo Form.	
			100											Precamb. (Dal.)	Doonamo Form.	
			052	60	NW	1.28								Precamb. (Dal.)	Doonamo Form.	
8i	064809	337578	**116**			**1.45**	1.43							Precamb. (Dal.)	Doonamo Form.	host rock jts 085, 050, 120
			121	86	SW	**1.36**								Precamb. (Dal.)	Doonamo Form.	
			114											Precamb. (Dal.)	Doonamo Form.	
			105			**1.5**								Precamb. (Dal.)	Doonamo Form.	

			085										Precamb. (Dal.)	Doonamo Form.	
			110			**1.4**							Precamb. (Dal.)	Doonamo Form.	
8	064710	337616											Precamb. (Dal.)	Doonamo Form.	
8ii	064809	337582	123	73	NE	**1.08**	1.09						Precamb. (Dal.)	Doonamo Form.	host rock jts 085, 050, 120
			115										Precamb. (Dal.)	Doonamo Form.	
			078										Precamb. (Dal.)	Doonamo Form.	
			114			**1.1**							Precamb. (Dal.)	Doonamo Form.	
			080										Precamb. (Dal.)	Doonamo Form.	
8iii	064809	337583	123	73	NE	**0.61**	0.76						Precamb. (Dal.)	Doonamo Form.	host rock jts 085, 050, 120
			122			**0.7**							Precamb. (Dal.)	Doonamo Form.	
			095										Precamb. (Dal.)	Doonamo Form.	
			114			**0.9**							Precamb. (Dal.)	Doonamo Form.	
			066										Precamb. (Dal.)	Doonamo Form.	
			109										Precamb. (Dal.)	Doonamo Form.	
			105			**0.8**							Precamb. (Dal.)	Doonamo Form.	
			105			**0.78**							Precamb. (Dal.)	Doonamo Form.	
			105	80	SW								Precamb. (Dal.)	Doonamo Form.	
			160										Precamb. (Dal.)	Doonamo Form.	
9	065176	337898	060			**0.74**	0.75	**090**					Precamb. (Dal.)	Aughernagalliagh Quartzite Memb.	host rock occasional jts 050 but no other
			060	82	NW	**0.75**							Precamb. (Dal.)	Aughernagalliagh Quartzite Memb.	
			120	71	SW	**0.75**							Precamb. (Dal.)	Aughernagalliagh Quartzite Memb.	
			090										Precamb. (Dal.)	Aughernagalliagh Quartzite Memb.	
10	065222	338252	065				0.38						Precamb. (Dal.)	Aughernagalliagh Quartzite Memb.	
			065										Precamb. (Dal.)	Aughernagalliagh Quartzite Memb.	
			059			0.38							Precamb. (Dal.)	Aughernagalliagh Quartzite Memb.	
			060										Precamb. (Dal.)	Aughernagalliagh Quartzite Memb.	
			095										Precamb. (Dal.)	Aughernagalliagh Quartzite Memb.	
11	066516	339105	035	65	NW	**0.68**	0.71						Precamb. (Dal.)	Doonamo Form.	follows foliation in places
			000	85	W	**0.46**							Precamb. (Dal.)	Doonamo Form.	
			030										Precamb. (Dal.)	Doonamo Form.	
			045	75	NW	**1**							Precamb. (Dal.)	Doonamo Form.	
			068										Precamb. (Dal.)	Doonamo Form.	
			034										Precamb. (Dal.)	Doonamo Form.	
			125	60	NE								Precamb. (Dal.)	Doonamo Form.	
			040										Precamb. (Dal.)	Doonamo Form.	
			076										Precamb. (Dal.)	Doonamo Form.	
			130	70	NE								Precamb. (Dal.)	Doonamo Form.	
12	066746	339230	040				0.58	**130**					Precamb. (Dal.)	Doonamo Form.	jogs across foliation
			040										Precamb. (Dal.)	Doonamo Form.	
			040	80	NW								Precamb. (Dal.)	Doonamo Form.	
			075	60	SE	*0.36*							Precamb. (Dal.)	Doonamo Form.	
			040			0.58							Precamb. (Dal.)	Doonamo Form.	
			040										Precamb. (Dal.)	Doonamo Form.	
			044										Precamb. (Dal.)	Doonamo Form.	
			037			*0.25*							Precamb. (Dal.)	Doonamo Form.	
			049	65	SE	*0.35*							Precamb. (Dal.)	Doonamo Form.	
13	068214	339457	*104*	*75*	*SW*	~1	1.00		104	75	SW		Precamb. (pre-Dal.)	Annagh Division	follows foliation
14	068540	340151	**083**	85	NW	1.25	1.25		100	35	SW		Precamb. (pre-Dal.)	Annagh Division	host rock jts 090, 070
15	069473	340181	133	82	NE	~0.45	0.45		081	46	SE		Precamb. (pre-Dal.)	Annagh Division	host rock jts 125
16	069443	340339	113	63	NE	0.98	0.98		087	78	SE		Precamb. (pre-Dal.)	Annagh Division	oblique to foliation
			126	63	NE								Precamb. (pre-Dal.)	Annagh Division	
16	069361	340376							111	75	SW		Precamb. (pre-Dal.)	Annagh Division	
17	069752	340477	018	81	NW	~0.7	0.70						Precamb. (pre-Dal.)	Annagh Division	
18	069498	340686	115	77	NE	1.3	1.3		015	20	SE		Precamb. (pre-Dal.)	Annagh Division	
19	069561	340750	084	76	SE	2.66	2.66		154	41	NE		Precamb. (pre-Dal.)	Annagh Division	
			072										Precamb. (pre-Dal.)	Annagh Division	
			083										Precamb. (pre-Dal.)	Annagh Division	
20	069538	340837	102	75	NE	0.15	0.15						Precamb. (pre-Dal.)	Annagh Division	no dyke// jt set
21	069467	341054	110	85	NE	**1.4-0.98**	1.19	**020**	035	75	SE		Precamb. (pre-Dal.)	Annagh Division	no strong dyke// set
			097										Precamb. (pre-Dal.)	Annagh Division	
			099										Precamb. (pre-Dal.)	Annagh Division	
			104										Precamb. (pre-Dal.)	Annagh Division	
			104	87	SW								Precamb. (pre-Dal.)	Annagh Division	
			104	87	SW								Precamb. (pre-Dal.)	Annagh Division	
22a	070476	340861	056	80	NW								Precamb. (pre-Dal.)	Annagh Division	dyke sub// jts at 050-060
22b	070499	340860	074	65	SE	2.5	2.50		008	60	SE		Precamb. (pre-Dal.)	Inishkea Division	dyke sub// jts at 050-060
			063										Precamb. (pre-Dal.)	Inishkea Division	
22c	070504	340851	098			*~1*							Precamb. (pre-Dal.)	Inishkea Division	no apparent dyke// jts
23	070849	340894	097	86	NE	0.93	0.93	**007**	164	37	NE		Precamb. (pre-Dal.)	Inishkea Division	no apparent dyke// jts
			097										Precamb. (pre-Dal.)	Inishkea Division	
			096										Precamb. (pre-Dal.)	Inishkea Division	
24a	071030	339656	*110*	*73*	*NE*	0.85	0.85		010	15	SE		Precamb. (Dal.)	Benmore / Broad Haven Form.	oblique to foliation, no dyke// jts
24b	071145	339631	102	65	NE				012	30	SE		Precamb. (Dal.)	Benmore / Broad Haven Form.	oblique to foliation, no dyke// jts
24	071426	339555											Precamb. (Dal.)	Benmore / Broad Haven Form.	oblique to foliation, no dyke// jts
25a	072036	338392	102	88	NE	>7.5	7.50		050	52	NW		Precamb. (Dal.)	Benmore / Broad Haven Form.	no apparent dyke// jts
25b	072104	338412	084	85	NW	*5-6*							Precamb. (Dal.)	Benmore / Broad Haven Form.	no apparent dyke// jts
			059										Precamb. (Dal.)	Benmore / Broad Haven Form.	
25c	072157	338383	**102**			*1-1.5*							Precamb. (Dal.)	Benmore / Broad Haven Form.	
26	073597	337260	003	64	SE	**0.3**	0.27		136	50	NE		Precamb. (Dal.)	Benmore / Broad Haven Form.	follows foliation

			136	50	NE	**0.24**		
			047	48	NW	*0.08*		
			179	65	NE			
27	074201	337445	097	80	NE	1.3	1.3	**011**
			098	83	NE			
			105					
			105					
			104					
			102					
			098					
			105					
			092					
27	074279	337423						
28	074326	337091	060				1.20	
			005	52	SE	*0.3*		
			060	89	NW	1.2		
			072					
29	074407	336935	106	87	NE	1.85	1.85	022
			110					
			122	80	NE			
			111					
30	074613	337197	*057*	*72*	*NW*	~1	1.00	
			065					
31	074690	337336	105	88	SW	1.29	1.29	
			114					
32	074728	337466	105	85	NE	1.13	1.13	013
			103					
			103					
33	074843	337482	102	75	NE	0.75	0.75	
34	074847	337314	108	80	NE	1.5	1.5	
35	075036	337279	049	60	NW	*0-0.3*		**145**
			083	86	NW	**0.86**	0.93	
			052	58	NW	**1**		
36	075016	337182	105	85	NE	**0.7-0.8**	0.75	
37	075149	336533	120	81	SW	1.85	1.85	
38a	075527	336424	060	60	SE	1.6	1.6	
38b	075622	336446	*085*	*55*	*SE*			
38c	075696	336359	153	83	SW			
39	076473	336745	090	60	N	1.7	1.7	
			082					
40	076567	336894	093				0.75	**013**
			037	57	SE	*0.35*		
			119	59	SW	*0.54*		
			107	58	SW			
			126	58	SW	*0.61*		
			118			0.75		
			076	63	SE			
			104	80	NE			
			120			*0.6*		
			086					
			060	74	SE	*0.53*		
			122	66	SW	*0.64*		
			130	85	NE			
			071	60	SE	*0.59*		
			140	80	NE			
41	076909	336750	096	45	SW	1.8	1.8	
			090					
42	078123	336095	051	50	SE	>3	3.00	
			078	49	SE			
43a	078002	336641	123			*1.25*		
			097	75	SW			
43b	078015	336676	020	70	SE	*0.8*		
43c	078041	336763	028	80	NW	1.8	1.80	
44	078135	336967	**100**			1.2	1.20	**022**
			100	83	NE			
			095					
			130			*0.55*		
45	079956	338203	153	75	NE	~4	4.00	
46	080352	338345	176	77	NE	1.1	1.1	
			170					
47a	080631	338397	087	48	SE	*0.1-0.07*	0.40	
47b	080646	338397	085			**0.37**		
47c	080689	338408	053			**0.42**		
48	080646	338388	000			0.55	0.55	
			165					
49i	080949	338452	080			0.66	0.66	
			082			*0.5*		
			070			*0.35*		
			082			*0.1*		

			Precamb. (Dal.)	Benmore / Broad Haven Form.	
			Precamb. (Dal.)	Benmore / Broad Haven Form.	
			Precamb. (Dal.)	Benmore / Broad Haven Form.	
008	55	SE	Precamb. (Dal.)	Benmore / Broad Haven Form.	dyke sub// jts
			Precamb. (Dal.)	Benmore / Broad Haven Form.	
			Precamb. (Dal.)	Benmore / Broad Haven Form.	
			Precamb. (Dal.)	Benmore / Broad Haven Form.	
			Precamb. (Dal.)	Benmore / Broad Haven Form.	
			Precamb. (Dal.)	Benmore / Broad Haven Form.	
			Precamb. (Dal.)	Benmore / Broad Haven Form.	
			Precamb. (Dal.)	Benmore / Broad Haven Form.	
			Precamb. (Dal.)	Benmore / Broad Haven Form.	
			Precamb. (Dal.)	Benmore / Broad Haven Form.	dyke sub// jts
014	45	SE	Precamb. (Dal.)	Benmore / Broad Haven Form.	jogs across foliation
			Precamb. (Dal.)	Benmore / Broad Haven Form.	
			Precamb. (Dal.)	Benmore / Broad Haven Form.	
			Precamb. (Dal.)	Benmore / Broad Haven Form.	
			Precamb. (Dal.)	Benmore / Broad Haven Form.	dyke sub// jts
			Precamb. (Dal.)	Benmore / Broad Haven Form.	
			Precamb. (Dal.)	Benmore / Broad Haven Form.	
			Precamb. (Dal.)	Benmore / Broad Haven Form.	
163	50	NE	Precamb. (Dal.)	Benmore / Broad Haven Form.	host rock jts 050-060
			Precamb. (Dal.)	Benmore / Broad Haven Form.	
028	43	SE	Precamb. (Dal.)	Benmore / Broad Haven Form.	
			Precamb. (Dal.)	Benmore / Broad Haven Form.	
004	55	SE	Precamb. (Dal.)	Benmore / Broad Haven Form.	dyke sub// jts in places
			Precamb. (Dal.)	Benmore / Broad Haven Form.	
			Precamb. (Dal.)	Benmore / Broad Haven Form.	
			Precamb. (Dal.)	Benmore / Broad Haven Form.	
			Precamb. (Dal.)	Benmore / Broad Haven Form.	dyke sub// jts
173	73	NE	Precamb. (Dal.)	Benmore / Broad Haven Form.	host rock jts 050
			Precamb. (Dal.)	Benmore / Broad Haven Form.	
			Precamb. (Dal.)	Benmore / Broad Haven Form.	
			Precamb. (Dal.)	Benmore / Broad Haven Form.	
024	53	SE	Precamb. (Dal.)	Benmore / Broad Haven Form.	dyke sub// jts
062	60	SE	Precamb. (Dal.)	Strahlaghy Quartzite Form.	follows foliation
			Precamb. (Dal.)	Pollacappul Form.	follows foliation
			Precamb. (Dal.)	Doon-na-Dell Schist Form.	oblique to foliation
042	58	SE	Precamb. (Dal.)	Inver Schist Form.	dyke sub// jts
			Precamb. (Dal.)	Inver Schist Form.	
			Precamb. (Dal.)	Inver Schist Form.	
			Precamb. (Dal.)	Inver Schist Form.	
			Precamb. (Dal.)	Inver Schist Form.	
			Precamb. (Dal.)	Inver Schist Form.	
			Precamb. (Dal.)	Inver Schist Form.	
			Precamb. (Dal.)	Inver Schist Form.	
			Precamb. (Dal.)	Inver Schist Form.	
			Precamb. (Dal.)	Inver Schist Form.	
			Precamb. (Dal.)	Inver Schist Form.	
			Precamb. (Dal.)	Inver Schist Form.	
			Precamb. (Dal.)	Inver Schist Form.	
			Precamb. (Dal.)	Inver Schist Form.	
			Precamb. (Dal.)	Inver Schist Form.	
			Precamb. (Dal.)	Inver Schist Form.	
			Precamb. (Dal.)	Inver Schist Form.	
088	50	SE	Precamb. (Dal.)	Inver Schist Form.	follows foliation
			Precamb. (Dal.)	Inver Schist Form.	
065	55	SE	Precamb. (Dal.)	Inver Schist Form.	dyke follows fault and foliation
			Precamb. (Dal.)	Inver Schist Form.	
076	47	SE	Precamb. (Dal.)	Inver Schist Form.	no apparent dyke// jts
			Precamb. (Dal.)	Inver Schist Form.	
065	50	SE	Precamb. (Dal.)	Inver Schist Form.	no apparent dyke// jts
			Precamb. (Dal.)	Inver Schist Form.	no apparent dyke// jts
081	65	SE	Precamb. (Dal.)	Inver Schist Form.	
			Precamb. (Dal.)	Inver Schist Form.	
			Precamb. (Dal.)	Inver Schist Form.	
			Precamb. (Dal.)	Inver Schist Form.	
			Precamb. (Dal.)	Benmore / Broad Haven Form.	
			Precamb. (Dal.)	Benmore / Broad Haven Form.	may be following N-S fault
			Precamb. (Dal.)	Benmore / Broad Haven Form.	
087	48	SE	Precamb. (Dal.)	Benmore / Broad Haven Form.	follows foliation
			Precamb. (Dal.)	Benmore / Broad Haven Form.	follows foliation
			Precamb. (Dal.)	Benmore / Broad Haven Form.	follows foliation
			Precamb. (Dal.)	Benmore / Broad Haven Form.	
			Precamb. (Dal.)	Benmore / Broad Haven Form.	
084	60	SE	Precamb. (Dal.)	Benmore / Broad Haven Form.	follows foliation and jogs across 050 jts
			Precamb. (Dal.)	Benmore / Broad Haven Form.	
			Precamb. (Dal.)	Benmore / Broad Haven Form.	
			Precamb. (Dal.)	Benmore / Broad Haven Form.	

			083			*0.45*		
49ii	080960	338489						
49ii	081040	338511	079	59	SE	1.1	1.1	
50	082278	338107	020	70	NW	1.77	1.77	**032**
			020	71	NW	*0.21*		
			138	73	SW			
			145			0.28	0.28	
			139					
			100	87	SW	*0.24*		
51	082389	337909	115	79	SW	0.22	0.22	
52	082338	339199	104	64	SW	1.98	1.98	
53	082398	339277	103	81	SW	2.02	2.02	
54	082506	339494	117	78	NE	1.2	1.2	
			129	76	NE			
55	085015	338904	124	66	SW	>2	2.00	
56	085011	338869	115	70	SW	>1.3	1.30	
57a	082044	339567	112	88	SW	**0.79**	0.52	
57b	081959	339566	107	89	SW	**0.37**		
			090					
57c	081884	339585	107	88	SW	**0.4**		
58	080079	340558	078	73	NW	5	5	
			083	82	NW			
59	079866	340101	144	80	NE	**0.3**	0.39	**056**
			148	75	NE	**0.37**		
			159	80	NE	**0.42**		
			130					
			143			**0.41**		
			152	82	NE	**0.43**		
59	079816	340176						
60	079829	340203	066	80	SE	**0.16**	0.13	
			088					
			082			**0.1**		
61	079897	340371	152	69	NE	**2.2**	2.05	**048**
			132	80	NE			
			144	80	NE			
			125					
			142					
			130			**1.9**		
61	079852	340433						
62	079967	340561	108	82	SW	4.3	4.3	
			139	85	SW			
			120	80	NE			
			104					
63	080002	340715	090	81	S	1.28	1.28	
			071	82	SE	1.5	1.5	
			110			*0.14*		
			080					
			117			*1.18*		
			124			*1.2*		
64	079659	340981	144	85	NE	1.88	1.88	
65	078888	341268	107	70	NE	~1	1.00	
			140	80	SW			
			107					
			115					
65	079188	341183						
66	082626	345069	117	87	SW	>2.5	2.50	
67	083139	344898						
67	083271	344804	*118*	*68*	*SW*	4.55	4.55	
68	084033	344541	126	76	SW	**~3.5-4**	3.75	
69	083965	344146	127			>2.1	2.10	
			104	85	NE			
			112					
70i	084378	344352	116			0.07	0.07	
70ii	084413	344351	117	80	NE	>3.5	3.50	
71	086068	344781	110			~3	3.00	
72i	088704	342749	*102*	*75*	*NE*	2 (total 72i/ii)	2.00	
72ii	088704	342748	*102*					
73	088951	342749	086	77	NW	1.6	1.60	
			085	80	NW			
			120					
			070	79	NW	*0.82*		
			065					
			103					
			065					
			103					
74	090119	340159	136	68	NE	>1.6	1.60	
75	091405	339335	113	79	SW	>3.3	3.30	
76	091645	339422	114			>3	3.00	
77	098363	342453	128	80	SW	3.6	3.6	

			Precamb. (Dal.)	Benmore / Broad Haven Form.	
			Precamb. (Dal.)	Benmore / Broad Haven Form.	
			Precamb. (Dal.)	Benmore / Broad Haven Form.	
105	85	SW	Precamb. (Dal.)	Benmore / Broad Haven Form.	host rock jts 028
			Precamb. (Dal.)	Benmore / Broad Haven Form.	
			Precamb. (Dal.)	Benmore / Broad Haven Form.	
			Precamb. (Dal.)	Benmore / Broad Haven Form.	
			Precamb. (Dal.)	Benmore / Broad Haven Form.	
			Precamb. (Dal.)	Benmore / Broad Haven Form.	
115	79	SW	Precamb. (Dal.)	Benmore / Broad Haven Form.	follows foliation
103	55	SW	Precamb. (Dal.)	Broad Haven Form.	follows foliation
109	72	SW	Precamb. (Dal.)	Broad Haven Form.	follows foliation
115	63	SW	Precamb. (Dal.)	Broad Haven Form.	follows foliation
			Precamb. (Dal.)	Broad Haven Form.	
123	68	SW	Precamb. (Dal.)	Broad Haven Form.	host rock jts 020; follows foliation
110	70	SW	Precamb. (Dal.)	Broad Haven Form.	follows foliation
112	88	SW	Precamb. (Dal.)	Broad Haven Form.	follows foliation
107	89	SW	Precamb. (Dal.)	Broad Haven Form.	mainly follows foliation
			Precamb. (Dal.)	Broad Haven Form.	
107	88	SW	Precamb. (Dal.)	Broad Haven Form.	follows foliation
083	84	NW	Precamb. (Dal.)	Broad Haven Form.	follows foliation
			Precamb. (Dal.)	Broad Haven Form.	
080	88	SE	Precamb. (Dal.)	Broad Haven Form.	host rock jts 130
			Precamb. (Dal.)	Broad Haven Form.	
			Precamb. (Dal.)	Broad Haven Form.	
			Precamb. (Dal.)	Broad Haven Form.	
			Precamb. (Dal.)	Broad Haven Form.	
			Precamb. (Dal.)	Broad Haven Form.	
			Precamb. (Dal.)	Broad Haven Form.	
			Precamb. (Dal.)	Broad Haven Form.	follows swings in foliation
			Precamb. (Dal.)	Broad Haven Form.	
			Precamb. (Dal.)	Broad Haven Form.	
083	84	NW	Precamb. (Dal.)	Broad Haven Form.	host rock jts 140-160; dyke follows these
			Precamb. (Dal.)	Broad Haven Form.	
			Precamb. (Dal.)	Broad Haven Form.	
			Precamb. (Dal.)	Broad Haven Form.	
			Precamb. (Dal.)	Broad Haven Form.	
			Precamb. (Dal.)	Broad Haven Form.	
			Precamb. (Dal.)	Broad Haven Form.	
065	85	SE	Precamb. (Dal.)	Broad Haven Form.	host rock jts 120
			Precamb. (Dal.)	Broad Haven Form.	
			Precamb. (Dal.)	Broad Haven Form.	
			Precamb. (Dal.)	Broad Haven Form.	
070	86	SE	Precamb. (Dal.)	Broad Haven Form.	
			Precamb. (Dal.)	Broad Haven Form.	
			Precamb. (Dal.)	Broad Haven Form.	
			Precamb. (Dal.)	Broad Haven Form.	
			Precamb. (Dal.)	Broad Haven Form.	
			Precamb. (Dal.)	Broad Haven Form.	
			Precamb. (Dal.)	Broad Haven Form.	follows foliation
107	60	SW	Precamb. (Dal.)	Broad Haven Form.	follows foliation
			Precamb. (Dal.)	Broad Haven Form.	
			Precamb. (Dal.)	Broad Haven Form.	
			Precamb. (Dal.)	Broad Haven Form.	
			Precamb. (Dal.)	Broad Haven Form.	follows foliation
060	35	NW	Precamb. (Dal.)	Benmore Form.	
			Precamb. (Dal.)	Benmore Form.	
			Precamb. (Dal.)	Benmore Form.	
037	48	NW	Precamb. (Dal.)	Benmore Form.	host rock jts 115-125
037	48	NW	Precamb. (Dal.)	Benmore Form.	host rock jts 115-120
			Precamb. (Dal.)	Benmore Form.	
			Precamb. (Dal.)	Benmore Form.	
			Precamb. (Dal.)	Benmore Form.	
034	38	SE	Precamb. (Dal.)	Benmore Form.	host rock jts 101 in some beds
			Precamb. (Dal.)	Benmore Form.	
025	35	SE	Precamb. (Dal.)	Benmore Form.	host rock jts 120
			Precamb. (Dal.)	Benmore Form.	
040	25	SE	Precamb. (Dal.)	Benmore Form.	host rock jts 065, 103, 084
			Precamb. (Dal.)	Benmore Form.	
			Precamb. (Dal.)	Benmore Form.	
			Precamb. (Dal.)	Benmore Form.	
			Precamb. (Dal.)	Benmore Form.	
			Precamb. (Dal.)	Benmore Form.	
			Precamb. (Dal.)	Benmore Form.	
			Precamb. (Dal.)	Benmore Form.	
060	82	SE	Precamb. (Dal.)	Broad Haven Form.	
035	50	NW	Precamb. (Dal.)	Broad Haven Form.	
			Precamb. (Dal.)	Broad Haven Form.	
128	27	SW	Precamb. (Dal.)	Broad Haven Form.	host rock jts 127

			117										Precamb. (Dal.)	Broad Haven Form.	
			097										Precamb. (Dal.)	Broad Haven Form.	
			123										Precamb. (Dal.)	Broad Haven Form.	
			142										Precamb. (Dal.)	Broad Haven Form.	
78	099316	341815	118				2.2					144	5 NE	Precamb. (Dal.)	Broad Haven Form.	host rock jts 118
			136											Precamb. (Dal.)	Broad Haven Form.	
			117	82	SW	2.2								Precamb. (Dal.)	Broad Haven Form.	
79	099372	339885	116	79	NE		6.00							Precamb. (Dal.)	Broad Haven Form.	
			114			>6								Precamb. (Dal.)	Broad Haven Form.	
80	100066	336177	*100*	*85*	*SW*	7	7							Precamb. (Dal.)	Broad Haven Form.	
81i	108831	332902	114	88	NE	0.75	0.75							Carboniferous	Downpatrick Form.	
81ii	108831	332897	085			0.88	0.88							Carboniferous	Downpatrick Form.	
82a	109519	340748	125			*0.01*	0.40							Carboniferous	Moyny Limestone Form.	
			127	85	SW	*0.05*								Carboniferous	Moyny Limestone Form.	
			120											Carboniferous	Moyny Limestone Form.	
			120											Carboniferous	Moyny Limestone Form.	
			120											Carboniferous	Moyny Limestone Form.	
			120											Carboniferous	Moyny Limestone Form.	
			122											Carboniferous	Moyny Limestone Form.	
			122											Carboniferous	Moyny Limestone Form.	
			122			*0.11*								Carboniferous	Moyny Limestone Form.	
			120											Carboniferous	Moyny Limestone Form.	
			113											Carboniferous	Moyny Limestone Form.	
			119			*0.15*								Carboniferous	Moyny Limestone Form.	
			117											Carboniferous	Moyny Limestone Form.	
			115	82	SW	*0.13*								Carboniferous	Moyny Limestone Form.	
			118											Carboniferous	Moyny Limestone Form.	
			112											Carboniferous	Moyny Limestone Form.	
			112											Carboniferous	Moyny Limestone Form.	
			115			*0.12*								Carboniferous	Moyny Limestone Form.	
			121											Carboniferous	Moyny Limestone Form.	
			121											Carboniferous	Moyny Limestone Form.	
			121			*0.06*								Carboniferous	Moyny Limestone Form.	
			114	85	SW									Carboniferous	Moyny Limestone Form.	
			134			*0.05*								Carboniferous	Moyny Limestone Form.	
			117	89	SW	*0.15*								Carboniferous	Moyny Limestone Form.	
			116											Carboniferous	Moyny Limestone Form.	
			115			*0.23*								Carboniferous	Moyny Limestone Form.	
			117			*0.29*								Carboniferous	Moyny Limestone Form.	
			123			*0.3*								Carboniferous	Moyny Limestone Form.	
			120			*0.32*								Carboniferous	Moyny Limestone Form.	
			121											Carboniferous	Moyny Limestone Form.	
			128			0.4								Carboniferous	Moyny Limestone Form.	
82b	109284	340936	050				0.24					026	9 NW	Carboniferous	Moyny Limestone Form.	dyke sub// jts in places
			100											Carboniferous	Moyny Limestone Form.	
			083											Carboniferous	Moyny Limestone Form.	
			094											Carboniferous	Moyny Limestone Form.	
			089											Carboniferous	Moyny Limestone Form.	
			093											Carboniferous	Moyny Limestone Form.	
			098	85	SW	**0.22**								Carboniferous	Moyny Limestone Form.	
			098											Carboniferous	Moyny Limestone Form.	
			092	85	SW									Carboniferous	Moyny Limestone Form.	
			095											Carboniferous	Moyny Limestone Form.	
			095											Carboniferous	Moyny Limestone Form.	
			092			**0.25**								Carboniferous	Moyny Limestone Form.	
			097											Carboniferous	Moyny Limestone Form.	
83	110796	340640	098	83	NE	0.73	0.73	**175**	ext.			045	4 NW	Carboniferous	Minnaun Sandstone Form.	dyke sub// jts in places
			096	82	NE	*0.73*								Carboniferous	Minnaun Sandstone Form.	
			083			*0.17*								Carboniferous	Minnaun Sandstone Form.	
			090			*0.15*								Carboniferous	Minnaun Sandstone Form.	
			073											Carboniferous	Minnaun Sandstone Form.	
			081											Carboniferous	Minnaun Sandstone Form.	
			081											Carboniferous	Minnaun Sandstone Form.	
			094											Carboniferous	Minnaun Sandstone Form.	
			096			*0.55*								Carboniferous	Minnaun Sandstone Form.	
			084											Carboniferous	Minnaun Sandstone Form.	
			084			*0.5*								Carboniferous	Minnaun Sandstone Form.	
			085	90T		*0.48*								Carboniferous	Minnaun Sandstone Form.	
			085											Carboniferous	Minnaun Sandstone Form.	
			085			*0.19*								Carboniferous	Minnaun Sandstone Form.	
			080			*0.15*								Carboniferous	Minnaun Sandstone Form.	
			077			*0.15*								Carboniferous	Minnaun Sandstone Form.	
			023											Carboniferous	Minnaun Sandstone Form.	
			069											Carboniferous	Minnaun Sandstone Form.	
			078			*0.27*								Carboniferous	Minnaun Sandstone Form.	
			083	82	NW	*0.45*								Carboniferous	Minnaun Sandstone Form.	
			082											Carboniferous	Minnaun Sandstone Form.	
			082			*0.46*								Carboniferous	Minnaun Sandstone Form.	
84	110987	340787												Carboniferous	Minnaun Sandstone Form.	

84	110881	340799												Carboniferous	Minnaun Sandstone Form.	
84	111237	340740	100	82	NE	**3.85**	3.68							Carboniferous	Minnaun Sandstone Form.	dyke sub// jts in places
			094											Carboniferous	Minnaun Sandstone Form.	
			102											Carboniferous	Minnaun Sandstone Form.	
			103											Carboniferous	Minnaun Sandstone Form.	
			105			**3.5**								Carboniferous	Minnaun Sandstone Form.	
			100											Carboniferous	Minnaun Sandstone Form.	
			104											Carboniferous	Minnaun Sandstone Form.	
85	111348	341172	079				1.77	169	ext.					Carboniferous	Minnaun Sandstone Form.	dyke sub// jts in places
			079											Carboniferous	Minnaun Sandstone Form.	
			079											Carboniferous	Minnaun Sandstone Form.	
			080	89	NW	**1.7**								Carboniferous	Minnaun Sandstone Form.	
			070											Carboniferous	Minnaun Sandstone Form.	
			083	78	SE	**1.55**								Carboniferous	Minnaun Sandstone Form.	
			073	78	SE									Carboniferous	Minnaun Sandstone Form.	
			079			**1.9**								Carboniferous	Minnaun Sandstone Form.	
			077	87	NW	**1.93**								Carboniferous	Minnaun Sandstone Form.	
86a	111997	341878	110				0.89							Carboniferous	Downpatrick Form.	
			106	83	SW	>0.89								Carboniferous	Downpatrick Form.	
			107											Carboniferous	Downpatrick Form.	
			106											Carboniferous	Downpatrick Form.	
86	112153	341835												Carboniferous	Downpatrick Form.	
86b	112235	341817	105	80	SW	**>0.8**	0.76		S side down 4 cm			127	5	NE	Carboniferous	Downpatrick Form.	
			102	80	NE	**0.71**									Carboniferous	Downpatrick Form.	
			101												Carboniferous	Downpatrick Form.	
			108												Carboniferous	Downpatrick Form.	
87	112381	342093	112				0.8	**018**	S side up 4 cm			127	5	NE	Carboniferous	Downpatrick Form.	host rock jts 105-112
			116												Carboniferous	Downpatrick Form.	
			116												Carboniferous	Downpatrick Form.	
			120												Carboniferous	Downpatrick Form.	
			116												Carboniferous	Downpatrick Form.	
			113												Carboniferous	Downpatrick Form.	
			111			0.8									Carboniferous	Downpatrick Form.	
			111												Carboniferous	Downpatrick Form.	
			112	85	SW										Carboniferous	Downpatrick Form.	
			116												Carboniferous	Downpatrick Form.	
			119												Carboniferous	Downpatrick Form.	
			105												Carboniferous	Downpatrick Form.	
			113												Carboniferous	Downpatrick Form.	
			113												Carboniferous	Downpatrick Form.	
			123												Carboniferous	Downpatrick Form.	
			116												Carboniferous	Downpatrick Form.	
			116												Carboniferous	Downpatrick Form.	
88	114180	341762	069	85	NW	**2.15**	2.08								Carboniferous	Downpatrick Form.	host rock jts 091, 070
			085			**2.3**									Carboniferous	Downpatrick Form.	
			091	85	NE										Carboniferous	Downpatrick Form.	
			088			**1.8**									Carboniferous	Downpatrick Form.	
89	114481	341645	*094*	*89*	*SW*	~0.9	0.90								Carboniferous	Moyny Limestone Form.	host rock jts 094
90a	120103	337424	096	87	SW		5.00	**006**	ext.						Carboniferous	Mullaghmore Sandstone Form.	host rock jts 160-173
90b	119972	337413	**093**	81	SW			001		0.75 N side					Carboniferous	Mullaghmore Sandstone Form.	host rock jts 160-172
90c	119866	337416	**092**			**5.1**									Carboniferous	Mullaghmore Sandstone Form.	host rock jts 160-171
90d	119806	337442	**083**	83	SE	**4.9**									Carboniferous	Mullaghmore Sandstone Form.	host rock jts 160-170
91a	120121	337497	081	87	SE	**2.9**	2.60								Carboniferous	Mullaghmore Sandstone Form.	
91b	119909	337524	**085**	86	SE	**2.3**		175				000	4	NE	Carboniferous	Mullaghmore Sandstone Form.	host rock jts 095, 104
92	120465	338124	091	86	SW	**0.82**	0.77	001							Carboniferous	Mullaghmore Sandstone Form.	host rock jts 065, 100
			091												Carboniferous	Mullaghmore Sandstone Form.	
			082												Carboniferous	Mullaghmore Sandstone Form.	
			095			**0.8**									Carboniferous	Mullaghmore Sandstone Form.	
			094												Carboniferous	Mullaghmore Sandstone Form.	
			095			**0.73**									Carboniferous	Mullaghmore Sandstone Form.	
			097			**0.73**									Carboniferous	Mullaghmore Sandstone Form.	
			098												Carboniferous	Mullaghmore Sandstone Form.	
93	120482	338154	096	87	SW		0.87	005	ext.						Carboniferous	Mullaghmore Sandstone Form.	host rock jts 101, 102
			094			**0.97**									Carboniferous	Mullaghmore Sandstone Form.	
			094												Carboniferous	Mullaghmore Sandstone Form.	
			103			**0.9**									Carboniferous	Mullaghmore Sandstone Form.	
			070												Carboniferous	Mullaghmore Sandstone Form.	
			101												Carboniferous	Mullaghmore Sandstone Form.	
			102												Carboniferous	Mullaghmore Sandstone Form.	
			090			**0.75**									Carboniferous	Mullaghmore Sandstone Form.	
			074												Carboniferous	Mullaghmore Sandstone Form.	
			100												Carboniferous	Mullaghmore Sandstone Form.	
94	120547	338212	101			**0.18**	0.21	**008**	S side up 2.5 cm			018	3	SE	Carboniferous	Mullaghmore Sandstone Form.	host rock jts 094-096
			102												Carboniferous	Mullaghmore Sandstone Form.	
			102												Carboniferous	Mullaghmore Sandstone Form.	
			102												Carboniferous	Mullaghmore Sandstone Form.	
			097												Carboniferous	Mullaghmore Sandstone Form.	
			104			**0.15**									Carboniferous	Mullaghmore Sandstone Form.	
			070												Carboniferous	Mullaghmore Sandstone Form.	

			102	79	SW							Carboniferous	Mullaghmore Sandstone Form.		
			093									Carboniferous	Mullaghmore Sandstone Form.		
			099									Carboniferous	Mullaghmore Sandstone Form.		
			120			**0.2**						Carboniferous	Mullaghmore Sandstone Form.		
			101									Carboniferous	Mullaghmore Sandstone Form.		
			102			**0.22**						Carboniferous	Mullaghmore Sandstone Form.		
			065									Carboniferous	Mullaghmore Sandstone Form.		
			108									Carboniferous	Mullaghmore Sandstone Form.		
			108									Carboniferous	Mullaghmore Sandstone Form.		
			104			**0.29**						Carboniferous	Mullaghmore Sandstone Form.		
			088									Carboniferous	Mullaghmore Sandstone Form.		
			101									Carboniferous	Mullaghmore Sandstone Form.		
			098									Carboniferous	Mullaghmore Sandstone Form.		
			068									Carboniferous	Mullaghmore Sandstone Form.		
			102	81	SW							Carboniferous	Mullaghmore Sandstone Form.		
95	121095	336052	103	87	SW	1.17	1.17	**013**	0.3	135	4	NE	Carboniferous	Mullaghmore Sandstone Form.	host rock jts 095-100, 099
			100										Carboniferous	Mullaghmore Sandstone Form.	
96	119939	333214	108	79	SW	1.4	1.4						Tertiary	Killala gabbro	
97i	120240	332743	094	90			3.6						Tertiary	Killala gabbro	host rock jts 087
			084	82	SE	3.6							Tertiary	Killala gabbro	
97ii	120240	332741	106	89	NE	2.3	2.3						Tertiary	Killala gabbro	
98	120274	332775	102	82	SW	1.59	1.59						Tertiary	Killala gabbro	host rock jts 085-097
99	122287	333312	*080*	*45*	*NW*	~2	2.00						Carboniferous	Mullaghmore Sandstone Form.	
100	122272	333183	107	58	SW	**1.08**	1.08	ext.					Tertiary	Killala gabbro	host rock jts 090
			107	58	SW	**1.08**							Tertiary	Killala gabbro	
			107										Tertiary	Killala gabbro	
101i	122299	333128	065			*0.55*	0.65						Tertiary	Killala gabbro	
			010										Tertiary	Killala gabbro	
			072	75	SE	*0.55*							Tertiary	Killala gabbro	
			020			*0.33*							Tertiary	Killala gabbro	
			064	50	NW								Tertiary	Killala gabbro	
			054	80	NW	*0-0.16*							Tertiary	Killala gabbro	
			061	50	SE	0.65							Tertiary	Killala gabbro	
101ii	122299	333118	045			**0.5**	0.58						Tertiary	Killala gabbro	host rock jts 053, 095
			060										Tertiary	Killala gabbro	
			052	52	SE								Tertiary	Killala gabbro	
			094	86	SW	**0.65**							Tertiary	Killala gabbro	
			098	83	SW								Tertiary	Killala gabbro	
102	122321	333084	068	78	SE	**0.14**	0.14						Tertiary	Killala gabbro	host rock jts 105, 040, 000
			073	76	SE	**0.14**							Tertiary	Killala gabbro	
			055										Tertiary	Killala gabbro	
103	122296	332915	108			**1.75**	1.72						Tertiary	Killala gabbro	
			096			1.6							Tertiary	Killala gabbro	
			103										Tertiary	Killala gabbro	
			108	83	SW	**1.8**							Tertiary	Killala gabbro	
			110										Tertiary	Killala gabbro	
			110										Tertiary	Killala gabbro	
			142										Tertiary	Killala gabbro	
			105										Tertiary	Killala gabbro	
			105	88	NE								Tertiary	Killala gabbro	
			106										Tertiary	Killala gabbro	
			108										Tertiary	Killala gabbro	
			104										Tertiary	Killala gabbro	
104i	122301	332796	125	90		**0.82**	0.81						Carboniferous	Mullaghmore Sandstone Form.	dyke sub// jts in places
			114										Carboniferous	Mullaghmore Sandstone Form.	
			130			**1**							Carboniferous	Mullaghmore Sandstone Form.	
			125										Carboniferous	Mullaghmore Sandstone Form.	
			122										Carboniferous	Mullaghmore Sandstone Form.	
			122										Carboniferous	Mullaghmore Sandstone Form.	
			122			**0.65**							Carboniferous	Mullaghmore Sandstone Form.	
			118	86	SW	**0.76**							Carboniferous	Mullaghmore Sandstone Form.	
			120			*0.3-0.15*							Carboniferous	Mullaghmore Sandstone Form.	
104ii	122301	332792	121	88	SW	*0.78-0.29*	1.02			037	5	NW	Carboniferous	Mullaghmore Sandstone Form.	dyke sub// jts
			116										Carboniferous	Mullaghmore Sandstone Form.	
			120			**0.96**							Carboniferous	Mullaghmore Sandstone Form.	
			118	87	SW	**1.07**							Carboniferous	Mullaghmore Sandstone Form.	
105	122237	332601	157	88	SW		0.50	**053**		045	3	NW	Carboniferous	Mullaghmore Sandstone Form.	host rock jts 097
			139	86	SW	*0.12*							Carboniferous	Mullaghmore Sandstone Form.	
			145										Carboniferous	Mullaghmore Sandstone Form.	
			128			*0.35*							Carboniferous	Mullaghmore Sandstone Form.	
			142	84	NE	**0.57**							Carboniferous	Mullaghmore Sandstone Form.	
			142	86	SW								Carboniferous	Mullaghmore Sandstone Form.	
			142			**0.43**							Carboniferous	Mullaghmore Sandstone Form.	
			148			*0.14*							Carboniferous	Mullaghmore Sandstone Form.	
			141			*0.3*							Carboniferous	Mullaghmore Sandstone Form.	
			144										Carboniferous	Mullaghmore Sandstone Form.	
106	123376	329115	*085*			~5	5.00			050	15	NW	Carboniferous	Mullaghmore Sandstone Form.	
107	123408	328928	096	79	SW	1.22	1.22			045	7	NW	Carboniferous	Mullaghmore Sandstone Form.	host rock jts 093-097, 100
108i	123408	328908	090	87	S	0.34	0.34						Carboniferous	Mullaghmore Sandstone Form.	host rock jts 085

108ii	123408	328906	090	80	S	1.9	1.9				051	6	NW	Carboniferous	Mullaghmore Sandstone Form.	host rock jts 095
109	123400	328846	078	86	NW	0.77	0.77				045	3	NW	Carboniferous	Mullaghmore Sandstone Form.	host rock jts 086
			082	76	NW	*0.16*								Carboniferous	Mullaghmore Sandstone Form.	
110	123400	328839	088	85	NW	1	1				045	3	NW	Carboniferous	Mullaghmore Sandstone Form.	
111	128596	330414	094	83	SW	1	1	033	S side up 20 cm		027	2	SE	Carboniferous	Ballina Limestone Form. (lower)	host rock jts 090, 150, 050
			094											Carboniferous	Ballina Limestone Form. (lower)	
112	128595	330455	103	85	SW	4	4	**013**	aext.	0.7 S side	027	2	SE	Carboniferous	Ballina Limestone Form. (lower)	host rock jts 100, 170
			103											Carboniferous	Ballina Limestone Form. (lower)	
113	128571	330530	099	83	SW	**1.6**	1.6	013		0.15	027	2	SE	Carboniferous	Ballina Limestone Form. (lower)	host rock jts 093, 164
			089											Carboniferous	Ballina Limestone Form. (lower)	
			093			**1.6**								Carboniferous	Ballina Limestone Form. (lower)	
			095											Carboniferous	Ballina Limestone Form. (lower)	
			096											Carboniferous	Ballina Limestone Form. (lower)	
114	128566	330558	094	88	SW	1	1	174	S side up 2 cm	0.2	000	2	NE	Carboniferous	Ballina Limestone Form. (lower)	host rock jts 094, 162
			096											Carboniferous	Ballina Limestone Form. (lower)	
115	128476	330762	082	87	SE		0.4	155		none seen				Carboniferous	Ballina Limestone Form. (lower)	host rock jts 065, 085, 156
			078											Carboniferous	Ballina Limestone Form. (lower)	
			078											Carboniferous	Ballina Limestone Form. (lower)	
			082			0.4								Carboniferous	Ballina Limestone Form. (lower)	
116i	128482	330812	089	86	SE	0.15	0.15			none seen	000	3	NE	Carboniferous	Ballina Limestone Form. (lower)	host rock jts 087, 170
116ii	128482	330820	099	84	SW	**0.7**	0.63			0.05-0.10				Carboniferous	Ballina Limestone Form. (lower)	host rock jts 086, 090, 163, 175
			081											Carboniferous	Ballina Limestone Form. (lower)	
			093											Carboniferous	Ballina Limestone Form. (lower)	
			089			**0.6**								Carboniferous	Ballina Limestone Form. (lower)	
			093											Carboniferous	Ballina Limestone Form. (lower)	
			099											Carboniferous	Ballina Limestone Form. (lower)	
			089											Carboniferous	Ballina Limestone Form. (lower)	
			102			**0.6**								Carboniferous	Ballina Limestone Form. (lower)	
			093											Carboniferous	Ballina Limestone Form. (lower)	
			091											Carboniferous	Ballina Limestone Form. (lower)	
			091											Carboniferous	Ballina Limestone Form. (lower)	
			086											Carboniferous	Ballina Limestone Form. (lower)	
			089			**0.6**								Carboniferous	Ballina Limestone Form. (lower)	
			095											Carboniferous	Ballina Limestone Form. (lower)	
117	128516	331106	099	84	SW	5.3	5.3			2.5 N side, 1 S side	000	2	NE	Carboniferous	Ballina Limestone Form. (lower)	host rock jts 182, 045, 180, 181, 185, 172
118i	128517	331245	105	82	SW	2.2	2.2	010						Carboniferous	Ballina Limestone Form. (lower)	host rock jts 056, 057, 058, 170, 173, 169
			105											Carboniferous	Ballina Limestone Form. (lower)	
			100	82	SW									Carboniferous	Ballina Limestone Form. (lower)	
			094	80	SW									Carboniferous	Ballina Limestone Form. (lower)	
			100			*0.9*								Carboniferous	Ballina Limestone Form. (lower)	
			089											Carboniferous	Ballina Limestone Form. (lower)	
			109											Carboniferous	Ballina Limestone Form. (lower)	
			088											Carboniferous	Ballina Limestone Form. (lower)	
			113											Carboniferous	Ballina Limestone Form. (lower)	
118ii	128525	331264	093	86	SW	0.35	0.35			0.05	162	3	NE	Carboniferous	Ballina Limestone Form. (lower)	host rock jts 182, 054, 166, 169, 054
			091											Carboniferous	Ballina Limestone Form. (lower)	
			049			*2.7*								Carboniferous	Ballina Limestone Form. (lower)	
			090											Carboniferous	Ballina Limestone Form. (lower)	
			055	82	SE									Carboniferous	Ballina Limestone Form. (lower)	
			089											Carboniferous	Ballina Limestone Form. (lower)	
			088											Carboniferous	Ballina Limestone Form. (lower)	
			091											Carboniferous	Ballina Limestone Form. (lower)	
			093											Carboniferous	Ballina Limestone Form. (lower)	
			096											Carboniferous	Ballina Limestone Form. (lower)	
			087											Carboniferous	Ballina Limestone Form. (lower)	
			091											Carboniferous	Ballina Limestone Form. (lower)	
			077											Carboniferous	Ballina Limestone Form. (lower)	
			069											Carboniferous	Ballina Limestone Form. (lower)	
119	128536	331279	099	87	SW	1.2	1.2			0.05-0.10				Carboniferous	Ballina Limestone Form. (lower)	host rock jts 165, 164, 168, 055, 057, 057
120	128582	331304	104	80	SW	0.28	0.28	ext.						Carboniferous	Ballina Limestone Form. (lower)	host rock jts 054, 165
			103											Carboniferous	Ballina Limestone Form. (lower)	
			108											Carboniferous	Ballina Limestone Form. (lower)	
			103											Carboniferous	Ballina Limestone Form. (lower)	
			112											Carboniferous	Ballina Limestone Form. (lower)	
			106											Carboniferous	Ballina Limestone Form. (lower)	
121	128663	331442	092				1.03	ext.	ext.	0.04				Carboniferous	Ballina Limestone Form. (lower)	dyke sub// jts in places
			103			**1.06**								Carboniferous	Ballina Limestone Form. (lower)	
			096											Carboniferous	Ballina Limestone Form. (lower)	
			104	88	SW									Carboniferous	Ballina Limestone Form. (lower)	
			099											Carboniferous	Ballina Limestone Form. (lower)	
			104											Carboniferous	Ballina Limestone Form. (lower)	
			090											Carboniferous	Ballina Limestone Form. (lower)	
			106											Carboniferous	Ballina Limestone Form. (lower)	
			103											Carboniferous	Ballina Limestone Form. (lower)	
			103											Carboniferous	Ballina Limestone Form. (lower)	
			101											Carboniferous	Ballina Limestone Form. (lower)	
			101											Carboniferous	Ballina Limestone Form. (lower)	
			096	85	SW	**1**								Carboniferous	Ballina Limestone Form. (lower)	
122	128821	331619	090			**3.1**	3.35			0.7				Carboniferous	Ballina Limestone Form. (lower)	dyke sub// jts in places

			086	85	SE								Carboniferous	Ballina Limestone Form. (lower)		
			085	85	SE	**3.6**							Carboniferous	Ballina Limestone Form. (lower)		
123i	128819	331641	092	72	SW	0.18	0.18			all CR marblised			Carboniferous	Ballina Limestone Form. (lower)		
			092										Carboniferous	Ballina Limestone Form. (lower)		
			092										Carboniferous	Ballina Limestone Form. (lower)		
			092										Carboniferous	Ballina Limestone Form. (lower)		
			092										Carboniferous	Ballina Limestone Form. (lower)		
123ii	128819	331644	092	82	SW		4.30			all CR marblised	027	2 NW	Carboniferous	Ballina Limestone Form. (lower)	dyke sub// jts in places	
			092										Carboniferous	Ballina Limestone Form. (lower)		
			092										Carboniferous	Ballina Limestone Form. (lower)		
			092										Carboniferous	Ballina Limestone Form. (lower)		
			092										Carboniferous	Ballina Limestone Form. (lower)		
			093	87	SW	**4.6**							Carboniferous	Ballina Limestone Form. (lower)		
			113										Carboniferous	Ballina Limestone Form. (lower)		
			100										Carboniferous	Ballina Limestone Form. (lower)		
			067			4							Carboniferous	Ballina Limestone Form. (lower)		
			080										Carboniferous	Ballina Limestone Form. (lower)		
			070										Carboniferous	Ballina Limestone Form. (lower)		
			103	58	SW								Carboniferous	Ballina Limestone Form. (lower)		
			096	70	SW								Carboniferous	Ballina Limestone Form. (lower)		
			096										Carboniferous	Ballina Limestone Form. (lower)		
124	128816	331658	138			46	46						Carboniferous	Ballina Limestone Form. (lower)		
			124										Carboniferous	Ballina Limestone Form. (lower)		
124	128812	331729	124	87	SW					14 N side	117	4 NE	Carboniferous	Ballina Limestone Form. (lower)		
			104										Carboniferous	Ballina Limestone Form. (lower)		
125	128861	331781	134	89	SW	1.7	1.7						Carboniferous	Ballina Limestone Form. (lower)	dyke sub// jts	
			103										Carboniferous	Ballina Limestone Form. (lower)		
			128	85	SW								Carboniferous	Ballina Limestone Form. (lower)		
126	128967	331941	**100**	87	SW	1	1	**010**	ext.	0.05			Carboniferous	Ballina Limestone Form. (lower)		
127	128996	332048	090	88	S	9	9			7-8 N side	162	3 NE	Carboniferous	Ballina Limestone Form. (lower)		
128i	129007	332110	086			1.5	1.5	ext.		0.08, 0.2			Carboniferous	Ballina Limestone Form. (lower)	dyke sub// jts	
			086										Carboniferous	Ballina Limestone Form. (lower)		
			090										Carboniferous	Ballina Limestone Form. (lower)		
			092	85	NE								Carboniferous	Ballina Limestone Form. (lower)		
128ii	129007	332113	098			0.1	0.1			none seen			Carboniferous	Ballina Limestone Form. (lower)		
			100	86	SW								Carboniferous	Ballina Limestone Form. (lower)		
			101										Carboniferous	Ballina Limestone Form. (lower)		
			102										Carboniferous	Ballina Limestone Form. (lower)		
			098	87	SW								Carboniferous	Ballina Limestone Form. (lower)		
129i	129126	332265	098	88	SW	4.6	4.6				146	4 NE	Carboniferous	Ballina Limestone Form. (lower)		
129ii	129126	332265	112	90		3	3						Carboniferous	Ballina Limestone Form. (lower)		
130	129540	332913	100	81	NE	>1.7	1.70						Carboniferous	Ballina Limestone Form. (lower)	dyke sub// jts	
131	129592	333016	077				0.22	ext.					Carboniferous	Ballina Limestone Form. (lower)	host rock jts oblique to dyke	
			080			*0.11-0.04*							Carboniferous	Ballina Limestone Form. (lower)		
			077										Carboniferous	Ballina Limestone Form. (lower)		
			069										Carboniferous	Ballina Limestone Form. (lower)		
			074			**0.3**							Carboniferous	Ballina Limestone Form. (lower)		
			077										Carboniferous	Ballina Limestone Form. (lower)		
			061			**0.16**							Carboniferous	Ballina Limestone Form. (lower)		
			074	80	NW	**0.19**							Carboniferous	Ballina Limestone Form. (lower)		
131	129512	332993											Carboniferous	Ballina Limestone Form. (lower)		
132i	129745	333335	104			1.1	1.1			0.05			Carboniferous	Ballina Limestone Form. (lower)		
			099										Carboniferous	Ballina Limestone Form. (lower)		
132ii	129745	333339	104	87	SW		0.11						Carboniferous	Ballina Limestone Form. (lower)		
			102			**0.13**		022					Carboniferous	Ballina Limestone Form. (lower)		
			104	84	SW	**0.1**							Carboniferous	Ballina Limestone Form. (lower)		
			097										Carboniferous	Ballina Limestone Form. (lower)		
			104			**0.07**							Carboniferous	Ballina Limestone Form. (lower)		
			092					157					Carboniferous	Ballina Limestone Form. (lower)		
			097										Carboniferous	Ballina Limestone Form. (lower)		
			099			**0.06**							Carboniferous	Ballina Limestone Form. (lower)		
			105	85	NE								Carboniferous	Ballina Limestone Form. (lower)		
			100	87	NE	**0.18**							Carboniferous	Ballina Limestone Form. (lower)		
			103	82	NE	**0.15**		014					Carboniferous	Ballina Limestone Form. (lower)		
			101	88	SW	**0.1**		036					Carboniferous	Ballina Limestone Form. (lower)		
133i	129789	333375	102	89	SW	2.55	2.55						Carboniferous	Ballina Limestone Form. (lower)		
133ii	129789	333375	102	89	SW	5.5	5.5			0.15-0.20			Carboniferous	Ballina Limestone Form. (lower)		
134	129780	333400	111	87	NE	1.7	1.7	022		0.1			Carboniferous	Ballina Limestone Form. (lower)		
			108	86	NE								Carboniferous	Ballina Limestone Form. (lower)		
			108	88	SW								Carboniferous	Ballina Limestone Form. (lower)		
			111	88	SW								Carboniferous	Ballina Limestone Form. (lower)		
			110										Carboniferous	Ballina Limestone Form. (lower)		
			112	88	SW								Carboniferous	Ballina Limestone Form. (lower)		
			110	88	SW								Carboniferous	Ballina Limestone Form. (lower)		
135i	129800	333497	105	78	NE	1.85 (135i/ii)	1.85						Carboniferous	Ballina Limestone Form. (lower)		
			065										Carboniferous	Ballina Limestone Form. (lower)		
			106										Carboniferous	Ballina Limestone Form. (lower)		
			061										Carboniferous	Ballina Limestone Form. (lower)		
			104										Carboniferous	Ballina Limestone Form. (lower)		

135ii	129800	333509	099	85	NE								Carboniferous	Ballina Limestone Form. (lower)	
			079										Carboniferous	Ballina Limestone Form. (lower)	
			099										Carboniferous	Ballina Limestone Form. (lower)	
			103	83	NE								Carboniferous	Ballina Limestone Form. (lower)	
136	130279	334520	099	86	SW	1.28	1.28	**175**	s side down 10 cm		162	3	NE	Carboniferous	Ballina Limestone Form. (upper)	host rock jts 160
			103											Carboniferous	Ballina Limestone Form. (upper)	
137	130435	334859	097	86	NE	1.25	1.25				146	4	NE	Carboniferous	Ballina Limestone Form. (upper)	host rock jts 050, 052, 159, 162, 155
			098	86	NE									Carboniferous	Ballina Limestone Form. (upper)	
138	130637	335177	098	85	NE	0.81	0.81	033, 024	s side up 10 cm		027	2	SE	Carboniferous	Ballina Limestone Form. (upper)	host rock jts 156
			101	85	NE									Carboniferous	Ballina Limestone Form. (upper)	
139	130693	335312	098	87	NE	0.05	0.05	010	ext.					Carboniferous	Ballina Limestone Form. (upper)	host rock jts 162, 150
			094											Carboniferous	Ballina Limestone Form. (upper)	
			098											Carboniferous	Ballina Limestone Form. (upper)	
			089					000						Carboniferous	Ballina Limestone Form. (upper)	
			092											Carboniferous	Ballina Limestone Form. (upper)	
			095											Carboniferous	Ballina Limestone Form. (upper)	
			090											Carboniferous	Ballina Limestone Form. (upper)	
140	130696	335331	101	82	NE	1.02	1.02		ext.		056	4	SE	Carboniferous	Ballina Limestone Form. (upper)	
141	130742	335820	105			**0.31**	0.32				146	4	NE	Carboniferous	Ballina Limestone Form. (upper)	host rock jts 164, 060
			105											Carboniferous	Ballina Limestone Form. (upper)	
			111	86	SW									Carboniferous	Ballina Limestone Form. (upper)	
			106			**0.32**								Carboniferous	Ballina Limestone Form. (upper)	
			104											Carboniferous	Ballina Limestone Form. (upper)	
			078					030						Carboniferous	Ballina Limestone Form. (upper)	
			105											Carboniferous	Ballina Limestone Form. (upper)	
			103											Carboniferous	Ballina Limestone Form. (upper)	
			112	83	SW									Carboniferous	Ballina Limestone Form. (upper)	
			110					037						Carboniferous	Ballina Limestone Form. (upper)	
			102											Carboniferous	Ballina Limestone Form. (upper)	
142	131382	336550	108	86	SW	0.28	0.28				000	3	NE	Carboniferous	Ballina Limestone Form. (upper)	host rock jts 052
143	131382	336630	107	86	SW	2.8	2.8				000	3	NE	Carboniferous	Ballina Limestone Form. (upper)	
144	131399	336649	103	86	SW	0.3	0.3							Carboniferous	Ballina Limestone Form. (upper)	
			101											Carboniferous	Ballina Limestone Form. (upper)	
145	131370	337010	111	88	NE	0.04-0.28	0.28	**017**						Carboniferous	Ballina Limestone Form. (lower)	
			113											Carboniferous	Ballina Limestone Form. (lower)	
			113											Carboniferous	Ballina Limestone Form. (lower)	
146	131541	338012	101			0.64	0.64	001			153	2	NE	Carboniferous	Ballina Limestone Form. (upper)	
			101	87	SW									Carboniferous	Ballina Limestone Form. (upper)	
			094											Carboniferous	Ballina Limestone Form. (upper)	
			096	86	SW	*0.015-0.12*								Carboniferous	Ballina Limestone Form. (upper)	
147	131594	338052	100			**0.85**	0.59	013	s side up 10 cm					Carboniferous	Ballina Limestone Form. (upper)	
			055											Carboniferous	Ballina Limestone Form. (upper)	
			087	88	SE									Carboniferous	Ballina Limestone Form. (upper)	
			086	78	SE	**0.32**								Carboniferous	Ballina Limestone Form. (upper)	
			057											Carboniferous	Ballina Limestone Form. (upper)	
			086											Carboniferous	Ballina Limestone Form. (upper)	
			088	83	SE									Carboniferous	Ballina Limestone Form. (upper)	
			073	70	SE									Carboniferous	Ballina Limestone Form. (upper)	
			087	74	SE									Carboniferous	Ballina Limestone Form. (upper)	
148	131581	338062	107			0.62	0.62	008, 011						Carboniferous	Ballina Limestone Form. (upper)	
			104											Carboniferous	Ballina Limestone Form. (upper)	
			099											Carboniferous	Ballina Limestone Form. (upper)	
			096											Carboniferous	Ballina Limestone Form. (upper)	
			107											Carboniferous	Ballina Limestone Form. (upper)	
			101											Carboniferous	Ballina Limestone Form. (upper)	
			096											Carboniferous	Ballina Limestone Form. (upper)	
			107											Carboniferous	Ballina Limestone Form. (upper)	
			098											Carboniferous	Ballina Limestone Form. (upper)	
			096											Carboniferous	Ballina Limestone Form. (upper)	
149	131378	338716	096	82	SW	1.34	1.34			0.3 S side				Carboniferous	Ballina Limestone Form. (lower)	host rock jts 162, 055
150	140909	337617	102			1.3max	1.30							Carboniferous	Glencar Limestone Form.	dyke sub// jts in places
			097	80	SW									Carboniferous	Glencar Limestone Form.	
			103											Carboniferous	Glencar Limestone Form.	
151	140949	337583	103	77	SW	2max	2.00							Carboniferous	Glencar Limestone Form.	
152	141390	336929	099	75	SW	**4-5**	4.50							Carboniferous	Glencar Limestone Form.	
153	142589	335921	104	85	SW	0.87	0.87			0.05				Carboniferous	Glencar Limestone Form.	dyke sub// jts
154	142608	335846	088	82	SE	1.2	1.2							Carboniferous	Glencar Limestone Form.	
155a	142685	335804	082	77	SE	**0.56**	0.58							Carboniferous	Glencar Limestone Form.	
			082											Carboniferous	Glencar Limestone Form.	
155b	142850	335819	084	86	SE	**0.6**					146	6	SW	Carboniferous	Glencar Limestone Form.	host rock jts 156, 167
			084	86	SE	**0.58**								Carboniferous	Glencar Limestone Form.	
156i	142917	335873	084	82	SE	1	1				119	10	SW	Carboniferous	Glencar Limestone Form.	
			087											Carboniferous	Glencar Limestone Form.	
156ii	142917	335878	083	82	SE	1.25	1.25				132	9	SW	Carboniferous	Glencar Limestone Form.	
157	142832	335950												Carboniferous	Glencar Limestone Form.	
157a	142958	335959	091	89	NE	**0.75**	0.77	**000**	ext.					Carboniferous	Glencar Limestone Form.	dyke sub// jts
			092											Carboniferous	Glencar Limestone Form.	
			092											Carboniferous	Glencar Limestone Form.	
			090	88	N									Carboniferous	Glencar Limestone Form.	

			091										Carboniferous	Glencar Limestone Form.		
			089										Carboniferous	Glencar Limestone Form.		
			089										Carboniferous	Glencar Limestone Form.		
			091										Carboniferous	Glencar Limestone Form.		
			090	89	S								Carboniferous	Glencar Limestone Form.		
			090										Carboniferous	Glencar Limestone Form.		
			093										Carboniferous	Glencar Limestone Form.		
			092										Carboniferous	Glencar Limestone Form.		
			088	88	NW								Carboniferous	Glencar Limestone Form.		
			086			**0.78**							Carboniferous	Glencar Limestone Form.		
			089										Carboniferous	Glencar Limestone Form.		
157b	143086	335948	085	80	NW	**0.62**	0.63			0.15	146	7	SW	Carboniferous	Glencar Limestone Form.	
			093											Carboniferous	Glencar Limestone Form.	
			091											Carboniferous	Glencar Limestone Form.	
			094											Carboniferous	Glencar Limestone Form.	
			091											Carboniferous	Glencar Limestone Form.	
			084	88	NW	**0.63**								Carboniferous	Glencar Limestone Form.	
			086	88	SE									Carboniferous	Glencar Limestone Form.	
158	143212	335851	085	83	SE	0.7	0.7	ext.	ext.					Carboniferous	Glencar Limestone Form.	dyke sub// jts
			084											Carboniferous	Glencar Limestone Form.	
			086											Carboniferous	Glencar Limestone Form.	
			083											Carboniferous	Glencar Limestone Form.	
			086	87	SE									Carboniferous	Glencar Limestone Form.	
159	143395	335655	099			~2	2.00							Carboniferous	Glencar Limestone Form.	dyke sub// jts
160	143495	335528	090			~1	1.00							Carboniferous	Glencar Limestone Form.	dyke sub// jts
161	143500	335515	098	85	SW	?								Carboniferous	Glencar Limestone Form.	dyke sub// jts
162	143572	335475	088	86	SE	0.84	0.84		ext.					Carboniferous	Glencar Limestone Form.	host rock jts 160-180
163	144261	335438	101	90		1.02	1.02				174	9	SW	Carboniferous	Mullaghmore Sandstone Form.	dyke sub// jts in places
			101											Carboniferous	Mullaghmore Sandstone Form.	
			094											Carboniferous	Mullaghmore Sandstone Form.	
			096	90										Carboniferous	Mullaghmore Sandstone Form.	
			096											Carboniferous	Mullaghmore Sandstone Form.	
			089			*0.72*								Carboniferous	Mullaghmore Sandstone Form.	
			087			*0.16-0*								Carboniferous	Mullaghmore Sandstone Form.	
			097											Carboniferous	Mullaghmore Sandstone Form.	
			095											Carboniferous	Mullaghmore Sandstone Form.	
			093											Carboniferous	Mullaghmore Sandstone Form.	
			118											Carboniferous	Mullaghmore Sandstone Form.	
			086	87	SE	*0.01*								Carboniferous	Mullaghmore Sandstone Form.	
			089			*0.05*								Carboniferous	Mullaghmore Sandstone Form.	
			087			*0.1*								Carboniferous	Mullaghmore Sandstone Form.	
			089											Carboniferous	Mullaghmore Sandstone Form.	
			091			*0.43*								Carboniferous	Mullaghmore Sandstone Form.	
			087	85	SE									Carboniferous	Mullaghmore Sandstone Form.	
			092											Carboniferous	Mullaghmore Sandstone Form.	
164i	144300	335475	087			1.7 total	1.70	004	ext.					Carboniferous	Mullaghmore Sandstone Form.	dyke sub// jts
			087											Carboniferous	Mullaghmore Sandstone Form.	
			087											Carboniferous	Mullaghmore Sandstone Form.	
			088											Carboniferous	Mullaghmore Sandstone Form.	
			087											Carboniferous	Mullaghmore Sandstone Form.	
			087											Carboniferous	Mullaghmore Sandstone Form.	
			087											Carboniferous	Mullaghmore Sandstone Form.	
			084											Carboniferous	Mullaghmore Sandstone Form.	
			091											Carboniferous	Mullaghmore Sandstone Form.	
			091											Carboniferous	Mullaghmore Sandstone Form.	
			088											Carboniferous	Mullaghmore Sandstone Form.	
			090											Carboniferous	Mullaghmore Sandstone Form.	
			087											Carboniferous	Mullaghmore Sandstone Form.	
			088											Carboniferous	Mullaghmore Sandstone Form.	
			088	86	NW									Carboniferous	Mullaghmore Sandstone Form.	
164ii	144300	335477	**091**								000	8	NW	Carboniferous	Mullaghmore Sandstone Form.	
			089	86	SE									Carboniferous	Mullaghmore Sandstone Form.	
165	144302	335479	095			0.18	0.18							Carboniferous	Mullaghmore Sandstone Form.	host rock jts 167
			093											Carboniferous	Mullaghmore Sandstone Form.	
			093	87	SW									Carboniferous	Mullaghmore Sandstone Form.	
			097											Carboniferous	Mullaghmore Sandstone Form.	
			085											Carboniferous	Mullaghmore Sandstone Form.	
			093											Carboniferous	Mullaghmore Sandstone Form.	
			088											Carboniferous	Mullaghmore Sandstone Form.	
			091											Carboniferous	Mullaghmore Sandstone Form.	
			092											Carboniferous	Mullaghmore Sandstone Form.	
			087											Carboniferous	Mullaghmore Sandstone Form.	
			087											Carboniferous	Mullaghmore Sandstone Form.	
			094											Carboniferous	Mullaghmore Sandstone Form.	
			093											Carboniferous	Mullaghmore Sandstone Form.	
			092											Carboniferous	Mullaghmore Sandstone Form.	
			092											Carboniferous	Mullaghmore Sandstone Form.	
			092											Carboniferous	Mullaghmore Sandstone Form.	
			092											Carboniferous	Mullaghmore Sandstone Form.	

			095											Carboniferous	Mullaghmore Sandstone Form.	
			092											Carboniferous	Mullaghmore Sandstone Form.	
166	144287	335545	089	87	NW	0.76	0.76							Carboniferous	Mullaghmore Sandstone Form.	dyke sub// jts
167	144326	335482	088	84	SE	0.21	0.21							Carboniferous	Mullaghmore Sandstone Form.	
			089											Carboniferous	Mullaghmore Sandstone Form.	
			081	87	NW	*0.19*								Carboniferous	Mullaghmore Sandstone Form.	
			084											Carboniferous	Mullaghmore Sandstone Form.	
			090											Carboniferous	Mullaghmore Sandstone Form.	
			090	88	N	*0.13*								Carboniferous	Mullaghmore Sandstone Form.	
			095			*0.025*								Carboniferous	Mullaghmore Sandstone Form.	
			089			*0.065*								Carboniferous	Mullaghmore Sandstone Form.	
			087	86	SE									Carboniferous	Mullaghmore Sandstone Form.	
			090	86	S									Carboniferous	Mullaghmore Sandstone Form.	
			091											Carboniferous	Mullaghmore Sandstone Form.	
			093											Carboniferous	Mullaghmore Sandstone Form.	
			091											Carboniferous	Mullaghmore Sandstone Form.	
			089	86	SE									Carboniferous	Mullaghmore Sandstone Form.	
			100											Carboniferous	Mullaghmore Sandstone Form.	
168	144325	335477	088	88	SE		1.6							Carboniferous	Mullaghmore Sandstone Form.	dyke sub// jts
			091			1.6								Carboniferous	Mullaghmore Sandstone Form.	
			087											Carboniferous	Mullaghmore Sandstone Form.	
			087											Carboniferous	Mullaghmore Sandstone Form.	
			088											Carboniferous	Mullaghmore Sandstone Form.	
			091			*0.13*								Carboniferous	Mullaghmore Sandstone Form.	
			092	88	SW									Carboniferous	Mullaghmore Sandstone Form.	
			093											Carboniferous	Mullaghmore Sandstone Form.	
			093											Carboniferous	Mullaghmore Sandstone Form.	
			088			*0.24*								Carboniferous	Mullaghmore Sandstone Form.	
169	144350	335404	104	82	SW	*0.82*	1	**011**						Carboniferous	Mullaghmore Sandstone Form.	
			094			*0.75*								Carboniferous	Mullaghmore Sandstone Form.	
			098											Carboniferous	Mullaghmore Sandstone Form.	
			092	88	NE	*0.23*								Carboniferous	Mullaghmore Sandstone Form.	
			116											Carboniferous	Mullaghmore Sandstone Form.	
			108			*0.01*								Carboniferous	Mullaghmore Sandstone Form.	
			093											Carboniferous	Mullaghmore Sandstone Form.	
			110											Carboniferous	Mullaghmore Sandstone Form.	
			090	88	N	1								Carboniferous	Mullaghmore Sandstone Form.	
170	144348	335397	096	82	SW		0.39	ext.						Carboniferous	Mullaghmore Sandstone Form.	
			102			**0.35**								Carboniferous	Mullaghmore Sandstone Form.	
			101			**0.4**								Carboniferous	Mullaghmore Sandstone Form.	
			110											Carboniferous	Mullaghmore Sandstone Form.	
			080											Carboniferous	Mullaghmore Sandstone Form.	
			113			**0.43**								Carboniferous	Mullaghmore Sandstone Form.	
			095											Carboniferous	Mullaghmore Sandstone Form.	
171	144356	335372	102	83	SW	*0.002*	0.44	ext.	ext.					Carboniferous	Mullaghmore Sandstone Form.	dyke sub// jts
			101			*0.3*								Carboniferous	Mullaghmore Sandstone Form.	
			120											Carboniferous	Mullaghmore Sandstone Form.	
			105											Carboniferous	Mullaghmore Sandstone Form.	
			097											Carboniferous	Mullaghmore Sandstone Form.	
			097											Carboniferous	Mullaghmore Sandstone Form.	
			093	85	SW									Carboniferous	Mullaghmore Sandstone Form.	
			094			0.44								Carboniferous	Mullaghmore Sandstone Form.	
			095			*0.06*								Carboniferous	Mullaghmore Sandstone Form.	
			092											Carboniferous	Mullaghmore Sandstone Form.	
			089											Carboniferous	Mullaghmore Sandstone Form.	
			096			*0.42*								Carboniferous	Mullaghmore Sandstone Form.	
			102											Carboniferous	Mullaghmore Sandstone Form.	
172a	144877	334711	095	87	SW	**0.89**	0.87		ext.					Carboniferous	Mullaghmore Sandstone Form.	dyke sub// jts
			095											Carboniferous	Mullaghmore Sandstone Form.	
172b	145159	334684	091	88	NE			ext.						Carboniferous	Mullaghmore Sandstone Form.	host rock jts oblique to dyke
			092			**0.85**								Carboniferous	Mullaghmore Sandstone Form.	
173	145392	334491	088	85	NW		2.48							Carboniferous	Mullaghmore Sandstone Form.	dyke sub// jts in places
			088											Carboniferous	Mullaghmore Sandstone Form.	
			087	83	NW									Carboniferous	Mullaghmore Sandstone Form.	
			084	82	NW	**2.27-2.82**								Carboniferous	Mullaghmore Sandstone Form.	
			086											Carboniferous	Mullaghmore Sandstone Form.	
			086											Carboniferous	Mullaghmore Sandstone Form.	
			086	85	NW									Carboniferous	Mullaghmore Sandstone Form.	
			084			**2.40**								Carboniferous	Mullaghmore Sandstone Form.	
			084											Carboniferous	Mullaghmore Sandstone Form.	
			084											Carboniferous	Mullaghmore Sandstone Form.	
174a	146554	334226	088				0.71							Carboniferous	Mullaghmore Sandstone Form.	dyke sub// jts in places
174b	146520	334222	092			**0.6**								Carboniferous	Mullaghmore Sandstone Form.	dyke sub// jts in places
174c	146410	334213	084	90										Carboniferous	Mullaghmore Sandstone Form.	dyke sub// jts in places
174d	146318	334208	093	87	NE	**0.73**								Carboniferous	Mullaghmore Sandstone Form.	dyke sub// jts in places
			091											Carboniferous	Mullaghmore Sandstone Form.	
			086	82	NW									Carboniferous	Mullaghmore Sandstone Form.	
			089			**0.77**								Carboniferous	Mullaghmore Sandstone Form.	
			088											Carboniferous	Mullaghmore Sandstone Form.	

174c	146227	334210	088										Carboniferous	Mullaghmore Sandstone Form.	dyke sub// jts in places
174f	146006	334203	092	85	SW								Carboniferous	Mullaghmore Sandstone Form.	dyke sub// jts in places
			089			**0.64**							Carboniferous	Mullaghmore Sandstone Form.	
			092										Carboniferous	Mullaghmore Sandstone Form.	
			088	85	NW								Carboniferous	Mullaghmore Sandstone Form.	
			094			**0.8**							Carboniferous	Mullaghmore Sandstone Form.	
			088										Carboniferous	Mullaghmore Sandstone Form.	
			103										Carboniferous	Mullaghmore Sandstone Form.	
			094										Carboniferous	Mullaghmore Sandstone Form.	
			120										Carboniferous	Mullaghmore Sandstone Form.	
			095										Carboniferous	Mullaghmore Sandstone Form.	
			090	82	N	**0.7**							Carboniferous	Mullaghmore Sandstone Form.	
174	145959	334204											Carboniferous	Mullaghmore Sandstone Form.	dyke sub// jts in places
174	145828	334183											Carboniferous	Mullaghmore Sandstone Form.	dyke sub// jts in places
175	146972	334357	093	83	NE	0.14-0	0.14	010					Carboniferous	Glencar Limestone Form.	dyke sub// jts in places
			086										Carboniferous	Glencar Limestone Form.	
			091	90									Carboniferous	Glencar Limestone Form.	
			090										Carboniferous	Glencar Limestone Form.	
			091										Carboniferous	Glencar Limestone Form.	
			092										Carboniferous	Glencar Limestone Form.	
			098										Carboniferous	Glencar Limestone Form.	
			098										Carboniferous	Glencar Limestone Form.	
			098										Carboniferous	Glencar Limestone Form.	
			098										Carboniferous	Glencar Limestone Form.	
			102										Carboniferous	Glencar Limestone Form.	
			102										Carboniferous	Glencar Limestone Form.	
			103										Carboniferous	Glencar Limestone Form.	
			090										Carboniferous	Glencar Limestone Form.	
			104										Carboniferous	Glencar Limestone Form.	
176	146990	334410	093	87	NE	2.5	2.5						Carboniferous	Glencar Limestone Form.	host rock jts oblique to dyke
			089										Carboniferous	Glencar Limestone Form.	
			091	87	NE								Carboniferous	Glencar Limestone Form.	
			089										Carboniferous	Glencar Limestone Form.	
			091										Carboniferous	Glencar Limestone Form.	
			097										Carboniferous	Glencar Limestone Form.	
			096	87	NE								Carboniferous	Glencar Limestone Form.	
			094										Carboniferous	Benbulben Shale Form.	
			099										Carboniferous	Benbulben Shale Form.	
			100										Carboniferous	Benbulben Shale Form.	
			099										Carboniferous	Benbulben Shale Form.	
			091										Carboniferous	Benbulben Shale Form.	
			088										Carboniferous	Benbulben Shale Form.	
			090										Carboniferous	Benbulben Shale Form.	
			094										Carboniferous	Benbulben Shale Form.	
			093										Carboniferous	Benbulben Shale Form.	
			096	87	NE								Carboniferous	Benbulben Shale Form.	
			098										Carboniferous	Benbulben Shale Form.	
			103										Carboniferous	Benbulben Shale Form.	
			112										Carboniferous	Benbulben Shale Form.	
			098										Carboniferous	Benbulben Shale Form.	
			100										Carboniferous	Benbulben Shale Form.	
176	146654	334434									004	8 SE	Carboniferous	Mullaghmore Sandstone Form.	host rock jts oblique to dyke
176	146564	334442											Carboniferous	Mullaghmore Sandstone Form.	host rock jts oblique to dyke
177	146579	334495	094	85	SW	0.3	0.3	**006**			177	9 NE	Carboniferous	Mullaghmore Sandstone Form.	dyke sub// jts in places
			095	85	SW								Carboniferous	Mullaghmore Sandstone Form.	
			094			*0.25*							Carboniferous	Mullaghmore Sandstone Form.	
			096										Carboniferous	Benbulben Shale Form.	
			097			*0.15*							Carboniferous	Benbulben Shale Form.	
			098			*0.11*							Carboniferous	Benbulben Shale Form.	
			094										Carboniferous	Benbulben Shale Form.	
			096										Carboniferous	Benbulben Shale Form.	
			096										Carboniferous	Benbulben Shale Form.	
			100										Carboniferous	Benbulben Shale Form.	
			096			*0.035*							Carboniferous	Benbulben Shale Form.	
			098			*0.027*							Carboniferous	Benbulben Shale Form.	
177	146714	334479									008	7 SE	Carboniferous	Benbulben Shale Form.	dyke sub// jts in places
177	146764	334473											Carboniferous	Benbulben Shale Form.	dyke sub// jts in places
178	147066	334567	096				2.5		0.15				Carboniferous	Glencar Limestone Form.	host rock jts 162
			094	89	SW								Carboniferous	Glencar Limestone Form.	
			094										Carboniferous	Glencar Limestone Form.	
			093			2.5							Carboniferous	Glencar Limestone Form.	
179	148414	335133	088	88	NW	0.135	0.135						Carboniferous	Glencar Limestone Form.	host rock jts 060, 103
			069			*0.07*							Carboniferous	Ballina Limestone Form. (upper)	
			124										Carboniferous	Ballina Limestone Form. (upper)	
			111										Carboniferous	Ballina Limestone Form. (upper)	
			107	88	NE	*0.06*							Carboniferous	Ballina Limestone Form. (upper)	
			105										Carboniferous	Ballina Limestone Form. (upper)	
			101										Carboniferous	Ballina Limestone Form. (upper)	
			095	82	SW	*0.02*							Carboniferous	Ballina Limestone Form. (upper)	

180	148418	335177	**096**	81	NE	**0.92**	1.10	**012**			040	17	SE	Carboniferous	Ballina Limestone Form. (upper)	host rock jts 052, 171, 120, 090-100
			058			*0.8*								Carboniferous	Ballina Limestone Form. (upper)	
			053											Carboniferous	Ballina Limestone Form. (upper)	
			080			**0.94**								Carboniferous	Ballina Limestone Form. (upper)	
			065											Carboniferous	Ballina Limestone Form. (upper)	
			093											Carboniferous	Ballina Limestone Form. (upper)	
			081			**1.45**								Carboniferous	Ballina Limestone Form. (upper)	
			093	82	NE									Carboniferous	Ballina Limestone Form. (upper)	
			090											Carboniferous	Ballina Limestone Form. (upper)	
181	148458	335274	095				0.88	ext.			038	28	SE	Carboniferous	Ballina Limestone Form. (upper)	host rock jts oblique to dyke
			086											Carboniferous	Ballina Limestone Form. (upper)	
			084			*0.45-0.13*								Carboniferous	Ballina Limestone Form. (upper)	
			085											Carboniferous	Ballina Limestone Form. (upper)	
			114											Carboniferous	Ballina Limestone Form. (upper)	
			117											Carboniferous	Ballina Limestone Form. (upper)	
			093			*0.42*								Carboniferous	Ballina Limestone Form. (upper)	
			099											Carboniferous	Ballina Limestone Form. (upper)	
			086	88	NW	*0.61*								Carboniferous	Ballina Limestone Form. (upper)	
			090	88	N	0.88								Carboniferous	Ballina Limestone Form. (upper)	
			084											Carboniferous	Ballina Limestone Form. (upper)	
			112											Carboniferous	Ballina Limestone Form. (upper)	
			090											Carboniferous	Ballina Limestone Form. (upper)	
			086											Carboniferous	Ballina Limestone Form. (upper)	
182	148649	335432	093	80	NE	?								Carboniferous	Ballina Limestone Form. (upper)	host rock jts oblique to dyke
			086											Carboniferous	Ballina Limestone Form. (upper)	
			090											Carboniferous	Ballina Limestone Form. (upper)	
183	149490	336474	101	86	NE	0.04	0.04				064	14	SE	Carboniferous	Ballina Limestone Form. (upper)	dyke sub// jts
184	149630	336618	103	88	SW	~1.5	1.50				064	14	SE	Carboniferous	Ballina Limestone Form. (upper)	dyke sub// jts
185i	150932	336447	098	84	SW	0.25	0.25	**008**	S side up 4 cm					Carboniferous	Ballina Limestone Form. (upper)	dyke sub// jts
185ii	150932	336443	097	85	NE	0.44	0.44		ext.		025	38	NW	Carboniferous	Ballina Limestone Form. (upper)	dyke sub// jts
186i	150869	336308	104	77	SW	1.02	1.02							Carboniferous	Ballina Limestone Form. (upper)	
			110											Carboniferous	Ballina Limestone Form. (upper)	
186ii	150869	336302	103	77	SW	0.1	0.1				016	35	NW	Carboniferous	Ballina Limestone Form. (upper)	dyke sub// jts
			104	74	SW									Carboniferous	Ballina Limestone Form. (upper)	
			104											Carboniferous	Ballina Limestone Form. (upper)	
187	157928	346894	108	76	NE	1.4	1.4				096	19	SW	Carboniferous	Dartry Limestone Form.	host rock jts 100-130

Structural data from Carboniferous host rock of the Killala swarm (plotted in Figure 2.12).

Dyke sub-parallel fractures			***NNW-SSE fractures (strike)***	***NE-SW fractures (strike)***	***Host rock bedding orientation***		
070			160	065	026	9	NW
079			173	053	045	4	NW
080			160	068	127	5	NE
081			172	048	127	5	NE
081	90		160	059	000	4	NW
082			171	060	018	3	SE
083	87	SE	160	061	135	4	NE
083	83	NW	170	057	037	5	NW
084			153	057	045	3	NW
084	88	SE	173	058	050	15	NW
085			167	060	045	7	NW
085			165	060	051	6	NW
085			159	057	045	3	NW
085	87	SE	173	053	045	3	NW
085	83	NW	166	055	027	2	SE
086			178	063	027	2	SE
086	70	NW	185	055	027	2	SE
087			183	058	000	2	NW
087			184	063	000	3	NW
087	90		188	055	000	2	NW
088			175	050	162	3	NE
088			173	058	027	2	NW
088			176	058	117	4	NE
088			172	062	162	3	NE
088	90		185		146	4	NE
088	84	SE	169		162	3	NE
089			172		146	4	NE
089	87	NW	168		027	2	SE
089	83	SE	167		056	4	SE
090			171		146	4	NE
090			168		000	3	NW
090			163		000	3	NW
090	90		162		153	2	NE
090	90		165		146	6	SW
090	85	NE	158		119	10	SW
090	90	NE	159		132	9	SW
091			165		146	7	SW
091	89	SW	153		174	9	SW
091	87	SW	167		000	8	NW
091	86	NE	165		162	6	SW
093			159		022	5	NW
093			170		000	1	NW
093			163		000	6	NW
093			183		156	10	NE
093	87	SW	170		004	8	SE
094			165		177	9	NE
094			174		008	7	SE
094			162		040	17	SE
094	90		165		038	28	SE
094	82	NE	157		064	14	SE
095			144		064	14	SE
095			147		025	38	NW
095			151		016	35	NW
095			163		096	19	SW
095			163				
095			173				
095			153				
095			173				
095	90						
096							
096							
096							
096							
096							
096	85	SW					
097							
097							
097							
097							
097							
097	88	SW					
097	88	SW					
097	88	NE					
097	88	SW					
097	85	NE					
097	90						
097	88	SW					
097	70	SW					
097	90						
097	81	NE					

097	87	SW					
098							
098							
098	86	SW					
098	88	SW					
098	88	SW					
098	90						
098	88	SW					
098	86	NE					
098	88	NE					
099							
099							
099							
099							
099							
099							
099							
099							
099	88	SW					
099	85	NE					
099	85	NE					
099	87	SW					
099	87	NE					
100							
100							
100							
100							
100							
100							
100							
100	88	SW					
100	90						
100	90						
100	85	NE					
100	90						
101							
101							
101							
102							
102							
102							
103							
103							
103							
103							
103	90						
103	86	SW					
103	84	NE					
104							
104							
104	86	NE					
105							
105	88	NE					
105	85	SW					
105	86	NE					
106							
106							
106							
109							
109	85	NE					
110	78	SW					
112							
112	84	SW					
115							
120	84	SW					
123							
123	87	SW					
126	85	SW					
127							

Tables showing en échelon array orientations, and geometric data (plotted in Figure 2.19), for segmented dykes.

* Segmentation form has been reconstructed due to loss of outcrop.

** The dyke segments have coalesced and segmentation is preserved as overlapping horns protruding from both margins of the dyke.

Length data for the segments was not always available. Where length is given for just one of the segments, a total length is estimated by doubling that length.

Dyke	Step geometry (RS = right-step; LS = left-step)	En échelon array strike
K82	RS	128
K85	RS	086
K87	RS	120
K92	RS	101
K93	RS	100
K100	LS	103
K103	RS	116
K117	RS	101
K121	LS	099
K123i	RS	101
K123ii	LS	081
K128i	LS	087
K128ii	RS	101
K134	RS	112
K157a	LS	088
K157b	LS	088
K173	LS	080
K176	RS	096
K178	RS	095
K181	RS	097

Dyke	Host rock lithology	Dyke width (m)	Segment overstep (m)	Segment overlap (m)	Aspect ratio (overlap/overstep)	Length of dyke segment 1 (m)	Length of dyke segment 2 (m)	Total length of the two dyke segments (m)	Step geometry (RS = right-step; LS = left-step)
K10	dal qtz	0.38**	0.6	1.5	2.5		14	28	RS
	dal qtz	0.38**	1.5	4.5	3.0		14	28	RS
K12	dal qtz/sch	0.58**	1.5	3	2.0	5.5	5	10.5	RS
K23	dal qtz/sch	0.93	1.65	4.5	2.7		13	26	LS
K27	dal qtz	1.3**	1	2.4	2.4		15.6	31.2	RS
	dal qtz	1.3**	0.51	1.4	2.7	15.6	11.1	26.7	RS
	dal qtz	1.3**	0.45	0.9	2.0	11.1	8.8	19.9	RS
K32	dal qtz	1.1	0.9	2.7	3.0				LS
K82b	carb lst	0.22	1.5	9	6.0		29	58	RS
	carb lst	0.25**	0.35	0.84	2.4		3.65	7.3	LS
	carb lst	0.25**	0.3	1.5	5.0		3.65	7.3	LS
K83	carb sst	0.5**	0.8	1.5	1.9	7.7	11	18.7	LS
	carb sst	0.45**	1.75	1.64	0.9				RS
K85*	carb sst	1.7	2.94	12.14	4.1	26.2	26.9	53.1	RS
K87	carb lst	0.8	0.64	1.65	2.6		7.7	15.4	RS
	carb lst	0.8**	0.23	0.4	1.7		7.7	15.4	RS
K92	carb sst	0.82	0.6	2.18	3.6				RS
	carb sst	0.82	1.52	6.6	4.3		14.2	28.4	RS
	carb sst	0.82	0.82	1.5	1.8	15.2	14.2	29.4	LS
K93*	carb sst	0.97	1.7	4.68	2.8				RS
	carb sst	0.9	2	9.28	4.6				RS
K100	tert gab	1.08	1.5	2.84	1.9		13.8	27.6	LS
	tert gab	1.08	0.78	1.44	1.8		13.8	27.6	LS
K103	tert gab	1.8	0.8	1.74	2.2				RS
K104i	carb sst	0.62	1.6	3.3	2.1	18.3	20.5	38.8	RS
K111	carb lst	1**	2	9.24	4.6				LS
K116ii	carb lst	0.6	0.4	1.5	3.8				LS
K118ii*	carb lst	0.35	1.2	5	4.2				LS
K118i/ii*	carb lst	2.7	10	30	3.0				RS
K120	carb lst	0.02	0.05	0.13	2.6	0.63	0.75	1.253	LS
K121	carb lst	1**	1.98	7.5	3.8				LS
K123i	carb lst	0.18	0.11	0.32	2.9		2.6	5.2	RS
K132ii	carb lst	0.13	0.46	0.73	1.6	6	16	22	LS
	carb lst	0.1	0.39	0.75	1.9	6.2	16	22.2	RS
	carb lst	0.014	0.04	0.11	2.8		0.32	0.64	RS
K135i	carb lst	0.0037	0.0065	0.019	2.9		0.062	0.124	LS
K137*	carb lst	1.25	2.2	9	4.1				LS
K141	carb lst	0.31	2.15	7.75	3.6				LS
K144	carb lst	0.3**	0.18	0.3	1.7				LS
K145	carb lst	0.28	1.2	3.5	2.9				LS
K148	carb lst	0.62**	0.24	0.48	2.0				RS
K155b	carb lst	0.58	0.42	1.13	2.7		5.33	10.66	LS
K157a	carb lst	0.75	1.65	4.5	2.7	3.5	10	13.5	LS
K157b	carb lst	0.018	0.045	0.122	2.7	0.23	0.36	0.59	LS
	carb lst	0.018	0.0056	0.02	3.6		0.23	0.46	LS
K158	carb lst	0.7	2.85	17	6.0				RS
K164i	carb sst	1	0.31	0.98	3.2		3.3	6.6	LS
K167	carb sst	0.065	0.0025	0.014	5.6	0.75	1.1	1.85	LS
K168	carb sst	0.13	0.35	1	2.9		4	8	RS
	carb sst	0.13	0.4	1.1	2.8		4	8	LS
K175	carb lst	0.053	0.059	0.165	2.8				LS
K181	carb lst	0.88	1.05	2.2	2.1		13	26	RS
DK15ii	carb lst	1	1.4	3.3	2.4				RS

Distances and dyke widths used to derive the amount of extension for the Killala swarm between Inishcrone and Lenadoon Point, east side of Killala Bay (Figure 2.20).

From		To		Distance (m)	Dyke	Dyke width (m)
128605	330283	128546	330626	350	K111	1
					K112	4
					K113	1.6
					K114	1
128471	330707	128529	331280	576	K115	0.4
					K116i	0.15
					K116ii	0.7
					K117	5.3
					K118i	2.2
					K118ii	0.35
					K119	1.2
					K120	0.28
128529	331280	128859	331781	601	K121	1.06
					K122	3.1
					K123i	0.18
					K123ii	4.6
					K124	46
					K125	1.7
BREAK ~100m						
128919	331853	129203	332300	530	K126	1
					K127	9
					K128i	1.5
					K128ii	0.1
					K129i	4.6
					K129ii	3
BREAK ~75m						
129288	332381	130798	335891	3818	K130	1.7
					K131	0.11
					K132i	1.1
					K132ii	0.13
					K133i	2.55
					K133ii	5.5
					K134	1.7
					K135i/ii	1.85
					K136	1.28
					K137	1.25
					K138	0.81
					K139	0.05
					K140	1.02
					K141	0.31
BREAK ~870m						
131359	336547	131368	339001	2454	K142	0.28
					K143	2.8
					K144	0.3
					K145	0.28
					K146	0.64
					K147	0.85
					K148	0.62
					K149	1.34
			TOTAL	8329		120.49
			EXTENSION		**1.45 %**	

Data for dykes of the Donegal-Kingscourt swarm. Dyke numbers are listed from the southern end of part of the swarm studied, northwards (see Figure 2.22). Dykes split into Xi, Xii etc. are situated in close proximity to each other and may be part of the same intrusion. Dykes listed as Xa, Xb etc. are different points along the same intrusion where the dyke outcrops over a relatively large distance. Dyke orientations apply to whole dykes, or segments of dykes when a list of orientations is given. Dip information was derived for only a proportion of the total number of dykes. Along coastal exposures strikes of segments are generally listed in the direction out to sea. In some cases only a grid reference is listed for a point along a dyke. Opening directions are given in the horizontal plane, and also sometimes in the vertical plane where exposure allowed. 'Ext.' refers to an extensional opening, i.e. no element of strike-slip (horizontal plane) or dip-slip (vertical plane). Where multiple opening directions are listed they do not correspond with the particular strike value to which they lie opposite in the table. Host rock orientation data refers to either bedding or metamorphic fabric.

DYKE NUMBER	EASTING	NORTHING	DYKE STRIKE	DYKE DIP	DYKE DIP DIRECTION	DYKE WIDTH (M)	OPENING DIRECTION (HORIZONTAL PLANE)	OPENING DIRECTION (VERTICAL PLANE)	HOST ROCK STRIKE	HOST ROCK DIP	HOST ROCK DIP DIRECTION	HOST ROCK AGE	HOST ROCK DETAIL
1	220571	344704	142	83	NE	19			170	11	SW	Carboniferous	Ballyshannon Limestone Form.
2	220227	347931	132									Carboniferous	Ballyshannon Limestone Form.
3	214840	352720	145									Carboniferous	Mullaghmore Sandstone Form.
4	207961	355779	132	85	NE	3.5						Carboniferous	Meenymore Form. & Quarry Sandstone Memb.
5a	219943	355911	135									Devonian	Shanmullagh Form.
5b	219580	356266	135									Devonian	Shanmullagh Form.
6	224335	357735	145									Devonian	Shanmullagh Form.
7	219967	361742	145									Carboniferous	Mullaghmore Sandstone Form.
8	224065	363265	150	85	NE	0.9						Carboniferous	Ballyshannon Limestone Form.
9	223080	363458	127	86	NE	2.1						Carboniferous	Ballyshannon Limestone Form.
			123	82	NE	1.95						Carboniferous	Ballyshannon Limestone Form.
			138	76	NE	2.8						Carboniferous	Ballyshannon Limestone Form.
			128	82	NE	4-5						Carboniferous	Ballyshannon Limestone Form.
			135	70	NE	1.9						Carboniferous	Ballyshannon Limestone Form.
			123	84	NE	3.1						Carboniferous	Ballyshannon Limestone Form.
10	222671	363433	130	83	NE	0.8						Carboniferous	Ballyshannon Limestone Form.
11	222303	363533	147			>5						Carboniferous	Ballyshannon Limestone Form.
12	231789	370637	087			>8			085	54	NW	Precambrian (Dal.)	Mullaghcarn Form.
13	195665	375005	150	86	NE	>3.5						Carboniferous	Ballyshannon Limestone Form.
14	185144	375062	133	83	NE	1.85	ext.		097	2	SW	Carboniferous	Bundoran Shale Form.
			141	85	NE							Carboniferous	Bundoran Shale Form.
			135	87	NE							Carboniferous	Bundoran Shale Form.
			135									Carboniferous	Bundoran Shale Form.
			137									Carboniferous	Bundoran Shale Form.
			137									Carboniferous	Bundoran Shale Form.
			137									Carboniferous	Bundoran Shale Form.
15i	185052	374741	176			1.05	ext.		081	12	NW	Carboniferous	Bundoran Shale Form.
			125	68	SW	1.4						Carboniferous	Bundoran Shale Form.
			136									Carboniferous	Bundoran Shale Form.
			123									Carboniferous	Bundoran Shale Form.
			003									Carboniferous	Bundoran Shale Form.
			122			1.35						Carboniferous	Bundoran Shale Form.
			123			1.02						Carboniferous	Bundoran Shale Form.
			125			1.02						Carboniferous	Bundoran Shale Form.
			125									Carboniferous	Bundoran Shale Form.
			125									Carboniferous	Bundoran Shale Form.
			123			1						Carboniferous	Bundoran Shale Form.
			123									Carboniferous	Bundoran Shale Form.
15ii	185045	374736	127			1	ext.		081	12	NW	Carboniferous	Bundoran Shale Form.
			123			1						Carboniferous	Bundoran Shale Form.
			123	80	NE	0.98						Carboniferous	Bundoran Shale Form.
			122			0.98						Carboniferous	Bundoran Shale Form.
			125									Carboniferous	Bundoran Shale Form.
			125			1.02						Carboniferous	Bundoran Shale Form.
			005	82	SE							Carboniferous	Bundoran Shale Form.
			177			0.90						Carboniferous	Bundoran Shale Form.
			150	75	NE	0.90						Carboniferous	Bundoran Shale Form.
16	185049	374704	127	68	NE	0.36	ext.		074	13	NW	Carboniferous	Bundoran Shale Form.
			136	80	NE							Carboniferous	Bundoran Shale Form.
			132	75	NE	1.2						Carboniferous	Bundoran Shale Form.
17a	184924	374493	125	77	NE	25			079	6	NW	Carboniferous	Bundoran Shale Form.
17b	184769	374596	126			>3						Carboniferous	Bundoran Shale Form.
			141									Carboniferous	Bundoran Shale Form.
17c	184654	374702	127			>7						Carboniferous	Bundoran Shale Form.
17d	184436	374822	125									Carboniferous	Bundoran Shale Form.
18a	174973	373241	016	88	SE	0.29	ext.	ext.	012	8	SE	Carboniferous	Ballyshannon Limestone Form.
			016			0.33						Carboniferous	Ballyshannon Limestone Form.
			006	89	SE							Carboniferous	Ballyshannon Limestone Form.
18b	175180	375287	175	88	SW	1	ext.		062	23	SE	Carboniferous	Banagher Sandstone Form.
			000									Carboniferous	Banagher Sandstone Form.
19	180464	382257	125	83	SW	>5-10						Carboniferous	Ballyshannon Limestone Form.
20	192157	385658	113	77	SW	13						Carboniferous	Bundoran Shale Form.
21	197084	386999	110									Precambrian (Dal.)	Lough Mourne Form.
22	200759	386948	140	90								Caledonian	Barnesmore granite, G3
			115									Caledonian	Barnesmore granite, G4
			152	85	SW	>1.5						Caledonian	Barnesmore granite, G5
23	200960	387009	120	72	NE	>4-5						Caledonian	Barnesmore granite, G4
24a	198485	390271	134	87	SW	0.5						Caledonian	Barnesmore granite, G2
24b	198367	390366	153	83	SW	0.45						Caledonian	Barnesmore granite, G2
25	175462	389495	130			>14						Caledonian	Appinite suite, undifferentiated
26ia	190096	394496	147			>2						Precambrian (Dal.)	Upper Crana Quartzite Form.
26ib	190157	394367	153	85	SW							Precambrian (Dal.)	Upper Crana Quartzite Form.
26ic	190365	394279	105									Precambrian (Dal.)	Upper Crana Quartzite Form.
26id	190569	394233	110									Precambrian (Dal.)	Upper Crana Quartzite Form.
26ie	190633	394196	147	80	NE	>4-5						Precambrian (Dal.)	Upper Crana Quartzite Form.
			012									Precambrian (Dal.)	Upper Crana Quartzite Form.
26if	190720	394116	139			>6						Precambrian (Dal.)	Upper Crana Quartzite Form.
			125									Precambrian (Dal.)	Upper Crana Quartzite Form.
26ig	190790	394041	148	82	NE	>6			011	40	NW	Precambrian (Dal.)	Slieve Tooey Quartzite Form.
26ii	190907	394064										Precambrian (Dal.)	Slieve Tooey Quartzite Form.
27	175839	404263	170	90		>1.65						Caledonian	Trawenagh Bay granite, G1
28	192068	419809	137	84	NE	3.7			000	14	W	Precambrian (Dal.)	Ards Quartzite Form.
29	192000	419826	145	80	NE	2.3			000	14	W	Precambrian (Dal.)	Ards Quartzite Form.
30ia	191448	422414	140	85	SW	>3.3						Precambrian (Dal.)	Sessiagh-Clonmass Form.
30ib	191563	422267	047	50	SE		060					Precambrian (Dal.)	Sessiagh-Clonmass Form.
30ic	191505	422215	056	64	SE							Precambrian (Dal.)	Sessiagh-Clonmass Form.
30id	191597	422216	148	87	NE	>2						Precambrian (Dal.)	Sessiagh-Clonmass Form.
30ie	191774	422018	143	85	NE	>2.4	045					Precambrian (Dal.)	Marble
30iia	191714	422349	148									Precambrian (Dal.)	Sessiagh-Clonmass Form.
			155	75	NE							Precambrian (Dal.)	Sessiagh-Clonmass Form.
			114									Precambrian (Dal.)	Sessiagh-Clonmass Form.
			135									Precambrian (Dal.)	Sessiagh-Clonmass Form.
			149	87	NE	>2.1						Precambrian (Dal.)	Sessiagh-Clonmass Form.

			150	85	NE						Precambrian (Dal.)	Sessiagh-Clonmass Form.
30iib	191890	422133	138	85	SW	>8.1					Precambrian (Dal.)	Sessiagh-Clonmass Form.
31	174339	419209	107	81	NE	>3.5					Caledonian	Thorr granite
			100								Caledonian	Thorr granite
32	174426	421094	158	64	NE	3.1					Caledonian	Thorr granite
33a	177228	421330	113	86	SW	6.2					Caledonian	Thorr granite
			105								Caledonian	Thorr granite
			138								Caledonian	Thorr granite
			134								Caledonian	Thorr granite
33b	177175	421354	100			~6					Caledonian	Thorr granite
33c	177133	421371	122	72	SW						Caledonian	Thorr granite
			085	77	SE						Caledonian	Thorr granite
33d	177024	421347	080	55	NW						Caledonian	Thorr granite
34i	178032	423241	133	85	SW	1.35	070				Caledonian	Thorr granite
			029								Caledonian	Thorr granite
			133			1.7					Caledonian	Thorr granite
			029								Caledonian	Thorr granite
34ii	178035	423243	155	90		2.85					Caledonian	Thorr granite
34iii	178039	423246	156	79	NE	1.05					Caledonian	Thorr granite
34iv	178041	423247	140	85	SW	0.16					Caledonian	Thorr granite
35	180002	423599	108	80	NE	6					Caledonian	Thorr granite
36	179776	424654	107	84	SW	2.35					Caledonian	Thorr granite
37	179238	426929	131	88	SW	1.2					Caledonian	Thorr granite
38	179926	429144	118				042				Caledonian	Thorr granite
			116	80	SW	3.4					Caledonian	Thorr granite
			173								Caledonian	Thorr granite
			140	70	SW						Caledonian	Thorr granite
			010								Caledonian	Thorr granite
39	179969	429651	130	89	SW	0.95					Caledonian	Thorr granite
40	180074	429687	122	57	NE	4					Caledonian	Thorr granite
41	180084	429701	128	70	SW	2					Caledonian	Thorr granite
42	180100	429730	123	86	NE		057				Caledonian	Thorr granite
			178	89	SW	2.1					Caledonian	Thorr granite
			116	80	SW	2.7					Caledonian	Thorr granite
43	180209	429889	163	72	NE	>3.2					Caledonian	Thorr granite
			177								Caledonian	Thorr granite
44	180238	430275	122	88	SW	1.3	030				Caledonian	Thorr granite
			122								Caledonian	Thorr granite
			117	80	SW	1.35					Caledonian	Thorr granite
45	180334	430329	121	87	NE	0.21	035				Caledonian	Thorr granite
			176			0.13	040				Caledonian	Thorr granite
			140			0.21					Caledonian	Thorr granite
46	180398	430310	171				042				Caledonian	Thorr granite
			122	87	NE	2.5					Caledonian	Thorr granite
			151								Caledonian	Thorr granite
			020								Caledonian	Thorr granite
47	180366	430410	139			46					Caledonian	Thorr granite
			117			45					Caledonian	Thorr granite
48	181621	433250	122			~4					Caledonian	Thorr granite
			092								Caledonian	Thorr granite
49	181557	433375	156	82	SW	1.6	050				Caledonian	Thorr granite
			104	90		1.5					Caledonian	Thorr granite
			144								Caledonian	Thorr granite
50	181260	433608	095	80	NE	1.3					Caledonian	Thorr granite
51	181485	434006	172	82	SW	2.55					Caledonian	Thorr granite
			090								Caledonian	Thorr granite
			153								Caledonian	Thorr granite
52	181539	434011	016	68	SE	1.15	056				Caledonian	Thorr granite
			132			1.39					Caledonian	Thorr granite
			016								Caledonian	Thorr granite
53	181602	434118	087	78	SE	1	052				Caledonian	Thorr granite
			130	90							Caledonian	Thorr granite
54	181922	434674	094	80	SW	1.6	036				Caledonian	Thorr granite
			095				042				Caledonian	Thorr granite
			093				038				Caledonian	Thorr granite
			093				040				Caledonian	Thorr granite
			096								Caledonian	Thorr granite
55	181958	434748	002	78	NW	2.1	070				Caledonian	Thorr granite
			097	81	SW	1					Caledonian	Thorr granite
			155			2.3					Caledonian	Thorr granite
			020			2					Caledonian	Thorr granite
			035			1.35					Caledonian	Thorr granite
			165	80	NE	2.5					Caledonian	Thorr granite
			035			1.35					Caledonian	Thorr granite
			158	88	SW	2.25					Caledonian	Thorr granite
56	182212	434590	094	73	SW	>3.3					Caledonian	Thorr granite
57	182400	434409	090	73	S	0.5					Caledonian	Thorr granite
58	182503	434287	164				046				Caledonian	Thorr granite
			147				052				Caledonian	Thorr granite
			095			2.45					Caledonian	Thorr granite
			160								Caledonian	Thorr granite
			102								Caledonian	Thorr granite
			165								Caledonian	Thorr granite
			124			2					Caledonian	Thorr granite
58	182615	434229									Caledonian	Thorr granite
59	183618	434071	134	83	SW		045				Caledonian	Thorr granite
			160			2.8	048				Caledonian	Thorr granite
			082				040				Caledonian	Thorr granite
			150								Caledonian	Thorr granite
			095	85	SW	2.4					Caledonian	Thorr granite
			107	78	SW	2.4					Caledonian	Thorr granite
59	183688	434047									Caledonian	Thorr granite
60	183715	434061	148	82	NE	6	067				Caledonian	Thorr granite
			163								Caledonian	Thorr granite
61	183723	434066	148			4					Caledonian	Thorr granite
62	183755	434038	106	83	NE	2.6					Caledonian	Thorr granite
63	183795	434083	097	82	SW	1	030				Caledonian	Thorr granite
			093			0.78					Caledonian	Thorr granite
			047			0.31					Caledonian	Thorr granite
			093			0.78					Caledonian	Thorr granite
64	183826	434118	137			0.7	047				Caledonian	Thorr granite
			080				030				Caledonian	Thorr granite
			142								Caledonian	Thorr granite
			120	88	NE	0.6					Caledonian	Thorr granite
			120								Caledonian	Thorr granite
65	183856	434153	109				050				Caledonian	Thorr granite
			005			0.66	050				Caledonian	Thorr granite
			100			0.71					Caledonian	Thorr granite
66	183937	434194	152			0.4	060				Caledonian	Thorr granite
			030				060				Caledonian	Thorr granite
			150								Caledonian	Thorr granite
			025			0.28					Caledonian	Thorr granite
			155			0.42					Caledonian	Thorr granite
67	184250	434203	010	82	SE	1.6	056				Caledonian	Thorr granite
			118			2					Caledonian	Thorr granite
			160								Caledonian	Thorr granite
68	184444	433898	158			1.4					Caledonian	Thorr granite
69	184532	433905	170			1.2	040				Caledonian	Thorr granite
			140								Caledonian	Thorr granite
			090								Caledonian	Thorr granite
70	185348	433647	147	85	NE	5					Caledonian	Thorr granite
			025								Caledonian	Thorr granite
71a	185970	433848	170	87	NE	2.95		037	90		Precambrian (Dal.)	Upper Falcarragh Pelite Form.
71b	185935	433889	127	80	NE	4					Precambrian (Dal.)	Upper Falcarragh Pelite Form.
72a	186252	433623	150								Precambrian (Dal.)	Upper Falcarragh Pelite Form.
			132								Precambrian (Dal.)	Upper Falcarragh Pelite Form.
			117								Precambrian (Dal.)	Upper Falcarragh Pelite Form.
			125								Precambrian (Dal.)	Upper Falcarragh Pelite Form.
			065								Precambrian (Dal.)	Upper Falcarragh Pelite Form.
			145			3.4					Precambrian (Dal.)	Upper Falcarragh Pelite Form.
72b	186314	433648	120								Precambrian (Dal.)	Upper Falcarragh Pelite Form.
			080								Precambrian (Dal.)	Upper Falcarragh Pelite Form.
73	192260	433566	174	75	SW	1.25		176	60	SW	Precambrian (Dal.)	Upper Falcarragh Pelite Form.
			169	72	SW	0.34					Precambrian (Dal.)	Upper Falcarragh Pelite Form.

Appendix 9 Background fracture orientations in the Rosses and Thorr granites (Donegal-Kingscourt swarm)

Fracture orientation data from the Rosses and Thorr granites, northwest Co. Donegal. Fifty measurements were taken at each point along the coast. Grid references are given. Entitling numbers are the locations as indicated in Figure 2.29 and Figure 2.30.

1a
(177228 421350)
000 75 NW
001 89 NW
002 80 NW
004 86 SE
005 65 NW
005 66 NW
006 82 NW
008 89 NW
009 80 NW
014 80 NW
020 83 NW
030 87 SE
038 80 NW
041 88 SE
042 85 SE
043 88 NW
044 85 SE
044 85 SE
045 84 SE
045 80 NW
088 85 NW
089 85 NW
093 85 SW
095 78 SW
096 83 SW
099 88 SW
105 80 SW
106 88 NE
108 85 SW
109 86 NE
115 85 NE
116 85 NE
125 88 SW
126 85 SW
130 90
132 82 SW
132 87 NE
133 82 SW
133 89 NE
133 89 NE
135 66 SW
136 80 SW
143 70 NE
148 90
171 84 SW
171 86 SW
174 76 SW
175 78 SW
176 88 SW
178 90

1b
(177991 422908)
001 83 NW
005 80 NW
005 85 NW
008 88 NW
010 85 NW
011 88 SE
012 85 SE
013 88 SE
015 90
016 85 SE
018 88 SE
020 84 NW
023 85 NW
027 80 NW
032 90
040 90
042 82 NW
048 80 NW
050 87 SE
054 80 NW
093 80 NE
097 75 NE
099 81 NE
100 83 NE
105 90
108 81 NE
113 89 SW
115 85 SW
117 82 NE
117 88 NE
128 85 SW
130 85 NE
133 82 NE
135 90
137 82 NE
138 83 NE
142 80 NE
144 80 SW
145 85 NE
145 83 NE
146 75 SW
148 89 SW
148 90
148 90
150 85 SW
151 82 NE
152 82 SW
155 83 SW
160 87 SW
164 83 SW

2a
(180100 429746)
000 77 SE
002 86 NW
005 68 SE
007 83 SE
008 80 SE
015 82 SE
019 72 SE
021 76 SE
022 80 SE
025 60 NW
025 83 NW
026 77 NW
027 80 SE
039 85 SE
039 71 SE
050 90
054 70 SE
055 87 SE
057 87 SE
065 80 NW
067 82 NW
070 83 NW
074 82 NW
080 82 NW
081 90
106 89 SW
108 86 SW
110 85 SW
111 85 SW
111 88 SW
112 86 SW
112 87 SW
113 85 SW
113 88 SW
115 77 SW
115 86 SW
117 89 SW
119 87 SW
119 86 SW
120 88 NE
120 73 SW
120 78 SW
121 79 SW
121 79 SW
123 80 SW
123 85 SW
124 80 SW
133 84 NE
139 90
142 85 NE

2b
(180221 430249)
027 83 SE
027 85 NW
031 80 SE
031 78 SE
031 82 SE
031 78 NW
032 87 NW
034 80 NW
035 72 SE
036 79 SE
037 84 NW
037 85 NW
037 83 SE
038 78 SE
038 78 SE
039 79 SE
042 75 SE
044 77 SE
108 82 SW
109 85 SW
109 75 SW
110 77 SW
113 81 SW
114 72 SW
115 81 SW
117 80 SW
117 80 SW
117 77 SW
117 78 SW
118 77 SW
118 83 SW
118 78 SW
118 85 SW
120 79 SW
120 78 SW
123 60 SW
123 79 SW
124 80 SW
124 80 SW
125 78 SW
127 85 SW
128 86 SW
128 84 SW
128 84 SW
147 72 NE
149 83 NE
157 86 NE
159 70 NE
162 79 NE
178 83 SW

2c
(180381 430314)
021 79 SE
024 82 NW
025 87 NW
029 86 NW
031 85 NW
032 83 NW
039 81 NW
040 82 SE
041 72 SE
041 84 NW
045 82 NW
048 90
049 85 NW
049 88 NW
054 88 NW
060 85 NW
068 84 NW
112 81 SW
113 85 SW
115 82 SW
115 76 SW
116 78 SW
116 79 SW
116 80 SW
116 83 SW
117 84 SW
117 79 SW
118 89 SW
118 83 SW
118 88 SW
119 80 SW
120 90
120 78 SW
121 82 SW
121 76 SW
123 82 SW
124 72 SW
125 83 SW
155 75 NE
167 86 NE
170 77 NE
170 85 NE
172 80 NE
172 81 NE
173 86 NE
173 80 NE
174 85 NE
176 78 SW
177 81 SW
178 76 SW

3a
(181449 433981)
003 82 SE
005 60 NW
010 65 NW
016 82 SE
021 83 SE
023 87 NW
029 75 SE
029 73 SE
031 81 SE
032 79 SE
032 78 SE
034 77 SE
085 80 SE
087 78 SE
090 90
090 85 SE
090 82 SE
092 82 NE
092 75 SW
092 90
092 80 NE
093 84 SW
093 82 SW
093 83 SW
093 80 SW
095 85 NE
095 79 SW
095 87 SW
095 85 NE
095 90
096 82 SW
096 85 NE
099 85 SW
099 85 SW
100 88 SW
102 83 NE
102 83 NE
103 86 SW
150 88 SW
160 81 NE
163 77 SW
164 80 NE
164 75 SW
166 77 SW
169 90
170 90
172 88 SW
172 75 NE
173 80 SW
179 85 NE

3b
(181902 434657)
000 75 NW
018 85 SE
020 80 SE
025 73 SE
028 79 SE
031 76 SE
031 90
066 73 NW
091 79 SW
091 78 SW
091 82 SW
092 80 SW
092 80 SW
092 86 NE
092 80 SW
093 84 SW
093 81 SW
094 77 SW
094 80 SW
095 85 SW
095 80 SW
095 82 SW
095 78 SW
096 82 SW
096 85 SW
097 82 SW
098 85 SW
102 84 SW
127 80 NE
133 80 SW
136 78 SW
145 78 SW
157 81 SW
157 78 SW
157 78 SW
157 90
158 86 SW
163 74 SW
163 88 SW
164 62 NE
165 81 SW
165 79 SW
166 75 SW
168 80 SW
170 67 SW
170 88 SW
171 80 SW
172 58 NE
172 90
174 81 SW

3c
(181990 434725)
003 83 SE
020 80 SE
025 81 SE
027 86 SE
028 83 SE
035 90
035 83 NW
035 78 NW
037 85 NW
037 85 SE
041 83 SE
045 77 SE
048 78 SE
049 83 NW
053 79 SE
054 80 SE
055 82 NW
055 90
055 82 NW
055 78 SE
073 60 NW
087 83 SE
088 85 SE
090 81 SE
091 88 SW
093 80 SW
093 81 SW
094 89 NE
095 85 NE
095 80 SW
096 78 SW
105 80 SW
120 78 SW
130 87 NE
133 75 NE
145 88 SW
150 82 NE
151 80 NE
153 80 NE
153 85 SW
153 87 SW
155 75 NE
155 81 NE
162 90
163 89 SW
164 76 SW
165 78 SW
170 84 SW
172 87 SW
177 81 SW

4
(183757 434069)
001 78 SE
002 84 SE
002 82 SE
003 80 SE
003 88 SE
005 90
005 80 SE
006 81 SE
015 90
020 84 SE
030 85 SE
030 90
044 86 SE
047 80 SE
052 90
088 86 SE
092 85 SW
092 87 SW
092 90
093 85 SW
093 83 SW
093 80 SW
095 83 NE
095 87 SW
095 85 SW
096 82 SW
096 90
097 89 SW
098 86 NE
098 80 NE
098 79 SW
099 86 NE
100 82 NE
103 87 SW
112 90
145 82 NE
161 70 NE
162 75 NE
162 85 NE
163 80 NE
163 83 SW
165 78 NE
169 80 SW
170 83 NE
170 82 NE
171 90
172 76 NE
173 80 NE
176 88 NE
179 75 NE

Raw field data expanded for binning and the construction of fracture frequency profiles.
Dyke numbers are as described in the text. Southern profiles listed first where fractures from both sides of dyke have been counted.
Numbers in italics in the form *X(Y)* represent the fracture counts and entitle blocks of expanded data. X = number of fractures; Y = interval of fracture count (in m). Where only X is listed, Y = 1 m. Data is listed from the dyke margin outwards. Where X = NO, there was no outcrop over distance Y. Note, for dykes K155b, WC25a and WC25c, individual fracture spacings were measured in the field. Dyke K127 is not listed since fractures were counted in 1 m bins.
Expanded data is in two columns. Left column: expanded individual fracture spacing based on *X(Y)* for that block (each value represents the spacing between it and the previous fracture in the same or previous block). Right column: cumulative distance away from the dyke margin based on left column values. Note, dyke K117 'AB' is an exception with cumulative data only listed (see below). The data blocks have been expanded in this way to allow re-binning into 25 cm distance bins for plotting (see Appendix 12).
Commas separate fracture counts, *X(Y)*, where a zero count for *X*, or several zero counts, is/are made before a non-zero count. Expanded and cumulative data then reflect this. Where several fracture counts with the same *Y* value exist in a comma-delimited list, *Y* is indicated at the end of the list.
Dyke numbers suffixed with 'x' or 'y' (K116ii and DK65) refer to separate profiles either on the same side of a dyke at the same orientation, or perpendicular to margins of different strike for the same dyke.
For dyke K117, suffix 'A' indicates 'major fractures' (type 2 fractures from the text) and 'B' indicates 'minor fractures' (type 1 fractures from the text), as explained in the text. Suffix 'AB' combines the cumulative data for the two fracture types.

K23
S
10(0.2)
0.020000 0.020000
0.020000 0.040000
0.020000 0.060000
0.020000 0.080000
0.020000 0.100000
0.020000 0.120000
0.020000 0.140000
0.020000 0.160000
0.020000 0.180000
0.020000 0.200000
8(0.2)
0.025000 0.225000
0.025000 0.250000
0.025000 0.275000
0.025000 0.300000
0.025000 0.325000
0.025000 0.350000
0.025000 0.375000
0.025000 0.400000
3(0.2)
0.066667 0.466667
0.066667 0.533333
0.066667 0.600000
1(0.2)
0.200000 0.800000
3(0.2)
0.066667 0.866667
0.066667 0.933333
0.066667 1.000000
3(0.2)
0.066667 1.066667
0.066667 1.133333
0.066667 1.200000
1(0.2)
0.200000 1.400000
2(0.2)
0.100000 1.500000
0.100000 1.600000

1(0.2)
0.200000 1.800000
0,2(0.2)
0.300000 2.100000
0.100000 2.200000
2(0.2)
0.100000 2.300000
0.100000 2.400000
1(0.2)
0.200000 2.600000
0,2(0.2)
0.300000 2.900000
0.100000 3.000000
1(0.2)
0.200000 3.200000
2(0.2)
0.100000 3.300000
0.100000 3.400000
1(0.5)
0.500000 3.900000
1(0.5)
0.500000 4.400000
1(0.5)
0.500000 4.900000
1(0.5)
0.500000 5.400000
0(1.5),2(0.5)
1.750000 7.150000
0.250000 7.400000
1(50)
0.500000 7.900000
0(2),3(0.5)
2.166667 10.066667
0.166667 10.233333
0.166667 10.400000
0(3),2(0.5)
3.250000 13.650000
0.250000 13.900000
0(0.5)
0(0.5)
0(0.5)

0(0.5)

K27
S
19(0.2)
0.010526 0.010526
0.010526 0.021053
0.010526 0.031579
0.010526 0.042105
0.010526 0.052632
0.010526 0.063158
0.010526 0.073684
0.010526 0.084211
0.010526 0.094737
0.010526 0.105263
0.010526 0.115789
0.010526 0.126316
0.010526 0.136842
0.010526 0.147368
0.010526 0.157895
0.010526 0.168421
0.010526 0.178947
0.010526 0.189474
0.010526 0.200000
10(0.2)
0.020000 0.220000
0.020000 0.240000
0.020000 0.260000
0.020000 0.280000
0.020000 0.300000
0.020000 0.320000
0.020000 0.340000
0.020000 0.360000
0.020000 0.380000
0.020000 0.400000
13(0.2)
0.015385 0.415385
0.015385 0.430769
0.015385 0.446154

0.015385 0.461538
0.015385 0.476923
0.015385 0.492308
0.015385 0.507692
0.015385 0.523077
0.015385 0.538462
0.015385 0.553846
0.015385 0.569231
0.015385 0.584615
0.015385 0.600000
12(0.2)
0.016667 0.616667
0.016667 0.633333
0.016667 0.650000
0.016667 0.666667
0.016667 0.683333
0.016667 0.700000
0.016667 0.716667
0.016667 0.733333
0.016667 0.750000
0.016667 0.766667
0.016667 0.783333
0.016667 0.800000
12(0.2)
0.016667 0.816667
0.016667 0.833333
0.016667 0.850000
0.016667 0.866667
0.016667 0.883333
0.016667 0.900000
0.016667 0.916667
0.016667 0.933333
0.016667 0.950000
0.016667 0.966667
0.016667 0.983333
0.016667 1.000000
9(0.2)
0.022222 1.022222
0.022222 1.044444
0.022222 1.066667
0.022222 1.088889

0.022222 1.111111
0.022222 1.133333
0.022222 1.155556
0.022222 1.177778
0.022222 1.200000
14(0.2)
0.014286 1.214286
0.014286 1.228571
0.014286 1.242857
0.014286 1.257143
0.014286 1.271429
0.014286 1.285714
0.014286 1.300000
0.014286 1.314286
0.014286 1.328571
0.014286 1.342857
0.014286 1.357143
0.014286 1.371429
0.014286 1.385714
0.014286 1.400000
14(0.2)
0.014286 1.414286
0.014286 1.428571
0.014286 1.442857
0.014286 1.457143
0.014286 1.471429
0.014286 1.485714
0.014286 1.500000
0.014286 1.514286
0.014286 1.528571
0.014286 1.542857
0.014286 1.557143
0.014286 1.571429
0.014286 1.585714
0.014286 1.600000
12(0.2)
0.016667 1.616667
0.016667 1.633333
0.016667 1.650000
0.016667 1.666667
0.016667 1.683333

0.016667 1.700000
0.016667 1.716667
0.016667 1.733333
0.016667 1.750000
0.016667 1.766667
0.016667 1.783333
0.016667 1.800000
13(0.2)
0.015385 1.815385
0.015385 1.830769
0.015385 1.846154
0.015385 1.861538
0.015385 1.876923
0.015385 1.892308
0.015385 1.907692
0.015385 1.923077
0.015385 1.938462
0.015385 1.953846
0.015385 1.969231
0.015385 1.984615
0.015385 2.000000
8(0.2)
0.025000 2.025000
0.025000 2.050000
0.025000 2.075000
0.025000 2.100000
0.025000 2.125000
0.025000 2.150000
0.025000 2.175000
0.025000 2.200000
8(0.2)
0.025000 2.225000
0.025000 2.250000
0.025000 2.275000
0.025000 2.300000
0.025000 2.325000
0.025000 2.350000
0.025000 2.375000
0.025000 2.400000
8(0.2)
0.025000 2.425000

0.025000 2.450000
0.025000 2.475000
0.025000 2.500000
0.025000 2.525000
0.025000 2.550000
0.025000 2.575000
0.025000 2.600000
6(0.2)
0.033333 2.633333
0.033333 2.666667
0.033333 2.700000
0.033333 2.733333
0.033333 2.766667
0.033333 2.800000
5(0.2)
0.040000 2.840000
0.040000 2.880000
0.040000 2.920000
0.040000 2.960000
0.040000 3.000000
12(0.5)
0.041667 3.041667
0.041667 3.083333
0.041667 3.125000
0.041667 3.166667
0.041667 3.208333
0.041667 3.250000
0.041667 3.291667
0.041667 3.333333
0.041667 3.375000
0.041667 3.416667
0.041667 3.458333
0.041667 3.500000
10(0.5)
0.050000 3.550000
0.050000 3.600000
0.050000 3.650000
0.050000 3.700000
0.050000 3.750000
0.050000 3.800000
0.050000 3.850000

0.050000 3.900000
0.050000 3.950000
0.050000 4.000000
3(0.5)
0.166667 4.166667
0.166667 4.333333
0.166667 4.500000
3(0.5)
0.166667 4.666667
0.166667 4.833333
0.166667 5.000000
2(0.5)
0.250000 5.250000
0.250000 5.500000
4(0.5)
0.125000 5.625000
0.125000 5.750000
0.125000 5.875000
0.125000 6.000000
13(0.5)
0.038462 6.038462
0.038462 6.076923
0.038462 6.115385
0.038462 6.153846
0.038462 6.192308
0.038462 6.230769
0.038462 6.269231
0.038462 6.307692
0.038462 6.346154
0.038462 6.384615
0.038462 6.423077
0.038462 6.461538
0.038462 6.500000
4(0.5)
0.125000 6.625000
0.125000 6.750000
0.125000 6.875000
0.125000 7.000000
0(0.5),2(0.5)
0.750000 7.750000
0.250000 8.000000

10(0.5)
0.050000 8.050000
0.050000 8.100000
0.050000 8.150000
0.050000 8.200000
0.050000 8.250000
0.050000 8.300000
0.050000 8.350000
0.050000 8.400000
0.050000 8.450000
0.050000 8.500000
8(0.5)
0.062500 8.562500
0.062500 8.625000
0.062500 8.687500
0.062500 8.750000
0.062500 8.812500
0.062500 8.875000
0.062500 8.937500
0.062500 9.000000
1(0.5)
0.500000 9.500000
3(0.5)
0.166667 9.666667
0.166667 9.833333
0.166667 10.000000
2(0.5)
0.250000 10.250000
0.250000 10.500000
0,0,1(0.5)
1.500000 12.000000
2(0.5)
0.250000 12.250000
0.250000 12.500000
1(0.5)
0.500000 13.000000
4(0.5)
0.125000 13.125000
0.125000 13.250000
0.125000 13.375000
0.125000 13.500000

6(0.5)
0.083333 13.583333
0.083333 13.666667
0.083333 13.750000
0.083333 13.833333
0.083333 13.916667
0.083333 14.000000
6(0.5)
0.083333 14.083333
0.083333 14.166667
0.083333 14.250000
0.083333 14.333333
0.083333 14.416667
0.083333 14.500000

N
13(0.2)
0.015385 0.015385
0.015385 0.030769
0.015385 0.046154
0.015385 0.061538
0.015385 0.076923
0.015385 0.092308
0.015385 0.107692
0.015385 0.123077
0.015385 0.138462
0.015385 0.153846
0.015385 0.169231
0.015385 0.184615
0.015385 0.200000
9(0.2)
0.022222 0.222222
0.022222 0.244444
0.022222 0.266667
0.022222 0.288889
0.022222 0.311111
0.022222 0.333333
0.022222 0.355556
0.022222 0.377778
0.022222 0.400000
12(0.2)

0.016667 0.416667
0.016667 0.433333
0.016667 0.450000
0.016667 0.466667
0.016667 0.483333
0.016667 0.500000
0.016667 0.516667
0.016667 0.533333
0.016667 0.550000
0.016667 0.566667
0.016667 0.583333
0.016667 0.600000
8(0.2)
0.025000 0.625000
0.025000 0.650000
0.025000 0.675000
0.025000 0.700000
0.025000 0.725000
0.025000 0.750000
0.025000 0.775000
0.025000 0.800000
21(0.2)
0.009524 0.809524
0.009524 0.819048
0.009524 0.828571
0.009524 0.838095
0.009524 0.847619
0.009524 0.857143
0.009524 0.866667
0.009524 0.876190
0.009524 0.885714
0.009524 0.895238
0.009524 0.904762
0.009524 0.914286
0.009524 0.923810
0.009524 0.933333
0.009524 0.942857
0.009524 0.952381
0.009524 0.961905
0.009524 0.971429
0.009524 0.980952

0.009524 0.990476
0.009524 1.000000
14(0.2)
0.014286 1.014286
0.014286 1.028571
0.014286 1.042857
0.014286 1.057143
0.014286 1.071429
0.014286 1.085714
0.014286 1.100000
0.014286 1.114286
0.014286 1.128571
0.014286 1.142857
0.014286 1.157143
0.014286 1.171429
0.014286 1.185714
0.014286 1.200000
8(0.2)
0.025000 1.225000
0.025000 1.250000
0.025000 1.275000
0.025000 1.300000
0.025000 1.325000
0.025000 1.350000
0.025000 1.375000
0.025000 1.400000
4(0.2)
0.050000 1.450000
0.050000 1.500000
0.050000 1.550000
0.050000 1.600000
9(0.2)
0.022222 1.622222
0.022222 1.644444
0.022222 1.666667
0.022222 1.688889
0.022222 1.711111
0.022222 1.733333
0.022222 1.755556
0.022222 1.777778
0.022222 1.800000

7(0.2)
0.028571 1.828571
0.028571 1.857143
0.028571 1.885714
0.028571 1.914286
0.028571 1.942857
0.028571 1.971429
0.028571 2.000000
1(0.2)
0.200000 2.200000
3(0.2)
0.066667 2.266667
0.066667 2.333333
0.066667 2.400000
2(0.5)
0.250000 2.650000
0.250000 2.900000
4(0.5)
0.125000 3.025000
0.125000 3.150000
0.125000 3.275000
0.125000 3.400000
8(0.5)
0.062500 3.462500
0.062500 3.525000
0.062500 3.587500
0.062500 3.650000
0.062500 3.712500
0.062500 3.775000
0.062500 3.837500
0.062500 3.900000
7(0.5)
0.071429 3.971429
0.071429 4.042857
0.071429 4.114286
0.071429 4.185714
0.071429 4.257143
0.071429 4.328571
0.071429 4.400000
7(0.5)
0.071429 4.471429

0.071429 4.542857
0.071429 4.614286
0.071429 4.685714
0.071429 4.757143
0.071429 4.828571
0.071429 4.900000
4(0.5)
0.125000 5.025000
0.125000 5.150000
0.125000 5.275000
0.125000 5.400000
10(0.5)
0.050000 5.450000
0.050000 5.500000
0.050000 5.550000
0.050000 5.600000
0.050000 5.650000
0.050000 5.700000
0.050000 5.750000
0.050000 5.800000
0.050000 5.850000
0.050000 5.900000
7(0.5)
0.071429 5.971429
0.071429 6.042857
0.071429 6.114286
0.071429 6.185714
0.071429 6.257143
0.071429 6.328571
0.071429 6.400000
10(0.5)
0.050000 6.450000
0.050000 6.500000
0.050000 6.550000
0.050000 6.600000
0.050000 6.650000
0.050000 6.700000
0.050000 6.750000
0.050000 6.800000
0.050000 6.850000
0.050000 6.900000
9(0.5)
0.055556 6.955556
0.055556 7.011111
0.055556 7.066667
0.055556 7.122222
0.055556 7.177778
0.055556 7.233333
0.055556 7.288889
0.055556 7.344444
0.055556 7.400000
2(0.5)
0.250000 7.650000
0.250000 7.900000
5(0.5)
0.100000 8.000000
0.100000 8.100000
0.100000 8.200000
0.100000 8.300000
0.100000 8.400000
7(0.5)
0.071429 8.471429
0.071429 8.542857
0.071429 8.614286
0.071429 8.685714
0.071429 8.757143
0.071429 8.828571
0.071429 8.900000
10(0.5)
0.050000 8.950000
0.050000 9.000000
0.050000 9.050000
0.050000 9.100000
0.050000 9.150000

0.050000 9.200000
0.050000 9.250000
0.050000 9.300000
0.050000 9.350000
0.050000 9.400000
8(0.5)
0.062500 9.462500
0.062500 9.525000
0.062500 9.587500
0.062500 9.650000
0.062500 9.712500
0.062500 9.775000
0.062500 9.837500
0.062500 9.900000
2
6(0.5)
0.083333 9.983333
0.083333 10.066667
0.083333 10.150000
0.083333 10.233333
0.083333 10.316667
0.083333 10.400000
2(0.5)
0.250000 10.650000
0.250000 10.900000
8(0.5)
0.062500 10.962500
0.062500 11.025000
0.062500 11.087500
0.062500 11.150000
0.062500 11.212500
0.062500 11.275000
0.062500 11.337500
0.062500 11.400000
10(0.5)
0.050000 11.450000
0.050000 11.500000
0.050000 11.550000
0.050000 11.600000
0.050000 11.650000
0.050000 11.700000
0.050000 11.750000
0.050000 11.800000
0.050000 11.850000
0.050000 11.900000
8(0.5)
0.062500 11.962500
0.062500 12.025000
0.062500 12.087500
0.062500 12.150000
0.062500 12.212500
0.062500 12.275000
0.062500 12.337500
0.062500 12.400000
6(0.5)
0.083333 12.483333
0.083333 12.566667
0.083333 12.650000
0.083333 12.733333
0.083333 12.816667
0.083333 12.900000
8(0.5)
0.062500 12.962500
0.062500 13.025000
0.062500 13.087500
0.062500 13.150000
0.062500 13.212500
0.062500 13.275000
0.062500 13.337500
0.062500 13.400000
6(0.5)
0.083333 13.483333
0.083333 13.566667
0.083333 13.650000
0.083333 13.733333

0.083333 13.816667
0.083333 13.900000
5(0.5)
0.100000 14.000000
0.100000 14.100000
0.100000 14.200000
0.100000 14.300000
0.100000 14.400000
4(0.5)
0.125000 14.525000
0.125000 14.650000
0.125000 14.775000
0.125000 14.900000
2
0.500000 15.400000
0.500000 15.900000
5
0.200000 16.100000
0.200000 16.300000
0.200000 16.500000
0.200000 16.700000
0.200000 16.900000
6
0.166667 17.066667
0.166667 17.233333
0.166667 17.400000
0.166667 17.566667
0.166667 17.733333
0.166667 17.900000
14
0.071429 17.971429
0.071429 18.042857
0.071429 18.114286
0.071429 18.185714
0.071429 18.257143
0.071429 18.328571
0.071429 18.400000
0.071429 18.471429
0.071429 18.542857
0.071429 18.614286
0.071429 18.685714
0.071429 18.757143
0.071429 18.828571
0.071429 18.900000
34
0.029412 18.929412
0.029412 18.958824
0.029412 18.988235
0.029412 19.017647
0.029412 19.047059
0.029412 19.076471
0.029412 19.105882
0.029412 19.135294
0.029412 19.164706
0.029412 19.194118
0.029412 19.223529
0.029412 19.252941
0.029412 19.282353
0.029412 19.311765
0.029412 19.341176
0.029412 19.370588
0.029412 19.400000
0.029412 19.429412
0.029412 19.458824
0.029412 19.488235
0.029412 19.517647
0.029412 19.547059
0.029412 19.576471
0.029412 19.605882
0.029412 19.635294
0.029412 19.664706
0.029412 19.694118
0.029412 19.723529
0.029412 19.752941

0.029412 19.782353
0.029412 19.811765
0.029412 19.841176
0.029412 19.870588
0.029412 19.900000
24
0.041667 19.941667
0.041667 19.983333
0.041667 20.025000
0.041667 20.066667
0.041667 20.108333
0.041667 20.150000
0.041667 20.191667
0.041667 20.233333
0.041667 20.275000
0.041667 20.316667
0.041667 20.358333
0.041667 20.400000
0.041667 20.441667
0.041667 20.483333
0.041667 20.525000
0.041667 20.566667
0.041667 20.608333
0.041667 20.650000
0.041667 20.691667
0.041667 20.733333
0.041667 20.775000
0.041667 20.816667
0.041667 20.858333
0.041667 20.900000
35
0.028571 20.928571
0.028571 20.957143
0.028571 20.985714
0.028571 21.014286
0.028571 21.042857
0.028571 21.071429
0.028571 21.100000
0.028571 21.128571
0.028571 21.157143
0.028571 21.185714
0.028571 21.214286
0.028571 21.242857
0.028571 21.271429
0.028571 21.300000
0.028571 21.328571
0.028571 21.357143
0.028571 21.385714
0.028571 21.414286
0.028571 21.442857
0.028571 21.471429
0.028571 21.500000
0.028571 21.528571
0.028571 21.557143
0.028571 21.585714
0.028571 21.614286
0.028571 21.642857
0.028571 21.671429
0.028571 21.700000
0.028571 21.728571
0.028571 21.757143
0.028571 21.785714
0.028571 21.814286
0.028571 21.842857
0.028571 21.871429
0.028571 21.900000
23
0.043478 21.943478
0.043478 21.986957
0.043478 22.030435
0.043478 22.073913
0.043478 22.117391
0.043478 22.160870
0.043478 22.204348

0.043478 22.247826
0.043478 22.291304
0.043478 22.334783
0.043478 22.378261
0.043478 22.421739
0.043478 22.465217
0.043478 22.508696
0.043478 22.552174
0.043478 22.595652
0.043478 22.639130
0.043478 22.682609
0.043478 22.726087
0.043478 22.769565
0.043478 22.813043
0.043478 22.856522
0.043478 22.900000
17
0.058824 22.958824
0.058824 23.017647
0.058824 23.076471
0.058824 23.135294
0.058824 23.194118
0.058824 23.252941
0.058824 23.311765
0.058824 23.370588
0.058824 23.429412
0.058824 23.488235
0.058824 23.547059
0.058824 23.605882
0.058824 23.664706
0.058824 23.723529
0.058824 23.782353
0.058824 23.841176
0.058824 23.900000
25
0.040000 23.940000
0.040000 23.980000
0.040000 24.020000
0.040000 24.060000
0.040000 24.100000
0.040000 24.140000
0.040000 24.180000
0.040000 24.220000
0.040000 24.260000
0.040000 24.300000
0.040000 24.340000
0.040000 24.380000
0.040000 24.420000
0.040000 24.460000
0.040000 24.500000
0.040000 24.540000
0.040000 24.580000
0.040000 24.620000
0.040000 24.660000
0.040000 24.700000
0.040000 24.740000
0.040000 24.780000
0.040000 24.820000
0.040000 24.860000
0.040000 24.900000
7
0.142857 25.042857
0.142857 25.185714
0.142857 25.328571
0.142857 25.471429
0.142857 25.614286
0.142857 25.757143
0.142857 25.900000
12
0.083333 25.983333
0.083333 26.066667
0.083333 26.150000
0.083333 26.233333
0.083333 26.316667

0.083333 26.400000
0.083333 26.483333
0.083333 26.566667
0.083333 26.650000
0.083333 26.733333
0.083333 26.816667
0.083333 26.900000

K32
S
5(0.2)
0.040000 0.040000
0.040000 0.080000
0.040000 0.120000
0.040000 0.160000
0.040000 0.200000
12(0.2)
0.016667 0.216667
0.016667 0.233333
0.016667 0.250000
0.016667 0.266667
0.016667 0.283333
0.016667 0.300000
0.016667 0.316667
0.016667 0.333333
0.016667 0.350000
0.016667 0.366667
0.016667 0.383333
0.016667 0.400000
18(0.2)
0.011111 0.411111
0.011111 0.422222
0.011111 0.433333
0.011111 0.444444
0.011111 0.455556
0.011111 0.466667
0.011111 0.477778
0.011111 0.488889
0.011111 0.500000
0.011111 0.511111
0.011111 0.522222
0.011111 0.533333
0.011111 0.544444
0.011111 0.555556
0.011111 0.566667
0.011111 0.577778
0.011111 0.588889
0.011111 0.600000
16(0.2)
0.012500 0.612500
0.012500 0.625000
0.012500 0.637500
0.012500 0.650000
0.012500 0.662500
0.012500 0.675000
0.012500 0.687500
0.012500 0.700000
0.012500 0.712500
0.012500 0.725000
0.012500 0.737500
0.012500 0.750000
0.012500 0.762500
0.012500 0.775000
0.012500 0.787500
0.012500 0.800000
15(0.2)
0.013333 0.813333
0.013333 0.826667
0.013333 0.840000
0.013333 0.853333
0.013333 0.866667
0.013333 0.880000
0.013333 0.893333

0.013333 0.906667
0.013333 0.920000
0.013333 0.933333
0.013333 0.946667
0.013333 0.960000
0.013333 0.973333
0.013333 0.986667
0.013333 1.000000
14(0.2)
0.014286 1.014286
0.014286 1.028571
0.014286 1.042857
0.014286 1.057143
0.014286 1.071429
0.014286 1.085714
0.014286 1.100000
0.014286 1.114286
0.014286 1.128571
0.014286 1.142857
0.014286 1.157143
0.014286 1.171429
0.014286 1.185714
0.014286 1.200000
3(0.2)
0.066667 1.266667
0.066667 1.333333
0.066667 1.400000
5(0.2)
0.040000 1.440000
0.040000 1.480000
0.040000 1.520000
0.040000 1.560000
0.040000 1.600000
9(0.2)
0.022222 1.622222
0.022222 1.644444
0.022222 1.666667
0.022222 1.688889
0.022222 1.711111
0.022222 1.733333
0.022222 1.755556
0.022222 1.777778
0.022222 1.800000
5(0.2)
0.040000 1.840000
0.040000 1.880000
0.040000 1.920000
0.040000 1.960000
0.040000 2.000000
10(0.2)
0.020000 2.020000
0.020000 2.040000
0.020000 2.060000
0.020000 2.080000
0.020000 2.100000
0.020000 2.120000
0.020000 2.140000
0.020000 2.160000
0.020000 2.180000
0.020000 2.200000
2(0.2)
0.100000 2.300000
0.100000 2.400000
0(0.7),1(0.5)
1.200000 3.600000
3(0.5)
0.166667 3.766667
0.166667 3.933333
0.166667 4.100000
1(0.5)
0.500000 4.600000
2(0.5)
0.250000 4.850000
0.250000 5.100000

7(0.5)
0.071429 5.171429
0.071429 5.242857
0.071429 5.314286
0.071429 5.385714
0.071429 5.457143
0.071429 5.528571
0.071429 5.600000
1(0.5)
0.500000 6.100000
1(0.5)
0.500000 6.600000
0(0.5)
0(0.5)
0(0.5)
0
0
0
0
0
0

N
15(0.2)
0.013333 0.013333
0.013333 0.026667
0.013333 0.040000
0.013333 0.053333
0.013333 0.066667
0.013333 0.080000
0.013333 0.093333
0.013333 0.106667
0.013333 0.120000
0.013333 0.133333
0.013333 0.146667
0.013333 0.160000
0.013333 0.173333
0.013333 0.186667
0.013333 0.200000
19(0.2)
0.010526 0.210526
0.010526 0.221053
0.010526 0.231579
0.010526 0.242105
0.010526 0.252632
0.010526 0.263158
0.010526 0.273684
0.010526 0.284211
0.010526 0.294737
0.010526 0.305263
0.010526 0.315789
0.010526 0.326316
0.010526 0.336842
0.010526 0.347368
0.010526 0.357895
0.010526 0.368421
0.010526 0.378947
0.010526 0.389474
0.010526 0.400000
19(0.2)
0.010526 0.410526
0.010526 0.421053
0.010526 0.431579
0.010526 0.442105
0.010526 0.452632
0.010526 0.463158
0.010526 0.473684
0.010526 0.484211
0.010526 0.494737
0.010526 0.505263
0.010526 0.515789
0.010526 0.526316
0.010526 0.536842
0.010526 0.547368

0.010526 0.557895
0.010526 0.568421
0.010526 0.578947
0.010526 0.589474
0.010526 0.600000
8(20)
0.025000 0.625000
0.025000 0.650000
0.025000 0.675000
0.025000 0.700000
0.025000 0.725000
0.025000 0.750000
0.025000 0.775000
0.025000 0.800000
4(0.2)
0.050000 0.850000
0.050000 0.900000
0.050000 0.950000
0.050000 1.000000
1(0.2)
0.200000 1.200000
2(0.2)
0.100000 1.300000
0.100000 1.400000
12(0.2)
0.016667 1.416667
0.016667 1.433333
0.016667 1.450000
0.016667 1.466667
0.016667 1.483333
0.016667 1.500000
0.016667 1.516667
0.016667 1.533333
0.016667 1.550000
0.016667 1.566667
0.016667 1.583333
0.016667 1.600000
5(0.2)
0.040000 1.640000
0.040000 1.680000
0.040000 1.720000
0.040000 1.760000
0.040000 1.800000
4(0.2)
0.050000 1.850000
0.050000 1.900000
0.050000 1.950000
0.050000 2.000000
3(0.2)
0.066667 2.066667
0.066667 2.133333
0.066667 2.200000
4(0.2)
0.050000 2.250000
0.050000 2.300000
0.050000 2.350000
0.050000 2.400000
3(0.2)
0.066667 2.466667
0.066667 2.533333
0.066667 2.600000
2(0.5)
0.250000 2.850000
0.250000 3.100000
1(0.5)
0.500000 3.600000
2(0.5)
0.250000 3.850000
0.250000 4.100000
1(0.5)
0.500000 4.600000
3(0.5)
0.166667 4.766667
0.166667 4.933333

0.166667 5.100000
3(0.5)
0.166667 5.266667
0.166667 5.433333
0.166667 5.600000
1(0.5)
0.500000 6.100000
1(0.5)
0.500000 6.600000
2(0.5)
0.250000 6.850000
0.250000 7.100000
1(0.5)
0.500000 7.600000
4(0.5)
0.125000 7.725000
0.125000 7.850000
0.125000 7.975000
0.125000 8.100000
2(0.5)
0.250000 8.350000
0.250000 8.600000
0,1
2.000000 10.600000
1
1.000000 11.600000
1
1.000000 12.600000
1
1.000000 13.600000
2
0.500000 14.100000
0.500000 14.600000
2
0.500000 15.100000
0.500000 15.600000
0,0,0,0,2
4.500000 20.100000
0.500000 20.600000
0
0
0

K84
S
26(0.5)
0.019231 0.019231
0.019231 0.038462
0.019231 0.057692
0.019231 0.076923
0.019231 0.096154
0.019231 0.115385
0.019231 0.134615
0.019231 0.153846
0.019231 0.173077
0.019231 0.192308
0.019231 0.211538
0.019231 0.230769
0.019231 0.250000
0.019231 0.269231
0.019231 0.288462
0.019231 0.307692
0.019231 0.326923
0.019231 0.346154
0.019231 0.365385
0.019231 0.384615
0.019231 0.403846
0.019231 0.423077
0.019231 0.442308
0.019231 0.461538
0.019231 0.480769
0.019231 0.500000
17(0.5)

0.029412 0.529412
0.029412 0.558824
0.029412 0.588235
0.029412 0.617647
0.029412 0.647059
0.029412 0.676471
0.029412 0.705882
0.029412 0.735294
0.029412 0.764706
0.029412 0.794118
0.029412 0.823529
0.029412 0.852941
0.029412 0.882353
0.029412 0.911765
0.029412 0.941176
0.029412 0.970588
0.029412 1.000000
17(0.5)
0.029412 1.029412
0.029412 1.058824
0.029412 1.088235
0.029412 1.117647
0.029412 1.147059
0.029412 1.176471
0.029412 1.205882
0.029412 1.235294
0.029412 1.264706
0.029412 1.294118
0.029412 1.323529
0.029412 1.352941
0.029412 1.382353
0.029412 1.411765
0.029412 1.441176
0.029412 1.470588
0.029412 1.500000
26(0.5)
0.019231 1.519231
0.019231 1.538462
0.019231 1.557692
0.019231 1.576923
0.019231 1.596154
0.019231 1.615385
0.019231 1.634615
0.019231 1.653846
0.019231 1.673077
0.019231 1.692308
0.019231 1.711538
0.019231 1.730769
0.019231 1.750000
0.019231 1.769231
0.019231 1.788462
0.019231 1.807692
0.019231 1.826923
0.019231 1.846154
0.019231 1.865385
0.019231 1.884615
0.019231 1.903846
0.019231 1.923077
0.019231 1.942308
0.019231 1.961538
0.019231 1.980769
0.019231 2.000000
29(0.5)
0.017241 2.017241
0.017241 2.034483
0.017241 2.051724
0.017241 2.068966
0.017241 2.086207
0.017241 2.103448
0.017241 2.120690
0.017241 2.137931
0.017241 2.155172
0.017241 2.172414
0.017241 2.189655

0.017241 2.206897
0.017241 2.224138
0.017241 2.241379
0.017241 2.258621
0.017241 2.275862
0.017241 2.293103
0.017241 2.310345
0.017241 2.327586
0.017241 2.344828
0.017241 2.362069
0.017241 2.379310
0.017241 2.396552
0.017241 2.413793
0.017241 2.431034
0.017241 2.448276
0.017241 2.465517
0.017241 2.482759
0.017241 2.500000
21(0.5)
0.023810 2.523810
0.023810 2.547619
0.023810 2.571429
0.023810 2.595238
0.023810 2.619048
0.023810 2.642857
0.023810 2.666667
0.023810 2.690476
0.023810 2.714286
0.023810 2.738095
0.023810 2.761905
0.023810 2.785714
0.023810 2.809524
0.023810 2.833333
0.023810 2.857143
0.023810 2.880952
0.023810 2.904762
0.023810 2.928571
0.023810 2.952381
0.023810 2.976190
0.023810 3.000000
24(0.5)
0.020833 3.020833
0.020833 3.041667
0.020833 3.062500
0.020833 3.083333
0.020833 3.104167
0.020833 3.125000
0.020833 3.145833
0.020833 3.166667
0.020833 3.187500
0.020833 3.208333
0.020833 3.229167
0.020833 3.250000
0.020833 3.270833
0.020833 3.291667
0.020833 3.312500
0.020833 3.333333
0.020833 3.354167
0.020833 3.375000
0.020833 3.395833
0.020833 3.416667
0.020833 3.437500
0.020833 3.458333
0.020833 3.479167
0.020833 3.500000
28(0.5)
0.017857 3.517857
0.017857 3.535714
0.017857 3.553571
0.017857 3.571429
0.017857 3.589286
0.017857 3.607143
0.017857 3.625000
0.017857 3.642857

0.017857 3.660714
0.017857 3.678571
0.017857 3.696429
0.017857 3.714286
0.017857 3.732143
0.017857 3.750000
0.017857 3.767857
0.017857 3.785714
0.017857 3.803571
0.017857 3.821429
0.017857 3.839286
0.017857 3.857143
0.017857 3.875000
0.017857 3.892857
0.017857 3.910714
0.017857 3.928571
0.017857 3.946429
0.017857 3.964286
0.017857 3.982143
0.017857 4.000000
21(0.5)
0.023810 4.023810
0.023810 4.047619
0.023810 4.071429
0.023810 4.095238
0.023810 4.119048
0.023810 4.142857
0.023810 4.166667
0.023810 4.190476
0.023810 4.214286
0.023810 4.238095
0.023810 4.261905
0.023810 4.285714
0.023810 4.309524
0.023810 4.333333
0.023810 4.357143
0.023810 4.380952
0.023810 4.404762
0.023810 4.428571
0.023810 4.452381
0.023810 4.476190
0.023810 4.500000
15(0.5)
0.033333 4.533333
0.033333 4.566667
0.033333 4.600000
0.033333 4.633333
0.033333 4.666667
0.033333 4.700000
0.033333 4.733333
0.033333 4.766667
0.033333 4.800000
0.033333 4.833333
0.033333 4.866667
0.033333 4.900000
0.033333 4.933333
0.033333 4.966667
0.033333 5.000000
18(0.5)
0.027778 5.027778
0.027778 5.055556
0.027778 5.083333
0.027778 5.111111
0.027778 5.138889
0.027778 5.166667
0.027778 5.194444
0.027778 5.222222
0.027778 5.250000
0.027778 5.277778
0.027778 5.305556
0.027778 5.333333
0.027778 5.361111
0.027778 5.388889
0.027778 5.416667

0.027778 5.444444
0.027778 5.472222
0.027778 5.500000
17(0.5)
0.029412 5.529412
0.029412 5.558824
0.029412 5.588235
0.029412 5.617647
0.029412 5.647059
0.029412 5.676471
0.029412 5.705882
0.029412 5.735294
0.029412 5.764706
0.029412 5.794118
0.029412 5.823529
0.029412 5.852941
0.029412 5.882353
0.029412 5.911765
0.029412 5.941176
0.029412 5.970588
0.029412 6.000000
9(0.5)
0.055556 6.055556
0.055556 6.111111
0.055556 6.166667
0.055556 6.222222
0.055556 6.277778
0.055556 6.333333
0.055556 6.388889
0.055556 6.444444
0.055556 6.500000
8(0.5)
0.062500 6.562500
0.062500 6.625000
0.062500 6.687500
0.062500 6.750000
0.062500 6.812500
0.062500 6.875000
0.062500 6.937500
0.062500 7.000000
5(0.5)
0.100000 7.100000
0.100000 7.200000
0.100000 7.300000
0.100000 7.400000
0.100000 7.500000
7(0.5)
0.071429 7.571429
0.071429 7.642857
0.071429 7.714286
0.071429 7.785714
0.071429 7.857143
0.071429 7.928571
0.071429 8.000000
7(0.5)
0.071429 8.071429
0.071429 8.142857
0.071429 8.214286
0.071429 8.285714
0.071429 8.357143
0.071429 8.428571
0.071429 8.500000
6(0.5)
0.083333 8.583333
0.083333 8.666667
0.083333 8.750000
0.083333 8.833333
0.083333 8.916667
0.083333 9.000000

N
NO(1)
12(0.5)
0.041667 0.041667
0.041667 0.083333
0.041667 0.125000
0.041667 0.166667
0.041667 0.208333
0.041667 0.250000
0.041667 0.291667
0.041667 0.333333
0.041667 0.375000
0.041667 0.416667
0.041667 0.458333
12(0.5)
0.041667 0.500000
0.041667 0.541667
0.041667 0.583333
0.041667 0.625000
0.041667 0.666667
0.041667 0.708333
0.041667 0.750000
0.041667 0.791667
0.041667 0.833333
0.041667 0.875000
0.041667 0.916667
12(0.5)
0.041667 0.958333
0.041667 1.000000
0.041667 1.041667
0.041667 1.083333
0.041667 1.125000
0.041667 1.166667
0.041667 1.208333
0.041667 1.250000
0.041667 1.291667
0.041667 1.333333
0.041667 1.375000
10(0.5)
0.050000 1.425000
0.050000 1.475000
0.050000 1.525000
0.050000 1.575000
0.050000 1.625000
0.050000 1.675000
0.050000 1.725000
0.050000 1.775000
0.050000 1.825000
0.050000 1.875000
9(0.5)
0.055556 1.930556
0.055556 1.986111
0.055556 2.041667
0.055556 2.097222
0.055556 2.152778
0.055556 2.208333
0.055556 2.263889
0.055556 2.319444
0.055556 2.375000
6(0.5)
0.083333 2.458333
0.083333 2.541667
0.083333 2.625000
0.083333 2.708333
0.083333 2.791667
0.083333 2.875000
7(0.5)
0.071429 2.946429
0.071429 3.017857
0.071429 3.089286
0.071429 3.160714
0.071429 3.232143
0.071429 3.303571
0.071429 3.375000
8(0.5)
0.062500 3.437500
0.062500 3.500000
0.062500 3.562500
0.062500 3.625000
0.062500 3.687500
0.062500 3.750000
0.062500 3.812500
0.062500 3.875000
4(0.5)
0.125000 4.000000
0.125000 4.125000
0.125000 4.250000
0.125000 4.375000
5(0.5)
0.100000 4.475000
0.100000 4.575000
0.100000 4.675000
0.100000 4.775000
0.100000 4.875000
9(0.5)
0.055556 4.930556
0.055556 4.986111
0.055556 5.041667
0.055556 5.097222
0.055556 5.152778
0.055556 5.208333
0.055556 5.263889
0.055556 5.319444
0.055556 5.375000
9(0.5)
0.055556 5.430556
0.055556 5.486111
0.055556 5.541667
0.055556 5.597222
0.055556 5.652778
0.055556 5.708333
0.055556 5.763889
0.055556 5.819444
0.055556 5.875000
5(0.5)
0.100000 5.975000
0.100000 6.075000
0.100000 6.175000
0.100000 6.275000
0.100000 6.375000
4(0.5)
0.125000 6.500000
0.125000 6.625000
0.125000 6.750000
0.125000 6.875000
5(0.5)
0.100000 6.975000
0.100000 7.075000
0.100000 7.175000
0.100000 7.275000
0.100000 7.375000
7
0.142857 7.517857
0.142857 7.660714
0.142857 7.803571
0.142857 7.946429
0.142857 8.089286
0.142857 8.232143
0.142857 8.375000
7
0.142857 8.517857
0.142857 8.660714
0.142857 8.803571
0.142857 8.946429
0.142857 9.089286
0.142857 9.232143
0.142857 9.375000
7
0.142857 9.517857
0.142857 9.660714
0.142857 9.803571
0.142857 9.946429
0.142857 10.089286
0.142857 10.232143
0.142857 10.375000
6
0.166667 10.541667
0.166667 10.708333
0.166667 10.875000
0.166667 11.041667
0.166667 11.208333
0.166667 11.375000
7
0.142857 11.517857
0.142857 11.660714
0.142857 11.803571
0.142857 11.946429
0.142857 12.089286
0.142857 12.232143
0.142857 12.375000
4
0.250000 12.625000
0.250000 12.875000
0.250000 13.125000
0.250000 13.375000
2
0.500000 13.875000
0.500000 14.375000
3
0.333333 14.708333
0.333333 15.041667
0.333333 15.375000
2
0.500000 15.875000
0.500000 16.375000
3
0.333333 16.708333
0.333333 17.041667
0.333333 17.375000
4
0.250000 17.625000
0.250000 17.875000
0.250000 18.125000
0.250000 18.375000
1
1.000000 19.375000
2
0.500000 19.875000
0.500000 20.375000
2
0.500000 20.875000
0.500000 21.375000
3
0.333333 21.708333
0.333333 22.041667
0.333333 22.375000
3
0.333333 22.708333
0.333333 23.041667
0.333333 23.375000
2
0.500000 23.875000
0.500000 24.375000
3
0.333333 24.708333
0.333333 25.041667
0.333333 25.375000

K90c
S
NO(2.5)
38(0.3)
0.007895 0.007895
0.007895 0.015789
0.007895 0.023684
0.007895 0.031579
0.007895 0.039474
0.007895 0.047368
0.007895 0.055263
0.007895 0.063158
0.007895 0.071053
0.007895 0.078947
0.007895 0.086842
0.007895 0.094737
0.007895 0.102632
0.007895 0.110526
0.007895 0.118421
0.007895 0.126316
0.007895 0.134211
0.007895 0.142105
0.007895 0.150000
0.007895 0.157895
0.007895 0.165789
0.007895 0.173684
0.007895 0.181579
0.007895 0.189474
0.007895 0.197368
0.007895 0.205263
0.007895 0.213158
0.007895 0.221053
0.007895 0.228947
0.007895 0.236842
0.007895 0.244737
0.007895 0.252632
0.007895 0.260526
0.007895 0.268421
0.007895 0.276316
0.007895 0.284211
0.007895 0.292105
0.007895 0.300000
13(0.3)
0.023077 0.323077
0.023077 0.346154
0.023077 0.369231
0.023077 0.392308
0.023077 0.415385
0.023077 0.438462
0.023077 0.461538
0.023077 0.484615
0.023077 0.507692
0.023077 0.530769
0.023077 0.553846
0.023077 0.576923
0.023077 0.600000
14(0.5)
0.035714 0.635714
0.035714 0.671429
0.035714 0.707143
0.035714 0.742857
0.035714 0.778571
0.035714 0.814286
0.035714 0.850000
0.035714 0.885714
0.035714 0.921429
0.035714 0.957143
0.035714 0.992857
0.035714 1.028571
0.035714 1.064286
0.035714 1.100000
6(0.5)
0.083333 1.183333
0.083333 1.266667
0.083333 1.350000
0.083333 1.433333
0.083333 1.516667
0.083333 1.600000
5(0.5)
0.100000 1.700000
0.100000 1.800000
0.100000 1.900000
0.100000 2.000000
0.100000 2.100000
3(0.5)
0.166667 2.266667
0.166667 2.433333
0.166667 2.600000

N
37(0.25)
0.006757 0.006757
0.006757 0.013514
0.006757 0.020270
0.006757 0.027027
0.006757 0.033784
0.006757 0.040541
0.006757 0.047297
0.006757 0.054054
0.006757 0.060811
0.006757 0.067568
0.006757 0.074324
0.006757 0.081081
0.006757 0.087838
0.006757 0.094595
0.006757 0.101351
0.006757 0.108108
0.006757 0.114865
0.006757 0.121622
0.006757 0.128378
0.006757 0.135135
0.006757 0.141892
0.006757 0.148649
0.006757 0.155405
0.006757 0.162162
0.006757 0.168919
0.006757 0.175676
0.006757 0.182432
0.006757 0.189189
0.006757 0.195946
0.006757 0.202703
0.006757 0.209459
0.006757 0.216216
0.006757 0.222973
0.006757 0.229730
0.006757 0.236486
0.006757 0.243243
0.006757 0.250000
21(0.25)
0.011905 0.261905
0.011905 0.273810
0.011905 0.285714
0.011905 0.297619
0.011905 0.309524
0.011905 0.321429
0.011905 0.333333
0.011905 0.345238
0.011905 0.357143
0.011905 0.369048
0.011905 0.380952
0.011905 0.392857
0.011905 0.404762
0.011905 0.416667
0.011905 0.428571
0.011905 0.440476
0.011905 0.452381
0.011905 0.464286
0.011905 0.476190
0.011905 0.488095
0.011905 0.500000
11(0.25)
0.022727 0.522727
0.022727 0.545455
0.022727 0.568182
0.022727 0.590909
0.022727 0.613636
0.022727 0.636364
0.022727 0.659091
0.022727 0.681818
0.022727 0.704545
0.022727 0.727273
0.022727 0.750000
12(0.25)
0.020833 0.770833
0.020833 0.791667
0.020833 0.812500
0.020833 0.833333
0.020833 0.854167
0.020833 0.875000
0.020833 0.895833
0.020833 0.916667
0.020833 0.937500
0.020833 0.958333
0.020833 0.979167
0.020833 1.000000
11(0.5)
0.045455 1.045455
0.045455 1.090909
0.045455 1.136364
0.045455 1.181818
0.045455 1.227273
0.045455 1.272727
0.045455 1.318182
0.045455 1.363636
0.045455 1.409091
0.045455 1.454545
0.045455 1.500000
15(0.5)
0.033333 1.533333
0.033333 1.566667
0.033333 1.600000
0.033333 1.633333
0.033333 1.666667
0.033333 1.700000
0.033333 1.733333
0.033333 1.766667
0.033333 1.800000
0.033333 1.833333
0.033333 1.866667
0.033333 1.900000
0.033333 1.933333
0.033333 1.966667
0.033333 2.000000
12(0.5)
0.041667 2.041667
0.041667 2.083333
0.041667 2.125000
0.041667 2.166667
0.041667 2.208333
0.041667 2.250000
0.041667 2.291667
0.041667 2.333333
0.041667 2.375000
0.041667 2.416667
0.041667 2.458333
0.041667 2.500000
21(0.5)
0.023810 2.523810
0.023810 2.547619
0.023810 2.571429
0.023810 2.595238
0.023810 2.619048
0.023810 2.642857
0.023810 2.666667
0.023810 2.690476
0.023810 2.714286
0.023810 2.738095
0.023810 2.761905
0.023810 2.785714
0.023810 2.809524
0.023810 2.833333
0.023810 2.857143
0.023810 2.880952
0.023810 2.904762
0.023810 2.928571
0.023810 2.952381
0.023810 2.976190
0.023810 3.000000
16(0.5)
0.031250 3.031250
0.031250 3.062500
0.031250 3.093750
0.031250 3.125000
0.031250 3.156250
0.031250 3.187500
0.031250 3.218750
0.031250 3.250000
0.031250 3.281250
0.031250 3.312500
0.031250 3.343750
0.031250 3.375000
0.031250 3.406250
0.031250 3.437500
0.031250 3.468750
0.031250 3.500000
18
0.055556 3.555556
0.055556 3.611111
0.055556 3.666667
0.055556 3.722222
0.055556 3.777778
0.055556 3.833333
0.055556 3.888889
0.055556 3.944444
0.055556 4.000000
0.055556 4.055556
0.055556 4.111111
0.055556 4.166667
0.055556 4.222222
0.055556 4.277778
0.055556 4.333333
0.055556 4.388889
0.055556 4.444444
0.055556 4.500000
6
0.166667 4.666667
0.166667 4.833333
0.166667 5.000000
0.166667 5.166667
0.166667 5.333333
0.166667 5.500000
4
0.250000 5.750000
0.250000 6.000000
0.250000 6.250000
0.250000 6.500000
0,3
1.333333 7.833333
0.333333 8.166667
0.333333 8.500000
0,1
2.000000 10.500000
4
0.250000 10.750000
0.250000 11.000000
0.250000 11.250000
0.250000 11.500000
8
0.125000 11.625000
0.125000 11.750000
0.125000 11.875000
0.125000 12.000000
0.125000 12.125000
0.125000 12.250000
0.125000 12.375000
0.125000 12.500000
7
0.142857 12.642857
0.142857 12.785714
0.142857 12.928571
0.142857 13.071429
0.142857 13.214286
0.142857 13.357143
0.142857 13.500000
3
0.333333 13.833333
0.333333 14.166667
0.333333 14.500000
2
0.500000 15.000000
0.500000 15.500000
0,1
2.000000 17.500000
0,2
1.500000 19.000000
0.500000 19.500000
6
0.166667 19.666667
0.166667 19.833333
0.166667 20.000000
0.166667 20.166667
0.166667 20.333333
0.166667 20.500000
2
0.500000 21.000000
0.500000 21.500000
4
0.250000 21.750000
0.250000 22.000000
0.250000 22.250000
0.250000 22.500000
7
0.142857 22.642857
0.142857 22.785714
0.142857 22.928571
0.142857 23.071429
0.142857 23.214286
0.142857 23.357143
0.142857 23.500000
2
0.500000 24.000000
0.500000 24.500000
0,0,2
2.500000 27.000000
0.500000 27.500000
0,1
2.000000 29.500000
1
1.000000 30.500000
1
1.000000 31.500000
4
0.250000 31.750000
0.250000 32.000000
0.250000 32.250000
0.250000 32.500000
2
0.500000 33.000000
0.500000 33.500000

K92
S
4(0.3)
0.075000 0.075000
0.075000 0.150000
0.075000 0.225000
0.075000 0.300000
4(0.3)
0.075000 0.375000
0.075000 0.450000
0.075000 0.525000
0.075000 0.600000
0(0.3),6(0.5)
0.383333 0.983333
0.083333 1.066667
0.083333 1.150000
0.083333 1.233333
0.083333 1.316667
0.083333 1.400000
3(0.5)
0.166667 1.566667
0.166667 1.733333
0.166667 1.900000
5
0.200000 2.100000
0.200000 2.300000
0.200000 2.500000
0.200000 2.700000
0.200000 2.900000
2
0.500000 3.400000
0.500000 3.900000
1
1.000000 4.900000
1
1.000000 5.900000
0,1
2.000000 7.900000
0,0,0,0,0,1
6.000000 13.900000
1
1.000000 14.900000
0,1
2.000000 16.900000
0
0
0
0
0
0
0
0

N
10(0.3)
0.030000 0.030000
0.030000 0.060000
0.030000 0.090000
0.030000 0.120000
0.030000 0.150000
0.030000 0.180000
0.030000 0.210000
0.030000 0.240000
0.030000 0.270000
0.030000 0.300000
3(0.3)
0.100000 0.400000
0.100000 0.500000
0.100000 0.600000
5(0.3)
0.060000 0.660000
0.060000 0.720000
0.060000 0.780000
0.060000 0.840000
0.060000 0.900000
5(0.3)
0.060000 0.960000
0.060000 1.020000
0.060000 1.080000
0.060000 1.140000
0.060000 1.200000
4
0.250000 1.450000
0.250000 1.700000
0.250000 1.950000
0.250000 2.200000
3
0.333333 2.533333
0.333333 2.866667
0.333333 3.200000
3
0.333333 3.533333
0.333333 3.866667
0.333333 4.200000
3
0.333333 4.533333
0.333333 4.866667
0.333333 5.200000
0,0,0,1
4.000000 9.200000
2
0.500000 9.700000
0.500000 10.200000
1
1.000000 11.200000
1
1.000000 12.200000
0,0,1
3.000000 15.200000
3
0.333333 15.533333
0.333333 15.866667
0.333333 16.200000
1
1.000000 17.200000

K93
S
9(0.3)
0.033333 0.033333
0.033333 0.066667
0.033333 0.100000
0.033333 0.133333
0.033333 0.166667
0.033333 0.200000
0.033333 0.233333
0.033333 0.266667
0.033333 0.300000
11(0.3)
0.027273 0.327273
0.027273 0.354545
0.027273 0.381818
0.027273 0.409091
0.027273 0.436364
0.027273 0.463636
0.027273 0.490909
0.027273 0.518182
0.027273 0.545455
0.027273 0.572727
0.027273 0.600000
5(0.3)
0.060000 0.660000
0.060000 0.720000
0.060000 0.780000
0.060000 0.840000
0.060000 0.900000
11(0.3)
0.027273 0.927273
0.027273 0.954545
0.027273 0.981818
0.027273 1.009091
0.027273 1.036364
0.027273 1.063636
0.027273 1.090909
0.027273 1.118182
0.027273 1.145455
0.027273 1.172727
0.027273 1.200000
7(0.3)
0.042857 1.242857
0.042857 1.285714
0.042857 1.328571
0.042857 1.371429
0.042857 1.414286
0.042857 1.457143
0.042857 1.500000
10(0.3)
0.030000 1.530000
0.030000 1.560000
0.030000 1.590000
0.030000 1.620000
0.030000 1.650000
0.030000 1.680000
0.030000 1.710000
0.030000 1.740000
0.030000 1.770000
0.030000 1.800000
4(0.5)
0.125000 1.925000
0.125000 2.050000
0.125000 2.175000
0.125000 2.300000
3(0.5)
0.166667 2.466667
0.166667 2.633333
0.166667 2.800000
3(0.5)
0.166667 2.966667
0.166667 3.133333
0.166667 3.300000
2(0.5)
0.250000 3.550000
0.250000 3.800000
1
1.000000 4.800000
8
0.125000 4.925000
0.125000 5.050000
0.125000 5.175000
0.125000 5.300000
0.125000 5.425000
0.125000 5.550000
0.125000 5.675000
0.125000 5.800000
3
0.333333 6.133333
0.333333 6.466667
0.333333 6.800000
3
0.333333 7.133333
0.333333 7.466667
0.333333 7.800000
0,1
2.000000 9.800000
2
0.500000 10.300000
0.500000 10.800000
1
1.000000 11.800000
0,0,0,0,1
5.000000 16.800000

N
10(0.3)
0.030000 0.030000
0.030000 0.060000
0.030000 0.090000
0.030000 0.120000
0.030000 0.150000
0.030000 0.180000
0.030000 0.210000
0.030000 0.240000
0.030000 0.270000
0.030000 0.300000
20(0.3)
0.015000 0.315000
0.015000 0.330000
0.015000 0.345000
0.015000 0.360000
0.015000 0.375000
0.015000 0.390000
0.015000 0.405000
0.015000 0.420000
0.015000 0.435000
0.015000 0.450000
0.015000 0.465000
0.015000 0.480000
0.015000 0.495000
0.015000 0.510000
0.015000 0.525000
0.015000 0.540000
0.015000 0.555000
0.015000 0.570000
0.015000 0.585000
0.015000 0.600000
18(0.3)
0.016667 0.616667
0.016667 0.633333
0.016667 0.650000
0.016667 0.666667
0.016667 0.683333
0.016667 0.700000
0.016667 0.716667
0.016667 0.733333
0.016667 0.750000
0.016667 0.766667
0.016667 0.783333
0.016667 0.800000
0.016667 0.816667
0.016667 0.833333
0.016667 0.850000
0.016667 0.866667
0.016667 0.883333
0.016667 0.900000
14(0.3)
0.021429 0.921429
0.021429 0.942857
0.021429 0.964286
0.021429 0.985714
0.021429 1.007143
0.021429 1.028571
0.021429 1.050000
0.021429 1.071429
0.021429 1.092857
0.021429 1.114286
0.021429 1.135714
0.021429 1.157143
0.021429 1.178571
0.021429 1.200000
9(0.3)
0.033333 1.233333
0.033333 1.266667
0.033333 1.300000
0.033333 1.333333
0.033333 1.366667
0.033333 1.400000
0.033333 1.433333
0.033333 1.466667
0.033333 1.500000
0.033333 1.533333
10(0.5)

0.050000 1.583333
0.050000 1.633333
0.050000 1.683333
0.050000 1.733333
0.050000 1.783333
0.050000 1.833333
0.050000 1.883333
0.050000 1.933333
0.050000 1.983333
0.050000 2.033333
13(0.5)
0.038462 2.071795
0.038462 2.110256
0.038462 2.148718
0.038462 2.187179
0.038462 2.225641
0.038462 2.264103
0.038462 2.302564
0.038462 2.341026
0.038462 2.379487
0.038462 2.417949
0.038462 2.456410
0.038462 2.494872
0.038462 2.533333
3(0.5)
0.166667 2.700000
0.166667 2.866667
0.166667 3.033333
2
0.500000 3.533333
0.500000 4.033333
2
0.500000 4.533333
0.500000 5.033333
0,0,1
3.000000 8.033333
1
1.000000 9.033333
2
0.500000 9.533333
0.500000 10.033333
2
0.500000 10.533333
0.500000 11.033333
3
0.333333 11.366667
0.333333 11.700000
0.333333 12.033333
0,0,0,3
3.333333 15.366667
0.333333 15.700000
0.333333 16.033333
2
0.500000 16.533333
0.500000 17.033333
3
0.333333 17.366667
0.333333 17.700000
0.333333 18.033333
0,1
2.000000 20.033333
1
1.000000 21.033333
0,1
2.000000 23.033333
1
1.000000 24.033333
1
1.000000 25.033333
2
0.500000 25.533333
0.500000 26.033333
1
1.000000 27.033333

K94

S

5(0.3)
0.060000 0.060000
0.060000 0.120000
0.060000 0.180000
0.060000 0.240000
0.060000 0.300000
5(0.3)
0.060000 0.360000
0.060000 0.420000
0.060000 0.480000
0.060000 0.540000
0.060000 0.600000
3(0.3)
0.100000 0.700000
0.100000 0.800000
0.100000 0.900000
2
0.500000 1.400000
0.500000 1.900000
2
0.500000 2.400000
0.500000 2.900000
2
0.500000 3.400000
0.500000 3.900000
0,1
2.000000 5.900000
1
1.000000 6.900000
0,0,2
2.500000 9.400000
0.500000 9.900000
0,1
2.000000 11.900000

N

12(0.3)
0.025000 0.025000
0.025000 0.050000
0.025000 0.075000
0.025000 0.100000
0.025000 0.125000
0.025000 0.150000
0.025000 0.175000
0.025000 0.200000
0.025000 0.225000
0.025000 0.250000
0.025000 0.275000
0.025000 0.300000
5(0.3)
0.060000 0.360000
0.060000 0.420000
0.060000 0.480000
0.060000 0.540000
0.060000 0.600000
3(0.3)
0.100000 0.700000
0.100000 0.800000
0.100000 0.900000
4
0.250000 1.150000
0.250000 1.400000
0.250000 1.650000
0.250000 1.900000
0,2
1.500000 3.400000
0.500000 3.900000
0,0,1
3.000000 6.900000
0,1
2.000000 8.900000
1
1.000000 9.900000
0,0,2
2.500000 12.400000
0.500000 12.900000

K111

S

57(0.17)
0.002982 0.002982
0.002982 0.005965
0.002982 0.008947
0.002982 0.011930
0.002982 0.014912
0.002982 0.017895
0.002982 0.020877
0.002982 0.023860
0.002982 0.026842
0.002982 0.029825
0.002982 0.032807
0.002982 0.035789
0.002982 0.038772
0.002982 0.041754
0.002982 0.044737
0.002982 0.047719
0.002982 0.050702
0.002982 0.053684
0.002982 0.056667
0.002982 0.059649
0.002982 0.062632
0.002982 0.065614
0.002982 0.068596
0.002982 0.071579
0.002982 0.074561
0.002982 0.077544
0.002982 0.080526
0.002982 0.083509
0.002982 0.086491
0.002982 0.089474
0.002982 0.092456
0.002982 0.095439
0.002982 0.098421
0.002982 0.101404
0.002982 0.104386
0.002982 0.107368
0.002982 0.110351
0.002982 0.113333
0.002982 0.116316
0.002982 0.119298
0.002982 0.122281
0.002982 0.125263
0.002982 0.128246
0.002982 0.131228
0.002982 0.134211
0.002982 0.137193
0.002982 0.140175
0.002982 0.143158
0.002982 0.146140
0.002982 0.149123
0.002982 0.152105
0.002982 0.155088
0.002982 0.158070
0.002982 0.161053
0.002982 0.164035
0.002982 0.167018
0.002982 0.170000
33(0.12)
0.003636 0.173636
0.003636 0.177273
0.003636 0.180909
0.003636 0.184545
0.003636 0.188182
0.003636 0.191818
0.003636 0.195455
0.003636 0.199091
0.003636 0.202727
0.003636 0.206364
0.003636 0.210000
0.003636 0.213636
0.003636 0.217273
0.003636 0.220909
0.003636 0.224545
0.003636 0.228182
0.003636 0.231818
0.003636 0.235455
0.003636 0.239091
0.003636 0.242727
0.003636 0.246364
0.003636 0.250000
0.003636 0.253636
0.003636 0.257273
0.003636 0.260909
0.003636 0.264545
0.003636 0.268182
0.003636 0.271818
0.003636 0.275455
0.003636 0.279091
0.003636 0.282727
0.003636 0.286364
0.003636 0.290000
4(0.38)
0.095000 0.385000
0.095000 0.480000
0.095000 0.575000
0.095000 0.670000
3(0.5)
0.166667 0.836667
0.166667 1.003333
0.166667 1.170000
2(0.5)
0.250000 1.420000
0.250000 1.670000
8(0.5)
0.062500 1.732500
0.062500 1.795000
0.062500 1.857500
0.062500 1.920000
0.062500 1.982500
0.062500 2.045000
0.062500 2.107500
0.062500 2.170000
6(0.5)
0.083333 2.253333
0.083333 2.336667
0.083333 2.420000
0.083333 2.503333
0.083333 2.586667
0.083333 2.670000
4(0.5)
0.125000 2.795000
0.125000 2.920000
0.125000 3.045000
0.125000 3.170000
12
0.083333 3.253333
0.083333 3.336667
0.083333 3.420000
0.083333 3.503333
0.083333 3.586667
0.083333 3.670000
0.083333 3.753333
0.083333 3.836667
0.083333 3.920000
0.083333 4.003333
0.083333 4.086667
0.083333 4.170000
13
0.076923 4.246923
0.076923 4.323846
0.076923 4.400769
0.076923 4.477692
0.076923 4.554615
0.076923 4.631538
0.076923 4.708462
0.076923 4.785385
0.076923 4.862308
0.076923 4.939231
0.076923 5.016154
0.076923 5.093077
0.076923 5.170000
9
0.111111 5.281111
0.111111 5.392222
0.111111 5.503333
0.111111 5.614444
0.111111 5.725556
0.111111 5.836667
0.111111 5.947778
0.111111 6.058889
0.111111 6.170000
7
0.142857 6.312857
0.142857 6.455714
0.142857 6.598571
0.142857 6.741429
0.142857 6.884286
0.142857 7.027143
0.142857 7.170000
9
0.111111 7.281111
0.111111 7.392222
0.111111 7.503333
0.111111 7.614444
0.111111 7.725556
0.111111 7.836667
0.111111 7.947778
0.111111 8.058889
0.111111 8.170000
9
0.111111 8.281111
0.111111 8.392222
0.111111 8.503333
0.111111 8.614444
0.111111 8.725556
0.111111 8.836667
0.111111 8.947778
0.111111 9.058889
0.111111 9.170000
5
0.200000 9.370000
0.200000 9.570000
0.200000 9.770000
0.200000 9.970000
0.200000 10.170000
3
0.333333 10.503333
0.333333 10.836667
0.333333 11.170000
4
0.250000 11.420000
0.250000 11.670000
0.250000 11.920000
0.250000 12.170000
5
0.200000 12.370000
0.200000 12.570000
0.200000 12.770000
0.200000 12.970000
0.200000 13.170000
3
0.333333 13.503333
0.333333 13.836667
0.333333 14.170000
5
0.200000 14.370000
0.200000 14.570000
0.200000 14.770000
0.200000 14.970000
0.200000 15.170000
4
0.250000 15.420000
0.250000 15.670000
0.250000 15.920000
0.250000 16.170000
5
0.200000 16.370000
0.200000 16.570000
0.200000 16.770000
0.200000 16.970000
0.200000 17.170000
4
0.250000 17.420000
0.250000 17.670000
0.250000 17.920000
0.250000 18.170000
5
0.200000 18.370000
0.200000 18.570000
0.200000 18.770000
0.200000 18.970000
0.200000 19.170000
4
0.250000 19.420000
0.250000 19.670000
0.250000 19.920000
0.250000 20.170000
4
0.250000 20.420000
0.250000 20.670000
0.250000 20.920000
0.250000 21.170000
3
0.333333 21.503333
0.333333 21.836667
0.333333 22.170000
4
0.250000 22.420000
0.250000 22.670000
0.250000 22.920000
0.250000 23.170000
7
0.142857 23.312857
0.142857 23.455714
0.142857 23.598571
0.142857 23.741429
0.142857 23.884286
0.142857 24.027143
0.142857 24.170000
4
0.250000 24.420000
0.250000 24.670000
0.250000 24.920000
0.250000 25.170000
6
0.166667 25.336667
0.166667 25.503333
0.166667 25.670000
0.166667 25.836667
0.166667 26.003333
0.166667 26.170000
9
0.111111 26.281111
0.111111 26.392222
0.111111 26.503333
0.111111 26.614444
0.111111 26.725556
0.111111 26.836667
0.111111 26.947778
0.111111 27.058889
0.111111 27.170000
5
0.200000 27.370000
0.200000 27.570000
0.200000 27.770000
0.200000 27.970000
0.200000 28.170000
6
0.166667 28.336667
0.166667 28.503333
0.166667 28.670000
0.166667 28.836667
0.166667 29.003333
0.166667 29.170000
5
0.200000 29.370000
0.200000 29.570000
0.200000 29.770000
0.200000 29.970000
0.200000 30.170000
8
0.125000 30.295000
0.125000 30.420000
0.125000 30.545000
0.125000 30.670000
0.125000 30.795000
0.125000 30.920000
0.125000 31.045000
0.125000 31.170000
5
0.200000 31.370000
0.200000 31.570000
0.200000 31.770000
0.200000 31.970000
0.200000 32.170000
5
0.200000 32.370000
0.200000 32.570000
0.200000 32.770000
0.200000 32.970000
0.200000 33.170000
4
0.250000 33.420000
0.250000 33.670000
0.250000 33.920000
0.250000 34.170000
3
0.333333 34.503333
0.333333 34.836667
0.333333 35.170000
5
0.200000 35.370000
0.200000 35.570000
0.200000 35.770000
0.200000 35.970000
0.200000 36.170000
5
0.200000 36.370000
0.200000 36.570000
0.200000 36.770000
0.200000 36.970000
0.200000 37.170000
6
0.166667 37.336667
0.166667 37.503333
0.166667 37.670000
0.166667 37.836667
0.166667 38.003333
0.166667 38.170000
4
0.250000 38.420000
0.250000 38.670000
0.250000 38.920000
0.250000 39.170000
5
0.200000 39.370000
0.200000 39.570000
0.200000 39.770000
0.200000 39.970000
0.200000 40.170000
5
0.200000 40.370000
0.200000 40.570000
0.200000 40.770000
0.200000 40.970000
0.200000 41.170000

N

56(0.16)
0.002857 0.002857
0.002857 0.005714
0.002857 0.008571
0.002857 0.011429
0.002857 0.014286
0.002857 0.017143
0.002857 0.020000
0.002857 0.022857
0.002857 0.025714
0.002857 0.028571
0.002857 0.031429
0.002857 0.034286
0.002857 0.037143
0.002857 0.040000
0.002857 0.042857
0.002857 0.045714
0.002857 0.048571
0.002857 0.051429
0.002857 0.054286
0.002857 0.057143
0.002857 0.060000
0.002857 0.062857
0.002857 0.065714
0.002857 0.068571
0.002857 0.071429
0.002857 0.074286
0.002857 0.077143
0.002857 0.080000
0.002857 0.082857
0.002857 0.085714
0.002857 0.088571
0.002857 0.091429
0.002857 0.094286
0.002857 0.097143
0.002857 0.100000
0.002857 0.102857
0.002857 0.105714
0.002857 0.108571
0.002857 0.111429
0.002857 0.114286
0.002857 0.117143
0.002857 0.120000
0.002857 0.122857
0.002857 0.125714
0.002857 0.128571
0.002857 0.131429
0.002857 0.134286
0.002857 0.137143
0.002857 0.140000
0.002857 0.142857
0.002857 0.145714
0.002857 0.148571
0.002857 0.151429
0.002857 0.154286
0.002857 0.157143
0.002857 0.160000
8(0.5)
0.062500 0.222500
0.062500 0.285000
0.062500 0.347500
0.062500 0.410000
0.062500 0.472500
0.062500 0.535000
0.062500 0.597500
0.062500 0.660000
3(0.5)
0.166667 0.826667
0.166667 0.993333
0.166667 1.160000
4(0.5)
0.125000 1.285000
0.125000 1.410000
0.125000 1.535000
0.125000 1.660000
5(0.5)
0.100000 1.760000
0.100000 1.860000
0.100000 1.960000
0.100000 2.060000
0.100000 2.160000
3(0.5)
0.166667 2.326667
0.166667 2.493333
0.166667 2.660000
6
0.166667 2.826667
0.166667 2.993333
0.166667 3.160000
0.166667 3.326667
0.166667 3.493333
0.166667 3.660000
6
0.166667 3.826667
0.166667 3.993333
0.166667 4.160000
0.166667 4.326667
0.166667 4.493333
0.166667 4.660000
7
0.142857 4.802857
0.142857 4.945714
0.142857 5.088571
0.142857 5.231429
0.142857 5.374286
0.142857 5.517143
0.142857 5.660000
6
0.166667 5.826667
0.166667 5.993333
0.166667 6.160000
0.166667 6.326667
0.166667 6.493333
0.166667 6.660000
6
0.166667 6.826667
0.166667 6.993333
0.166667 7.160000
0.166667 7.326667
0.166667 7.493333
0.166667 7.660000
4
0.250000 7.910000
0.250000 8.160000
0.250000 8.410000
0.250000 8.660000
5
0.200000 8.860000
0.200000 9.060000
0.200000 9.260000
0.200000 9.460000
0.200000 9.660000
7
0.142857 9.802857
0.142857 9.945714
0.142857 10.088571
0.142857 10.231429
0.142857 10.374286
0.142857 10.517143
0.142857 10.660000
4
0.250000 10.910000
0.250000 11.160000
0.250000 11.410000
0.250000 11.660000
4
0.250000 11.910000
0.250000 12.160000
0.250000 12.410000
0.250000 12.660000
7
0.142857 12.802857
0.142857 12.945714
0.142857 13.088571
0.142857 13.231429
0.142857 13.374286
0.142857 13.517143
0.142857 13.660000
5
0.200000 13.860000
0.200000 14.060000
0.200000 14.260000
0.200000 14.460000
0.200000 14.660000
7
0.142857 14.802857
0.142857 14.945714
0.142857 15.088571
0.142857 15.231429
0.142857 15.374286
0.142857 15.517143
0.142857 15.660000
7
0.142857 15.802857
0.142857 15.945714
0.142857 16.088571
0.142857 16.231429
0.142857 16.374286
0.142857 16.517143
0.142857 16.660000
6
0.166667 16.826667
0.166667 16.993333
0.166667 17.160000
0.166667 17.326667
0.166667 17.493333
0.166667 17.660000
7
0.142857 17.802857
0.142857 17.945714
0.142857 18.088571
0.142857 18.231429
0.142857 18.374286
0.142857 18.517143
0.142857 18.660000
8
0.125000 18.785000
0.125000 18.910000
0.125000 19.035000
0.125000 19.160000
0.125000 19.285000
0.125000 19.410000
0.125000 19.535000
0.125000 19.660000
7
0.142857 19.802857
0.142857 19.945714
0.142857 20.088571
0.142857 20.231429
0.142857 20.374286
0.142857 20.517143
0.142857 20.660000
9
0.111111 20.771111
0.111111 20.882222
0.111111 20.993333
0.111111 21.104444
0.111111 21.215556
0.111111 21.326667
0.111111 21.437778
0.111111 21.548889
0.111111 21.660000
10
0.100000 21.760000
0.100000 21.860000
0.100000 21.960000
0.100000 22.060000
0.100000 22.160000
0.100000 22.260000
0.100000 22.360000
0.100000 22.460000
0.100000 22.560000
0.100000 22.660000
10
0.100000 22.760000
0.100000 22.860000
0.100000 22.960000
0.100000 23.060000
0.100000 23.160000
0.100000 23.260000
0.100000 23.360000
0.100000 23.460000
0.100000 23.560000
0.100000 23.660000
8
0.125000 23.785000
0.125000 23.910000
0.125000 24.035000
0.125000 24.160000
0.125000 24.285000
0.125000 24.410000
0.125000 24.535000
0.125000 24.660000
10
0.100000 24.760000
0.100000 24.860000
0.100000 24.960000
0.100000 25.060000
0.100000 25.160000
0.100000 25.260000
0.100000 25.360000
0.100000 25.460000
0.100000 25.560000
0.100000 25.660000
8
0.125000 25.785000
0.125000 25.910000
0.125000 26.035000
0.125000 26.160000
0.125000 26.285000
0.125000 26.410000
0.125000 26.535000
0.125000 26.660000
9
0.111111 26.771111
0.111111 26.882222
0.111111 26.993333
0.111111 27.104444
0.111111 27.215556
0.111111 27.326667
0.111111 27.437778
0.111111 27.548889
0.111111 27.660000
6
0.166667 27.826667
0.166667 27.993333
0.166667 28.160000
0.166667 28.326667
0.166667 28.493333
0.166667 28.660000
7
0.142857 28.802857
0.142857 28.945714
0.142857 29.088571
0.142857 29.231429
0.142857 29.374286
0.142857 29.517143
0.142857 29.660000
7
0.142857 29.802857
0.142857 29.945714
0.142857 30.088571
0.142857 30.231429
0.142857 30.374286
0.142857 30.517143
0.142857 30.660000
10
0.100000 30.760000
0.100000 30.860000
0.100000 30.960000
0.100000 31.060000
0.100000 31.160000
0.100000 31.260000
0.100000 31.360000
0.100000 31.460000
0.100000 31.560000
0.100000 31.660000
13
0.076923 31.736923
0.076923 31.813846
0.076923 31.890769
0.076923 31.967692
0.076923 32.044615
0.076923 32.121538
0.076923 32.198462
0.076923 32.275385
0.076923 32.352308
0.076923 32.429231
0.076923 32.506154
0.076923 32.583077
0.076923 32.660000

K112

S

NO(0.2)
50(0.16)
0.003200 0.003200
0.003200 0.006400
0.003200 0.009600
0.003200 0.012800
0.003200 0.016000
0.003200 0.019200
0.003200 0.022400
0.003200 0.025600
0.003200 0.028800
0.003200 0.032000
0.003200 0.035200
0.003200 0.038400
0.003200 0.041600
0.003200 0.044800
0.003200 0.048000
0.003200 0.051200
0.003200 0.054400
0.003200 0.057600
0.003200 0.060800
0.003200 0.064000
0.003200 0.067200
0.003200 0.070400
0.003200 0.073600
0.003200 0.076800
0.003200 0.080000
0.003200 0.083200
0.003200 0.086400
0.003200 0.089600
0.003200 0.092800
0.003200 0.096000
0.003200 0.099200
0.003200 0.102400
0.003200 0.105600
0.003200 0.108800
0.003200 0.112000
0.003200 0.115200
0.003200 0.118400
0.003200 0.121600
0.003200 0.124800
0.003200 0.128000
0.003200 0.131200
0.003200 0.134400
0.003200 0.137600
0.003200 0.140800
0.003200 0.144000
0.003200 0.147200
0.003200 0.150400
0.003200 0.153600
0.003200 0.156800
0.003200 0.160000
37(0.17)
0.004595 0.164595
0.004595 0.169189
0.004595 0.173784
0.004595 0.178378
0.004595 0.182973
0.004595 0.187568
0.004595 0.192162
0.004595 0.196757
0.004595 0.201351
0.004595 0.205946
0.004595 0.210541
0.004595 0.215135
0.004595 0.219730
0.004595 0.224324
0.004595 0.228919
0.004595 0.233514
0.004595 0.238108
0.004595 0.242703
0.004595 0.247297
0.004595 0.251892
0.004595 0.256486
0.004595 0.261081
0.004595 0.265676
0.004595 0.270270
0.004595 0.274865
0.004595 0.279459
0.004595 0.284054
0.004595 0.288649
0.004595 0.293243
0.004595 0.297838
0.004595 0.302432
0.004595 0.307027
0.004595 0.311622
0.004595 0.316216
0.004595 0.320811
0.004595 0.325405
0.004595 0.330000

50(0.5)
0.010000 0.340000
0.010000 0.350000
0.010000 0.360000
0.010000 0.370000
0.010000 0.380000
0.010000 0.390000
0.010000 0.400000
0.010000 0.410000
0.010000 0.420000
0.010000 0.430000
0.010000 0.440000
0.010000 0.450000
0.010000 0.460000
0.010000 0.470000
0.010000 0.480000
0.010000 0.490000
0.010000 0.500000
0.010000 0.510000
0.010000 0.520000
0.010000 0.530000
0.010000 0.540000
0.010000 0.550000
0.010000 0.560000
0.010000 0.570000
0.010000 0.580000
0.010000 0.590000
0.010000 0.600000
0.010000 0.610000
0.010000 0.620000
0.010000 0.630000
0.010000 0.640000
0.010000 0.650000
0.010000 0.660000
0.010000 0.670000
0.010000 0.680000
0.010000 0.690000
0.010000 0.700000
0.010000 0.710000
0.010000 0.720000
0.010000 0.730000
0.010000 0.740000
0.010000 0.750000
0.010000 0.760000
0.010000 0.770000
0.010000 0.780000
0.010000 0.790000
0.010000 0.800000
0.010000 0.810000
0.010000 0.820000
0.010000 0.830000
40(0.5)
0.012500 0.842500
0.012500 0.855000
0.012500 0.867500
0.012500 0.880000
0.012500 0.892500
0.012500 0.905000
0.012500 0.917500
0.012500 0.930000
0.012500 0.942500
0.012500 0.955000
0.012500 0.967500
0.012500 0.980000
0.012500 0.992500
0.012500 1.005000
0.012500 1.017500
0.012500 1.030000
0.012500 1.042500
0.012500 1.055000
0.012500 1.067500
0.012500 1.080000
0.012500 1.092500
0.012500 1.105000
0.012500 1.117500
0.012500 1.130000
0.012500 1.142500
0.012500 1.155000
0.012500 1.167500
0.012500 1.180000
0.012500 1.192500
0.012500 1.205000
0.012500 1.217500
0.012500 1.230000
0.012500 1.242500
0.012500 1.255000
0.012500 1.267500
0.012500 1.280000
0.012500 1.292500
0.012500 1.305000
0.012500 1.317500
0.012500 1.330000
28(0.5)
0.017857 1.347857
0.017857 1.365714
0.017857 1.383571
0.017857 1.401429
0.017857 1.419286
0.017857 1.437143
0.017857 1.455000
0.017857 1.472857
0.017857 1.490714
0.017857 1.508571
0.017857 1.526429
0.017857 1.544286
0.017857 1.562143
0.017857 1.580000
0.017857 1.597857
0.017857 1.615714
0.017857 1.633571
0.017857 1.651429
0.017857 1.669286
0.017857 1.687143
0.017857 1.705000
0.017857 1.722857
0.017857 1.740714
0.017857 1.758571
0.017857 1.776429
0.017857 1.794286
0.017857 1.812143
0.017857 1.830000
3(0.5)
0.166667 1.996667
0.166667 2.163333
0.166667 2.330000
5
0.200000 2.530000
0.200000 2.730000
0.200000 2.930000
0.200000 3.130000
0.200000 3.330000
4
0.250000 3.580000
0.250000 3.830000
0.250000 4.080000
0.250000 4.330000
4
0.250000 4.580000
0.250000 4.830000
0.250000 5.080000
0.250000 5.330000
8
0.125000 5.455000
0.125000 5.580000
0.125000 5.705000
0.125000 5.830000
0.125000 5.955000
0.125000 6.080000
0.125000 6.205000
0.125000 6.330000
4
0.250000 6.580000
0.250000 6.830000
0.250000 7.080000
0.250000 7.330000
5
0.200000 7.530000
0.200000 7.730000
0.200000 7.930000
0.200000 8.130000
0.200000 8.330000
4
0.250000 8.580000
0.250000 8.830000
0.250000 9.080000
0.250000 9.330000
7
0.142857 9.472857
0.142857 9.615714
0.142857 9.758571
0.142857 9.901429
0.142857 10.044286
0.142857 10.187143
0.142857 10.330000
5
0.200000 10.530000
0.200000 10.730000
0.200000 10.930000
0.200000 11.130000
0.200000 11.330000
5
0.200000 11.530000
0.200000 11.730000
0.200000 11.930000
0.200000 12.130000
0.200000 12.330000
4
0.250000 12.580000
0.250000 12.830000
0.250000 13.080000
0.250000 13.330000
5
0.200000 13.530000
0.200000 13.730000
0.200000 13.930000
0.200000 14.130000
0.200000 14.330000
3
0.333333 14.663333
0.333333 14.996667
0.333333 15.330000
5
0.200000 15.530000
0.200000 15.730000
0.200000 15.930000
0.200000 16.130000
0.200000 16.330000
4
0.250000 16.580000
0.250000 16.830000
0.250000 17.080000
0.250000 17.330000
4
0.250000 17.580000
0.250000 17.830000
0.250000 18.080000
0.250000 18.330000
5
0.200000 18.530000
0.200000 18.730000
0.200000 18.930000
0.200000 19.130000
0.200000 19.330000
4
0.250000 19.580000
0.250000 19.830000
0.250000 20.080000
0.250000 20.330000
3
0.333333 20.663333
0.333333 20.996667
0.333333 21.330000

N
55(0.25)
0.004545 0.004545
0.004545 0.009091
0.004545 0.013636
0.004545 0.018182
0.004545 0.022727
0.004545 0.027273
0.004545 0.031818
0.004545 0.036364
0.004545 0.040909
0.004545 0.045455
0.004545 0.050000
0.004545 0.054545
0.004545 0.059091
0.004545 0.063636
0.004545 0.068182
0.004545 0.072727
0.004545 0.077273
0.004545 0.081818
0.004545 0.086364
0.004545 0.090909
0.004545 0.095455
0.004545 0.100000
0.004545 0.104545
0.004545 0.109091
0.004545 0.113636
0.004545 0.118182
0.004545 0.122727
0.004545 0.127273
0.004545 0.131818
0.004545 0.136364
0.004545 0.140909
0.004545 0.145455
0.004545 0.150000
0.004545 0.154545
0.004545 0.159091
0.004545 0.163636
0.004545 0.168182
0.004545 0.172727
0.004545 0.177273
0.004545 0.181818
0.004545 0.186364
0.004545 0.190909
0.004545 0.195455
0.004545 0.200000
0.004545 0.204545
0.004545 0.209091
0.004545 0.213636
0.004545 0.218182
0.004545 0.222727
0.004545 0.227273
0.004545 0.231818
0.004545 0.236364
0.004545 0.240909
0.004545 0.245455
0.004545 0.250000
9(0.25)
0.027778 0.277778
0.027778 0.305556
0.027778 0.333333
0.027778 0.361111
0.027778 0.388889
0.027778 0.416667
0.027778 0.444444
0.027778 0.472222
0.027778 0.500000
69(0.5)
0.007246 0.507246
0.007246 0.514493
0.007246 0.521739
0.007246 0.528986
0.007246 0.536232
0.007246 0.543478
0.007246 0.550725
0.007246 0.557971
0.007246 0.565217
0.007246 0.572464
0.007246 0.579710
0.007246 0.586957
0.007246 0.594203
0.007246 0.601449
0.007246 0.608696
0.007246 0.615942
0.007246 0.623188
0.007246 0.630435
0.007246 0.637681
0.007246 0.644928
0.007246 0.652174
0.007246 0.659420
0.007246 0.666667
0.007246 0.673913
0.007246 0.681159
0.007246 0.688406
0.007246 0.695652
0.007246 0.702899
0.007246 0.710145
0.007246 0.717391
0.007246 0.724638
0.007246 0.731884
0.007246 0.739130
0.007246 0.746377
0.007246 0.753623
0.007246 0.760870
0.007246 0.768116
0.007246 0.775362
0.007246 0.782609
0.007246 0.789855
0.007246 0.797101
0.007246 0.804348
0.007246 0.811594
0.007246 0.818841
0.007246 0.826087
0.007246 0.833333
0.007246 0.840580
0.007246 0.847826
0.007246 0.855072
0.007246 0.862319
0.007246 0.869565
0.007246 0.876812
0.007246 0.884058
0.007246 0.891304
0.007246 0.898551
0.007246 0.905797
0.007246 0.913043
0.007246 0.920290
0.007246 0.927536
0.007246 0.934783
0.007246 0.942029
0.007246 0.949275
0.007246 0.956522
0.007246 0.963768
0.007246 0.971014
0.007246 0.978261
0.007246 0.985507
0.007246 0.992754
0.007246 1.000000
51(0.5)
0.009804 1.009804
0.009804 1.019608
0.009804 1.029412
0.009804 1.039216
0.009804 1.049020
0.009804 1.058824
0.009804 1.068627
0.009804 1.078431
0.009804 1.088235
0.009804 1.098039
0.009804 1.107843
0.009804 1.117647
0.009804 1.127451
0.009804 1.137255
0.009804 1.147059
0.009804 1.156863
0.009804 1.166667
0.009804 1.176471
0.009804 1.186275
0.009804 1.196078
0.009804 1.205882
0.009804 1.215686
0.009804 1.225490
0.009804 1.235294
0.009804 1.245098
0.009804 1.254902
0.009804 1.264706
0.009804 1.274510
12(0.5)
0.041667 1.041667
0.041667 1.083333
0.041667 1.125000
0.041667 1.166667
0.041667 1.208333
0.041667 1.250000
0.041667 1.291667
0.041667 1.333333
0.041667 1.375000
0.041667 1.416667
0.041667 1.458333
0.041667 1.500000
11(0.5)
0.045455 2.545455
0.045455 2.590909
0.045455 2.636364
0.045455 2.681818
0.045455 2.727273
0.045455 2.772727
0.045455 2.818182
0.045455 2.863636
0.045455 2.909091
0.045455 2.954545
0.045455 3.000000
12(0.5)
0.041667 3.041667
0.041667 3.083333
0.041667 3.125000
0.041667 3.166667
0.041667 3.208333
0.041667 3.250000
0.041667 3.291667
0.041667 3.333333
0.041667 3.375000
0.041667 3.416667
0.041667 3.458333
0.041667 3.500000
0.041667 3.541667
4(0.5)
0.125000 3.666667
0.125000 3.791667
0.125000 3.916667
0.125000 4.041667
1(0.5)
0.500000 4.541667
1
1.000000 5.541667
7
0.142857 5.684524
0.142857 5.827381
0.142857 5.970238
0.142857 6.113095
0.142857 6.255952
0.142857 6.398810
0.142857 6.541667
2
0.500000 7.041667
0.500000 7.541667
4
0.250000 7.791667
0.250000 8.041667
0.250000 8.291667
0.250000 8.541667
4
0.250000 8.791667
0.250000 9.041667
0.250000 9.291667
0.250000 9.541667
3
0.333333 9.875000
0.020833 1.958333
0.020833 1.979167
0.020833 2.000000
12(0.5)
0.041667 2.041667
0.041667 2.083333
0.041667 2.125000
0.041667 2.166667
0.041667 2.208333
0.041667 2.250000
0.041667 2.291667
2
0.041667 2.333333
0.041667 2.375000
0.041667 2.416667
0.041667 2.458333
0.041667 2.500000
11(0.5)
0.045455 2.545455
0.045455 2.590909
0.045455 2.636364
0.045455 2.681818
0.045455 2.727273
0.045455 2.772727
0.045455 2.818182
0.045455 2.863636
0.045455 2.909091
0.045455 2.954545
0.045455 3.000000
12(0.5)
0.041667 3.041667
0.041667 3.083333
0.041667 3.125000
0.041667 3.166667
0.041667 3.208333
0.041667 3.250000
0.041667 3.291667
0.041667 3.333333
0.041667 3.375000
0.041667 3.416667
0.041667 3.458333
0.041667 3.500000
0.041667 3.541667
4(0.5)
0.125000 3.666667
0.125000 3.791667
0.125000 3.916667
0.125000 4.041667
1(0.5)
0.500000 4.541667
1
1.000000 5.541667
7
0.142857 5.684524
0.142857 5.827381
0.142857 5.970238
0.142857 6.113095
0.142857 6.255952
0.142857 6.398810
0.142857 6.541667
2
0.500000 7.041667
0.500000 7.541667
4
0.250000 7.791667
0.250000 8.041667
0.250000 8.291667
0.250000 8.541667
4
0.250000 8.791667
0.250000 9.041667
0.250000 9.291667
0.250000 9.541667
3
0.333333 9.875000
0.333333 10.208333
0.333333 10.541667
1
1.000000 11.541667
2
0.500000 12.041667
0.500000 12.541667
3
0.333333 12.875000
0.333333 13.208333
0.333333 13.541667
2
0.500000 14.041667
0.500000 14.541667
3
0.333333 14.875000
0.333333 15.208333
0.333333 15.541667
1
1.000000 16.541667
2
0.500000 17.041667
0.500000 17.541667
1
1.000000 18.541667
3
0.333333 18.875000
0.333333 19.208333
0.333333 19.541667
1
1.000000 20.541667
1
1.000000 21.541667
3
0.333333 21.875000
0.333333 22.208333
0.333333 22.541667
5
0.200000 22.741667
0.200000 22.941667
0.200000 23.141667
0.200000 23.341667
0.200000 23.541667
3
0.333333 23.875000
0.333333 24.208333
0.333333 24.541667
0,1
2.000000 26.541667
2
0.500000 27.041667
0.500000 27.541667
0,1
2.000000 29.541667
3
0.333333 29.875000
0.333333 30.208333
0.333333 30.541667
1
1.000000 31.541667
2
0.500000 32.041667
0.500000 32.541667
2
0.500000 33.041667
0.500000 33.541667

K113 S
32(0.14)
0.004375 0.004375
0.004375 0.008750
0.004375 0.013125
0.004375 0.017500
0.004375 0.021875
0.004375 0.026250
0.004375 0.030625
0.004375 0.035000
0.004375 0.039375
0.004375 0.043750
0.004375 0.048125
0.004375 0.052500
0.004375 0.056875
0.004375 0.061250
0.004375 0.065625
0.004375 0.070000
0.004375 0.074375
0.004375 0.078750
0.004375 0.083125
0.004375 0.087500
0.004375 0.091875
22(0.5)
0.022727 0.662727
0.022727 0.685455
0.022727 0.708182
0.022727 0.730909
0.022727 0.753636
0.022727 0.776364
0.022727 0.799091
0.022727 0.821818
0.022727 0.844545
0.022727 0.867273
0.022727 0.890000
0.022727 0.912727
0.022727 0.935455
0.022727 0.958182
0.022727 0.980909
0.022727 1.003636
0.022727 1.026364
0.022727 1.049091
0.022727 1.071818
0.022727 1.094545
0.022727 1.117273
0.022727 1.140000
13(0.1)
0.007692 1.147692
0.007692 1.155385
0.007692 1.163077
0.007692 1.170769
0.007692 1.178462
0.007692 1.186154
0.007692 1.193846
0.007692 1.201538
0.007692 1.209231
0.007692 1.216923
0.007692 1.224615
0.007692 1.232308
0.007692 1.240000
46(0.5)
0.010870 1.250870
0.010870 1.261739
0.010870 1.272609
0.010870 1.283478
0.010870 1.294348
0.010870 1.305217
0.010870 1.316087
0.010870 1.326957
0.010870 1.337826
0.010870 1.348696
0.010870 1.359565
0.010870 1.370435
0.010870 1.381304
0.010870 1.392174
0.010870 1.403043
0.010870 1.413913
0.010870 1.424783
0.010870 1.435652
0.010870 1.446522
0.010870 1.457391
0.010870 1.468261
0.010870 1.479130
0.010870 1.490000
0.010870 1.500870
0.010870 1.511739
0.010870 1.522609
0.010870 1.533478
0.010870 1.544348
0.010870 1.555217
0.010870 1.566087
0.010870 1.576957
0.010870 1.587826
0.010870 1.598696
0.010870 1.609565
0.010870 1.620435
0.010870 1.631304
0.010870 1.642174
0.010870 1.653043
0.010870 1.663913
0.010870 1.674783
0.010870 1.685652
0.010870 1.696522
0.010870 1.707391
0.010870 1.718261
0.010870 1.729130
0.010870 1.740000
5
0.200000 1.940000
0.200000 2.140000
0.200000 2.340000
0.200000 2.540000
0.200000 2.740000
1
1.000000 3.740000
3
0.333333 4.073333
0.333333 4.406667
0.333333 4.740000
4
0.250000 4.990000
0.250000 5.240000
0.250000 5.490000
0.250000 5.740000
2
0.500000 6.240000
0.500000 6.740000
1
1.000000 7.740000
2
0.500000 8.240000
0.500000 8.740000
4
0.250000 8.990000
0.250000 9.240000
0.250000 9.490000
0.250000 9.740000
3
0.333333 10.073333
0.333333 10.406667
0.333333 10.740000
4
0.250000 10.990000
0.250000 11.240000
0.250000 11.490000
0.250000 11.740000
3
0.333333 12.073333
0.333333 12.406667
0.333333 12.740000
2
0.500000 13.240000
0.500000 13.740000
1
1.000000 14.740000
1
1.000000 15.740000
2
0.500000 16.240000
0.500000 16.740000
1
1.000000 17.740000
1
1.000000 18.740000
2
0.500000 19.240000
0.500000 19.740000
0,1
2.000000 21.740000
0,2
1.500000 23.240000
0.500000 23.740000
2
0.500000 24.240000
0.500000 24.740000
2
0.500000 25.240000
0.500000 25.740000
2
0.500000 26.240000
0.500000 26.740000
3
0.333333 27.073333
0.333333 27.406667
0.333333 27.740000
2
0.500000 28.240000
0.500000 28.740000
1
1.000000 29.740000
1
1.000000 30.740000

N
30(0.28)
0.009333 0.009333
0.009333 0.018667
0.009333 0.028000
0.009333 0.037333
0.009333 0.046667
0.009333 0.056000
0.009333 0.065333
0.009333 0.074667
0.009333 0.084000
0.009333 0.093333
0.009333 0.102667
0.009333 0.112000
0.009333 0.121333
0.009333 0.130667
0.009333 0.140000
0.009333 0.149333
0.009333 0.158667
0.009333 0.168000
0.009333 0.177333
0.009333 0.186667
0.009333 0.196000
0.009333 0.205333
0.009333 0.214667
0.009333 0.224000
0.009333 0.233333
0.009333 0.242667
0.009333 0.252000
0.009333 0.261333
0.009333 0.270667
0.009333 0.280000
8(0.22)
0.027500 0.307500
0.027500 0.335000
0.027500 0.362500
0.027500 0.390000
0.027500 0.417500
0.027500 0.445000
0.027500 0.472500
0.027500 0.500000
32(0.3)
0.009375 0.509375
0.009375 0.518750
0.009375 0.528125
0.009375 0.537500
0.009375 0.546875
0.009375 0.556250
0.009375 0.565625
0.009375 0.575000
0.009375 0.584375
0.009375 0.593750
0.009375 0.603125
0.009375 0.612500
0.009375 0.621875
0.009375 0.631250
0.009375 0.640625
0.009375 0.650000
0.009375 0.659375
0.009375 0.668750
0.009375 0.678125
0.009375 0.687500
0.009375 0.696875
0.009375 0.706250
0.009375 0.715625
0.009375 0.725000
0.009375 0.734375
0.009375 0.743750
0.009375 0.753125
0.009375 0.762500
0.009375 0.771875
0.009375 0.781250
0.009375 0.790625
0.009375 0.800000
2(0.2)
0.100000 0.900000
0.100000 1.000000
5(0.5)
0.100000 1.100000
0.100000 1.200000
0.100000 1.300000
0.100000 1.400000
0.100000 1.500000
2
0.500000 2.000000
0.500000 2.500000
1
1.000000 3.500000
1
1.000000 4.500000
2
0.500000 5.000000
0.500000 5.500000
2
0.500000 6.000000
0.500000 6.500000
1
1.000000 7.500000
3
0.333333 7.833333
0.333333 8.166667
0.333333 8.500000
2
0.500000 9.000000
0.500000 9.500000
1
1.000000 10.500000
3
0.333333 10.833333

0.333333 11.166667
0.333333 11.500000
2
0.500000 12.000000
0.500000 12.500000
1
1.000000 13.500000

K114
S
83(0.39)
0.004699 0.004699
0.004699 0.009398
0.004699 0.014096
0.004699 0.018795
0.004699 0.023494
0.004699 0.028193
0.004699 0.032892
0.004699 0.037590
0.004699 0.042289
0.004699 0.046988
0.004699 0.051687
0.004699 0.056386
0.004699 0.061084
0.004699 0.065783
0.004699 0.070482
0.004699 0.075181
0.004699 0.079880
0.004699 0.084578
0.004699 0.089277
0.004699 0.093976
0.004699 0.098675
0.004699 0.103373
0.004699 0.108072
0.004699 0.112771
0.004699 0.117470
0.004699 0.122169
0.004699 0.126867
0.004699 0.131566
0.004699 0.136265
0.004699 0.140964
0.004699 0.145663
0.004699 0.150361
0.004699 0.155060
0.004699 0.159759
0.004699 0.164458
0.004699 0.169157
0.004699 0.173855
0.004699 0.178554
0.004699 0.183253
0.004699 0.187952
0.004699 0.192651
0.004699 0.197349
0.004699 0.202048
0.004699 0.206747
0.004699 0.211446
0.004699 0.216145
0.004699 0.220843
0.004699 0.225542
0.004699 0.230241
0.004699 0.234940
0.004699 0.239639
0.004699 0.244337
0.004699 0.249036
0.004699 0.253735
0.004699 0.258434
0.004699 0.263133
0.004699 0.267831
0.004699 0.272530
0.004699 0.277229
0.004699 0.281928
0.004699 0.286627
0.004699 0.291325

0.004699 0.296024
0.004699 0.300723
0.004699 0.305422
0.004699 0.310120
0.004699 0.314819
0.004699 0.319518
0.004699 0.324217
0.004699 0.328916
0.004699 0.333614
0.004699 0.338313
0.004699 0.343012
0.004699 0.347711
0.004699 0.352410
0.004699 0.357108
0.004699 0.361807
0.004699 0.366506
0.004699 0.371205
0.004699 0.375904
0.004699 0.380602
0.004699 0.385301
0.004699 0.390000
11(0.2)
0.018182 0.408182
0.018182 0.426364
0.018182 0.444545
0.018182 0.462727
0.018182 0.480909
0.018182 0.499091
0.018182 0.517273
0.018182 0.535455
0.018182 0.553636
0.018182 0.571818
0.018182 0.590000
0.018182 0.608182
2(0.3)
0.150000 0.758182
0.150000 0.908182
3(0.5)
0.166667 1.074848
0.166667 1.241515
0.166667 1.408182
5
0.200000 1.608182
0.200000 1.808182
0.200000 2.008182
0.200000 2.208182
0.200000 2.408182
2
0.500000 2.908182
0.500000 3.408182
2
0.500000 3.908182
0.500000 4.408182
1
1.000000 5.408182
2
0.500000 5.908182
0.500000 6.408182
1
1.000000 7.408182
3
0.333333 7.741515
0.333333 8.074848
0.333333 8.408182
1
1.000000 9.408182
0,0,1
3.000000 12.408182
1
1.000000 13.408182

N
96(0.37)
0.003854 0.003854

0.003854 0.007708
0.003854 0.011563
0.003854 0.015417
0.003854 0.019271
0.003854 0.023125
0.003854 0.026979
0.003854 0.030833
0.003854 0.034688
0.003854 0.038542
0.003854 0.042396
0.003854 0.046250
0.003854 0.050104
0.003854 0.053958
0.003854 0.057813
0.003854 0.061667
0.003854 0.065521
0.003854 0.069375
0.003854 0.073229
0.003854 0.077083
0.003854 0.080938
0.003854 0.084792
0.003854 0.088646
0.003854 0.092500
0.003854 0.096354
0.003854 0.100208
0.003854 0.104063
0.003854 0.107917
0.003854 0.111771
0.003854 0.115625
0.003854 0.119479
0.003854 0.123333
0.003854 0.127188
0.003854 0.131042
0.003854 0.134896
0.003854 0.138750
0.003854 0.142604
0.003854 0.146458
0.003854 0.150313
0.003854 0.154167
0.003854 0.158021
0.003854 0.161875
0.003854 0.165729
0.003854 0.169583
0.003854 0.173438
0.003854 0.177292
0.003854 0.181146
0.003854 0.185000
0.003854 0.188854
0.003854 0.192708
0.003854 0.196563
0.003854 0.200417
0.003854 0.204271
0.003854 0.208125
0.003854 0.211979
0.003854 0.215833
0.003854 0.219688
0.003854 0.223542
0.003854 0.227396
0.003854 0.231250
0.003854 0.235104
0.003854 0.238958
0.003854 0.242813
0.003854 0.246667
0.003854 0.250521
0.003854 0.254375
0.003854 0.258229
0.003854 0.262083
0.003854 0.265938
0.003854 0.269792
0.003854 0.273646
0.003854 0.277500
0.003854 0.281354
0.003854 0.285208
0.003854 0.289063

0.003854 0.292917
0.003854 0.296771
0.003854 0.300625
0.003854 0.304479
0.003854 0.308333
0.003854 0.312188
0.003854 0.316042
0.003854 0.319896
0.003854 0.323750
0.003854 0.327604
0.003854 0.331458
0.003854 0.335313
0.003854 0.339167
0.003854 0.343021
0.003854 0.346875
0.003854 0.350729
0.003854 0.354583
0.003854 0.358438
0.003854 0.362292
0.003854 0.366146
0.003854 0.370000
8(0.5)
0.062500 0.432500
0.062500 0.495000
0.062500 0.557500
0.062500 0.620000
0.062500 0.682500
0.062500 0.745000
0.062500 0.807500
0.062500 0.870000
3(0.5)
0.166667 1.036667
0.166667 1.203333
0.166667 1.370000
3
0.333333 1.703333
0.333333 2.036667
0.333333 2.370000
3
0.333333 2.703333
0.333333 3.036667
0.333333 3.370000
0,1
2.000000 5.370000
2
0.500000 5.870000
0.500000 6.370000
2
0.500000 6.870000
0.500000 7.370000
2
0.500000 7.870000
0.500000 8.370000
2
0.500000 8.870000
0.500000 9.370000
2
0.500000 9.870000
0.500000 10.370000

K115
S
3(0.5)
0.166667 0.166667
0.166667 0.333333
0.166667 0.500000
2(0.5)
0.250000 0.750000
0.250000 1.000000
2
0.500000 1.500000
0.500000 2.000000
1
1.000000 3.000000
1
1.000000 4.000000
1
1.000000 5.000000

N
3(0.5)
0.166667 0.000600
0.166667 0.167267
0.166667 0.333933
1(0.5)
0.500000 0.833933
3(0.5)
0.166667 1.000600
0.166667 1.167267
0.166667 1.333933
3(0.5)
0.166667 1.500600
0.166667 1.667267
0.166667 1.833933
5
0.200000 2.033933
0.200000 2.233933
0.200000 2.433933
0.200000 2.633933
0.200000 2.833933
3
0.333333 3.167267
0.333333 3.500600
0.333333 3.833933
5
0.200000 4.033933
0.200000 4.233933
0.200000 4.433933
0.200000 4.633933
0.200000 4.833933
3
0.333333 5.167267
0.333333 5.500600
0.333333 5.833933
4
0.250000 6.083933
0.250000 6.333933
0.250000 6.583933
0.250000 6.833933
6
0.166667 7.000600
0.166667 7.167267
0.166667 7.333933
0.166667 7.500600
0.166667 7.667267
0.166667 7.833933
3
0.333333 8.167267
0.333333 8.500600
0.333333 8.833933
2
0.500000 9.333933
0.500000 9.833933
2
0.500000 10.333933
0.500000 10.833933
1
1.000000 11.833933
0,1
2.000000 13.833933
1
1.000000 14.833933
2
0.500000 15.333933
0.500000 15.833933
3
0.333333 16.167267

0.333333 16.500600
0.333333 16.833933
1
1.000000 17.833933
0,1
2.000000 19.833933
6
0.166667 20.000600
0.166667 20.167267
0.166667 20.333933
0.166667 20.500600
0.166667 20.667267
0.166667 20.833933
1
1.000000 21.833933
1
1.000000 22.833933
1
1.000000 23.833933

K116i
S
2(0.5)
0.250000 0.250000
0.250000 0.500000
3(0.5)
0.166667 0.666667
0.166667 0.833333
0.166667 1.000000
4
0.250000 1.250000
0.250000 1.500000
0.250000 1.750000
0.250000 2.000000
7
0.142857 2.142857
0.142857 2.285714
0.142857 2.428571
0.142857 2.571429
0.142857 2.714286
0.142857 2.857143
0.142857 3.000000
4
0.250000 3.250000
0.250000 3.500000
0.250000 3.750000
0.250000 4.000000
2
0.500000 4.500000
0.500000 5.000000
5
0.200000 5.200000
0.200000 5.400000
0.200000 5.600000
0.200000 5.800000
0.200000 6.000000
0.200000 6.200000
1
1.000000 7.200000
3
0.333333 7.533333
0.333333 7.866667
0.333333 8.200000
0,2
1.500000 9.700000
0.500000 10.200000
2
0.500000 10.700000
0.500000 11.200000
1
1.000000 12.200000
0,2
1.500000 13.700000

0.500000 14.200000
4
0.250000 14.450000
0.250000 14.700000
0.250000 14.950000
0.250000 15.200000
1
1.000000 16.200000
1
1.000000 17.200000
1
1.000000 18.200000
2
0.500000 18.700000
0.500000 19.200000
0,1
2.000000 21.200000
0,1
2.000000 23.200000
1
1.000000 24.200000

N
3(0.5)
0.166667 0.166667
0.166667 0.333333
0.166667 0.500000
2(0.5)
0.250000 0.750000
0.250000 1.000000
1
1.000000 2.000000
1
1.000000 3.000000
4
0.250000 3.250000
0.250000 3.500000
0.250000 3.750000
0.250000 4.000000
3
0.333333 4.333333
0.333333 4.666667
0.333333 5.000000

K116iix
S
37(0.09)
0.002432 0.002432
0.002432 0.004865
0.002432 0.007297
0.002432 0.009730
0.002432 0.012162
0.002432 0.014595
0.002432 0.017027
0.002432 0.019459
0.002432 0.021892
0.002432 0.024324
0.002432 0.026757
0.002432 0.029189
0.002432 0.031622
0.002432 0.034054
0.002432 0.036486
0.002432 0.038919
0.002432 0.041351
0.002432 0.043784
0.002432 0.046216
0.002432 0.048649
0.002432 0.051081
0.002432 0.053514
0.002432 0.055946
0.002432 0.058378
0.002432 0.060811
0.002432 0.063243

0.002432 0.065676
0.002432 0.068108
0.002432 0.070541
0.002432 0.072973
0.002432 0.075405
0.002432 0.077838
0.002432 0.080270
0.002432 0.082703
0.002432 0.085135
0.002432 0.087568
0.002432 0.090000
0(0.16),1(0.5)
0.660000 0.750000
2
0.500000 1.250000
0.500000 1.750000
1
0.010000 1.760000
5
0.200000 1.960000
0.200000 2.160000
0.200000 2.360000
0.200000 2.560000
0.200000 2.760000
3
0.333333 3.093333
0.333333 3.426667
0.333333 3.760000

N
37(0.1)
0.002703 0.002703
0.002703 0.005405
0.002703 0.008108
0.002703 0.010811
0.002703 0.013514
0.002703 0.016216
0.002703 0.018919
0.002703 0.021622
0.002703 0.024324
0.002703 0.027027
0.002703 0.029730
0.002703 0.032432
0.002703 0.035135
0.002703 0.037838
0.002703 0.040541
0.002703 0.043243
0.002703 0.045946
0.002703 0.048649
0.002703 0.051351
0.002703 0.054054
0.002703 0.056757
0.002703 0.059459
0.002703 0.062162
0.002703 0.064865
0.002703 0.067568
0.002703 0.070270
0.002703 0.072973
0.002703 0.075676
0.002703 0.078378
0.002703 0.081081
0.002703 0.083784
0.002703 0.086486
0.002703 0.089189
0.002703 0.091892
0.002703 0.094595
0.002703 0.097297
0.002703 0.100000
6(0.4)
0.066667 0.166667
0.066667 0.233333
0.066667 0.300000
0.066667 0.366667
0.066667 0.433333

0.066667 0.500000
3
0.333333 0.833333
0.333333 1.166667
0.333333 1.500000
1
1.000000 2.500000
2
0.500000 3.000000
0.500000 3.500000
1
1.000000 4.500000
0,0,1
3.000000 7.500000
1
1.000000 8.500000
1
1.000000 9.500000
0,1
2.000000 11.500000

K116iiy
N
30(0.1)
0.003333 0.003333
0.003333 0.006667
0.003333 0.010000
0.003333 0.013333
0.003333 0.016667
0.003333 0.020000
0.003333 0.023333
0.003333 0.026667
0.003333 0.030000
0.003333 0.033333
0.003333 0.036667
0.003333 0.040000
0.003333 0.043333
0.003333 0.046667
0.003333 0.050000
0.003333 0.053333
0.003333 0.056667
0.003333 0.060000
0.003333 0.063333
0.003333 0.066667
0.003333 0.070000
0.003333 0.073333
0.003333 0.076667
0.003333 0.080000
0.003333 0.083333
0.003333 0.086667
42(0.4)
0.009524 0.096190
0.009524 0.105714
0.009524 0.115238
0.009524 0.124762
0.009524 0.134286
0.009524 0.143810
0.009524 0.153333
0.009524 0.162857
0.009524 0.172381
0.009524 0.181905
0.009524 0.191429
0.009524 0.200952
0.009524 0.210476
0.009524 0.220000
0.009524 0.229524
0.009524 0.239048
0.009524 0.248571
0.009524 0.258095
0.009524 0.267619
0.009524 0.277143
0.009524 0.286667
0.009524 0.296190
0.009524 0.305714

0.009524 0.315238
0.009524 0.324762
0.009524 0.334286
0.009524 0.343810
0.009524 0.353333
0.009524 0.362857
0.009524 0.372381
0.009524 0.381905
0.009524 0.391429
0.009524 0.400952
0.009524 0.410476
0.009524 0.420000
0.009524 0.429524
0.009524 0.439048
0.009524 0.448571
0.009524 0.458095
0.009524 0.467619
0.009524 0.477143
0.009524 0.486667
30(0.5)
0.016667 0.503333
0.016667 0.520000
0.016667 0.536667
0.016667 0.553333
0.016667 0.570000
0.016667 0.586667
0.016667 0.603333
0.016667 0.620000
0.016667 0.636667
0.016667 0.653333
0.016667 0.670000
0.016667 0.686667
0.016667 0.703333
0.016667 0.720000
0.016667 0.736667
0.016667 0.753333
0.016667 0.770000
0.016667 0.786667
0.016667 0.803333
0.016667 0.820000
0.016667 0.836667
0.016667 0.853333
0.016667 0.870000
0.016667 0.886667
0.016667 0.903333
0.016667 0.920000
0.016667 0.936667
0.016667 0.953333
0.016667 0.970000
0.016667 0.986667
29(0.5)
0.017241 1.003908
0.017241 1.021149
0.017241 1.038391
0.017241 1.055632
0.017241 1.072874
0.017241 1.090115
0.017241 1.107356
0.017241 1.124598
0.017241 1.141839
0.017241 1.159080
0.017241 1.176322
0.017241 1.193563
0.017241 1.210805
0.017241 1.228046
0.017241 1.245287
0.017241 1.262529
0.017241 1.279770
0.017241 1.297011
0.017241 1.314253
0.017241 1.331494
0.017241 1.348736
0.017241 1.365977
0.017241 1.383218

0.017241 1.400460
0.017241 1.417701
0.017241 1.434943
0.017241 1.452184
0.017241 1.469425
0.017241 1.486667
14(0.5)
0.035714 1.522381
0.035714 1.558095
0.035714 1.593810
0.035714 1.629524
0.035714 1.665238
0.035714 1.700952
0.035714 1.736667
0.035714 1.772381
0.035714 1.808095
0.035714 1.843810
0.035714 1.879524
0.035714 1.915238
0.035714 1.950952
0.035714 1.986667
10(0.5)
0.050000 2.036667
0.050000 2.086667
0.050000 2.136667
0.050000 2.186667
0.050000 2.236667
0.050000 2.286667
0.050000 2.336667
0.050000 2.386667
0.050000 2.436667
0.050000 2.486667
11(0.5)
0.045455 2.532121
0.045455 2.577576
0.045455 2.623030
0.045455 2.668485
0.045455 2.713939
0.045455 2.759394
0.045455 2.804848
0.045455 2.850303
0.045455 2.895758
0.045455 2.941212
0.045455 2.986667
9(0.5)
0.055556 3.042222
0.055556 3.097778
0.055556 3.153333
0.055556 3.208889
0.055556 3.264444
0.055556 3.320000
0.055556 3.375556
0.055556 3.431111
0.055556 3.486667
0.055556 3.542222
2(0.5)
0.250000 3.792222
0.250000 4.042222
0,0,0,1
4.000000 8.042222
1
1.000000 9.042222
0
0
0
0
0
0

K117A
S
3(0.35)
0.116667 0.116667

0.116667 0.233333
0.116667 0.350000
5(0.5)
0.100000 0.450000
0.100000 0.550000
0.100000 0.650000
0.100000 0.750000
0.100000 0.850000
8(0.5)
0.062500 0.912500
0.062500 0.975000
0.062500 1.037500
0.062500 1.100000
0.062500 1.162500
0.062500 1.225000
0.062500 1.287500
0.062500 1.350000
10(0.5)
0.050000 1.400000
0.050000 1.450000
0.050000 1.500000
0.050000 1.550000
0.050000 1.600000
0.050000 1.650000
0.050000 1.700000
0.050000 1.750000
0.050000 1.800000
0.050000 1.850000
8(0.5)
0.062500 1.912500
0.062500 1.975000
0.062500 2.037500
0.062500 2.100000
0.062500 2.162500
0.062500 2.225000
0.062500 2.287500
0.062500 2.350000
9
0.111111 2.461111
0.111111 2.572222
0.111111 2.683333
0.111111 2.794444
0.111111 2.905556
0.111111 3.016667
0.111111 3.127778
0.111111 3.238889
0.111111 3.350000
0.111111 3.461111
5
0.200000 3.661111
0.200000 3.861111
0.200000 4.061111
0.200000 4.261111
0.200000 4.461111
2
0.500000 4.961111
0.500000 5.461111
2
0.500000 5.961111
0.500000 6.461111
1
1.000000 7.461111
1
1.000000 8.461111
1
1.000000 9.461111
2
0.500000 9.961111
0.500000 10.461111
1
1.000000 11.461111
0,1
2.000000 13.461111
0,0,1

3.000000 16.461111

N
4(0.5)
0.125000 0.125000
0.125000 0.250000
0.125000 0.375000
0.125000 0.500000
4(0.5)
0.125000 0.625000
0.125000 0.750000
0.125000 0.875000
0.125000 1.000000
3(0.5)
0.166667 1.166667
0.166667 1.333333
0.166667 1.500000
5(0.5)
0.100000 1.600000
0.100000 1.700000
0.100000 1.800000
0.100000 1.900000
0.100000 2.000000
5(0.5)
0.100000 2.100000
0.100000 2.200000
0.100000 2.300000
0.100000 2.400000
0.100000 2.500000
9
0.111111 2.611111
0.111111 2.722222
0.111111 2.833333
0.111111 2.944444
0.111111 3.055556
0.111111 3.166667
0.111111 3.277778
0.111111 3.388889
0.111111 3.500000
5
0.200000 3.700000
0.200000 3.900000
0.200000 4.100000
0.200000 4.300000
0.200000 4.500000
6
0.166667 4.666667
0.166667 4.833333
0.166667 5.000000
0.166667 5.166667
0.166667 5.333333
0.166667 5.500000
3
0.333333 5.833333
0.333333 6.166667
0.333333 6.500000
4
0.250000 6.750000
0.250000 7.000000
0.250000 7.250000
0.250000 7.500000
1
1.000000 8.500000
2
0.500000 9.000000
0.500000 9.500000
4
0.250000 9.750000
0.250000 10.000000
0.250000 10.250000
0.250000 10.500000
2
0.500000 11.000000
0.500000 11.500000

4
0.250000 11.750000
0.250000 12.000000
0.250000 12.250000
0.250000 12.500000
5
0.200000 12.700000
0.200000 12.900000
0.200000 13.100000
0.200000 13.300000
0.200000 13.500000
2
0.500000 14.000000
0.500000 14.500000
4
0.250000 14.750000
0.250000 15.000000
0.250000 15.250000
0.250000 15.500000
2
0.500000 16.000000
0.500000 16.500000
3
0.333333 16.833333
0.333333 17.166667
0.333333 17.500000
3
0.333333 17.833333
0.333333 18.166667
0.333333 18.500000
2
0.500000 19.000000
0.500000 19.500000
2
0.500000 20.000000
0.500000 20.500000
1
1.000000 21.500000
0.2
1.500000 23.000000
0.500000 23.500000
2
0.500000 24.000000
0.500000 24.500000
3
0.333333 24.833333
0.333333 25.166667
0.333333 25.500000
0.1
2.000000 27.500000
1
1.000000 28.500000
2
0.500000 29.000000
0.500000 29.500000
2
0.500000 30.000000
0.500000 30.500000
0.1
2.000000 32.500000
1
1.000000 33.500000
1
1.000000 34.500000
1
1.000000 35.500000
1
1.000000 36.500000
2
0.500000 37.000000
0.500000 37.500000
2
0.500000 38.000000
0.500000 38.500000

K117B

S

53(0.25)
0.004717 0.004717
0.004717 0.009434
0.004717 0.014151
0.004717 0.018868
0.004717 0.023585
0.004717 0.028302
0.004717 0.033019
0.004717 0.037736
0.004717 0.042453
0.004717 0.047170
0.004717 0.051887
0.004717 0.056604
0.004717 0.061321
0.004717 0.066038
0.004717 0.070755
0.004717 0.075472
0.004717 0.080189
0.004717 0.084906
0.004717 0.089623
0.004717 0.094340
0.004717 0.099057
0.004717 0.103774
0.004717 0.108491
0.004717 0.113208
0.004717 0.117925
0.004717 0.122642
0.004717 0.127358
0.004717 0.132075
0.004717 0.136792
0.004717 0.141509
0.004717 0.146226
0.004717 0.150943
0.004717 0.155660
0.004717 0.160377
0.004717 0.165094
0.004717 0.169811
0.004717 0.174528
0.004717 0.179245
0.004717 0.183962
0.004717 0.188679
0.004717 0.193396
0.004717 0.198113
0.004717 0.202830
0.004717 0.207547
0.004717 0.212264
0.004717 0.216981
0.004717 0.221698
0.004717 0.226415
0.004717 0.231132
0.004717 0.235849
0.004717 0.240566
0.004717 0.245283
0.004717 0.250000
30(0.25)
0.008333 0.258333
0.008333 0.266667
0.008333 0.275000
0.008333 0.283333
0.008333 0.291667
0.008333 0.300000
0.008333 0.308333
0.008333 0.316667
0.008333 0.325000
0.008333 0.333333
0.008333 0.341667
0.008333 0.350000
0.008333 0.358333
0.008333 0.366667
0.008333 0.375000
0.008333 0.383333
0.008333 0.391667
0.008333 0.400000
0.008333 0.408333
0.008333 0.416667
0.008333 0.425000
0.008333 0.433333
0.008333 0.441667
0.008333 0.450000
0.008333 0.458333
0.008333 0.466667
0.008333 0.475000
0.008333 0.483333
0.008333 0.491667
0.008333 0.500000
22(0.25)
0.011364 0.511364
0.011364 0.522727
0.011364 0.534091
0.011364 0.545455
0.011364 0.556818
0.011364 0.568182
0.011364 0.579545
0.011364 0.590909
0.011364 0.602273
0.011364 0.613636
0.011364 0.625000
0.011364 0.636364
0.011364 0.647727
0.011364 0.659091
0.011364 0.670455
0.011364 0.681818
0.011364 0.693182
0.011364 0.704545
0.011364 0.715909
0.011364 0.727273
0.011364 0.738636
0.011364 0.750000
16(0.25)
0.015625 0.765625
0.015625 0.781250
0.015625 0.796875
0.015625 0.812500
0.015625 0.828125
0.015625 0.843750
0.015625 0.859375
0.015625 0.875000
0.015625 0.890625
0.015625 0.906250
0.015625 0.921875
0.015625 0.937500
0.015625 0.953125
0.015625 0.968750
0.015625 0.984375
0.015625 1.000000
14(0.25)
0.017857 1.017857
0.017857 1.035714
0.017857 1.053571
0.017857 1.071429
0.017857 1.089286
0.017857 1.107143
0.017857 1.125000
0.017857 1.142857
0.017857 1.160714
0.017857 1.178571
0.017857 1.196429
0.017857 1.214286
0.017857 1.232143
0.017857 1.250000
7(0.1)
0.014286 1.264286
0.014286 1.278571
0.014286 1.292857
0.014286 1.307143
0.014286 1.321429
0.014286 1.335714
0.014286 1.350000

N

15(0.08)
0.005333 0.005333
0.005333 0.010667
0.005333 0.016000
0.005333 0.021333
0.005333 0.026667
0.005333 0.032000
0.005333 0.037333
0.005333 0.042667
0.005333 0.048000
0.005333 0.053333
0.005333 0.058667
0.005333 0.064000
0.005333 0.069333
0.005333 0.074667
0.005333 0.080000
11(0.42)
0.038182 0.118182
0.038182 0.156364
0.038182 0.194545
0.038182 0.232727
0.038182 0.270909
0.038182 0.309091
0.038182 0.347273
0.038182 0.385455
0.038182 0.423636
0.038182 0.461818
0.038182 0.500000
0
1.000000 1.500000
7(0.07)
0.010000 1.510000
0.010000 1.520000
0.010000 1.530000
0.010000 1.540000
0.010000 1.550000
0.010000 1.560000
0.010000 1.570000
0(0.18)
0.180000 1.750000
22(0.3)
0.013636 1.763636
0.013636 1.777273
0.013636 1.790909
0.013636 1.804545
0.013636 1.818182
0.013636 1.831818
0.013636 1.845455
0.013636 1.859091
0.013636 1.872727
0.013636 1.886364
0.013636 1.900000
0.013636 1.913636
0.013636 1.927273
0.013636 1.940909
0.013636 1.954545
0.013636 1.968182
0.013636 1.981818
0.013636 1.995455
0.013636 2.009091
0.013636 2.022727
0.013636 2.036364
0.013636 2.050000
0(0.2)
0.200000 2.250000
27(0.17)
0.006296 2.256296
0.006296 2.262593
0.006296 2.268889
0.006296 2.275185
0.006296 2.281481
0.006296 2.287778
0.006296 2.294074
0.006296 2.300370
0.006296 2.306667
0.006296 2.312963
0.006296 2.319259
0.006296 2.325556
0.006296 2.331852
0.006296 2.338148
0.006296 2.344444
0.006296 2.350741
0.006296 2.357037
0.006296 2.363333
0.006296 2.369630
0.006296 2.375926
0.006296 2.382222
0.006296 2.388519
0.006296 2.394815
0.006296 2.401111
0.006296 2.407407
0.006296 2.413704
0.006296 2.420000
0.006296 2.426296
0(0.53)
0.530000 2.956296
40(0.25)
0.006250 2.962546
0.006250 2.968796
0.006250 2.975046
0.006250 2.981296
0.006250 2.987546
0.006250 2.993796
0.006250 3.000046
0.006250 3.006296
0.006250 3.012546
0.006250 3.018796
0.006250 3.025046
0.006250 3.031296
0.006250 3.037546
0.006250 3.043796
0.006250 3.050046
0.006250 3.056296
0.006250 3.062546
0.006250 3.068796
0.006250 3.075046
0.006250 3.081296
0.006250 3.087546
0.006250 3.093796
0.006250 3.100046
0.006250 3.106296
0.006250 3.112546
0.006250 3.118796
0.006250 3.125046
0.006250 3.131296
0.006250 3.137546
0.006250 3.143796
0.006250 3.150046
0.006250 3.156296
0.006250 3.162546
0.006250 3.168796
0.006250 3.175046
0.006250 3.181296
0.006250 3.187546
0.006250 3.193796
0.006250 3.200046
0.006250 3.206296
34(0.25)
0.007353 3.213649
0.007353 3.221002
0.007353 3.228355
0.007353 3.235708
0.007353 3.243061
0.007353 3.250414
0.007353 3.257767
0.007353 3.265120
0.007353 3.272473
0.007353 3.279826
0.007353 3.287179
0.007353 3.294532
0.007353 3.301885
0.007353 3.309237
0.007353 3.316590
0.007353 3.323943
0.007353 3.331296
0.007353 3.338649
0.007353 3.346002
0.007353 3.353355
0.007353 3.360708
0.007353 3.368061
0.007353 3.375414
0.007353 3.382767
0.007353 3.390120
0.007353 3.397473
0.007353 3.404826
0.007353 3.412179
0.007353 3.419532
0.007353 3.426885
0.007353 3.434237
0.007353 3.441590
0.007353 3.448943
0.007353 3.456296
24(0.5)
0.020833 3.477130
0.020833 3.497963
0.020833 3.518796
0.020833 3.539630
0.020833 3.560463
0.020833 3.581296
0.020833 3.602130
0.020833 3.622963
0.020833 3.643796
0.020833 3.664630
0.020833 3.685463
0.020833 3.706296
0.020833 3.727130
0.020833 3.747963
0.020833 3.768796
0.020833 3.789630
0.020833 3.810463
0.020833 3.831296
0.020833 3.852130
0.020833 3.872963
0.020833 3.893796
0.020833 3.914630
0.020833 3.935463
0.020833 3.956296
20(0.5)
0.025000 3.981296
0.025000 4.006296
0.025000 4.031296
0.025000 4.056296
0.025000 4.081296
0.025000 4.106296
0.025000 4.131296
0.025000 4.156296
0.025000 4.181296
0.025000 4.206296
0.025000 4.231296
0.025000 4.256296
0.025000 4.281296
0.025000 4.306296
0.025000 4.331296
0.025000 4.356296
0.025000 4.381296
0.025000 4.406296
0.025000 4.431296
0.025000 4.456296
10(0.5)
0.050000 4.506296
0.050000 4.556296
0.050000 4.606296
0.050000 4.656296
0.050000 4.706296
0.050000 4.756296
0.050000 4.806296
0.050000 4.856296
0.050000 4.906296
0.050000 4.956296
3(0.5)
0.166667 5.122963
0.166667 5.289630
0.166667 5.456296

K117AB

S

0.004717
0.009434
0.014151
0.018868
0.023585
0.028302
0.033019
0.037736
0.042453
0.047170
0.051887
0.056604
0.061321
0.066038
0.070755
0.075472
0.080189
0.084906
0.089623
0.094340
0.099057
0.103774
0.108491
0.113208
0.116667
0.117925
0.122642
0.127358
0.132075
0.136792
0.141509
0.146226
0.150943
0.155660
0.160377
0.165094
0.169811
0.174528
0.179245
0.183962
0.188679
0.193396
0.198113
0.202830
0.207547
0.212264
0.216981
0.221698
0.226415
0.231132
0.233333
0.235849
0.240566
0.245283
0.250000
0.258333
0.266667
0.275000
0.283333
0.291667
0.300000
0.308333
0.316667
0.325000
0.333333
0.341667
0.350000
0.350000
0.358333
0.366667
0.375000
0.383333
0.391667
0.400000
0.408333
0.416667
0.425000
0.433333
0.441667
0.450000
0.450000
0.458333
0.466667
0.475000
0.483333
0.491667
0.500000
0.511364
0.522727
0.534091
0.545455
0.550000
0.556818
0.568182
0.579545
0.590909
0.602273
0.613636
0.625000
0.636364
0.647727
0.650000
0.659091
0.670455
0.681818
0.693182
0.704545
0.715909
0.727273
0.738636
0.750000
0.750000
0.765625
0.781250
0.796875
0.812500
0.828125
0.843750
0.850000
0.859375
0.875000
0.890625
0.906250
0.912500
0.921875
0.937500
0.953125
0.968750
0.975000
0.984375
1.000000
1.017857
1.035714
1.037500
1.053571
1.071429
1.089286
1.100000
1.107143
1.125000
1.142857
1.160714
1.162500
1.178571
1.196429
1.214286
1.225000
1.232143
1.250000
1.264286
1.278571
1.287500
1.292857
1.307143
1.321429
1.335714
1.350000
1.350000
1.400000
1.450000
1.500000
1.500000
1.550000
1.600000
1.650000
1.700000
1.750000
1.800000
1.850000
1.912500
1.975000
2.037500
2.100000
2.162500
2.225000
2.287500
2.350000
2.461111
2.572222
2.683333
2.794444
2.905556
3.016667
3.127778
3.238889
3.350000
3.461111
3.661111
3.861111
4.061111
4.261111
4.461111
4.961111
5.461111
5.961111
6.461111
7.461111
8.461111
9.461111
9.961111
10.461111
11.461111
13.461111
16.461111

N

0.005333
0.010667
0.016000
0.021333
0.026667
0.032000
0.037333
0.042667
0.048000
0.053333
0.058667
0.064000
0.069333
0.074667
0.080000
0.118182
0.125000
0.156364
0.194545
0.232727
0.250000
0.270909
0.309091
0.347273
0.375000
0.385455
0.423636
0.461818
0.500000
0.500000
0.625000
0.750000
0.875000
1.000000
1.166667
1.333333
1.500000
1.500000
1.510000
1.520000
1.530000
1.540000
1.550000
1.560000
1.570000
1.600000
1.700000
1.750000
1.763636
1.777273
1.790909
1.800000
1.804545
1.818182
1.831818
1.845455
1.859091
1.872727
1.886364
1.900000
1.900000
1.913636
1.927273
1.940909
1.954545
1.968182
1.981818
1.995455
2.000000
2.009091
2.022727
2.036364
2.050000
2.100000
2.200000
2.250000
2.256296
2.262593
2.268889
2.275185
2.281481
2.287778
2.294074
2.300000
2.300370
2.306667
2.312963
2.319259
2.325556
2.331852
2.338148
2.344444
2.350741
2.357037
2.363333
2.369630
2.375926
2.382222
2.388519
2.394815
2.400000
2.401111
2.407407
2.413704
2.420000
2.426296
2.500000
2.611111
2.722222
2.833333
2.944444
2.956296
2.962546
2.968796
2.975046
2.981296
2.987546
2.993796
3.000046
3.006296
3.012546
3.018796
3.025046
3.031296
3.037546
3.043796
3.050046
3.055556
3.056296
3.062546
3.068796
3.075046
3.081296
3.087546
3.093796
3.100046
3.106296
3.112546
3.118796
3.125046
3.131296
3.137546
3.143796
3.150046
3.156296
3.162546
3.166667
3.168796
3.175046
3.181296
3.187546
3.193796
3.200046
3.206296
3.213649
3.221002
3.228355
3.235708
3.243061
3.250414
3.257767
3.265120
3.272473
3.277778
3.279826
3.287179
3.294532
3.301885
3.309237
3.316590
3.323943
3.331296
3.338649
3.346002
3.353355
3.360708
3.368061
3.375414
3.382767
3.388889
3.390120
3.397473
3.404826
3.412179
3.419532
3.426885
3.434237
3.441590
3.448943
3.456296
3.477130
3.497963
3.500000
3.518796
3.539630
3.560463
3.581296
3.602130
3.622963
3.643796
3.664630
3.685463
3.700000
3.706296
3.727130
3.747963
3.768796
3.789630
3.810463
3.831296
3.852130
3.872963
3.893796
3.900000
3.914630
3.935463
3.956296
3.981296
4.006296
4.031296
4.056296
4.081296
4.100000
4.106296
4.131296
4.156296
4.181296
4.206296
4.231296
4.256296
4.281296
4.300000
4.306296
4.331296
4.356296
4.381296
4.400000
4.456296
4.481296
4.500000
4.506296
4.556296
4.606296
4.656296
4.666667
4.706296
4.756296
4.806296
4.833333
4.856296
4.906296
4.956296
5.000000
5.122963
5.166667
5.289630
5.333333
5.456296
5.500000
5.833333
6.166667
6.500000
6.750000
7.000000
7.250000
7.500000
8.500000
9.000000
9.500000
9.750000
10.000000
10.250000
10.500000
11.000000
11.500000
11.750000
12.000000
12.250000
12.500000
12.700000
12.900000
13.100000
13.300000
13.500000
14.000000
14.500000
14.750000
15.000000
15.250000
15.500000
16.000000
16.500000
16.833333
17.166667

17.500000
17.833333
18.166667
18.500000
19.000000
19.500000
20.000000
20.500000
21.500000
23.000000
23.500000
24.000000
24.500000
24.833333
25.166667
25.500000
27.500000
28.500000
29.000000
29.500000
30.000000
30.500000
32.500000
33.500000
34.500000
35.500000
36.500000
37.000000
37.500000
38.000000
38.500000

K118i
S
56(0.19)
0.003393 0.003393
0.003393 0.006786
0.003393 0.010179
0.003393 0.013571
0.003393 0.016964
0.003393 0.020357
0.003393 0.023750
0.003393 0.027143
0.003393 0.030536
0.003393 0.033929
0.003393 0.037321
0.003393 0.040714
0.003393 0.044107
0.003393 0.047500
0.003393 0.050893
0.003393 0.054286
0.003393 0.057679
0.003393 0.061071
0.003393 0.064464
0.003393 0.067857
0.003393 0.071250
0.003393 0.074643
0.003393 0.078036
0.003393 0.081429
0.003393 0.084821
0.003393 0.088214
0.003393 0.091607
0.003393 0.095000
0.003393 0.098393
0.003393 0.101786
0.003393 0.105179
0.003393 0.108571
0.003393 0.111964
0.003393 0.115357
0.003393 0.118750
0.003393 0.122143
0.003393 0.125536
0.003393 0.128929

0.003393 0.132321
0.003393 0.135714
0.003393 0.139107
0.003393 0.142500
0.003393 0.145893
0.003393 0.149286
0.003393 0.152679
0.003393 0.156071
0.003393 0.159464
0.003393 0.162857
0.003393 0.166250
0.003393 0.169643
0.003393 0.173036
0.003393 0.176429
0.003393 0.179821
0.003393 0.183214
0.003393 0.186607
0.003393 0.190000
22(0.12)
0.005455 0.195455
0.005455 0.200909
0.005455 0.206364
0.005455 0.211818
0.005455 0.217273
0.005455 0.222727
0.005455 0.228182
0.005455 0.233636
0.005455 0.239091
0.005455 0.244545
0.005455 0.250000
0.005455 0.255455
0.005455 0.260909
0.005455 0.266364
0.005455 0.271818
0.005455 0.277273
0.005455 0.282727
0.005455 0.288182
0.005455 0.293636
0.005455 0.299091
0.005455 0.304545
0.005455 0.310000
27(0.5)
0.018519 0.328519
0.018519 0.347037
0.018519 0.365556
0.018519 0.384074
0.018519 0.402593
0.018519 0.421111
0.018519 0.439630
0.018519 0.458148
0.018519 0.476667
0.018519 0.495185
0.018519 0.513704
0.018519 0.532222
0.018519 0.550741
0.018519 0.569259
0.018519 0.587778
0.018519 0.606296
0.018519 0.624815
0.018519 0.643333
0.018519 0.661852
0.018519 0.680370
0.018519 0.698889
0.018519 0.717407
0.018519 0.735926
0.018519 0.754444
0.018519 0.772963
0.018519 0.791481
0.018519 0.810000
23(0.5)
0.021739 0.831739
0.021739 0.853478
0.021739 0.875217
0.021739 0.896957

0.021739 0.918696
0.021739 0.940435
0.021739 0.962174
0.021739 0.983913
0.021739 1.005652
0.021739 1.027391
0.021739 1.049130
0.021739 1.070870
0.021739 1.092609
0.021739 1.114348
0.021739 1.136087
0.021739 1.157826
0.021739 1.179565
0.021739 1.201304
0.021739 1.223043
0.021739 1.244783
0.021739 1.266522
0.021739 1.288261
0.021739 1.310000
18(0.5)
0.027778 1.337778
0.027778 1.365556
0.027778 1.393333
0.027778 1.421111
0.027778 1.448889
0.027778 1.476667
0.027778 1.504444
0.027778 1.532222
0.027778 1.560000
0.027778 1.587778
0.027778 1.615556
0.027778 1.643333
0.027778 1.671111
0.027778 1.698889
0.027778 1.726667
0.027778 1.754444
0.027778 1.782222
0.027778 1.810000
33
0.030303 1.840303
0.030303 1.870606
0.030303 1.900909
0.030303 1.931212
0.030303 1.961515
0.030303 1.991818
0.030303 2.022121
0.030303 2.052424
0.030303 2.082727
0.030303 2.113030
0.030303 2.143333
0.030303 2.173636
0.030303 2.203939
0.030303 2.234242
0.030303 2.264545
0.030303 2.294848
0.030303 2.325152
0.030303 2.355455
0.030303 2.385758
0.030303 2.416061
0.030303 2.446364
0.030303 2.476667
0.030303 2.506970
0.030303 2.537273
0.030303 2.567576
0.030303 2.597879
0.030303 2.628182
0.030303 2.658485
0.030303 2.688788
0.030303 2.719091
0.030303 2.749394
0.030303 2.779697
0.030303 2.810000
20
0.050000 2.860000

0.050000 2.910000
0.050000 2.960000
0.050000 3.010000
0.050000 3.060000
0.050000 3.110000
0.050000 3.160000
0.050000 3.210000
0.050000 3.260000
0.050000 3.310000
0.050000 3.360000
0.050000 3.410000
0.050000 3.460000
0.050000 3.510000
0.050000 3.560000
0.050000 3.610000
0.050000 3.660000
0.050000 3.710000
0.050000 3.760000
0.050000 3.810000
11
0.090909 3.900909
0.090909 3.991818
0.090909 4.082727
0.090909 4.173636
0.090909 4.264545
0.090909 4.355455
0.090909 4.446364
0.090909 4.537273
0.090909 4.628182
0.090909 4.719091
0.090909 4.810000
12
0.083333 4.893333
0.083333 4.976667
0.083333 5.060000
0.083333 5.143333
0.083333 5.226667
0.083333 5.310000
0.083333 5.393333
0.083333 5.476667
0.083333 5.560000
0.083333 5.643333
0.083333 5.726667
0.083333 5.810000
12
0.083333 5.893333
0.083333 5.976667
0.083333 6.060000
0.083333 6.143333
0.083333 6.226667
0.083333 6.310000
0.083333 6.393333
0.083333 6.476667
0.083333 6.560000
0.083333 6.643333
0.083333 6.726667
0.083333 6.810000
12
0.083333 6.893333
0.083333 6.976667
0.083333 7.060000
0.083333 7.143333
0.083333 7.226667
0.083333 7.310000
0.083333 7.393333
0.083333 7.476667
0.083333 7.560000
0.083333 7.643333
0.083333 7.726667
0.083333 7.810000
8
0.125000 7.935000
0.125000 8.060000
0.125000 8.185000

0.125000 8.310000
0.125000 8.435000
0.125000 8.560000
0.125000 8.685000
0.125000 8.810000
6
0.166667 8.976667
0.166667 9.143333
0.166667 9.310000
0.166667 9.476667
0.166667 9.643333
0.166667 9.810000
5
0.200000 10.010000
0.200000 10.210000
0.200000 10.410000
0.200000 10.610000
0.200000 10.810000
5
0.200000 11.010000
0.200000 11.210000
0.200000 11.410000
0.200000 11.610000
0.200000 11.810000
6
0.166667 11.976667
0.166667 12.143333
0.166667 12.310000
0.166667 12.476667
0.166667 12.643333
0.166667 12.810000
12
0.083333 12.893333
0.083333 12.976667
0.083333 13.060000
0.083333 13.143333
0.083333 13.226667
0.083333 13.310000
0.083333 13.393333
0.083333 13.476667
0.083333 13.560000
0.083333 13.643333
0.083333 13.726667
0.083333 13.810000
7
0.142857 13.952857
0.142857 14.095714
0.142857 14.238571
0.142857 14.381429
0.142857 14.524286
0.142857 14.667143
0.142857 14.810000
8
0.125000 14.935000
0.125000 15.060000
0.125000 15.185000
0.125000 15.310000
0.125000 15.435000
0.125000 15.560000
0.125000 15.685000
0.125000 15.810000
8
0.125000 15.935000
0.125000 16.060000
0.125000 16.185000
0.125000 16.310000
0.125000 16.435000
0.125000 16.560000
0.125000 16.685000
0.125000 16.810000
7
0.142857 16.952857
0.142857 17.095714
0.142857 17.238571

0.142857 17.381429
0.142857 17.524286
0.142857 17.667143
0.142857 17.810000
6
0.166667 17.976667
0.166667 18.143333
0.166667 18.310000
0.166667 18.476667
0.166667 18.643333
0.166667 18.810000
5
0.200000 19.010000
0.200000 19.210000
0.200000 19.410000
0.200000 19.610000
0.200000 19.810000
6
0.166667 19.976667
0.166667 20.143333
0.166667 20.310000
0.166667 20.476667
0.166667 20.643333
0.166667 20.810000
8
0.125000 20.935000
0.125000 21.060000
0.125000 21.185000
0.125000 21.310000
0.125000 21.435000
0.125000 21.560000
0.125000 21.685000
0.125000 21.810000
5
0.200000 22.010000
0.200000 22.210000
0.200000 22.410000
0.200000 22.610000
0.200000 22.810000
5
0.200000 23.010000
0.200000 23.210000
0.200000 23.410000
0.200000 23.610000
0.200000 23.810000
6
0.166667 23.976667
0.166667 24.143333
0.166667 24.310000
0.166667 24.476667
0.166667 24.643333
0.166667 24.810000
3
0.333333 25.143333
0.333333 25.476667
0.333333 25.810000
5
0.200000 26.010000
0.200000 26.210000
0.200000 26.410000
0.200000 26.610000
0.200000 26.810000
3
0.333333 27.143333
0.333333 27.476667
0.333333 27.810000

N
78(0.2)
0.002564 0.002564
0.002564 0.005128
0.002564 0.007692
0.002564 0.010256
0.002564 0.012821

0.002564 0.015385
0.002564 0.017949
0.002564 0.020513
0.002564 0.023077
0.002564 0.025641
0.002564 0.028205
0.002564 0.030769
0.002564 0.033333
0.002564 0.035897
0.002564 0.038462
0.002564 0.041026
0.002564 0.043590
0.002564 0.046154
0.002564 0.048718
0.002564 0.051282
0.002564 0.053846
0.002564 0.056410
0.002564 0.058974
0.002564 0.061538
0.002564 0.064103
0.002564 0.066667
0.002564 0.069231
0.002564 0.071795
0.002564 0.074359
0.002564 0.076923
0.002564 0.079487
0.002564 0.082051
0.002564 0.084615
0.002564 0.087179
0.002564 0.089744
0.002564 0.092308
0.002564 0.094872
0.002564 0.097436
0.002564 0.100000
0.002564 0.102564
0.002564 0.105128
0.002564 0.107692
0.002564 0.110256
0.002564 0.112821
0.002564 0.115385
0.002564 0.117949
0.002564 0.120513
0.002564 0.123077
0.002564 0.125641
0.002564 0.128205
0.002564 0.130769
0.002564 0.133333
0.002564 0.135897
0.002564 0.138462
0.002564 0.141026
0.002564 0.143590
0.002564 0.146154
0.002564 0.148718
0.002564 0.151282
0.002564 0.153846
0.002564 0.156410
0.002564 0.158974
0.002564 0.161538
0.002564 0.164103
0.002564 0.166667
0.002564 0.169231
0.002564 0.171795
0.002564 0.174359
0.002564 0.176923
0.002564 0.179487
0.002564 0.182051
0.002564 0.184615
0.002564 0.187179
0.002564 0.189744
0.002564 0.192308
0.002564 0.194872
0.002564 0.197436
0.002564 0.200000
57(0.4)

0.007018 0.207018
0.007018 0.214035
0.007018 0.221053
0.007018 0.228070
0.007018 0.235088
0.007018 0.242105
0.007018 0.249123
0.007018 0.256140
0.007018 0.263158
0.007018 0.270175
0.007018 0.277193
0.007018 0.284211
0.007018 0.291228
0.007018 0.298246
0.007018 0.305263
0.007018 0.312281
0.007018 0.319298
0.007018 0.326316
0.007018 0.333333
0.007018 0.340351
0.007018 0.347368
0.007018 0.354386
0.007018 0.361404
0.007018 0.368421
0.007018 0.375439
0.007018 0.382456
0.007018 0.389474
0.007018 0.396491
0.007018 0.403509
0.007018 0.410526
0.007018 0.417544
0.007018 0.424561
0.007018 0.431579
0.007018 0.438596
0.007018 0.445614
0.007018 0.452632
0.007018 0.459649
0.007018 0.466667
0.007018 0.473684
0.007018 0.480702
0.007018 0.487719
0.007018 0.494737
0.007018 0.501754
0.007018 0.508772
0.007018 0.515789
0.007018 0.522807
0.007018 0.529825
0.007018 0.536842
0.007018 0.543860
0.007018 0.550877
0.007018 0.557895
0.007018 0.564912
0.007018 0.571930
0.007018 0.578947
0.007018 0.585965
0.007018 0.592982
0.007018 0.600000
65(0.5)
0.007692 0.607692
0.007692 0.615385
0.007692 0.623077
0.007692 0.630769
0.007692 0.638462
0.007692 0.646154
0.007692 0.653846
0.007692 0.661538
0.007692 0.669231
0.007692 0.676923
0.007692 0.684615
0.007692 0.692308
0.007692 0.700000
0.007692 0.707692
0.007692 0.715385
0.007692 0.723077

0.007692 0.730769
0.007692 0.738462
0.007692 0.746154
0.007692 0.753846
0.007692 0.761538
0.007692 0.769231
0.007692 0.776923
0.007692 0.784615
0.007692 0.792308
0.007692 0.800000
0.007692 0.807692
0.007692 0.815385
0.007692 0.823077
0.007692 0.830769
0.007692 0.838462
0.007692 0.846154
0.007692 0.853846
0.007692 0.861538
0.007692 0.869231
0.007692 0.876923
0.007692 0.884615
0.007692 0.892308
0.007692 0.900000
0.007692 0.907692
0.007692 0.915385
0.007692 0.923077
0.007692 0.930769
0.007692 0.938462
0.007692 0.946154
0.007692 0.953846
0.007692 0.961538
0.007692 0.969231
0.007692 0.976923
0.007692 0.984615
0.007692 0.992308
0.007692 1.000000
0.007692 1.007692
0.007692 1.015385
0.007692 1.023077
0.007692 1.030769
0.007692 1.038462
0.007692 1.046154
0.007692 1.053846
0.007692 1.061538
0.007692 1.069231
0.007692 1.076923
0.007692 1.084615
0.007692 1.092308
0.007692 1.100000
24(0.5)
0.020833 1.120833
0.020833 1.141667
0.020833 1.162500
0.020833 1.183333
0.020833 1.204167
0.020833 1.225000
0.020833 1.245833
0.020833 1.266667
0.020833 1.287500
0.020833 1.308333
0.020833 1.329167
0.020833 1.350000
0.020833 1.370833
0.020833 1.391667
0.020833 1.412500
0.020833 1.433333
0.020833 1.454167
0.020833 1.475000
0.020833 1.495833
0.020833 1.516667
0.020833 1.537500
0.020833 1.558333
0.020833 1.579167
0.020833 1.600000

11(0.5)
0.045455 1.645455
0.045455 1.690909
0.045455 1.736364
0.045455 1.781818
0.045455 1.827273
0.045455 1.872727
0.045455 1.918182
0.045455 1.963636
0.045455 2.009091
0.045455 2.054545
0.045455 2.100000
9(0.5)
0.055556 2.155556
0.055556 2.211111
0.055556 2.266667
0.055556 2.322222
0.055556 2.377778
0.055556 2.433333
0.055556 2.488889
0.055556 2.544444
0.055556 2.600000
17
0.058824 2.658824
0.058824 2.717647
0.058824 2.776471
0.058824 2.835294
0.058824 2.894118
0.058824 2.952941
0.058824 3.011765
0.058824 3.070588
0.058824 3.129412
0.058824 3.188235
0.058824 3.247059
0.058824 3.305882
0.058824 3.364706
0.058824 3.423529
0.058824 3.482353
0.058824 3.541176
0.058824 3.600000
6
0.166667 3.766667
0.166667 3.933333
0.166667 4.100000
0.166667 4.266667
0.166667 4.433333
0.166667 4.600000
5
0.200000 4.800000
0.200000 5.000000
0.200000 5.200000
0.200000 5.400000
0.200000 5.600000
5
0.200000 5.800000
0.200000 6.000000
0.200000 6.200000
0.200000 6.400000
0.200000 6.600000
5
0.200000 6.800000
0.200000 7.000000
0.200000 7.200000
0.200000 7.400000
0.200000 7.600000
3
0.333333 7.933333
0.333333 8.266667
0.333333 8.600000

K118ii
S
36(0.1)

0.002778 0.002778
0.002778 0.005556
0.002778 0.008333
0.002778 0.011111
0.002778 0.013889
0.002778 0.016667
0.002778 0.019444
0.002778 0.022222
0.002778 0.025000
0.002778 0.027778
0.002778 0.030556
0.002778 0.033333
0.002778 0.036111
0.002778 0.038889
0.002778 0.041667
0.002778 0.044444
0.002778 0.047222
0.002778 0.050000
0.002778 0.052778
0.002778 0.055556
0.002778 0.058333
0.002778 0.061111
0.002778 0.063889
0.002778 0.066667
0.002778 0.069444
0.002778 0.072222
0.002778 0.075000
0.002778 0.077778
0.002778 0.080556
0.002778 0.083333
0.002778 0.086111
0.002778 0.088889
0.002778 0.091667
0.002778 0.094444
0.002778 0.097222
0.002778 0.100000
16(0.15)
0.009375 0.109375
0.009375 0.118750
0.009375 0.128125
0.009375 0.137500
0.009375 0.146875
0.009375 0.156250
0.009375 0.165625
0.009375 0.175000
0.009375 0.184375
0.009375 0.193750
0.009375 0.203125
0.009375 0.212500
0.009375 0.221875
0.009375 0.231250
0.009375 0.240625
0.009375 0.250000
8(0.3)
0.037500 0.287500
0.037500 0.325000
0.037500 0.362500
0.037500 0.400000
0.037500 0.437500
0.037500 0.475000
0.037500 0.512500
0.037500 0.550000
9(0.5)
0.055556 0.605556
0.055556 0.661111
0.055556 0.716667
0.055556 0.772222
0.055556 0.827778
0.055556 0.883333
0.055556 0.938889
0.055556 0.994444
0.055556 1.050000
3(0.5)
0.166667 1.216667

0.166667 1.383333
0.166667 1.550000
4
0.250000 1.800000
0.250000 2.050000
0.250000 2.300000
0.250000 2.550000
4
0.250000 2.800000
0.250000 3.050000
0.250000 3.300000
0.250000 3.550000
3
0.333333 3.883333
0.333333 4.216667
0.333333 4.550000
3
0.333333 4.883333
0.333333 5.216667
0.333333 5.550000
4
0.250000 5.800000
0.250000 6.050000
0.250000 6.300000
0.250000 6.550000
3
0.333333 6.883333
0.333333 7.216667
0.333333 7.550000

N
28(0.07)
0.002500 0.002500
0.002500 0.005000
0.002500 0.007500
0.002500 0.010000
0.002500 0.012500
0.002500 0.015000
0.002500 0.017500
0.002500 0.020000
0.002500 0.022500
0.002500 0.025000
0.002500 0.027500
0.002500 0.030000
0.002500 0.032500
0.002500 0.035000
0.002500 0.037500
0.002500 0.040000
0.002500 0.042500
0.002500 0.045000
0.002500 0.047500
0.002500 0.050000
0.002500 0.052500
0.002500 0.055000
0.002500 0.057500
0.002500 0.060000
0.002500 0.062500
0.002500 0.065000
0.002500 0.067500
0.002500 0.070000
18(0.13)
0.007222 0.077222
0.007222 0.084444
0.007222 0.091667
0.007222 0.098889
0.007222 0.106111
0.007222 0.113333
0.007222 0.120556
0.007222 0.127778
0.007222 0.135000
0.007222 0.142222
0.007222 0.149444
0.007222 0.156667
0.007222 0.163889

0.007222 0.171111
0.007222 0.178333
0.007222 0.185556
0.007222 0.192778
0.007222 0.200000
28(0.3)
0.010714 0.210714
0.010714 0.221429
0.010714 0.232143
0.010714 0.242857
0.010714 0.253571
0.010714 0.264286
0.010714 0.275000
0.010714 0.285714
0.010714 0.296429
0.010714 0.307143
0.010714 0.317857
0.010714 0.328571
0.010714 0.339286
0.010714 0.350000
0.010714 0.360714
0.010714 0.371429
0.010714 0.382143
0.010714 0.392857
0.010714 0.403571
0.010714 0.414286
0.010714 0.425000
0.010714 0.435714
0.010714 0.446429
0.010714 0.457143
0.010714 0.467857
0.010714 0.478571
0.010714 0.489286
0.010714 0.500000
53(0.5)
0.009434 0.509434
0.009434 0.518868
0.009434 0.528302
0.009434 0.537736
0.009434 0.547170
0.009434 0.556604
0.009434 0.566038
0.009434 0.575472
0.009434 0.584906
0.009434 0.594340
0.009434 0.603774
0.009434 0.613208
0.009434 0.622642
0.009434 0.632075
0.009434 0.641509
0.009434 0.650943
0.009434 0.660377
0.009434 0.669811
0.009434 0.679245
0.009434 0.688679
0.009434 0.698113
0.009434 0.707547
0.009434 0.716981
0.009434 0.726415
0.009434 0.735849
0.009434 0.745283
0.009434 0.754717
0.009434 0.764151
0.009434 0.773585
0.009434 0.783019
0.009434 0.792453
0.009434 0.801887
0.009434 0.811321
0.009434 0.820755
0.009434 0.830189
0.009434 0.839623
0.009434 0.849057
0.009434 0.858491
0.009434 0.867925

0.009434 0.877358
0.009434 0.886792
0.009434 0.896226
0.009434 0.905660
0.009434 0.915094
0.009434 0.924528
0.009434 0.933962
0.009434 0.943396
0.009434 0.952830
0.009434 0.962264
0.009434 0.971698
0.009434 0.981132
0.009434 0.990566
0.009434 1.000000
34(0.5)
0.014706 1.014706
0.014706 1.029412
0.014706 1.044118
0.014706 1.058824
0.014706 1.073529
0.014706 1.088235
0.014706 1.102941
0.014706 1.117647
0.014706 1.132353
0.014706 1.147059
0.014706 1.161765
0.014706 1.176471
0.014706 1.191176
0.014706 1.205882
0.014706 1.220588
0.014706 1.235294
0.014706 1.250000
0.014706 1.264706
0.014706 1.279412
0.014706 1.294118
0.014706 1.308824
0.014706 1.323529
0.014706 1.338235
0.014706 1.352941
0.014706 1.367647
0.014706 1.382353
0.014706 1.397059
0.014706 1.411765
0.014706 1.426471
0.014706 1.441176
0.014706 1.455882
0.014706 1.470588
0.014706 1.485294
0.014706 1.500000
19(0.5)
0.026316 1.526316
0.026316 1.552632
0.026316 1.578947
0.026316 1.605263
0.026316 1.631579
0.026316 1.657895
0.026316 1.684211
0.026316 1.710526
0.026316 1.736842
0.026316 1.763158
0.026316 1.789474
0.026316 1.815789
0.026316 1.842105
0.026316 1.868421
0.026316 1.894737
0.026316 1.921053
0.026316 1.947368
0.026316 1.973684
0.026316 2.000000
16(0.5)
0.031250 2.031250
0.031250 2.062500
0.031250 2.093750
0.031250 2.125000

0.031250 2.156250
0.031250 2.187500
0.031250 2.218750
0.031250 2.250000
0.031250 2.281250
0.031250 2.312500
0.031250 2.343750
0.031250 2.375000
0.031250 2.406250
0.031250 2.437500
0.031250 2.468750
0.031250 2.500000
21
0.047619 2.547619
0.047619 2.595238
0.047619 2.642857
0.047619 2.690476
0.047619 2.738095
0.047619 2.785714
0.047619 2.833333
0.047619 2.880952
0.047619 2.928571
0.047619 2.976190
0.047619 3.023810
0.047619 3.071429
0.047619 3.119048
0.047619 3.166667
0.047619 3.214286
0.047619 3.261905
0.047619 3.309524
0.047619 3.357143
0.047619 3.404762
0.047619 3.452381
0.047619 3.500000
12
0.083333 3.583333
0.083333 3.666667
0.083333 3.750000
0.083333 3.833333
0.083333 3.916667
0.083333 4.000000
0.083333 4.083333
0.083333 4.166667
0.083333 4.250000
0.083333 4.333333
0.083333 4.416667
0.083333 4.500000
9
0.111111 4.611111
0.111111 4.722222
0.111111 4.833333
0.111111 4.944444
0.111111 5.055556
0.111111 5.166667
0.111111 5.277778
0.111111 5.388889
0.111111 5.500000
8
0.125000 5.625000
0.125000 5.750000
0.125000 5.875000
0.125000 6.000000
0.125000 6.125000
0.125000 6.250000
0.125000 6.375000
0.125000 6.500000
10
0.100000 6.600000
0.100000 6.700000
0.100000 6.800000
0.100000 6.900000
0.100000 7.000000
0.100000 7.100000
0.100000 7.200000

0.100000 7.300000
0.100000 7.400000
0.100000 7.500000
8
0.125000 7.625000
0.125000 7.750000
0.125000 7.875000
0.125000 8.000000
0.125000 8.125000
0.125000 8.250000
0.125000 8.375000
0.125000 8.500000
7
0.142857 8.642857
0.142857 8.785714
0.142857 8.928571
0.142857 9.071429
0.142857 9.214286
0.142857 9.357143
0.142857 9.500000
7
0.142857 9.642857
0.142857 9.785714
0.142857 9.928571
0.142857 10.071429
0.142857 10.214286
0.142857 10.357143
0.142857 10.500000

K119
S
37(0.25)
0.006757 0.006757
0.006757 0.013514
0.006757 0.020270
0.006757 0.027027
0.006757 0.033784
0.006757 0.040541
0.006757 0.047297
0.006757 0.054054
0.006757 0.060811
0.006757 0.067568
0.006757 0.074324
0.006757 0.081081
0.006757 0.087838
0.006757 0.094595
0.006757 0.101351
0.006757 0.108108
0.006757 0.114865
0.006757 0.121622
0.006757 0.128378
0.006757 0.135135
0.006757 0.141892
0.006757 0.148649
0.006757 0.155405
0.006757 0.162162
0.006757 0.168919
0.006757 0.175676
0.006757 0.182432
0.006757 0.189189
0.006757 0.195946
0.006757 0.202703
0.006757 0.209459
0.006757 0.216216
0.006757 0.222973
0.006757 0.229730
0.006757 0.236486
0.006757 0.243243
0.006757 0.250000
44(0.25)
0.005682 0.255682
0.005682 0.261364
0.005682 0.267045

0.005682 0.272727
0.005682 0.278409
0.005682 0.284091
0.005682 0.289773
0.005682 0.295455
0.005682 0.301136
0.005682 0.306818
0.005682 0.312500
0.005682 0.318182
0.005682 0.323864
0.005682 0.329545
0.005682 0.335227
0.005682 0.340909
0.005682 0.346591
0.005682 0.352273
0.005682 0.357955
0.005682 0.363636
0.005682 0.369318
0.005682 0.375000
0.005682 0.380682
0.005682 0.386364
0.005682 0.392045
0.005682 0.397727
0.005682 0.403409
0.005682 0.409091
0.005682 0.414773
0.005682 0.420455
0.005682 0.426136
0.005682 0.431818
0.005682 0.437500
0.005682 0.443182
0.005682 0.448864
0.005682 0.454545
0.005682 0.460227
0.005682 0.465909
0.005682 0.471591
0.005682 0.477273
0.005682 0.482955
0.005682 0.488636
0.005682 0.494318
0.005682 0.500000
31(0.25)
0.008065 0.508065
0.008065 0.516129
0.008065 0.524194
0.008065 0.532258
0.008065 0.540323
0.008065 0.548387
0.008065 0.556452
0.008065 0.564516
0.008065 0.572581
0.008065 0.580645
0.008065 0.588710
0.008065 0.596774
0.008065 0.604839
0.008065 0.612903
0.008065 0.620968
0.008065 0.629032
0.008065 0.637097
0.008065 0.645161
0.008065 0.653226
0.008065 0.661290
0.008065 0.669355
0.008065 0.677419
0.008065 0.685484
0.008065 0.693548
0.008065 0.701613
0.008065 0.709677
0.008065 0.717742
0.008065 0.725806
0.008065 0.733871
0.008065 0.741935
16(0.25)
0.015625 0.757560

0.015625 0.773185
0.015625 0.788810
0.015625 0.804435
0.015625 0.820060
0.015625 0.835685
0.015625 0.851310
0.015625 0.866935
0.015625 0.882560
0.015625 0.898185
0.015625 0.913810
0.015625 0.929435
0.015625 0.945060
0.015625 0.960685
0.015625 0.976310
0.015625 0.991935
10(0.25)
0.025000 1.016935
0.025000 1.041935
0.025000 1.066935
0.025000 1.091935
0.025000 1.116935
0.025000 1.141935
0.025000 1.166935
0.025000 1.191935
0.025000 1.216935
0.025000 1.241935
13(0.5)
0.038462 1.280397
0.038462 1.318859
0.038462 1.357320
0.038462 1.395782
0.038462 1.434243
0.038462 1.472705
0.038462 1.511166
0.038462 1.549628
0.038462 1.588089
0.038462 1.626551
0.038462 1.665012
0.038462 1.703474
0.038462 1.741935
8(0.5)
0.062500 1.804435
0.062500 1.866935
0.062500 1.929435
0.062500 1.991935
0.062500 2.054435
0.062500 2.116935
0.062500 2.179435
0.062500 2.241935
6
0.166667 2.408602
0.166667 2.575269
0.166667 2.741935
0.166667 2.908602
0.166667 3.075269
0.166667 3.241935
6
0.166667 3.408602
0.166667 3.575269
0.166667 3.741935
0.166667 3.908602
0.166667 4.075269
0.166667 4.241935
4
0.250000 4.491935
0.250000 4.741935
0.250000 4.991935
0.250000 5.241935
NO(3)
3.000000 8.241935
8
0.125000 8.366935
0.125000 8.491935
0.125000 8.616935

0.125000 8.741935
0.125000 8.866935
0.125000 8.991935
0.125000 9.116935
0.125000 9.241935
7
0.142857 9.384793
0.142857 9.527650
0.142857 9.670507
0.142857 9.813364
0.142857 9.956221
0.142857 10.099078
0.142857 10.241935

N
56(0.25)
0.004464 0.004464
0.004464 0.008929
0.004464 0.013393
0.004464 0.017857
0.004464 0.022321
0.004464 0.026786
0.004464 0.031250
0.004464 0.035714
0.004464 0.040179
0.004464 0.044643
0.004464 0.049107
0.004464 0.053571
0.004464 0.058036
0.004464 0.062500
0.004464 0.066964
0.004464 0.071429
0.004464 0.075893
0.004464 0.080357
0.004464 0.084821
0.004464 0.089286
0.004464 0.093750
0.004464 0.098214
0.004464 0.102679
0.004464 0.107143
0.004464 0.111607
0.004464 0.116071
0.004464 0.120536
0.004464 0.125000
0.004464 0.129464
0.004464 0.133929
0.004464 0.138393
0.004464 0.142857
0.004464 0.147321
0.004464 0.151786
0.004464 0.156250
0.004464 0.160714
0.004464 0.165179
0.004464 0.169643
0.004464 0.174107
0.004464 0.178571
0.004464 0.183036
0.004464 0.187500
0.004464 0.191964
0.004464 0.196429
0.004464 0.200893
0.004464 0.205357
0.004464 0.209821
0.004464 0.214286
0.004464 0.218750
0.004464 0.223214
0.004464 0.227679
0.004464 0.232143
0.004464 0.236607
0.004464 0.241071
0.004464 0.245536
0.004464 0.250000
32(0.25)
0.007813 0.257813

0.007813 0.265625
0.007813 0.273438
0.007813 0.281250
0.007813 0.289063
0.007813 0.296875
0.007813 0.304688
0.007813 0.312500
0.007813 0.320313
0.007813 0.328125
0.007813 0.335938
0.007813 0.343750
0.007813 0.351563
0.007813 0.359375
0.007813 0.367188
0.007813 0.375000
0.007813 0.382813
0.007813 0.390625
0.007813 0.398438
0.007813 0.406250
0.007813 0.414063
0.007813 0.421875
0.007813 0.429688
0.007813 0.437500
0.007813 0.445313
0.007813 0.453125
0.007813 0.460938
0.007813 0.468750
0.007813 0.476563
0.007813 0.484375
0.007813 0.492188
0.007813 0.500000
23(0.25)
0.010870 0.510870
0.010870 0.521739
0.010870 0.532609
0.010870 0.543478
0.010870 0.554348
0.010870 0.565217
0.010870 0.576087
0.010870 0.586957
0.010870 0.597826
0.010870 0.608696
0.010870 0.619565
0.010870 0.630435
0.010870 0.641304
0.010870 0.652174
0.010870 0.663043
0.010870 0.673913
0.010870 0.684783
0.010870 0.695652
0.010870 0.706522
0.010870 0.717391
0.010870 0.728261
0.010870 0.739130
0.010870 0.750000
10(0.25)
0.025000 0.775000
0.025000 0.800000
0.025000 0.825000
0.025000 0.850000
0.025000 0.875000
0.025000 0.900000
0.025000 0.925000
0.025000 0.950000
0.025000 0.975000
0.025000 1.000000
9(0.25)
0.027778 1.027778
0.027778 1.055556
0.027778 1.083333
0.027778 1.111111
0.027778 1.138889
0.027778 1.166667
0.027778 1.194444

0.027778 1.222222
0.027778 1.250000
8(0.5)
0.062500 1.312500
0.062500 1.375000
0.062500 1.437500
0.062500 1.500000
0.062500 1.562500
0.062500 1.625000
0.062500 1.687500
0.062500 1.750000
13(0.5)
0.038462 1.788462
0.038462 1.826923
0.038462 1.865385
0.038462 1.903846
0.038462 1.942308
0.038462 1.980769
0.038462 2.019231
0.038462 2.057692
0.038462 2.096154
0.038462 2.134615
0.038462 2.173077
0.038462 2.211538
0.038462 2.250000
11(0.5)
0.045455 2.295455
0.045455 2.340909
0.045455 2.386364
0.045455 2.431818
0.045455 2.477273
0.045455 2.522727
0.045455 2.568182
0.045455 2.613636
0.045455 2.659091
0.045455 2.704545
0.045455 2.750000
9
0.111111 2.861111
0.111111 2.972222
0.111111 3.083333
0.111111 3.194444
0.111111 3.305556
0.111111 3.416667
0.111111 3.527778
0.111111 3.638889
0.111111 3.750000
4
0.250000 4.000000
0.250000 4.250000
0.250000 4.500000
0.250000 4.750000
4
0.250000 5.000000
0.250000 5.250000
0.250000 5.500000
0.250000 5.750000
2
0.500000 6.250000
0.500000 6.750000
4
0.250000 7.000000
0.250000 7.250000
0.250000 7.500000
0.250000 7.750000
5
0.200000 7.950000
0.200000 8.150000
0.200000 8.350000
0.200000 8.550000
0.200000 8.750000
4
0.250000 9.000000
0.250000 9.250000

0.250000 9.500000
0.250000 9.750000
2
0.500000 10.250000
0.500000 10.750000
3
0.333333 11.083333
0.333333 11.416667
0.333333 11.750000
4
0.250000 12.000000
0.250000 12.250000
0.250000 12.500000
0.250000 12.750000
3
0.333333 13.083333
0.333333 13.416667
0.333333 13.750000
4
0.250000 14.000000
0.250000 14.250000
0.250000 14.500000
0.250000 14.750000
4
0.250000 15.000000
0.250000 15.250000
0.250000 15.500000
0.250000 15.750000
4
0.250000 16.000000
0.250000 16.250000
0.250000 16.500000
0.250000 16.750000

K126
S
85(0.3)
0.003529 0.003529
0.003529 0.007059
0.003529 0.010588
0.003529 0.014118
0.003529 0.017647
0.003529 0.021176
0.003529 0.024706
0.003529 0.028235
0.003529 0.031765
0.003529 0.035294
0.003529 0.038824
0.003529 0.042353
0.003529 0.045882
0.003529 0.049412
0.003529 0.052941
0.003529 0.056471
0.003529 0.060000
0.003529 0.063529
0.003529 0.067059
0.003529 0.070588
0.003529 0.074118
0.003529 0.077647
0.003529 0.081176
0.003529 0.084706
0.003529 0.088235
0.003529 0.091765
0.003529 0.095294
0.003529 0.098824
0.003529 0.102353
0.003529 0.105882
0.003529 0.109412
0.003529 0.112941
0.003529 0.116471
0.003529 0.120000
0.003529 0.123529
0.003529 0.127059

0.003529 0.130588
0.003529 0.134118
0.003529 0.137647
0.003529 0.141176
0.003529 0.144706
0.003529 0.148235
0.003529 0.151765
0.003529 0.155294
0.003529 0.158824
0.003529 0.162353
0.003529 0.165882
0.003529 0.169412
0.003529 0.172941
0.003529 0.176471
0.003529 0.180000
0.003529 0.183529
0.003529 0.187059
0.003529 0.190588
0.003529 0.194118
0.003529 0.197647
0.003529 0.201176
0.003529 0.204706
0.003529 0.208235
0.003529 0.211765
0.003529 0.215294
0.003529 0.218824
0.003529 0.222353
0.003529 0.225882
0.003529 0.229412
0.003529 0.232941
0.003529 0.236471
0.003529 0.240000
0.003529 0.243529
0.003529 0.247059
0.003529 0.250588
0.003529 0.254118
0.003529 0.257647
0.003529 0.261176
0.003529 0.264706
0.003529 0.268235
0.003529 0.271765
0.003529 0.275294
0.003529 0.278824
0.003529 0.282353
0.003529 0.285882
0.003529 0.289412
0.003529 0.292941
0.003529 0.296471
0.003529 0.300000
45(0.25)
0.005556 0.305556
0.005556 0.311111
0.005556 0.316667
0.005556 0.322222
0.005556 0.327778
0.005556 0.333333
0.005556 0.338889
0.005556 0.344444
0.005556 0.350000
0.005556 0.355556
0.005556 0.361111
0.005556 0.366667
0.005556 0.372222
0.005556 0.377778
0.005556 0.383333
0.005556 0.388889
0.005556 0.394444
0.005556 0.400000
0.005556 0.405556
0.005556 0.411111
0.005556 0.416667
0.005556 0.422222
0.005556 0.427778
0.005556 0.433333

0.005556 0.438889
0.005556 0.444444
0.005556 0.450000
0.005556 0.455556
0.005556 0.461111
0.005556 0.466667
0.005556 0.472222
0.005556 0.477778
0.005556 0.483333
0.005556 0.488889
0.005556 0.494444
0.005556 0.500000
0.005556 0.505556
0.005556 0.511111
0.005556 0.516667
0.005556 0.522222
0.005556 0.527778
0.005556 0.533333
0.005556 0.538889
0.005556 0.544444
0.005556 0.550000
19(0.22)
0.011579 0.561579
0.011579 0.573158
0.011579 0.584737
0.011579 0.596316
0.011579 0.607895
0.011579 0.619474
0.011579 0.631053
0.011579 0.642632
0.011579 0.654211
0.011579 0.665789
0.011579 0.677368
0.011579 0.688947
0.011579 0.700526
0.011579 0.712105
0.011579 0.723684
0.011579 0.735263
0.011579 0.746842
0.011579 0.758421
0.011579 0.770000
2(0.28)
0.140000 0.910000
0.140000 1.050000
5
0.200000 1.250000
0.200000 1.450000
0.200000 1.650000
0.200000 1.850000
0.200000 2.050000
3
0.333333 2.383333
0.333333 2.716667
0.333333 3.050000
5
0.200000 3.250000
0.200000 3.450000
0.200000 3.650000
0.200000 3.850000
0.200000 4.050000
2
0.500000 4.550000
0.500000 5.050000
3
0.333333 5.383333
0.333333 5.716667
0.333333 6.050000
3
0.333333 6.383333
0.333333 6.716667
0.333333 7.050000
1
1.000000 8.050000
2

0.500000 8.550000
0.500000 9.050000
3
0.333333 9.383333
0.333333 9.716667
0.333333 10.050000
3
0.333333 10.383333
0.333333 10.716667
0.333333 11.050000
1
1.000000 12.050000
2
0.500000 12.550000
0.500000 13.050000
3
0.333333 13.383333
0.333333 13.716667
0.333333 14.050000
4
0.250000 14.300000
0.250000 14.550000
0.250000 14.800000
0.250000 15.050000
2
0.500000 15.550000
0.500000 16.050000
3
0.333333 16.383333
0.333333 16.716667
0.333333 17.050000
5
0.200000 17.250000
0.200000 17.450000
0.200000 17.650000
0.200000 17.850000
0.200000 18.050000
2
0.500000 18.550000
0.500000 19.050000
1
1.000000 20.050000
1
1.000000 21.050000
2
0.500000 21.550000
0.500000 22.050000
2
0.500000 22.550000
0.500000 23.050000
2
0.500000 23.550000
0.500000 24.050000
3
0.333333 24.383333
0.333333 24.716667
0.333333 25.050000

N
98(0.3)
0.003061 0.003061
0.003061 0.006122
0.003061 0.009184
0.003061 0.012245
0.003061 0.015306
0.003061 0.018367
0.003061 0.021429
0.003061 0.024490
0.003061 0.027551
0.003061 0.030612
0.003061 0.033673
0.003061 0.036735
0.003061 0.039796
0.003061 0.042857

0.003061 0.045918
0.003061 0.048980
0.003061 0.052041
0.003061 0.055102
0.003061 0.058163
0.003061 0.061224
0.003061 0.064286
0.003061 0.067347
0.003061 0.070408
0.003061 0.073469
0.003061 0.076531
0.003061 0.079592
0.003061 0.082653
0.003061 0.085714
0.003061 0.088776
0.003061 0.091837
0.003061 0.094898
0.003061 0.097959
0.003061 0.101020
0.003061 0.104082
0.003061 0.107143
0.003061 0.110204
0.003061 0.113265
0.003061 0.116327
0.003061 0.119388
0.003061 0.122449
0.003061 0.125510
0.003061 0.128571
0.003061 0.131633
0.003061 0.134694
0.003061 0.137755
0.003061 0.140816
0.003061 0.143878
0.003061 0.146939
0.003061 0.150000
0.003061 0.153061
0.003061 0.156122
0.003061 0.159184
0.003061 0.162245
0.003061 0.165306
0.003061 0.168367
0.003061 0.171429
0.003061 0.174490
0.003061 0.177551
0.003061 0.180612
0.003061 0.183673
0.003061 0.186735
0.003061 0.189796
0.003061 0.192857
0.003061 0.195918
0.003061 0.198980
0.003061 0.202041
0.003061 0.205102
0.003061 0.208163
0.003061 0.211224
0.003061 0.214286
0.003061 0.217347
0.003061 0.220408
0.003061 0.223469
0.003061 0.226531
0.003061 0.229592
0.003061 0.232653
0.003061 0.235714
0.003061 0.238776
0.003061 0.241837
0.003061 0.244898
0.003061 0.247959
0.003061 0.251020
0.003061 0.254082
0.003061 0.257143
0.003061 0.260204
0.003061 0.263265
0.003061 0.266327
0.003061 0.269388

0.003061 0.272449
0.003061 0.275510
0.003061 0.278571
0.003061 0.281633
0.003061 0.284694
0.003061 0.287755
0.003061 0.290816
0.003061 0.293878
0.003061 0.296939
0.003061 0.300000
37(0.2)
0.005405 0.305405
0.005405 0.310811
0.005405 0.316216
0.005405 0.321622
0.005405 0.327027
0.005405 0.332432
0.005405 0.337838
0.005405 0.343243
0.005405 0.348649
0.005405 0.354054
0.005405 0.359459
0.005405 0.364865
0.005405 0.370270
0.005405 0.375676
0.005405 0.381081
0.005405 0.386486
0.005405 0.391892
0.005405 0.397297
0.005405 0.402703
0.005405 0.408108
0.005405 0.413514
0.005405 0.418919
0.005405 0.424324
0.005405 0.429730
0.005405 0.435135
0.005405 0.440541
0.005405 0.445946
0.005405 0.451351
0.005405 0.456757
0.005405 0.462162
0.005405 0.467568
0.005405 0.472973
0.005405 0.478378
0.005405 0.483784
0.005405 0.489189
0.005405 0.494595
0.005405 0.500000
23(0.25)
0.010870 0.510870
0.010870 0.521739
0.010870 0.532609
0.010870 0.543478
0.010870 0.554348
0.010870 0.565217
0.010870 0.576087
0.010870 0.586957
0.010870 0.597826
0.010870 0.608696
0.010870 0.619565
0.010870 0.630435
0.010870 0.641304
0.010870 0.652174
0.010870 0.663043
0.010870 0.673913
0.010870 0.684783
0.010870 0.695652
0.010870 0.706522
0.010870 0.717391
0.010870 0.728261
0.010870 0.739130
0.010870 0.750000
2(0.25)
0.125000 0.875000
0.125000 1.000000
4(0.5)
0.125000 1.125000
0.125000 1.250000
0.125000 1.375000
0.125000 1.500000
3(0.5)
0.166667 1.666667
0.166667 1.833333
0.166667 2.000000
4
0.250000 2.250000
0.250000 2.500000
0.250000 2.750000
0.250000 3.000000
4
0.250000 3.250000
0.250000 3.500000
0.250000 3.750000
0.250000 4.000000
4
0.250000 4.250000
0.250000 4.500000
0.250000 4.750000
0.250000 5.000000
2
0.500000 5.500000
0.500000 6.000000
4
0.250000 6.250000
0.250000 6.500000
0.250000 6.750000
0.250000 7.000000
3
0.333333 7.333333
0.333333 7.666667
0.333333 8.000000
3
0.333333 8.333333
0.333333 8.666667
0.333333 9.000000
2
0.500000 9.500000
0.500000 10.000000
4
0.250000 10.250000
0.250000 10.500000
0.250000 10.750000
0.250000 11.000000
5
0.200000 11.200000
0.200000 11.400000
0.200000 11.600000
0.200000 11.800000
0.200000 12.000000
2
0.500000 12.500000
0.500000 13.000000
3
0.333333 13.333333
0.333333 13.666667
0.333333 14.000000
4
0.250000 14.250000
0.250000 14.500000
0.250000 14.750000
0.250000 15.000000
3
0.333333 15.333333
0.333333 15.666667
0.333333 16.000000
3
0.333333 16.333333
0.333333 16.666667
0.333333 17.000000

K132i
S
NO(0.4)
59(0.25)
0.004237 0.004237
0.004237 0.008475
0.004237 0.012712
0.004237 0.016949
0.004237 0.021186
0.004237 0.025424
0.004237 0.029661
0.004237 0.033898
0.004237 0.038136
0.004237 0.042373
0.004237 0.046610
0.004237 0.050847
0.004237 0.055085
0.004237 0.059322
0.004237 0.063559
0.004237 0.067797
0.004237 0.072034
0.004237 0.076271
0.004237 0.080508
0.004237 0.084746
0.004237 0.088983
0.004237 0.093220
0.004237 0.097458
0.004237 0.101695
0.004237 0.105932
0.004237 0.110169
0.004237 0.114407
0.004237 0.118644
0.004237 0.122881
0.004237 0.127119
0.004237 0.131356
0.004237 0.135593
0.004237 0.139831
0.004237 0.144068
0.004237 0.148305
0.004237 0.152542
0.004237 0.156780
0.004237 0.161017
0.004237 0.165254
0.004237 0.169492
0.004237 0.173729
0.004237 0.177966
0.004237 0.182203
0.004237 0.186441
0.004237 0.190678
0.004237 0.194915
0.004237 0.199153
0.004237 0.203390
0.004237 0.207627
0.004237 0.211864
0.004237 0.216102
0.004237 0.220339
0.004237 0.224576
0.004237 0.228814
0.004237 0.233051
0.004237 0.237288
0.004237 0.241525
0.004237 0.245763
0.004237 0.250000
57(0.25)
0.004386 0.254386
0.004386 0.258772
0.004386 0.263158
0.004386 0.267544
0.004386 0.271930
0.004386 0.276316
0.004386 0.280702
0.004386 0.285088
0.004386 0.289474
0.004386 0.293860
0.004386 0.298246
0.004386 0.302632
0.004386 0.307018
0.004386 0.311404
0.004386 0.315789
0.004386 0.320175
0.004386 0.324561
0.004386 0.328947
0.004386 0.333333
0.004386 0.337719
0.004386 0.342105
0.004386 0.346491
0.004386 0.350877
0.004386 0.355263
0.004386 0.359649
0.004386 0.364035
0.004386 0.368421
0.004386 0.372807
0.004386 0.377193
0.004386 0.381579
0.004386 0.385965
0.004386 0.390351
0.004386 0.394737
0.004386 0.399123
0.004386 0.403509
0.004386 0.407895
0.004386 0.412281
0.004386 0.416667
0.004386 0.421053
0.004386 0.425439
0.004386 0.429825
0.004386 0.434211
0.004386 0.438596
0.004386 0.442982
0.004386 0.447368
0.004386 0.451754
0.004386 0.456140
0.004386 0.460526
0.004386 0.464912
0.004386 0.469298
0.004386 0.473684
0.004386 0.478070
0.004386 0.482456
0.004386 0.486842
0.004386 0.491228
0.004386 0.495614
0.004386 0.500000
45(0.25)
0.005556 0.505556
0.005556 0.511111
0.005556 0.516667
0.005556 0.522222
0.005556 0.527778
0.005556 0.533333
0.005556 0.538889
0.005556 0.544444
0.005556 0.550000
0.005556 0.555556
0.005556 0.561111
0.005556 0.566667
0.005556 0.572222
0.005556 0.577778
0.005556 0.583333
0.005556 0.588889
0.005556 0.594444
0.005556 0.600000
0.005556 0.605556
0.005556 0.611111
0.005556 0.616667
0.005556 0.622222
0.005556 0.627778
0.005556 0.633333
0.005556 0.638889
0.005556 0.644444
0.005556 0.650000
0.005556 0.655556
0.005556 0.661111
0.005556 0.666667
0.005556 0.672222
0.005556 0.677778
0.005556 0.683333
0.005556 0.688889
0.005556 0.694444
0.005556 0.700000
0.005556 0.705556
0.005556 0.711111
0.005556 0.716667
0.005556 0.722222
0.005556 0.727778
0.005556 0.733333
0.005556 0.738889
0.005556 0.744444
0.005556 0.750000
36(0.5)
0.013889 0.763889
0.013889 0.777778
0.013889 0.791667
0.013889 0.805556
0.013889 0.819444
0.013889 0.833333
0.013889 0.847222
0.013889 0.861111
0.013889 0.875000
0.013889 0.888889
0.013889 0.902778
0.013889 0.916667
0.013889 0.930556
0.013889 0.944444
0.013889 0.958333
0.013889 0.972222
0.013889 0.986111
0.013889 1.000000
0.013889 1.013889
0.013889 1.027778
0.013889 1.041667
0.013889 1.055556
0.013889 1.069444
0.013889 1.083333
0.013889 1.097222
0.013889 1.111111
0.013889 1.125000
0.013889 1.138889
0.013889 1.152778
0.013889 1.166667
0.013889 1.180556
0.013889 1.194444
0.013889 1.208333
0.013889 1.222222
0.013889 1.236111
0.013889 1.250000
10(0.5)
0.050000 1.300000
0.050000 1.350000
0.050000 1.400000
0.050000 1.450000
0.050000 1.500000
0.050000 1.550000
0.050000 1.600000
0.050000 1.650000
0.050000 1.700000
0.050000 1.750000
6(0.5)
0.083333 1.833333
0.083333 1.916667
0.083333 2.000000
0.083333 2.083333
0.083333 2.166667
0.083333 2.250000
9
0.111111 2.361111
0.111111 2.472222
0.111111 2.583333
0.111111 2.694444
0.111111 2.805556
0.111111 2.916667
0.111111 3.027778
0.111111 3.138889
0.111111 3.250000
4
0.250000 3.500000
0.250000 3.750000
0.250000 4.000000
0.250000 4.250000
8
0.125000 4.375000
0.125000 4.500000
0.125000 4.625000
0.125000 4.750000
0.125000 4.875000
0.125000 5.000000
0.125000 5.125000
0.125000 5.250000
4
0.250000 5.500000
0.250000 5.750000
0.250000 6.000000
0.250000 6.250000
10
0.100000 6.350000
0.100000 6.450000
0.100000 6.550000
0.100000 6.650000
0.100000 6.750000
0.100000 6.850000
0.100000 6.950000
0.100000 7.050000
0.100000 7.150000
0.100000 7.250000
2
0.500000 7.750000
0.500000 8.250000
7
0.142857 8.392857
0.142857 8.535714
0.142857 8.678571
0.142857 8.821429
0.142857 8.964286
0.142857 9.107143
0.142857 9.250000
3
0.333333 9.583333
0.333333 9.916667
0.333333 10.250000
6
0.166667 10.416667
0.166667 10.583333
0.166667 10.750000
0.166667 10.916667
0.166667 11.083333
0.166667 11.250000
8
0.125000 11.375000
0.125000 11.500000
0.125000 11.625000
0.125000 11.750000
0.125000 11.875000
0.125000 12.000000
0.125000 12.125000
0.125000 12.250000
5
0.200000 12.450000
0.200000 12.650000
0.200000 12.850000
0.200000 13.050000
0.200000 13.250000
3
0.333333 13.583333
0.333333 13.916667
0.333333 14.250000
3
0.333333 14.583333
0.333333 14.916667
0.333333 15.250000
5
0.200000 15.450000
0.200000 15.650000
0.200000 15.850000
0.200000 16.050000
0.200000 16.250000
5
0.200000 16.450000
0.200000 16.650000
0.200000 16.850000
0.200000 17.050000
0.200000 17.250000
4
0.250000 17.500000
0.250000 17.750000
0.250000 18.000000
0.250000 18.250000
2
0.500000 18.750000
0.500000 19.250000
5
0.200000 19.450000
0.200000 19.650000
0.200000 19.850000
0.200000 20.050000
0.200000 20.250000
3
0.333333 20.583333
0.333333 20.916667
0.333333 21.250000
3
0.333333 21.583333
0.333333 21.916667
0.333333 22.250000
4
0.250000 22.500000
0.250000 22.750000
0.250000 23.000000
0.250000 23.250000
6
0.166667 23.416667
0.166667 23.583333
0.166667 23.750000
0.166667 23.916667
0.166667 24.083333
0.166667 24.250000
5
0.200000 24.450000
0.200000 24.650000
0.200000 24.850000
0.200000 25.050000
0.200000 25.250000
5
0.200000 25.450000
0.200000 25.650000
0.200000 25.850000
0.200000 26.050000
0.200000 26.250000
5
0.200000 26.450000
0.200000 26.650000
0.200000 26.850000
0.200000 27.050000
0.200000 27.250000
8
0.125000 27.375000
0.125000 27.500000
0.125000 27.625000
0.125000 27.750000
0.125000 27.875000
0.125000 28.000000
0.125000 28.125000
0.125000 28.250000
4
0.250000 28.500000
0.250000 28.750000
0.250000 29.000000
0.250000 29.250000
4
0.250000 29.500000
0.250000 29.750000
0.250000 30.000000
0.250000 30.250000
3
0.333333 30.583333
0.333333 30.916667
0.333333 31.250000
6
0.166667 31.416667
0.166667 31.583333
0.166667 31.750000
0.166667 31.916667
0.166667 32.083333
0.166667 32.250000
3
0.333333 32.583333
0.333333 32.916667
0.333333 33.250000
5
0.200000 33.450000
0.200000 33.650000
0.200000 33.850000
0.200000 34.050000
0.200000 34.250000
4
0.250000 34.500000
0.250000 34.750000
0.250000 35.000000
0.250000 35.250000

N
NO(0.2)
108(0.5)
0.004630 0.004630
0.004630 0.009259
0.004630 0.013889
0.004630 0.018519
0.004630 0.023148
0.004630 0.027778
0.004630 0.032407
0.004630 0.037037
0.004630 0.041667
0.004630 0.046296
0.004630 0.050926
0.004630 0.055556
0.004630 0.060185
0.004630 0.064815
0.004630 0.069444
0.004630 0.074074
0.004630 0.078704
0.004630 0.083333
0.004630 0.087963
0.004630 0.092593
0.004630 0.097222
0.004630 0.101852
0.004630 0.106481
0.004630 0.111111
0.004630 0.115741
0.004630 0.120370
0.004630 0.125000
0.004630 0.129630
0.004630 0.134259
0.004630 0.138889
0.004630 0.143519
0.004630 0.148148
0.004630 0.152778
0.004630 0.157407
0.004630 0.162037
0.004630 0.166667
0.004630 0.171296
0.004630 0.175926
0.004630 0.180556
0.004630 0.185185
0.004630 0.189815
0.004630 0.194444
0.004630 0.199074
0.004630 0.203704
0.004630 0.208333
0.004630 0.212963
0.004630 0.217593
0.004630 0.222222
0.004630 0.226852
0.004630 0.231481
0.004630 0.236111
0.004630 0.240741
0.004630 0.245370
0.004630 0.250000
0.004630 0.254630
0.004630 0.259259
0.004630 0.263889
0.004630 0.268519
0.004630 0.273148
0.004630 0.277778
0.004630 0.282407
0.004630 0.287037
0.004630 0.291667
0.004630 0.296296
0.004630 0.300926
0.004630 0.305556
0.004630 0.310185
0.004630 0.314815
0.004630 0.319444
0.004630 0.324074
0.004630 0.328704
0.004630 0.333333
0.004630 0.337963
0.004630 0.342593
0.004630 0.347222
0.004630 0.351852
0.004630 0.356481
0.004630 0.361111
0.004630 0.365741
0.004630 0.370370
0.004630 0.375000
0.004630 0.379630
0.004630 0.384259
0.004630 0.388889
0.004630 0.393519
0.004630 0.398148
0.004630 0.402778
0.004630 0.407407
0.004630 0.412037
0.004630 0.416667
0.004630 0.421296
0.004630 0.425926
0.004630 0.430556
0.004630 0.435185
0.004630 0.439815
0.004630 0.444444
0.004630 0.449074
0.004630 0.453704
0.004630 0.458333
0.004630 0.462963
0.004630 0.467593
0.004630 0.472222
0.004630 0.476852
0.004630 0.481481
0.004630 0.486111
0.004630 0.490741
0.004630 0.495370
0.004630 0.500000
49(0.5)
0.010204 0.510204
0.010204 0.520408
0.010204 0.530612
0.010204 0.540816
0.010204 0.551020
0.010204 0.561224
0.010204 0.571429
0.010204 0.581633
0.010204 0.591837
0.010204 0.602041
0.010204 0.612245
0.010204 0.622449
0.010204 0.632653
0.010204 0.642857
0.010204 0.653061
0.010204 0.663265
0.010204 0.673469
0.010204 0.683673
0.010204 0.693878
0.010204 0.704082
0.010204 0.714286
0.010204 0.724490
0.010204 0.734694
0.010204 0.744898
0.010204 0.755102
0.010204 0.765306
0.010204 0.775510
0.010204 0.785714
0.010204 0.795918
0.010204 0.806122
0.010204 0.816327
0.010204 0.826531
0.010204 0.836735
0.010204 0.846939
0.010204 0.857143
0.010204 0.867347
0.010204 0.877551
0.010204 0.887755
0.010204 0.897959
0.010204 0.908163
0.010204 0.918367
0.010204 0.928571
0.010204 0.938776
0.010204 0.948980
0.010204 0.959184
0.010204 0.969388
0.010204 0.979592
0.010204 0.989796
0.010204 1.000000
25(0.5)
0.020000 1.020000
0.020000 1.040000
0.020000 1.060000
0.020000 1.080000
0.020000 1.100000
0.020000 1.120000
0.020000 1.140000
0.020000 1.160000
0.020000 1.180000
0.020000 1.200000
0.020000 1.220000
0.020000 1.240000
0.020000 1.260000
0.020000 1.280000
0.020000 1.300000
0.020000 1.320000
0.020000 1.340000
0.020000 1.360000
0.020000 1.380000
0.020000 1.400000
0.020000 1.420000
0.020000 1.440000
0.020000 1.460000
0.020000 1.480000
0.020000 1.500000
16(0.5)
0.031250 1.531250
0.031250 1.562500
0.031250 1.593750
0.031250 1.625000
0.031250 1.656250
0.031250 1.687500
0.031250 1.718750
0.031250 1.750000
0.031250 1.781250
0.031250 1.812500
0.031250 1.843750
0.031250 1.875000
0.031250 1.906250
0.031250 1.937500
0.031250 1.968750
0.031250 2.000000
10
0.100000 2.100000
0.100000 2.200000
0.100000 2.300000
0.100000 2.400000
0.100000 2.500000
0.100000 2.600000
0.100000 2.700000
0.100000 2.800000
0.100000 2.900000
0.100000 3.000000

K132ii
S
10(0.06)
0.006000 0.006000
0.006000 0.012000
0.006000 0.018000
0.006000 0.024000
0.006000 0.030000
0.006000 0.036000
0.006000 0.042000
0.006000 0.048000
0.006000 0.054000
0.006000 0.060000
61(0.25)
0.004098 0.064098
0.004098 0.068197
0.004098 0.072295
0.004098 0.076393
0.004098 0.080492
0.004098 0.084590
0.004098 0.088689
0.004098 0.092787
0.004098 0.096885
0.004098 0.100984
0.004098 0.105082
0.004098 0.109180
0.004098 0.113279
0.004098 0.117377
0.004098 0.121475
0.004098 0.125574
0.004098 0.129672
0.004098 0.133770
0.004098 0.137869
0.004098 0.141967
0.004098 0.146066
0.004098 0.150164
0.004098 0.154262
0.004098 0.158361
0.004098 0.162459
0.004098 0.166557
0.004098 0.170656
0.004098 0.174754
0.004098 0.178852
0.004098 0.182951
0.004098 0.187049
0.004098 0.191148
0.004098 0.195246
0.004098 0.199344
0.004098 0.203443
0.004098 0.207541
0.004098 0.211639
0.004098 0.215738
0.004098 0.219836
32(0.25)
0.007813 0.567813
0.007813 0.575625
0.007813 0.583438
0.007813 0.591250
0.007813 0.599063
0.007813 0.606875
0.007813 0.614688
0.007813 0.622500
0.007813 0.630313
0.007813 0.638125
0.007813 0.645938
0.007813 0.653750
0.007813 0.661563
0.007813 0.669375
0.007813 0.677188
0.007813 0.685000
0.007813 0.692813
0.007813 0.700625
0.007813 0.708438
0.007813 0.716250
0.007813 0.724063
0.007813 0.731875
0.007813 0.739688
0.007813 0.747500
0.007813 0.755313
0.007813 0.763125
0.007813 0.770938
0.007813 0.778750
0.007813 0.786563
0.007813 0.794375
0.007813 0.802188
0.007813 0.810000
25(0.5)
0.020000 0.830000
0.020000 0.850000
0.020000 0.870000
0.020000 0.890000
0.020000 0.910000
0.020000 0.930000
0.020000 0.950000
0.020000 0.970000
0.020000 0.990000
0.020000 1.010000
0.020000 1.030000
0.020000 1.050000
0.020000 1.070000
0.020000 1.090000
0.020000 1.110000
0.020000 1.130000
0.020000 1.150000
0.005000 0.450000
0.005000 0.455000
0.005000 0.460000
0.005000 0.465000
0.005000 0.470000
0.005000 0.475000
0.005000 0.480000
0.005000 0.485000
0.005000 0.490000
0.005000 0.495000
0.005000 0.500000
0.005000 0.505000
0.005000 0.510000
0.005000 0.515000
0.005000 0.520000
0.005000 0.525000
0.005000 0.530000
0.005000 0.535000
0.005000 0.540000
0.005000 0.545000
0.005000 0.550000
0.005000 0.555000
0.005000 0.560000
32(0.25)
0.007813 0.567813
0.007813 0.575625
0.007813 0.583438
0.007813 0.591250
0.007813 0.599063
0.007813 0.606875
0.007813 0.614688
0.007813 0.622500
0.007813 0.630313
0.007813 0.638125
0.007813 0.645938
0.007813 0.653750
0.007813 0.661563
0.007813 0.669375
0.007813 0.677188
0.007813 0.685000
0.007813 0.692813
0.007813 0.700625
0.007813 0.708438
0.007813 0.716250
0.007813 0.724063
0.007813 0.731875
0.007813 0.739688
0.007813 0.747500
0.007813 0.755313
0.007813 0.763125
0.007813 0.770938
0.007813 0.778750
0.007813 0.786563
0.007813 0.794375
0.007813 0.802188
0.007813 0.810000
25(0.5)
0.020000 0.830000
0.020000 0.850000
0.020000 0.870000
0.020000 0.890000
0.020000 0.910000
0.020000 0.930000
0.020000 0.950000
0.020000 0.970000
0.020000 0.990000
0.020000 1.010000
0.020000 1.030000
0.020000 1.050000
0.020000 1.070000
0.020000 1.090000
0.020000 1.110000
0.020000 1.130000
0.020000 1.150000

0.020000 1.170000
0.020000 1.190000
0.020000 1.210000
0.020000 1.230000
0.020000 1.250000
0.020000 1.270000
0.020000 1.290000
0.020000 1.310000
12
0.083333 1.393333
0.083333 1.476667
0.083333 1.560000
0.083333 1.643333
0.083333 1.726667
0.083333 1.810000
0.083333 1.893333
0.083333 1.976667
0.083333 2.060000
0.083333 2.143333
0.083333 2.226667
0.083333 2.310000

N
8(0.5)
0.062500 0.062500
0.062500 0.125000
0.062500 0.187500
0.062500 0.250000
0.062500 0.312500
0.062500 0.375000
0.062500 0.437500
0.062500 0.500000
7(0.5)
0.071429 0.571429
0.071429 0.642857
0.071429 0.714286
0.071429 0.785714
0.071429 0.857143
0.071429 0.928571
0.071429 1.000000
5
0.200000 1.200000
0.200000 1.400000
0.200000 1.600000
0.200000 1.800000
0.200000 2.000000
8
0.125000 2.125000
0.125000 2.250000
0.125000 2.375000
0.125000 2.500000
0.125000 2.625000
0.125000 2.750000
0.125000 2.875000
0.125000 3.000000
3
0.333333 3.333333
0.333333 3.666667
0.333333 4.000000
6
0.166667 4.166667
0.166667 4.333333
0.166667 4.500000
0.166667 4.666667
0.166667 4.833333
0.166667 5.000000
3
0.333333 5.333333
0.333333 5.666667
0.333333 6.000000
2
0.500000 6.500000
0.500000 7.000000
6
0.166667 7.166667
0.166667 7.333333
0.166667 7.500000
0.166667 7.666667
0.166667 7.833333
0.166667 8.000000
6
0.166667 8.166667
0.166667 8.333333
0.166667 8.500000
0.166667 8.666667
0.166667 8.833333
0.166667 9.000000

K134
S
36(0.1)
0.002778 0.002778
0.002778 0.005556
0.002778 0.008333
0.002778 0.011111
0.002778 0.013889
0.002778 0.016667
0.002778 0.019444
0.002778 0.022222
0.002778 0.025000
0.002778 0.027778
0.002778 0.030556
0.002778 0.033333
0.002778 0.036111
0.002778 0.038889
0.002778 0.041667
0.002778 0.044444
0.002778 0.047222
0.002778 0.050000
0.002778 0.052778
0.002778 0.055556
0.002778 0.058333
0.002778 0.061111
0.002778 0.063889
0.002778 0.066667
0.002778 0.069444
0.002778 0.072222
0.002778 0.075000
0.002778 0.077778
0.002778 0.080556
0.002778 0.083333
0.002778 0.086111
0.002778 0.088889
0.002778 0.091667
0.002778 0.094444
0.002778 0.097222
0.002778 0.100000
70(0.3)
0.004286 0.104286
0.004286 0.108571
0.004286 0.112857
0.004286 0.117143
0.004286 0.121429
0.004286 0.125714
0.004286 0.130000
0.004286 0.134286
0.004286 0.138571
0.004286 0.142857
0.004286 0.147143
0.004286 0.151429
0.004286 0.155714
0.004286 0.160000
0.004286 0.164286
0.004286 0.168571
0.004286 0.172857
0.004286 0.177143
0.004286 0.181429
0.004286 0.185714
0.004286 0.190000
0.004286 0.194286
0.004286 0.198571
0.004286 0.202857
0.004286 0.207143
0.004286 0.211429
0.004286 0.215714
0.004286 0.220000
0.004286 0.224286
0.004286 0.228571
0.004286 0.232857
0.004286 0.237143
0.004286 0.241429
0.004286 0.245714
0.004286 0.250000
0.004286 0.254286
0.004286 0.258571
0.004286 0.262857
0.004286 0.267143
0.004286 0.271429
0.004286 0.275714
0.004286 0.280000
0.004286 0.284286
0.004286 0.288571
0.004286 0.292857
0.004286 0.297143
0.004286 0.301429
0.004286 0.305714
0.004286 0.310000
0.004286 0.314286
0.004286 0.318571
0.004286 0.322857
0.004286 0.327143
0.004286 0.331429
0.004286 0.335714
0.004286 0.340000
0.004286 0.344286
0.004286 0.348571
0.004286 0.352857
0.004286 0.357143
0.004286 0.361429
0.004286 0.365714
0.004286 0.370000
0.004286 0.374286
0.004286 0.378571
0.004286 0.382857
0.004286 0.387143
0.004286 0.391429
0.004286 0.395714
0.004286 0.400000
47(0.3)
0.006383 0.406383
0.006383 0.412766
0.006383 0.419149
0.006383 0.425532
0.006383 0.431915
0.006383 0.438298
0.006383 0.444681
0.006383 0.451064
0.006383 0.457447
0.006383 0.463830
0.006383 0.470213
0.006383 0.476596
0.006383 0.482979
0.006383 0.489362
0.006383 0.495745
0.006383 0.502128
0.006383 0.508511
0.006383 0.514894
0.006383 0.521277
0.006383 0.527660
0.006383 0.534043
0.006383 0.540426
0.006383 0.546809
0.006383 0.553191
0.006383 0.559574
0.006383 0.565957
0.006383 0.572340
0.006383 0.578723
0.006383 0.585106
0.006383 0.591489
0.006383 0.597872
0.006383 0.604255
0.006383 0.610638
0.006383 0.617021
0.006383 0.623404
0.006383 0.629787
0.006383 0.636170
0.006383 0.642553
0.006383 0.648936
0.006383 0.655319
0.006383 0.661702
0.006383 0.668085
0.006383 0.674468
0.006383 0.680851
0.006383 0.687234
0.006383 0.693617
0.006383 0.700000
35(0.3)
0.008571 0.708571
0.008571 0.717143
0.008571 0.725714
0.008571 0.734286
0.008571 0.742857
0.008571 0.751429
0.008571 0.760000
0.008571 0.768571
0.008571 0.777143
0.008571 0.785714
0.008571 0.794286
0.008571 0.802857
0.008571 0.811429
0.008571 0.820000
0.008571 0.828571
0.008571 0.837143
0.008571 0.845714
0.008571 0.854286
0.008571 0.862857
0.008571 0.871429
0.008571 0.880000
0.008571 0.888571
0.008571 0.897143
0.008571 0.905714
0.008571 0.914286
0.008571 0.922857
0.008571 0.931429
0.008571 0.940000
0.008571 0.948571
0.008571 0.957143
0.008571 0.965714
0.008571 0.974286
0.008571 0.982857
0.008571 0.991429
0.008571 1.000000
41(0.5)
0.012195 1.012195
0.012195 1.024390
0.012195 1.036585
0.012195 1.048780
0.012195 1.060976
0.012195 1.073171
0.012195 1.085366
0.012195 1.097561
0.012195 1.109756
0.012195 1.121951
0.012195 1.134146
0.012195 1.146341
0.012195 1.158537
0.012195 1.170732
0.012195 1.182927
0.012195 1.195122
0.012195 1.207317
0.012195 1.219512
0.012195 1.231707
0.012195 1.243902
0.012195 1.256098
0.012195 1.268293
0.012195 1.280488
0.012195 1.292683
0.012195 1.304878
0.012195 1.317073
0.012195 1.329268
0.012195 1.341463
0.012195 1.353659
0.012195 1.365854
0.012195 1.378049
0.012195 1.390244
0.012195 1.402439
0.012195 1.414634
0.012195 1.426829
0.012195 1.439024
0.012195 1.451220
0.012195 1.463415
0.012195 1.475610
0.012195 1.487805
0.012195 1.500000
7(0.5)
0.071429 1.571429
0.071429 1.642857
0.071429 1.714286
0.071429 1.785714
0.071429 1.857143
0.071429 1.928571
0.071429 2.000000
7
0.142857 2.142857
0.142857 2.285714
0.142857 2.428571
0.142857 2.571429
0.142857 2.714286
0.142857 2.857143
0.142857 3.000000
6
0.166667 3.166667
0.166667 3.333333
0.166667 3.500000
0.166667 3.666667
0.166667 3.833333
0.166667 4.000000
6
0.166667 4.166667
0.166667 4.333333
0.166667 4.500000
0.166667 4.666667
0.166667 4.833333
0.166667 5.000000
3
0.333333 5.333333
0.333333 5.666667
0.333333 6.000000
4
0.250000 6.250000
0.250000 6.500000
0.250000 6.750000
0.250000 7.000000
3
0.333333 7.333333
0.333333 7.666667
0.333333 8.000000
4
0.250000 8.250000
0.250000 8.500000
0.250000 8.750000
0.250000 9.000000
2
0.500000 9.500000
0.500000 10.000000

N
37(0.1)
0.002703 0.002703
0.002703 0.005405
0.002703 0.008108
0.002703 0.010811
0.002703 0.013514
0.002703 0.016216
0.002703 0.018919
0.002703 0.021622
0.002703 0.024324
0.002703 0.027027
0.002703 0.029730
0.002703 0.032432
0.002703 0.035135
0.002703 0.037838
0.002703 0.040541
0.002703 0.043243
0.002703 0.045946
0.002703 0.048649
0.002703 0.051351
0.002703 0.054054
0.002703 0.056757
0.002703 0.059459
0.002703 0.062162
0.002703 0.064865
0.002703 0.067568
0.002703 0.070270
0.002703 0.072973
0.002703 0.075676
0.002703 0.078378
0.002703 0.081081
0.002703 0.083784
0.002703 0.086486
0.002703 0.089189
0.002703 0.091892
0.002703 0.094595
0.002703 0.097297
0.002703 0.100000
80(0.3)
0.003750 0.103750
0.003750 0.107500
0.003750 0.111250
0.003750 0.115000
0.003750 0.118750
0.003750 0.122500
0.003750 0.126250
0.003750 0.130000
0.003750 0.133750
0.003750 0.137500
0.003750 0.141250
0.003750 0.145000
0.003750 0.148750
0.003750 0.152500
0.003750 0.156250
0.003750 0.160000
0.003750 0.163750
0.003750 0.167500
0.003750 0.171250
0.003750 0.175000
0.003750 0.178750
0.003750 0.182500
0.003750 0.186250
0.003750 0.190000
0.003750 0.193750
0.003750 0.197500
0.003750 0.201250
0.003750 0.205000
0.003750 0.208750
0.003750 0.212500
0.003750 0.216250
0.003750 0.220000
0.003750 0.223750
0.003750 0.227500
0.003750 0.231250
0.003750 0.235000
0.003750 0.238750
0.003750 0.242500
0.003750 0.246250
0.003750 0.250000
0.003750 0.253750
0.003750 0.257500
0.003750 0.261250
0.003750 0.265000
0.003750 0.268750
0.003750 0.272500
0.003750 0.276250
0.003750 0.280000
0.003750 0.283750
0.003750 0.287500
0.003750 0.291250
0.003750 0.295000
0.003750 0.298750
0.003750 0.302500
0.003750 0.306250
0.003750 0.310000
0.003750 0.313750
0.003750 0.317500
0.003750 0.321250
0.003750 0.325000
0.003750 0.328750
0.003750 0.332500
0.003750 0.336250
0.003750 0.340000
0.003750 0.343750
0.003750 0.347500
0.003750 0.351250
0.003750 0.355000
0.003750 0.358750
0.003750 0.362500
0.003750 0.366250
0.003750 0.370000
0.003750 0.373750
0.003750 0.377500
0.003750 0.381250
0.003750 0.385000
0.003750 0.388750
0.003750 0.392500
0.003750 0.396250
0.003750 0.400000
70(0.3)
0.004286 0.404286
0.004286 0.408571
0.004286 0.412857
0.004286 0.417143
0.004286 0.421429
0.004286 0.425714
0.004286 0.430000
0.004286 0.434286
0.004286 0.438571
0.004286 0.442857
0.004286 0.447143
0.004286 0.451429
0.004286 0.455714
0.004286 0.460000
0.004286 0.464286
0.004286 0.468571
0.004286 0.472857
0.004286 0.477143
0.004286 0.481429
0.004286 0.485714
0.004286 0.490000
0.004286 0.494286
0.004286 0.498571
0.004286 0.502857
0.004286 0.507143
0.004286 0.511429
0.004286 0.515714
0.004286 0.520000
0.004286 0.524286
0.004286 0.528571
0.004286 0.532857
0.004286 0.537143
0.004286 0.541429
0.004286 0.545714
0.004286 0.550000
0.004286 0.554286
0.004286 0.558571
0.004286 0.562857
0.004286 0.567143
0.004286 0.571429
0.004286 0.575714
0.004286 0.580000
0.004286 0.584286
0.004286 0.588571
0.004286 0.592857
0.004286 0.597143
0.004286 0.601429
0.004286 0.605714
0.004286 0.610000
0.004286 0.614286
0.004286 0.618571
0.004286 0.622857
0.004286 0.627143
0.004286 0.631429
0.004286 0.635714
0.004286 0.640000
0.004286 0.644286
0.004286 0.648571
0.004286 0.652857
0.004286 0.657143
0.004286 0.661429
0.004286 0.665714
0.004286 0.670000
0.004286 0.674286
0.004286 0.678571
0.004286 0.682857
0.004286 0.687143
0.004286 0.691429
0.004286 0.695714
0.004286 0.700000
79(0.5)
0.006329 0.706329
0.006329 0.712658
0.006329 0.718987
0.006329 0.725316
0.006329 0.731646
0.006329 0.737975
0.006329 0.744304
0.006329 0.750633
0.006329 0.756962
0.006329 0.763291
0.006329 0.769620
0.006329 0.775949
0.006329 0.782278
0.006329 0.788608
0.006329 0.794937
0.006329 0.801266
0.006329 0.807595
0.006329 0.813924
0.006329 0.820253
0.006329 0.826582
0.006329 0.832911
0.006329 0.839241
0.006329 0.845570
0.006329 0.851899
0.006329 0.858228
0.006329 0.864557
0.006329 0.870886
0.006329 0.877215
0.006329 0.883544
0.006329 0.889873
0.006329 0.896203
0.006329 0.902532
0.006329 0.908861
0.006329 0.915190
0.006329 0.921519
0.006329 0.927848
0.006329 0.934177
0.006329 0.940506
0.006329 0.946835
0.006329 0.953165
0.006329 0.959494
0.006329 0.965823
0.006329 0.972152
0.006329 0.978481
0.006329 0.984810
0.006329 0.991139
0.006329 0.997468
0.006329 1.003797
0.006329 1.010127
0.006329 1.016456
0.006329 1.022785
0.006329 1.029114
0.006329 1.035443
0.006329 1.041772
0.006329 1.048101
0.006329 1.054430
0.006329 1.060759
0.006329 1.067089
0.006329 1.073418
0.006329 1.079747
0.006329 1.086076
0.006329 1.092405
0.006329 1.098734
0.006329 1.105063
0.006329 1.111392
0.006329 1.117722
0.006329 1.124051
0.006329 1.130380
0.006329 1.136709
0.006329 1.143038
0.006329 1.149367
0.006329 1.155696
0.006329 1.162025
0.006329 1.168354
0.006329 1.174684
0.006329 1.181013
0.006329 1.187342
0.006329 1.193671
0.006329 1.200000
24(0.5)
0.020833 1.220833
0.020833 1.241667
0.020833 1.262500
0.020833 1.283333
0.020833 1.304167
0.020833 1.325000
0.020833 1.345833
0.020833 1.366667
0.020833 1.387500
0.020833 1.408333
0.020833 1.429167
0.020833 1.450000
0.020833 1.470833
0.020833 1.491667
0.020833 1.512500
0.020833 1.533333
0.020833 1.554167
0.020833 1.575000
0.020833 1.595833
0.020833 1.616667
0.020833 1.637500
0.020833 1.658333
0.020833 1.679167
0.020833 1.700000
6
0.166667 1.866667
0.166667 2.033333
0.166667 2.200000
0.166667 2.366667
0.166667 2.533333
0.166667 2.700000
1
0.500000 3.200000
6
0.166667 3.366667
0.166667 3.533333
0.166667 3.700000
0.166667 3.866667
0.166667 4.033333
0.166667 4.200000
3
0.333333 4.533333
0.333333 4.866667
0.333333 5.200000
3
0.333333 5.533333
0.333333 5.866667
0.333333 6.200000
2
0.500000 6.700000
0.500000 7.200000
3
0.333333 7.533333
0.333333 7.866667
0.333333 8.200000
5
0.200000 8.400000
0.200000 8.600000
0.200000 8.800000
0.200000 9.000000
0.200000 9.200000
2
0.500000 9.700000
0.500000 10.200000

K136
S
82(0.25)
0.003049 0.003049
0.003049 0.006098
0.003049 0.009146
0.003049 0.012195
0.003049 0.015244
0.003049 0.018293
0.003049 0.021341
0.003049 0.024390
0.003049 0.027439
0.003049 0.030488
0.003049 0.033537
0.003049 0.036585
0.003049 0.039634
0.003049 0.042683
0.003049 0.045732
0.003049 0.048780
0.003049 0.051829
0.003049 0.054878
0.003049 0.057927
0.003049 0.060976
0.003049 0.064024
0.003049 0.067073
0.003049 0.070122
0.003049 0.073171
0.003049 0.076220
0.003049 0.079268
0.003049 0.082317
0.003049 0.085366
0.003049 0.088415
0.003049 0.091463
0.003049 0.094512
0.003049 0.097561
0.003049 0.100610
0.003049 0.103659
0.003049 0.106707
0.003049 0.109756
0.003049 0.112805
0.003049 0.115854
0.003049 0.118902
0.003049 0.121951
0.003049 0.125000
0.003049 0.128049
0.003049 0.131098
0.003049 0.134146
0.003049 0.137195
0.003049 0.140244
0.003049 0.143293
0.003049 0.146341
0.003049 0.149390
0.003049 0.152439
0.003049 0.155488
0.003049 0.158537
0.003049 0.161585
0.003049 0.164634
0.003049 0.167683
0.003049 0.170732
0.003049 0.173780
0.003049 0.176829
0.003049 0.179878
0.003049 0.182927
0.003049 0.185976
0.003049 0.189024
0.003049 0.192073
0.003049 0.195122
0.003049 0.198171
0.003049 0.201220
0.003049 0.204268
0.003049 0.207317
0.003049 0.210366
0.003049 0.213415
0.003049 0.216463
0.003049 0.219512
0.003049 0.222561
0.003049 0.225610
0.003049 0.228659
0.003049 0.231707
0.003049 0.234756
0.003049 0.237805
0.003049 0.240854
0.003049 0.243902
0.003049 0.246951
0.003049 0.250000
64(0.25)
0.003906 0.253906
0.003906 0.257813
0.003906 0.261719
0.003906 0.265625
0.003906 0.269531
0.003906 0.273438
0.003906 0.277344
0.003906 0.281250
0.003906 0.285156
0.003906 0.289063
0.003906 0.292969
0.003906 0.296875
0.003906 0.300781
0.003906 0.304688
0.003906 0.308594
0.003906 0.312500
0.003906 0.316406
0.003906 0.320313
0.003906 0.324219
0.003906 0.328125
0.003906 0.332031
0.003906 0.335938
0.003906 0.339844
0.003906 0.343750
0.003906 0.347656
0.003906 0.351563
0.003906 0.355469
0.003906 0.359375
0.003906 0.363281
0.003906 0.367188
0.003906 0.371094
0.003906 0.375000
0.003906 0.378906
0.003906 0.382813
0.003906 0.386719
0.003906 0.390625
0.003906 0.394531
0.003906 0.398438
22(0.25)
0.011364 0.761364
0.011364 0.772727
0.011364 0.784091
0.011364 0.795455
0.011364 0.806818
0.011364 0.818182
0.011364 0.829545
0.011364 0.840909
0.011364 0.852273
0.011364 0.863636
0.011364 0.875000
0.011364 0.886364
0.011364 0.897727
0.011364 0.909091
0.011364 0.920455
0.011364 0.931818
0.011364 0.943182
0.011364 0.954545
0.011364 0.965909
0.011364 0.977273
0.011364 0.988636
0.011364 1.000000
6(0.25)
0.041667 1.041667
0.041667 1.083333
0.041667 1.125000
0.041667 1.166667
0.041667 1.208333
0.041667 1.250000
2
0.500000 1.750000
0.500000 2.250000
2
0.500000 2.750000
0.500000 3.250000
4
0.250000 3.500000
0.250000 3.750000
0.250000 4.000000
0.250000 4.250000
4
0.250000 4.500000
0.250000 4.750000
0.250000 5.000000
0.250000 5.250000
2
0.500000 5.750000
0.500000 6.250000
3
0.005435 0.625000
0.005435 0.630435
0.005435 0.635870
0.005435 0.641304
0.005435 0.646739
0.005435 0.652174
0.005435 0.657609
0.005435 0.663043
0.005435 0.668478
0.005435 0.673913
0.005435 0.679348
0.005435 0.684783
0.005435 0.690217
0.005435 0.695652
0.005435 0.701087
0.005435 0.706522
0.005435 0.711957
0.005435 0.717391
0.005435 0.722826
0.005435 0.728261
0.005435 0.733696
0.005435 0.739130
0.005435 0.744565
0.005435 0.750000
22(0.25)
0.011364 0.761364
0.011364 0.772727
0.011364 0.784091
0.011364 0.795455
0.011364 0.806818
0.011364 0.818182
0.011364 0.829545
0.011364 0.840909
0.011364 0.852273
0.011364 0.863636
0.011364 0.875000
0.011364 0.886364
0.011364 0.897727
0.011364 0.909091
0.011364 0.920455
0.011364 0.931818
0.011364 0.943182
0.011364 0.954545
0.011364 0.965909
0.011364 0.977273
0.011364 0.988636
0.011364 1.000000
6(0.25)
0.041667 1.041667
0.041667 1.083333
0.041667 1.125000
0.041667 1.166667
0.041667 1.208333
0.041667 1.250000
2
0.500000 1.750000
0.500000 2.250000
2
0.500000 2.750000
0.500000 3.250000
4
0.250000 3.500000
0.250000 3.750000
0.250000 4.000000
0.250000 4.250000
4
0.250000 4.500000
0.250000 4.750000
0.250000 5.000000
0.250000 5.250000
2
0.500000 5.750000
0.500000 6.250000
3

0.333333 6.583333
0.333333 6.916667
0.333333 7.250000
2
0.500000 7.750000
0.500000 8.250000
3
0.333333 8.583333
0.333333 8.916667
0.333333 9.250000
2
0.500000 9.750000
0.500000 10.250000
2
0.500000 10.750000
0.500000 11.250000
4
0.250000 11.500000
0.250000 11.750000
0.250000 12.000000
0.250000 12.250000
1
1.000000 13.250000
3
0.333333 13.583333
0.333333 13.916667
0.333333 14.250000
3
0.333333 14.583333
0.333333 14.916667
0.333333 15.250000
3
0.333333 15.583333
0.333333 15.916667
0.333333 16.250000
3
0.333333 16.583333
0.333333 16.916667
0.333333 17.250000
5
0.200000 17.450000
0.200000 17.650000
0.200000 17.850000
0.200000 18.050000
0.200000 18.250000
4
0.250000 18.500000
0.250000 18.750000
0.250000 19.000000
0.250000 19.250000
2
0.500000 19.750000
0.500000 20.250000

N
83(0.25)
0.003012 0.003012
0.003012 0.006024
0.003012 0.009036
0.003012 0.012048
0.003012 0.015060
0.003012 0.018072
0.003012 0.021084
0.003012 0.024096
0.003012 0.027108
0.003012 0.030120
0.003012 0.033133
0.003012 0.036145
0.003012 0.039157
0.003012 0.042169
0.003012 0.045181
0.003012 0.048193
0.003012 0.051205
0.003012 0.054217

0.003012 0.057229
0.003012 0.060241
0.003012 0.063253
0.003012 0.066265
0.003012 0.069277
0.003012 0.072289
0.003012 0.075301
0.003012 0.078313
0.003012 0.081325
0.003012 0.084337
0.003012 0.087349
0.003012 0.090361
0.003012 0.093373
0.003012 0.096386
0.003012 0.099398
0.003012 0.102410
0.003012 0.105422
0.003012 0.108434
0.003012 0.111446
0.003012 0.114458
0.003012 0.117470
0.003012 0.120482
0.003012 0.123494
0.003012 0.126506
0.003012 0.129518
0.003012 0.132530
0.003012 0.135542
0.003012 0.138554
0.003012 0.141566
0.003012 0.144578
0.003012 0.147590
0.003012 0.150602
0.003012 0.153614
0.003012 0.156627
0.003012 0.159639
0.003012 0.162651
0.003012 0.165663
0.003012 0.168675
0.003012 0.171687
0.003012 0.174699
0.003012 0.177711
0.003012 0.180723
0.003012 0.183735
0.003012 0.186747
0.003012 0.189759
0.003012 0.192771
0.003012 0.195783
0.003012 0.198795
0.003012 0.201807
0.003012 0.204819
0.003012 0.207831
0.003012 0.210843
0.003012 0.213855
0.003012 0.216867
0.003012 0.219880
0.003012 0.222892
0.003012 0.225904
0.003012 0.228916
0.003012 0.231928
0.003012 0.234940
0.003012 0.237952
0.003012 0.240964
0.003012 0.243976
0.003012 0.246988
0.003012 0.250000
68(0.25)
0.003676 0.253676
0.003676 0.257353
0.003676 0.261029
0.003676 0.264706
0.003676 0.268382
0.003676 0.272059
0.003676 0.275735
0.003676 0.279412

0.003676 0.283088
0.003676 0.286765
0.003676 0.290441
0.003676 0.294118
0.003676 0.297794
0.003676 0.301471
0.003676 0.305147
0.003676 0.308824
0.003676 0.312500
0.003676 0.316176
0.003676 0.319853
0.003676 0.323529
0.003676 0.327206
0.003676 0.330882
0.003676 0.334559
0.003676 0.338235
0.003676 0.341912
0.003676 0.345588
0.003676 0.349265
0.003676 0.352941
0.003676 0.356618
0.003676 0.360294
0.003676 0.363971
0.003676 0.367647
0.003676 0.371324
0.003676 0.375000
0.003676 0.378676
0.003676 0.382353
0.003676 0.386029
0.003676 0.389706
0.003676 0.393382
0.003676 0.397059
0.003676 0.400735
0.003676 0.404412
0.003676 0.408088
0.003676 0.411765
0.003676 0.415441
0.003676 0.419118
0.003676 0.422794
0.003676 0.426471
0.003676 0.430147
0.003676 0.433824
0.003676 0.437500
0.003676 0.441176
0.003676 0.444853
0.003676 0.448529
0.003676 0.452206
0.003676 0.455882
0.003676 0.459559
0.003676 0.463235
0.003676 0.466912
0.003676 0.470588
0.003676 0.474265
0.003676 0.477941
0.003676 0.481618
0.003676 0.485294
0.003676 0.488971
0.003676 0.492647
0.003676 0.496324
0.003676 0.500000
44(0.25)
0.005682 0.505682
0.005682 0.511364
0.005682 0.517045
0.005682 0.522727
0.005682 0.528409
0.005682 0.534091
0.005682 0.539773
0.005682 0.545455
0.005682 0.551136
0.005682 0.556818
0.005682 0.562500
0.005682 0.568182
0.005682 0.573864

0.005682 0.579545
0.005682 0.585227
0.005682 0.590909
0.005682 0.596591
0.005682 0.602273
0.005682 0.607955
0.005682 0.613636
0.005682 0.619318
0.005682 0.625000
0.005682 0.630682
0.005682 0.636364
0.005682 0.642045
0.005682 0.647727
0.005682 0.653409
0.005682 0.659091
0.005682 0.664773
0.005682 0.670455
0.005682 0.676136
0.005682 0.681818
0.005682 0.687500
0.005682 0.693182
0.005682 0.698864
0.005682 0.704545
0.005682 0.710227
0.005682 0.715909
0.005682 0.721591
0.005682 0.727273
0.005682 0.732955
0.005682 0.738636
0.005682 0.744318
0.005682 0.750000
25(0.25)
0.010000 0.760000
0.010000 0.770000
0.010000 0.780000
0.010000 0.790000
0.010000 0.800000
0.010000 0.810000
0.010000 0.820000
0.010000 0.830000
0.010000 0.840000
0.010000 0.850000
0.010000 0.860000
0.010000 0.870000
0.010000 0.880000
0.010000 0.890000
0.010000 0.900000
0.010000 0.910000
0.010000 0.920000
0.010000 0.930000
0.010000 0.940000
0.010000 0.950000
0.010000 0.960000
0.010000 0.970000
0.010000 0.980000
0.010000 0.990000
0.010000 1.000000
5(0.25)
0.050000 1.050000
0.050000 1.100000
0.050000 1.150000
0.050000 1.200000
0.050000 1.250000
5
0.200000 1.450000
0.200000 1.650000
0.200000 1.850000
0.200000 2.050000
0.200000 2.250000
3
0.333333 2.583333
0.333333 2.916667
0.333333 3.250000
1
1.000000 4.250000
3
0.333333 4.583333
0.333333 4.916667
0.333333 5.250000
2
0.500000 5.750000
0.500000 6.250000
3
0.333333 6.583333
0.333333 6.916667
0.333333 7.250000
4
0.250000 7.500000
0.250000 7.750000
0.250000 8.000000
0.250000 8.250000
3
0.333333 8.583333
0.333333 8.916667
0.333333 9.250000
2
0.500000 9.750000
0.500000 10.250000
0,2
1.500000 11.750000
0.500000 12.250000
1
1.000000 13.250000
3
0.333333 13.583333
0.333333 13.916667
0.333333 14.250000
2
0.500000 14.750000
0.500000 15.250000
1
1.000000 16.250000
3
0.333333 16.583333
0.333333 16.916667
0.333333 17.250000
1
1.000000 18.250000

K138
S
27(0.14)
0.005185 0.005185
0.005185 0.010370
0.005185 0.015556
0.005185 0.020741
0.005185 0.025926
0.005185 0.031111
0.005185 0.036296
0.005185 0.041481
0.005185 0.046667
0.005185 0.051852
0.005185 0.057037
0.005185 0.062222
0.005185 0.067407
0.005185 0.072593
0.005185 0.077778
0.005185 0.082963
0.005185 0.088148
0.005185 0.093333
0.005185 0.098519
0.005185 0.103704
0.005185 0.108889
0.005185 0.114074
0.005185 0.119259
0.005185 0.124444
0.005185 0.129630

0.005185 0.134815
0.005185 0.140000
17(0.45)
0.026471 0.166471
0.026471 0.192941
0.026471 0.219412
0.026471 0.245882
0.026471 0.272353
0.026471 0.298824
0.026471 0.325294
0.026471 0.351765
0.026471 0.378235
0.026471 0.404706
0.026471 0.431176
0.026471 0.457647
0.026471 0.484118
0.026471 0.510588
0.026471 0.537059
0.026471 0.563529
0.026471 0.590000
10(0.5)
0.050000 0.640000
0.050000 0.690000
0.050000 0.740000
0.050000 0.790000
0.050000 0.840000
0.050000 0.890000
0.050000 0.940000
0.050000 0.990000
0.050000 1.040000
0.050000 1.090000
8(0.5)
0.062500 1.152500
0.062500 1.215000
0.062500 1.277500
0.062500 1.340000
0.062500 1.402500
0.062500 1.465000
0.062500 1.527500
0.062500 1.590000
7(0.5)
0.071429 1.661429
0.071429 1.732857
0.071429 1.804286
0.071429 1.875714
0.071429 1.947143
0.071429 2.018571
0.071429 2.090000
7(0.5)
0.071429 2.161429
0.071429 2.232857
0.071429 2.304286
0.071429 2.375714
0.071429 2.447143
0.071429 2.518571
0.071429 2.590000
3
0.333333 2.923333
0.333333 3.256667
0.333333 3.590000
5
0.200000 3.790000
0.200000 3.990000
0.200000 4.190000
0.200000 4.390000
0.200000 4.590000
5
0.200000 4.790000
0.200000 4.990000
0.200000 5.190000
0.200000 5.390000
0.200000 5.590000
3
0.333333 5.923333

0.333333 6.256667
0.333333 6.590000
6
0.166667 6.756667
0.166667 6.923333
0.166667 7.090000
0.166667 7.256667
0.166667 7.423333
0.166667 7.590000
4
0.250000 7.840000
0.250000 8.090000
0.250000 8.340000
0.250000 8.590000
4
0.250000 8.840000
0.250000 9.090000
0.250000 9.340000
0.250000 9.590000
2
0.500000 10.090000
0.500000 10.590000
6
0.166667 10.756667
0.166667 10.923333
0.166667 11.090000
0.166667 11.256667
0.166667 11.423333
0.166667 11.590000
5
0.200000 11.790000
0.200000 11.990000
0.200000 12.190000
0.200000 12.390000
0.200000 12.590000
6
0.166667 12.756667
0.166667 12.923333
0.166667 13.090000
0.166667 13.256667
0.166667 13.423333
0.166667 13.590000
5
0.200000 13.790000
0.200000 13.990000
0.200000 14.190000
0.200000 14.390000
0.200000 14.590000
4
0.250000 14.840000
0.250000 15.090000
0.250000 15.340000
0.250000 15.590000
2
0.500000 16.090000
0.500000 16.590000
2
0.500000 17.090000
0.500000 17.590000
4
0.250000 17.840000
0.250000 18.090000
0.250000 18.340000
0.250000 18.590000
9
0.111111 18.701111
0.111111 18.812222
0.111111 18.923333
0.111111 19.034444
0.111111 19.145556
0.111111 19.256667
0.111111 19.367778
0.111111 19.478889
0.111111 19.590000

5
0.200000 19.790000
0.200000 19.990000
0.200000 20.190000
0.200000 20.390000
0.200000 20.590000
2
0.500000 21.090000
0.500000 21.590000
5
0.200000 21.790000
0.200000 21.990000
0.200000 22.190000
0.200000 22.390000
0.200000 22.590000
3
0.333333 22.923333
0.333333 23.256667
0.333333 23.590000
3
0.333333 23.923333
0.333333 24.256667
0.333333 24.590000
2
0.500000 25.090000
0.500000 25.590000
4
0.250000 25.840000
0.250000 26.090000
0.250000 26.340000
0.250000 26.590000
4
0.250000 26.840000
0.250000 27.090000
0.250000 27.340000
0.250000 27.590000

N
30(0.16)
0.005333 0.005333
0.005333 0.010667
0.005333 0.016000
0.005333 0.021333
0.005333 0.026667
0.005333 0.032000
0.005333 0.037333
0.005333 0.042667
0.005333 0.048000
0.005333 0.053333
0.005333 0.058667
0.005333 0.064000
0.005333 0.069333
0.005333 0.074667
0.005333 0.080000
0.005333 0.085333
0.005333 0.090667
0.005333 0.096000
0.005333 0.101333
0.005333 0.106667
0.005333 0.112000
0.005333 0.117333
0.005333 0.122667
0.005333 0.128000
0.005333 0.133333
0.005333 0.138667
0.005333 0.144000
0.005333 0.149333
0.005333 0.154667
0.005333 0.160000
17(0.34)
0.020000 0.180000
0.020000 0.200000
0.020000 0.220000
0.020000 0.240000

0.020000 0.260000
0.020000 0.280000
0.020000 0.300000
0.020000 0.320000
0.020000 0.340000
0.020000 0.360000
0.020000 0.380000
0.020000 0.400000
0.020000 0.420000
0.020000 0.440000
0.020000 0.460000
0.020000 0.480000
0.020000 0.500000
15(0.5)
0.033333 0.533333
0.033333 0.566667
0.033333 0.600000
0.033333 0.633333
0.033333 0.666667
0.033333 0.700000
0.033333 0.733333
0.033333 0.766667
0.033333 0.800000
0.033333 0.833333
0.033333 0.866667
0.033333 0.900000
0.033333 0.933333
0.033333 0.966667
0.033333 1.000000
7(0.5)
0.071429 1.071429
0.071429 1.142857
0.071429 1.214286
0.071429 1.285714
0.071429 1.357143
0.071429 1.428571
0.071429 1.500000
2(0.5)
0.250000 1.750000
0.250000 2.000000
5(0.5)
0.100000 2.100000
0.100000 2.200000
0.100000 2.300000
0.100000 2.400000
0.100000 2.500000
4(0.5)
0.125000 2.625000
0.125000 2.750000
0.125000 2.875000
0.125000 3.000000
7
0.142857 3.142857
0.142857 3.285714
0.142857 3.428571
0.142857 3.571429
0.142857 3.714286
0.142857 3.857143
0.142857 4.000000
3
0.333333 4.333333
0.333333 4.666667
0.333333 5.000000
3
0.333333 5.333333
0.333333 5.666667
0.333333 6.000000
3
0.333333 6.333333
0.333333 6.666667
0.333333 7.000000
4
0.250000 7.250000
0.250000 7.500000

0.250000 7.750000
0.250000 8.000000
4
0.250000 8.250000
0.250000 8.500000
0.250000 8.750000
0.250000 9.000000
6
0.166667 9.166667
0.166667 9.333333
0.166667 9.500000
0.166667 9.666667
0.166667 9.833333
0.166667 10.000000
7
0.142857 10.142857
0.142857 10.285714
0.142857 10.428571
0.142857 10.571429
0.142857 10.714286
0.142857 10.857143
0.142857 11.000000
4
0.250000 11.250000
0.250000 11.500000
0.250000 11.750000
0.250000 12.000000
4
0.250000 12.250000
0.250000 12.500000
0.250000 12.750000
0.250000 13.000000
5
0.200000 13.200000
0.200000 13.400000
0.200000 13.600000
0.200000 13.800000
0.200000 14.000000
6
0.166667 14.166667
0.166667 14.333333
0.166667 14.500000
0.166667 14.666667
0.166667 14.833333
0.166667 15.000000
7
0.142857 15.142857
0.142857 15.285714
0.142857 15.428571
0.142857 15.571429
0.142857 15.714286
0.142857 15.857143
0.142857 16.000000
6
0.166667 16.166667
0.166667 16.333333
0.166667 16.500000
0.166667 16.666667
0.166667 16.833333
0.166667 17.000000
6
0.166667 17.166667
0.166667 17.333333
0.166667 17.500000
0.166667 17.666667
0.166667 17.833333
0.166667 18.000000
4
0.250000 18.250000
0.250000 18.500000
0.250000 18.750000
0.250000 19.000000
2
0.500000 19.500000

0.500000 20.000000

K147
S
15(0.15)
0.010000 0.010000
0.010000 0.020000
0.010000 0.030000
0.010000 0.040000
0.010000 0.050000
0.010000 0.060000
0.010000 0.070000
0.010000 0.080000
0.010000 0.090000
0.010000 0.100000
0.010000 0.110000
0.010000 0.120000
0.010000 0.130000
0.010000 0.140000
0.010000 0.150000
11(0.5)
0.045455 0.195455
0.045455 0.240909
0.045455 0.286364
0.045455 0.331818
0.045455 0.377273
0.045455 0.422727
0.045455 0.468182
0.045455 0.513636
0.045455 0.559091
0.045455 0.604545
0.045455 0.650000
8(0.5)
0.062500 0.712500
0.062500 0.775000
0.062500 0.837500
0.062500 0.900000
0.062500 0.962500
0.062500 1.025000
0.062500 1.087500
0.062500 1.150000
12
0.083333 1.233333
0.083333 1.316667
0.083333 1.400000
0.083333 1.483333
0.083333 1.566667
0.083333 1.650000
0.083333 1.733333
0.083333 1.816667
0.083333 1.900000
0.083333 1.983333
0.083333 2.066667
0.083333 2.150000
9
0.111111 2.261111
0.111111 2.372222
0.111111 2.483333
0.111111 2.594444
0.111111 2.705556
0.111111 2.816667
0.111111 2.927778
0.111111 3.038889
4
0.250000 3.288889
0.250000 3.538889
0.250000 3.788889
0.250000 4.038889
5
0.200000 4.238889
0.200000 4.438889
0.200000 4.638889
0.200000 4.838889

0.200000 5.038889
9
0.111111 5.150000
0.111111 5.261111
0.111111 5.372222
0.111111 5.483333
0.111111 5.594444
0.111111 5.705556
0.111111 5.816667
0.111111 5.927778
6
0.166667 6.094444
0.166667 6.261111
0.166667 6.427778
0.166667 6.594444
0.166667 6.761111
0.166667 6.927778
3
0.333333 7.261111
0.333333 7.594444
0.333333 7.927778
6
0.166667 8.094444
0.166667 8.261111
0.166667 8.427778
0.166667 8.594444
0.166667 8.761111
0.166667 8.927778
7
0.142857 9.070635
0.142857 9.213492
0.142857 9.356349
0.142857 9.499206
0.142857 9.642063
0.142857 9.784921
0.142857 9.927778
5
0.200000 10.127778
0.200000 10.327778
0.200000 10.527778
0.200000 10.727778
0.200000 10.927778
4
0.250000 11.177778
0.250000 11.427778
0.250000 11.677778
0.250000 11.927778
2
0.500000 12.427778
0.500000 12.927778
5
0.200000 13.127778
0.200000 13.327778
0.200000 13.527778
0.200000 13.727778
0.200000 13.927778

N
8(0.15)
0.018750 0.018750
0.018750 0.037500
0.018750 0.056250
0.018750 0.075000
0.018750 0.093750
0.018750 0.112500
0.018750 0.131250
0.018750 0.150000
14(0.5)
0.035714 0.185714
0.035714 0.221429
0.035714 0.257143
0.035714 0.292857
0.035714 0.328571
0.035714 0.364286

0.035714 0.400000
0.035714 0.435714
0.035714 0.471429
0.035714 0.507143
0.035714 0.542857
0.035714 0.578571
0.035714 0.614286
0.035714 0.650000
5(0.5)
0.100000 0.750000
0.100000 0.850000
0.100000 0.950000
0.100000 1.050000
0.100000 1.150000
5
0.200000 1.350000
0.200000 1.550000
0.200000 1.750000
0.200000 1.950000
0.200000 2.150000
2
0.500000 2.650000
0.500000 3.150000
4
0.250000 3.400000
0.250000 3.650000
0.250000 3.900000
0.250000 4.150000
2
0.500000 4.650000
0.500000 5.150000
3
0.333333 5.483333
0.333333 5.816667
0.333333 6.150000
3
0.333333 6.483333
0.333333 6.816667
0.333333 7.150000
3
0.333333 7.483333
0.333333 7.816667
0.333333 8.150000
5
0.200000 8.350000
0.200000 8.550000
0.200000 8.750000
0.200000 8.950000
0.200000 9.150000
6
0.166667 9.316667
0.166667 9.483333
0.166667 9.650000
0.166667 9.816667
0.166667 9.983333
0.166667 10.150000

K148
S
38(0.15)
0.003947 0.003947
0.003947 0.007895
0.003947 0.011842
0.003947 0.015789
0.003947 0.019737
0.003947 0.023684
0.003947 0.027632
0.003947 0.031579
0.003947 0.035526
0.003947 0.039474
0.003947 0.043421
0.003947 0.047368
0.003947 0.051316

0.003947 0.055263
0.003947 0.059211
0.003947 0.063158
0.003947 0.067105
0.003947 0.071053
0.003947 0.075000
0.003947 0.078947
0.003947 0.082895
0.003947 0.086842
0.003947 0.090789
0.003947 0.094737
0.003947 0.098684
0.003947 0.102632
0.003947 0.106579
0.003947 0.110526
0.003947 0.114474
0.003947 0.118421
0.003947 0.122368
0.003947 0.126316
0.003947 0.130263
0.003947 0.134211
0.003947 0.138158
0.003947 0.142105
0.003947 0.146053
0.003947 0.150000
1
1.000000 1.150000
1
1.000000 2.150000
3
0.333333 2.483333
0.333333 2.816667
0.333333 3.150000
3
0.333333 3.483333
0.333333 3.816667
0.333333 4.150000
3
0.333333 4.483333
0.333333 4.816667
0.333333 5.150000

N
43(0.15)
0.003488 0.003488
0.003488 0.006977
0.003488 0.010465
0.003488 0.013953
0.003488 0.017442
0.003488 0.020930
0.003488 0.024419
0.003488 0.027907
0.003488 0.031395
0.003488 0.034884
0.003488 0.038372
0.003488 0.041860
0.003488 0.045349
0.003488 0.048837
0.003488 0.052326
0.003488 0.055814
0.003488 0.059302
0.003488 0.062791
0.003488 0.066279
0.003488 0.069767
0.003488 0.073256
0.003488 0.076744
0.003488 0.080233
0.003488 0.083721
0.003488 0.087209
0.003488 0.090698
0.003488 0.094186
0.003488 0.097674
0.003488 0.101163
0.003488 0.104651

0.003488 0.108140
0.003488 0.111628
0.003488 0.115116
0.003488 0.118605
0.003488 0.122093
0.003488 0.125581
0.003488 0.129070
0.003488 0.132558
0.003488 0.136047
0.003488 0.139535
0.003488 0.143023
0.003488 0.146512
0.003488 0.150000
7
0.142857 0.292857
0.142857 0.435714
0.142857 0.578571
0.142857 0.721429
0.142857 0.864286
0.142857 1.007143
0.142857 1.150000
2
0.500000 1.650000
0.500000 2.150000
4
0.250000 2.400000
0.250000 2.650000
0.250000 2.900000
0.250000 3.150000
6
0.166667 3.316667
0.166667 3.483333
0.166667 3.650000
0.166667 3.816667
0.166667 3.983333
0.166667 4.150000
2
0.500000 4.650000
0.500000 5.150000

K155b
S
0.004 0.004
0.002 0.006
0.001 0.007
0.002 0.009
0.001 0.010
0.004 0.014
0.004 0.018
0.004 0.022
0.005 0.027
0.003 0.030
0.002 0.032
0.003 0.035
0.001 0.036
0.001 0.037
0.001 0.038
0.004 0.042
0.003 0.045
0.002 0.047
0.001 0.048
0.001 0.049
0.003 0.052
0.003 0.055
0.002 0.057
0.001 0.058
0.003 0.061
0.002 0.063
0.001 0.064
0.001 0.065
0.002 0.067
0.002 0.069
0.004 0.073

0.003 0.076
0.003 0.079
0.004 0.083
0.003 0.086
0.002 0.088
0.004 0.092
0.005 0.097
0.003 0.100
0.001 0.101
0.002 0.103
0.003 0.106
0.002 0.108
0.003 0.111
0.002 0.113
0.003 0.116
0.003 0.119
0.001 0.120
0.001 0.121
0.002 0.123
0.004 0.127
0.001 0.128
0.004 0.132
0.003 0.135
0.002 0.137
0.002 0.139
0.004 0.143
0.002 0.145
0.002 0.147
0.002 0.149
0.003 0.152
0.002 0.154
0.001 0.155
0.001 0.156
0.002 0.158
0.002 0.160
0.005 0.165
0.001 0.166
0.005 0.171
0.002 0.173
0.004 0.177
0.005 0.182
0.001 0.183
0.002 0.185
0.003 0.188
0.006 0.194
0.006 0.200
0.006 0.206
0.004 0.210
0.010 0.220
0.007 0.227
0.007 0.234
0.006 0.240
0.012 0.252
0.019 0.271
0.035 0.306
0.012 0.318
0.067 0.385
0.025 0.410
0.010 0.420
0.003 0.423
0.007 0.430
0.002 0.432
0.010 0.442
0.003 0.445
0.003 0.448
0.007 0.455
0.004 0.459
0.026 0.485
0.004 0.489
0.015 0.504
0.034 0.538
0.031 0.569
0.020 0.589
0.003 0.592

0.004 0.596
0.003 0.599
0.004 0.603
0.010 0.613
0.011 0.624
0.003 0.627
0.003 0.630
0.008 0.638
0.006 0.644
0.005 0.649
0.006 0.655
0.002 0.657
0.003 0.660
0.005 0.665
0.002 0.667
0.005 0.672
0.010 0.682
0.016 0.698
0.011 0.709
0.017 0.726
0.030 0.756
0.026 0.782
0.009 0.791
0.011 0.802
0.012 0.814
0.013 0.827
0.008 0.835
0.005 0.840
0.021 0.861
0.003 0.864
0.012 0.876
0.030 0.906
0.008 0.914
0.018 0.932
0.010 0.942
0.020 0.962
0.040 1.002
0.007 1.009
0.001 1.010
0.009 1.019
0.006 1.025
0.031 1.056
0.015 1.071
0.016 1.087
0.007 1.094
0.006 1.100
0.002 1.102
0.009 1.111
0.023 1.134
0.026 1.160
0.007 1.167
0.020 1.187
0.035 1.222
0.015 1.237
0.040 1.277
0.032 1.309
0.078 1.387
0.060 1.447
0.055 1.502
0.026 1.528
0.031 1.559
0.036 1.595
0.045 1.640
0.038 1.678
0.065 1.743
0.021 1.764
0.050 1.814
0.042 1.856
0.085 1.941
0.092 2.033
0.040 2.073
0.050 2.123
0.065 2.188
0.069 2.257

0.054 2.311
0.027 2.338
0.045 2.383
0.029 2.412
0.155 2.567
0.105 2.672
0.090 2.762
0.120 2.882
0.085 2.967
0.060 3.027
0.050 3.077
0.062 3.139
0.165 3.304
0.138 3.442
0.055 3.497
0.060 3.557
0.130 3.687
0.066 3.753
0.121 3.874
0.075 3.949
0.195 4.144
0.060 4.204
0.435 4.639
0.120 4.759
0.260 5.019
0.150 5.169
0.125 5.294
0.310 5.604
0.158 5.762
0.870 6.632
0.155 6.787
0.395 7.182
0.190 7.372
0.065 7.437
0.265 7.702
0.070 7.772
0.135 7.907

N
0.004 0.004
0.004 0.008
0.007 0.015
0.003 0.018
0.003 0.021
0.007 0.028
0.006 0.034
0.005 0.039
0.005 0.044
0.005 0.049
0.005 0.054
0.004 0.058
0.008 0.066
0.005 0.071
0.005 0.076
0.003 0.079
0.006 0.085
0.008 0.093
0.005 0.098
0.004 0.102
0.003 0.105
0.003 0.108
0.004 0.112
0.003 0.115
0.003 0.118
0.007 0.125
0.007 0.132
0.005 0.137
0.008 0.145
0.005 0.150
0.005 0.155
0.005 0.160
0.006 0.166
0.006 0.172
0.009 0.181

0.008 0.189
0.009 0.198
0.010 0.208
0.008 0.216
0.010 0.226
0.012 0.238
0.014 0.252
0.010 0.262
0.011 0.273
0.018 0.291
0.017 0.308
0.010 0.318
0.018 0.336
0.010 0.346
0.002 0.348
0.001 0.349
0.002 0.351
0.002 0.353
0.001 0.354
0.001 0.355
0.012 0.367
0.015 0.382
0.005 0.387
0.007 0.394
0.007 0.401
0.011 0.412
0.012 0.424
0.015 0.439
0.005 0.444
0.007 0.451
0.005 0.456
0.006 0.462
0.006 0.468
0.010 0.478
0.005 0.483
0.026 0.509
0.011 0.520
0.010 0.530
0.004 0.534
0.085 0.619
0.014 0.633
0.042 0.675
0.012 0.687
0.020 0.707
0.020 0.727
0.035 0.762
0.010 0.772
0.010 0.782
0.020 0.802
0.010 0.812
0.030 0.842
0.120 0.962
0.005 0.967
0.020 0.987
0.024 1.011
0.005 1.016
0.020 1.036
0.014 1.050
0.010 1.060
0.025 1.085
0.012 1.097
0.040 1.137
0.025 1.162
0.040 1.202
0.026 1.228
0.022 1.250
0.004 1.254
0.065 1.319
0.042 1.361
0.030 1.391
0.037 1.428
0.031 1.459
0.060 1.519
0.018 1.537

0.020 1.557
0.060 1.617
0.034 1.651
0.016 1.667
0.036 1.703
0.045 1.748
0.032 1.780
0.012 1.792
0.014 1.806
0.050 1.856
0.010 1.866
0.034 1.900
0.032 1.932
0.034 1.966
0.026 1.992
0.063 2.055
0.072 2.127
0.013 2.140
0.045 2.185
0.021 2.206
0.015 2.221
0.050 2.271
0.060 2.331
0.070 2.401
0.017 2.418
0.020 2.438
0.020 2.458
0.025 2.483
0.080 2.563
0.020 2.583
0.021 2.604
0.055 2.659
0.055 2.714
0.090 2.804
0.048 2.852
0.052 2.904
0.055 2.959
0.020 2.979
0.030 3.009
0.045 3.054
0.017 3.071
0.064 3.135
0.046 3.181
0.080 3.261
0.055 3.316
0.036 3.352
0.040 3.392
0.032 3.424
0.060 3.484
0.060 3.544
0.150 3.694
0.050 3.744
0.083 3.827
0.098 3.925
0.075 4.000
0.110 4.110
0.245 4.355
0.103 4.458
0.065 4.523
0.150 4.673
0.062 4.735
0.190 4.925
0.200 5.125
0.160 5.285
0.210 5.495
0.150 5.645
0.285 5.930
0.110 6.040
0.100 6.140
0.170 6.310
0.075 6.385
0.065 6.450
0.230 6.680
0.145 6.825

0.250 7.075
0.220 7.295
0.085 7.380
0.230 7.610
0.050 7.660
0.120 7.780
0.140 7.920
0.170 8.090
0.210 8.300
0.190 8.490
0.205 8.695
0.220 8.915
0.330 9.245
0.230 9.475
0.390 9.865
0.560 10.425
0.230 10.655
0.730 11.385
0.390 11.775
0.290 12.065
0.280 12.345
0.130 12.475
0.095 12.570
0.560 13.130
0.400 13.530
0.750 14.280
0.360 14.640
0.280 14.920
0.140 15.060
0.160 15.220
0.040 15.260
0.110 15.370
0.080 15.450
0.140 15.590
0.370 15.960
0.120 16.080
0.380 16.460
0.220 16.680
0.110 16.790
0.350 17.140

K157a
S
66(0.25)
0.003788 0.003788
0.003788 0.007576
0.003788 0.011364
0.003788 0.015152
0.003788 0.018939
0.003788 0.022727
0.003788 0.026515
0.003788 0.030303
0.003788 0.034091
0.003788 0.037879
0.003788 0.041667
0.003788 0.045455
0.003788 0.049242
0.003788 0.053030
0.003788 0.056818
0.003788 0.060606
0.003788 0.064394
0.003788 0.068182
0.003788 0.071970
0.003788 0.075758
0.003788 0.079545
0.003788 0.083333
0.003788 0.087121
0.003788 0.090909
0.003788 0.094697
0.003788 0.098485
0.003788 0.102273
0.003788 0.106061
0.003788 0.109848

0.003788 0.113636
0.003788 0.117424
0.003788 0.121212
0.003788 0.125000
0.003788 0.128788
0.003788 0.132576
0.003788 0.136364
0.003788 0.140152
0.003788 0.143939
0.003788 0.147727
0.003788 0.151515
0.003788 0.155303
0.003788 0.159091
0.003788 0.162879
0.003788 0.166667
0.003788 0.170455
0.003788 0.174242
0.003788 0.178030
0.003788 0.181818
0.003788 0.185606
0.003788 0.189394
0.003788 0.193182
0.003788 0.196970
0.003788 0.200758
0.003788 0.204545
0.003788 0.208333
0.003788 0.212121
0.003788 0.215909
0.003788 0.219697
0.003788 0.223485
0.003788 0.227273
0.003788 0.231061
0.003788 0.234848
0.003788 0.238636
0.003788 0.242424
0.003788 0.246212
0.003788 0.250000
32(0.25)
0.007813 0.257813
0.007813 0.265625
0.007813 0.273438
0.007813 0.281250
0.007813 0.289063
0.007813 0.296875
0.007813 0.304688
0.007813 0.312500
0.007813 0.320313
0.007813 0.328125
0.007813 0.335938
0.007813 0.343750
0.007813 0.351563
0.007813 0.359375
0.007813 0.367188
0.007813 0.375000
0.007813 0.382813
0.007813 0.390625
0.007813 0.398438
0.007813 0.406250
0.007813 0.414063
0.007813 0.421875
0.007813 0.429688
0.007813 0.437500
0.007813 0.445313
0.007813 0.453125
0.007813 0.460938
0.007813 0.468750
0.007813 0.476563
0.007813 0.484375
0.007813 0.492188
0.007813 0.500000
8(0.25)
0.031250 0.531250
0.031250 0.562500
0.031250 0.593750

0.031250 0.625000
0.031250 0.656250
0.031250 0.687500
0.031250 0.718750
0.031250 0.750000
6(0.25)
0.041667 0.791667
0.041667 0.833333
0.041667 0.875000
0.041667 0.916667
0.041667 0.958333
0.041667 1.000000
11(0.5)
0.045455 1.045455
0.045455 1.090909
0.045455 1.136364
0.045455 1.181818
0.045455 1.227273
0.045455 1.272727
0.045455 1.318182
0.045455 1.363636
0.045455 1.409091
0.045455 1.454545
0.045455 1.500000
12(0.5)
0.041667 1.541667
0.041667 1.583333
0.041667 1.625000
0.041667 1.666667
0.041667 1.708333
0.041667 1.750000
0.041667 1.791667
0.041667 1.833333
0.041667 1.875000
0.041667 1.916667
0.041667 1.958333
0.041667 2.000000
10(0.5)
0.050000 2.050000
0.050000 2.100000
0.050000 2.150000
0.050000 2.200000
0.050000 2.250000
0.050000 2.300000
0.050000 2.350000
0.050000 2.400000
0.050000 2.450000
0.050000 2.500000
10
0.100000 2.600000
0.100000 2.700000
0.100000 2.800000
0.100000 2.900000
0.100000 3.000000
0.100000 3.100000
0.100000 3.200000
0.100000 3.300000
0.100000 3.400000
0.100000 3.500000
18
0.055556 3.555556
0.055556 3.611111
0.055556 3.666667
0.055556 3.722222
0.055556 3.777778
0.055556 3.833333
0.055556 3.888889
0.055556 3.944444
0.055556 4.000000
0.055556 4.055556
0.055556 4.111111
0.055556 4.166667
0.055556 4.222222
0.055556 4.277778

0.055556 4.333333
0.055556 4.388889
0.055556 4.444444
0.055556 4.500000
13
0.076923 4.576923
0.076923 4.653846
0.076923 4.730769
0.076923 4.807692
0.076923 4.884615
0.076923 4.961538
0.076923 5.038462
0.076923 5.115385
0.076923 5.192308
0.076923 5.269231
0.076923 5.346154
0.076923 5.423077
0.076923 5.500000
14
0.071429 5.571429
0.071429 5.642857
0.071429 5.714286
0.071429 5.785714
0.071429 5.857143
0.071429 5.928571
0.071429 6.000000
0.071429 6.071429
0.071429 6.142857
0.071429 6.214286
0.071429 6.285714
0.071429 6.357143
0.071429 6.428571
0.071429 6.500000
11
0.090909 6.590909
0.090909 6.681818
0.090909 6.772727
0.090909 6.863636
0.090909 6.954545
0.090909 7.045455
0.090909 7.136364
0.090909 7.227273
0.090909 7.318182
0.090909 7.409091
0.090909 7.500000
10
0.100000 7.600000
0.100000 7.700000
0.100000 7.800000
0.100000 7.900000
0.100000 8.000000
0.100000 8.100000
0.100000 8.200000
0.100000 8.300000
0.100000 8.400000
0.100000 8.500000
10
0.100000 8.600000
0.100000 8.700000
0.100000 8.800000
0.100000 8.900000
0.100000 9.000000
0.100000 9.100000
0.100000 9.200000
0.100000 9.300000
0.100000 9.400000
0.100000 9.500000
8
0.125000 9.625000
0.125000 9.750000
0.125000 9.875000
0.125000 10.000000
0.125000 10.125000
0.125000 10.250000

0.125000 10.375000
0.125000 10.500000
11
0.090909 10.590909
0.090909 10.681818
0.090909 10.772727
0.090909 10.863636
0.090909 10.954545
0.090909 11.045455
0.090909 11.136364
0.090909 11.227273
0.090909 11.318182
0.090909 11.409091
0.090909 11.500000
0.090909 11.590909
13
0.076923 11.667832
0.076923 11.744755
0.076923 11.821678
0.076923 11.898601
0.076923 11.975524
0.076923 12.052448
0.076923 12.129371
0.076923 12.206294
0.076923 12.283217
0.076923 12.360140
0.076923 12.437063
0.076923 12.513986
0.076923 12.590909
0.076923 12.667832

N
61(0.25)
0.004098 0.004098
0.004098 0.008197
0.004098 0.012295
0.004098 0.016393
0.004098 0.020492
0.004098 0.024590
0.004098 0.028689
0.004098 0.032787
0.004098 0.036885
0.004098 0.040984
0.004098 0.045082
0.004098 0.049180
0.004098 0.053279
0.004098 0.057377
0.004098 0.061475
0.004098 0.065574
0.004098 0.069672
0.004098 0.073770
0.004098 0.077869
0.004098 0.081967
0.004098 0.086066
0.004098 0.090164
0.004098 0.094262
0.004098 0.098361
0.004098 0.102459
0.004098 0.106557
0.004098 0.110656
0.004098 0.114754
0.004098 0.118852
0.004098 0.122951
0.004098 0.127049
0.004098 0.131148
0.004098 0.135246
0.004098 0.139344
0.004098 0.143443
0.004098 0.147541
0.004098 0.151639
0.004098 0.155738
0.004098 0.159836
0.004098 0.163934
0.004098 0.168033

0.004098 0.172131
0.004098 0.176230
0.004098 0.180328
0.004098 0.184426
0.004098 0.188525
0.004098 0.192623
0.004098 0.196721
0.004098 0.200820
0.004098 0.204918
0.004098 0.209016
0.004098 0.213115
0.004098 0.217213
0.004098 0.221311
0.004098 0.225410
0.004098 0.229508
0.004098 0.233607
0.004098 0.237705
0.004098 0.241803
0.004098 0.245902
0.004098 0.250000
41(0.25)
0.006098 0.256098
0.006098 0.262195
0.006098 0.268293
0.006098 0.274390
0.006098 0.280488
0.006098 0.286585
0.006098 0.292683
0.006098 0.298780
0.006098 0.304878
0.006098 0.310976
0.006098 0.317073
0.006098 0.323171
0.006098 0.329268
0.006098 0.335366
0.006098 0.341463
0.006098 0.347561
0.006098 0.353659
0.006098 0.359756
0.006098 0.365854
0.006098 0.371951
0.006098 0.378049
0.006098 0.384146
0.006098 0.390244
0.006098 0.396341
0.006098 0.402439
0.006098 0.408537
0.006098 0.414634
0.006098 0.420732
0.006098 0.426829
0.006098 0.432927
0.006098 0.439024
0.006098 0.445122
0.006098 0.451220
0.006098 0.457317
0.006098 0.463415
0.006098 0.469512
0.006098 0.475610
0.006098 0.481707
0.006098 0.487805
0.006098 0.493902
0.006098 0.500000
16(0.25)
0.015625 0.515625
0.015625 0.531250
0.015625 0.546875
0.015625 0.562500
0.015625 0.578125
0.015625 0.593750
0.015625 0.609375
0.015625 0.625000
0.015625 0.640625
0.015625 0.656250
0.015625 0.671875

0.015625 0.687500
0.015625 0.703125
0.015625 0.718750
0.015625 0.734375
0.015625 0.750000
4(0.5)
0.125000 0.875000
0.125000 1.000000
0.125000 1.125000
0.125000 1.250000
4(0.5)
0.125000 1.375000
0.125000 1.500000
0.125000 1.625000
0.125000 1.750000
7(0.5)
0.071429 1.821429
0.071429 1.892857
0.071429 1.964286
0.071429 2.035714
0.071429 2.107143
0.071429 2.178571
0.071429 2.250000
5(0.5)
0.100000 2.350000
0.100000 2.450000
0.100000 2.550000
0.100000 2.650000
0.100000 2.750000
8(0.5)
0.062500 2.812500
0.062500 2.875000
0.062500 2.937500
0.062500 3.000000
0.062500 3.062500
0.062500 3.125000
0.062500 3.187500
0.062500 3.250000
2(0.5)
0.250000 3.500000
0.250000 3.750000
11
0.090909 3.840909
0.090909 3.931818
0.090909 4.022727
0.090909 4.113636
0.090909 4.204545
0.090909 4.295455
0.090909 4.386364
0.090909 4.477273
0.090909 4.568182
0.090909 4.659091
0.090909 4.750000
11
0.090909 4.840909
0.090909 4.931818
0.090909 5.022727
0.090909 5.113636
0.090909 5.204545
0.090909 5.295455
0.090909 5.386364
0.090909 5.477273
0.090909 5.568182
0.090909 5.659091
0.090909 5.750000
6
0.166667 5.916667
0.166667 6.083333
0.166667 6.250000
0.166667 6.416667
0.166667 6.583333
0.166667 6.750000
8
0.125000 6.875000

0.125000 7.000000
0.125000 7.125000
0.125000 7.250000
0.125000 7.375000
0.125000 7.500000
0.125000 7.625000
0.125000 7.750000
6
0.166667 7.916667
0.166667 8.083333
0.166667 8.250000
0.166667 8.416667
0.166667 8.583333
0.166667 8.750000
11
0.090909 8.840909
0.090909 8.931818
0.090909 9.022727
0.090909 9.113636
0.090909 9.204545
0.090909 9.295455
0.090909 9.386364
0.090909 9.477273
0.090909 9.568182
0.090909 9.659091
0.090909 9.750000
10
0.100000 9.850000
0.100000 9.950000
0.100000 10.050000
0.100000 10.150000
0.100000 10.250000
0.100000 10.350000
0.100000 10.450000
0.100000 10.550000
0.100000 10.650000
0.100000 10.750000

K176
S
NO(0.2)
56(0.25)
0.004464 0.004464
0.004464 0.008929
0.004464 0.013393
0.004464 0.017857
0.004464 0.022321
0.004464 0.026786
0.004464 0.031250
0.004464 0.035714
0.004464 0.040179
0.004464 0.044643
0.004464 0.049107
0.004464 0.053571
0.004464 0.058036
0.004464 0.062500
0.004464 0.066964
0.004464 0.071429
0.004464 0.075893
0.004464 0.080357
0.004464 0.084821
0.004464 0.089286
0.004464 0.093750
0.004464 0.098214
0.004464 0.102679
0.004464 0.107143
0.004464 0.111607
0.004464 0.116071
0.004464 0.120536
0.004464 0.125000
0.004464 0.129464
0.004464 0.133929
0.004464 0.138393

0.004464 0.142857
0.004464 0.147321
0.004464 0.151786
0.004464 0.156250
0.004464 0.160714
0.004464 0.165179
0.004464 0.169643
0.004464 0.174107
0.004464 0.178571
0.004464 0.183036
0.004464 0.187500
0.004464 0.191964
0.004464 0.196429
0.004464 0.200893
0.004464 0.205357
0.004464 0.209821
0.004464 0.214286
0.004464 0.218750
0.004464 0.223214
0.004464 0.227679
0.004464 0.232143
0.004464 0.236607
0.004464 0.241071
0.004464 0.245536
0.004464 0.250000
39(0.25)
0.006410 0.256410
0.006410 0.262821
0.006410 0.269231
0.006410 0.275641
0.006410 0.282051
0.006410 0.288462
0.006410 0.294872
0.006410 0.301282
0.006410 0.307692
0.006410 0.314103
0.006410 0.320513
0.006410 0.326923
0.006410 0.333333
0.006410 0.339744
0.006410 0.346154
0.006410 0.352564
0.006410 0.358974
0.006410 0.365385
0.006410 0.371795
0.006410 0.378205
0.006410 0.384615
0.006410 0.391026
0.006410 0.397436
0.006410 0.403846
0.006410 0.410256
0.006410 0.416667
0.006410 0.423077
0.006410 0.429487
0.006410 0.435897
0.006410 0.442308
0.006410 0.448718
0.006410 0.455128
0.006410 0.461538
0.006410 0.467949
0.006410 0.474359
0.006410 0.480769
0.006410 0.487179
0.006410 0.493590
0.006410 0.500000
42(0.25)
0.005952 0.505952
0.005952 0.511905
0.005952 0.517857
0.005952 0.523810
0.005952 0.529762
0.005952 0.535714
0.005952 0.541667
0.005952 0.547619

0.005952 0.553571
0.005952 0.559524
0.005952 0.565476
0.005952 0.571429
0.005952 0.577381
0.005952 0.583333
0.005952 0.589286
0.005952 0.595238
0.005952 0.601190
0.005952 0.607143
0.005952 0.613095
0.005952 0.619048
0.005952 0.625000
0.005952 0.630952
0.005952 0.636905
0.005952 0.642857
0.005952 0.648810
0.005952 0.654762
0.005952 0.660714
0.005952 0.666667
0.005952 0.672619
0.005952 0.678571
0.005952 0.684524
0.005952 0.690476
0.005952 0.696429
0.005952 0.702381
0.005952 0.708333
0.005952 0.714286
0.005952 0.720238
0.005952 0.726190
0.005952 0.732143
0.005952 0.738095
0.005952 0.744048
0.005952 0.750000
25(0.25)
0.010000 0.760000
0.010000 0.770000
0.010000 0.780000
0.010000 0.790000
0.010000 0.800000
0.010000 0.810000
0.010000 0.820000
0.010000 0.830000
0.010000 0.840000
0.010000 0.850000
0.010000 0.860000
0.010000 0.870000
0.010000 0.880000
0.010000 0.890000
0.010000 0.900000
0.010000 0.910000
0.010000 0.920000
0.010000 0.930000
0.010000 0.940000
0.010000 0.950000
0.010000 0.960000
0.010000 0.970000
0.010000 0.980000
0.010000 0.990000
0.010000 1.000000
15(0.25)
0.016667 1.016667
0.016667 1.033333
0.016667 1.050000
0.016667 1.066667
0.016667 1.083333
0.016667 1.100000
0.016667 1.116667
0.016667 1.133333
0.016667 1.150000
0.016667 1.166667
0.016667 1.183333
0.016667 1.200000
0.016667 1.216667

0.016667 1.233333
0.016667 1.250000
6(0.5)
0.083333 1.333333
0.083333 1.416667
0.083333 1.500000
0.083333 1.583333
0.083333 1.666667
0.083333 1.750000
2
0.500000 2.250000
0.500000 2.750000
2
0.500000 3.250000
0.500000 3.750000
7
0.142857 3.892857
0.142857 4.035714
0.142857 4.178571
0.142857 4.321429
0.142857 4.464286
0.142857 4.607143
0.142857 4.750000
6
0.166667 4.916667
0.166667 5.083333
0.166667 5.250000
0.166667 5.416667
0.166667 5.583333
0.166667 5.750000
4
0.250000 6.000000
0.250000 6.250000
0.250000 6.500000
0.250000 6.750000
4
0.250000 7.000000
0.250000 7.250000
0.250000 7.500000
0.250000 7.750000
3
0.333333 8.083333
0.333333 8.416667
0.333333 8.750000
3
0.333333 9.083333
0.333333 9.416667
0.333333 9.750000

N
NO(0.2)
47(0.25)
0.005319 0.005319
0.005319 0.010638
0.005319 0.015957
0.005319 0.021277
0.005319 0.026596
0.005319 0.031915
0.005319 0.037234
0.005319 0.042553
0.005319 0.047872
0.005319 0.053191
0.005319 0.058511
0.005319 0.063830
0.005319 0.069149
0.005319 0.074468
0.005319 0.079787
0.005319 0.085106
0.005319 0.090426
0.005319 0.095745
0.005319 0.101064
0.005319 0.106383
0.005319 0.111702
0.005319 0.117021

0.005319 0.122340
0.005319 0.127660
0.005319 0.132979
0.005319 0.138298
0.005319 0.143617
0.005319 0.148936
0.005319 0.154255
0.005319 0.159574
0.005319 0.164894
0.005319 0.170213
0.005319 0.175532
0.005319 0.180851
0.005319 0.186170
0.005319 0.191489
0.005319 0.196809
0.005319 0.202128
0.005319 0.207447
0.005319 0.212766
0.005319 0.218085
0.005319 0.223404
0.005319 0.228723
0.005319 0.234043
0.005319 0.239362
0.005319 0.244681
0.005319 0.250000
33(0.25)
0.007576 0.257576
0.007576 0.265152
0.007576 0.272727
0.007576 0.280303
0.007576 0.287879
0.007576 0.295455
0.007576 0.303030
0.007576 0.310606
0.007576 0.318182
0.007576 0.325758
0.007576 0.333333
0.007576 0.340909
0.007576 0.348485
0.007576 0.356061
0.007576 0.363636
0.007576 0.371212
0.007576 0.378788
0.007576 0.386364
0.007576 0.393939
0.007576 0.401515
0.007576 0.409091
0.007576 0.416667
0.007576 0.424242
0.007576 0.431818
0.007576 0.439394
0.007576 0.446970
0.007576 0.454545
0.007576 0.462121
0.007576 0.469697
0.007576 0.477273
0.007576 0.484848
0.007576 0.492424
0.007576 0.500000
25(0.25)
0.010000 0.510000
0.010000 0.520000
0.010000 0.530000
0.010000 0.540000
0.010000 0.550000
0.010000 0.560000
0.010000 0.570000
0.010000 0.580000
0.010000 0.590000
0.010000 0.600000
0.010000 0.610000
0.010000 0.620000
0.010000 0.630000
0.010000 0.640000

0.010000 0.650000
0.010000 0.660000
0.010000 0.670000
0.010000 0.680000
0.010000 0.690000
0.010000 0.700000
0.010000 0.710000
0.010000 0.720000
0.010000 0.730000
0.010000 0.740000
0.010000 0.750000
22(0.25)
0.011364 0.761364
0.011364 0.772727
0.011364 0.784091
0.011364 0.795455
0.011364 0.806818
0.011364 0.818182
0.011364 0.829545
0.011364 0.840909
0.011364 0.852273
0.011364 0.863636
0.011364 0.875000
0.011364 0.886364
0.011364 0.897727
0.011364 0.909091
0.011364 0.920455
0.011364 0.931818
0.011364 0.943182
0.011364 0.954545
0.011364 0.965909
0.011364 0.977273
0.011364 0.988636
0.011364 1.000000
16(0.25)
0.015625 1.015625
0.015625 1.031250
0.015625 1.046875
0.015625 1.062500
0.015625 1.078125
0.015625 1.093750
0.015625 1.109375
0.015625 1.125000
0.015625 1.140625
0.015625 1.156250
0.015625 1.171875
0.015625 1.187500
0.015625 1.203125
0.015625 1.218750
0.015625 1.234375
0.015625 1.250000
4(0.5)
0.125000 1.375000
0.125000 1.500000
0.125000 1.625000
0.125000 1.750000
4
0.250000 2.000000
0.250000 2.250000
0.250000 2.500000
0.250000 2.750000
3
0.333333 3.083333
0.333333 3.416667
0.333333 3.750000
4
0.250000 4.000000
0.250000 4.250000
0.250000 4.500000
0.250000 4.750000
1
1.000000 5.750000
3
0.333333 6.083333

0.333333 6.416667
0.333333 6.750000
3
0.333333 7.083333
0.333333 7.416667
0.333333 7.750000
3
0.333333 8.083333
0.333333 8.416667
0.333333 8.750000
5
0.200000 8.950000
0.200000 9.150000
0.200000 9.350000
0.200000 9.550000
0.200000 9.750000
4
0.250000 10.000000
0.250000 10.250000
0.250000 10.500000
0.250000 10.750000
4
0.250000 11.000000
0.250000 11.250000
0.250000 11.500000
0.250000 11.750000
4
0.250000 12.000000
0.250000 12.250000
0.250000 12.500000
0.250000 12.750000
3
0.333333 13.083333
0.333333 13.416667
0.333333 13.750000
4
0.250000 14.000000
0.250000 14.250000
0.250000 14.500000
0.250000 14.750000

K178
S
50(0.25)
0.005000 0.005000
0.005000 0.010000
0.005000 0.015000
0.005000 0.020000
0.005000 0.025000
0.005000 0.030000
0.005000 0.035000
0.005000 0.040000
0.005000 0.045000
0.005000 0.050000
0.005000 0.055000
0.005000 0.060000
0.005000 0.065000
0.005000 0.070000
0.005000 0.075000
0.005000 0.080000
0.005000 0.085000
0.005000 0.090000
0.005000 0.095000
0.005000 0.100000
0.005000 0.105000
0.005000 0.110000
0.005000 0.115000
0.005000 0.120000
0.005000 0.125000
0.005000 0.130000
0.005000 0.135000
0.005000 0.140000
0.005000 0.145000

0.005000 0.150000
0.005000 0.155000
0.005000 0.160000
0.005000 0.165000
0.005000 0.170000
0.005000 0.175000
0.005000 0.180000
0.005000 0.185000
0.005000 0.190000
0.005000 0.195000
0.005000 0.200000
0.005000 0.205000
0.005000 0.210000
0.005000 0.215000
0.005000 0.220000
0.005000 0.225000
0.005000 0.230000
0.005000 0.235000
0.005000 0.240000
0.005000 0.245000
0.005000 0.250000
37(0.25)
0.006757 0.256757
0.006757 0.263514
0.006757 0.270270
0.006757 0.277027
0.006757 0.283784
0.006757 0.290541
0.006757 0.297297
0.006757 0.304054
0.006757 0.310811
0.006757 0.317568
0.006757 0.324324
0.006757 0.331081
0.006757 0.337838
0.006757 0.344595
0.006757 0.351351
0.006757 0.358108
0.006757 0.364865
0.006757 0.371622
0.006757 0.378378
0.006757 0.385135
0.006757 0.391892
0.006757 0.398649
0.006757 0.405405
0.006757 0.412162
0.006757 0.418919
0.006757 0.425676
0.006757 0.432432
0.006757 0.439189
0.006757 0.445946
0.006757 0.452703
0.006757 0.459459
0.006757 0.466216
0.006757 0.472973
0.006757 0.479730
0.006757 0.486486
0.006757 0.493243
0.006757 0.500000
30(0.25)
0.008333 0.508333
0.008333 0.516667
0.008333 0.525000
0.008333 0.533333
0.008333 0.541667
0.008333 0.550000
0.008333 0.558333
0.008333 0.566667
0.008333 0.575000
0.008333 0.583333
0.008333 0.591667
0.008333 0.600000
0.008333 0.608333
0.008333 0.616667

0.008333 0.625000
0.008333 0.633333
0.008333 0.641667
0.008333 0.650000
0.008333 0.658333
0.008333 0.666667
0.008333 0.675000
0.008333 0.683333
0.008333 0.691667
0.008333 0.700000
0.008333 0.708333
0.008333 0.716667
0.008333 0.725000
0.008333 0.733333
0.008333 0.741667
0.008333 0.750000
23(0.25)
0.010870 0.760870
0.010870 0.771739
0.010870 0.782609
0.010870 0.793478
0.010870 0.804348
0.010870 0.815217
0.010870 0.826087
0.010870 0.836957
0.010870 0.847826
0.010870 0.858696
0.010870 0.869565
0.010870 0.880435
0.010870 0.891304
0.010870 0.902174
0.010870 0.913043
0.010870 0.923913
0.010870 0.934783
0.010870 0.945652
0.010870 0.956522
0.010870 0.967391
0.010870 0.978261
0.010870 0.989130
0.010870 1.000000
12(0.25)
0.020833 1.020833
0.020833 1.041667
0.020833 1.062500
0.020833 1.083333
0.020833 1.104167
0.020833 1.125000
0.020833 1.145833
0.020833 1.166667
0.020833 1.187500
0.020833 1.208333
0.020833 1.229167
0.020833 1.250000
10(0.5)
0.050000 1.300000
0.050000 1.350000
0.050000 1.400000
0.050000 1.450000
0.050000 1.500000
0.050000 1.550000
0.050000 1.600000
0.050000 1.650000
0.050000 1.700000
0.050000 1.750000
7(0.5)
0.071429 1.821429
0.071429 1.892857
0.071429 1.964286
0.071429 2.035714
0.071429 2.107143
0.071429 2.178571
0.071429 2.250000
4(0.5)
0.125000 2.375000

0.125000 2.500000
0.125000 2.625000
0.125000 2.750000
4(0.5)
0.125000 2.875000
0.125000 3.000000
0.125000 3.125000
0.125000 3.250000
5(0.5)
0.100000 3.350000
0.100000 3.450000
0.100000 3.550000
0.100000 3.650000
0.100000 3.750000
5(0.5)
0.100000 3.850000
0.100000 3.950000
0.100000 4.050000
0.100000 4.150000
0.100000 4.250000
6(0.5)
0.083333 4.333333
0.083333 4.416667
0.083333 4.500000
0.083333 4.583333
0.083333 4.666667
0.083333 4.750000
5(0.5)
0.100000 4.850000
0.100000 4.950000
0.100000 5.050000
0.100000 5.150000
0.100000 5.250000
7(0.5)
0.071429 5.321429
0.071429 5.392857
0.071429 5.464286
0.071429 5.535714
0.071429 5.607143
0.071429 5.678571
0.071429 5.750000
5(0.5)
0.100000 5.850000
0.100000 5.950000
0.100000 6.050000
0.100000 6.150000
0.100000 6.250000
4(0.5)
0.125000 6.375000
0.125000 6.500000
0.125000 6.625000
0.125000 6.750000
3(0.5)
0.166667 6.916667
0.166667 7.083333
0.166667 7.250000
3(0.5)
0.166667 7.416667
0.166667 7.583333
0.166667 7.750000
4
0.250000 8.000000
0.250000 8.250000
0.250000 8.500000
0.250000 8.750000
5
0.200000 8.950000
0.200000 9.150000
0.200000 9.350000
0.200000 9.550000
0.200000 9.750000
5
0.200000 9.950000
0.200000 10.150000

0.200000 10.350000
0.200000 10.550000
0.200000 10.750000
5
0.200000 10.950000
0.200000 11.150000
0.200000 11.350000
0.200000 11.550000
0.200000 11.750000
4
0.250000 12.000000
0.250000 12.250000
0.250000 12.500000
0.250000 12.750000
2
0.500000 13.250000
0.500000 13.750000
4
0.250000 14.000000
0.250000 14.250000
0.250000 14.500000
0.250000 14.750000
5
0.200000 14.950000
0.200000 15.150000
0.200000 15.350000
0.200000 15.550000
0.200000 15.750000
3
0.333333 16.083333
0.333333 16.416667
0.333333 16.750000
2
0.500000 17.250000
0.500000 17.750000
3
0.333333 18.083333
0.333333 18.416667
0.333333 18.750000
2
0.500000 19.250000
0.500000 19.750000
1
1.000000 20.750000
3
0.333333 21.083333
0.333333 21.416667
0.333333 21.750000
4
0.250000 22.000000
0.250000 22.250000
0.250000 22.500000
0.250000 22.750000
2
0.500000 23.250000
0.500000 23.750000
4
0.250000 24.000000
0.250000 24.250000
0.250000 24.500000
0.250000 24.750000
2
0.500000 25.250000
0.500000 25.750000
4
0.250000 26.000000
0.250000 26.250000
0.250000 26.500000
0.250000 26.750000
3
0.333333 27.083333
0.333333 27.416667
0.333333 27.750000
2

0.500000 28.250000
0.500000 28.750000
3
0.333333 29.083333
0.333333 29.416667
0.333333 29.750000

N
65(0.25)
0.003846 0.003846
0.003846 0.007692
0.003846 0.011538
0.003846 0.015385
0.003846 0.019231
0.003846 0.023077
0.003846 0.026923
0.003846 0.030769
0.003846 0.034615
0.003846 0.038462
0.003846 0.042308
0.003846 0.046154
0.003846 0.050000
0.003846 0.053846
0.003846 0.057692
0.003846 0.061538
0.003846 0.065385
0.003846 0.069231
0.003846 0.073077
0.003846 0.076923
0.003846 0.080769
0.003846 0.084615
0.003846 0.088462
0.003846 0.092308
0.003846 0.096154
0.003846 0.100000
0.003846 0.103846
0.003846 0.107692
0.003846 0.111538
0.003846 0.115385
0.003846 0.119231
0.003846 0.123077
0.003846 0.126923
0.003846 0.130769
0.003846 0.134615
0.003846 0.138462
0.003846 0.142308
0.003846 0.146154
0.003846 0.150000
0.003846 0.153846
0.003846 0.157692
0.003846 0.161538
0.003846 0.165385
0.003846 0.169231
0.003846 0.173077
0.003846 0.176923
0.003846 0.180769
0.003846 0.184615
0.003846 0.188462
0.003846 0.192308
0.003846 0.196154
0.003846 0.200000
0.003846 0.203846
0.003846 0.207692
0.003846 0.211538
0.003846 0.215385
0.003846 0.219231
0.003846 0.223077
0.003846 0.226923
0.003846 0.230769
0.003846 0.234615
0.003846 0.238462
0.003846 0.242308
0.003846 0.246154
0.003846 0.250000

50(0.25)
0.005000 0.255000
0.005000 0.260000
0.005000 0.265000
0.005000 0.270000
0.005000 0.275000
0.005000 0.280000
0.005000 0.285000
0.005000 0.290000
0.005000 0.295000
0.005000 0.300000
0.005000 0.305000
0.005000 0.310000
0.005000 0.315000
0.005000 0.320000
0.005000 0.325000
0.005000 0.330000
0.005000 0.335000
0.005000 0.340000
0.005000 0.345000
0.005000 0.350000
0.005000 0.355000
0.005000 0.360000
0.005000 0.365000
0.005000 0.370000
0.005000 0.375000
0.005000 0.380000
0.005000 0.385000
0.005000 0.390000
0.005000 0.395000
0.005000 0.400000
0.005000 0.405000
0.005000 0.410000
0.005000 0.415000
0.005000 0.420000
0.005000 0.425000
0.005000 0.430000
0.005000 0.435000
0.005000 0.440000
0.005000 0.445000
0.005000 0.450000
0.005000 0.455000
0.005000 0.460000
0.005000 0.465000
0.005000 0.470000
0.005000 0.475000
0.005000 0.480000
0.005000 0.485000
0.005000 0.490000
0.005000 0.495000
0.005000 0.500000
31(0.25)
0.008065 0.508065
0.008065 0.516129
0.008065 0.524194
0.008065 0.532258
0.008065 0.540323
0.008065 0.548387
0.008065 0.556452
0.008065 0.564516
0.008065 0.572581
0.008065 0.580645
0.008065 0.588710
0.008065 0.596774
0.008065 0.604839
0.008065 0.612903
0.008065 0.620968
0.008065 0.629032
0.008065 0.637097
0.008065 0.645161
0.008065 0.653226
0.008065 0.661290
0.008065 0.669355
0.008065 0.677419

0.008065 0.685484
0.008065 0.693548
0.008065 0.701613
0.008065 0.709677
0.008065 0.717742
0.008065 0.725806
0.008065 0.733871
0.008065 0.741935
0.008065 0.750000
21(0.25)
0.011905 0.761905
0.011905 0.773810
0.011905 0.785714
0.011905 0.797619
0.011905 0.809524
0.011905 0.821429
0.011905 0.833333
0.011905 0.845238
0.011905 0.857143
0.011905 0.869048
0.011905 0.880952
0.011905 0.892857
0.011905 0.904762
0.011905 0.916667
0.011905 0.928571
0.011905 0.940476
0.011905 0.952381
0.011905 0.964286
0.011905 0.976190
0.011905 0.988095
0.011905 1.000000
21(0.25)
0.011905 1.011905
0.011905 1.023810
0.011905 1.035714
0.011905 1.047619
0.011905 1.059524
0.011905 1.071429
0.011905 1.083333
0.011905 1.095238
0.011905 1.107143
0.011905 1.119048
0.011905 1.130952
0.011905 1.142857
0.011905 1.154762
0.011905 1.166667
0.011905 1.178571
0.011905 1.190476
0.011905 1.202381
0.011905 1.214286
0.011905 1.226190
0.011905 1.238095
0.011905 1.250000
11(0.25)
0.022727 1.272727
0.022727 1.295455
0.022727 1.318182
0.022727 1.340909
0.022727 1.363636
0.022727 1.386364
0.022727 1.409091
0.022727 1.431818
0.022727 1.454545
0.022727 1.477273
0.022727 1.500000
18(0.5)
0.027778 1.527778
0.027778 1.555556
0.027778 1.583333
0.027778 1.611111
0.027778 1.638889
0.027778 1.666667
0.027778 1.694444
0.027778 1.722222

0.027778 1.750000
0.027778 1.777778
0.027778 1.805556
0.027778 1.833333
0.027778 1.861111
0.027778 1.888889
0.027778 1.916667
0.027778 1.944444
0.027778 1.972222
0.027778 2.000000
12(0.5)
0.041667 2.041667
0.041667 2.083333
0.041667 2.125000
0.041667 2.166667
0.041667 2.208333
0.041667 2.250000
0.041667 2.291667
0.041667 2.333333
0.041667 2.375000
0.041667 2.416667
0.041667 2.458333
0.041667 2.500000
13(0.5)
0.038462 2.538462
0.038462 2.576923
0.038462 2.615385
0.038462 2.653846
0.038462 2.692308
0.038462 2.730769
0.038462 2.769231
0.038462 2.807692
0.038462 2.846154
0.038462 2.884615
0.038462 2.923077
0.038462 2.961538
0.038462 3.000000
14(0.5)
0.035714 3.035714
0.035714 3.071429
0.035714 3.107143
0.035714 3.142857
0.035714 3.178571
0.035714 3.214286
0.035714 3.250000
0.035714 3.285714
0.035714 3.321429
0.035714 3.357143
0.035714 3.392857
0.035714 3.428571
0.035714 3.464286
0.035714 3.500000
8(0.5)
0.062500 3.562500
0.062500 3.625000
0.062500 3.687500
0.062500 3.750000
0.062500 3.812500
0.062500 3.875000
0.062500 3.937500
0.062500 4.000000
12(0.5)
0.041667 4.041667
0.041667 4.083333
0.041667 4.125000
0.041667 4.166667
0.041667 4.208333
0.041667 4.250000
0.041667 4.291667
0.041667 4.333333
0.041667 4.375000
0.041667 4.416667
0.041667 4.458333
0.041667 4.500000

10(0.5)
0.050000 4.550000
0.050000 4.600000
0.050000 4.650000
0.050000 4.700000
0.050000 4.750000
0.050000 4.800000
0.050000 4.850000
0.050000 4.900000
0.050000 4.950000
0.050000 5.000000
7(0.5)
0.071429 5.071429
0.071429 5.142857
0.071429 5.214286
0.071429 5.285714
0.071429 5.357143
0.071429 5.428571
0.071429 5.500000
7
0.142857 5.642857
0.142857 5.785714
0.142857 5.928571
0.142857 6.071429
0.142857 6.214286
0.142857 6.357143
0.142857 6.500000
6
0.166667 6.666667
0.166667 6.833333
0.166667 7.000000
0.166667 7.166667
0.166667 7.333333
0.166667 7.500000
4
0.250000 7.750000
0.250000 8.000000
0.250000 8.250000
0.250000 8.500000
4
0.250000 8.750000
0.250000 9.000000
0.250000 9.250000
0.250000 9.500000
5
0.200000 9.700000
0.200000 9.900000
0.200000 10.100000
0.200000 10.300000
0.200000 10.500000
4
0.250000 10.750000
0.250000 11.000000
0.250000 11.250000
0.250000 11.500000
5
0.200000 11.700000
0.200000 11.900000
0.200000 12.100000
0.200000 12.300000
0.200000 12.500000
4
0.250000 12.750000
0.250000 13.000000
0.250000 13.250000
0.250000 13.500000
5
0.200000 13.700000
0.200000 13.900000
0.200000 14.100000
0.200000 14.300000
0.200000 14.500000
7
0.142857 14.642857

0.142857 14.785714
0.142857 14.928571
0.142857 15.071429
0.142857 15.214286
0.142857 15.357143
0.142857 15.500000
5
0.200000 15.700000
0.200000 15.900000
0.200000 16.100000
0.200000 16.300000
0.200000 16.500000
3
0.333333 16.833333
0.333333 17.166667
0.333333 17.500000
4
0.250000 17.750000
0.250000 18.000000
0.250000 18.250000
0.250000 18.500000
5
0.200000 18.700000
0.200000 18.900000
0.200000 19.100000
0.200000 19.300000
0.200000 19.500000

K180
S
50(0.1)
0.002000 0.002000
0.002000 0.004000
0.002000 0.006000
0.002000 0.008000
0.002000 0.010000
0.002000 0.012000
0.002000 0.014000
0.002000 0.016000
0.002000 0.018000
0.002000 0.020000
0.002000 0.022000
0.002000 0.024000
0.002000 0.026000
0.002000 0.028000
0.002000 0.030000
0.002000 0.032000
0.002000 0.034000
0.002000 0.036000
0.002000 0.038000
0.002000 0.040000
0.002000 0.042000
0.002000 0.044000
0.002000 0.046000
0.002000 0.048000
0.002000 0.050000
0.002000 0.052000
0.002000 0.054000
0.002000 0.056000
0.002000 0.058000
0.002000 0.060000
0.002000 0.062000
0.002000 0.064000
0.002000 0.066000
0.002000 0.068000
0.002000 0.070000
0.002000 0.072000
0.002000 0.074000
0.002000 0.076000
0.002000 0.078000
0.002000 0.080000
0.002000 0.082000
0.002000 0.084000

0.002000 0.086000
0.002000 0.088000
0.002000 0.090000
0.002000 0.092000
0.002000 0.094000
0.002000 0.096000
0.002000 0.098000
0.002000 0.100000
25(0.1)
0.004000 0.104000
0.004000 0.108000
0.004000 0.112000
0.004000 0.116000
0.004000 0.120000
0.004000 0.124000
0.004000 0.128000
0.004000 0.132000
0.004000 0.136000
0.004000 0.140000
0.004000 0.144000
0.004000 0.148000
0.004000 0.152000
0.004000 0.156000
0.004000 0.160000
0.004000 0.164000
0.004000 0.168000
0.004000 0.172000
0.004000 0.176000
0.004000 0.180000
0.004000 0.184000
0.004000 0.188000
0.004000 0.192000
0.004000 0.196000
0.004000 0.200000
15(0.3)
0.020000 0.220000
0.020000 0.240000
0.020000 0.260000
0.020000 0.280000
0.020000 0.300000
0.020000 0.320000
0.020000 0.340000
0.020000 0.360000
0.020000 0.380000
0.020000 0.400000
0.020000 0.420000
0.020000 0.440000
0.020000 0.460000
0.020000 0.480000
0.020000 0.500000
5(0.5)
0.100000 0.600000
0.100000 0.700000
0.100000 0.800000
0.100000 0.900000
0.100000 1.000000
1(0.5)
0.500000 1.500000
3
0.333333 1.833333
0.333333 2.166667
0.333333 2.500000
5
0.200000 2.700000
0.200000 2.900000
0.200000 3.100000
0.200000 3.300000
0.200000 3.500000
4
0.250000 3.750000
0.250000 4.000000
0.250000 4.250000
0.250000 4.500000
3

0.333333 4.833333
0.333333 5.166667
0.333333 5.500000
5
0.200000 5.700000
0.200000 5.900000
0.200000 6.100000
0.200000 6.300000
0.200000 6.500000
3
0.333333 6.833333
0.333333 7.166667
0.333333 7.500000
3
0.333333 7.833333
0.333333 8.166667
0.333333 8.500000
3
0.333333 8.833333
0.333333 9.166667
0.333333 9.500000
5
0.200000 9.700000
0.200000 9.900000
0.200000 10.100000
0.200000 10.300000
0.200000 10.500000
4
0.250000 10.750000
0.250000 11.000000
0.250000 11.250000
0.250000 11.500000
4
0.250000 11.750000
0.250000 12.000000
0.250000 12.250000
0.250000 12.500000
2
0.500000 13.000000
0.500000 13.500000
2
0.500000 14.000000
0.500000 14.500000
3
0.333333 14.833333
0.333333 15.166667
0.333333 15.500000
5
0.200000 15.700000
0.200000 15.900000
0.200000 16.100000
0.200000 16.300000
0.200000 16.500000
5
0.200000 16.700000
0.200000 16.900000
0.200000 17.100000
0.200000 17.300000
0.200000 17.500000
3
0.333333 17.833333
0.333333 18.166667
0.333333 18.500000
4
0.250000 18.750000
0.250000 19.000000
0.250000 19.250000
0.250000 19.500000

N
29(0.06)
0.002069 0.002069
0.002069 0.004138
0.002069 0.006207

0.002069 0.008276
0.002069 0.010345
0.002069 0.012414
0.002069 0.014483
0.002069 0.016552
0.002069 0.018621
0.002069 0.020690
0.002069 0.022759
0.002069 0.024828
0.002069 0.026897
0.002069 0.028966
0.002069 0.031034
0.002069 0.033103
0.002069 0.035172
0.002069 0.037241
0.002069 0.039310
0.002069 0.041379
0.002069 0.043448
0.002069 0.045517
0.002069 0.047586
0.002069 0.049655
0.002069 0.051724
0.002069 0.053793
0.002069 0.055862
0.002069 0.057931
0.002069 0.060000
20(0.08)
0.004000 0.064000
0.004000 0.068000
0.004000 0.072000
0.004000 0.076000
0.004000 0.080000
0.004000 0.084000
0.004000 0.088000
0.004000 0.092000
0.004000 0.096000
0.004000 0.100000
0.004000 0.104000
0.004000 0.108000
0.004000 0.112000
0.004000 0.116000
0.004000 0.120000
0.004000 0.124000
0.004000 0.128000
0.004000 0.132000
0.004000 0.136000
0.004000 0.140000
6(0.1)
0.016667 0.156667
0.016667 0.173333
0.016667 0.190000
0.016667 0.206667
0.016667 0.223333
0.016667 0.240000
7(0.3)
0.042857 0.282857
0.042857 0.325714
0.042857 0.368571
0.042857 0.411429
0.042857 0.454286
0.042857 0.497143
0.042857 0.540000
4
0.250000 0.790000
0.250000 1.040000
0.250000 1.290000
0.250000 1.540000
1
1.000000 2.540000
0,1
2.000000 4.540000
2
0.500000 5.040000
0.500000 5.540000

5
0.200000 5.740000
0.200000 5.940000
0.200000 6.140000
0.200000 6.340000
0.200000 6.540000
3
0.333333 6.873333
0.333333 7.206667
0.333333 7.540000
3
0.333333 7.873333
0.333333 8.206667
0.333333 8.540000
3
0.333333 8.873333
0.333333 9.206667
0.333333 9.540000
3
0.333333 9.873333
0.333333 10.206667
0.333333 10.540000
1
1.000000 11.540000
1
1.000000 12.540000
4
0.250000 12.790000
0.250000 13.040000
0.250000 13.290000
0.250000 13.540000
2
0.500000 14.040000
0.500000 14.540000
4
0.250000 14.790000
0.250000 15.040000
0.250000 15.290000
0.250000 15.540000
3
0.333333 15.873333
0.333333 16.206667
0.333333 16.540000
3
0.333333 16.873333
0.333333 17.206667
0.333333 17.540000
3
0.333333 17.873333
0.333333 18.206667
0.333333 18.540000

WC25a
SE
0.020 0.020
0.030 0.050
0.020 0.070
0.020 0.090
0.005 0.095
0.010 0.105
0.020 0.125
0.020 0.145
0.015 0.160
0.010 0.170
0.010 0.180
0.020 0.200
0.030 0.230
0.015 0.245
0.015 0.260
0.020 0.280
0.100 0.380
0.025 0.405
0.010 0.415

0.010 0.425
0.010 0.435
0.035 0.470
0.100 0.570
0.060 0.630
0.020 0.650
0.010 0.660
0.010 0.670
0.060 0.730
0.010 0.740
0.060 0.800
0.080 0.880
0.040 0.920
0.010 0.930
0.160 1.090
0.200 1.290
0.200 1.490
0.020 1.510
0.015 1.525
0.060 1.585
0.200 1.785
0.150 1.935
0.150 2.085
0.050 2.135
0.120 2.255
0.110 2.365
0.015 2.380
0.020 2.400
0.025 2.425
0.030 2.455
0.020 2.475
0.030 2.505
0.020 2.525
0.200 2.725
0.080 2.805
0.040 2.845
0.040 2.885
0.050 2.935
0.030 2.965
0.040 3.005
0.020 3.025
0.130 3.155
0.290 3.445
0.060 3.505
0.090 3.595
0.060 3.655
0.050 3.705
0.040 3.745
0.180 3.925
0.190 4.115
0.100 4.215
0.040 4.255
0.150 4.405
0.200 4.605
0.050 4.655
0.350 5.005
0.400 5.405
0.030 5.435
0.030 5.465
0.050 5.515
0.060 5.575
0.040 5.615
0.100 5.715
0.350 6.065
0.100 6.165
0.850 7.015
0.700 7.715
0.400 8.115
1.500 9.615

NW
0.010 0.010
0.020 0.030
0.050 0.080

0.060 0.140
0.050 0.190
0.010 0.200
0.005 0.205
0.070 0.275
0.010 0.285
0.015 0.300
0.015 0.315
0.005 0.320
0.020 0.340
0.015 0.355
0.010 0.365
0.010 0.375
0.010 0.385
0.020 0.405
0.010 0.415
0.010 0.425
0.020 0.445
0.005 0.450
0.010 0.460
0.035 0.495
0.020 0.515
0.025 0.540
0.030 0.570
0.015 0.585
0.010 0.595
0.010 0.605
0.040 0.645
0.050 0.695
0.080 0.775
0.060 0.835
0.040 0.875
0.090 0.965
0.140 1.105
0.090 1.195
0.050 1.245
0.040 1.285
0.010 1.295
0.015 1.310
0.010 1.320
0.100 1.420
0.070 1.490
0.030 1.520
0.015 1.535
0.070 1.605
0.015 1.620
0.015 1.635
0.070 1.705
0.050 1.755
0.060 1.815
0.030 1.845
0.060 1.905
0.030 1.935
0.060 1.995
0.020 2.015
0.040 2.055
0.150 2.205
0.010 2.215
0.020 2.235
0.040 2.275
0.050 2.325
0.020 2.345
0.015 2.360
0.015 2.375
0.010 2.385
0.020 2.405
0.005 2.410
0.020 2.430
0.040 2.470
0.030 2.500
0.020 2.520
0.110 2.630
0.040 2.670
0.030 2.700

0.040 2.740
0.030 2.770
0.030 2.800
0.010 2.810
0.010 2.820
0.030 2.850
0.010 2.860
0.030 2.890
0.015 2.905
0.050 2.955
0.040 2.995
0.040 3.035
0.040 3.075
0.090 3.165
0.120 3.285
0.070 3.355
0.070 3.425
0.020 3.445
0.050 3.495
0.030 3.525
0.030 3.555
0.010 3.565
0.080 3.645
0.050 3.695
0.040 3.735
0.130 3.865
0.040 3.905
0.020 3.925
0.140 4.065
0.040 4.105
0.070 4.175
0.010 4.185
0.010 4.195
0.020 4.215
0.050 4.265
0.060 4.325
0.030 4.355
0.030 4.385
0.010 4.395
0.010 4.405
0.010 4.415
0.010 4.425
0.010 4.435
0.010 4.445
0.030 4.475
0.030 4.505
0.010 4.515
0.020 4.535
0.030 4.565
0.150 4.715
0.020 4.735
0.060 4.795
0.140 4.935
0.070 5.005
0.020 5.025
0.020 5.045
0.070 5.115
0.040 5.155
0.270 5.425
0.120 5.545
0.080 5.625
0.120 5.745
0.040 5.785
0.080 5.865
0.220 6.085
0.160 6.245
0.160 6.405
0.200 6.605
0.050 6.655
0.070 6.725
0.050 6.775
0.380 7.155
0.090 7.245
0.280 7.525

0.220 7.745
0.110 7.855
0.100 7.955
0.060 8.015
0.120 8.135
0.100 8.235
0.090 8.325
0.180 8.505
0.050 8.555
0.200 8.755
0.080 8.835
0.140 8.975
0.060 9.035
0.350 9.385
0.300 9.685
0.090 9.775
0.050 9.825
0.680 10.505
0.300 10.805
1.900 12.705
1.100 13.805
0.070 13.875
0.060 13.935
0.060 13.995
0.060 14.055
0.040 14.095
0.040 14.135
0.270 14.405
0.040 14.445
0.050 14.495
0.070 14.565
0.500 15.065
1.700 16.765
0.060 16.825
0.100 16.925
0.030 16.955
0.120 17.075
0.700 17.775
0.100 17.875
0.500 18.375
0.300 18.675
0.500 19.175
0.050 19.225
0.050 19.275
0.200 19.475
0.130 19.605
0.130 19.735
0.300 20.035
0.270 20.305
0.070 20.375
0.270 20.645
0.080 20.725
0.130 20.855
0.130 20.985
0.070 21.055
0.020 21.075
0.030 21.105
0.050 21.155

WC25c
SE
NO(0.4)
0.110 0.110
0.030 0.140
0.005 0.145
0.005 0.150
0.015 0.165
0.035 0.200
0.085 0.285
0.120 0.405
0.090 0.495
0.050 0.545
0.140 0.685

0.080 0.765
0.070 0.835
0.010 0.845
0.120 0.965
0.020 0.985
0.020 1.005
0.015 1.020
0.100 1.120
0.020 1.140
0.050 1.190
0.110 1.300
0.060 1.360
0.100 1.460
0.005 1.465
0.015 1.480
0.005 1.485
0.005 1.490
0.050 1.540
0.020 1.560
0.020 1.580
0.015 1.595
0.010 1.605
0.005 1.610
0.005 1.615
0.020 1.635
0.010 1.645
0.015 1.660
0.015 1.675
0.015 1.690
0.015 1.705
0.015 1.720
0.010 1.730
0.010 1.740
0.015 1.755
0.010 1.765
0.020 1.785
0.015 1.800
0.050 1.850
0.060 1.910
0.025 1.935
0.010 1.945
0.025 1.970
0.010 1.980
0.010 1.990
0.010 2.000
0.010 2.010
0.015 2.025
0.020 2.045
0.040 2.085
0.015 2.100
0.020 2.120
0.055 2.175
0.080 2.255
0.005 2.260
0.005 2.265
0.060 2.325
0.020 2.345
0.010 2.355
0.060 2.415
0.020 2.435
0.030 2.465
0.020 2.485
0.020 2.505
0.030 2.535
0.040 2.575
0.010 2.585
0.030 2.615
0.020 2.635
0.130 2.765
0.210 2.975
0.040 3.015
0.060 3.075
0.020 3.095
0.010 3.105

0.020 3.125
0.015 3.140
0.070 3.210
0.020 3.230
0.010 3.240
0.030 3.270
0.030 3.300
0.065 3.365
0.040 3.405
0.040 3.445
0.080 3.525
0.040 3.565
0.065 3.630
0.040 3.670
0.050 3.720
0.040 3.760
0.080 3.840
0.090 3.930
0.010 3.940
0.005 3.945
0.015 3.960
0.080 4.040
0.015 4.055
0.015 4.070
0.015 4.085
0.020 4.105
0.020 4.125
0.015 4.140
0.150 4.290
0.015 4.305
0.030 4.335
0.015 4.350
0.040 4.390
0.030 4.420
0.010 4.430
0.050 4.480
0.020 4.500
0.040 4.540
0.010 4.550
0.015 4.565
0.010 4.575
0.030 4.605
0.060 4.665
0.010 4.675
0.050 4.725
0.030 4.755
0.020 4.775
0.015 4.790
0.035 4.825
0.010 4.835
0.020 4.855
0.040 4.895
0.020 4.915
0.050 4.965
0.060 5.025
0.020 5.045
0.040 5.085
0.030 5.115
0.030 5.145
0.040 5.185
0.030 5.215
0.010 5.225
0.010 5.235
0.040 5.275
0.030 5.305
0.070 5.375
0.010 5.385
0.020 5.405
0.025 5.430
0.025 5.455
0.120 5.575
0.040 5.615
0.120 5.735
0.070 5.805

0.100 5.905
0.020 5.925
0.080 6.005
0.100 6.105
0.120 6.225
0.070 6.295
0.070 6.365
0.060 6.425
0.120 6.545
0.100 6.645
0.040 6.685
0.070 6.755
0.050 6.805
0.050 6.855
0.060 6.915
0.030 6.945
0.040 6.985
0.280 7.265
0.110 7.375
0.160 7.535
0.080 7.615
0.030 7.645
0.030 7.675
0.120 7.795
0.030 7.825
0.030 7.855
0.040 7.895
0.040 7.935
0.065 8.000
0.035 8.035
0.050 8.085
0.100 8.185
0.005 8.190
0.010 8.200
0.150 8.350
0.070 8.420
0.120 8.540
0.030 8.570
0.050 8.620
0.060 8.680
0.200 8.880
0.040 8.920
0.090 9.010
0.080 9.090
0.050 9.140
0.070 9.210
0.070 9.280
0.040 9.320
0.040 9.360
0.200 9.560
0.010 9.570
0.020 9.590
0.060 9.650
0.140 9.790
0.150 9.940
0.180 10.120
0.520 10.640
0.160 10.800
0.240 11.040
0.140 11.180
0.570 11.750
0.650 12.400
1.100 13.500
1.000 14.500
0.770 15.270
0.300 15.570
2.800 18.370
0.250 18.620
0.200 18.820
1.500 20.320
0.400 20.720
0.220 20.940
0.170 21.110
0.170 21.280

0.400 21.680
0.900 22.580
0.300 22.880
2.000 24.880
0.320 25.200
0.600 25.800
0.450 26.250
0.750 27.000
0.950 27.950
0.200 28.150
0.400 28.550
0.550 29.100
0.250 29.350
0.400 29.750
0.100 29.850
0.180 30.030
0.200 30.230
0.130 30.360
0.300 30.660
0.400 31.060
0.250 31.310
0.350 31.660
1.700 33.360
1.400 34.760
2.400 37.160
0.800 37.960
0.280 38.240
0.400 38.640
0.700 39.340
0.600 39.940
0.700 40.640
0.700 41.340
0.400 41.740
2.000 43.740
0.600 44.340
0.600 44.940
0.300 45.240
0.320 45.560
0.120 45.680
0.240 45.920
0.600 46.520

NW
NO(0.9)
0.010 0.010
0.010 0.020
0.010 0.030
0.005 0.035
0.005 0.040
0.005 0.045
0.010 0.055
0.010 0.065
0.010 0.075
0.005 0.080
0.010 0.090
0.005 0.095
0.005 0.100
0.015 0.115
0.010 0.125
0.015 0.140
0.005 0.145
0.010 0.155
0.005 0.160
0.005 0.165
0.020 0.185
0.010 0.195
0.005 0.200
0.020 0.220
0.020 0.240
0.020 0.260
0.005 0.265
0.010 0.275
0.010 0.285
0.030 0.315

0.005 0.320
0.020 0.340
0.025 0.365
0.025 0.390
0.025 0.415
0.010 0.425
0.010 0.435
0.005 0.440
0.005 0.445
0.015 0.460
0.005 0.465
0.005 0.470
0.025 0.495
0.020 0.515
0.005 0.520
0.005 0.525
0.010 0.535
0.010 0.545
0.020 0.565
0.035 0.600
0.010 0.610
0.020 0.630
0.025 0.655
0.010 0.665
0.025 0.690
0.010 0.700
0.010 0.710
0.010 0.720
0.010 0.730
0.005 0.735
0.005 0.740
0.005 0.745
0.005 0.750
0.010 0.760
0.020 0.780
0.010 0.790
0.005 0.795
0.005 0.800
0.005 0.805
0.020 0.825
0.010 0.835
0.020 0.855
0.010 0.865
0.010 0.875
0.040 0.915
0.030 0.945
0.025 0.970
0.010 0.980
0.005 0.985
0.010 0.995
0.015 1.010
0.015 1.025
0.020 1.045
0.005 1.050
0.010 1.060
0.010 1.070
0.010 1.080
0.010 1.090
0.005 1.095
0.025 1.120
0.035 1.155
0.020 1.175
0.015 1.190
0.020 1.210
0.020 1.230
0.020 1.250
0.025 1.275
0.020 1.295
0.010 1.305
0.030 1.335
0.030 1.365
0.025 1.390
0.030 1.420
0.025 1.445

0.030 1.475
0.030 1.505
0.035 1.540
0.015 1.555
0.020 1.575
0.020 1.595
0.015 1.610
0.015 1.625
0.015 1.640
0.010 1.650
0.015 1.665
0.010 1.675
0.015 1.690
0.020 1.710
0.015 1.725
0.015 1.740
0.020 1.760
0.010 1.770
0.010 1.780
0.020 1.800
0.020 1.820
0.015 1.835
0.005 1.840
0.020 1.860
0.015 1.875
0.020 1.895
0.020 1.915
0.005 1.920
0.015 1.935
0.015 1.950
0.020 1.970
0.020 1.990
0.030 2.020
0.030 2.050
0.030 2.080
0.020 2.100
0.025 2.125
0.040 2.165
0.060 2.225
0.040 2.265
0.030 2.295
0.040 2.335
0.030 2.365
0.030 2.395
0.030 2.425
0.050 2.475
0.040 2.515
0.010 2.525
0.030 2.555
0.010 2.565
0.030 2.595
0.040 2.635
0.040 2.675
0.030 2.705
0.035 2.740
0.025 2.765
0.020 2.785
0.035 2.820
0.015 2.835
0.020 2.855
0.045 2.900
0.035 2.935
0.025 2.960
0.020 2.980
0.060 3.040
0.035 3.075
0.045 3.120
0.025 3.145
0.020 3.165
0.030 3.195
0.025 3.220
0.045 3.265
0.025 3.290
0.010 3.300

0.010 3.310
0.015 3.325
0.015 3.340
0.020 3.360
0.015 3.375
0.010 3.385
0.015 3.400
0.010 3.410
0.020 3.430
0.010 3.440
0.030 3.470
0.010 3.480
0.050 3.530
0.020 3.550
0.025 3.575
0.035 3.610
0.040 3.650
0.015 3.665
0.050 3.715
0.010 3.725
0.010 3.735
0.040 3.775
0.010 3.785
0.020 3.805
0.060 3.865
0.025 3.890
0.010 3.900
0.025 3.925
0.040 3.965
0.030 3.995
0.030 4.025
0.040 4.065
0.040 4.105
0.010 4.115
0.010 4.125
0.015 4.140
0.040 4.180
0.040 4.220
0.030 4.250
0.040 4.290
0.010 4.300
0.020 4.320
0.100 4.420
0.030 4.450
0.030 4.480
0.060 4.540
0.045 4.585
0.035 4.620
0.010 4.630
0.015 4.645
0.180 4.825
0.200 5.025
0.025 5.050
0.050 5.100
0.055 5.155
0.075 5.230
0.105 5.335
0.085 5.420
0.075 5.495
0.040 5.535
0.060 5.595
0.010 5.605
0.110 5.715
0.270 5.985
0.100 6.085
0.750 6.835
0.180 7.015
0.530 7.545
0.070 7.615
0.060 7.675
0.650 8.325
0.600 8.925
0.350 9.275
0.250 9.525

0.450 9.975
0.150 10.125
0.100 10.225
0.050 10.275
0.050 10.325
0.110 10.435
0.050 10.485
0.350 10.835
0.650 11.485
0.320 11.805
0.170 11.975
0.200 12.175
0.150 12.325
0.030 12.355
0.200 12.555
0.450 13.005
0.050 13.055
0.050 13.105
0.150 13.255
0.600 13.855
0.160 14.015
0.090 14.105
0.500 14.605
1.100 15.705
0.400 16.105
0.250 16.355
0.050 16.405
1.100 17.505
0.420 17.925
0.370 18.295
0.250 18.545
0.370 18.915
0.240 19.155
0.330 19.485
0.460 19.945
0.460 20.405
0.400 20.805
0.300 21.105
0.450 21.555
0.050 21.605
0.050 21.655
0.400 22.055
2.000 24.055
0.240 24.295
1.000 25.295
0.200 25.495
0.200 25.695
0.070 25.765
2.450 28.215
0.150 28.365
2.000 30.365
0.320 30.685
1.100 31.785
0.700 32.485
0.620 33.105
0.400 33.505
1.000 34.505
2.900 37.405
0.300 37.705
1.600 39.305
0.300 39.605
5.800 45.405
0.960 46.365
3.500 49.865
1.480 51.345
0.450 51.795
0.150 51.945
0.120 52.065
0.180 52.245

WC33a
SE
NO(0.2)
14(0.2)
0.014286 0.014286
0.014286 0.028571
0.014286 0.042857
0.014286 0.057143
0.014286 0.071429
0.014286 0.085714
0.014286 0.100000
0.014286 0.114286
0.014286 0.128571
0.014286 0.142857
0.014286 0.157143
0.014286 0.171429
0.014286 0.185714
0.014286 0.200000
21(0.2)
0.009524 0.209524
0.009524 0.219048
0.009524 0.228571
0.009524 0.238095
0.009524 0.247619
0.009524 0.257143
0.009524 0.266667
0.009524 0.276190
0.009524 0.285714
0.009524 0.295238
0.009524 0.304762
0.009524 0.314286
0.009524 0.323810
0.009524 0.333333
0.009524 0.342857
0.009524 0.352381
0.009524 0.361905
0.009524 0.371429
0.009524 0.380952
0.009524 0.390476
0.009524 0.400000
14(0.2)
0.014286 0.414286
0.014286 0.428571
0.014286 0.442857
0.014286 0.457143
0.014286 0.471429
0.014286 0.485714
0.014286 0.500000
0.014286 0.514286
0.014286 0.528571
0.014286 0.542857
0.014286 0.557143
0.014286 0.571429
0.014286 0.585714
0.014286 0.600000
19(0.2)
0.010526 0.610526
0.010526 0.621053
0.010526 0.631579
0.010526 0.642105
0.010526 0.652632
0.010526 0.663158
0.010526 0.673684
0.010526 0.684211
0.010526 0.694737
0.010526 0.705263
0.010526 0.715789
0.010526 0.726316
0.010526 0.736842
0.010526 0.747368
0.010526 0.757895
0.010526 0.768421
0.010526 0.778947
0.010526 0.789474
0.010526 0.800000
16(0.2)
0.012500 0.812500

0.012500 0.825000
0.012500 0.837500
0.012500 0.850000
0.012500 0.862500
0.012500 0.875000
0.012500 0.887500
0.012500 0.900000
0.012500 0.912500
0.012500 0.925000
0.012500 0.937500
0.012500 0.950000
0.012500 0.962500
0.012500 0.975000
0.012500 0.987500
0.012500 1.000000
15(0.2)
0.013333 1.013333
0.013333 1.026667
0.013333 1.040000
0.013333 1.053333
0.013333 1.066667
0.013333 1.080000
0.013333 1.093333
0.013333 1.106667
0.013333 1.120000
0.013333 1.133333
0.013333 1.146667
0.013333 1.160000
0.013333 1.173333
0.013333 1.186667
0.013333 1.200000
15(0.2)
0.013333 1.213333
0.013333 1.226667
0.013333 1.240000
0.013333 1.253333
0.013333 1.266667
0.013333 1.280000
0.013333 1.293333
0.013333 1.306667
0.013333 1.320000
0.013333 1.333333
0.013333 1.346667
0.013333 1.360000
0.013333 1.373333
0.013333 1.386667
0.013333 1.400000
16(0.2)
0.012500 1.412500
0.012500 1.425000
0.012500 1.437500
0.012500 1.450000
0.012500 1.462500
0.012500 1.475000
0.012500 1.487500
0.012500 1.500000
0.012500 1.512500
0.012500 1.525000
0.012500 1.537500
0.012500 1.550000
0.012500 1.562500
0.012500 1.575000
0.012500 1.587500
0.012500 1.600000
18(0.2)
0.011111 1.611111
0.011111 1.622222
0.011111 1.633333
0.011111 1.644444
0.011111 1.655556
0.011111 1.666667
0.011111 1.677778
0.011111 1.688889
0.011111 1.700000

0.011111 1.711111
0.011111 1.722222
0.011111 1.733333
0.011111 1.744444
0.011111 1.755556
0.011111 1.766667
0.011111 1.777778
0.011111 1.788889
0.011111 1.800000
51(0.4)
0.007843 1.807843
0.007843 1.815686
0.007843 1.823529
0.007843 1.831373
0.007843 1.839216
0.007843 1.847059
0.007843 1.854902
0.007843 1.862745
0.007843 1.870588
0.007843 1.878431
0.007843 1.886275
0.007843 1.894118
0.007843 1.901961
0.007843 1.909804
0.007843 1.917647
0.007843 1.925490
0.007843 1.933333
0.007843 1.941176
0.007843 1.949020
0.007843 1.956863
0.007843 1.964706
0.007843 1.972549
0.007843 1.980392
0.007843 1.988235
0.007843 1.996078
0.007843 2.003922
0.007843 2.011765
0.007843 2.019608
0.007843 2.027451
0.007843 2.035294
0.007843 2.043137
0.007843 2.050980
0.007843 2.058824
0.007843 2.066667
0.007843 2.074510
0.007843 2.082353
0.007843 2.090196
0.007843 2.098039
0.007843 2.105882
0.007843 2.113725
0.007843 2.121569
0.007843 2.129412
0.007843 2.137255
0.007843 2.145098
0.007843 2.152941
0.007843 2.160784
0.007843 2.168627
0.007843 2.176471
0.007843 2.184314
0.007843 2.192157
0.007843 2.200000
49(0.4)
0.008163 2.208163
0.008163 2.216327
0.008163 2.224490
0.008163 2.232653
0.008163 2.240816
0.008163 2.248980
0.008163 2.257143
0.008163 2.265306
0.008163 2.273469
0.008163 2.281633
0.008163 2.289796
0.008163 2.297959

0.008163 2.306122
0.008163 2.314286
0.008163 2.322449
0.008163 2.330612
0.008163 2.338776
0.008163 2.346939
0.008163 2.355102
0.008163 2.363265
0.008163 2.371429
0.008163 2.379592
0.008163 2.387755
0.008163 2.395918
0.008163 2.404082
0.008163 2.412245
0.008163 2.420408
0.008163 2.428571
0.008163 2.436735
0.008163 2.444898
0.008163 2.453061
0.008163 2.461224
0.008163 2.469388
0.008163 2.477551
0.008163 2.485714
0.008163 2.493878
0.008163 2.502041
39(0.4)
0.010256 3.010256
0.010256 3.020513
0.010256 3.030769
0.010256 3.041026
0.010256 3.051282
0.010256 3.061538
0.010256 3.071795
0.010256 3.082051
0.010256 3.092308
0.010256 3.102564
0.010256 3.112821
0.010256 3.123077
0.010256 3.133333
0.010256 3.143590
0.010256 3.153846
0.010256 3.164103
0.010256 3.174359
0.010256 3.184615
0.010256 3.194872
0.010256 3.205128
0.010256 3.215385
0.010256 3.225641
0.010256 3.235897
0.010256 3.246154
0.010256 3.256410
0.010256 3.266667
0.010256 3.276923
0.010256 3.287179
0.010256 3.297436
0.010256 3.307692
0.010256 3.317949
0.010256 3.328205
0.010256 3.338462
0.010256 3.348718
0.010256 3.358974
0.010256 3.369231
0.010256 3.379487
0.010256 3.389744
0.010256 3.400000
48(0.4)
0.008333 3.408333
0.008333 3.416667
0.008333 3.425000
0.008333 3.433333
0.008333 3.441667
0.008333 3.450000
0.008333 3.458333
0.008333 3.466667
0.008333 3.475000

0.006667 2.846667
0.006667 2.853333
0.006667 2.860000
0.006667 2.866667
0.006667 2.873333
0.006667 2.880000
0.006667 2.886667
0.006667 2.893333
0.006667 2.900000
0.006667 2.906667
0.006667 2.913333
0.006667 2.920000
0.006667 2.926667
0.006667 2.933333
0.006667 2.940000
0.006667 2.946667
0.006667 2.953333
0.006667 2.960000
0.006667 2.966667
0.006667 2.973333
0.006667 2.980000
0.006667 2.986667
0.006667 2.993333
0.006667 3.000000
39(0.4)
0.010256 3.010256
0.010256 3.020513
0.010256 3.030769
0.010256 3.041026
0.010256 3.051282
0.010256 3.061538
0.010256 3.071795
0.010256 3.082051
0.010256 3.092308
0.010256 3.102564
0.010256 3.112821
0.010256 3.123077
0.010256 3.133333
0.010256 3.143590
0.010256 3.153846
0.010256 3.164103
0.010256 3.174359
0.010256 3.184615
0.010256 3.194872
0.010256 3.205128
0.010256 3.215385
0.010256 3.225641
0.010256 3.235897
0.010256 3.246154
0.010256 3.256410
0.010256 3.266667
0.010256 3.276923
0.010256 3.287179
0.010256 3.297436
0.010256 3.307692
0.010256 3.317949
0.010256 3.328205
0.010256 3.338462
0.010256 3.348718
0.010256 3.358974
0.010256 3.369231
0.010256 3.379487
0.010256 3.389744
0.010256 3.400000
48(0.4)
0.008333 3.408333
0.008333 3.416667
0.008333 3.425000
0.008333 3.433333
0.008333 3.441667
0.008333 3.450000
0.008333 3.458333
0.008333 3.466667
0.008333 3.475000

0.008333 3.483333
0.008333 3.491667
0.008333 3.500000
0.008333 3.508333
0.008333 3.516667
0.008333 3.525000
0.008333 3.533333
0.008333 3.541667
0.008333 3.550000
0.008333 3.558333
0.008333 3.566667
0.008333 3.575000
0.008333 3.583333
0.008333 3.591667
0.008333 3.600000
0.008333 3.608333
0.008333 3.616667
0.008333 3.625000
0.008333 3.633333
0.008333 3.641667
0.008333 3.650000
0.008333 3.658333
0.008333 3.666667
0.008333 3.675000
0.008333 3.683333
0.008333 3.691667
0.008333 3.700000
0.008333 3.708333
0.008333 3.716667
0.008333 3.725000
0.008333 3.733333
0.008333 3.741667
0.008333 3.750000
0.008333 3.758333
0.008333 3.766667
0.008333 3.775000
0.008333 3.783333
0.008333 3.791667
0.008333 3.800000
53(0.4)
0.007547 3.807547
0.007547 3.815094
0.007547 3.822642
0.007547 3.830189
0.007547 3.837736
0.007547 3.845283
0.007547 3.852830
0.007547 3.860377
0.007547 3.867925
0.007547 3.875472
0.007547 3.883019
0.007547 3.890566
0.007547 3.898113
0.007547 3.905660
0.007547 3.913208
0.007547 3.920755
0.007547 3.928302
0.007547 3.935849
0.007547 3.943396
0.007547 3.950943
0.007547 3.958491
0.007547 3.966038
0.007547 3.973585
0.007547 3.981132
0.007547 3.988679
0.007547 3.996226
0.007547 4.003774
0.007547 4.011321
0.007547 4.018868
0.007547 4.026415
0.007547 4.033962
0.007547 4.041509
0.007547 4.049057
0.007547 4.056604

0.007547 4.064151
0.007547 4.071698
0.007547 4.079245
0.007547 4.086792
0.007547 4.094340
0.007547 4.101887
0.007547 4.109434
0.007547 4.116981
0.007547 4.124528
0.007547 4.132075
0.007547 4.139623
0.007547 4.147170
0.007547 4.154717
0.007547 4.162264
0.007547 4.169811
0.007547 4.177358
0.007547 4.184906
0.007547 4.192453
0.007547 4.200000
40(0.4)
0.010000 4.210000
0.010000 4.220000
0.010000 4.230000
0.010000 4.240000
0.010000 4.250000
0.010000 4.260000
0.010000 4.270000
0.010000 4.280000
0.010000 4.290000
0.010000 4.300000
0.010000 4.310000
0.010000 4.320000
0.010000 4.330000
0.010000 4.340000
0.010000 4.350000
0.010000 4.360000
0.010000 4.370000
0.010000 4.380000
0.010000 4.390000
0.010000 4.400000
0.010000 4.410000
0.010000 4.420000
0.010000 4.430000
0.010000 4.440000
0.010000 4.450000
0.010000 4.460000
0.010000 4.470000
0.010000 4.480000
0.010000 4.490000
0.010000 4.500000
0.010000 4.510000
0.010000 4.520000
0.010000 4.530000
0.010000 4.540000
0.010000 4.550000
0.010000 4.560000
0.010000 4.570000
0.010000 4.580000
0.010000 4.590000
0.010000 4.600000
38(0.4)
0.010526 4.610526
0.010526 4.621053
0.010526 4.631579
0.010526 4.642105
0.010526 4.652632
0.010526 4.663158
0.010526 4.673684
0.010526 4.684211
0.010526 4.694737
0.010526 4.705263
0.010526 4.715789
0.010526 4.726316
0.010526 4.736842

0.010526 4.747368
0.010526 4.757895
0.010526 4.768421
0.010526 4.778947
0.010526 4.789474
0.010526 4.800000
0.010526 4.810526
0.010526 4.821053
0.010526 4.831579
0.010526 4.842105
0.010526 4.852632
0.010526 4.863158
0.010526 4.873684
0.010526 4.884211
0.010526 4.894737
0.010526 4.905263
0.010526 4.915789
0.010526 4.926316
0.010526 4.936842
0.010526 4.947368
0.010526 4.957895
0.010526 4.968421
0.010526 4.978947
0.010526 4.989474
0.010526 5.000000
38(0.4)
0.010526 5.010526
0.010526 5.021053
45(0.4)
0.010526 5.031579
0.010526 5.042105
0.010526 5.052632
0.010526 5.063158
0.010526 5.073684
0.010526 5.084211
0.010526 5.094737
0.010526 5.105263
0.010526 5.115789
0.010526 5.126316
0.010526 5.136842
0.010526 5.147368
0.010526 5.157895
0.010526 5.168421
0.010526 5.178947
0.010526 5.189474
0.010526 5.200000
0.010526 5.210526
0.010526 5.221053
0.010526 5.231579
0.010526 5.242105
0.010526 5.252632
0.010526 5.263158
0.010526 5.273684
0.010526 5.284211
0.010526 5.294737
0.010526 5.305263
0.010526 5.315789
0.010526 5.326316
0.010526 5.336842
0.010526 5.347368
0.010526 5.357895
0.010526 5.368421
0.010526 5.378947
0.010526 5.389474
0.010526 5.400000
36(0.4)
0.011111 5.411111
0.011111 5.422222
0.011111 5.433333
0.011111 5.444444
0.011111 5.455556
0.011111 5.466667
0.011111 5.477778
0.011111 5.488889
0.011111 5.500000

0.011111 5.511111
0.011111 5.522222
0.011111 5.533333
0.011111 5.544444
0.011111 5.555556
0.011111 5.566667
0.011111 5.577778
0.011111 5.588889
0.011111 5.600000
0.011111 5.611111
0.011111 5.622222
0.011111 5.633333
0.011111 5.644444
0.011111 5.655556
0.011111 5.666667
0.011111 5.677778
0.011111 5.688889
0.011111 5.700000
0.011111 5.711111
0.011111 5.722222
0.011111 5.733333
0.011111 5.744444
0.011111 5.755556
0.011111 5.766667
0.011111 5.777778
0.011111 5.788889
0.011111 5.800000
45(0.4)
0.008889 5.808889
0.008889 5.817778
0.008889 5.826667
0.008889 5.835556
0.008889 5.844444
0.008889 5.853333
0.008889 5.862222
0.008889 5.871111
0.008889 5.880000
0.008889 5.888889
0.008889 5.897778
0.008889 5.906667
0.008889 5.915556
0.008889 5.924444
0.008889 5.933333
0.008889 5.942222
0.008889 5.951111
0.008889 5.960000
0.008889 5.968889
0.008889 5.977778
0.008889 5.986667
0.008889 5.995556
0.008889 6.004444
0.008889 6.013333
0.008889 6.022222
0.008889 6.031111
0.008889 6.040000
0.008889 6.048889
0.008889 6.057778
0.008889 6.066667
0.008889 6.075556
0.008889 6.084444
0.008889 6.093333
0.008889 6.102222
0.008889 6.111111
0.008889 6.120000
0.008889 6.128889
0.008889 6.137778
0.008889 6.146667
0.008889 6.155556
0.008889 6.164444
0.008889 6.173333
0.008889 6.182222
0.008889 6.191111
0.008889 6.200000
40(0.4)

0.010000 6.210000
0.010000 6.220000
0.010000 6.230000
0.010000 6.240000
0.010000 6.250000
0.010000 6.260000
0.010000 6.270000
0.010000 6.280000
0.010000 6.290000
0.010000 6.300000
0.010000 6.310000
0.010000 6.320000
0.010000 6.330000
0.010000 6.340000
0.010000 6.350000
0.010000 6.360000
0.010000 6.370000
0.010000 6.380000
0.010000 6.390000
0.010000 6.400000
0.010000 6.410000
0.010000 6.420000
0.010000 6.430000
0.010000 6.440000
0.010000 6.450000
0.010000 6.460000
0.010000 6.470000
0.010000 6.480000
0.010000 6.490000
0.010000 6.500000
0.010000 6.510000
0.010000 6.520000
0.010000 6.530000
0.010000 6.540000
0.010000 6.550000
0.010000 6.560000
0.010000 6.570000
0.010000 6.580000
0.010000 6.590000
0.010000 6.600000
43(0.4)
0.009302 6.609302
0.009302 6.618605
0.009302 6.627907
0.009302 6.637209
0.009302 6.646512
40(0.4)
0.009302 6.655814
0.009302 6.665116
0.009302 6.674419
0.009302 6.683721
0.009302 6.693023
0.009302 6.702326
0.009302 6.711628
0.009302 6.720930
0.009302 6.730233
0.009302 6.739535
0.009302 6.748837
0.009302 6.758140
0.009302 6.767442
0.009302 6.776744
0.009302 6.786047
0.009302 6.795349
0.009302 6.804651
0.009302 6.813953
0.009302 6.823256
0.009302 6.832558
0.009302 6.841860
0.009302 6.851163
0.009302 6.860465
0.009302 6.869767
0.009302 6.879070
0.009302 6.888372
0.009302 6.897674
0.009302 6.906977

0.009302 6.916279
0.009302 6.925581
0.009302 6.934884
0.009302 6.944186
0.009302 6.953488
0.009302 6.962791
0.009302 6.972093
0.009302 6.981395
0.009302 6.990698
0.009302 7.000000
34(0.4)
0.011765 7.011765
0.011765 7.023529
0.011765 7.035294
0.011765 7.047059
0.011765 7.058824
0.011765 7.070588
0.011765 7.082353
0.011765 7.094118
0.011765 7.105882
0.011765 7.117647
0.011765 7.129412
0.011765 7.141176
0.011765 7.152941
0.011765 7.164706
0.011765 7.176471
0.011765 7.188235
0.011765 7.200000
0.011765 7.211765
0.011765 7.223529
0.011765 7.235294
0.011765 7.247059
0.011765 7.258824
0.011765 7.270588
0.011765 7.282353
0.011765 7.294118
0.011765 7.305882
0.011765 7.317647
0.011765 7.329412
0.011765 7.341176
0.011765 7.352941
0.011765 7.364706
0.011765 7.376471
0.011765 7.388235
0.011765 7.400000
40(0.4)
0.010000 7.410000
0.010000 7.420000
0.010000 7.430000
0.010000 7.440000
0.010000 7.450000
0.010000 7.460000
0.010000 7.470000
0.010000 7.480000
0.010000 7.490000
0.010000 7.500000
0.010000 7.510000
0.010000 7.520000
0.010000 7.530000
0.010000 7.540000
0.010000 7.550000
0.010000 7.560000
0.010000 7.570000
0.010000 7.580000
0.010000 7.590000
0.010000 7.600000
0.010000 7.610000
0.010000 7.620000
0.010000 7.630000
0.010000 7.640000
0.010000 7.650000
0.010000 7.660000
0.010000 7.670000
0.010000 7.680000

0.010000 7.690000
0.010000 7.700000
0.010000 7.710000
0.010000 7.720000
0.010000 7.730000
0.010000 7.740000
0.010000 7.750000
0.010000 7.760000
0.010000 7.770000
0.010000 7.780000
0.010000 7.790000
0.010000 7.800000
46(0.4)
0.008696 7.808696
0.008696 7.817391
0.008696 7.826087
0.008696 7.834783
0.008696 7.843478
0.008696 7.852174
0.008696 7.860870
0.008696 7.869565
0.008696 7.878261
0.008696 7.886957
0.008696 7.895652
0.008696 7.904348
0.008696 7.913043
0.008696 7.921739
0.008696 7.930435
0.008696 7.939130
0.008696 7.947826
0.008696 7.956522
0.008696 7.965217
0.008696 7.973913
0.008696 7.982609
0.008696 7.991304
0.008696 8.000000
0.008696 8.008696
0.008696 8.017391
0.008696 8.026087
0.008696 8.034783
0.008696 8.043478
0.008696 8.052174
0.008696 8.060870
0.008696 8.069565
0.008696 8.078261
0.008696 8.086957
0.008696 8.095652
0.008696 8.104348
0.008696 8.113043
0.008696 8.121739
0.008696 8.130435
0.008696 8.139130
0.008696 8.147826
0.008696 8.156522
0.008696 8.165217
0.008696 8.173913
0.008696 8.182609
0.008696 8.191304
0.008696 8.200000
43(0.4)
0.009302 8.209302
0.009302 8.218605
0.009302 8.227907
0.009302 8.237209
0.009302 8.246512
0.009302 8.255814
0.009302 8.265116
0.009302 8.274419
0.009302 8.283721
0.009302 8.293023
0.009302 8.302326
0.009302 8.311628
0.009302 8.320930
0.009302 8.330233

0.009302 8.339535
0.009302 8.348837
0.009302 8.358140
0.009302 8.367442
0.009302 8.376744
0.009302 8.386047
0.009302 8.395349
0.009302 8.404651
0.009302 8.413953
0.009302 8.423256
0.009302 8.432558
54(0.4)
0.009302 8.441860
0.009302 8.451163
0.009302 8.460465
0.009302 8.469767
0.009302 8.479070
0.009302 8.488372
0.009302 8.497674
0.009302 8.506977
0.009302 8.516279
0.009302 8.525581
0.009302 8.534884
0.009302 8.544186
0.009302 8.553488
0.009302 8.562791
0.009302 8.572093
0.009302 8.581395
0.009302 8.590698
0.009302 8.600000
54(0.4)
0.007407 8.607407
0.007407 8.614815
0.007407 8.622222
0.007407 8.629630
0.007407 8.637037
0.007407 8.644444
0.007407 8.651852
0.007407 8.659259
0.007407 8.666667
0.007407 8.674074
0.007407 8.681481
0.007407 8.688889
0.007407 8.696296
0.007407 8.703704
0.007407 8.711111
0.007407 8.718519
0.007407 8.725926
0.007407 8.733333
0.007407 8.740741
0.007407 8.748148
0.007407 8.755556
0.007407 8.762963
0.007407 8.770370
0.007407 8.777778
0.007407 8.785185
0.007407 8.792593
0.007407 8.800000
0.007407 8.807407
0.007407 8.814815
0.007407 8.822222
0.007407 8.829630
0.007407 8.837037
0.007407 8.844444
0.007407 8.851852
0.007407 8.859259
0.007407 8.866667
65(0.4)
0.006154 9.406154
0.006154 9.412308
0.006154 9.418462
0.006154 9.424615
0.006154 9.430769
0.006154 9.436923
0.006154 9.443077
0.006154 9.449231

0.007407 8.933333
0.007407 8.940741
0.007407 8.948148
0.007407 8.955556
0.007407 8.962963
0.007407 8.970370
0.007407 8.977778
0.007407 8.985185
0.007407 8.992593
0.007407 9.000000
54(0.4)
0.007407 9.007407
0.007407 9.014815
0.007407 9.022222
0.007407 9.029630
0.007407 9.037037
0.007407 9.044444
0.007407 9.051852
0.007407 9.059259
0.007407 9.066667
0.007407 9.074074
0.007407 9.081481
0.007407 9.088889
0.007407 9.096296
0.007407 9.103704
0.007407 9.111111
0.007407 9.118519
0.007407 9.125926
0.007407 9.133333
0.007407 9.140741
0.007407 9.148148
0.007407 9.155556
0.007407 9.162963
0.007407 9.170370
0.007407 9.177778
0.007407 9.185185
0.007407 9.192593
0.007407 9.200000
0.007407 9.207407
0.007407 9.214815
0.007407 9.222222
0.007407 9.229630
0.007407 9.237037
0.007407 9.244444
0.007407 9.251852
0.007407 9.259259
0.007407 9.266667
0.007407 9.274074
0.007407 9.281481
0.007407 9.288889
0.007407 9.296296
0.007407 9.303704
0.007407 9.311111
0.007407 9.318519
0.007407 9.325926
0.007407 9.333333
0.007407 9.340741
0.007407 9.348148
72(0.4)
0.005556 9.805556
0.005556 9.811111
0.005556 9.816667
0.005556 9.822222
0.005556 9.827778
0.005556 9.833333
0.005556 9.838889
0.005556 9.844444
0.005556 9.850000
0.005556 9.855556
0.005556 9.861111
0.005556 9.866667
0.005556 9.872222
0.005556 9.877778
0.005556 9.883333
0.005556 9.888889

0.006154 9.455385
0.006154 9.461538
0.006154 9.467692
0.006154 9.473846
0.006154 9.480000
0.006154 9.486154
0.006154 9.492308
0.006154 9.498462
0.006154 9.504615
0.006154 9.510769
0.006154 9.516923
0.006154 9.523077
0.006154 9.529231
0.006154 9.535385
0.006154 9.541538
0.006154 9.547692
0.006154 9.553846
0.006154 9.560000
0.006154 9.566154
0.006154 9.572308
0.006154 9.578462
0.006154 9.584615
0.006154 9.590769
0.006154 9.596923
0.006154 9.603077
0.006154 9.609231
0.006154 9.615385
0.006154 9.621538
0.006154 9.627692
0.006154 9.633846
0.006154 9.640000
0.006154 9.646154
0.006154 9.652308
0.006154 9.658462
0.006154 9.664615
0.006154 9.670769
0.006154 9.676923
0.006154 9.683077
0.006154 9.689231
0.006154 9.695385
0.006154 9.701538
0.006154 9.707692
0.006154 9.713846
0.006154 9.720000
0.006154 9.726154
0.006154 9.732308
0.006154 9.738462
0.006154 9.744615
0.006154 9.750769
0.006154 9.756923
0.006154 9.763077
0.006154 9.769231
0.006154 9.775385
0.006154 9.781538
0.006154 9.787692
0.006154 9.793846
0.006154 9.800000
65(0.4)
0.006154 10.206154
0.006154 10.212308
0.006154 10.218462
0.006154 10.224615
0.006154 10.230769
0.006154 10.236923
0.006154 10.243077
0.006154 10.249231
0.006154 10.255385
0.006154 10.261538
0.006154 10.267692
0.006154 10.273846
0.006154 10.280000
0.006154 10.286154
0.006154 10.292308
0.006154 10.298462
0.006154 10.304615

0.006154 9.894444
0.005556 9.900000
0.005556 9.905556
0.005556 9.911111
0.005556 9.916667
0.005556 9.922222
0.005556 9.927778
0.005556 9.933333
0.005556 9.938889
0.005556 9.944444
0.005556 9.950000
0.005556 9.955556
0.005556 9.961111
0.005556 9.966667
0.005556 9.972222
0.005556 9.977778
0.005556 9.983333
0.005556 9.988889
0.005556 9.994444
0.005556 10.000000
0.005556 10.005556
0.005556 10.011111
0.005556 10.016667
0.005556 10.022222
0.005556 10.027778
0.005556 10.033333
0.005556 10.038889
0.005556 10.044444
0.005556 10.050000
0.005556 10.055556
0.005556 10.061111
0.005556 10.066667
0.005556 10.072222
0.005556 10.077778
0.005556 10.083333
0.005556 10.088889
0.005556 10.094444
0.005556 10.100000
0.005556 10.105556
0.005556 10.111111
0.005556 10.116667
0.005556 10.122222
0.005556 10.127778
0.005556 10.133333
0.005556 10.138889
0.005556 10.144444
0.005556 10.150000
0.005556 10.155556
0.005556 10.161111
90(0.4)
0.004444 10.604444
0.004444 10.608889
0.004444 10.613333
0.004444 10.617778
0.004444 10.622222
0.004444 10.626667
0.004444 10.631111
0.004444 10.635556
0.004444 10.640000
0.004444 10.644444
0.004444 10.648889
0.004444 10.653333
0.004444 10.657778
0.004444 10.662222
0.004444 10.666667
0.004444 10.671111
79(0.4)
0.005063 11.005063
0.005063 11.010127
0.005063 11.015190
0.005063 11.020253
0.005063 11.025316
0.005063 11.030380
0.005063 11.035443
0.005063 11.040506

0.006154 10.310769
0.006154 10.316923
0.006154 10.323077
0.006154 10.329231
0.006154 10.335385
0.006154 10.341538
0.006154 10.347692
0.006154 10.353846
0.006154 10.360000
0.006154 10.366154
0.006154 10.372308
0.006154 10.378462
0.006154 10.384615
0.006154 10.390769
0.006154 10.396923
0.006154 10.403077
0.006154 10.409231
0.006154 10.415385
0.006154 10.421538
0.006154 10.427692
0.006154 10.433846
0.006154 10.440000
0.006154 10.446154
0.006154 10.452308
0.006154 10.458462
0.006154 10.464615
0.006154 10.470769
0.006154 10.476923
0.006154 10.483077
0.006154 10.489231
0.006154 10.495385
0.006154 10.501538
0.006154 10.507692
0.006154 10.513846
0.006154 10.520000
0.006154 10.526154
0.006154 10.532308
0.006154 10.538462
0.006154 10.544615
0.006154 10.550769
0.006154 10.556923
0.006154 10.563077
0.006154 10.569231
0.006154 10.575385
0.006154 10.581538
0.006154 10.587692
0.006154 10.593846
0.006154 10.600000
90(0.4)
0.004444 10.604444
0.004444 10.608889
0.004444 10.613333
0.004444 10.617778
0.004444 10.622222
0.004444 10.626667
0.004444 10.631111
0.004444 10.635556
0.004444 10.640000
0.004444 10.644444
0.004444 10.648889
0.004444 10.653333
0.004444 10.657778
0.004444 10.662222
0.004444 10.666667
0.004444 10.671111
0.004444 10.675556
0.004444 10.680000
0.004444 10.684444
0.004444 10.688889
0.004444 10.693333
0.004444 10.697778
0.004444 10.702222
0.004444 10.706667
0.004444 10.711111

0.004444 10.715556
0.004444 10.720000
0.004444 10.724444
0.004444 10.728889
0.004444 10.733333
0.004444 10.737778
0.004444 10.742222
0.004444 10.746667
0.004444 10.751111
0.004444 10.755556
0.004444 10.760000
0.004444 10.764444
0.004444 10.768889
0.004444 10.773333
0.004444 10.777778
0.004444 10.782222
0.004444 10.786667
0.004444 10.791111
0.004444 10.795556
0.004444 10.800000
0.004444 10.804444
0.004444 10.808889
0.004444 10.813333
0.004444 10.817778
0.004444 10.822222
0.004444 10.826667
0.004444 10.831111
0.004444 10.835556
0.004444 10.840000
0.004444 10.844444
0.004444 10.848889
0.004444 10.853333
0.004444 10.857778
0.004444 10.862222
0.004444 10.866667
0.004444 10.871111
0.004444 10.875556
0.004444 10.880000
0.004444 10.884444
0.004444 10.888889
0.004444 10.893333
0.004444 10.897778
0.004444 10.902222
0.004444 10.906667
0.004444 10.911111
0.004444 10.915556
0.004444 10.920000
0.004444 10.924444
0.004444 10.928889
0.004444 10.933333
0.004444 10.937778
0.004444 10.942222
0.004444 10.946667
0.004444 10.951111
0.004444 10.955556
0.004444 10.960000
0.004444 10.964444
0.004444 10.968889
0.004444 10.973333
0.004444 10.977778
0.004444 10.982222
0.004444 10.986667
0.004444 10.991111
0.004444 10.995556
0.004444 11.000000

0.005063 11.045570
0.005063 11.050633
0.005063 11.055696
0.005063 11.060759
0.005063 11.065823
0.005063 11.070886
0.005063 11.075949
0.005063 11.081013
0.005063 11.086076
0.005063 11.091139
0.005063 11.096203
0.005063 11.101266
0.005063 11.106329
0.005063 11.111392
0.005063 11.116456
0.005063 11.121519
0.005063 11.126582
0.005063 11.131646
0.005063 11.136709
0.005063 11.141772
0.005063 11.146835
0.005063 11.151899
0.005063 11.156962
0.005063 11.162025
0.005063 11.167089
0.005063 11.172152
0.005063 11.177215
0.005063 11.182278
0.005063 11.187342
0.005063 11.192405
0.005063 11.197468
0.005063 11.202532
0.005063 11.207595
0.005063 11.212658
0.005063 11.217722
0.005063 11.222785
0.005063 11.227848
0.005063 11.232911
0.005063 11.237975
0.005063 11.243038
0.005063 11.248101
0.005063 11.253165
0.005063 11.258228
0.005063 11.263291
0.005063 11.268354
0.005063 11.273418
0.005063 11.278481
0.005063 11.283544
0.005063 11.288608
0.005063 11.293671
0.005063 11.298734
0.005063 11.303797
0.005063 11.308861
0.005063 11.313924
0.005063 11.318987
0.005063 11.324051
0.005063 11.329114
0.005063 11.334177
0.005063 11.339241
0.005063 11.344304
0.005063 11.349367
0.005063 11.354430
0.005063 11.359494
0.005063 11.364557
0.005063 11.369620
0.005063 11.374684
0.005063 11.379747
0.005063 11.384810
0.005063 11.389873
0.005063 11.394937
0.005063 11.400000
74(0.4)
0.005405 11.405405
0.005405 11.410811

0.005405 11.416216
0.005405 11.421622
0.005405 11.427027
0.005405 11.432432
0.005405 11.437838
0.005405 11.443243
0.005405 11.448649
0.005405 11.454054
0.005405 11.459459
0.005405 11.464865
0.005405 11.470270
0.005405 11.475676
0.005405 11.481081
0.005405 11.486486
0.005405 11.491892
0.005405 11.497297
0.005405 11.502703
0.005405 11.508108
0.005405 11.513514
0.005405 11.518919
0.005405 11.524324
0.005405 11.529730
0.005405 11.535135
0.005405 11.540541
0.005405 11.545946
0.005405 11.551351
0.005405 11.556757
0.005405 11.562162
0.005405 11.567568
0.005405 11.572973
0.005405 11.578378
0.005405 11.583784
0.005405 11.589189
0.005405 11.594595
0.005405 11.600000
0.005405 11.605405
0.005405 11.610811
0.005405 11.616216
0.005405 11.621622
0.005405 11.627027
0.005405 11.632432
0.005405 11.637838
0.005405 11.643243
0.005405 11.648649
0.005405 11.654054
0.005405 11.659459
0.005405 11.664865
0.005405 11.670270
0.005405 11.675676
0.005405 11.681081
0.005405 11.686486
0.005405 11.691892
0.005405 11.697297
0.005405 11.702703
0.005405 11.708108
0.005405 11.713514
0.005405 11.718919
0.005405 11.724324
0.005405 11.729730
0.005405 11.735135
0.005405 11.740541
0.005405 11.745946
0.005405 11.751351
0.005405 11.756757
0.005405 11.762162
0.005405 11.767568
0.005405 11.772973
0.005405 11.778378
0.005405 11.783784
0.005405 11.789189
0.005405 11.794595
0.005405 11.800000
74(0.4)
0.005405 11.805405

0.005405 11.810811
0.005405 11.816216
0.005405 11.821622
0.005405 11.827027
0.005405 11.832432
0.005405 11.837838
0.005405 11.843243
0.005405 11.848649
0.005405 11.854054
0.005405 11.859459
0.005405 11.864865
0.005405 11.870270
0.005405 11.875676
0.005405 11.881081
0.005405 11.886486
0.005405 11.891892
0.005405 11.897297
0.005405 11.902703
0.005405 11.908108
0.005405 11.913514
0.005405 11.918919
0.005405 11.924324
0.005405 11.929730
0.005405 11.935135
0.005405 11.940541
0.005405 11.945946
0.005405 11.951351
0.005405 11.956757
0.005405 11.962162
0.005405 11.967568
0.005405 11.972973
0.005405 11.978378
0.005405 11.983784
0.005405 11.989189
0.005405 11.994595
0.005405 12.000000
0.005405 12.005405
0.005405 12.010811
0.005405 12.016216
0.005405 12.021622
0.005405 12.027027
0.005405 12.032432
0.005405 12.037838
0.005405 12.043243
0.005405 12.048649
0.005405 12.054054
0.005405 12.059459
0.005405 12.064865
0.005405 12.070270
0.005405 12.075676
0.005405 12.081081
0.005405 12.086486
0.005405 12.091892
0.005405 12.097297
0.005405 12.102703
0.005405 12.108108
0.005405 12.113514
0.005405 12.118919
0.005405 12.124324
0.005405 12.129730
0.005405 12.135135
0.005405 12.140541
0.005405 12.145946
0.005405 12.151351
0.005405 12.156757
0.005405 12.162162
0.005405 12.167568
0.005405 12.172973
0.005405 12.178378
0.005405 12.183784
0.005405 12.189189
0.005405 12.194595
0.005405 12.200000
69(0.4)

0.005797 12.205797
0.005797 12.211594
0.005797 12.217391
0.005797 12.223188
0.005797 12.228986
0.005797 12.234783
0.005797 12.240580
0.005797 12.246377
0.005797 12.252174
0.005797 12.257971
0.005797 12.263768
0.005797 12.269565
0.005797 12.275362
0.005797 12.281159
0.005797 12.286957
0.005797 12.292754
0.005797 12.298551
0.005797 12.304348
0.005797 12.310145
0.005797 12.315942
0.005797 12.321739
0.005797 12.327536
0.005797 12.333333
0.005797 12.339130
0.005797 12.344928
0.005797 12.350725
0.005797 12.356522
0.005797 12.362319
0.005797 12.368116
0.005797 12.373913
0.005797 12.379710
0.005797 12.385507
0.005797 12.391304
0.005797 12.397101
0.005797 12.402899
0.005797 12.408696
0.005797 12.414493
0.005797 12.420290
0.005797 12.426087
0.005797 12.431884
0.005797 12.437681
0.005797 12.443478
0.005797 12.449275
0.005797 12.455072
0.005797 12.460870
0.005797 12.466667
0.005797 12.472464
0.005797 12.478261
0.005797 12.484058
0.005797 12.489855
0.005797 12.495652
0.005797 12.501449
0.005797 12.507246
0.005797 12.513043
0.005797 12.518841
0.005797 12.524638
0.005797 12.530435
0.005797 12.536232
0.005797 12.542029
0.005797 12.547826
0.005797 12.553623
0.005797 12.559420
0.005797 12.565217
0.005797 12.571014
0.005797 12.576812
0.005797 12.582609
0.005797 12.588406
0.005797 12.594203
0.005797 12.600000
73(0.4)
0.005479 12.605479
0.005479 12.610959
0.005479 12.616438
0.005479 12.621918

0.005479 12.627397
0.005479 12.632877
0.005479 12.638356
0.005479 12.643836
0.005479 12.649315
0.005479 12.654795
0.005479 12.660274
0.005479 12.665753
0.005479 12.671233
0.005479 12.676712
0.005479 12.682192
0.005479 12.687671
0.005479 12.693151
0.005479 12.698630
0.005479 12.704110
0.005479 12.709589
0.005479 12.715068
0.005479 12.720548
0.005479 12.726027
0.005479 12.731507
0.005479 12.736986
0.005479 12.742466
0.005479 12.747945
0.005479 12.753425
0.005479 12.758904
0.005479 12.764384
0.005479 12.769863
0.005479 12.775342
0.005479 12.780822
0.005479 12.786301
0.005479 12.791781
0.005479 12.797260
0.005479 12.802740
0.005479 12.808219
0.005479 12.813699
0.005479 12.819178
0.005479 12.824658
0.005479 12.830137
0.005479 12.835616
0.005479 12.841096
0.005479 12.846575
0.005479 12.852055
0.005479 12.857534
0.005479 12.863014
0.005479 12.868493
0.005479 12.873973
0.005479 12.879452
0.005479 12.884932
0.005479 12.890411
0.005479 12.895890
0.005479 12.901370
0.005479 12.906849
0.005479 12.912329
0.005479 12.917808
0.005479 12.923288
0.005479 12.928767
0.005479 12.934247
0.005479 12.939726
0.005479 12.945205
0.005479 12.950685
0.005479 12.956164
0.005479 12.961644
0.005479 12.967123
0.005479 12.972603
0.005479 12.978082
0.005479 12.983562
0.005479 12.989041
0.005479 12.994521
0.005479 13.000000
76(0.4)
0.005263 13.005263
0.005263 13.010526
0.005263 13.015789
0.005263 13.021053

0.005263 13.026316
0.005263 13.031579
0.005263 13.036842
0.005263 13.042105
0.005263 13.047368
0.005263 13.052632
0.005263 13.057895
0.005263 13.063158
0.005263 13.068421
0.005263 13.073684
0.005263 13.078947
0.005263 13.084211
0.005263 13.089474
0.005263 13.094737
0.005263 13.100000
0.005263 13.105263
0.005263 13.110526
0.005263 13.115789
0.005263 13.121053
0.005263 13.126316
0.005263 13.131579
0.005263 13.136842
0.005263 13.142105
0.005263 13.147368
0.005263 13.152632
0.005263 13.157895
0.005263 13.163158
0.005263 13.168421
0.005263 13.173684
0.005263 13.178947
0.005263 13.184211
0.005263 13.189474
0.005263 13.194737
0.005263 13.200000
0.005263 13.205263
0.005263 13.210526
0.005263 13.215789
0.005263 13.221053
0.005263 13.226316
0.005263 13.231579
0.005263 13.236842
0.005263 13.242105
0.005263 13.247368
0.005263 13.252632
0.005263 13.257895
0.005263 13.263158
0.005263 13.268421
0.005263 13.273684
0.005263 13.278947
0.005263 13.284211
0.005263 13.289474
0.005263 13.294737
0.005263 13.300000
0.005263 13.305263
0.005263 13.310526
0.005263 13.315789
0.005263 13.321053
0.005263 13.326316
0.005263 13.331579
0.005263 13.336842
0.005263 13.342105
0.005263 13.347368
0.005263 13.352632
0.005263 13.357895
0.005263 13.363158
0.005263 13.368421
0.005263 13.373684
0.005263 13.378947
0.005263 13.384211
0.005263 13.389474
0.005263 13.394737
0.005263 13.400000
79(0.4)
0.005063 13.405063

0.005063 13.410127
0.005063 13.415190
0.005063 13.420253
0.005063 13.425316
0.005063 13.430380
70(0.4)
0.005714 13.805714
0.005714 13.811429
0.005714 13.817143
0.005714 13.822857
0.005714 13.828571
0.005714 13.834286
0.005714 13.840000
0.005714 13.845714
0.005714 13.851429
0.005714 13.857143
0.005714 13.862857
0.005714 13.868571
0.005714 13.874286
0.005714 13.880000
0.005714 13.885714
0.005714 13.891429
0.005714 13.897143
0.005714 13.902857
0.005714 13.908571
0.005714 13.914286
0.005714 13.920000
0.005714 13.925714
0.005714 13.931429
0.005714 13.937143
0.005714 13.942857
0.005714 13.948571
0.005714 13.954286
0.005714 13.960000
0.005714 13.965714
0.005714 13.971429
0.005714 13.977143
0.005714 13.982857
0.005714 13.988571
0.005714 13.994286
0.005714 14.000000
0.005714 14.005714
0.005714 14.011429
0.005714 14.017143
0.005714 14.022857
0.005714 14.028571
0.005714 14.034286
0.005714 14.040000
0.005714 14.045714
0.005714 14.051429
0.005714 14.057143
0.005714 14.062857
0.005714 14.068571
0.005714 14.074286
0.005714 14.080000
0.005714 14.085714
0.005714 14.091429
0.005714 14.097143
0.005714 14.102857
0.005714 14.108571
0.005714 14.114286
0.005714 14.120000
0.005714 14.125714
0.005714 14.131429
0.005714 14.137143
0.005714 14.142857
0.005714 14.148571
0.005714 14.154286
0.005714 14.160000
0.005714 14.165714
0.005714 14.171429
0.005714 14.177143
67(0.4)
0.005714 14.182857
0.005714 14.188571
0.005714 14.194286

0.005714 14.200000
68(0.4)
0.005882 14.205882
0.005882 14.211765
0.005882 14.217647
0.005882 14.223529
0.005882 14.229412
0.005882 14.235294
0.005882 14.241176
0.005882 14.247059
0.005882 14.252941
0.005882 14.258824
0.005882 14.264706
0.005882 14.270588
0.005882 14.276471
0.005882 14.282353
0.005882 14.288235
0.005882 14.294118
0.005882 14.300000
0.005882 14.305882
0.005882 14.311765
0.005882 14.317647
0.005882 14.323529
0.005882 14.329412
0.005882 14.335294
0.005882 14.341176
0.005882 14.347059
0.005882 14.352941
0.005882 14.358824
0.005882 14.364706
0.005882 14.370588
0.005882 14.376471
0.005882 14.382353
0.005882 14.388235
0.005882 14.394118
0.005882 14.400000
0.005882 14.405882
0.005882 14.411765
0.005882 14.417647
0.005882 14.423529
0.005882 14.429412
0.005882 14.435294
0.005882 14.441176
0.005882 14.447059
0.005882 14.452941
0.005882 14.458824
0.005882 14.464706
0.005882 14.470588
0.005882 14.476471
0.005882 14.482353
0.005882 14.488235
0.005882 14.494118
0.005882 14.500000
0.005882 14.505882
0.005882 14.511765
0.005882 14.517647
0.005882 14.523529
0.005882 14.529412
0.005882 14.535294
0.005882 14.541176
0.005882 14.547059
0.005882 14.552941
0.005882 14.558824
0.005882 14.564706
0.005882 14.570588
58(0.4)
0.005882 14.576471
0.005882 14.582353
0.005882 14.588235
0.005882 14.594118
0.005882 14.600000
0.005970 14.605970
0.005970 14.611940
0.005970 14.617910

0.005970 14.623881
0.005970 14.629851
0.005970 14.635821
0.005970 14.641791
0.005970 14.647761
0.005970 14.653731
0.005970 14.659701
0.005970 14.665672
0.005970 14.671642
0.005970 14.677612
0.005970 14.683582
0.005970 14.689552
0.005970 14.695522
0.005970 14.701493
0.005970 14.707463
0.005970 14.713433
0.005970 14.719403
0.005970 14.725373
0.005970 14.731343
0.005970 14.737313
0.005970 14.743284
0.005970 14.749254
0.005970 14.755224
0.005970 14.761194
0.005970 14.767164
0.005970 14.773134
0.005970 14.779104
0.005970 14.785075
0.005970 14.791045
0.005970 14.797015
0.005970 14.802985
0.005970 14.808955
0.005970 14.814925
0.005970 14.820896
0.005970 14.826866
0.005970 14.832836
0.005970 14.838806
0.005970 14.844776
0.005970 14.850746
0.005970 14.856716
0.005970 14.862687
0.005970 14.868657
0.005970 14.874627
0.005970 14.880597
0.005970 14.886567
0.005970 14.892537
0.005970 14.898507
0.005970 14.904478
0.005970 14.910448
0.005970 14.916418
0.005970 14.922388
0.005970 14.928358
0.005970 14.934328
0.005970 14.940299
0.005970 14.946269
0.005970 14.952239
0.005970 14.958209
0.005970 14.964179
0.005970 14.970149
0.005970 14.976119
0.005970 14.982090
0.005970 14.988060
0.005970 14.994030
0.005970 15.000000
58(0.4)
0.006897 15.006897
0.006897 15.013793
0.006897 15.020690
0.006897 15.027586
0.006897 15.034483
0.006897 15.041379
0.006897 15.048276
0.006897 15.055172
0.006897 15.062069

0.006897 15.068966
0.006897 15.075862
0.006897 15.082759
0.006897 15.089655
0.006897 15.096552
0.006897 15.103448
0.006897 15.110345
0.006897 15.117241
0.006897 15.124138
0.006897 15.131034
0.006897 15.137931
0.006897 15.144828
0.006897 15.151724
0.006897 15.158621
0.006897 15.165517
0.006897 15.172414
0.006897 15.179310
0.006897 15.186207
0.006897 15.193103
0.006897 15.200000
0.006897 15.206897
0.006897 15.213793
0.006897 15.220690
0.006897 15.227586
0.006897 15.234483
0.006897 15.241379
0.006897 15.248276
0.006897 15.255172
0.006897 15.262069
0.006897 15.268966
0.006897 15.275862
0.006897 15.282759
0.006897 15.289655
0.007018 15.800000
45(0.4)
0.008889 15.808889
0.008889 15.817778
0.008889 15.826667
0.008889 15.835556
0.008889 15.844444
0.008889 15.853333
0.008889 15.862222
39(0.4)
0.010256 15.871111
0.008889 15.880000
0.008889 15.888889
0.008889 15.897778
0.008889 15.906667
0.008889 15.915556
0.008889 15.924444
0.008889 15.933333
0.008889 15.942222
0.008889 15.951111
0.008889 15.960000
0.008889 15.968889
0.008889 15.977778
0.008889 15.986667
0.008889 15.995556
0.008889 16.004444
0.008889 16.013333
0.008889 16.022222
0.008889 16.031111
0.008889 16.040000
0.008889 16.048889
0.008889 16.057778
0.008889 16.066667
0.008889 16.075556
0.008889 16.084444
0.008889 16.093333
0.008889 16.102222
0.008889 16.111111
0.008889 16.120000
0.008889 16.128889
0.008889 16.137778
0.008889 16.146667
0.008889 16.155556

0.007018 15.575439
0.007018 15.582456
0.007018 15.589474
0.007018 15.596491
0.007018 15.603509
0.007018 15.610526
34(0.4)
0.011765 16.211765
0.011765 16.223529
0.011765 16.235294
0.011765 16.247059
0.011765 16.258824
0.011765 16.270588
0.011765 16.282353
0.011765 16.294118
0.011765 16.305882
0.011765 16.317647
0.011765 16.329412
0.011765 16.341176
0.011765 16.352941
0.011765 16.364706
0.011765 16.376471
0.011765 16.388235
0.011765 16.400000
0.011765 16.411765
0.011765 16.423529
0.011765 16.435294
0.011765 16.447059
0.011765 16.458824
0.011765 16.470588
0.011765 16.482353
0.011765 16.494118
0.011765 16.505882
0.011765 16.517647
0.011765 16.529412
0.011765 16.541176
0.011765 16.552941
0.011765 16.564706
0.011765 16.576471
0.011765 16.588235
0.011765 16.600000
39(0.4)
0.010256 16.610256
0.010256 16.620513
0.010256 16.630769
0.010256 16.641026
0.010256 16.651282
0.010256 16.661538
0.010256 16.671795
0.010256 16.682051
0.010256 16.692308
0.010256 16.702564
0.010256 16.712821
0.010256 16.723077
0.010256 16.733333
0.010256 16.743590
0.010256 16.753846
0.010256 16.764103
0.010256 16.774359
0.010256 16.784615
0.010256 16.794872
0.010256 16.805128
0.010256 16.815385
0.010256 16.825641
0.010256 16.835897
0.010256 16.846154
0.010256 16.856410
0.010256 16.866667
0.010256 16.876923
0.010256 16.887179
0.010256 16.897436
0.010256 16.907692
0.010256 16.917949
0.010256 16.928205
0.010256 16.938462

0.010256 16.948718
0.010256 16.958974
0.010256 16.969231
0.010256 16.979487
0.010256 16.989744
0.010256 17.000000
42(0.4)
0.009524 17.009524
0.009524 17.019048
0.009524 17.028571
0.009524 17.038095
0.009524 17.047619
0.009524 17.057143
0.009524 17.066667
0.009524 17.076190
0.009524 17.085714
0.009524 17.095238
0.009524 17.104762
0.009524 17.114286
0.009524 17.123810
0.009524 17.133333
0.009524 17.142857
0.009524 17.152381
0.009524 17.161905
0.009524 17.171429
0.009524 17.180952
0.009524 17.190476
0.009524 17.200000
0.009524 17.209524
0.009524 17.219048
0.009524 17.228571
0.009524 17.238095
0.009524 17.247619
0.009524 17.257143
0.009524 17.266667
0.009524 17.276190
0.009524 17.285714
0.009524 17.295238
0.009524 17.304762
0.009524 17.314286
0.009524 17.323810
0.009524 17.333333
0.009524 17.342857
0.009524 17.352381
0.009524 17.361905
0.009524 17.371429
0.009524 17.380952
0.009524 17.390476
0.009524 17.400000
58(0.4)
0.006897 17.406897
0.006897 17.413793
0.006897 17.420690
0.006897 17.427586
0.006897 17.434483
0.006897 17.441379
0.006897 17.448276
0.006897 17.455172
0.006897 17.462069
0.006897 17.468966
0.006897 17.475862
0.006897 17.482759
0.006897 17.489655
0.006897 17.496552
0.006897 17.503448
0.006897 17.510345
0.006897 17.517241
0.006897 17.524138
0.006897 17.531034
0.006897 17.537931
0.006897 17.544828
0.006897 17.551724
0.006897 17.558621
0.006897 17.565517

0.006897 17.572414
0.006897 17.579310
0.006897 17.586207
0.006897 17.593103
0.006897 17.600000
0.006897 17.606897
0.006897 17.613793
0.006897 17.620690
0.006897 17.627586
0.006897 17.634483
41(0.4)
0.006897 17.641379
0.006897 17.648276
0.006897 17.655172
0.006897 17.662069
0.006897 17.668966
0.006897 17.675862
0.006897 17.682759
0.006897 17.689655
0.006897 17.696552
0.006897 17.703448
0.006897 17.710345
0.006897 17.717241
0.006897 17.724138
0.006897 17.731034
0.006897 17.737931
0.006897 17.744828
0.006897 17.751724
0.006897 17.758621
0.006897 17.765517
0.006897 17.772414
0.006897 17.779310
0.006897 17.786207
0.006897 17.793103
0.006897 17.800000
48(0.4)
0.008333 17.808333
0.008333 17.816667
0.008333 17.825000
0.008333 17.833333
0.008333 17.841667
0.008333 17.850000
0.008333 17.858333
0.008333 17.866667
0.008333 17.875000
0.008333 17.883333
0.008333 17.891667
0.008333 17.900000
0.008333 17.908333
0.008333 17.916667
0.008333 17.925000
0.008333 17.933333
0.008333 17.941667
0.008333 17.950000
0.008333 17.958333
0.008333 17.966667
0.008333 17.975000
0.008333 17.983333
0.008333 17.991667
0.008333 18.000000
0.008333 18.008333
0.008333 18.016667
0.008333 18.025000
0.008333 18.033333
0.008333 18.041667
0.008333 18.050000
0.008333 18.058333
0.008333 18.066667
0.008333 18.075000
0.008333 18.083333
0.008333 18.091667
0.008333 18.100000
0.008333 18.108333
0.008333 18.116667
0.008333 18.125000

0.008333 18.133333
0.008333 18.141667
0.008333 18.150000
0.008333 18.158333
0.008333 18.166667
0.008333 18.175000
0.008333 18.183333
0.008333 18.191667
0.008333 18.200000
41(0.4)
0.009756 18.209756
0.009756 18.219512
0.009756 18.229268
0.009756 18.239024
0.009756 18.248780
35(0.4)
0.009756 18.258537
0.009756 18.268293
0.009756 18.278049
0.009756 18.287805
0.009756 18.297561
0.009756 18.307317
0.009756 18.317073
0.009756 18.326829
0.009756 18.336585
0.009756 18.346341
0.009756 18.356098
0.009756 18.365854
0.009756 18.375610
0.009756 18.385366
0.009756 18.395122
0.009756 18.404878
0.009756 18.414634
0.009756 18.424390
0.009756 18.434146
0.009756 18.443902
0.009756 18.453659
0.009756 18.463415
0.009756 18.473171
0.009756 18.482927
0.009756 18.492683
0.009756 18.502439
0.009756 18.512195
0.009756 18.521951
0.009756 18.531707
0.009756 18.541463
0.009756 18.551220
0.009756 18.560976
0.009756 18.570732
0.009756 18.580488
0.009756 18.590244
0.009756 18.600000
36(0.4)
0.011111 18.611111
0.011111 18.622222
0.011111 18.633333
0.011111 18.644444
0.011111 18.655556
0.011111 18.666667
0.011111 18.677778
0.011111 18.688889
0.011111 18.700000
0.011111 18.711111
0.011111 18.722222
0.011111 18.733333
0.011111 18.744444
0.011111 18.755556
0.011111 18.766667
0.011111 18.777778
0.011111 18.788889
0.011111 18.800000
0.011111 18.811111
0.011111 18.822222
0.011111 18.833333
0.011111 18.844444

0.011111 18.855556
0.011111 18.866667
0.011111 18.877778
0.011111 18.888889
0.011111 18.900000
0.011111 18.911111
0.011111 18.922222
0.011111 18.933333
0.011111 18.944444
0.011111 18.955556
0.011111 18.966667
0.011111 18.977778
0.011111 18.988889
0.011111 19.000000
35(0.4)
0.011429 19.011429
0.011429 19.022857
0.011429 19.034286
0.011429 19.045714
0.011429 19.057143
0.011429 19.068571
0.011429 19.080000
0.011429 19.091429
0.011429 19.102857
0.011429 19.114286
0.011429 19.125714
0.011429 19.137143
0.011429 19.148571
0.011429 19.160000
0.011429 19.171429
0.011429 19.182857
0.011429 19.194286
0.011429 19.205714
0.011429 19.217143
0.011429 19.228571
0.011429 19.240000
0.011429 19.251429
0.011429 19.262857
0.011429 19.274286
0.011429 19.285714
0.011429 19.297143
0.011429 19.308571
0.011429 19.320000
0.011429 19.331429
0.011429 19.342857
0.011429 19.354286
0.011429 19.365714
0.011429 19.377143
0.011429 19.388571
0.011429 19.400000
30(0.4)
0.013333 19.413333
0.013333 19.426667
0.013333 19.440000
0.013333 19.453333
0.013333 19.466667
0.013333 19.480000
0.013333 19.493333
0.013333 19.506667
0.013333 19.520000
0.013333 19.533333
0.013333 19.546667
0.013333 19.560000
0.013333 19.573333
0.013333 19.586667
0.013333 19.600000
0.013333 19.613333
0.013333 19.626667
0.013333 19.640000
0.013333 19.653333
0.013333 19.666667
0.013333 19.680000
0.013333 19.693333
0.013333 19.706667

0.013333 19.720000
0.013333 19.733333
0.013333 19.746667
0.013333 19.760000
0.013333 19.773333
0.013333 19.786667
0.013333 19.800000
36(0.4)
0.011111 19.811111
0.011111 19.822222
0.011111 19.833333
0.011111 19.844444
0.011111 19.855556
0.011111 19.866667
0.011111 19.877778
0.011111 19.888889
0.011111 19.900000
0.011111 19.911111
0.011111 19.922222
0.011111 19.933333
0.011111 19.944444
0.011111 19.955556
0.011111 19.966667
0.011111 19.977778
0.011111 19.988889
0.011111 20.000000
0.011111 20.011111
0.011111 20.022222
0.011111 20.033333
0.011111 20.044444
0.011111 20.055556
0.011111 20.066667
0.011111 20.077778
0.011111 20.088889
0.011111 20.100000
0.011111 20.111111
0.011111 20.122222
0.011111 20.133333
0.011111 20.144444
0.011111 20.155556
0.011111 20.166667
0.011111 20.177778
0.011111 20.188889
0.011111 20.200000
36(0.4)
0.011111 20.211111
0.011111 20.222222
0.011111 20.233333
0.011111 20.244444
0.011111 20.255556
0.011111 20.266667
0.011111 20.277778
0.011111 20.288889
0.011111 20.300000
0.011111 20.311111
0.011111 20.322222
0.011111 20.333333
0.011111 20.344444
0.011111 20.355556
0.011111 20.366667
0.011111 20.377778
0.011111 20.388889
0.011111 20.400000
0.011111 20.411111
0.011111 20.422222
0.011111 20.433333
0.011111 20.444444
0.011111 20.455556
0.011111 20.466667
0.011111 20.477778
0.011111 20.488889
0.011111 20.500000
0.011111 20.511111
0.011111 20.522222

0.011111 20.533333
0.011111 20.544444
0.011111 20.555556
0.011111 20.566667
0.011111 20.577778
0.011111 20.588889
0.011111 20.600000
33(0.4)
0.012121 20.612121
0.012121 20.624242
0.012121 20.636364
0.012121 20.648485
0.012121 20.660606
0.012121 20.672727
0.012121 20.684848
0.012121 20.696970
0.012121 20.709091
0.012121 20.721212
0.012121 20.733333
0.012121 20.745455
0.012121 20.757576
0.012121 20.769697
0.012121 20.781818
0.012121 20.793939
0.012121 20.806061
0.012121 20.818182
0.012121 20.830303
0.012121 20.842424
0.012121 20.854545
0.012121 20.866667
0.012121 20.878788
0.012121 20.890909
0.012121 20.903030
0.012121 20.915152
0.012121 20.927273
0.012121 20.939394
0.012121 20.951515
0.012121 20.963636
0.012121 20.975758
0.012121 20.987879
0.012121 21.000000
42(0.4)
0.009524 21.009524
0.009524 21.019048
0.009524 21.028571
0.009524 21.038095
0.009524 21.047619
0.009524 21.057143
0.009524 21.066667
0.009524 21.076190
0.009524 21.085714
0.009524 21.095238
0.009524 21.104762
0.009524 21.114286
0.009524 21.123810
0.009524 21.133333
0.009524 21.142857
0.009524 21.152381
0.009524 21.161905
0.009524 21.171429
0.009524 21.180952
0.009524 21.190476
0.009524 21.200000
0.009524 21.209524
0.009524 21.219048
0.009524 21.228571
0.009524 21.238095
0.009524 21.247619
0.009524 21.257143
0.009524 21.266667
0.009524 21.276190
0.009524 21.285714
0.009524 21.295238
0.009524 21.304762

0.009524 21.314286
0.009524 21.323810
0.009524 21.333333
0.009524 21.342857
0.009524 21.352381
0.009524 21.361905
0.009524 21.371429
0.009524 21.380952
0.009524 21.390476
0.009524 21.400000
51(0.4)
0.007843 21.407843
0.007843 21.415686
0.007843 21.423529
0.007843 21.431373
0.007843 21.439216
0.007843 21.447059
0.007843 21.454902
0.007843 21.462745
0.007843 21.470588
0.007843 21.478431
0.007843 21.486275
0.007843 21.494118
0.007843 21.501961
0.007843 21.509804
0.007843 21.517647
0.007843 21.525490
0.007843 21.533333
0.007843 21.541176
0.007843 21.549020
0.007843 21.556863
0.007843 21.564706
0.007843 21.572549
0.007843 21.580392
0.007843 21.588235
0.007843 21.596078
0.007843 21.603922
0.007843 21.611765
0.007843 21.619608
0.007843 21.627451
0.007843 21.635294
0.007843 21.643137
0.007843 21.650980
0.007843 21.658824
0.007843 21.666667
0.007843 21.674510
0.007843 21.682353
0.007843 21.690196
0.007843 21.698039
0.007843 21.705882
0.007843 21.713725
0.007843 21.721569
0.007843 21.729412
0.007843 21.737255
0.007843 21.745098
0.007843 21.752941
0.007843 21.760784
0.007843 21.768627
0.007843 21.776471
0.007843 21.784314
0.007843 21.792157
0.007843 21.800000
51(0.4)
0.012903 21.812903
0.012903 21.825806
0.012903 21.838710
0.012903 21.851613
0.012903 21.864516
0.012903 21.877419
0.012903 21.890323
0.012903 21.903226
0.012903 21.916129
0.012903 21.929032
0.012903 21.941935

0.012903 21.954839
0.012903 21.967742
0.012903 21.980645
0.012903 21.993548
0.012903 22.006452
0.012903 22.019355
0.012903 22.032258
0.012903 22.045161
32(0.4)
0.012903 22.058065
0.012903 22.070968
0.012903 22.083871
0.012903 22.096774
0.012903 22.109677
0.012903 22.122581
0.012903 22.135484
0.012903 22.148387
0.012903 22.161290
0.012903 22.174194
0.012903 22.187097
0.012903 22.200000
27(0.4)
0.014815 22.214815
0.014815 22.229630
0.014815 22.244444
0.014815 22.259259
0.014815 22.274074
0.014815 22.288889
0.014815 22.303704
0.014815 22.318519
0.014815 22.333333
0.014815 22.348148
0.014815 22.362963
0.014815 22.377778
0.014815 22.392593
0.014815 22.407407
0.014815 22.422222
0.014815 22.437037
0.014815 22.451852
0.014815 22.466667
0.014815 22.481481
0.014815 22.496296
0.014815 22.511111
0.014815 22.525926
0.014815 22.540741
0.014815 22.555556
0.014815 22.570370
0.014815 22.585185
0.014815 22.600000
32(0.4)
0.012500 22.612500
0.012500 22.625000
0.012500 22.637500
0.012500 22.650000
0.012500 22.662500
0.012500 22.675000
0.012500 22.687500
0.012500 22.700000
0.012500 22.712500
0.012500 22.725000
0.012500 22.737500
0.012500 22.750000
0.012500 22.762500
0.012500 22.775000
0.012500 22.787500
0.012500 22.800000
0.012500 22.812500
0.012500 22.825000
0.012500 22.837500
0.012500 22.850000
0.012500 22.862500
0.012500 22.875000
0.012500 22.887500
0.012500 22.900000
0.012500 22.912500

0.012500 22.925000
0.012500 22.937500
0.012500 22.950000
0.012500 22.962500
0.012500 22.975000
0.012500 22.987500
0.012500 23.000000
32(0.4)
0.012500 23.012500
0.012500 23.025000
0.012500 23.037500
0.012500 23.050000
0.012500 23.062500
0.012500 23.075000
0.012500 23.087500
0.012500 23.100000
0.012500 23.112500
0.012500 23.125000
0.012500 23.137500
0.012500 23.150000
0.012500 23.162500
0.012500 23.175000
0.012500 23.187500
0.012500 23.200000
25(0.4)
0.016000 24.216000
0.016000 24.232000
0.016000 24.248000
0.016000 24.264000
0.016000 24.280000
0.016000 24.296000
0.016000 24.312000
0.016000 24.328000
0.016000 24.344000
0.016000 24.360000
0.016000 24.376000
0.016000 24.392000
0.016000 24.408000
0.016000 24.424000
0.016000 24.440000
0.016000 24.456000
0.016000 24.472000
0.016000 24.488000
0.016000 24.504000
0.016000 24.520000
0.016000 24.536000
0.016000 24.552000
0.016000 24.568000
0.016000 24.584000
0.016000 24.600000
23(0.4)
0.017391 24.617391
0.017391 24.634783
0.017391 24.652174
0.017391 24.669565
0.017391 24.686957
0.017391 24.704348
0.017391 24.721739
0.017391 24.739130
0.017391 24.756522
0.017391 24.773913
0.017391 24.791304
0.017391 24.808696
0.017391 24.826087
0.017391 24.843478
0.017391 24.860870
13(0.4)
0.017391 24.878261
0.017391 24.895652
0.017391 24.913043
0.017391 24.930435
0.017391 24.947826
0.017391 24.965217
0.017391 24.982609
0.017391 25.000000
24(0.4)

0.014815 23.874074
0.014815 23.888889
0.014815 23.903704
0.014815 23.918519
0.014815 23.933333
0.014815 23.948148
0.014815 23.962963
0.014815 23.977778
0.014815 23.992593
0.014815 24.007407
0.014815 24.022222
0.014815 24.037037
0.014815 24.051852
0.014815 24.066667
0.014815 24.081481
0.014815 24.096296
0.014815 24.111111
0.014815 24.125926
0.014815 24.140741
0.014815 24.155556
0.014815 24.170370
0.014815 24.185185
0.014815 24.200000
25(0.4)
0.016000 24.216000
0.016000 24.232000
0.016000 24.248000
0.016000 24.264000
0.016000 24.280000
0.016000 24.296000
0.016000 24.312000
0.016000 24.328000
0.016000 24.344000
0.016000 24.360000
0.016000 24.376000
0.016000 24.392000
0.016000 24.408000
0.016000 24.424000
0.016000 24.440000
0.016000 24.456000
0.016000 24.472000
0.016000 24.488000
0.016000 24.504000
0.016000 24.520000
0.016000 24.536000
0.016000 24.552000
0.016000 24.568000
0.016000 24.584000
0.016000 24.600000
23(0.4)
0.017391 24.617391
0.017391 24.634783
0.017391 24.652174
0.017391 24.669565
0.017391 24.686957
0.017391 24.704348
0.017391 24.721739
0.017391 24.739130
0.017391 24.756522
0.017391 24.773913
0.017391 24.791304
0.017391 24.808696
0.017391 24.826087
0.017391 24.843478
0.017391 24.860870
13(0.4)
0.017391 24.878261
0.017391 24.895652
0.017391 24.913043
0.017391 24.930435
0.017391 24.947826
0.017391 24.965217
0.017391 24.982609
0.017391 25.000000
24(0.4)

0.016667 25.016667
0.016667 25.033333
0.016667 25.050000
0.016667 25.066667
0.016667 25.083333
0.016667 25.100000
0.016667 25.116667
0.016667 25.133333
0.016667 25.150000
0.016667 25.166667
0.016667 25.183333
0.016667 25.200000
0.016667 25.216667
0.016667 25.233333
0.016667 25.250000
0.016667 25.266667
0.016667 25.283333
0.016667 25.300000
0.016667 25.316667
0.016667 25.333333
0.016667 25.350000
0.016667 25.366667
0.016667 25.383333
0.016667 25.400000
19(0.4)
0.016667 25.416667
0.016667 25.433333
0.016667 25.450000
0.016667 25.466667
0.016667 25.483333
0.016667 25.500000
0.016667 25.516667
0.016667 25.533333
0.016667 25.550000
0.016667 25.566667
0.016667 25.583333
0.016667 25.600000
0.016667 25.616667
0.016667 25.633333
0.016667 25.650000
0.016667 25.666667
0.016667 25.683333
0.016667 25.700000
0.016667 25.716667
0.016667 25.733333
0.016667 25.750000
0.016667 25.766667
0.016667 25.783333
0.016667 25.800000
14(0.4)
0.028571 25.828571
0.028571 25.857143
0.028571 25.885714
0.028571 25.914286
0.028571 25.942857
0.028571 25.971429
0.028571 26.000000
0.028571 26.028571
0.028571 26.057143
0.028571 26.085714
0.028571 26.114286
0.028571 26.142857
0.028571 26.171429
0.028571 26.200000
13(0.4)
0.030769 26.230769
0.030769 26.261538
0.030769 26.292308
0.030769 26.323077
0.030769 26.353846
0.030769 26.384615
0.030769 26.415385
0.030769 26.446154
0.030769 26.476923

0.030769 26.507692
0.030769 26.538462
0.030769 26.569231
0.030769 26.600000
18(0.4)
0.022222 26.622222
0.022222 26.644444
0.022222 26.666667
0.022222 26.688889
0.022222 26.711111
0.022222 26.733333
19(0.4)
0.022222 26.755556
0.022222 26.777778
0.022222 26.800000
0.022222 26.822222
0.022222 26.844444
0.022222 26.866667
0.022222 26.888889
0.022222 26.911111
0.022222 26.933333
0.022222 26.955556
0.022222 26.977778
0.022222 27.000000
19(0.4)
0.021053 27.021053
0.021053 27.042105
0.021053 27.063158
0.021053 27.084211
0.021053 27.105263
0.021053 27.126316
0.021053 27.147368
20(0.4)
0.021053 27.168421
0.021053 27.189474
0.021053 27.210526
0.021053 27.231579
0.021053 27.252632
0.021053 27.273684
0.021053 27.294737
0.021053 27.315789
0.021053 27.336842
0.021053 27.357895
0.021053 27.378947
0.021053 27.400000
21(0.4)
0.019048 27.419048
0.019048 27.438095
0.019048 27.457143
0.019048 27.476190
0.019048 27.495238
0.019048 27.514286
0.019048 27.533333
0.019048 27.552381
14(0.4)
0.028571 27.571429
0.028571 27.590476
0.028571 27.609524
0.028571 27.628571
0.028571 27.647619
0.028571 27.666667
0.028571 27.685714
0.028571 27.704762
0.028571 27.723810
0.028571 27.742857
0.028571 27.761905
0.028571 27.780952
0.028571 27.800000
18(0.4)
0.022222 27.822222
0.022222 27.844444
0.022222 27.866667
0.022222 27.888889
0.022222 27.911111
0.022222 27.933333
0.022222 27.955556
0.022222 27.977778

0.022222 28.000000
0.022222 28.022222
0.022222 28.044444
0.022222 28.066667
0.022222 28.088889
0.022222 28.111111
0.022222 28.133333
0.022222 28.155556
0.022222 28.177778
0.022222 28.200000
19(0.4)
0.021053 28.221053
0.021053 28.242105
0.021053 28.263158
0.021053 28.284211
0.021053 28.305263
0.021053 28.326316
0.021053 28.347368
0.021053 28.368421
0.021053 28.389474
0.021053 28.410526
0.021053 28.431579
0.021053 28.452632
0.021053 28.473684
0.021053 28.494737
0.021053 28.515789
0.021053 28.536842
0.021053 28.557895
0.021053 28.578947
0.021053 28.600000
20(0.4)
0.020000 28.620000
0.020000 28.640000
0.020000 28.660000
0.020000 28.680000
0.020000 28.700000
0.020000 28.720000
0.020000 28.740000
0.020000 28.760000
0.020000 28.780000
0.020000 28.800000
0.020000 28.820000
0.020000 28.840000
0.020000 28.860000
0.020000 28.880000
0.020000 28.900000
0.020000 28.920000
0.020000 28.940000
0.020000 28.960000
0.020000 28.980000
0.020000 29.000000
14(0.4)
0.028571 29.028571
0.028571 29.057143
0.028571 29.085714
0.028571 29.114286
0.028571 29.142857
0.028571 29.171429
0.028571 29.200000
0.028571 29.228571
0.028571 29.257143
0.028571 29.285714
0.028571 29.314286
0.028571 29.342857
0.028571 29.371429
0.028571 29.400000
13(0.4)
0.030769 29.430769
0.030769 29.461538
0.030769 29.492308
0.030769 29.523077
0.030769 29.553846
0.030769 29.584615
0.030769 29.615385

0.030769 29.646154
0.030769 29.676923
0.030769 29.707692
0.030769 29.738462
0.030769 29.769231
0.030769 29.800000
14(0.4)
0.028571 29.828571
0.028571 29.857143
0.028571 29.885714
0.028571 29.914286
0.028571 29.942857
0.028571 29.971429
0.028571 30.000000
0.028571 30.028571
0.028571 30.057143
0.028571 30.085714
0.028571 30.114286
0.028571 30.142857
0.028571 30.171429
0.028571 30.200000
9(0.4)
0.044444 30.244444
0.044444 30.288889
0.044444 30.333333
0.044444 30.377778
0.044444 30.422222
0.044444 30.466667
0.044444 30.511111
0.044444 30.555556
0.044444 30.600000
8(0.4)
0.050000 30.650000
0.050000 30.700000
0.050000 30.750000
0.050000 30.800000
0.050000 30.850000
0.050000 30.900000
0.050000 30.950000
0.050000 31.000000
10(0.4)
0.040000 31.040000
0.040000 31.080000
0.040000 31.120000
0.040000 31.160000
0.040000 31.200000
0.040000 31.240000
0.040000 31.280000
0.040000 31.320000
0.040000 31.360000
0.040000 31.400000
14(0.4)
0.028571 31.428571
0.028571 31.457143
0.028571 31.485714
0.028571 31.514286
0.028571 31.542857
0.028571 31.571429
0.028571 31.600000
0.028571 31.628571
0.028571 31.657143
0.028571 31.685714
0.028571 31.714286
0.028571 31.742857
0.028571 31.771429
0.028571 31.800000
16(0.4)
0.025000 31.825000
0.025000 31.850000
0.025000 31.875000
0.025000 31.900000
0.025000 31.925000
0.025000 31.950000
0.025000 31.975000

0.025000 32.000000
0.025000 32.025000
0.025000 32.050000
0.025000 32.075000
0.025000 32.100000
0.025000 32.125000
0.025000 32.150000
0.025000 32.175000
0.025000 32.200000
15(0.4)
0.026667 32.226667
0.026667 32.253333
0.026667 32.280000
0.026667 32.306667
0.026667 32.333333
0.026667 32.360000
0.026667 32.386667
0.026667 32.413333
0.026667 32.440000
0.026667 32.466667
0.026667 32.493333
0.026667 32.520000
0.026667 32.546667
0.026667 32.573333
0.026667 32.600000
13(0.4)
0.030769 32.630769
0.030769 32.661538
0.030769 32.692308
0.030769 32.723077
0.030769 32.753846
0.030769 32.784615
0.030769 32.815385
0.030769 32.846154
0.030769 32.876923
0.030769 32.907692
0.030769 32.938462
0.030769 32.969231
0.030769 33.000000
7(0.4)
0.057143 33.057143
0.057143 33.114286
0.057143 33.171429
0.057143 33.228571
0.057143 33.285714
0.057143 33.342857
0.057143 33.400000
6(0.4)
0.066667 33.466667
0.066667 33.533333
0.066667 33.600000
0.066667 33.666667
0.066667 33.733333
0.066667 33.800000
9(0.4)
0.044444 33.844444
0.044444 33.888889
0.044444 33.933333
0.044444 33.977778
0.044444 34.022222
0.044444 34.066667
0.044444 34.111111
0.044444 34.155556
0.044444 34.200000
7(0.4)
0.057143 34.257143
0.057143 34.314286
0.057143 34.371429
0.057143 34.428571
0.057143 34.485714
0.057143 34.542857
0.057143 34.600000
7(0.4)
0.057143 34.657143

0.057143 34.714286
0.057143 34.771429
0.057143 34.828571
0.057143 34.885714
0.057143 34.942857
0.057143 35.000000
5(0.4)
0.080000 35.080000
0.080000 35.160000
0.080000 35.240000
0.080000 35.320000
0.080000 35.400000
7(0.4)
0.057143 35.457143
0.057143 35.514286
0.057143 35.571429
0.057143 35.628571
0.057143 35.685714
0.057143 35.742857
0.057143 35.800000
5(0.4)
0.080000 35.880000
0.080000 35.960000
0.080000 36.040000
0.080000 36.120000
0.080000 36.200000
3(0.4)
0.133333 36.333333
0.133333 36.466667
0.133333 36.600000
11(0.4)
0.036364 36.636364
0.036364 36.672727
0.036364 36.709091
0.036364 36.745455
0.036364 36.781818
0.036364 36.818182
0.036364 36.854545
0.036364 36.890909
0.036364 36.927273
0.036364 36.963636
0.036364 37.000000
5(0.4)
0.080000 37.080000
0.080000 37.160000
0.080000 37.240000
0.080000 37.320000
0.080000 37.400000
3(0.4)
0.133333 37.533333
0.133333 37.666667
0.133333 37.800000
4(0.4)
0.100000 37.900000
0.100000 38.000000
0.100000 38.100000
0.100000 38.200000
7(0.4)
0.057143 38.257143
0.057143 38.314286
0.057143 38.371429
0.057143 38.428571
0.057143 38.485714
0.057143 38.542857
0.057143 38.600000
8(0.4)
0.050000 38.650000
0.050000 38.700000
0.050000 38.750000
0.050000 38.800000
0.050000 38.850000
0.050000 38.900000
0.050000 38.950000
0.050000 39.000000

6(0.4)
0.066667 39.066667
0.066667 39.133333
0.066667 39.200000
0.066667 39.266667
0.066667 39.333333
0.066667 39.400000
8(0.4)
0.050000 39.450000
0.050000 39.500000
0.050000 39.550000
0.050000 39.600000
0.050000 39.650000
0.050000 39.700000
0.050000 39.750000
0.050000 39.800000
2(0.4)
0.200000 40.000000
0.200000 40.200000
3(0.4)
0.133333 40.333333
0.133333 40.466667
0.133333 40.600000
2(0.4)
0.200000 40.800000
0.200000 41.000000
0,3(0.4)
0.533333 41.533333
0.133333 41.666667
0.133333 41.800000
2(0.4)
0.200000 42.000000
0.200000 42.200000
2(0.4)
0.200000 42.400000
0.200000 42.600000
0,2(0.4)
0.600000 43.200000
0.200000 43.400000
2(0.4)
0.200000 43.600000
0.200000 43.800000
2(0.4)
0.200000 44.000000
0.200000 44.200000
1(0.4)
0.400000 44.600000
2(0.4)
0.200000 44.800000
0.200000 45.000000
1(0.4)
0.400000 45.400000
3(0.4)
0.133333 45.533333
0.133333 45.666667
0.133333 45.800000
2(0.4)
0.200000 46.000000
0.200000 46.200000
1(0.4)
0.400000 46.600000
2(0.4)
0.200000 46.800000
0.200000 47.000000
1(0.4)
0.400000 47.400000
2(0.4)
0.200000 47.600000
0.200000 47.800000
0,0,3(0.4)
0.933333 48.733333
0.133333 48.866667
0.133333 49.000000
2(0.4)

0.200000 49.200000
0.200000 49.400000
1(0.4)
0.400000 49.800000
7(0.4)
0.057143 49.857143
0.057143 49.914286
0.057143 49.971429
0.057143 50.028571
0.057143 50.085714
0.057143 50.142857
0.057143 50.200000
5(0.4)
0.080000 50.280000
0.080000 50.360000
0.080000 50.440000
0.080000 50.520000
0.080000 50.600000
2(0.4)
0.200000 50.800000
0.200000 51.000000
0,1(0.4)
0.800000 51.800000
2(0.4)
0.200000 52.000000
0.200000 52.200000
0,3(0.4)
0.533333 52.733333
0.133333 52.866667
0.133333 53.000000
1(0.4)
0.400000 53.400000
2(0.4)
0.200000 53.600000
0.200000 53.800000
2(0.4)
0.200000 54.000000
0.200000 54.200000
3(0.4)
0.133333 54.333333
0.133333 54.466667
0.133333 54.600000
1(0.4)
0.400000 55.000000
0,0,0,1(0.4)
2.000000 57.000000
1(0.4)
0.400000 57.400000
2(0.4)
0.200000 57.600000
0.200000 57.800000
1(0.4)
0.400000 58.200000
1(0.4)
0.400000 58.600000
0,0,0,4(0.4)
1.300000 59.900000
0.100000 60.000000
0.100000 60.100000
0.100000 60.200000
3(0.4)
0.133333 60.333333
0.133333 60.466667
0.133333 60.600000
2(0.4)
0.200000 60.800000
0.200000 61.000000
3(0.4)
0.133333 61.133333
0.133333 61.266667
0.133333 61.400000
1(0.4)
0.400000 61.800000
0,2(0.4)

0.600000 62.400000
0.200000 62.600000
0,2(0.4)
0.600000 63.200000
0.200000 63.400000
0,0,1(0.4)
1.200000 64.600000
0,2(0.4)
0.600000 65.200000
0.200000 65.400000

DK1
SW
56(0.2)
0.003571 0.003571
0.003571 0.007143
0.003571 0.010714
0.003571 0.014286
0.003571 0.017857
0.003571 0.021429
0.003571 0.025000
0.003571 0.028571
0.003571 0.032143
0.003571 0.035714
0.003571 0.039286
0.003571 0.042857
0.003571 0.046429
0.003571 0.050000
0.003571 0.053571
0.003571 0.057143
0.003571 0.060714
0.003571 0.064286
0.003571 0.067857
0.003571 0.071429
0.003571 0.075000
0.003571 0.078571
0.003571 0.082143
0.003571 0.085714
0.003571 0.089286
0.003571 0.092857
0.003571 0.096429
0.003571 0.100000
0.003571 0.103571
0.003571 0.107143
0.003571 0.110714
0.003571 0.114286
0.003571 0.117857
0.003571 0.121429
0.003571 0.125000
0.003571 0.128571
0.003571 0.132143
0.003571 0.135714
0.003571 0.139286
0.003571 0.142857
0.003571 0.146429
0.003571 0.150000
0.003571 0.153571
0.003571 0.157143
0.003571 0.160714
0.003571 0.164286
0.003571 0.167857
0.003571 0.171429
0.003571 0.175000
0.003571 0.178571
0.003571 0.182143
0.003571 0.185714
0.003571 0.189286
0.003571 0.192857
0.003571 0.196429
0.003571 0.200000
41(0.2)
0.004878 0.204878
0.004878 0.209756

0.004878 0.214634
0.004878 0.219512
0.004878 0.224390
0.004878 0.229268
0.004878 0.234146
0.004878 0.239024
0.004878 0.243902
0.004878 0.248780
0.004878 0.253659
0.004878 0.258537
0.004878 0.263415
0.004878 0.268293
0.004878 0.273171
0.004878 0.278049
0.004878 0.282927
0.004878 0.287805
0.004878 0.292683
0.004878 0.297561
0.004878 0.302439
0.004878 0.307317
0.004878 0.312195
0.004878 0.317073
0.004878 0.321951
0.004878 0.326829
0.004878 0.331707
0.004878 0.336585
0.004878 0.341463
0.004878 0.346341
0.004878 0.351220
0.004878 0.356098
0.004878 0.360976
0.004878 0.365854
0.004878 0.370732
0.004878 0.375610
0.004878 0.380488
0.004878 0.385366
0.004878 0.390244
0.004878 0.395122
0.004878 0.400000
18(0.2)
0.011111 0.411111
0.011111 0.422222
0.011111 0.433333
0.011111 0.444444
0.011111 0.455556
0.011111 0.466667
0.011111 0.477778
0.011111 0.488889
0.011111 0.500000
0.011111 0.511111
0.011111 0.522222
0.011111 0.533333
0.011111 0.544444
0.011111 0.555556
0.011111 0.566667
0.011111 0.577778
0.011111 0.588889
0.011111 0.600000
18(0.2)
0.011111 0.611111
0.011111 0.622222
0.011111 0.633333
0.011111 0.644444
0.011111 0.655556
0.011111 0.666667
0.011111 0.677778
0.011111 0.688889
0.011111 0.700000
0.011111 0.711111
0.011111 0.722222
0.011111 0.733333
0.011111 0.744444
0.011111 0.755556
0.011111 0.766667

0.011111 0.777778
0.011111 0.788889
0.011111 0.800000
14(0.2)
0.014286 0.814286
0.014286 0.828571
0.014286 0.842857
0.014286 0.857143
0.014286 0.871429
0.014286 0.885714
0.014286 0.900000
0.014286 0.914286
0.014286 0.928571
0.014286 0.942857
0.014286 0.957143
0.014286 0.971429
0.014286 0.985714
0.014286 1.000000
15(0.2)
0.013333 1.013333
0.013333 1.026667
0.013333 1.040000
0.013333 1.053333
0.013333 1.066667
0.013333 1.080000
0.013333 1.093333
0.013333 1.106667
0.013333 1.120000
0.013333 1.133333
0.013333 1.146667
0.013333 1.160000
0.013333 1.173333
0.013333 1.186667
0.013333 1.200000
13(0.2)
0.015385 1.215385
0.015385 1.230769
0.015385 1.246154
0.015385 1.261538
0.015385 1.276923
0.015385 1.292308
0.015385 1.307692
0.015385 1.323077
0.015385 1.338462
0.015385 1.353846
0.015385 1.369231
0.015385 1.384615
0.015385 1.400000
8(0.2)
0.025000 1.425000
0.025000 1.450000
0.025000 1.475000
0.025000 1.500000
0.025000 1.525000
0.025000 1.550000
0.025000 1.575000
0.025000 1.600000
8(0.2)
0.025000 1.625000
0.025000 1.650000
0.025000 1.675000
0.025000 1.700000
0.025000 1.725000
0.025000 1.750000
0.025000 1.775000
0.025000 1.800000
6(0.2)
0.033333 1.833333
0.033333 1.866667
0.033333 1.900000
0.033333 1.933333
0.033333 1.966667
0.033333 2.000000
10(0.2)

0.020000 2.020000
0.020000 2.040000
0.020000 2.060000
0.020000 2.080000
0.020000 2.100000
0.020000 2.120000
0.020000 2.140000
0.020000 2.160000
0.020000 2.180000
0.020000 2.200000
7(0.2)
0.028571 2.228571
0.028571 2.257143
0.028571 2.285714
0.028571 2.314286
0.028571 2.342857
0.028571 2.371429
0.028571 2.400000
6(0.2)
0.033333 2.433333
0.033333 2.466667
0.033333 2.500000
0.033333 2.533333
0.033333 2.566667
0.033333 2.600000
7(0.2)
0.028571 2.628571
0.028571 2.657143
0.028571 2.685714
0.028571 2.714286
0.028571 2.742857
0.028571 2.771429
0.028571 2.800000
5(0.2)
0.040000 2.840000
0.040000 2.880000
0.040000 2.920000
0.040000 2.960000
0.040000 3.000000
7(0.2)
0.028571 3.028571
0.028571 3.057143
0.028571 3.085714
0.028571 3.114286
0.028571 3.142857
0.028571 3.171429
0.028571 3.200000
9(0.2)
0.022222 3.222222
0.022222 3.244444
0.022222 3.266667
0.022222 3.288889
0.022222 3.311111
0.022222 3.333333
0.022222 3.355556
0.022222 3.377778
0.022222 3.400000
5(0.2)
0.040000 3.440000
0.040000 3.480000
0.040000 3.520000
0.040000 3.560000
0.040000 3.600000
5(0.2)
0.040000 3.640000
0.040000 3.680000
0.040000 3.720000
0.040000 3.760000
0.040000 3.800000
7(0.2)
0.028571 3.828571
0.028571 3.857143
0.028571 3.885714
0.028571 3.914286

0.028571 3.942857
0.028571 3.971429
0.028571 4.000000
7(0.2)
0.028571 4.028571
0.028571 4.057143
0.028571 4.085714
0.028571 4.114286
0.028571 4.142857
0.028571 4.171429
0.028571 4.200000
5(0.2)
0.040000 4.240000
0.040000 4.280000
0.040000 4.320000
0.040000 4.360000
0.040000 4.400000
6(0.2)
0.033333 4.433333
0.033333 4.466667
0.033333 4.500000
0.033333 4.533333
0.033333 4.566667
0.033333 4.600000
4(0.2)
0.050000 4.650000
0.050000 4.700000
0.050000 4.750000
0.050000 4.800000
5(0.2)
0.040000 4.840000
0.040000 4.880000
0.040000 4.920000
0.040000 4.960000
0.040000 5.000000
4(0.2)
0.050000 5.050000
0.050000 5.100000
0.050000 5.150000
0.050000 5.200000
4(0.2)
0.050000 5.250000
0.050000 5.300000
0.050000 5.350000
0.050000 5.400000
3(0.2)
0.066667 5.466667
0.066667 5.533333
0.066667 5.600000
4(0.2)
0.050000 5.650000
0.050000 5.700000
0.050000 5.750000
0.050000 5.800000
3(0.2)
0.066667 5.866667
0.066667 5.933333
0.066667 6.000000
4(0.2)
0.050000 6.050000
0.050000 6.100000
0.050000 6.150000
0.050000 6.200000
3(0.2)
0.066667 6.266667
0.066667 6.333333
0.066667 6.400000
3(0.2)
0.066667 6.466667
0.066667 6.533333
0.066667 6.600000
2(0.2)
0.100000 6.700000
0.100000 6.800000

6(0.5)
0.083333 6.883333
0.083333 6.966667
0.083333 7.050000
0.083333 7.133333
0.083333 7.216667
0.083333 7.300000
3(0.5)
0.166667 7.466667
0.166667 7.633333
0.166667 7.800000
4(0.5)
0.125000 7.925000
0.125000 8.050000
0.125000 8.175000
0.125000 8.300000
3(0.5)
0.166667 8.466667
0.166667 8.633333
0.166667 8.800000
2(0.5)
0.250000 9.050000
0.250000 9.300000
3(0.5)
0.166667 9.466667
0.166667 9.633333
0.166667 9.800000
2(0.5)
0.250000 10.050000
0.250000 10.300000
5
0.200000 10.500000
0.200000 10.700000
0.200000 10.900000
0.200000 11.100000
0.200000 11.300000
6
0.166667 11.466667
0.166667 11.633333
0.166667 11.800000
0.166667 11.966667
0.166667 12.133333
0.166667 12.300000
1
1.000000 13.300000
1
1.000000 14.300000
1
1.000000 15.300000
2
0.500000 15.800000
0.500000 16.300000
2
0.500000 16.800000
0.500000 17.300000
1
1.000000 18.300000
3
0.333333 18.633333
0.333333 18.966667
0.333333 19.300000
3
0.333333 19.633333
0.333333 19.966667
0.333333 20.300000
0,2
1.500000 21.800000
0.500000 22.300000
1
1.000000 23.300000
1
1.000000 24.300000
2
0.500000 24.800000

0.500000 25.300000
2
0.500000 25.800000
0.500000 26.300000
1
1.000000 27.300000
1
1.000000 28.300000
1
1.000000 29.300000
1
1.000000 30.300000
2
0.500000 30.800000
0.500000 31.300000
1
1.000000 32.300000
2
0.500000 32.800000
0.500000 33.300000
0,1
2.000000 35.300000
1
1.000000 36.300000

DK14
NE
3(0.2)
0.066667 0.066667
0.066667 0.133333
0.066667 0.200000
13(0.2)
0.015385 0.215385
0.015385 0.230769
0.015385 0.246154
0.015385 0.261538
0.015385 0.276923
0.015385 0.292308
0.015385 0.307692
0.015385 0.323077
0.015385 0.338462
0.015385 0.353846
0.015385 0.369231
0.015385 0.384615
0.015385 0.400000
15(0.2)
0.013333 0.413333
0.013333 0.426667
0.013333 0.440000
0.013333 0.453333
0.013333 0.466667
0.013333 0.480000
0.013333 0.493333
0.013333 0.506667
0.013333 0.520000
0.013333 0.533333
0.013333 0.546667
0.013333 0.560000
0.013333 0.573333
0.013333 0.586667
0.013333 0.600000
44(0.2)
0.004545 0.604545
0.004545 0.609091
0.004545 0.613636
0.004545 0.618182
0.004545 0.622727
0.004545 0.627273
0.004545 0.631818
0.004545 0.636364
0.004545 0.640909
0.004545 0.645455
0.004545 0.650000
0.004545 0.654545

0.004545 0.659091
0.004545 0.663636
0.004545 0.668182
0.004545 0.672727
0.004545 0.677273
0.004545 0.681818
0.004545 0.686364
0.004545 0.690909
0.004545 0.695455
0.004545 0.700000
0.004545 0.704545
0.004545 0.709091
0.004545 0.713636
0.004545 0.718182
0.004545 0.722727
0.004545 0.727273
0.004545 0.731818
0.004545 0.736364
0.004545 0.740909
0.004545 0.745455
0.004545 0.750000
0.004545 0.754545
0.004545 0.759091
0.004545 0.763636
0.004545 0.768182
0.004545 0.772727
0.004545 0.777273
0.004545 0.781818
0.004545 0.786364
0.004545 0.790909
0.004545 0.795455
0.004545 0.800000
37(0.2)
0.005405 0.805405
0.005405 0.810811
0.005405 0.816216
0.005405 0.821622
0.005405 0.827027
0.005405 0.832432
0.005405 0.837838
0.005405 0.843243
0.005405 0.848649
0.005405 0.854054
0.005405 0.859459
0.005405 0.864865
0.005405 0.870270
0.005405 0.875676
0.005405 0.881081
0.005405 0.886486
0.005405 0.891892
0.005405 0.897297
0.005405 0.902703
0.005405 0.908108
0.005405 0.913514
0.005405 0.918919
0.005405 0.924324
0.005405 0.929730
0.005405 0.935135
0.005405 0.940541
0.005405 0.945946
0.005405 0.951351
0.005405 0.956757
0.005405 0.962162
0.005405 0.967568
0.005405 0.972973
0.005405 0.978378
0.005405 0.983784
0.005405 0.989189
0.005405 0.994595
0.005405 1.000000
19(0.2)
0.010526 1.010526
0.010526 1.021053
0.010526 1.031579

0.005063 11.045570
0.005063 11.050633
0.005063 11.055696
0.005063 11.060759
0.005063 11.065823
0.005063 11.070886
0.005063 11.075949
0.005063 11.081013
0.005063 11.086076
0.005063 11.091139
0.005063 11.096203
0.005063 11.101266
0.005063 11.106329
0.005063 11.111392
0.005063 11.116456
0.005063 11.121519
0.005063 11.126582
0.005063 11.131646
0.005063 11.136709
0.005063 11.141772
0.005063 11.146835
0.005063 11.151899
0.005063 11.156962
0.005063 11.162025
0.005063 11.167089
0.005063 11.172152
0.005063 11.177215
0.005063 11.182278
0.005063 11.187342
0.005063 11.192405
0.005063 11.197468
0.005063 11.202532
0.005063 11.207595
0.005063 11.212658
0.005063 11.217722
0.005063 11.222785
0.005063 11.227848
0.005063 11.232911
0.005063 11.237975
0.005063 11.243038
0.005063 11.248101
0.005063 11.253165
0.005063 11.258228
0.005063 11.263291
0.005063 11.268354
0.005063 11.273418
0.005063 11.278481
0.005063 11.283544
0.005063 11.288608
0.005063 11.293671
0.005063 11.298734
0.005063 11.303797
0.005063 11.308861
0.005063 11.313924
0.005063 11.318987
0.005063 11.324051
0.005063 11.329114
0.005063 11.334177
0.005063 11.339241
0.005063 11.344304
0.005063 11.349367
0.005063 11.354430
0.005063 11.359494
0.005063 11.364557
0.005063 11.369620
0.005063 11.374684
0.005063 11.379747
0.005063 11.384810
0.005063 11.389873
0.005063 11.394937
0.005063 11.400000
74(0.4)
0.005405 11.405405
0.005405 11.410811

0.005405 11.416216
0.005405 11.421622
0.005405 11.427027
0.005405 11.432432
0.005405 11.437838
0.005405 11.443243
0.005405 11.448649
0.005405 11.454054
0.005405 11.459459
0.005405 11.464865
0.005405 11.470270
0.005405 11.475676
0.005405 11.481081
0.005405 11.486486
0.005405 11.491892
0.005405 11.497297
0.005405 11.502703
0.005405 11.508108
0.005405 11.513514
0.005405 11.518919
0.005405 11.524324
0.005405 11.529730
0.005405 11.535135
0.005405 11.540541
0.005405 11.545946
0.005405 11.551351
0.005405 11.556757
0.005405 11.562162
0.005405 11.567568
0.005405 11.572973
0.005405 11.578378
0.005405 11.583784
0.005405 11.589189
0.005405 11.594595
0.005405 11.600000
0.005405 11.605405
0.005405 11.610811
0.005405 11.616216
0.005405 11.621622
0.005405 11.627027
0.005405 11.632432
0.005405 11.637838
0.005405 11.643243
0.005405 11.648649
0.005405 11.654054
0.005405 11.659459
0.005405 11.664865
0.005405 11.670270
0.005405 11.675676
0.005405 11.681081
0.005405 11.686486
0.005405 11.691892
0.005405 11.697297
0.005405 11.702703
0.005405 11.708108
0.005405 11.713514
0.005405 11.718919
0.005405 11.724324
0.005405 11.729730
0.005405 11.735135
0.005405 11.740541
0.005405 11.745946
0.005405 11.751351
0.005405 11.756757
0.005405 11.762162
0.005405 11.767568
0.005405 11.772973
0.005405 11.778378
0.005405 11.783784
0.005405 11.789189
0.005405 11.794595
0.005405 11.800000
74(0.4)
0.005405 11.805405

0.005405 11.810811
0.005405 11.816216
0.005405 11.821622
0.005405 11.827027
0.005405 11.832432
0.005405 11.837838
0.005405 11.843243
0.005405 11.848649
0.005405 11.854054
0.005405 11.859459
0.005405 11.864865
0.005405 11.870270
0.005405 11.875676
0.005405 11.881081
0.005405 11.886486
0.005405 11.891892
0.005405 11.897297
0.005405 11.902703
0.005405 11.908108
0.005405 11.913514
0.005405 11.918919
0.005405 11.924324
0.005405 11.929730
0.005405 11.935135
0.005405 11.940541
0.005405 11.945946
0.005405 11.951351
0.005405 11.956757
0.005405 11.962162
0.005405 11.967568
0.005405 11.972973
0.005405 11.978378
0.005405 11.983784
0.005405 11.989189
0.005405 11.994595
0.005405 12.000000
0.005405 12.005405
0.005405 12.010811
0.005405 12.016216
0.005405 12.021622
0.005405 12.027027
0.005405 12.032432
0.005405 12.037838
0.005405 12.043243
0.005405 12.048649
0.005405 12.054054
0.005405 12.059459
0.005405 12.064865
0.005405 12.070270
0.005405 12.075676
0.005405 12.081081
0.005405 12.086486
0.005405 12.091892
0.005405 12.097297
0.005405 12.102703
0.005405 12.108108
0.005405 12.113514
0.005405 12.118919
0.005405 12.124324
0.005405 12.129730
0.005405 12.135135
0.005405 12.140541
0.005405 12.145946
0.005405 12.151351
0.005405 12.156757
0.005405 12.162162
0.005405 12.167568
0.005405 12.172973
0.005405 12.178378
0.005405 12.183784
0.005405 12.189189
0.005405 12.194595
0.005405 12.200000
69(0.4)

0.005797 12.205797
0.005797 12.211594
0.005797 12.217391
0.005797 12.223188
0.005797 12.228986
0.005797 12.234783
0.005797 12.240580
0.005797 12.246377
0.005797 12.252174
0.005797 12.257971
0.005797 12.263768
0.005797 12.269565
0.005797 12.275362
0.005797 12.281159
0.005797 12.286957
0.005797 12.292754
0.005797 12.298551
0.005797 12.304348
0.005797 12.310145
0.005797 12.315942
0.005797 12.321739
0.005797 12.327536
0.005797 12.333333
0.005797 12.339130
0.005797 12.344928
0.005797 12.350725
0.005797 12.356522
0.005797 12.362319
0.005797 12.368116
0.005797 12.373913
0.005797 12.379710
0.005797 12.385507
0.005797 12.391304
0.005797 12.397101
0.005797 12.402899
0.005797 12.408696
0.005797 12.414493
0.005797 12.420290
0.005797 12.426087
0.005797 12.431884
0.005797 12.437681
0.005797 12.443478
0.005797 12.449275
0.005797 12.455072
0.005797 12.460870
0.005797 12.466667
0.005797 12.472464
0.005797 12.478261
0.005797 12.484058
0.005797 12.489855
0.005797 12.495652
0.005797 12.501449
0.005797 12.507246
0.005797 12.513043
0.005797 12.518841
0.005797 12.524638
0.005797 12.530435
0.005797 12.536232
0.005797 12.542029
0.005797 12.547826
0.005797 12.553623
0.005797 12.559420
0.005797 12.565217
0.005797 12.571014
0.005797 12.576812
0.005797 12.582609
0.005797 12.588406
0.005797 12.594203
0.005797 12.600000
73(0.4)
0.005479 12.605479
0.005479 12.610959
0.005479 12.616438
0.005479 12.621918

0.005479 12.627397
0.005479 12.632877
0.005479 12.638356
0.005479 12.643836
0.005479 12.649315
0.005479 12.654795
0.005479 12.660274
0.005479 12.665753
0.005479 12.671233
0.005479 12.676712
0.005479 12.682192
0.005479 12.687671
0.005479 12.693151
0.005479 12.698630
0.005479 12.704110
0.005479 12.709589
0.005479 12.715068
0.005479 12.720548
0.005479 12.726027
0.005479 12.731507
0.005479 12.736986
0.005479 12.742466
0.005479 12.747945
0.005479 12.753425
0.005479 12.758904
0.005479 12.764384
0.005479 12.769863
0.005479 12.775342
0.005479 12.780822
0.005479 12.786301
0.005479 12.791781
0.005479 12.797260
0.005479 12.802740
0.005479 12.808219
0.005479 12.813699
0.005479 12.819178
0.005479 12.824658
0.005479 12.830137
0.005479 12.835616
0.005479 12.841096
0.005479 12.846575
0.005479 12.852055
0.005479 12.857534
0.005479 12.863014
0.005479 12.868493
0.005479 12.873973
0.005479 12.879452
0.005479 12.884932
0.005479 12.890411
0.005479 12.895890
0.005479 12.901370
0.005479 12.906849
0.005479 12.912329
0.005479 12.917808
0.005479 12.923288
0.005479 12.928767
0.005479 12.934247
0.005479 12.939726
0.005479 12.945205
0.005479 12.950685
0.005479 12.956164
0.005479 12.961644
0.005479 12.967123
0.005479 12.972603
0.005479 12.978082
0.005479 12.983562
0.005479 12.989041
0.005479 12.994521
0.005479 13.000000
76(0.4)
0.005263 13.005263
0.005263 13.010526
0.005263 13.015789
0.005263 13.021053

0.005263 13.026316
0.005263 13.031579
0.005263 13.036842
0.005263 13.042105
0.005263 13.047368
0.005263 13.052632
0.005263 13.057895
0.005263 13.063158
0.005263 13.068421
0.005263 13.073684
0.005263 13.078947
0.005263 13.084211
0.005263 13.089474
0.005263 13.094737
0.005263 13.100000
0.005263 13.105263
0.005263 13.110526
0.005263 13.115789
0.005263 13.121053
0.005263 13.126316
0.005263 13.131579
0.005263 13.136842
0.005263 13.142105
0.005263 13.147368
0.005263 13.152632
0.005263 13.157895
0.005263 13.163158
0.005263 13.168421
0.005263 13.173684
0.005263 13.178947
0.005263 13.184211
0.005263 13.189474
0.005263 13.194737
0.005263 13.200000
0.005263 13.205263
0.005263 13.210526
0.005263 13.215789
0.005263 13.221053
0.005263 13.226316
0.005263 13.231579
0.005263 13.236842
0.005263 13.242105
0.005263 13.247368
0.005263 13.252632
0.005263 13.257895
0.005263 13.263158
0.005263 13.268421
0.005263 13.273684
0.005263 13.278947
0.005263 13.284211
0.005263 13.289474
0.005263 13.294737
0.005263 13.300000
0.005263 13.305263
0.005263 13.310526
0.005263 13.315789
0.005263 13.321053
0.005263 13.326316
0.005263 13.331579
0.005263 13.336842
0.005263 13.342105
0.005263 13.347368
0.005263 13.352632
0.005263 13.357895
0.005263 13.363158
0.005263 13.368421
0.005263 13.373684
0.005263 13.378947
0.005263 13.384211
0.005263 13.389474
0.005263 13.394737
0.005263 13.400000
79(0.4)
0.005063 13.405063

0.005063 13.410127
0.005063 13.415190
0.005063 13.420253
0.005063 13.425316
0.005063 13.430380
70(0.4)
0.005714 13.805714
0.005714 13.811429
0.005714 13.817143
0.005714 13.822857
0.005714 13.828571
0.005714 13.834286
0.005714 13.840000
0.005714 13.845714
0.005714 13.851429
0.005714 13.857143
0.005714 13.862857
0.005714 13.868571
0.005714 13.874286
0.005714 13.880000
0.005714 13.885714
0.005714 13.891429
0.005714 13.897143
0.005714 13.902857
0.005714 13.908571
0.005714 13.914286
0.005714 13.920000
0.005714 13.925714
0.005714 13.931429
0.005714 13.937143
0.005714 13.942857
0.005714 13.948571
0.005714 13.954286
0.005714 13.960000
0.005714 13.965714
0.005714 13.971429
0.005714 13.977143
0.005714 13.982857
0.005714 13.988571
0.005714 13.994286
0.005714 14.000000
0.005714 14.005714
0.005714 14.011429
0.005714 14.017143
0.005714 14.022857
0.005714 14.028571
0.005714 14.034286
0.005714 14.040000
0.005714 14.045714
0.005714 14.051429
0.005714 14.057143
0.005714 14.062857
0.005714 14.068571
0.005714 14.074286
0.005714 14.080000
0.005714 14.085714
0.005714 14.091429
0.005714 14.097143
0.005714 14.102857
0.005714 14.108571
0.005714 14.114286
0.005714 14.120000
0.005714 14.125714
0.005714 14.131429
0.005714 14.137143
0.005714 14.142857
0.005714 14.148571
0.005714 14.154286
0.005714 14.160000
0.005714 14.165714
0.005714 14.171429
0.005714 14.177143
67(0.4)
0.005714 14.182857
0.005714 14.188571
0.005714 14.194286

0.005714 14.200000
68(0.4)
0.005882 14.205882
0.005882 14.211765
0.005882 14.217647
0.005882 14.223529
0.005882 14.229412
0.005882 14.235294
0.005882 14.241176
0.005882 14.247059
0.005882 14.252941
0.005882 14.258824
0.005882 14.264706
0.005882 14.270588
0.005882 14.276471
0.005882 14.282353
0.005882 14.288235
0.005882 14.294118
0.005882 14.300000
0.005882 14.305882
0.005882 14.311765
0.005882 14.317647
0.005882 14.323529
0.005882 14.329412
0.005882 14.335294
0.005882 14.341176
0.005882 14.347059
0.005882 14.352941
0.005882 14.358824
0.005882 14.364706
0.005882 14.370588
0.005882 14.376471
0.005882 14.382353
0.005882 14.388235
0.005882 14.394118
0.005882 14.400000
0.005882 14.405882
0.005882 14.411765
0.005882 14.417647
0.005882 14.423529
0.005882 14.429412
0.005882 14.435294
0.005882 14.441176
0.005882 14.447059
0.005882 14.452941
0.005882 14.458824
0.005882 14.464706
0.005882 14.470588
0.005882 14.476471
0.005882 14.482353
0.005882 14.488235
0.005882 14.494118
0.005882 14.500000
0.005882 14.505882
0.005882 14.511765
0.005882 14.517647
0.005882 14.523529
0.005882 14.529412
0.005882 14.535294
0.005882 14.541176
0.005882 14.547059
0.005882 14.552941
0.005882 14.558824
0.005882 14.564706
0.005882 14.570588
58(0.4)
0.005882 14.576471
0.005882 14.582353
0.005882 14.588235
0.005882 14.594118
0.005882 14.600000
67(0.4)
0.005970 14.605970
0.005970 14.611940
0.005970 14.617910

0.005970 14.623881
0.005970 14.629851
0.005970 14.635821
0.005970 14.641791
0.005970 14.647761
0.005970 14.653731
0.005970 14.659701
0.005970 14.665672
0.005970 14.671642
0.005970 14.677612
0.005970 14.683582
0.005970 14.689552
0.005970 14.695522
0.005970 14.701493
0.005970 14.707463
0.005970 14.713433
0.005970 14.719403
0.005970 14.725373
0.005970 14.731343
0.005970 14.737313
0.005970 14.743284
0.005970 14.749254
0.005970 14.755224
0.005970 14.761194
0.005970 14.767164
0.005970 14.773134
0.005970 14.779104
0.005970 14.785075
0.005970 14.791045
0.005970 14.797015
0.005970 14.802985
0.005970 14.808955
0.005970 14.814925
0.005970 14.820896
0.005970 14.826866
0.005970 14.832836
0.005970 14.838806
0.005970 14.844776
0.005970 14.850746
0.005970 14.856716
0.005970 14.862687
0.005970 14.868657
0.005970 14.874627
0.005970 14.880597
0.005970 14.886567
0.005970 14.892537
0.005970 14.898507
0.005970 14.904478
0.005970 14.910448
0.005970 14.916418
57(0.4)
0.005970 14.922388
0.005970 14.928358
0.005970 14.934328
0.005970 14.940299
0.005970 14.946269
0.005970 14.952239
0.005970 14.958209
0.005970 14.964179
0.005970 14.970149
0.005970 14.976119
0.005970 14.982090
0.005970 14.988060
0.005970 14.994030
0.005970 15.000000
58(0.4)
0.006897 15.006897
0.006897 15.013793
0.006897 15.020690
0.006897 15.027586
0.006897 15.034483
0.006897 15.041379
0.006897 15.048276
0.006897 15.055172
0.006897 15.062069

0.006897 15.068966
0.006897 15.075862
0.006897 15.082759
0.006897 15.089655
0.006897 15.096552
0.006897 15.103448
0.006897 15.110345
0.006897 15.117241
0.006897 15.124138
0.006897 15.131034
0.006897 15.137931
0.006897 15.144828
0.006897 15.151724
0.006897 15.158621
0.006897 15.165517
0.006897 15.172414
0.006897 15.179310
0.006897 15.186207
0.006897 15.193103
0.006897 15.200000
0.006897 15.206897
0.006897 15.213793
0.006897 15.220690
0.006897 15.227586
0.006897 15.234483
0.006897 15.241379
0.006897 15.248276
0.006897 15.255172
0.006897 15.262069
0.006897 15.268966
0.006897 15.275862
0.006897 15.282759
0.006897 15.289655
0.007018 15.800000
45(0.4)
0.008889 15.808889
0.008889 15.817778
0.008889 15.826667
0.008889 15.835556
0.008889 15.844444
0.008889 15.853333
0.008889 15.862222
39(0.4)
0.010256 15.871111
0.010256 15.880000
0.010256 15.888889
0.010256 15.897778
0.010256 15.906667
0.010256 15.915556
0.010256 15.924444
0.010256 15.933333
0.010256 15.942222
0.010256 15.951111
0.010256 15.960000
0.010256 15.968889
0.010256 15.977778
0.010256 15.986667
0.010256 15.995556
0.008889 16.004444
0.008889 16.013333
0.008889 16.022222
0.008889 16.031111
0.008889 16.040000
0.008889 16.048889
0.008889 16.057778
0.008889 16.066667
0.008889 16.075556
0.008889 16.084444
0.008889 16.093333
0.008889 16.102222
0.008889 16.111111
0.008889 16.120000
0.008889 16.128889
0.008889 16.137778
0.008889 16.146667
0.008889 16.155556

0.008889 16.164444
0.008889 16.173333
0.008889 16.182222
0.008889 16.191111
0.008889 16.200000
34(0.4)
0.011765 16.211765
0.011765 16.223529
0.011765 16.235294
0.011765 16.247059
0.011765 16.258824
0.011765 16.270588
0.011765 16.282353
0.011765 16.294118
0.011765 16.305882
0.011765 16.317647
0.011765 16.329412
0.011765 16.341176
0.011765 16.352941
0.011765 16.364706
0.011765 16.376471
0.011765 16.388235
0.011765 16.400000
0.011765 16.411765
0.011765 16.423529
0.011765 16.435294
0.011765 16.447059
0.011765 16.458824
0.011765 16.470588
0.011765 16.482353
0.011765 16.494118
0.011765 16.505882
0.011765 16.517647
0.011765 16.529412
0.011765 16.541176
0.011765 16.552941
0.011765 16.564706
0.011765 16.576471
0.011765 16.588235
0.011765 16.600000
39(0.4)
0.010256 16.610256
0.010256 16.620513
0.010256 16.630769
0.010256 16.641026
0.010256 16.651282
0.010256 16.661538
0.010256 16.671795
0.010256 16.682051
0.010256 16.692308
0.010256 16.702564
0.010256 16.712821
0.010256 16.723077
0.010256 16.733333
0.010256 16.743590
0.010256 16.753846
0.010256 16.764103
0.010256 16.774359
0.010256 16.784615
0.010256 16.794872
0.010256 16.805128
0.010256 16.815385
0.010256 16.825641
0.010256 16.835897
0.010256 16.846154
0.010256 16.856410
0.010256 16.866667
0.010256 16.876923
0.010256 16.887179
0.010256 16.897436
0.010256 16.907692
0.010256 16.917949
0.010256 16.928205
0.010256 16.938462

0.010256 16.948718
0.010256 16.958974
0.010256 16.969231
0.010256 16.979487
0.010256 16.989744
0.010256 17.000000
42(0.4)
0.009524 17.009524
0.009524 17.019048
0.009524 17.028571
0.009524 17.038095
0.009524 17.047619
0.009524 17.057143
0.009524 17.066667
0.009524 17.076190
0.009524 17.085714
0.009524 17.095238
0.009524 17.104762
0.009524 17.114286
0.009524 17.123810
0.009524 17.133333
0.009524 17.142857
0.009524 17.152381
0.009524 17.161905
0.009524 17.171429
0.009524 17.180952
0.009524 17.190476
0.009524 17.200000
0.009524 17.209524
0.009524 17.219048
0.009524 17.228571
0.009524 17.238095
0.009524 17.247619
0.009524 17.257143
0.009524 17.266667
0.009524 17.276190
0.009524 17.285714
0.009524 17.295238
0.009524 17.304762
0.009524 17.314286
0.009524 17.323810
0.009524 17.333333
0.009524 17.342857
0.009524 17.352381
0.009524 17.361905
0.009524 17.371429
0.009524 17.380952
0.009524 17.390476
0.009524 17.400000
58(0.4)
0.006897 17.406897
0.006897 17.413793
0.006897 17.420690
0.006897 17.427586
0.006897 17.434483
0.006897 17.441379
0.006897 17.448276
0.006897 17.455172
0.006897 17.462069
0.006897 17.468966
0.006897 17.475862
0.006897 17.482759
0.006897 17.489655
0.006897 17.496552
0.006897 17.503448
0.006897 17.510345
0.006897 17.517241
0.006897 17.524138
0.006897 17.531034
0.006897 17.537931
0.006897 17.544828
0.006897 17.551724
0.006897 17.558621
0.006897 17.565517

0.006897 17.572414
0.006897 17.579310
0.006897 17.586207
0.006897 17.593103
0.006897 17.600000
0.006897 17.606897
0.006897 17.613793
0.006897 17.620690
0.006897 17.627586
0.006897 17.634483
0.006897 17.641379
0.006897 17.648276
0.006897 17.655172
0.006897 17.662069
0.006897 17.668966
0.006897 17.675862
0.006897 17.682759
0.006897 17.689655
0.006897 17.696552
0.006897 17.703448
0.006897 17.710345
0.006897 17.717241
0.006897 17.724138
0.006897 17.731034
0.006897 17.737931
0.006897 17.744828
0.006897 17.751724
0.006897 17.758621
0.006897 17.765517
0.006897 17.772414
0.006897 17.779310
0.006897 17.786207
0.006897 17.793103
0.006897 17.800000
48(0.4)
0.008333 17.808333
0.008333 17.816667
0.008333 17.825000
0.008333 17.833333
0.008333 17.841667
0.008333 17.850000
0.008333 17.858333
0.008333 17.866667
0.008333 17.875000
0.008333 17.883333
0.008333 17.891667
0.008333 17.900000
0.008333 17.908333
0.008333 17.916667
0.008333 17.925000
0.008333 17.933333
0.008333 17.941667
0.008333 17.950000
0.008333 17.958333
0.008333 17.966667
0.008333 17.975000
0.008333 17.983333
0.008333 17.991667
0.008333 18.000000
0.008333 18.008333
0.008333 18.016667
0.008333 18.025000
0.008333 18.033333
0.008333 18.041667
0.008333 18.050000
0.008333 18.058333
0.008333 18.066667
0.008333 18.075000
0.008333 18.083333
0.008333 18.091667
0.008333 18.100000
0.008333 18.108333
0.008333 18.116667
0.008333 18.125000

0.008333 18.133333
0.008333 18.141667
0.008333 18.150000
0.008333 18.158333
0.008333 18.166667
0.008333 18.175000
0.008333 18.183333
0.008333 18.191667
0.008333 18.200000
41(0.4)
0.009756 18.209756
0.009756 18.219512
0.009756 18.229268
0.009756 18.239024
0.009756 18.248780
0.009756 18.258537
0.009756 18.268293
0.009756 18.278049
0.009756 18.287805
0.009756 18.297561
0.009756 18.307317
0.009756 18.317073
0.009756 18.326829
0.009756 18.336585
0.009756 18.346341
0.009756 18.356098
0.009756 18.365854
0.009756 18.375610
0.009756 18.385366
0.009756 18.395122
0.009756 18.404878
0.009756 18.414634
0.009756 18.424390
0.009756 18.434146
0.009756 18.443902
0.009756 18.453659
0.009756 18.463415
0.009756 18.473171
0.009756 18.482927
0.009756 18.492683
0.009756 18.502439
0.009756 18.512195
0.009756 18.521951
0.009756 18.531707
0.009756 18.541463
0.009756 18.551220
0.009756 18.560976
0.009756 18.570732
0.009756 18.580488
0.009756 18.590244
0.009756 18.600000
30(0.4)
0.013333 19.413333
0.013333 19.426667
0.013333 19.440000
0.013333 19.453333
0.013333 19.466667
0.013333 19.480000
0.013333 19.493333
0.013333 19.506667
0.013333 19.520000
0.013333 19.533333
0.013333 19.546667
0.013333 19.560000
0.013333 19.573333
0.013333 19.586667
0.013333 19.600000
0.013333 19.613333
0.013333 19.626667
0.013333 19.640000
0.013333 19.653333
0.013333 19.666667
0.013333 19.680000
0.013333 19.693333
0.013333 19.706667

0.011111 18.855556
0.011111 18.866667
0.011111 18.877778
0.011111 18.888889
0.011111 18.900000
0.011111 18.911111
0.011111 18.922222
0.011111 18.933333
0.011111 18.944444
0.011111 18.955556
0.011111 18.966667
0.011111 18.977778
0.011111 18.988889
0.011111 19.000000
35(0.4)
0.011429 19.011429
0.011429 19.022857
0.011429 19.034286
0.011429 19.045714
0.011429 19.057143
0.011429 19.068571
0.011429 19.080000
0.011429 19.091429
0.011429 19.102857
0.011429 19.114286
0.011429 19.125714
0.011429 19.137143
0.011429 19.148571
0.011429 19.160000
0.011429 19.171429
0.011429 19.182857
0.011429 19.194286
0.011429 19.205714
0.011429 19.217143
0.011429 19.228571
0.011429 19.240000
0.011429 19.251429
0.011429 19.262857
0.011429 19.274286
0.011429 19.285714
0.011429 19.297143
0.011429 19.308571
0.011429 19.320000
0.011429 19.331429
0.011429 19.342857
0.011429 19.354286
0.011429 19.365714
0.011429 19.377143
0.011429 19.388571
0.011429 19.400000
36(0.4)
0.011111 18.611111
0.011111 18.622222
0.011111 18.633333
0.011111 18.644444
0.011111 18.655556
0.011111 18.666667
0.011111 18.677778
0.011111 18.688889
0.011111 18.700000
0.011111 18.711111
0.011111 18.722222
0.011111 18.733333
0.011111 18.744444
0.011111 18.755556
0.011111 18.766667
0.011111 18.777778
0.011111 18.788889
0.011111 18.800000
0.011111 18.811111
0.011111 18.822222
0.011111 18.833333
0.011111 18.844444

0.013333 19.720000
0.013333 19.733333
0.013333 19.746667
0.013333 19.760000
0.013333 19.773333
0.013333 19.786667
0.013333 19.800000
36(0.4)
0.011111 19.811111
0.011111 19.822222
0.011111 19.833333
0.011111 19.844444
0.011111 19.855556
0.011111 19.866667
0.011111 19.877778
0.011111 19.888889
0.011111 19.900000
0.011111 19.911111
0.011111 19.922222
0.011111 19.933333
0.011111 19.944444
0.011111 19.955556
0.011111 19.966667
0.011111 19.977778
0.011111 19.988889
0.011111 20.000000
0.011111 20.011111
0.011111 20.022222
0.011111 20.033333
0.011111 20.044444
0.011111 20.055556
0.011111 20.066667
0.011111 20.077778
0.011111 20.088889
0.011111 20.100000
0.011111 20.111111
0.011111 20.122222
0.011111 20.133333
0.011111 20.144444
0.011111 20.155556
0.011111 20.166667
0.011111 20.177778
0.011111 20.188889
0.011111 20.200000
36(0.4)
0.011111 20.211111
0.011111 20.222222
0.011111 20.233333
0.011111 20.244444
0.011111 20.255556
0.011111 20.266667
0.011111 20.277778
0.011111 20.288889
0.011111 20.300000
0.011111 20.311111
0.011111 20.322222
0.011111 20.333333
0.011111 20.344444
0.011111 20.355556
0.011111 20.366667
0.011111 20.377778
0.011111 20.388889
0.011111 20.400000
0.011111 20.411111
0.011111 20.422222
0.011111 20.433333
0.011111 20.444444
0.011111 20.455556
0.011111 20.466667
0.011111 20.477778
0.011111 20.488889
0.011111 20.500000
0.011111 20.511111
0.011111 20.522222

0.011111 20.533333
0.011111 20.544444
0.011111 20.555556
0.011111 20.566667
0.011111 20.577778
0.011111 20.588889
0.011111 20.600000
33(0.4)
0.012121 20.612121
0.012121 20.624242
0.012121 20.636364
0.012121 20.648485
0.012121 20.660606
0.012121 20.672727
0.012121 20.684848
0.012121 20.696970
0.012121 20.709091
0.012121 20.721212
0.012121 20.733333
0.012121 20.745455
0.012121 20.757576
0.012121 20.769697
0.012121 20.781818
0.012121 20.793939
0.012121 20.806061
0.012121 20.818182
0.012121 20.830303
0.012121 20.842424
0.012121 20.854545
0.012121 20.866667
0.012121 20.878788
0.012121 20.890909
0.012121 20.903030
0.012121 20.915152
0.012121 20.927273
0.012121 20.939394
0.012121 20.951515
0.012121 20.963636
0.012121 20.975758
0.012121 20.987879
0.012121 21.000000
42(0.4)
0.009524 21.009524
0.009524 21.019048
0.009524 21.028571
0.009524 21.038095
0.009524 21.047619
0.009524 21.057143
0.009524 21.066667
0.009524 21.076190
0.009524 21.085714
0.009524 21.095238
0.009524 21.104762
0.009524 21.114286
0.009524 21.123810
0.009524 21.133333
0.009524 21.142857
0.009524 21.152381
0.009524 21.161905
0.009524 21.171429
0.009524 21.180952
0.009524 21.190476
0.009524 21.200000
0.009524 21.209524
0.009524 21.219048
0.009524 21.228571
0.009524 21.238095
0.009524 21.247619
0.009524 21.257143
0.009524 21.266667
0.009524 21.276190
0.009524 21.285714
0.009524 21.295238
0.009524 21.304762

0.009524 21.314286
0.009524 21.323810
0.009524 21.333333
0.009524 21.342857
0.009524 21.352381
0.009524 21.361905
0.009524 21.371429
0.009524 21.380952
0.009524 21.390476
0.009524 21.400000
51(0.4)
0.007843 21.407843
0.007843 21.415686
0.007843 21.423529
0.007843 21.431373
0.007843 21.439216
0.007843 21.447059
0.007843 21.454902
0.007843 21.462745
0.007843 21.470588
0.007843 21.478431
0.007843 21.486275
0.007843 21.494118
0.007843 21.501961
0.007843 21.509804
0.007843 21.517647
0.007843 21.525490
0.007843 21.533333
0.007843 21.541176
0.007843 21.549020
0.007843 21.556863
0.007843 21.564706
0.007843 21.572549
0.007843 21.580392
0.007843 21.588235
0.007843 21.596078
0.007843 21.603922
0.007843 21.611765
0.007843 21.619608
0.007843 21.627451
0.007843 21.635294
0.007843 21.643137
0.007843 21.650980
0.007843 21.658824
0.007843 21.666667
0.007843 21.674510
0.007843 21.682353
0.007843 21.690196
0.007843 21.698039
0.007843 21.705882
0.007843 21.713725
0.007843 21.721569
0.007843 21.729412
0.007843 21.737255
0.007843 21.745098
0.007843 21.752941
0.007843 21.760784
0.007843 21.768627
0.007843 21.776471
0.007843 21.784314
0.007843 21.792157
0.007843 21.800000
31(0.4)
0.012903 21.812903
0.012903 21.825806
0.012903 21.838710
0.012903 21.851613
0.012903 21.864516
0.012903 21.877419
0.012903 21.890323
0.012903 21.903226
0.012903 21.916129
0.012903 21.929032
0.012903 21.941935

0.012903 21.954839
0.012903 21.967742
0.012903 21.980645
0.012903 21.993548
0.012903 22.006452
0.012903 22.019355
0.012903 22.032258
0.012903 22.045161
32(0.4)
0.012903 22.058065
0.012903 22.070968
0.012903 22.083871
0.012903 22.096774
0.012903 22.109677
0.012903 22.122581
0.012903 22.135484
0.012903 22.148387
0.012903 22.161290
0.012903 22.174194
0.012903 22.187097
0.012903 22.200000
27(0.4)
0.014815 22.214815
0.014815 22.229630
0.014815 22.244444
0.014815 22.259259
0.014815 22.274074
0.014815 22.288889
0.014815 22.303704
0.014815 22.318519
0.014815 22.333333
0.014815 22.348148
0.014815 22.362963
0.014815 22.377778
0.014815 22.392593
0.014815 22.407407
0.014815 22.422222
0.014815 22.437037
0.014815 22.451852
0.014815 22.466667
0.014815 22.481481
0.014815 22.496296
28(0.4)
0.014286 23.414286
0.014286 23.428571
0.014286 23.442857
0.014286 23.457143
0.014286 23.471429
0.014286 23.485714
0.014286 23.500000
0.014286 23.514286
0.014286 23.528571
0.014286 23.542857
0.014286 23.557143
0.014286 23.571429
0.014286 23.585714
0.014286 23.600000
0.014286 23.614286
0.014286 23.628571
0.014286 23.642857
0.014286 23.657143
0.014286 23.671429
0.014286 23.685714
0.014286 23.700000
0.014286 23.714286
0.014286 23.728571
0.014286 23.742857
0.014286 23.757143
0.014286 23.771429
0.014286 23.785714
0.014286 23.800000
27(0.4)
0.014815 23.814815
0.014815 23.829630
0.014815 23.844444
0.014815 23.859259

0.012500 22.925000
0.012500 22.937500
0.012500 22.950000
0.012500 22.962500
0.012500 22.975000
0.012500 22.987500
0.012500 23.000000
32(0.4)
0.012500 23.012500
0.012500 23.025000
0.012500 23.037500
0.012500 23.050000
0.012500 23.062500
0.012500 23.075000
0.012500 23.087500
0.012500 23.100000
0.012500 23.112500
0.012500 23.125000
0.012500 23.137500
0.012500 23.150000
0.012500 23.162500
0.012500 23.175000
0.012500 23.187500
0.012500 23.200000
25(0.4)
0.012500 23.212500
0.012500 23.225000
0.012500 23.237500
0.012500 23.250000
0.012500 23.262500
0.012500 23.275000
0.012500 23.287500
0.012500 23.300000
0.012500 23.312500
0.012500 23.325000
0.012500 23.337500
0.012500 23.350000
0.012500 23.362500
0.012500 23.375000
0.012500 23.387500
0.012500 23.400000
28(0.4)
0.014286 23.414286
0.014286 23.428571
0.014286 23.442857
0.014286 23.457143
0.014286 23.471429
0.014286 23.485714
0.014286 23.500000
0.014286 23.514286
0.014286 23.528571
0.014286 23.542857
0.014286 23.557143
0.014286 23.571429
0.014286 23.585714
0.014286 23.600000
0.014286 23.614286
0.014286 23.628571
0.014286 23.642857
0.014286 23.657143
0.014286 23.671429
0.014286 23.685714
0.014286 23.700000
0.014286 23.714286
0.014286 23.728571
0.014286 23.742857
0.014286 23.757143
0.014286 23.771429
0.014286 23.785714
0.014286 23.800000
27(0.4)
0.014815 23.814815
0.014815 23.829630
0.014815 23.844444
0.014815 23.859259

0.014815 23.874074
0.014815 23.888889
0.014815 23.903704
0.014815 23.918519
0.014815 23.933333
0.014815 23.948148
0.014815 23.962963
0.014815 23.977778
0.014815 23.992593
0.014815 24.007407
0.014815 24.022222
0.014815 24.037037
0.014815 24.051852
0.014815 24.066667
0.014815 24.081481
0.014815 24.096296
0.014815 24.111111
0.014815 24.125926
0.014815 24.140741
0.014815 24.155556
0.014815 24.170370
0.014815 24.185185
0.014815 24.200000
25(0.4)
0.016000 24.216000
0.016000 24.232000
0.016000 24.248000
0.016000 24.264000
0.016000 24.280000
0.016000 24.296000
0.016000 24.312000
0.016000 24.328000
0.016000 24.344000
0.016000 24.360000
0.016000 24.376000
0.016000 24.392000
0.016000 24.408000
0.016000 24.424000
0.016000 24.440000
0.016000 24.456000
0.016000 24.472000
0.016000 24.488000
0.016000 24.504000
0.016000 24.520000
0.016000 24.536000
0.016000 24.552000
0.016000 24.568000
0.016000 24.584000
0.016000 24.600000
23(0.4)
0.017391 24.617391
0.017391 24.634783
0.017391 24.652174
0.017391 24.669565
0.017391 24.686957
0.017391 24.704348
0.017391 24.721739
0.017391 24.739130
0.017391 24.756522
0.017391 24.773913
0.017391 24.791304
0.017391 24.808696
0.017391 24.826087
0.017391 24.843478
0.017391 24.860870
0.017391 24.878261
0.017391 24.895652
0.017391 24.913043
0.017391 24.930435
0.017391 24.947826
0.017391 24.965217
0.017391 24.982609
0.017391 25.000000
24(0.4)

0.016667 25.016667
0.016667 25.033333
0.016667 25.050000
0.016667 25.066667
0.016667 25.083333
0.016667 25.100000
0.016667 25.116667
0.016667 25.133333
0.016667 25.150000
0.016667 25.166667
0.016667 25.183333
0.016667 25.200000
0.016667 25.216667
0.016667 25.233333
0.016667 25.250000
0.016667 25.266667
0.016667 25.283333
0.016667 25.300000
0.016667 25.316667
0.016667 25.333333
0.016667 25.350000
0.016667 25.366667
0.016667 25.383333
0.016667 25.400000
19(0.4)
0.021053 27.021053
0.021053 27.042105
0.021053 27.063158
0.021053 27.084211
0.021053 27.105263
0.021053 27.126316
0.021053 27.147368
20(0.4)
0.021053 27.168421
0.021053 27.189474
0.021053 27.210526
0.021053 27.231579
0.021053 27.252632
0.021053 27.273684
0.021053 27.294737
0.021053 27.315789
0.021053 27.336842
0.021053 27.357895
0.021053 27.378947
0.021053 27.400000
21(0.4)
0.019048 27.419048
0.019048 27.438095
0.019048 27.457143
0.019048 27.476190
0.019048 27.495238
0.019048 27.514286
0.019048 27.533333
0.019048 27.552381
14(0.4)
0.028571 28.571429
0.028571 28.585714
0.028571 28.600000
0.028571 28.614286
0.028571 28.628571
0.028571 28.642857
0.028571 28.657143
0.028571 28.671429
0.028571 28.685714
0.028571 28.700000
0.028571 28.714286
0.028571 28.728571
0.028571 28.742857
0.028571 28.757143
0.028571 28.771429
0.028571 28.785714
0.028571 28.800000
13(0.4)
0.030769 28.815385
0.030769 28.830769
0.030769 28.846154
0.030769 28.861538
0.030769 28.876923
0.030769 28.892308
0.030769 28.907692
0.030769 28.923077
0.030769 28.938462
0.030769 28.953846
0.030769 28.969231
0.030769 28.984615
0.030769 29.000000
13(0.4)
0.030769 29.015385
0.030769 29.030769
0.030769 29.046154
0.030769 29.061538
0.030769 29.076923
0.030769 29.092308
0.030769 29.107692
0.030769 29.123077
0.030769 29.138462
0.030769 29.153846
0.030769 29.169231
0.030769 29.184615
0.030769 29.200000
13(0.4)
0.030769 29.215385
0.030769 29.230769
0.030769 29.246154
0.030769 29.261538
0.030769 29.276923
0.030769 29.292308
0.030769 29.307692
0.030769 29.323077
0.030769 29.338462
0.030769 29.353846
0.030769 29.369231
0.030769 29.384615
0.030769 29.400000
13(0.4)
0.030769 29.415385
0.030769 29.430769
0.030769 29.446154
0.030769 29.461538
0.030769 29.476923

0.030769 26.507692
0.030769 26.538462
0.030769 26.569231
0.030769 26.600000
18(0.4)
0.022222 26.622222
0.022222 26.644444
0.022222 26.666667
0.022222 26.688889
0.022222 26.711111
0.022222 26.733333
19(0.4)
0.022222 26.755556
0.022222 26.777778
0.022222 26.800000
0.022222 26.822222
0.022222 26.844444
0.022222 26.866667
0.022222 26.888889
0.022222 26.911111
0.022222 26.933333
0.022222 26.955556
0.022222 26.977778
0.022222 27.000000
19(0.4)
0.021053 27.021053
0.021053 27.042105
0.021053 27.063158
0.021053 27.084211
0.021053 27.105263
0.021053 27.126316
0.021053 27.147368
20(0.4)
0.021053 27.168421
0.021053 27.189474
0.021053 27.210526
0.021053 27.231579
0.021053 27.252632
0.021053 27.273684
0.021053 27.294737
0.021053 27.315789
0.021053 27.336842
0.021053 27.357895
0.021053 27.378947
0.021053 27.400000
21(0.4)
0.019048 27.419048
0.019048 27.438095
0.019048 27.457143
0.019048 27.476190
0.019048 27.495238
0.019048 27.514286
0.019048 27.533333
0.019048 27.552381
14(0.4)
0.028571 29.028571
0.028571 29.057143
0.028571 29.085714
0.028571 29.114286
0.028571 29.142857
0.028571 29.171429
0.028571 29.200000
0.028571 29.228571
0.028571 29.257143
0.028571 29.285714
0.028571 29.314286
0.028571 29.342857
0.028571 29.371429
0.028571 29.400000
13(0.4)
0.030769 29.430769
0.030769 29.461538
0.030769 29.492308
0.030769 29.523077
0.030769 29.553846
0.030769 29.584615
0.030769 29.615385

0.022222 28.000000
0.022222 28.022222
0.022222 28.044444
0.022222 28.066667
0.022222 28.088889
0.022222 28.111111
0.022222 28.133333
0.022222 28.155556
0.022222 28.177778
0.022222 28.200000
19(0.4)
0.021053 28.221053
0.021053 28.242105
0.021053 28.263158
0.021053 28.284211
0.021053 28.305263
0.021053 28.326316
0.021053 28.347368
0.021053 28.368421
0.021053 28.389474
0.021053 28.410526
0.021053 28.431579
0.021053 28.452632
0.021053 28.473684
0.021053 28.494737
0.021053 28.515789
0.021053 28.536842
0.021053 28.557895
0.021053 28.578947
0.021053 28.600000
20(0.4)
0.020000 28.620000
0.020000 28.640000
0.020000 28.660000
0.020000 28.680000
0.020000 28.700000
0.020000 28.720000
0.020000 28.740000
0.020000 28.760000
0.020000 28.780000
0.020000 28.800000
0.020000 28.820000
0.020000 28.840000
0.020000 28.860000
0.020000 28.880000
0.020000 28.900000
0.020000 28.920000
0.020000 28.940000
0.020000 28.960000
0.020000 28.980000
0.020000 29.000000
14(0.4)
0.028571 29.028571
0.028571 29.057143
0.028571 29.085714
0.028571 29.114286
0.028571 29.142857
0.028571 29.171429
0.028571 29.200000
0.028571 29.228571
0.028571 29.257143
0.028571 29.285714
0.028571 29.314286
0.028571 29.342857
0.028571 29.371429
0.028571 29.400000
13(0.4)
0.030769 29.430769
0.030769 29.461538
0.030769 29.492308
0.030769 29.523077
0.030769 29.553846
0.030769 29.584615
0.030769 29.615385

0.030769 29.646154
0.030769 29.676923
0.030769 29.707692
0.030769 29.738462
0.030769 29.769231
0.030769 29.800000
14(0.4)
0.028571 29.828571
0.028571 29.857143
0.028571 29.885714
0.028571 29.914286
0.028571 29.942857
0.028571 29.971429
0.028571 30.000000
0.028571 30.028571
0.028571 30.057143
0.028571 30.085714
0.028571 30.114286
0.028571 30.142857
0.028571 30.171429
0.028571 30.200000
9(0.4)
0.044444 30.244444
0.044444 30.288889
0.044444 30.333333
0.044444 30.377778
0.044444 30.422222
0.044444 30.466667
0.044444 30.511111
0.044444 30.555556
0.044444 30.600000
8(0.4)
0.050000 30.650000
0.050000 30.700000
0.050000 30.750000
0.050000 30.800000
0.050000 30.850000
0.050000 30.900000
0.050000 30.950000
0.050000 31.000000
10(0.4)
0.040000 31.040000
0.040000 31.080000
0.040000 31.120000
0.040000 31.160000
0.040000 31.200000
0.040000 31.240000
0.040000 31.280000
0.040000 31.320000
0.040000 31.360000
0.040000 31.400000
14(0.4)
0.028571 31.428571
0.028571 31.457143
0.028571 31.485714
0.028571 31.514286
0.028571 31.542857
0.028571 31.571429
0.028571 31.600000
0.028571 31.628571
0.028571 31.657143
0.028571 31.685714
0.028571 31.714286
0.028571 31.742857
0.028571 31.771429
0.028571 31.800000
16(0.4)
0.025000 31.825000
0.025000 31.850000
0.025000 31.875000
0.025000 31.900000
0.025000 31.925000
0.025000 31.950000
0.025000 31.975000

0.025000 32.000000
0.025000 32.025000
0.025000 32.050000
0.025000 32.075000
0.025000 32.100000
0.025000 32.125000
0.025000 32.150000
0.025000 32.175000
0.025000 32.200000
15(0.4)
0.026667 32.226667
0.026667 32.253333
0.026667 32.280000
0.026667 32.306667
0.026667 32.333333
0.026667 32.360000
0.026667 32.386667
0.026667 32.413333
0.026667 32.440000
0.026667 32.466667
0.026667 32.493333
0.026667 32.520000
0.026667 32.546667
0.026667 32.573333
0.026667 32.600000
13(0.4)
0.030769 32.630769
0.030769 32.661538
0.030769 32.692308
0.030769 32.723077
0.030769 32.753846
0.030769 32.784615
0.030769 32.815385
0.030769 32.846154
0.030769 32.876923
0.030769 32.907692
0.030769 32.938462
0.030769 32.969231
0.030769 33.000000
7(0.4)
0.057143 33.057143
0.057143 33.114286
0.057143 33.171429
0.057143 33.228571
0.057143 33.285714
0.057143 33.342857
0.057143 33.400000
6(0.4)
0.066667 33.466667
0.066667 33.533333
0.066667 33.600000
0.066667 33.666667
0.066667 33.733333
0.066667 33.800000
9(0.4)
0.044444 33.844444
0.044444 33.888889
0.044444 33.933333
0.044444 33.977778
0.044444 34.022222
0.044444 34.066667
0.044444 34.111111
0.044444 34.155556
0.044444 34.200000
7(0.4)
0.057143 34.257143
0.057143 34.314286
0.057143 34.371429
0.057143 34.428571
0.057143 34.485714
0.057143 34.542857
0.057143 34.600000
7(0.4)
0.057143 34.657143

0.057143 34.714286
0.057143 34.771429
0.057143 34.828571
0.057143 34.885714
0.057143 34.942857
0.057143 35.000000
5(0.4)
0.080000 35.080000
0.080000 35.160000
0.080000 35.240000
0.080000 35.320000
0.080000 35.400000
7(0.4)
0.057143 35.457143
0.057143 35.514286
0.057143 35.571429
0.057143 35.628571
0.057143 35.685714
0.057143 35.742857
0.057143 35.800000
5(0.4)
0.080000 35.880000
0.080000 35.960000
0.080000 36.040000
0.080000 36.120000
0.080000 36.200000
3(0.4)
0.133333 36.333333
0.133333 36.466667
0.133333 36.600000
11(0.4)
0.036364 36.636364
0.036364 36.672727
0.036364 36.709091
0.036364 36.745455
0.036364 36.781818
0.036364 36.818182
0.036364 36.854545
0.036364 36.890909
0.036364 36.927273
0.036364 36.963636
0.036364 37.000000
5(0.4)
0.080000 37.080000
0.080000 37.160000
0.080000 37.240000
0.080000 37.320000
0.080000 37.400000
3(0.4)
0.133333 37.533333
0.133333 37.666667
0.133333 37.800000
4(0.4)
0.100000 37.900000
0.100000 38.000000
0.100000 38.100000
0.100000 38.200000
7(0.4)
0.057143 38.257143
0.057143 38.314286
0.057143 38.371429
0.057143 38.428571
0.057143 38.485714
0.057143 38.542857
0.057143 38.600000
8(0.4)
0.050000 38.650000
0.050000 38.700000
0.050000 38.750000
0.050000 38.800000
0.050000 38.850000
0.050000 38.900000
0.050000 38.950000
0.050000 39.000000

6(0.4)
0.066667 39.066667
0.066667 39.133333
0.066667 39.200000
0.066667 39.266667
0.066667 39.333333
0.066667 39.400000
8(0.4)
0.050000 39.450000
0.050000 39.500000
0.050000 39.550000
0.050000 39.600000
0.050000 39.650000
0.050000 39.700000
0.050000 39.750000
0.050000 39.800000
2(0.4)
0.200000 40.000000
0.200000 40.200000
3(0.4)
0.133333 40.333333
0.133333 40.466667
0.133333 40.600000
2(0.4)
0.200000 40.800000
0.200000 41.000000
0,3(0.4)
0.533333 41.533333
0.133333 41.666667
0.133333 41.800000
2(0.4)
0.200000 42.000000
0.200000 42.200000
2(0.4)
0.200000 42.400000
0.200000 42.600000
0,2(0.4)
0.600000 43.200000
0.200000 43.400000
2(0.4)
0.200000 43.600000
0.200000 43.800000
2(0.4)
0.200000 44.000000
0.200000 44.200000
1(0.4)
0.400000 44.600000
2(0.4)
0.200000 44.800000
0.200000 45.000000
1(0.4)
0.400000 45.400000
3(0.4)
0.133333 45.533333
0.133333 45.666667
0.133333 45.800000
2(0.4)
0.200000 46.000000
0.200000 46.200000
1(0.4)
0.400000 46.600000
2(0.4)
0.200000 46.800000
0.200000 47.000000
1(0.4)
0.400000 47.400000
2(0.4)
0.200000 47.600000
0.200000 47.800000
0,3,3(0.4)
0.933333 48.733333
0.133333 48.866667
0.133333 49.000000
2(0.4)

0.200000 49.200000
0.200000 49.400000
1(0.4)
0.400000 49.800000
7(0.4)
0.057143 49.857143
0.057143 49.914286
0.057143 49.971429
0.057143 50.028571
0.057143 50.085714
0.057143 50.142857
0.057143 50.200000
5(0.4)
0.080000 50.280000
0.080000 50.360000
0.080000 50.440000
0.080000 50.520000
0.080000 50.600000
2(0.4)
0.200000 50.800000
0.200000 51.000000
0,1(0.4)
0.800000 51.800000
2(0.4)
0.200000 52.000000
0.200000 52.200000
0,3(0.4)
0.533333 52.733333
0.133333 52.866667
0.133333 53.000000
1(0.4)
0.400000 53.400000
2(0.4)
0.200000 53.600000
0.200000 53.800000
2(0.4)
0.200000 54.000000
0.200000 54.200000
3(0.4)
0.133333 54.333333
0.133333 54.466667
0.133333 54.600000
1(0.4)
0.400000 55.000000
0,0,0,0,1(0.4)
2.000000 57.000000
1(0.4)
0.400000 57.400000
2(0.4)
0.200000 57.600000
0.200000 57.800000
1(0.4)
0.400000 58.200000
1(0.4)
0.400000 58.600000
0,0,0,4(0.4)
1.300000 59.900000
0.100000 60.000000
0.100000 60.100000
0.100000 60.200000
3(0.4)
0.133333 60.333333
0.133333 60.466667
0.133333 60.600000
2(0.4)
0.200000 60.800000
0.200000 61.000000
3(0.4)
0.133333 61.133333
0.133333 61.266667
0.133333 61.400000
1(0.4)
0.400000 61.800000
0,2(0.4)

0.600000 62.400000
0.200000 62.600000
0,2(0.4)
0.600000 63.200000
0.200000 63.400000
0,0,1(0.4)
1.200000 64.600000
0,2(0.4)
0.600000 65.200000
0.200000 65.400000

DK1
SW
56(0.2)
0.003571 0.003571
0.003571 0.007143
0.003571 0.010714
0.003571 0.014286
0.003571 0.017857
0.003571 0.021429
0.003571 0.025000
0.003571 0.028571
0.003571 0.032143
0.003571 0.035714
0.003571 0.039286
0.003571 0.042857
0.003571 0.046429
0.003571 0.050000
0.003571 0.053571
0.003571 0.057143
0.003571 0.060714
0.003571 0.064286
0.003571 0.067857
0.003571 0.071429
0.003571 0.075000
0.003571 0.078571
0.003571 0.082143
0.003571 0.085714
0.003571 0.089286
0.003571 0.092857
0.003571 0.096429
0.003571 0.100000
0.003571 0.103571
0.003571 0.107143
0.003571 0.110714
0.003571 0.114286
0.003571 0.117857
0.003571 0.121429
0.003571 0.125000
0.003571 0.128571
0.003571 0.132143
0.003571 0.135714
0.003571 0.139286
0.003571 0.142857
0.003571 0.146429
0.003571 0.150000
0.003571 0.153571
0.003571 0.157143
0.003571 0.160714
0.003571 0.164286
0.003571 0.167857
0.003571 0.171429
0.003571 0.175000
0.003571 0.178571
0.003571 0.182143
0.003571 0.185714
0.003571 0.189286
0.003571 0.192857
0.003571 0.196429
0.003571 0.200000
41(0.2)
0.004878 0.204878
0.004878 0.209756

0.004878 0.214634
0.004878 0.219512
0.004878 0.224390
0.004878 0.229268
0.004878 0.234146
0.004878 0.239024
0.004878 0.243902
0.004878 0.248780
0.004878 0.253659
0.004878 0.258537
0.004878 0.263415
0.004878 0.268293
0.004878 0.273171
0.004878 0.278049
0.004878 0.282927
0.004878 0.287805
0.004878 0.292683
0.004878 0.297561
0.004878 0.302439
0.004878 0.307317
0.004878 0.312195
0.004878 0.317073
0.004878 0.321951
0.004878 0.326829
0.004878 0.331707
0.004878 0.336585
0.004878 0.341463
0.004878 0.346341
0.004878 0.351220
0.004878 0.356098
0.004878 0.360976
0.004878 0.365854
0.004878 0.370732
0.004878 0.375610
0.004878 0.380488
0.004878 0.385366
0.004878 0.390244
0.004878 0.395122
0.004878 0.400000
18(0.2)
0.011111 0.411111
0.011111 0.422222
0.011111 0.433333
0.011111 0.444444
0.011111 0.455556
0.011111 0.466667
0.011111 0.477778
0.011111 0.488889
0.011111 0.500000
0.011111 0.511111
0.011111 0.522222
0.011111 0.533333
0.011111 0.544444
0.011111 0.555556
0.011111 0.566667
0.011111 0.577778
0.011111 0.588889
0.011111 0.600000
18(0.2)
0.011111 0.611111
0.011111 0.622222
0.011111 0.633333
0.011111 0.644444
0.011111 0.655556
0.011111 0.666667
0.011111 0.677778
0.011111 0.688889
0.011111 0.700000
0.011111 0.711111
0.011111 0.722222
0.011111 0.733333
0.011111 0.744444
0.011111 0.755556
0.011111 0.766667

0.011111 0.777778
0.011111 0.788889
0.011111 0.800000
14(0.2)
0.014286 0.814286
0.014286 0.828571
0.014286 0.842857
0.014286 0.857143
0.014286 0.871429
0.014286 0.885714
0.014286 0.900000
0.014286 0.914286
0.014286 0.928571
0.014286 0.942857
0.014286 0.957143
0.014286 0.971429
0.014286 0.985714
0.014286 1.000000
15(0.2)
0.013333 1.013333
0.013333 1.026667
0.013333 1.040000
0.013333 1.053333
0.013333 1.066667
0.013333 1.080000
0.013333 1.093333
0.013333 1.106667
0.013333 1.120000
0.013333 1.133333
0.013333 1.146667
0.013333 1.160000
0.013333 1.173333
0.013333 1.186667
0.013333 1.200000
13(0.2)
0.015385 1.215385
0.015385 1.230769
0.015385 1.246154
0.015385 1.261538
0.015385 1.276923
0.015385 1.292308
0.015385 1.307692
0.015385 1.323077
0.015385 1.338462
0.015385 1.353846
0.015385 1.369231
0.015385 1.384615
0.015385 1.400000
8(0.2)
0.025000 1.425000
0.025000 1.450000
0.025000 1.475000
0.025000 1.500000
0.025000 1.525000
0.025000 1.550000
0.025000 1.575000
0.025000 1.600000
8(0.2)
0.025000 1.625000
0.025000 1.650000
0.025000 1.675000
0.025000 1.700000
0.025000 1.725000
0.025000 1.750000
0.025000 1.775000
0.025000 1.800000
6(0.2)
0.033333 1.833333
0.033333 1.866667
0.033333 1.900000
0.033333 1.933333
0.033333 1.966667
0.033333 2.000000
10(0.2)

0.020000 2.020000
0.020000 2.040000
0.020000 2.060000
0.020000 2.080000
0.020000 2.100000
0.020000 2.120000
0.020000 2.140000
0.020000 2.160000
0.020000 2.180000
0.020000 2.200000
7(0.2)
0.028571 2.228571
0.028571 2.257143
0.028571 2.285714
0.028571 2.314286
0.028571 2.342857
0.028571 2.371429
0.028571 2.400000
6(0.2)
0.033333 2.433333
0.033333 2.466667
0.033333 2.500000
0.033333 2.533333
0.033333 2.566667
0.033333 2.600000
7(0.2)
0.028571 2.628571
0.028571 2.657143
0.028571 2.685714
0.028571 2.714286
0.028571 2.742857
0.028571 2.771429
0.028571 2.800000
5(0.2)
0.040000 2.840000
0.040000 2.880000
0.040000 2.920000
0.040000 2.960000
0.040000 3.000000
7(0.2)
0.028571 3.028571
0.028571 3.057143
0.028571 3.085714
0.028571 3.114286
0.028571 3.142857
0.028571 3.171429
0.028571 3.200000
9(0.2)
0.022222 3.222222
0.022222 3.244444
0.022222 3.266667
0.022222 3.288889
0.022222 3.311111
0.022222 3.333333
0.022222 3.355556
0.022222 3.377778
0.022222 3.400000
5(0.2)
0.040000 3.440000
0.040000 3.480000
0.040000 3.520000
0.040000 3.560000
0.040000 3.600000
5(0.2)
0.040000 3.640000
0.040000 3.680000
0.040000 3.720000
0.040000 3.760000
0.040000 3.800000
7(0.2)
0.028571 3.828571
0.028571 3.857143
0.028571 3.885714
0.028571 3.914286

0.028571 3.942857
0.028571 3.971429
0.028571 4.000000
7(0.2)
0.028571 4.028571
0.028571 4.057143
0.028571 4.085714
0.028571 4.114286
0.028571 4.142857
0.028571 4.171429
0.028571 4.200000
5(0.2)
0.040000 4.240000
0.040000 4.280000
0.040000 4.320000
0.040000 4.360000
0.040000 4.400000
6(0.2)
0.033333 4.433333
0.033333 4.466667
0.033333 4.500000
0.033333 4.533333
0.033333 4.566667
0.033333 4.600000
4(0.2)
0.050000 4.650000
0.050000 4.700000
0.050000 4.750000
0.050000 4.800000
5(0.2)
0.040000 4.840000
0.040000 4.880000
0.040000 4.920000
0.040000 4.960000
0.040000 5.000000
4(0.2)
0.050000 5.050000
0.050000 5.100000
0.050000 5.150000
0.050000 5.200000
4(0.2)
0.050000 5.250000
0.050000 5.300000
0.050000 5.350000
0.050000 5.400000
3(0.2)
0.066667 5.466667
0.066667 5.533333
0.066667 5.600000
4(0.2)
0.050000 5.650000
0.050000 5.700000
0.050000 5.750000
0.050000 5.800000
3(0.2)
0.066667 5.866667
0.066667 5.933333
0.066667 6.000000
4(0.2)
0.050000 6.050000
0.050000 6.100000
0.050000 6.150000
0.050000 6.200000
3(0.2)
0.066667 6.266667
0.066667 6.333333
0.066667 6.400000
3(0.2)
0.066667 6.466667
0.066667 6.533333
0.066667 6.600000
2(0.2)
0.100000 6.700000
0.100000 6.800000

6(0.5)
0.083333 6.883333
0.083333 6.966667
0.083333 7.050000
0.083333 7.133333
0.083333 7.216667
0.083333 7.300000
3(0.5)
0.166667 7.466667
0.166667 7.633333
0.166667 7.800000
4(0.5)
0.125000 7.925000
0.125000 8.050000
0.125000 8.175000
0.125000 8.300000
3(0.5)
0.166667 8.466667
0.166667 8.633333
0.166667 8.800000
2(0.5)
0.250000 9.050000
0.250000 9.300000
3(0.5)
0.166667 9.466667
0.166667 9.633333
0.166667 9.800000
2(0.5)
0.250000 10.050000
0.250000 10.300000
5
0.200000 10.500000
0.200000 10.700000
0.200000 10.900000
0.200000 11.100000
0.200000 11.300000
6
0.166667 11.466667
0.166667 11.633333
0.166667 11.800000
0.166667 11.966667
0.166667 12.133333
0.166667 12.300000
1
1.000000 13.300000
1
1.000000 14.300000
1
1.000000 15.300000
2
0.500000 15.800000
0.500000 16.300000
2
0.500000 16.800000
0.500000 17.300000
1
1.000000 18.300000
3
0.333333 18.633333
0.333333 18.966667
0.333333 19.300000
3
0.333333 19.633333
0.333333 19.966667
0.333333 20.300000
0,2
1.500000 21.800000
0.500000 22.300000
1
1.000000 23.300000
1
1.000000 24.300000
2
0.500000 24.800000

0.500000 25.300000
2
0.500000 25.800000
0.500000 26.300000
1
1.000000 27.300000
1
1.000000 28.300000
1
1.000000 29.300000
1
1.000000 30.300000
2
0.500000 30.800000
0.500000 31.300000
1
1.000000 32.300000
2
0.500000 32.800000
0.500000 33.300000
0,1
2.000000 35.300000
1
1.000000 36.300000

DK14
NE
3(0.2)
0.066667 0.066667
0.066667 0.133333
0.066667 0.200000
13(0.2)
0.015385 0.215385
0.015385 0.230769
0.015385 0.246154
0.015385 0.261538
0.015385 0.276923
0.015385 0.292308
0.015385 0.307692
0.015385 0.323077
0.015385 0.338462
0.015385 0.353846
0.015385 0.369231
0.015385 0.384615
0.015385 0.400000
15(0.2)
0.013333 0.413333
0.013333 0.426667
0.013333 0.440000
0.013333 0.453333
0.013333 0.466667
0.013333 0.480000
0.013333 0.493333
0.013333 0.506667
0.013333 0.520000
0.013333 0.533333
0.013333 0.546667
0.013333 0.560000
0.013333 0.573333
0.013333 0.586667
0.013333 0.600000
44(0.2)
0.004545 0.604545
0.004545 0.609091
0.004545 0.613636
0.004545 0.618182
0.004545 0.622727
0.004545 0.627273
0.004545 0.631818
0.004545 0.636364
0.004545 0.640909
0.004545 0.645455
0.004545 0.650000
0.004545 0.654545

0.004545 0.659091
0.004545 0.663636
0.004545 0.668182
0.004545 0.672727
0.004545 0.677273
0.004545 0.681818
0.004545 0.686364
0.004545 0.690909
0.004545 0.695455
0.004545 0.700000
0.004545 0.704545
0.004545 0.709091
0.004545 0.713636
0.004545 0.718182
0.004545 0.722727
0.004545 0.727273
0.004545 0.731818
0.004545 0.736364
0.004545 0.740909
0.004545 0.745455
0.004545 0.750000
0.004545 0.754545
0.004545 0.759091
0.004545 0.763636
0.004545 0.768182
0.004545 0.772727
0.004545 0.777273
0.004545 0.781818
0.004545 0.786364
0.004545 0.790909
0.004545 0.795455
0.004545 0.800000
37(0.2)
0.005405 0.805405
0.005405 0.810811
0.005405 0.816216
0.005405 0.821622
0.005405 0.827027
0.005405 0.832432
0.005405 0.837838
0.005405 0.843243
0.005405 0.848649
0.005405 0.854054
0.005405 0.859459
0.005405 0.864865
0.005405 0.870270
0.005405 0.875676
0.005405 0.881081
0.005405 0.886486
0.005405 0.891892
0.005405 0.897297
0.005405 0.902703
0.005405 0.908108
0.005405 0.913514
0.005405 0.918919
0.005405 0.924324
0.005405 0.929730
0.005405 0.935135
0.005405 0.940541
0.005405 0.945946
0.005405 0.951351
0.005405 0.956757
0.005405 0.962162
0.005405 0.967568
0.005405 0.972973
0.005405 0.978378
0.005405 0.983784
0.005405 0.989189
0.005405 0.994595
0.005405 1.000000
19(0.2)
0.010526 1.010526
0.010526 1.021053
0.010526 1.031579

0.010526 1.042105
0.010526 1.052632
0.010526 1.063158
0.010526 1.073684
0.010526 1.084211
0.010526 1.094737
0.010526 1.105263
0.010526 1.115789
0.010526 1.126316
0.010526 1.136842
0.010526 1.147368
0.010526 1.157895
0.010526 1.168421
0.010526 1.178947
0.010526 1.189474
0.010526 1.200000
10(0.2)
0.020000 1.220000
0.020000 1.240000
0.020000 1.260000
0.020000 1.280000
0.020000 1.300000
0.020000 1.320000
0.020000 1.340000
0.020000 1.360000
0.020000 1.380000
0.020000 1.400000
11(0.2)
0.018182 1.418182
0.018182 1.436364
0.018182 1.454545
0.018182 1.472727
0.018182 1.490909
0.018182 1.509091
0.018182 1.527273
0.018182 1.545455
0.018182 1.563636
0.018182 1.581818
0.018182 1.600000
8(0.2)
0.025000 1.625000
0.025000 1.650000
0.025000 1.675000
0.025000 1.700000
0.025000 1.725000
0.025000 1.750000
0.025000 1.775000
0.025000 1.800000
7(0.2)
0.028571 1.828571
0.028571 1.857143
0.028571 1.885714
0.028571 1.914286
0.028571 1.942857
0.028571 1.971429
0.028571 2.000000
7(0.2)
0.028571 2.028571
0.028571 2.057143
0.028571 2.085714
0.028571 2.114286
0.028571 2.142857
0.028571 2.171429
0.028571 2.200000
6(0.2)
0.033333 2.233333
0.033333 2.266667
0.033333 2.300000
0.033333 2.333333
0.033333 2.366667
0.033333 2.400000
7(0.2)
0.028571 2.428571
0.028571 2.457143

0.028571 2.485714
0.028571 2.514286
0.028571 2.542857
0.028571 2.571429
0.028571 2.600000
5(0.2)
0.040000 2.640000
0.040000 2.680000
0.040000 2.720000
0.040000 2.760000
0.040000 2.800000
2(0.2)
0.100000 2.900000
0.100000 3.000000
4(0.2)
0.050000 3.050000
0.050000 3.100000
0.050000 3.150000
0.050000 3.200000
4(0.2)
0.050000 3.250000
0.050000 3.300000
0.050000 3.350000
0.050000 3.400000
5(0.2)
0.040000 3.440000
0.040000 3.480000
0.040000 3.520000
0.040000 3.560000
0.040000 3.600000
7(0.2)
0.028571 3.628571
0.028571 3.657143
0.028571 3.685714
0.028571 3.714286
0.028571 3.742857
0.028571 3.771429
0.028571 3.800000
6(0.2)
0.033333 3.833333
0.033333 3.866667
0.033333 3.900000
0.033333 3.933333
0.033333 3.966667
0.033333 4.000000
7(0.2)
0.028571 4.028571
0.028571 4.057143
0.028571 4.085714
0.028571 4.114286
0.028571 4.142857
0.028571 4.171429
0.028571 4.200000
7(0.2)
0.028571 4.228571
0.028571 4.257143
0.028571 4.285714
0.028571 4.314286
0.028571 4.342857
0.028571 4.371429
0.028571 4.400000
8(0.2)
0.025000 4.425000
0.025000 4.450000
0.025000 4.475000
0.025000 4.500000
0.025000 4.525000
0.025000 4.550000
0.025000 4.575000
0.025000 4.600000
5(0.2)
0.040000 4.640000
0.040000 4.680000
0.040000 4.720000

0.040000 4.760000
0.040000 4.800000
5(0.2)
0.040000 4.840000
0.040000 4.880000
0.040000 4.920000
0.040000 4.960000
0.040000 5.000000
6(0.2)
0.033333 5.033333
0.033333 5.066667
0.033333 5.100000
0.033333 5.133333
0.033333 5.166667
0.033333 5.200000
5(0.2)
0.040000 5.240000
0.040000 5.280000
0.040000 5.320000
0.040000 5.360000
0.040000 5.400000
4(0.2)
0.050000 5.450000
0.050000 5.500000
0.050000 5.550000
0.050000 5.600000
4(0.2)
0.050000 5.650000
0.050000 5.700000
0.050000 5.750000
0.050000 5.800000
6(0.2)
0.033333 5.833333
0.033333 5.866667
0.033333 5.900000
0.033333 5.933333
0.033333 5.966667
0.033333 6.000000
7(0.2)
0.028571 6.028571
0.028571 6.057143
0.028571 6.085714
0.028571 6.114286
0.028571 6.142857
0.028571 6.171429
0.028571 6.200000
5(0.2)
0.040000 6.240000
0.040000 6.280000
0.040000 6.320000
0.040000 6.360000
0.040000 6.400000
5(0.2)
0.040000 6.440000
0.040000 6.480000
0.040000 6.520000
0.040000 6.560000
0.040000 6.600000
6(0.2)
0.033333 6.633333
0.033333 6.666667
0.033333 6.700000
0.033333 6.733333
0.033333 6.766667
0.033333 6.800000
12(0.5)
0.041667 6.841667
0.041667 6.883333
0.041667 6.925000
0.041667 6.966667
0.041667 7.008333
0.041667 7.050000
0.041667 7.091667
0.041667 7.133333

0.041667 7.175000
0.041667 7.216667
0.041667 7.258333
0.041667 7.300000
9(0.5)
0.055556 7.355556
0.055556 7.411111
0.055556 7.466667
0.055556 7.522222
0.055556 7.577778
0.055556 7.633333
0.055556 7.688889
0.055556 7.744444
0.055556 7.800000
9(0.5)
0.055556 7.855556
0.055556 7.911111
0.055556 7.966667
0.055556 8.022222
0.055556 8.077778
0.055556 8.133333
0.055556 8.188889
0.055556 8.244444
0.055556 8.300000
8(0.5)
0.062500 8.362500
0.062500 8.425000
0.062500 8.487500
0.062500 8.550000
0.062500 8.612500
0.062500 8.675000
0.062500 8.737500
0.062500 8.800000
7(0.5)
0.071429 8.871429
0.071429 8.942857
0.071429 9.014286
0.071429 9.085714
0.071429 9.157143
0.071429 9.228571
0.071429 9.300000
6(0.5)
0.083333 9.383333
0.083333 9.466667
0.083333 9.550000
0.083333 9.633333
0.083333 9.716667
0.083333 9.800000
3(0.5)
0.166667 9.966667
0.166667 10.133333
0.166667 10.300000
6
0.166667 10.466667
0.166667 10.633333
0.166667 10.800000
0.166667 10.966667
0.166667 11.133333
0.166667 11.300000
4
0.250000 11.550000
0.250000 11.800000
0.250000 12.050000
0.250000 12.300000
1
1.000000 13.300000
2
0.500000 13.800000
0.500000 14.300000
1
1.000000 15.300000
3
0.333333 15.633333
0.333333 15.966667

0.333333 16.300000
3
0.333333 16.633333
0.333333 16.966667
0.333333 17.300000
2
0.500000 17.800000
0.500000 18.300000
1
1.000000 19.300000
1
1.000000 20.300000
2
0.500000 20.800000
0.500000 21.300000
1
1.000000 22.300000
2
0.500000 22.800000
0.500000 23.300000
4
0.250000 23.550000
0.250000 23.800000
0.250000 24.050000
0.250000 24.300000
2
0.500000 24.800000
0.500000 25.300000
2
0.500000 25.800000
0.500000 26.300000
1
1.000000 27.300000
1
1.000000 28.300000
2
0.500000 28.800000
0.500000 29.300000
1
1.000000 30.300000

DK17a
SW
15(0.2)
0.013333 0.013333
0.013333 0.026667
0.013333 0.040000
0.013333 0.053333
0.013333 0.066667
0.013333 0.080000
0.013333 0.093333
0.013333 0.106667
0.013333 0.120000
0.013333 0.133333
0.013333 0.146667
0.013333 0.160000
0.013333 0.173333
0.013333 0.186667
0.013333 0.200000
24(0.2)
0.008333 0.208333
0.008333 0.216667
0.008333 0.225000
0.008333 0.233333
0.008333 0.241667
0.008333 0.250000
0.008333 0.258333
0.008333 0.266667
0.008333 0.275000
0.008333 0.283333
0.008333 0.291667
0.008333 0.300000
0.008333 0.308333

0.008333 0.316667
0.008333 0.325000
0.008333 0.333333
0.008333 0.341667
0.008333 0.350000
0.008333 0.358333
0.008333 0.366667
0.008333 0.375000
0.008333 0.383333
0.008333 0.391667
0.008333 0.400000
25(0.2)
0.008000 0.408000
0.008000 0.416000
0.008000 0.424000
0.008000 0.432000
0.008000 0.440000
0.008000 0.448000
0.008000 0.456000
0.008000 0.464000
0.008000 0.472000
0.008000 0.480000
0.008000 0.488000
0.008000 0.496000
0.008000 0.504000
0.008000 0.512000
0.008000 0.520000
0.008000 0.528000
0.008000 0.536000
0.008000 0.544000
0.008000 0.552000
0.008000 0.560000
0.008000 0.568000
0.008000 0.576000
0.008000 0.584000
0.008000 0.592000
0.008000 0.600000
20(0.2)
0.010000 0.610000
0.010000 0.620000
0.010000 0.630000
0.010000 0.640000
0.010000 0.650000
0.010000 0.660000
0.010000 0.670000
0.010000 0.680000
0.010000 0.690000
0.010000 0.700000
0.010000 0.710000
0.010000 0.720000
0.010000 0.730000
0.010000 0.740000
0.010000 0.750000
0.010000 0.760000
0.010000 0.770000
0.010000 0.780000
0.010000 0.790000
0.010000 0.800000
24(0.2)
0.008333 0.808333
0.008333 0.816667
0.008333 0.825000
0.008333 0.833333
0.008333 0.841667
0.008333 0.850000
0.008333 0.858333
0.008333 0.866667
0.008333 0.875000
0.008333 0.883333
0.008333 0.891667
0.008333 0.900000
0.008333 0.908333
0.008333 0.916667
0.008333 0.925000

0.008333 0.933333
0.008333 0.941667
0.008333 0.950000
0.008333 0.958333
0.008333 0.966667
0.008333 0.975000
0.008333 0.983333
0.008333 0.991667
0.008333 1.000000
24(0.2)
0.008333 1.008333
0.008333 1.016667
0.008333 1.025000
0.008333 1.033333
0.008333 1.041667
0.008333 1.050000
0.008333 1.058333
0.008333 1.066667
0.008333 1.075000
0.008333 1.083333
0.008333 1.091667
0.008333 1.100000
0.008333 1.108333
0.008333 1.116667
0.008333 1.125000
0.008333 1.133333
0.008333 1.141667
0.008333 1.150000
0.008333 1.158333
0.008333 1.166667
0.008333 1.175000
0.008333 1.183333
0.008333 1.191667
0.008333 1.200000
14(0.2)
0.014286 1.214286
0.014286 1.228571
0.014286 1.242857
0.014286 1.257143
0.014286 1.271429
0.014286 1.285714
0.014286 1.300000
0.014286 1.314286
0.014286 1.328571
0.014286 1.342857
0.014286 1.357143
0.014286 1.371429
0.014286 1.385714
0.014286 1.400000
13(0.2)
0.015385 1.415385
0.015385 1.430769
0.015385 1.446154
0.015385 1.461538
0.015385 1.476923
0.015385 1.492308
0.015385 1.507692
0.015385 1.523077
0.015385 1.538462
0.015385 1.553846
0.015385 1.569231
0.015385 1.584615
0.015385 1.600000
10(0.2)
0.020000 1.620000
0.020000 1.640000
0.020000 1.660000
0.020000 1.680000
0.020000 1.700000
0.020000 1.720000
0.020000 1.740000
0.020000 1.760000
0.020000 1.780000
0.020000 1.800000

9(0.2)
0.022222 1.822222
0.022222 1.844444
0.022222 1.866667
0.022222 1.888889
0.022222 1.911111
4(0.2)
0.050000 3.850000
0.050000 3.900000
0.050000 3.950000
0.050000 4.000000
4(0.2)
0.050000 4.050000
0.050000 4.100000
0.050000 4.150000
0.050000 4.200000
6(0.2)
0.033333 4.233333
0.033333 4.266667
0.033333 4.300000
0.033333 4.333333
0.033333 4.366667
0.033333 4.400000
4(0.2)
0.050000 4.450000
0.050000 4.500000
0.050000 4.550000
0.050000 4.600000
7(0.2)
0.028571 4.628571
0.028571 4.657143
0.028571 4.685714
0.028571 4.714286
0.028571 4.742857
0.028571 4.771429
0.028571 4.800000
7(0.2)
0.028571 4.828571
0.028571 4.857143
0.028571 4.885714
0.028571 4.914286
0.028571 4.942857
0.028571 4.971429
0.028571 5.000000
8(0.2)
0.025000 5.025000
0.025000 5.050000
0.025000 5.075000
0.025000 5.100000
0.025000 5.125000
0.025000 5.150000
0.025000 5.175000
0.025000 5.200000
7(0.2)
0.028571 5.228571
0.028571 5.257143
0.028571 5.285714
0.028571 5.314286
0.028571 5.342857
0.028571 5.371429
0.028571 5.400000
7(0.2)
0.028571 5.428571
0.028571 5.457143
0.028571 5.485714
0.028571 5.514286
0.028571 5.542857
0.028571 5.571429
0.028571 5.600000
4(0.2)
0.050000 5.650000
0.050000 5.700000
0.050000 5.750000
0.050000 5.800000
4(0.2)

0.033333 3.666667
0.033333 3.700000
0.033333 3.733333
0.033333 3.766667
0.033333 3.800000
5(0.2)
0.040000 6.040000
0.040000 6.080000
0.040000 6.120000
0.040000 6.160000
0.040000 6.200000
5(0.2)
0.040000 6.240000
0.040000 6.280000
0.040000 6.320000
0.040000 6.360000
0.040000 6.400000
5(0.2)
0.040000 6.440000
0.040000 6.480000
0.040000 6.520000
0.040000 6.560000
0.040000 6.600000
5(0.2)
0.040000 6.640000
0.040000 6.680000
0.040000 6.720000
0.040000 6.760000
0.040000 6.800000
6(0.2)
0.033333 6.833333
0.033333 6.866667
0.033333 6.900000
0.033333 6.933333
0.033333 6.966667
0.033333 7.000000
6(0.2)
0.033333 7.033333
0.033333 7.066667
0.033333 7.100000
0.033333 7.133333
0.033333 7.166667
0.033333 7.200000
6(0.2)
0.033333 7.233333
0.033333 7.266667
0.033333 7.300000
0.033333 7.333333
0.033333 7.366667
0.033333 7.400000
4(0.2)
0.050000 7.450000
0.050000 7.500000
0.050000 7.550000
0.050000 7.600000
4(0.2)
0.050000 7.650000
0.050000 7.700000
0.050000 7.750000
0.050000 7.800000
5(0.2)
0.040000 7.840000
0.040000 7.880000
0.040000 7.920000
0.040000 8.000000
4(0.2)
0.050000 8.050000
0.050000 8.100000
0.050000 8.150000
0.050000 8.200000
5(0.2)
0.040000 8.240000
0.040000 8.280000
0.040000 8.320000

0.040000 8.360000
0.040000 8.400000
6(0.2)
0.033333 8.433333
0.033333 8.466667
0.033333 8.500000
0.033333 8.533333
0.033333 8.566667
0.033333 8.600000
5(0.2)
0.040000 8.640000
0.040000 8.680000
0.040000 8.720000
0.040000 8.760000
0.040000 8.800000
5(0.2)
0.040000 8.840000
0.040000 8.880000
0.040000 8.920000
0.040000 8.960000
0.040000 9.000000
5(0.2)
0.040000 9.040000
0.040000 9.080000
0.040000 9.120000
0.040000 9.160000
0.040000 9.200000
9(0.2)
0.022222 9.222222
0.022222 9.244444
0.022222 9.266667
0.022222 9.288889
0.022222 9.311111
0.022222 9.333333
0.022222 9.355556
0.022222 9.377778
0.022222 9.400000
5(0.2)
0.040000 9.440000
0.040000 9.480000
0.040000 9.520000
0.040000 9.560000
0.040000 9.600000
5(0.2)
0.040000 9.640000
0.040000 9.680000
0.040000 9.720000
0.040000 9.760000
0.040000 9.800000
4(0.2)
0.050000 9.850000
0.050000 9.900000
0.050000 9.950000
0.050000 10.000000
3(0.2)
0.066667 10.066667
0.066667 10.133333
0.066667 10.200000
4(0.2)
0.050000 10.250000
0.050000 10.300000
0.050000 10.350000
0.050000 10.400000
3(0.2)
0.066667 10.466667
0.066667 10.533333
0.066667 10.600000
3(0.2)
0.066667 10.666667
0.066667 10.733333
0.066667 10.800000
5(0.2)
0.040000 10.840000
0.040000 10.880000

0.040000 10.920000
0.040000 10.960000
0.040000 11.000000
4(0.2)
0.050000 11.050000
0.050000 11.100000
0.050000 11.150000
0.050000 11.200000
5(0.2)
0.040000 11.240000
0.040000 11.280000
0.040000 11.320000
0.040000 11.360000
0.040000 11.400000
3(0.2)
0.066667 11.466667
0.066667 11.533333
0.066667 11.600000
4(0.2)
0.050000 11.650000
0.050000 11.700000
0.050000 11.750000
0.050000 11.800000
3(0.2)
0.066667 11.866667
0.066667 11.933333
0.066667 12.000000
2(0.2)
0.100000 12.100000
0.100000 12.200000
4(0.2)
0.050000 12.250000
0.050000 12.300000
0.050000 12.350000
0.050000 12.400000
3(0.2)
0.066667 12.466667
0.066667 12.533333
0.066667 12.600000
5(0.2)
0.040000 12.640000
0.040000 12.680000
0.040000 12.720000
0.040000 12.760000
0.040000 12.800000
4(0.2)
0.050000 12.850000
0.050000 12.900000
0.050000 12.950000
0.050000 13.000000
3(0.2)
0.066667 13.066667
0.066667 13.133333
0.066667 13.200000
3(0.2)
0.066667 13.266667
0.066667 13.333333
0.066667 13.400000
4(0.2)
0.050000 13.450000
0.050000 13.500000
0.050000 13.550000
0.050000 13.600000
4(0.2)
0.050000 13.650000
0.050000 13.700000
0.050000 13.750000
0.050000 13.800000
2(0.2)
0.100000 13.900000
0.100000 14.000000
0(0.2),1(0.2)
0.400000 14.400000
1(0.2)

0.200000 14.600000
2(0.2)
0.100000 14.700000
0.100000 14.800000
3(0.2)
0.066667 14.866667
0.066667 14.933333
0.066667 15.000000
4(0.2)
0.050000 15.050000
0.050000 15.100000
0.050000 15.150000
0.050000 15.200000
5(0.2)
0.040000 15.240000
0.040000 15.280000
0.040000 15.320000
0.040000 15.360000
0.040000 15.400000
2(0.2)
0.100000 15.500000
0.100000 15.600000
1(0.2)
0.200000 15.800000
2(0.2)
0.100000 15.900000
0.100000 16.000000
1(0.2)
0.200000 16.200000
3(0.5)
0.166667 16.366667
0.166667 16.533333
0.166667 16.700000
2(0.5)
0.250000 16.950000
0.250000 17.200000
2(0.5)
0.250000 17.450000
0.250000 17.700000
5(0.5)
0.100000 17.800000
0.100000 17.900000
0.100000 18.000000
0.100000 18.100000
0.100000 18.200000
2(0.5)
0.250000 18.450000
0.250000 18.700000
3(0.5)
0.166667 18.866667
0.166667 19.033333
0.166667 19.200000
3(0.5)
0.166667 19.366667
0.166667 19.533333
0.166667 19.700000
2(0.5)
0.250000 19.950000
0.250000 20.200000
2(0.5)
0.250000 20.450000
0.250000 20.700000
4(0.5)
0.125000 20.825000
0.125000 20.950000
0.125000 21.075000
0.125000 21.200000
4(0.5)
0.125000 21.325000
0.125000 21.450000
0.125000 21.575000
0.125000 21.700000
6(0.5)
0.083333 21.783333

0.083333 21.866667
0.083333 21.950000
0.083333 22.033333
0.083333 22.116667
0.083333 22.200000
4(0.5)
0.125000 22.325000
0.125000 22.450000
0.125000 22.575000
0.125000 22.700000
4(0.5)
0.125000 22.825000
0.125000 22.950000
0.125000 23.075000
0.125000 23.200000
2(0.5)
0.250000 23.450000
0.250000 23.700000
2(0.5)
0.250000 23.950000
0.250000 24.200000
3(0.5)
0.166667 24.366667
0.166667 24.533333
0.166667 24.700000
3(0.5)
0.166667 24.866667
0.166667 25.033333
0.166667 25.200000
3(0.5)
0.166667 25.366667
0.166667 25.533333
0.166667 25.700000
2(0.5)
0.250000 25.950000
0.250000 26.200000
1(0.5)
0.500000 26.700000
3(0.5)
0.166667 26.866667
0.166667 27.033333
0.166667 27.200000
2(0.5)
0.250000 27.450000
0.250000 27.700000
1(0.5)
0.500000 28.200000
2(0.5)
0.250000 28.450000
0.250000 28.700000
0(0.5),2(0.5)
0.750000 29.450000
0.250000 29.700000
4(0.5)
0.125000 29.825000
0.125000 29.950000
0.125000 30.075000
0.125000 30.200000
2(0.5)
0.250000 30.450000
0.250000 30.700000
3(0.5)
0.166667 30.866667
0.166667 31.033333
0.166667 31.200000
2(0.5)
0.250000 31.450000
0.250000 31.700000
2(0.5)
0.250000 31.950000
0.250000 32.200000
1(0.5)
0.500000 32.700000
0(0.5),2(0.5)

0.750000 33.450000
0.250000 33.700000
1(0.5)
0.500000 34.200000
2(0.5)
0.250000 34.450000
0.250000 34.700000
1(0.5)
0.500000 35.200000
1(0.5)
0.500000 35.700000
1(0.5)
0.500000 36.200000
3
0.333333 36.533333
0.333333 36.866667
0.333333 37.200000
4
0.250000 37.450000
0.250000 37.700000
0.250000 37.950000
0.250000 38.200000
3
0.333333 38.533333
0.333333 38.866667
0.333333 39.200000
3
0.333333 39.533333
0.333333 39.866667
0.333333 40.200000
3
0.333333 40.533333
0.333333 40.866667
0.333333 41.200000
3
0.333333 41.533333
0.333333 41.866667
0.333333 42.200000
2
0.500000 42.700000
0.500000 43.200000
3
0.333333 43.533333
0.333333 43.866667
0.333333 44.200000
3
0.333333 44.533333
0.333333 44.866667
0.333333 45.200000
1
1.000000 46.200000
3
0.333333 46.533333
0.333333 46.866667
0.333333 47.200000
1
1.000000 48.200000
1
1.000000 49.200000
2
0.500000 49.700000
0.500000 50.200000
1
1.000000 51.200000
3
0.333333 51.533333
0.333333 51.866667
0.333333 52.200000
2
0.500000 52.700000
0.500000 53.200000
0,1
2.000000 55.200000
1

1.000000 56.200000
0
0
0
0
0
0
0
0
0
0
0
0

DK33a
N
90(0.5)
0.005556 0.005556
0.005556 0.011111
0.005556 0.016667
0.005556 0.022222
0.005556 0.027778
0.005556 0.033333
0.005556 0.038889
0.005556 0.044444
0.005556 0.050000
0.005556 0.055556
0.005556 0.061111
0.005556 0.066667
0.005556 0.072222
0.005556 0.077778
0.005556 0.083333
0.005556 0.088889
0.005556 0.094444
0.005556 0.100000
0.005556 0.105556
0.005556 0.111111
0.005556 0.116667
0.005556 0.122222
0.005556 0.127778
0.005556 0.133333
0.005556 0.138889
0.005556 0.144444
0.005556 0.150000
0.005556 0.155556
0.005556 0.161111
0.005556 0.166667
0.005556 0.172222
0.005556 0.177778
0.005556 0.183333
0.005556 0.188889
0.005556 0.194444
0.005556 0.200000
0.005556 0.205556
0.005556 0.211111
0.005556 0.216667
0.005556 0.222222
0.005556 0.227778
0.005556 0.233333
0.005556 0.238889
0.005556 0.244444
0.005556 0.250000
0.005556 0.255556
0.005556 0.261111
0.005556 0.266667
0.005556 0.272222
0.005556 0.277778
0.005556 0.283333
0.005556 0.288889
0.005556 0.294444
0.005556 0.300000
0.005556 0.305556
0.005556 0.311111

0.005556 0.316667
0.005556 0.322222
0.005556 0.327778
0.005556 0.333333
0.005556 0.338889
0.005556 0.344444
0.005556 0.350000
0.005556 0.355556
0.005556 0.361111
0.005556 0.366667
0.005556 0.372222
0.005556 0.377778
0.005556 0.383333
0.005556 0.388889
0.005556 0.394444
0.005556 0.400000
0.005556 0.405556
0.005556 0.411111
0.005556 0.416667
0.005556 0.422222
0.005556 0.427778
0.005556 0.433333
0.005556 0.438889
0.005556 0.444444
0.005556 0.450000
0.005556 0.455556
0.005556 0.461111
0.005556 0.466667
0.005556 0.472222
0.005556 0.477778
0.005556 0.483333
0.005556 0.488889
0.005556 0.494444
0.005556 0.500000
70(0.5)
0.007143 0.507143
0.007143 0.514286
0.007143 0.521429
0.007143 0.528571
0.007143 0.535714
0.007143 0.542857
0.007143 0.550000
0.007143 0.557143
0.007143 0.564286
0.007143 0.571429
0.007143 0.578571
0.007143 0.585714
0.007143 0.592857
0.007143 0.600000
0.007143 0.607143
0.007143 0.614286
0.007143 0.621429
0.007143 0.628571
0.007143 0.635714
0.007143 0.642857
0.007143 0.650000
0.007143 0.657143
0.007143 0.664286
0.007143 0.671429
0.007143 0.678571
0.007143 0.685714
0.007143 0.692857
0.007143 0.700000
0.007143 0.707143
0.007143 0.714286
0.007143 0.721429
0.007143 0.728571
0.007143 0.735714
0.007143 0.742857
0.007143 0.750000
0.007143 0.757143
0.007143 0.764286
0.007143 0.771429
0.007143 0.778571

0.007143 0.785714
0.007143 0.792857
0.007143 0.800000
0.007143 0.807143
0.007143 0.814286
0.007143 0.821429
0.007143 0.828571
0.007143 0.835714
0.007143 0.842857
0.007143 0.850000
0.007143 0.857143
0.007143 0.864286
0.007143 0.871429
0.007143 0.878571
0.007143 0.885714
0.007143 0.892857
0.007143 0.900000
0.007143 0.907143
0.007143 0.914286
0.007143 0.921429
0.007143 0.928571
0.007143 0.935714
0.007143 0.942857
0.007143 0.950000
0.007143 0.957143
0.007143 0.964286
0.007143 0.971429
0.007143 0.978571
0.007143 0.985714
0.007143 0.992857
0.007143 1.000000
44(0.5)
0.011364 1.011364
0.011364 1.022727
0.011364 1.034091
0.011364 1.045455
0.011364 1.056818
0.011364 1.068182
0.011364 1.079545
0.011364 1.090909
0.011364 1.102273
0.011364 1.113636
0.011364 1.125000
0.011364 1.136364
0.011364 1.147727
0.011364 1.159091
0.011364 1.170455
0.011364 1.181818
0.011364 1.193182
0.011364 1.204545
0.011364 1.215909
0.011364 1.227273
0.011364 1.238636
0.011364 1.250000
0.011364 1.261364
0.011364 1.272727
0.011364 1.284091
0.011364 1.295455
0.011364 1.306818
0.011364 1.318182
0.011364 1.329545
0.011364 1.340909
0.011364 1.352273
0.011364 1.363636
0.011364 1.375000
0.011364 1.386364
0.011364 1.397727
0.011364 1.409091
0.011364 1.420455
0.011364 1.431818
0.011364 1.443182
0.011364 1.454545
0.011364 1.465909
0.011364 1.477273

0.011364 1.488636
0.011364 1.500000
42(0.5)
0.011905 1.511905
0.011905 1.523810
0.011905 1.535714
0.011905 1.547619
0.011905 1.559524
0.011905 1.571429
0.011905 1.583333
0.011905 1.595238
0.011905 1.607143
0.011905 1.619048
0.011905 1.630952
0.011905 1.642857
0.011905 1.654762
0.011905 1.666667
0.011905 1.678571
0.011905 1.690476
0.011905 1.702381
0.011905 1.714286
0.011905 1.726190
0.011905 1.738095
0.011905 1.750000
0.011905 1.761905
0.011905 1.773810
0.011905 1.785714
0.011905 1.797619
0.011905 1.809524
0.011905 1.821429
0.011905 1.833333
0.011905 1.845238
0.011905 1.857143
0.011905 1.869048
0.011905 1.880952
0.011905 1.892857
0.011905 1.904762
0.011905 1.916667
0.011905 1.928571
0.011905 1.940476
0.011905 1.952381
0.011905 1.964286
0.011905 1.976190
0.011905 1.988095
0.011905 2.000000
8(0.5)
0.062500 2.062500
0.062500 2.125000
0.062500 2.187500
0.062500 2.250000
0.062500 2.312500
0.062500 2.375000
0.062500 2.437500
0.062500 2.500000
8(0.5)
0.062500 2.562500
0.062500 2.625000
0.062500 2.687500
0.062500 2.750000
0.062500 2.812500
0.062500 2.875000
0.062500 2.937500
0.062500 3.000000
4(0.5)
0.125000 3.125000
0.125000 3.250000
0.125000 3.375000
0.125000 3.500000
1(0.5)
0.500000 4.000000
2(0.5)
0.250000 4.250000
0.250000 4.500000
0,1(0.5)

1.000000 5.500000
1(0.5)
0.500000 6.000000
2(0.5)
0.250000 6.250000
0.250000 6.500000
17(0.5)
0.029412 6.529412
0.029412 6.558824
0.029412 6.588235
0.029412 6.617647
0.029412 6.647059
0.029412 6.676471
0.029412 6.705882
0.029412 6.735294
0.029412 6.764706
0.029412 6.794118
0.029412 6.823529
0.029412 6.852941
0.029412 6.882353
0.029412 6.911765
0.029412 6.941176
0.029412 6.970588
0.029412 7.000000
2(0.5)
0.250000 7.250000
0.250000 7.500000
1(0.5)
0.500000 8.000000
3(0.5)
0.166667 8.166667
0.166667 8.333333
0.166667 8.500000
1(0.5)
0.500000 9.000000
0,0,0,1(0.5)
2.000000 11.000000
0,1(0.5)
1.000000 12.000000
1(0.5)
0.500000 12.500000
0,1(0.5)
1.000000 13.500000
3(0.5)
0.166667 13.666667
0.166667 13.833333
0.166667 14.000000
0(0.5)

DK42
S
28(0.1)
0.003571 0.003571
0.003571 0.007143
0.003571 0.010714
0.003571 0.014286
0.003571 0.017857
0.003571 0.021429
0.003571 0.025000
0.003571 0.028571
0.003571 0.032143
0.003571 0.035714
0.003571 0.039286
0.003571 0.042857
0.003571 0.046429
0.003571 0.050000
0.003571 0.053571
0.003571 0.057143
0.003571 0.060714
0.003571 0.064286
0.003571 0.067857
0.003571 0.071429
0.003571 0.075000

0.003571 0.078571
0.003571 0.082143
0.003571 0.085714
0.003571 0.089286
0.003571 0.092857
0.003571 0.096429
0.003571 0.100000
19(0.1)
0.005263 0.105263
0.005263 0.110526
0.005263 0.115789
0.005263 0.121053
0.005263 0.126316
0.005263 0.131579
0.005263 0.136842
0.005263 0.142105
0.005263 0.147368
0.005263 0.152632
0.005263 0.157895
0.005263 0.163158
0.005263 0.168421
0.005263 0.173684
0.005263 0.178947
0.005263 0.184211
0.005263 0.189474
0.005263 0.194737
0.005263 0.200000
11(0.1)
0.009091 0.209091
0.009091 0.218182
0.009091 0.227273
0.009091 0.236364
0.009091 0.245455
0.009091 0.254545
0.009091 0.263636
0.009091 0.272727
0.009091 0.281818
0.009091 0.290909
0.009091 0.300000
2(0.1)
0.050000 0.350000
0.050000 0.400000
2(0.1)
0.050000 0.450000
0.050000 0.500000
3(0.1)
0.033333 0.533333
0.033333 0.566667
0.033333 0.600000
2(0.1)
0.050000 0.650000
0.050000 0.700000
1(0.1)
0.100000 0.800000
0,0,1(0.1)
0.300000 1.100000
2(0.1)
0.050000 1.150000
0.050000 1.200000
0,0,1(0.1)
0.300000 1.500000
1(0.1)
0.100000 1.600000
1(0.1)
0.100000 1.700000
0,0,1(0.1)
0.300000 2.000000
4(0.5)
0.125000 2.125000
0.125000 2.250000
0.125000 2.375000
0.125000 2.500000
3(0.5)
0.166667 2.666667

0.166667 2.833333
0.166667 3.000000
0,4(0.5)
0.625000 3.625000
0.125000 3.750000
0.125000 3.875000
0.125000 4.000000
3(0.5)
0.166667 4.166667
0.166667 4.333333
0.166667 4.500000
3(0.5)
0.166667 4.666667
0.166667 4.833333
0.166667 5.000000
0,0,0,1(0.5)
2.000000 7.000000
0,2(0.5)
0.750000 7.750000
0.250000 8.000000
1(0.5)
1.000000 9.000000
0(0.5)

DK44
S
27(0.1)
0.003704 0.003704
0.003704 0.007407
0.003704 0.011111
0.003704 0.014815
0.003704 0.018519
0.003704 0.022222
0.003704 0.025926
0.003704 0.029630
0.003704 0.033333
0.003704 0.037037
0.003704 0.040741
0.003704 0.044444
0.003704 0.048148
0.003704 0.051852
0.003704 0.055556
0.003704 0.059259
0.003704 0.062963
0.003704 0.066667
0.003704 0.070370
0.003704 0.074074
0.003704 0.077778
0.003704 0.081481
0.003704 0.085185
0.003704 0.088889
0.003704 0.092593
0.003704 0.096296
0.003704 0.100000
24(0.1)
0.004167 0.104167
0.004167 0.108333
0.004167 0.112500
0.004167 0.116667
0.004167 0.120833
0.004167 0.125000
0.004167 0.129167
0.004167 0.133333
0.004167 0.137500
0.004167 0.141667
0.004167 0.145833
0.004167 0.150000
0.004167 0.154167
0.004167 0.158333
0.004167 0.162500
0.004167 0.166667
0.004167 0.170833
0.004167 0.175000

0.004167 0.179167
0.004167 0.183333
0.004167 0.187500
0.004167 0.191667
0.004167 0.195833
0.004167 0.200000
12(0.1)
0.008333 0.208333
0.008333 0.216667
0.008333 0.225000
0.008333 0.233333
0.008333 0.241667
0.008333 0.250000
0.008333 0.258333
0.008333 0.266667
0.008333 0.275000
0.008333 0.283333
0.008333 0.291667
0.008333 0.300000
11(0.1)
0.009091 0.309091
0.009091 0.318182
0.009091 0.327273
0.009091 0.336364
0.009091 0.345455
0.009091 0.354545
0.009091 0.363636
0.009091 0.372727
0.009091 0.381818
0.009091 0.390909
0.009091 0.400000
0,0,1(0.1)
0.300000 0.700000
4(0.1)
0.025000 0.725000
0.025000 0.750000
0.025000 0.775000
0.025000 0.800000
1(0.1)
0.100000 0.900000
0,4(0.5)
0.625000 1.525000
0.125000 1.650000
0.125000 1.775000
0.125000 1.900000
3(0.5)
0.166667 2.066667
0.166667 2.233333
0.166667 2.400000
12(0.5)
0.041667 2.441667
0.041667 2.483333
0.041667 2.525000
0.041667 2.566667
0.041667 2.608333
0.041667 2.650000
0.041667 2.691667
0.041667 2.733333
0.041667 2.775000
0.041667 2.816667
0.041667 2.858333
0.041667 2.900000
2(0.5)
0.250000 3.150000
0.250000 3.400000
2(0.5)
0.250000 3.650000
0.250000 3.900000
0,1(0.5)
1.000000 4.900000
0,3(0.5)
0.666667 5.566667
0.166667 5.733333
0.166667 5.900000

1(0.5)
0.500000 6.400000

N
19(0.1)
0.005263 0.005263
0.005263 0.010526
0.005263 0.015789
0.005263 0.021053
0.005263 0.026316
0.005263 0.031579
0.005263 0.036842
0.005263 0.042105
0.005263 0.047368
0.005263 0.052632
0.005263 0.057895
0.005263 0.063158
0.005263 0.068421
0.005263 0.073684
0.005263 0.078947
0.005263 0.084211
0.005263 0.089474
0.005263 0.094737
0.005263 0.100000
12(0.1)
0.008333 0.108333
0.008333 0.116667
0.008333 0.125000
0.008333 0.133333
0.008333 0.141667
0.008333 0.150000
0.008333 0.158333
0.008333 0.166667
0.008333 0.175000
0.008333 0.183333
0.008333 0.191667
0.008333 0.200000
6(0.1)
0.016667 0.216667
0.016667 0.233333
0.016667 0.250000
0.016667 0.266667
0.016667 0.283333
0.016667 0.300000
0,1(0.1)
0.200000 0.500000
0,0,1(0.1)
0.300000 0.800000
0(0.1),2(0.5)
0.350000 1.150000
0.250000 1.400000
4(0.5)
0.125000 1.525000
0.125000 1.650000
0.125000 1.775000
0.125000 1.900000
10(0.5)
0.050000 1.950000
0.050000 2.000000
0.050000 2.050000
0.050000 2.100000
0.050000 2.150000
0.050000 2.200000
0.050000 2.250000
0.050000 2.300000
0.050000 2.350000
0.050000 2.400000
19(0.5)
0.026316 2.426316
0.026316 2.452632
0.026316 2.478947
0.026316 2.505263
0.026316 2.531579
0.026316 2.557895

0.026316 2.584211
0.026316 2.610526
0.026316 2.636842
0.026316 2.663158
0.026316 2.689474
0.026316 2.715789
0.026316 2.742105
0.026316 2.768421
0.026316 2.794737
0.026316 2.821053
0.026316 2.847368
0.026316 2.873684
0.026316 2.900000
20(0.5)
0.025000 2.925000
0.025000 2.950000
0.025000 2.975000
0.025000 3.000000
0.025000 3.025000
0.025000 3.050000
0.025000 3.075000
0.025000 3.100000
0.025000 3.125000
0.025000 3.150000
0.025000 3.175000
0.025000 3.200000
0.025000 3.225000
0.025000 3.250000
0.025000 3.275000
0.025000 3.300000
0.025000 3.325000
0.025000 3.350000
0.025000 3.375000
0.025000 3.400000
15(0.5)
0.033333 3.433333
0.033333 3.466667
0.033333 3.500000
0.033333 3.533333
0.033333 3.566667
0.033333 3.600000
0.033333 3.633333
0.033333 3.666667
0.033333 3.700000
0.033333 3.733333
0.033333 3.766667
0.033333 3.800000
0.033333 3.833333
0.033333 3.866667
0.033333 3.900000
4(0.5)
0.125000 4.025000
0.125000 4.150000
0.125000 4.275000
0.125000 4.400000
1(0.5)
0.500000 4.900000
4(0.5)
0.125000 5.025000
0.125000 5.150000
0.125000 5.275000
0.125000 5.400000

DK54
S
35(0.1)
0.002857 0.002857
0.002857 0.005714
0.002857 0.008571
0.002857 0.011429
0.002857 0.014286
0.002857 0.017143
0.002857 0.020000

0.002857 0.022857
0.002857 0.025714
0.002857 0.028571
0.002857 0.031429
0.002857 0.034286
0.002857 0.037143
0.002857 0.040000
0.002857 0.042857
0.002857 0.045714
0.002857 0.048571
0.002857 0.051429
0.002857 0.054286
0.002857 0.057143
0.002857 0.060000
0.002857 0.062857
0.002857 0.065714
0.002857 0.068571
0.002857 0.071429
0.002857 0.074286
0.002857 0.077143
0.002857 0.080000
0.002857 0.082857
0.002857 0.085714
0.002857 0.088571
0.002857 0.091429
0.002857 0.094286
0.002857 0.097143
0.002857 0.100000
30(0.1)
0.003333 0.103333
0.003333 0.106667
0.003333 0.110000
0.003333 0.113333
0.003333 0.116667
0.003333 0.120000
0.003333 0.123333
0.003333 0.126667
0.003333 0.130000
0.003333 0.133333
0.003333 0.136667
0.003333 0.140000
0.003333 0.143333
0.003333 0.146667
0.003333 0.150000
0.003333 0.153333
0.003333 0.156667
0.003333 0.160000
0.003333 0.163333
0.003333 0.166667
0.003333 0.170000
0.003333 0.173333
0.003333 0.176667
0.003333 0.180000
0.003333 0.183333
0.003333 0.186667
0.003333 0.190000
0.003333 0.193333
0.003333 0.196667
0.003333 0.200000
26(0.1)
0.003846 0.203846
0.003846 0.207692
0.003846 0.211538
0.003846 0.215385
0.003846 0.219231
0.003846 0.223077
0.003846 0.226923
0.003846 0.230769
0.003846 0.234615
0.003846 0.238462
0.003846 0.242308
0.003846 0.246154
0.003846 0.250000
0.003846 0.253846

0.003846 0.257692
0.003846 0.261538
0.003846 0.265385
0.003846 0.269231
0.003846 0.273077
0.003846 0.276923
0.003846 0.280769
0.003846 0.284615
0.003846 0.288462
0.003846 0.292308
0.003846 0.296154
0.003846 0.300000
20(0.1)
0.005000 0.305000
0.005000 0.310000
0.005000 0.315000
0.005000 0.320000
0.005000 0.325000
0.005000 0.330000
0.005000 0.335000
0.005000 0.340000
0.005000 0.345000
0.005000 0.350000
0.005000 0.355000
0.005000 0.360000
0.005000 0.365000
0.005000 0.370000
0.005000 0.375000
0.005000 0.380000
0.005000 0.385000
0.005000 0.390000
0.005000 0.395000
0.005000 0.400000
20(0.1)
0.005000 0.405000
0.005000 0.410000
0.005000 0.415000
0.005000 0.420000
0.005000 0.425000
0.005000 0.430000
0.005000 0.435000
0.005000 0.440000
0.005000 0.445000
0.005000 0.450000
0.005000 0.455000
0.005000 0.460000
0.005000 0.465000
0.005000 0.470000
0.005000 0.475000
0.005000 0.480000
0.005000 0.485000
0.005000 0.490000
0.005000 0.495000
0.005000 0.500000
15(0.1)
0.006667 0.506667
0.006667 0.513333
0.006667 0.520000
0.006667 0.526667
0.006667 0.533333
0.006667 0.540000
0.006667 0.546667
0.006667 0.553333
0.006667 0.560000
0.006667 0.566667
0.006667 0.573333
0.006667 0.580000
0.006667 0.586667
0.006667 0.593333
0.006667 0.600000
16(0.1)
0.006250 0.606250
0.006250 0.612500
0.006250 0.618750

0.006250 0.625000
0.006250 0.631250
0.006250 0.637500
0.006250 0.643750
0.006250 0.650000
0.006250 0.656250
0.006250 0.662500
0.006250 0.668750
0.006250 0.675000
0.006250 0.681250
0.006250 0.687500
0.006250 0.693750
0.006250 0.700000
17(0.1)
0.005882 0.705882
0.005882 0.711765
0.005882 0.717647
0.005882 0.723529
0.005882 0.729412
0.005882 0.735294
0.005882 0.741176
0.005882 0.747059
0.005882 0.752941
0.005882 0.758824
0.005882 0.764706
0.005882 0.770588
0.005882 0.776471
0.005882 0.782353
0.005882 0.788235
0.005882 0.794118
0.005882 0.800000
8(0.1)
0.012500 0.812500
0.012500 0.825000
0.012500 0.837500
0.012500 0.850000
0.012500 0.862500
0.012500 0.875000
0.012500 0.887500
0.012500 0.900000
2(0.1)
0.050000 0.950000
0.050000 1.000000
3(0.1)
0.033333 1.033333
0.033333 1.066667
0.033333 1.100000
2(0.1)
0.050000 1.150000
0.050000 1.200000
3(0.1)
0.033333 1.233333
0.033333 1.266667
0.033333 1.300000
0,0,0(0.1),1(0.5)
0.800000 2.100000
0,0,1(0.5)
1.500000 3.600000
0(0.5)

N

36(0.1)
0.002778 0.002778
0.002778 0.005556
0.002778 0.008333
0.002778 0.011111
0.002778 0.013889
0.002778 0.016667
0.002778 0.019444
0.002778 0.022222
0.002778 0.025000
0.002778 0.027778
0.002778 0.030556
0.002778 0.033333

0.002778 0.036111
0.002778 0.038889
0.002778 0.041667
0.002778 0.044444
0.002778 0.047222
0.002778 0.050000
0.002778 0.052778
0.002778 0.055556
0.002778 0.058333
0.002778 0.061111
0.002778 0.063889
0.002778 0.066667
0.002778 0.069444
0.002778 0.072222
0.002778 0.075000
0.002778 0.077778
0.002778 0.080556
0.002778 0.083333
0.002778 0.086111
0.002778 0.088889
0.002778 0.091667
0.002778 0.094444
0.002778 0.097222
0.002778 0.100000
29(0.1)
0.003448 0.103448
0.003448 0.106897
0.003448 0.110345
0.003448 0.113793
0.003448 0.117241
0.003448 0.120690
0.003448 0.124138
0.003448 0.127586
0.003448 0.131034
0.003448 0.134483
0.003448 0.137931
0.003448 0.141379
0.003448 0.144828
0.003448 0.148276
0.003448 0.151724
0.003448 0.155172
0.003448 0.158621
0.003448 0.162069
0.003448 0.165517
0.003448 0.168966
0.003448 0.172414
0.003448 0.175862
0.003448 0.179310
0.003448 0.182759
0.003448 0.186207
0.003448 0.189655
0.003448 0.193103
0.003448 0.196552
0.003448 0.200000
23(0.1)
0.004348 0.204348
0.004348 0.208696
0.004348 0.213043
0.004348 0.217391
0.004348 0.221739
0.004348 0.226087
0.004348 0.230435
0.004348 0.234783
0.004348 0.239130
0.004348 0.243478
0.004348 0.247826
0.004348 0.252174
0.004348 0.256522
0.004348 0.260870
0.004348 0.265217
0.004348 0.269565
0.004348 0.273913
0.004348 0.278261
0.004348 0.282609

0.004348 0.286957
0.004348 0.291304
0.004348 0.295652
0.004348 0.300000
19(0.1)
0.005263 0.305263
0.005263 0.310526
0.005263 0.315789
0.005263 0.321053
0.005263 0.326316
0.005263 0.331579
0.005263 0.336842
0.005263 0.342105
0.005263 0.347368
0.005263 0.352632
0.005263 0.357895
0.005263 0.363158
0.005263 0.368421
0.005263 0.373684
0.005263 0.378947
0.005263 0.384211
0.005263 0.389474
0.005263 0.394737
0.005263 0.400000
21(0.1)
0.004762 0.404762
0.004762 0.409524
0.004762 0.414286
0.004762 0.419048
0.004762 0.423810
0.004762 0.428571
0.004762 0.433333
0.004762 0.438095
0.004762 0.442857
0.004762 0.447619
0.004762 0.452381
0.004762 0.457143
0.004762 0.461905
0.004762 0.466667
0.004762 0.471429
0.004762 0.476190
0.004762 0.480952
0.004762 0.485714
0.004762 0.490476
0.004762 0.495238
0.004762 0.500000
15(0.1)
0.006667 0.506667
0.006667 0.513333
0.006667 0.520000
0.006667 0.526667
0.006667 0.533333
0.006667 0.540000
0.006667 0.546667
0.006667 0.553333
0.006667 0.560000
0.006667 0.566667
0.006667 0.573333
0.006667 0.580000
0.006667 0.586667
0.006667 0.593333
0.006667 0.600000
7(0.1)
0.014286 0.614286
0.014286 0.628571
0.014286 0.642857
0.014286 0.657143
0.014286 0.671429
0.014286 0.685714
0.014286 0.700000
6(0.1)
0.016667 0.716667
0.016667 0.733333
0.016667 0.750000

0.016667 0.766667
0.016667 0.783333
0.016667 0.800000
14(0.1)
0.007143 0.807143
0.007143 0.814286
0.007143 0.821429
0.007143 0.828571
0.007143 0.835714
0.007143 0.842857
0.007143 0.850000
0.007143 0.857143
0.007143 0.864286
0.007143 0.871429
0.007143 0.878571
0.007143 0.885714
0.007143 0.892857
0.007143 0.900000
17(0.1)
0.005882 0.905882
0.005882 0.911765
0.005882 0.917647
0.005882 0.923529
0.005882 0.929412
0.005882 0.935294
0.005882 0.941176
0.005882 0.947059
0.005882 0.952941
0.005882 0.958824
0.005882 0.964706
0.005882 0.970588
0.005882 0.976471
0.005882 0.982353
0.005882 0.988235
0.005882 0.994118
0.005882 1.000000
3(0.1)
0.033333 1.033333
0.033333 1.066667
0.033333 1.100000
1(0.1)
0.100000 1.200000
0,0,0(0.1),3(0.5)
0.466667 1.666667
0.166667 1.833333
0.166667 2.000000
0,0,1(0.5)
1.500000 3.500000
0(0.5)

DK65x
S

30(0.1)
0.003333 0.003333
0.003333 0.006667
0.003333 0.010000
0.003333 0.013333
0.003333 0.016667
0.003333 0.020000
0.003333 0.023333
0.003333 0.026667
0.003333 0.030000
0.003333 0.033333
0.003333 0.036667
0.003333 0.040000
0.003333 0.043333
0.003333 0.046667
0.003333 0.050000
0.003333 0.053333
0.003333 0.056667
0.003333 0.060000
0.003333 0.063333
0.003333 0.066667

0.003333 0.070000
0.003333 0.073333
0.003333 0.076667
0.003333 0.080000
0.003333 0.083333
0.003333 0.086667
0.003333 0.090000
0.003333 0.093333
0.003333 0.096667
0.003333 0.100000
24(0.1)
0.004167 0.104167
0.004167 0.108333
0.004167 0.112500
0.004167 0.116667
0.004167 0.120833
0.004167 0.125000
0.004167 0.129167
0.004167 0.133333
0.004167 0.137500
0.004167 0.141667
0.004167 0.145833
0.004167 0.150000
0.004167 0.154167
0.004167 0.158333
0.004167 0.162500
0.004167 0.166667
0.004167 0.170833
0.004167 0.175000
0.004167 0.179167
0.004167 0.183333
0.004167 0.187500
0.004167 0.191667
0.004167 0.195833
0.004167 0.200000
20(0.1)
0.005000 0.205000
0.005000 0.210000
0.005000 0.215000
0.005000 0.220000
0.005000 0.225000
0.005000 0.230000
0.005000 0.235000
0.005000 0.240000
0.005000 0.245000
0.005000 0.250000
0.005000 0.255000
0.005000 0.260000
0.005000 0.265000
0.005000 0.270000
0.005000 0.275000
0.005000 0.280000
0.005000 0.285000
0.005000 0.290000
0.005000 0.295000
0.005000 0.300000
6(0.1)
0.016667 0.316667
0.016667 0.333333
0.016667 0.350000
0.016667 0.366667
0.016667 0.383333
0.016667 0.400000
2(0.1)
0.050000 0.450000
0.050000 0.500000
0,0,1(0.1)
0.300000 0.800000
0(0.1),0,1(0.5)
1.100000 1.900000
1(0.5)
0.500000 2.400000
0,1(0.5)
0.550000 2.950000

0.050000 3.000000
0.050000 3.050000
0.050000 3.100000
0.050000 3.150000
0.050000 3.200000
0.050000 3.250000
0.050000 3.300000
0.050000 3.350000
0.050000 3.400000
0(0.5)
0(0.5)

DK65y
W

33(0.1)
0.003030 0.003030
0.003030 0.006061
0.003030 0.009091
0.003030 0.012121
0.003030 0.015152
0.003030 0.018182
0.003030 0.021212
0.003030 0.024242
0.003030 0.027273
0.003030 0.030303
0.003030 0.033333
0.003030 0.036364
0.003030 0.039394
0.003030 0.042424
0.003030 0.045455
0.003030 0.048485
0.003030 0.051515
0.003030 0.054545
0.003030 0.057576
0.003030 0.060606
0.003030 0.063636
0.003030 0.066667
0.003030 0.069697
0.003030 0.072727
0.003030 0.075758
0.003030 0.078788
0.003030 0.081818
0.003030 0.084848
0.003030 0.087879
0.003030 0.090909
0.003030 0.093939
0.003030 0.096970
0.003030 0.100000
26(0.1)
0.003846 0.103846
0.003846 0.107692
0.003846 0.111538
0.003846 0.115385
0.003846 0.119231
0.003846 0.123077
0.003846 0.126923
0.003846 0.130769
0.003846 0.134615
0.003846 0.138462
0.003846 0.142308
0.003846 0.146154
0.003846 0.150000
0.003846 0.153846
0.003846 0.157692
0.003846 0.161538
0.003846 0.165385
0.003846 0.169231
0.003846 0.173077
0.003846 0.176923
0.003846 0.180769
0.003846 0.184615
0.003846 0.188462
0.003846 0.192308
0.003846 0.196154

0.003846 0.200000
15(0.1)
0.006667 0.206667
0.006667 0.213333
0.006667 0.220000
0.006667 0.226667
0.006667 0.233333
0.006667 0.240000
0.006667 0.246667
0.006667 0.253333
0.006667 0.260000
0.006667 0.266667
0.006667 0.273333
0.006667 0.280000
0.006667 0.286667
0.006667 0.293333
0.006667 0.300000
8(0.1)
0.012500 0.312500
0.012500 0.325000
0.012500 0.337500
0.012500 0.350000
0.012500 0.362500
0.012500 0.375000
0.012500 0.387500
0.012500 0.400000
5(0.1)
0.020000 0.420000
0.020000 0.440000
0.020000 0.460000
0.020000 0.480000
0.020000 0.500000
2(0.1)
0.050000 0.550000
0.050000 0.600000
1(0.1)
0.100000 0.700000
1(0.1)
0.100000 0.800000
0,6(0.1)
0.116667 0.916667
0.016667 0.933333
0.016667 0.950000
0.016667 0.966667
0.016667 0.983333
0.016667 1.000000
0,0,0,2(0.5)
1.750000 2.750000
0.250000 3.000000
0,1(0.5)
1.000000 4.000000

Dyke-parallel fracture strike data for the fracture frequency profiles.
X = distance from dyke margin. Y = strike of fracture.
Z = angular deflection of fracture strike from strike of dyke (the strike of the dyke is indicated in brackets after the dyke number). Negative values indicate the fracture is *anticlockwise* from the strike of dyke, positive values indicate the fracture is *clockwise* from the strike of dyke. This deflection is depicted in Figure 3.4 as part of the fracture frequency profiles.

X	Y	Z
K23 (097)		
S		
3.25	108	11
7.25	109	12
10.25	125	28
13.75	099	2
K27 (104)		
S		
0.25	103	-1
1	111	7
3.25	126	22
4.25	104	0
5.75	118	14
8.25	124	20
10.5	079	-25
13.25	076	-28
N		
3.75	103	-1
4.75	098	-6
7.25	101	-3
9.75	095	-9
14.25	124	20
19.5	117	13
21.5	113	9
26.5	125	21
K32 (103)		
S		
1	103	0
2	112	9
N		
7.5	103	0
K84 (104)		
S		
1.25	103	-1
2.75	104	0
4.75	106	2
6.25	104	0
8.25	104	0
N		
0.75	102	-2
3.25	102	-2
6.75	103	-1
10	105	1
12	106	2
19.25	103	-1
23	103	-1
K90c (098)		
N		
0.5	098	0
2.25	099	1
5	101	3
8.25	092	-6
10.5	107	9
12	100	2
20	114	16
23	098	0
30.5	093	-5
33.25	093	-5
K92 (095)		
S		
1.25	093	-2
2.5	095	0
3.5	095	0
13.75	116	21
14.75	103	8
N		
0.25	093	-2
0.75	093	-2
1.75	096	1
3	101	6
4	101	6
5	099	4
11	098	3
16	102	7
K93 (103)		
S		
0.5	103	0
1.5	106	3
3.75	106	3
5.5	105	2
7.5	111	8
12	109	6
16.75	102	-1
N		
1	104	1
4	102	-1
5	105	2
9	105	2
11	103	0
15.25	099	-4
17.5	101	-2
20	099	-4
21	094	-9
24	100	-3
26	100	-3
K94 (101)		
S		
0.75	102	1
1.5	102	1
3.5	094	-7
7	093	-8
9.5	093	-8
11.75	096	-5
N		
0.5	098	-3
3.5	095	-6
9	092	-9
12.75	093	-8
K111 (094)		
S		
0.5	095	1
2	096	2
5	094	0
10	096	2
17	101	7
23	102	8
27	099	5
32	095	1
38	092	-2
N		
1.4	096	2
5	099	5
16	101	7
25	106	12
32	104	10
K112 (103)		
S		
1	099	-4
4	099	-4
14	097	-6
21	099	-4
N		
2.25	099	-4
10.25	093	-10
18.5	099	-4
20.5	097	-6
27	099	-4
K113 (089)		
S		
1	091	2
10.5	092	3
26.5	097	8
N		
1.25	091	2
K114 (096)		
S		
0.75	098	2
2	100	4
4	097	1
N		
1.25	096	0
10	093	-3
K115 (081)		
S		
1.75	083	2
4	087	6
5	093	12
N		
0.25	089	8
1.25	089	8
4.5	084	3
6.5	084	3
8.5	072	-9
12	094	13
14	094	13
15	084	3
18	084	3
20.5	086	5
K116i (089)		
S		
0.25	089	0
0.75	089	0
1.75	088	-1
3.75	091	2
5.75	089	0
8	092	3
11	086	-3
14.75	094	5

16	099	10
19	096	7
23	090	1
N		
3	088	-1
3.75	088	-1

K116iix (093)

S		
0.75	100	7
1.5	100	7
2.5	092	-1
N		
3.25	095	2
11.25	097	4

K117 (099)

S		
2.25	101	2
4	101	2
6.25	101	2
13.25	096	-3
16.25	093	-6
N		
3	100	1
10	100	1
15	097	-2
19	098	-1
23	106	7
33.5	102	3

K118i (105)

S		
0.5	102	-3
1	102	-3
1.5	090	-15
2.25	094	-11
4.5	100	-5
5.5	100	-5
6.5	098	-7
11.5	100	-5
14.5	096	-9
15.5	090	-15
20.5	096	-9
26.5	096	-9
N		
0.5	114	9
0.75	096	-9
1.5	098	-7
2	106	1
2.5	096	-9
4	089	-16
6.25	089	-16
8.25	094	-11

K118ii (093)

S		
2	094	1
3	094	1
5.5	094	1
7.5	094	1
N		
1.25	094	1
3	094	1
7	094	1

K119 (100)

S		
0.25	100	0
1	094, 100	-6, 0
3.75	094	-6
N		
0.75	100	0
2.5	094, 100	-6, 0
5.5	094	-6
9.5	094	-6
16.5	094	-6

K126 (096)

S		
0.5	095	-1
1	093	-3
1.5	093	-3
3.5	099	3
5	099	3
5.75	108	12
9	109, 088	13, -8
13	088	-8
13.75	109	13
16.5	090	-6
19	099	3
23.5	085	-11
24.5	109	13
N		
0.25	096	0
1	096	0
1.75	092	-4
3.5	107	11
6.5	089, 112	-13, 16
16.5	089, 104	-13, 16

K127 (090)

S		
3	089	-1
8	089	-1
14	089	-1
20	089	-1
25	089	-1
42	089	-1
50	087	-3
N		
7	089	-1
12	089	-1
19	093	3
26	089	-1

K132i (104)

S		
3	102	-2
5	099	-5
19	099	-5
32	099	-5

K132ii (104)

N		
3.5	101	-3

K134 (108)

S		
0.5	109	1
8.5	104	-4
N		
0.25	109	1
6	102	-6

K136 (103)

S		
0.5	104	1
1.25	104	1
2.25	101	-2
7	100	-3
12	102	-1
20	100	-3
N		
0.5	104	1
2	101	-2
5	099	-4
6	099	-4
8.25	103	0
14	103	0
17	096	-7

K138 (101)

S		
1.25	102	1
5.25	102	1
9.25	099	-2
14	099	-2
22	103	2
N		
3.5	102	1
12.5	101	0
16.5	102	1
19.75	101	0

K147 (092)

S		
0.5	091	-1
2.75	089	-3
8.5	087	-5
13.5	081	-11
N		
0.5	092	0
1.75	089	-3
4	094	2
8.5	094	2

K155b (084)

S		
0.5	087	3
1.5	089	5
7.75	089	5
N		
2.25	087	3
16.75	089	5

K157a (091)

S		
0.25	089	-2
11	091	0
N		
3.5	091	0
10.25	097	6

K176 (099)

S		
0.5	099	0
2.5	099	0
6.5	109	10
8.5	109	10
N		
0.5	099	0
3.5	094	-5
5.75	096	-3
13.5	096	-3

K178 (094)

S		
0.5	095	1
2	095	1
4	095	1
6.5	095	1
11.5	095	1
26.5	095	1
29.5	095	1
N		
0.5	095	1

1.75	095	1
5.25	095	1
10	095	1
19	095	1

K180 (094)

S

0.25	094	0
3	105	11
5.25	093	-1
7.25	096	2
9	091	-3
10	090	-4
12.25	092	-2
14.5	094	0
16	100	6
18	103	9

N

0.5	092	-2
2.5	103	9
4.5	109	15
6.25	102	8
8.25	102	8
10.25	116	22
11.5	116	22
13.25	087	-7
15.25	093	-1
17.5	098	4

WC25a (036)

SE

0.4	011	-25
0.5	034	-2
0.6	024	-12
0.7	039	3
0.75	025	-11
1	011	-25
1.5	038	2
2	019	-17
2.25	036	0
2.35	024	-12
2.75	036	0
3	019	-17
3.5	029	-7
4	025	-11
4.5	031	-5
4.75	029	-7
5.5	039	3
7	027	-9
9.5	027	-9

NW

0.25	034	-2
0.5	023	-13
0.75	004	-32
0.85	029	-7
0.9	174	138
1	031	-5
1.1	007	-29
1.2	017	-19
1.25	036	0
1.3	036	0
1.35	003	-33
1.4	003	-33
1.5	019	-17
1.6	019	-17
1.7	024	-12
2	024	-12
2.25	009	-27
2.5	009	-27
2.6	024	-12
2.75	021	-15
3	021	-15
3.25	019	-17
3.5	034	-2
4	039	3
4.75	043	7
5	044	8
5.5	049	13
6.5	054	18
9	051	15
10.75	034	-2
12.75	026	-10
13.75	021	-15
14.5	027	-9
16.75	029	-7
17.75	042	6
18.5	037	1
20.5	042	6
21	042	6

WC25c (032)

SE

0.25	022	-10
1	034	2
1.75	035	3
4	044	12
7.5	039	7
13.5	044	12
18.75	039	7
28.5	027	-5
31	029	-3
46.5	038	6

NW

1	032	0
2.5	040	8
6.75	043	11
20	034	2
32.5	034	2

WC33a (038)

SE

12.75	040	2
32.75	038	0
40.5	043	5
50	044	6
52	033	-5
53	039	1
60	039	1
63	036	-2

DK14 (133)

SW

0.75	132	-1
2.5	132	-1
5	127	-6
9.5	127	-6
12	098	-35
24	098	-35
29	131	-2

NE

1.25	129	-4
2.5	131	-2
5.5	129	-4
8.75	136	3
14.25	136	3
19	134	1
27.25	135	2
36.25	137	4

DK17a (125)

SW

1	126	1
3	127	2
5	124	-1
10	124	-1
14.5	124	-1
19	124	-1
25.5	127	2
31	124	-1
43	132	7
50	129	4

DK33a (100)

S

6.75	094	-6
13.75	104	4

DK42 (116)

S

3.75	122	6
8.75	116	0

Binned data for the construction of fracture frequency profiles.
Data is in two columns. Left column: bins of 0.25 m (except for shaded sections of 1 m bins). Right column: frequency of fractures.
Dyke numbers suffixed with 'x' or 'y' (K116ii and DK65) refer to separate profiles either on the same side of a dyke at the same orientation, or perpendicular to margins of different strike for the same dyke.
For dyke K117, suffix 'A' indicates 'major fractures' (type 2 fractures from the text) and 'B' indicates 'minor fractures' (type 1 fractures from the text), as explained in the text. Suffix 'AB' combines data for the two fracture types.
For dyke K127, NO = no outcrop. The numbers marked with * are used to 'fill in' the profile (where there was no outcrop) for comparison with the modelled thermal history in Figure 3.28.

K23

S	
0.25	12
0.50	7
0.75	2
1.00	4
1.25	3
1.50	2
1.75	1
2.00	1
2.25	2
2.50	2
2.75	1
3.00	1
3.25	2
3.50	2
3.75	0
4.00	1
4.25	0
4.50	1
4.75	0
5.00	1
5.25	0
5.50	1
5.75	0
6.00	0
6.25	0
6.50	0
6.75	0
7.00	0
7.25	1
7.50	1
7.75	0
8.00	1
8.25	0
8.50	0
8.75	0
9.00	0
9.25	0
9.50	0
9.75	0
10.00	0
10.25	2
10.50	1
10.75	0
11.00	0
11.25	0
11.50	0
11.75	0
12.00	0
12.25	0
12.50	0
12.75	0
13.00	0
13.25	0
13.50	0
13.75	1
14.00	1
14.25	0
14.50	0
14.75	0
15.00	0
15.25	0
15.50	0
15.75	0
16.00	0

K27

S	
0.25	21
0.50	14
0.75	15
1.00	15
1.25	13
1.50	18
1.75	16
2.00	16
2.25	10
2.50	10
2.75	8
3.00	7
3.25	6
3.50	6
3.75	5
4.00	5
4.25	1
4.50	2
4.75	1
5.00	2
5.25	1
5.50	1
5.75	2
6.00	2
6.25	6
6.50	7
6.75	2
7.00	2
7.25	0
7.50	0
7.75	1
8.00	1
8.25	5
8.50	5
8.75	4
9.00	4
9.25	0
9.50	1
9.75	1
10.00	2
10.25	1
10.50	1
10.75	0
11.00	0
11.25	0
11.50	0
11.75	0
12.00	1
12.25	1
12.50	1
12.75	0
13.00	1
13.25	2
13.50	2
13.75	3
14.00	3
14.25	2
14.50	3
14.75	1

N

0.25	15
0.50	13
0.75	11
1.00	24
1.25	16
1.50	8
1.75	8
2.00	10
2.25	1
2.50	3
2.75	1
3.00	1
3.25	2
3.50	3
3.75	4
4.00	4
4.25	3
4.50	4
4.75	3
5.00	3
5.25	2
5.50	4
5.75	5
6.00	4
6.25	3
6.50	5
6.75	5
7.00	4
7.25	5
7.50	3
7.75	1
8.00	2
8.25	2
8.50	3
8.75	3
9.00	5
9.25	5
9.50	4
9.75	4
10.00	4
10.25	3
10.50	2
10.75	1
11.00	2
11.25	4
11.50	5
11.75	5
12.00	4
12.25	4
12.50	4
12.75	3
13.00	3
13.25	4
13.50	4
13.75	3
14.00	2
14.25	3
14.50	2
14.75	2
15.00	2
15.25	0
15.50	1
15.75	0
16.00	1
16.25	1
16.50	1
16.75	2
17.00	1
17.25	2
17.50	1
17.75	2
18.00	2
18.25	3
18.50	4
18.75	3
19.00	6
19.25	8
19.50	9
19.75	8
20.00	8
20.25	6
20.50	6
20.75	6
21.00	7
21.25	9
21.50	8
21.75	9
22.00	8
22.25	6
22.50	5
22.75	6
23.00	5
23.25	4
23.50	5
23.75	4
24.00	5
24.25	6
24.50	6
24.75	7
25.00	4
25.25	2
25.50	2
25.75	1
26.00	3
26.25	3
26.50	3
26.75	3
27.00	2

K32

S	
0.25	8
0.50	17
0.75	22
1.00	19
1.25	14
1.50	5
1.75	9
2.00	8
2.25	10
2.50	2
2.75	0
3.00	0
3.25	0
3.50	0
3.75	1
4.00	2
4.25	1
4.50	0
4.75	1
5.00	1
5.25	3
5.50	3
5.75	2
6.00	0
6.25	1
6.50	0
6.75	1
7.00	0
7.25	0
7.50	0
7.75	0
8.00	0
8.25	0
8.50	0
8.75	0
9.00	0
9.25	0
9.50	0
9.75	0
10.00	0
10.25	0
10.50	0
10.75	0
11.00	0
11.25	0
11.50	0
11.75	0
12.00	0
12.25	0
12.50	0
12.75	0
13.00	0
13.25	0
13.50	0
13.75	0
14.00	0

N

0.25	19
0.50	24
0.75	16
1.00	6
1.25	1
1.50	8
1.75	9
2.00	6
2.25	4
2.50	4
2.75	2
3.00	1
3.25	1
3.50	0
3.75	1
4.00	1
4.25	1
4.50	0
4.75	1
5.00	2
5.25	1
5.50	2
5.75	1
6.00	0
6.25	1
6.50	0
6.75	1
7.00	1
7.25	1
7.50	0
7.75	2
8.00	2
8.25	1
8.50	1
8.75	1
9.00	0
9.25	0
9.50	0
9.75	0
10.00	0
10.25	0
10.50	0
10.75	1
11.00	0
11.25	0
11.50	0
11.75	1
12.00	0
12.25	0
12.50	0
12.75	1
13.00	0
13.25	0
13.50	0
13.75	1
14.00	0
14.25	0
14.50	0
14.75	1
15.00	0
15.25	1
15.50	0
15.75	1
16.00	0
16.25	0
16.50	0
16.75	0
17.00	0
17.25	0
17.50	0
17.75	0
18.00	0
18.25	0
18.50	0
18.75	0
19.00	0
19.25	0
19.50	0
19.75	0
20.00	0
20.25	1
20.50	0
20.75	1
21.00	0
21.25	0
21.50	0
21.75	0
22.00	0
22.25	0
22.50	0
22.75	0
23.00	0
23.25	0
23.50	0
23.75	0
24.00	0

K84

S	
0.25	13
0.50	13
0.75	8
1.00	9
1.25	8
1.50	9
1.75	13
2.00	13
2.25	14
2.50	15
2.75	10
3.00	11
3.25	12
3.50	12
3.75	14
4.00	14
4.25	10
4.50	11
4.75	7
5.00	8
5.25	9
5.50	9
5.75	8
6.00	9
6.25	4
6.50	5
6.75	4
7.00	4
7.25	2
7.50	3
7.75	3
8.00	4
8.25	3
8.50	4
8.75	3
9.00	3

N

0.25	5
0.50	6
0.75	7
1.00	6
1.25	6
1.50	5
1.75	5
2.00	5
2.25	4
2.50	4
2.75	3
3.00	3
3.25	4
3.50	3
3.75	4
4.00	3
4.25	2
4.50	3
4.75	2
5.00	4
5.25	4
5.50	5
5.75	4
6.00	4
6.25	2
6.50	3
6.75	2
7.00	2
7.25	2
7.50	2
7.75	2
8.00	2
8.25	2
8.50	1
8.75	2
9.00	2
9.25	2
9.50	1
9.75	2
10.00	2
10.25	2
10.50	1
10.75	2
11.00	1
11.25	2
11.50	1
11.75	2
12.00	2
12.25	2
12.50	1
12.75	1
13.00	1
13.25	1
13.50	1
13.75	0
14.00	1
14.25	1
14.50	1
14.75	1
15.00	0
15.25	1
15.50	1
15.75	0
16.00	1
16.25	0
16.50	1
16.75	1
17.00	0
17.25	1
17.50	1
17.75	1
18.00	1
18.25	1
18.50	1
18.75	0
19.00	0
19.25	0
19.50	1
19.75	0
20.00	1
20.25	0
20.50	1
20.75	0
21.00	1
21.25	0
21.50	1
21.75	1
22.00	0
22.25	1
22.50	1
22.75	1
23.00	0
23.25	1
23.50	1
23.75	0
24.00	1
24.25	0
24.50	1
24.75	1
25.00	0
25.25	1
25.50	1

K90c

S	
0.25	31
0.50	15
0.75	9
1.00	7
1.25	4
1.50	3
1.75	3
2.00	3
2.25	1
2.50	2
2.75	1

N

0.25	37
0.50	21
0.75	11
1.00	11
1.25	6
1.50	6

1.75	7
2.00	7
2.25	6
2.50	7
2.75	10
3.00	11
3.25	8
3.50	8
3.75	4
4.00	5
4.25	4
4.50	5
4.75	1
5.00	2
5.25	1
5.50	2
5.75	1
6.00	1
6.25	1
6.50	1
6.75	0
7.00	0
7.25	0
7.50	0
7.75	0
8.00	1
8.25	1
8.50	1
8.75	0
9.00	0
9.25	0
9.50	0
9.75	0
10.00	0
10.25	0
10.50	1
10.75	1
11.00	1
11.25	1
11.50	1
11.75	2
12.00	2
12.25	2
12.50	2
12.75	1
13.00	2

13.25	2
13.50	2
13.75	0
14.00	1
14.25	1
14.50	1
14.75	0
15.00	1
15.25	0
15.50	1
15.75	0
16.00	0
16.25	0
16.50	0
16.75	0
17.00	0
17.25	0
17.50	0
17.75	0
18.00	0
18.25	0
18.50	0
18.75	0
19.00	1
19.25	0
19.50	1
19.75	1
20.00	2
20.25	1
20.50	1
20.75	1
21.00	0
21.25	1
21.50	0
21.75	1
22.00	1
22.25	1
22.50	1
22.75	2
23.00	2
23.25	2
23.50	2
23.75	0
24.00	1
24.25	0
24.50	1

24.75	0
25.00	0
25.25	0
25.50	0
25.75	0
26.00	0
26.25	0
26.50	0
26.75	0
27.00	1
27.25	0
27.50	1
27.75	0
28.00	0
28.25	0
28.50	0
28.75	0
29.00	0
29.25	0
29.50	1
29.75	0
30.00	0
30.25	0
30.50	1
30.75	0
31.00	0
31.25	0
31.50	1
31.75	1
32.00	1
32.25	1
32.50	1
32.75	0
33.00	1
33.25	0
33.50	1

K92

S	
0.25	3
0.50	3
0.75	2
1.00	1
1.25	3
1.50	2
1.75	2

2.00	1
2.25	1
2.50	1
2.75	2
3.00	1
3.25	0
3.50	1
3.75	0
4.00	1
4.25	0
4.50	0
4.75	0
5.00	1
5.25	0
5.50	0
5.75	0
6;00	1
6.25	0
6.50	0
6.75	0
7.00	0
7.25	0
7.50	0
7.75	0
8.00	1
8.25	0
8.50	0
8.75	0
9.00	0
9.25	0
9.50	0
9.75	0
10.00	0
10.25	0
10.50	0
10.75	0
11.00	0
11.25	0
11.50	0
11.75	0
12.00	0
12.25	0
12.50	0
12.75	0
13.00	0
13.25	0

13.50	0
13.75	0
14.00	1
14.25	0
14.50	0
14.75	0
15.00	1
15.25	0
15.50	0
15.75	0
16.00	0
16.25	0
16.50	0
16.75	0
17.00	1
17.25	0
17.50	0
17.75	0
18.00	0
18.25	0
18.50	0
18.75	0
19.00	0
19.25	0
19.50	0
19.75	0
20.00	0
20.25	0
20.50	0
20.75	0
21.00	0
21.25	0
21.50	0
21.75	0
22.00	0
22.25	0
22.50	0
22.75	0
23.00	0
23.25	0
23.50	0
23.75	0
24.00	0
24.25	0
24.50	0
24.75	0

25.00	0

N	
0.25	8
0.50	4
0.75	3
1.00	4
1.25	4
1.50	1
1.75	1
2.00	1
2.25	1
2.50	0
2.75	1
3.00	1
3.25	1
3.50	0
3.75	1
4.00	1
4.25	1
4.50	0
4.75	1
5.00	1
5.25	1
5.50	0
5.75	0
6.00	0
6.25	0
6.50	0
6.75	0
7.00	0
7.25	0
7.50	0
7.75	0
8.00	0
8.25	0
8.50	0
8.75	0
9.00	0
9.25	1
9.50	0
9.75	1
10.00	0
10.25	1
10.50	0
10.75	0

11.00	0
11.25	1
11.50	0
11.75	0
12.00	0
12.25	1
12.50	0
12.75	0
13.00	0
13.25	0
13.50	0
13.75	0
14.00	0
14.25	0
14.50	0
14.75	0
15.00	0
15.25	0
15.50	0
15.75	0
16.00	1
16.25	1
16.50	0
16.75	0
17.00	0
17.25	1

K93

S	
0.25	7
0.50	9
0.75	6
1.00	6
1.25	9
1.50	5
1.75	9
2.00	3
2.25	2
2.50	2
2.75	1
3.00	2
3.25	1
3.50	1
3.75	1
4.00	1
4.25	0

4.50	0
4.75	0
5.00	2
5.25	2
5.50	2
5.75	2
6.00	1
6.25	1
6.50	1
6.75	0
7.00	1
7.25	1
7.50	1
7.75	0
8.00	1
8.25	0
8.50	0
8.75	0
9.00	0
9.25	0
9.50	0
9.75	0
10.00	1
10.25	0
10.50	1
10.75	0
11.00	1
11.25	0
11.50	0
11.75	0
12.00	1
12.25	0
12.50	0
12.75	0
13.00	0
13.25	0
13.50	0
13.75	0
14.00	0
14.25	0
14.50	0
14.75	0
15.00	0
15.25	0
15.50	0
15.75	0

16.00	0
16.25	0
16.50	0
16.75	0
17.00	1

N	
0.25	8
0.50	15
0.75	15
1.00	14
1.25	11
1.50	7
1.75	6
2.00	5
2.25	6
2.50	7
2.75	2
3.00	1
3.25	1
3.50	0
3.75	1
4.00	0
4.25	1
4.50	0
4.75	1
5.00	0
5.25	1
5.50	0
5.75	0
6.00	0
6.25	0
6.50	0
6.75	0
7.00	0
7.25	0
7.50	0
7.75	0
8.00	0
8.25	1
8.50	0
8.75	0
9.00	0
9.25	1
9.50	0
9.75	1

10.00	0
10.25	1
10.50	0
10.75	1
11.00	0
11.25	1
11.50	1
11.75	1
12.00	0
12.25	1
12.50	0
12.75	0
13.00	0
13.25	1
13.50	0
13.75	0
14.00	0
14.25	0
14.50	0
14.75	0
15.00	0
15.25	0
15.50	0
15.75	0
16.00	0
16.25	1
16.50	0
16.75	1
17.00	0
17.25	1
17.50	1
17.75	1
18.00	0
18.25	1
18.50	0
18.75	0
19.00	0
19.25	0
19.50	0
19.75	0
20.00	0
20.25	1
20.50	0
20.75	0
21.00	0
21.25	1

21.50	0
21.75	0
22.00	0
22.25	0
22.50	0
22.75	0
23.00	0
23.25	1
23.50	0
23.75	0
24.00	0
24.25	1
24.50	0
24.75	0
25.00	0
25.25	1
25.50	0
25.75	1
26.00	0
26.25	1
26.50	0
26.75	0
27.00	0
27.25	1

K94

S	
0.25	4
0.50	4
0.75	3
1.00	2
1.25	0
1.50	1
1.75	0
2.00	1
2.25	0
2.50	1
2.75	0
3.00	1
3.25	0
3.50	1
3.75	0
4.00	1
4.25	0
4.50	0
4.75	0

5.00	0
5.25	0
5.50	0
5.75	0
6.00	1
6.25	0
6.50	0
6.75	0
7.00	1
7.25	0
7.50	0
7.75	0
8.00	0
8.25	0
8.50	0
8.75	0
9.00	0
9.25	0
9.50	1
9.75	0
10.00	1
10.25	0
10.50	0
10.75	0
11.00	0
11.25	0
11.50	0
11.75	0
12.00	1

N	
0.25	10
0.50	5
0.75	3
1.00	2
1.25	1
1.50	1
1.75	1
2.00	1
2.25	0
2.50	0
2.75	0
3.00	0
3.25	0
3.50	1
3.75	0

4.00	1
4.25	0
4.50	0
4.75	0
5.00	0
5.25	0
5.50	0
5.75	0
6.00	1
6.25	0
6.50	0
6.75	0
7.00	1
7.25	0
7.50	0
7.75	0
8.00	0
8.25	0
8.50	0
8.75	0
9.00	0
9.25	0
9.50	0
9.75	0
10.00	1
10.25	0
10.50	0
10.75	0
11.00	0
11.25	0
11.50	0
11.75	0
12.00	0
12.25	0
12.50	1
12.75	0
13.00	1

K111

S	
0.25	79
0.50	13
0.75	2
1.00	1
1.25	2
1.50	1

1.75	2
2.00	4
2.25	3
2.50	3
2.75	3
3.00	2
3.25	2
3.50	3
3.75	3
4.00	3
4.25	4
4.50	3
4.75	3
5.00	3
5.25	3
5.50	2
5.75	3
6.00	2
6.25	2
6.50	2
6.75	2
7.00	1
7.25	2
7.50	2
7.75	3
8.00	2
8.25	2
8.50	2
8.75	3
9.00	2
9.25	2
9.50	1
9.75	1
10.00	2
10.25	1
10.50	0
10.75	1
11.00	1
11.25	1
11.50	1
11.75	1
12.00	1
12.25	1
12.50	1
12.75	1
13.00	2

13.25	1
13.50	0
13.75	1
14.00	1
14.25	2
14.50	1
14.75	1
15.00	2
15.25	1
15.50	1
15.75	1
16.00	1
16.25	1
16.50	1
16.75	1
17.00	2
17.25	1
17.50	1
17.75	1
18.00	1
18.25	1
18.50	1
18.75	1
19.00	2
19.25	1
19.50	1
19.75	1
20.00	1
20.25	1
20.50	1
20.75	1
21.00	1
21.25	1
21.50	0
21.75	1
22.00	1
22.25	1
22.50	1
22.75	1
23.00	1
23.25	1
23.50	2
23.75	2
24.00	1
24.25	2
24.50	1

24.75	1
25.00	1
25.25	1
25.50	1
25.75	2
26.00	1
26.25	2
26.50	2
26.75	3
27.00	2
27.25	2
27.50	1
27.75	1
28.00	2
28.25	1
28.50	1
28.75	2
29.00	1
29.25	2
29.50	1
29.75	1
30.00	2
30.25	1
30.50	2
30.75	2
31.00	2
31.25	2
31.50	1
31.75	1
32.00	2
32.25	1
32.50	1
32.75	1
33.00	2
33.25	1
33.50	1
33.75	1
34.00	1
34.25	1
34.50	0
34.75	1
35.00	1
35.25	1
35.50	1
35.75	1
36.00	2

36.25	1
36.50	1
36.75	1
37.00	2
37.25	1
37.50	1
37.75	2
38.00	1
38.25	2
38.50	1
38.75	1
39.00	1
39.25	1
39.50	1
39.75	1
40.00	2
40.25	1
40.50	1
40.75	1
41.00	2
41.25	1

N	
0.25	57
0.50	4
0.75	3
1.00	2
1.25	1
1.50	2
1.75	2
2.00	3
2.25	2
2.50	2
2.75	1
3.00	2
3.25	1
3.50	2
3.75	1
4.00	2
4.25	1
4.50	2
4.75	1
5.00	2
5.25	2
5.50	1
5.75	2

6.00	2
6.25	1
6.50	2
6.75	1
7.00	2
7.25	1
7.50	2
7.75	1
8.00	1
8.25	1
8.50	1
8.75	1
9.00	1
9.25	1
9.50	2
9.75	1
10.00	2
10.25	2
10.50	1
10.75	2
11.00	1
11.25	1
11.50	1
11.75	2
12.00	1
12.25	1
12.50	1
12.75	1
13.00	1
13.25	1
13.50	1
13.75	2
14.00	1
14.25	1
14.50	1
14.75	1
15.00	1
15.25	0
15.50	1
15.75	2
16.00	1
16.25	1
16.50	1
16.75	1
17.00	1
17.25	1
17.50	1
17.75	1
18.00	1
18.25	1

17.50	2
17.75	1
18.00	2
18.25	2
18.50	1
18.75	2
19.00	2
19.25	2
19.50	2
19.75	2
20.00	2
20.25	2
20.50	1
20.75	2
21.00	3
21.25	2
21.50	2
21.75	2
22.00	3
22.25	2
22.50	3
22.75	2
23.00	3
23.25	2
23.50	3
23.75	2
24.00	2
24.25	2
24.50	2
24.75	2
25.00	3
25.25	2
25.50	3
25.75	2
26.00	2
26.25	2
26.50	2
26.75	2
27.00	3
27.25	2
27.50	2
27.75	2
28.00	2
28.25	1
28.50	2
28.75	1

29.00	2
29.25	2
29.50	1
29.75	2
30.00	2
30.25	2
30.50	1
30.75	2
31.00	3
31.25	2
31.50	3
31.75	3
32.00	3
32.25	3
32.50	3
32.75	3

K112

S	
0.25	69
0.50	34
0.75	25
1.00	22
1.25	20
1.50	16
1.75	14
2.00	6
2.25	1
2.50	1
2.75	2
3.00	1
3.25	1
3.50	1
3.75	1
4.00	1
4.25	1
4.50	1
4.75	1
5.00	1
5.25	1
5.50	2
5.75	2
6.00	2
6.25	2
6.50	1
6.75	1

7.00	1
7.25	1
7.50	1
7.75	2
8.00	1
8.25	1
8.50	1
8.75	1
9.00	1
9.25	1
9.50	2
9.75	1
10.00	2
10.25	2
10.50	1
10.75	2
11.00	1
11.25	1
11.50	1
11.75	2
12.00	1
12.25	1
12.50	1
12.75	1
13.00	1
13.25	1
13.50	1
13.75	2
14.00	1
14.25	1
14.50	1
14.75	1
15.00	1
15.25	0
15.50	1
15.75	2
16.00	1
16.25	1
16.50	1
16.75	1
17.00	1
17.25	1
17.50	1
17.75	1
18.00	1
18.25	1

18.50	1
18.75	2
19.00	1
19.25	1
19.50	1
19.75	1
20.00	1
20.25	1
20.50	1
20.75	1
21.00	1
21.25	1
21.50	1

N	
0.25	54
0.50	9
0.75	35
1.00	34
1.25	26
1.50	25
1.75	13
2.00	12
2.25	6
2.50	6
2.75	5
3.00	6
3.25	6
3.50	6
3.75	2
4.00	2
4.25	1
4.50	0
4.75	1
5.00	0
5.25	0
5.50	0
5.75	2
6.00	2
6.25	1
6.50	2
6.75	1
7.00	0
7.25	1
7.50	0
7.75	1

8.00	1
8.25	1
8.50	1
8.75	1
9.00	1
9.25	1
9.50	1
9.75	1
10.00	1
10.25	1
10.50	0
10.75	1
11.00	0
11.25	0
11.50	0
11.75	1
12.00	0
12.25	1
12.50	0
12.75	1
13.00	0
13.25	1
13.50	0
13.75	1
14.00	0
14.25	0
14.50	0
14.75	1
15.00	0
15.25	0
15.50	0
15.75	1
16.00	0
16.25	0
16.50	0
16.75	1
17.00	0
17.25	1
17.50	0
17.75	1
18.00	0
18.25	0
18.50	0
18.75	1
19.00	1
19.25	1

19.50	0
19.75	1
20.00	0
20.25	0
20.50	0
20.75	1
21.00	0
21.25	0
21.50	0
21.75	1
22.00	1
22.25	1
22.50	0
22.75	2
23.00	1
23.25	1
23.50	1
23.75	1
24.00	1
24.25	1
24.50	0
24.75	1
25.00	0
25.25	0
25.50	0
25.75	0
26.00	0
26.25	0
26.50	0
26.75	1
27.00	0
27.25	1
27.50	0
27.75	1
28.00	0
28.25	0
28.50	0
28.75	1
29.00	0
29.25	0
29.50	0
29.75	1
30.00	1
30.25	1
30.50	0
30.75	1

31.00	0
31.25	0
31.50	0
31.75	1
32.00	0
32.25	1
32.50	0
32.75	1
33.00	0
33.25	1
33.50	0
33.75	1

K113

S	
0.25	45
0.50	30
0.75	22
1.00	11
1.25	20
1.50	23
1.75	23
2.00	1
2.25	1
2.50	1
2.75	2
3.00	0
3.25	0
3.50	0
3.75	1
4.00	0
4.25	1
4.50	1
4.75	1
5.00	1
5.25	1
5.50	1
5.75	1
6.00	1
6.25	1
6.50	1
6.75	1
7.00	1
7.25	1
7.50	1
7.75	1

8.00	0
8.25	1
8.50	0
8.75	1
9.00	1
9.25	1
9.50	1
9.75	1
10.00	0
10.25	1
10.50	1
10.75	1
11.00	1
11.25	1
11.50	1
11.75	1
12.00	0
12.25	1
12.50	1
12.75	1
13.00	0
13.25	1
13.50	0
13.75	1
14.00	0
14.25	0
14.50	0
14.75	1
15.00	0
15.25	0
15.50	0
15.75	1
16.00	0
16.25	1
16.50	0
16.75	1
17.00	0
17.25	1
17.50	0
17.75	1
18.00	0
18.25	0
18.50	0
18.75	1
19.00	0
19.25	1

19.50	0
19.75	1
20.00	0
20.25	0
20.50	0
20.75	0
21.00	0
21.25	0
21.50	0
21.75	1
22.00	0
22.25	0
22.50	0
22.75	0
23.00	0
23.25	1
23.50	0
23.75	1
24.00	0
24.25	1
24.50	0
24.75	1
25.00	0
25.25	1
25.50	0
25.75	1
26.00	0
26.25	1
26.50	0
26.75	1
27.00	0
27.25	1
27.50	1
27.75	1
28.00	0
28.25	1
28.50	0
28.75	1
29.00	0
29.25	0
29.50	0
29.75	1
30.00	0
30.25	0
30.50	0
30.75	1

N	
0.25	26
0.50	11
0.75	27
1.00	7
1.25	3
1.50	2
1.75	1
2.00	0
2.25	1
2.50	0
2.75	1
3.00	0
3.25	0
3.50	0
3.75	1
4.00	0
4.25	0
4.50	0
4.75	1
5.00	0
5.25	1
5.50	0
5.75	1
6.00	0
6.25	1
6.50	0
6.75	1
7.00	0
7.25	0
7.50	0
7.75	1
8.00	1
8.25	1
8.50	0
8.75	1
9.00	0
9.25	1
9.50	0
9.75	1
10.00	0
10.25	0
10.50	0
10.75	1
11.00	1

11.25	1
11.50	0
11.75	1
12.00	0
12.25	1
12.50	0
12.75	1
13.00	0
13.25	0
13.50	0
13.75	1

K114

S	
0.25	53
0.50	36
0.75	6
1.00	2
1.25	2
1.50	1
1.75	1
2.00	1
2.25	2
2.50	1
2.75	0
3.00	1
3.25	0
3.50	1
3.75	0
4.00	1
4.25	0
4.50	1
4.75	0
5.00	0
5.25	0
5.50	1
5.75	0
6.00	1
6.25	0
6.50	1
6.75	0
7.00	0
7.25	0
7.50	1
7.75	1
8.00	0

8.25	1
8.50	1
8.75	0
9.00	0
9.25	0
9.50	1
9.75	0
10.00	0
10.25	0
10.50	0
10.75	0
11.00	0
11.25	0
11.50	0
11.75	0
12.00	0
12.25	0
12.50	1
12.75	0
13.00	0
13.25	0
13.50	1

N	
0.25	64
0.50	34
0.75	4
1.00	2
1.25	2
1.50	1
1.75	1
2.00	0
2.25	1
2.50	1
2.75	1
3.00	0
3.25	1
3.50	1
3.75	0
4.00	0
4.25	0
4.50	0
4.75	0
5.00	0
5.25	0
5.50	1

5.75	0
6.00	1
6.25	0
6.50	1
6.75	0
7.00	1
7.25	0
7.50	1
7.75	0
8.00	1
8.25	0
8.50	1
8.75	0
9.00	1
9.25	0
9.50	1
9.75	0
10.00	1
10.25	0
10.50	1

K115

S	
0.25	1
0.50	2
0.75	1
1.00	1
1.25	0
1.50	1
1.75	0
2.00	1
2.25	0
2.50	0
2.75	0
3.00	1
3.25	0
3.50	0
3.75	0
4.00	1
4.25	0
4.50	0
4.75	0
5.00	1

N	
0.25	2

0.50	1
0.75	0
1.00	1
1.25	2
1.50	1
1.75	2
2.00	1
2.25	2
2.50	1
2.75	1
3.00	1
3.25	0
3.50	0
3.75	0
4.00	1
4.25	0
4.50	0
4.75	0
5.00	1
5.25	0
5.50	1
5.75	1
6.00	1
6.25	1
6.50	1
6.75	1
7.00	1
7.25	2
7.50	1
7.75	2
8.00	1
8.25	1
8.50	0
8.75	1
9.00	1
9.25	0
9.50	1
9.75	0
10.00	1
10.25	0
10.50	1
10.75	0
11.00	1
11.25	0
11.50	0
11.75	0

12.00	1
12.25	0
12.50	0
12.75	0
13.00	0
13.25	0
13.50	0
13.75	0
14.00	1
14.25	0
14.50	0
14.75	0
15.00	1
15.25	0
15.50	1
15.75	0
16.00	1
16.25	1
16.50	0
16.75	1
17.00	1
17.25	0
17.50	0
17.75	0
18.00	1
18.25	0
18.50	0
18.75	0
19.00	0
19.25	0
19.50	0
19.75	0
20.00	1
20.25	2
20.50	1
20.75	2
21.00	1
21.25	0
21.50	0
21.75	0
22.00	1
22.25	0
22.50	0
22.75	0
23.00	1
23.25	0
23.50	0
23.75	0
24.00	1

K116i

S

0.25	1
0.50	1
0.75	1
1.00	1
1.25	1
1.50	1
1.75	1
2.00	2
2.25	1
2.50	2
2.75	2
3.00	2
3.25	1
3.50	1
3.75	1
4.00	1
4.25	0
4.50	1
4.75	0
5.00	1
5.25	1
5.50	1
5.75	1
6.00	1
6.25	2
6.50	0
6.75	0
7.00	0
7.25	1
7.50	0
7.75	1
8.00	1
8.25	1
8.50	0
8.75	0
9.00	0
9.25	0
9.50	0
9.75	1
10.00	0

10.25	1
10.50	0
10.75	1
11.00	0
11.25	1
11.50	0
11.75	0
12.00	0
12.25	1
12.50	0
12.75	0
13.00	0
13.25	0
13.50	0
13.75	1
14.00	0
14.25	1
14.50	0
14.75	1
15.00	1
15.25	0
15.50	0
15.75	0
16.00	1
16.25	1
16.50	0
16.75	0
17.00	0
17.25	1
17.50	0
17.75	0
18.00	0
18.25	1
18.50	0
18.75	1
19.00	0
19.25	1
19.50	0
19.75	0
20.00	0
20.25	0
20.50	0
20.75	0
21.00	0
21.25	1
21.50	0

21.75	0
22.00	0
22.25	0
22.50	0
22.75	0
23.00	0
23.25	1
23.50	0
23.75	0
24.00	0
24.25	1

N

0.25	1
0.50	2
0.75	1
1.00	1
1.25	0
1.50	0
1.75	0
2.00	1
2.25	0
2.50	0
2.75	0
3.00	1
3.25	1
3.50	1
3.75	1
4.00	1
4.25	0
4.50	1
4.75	1
5.00	1

K116iix

S

0.25	37
0.50	0
0.75	0
1.00	1
1.25	1
1.50	0
1.75	1
2.00	2
2.25	1
2.50	1

2.75	1
3.00	1
3.25	1
3.50	1
3.75	0
4.00	1

N

0.25	39
0.50	4
0.75	0
1.00	1
1.25	1
1.50	1
1.75	0
2.00	0
2.25	0
2.50	1
2.75	0
3.00	1
3.25	0
3.50	1
3.75	0
4.00	0
4.25	0
4.50	1
4.75	0
5.00	0
5.25	0
5.50	0
5.75	0
6.00	0
6.25	0
6.50	0
6.75	0
7.00	0
7.25	0
7.50	1
7.75	0
8.00	0
8.25	0
8.50	1
8.75	0
9.00	0
9.25	0
9.50	1

9.75	0
10.00	0
10.25	0
10.50	0
10.75	0
11.00	0
11.25	0
11.50	1

K116iiy

N

0.25	43
0.50	25
0.75	15
1.00	15
1.25	15
1.50	14
1.75	7
2.00	7
2.25	5
2.50	5
2.75	5
3.00	6
3.25	4
3.50	5
3.75	1
4.00	1
4.25	1
4.50	0
4.75	0
5.00	0
5.25	0
5.50	0
5.75	0
6.00	0
6.25	0
6.50	0
6.75	0
7.00	0
7.25	0
7.50	0
7.75	0
8.00	0
8.25	1
8.50	0
8.75	0

9.00	0
9.25	1
9.50	0
9.75	0
10.00	0
10.25	0
10.50	0
10.75	0
11.00	0
11.25	0
11.50	0
11.75	0
12.00	0
12.25	0
12.50	0
12.75	0
13.00	0
13.25	0
13.50	0
13.75	0
14.00	0
14.25	0
14.50	0
14.75	0
15.00	0
15.25	0

K117A

S

0.25	2
0.50	2
0.75	3
1.00	3
1.25	4
1.50	5
1.75	4
2.00	5
2.25	4
2.50	3
2.75	2
3.00	2
3.25	3
3.50	2
3.75	1
4.00	1
4.25	1

4.50	2
4.75	0
5.00	1
5.25	0
5.50	1
5.75	0
6.00	1
6.25	0
6.50	0
6.75	0
7.00	0
7.25	0
7.50	1
7.75	0
8.00	0
8.25	0
8.50	1
8.75	0
9.00	0
9.25	0
9.50	1
9.75	0
10.00	1
10.25	0
10.50	1
10.75	0
11.00	0
11.25	0
11.50	1
11.75	0
12.00	0
12.25	0
12.50	0
12.75	0
13.00	0
13.25	0
13.50	1
13.75	0
14.00	0
14.25	0
14.50	0
14.75	0
15.00	0
15.25	0
15.50	0
15.75	0

16.00	0
16.25	0
16.50	1
1	10
2	18
3	11
4	7
5	4
6	2
7	1
8	1
9	1
10	2
11	1
12	1
13	0
14	1
15	0
16	0
17	1

N

0.25	2
0.50	2
0.75	2
1.00	2
1.25	1
1.50	1
1.75	3
2.00	2
2.25	3
2.50	2
2.75	3
3.00	2
3.25	2
3.50	2
3.75	2
4.00	1
4.25	1
4.50	1
4.75	2
5.00	1
5.25	2
5.50	1
5.75	1
6.00	1

6.25	1
6.50	0
6.75	1
7.00	1
7.25	1
7.50	1
7.75	1
8.00	0
8.25	0
8.50	0
8.75	1
9.00	0
9.25	1
9.50	0
9.75	1
10.00	1
10.25	1
10.50	1
10.75	1
11.00	0
11.25	1
11.50	0
11.75	1
12.00	1
12.25	1
12.50	1
12.75	2
13.00	1
13.25	1
13.50	2
13.75	0
14.00	1
14.25	0
14.50	1
14.75	0
15.00	1
15.25	0
15.50	0
15.75	0
16.00	1
16.25	0
16.50	1
16.75	0
17.00	1
17.25	1
17.50	1

17.75	0
18.00	1
18.25	1
18.50	1
18.75	0
19.00	1
19.25	0
19.50	1
19.75	0
20.00	1
20.25	0
20.50	1
20.75	0
21.00	0
21.25	0
21.50	1
21.75	0
22.00	0
22.25	0
22.50	0
22.75	0
23.00	0
23.25	0
23.50	0
23.75	0
24.00	0
24.25	0
24.50	0
24.75	0
25.00	1
25.25	1
25.50	1
25.75	0
26.00	0
26.25	0
26.50	0
26.75	0
27.00	0
27.25	0
27.50	1
27.75	0
28.00	0
28.25	0
28.50	1
28.75	0
29.00	1

29.25	0
29.50	1
29.75	0
30.00	1
30.25	0
30.50	1
30.75	0
31.00	0
31.25	0
31.50	0
31.75	0
32.00	0
32.25	0
32.50	1
32.75	0
33.00	0
33.25	0
33.50	1
33.75	0
34.00	0
34.25	0
34.50	1
34.75	0
35.00	0
35.25	0
35.50	1
35.75	0
36.00	0
36.25	0
36.50	1
36.75	0
37.00	1
37.25	0
37.50	1
37.75	0
38.00	1
38.25	0
38.50	1
1	8
2	7
3	10
4	7
5	5
6	5
7	3
8	3

9	1
10	3
11	3
12	3
13	5
14	4
15	3
16	3
17	2
18	3
19	3
20	2
21	1
22	1
23	1
24	2
25	2
26	2
27	0
28	1
29	2
30	2
31	1
32	0
33	1
34	1
35	1
36	1
37	2
38	2
39	1

K117B

S

0.25	53
0.50	29
0.75	22
1.00	16
1.25	15
1.50	7

N

0.25	19
0.50	6
0.75	1
1.00	0

1.25	0
1.50	1
1.75	8
2.00	18
2.25	4
2.50	29
2.75	0
3.00	7
3.25	39
3.50	31
3.75	12
4.00	11
4.25	10
4.50	9
4.75	5
5.00	5
5.25	1
5.50	2

K117AB

S

0.25	55
0.50	31
0.75	26
1.00	19
1.25	18
1.50	12
1.75	5
2.00	4
2.25	4
2.50	3
2.75	2
3.00	2
3.25	3
3.50	2
3.75	1
4.00	1
4.25	1
4.50	2
4.75	0
5.00	1
5.25	0
5.50	1
5.75	0
6.00	1
6.25	0

6.50	1
6.75	0
7.00	0
7.25	0
7.50	1
7.75	0
8.00	0
8.25	0
8.50	1
8.75	0
9.00	0
9.25	0
9.50	1
9.75	0
10.00	1
10.25	0
10.50	1
10.75	0
11.00	0
11.25	0
11.50	1
11.75	0
12.00	0
12.25	0
12.50	0
12.75	0
13.00	0
13.25	0
13.50	1
13.75	0
14.00	0
14.25	0
14.50	0
14.75	0
15.00	0
15.25	0
15.50	0
15.75	0
16.00	0
16.25	0
16.50	1

N

0.25	21
0.50	9
0.75	2

1.00	2
1.25	1
1.50	3
1.75	10
2.00	21
2.25	7
2.50	31
2.75	2
3.00	9
3.25	41
3.50	34
3.75	13
4.00	12
4.25	11
4.50	11
4.75	6
5.00	7
5.25	2
5.50	4
5.75	0
6.00	1
6.25	1
6.50	1
6.75	1
7.00	1
7.25	1
7.50	1
7.75	0
8.00	0
8.25	0
8.50	1
8.75	0
9.00	1
9.25	0
9.50	1
9.75	1
10.00	1
10.25	1
10.50	1
10.75	0
11.00	1
11.25	0
11.50	1
11.75	1
12.00	1
12.25	1

12.50	1
12.75	1
13.00	1
13.25	1
13.50	2
13.75	0
14.00	1
14.25	0
14.50	1
14.75	1
15.00	1
15.25	1
15.50	1
15.75	0
16.00	1
16.25	0
16.50	1
16.75	0
17.00	1
17.25	1
17.50	1
17.75	0
18.00	1
18.25	1
18.50	1
18.75	0
19.00	1
19.25	0
19.50	1
19.75	0
20.00	1
20.25	0
20.50	1
20.75	0
21.00	0
21.25	0
21.50	1
21.75	0
22.00	0
22.25	0
22.50	0
22.75	0
23.00	1
23.25	0
23.50	1
23.75	0

24.00	1
24.25	0
24.50	1
24.75	0
25.00	1
25.25	1
25.50	1
25.75	0
26.00	0
26.25	0
26.50	0
26.75	0
27.00	0
27.25	0
27.50	1
27.75	0
28.00	0
28.25	0
28.50	1
28.75	0
29.00	1
29.25	0
29.50	1
29.75	0
30.00	1
30.25	0
30.50	1
30.75	0
31.00	0
31.25	0
31.50	0
31.75	0
32.00	0
32.25	0
32.50	1
32.75	0
33.00	0
33.25	0
33.50	1
33.75	0
34.00	0
34.25	0
34.50	1
34.75	0
35.00	0
35.25	0

35.50	1
35.75	0
36.00	0
36.25	0
36.50	1
36.75	0
37.00	1
37.25	0
37.50	1
37.75	0
38.00	1
38.25	0
38.50	1

K118i

S	
0.25	66
0.50	22
0.75	13
1.00	12
1.25	12
1.50	9
1.75	9
2.00	9
2.25	8
2.50	8
2.75	9
3.00	5
3.25	5
3.50	5
3.75	5
4.00	4
4.25	2
4.50	3
4.75	3
5.00	3
5.25	3
5.50	3
5.75	3
6.00	3
6.25	3
6.50	3
6.75	3

7.00	3
7.25	3
7.50	3
7.75	3
8.00	2
8.25	2
8.50	2
8.75	2
9.00	2
9.25	1
9.50	2
9.75	1
10.00	1
10.25	2
10.50	1
10.75	1
11.00	1
11.25	2
11.50	1
11.75	1
12.00	2
12.25	1
12.50	2
12.75	1
13.00	3
13.25	3
13.50	3
13.75	3
14.00	2
14.25	2
14.50	1
14.75	2
15.00	2
15.25	2
15.50	2
15.75	2
16.00	2
16.25	2
16.50	2
16.75	2
17.00	2

17.25	2
17.50	1
17.75	2
18.00	2
18.25	1
18.50	2
18.75	1
19.00	1
19.25	2
19.50	1
19.75	1
20.00	2
20.25	1
20.50	2
20.75	1
21.00	2
21.25	2
21.50	2
21.75	2
22.00	1
22.25	2
22.50	1
22.75	1
23.00	1
23.25	2
23.50	1
23.75	1
24.00	2
24.25	1
24.50	2
24.75	1
25.00	1
25.25	1
25.50	1
25.75	0
26.00	1
26.25	2
26.50	1
26.75	1
27.00	1
27.25	1

27.50	1
27.75	0
28.00	1

N	
0.25	85
0.50	35
0.75	34
1.00	33
1.25	20
1.50	12
1.75	8
2.00	5
2.25	5
2.50	5
2.75	4
3.00	4
3.25	5
3.50	4
3.75	2
4.00	2
4.25	1
4.50	2
4.75	1
5.00	2
5.25	1
5.50	1
5.75	1
6.00	2
6.25	1
6.50	1
6.75	1
7.00	2
7.25	1
7.50	1
7.75	1
8.00	1
8.25	0
8.50	1
8.75	1

K118ii

S	
0.25	52
0.50	6
0.75	5

1.00	5
1.25	2
1.50	1
1.75	1
2.00	1
2.25	1
2.50	1
2.75	1
3.00	1
3.25	1
3.50	1
3.75	1
4.00	1
4.25	1
4.50	0
4.75	1
5.00	1
5.25	1
5.50	0
5.75	1
6.00	1
6.25	1
6.50	1
6.75	1
7.00	1
7.25	1
7.50	0
7.75	1

N	
0.25	50
0.50	23
0.75	27
1.00	26
1.25	18
1.50	17
1.75	9
2.00	10
2.25	8
2.50	8
2.75	5
3.00	5
3.25	5
3.50	6
3.75	3
4.00	3

4.25	3
4.50	3
4.75	2
5.00	2
5.25	2
5.50	3
5.75	2
6.00	2
6.25	2
6.50	2
6.75	2
7.00	3
7.25	2
7.50	3
7.75	2
8.00	2
8.25	2
8.50	2
8.75	1
9.00	2
9.25	2
9.50	2
9.75	1
10.00	2
10.25	2
10.50	2

K119

S	
0.25	37
0.50	44
0.75	30
1.00	16
1.25	10
1.50	6
1.75	7
2.00	4
2.25	4
2.50	1
2.75	2
3.00	1
3.25	2
3.50	1
3.75	2
4.00	1
4.25	2

4.50	1
4.75	1
5.00	1
5.25	1
5.50	0
5.75	0
6.00	0
6.25	0
6.50	0
6.75	0
7.00	0
7.25	0
7.50	0
7.75	0
8.00	0
8.25	1
8.50	2
8.75	2
9.00	2
9.25	2
9.50	1
9.75	2
10.00	2
10.25	2

N	
0.25	55
0.50	32
0.75	23
1.00	10
1.25	9
1.50	4
1.75	4
2.00	7
2.25	6
2.50	6
2.75	6
3.00	2
3.25	2
3.50	2
3.75	2
4.00	2
4.25	1
4.50	1
4.75	1
5.00	1

5.25	1
5.50	1
5.75	1
6.00	0
6.25	1
6.50	0
6.75	1
7.00	1
7.25	1
7.50	1
7.75	1
8.00	1
8.25	1
8.50	1
8.75	2
9.00	1
9.25	1
9.50	1
9.75	1
10.00	0
10.25	1
10.50	0
10.75	1
11.00	0
11.25	1
11.50	1
11.75	1
12.00	1
12.25	1
12.50	1
12.75	1
13.00	0
13.25	1
13.50	1
13.75	0
14.00	1
14.25	1
14.50	1
14.75	1
15.00	1
15.25	1
15.50	1
15.75	1
16.00	2
16.25	1
16.50	1

16.75	1

K126

S	
0.25	70
0.50	51
0.75	26
1.00	3
1.25	2
1.50	1
1.75	1
2.00	1
2.25	1
2.50	1
2.75	1
3.00	0
3.25	2
3.50	1
3.75	1
4.00	1
4.25	1
4.50	0
4.75	1
5.00	0
5.25	1
5.50	1
5.75	1
6.00	0
6.25	1
6.50	1
6.75	1
7.00	0
7.25	1
7.50	0
7.75	0
8.00	0
8.25	1
8.50	0
8.75	1
9.00	0
9.25	1
9.50	1
9.75	1
10.00	0
10.25	1
10.50	1

10.75	1
11.00	0
11.25	1
11.50	0
11.75	0
12.00	0
12.25	1
12.50	0
12.75	1
13.00	0
13.25	1
13.50	1
13.75	1
14.00	0
14.25	1
14.50	1
14.75	1
15.00	1
15.25	1
15.50	0
15.75	1
16.00	0
16.25	1
16.50	0
16.75	1
17.00	0
17.25	2
17.50	1
17.75	1
18.00	1
18.25	1
18.50	0
18.75	1
19.00	0
19.25	1
19.50	0
19.75	0
20.00	0
20.25	1
20.50	0
20.75	0
21.00	0
21.25	1
21.50	0
21.75	1
22.00	0

22.25	1
22.50	0
22.75	1
23.00	0
23.25	1
23.50	0
23.75	1
24.00	0
24.25	1
24.50	1
24.75	1
25.00	0
25.25	1

N	
0.25	81
0.50	54
0.75	22
1.00	2
1.25	2
1.50	2
1.75	2
2.00	1
2.25	1
2.50	1
2.75	1
3.00	1
3.25	1
3.50	1
3.75	1
4.00	1
4.25	1
4.50	1
4.75	1
5.00	1
5.25	1
5.50	1
5.75	1
6.00	1
6.25	1
6.50	1
6.75	1
7.00	1
7.25	1
7.50	1
7.75	1

8.00	0
8.25	1
8.50	1
8.75	1
9.00	0
9.25	1
9.50	0
9.75	1
10.00	0
10.25	1
10.50	1
10.75	1
11.00	1
11.25	2
11.50	1
11.75	1
12.00	2
12.25	0
12.50	1
12.75	0
13.00	1
13.25	0
13.50	1
13.75	1
14.00	0
14.25	1
14.50	1
14.75	1
15.00	1
15.25	1
15.50	1
15.75	1
16.00	0
16.25	1
16.50	1
16.75	1
17.00	1

K127

S	
1	140*
2	110*
3	95
4	98
5	60
6	50*

7	45*
8	33
9	34
10	32
11	37
12	40
13	34
14	40
15	31
16	22
17	25
18	35
19	32
20	28
21	15
22	12
23	8
24	8
25	6
26	7
27	6
28	4
29	8
30	4
31	6
32	9
33	7
34	5
35	6
36	5
37	6
38	6
39	5
40	5
41	4
42	6
43	5
44	5
45	5
46	6
47	6
48	5
49	5
50	5
51	5
52	5

N	
1	7
2	9
3	7
4	9
5	4
6	104
7	71
8	47
9	42
10	30
11	23
12	28
13	20
14	19
15	14
16	17
17	19
18	13
19	17
20	10
21	9
22	5
23	5
24	5
25	5
26	4
27	6
28	3
29	4
30	7
31	5
32	5
33	6
34	4
35	4
36	5
37	4
38	4

K132i

S	
0.25	59
0.50	56
0.75	46

1.00	18
1.25	18
1.50	5
1.75	5
2.00	3
2.25	3
2.50	2
2.75	2
3.00	2
3.25	3
3.50	1
3.75	1
4.00	1
4.25	1
4.50	2
4.75	2
5.00	2
5.25	2
5.50	1
5.75	1
6.00	1
6.25	1
6.50	2
6.75	3
7.00	2
7.25	3
7.50	0
7.75	1
8.00	0
8.25	1
8.50	1
8.75	2
9.00	2
9.25	2
9.50	0
9.75	1
10.00	1
10.25	1
10.50	1
10.75	2
11.00	1
11.25	2
11.50	2
11.75	2
12.00	2
12.25	2

12.50	1
12.75	1
13.00	1
13.25	2
13.50	0
13.75	1
14.00	1
14.25	1
14.50	0
14.75	1
15.00	1
15.25	1
15.50	1
15.75	1
16.00	1
16.25	2
16.50	1
16.75	1
17.00	1
17.25	2
17.50	1
17.75	1
18.00	1
18.25	1
18.50	0
18.75	1
19.00	0
19.25	1
19.50	1
19.75	1
20.00	1
20.25	2
20.50	0
20.75	1
21.00	1
21.25	1
21.50	0
21.75	1
22.00	1
22.25	1
22.50	1
22.75	1
23.00	1
23.25	1
23.50	1
23.75	2

24.00	1
24.25	2
24.50	1
24.75	1
25.00	1
25.25	2
25.50	1
25.75	1
26.00	1
26.25	2
26.50	1
26.75	1
27.00	1
27.25	2
27.50	2
27.75	2
28.00	2
28.25	2
28.50	1
28.75	1
29.00	1
29.25	1
29.50	1
29.75	1
30.00	1
30.25	1
30.50	0
30.75	1
31.00	1
31.25	1
31.50	1
31.75	2
32.00	1
32.25	2
32.50	0
32.75	1
33.00	1
33.25	1
33.50	1
33.75	1
34.00	1
34.25	2
34.50	1
34.75	1
35.00	1
35.25	1

N	
0.25	54
0.50	53
0.75	25
1.00	24
1.25	13
1.50	12
1.75	8
2.00	8
2.25	3
2.50	2
2.75	3
3.00	2
3.25	1

K132ii

S	
0.25	56
0.50	52
0.75	37
1.00	17
1.25	12
1.50	6
1.75	3
2.00	3
2.25	3
2.50	1

N	
0.25	4
0.50	4
0.75	3
1.00	4
1.25	1
1.50	1
1.75	1
2.00	2
2.25	2
2.50	2
2.75	2
3.00	2
3.25	0
3.50	1
3.75	1
4.00	1

4.25	1
4.50	1
4.75	2
5.00	1
5.25	1
5.50	1
5.75	1
6.00	0
6.25	1
6.50	0
6.75	1
7.00	0
7.25	2
7.50	1
7.75	2
8.00	1
8.25	2
8.50	2
8.75	1
9.00	2

K134

S	
0.25	71
0.50	50
0.75	37
1.00	30
1.25	20
1.50	21
1.75	3
2.00	4
2.25	1
2.50	2
2.75	2
3.00	2
3.25	1
3.50	2
3.75	1
4.00	2
4.25	1
4.50	2
4.75	1
5.00	2
5.25	0
5.50	1
5.75	1

6.00	1
6.25	1
6.50	1
6.75	1
7.00	1
7.25	0
7.50	1
7.75	1
8.00	1
8.25	1
8.50	1
8.75	1
9.00	1
9.25	0
9.50	1
9.75	0
10.00	1

N	
0.25	76
0.50	64
0.75	54
1.00	40
1.25	34
1.50	12
1.75	10
2.00	1
2.25	2
2.50	1
2.75	2
3.00	0
3.25	1
3.50	1
3.75	2
4.00	1
4.25	2
4.50	0
4.75	1
5.00	1
5.25	1
5.50	0
5.75	1
6.00	1
6.25	1
6.50	0
6.75	1

7.00	0
7.25	1
7.50	0
7.75	1
8.00	1
8.25	1
8.50	1
8.75	1
9.00	2
9.25	1
9.50	0
9.75	1
10.00	0
10.25	1

K136

S	
0.25	81
0.50	64
0.75	46
1.00	22
1.25	6
1.50	1
1.75	0
2.00	1
2.25	0
2.50	1
2.75	0
3.00	1
3.25	0
3.50	1
3.75	1
4.00	1
4.25	1
4.50	1
4.75	1
5.00	1
5.25	1
5.50	1
5.75	0
6.00	1
6.25	0
6.50	1
6.75	1
7.00	1
7.25	0

7.50	1
7.75	0
8.00	1
8.25	1
8.50	0
8.75	1
9.00	1
9.25	0
9.50	1
9.75	0
10.00	1
10.25	0
10.50	1
10.75	0
11.00	1
11.25	0
11.50	1
11.75	1
12.00	1
12.25	1
12.50	1
12.75	0
13.00	0
13.25	0
13.50	1
13.75	1
14.00	1
14.25	0
14.50	1
14.75	1
15.00	1
15.25	0
15.50	1
15.75	1
16.00	1
16.25	0
16.50	1
16.75	1
17.00	1
17.25	0
17.50	2
17.75	1
18.00	1
18.25	2
18.50	1
18.75	1

19.00	1
19.25	1
19.50	0
19.75	1
20.00	0
20.25	1

N	
0.25	82
0.50	69
0.75	43
1.00	25
1.25	5
1.50	2
1.75	1
2.00	1
2.25	1
2.50	1
2.75	1
3.00	1
3.25	0
3.50	1
3.75	0
4.00	0
4.25	0
4.50	1
4.75	1
5.00	1
5.25	0
5.50	1
5.75	0
6.00	1
6.25	0
6.50	1
6.75	1
7.00	1
7.25	0
7.50	1
7.75	1
8.00	2
8.25	1
8.50	0
8.75	1
9.00	1
9.25	0
9.50	1

9.75	0
10.00	1
10.25	0
10.50	1
10.75	0
11.00	0
11.25	0
11.50	0
11.75	0
12.00	1
12.25	0
12.50	1
12.75	0
13.00	0
13.25	0
13.50	1
13.75	1
14.00	1
14.25	0
14.50	1
14.75	0
15.00	1
15.25	0
15.50	1
15.75	0
16.00	0
16.25	0
16.50	1
16.75	1
17.00	1
17.25	1
17.50	0
17.75	0
18.00	0
18.25	1

K138

S	
0.25	31
0.50	9
0.75	7
1.00	5
1.25	4
1.50	4
1.75	4
2.00	3

2.25	4
2.50	3
2.75	2
3.00	1
3.25	0
3.50	1
3.75	1
4.00	2
4.25	1
4.50	1
4.75	1
5.00	2
5.25	1
5.50	1
5.75	1
6.00	1
6.25	1
6.50	1
6.75	1
7.00	1
7.25	1
7.50	1
7.75	1
8.00	2
8.25	1
8.50	1
8.75	1
9.00	1
9.25	1
9.50	2
9.75	1
10.00	2
10.25	1
10.50	1
10.75	2
11.00	1
11.25	1
11.50	1
11.75	1
12.00	1
12.25	1
12.50	1
12.75	1
13.00	1
13.25	1
13.50	1
13.75	1
14.00	2
14.25	1
14.50	2
14.75	1
15.00	2
15.25	1
15.50	2
15.75	2
16.00	2
16.25	1
16.50	2
16.75	1
17.00	2
17.25	1
17.50	2
17.75	1
18.00	2
18.25	1
18.50	1
18.75	1
19.00	1
19.25	0
19.50	1
19.75	0

20.00	1

K147

S	
0.25	17
0.50	5
0.75	5
1.00	4
1.25	4
1.50	3
1.75	3
2.00	3
2.25	2
2.50	3
2.75	2
3.00	2
3.25	1
3.50	1
3.75	1
4.00	1
4.25	2
4.50	1
4.75	1
5.00	1
5.25	2
5.50	3
5.75	2
6.00	2
6.25	1
6.50	2
6.75	1
7.00	2
7.25	0
7.50	1
7.75	1
8.00	1
8.25	1
8.50	2
8.75	1
9.00	2
9.25	2
9.50	2
9.75	1
10.00	2
10.25	1
10.50	1

N	
0.25	34
0.50	12
0.75	8
1.00	8
1.25	3
1.50	4
1.75	1
2.00	1
2.25	2
2.50	3
2.75	2
3.00	2
3.25	1
3.50	2
3.75	2
4.00	2
4.25	0
4.50	1
4.75	1
5.00	1
5.25	0
5.50	1
5.75	1
6.00	1
6.25	0
6.50	1
6.75	1
7.00	1
7.25	1
7.50	1
7.75	1
8.00	1
8.25	1

8.50	1
8.75	1
9.00	1
9.25	1
9.50	2
9.75	1
10.00	2
10.25	1
10.50	2
10.75	2
11.00	2
11.25	1
11.50	1
11.75	1
12.00	1
12.25	1
12.50	1
12.75	1
13.00	1
13.25	1
13.50	1
13.75	1
14.00	2
14.25	1
14.50	2
14.75	1
15.00	2
15.25	1
15.50	2
15.75	2
16.00	2
16.25	1
16.50	2
16.75	1
17.00	2
17.25	1
17.50	2
17.75	1
18.00	2
18.25	1
18.50	1
18.75	1
19.00	1
19.25	0
19.50	1
19.75	0

10.75	2
11.00	1
11.25	1
11.50	1
11.75	1
12.00	1
12.25	0
12.50	1
12.75	0
13.00	1
13.25	1
13.50	1
13.75	2
14.00	1

N	
0.25	10
0.50	7
0.75	6
1.00	2
1.25	2
1.50	1
1.75	2
2.00	1
2.25	1
2.50	0
2.75	1
3.00	0
3.25	1
3.50	1
3.75	1
4.00	1
4.25	1
4.50	0
4.75	1
5.00	0
5.25	1
5.50	1
5.75	0
6.00	1
6.25	1
6.50	1
6.75	0
7.00	1
7.25	1
7.50	1

7.75	0
8.00	1
8.25	1
8.50	1
8.75	2
9.00	1
9.25	1
9.50	2
9.75	1
10.00	2
10.25	1

K148

S	
0.25	38
0.50	0
0.75	0
1.00	0
1.25	1
1.50	0
1.75	0
2.00	0
2.25	1
2.50	1
2.75	0
3.00	1
3.25	1
3.50	1
3.75	0
4.00	1
4.25	1
4.50	1
4.75	0
5.00	1
5.25	1

N	
0.25	43
0.50	2
0.75	2
1.00	1
1.25	2
1.50	0
1.75	1
2.00	0
2.25	1

2.50	1
2.75	1
3.00	1
3.25	1
3.50	2
3.75	1
4.00	2
4.25	1
4.50	0
4.75	1
5.00	0
5.25	1

K155b

S	
0.25	83
0.50	17
0.75	25
1.00	16
1.25	18
1.50	4
1.75	7
2.00	4
2.25	4
2.50	5
2.75	2
3.00	3
3.25	3
3.50	3
3.75	2
4.00	3
4.25	2
4.50	0
4.75	1
5.00	1
5.25	2
5.50	1
5.75	1
6.00	1
6.25	0
6.50	0
6.75	1
7.00	1
7.25	1
7.50	2
7.75	1

8.00	2

N	
0.25	41
0.50	29
0.75	10
1.00	9
1.25	11
1.50	7
1.75	8
2.00	9
2.25	6
2.50	7
2.75	5
3.00	5
3.25	5
3.50	6
3.75	3
4.00	3
4.25	1
4.50	2
4.75	3
5.00	1
5.25	1
5.50	2
5.75	1
6.00	1
6.25	2
6.50	3
6.75	1
7.00	1
7.25	1
7.50	2
7.75	2
8.00	2
8.25	1
8.50	2
8.75	1
9.00	1
9.25	1
9.50	1
9.75	0
10.00	1
10.25	0
10.50	1
10.75	1

11.00	0
11.25	0
11.50	1
11.75	0
12.00	1
12.25	1
12.50	2
12.75	1
13.00	0
13.25	1
13.50	0
13.75	1
14.00	0
14.25	0
14.50	1
14.75	1
15.00	1
15.25	2
15.50	3
15.75	1
16.00	1
16.25	1
16.50	1
16.75	1
17.00	1
17.25	1

K157a

S	
0.25	66
0.50	32
0.75	8
1.00	6
1.25	5
1.50	6
1.75	6
2.00	6
2.25	5
2.50	5
2.75	2
3.00	3
3.25	2
3.50	3
3.75	4
4.00	5
4.25	4

4.50	5
4.75	3
5.00	3
5.25	3
5.50	4
5.75	3
6.00	4
6.25	3
6.50	4
6.75	2
7.00	3
7.25	3
7.50	3
7.75	2
8.00	3
8.25	2
8.50	3
8.75	2
9.00	3
9.25	2
9.50	3
9.75	2
10.00	2
10.25	2
10.50	2
10.75	2
11.00	3
11.25	3
11.50	3
11.75	3
12.00	3
12.25	3
12.50	3
12.75	3

N	
0.25	60
0.50	41
0.75	16
1.00	2
1.25	2
1.50	2
1.75	2
2.00	4
2.25	3
2.50	3

2.75	2
3.00	4
3.25	4
3.50	1
3.75	1
4.00	3
4.25	3
4.50	3
4.75	2
5.00	3
5.25	3
5.50	3
5.75	3
6.00	1
6.25	1
6.50	2
6.75	1
7.00	2
7.25	2
7.50	2
7.75	2
8.00	2
8.25	1
8.50	2
8.75	2
9.00	2
9.25	3
9.50	3
9.75	2
10.00	3
10.25	2
10.50	3
10.75	2
11.00	1

K176

S	
0.25	55
0.50	40
0.75	42
1.00	25
1.25	15
1.50	3
1.75	3
2.00	0
2.25	1

2.50	0
2.75	1
3.00	0
3.25	1
3.50	0
3.75	1
4.00	1
4.25	2
4.50	2
4.75	2
5.00	1
5.25	2
5.50	1
5.75	1
6.00	2
6.25	1
6.50	1
6.75	1
7.00	0
7.25	1
7.50	1
7.75	1
8.00	0
8.25	1
8.50	1
8.75	1
9.00	1
9.25	1
9.50	1
9.75	0

N	
0.25	46
0.50	34
0.75	24
1.00	23
1.25	16
1.50	2
1.75	2
2.00	1
2.25	1
2.50	1
2.75	1
3.00	0
3.25	1
3.50	1

3.75	0
4.00	2
4.25	1
4.50	1
4.75	1
5.00	0
5.25	0
5.50	0
5.75	1
6.00	0
6.25	1
6.50	1
6.75	1
7.00	0
7.25	1
7.50	1
7.75	1
8.00	0
8.25	1
8.50	1
8.75	1
9.00	1
9.25	1
9.50	1
9.75	2
10.00	1
10.25	1
10.50	1
10.75	1
11.00	1
11.25	1
11.50	1
11.75	1
12.00	1
12.25	1
12.50	1
12.75	1
13.00	0
13.25	1
13.50	1
13.75	1
14.00	1
14.25	1
14.50	1
14.75	1

K178

S	
0.25	49
0.50	38
0.75	30
1.00	23
1.25	12
1.50	5
1.75	5
2.00	3
2.25	4
2.50	2
2.75	2
3.00	2
3.25	2
3.50	2
3.75	2
4.00	3
4.25	3
4.50	3
4.75	3
5.00	2
5.25	3
5.50	3
5.75	4
6.00	2
6.25	3
6.50	2
6.75	2
7.00	1
7.25	2
7.50	1
7.75	2
8.00	1
8.25	1
8.50	1
8.75	1
9.00	1
9.25	1
9.50	1
9.75	2
10.00	1
10.25	1
10.50	1
10.75	2

11.00	1
11.25	1
11.50	1
11.75	2
12.00	1
12.25	1
12.50	1
12.75	1
13.00	0
13.25	1
13.50	0
13.75	1
14.00	1
14.25	2
14.50	1
14.75	1
15.00	2
15.25	2
15.50	2
15.75	1
16.00	1
16.25	1
16.50	2
16.75	0
17.00	1
17.25	1
17.50	1
17.75	1
18.00	1
18.25	1
18.50	1
18.75	1
19.00	1
19.25	1
19.50	2

K180

S	
0.25	77
0.50	12
0.75	3
1.00	2
1.25	1
1.50	0
1.75	1
2.00	1
2.25	1
2.50	0
2.75	2
3.00	1
3.25	1
3.50	1
3.75	1
4.00	1
4.25	1
4.50	1
4.75	1
5.00	1
5.25	1
5.50	0
5.75	2
6.00	1
6.25	1

6.50	1
6.75	1
7.00	1
7.25	1
7.50	0
7.75	1
8.00	1
8.25	1
8.50	0
8.75	1
9.00	1
9.25	1
9.50	0
9.75	2
10.00	1
10.25	1
10.50	2
10.75	1
11.00	1
11.25	1
11.50	1
11.75	1
12.00	1
12.25	1
12.50	1
12.75	0
13.00	1
13.25	0
13.50	1
13.75	0
14.00	1
14.25	0
14.50	1
14.75	1
15.00	1
15.25	1
15.50	0
15.75	2
16.00	1
16.25	1
16.50	2
16.75	1
17.00	1
17.25	1
17.50	2
17.75	0

18.00	1
18.25	1
18.50	1
18.75	1
19.00	1
19.25	1
19.50	1

N	
0.25	55
0.50	6
0.75	1
1.00	1
1.25	1
1.50	1
1.75	1
2.00	0
2.25	0
2.50	0
2.75	1
3.00	0
3.25	0
3.50	0
3.75	0
4.00	0
4.25	0
4.50	0
4.75	1
5.00	0
5.25	1
5.50	0
5.75	2
6.00	1
6.25	1
6.50	1
6.75	1
7.00	1
7.25	1
7.50	0
7.75	1
8.00	1
8.25	1
8.50	0
8.75	1
9.00	1
9.25	1

9.50	0
9.75	1
10.00	1
10.25	1
10.50	0
10.75	1
11.00	0
11.25	0
11.50	0
11.75	1
12.00	0
12.25	0
12.50	0
12.75	1
13.00	1
13.25	1
13.50	1
13.75	1
14.00	0
14.25	1
14.50	0
14.75	1
15.00	1
15.25	1
15.50	1
15.75	1
16.00	1
16.25	1
16.50	0
16.75	1
17.00	1
17.25	1
17.50	0
17.75	1
18.00	1
18.25	1
18.50	0
18.75	1

WC25a

SE	
0.25	14
0.50	8
0.75	7
1.00	4
1.25	1

1.50	2	2.75	5	14.25	3	3.75	5	15.25	0	26.75	0	38.25	1	2.50	7	14.00	1	25.50	2	37.00	0	48.50	0	7.00	27	18.50	25	30.00	9	41.50	0
1.75	3	3.00	10	14.50	3	4.00	6	15.50	1	27.00	1	38.50	0	2.75	9	14.25	2	25.75	1	37.25	0	48.75	0	7.25	21	18.75	24	30.25	8	41.75	2
2.00	2	3.25	3	14.75	1	4.25	7	15.75	1	27.25	0	38.75	1	3.00	9	14.50	0	26.00	1	37.50	1	49.00	0	7.50	23	19.00	22	30.50	5	42.00	2
2.25	2	3.50	5	15.00	0	4.50	9	16.00	0	27.50	0	39.00	0	3.25	7	14.75	1	26.25	0	37.75	1	49.25	0	7.75	25	19.25	22	30.75	6	42.25	1
2.50	7	3.75	6	15.25	1	4.75	8	16.25	0	27.75	0	39.25	0	3.50	15	15.00	0	26.50	0	38.00	0	49.50	0	8.00	28	19.50	21	31.00	5	42.50	1
2.75	3	4.00	3	15.50	0	5.00	9	16.50	0	28.00	1	39.50	1	3.75	9	15.25	0	26.75	0	38.25	0	49.75	0	8.25	28	19.75	19	31.25	6	42.75	1
3.00	5	4.25	6	15.75	0	5.25	9	16.75	0	28.25	1	39.75	0	4.00	9	15.50	0	27.00	0	38.50	0	50.00	1	8.50	27	20.00	21	31.50	7	43.00	0
3.25	3	4.50	11	16.00	0	5.50	7	17.00	0	28.50	0	40.00	1	4.25	9	15.75	1	27.25	0	38.75	0	50.25	0	8.75	31	20.25	23	31.75	9	43.25	1
3.50	1	4.75	6	16.25	0	5.75	3	17.25	0	28.75	1	40.25	0	4.50	6	16.00	0	27.50	0	39.00	0	50.50	0	9.00	34	20.50	22	32.00	10	43.50	1
3.75	5	5.00	2	16.50	0	6.00	3	17.50	0	29.00	0	40.50	0	4.75	5	16.25	1	27.75	0	39.25	0	50.75	0	9.25	33	20.75	22	32.25	9	43.75	1
4.00	1	5.25	5	16.75	0	6.25	3	17.75	0	29.25	1	40.75	1	5.00	1	16.50	2	28.00	0	39.50	1	51.00	0	9.50	37	21.00	20	32.50	10	44.00	2
4.25	2	5.50	1	17.00	4	6.50	3	18.00	0	29.50	1	41.00	0	5.25	5	16.75	0	28.25	1	39.75	1	51.25	0	9.75	40	21.25	27	32.75	8	44.25	1
4.50	2	5.75	3	17.25	1	6.75	3	18.25	0	29.75	1	41.25	0	5.50	3	17.00	0	28.50	1	40.00	0	51.50	1	10.00	44	21.50	28	33.00	9	44.50	0
4.75	2	6.00	2	17.50	0	7.00	6	18.50	1	30.00	1	41.50	1	5.75	4	17.25	0	28.75	0	40.25	0	51.75	0	10.25	45	21.75	32	33.25	4	44.75	1
5.00	0	6.25	2	17.75	0	7.25	0	18.75	1	30.25	2	41.75	1	6.00	1	17.50	0	29.00	0	40.50	0	52.00	2	10.50	40	22.00	22	33.50	4	45.00	2
5.25	1	6.50	1	18.00	2	7.50	2	19.00	1	30.50	1	42.00	0	6.25	1	17.75	1	29.25	0	40.75	0	52.25	2	10.75	50	22.25	19	33.75	4	45.25	0
5.50	3	6.75	3	18.25	0	7.75	4	19.25	0	30.75	1	42.25	0	6.50	0	18.00	1	29.50	0	41.00	0			11.00	56	22.50	17	34.00	5	45.50	1
5.75	4	7.00	1	18.50	1	8.00	6	19.50	0	31.00	0	42.50	0	6.75	0	18.25	0	29.75	0	41.25	0	**WC33a**		11.25	50	22.75	18	34.25	5	45.75	2
6.00	0	7.25	2	18.75	1	8.25	5	19.75	0	31.25	1	42.75	0	7.00	1	18.50	1	30.00	0	41.50	0	***SE***		11.50	48	23.00	20	34.50	5	46.00	2
6.25	2	7.50	0	19.00	0	8.50	2	20.00	0	31.50	1	43.00	0	7.25	1	18.75	1	30.25	0	41.75	0	0.25	19	11.75	46	23.25	20	34.75	4	46.25	1
6.50	0	7.75	2	19.25	2	8.75	4	20.25	0	31.75	1	43.25	0	7.50	0	19.00	1	30.50	1	42.00	0	0.50	22	12.00	46	23.50	19	35.00	5	46.50	0
6.75	0	8.00	2	19.50	2	9.00	2	20.50	1	32.00	0	43.50	0	7.75	3	19.25	1	30.75	1	42.25	0	0.75	22	12.25	46	23.75	18	35.25	3	46.75	1
7.00	0	8.25	3	19.75	2	9.25	4	20.75	1	32.25	0	43.75	1	8.00	0	19.50	1	31.00	0	42.50	0	1.00	21	12.50	43	24.00	17	35.50	3	47.00	2
7.25	1	8.50	1	20.00	0	9.50	3	21.00	1	32.50	0	44.00	0	8.25	0	19.75	0	31.25	0	42.75	0	1.25	18	12.75	45	24.25	17	35.75	5	47.25	0
7.50	0	8.75	2	20.25	1	9.75	4	21.25	1	32.75	0	44.25	0	8.50	1	20.00	1	31.50	0	43.00	0	1.50	19	13.00	45	24.50	15	36.00	3	47.50	1
7.75	1	9.00	3	20.50	2	10.00	2	21.50	1	33.00	0	44.50	1	8.75	0	20.25	0	31.75	0	43.25	0	1.75	22	13.25	48	24.75	15	36.25	3	47.75	1
8.00	0	9.25	1	20.75	2	10.25	1	21.75	1	33.25	0	44.75	0	9.00	1	20.50	1	32.00	1	43.50	0	2.00	30	13.50	48	25.00	14	36.50	2	48.00	1
8.25	1	9.50	1	21.00	2	10.50	0	22.00	0	33.50	1	45.00	1	9.25	0	20.75	0	32.25	0	43.75	0	2.25	32	13.75	50	25.25	15	36.75	5	48.25	0
8.50	0	9.75	1	21.25	4	10.75	1	22.25	0	33.75	0	45.25	1	9.50	1	21.00	1	32.50	1	44.00	0	2.50	30	14.00	44	25.50	15	37.00	7	48.50	0
8.75	0	10.00	2			11.00	1	22.50	0	34.00	0	45.50	0	9.75	1	21.25	1	32.75	0	44.25	0	2.75	35	14.25	44	25.75	15	37.25	3	48.75	1
9.00	0	10.25	0	**WC25c**		11.25	2	22.75	1	34.25	0	45.75	2	10.00	1	21.50	0	33.00	0	44.50	0	3.00	37	14.50	42	26.00	10	37.50	2	49.00	2
9.25	0	10.50	0	***SE***		11.50	0	23.00	1	34.50	0	46.00	1	10.25	2	21.75	3	33.25	1	44.75	0	3.25	25	14.75	43	26.25	9	37.75	2	49.25	1
9.50	0	10.75	1	0.25	6	11.75	1	23.25	0	34.75	0	46.25	0	10.50	4	22.00	0	33.50	0	45.00	0	3.50	26	15.00	41	26.50	8	38.00	3	49.50	1
9.75	1	11.00	1	0.50	3	12.00	0	23.50	0	35.00	1	46.50	0	10.75	0	22.25	1	33.75	1	45.25	0	3.75	30	15.25	37	26.75	10	38.25	2	49.75	0
		11.25	0	0.75	2	12.25	0	23.75	0	35.25	0	46.75	1	11.00	1	22.50	0	34.00	0	45.50	1	4.00	33	15.50	36	27.00	11	38.50	5	50.00	4
NW		11.50	0	1.00	5	12.50	1	24.00	0	35.50	0			11.25	0	22.75	0	34.25	0	45.75	0	4.25	31	15.75	35	27.25	12	38.75	5	50.25	4
0.25	7	11.75	0	1.25	5	12.75	0	24.25	0	35.75	0	***NW***		11.50	1	23.00	0	34.50	0	46.00	0	4.50	25	16.00	30	27.50	13	39.00	5	50.50	3
0.50	17	12.00	0	1.50	7	13.00	0	24.50	0	36.00	0	0.25	25	11.75	0	23.25	0	34.75	1	46.25	0	4.75	25	16.25	27	27.75	13	39.25	3	50.75	2
0.75	8	12.25	0	1.75	16	13.25	0	24.75	0	36.25	0	0.50	18	12.00	2	23.50	0	35.00	0	46.50	1	5.00	24	16.50	21	28.00	12	39.50	5	51.00	2
1.00	4	12.50	0	2.00	12	13.50	1	25.00	1	36.50	0	0.75	19	12.25	1	23.75	0	35.25	0	46.75	0	5.25	23	16.75	23	28.25	11	39.75	5	51.25	0
1.25	3	12.75	1	2.25	7	13.75	0	25.25	1	36.75	0	1.00	18	12.50	2	24.00	0	35.50	0	47.00	0	5.50	24	17.00	25	28.50	12	40.00	2	51.50	0
1.50	6	13.00	0	2.50	10	14.00	0	25.50	0	37.00	0	1.25	15	12.75	1	24.25	1	35.75	0	47.25	0	5.75	22	17.25	26	28.75	12	40.25	1	51.75	0
1.75	6	13.25	0	2.75	6	14.25	0	25.75	0	37.25	1	1.50	10	13.00	0	24.50	1	36.00	0	47.50	0	6.00	27	17.50	30	29.00	13	40.50	2	52.00	2
2.00	6	13.50	0	3.00	2	14.50	1	26.00	1	37.50	0	1.75	15	13.25	3	24.75	0	36.25	0	47.75	0	6.25	28	17.75	36	29.25	8	40.75	1	52.25	1
2.25	5	13.75	0	3.25	9	14.75	0	26.25	1	37.75	0	2.00	16	13.50	1	25.00	0	36.50	0	48.00	0	6.50	25	18.00	31	29.50	9	41.00	2	52.50	0
2.50	11	14.00	4	3.50	5	15.00	0	26.50	0	38.00	1	2.25	7	13.75	0	25.25	0	36.75	0	48.25	0	6.75	26	18.25	30	29.75	8	41.25	0	52.75	1

53.00	2
53.25	0
53.50	1
53.75	1
54.00	2
54.25	1
54.50	2
54.75	1
55.00	1
55.25	0
55.50	0
55.75	0
56.00	0
56.25	0
56.50	0
56.75	0
57.00	1
57.25	0
57.50	1
57.75	1
58.00	1
58.25	1
58.50	0
58.75	1
59.00	0
59.25	0
59.50	0
59.75	0
60.00	2
60.25	2
60.50	2
60.75	1
61.00	2
61.25	1
61.50	2
61.75	0
62.00	1
62.25	0
62.50	1
62.75	1
63.00	0
63.25	1
63.50	1
63.75	0
64.00	0
64.25	0
64.50	0
64.75	1
65.00	0
65.25	1
65.50	1

DK14

SW

0.25	66
0.5	40
0.75	22
1	19
1.25	18
1.5	14
1.75	10
2	8
2.25	11
2.5	9
2.75	8
3	7
3.25	9
3.5	9
3.75	6
4	9
4.25	8
4.5	7
4.75	6
5	6
5.25	5
5.5	4
5.75	5
6	4
6.25	4
6.5	4
6.75	3
7	3
7.25	3
7.5	2
7.75	1
8	2
8.25	2
8.5	2
8.75	1
9	1
9.25	1
9.5	2
9.75	1
10	1
10.25	1
10.5	2
10.75	1
11	1
11.25	1
11.5	2
11.75	1
12	2
12.25	1
12.5	1
12.75	0
13	0
13.25	0
13.5	1
13.75	0
14	0
14.25	0
14.5	1
14.75	0
15	0
15.25	0
15.5	1
15.75	0
16	1
16.25	0
16.5	1
16.75	0
17	1
17.25	0
17.5	1
17.75	0
18	0
18.25	0
18.5	1
18.75	1
19	1
19.25	0
19.5	1
19.75	1
20	1
20.25	0
20.5	1
20.75	0
21	0
21.25	0
21.5	0
21.75	0
22	1
22.25	0
22.5	0
22.75	0
23	0
23.25	0
23.5	1
23.75	0
24	0
24.25	0
24.5	1
24.75	0
25	1
25.25	0
25.5	1
25.75	0
26	1
26.25	0
26.5	1
26.75	0
27	0
27.25	0
27.5	1
27.75	0
28	0
28.25	0
28.5	1
28.75	0
29	0
29.25	0
29.5	1
29.75	0
30	0
32.75	0
33	1
33.25	0
33.5	1
33.75	0
34	0
34.25	0
34.5	0
34.75	0
35	0
35.25	0
35.5	1
35.75	0
36	0
36.25	0
36.5	1

NE

0.25	6
0.5	17
0.75	41
1	48
1.25	21
1.5	13
1.75	12
2	9
2.25	8
2.5	8
2.75	7
3	4
3.25	5
3.5	5
3.75	8
4	8
4.25	8
4.5	10
4.75	7
5	7
5.25	7
5.5	6
5.75	5
6	7
6.25	8
6.5	6
6.75	7
7	6
7.25	6
7.5	5
7.75	5
8	4
8.25	5
8.5	4
8.75	4
9	3
9.25	4
9.5	3
9.75	3
10	2
10.25	1
10.5	2
10.75	1
11	2
11.25	1
11.5	1
11.75	1
12	1
12.25	1
12.5	1
12.75	1
13	2
13.25	1
13.5	1
13.75	1
14	1
14.25	0
14.5	1
14.75	2
15	4
15.25	5
15.5	5
15.75	1
16	3
16.25	1
16.5	1
16.75	2
17	1
17.25	1
17.5	1
17.75	1
18	3
18.25	2
18.5	1
18.75	1
19	1
19.25	2
19.5	1
19.75	2
20	1
20.25	1
20.5	1
20.75	1
21	2
21.25	2
21.5	2
21.75	2
22	3
22.25	3
22.5	2
22.75	2
23	2
23.25	2
23.5	1
23.75	1
24	1
24.25	1
24.5	1
24.75	2
25	1
25.25	2
25.5	1
25.75	2
26	1
26.25	1
26.5	0
26.75	1
27	1
27.25	2
27.5	1
27.75	1
28	0
28.25	1
28.5	1
28.75	1
29	0
29.25	0
29.5	1
29.75	1
30	2
30.25	2
30.5	1
30.75	1
31	1
31.25	2
31.5	1
31.75	1
32	1
32.25	1
32.5	0
32.75	1
33	0
33.25	0
33.5	1
33.75	1
34	0
34.25	1
34.5	0
34.75	1
35	0
35.25	1
35.5	0
35.75	1
36	0
36.25	1
36.5	0
36.75	1
37	1
37.25	1
37.5	1
37.75	1
38	1
38.25	1
38.5	0
38.75	1
39	1
39.25	1
39.5	0
39.75	1
40	1
40.25	1
40.5	0
40.75	1
41	1
41.25	1
41.5	0
41.75	1
42	1
42.25	1
42.5	0
42.75	1
43	0
43.25	1
43.5	0
43.75	1
44	1
44.25	1
44.5	0
44.75	1
45	1
45.25	1
45.5	0
45.75	0
46	0
46.25	1
46.5	0
46.75	1
47	1
47.25	1
47.5	0
47.75	0
48	0
48.25	1
48.5	0
48.75	0
49	0
49.25	1
49.5	0
49.75	1
50	0
50.25	1
50.5	0
50.75	0
51	0
51.25	1
51.5	0
51.75	1
52	1
52.25	1
52.5	0
52.75	1
53	0
53.25	1
53.5	0
53.75	0
54	0
54.25	0
54.5	0
54.75	0
55	0
55.25	1
55.5	0
55.75	0
56	0
56.25	1
56.5	0
56.75	0
57	0
57.25	0
57.5	0
57.75	0
58	0
58.25	0
58.5	0
58.75	0
59	0
59.25	0
59.5	0
59.75	0
60	0
60.25	0
60.5	0
60.75	0
61	0
61.25	0
61.5	0
61.75	0
62	0
62.25	0
62.5	0
62.75	0
63	0
63.25	0
63.5	0
63.75	0
64	0
64.25	0
64.5	0
64.75	0
65	0
65.25	0
65.5	0
65.75	0
66	0
66.25	0
66.5	0
66.75	0
67	0
67.25	0
67.5	0
67.75	0
68	0
68.25	0
68.5	0
68.75	0
69	0

DK17a

SW

0.25	21
0.5	30
0.75	27
1	29
1.25	28
1.5	17
1.75	14
2	12
2.25	10
2.5	7
2.75	9
3	10
3.25	9
3.5	6
3.75	7
4	6
4.25	5
4.5	7
4.75	7
5	9
5.25	9
5.5	9
5.75	7
6	5
6.25	6
6.5	6
6.75	6
7	8
7.25	7
7.5	7
7.75	5
8	6
8.25	5
8.5	7
8.75	6
9	7
9.25	7
9.5	9
9.75	6
10	6
10.25	4

DK33a

N

0.25	44
0.5	46
0.75	35
1	35
1.25	22
1.5	21
1.75	21
2	22
2.25	4
2.5	4
2.75	4
3	4
3.25	2
3.5	2
3.75	0
4	1
4.25	1
4.5	1
4.75	0
5	0
5.25	0
5.5	1
5.75	0
6	1
6.25	1
6.5	1
6.75	8
7	9
7.25	1
7.5	1
7.75	0
8	1
8.25	1
8.5	2
8.75	0
9	1
9.25	0
9.5	0
9.75	0
10	0
10.25	0
10.5	0
10.75	0
11	1
11.25	0
11.5	0
11.75	0
12	1
12.25	0
12.5	1
12.75	0
13	0
13.25	0
13.5	1
13.75	1
14	2
14.25	0
14.5	0

DK42

S

0.25	52
0.50	10
0.75	5
1.00	1
1.25	3
1.50	1
1.75	2
2.00	1
2.25	2
2.50	2
2.75	1
3.00	2
3.25	0
3.50	0
3.75	2
4.00	2
4.25	1
4.50	2
4.75	1
5.00	1
5.25	1
5.50	0
5.75	0
6.00	0
6.25	0
6.50	0
6.75	0
7.00	0
7.25	1
7.50	0
7.75	0
8.00	2
8.25	0
8.50	0
8.75	0
9.00	1
9.25	0
9.50	0

DK44

S

0.25	56
0.50	18
0.75	2
1.00	4
1.25	0
1.50	0
1.75	2
2.00	2
2.25	2
2.50	3
2.75	6
3.00	4
3.25	1
3.50	1
3.75	1
4.00	1
4.25	0
4.50	0
4.75	0
5.00	1
5.25	0
5.50	0
5.75	2
6.00	1
6.25	0
6.50	1

N

0.25	34
0.50	4
0.75	0
1.00	1
1.25	1
1.50	1
1.75	2
2.00	4
2.25	5
2.50	6
2.75	10
3.00	10
3.25	10
3.50	9
3.75	7
4.00	5
4.25	2
4.50	2
4.75	0
5.00	1
5.25	2
5.50	2

DK54

S

0.25	78
0.50	53
0.75	39
1.00	19
1.25	6
1.50	2
1.75	0
2.00	0
2.25	1
2.50	0
2.75	0
3.00	0
3.25	0
3.50	0
3.75	1
4.00	0
4.25	0

N

0.25	76
0.50	52
0.75	24
1.00	35
1.25	4
1.50	0
1.75	1
2.00	1
2.25	1
2.50	0
2.75	0
3.00	0
3.25	0
3.50	0
3.75	1
4.00	0

DK65x

S

0.25	63
0.50	18
0.75	1
1.00	1
1.25	0
1.50	0
1.75	0
2.00	1
2.25	0
2.50	1
2.75	0
3.00	2
3.25	5
3.50	3
3.75	0
4.00	0
4.25	0
4.50	0

DK65y

W

0.25	66
0.50	21
0.75	3
1.00	7
1.25	0
1.50	0
1.75	0
2.00	0
2.25	0
2.50	0
2.75	1
3.00	1
3.25	0
3.50	0
3.75	0
4.00	1

Appendix 13 Fracture count data re-binned for the plotting of individual profiles (dyke-parallel fracture frequency in the host rock)

Fracture frequency data binned for the plotting of individual profiles with subtraction of the background fracture frequency.
The data binned is the expanded fracture data listed in Appendix 10. The fracture data used was that between the dyke margin and the edge of the dyke-associated fracture zone. This data was then binned to 15 distance bins per profile.
X = distance bins; Y = fracture numbers; Z = fracture numbers after subtraction of the background fracture frequency.
For subtraction of background fracture frequency: a = background frequency per metre; b = number of background fractures per bin for subtraction. The text following is the number of background fractures to subtract from the newly binned data.
The number at the bottom of column Z or Y is the total number of fractures. Where there is no column Z, there is no background fracture frequency for subtraction.
For the south side of dyke K127, the data includes the assumed fracture counts (detailed in Appendix 12) where there is no outcrop.

X	Y	Z
K23 S		
0.294	13	13
0.588	7	6
0.882	3	3
1.176	4	3
1.47	2	2
1.764	2	1
2.058	1	1
2.352	3	2
2.646	2	2
2.94	1	0
3.234	2	2
3.528	2	1
3.822	0	0
4.116	1	0
4.41	1	1
		37
a	2	
b	0.588	
1 per 2 bins		
K32 S		
0.44	20	
0.88	37	
1.32	24	
1.76	14	
2.2	17	
2.64	2	
3.08	0	
3.52	0	
3.96	3	
4.4	1	
4.84	1	
5.28	4	
5.72	5	
6.16	1	
6.6	1	
	130	
K32 N		
0.574	50	49
1.148	15	14
1.722	18	17
2.296	10	9
2.87	7	6
3.444	1	0
4.018	2	1
4.592	1	0
5.166	4	3
5.74	3	2
6.314	1	0
6.888	2	1
7.462	1	0
8.036	4	3
8.61	3	2
		107
a	2	
b	1.148	
1 per bin		
K90c N		
0.417	51	50
0.834	22	21
1.251	13	12
1.668	11	10
2.085	12	11
2.502	10	9
2.919	17	16
3.336	14	13
3.753	10	9
4.17	8	7
4.587	6	5
5.004	3	2
5.421	2	1
5.838	2	1
6.255	2	1
		168
a	2	
b	0.834	
1 per bin		
K93 S		
0.254	7	7
0.508	9	9
0.762	6	6
1.016	7	7
1.27	8	7
1.524	6	6
1.778	9	8
2.032	2	2
2.286	2	2
2.54	2	2
2.794	1	1
3.048	2	2
3.302	2	1
3.556	1	1
3.81	1	1
		62
a	0.8	
b	0.2032	
1 per 5 bins		
K93 N		
0.269	8	8
0.538	17	17
0.807	17	16
1.076	14	14
1.345	10	10
1.614	7	7
1.883	5	5
2.152	7	7
2.421	7	6
2.69	3	3
2.959	2	2
3.228	1	1
3.497	0	0
3.766	1	0
4.035	1	1
		97
a	0.8	
b	0.2152	
1 per 5 bins		
K112 N		
0.437	61	60
0.874	54	53
1.311	49	48
1.748	31	30
2.185	17	16
2.622	10	9
3.059	10	9
3.496	10	9
3.933	5	4
4.37	1	0
4.807	1	0
5.244	0	0
5.681	1	0
6.118	4	3
6.555	3	2
		243
a	2.2	
b	0.9614	
1 per bin		
K114 S		
0.161	34	34
0.322	34	33
0.483	20	20
0.644	7	7
0.805	1	1
0.966	1	0
1.127	1	1
1.288	1	1
1.449	1	1
1.61	1	0
1.771	0	0
1.932	1	1
2.093	1	1
2.254	1	0
2.415	1	1
		101
a	1.44	
b	0.23184	
1 per 4 bins		
K114 N		
0.159	41	41
0.318	41	40
0.477	15	15
0.636	3	3
0.795	2	2
0.954	2	1
1.113	1	1
1.272	1	1
1.431	1	0
1.59	0	0
1.749	1	1
1.908	0	0
2.067	1	1
2.226	0	0
2.385	1	1
		107
a	1.44	
b	0.22896	
1 per 4 bins		
K116iiy N		
0.27	45	
0.54	26	
0.81	16	
1.08	16	
1.35	16	
1.62	11	
1.89	8	
2.16	6	
2.43	5	
2.7	6	
2.97	6	
3.24	5	
3.51	5	
3.78	1	
4.05	2	
	174	
K117 S		
0.698	106	
1.396	52	

2.094	13	
2.792	8	
3.49	7	
4.188	3	
4.886	2	
5.584	2	
6.282	1	
6.98	1	
7.678	1	
8.376	0	
9.074	1	
9.772	1	
10.47	2	
	200	

K117 N

1.234	35	34
2.468	71	69
3.702	97	95
4.936	48	46
6.17	10	8
7.404	4	2
8.638	2	1
9.872	3	1
11.106	4	2
12.34	4	2
13.574	6	4
14.808	3	2
16.042	4	3
17.276	3	2
18.51	4	1
		272
a	1.4	
b	1.7276	

1 per bin and 3 per 4 bins

K118i S

0.285	73	71
0.57	19	18
0.855	15	13
1.14	13	11
1.425	12	11
1.71	10	8
1.995	10	8
2.28	9	8
2.565	9	7
2.85	9	7
3.135	6	5
3.42	6	4
3.705	5	3
3.99	4	3
4.275	4	2
		179
a	5.76	
b	1.6416	

1 per bin and 2 per 3 bins

K118i N

0.263	86	85
0.526	38	36
0.789	35	34
1.052	34	32
1.315	17	16
1.578	12	10
1.841	7	6
2.104	6	4
2.367	4	3
2.63	5	3
2.893	4	3
3.156	5	3
3.419	4	3
3.682	4	2
3.945	2	1
		241
a	5.76	
b	1.51488	

1 per bin and 1 per 2 bins

K118ii S

0.082	29	28
0.164	13	13
0.246	9	8
0.328	3	3
0.41	2	2
0.492	2	1
0.574	2	2
0.656	1	0
0.738	2	1
0.82	1	1
0.902	2	1
0.984	1	1
1.066	2	1
1.148	0	0
1.23	1	1
		63
a	5.68	
b	0.46576	

I per 2 bins

K118ii N

0.284	53	52
0.568	28	26
0.852	30	28
1.136	25	24
1.42	19	17
1.704	13	11
1.988	11	10
2.272	9	7
2.556	9	7
2.84	6	5
3.124	6	4
3.408	6	4
3.692	4	3
3.976	3	1
4.26	4	2
		201
a	5.68	
b	1.61312	

1 per bin and 2 per 3 bins

K119 S

0.217	32	30
0.434	37	36
0.651	30	29
0.868	20	19
1.085	11	10
1.302	8	6
1.519	6	5
1.736	5	4
1.953	4	3
2.17	3	2
2.387	2	0
2.604	2	1
2.821	1	0
3.038	1	0
3.255	2	1
		146
a	5.52	
b	1.19784	

1 per bin and 1 per 5 bins

K119 N

0.267	58	57
0.534	33	31
0.801	22	21
1.068	10	8
1.335	8	7
1.602	4	2
1.869	6	5
2.136	7	5
2.403	6	5
2.67	6	4
2.937	3	2
3.204	3	1
3.471	2	1
3.738	2	0
4.005	2	1
		150
a	5.52	
b	1.47384	

1 per bin and 1 per 2 bins

K126 S

0.11	31	31
0.22	31	30
0.33	28	28
0.44	20	20
0.55	20	19
0.66	9	9
0.77	10	9
0.88	0	0
0.99	1	1
1.1	1	0
1.21	0	0
1.32	1	1
1.43	0	0
1.54	1	0
1.65	1	1
		149
a	2.9	
b	0.319	

1 per 3 bins

K126 N

0.134	43	43
0.268	44	42
0.402	29	29
0.536	22	22
0.67	12	12
0.804	8	7
0.938	1	1
1.072	1	1
1.206	1	0
1.34	1	1
1.474	1	1
1.608	1	0
1.742	1	1
1.876	1	0
2.01	1	1
		161
a	2.9	
b	0.3886	

2 per 5 bins

K127 S

2.2	269	257
4.4	198	186
6.6	113	101
8.8	78	66
11	76	64
13.2	82	70
15.4	71	59
17.6	60	48
19.8	68	56
22	33	21
24.2	17	5
26.4	14	2
28.6	12	0
30.8	12	0
33	18	6
		941
a	5.4	
b	11.88	

12 per bin

K127 N

1.534	11	4
3.068	12	5
4.602	11	4
6.136	115	107
7.67	93	85
9.204	64	56
10.738	40	33
12.272	40	32
13.806	30	23
15.34	23	16
16.874	28	20
18.408	22	15
19.942	20	12
21.476	12	5
23.01	8	1
		418
a	4.8	
b	7.3632	

7 per bin and 2 per 5 bins

K132ii S

0.149	31	31
0.298	37	36
0.447	30	29
0.596	27	26
0.745	19	18
0.894	13	12
1.043	7	7
1.192	8	7
1.341	6	5
1.49	2	2
1.639	1	0
1.788	2	1
1.937	2	2
2.086	2	1
2.235	2	2
		179
a	4.88	
b	0.72712	

3 per 4 bins

K134 S

0.267	74	73
0.534	52	51
0.801	38	37
1.068	29	28
1.335	22	22
1.602	15	14
1.869	4	4
2.136	2	1
2.403	2	1

Appendix 13 Fracture count data re-binned for the plotting of individual profiles (dyke-parallel fracture frequency in the host rock)

2.67	2	1
2.937	2	2
3.204	2	2
3.471	1	1
3.738	2	2
4.005	2	1
		240
a	3.12	
b	0.83304	
4 per 5 bins		

K134 N

0.247	76	75
0.494	62	61
0.741	55	54
0.988	39	39
1.235	35	34
1.482	12	11
1.729	11	10
1.976	1	1
2.223	2	2
2.47	1	0
2.717	2	1
2.964	0	0
3.211	1	1
3.458	1	0
3.705	2	1
		290
a	3.12	
b	0.77064	
3 per 4 bins		

K136 S

0.084	27	27
0.168	28	28
0.252	27	26
0.336	22	22
0.42	21	21
0.504	21	21
0.588	16	16
0.672	15	15
0.756	15	14
0.84	7	7
0.924	8	8
1.008	7	7
1.092	2	2
1.176	2	2
1.26	2	1
		217
a	2.52	
b	0.21168	
1 per 5 bins		

K136 N

0.137	45	45
0.274	44	43
0.411	37	37
0.548	33	33
0.685	24	23
0.822	19	19
0.959	13	12
1.096	6	6
1.233	3	3
1.37	1	1
1.507	1	0
1.644	0	0
1.781	1	1
1.918	1	0
2.055	1	1
		224
a	2.52	
b	0.34524	
1 per 3 bins		

K138 S

0.173	28	28
0.346	6	6
0.519	7	7
0.692	5	4
0.865	3	3
1.038	3	3
1.211	3	3
1.384	3	2
1.557	3	3
1.73	2	2
1.903	3	3
2.076	2	2
2.249	3	3
2.422	2	2
2.595	3	2
		73
a	4.6	
b	0.7958	
4 per 5 bins		

K138 N

0.267	35	34
0.534	13	12
0.801	8	7
1.068	6	4
1.335	4	2
1.602	3	2
1.869	1	0
2.136	2	1
2.403	3	2
2.67	2	1
2.937	2	0
3.204	2	1
3.471	2	1
3.738	2	0
4.005	2	1
		68
a	4.6	
b	1.2282	
1 per bin and 1 per 4 bins		

K155b S

0.281	85	84
0.562	17	16
0.843	31	29
1.124	20	19
1.405	9	8
1.686	7	6
1.967	5	4
2.248	4	3
2.529	5	3
2.81	3	2
3.091	4	3
3.372	2	1
3.653	3	2
3.934	3	2
4.215	3	1
		183
a	4.16	
b	1.16896	
1 per bin and 1 per 5 bins		

K155b N

0.421	61	59
0.842	24	22
1.263	17	15
1.684	11	10
2.105	12	10
2.526	12	10
2.947	8	7
3.368	10	8
3.789	6	4
4.21	4	2
4.631	3	1
5.052	3	2
5.473	2	1
5.894	2	0
6.315	4	1
		152
a	4.16	
b	1.75136	
1 per bin and 3 per 4 bins		

K157a S

0.434	89	85
0.868	19	15
1.302	10	6
1.736	10	6
2.17	10	6
2.604	8	4
3.038	4	0
3.472	4	0
3.906	8	4
4.34	8	4
4.774	6	2
5.208	6	2
5.642	5	1
6.076	7	3
6.51	6	2
		140
a	8.76	
b	3.80184	
4 per bin		

K157a N

0.299	69	66
0.598	39	36
0.897	11	8
1.196	2	0
1.495	2	0
1.794	3	1
2.093	4	1
2.392	4	1
2.691	3	0
2.99	4	1
3.289	5	2
3.588	1	0
3.887	2	0
4.186	3	1
4.485	4	1
		118
a	8.76	
b	2.61924	
2 per bin and 3 per 5 bins		

K178 S

0.484	84	82
0.968	53	51
1.452	19	17
1.936	8	6
2.42	6	4
2.904	4	2
3.388	4	2
3.872	5	3
4.356	5	3
4.84	5	3
5.324	6	4
5.808	6	4
6.292	5	3
6.776	4	2
7.26	3	1
		187
a	4.12	
b	1.99408	
2 per bin		

K178 N

0.467	108	106
0.934	53	51
1.401	33	31
1.868	18	16
2.335	13	11
2.802	11	9
3.269	13	11
3.736	10	8
4.203	9	7
4.67	11	9
5.137	8	6
5.604	6	4
6.071	3	1
6.538	4	2
7.005	3	1
		273
a	4.12	
b	1.92404	
2 per bin		

WC25a NW

0.626	30	28
1.252	9	7
1.878	15	13
2.504	19	17
3.13	17	15
3.756	12	10
4.382	12	10
5.008	17	15
5.634	7	5
6.26	5	3
6.886	5	3
7.512	2	0
8.138	6	4
8.764	5	3
9.39	4	2
		135
a	3.2	
b	2.0032	
2 per bin		

DK14 NE

0.787	72	71
1.574	78	76
2.361	28	27
3.148	18	17
3.935	22	21
4.722	27	25
5.509	20	19
6.296	21	20
7.083	20	18
7.87	16	15
8.657	13	12
9.444	11	10
10.231	7	6

Appendix 13 Fracture count data re-binned for the plotting of individual profiles (dyke-parallel fracture frequency in the host rock)

11.018	5	4
11.805	4	2
		343
a	1.6	
b	1.2592	

1 per bin and 1 per 4 bins

DK14 SW

0.82	134	133
1.64	50	49
2.46	31	29
3.28	27	26
4.1	26	25
4.92	22	20
5.74	15	14
6.56	14	13
7.38	9	7
8.2	6	5
9.02	4	3
9.84	5	3
10.66	3	2
11.48	5	4
12.3	5	3
		336
a	1.6	
b	1.312	

1 per bin and 1 per 3 bins

DK17a SW

3.747	236
7.494	103
11.241	88
14.988	54
18.735	30
22.482	26
26.229	21
29.976	13
33.723	14
37.47	10
41.217	12
44.964	10
48.711	6
52.458	7
56.205	4
	634

DK33a N

0.234	42
0.468	42
0.702	34
0.936	33
1.17	23
1.404	21
1.638	20
1.872	20
2.106	12
2.34	4
2.574	4
2.808	3
3.042	4
3.276	2
3.51	2
	266

DK42 S

0.134	34
0.268	20
0.402	6
0.536	3
0.67	3
0.804	2
0.938	0
1.072	0
1.206	3
1.34	0
1.474	0
1.608	2
1.742	1
1.876	0
2.01	1
	75

DK54 S

0.087	30
0.174	27
0.261	23
0.348	20
0.435	17
0.522	17
0.609	13
0.696	14
0.783	15
0.87	8
0.957	4
1.044	2
1.131	2
1.218	2
1.305	3
	197

DK54 N

0.08	28
0.16	25
0.24	21
0.32	17
0.4	16
0.48	16
0.56	14
0.64	8
0.72	6
0.8	4
0.88	12
0.96	13
1.04	8
1.12	2
1.2	1
	191

DK65y W

0.067	22
0.134	19
0.201	18
0.268	10
0.335	7
0.402	6
0.469	3
0.536	2
0.603	2
0.67	0
0.737	1
0.804	1
0.871	0
0.938	2
1.005	4
	97

Data plotted in Figure 3.13 (for dyke K141).
The orientations that are italicised have been injected with magma. * There are two distinct groups (in orientation) of mineralised fractures. The kinematics are what would be expected if the fractures were seen to have accommodated shear.

Block number (as described in Figure 3.13)	Orientation	*Kinematics (S = sinistral; D = dextral)	Orientation of acute and obtuse conjugate bisectors of the average orientations	Acute and obtuse dihedral angles for the conjugate pairs
1	035/70NW	D		
	035/70NW	D		
	034/70NW	D		
	084/88SE	S		
	085/89SE	S		
	089/86SE	S		
	086/90	S		
	084/90	S		
	039/70NW	D		
	033/76NW	D		
	027/82NW	D		
	021/53NW	D		
	021/48NW	D		
	023/68NW	D		
	023/66NW	D		
	043/58NW	D		
	036/68NW	D		
	029/73NW	D		
	038/80NW	D		
	037/80NW	D		
Means	086/89SE	S	055/23 (acute)	57.15
	032/69NW	D	150/11 (obtuse)	122.85
2	041/58NW	D		
	036/58NW	D		
	038/58NW	D		
	033/70NW	D		
	034/68NW	D		
	034/60NW	D		
Means	036/62NW	D		
3	043/70NW	D		
	031/70NW	D		
	025/70NW	D		
	023/57NW	D		
	021/57NW	D		
	022/57NW	D		
	024/90	D		
	043/60NW	D		
	034/72NW	D		
	057/60NW	S		
	025/72NW	D		
	038/72NW	D		
	090/68NW	S		
	091/69NE	S		
	089/67NW	S		
	027/76NW	D		
	030/78NW	D		
	025/80NW	D		
	027/86NW	D		
	024/86NW	D		
	072/65NW	S		
	068/68NW	S		
	039/80NW	D		
	025/78NW	D		
	021/77NW	D		
	082/50NW	S		
	073/64NW	D		
Means	076/63NW	S	237/12 (acute)	44.45
	029/73NW	D	142/24 (obtuse)	135.55

4	029/83NW	D		
	030/84NW	D		
	027/83NW	D		
	024/80NW	D		
	028/81NW	D		
	035/83NW	D		
	070/64NW	S		
	025/78NW	D		
	028/77NW	D		
	067/60NW	S		
	065/65NW	S		
	070/70NW	S		
Means	068/65NW	S	235/22 (acute)	41.25
	028/81NW	D	137/18 (obtuse)	138.75
5	031/77NW	D		
	035/77NW	D		
	031/77NW	D		
	034/83NW	D		
Means	033/78NW	D		
Sin. dyke// shear	113/70SW			
Sin. dyke// shear	112/68SW			
Dyke	111/86SW			

Data plotted in Figure 3.16 (for dyke K135i/ii).
See column headings for explanations.

HIGH ANGLE FRACTURES	**SHEARS**			
Orientation (bold - exploited by magma; italics - accommodates dextral slip)	**Orientation**	**Kinematics (S = sinistral; D = dextral). Conjugate pairs in bold.**	**Orientation of acute conjugate bisector**	**Comment**
061/70SE	069/57SE	D		follows cuspate fracture
055/46SE	063/60SE	D		follows cuspate fracture
060/47SE	115/82SW	S		
071/40SE	105/83NE	S		reactivated
055/60SE	104/85NE	S		reactivated
047/42SE	103/83NE	S		reactivated
059/45SE	103/85NE	S		reactivated
070/36SE	102/84NE	S		reactivated
053/48SE	106/74SW	S		reactivated
055/58SE	120/67SW	S		
067/30SE	108/84NE	S		reactivated
067/40SE	117/85SW	S		exploited by dyke
073/44SE	103/80NE	**S**	092/23	reactivated
069/57SE	091/75NE	**D**		
063/60SE				
066/30SE	103/84NE	**S**	076/35	reactivated
065/30SE	073/63NW	**D**		
069/36SE				
051/23SE	068/75SE			dyke injection
054/40SE	097/83SW			dyke injection
048/30SE	066/55NW	D		
054/36SE	102/76SW	D		reactivated
062/25SE	086/80SE	D		
046/23SE	123/67SW	S		
044/29SE	144/85NE	S		
060/23SE	125/88SW	S		
070/36SE	118/32SW	S		

030/32SE	122/68SW	**S**	237/46	
055/28SE	102/34SW	**D**		
069/29SE				
038/23SE	118/86SW	**S**	277/48	
058/31SE	104/70SW	**D**		
043/22SE				
078/24SE	073/24SE			dyke injection
068/24SE	063/24SE			dyke injection
053/30SE	086/32SE			dyke injection
086/25SE	107/56SW			dyke injection
081/25SE	120/87SW	S		
063/24SE	126/74SW	S		
068/67SE	131/74SW	S		
051/23SE	103/85SW	S		reactivated

Host rock shear data, as plotted in Figure 3.19 and Figure 3.20.
See column headings for explanations. The shaded areas indicate shears not plotted in Figure 3.19, given their proximity to dyke segmentation zones. The rotated data is plotted in Figure 3.20. The shears that are italicised for dyke K147 are plotted but are not shown in the extent of the map in Figure 3.19.

Dyke number	Orientation (either strike/dip, or just strike)	Kinematics (S = sinistral; D = dextral). Conjugate pairs in bold.	Orientation of acute conjugate bisector (either azimuth/plunge, or just azimuth). In brackets, strike of bisector taking planes as vertical	Dihedral angle for conjugate pairs. In brackets, dihedral angle taking planes as vertical)	Angle between shear and dyke	Displacement (mm)
K117	109	S				
	099	S				
	109	S				
	113	S				2
	098	S				3
	101	S				
	111	S				
	105	S				
	096	S				
	102	S				20
	099	S				
	101	S				
	103	S				20
	106	S				30
	103	S				1.5
	109	S				1
	108	S				6
	113	S				
	101	S				
	103	S				
	102	S				0.5
	103	S				0.5
	084	D				
	097	D				3.5
	092	D				3
	098	D				
	087	D				
	101	D				
	108	**S**	104.5	7		1.5
	101	**D**				3.5
	116	**S**	112	8		
	108	**D**				
	103	**S**	93	20		
	083	**D**				
	123	**S**	106	34		
	089	**D**				
	108	**S**	100	16		
	092	**D**				
	101	**S**	92	18		5
	083	**D**				
	109	**S**	101	16		
	093	**D**				
	089/82SE	D			10.1	
	091/90	D			10.0	
	102/87SW	**S**	278/18 (099)	6.31 (6)	4.2	15
	096/85SW	**D**			3.2	20
	104/89SW	**S**	278/10 (098.5)	11.17 (11)	7.1	
	093/87SW	**D**			6.7	
	103/87SW	**S**	272/49 (100)	9.19 (6)	5.0	
	097/80SW	**D**			4.5	
Means	105	S	099	12		
	093	D				
Rotated	080.1/87.9SE	D				
	082/84.1NW	D				
	093/87NE	**S**	270.1/10	11.17		
	087/89NW	**D**				
	095/85NE	**S**	269.9/49.4	9.19		

	084/87NW	**D**				
	094/87NE	**S**	271/18	6.31		
	088/86SE	**D**				
Dyke	099/84SW					
K118i	***105***					
	105	S				
	093	D				2
	089	D				20
	119	S				
	111	S				2
	118	S				1
	101	D				
	108/86SW	S				3
	108/86SW	S				3
	094					
	103	**S**	100.5	5		
	098	**D**				
	103/80SW	S			8.86	5
	106/82SW	S			12.02	0.5
	093/77SW	D			3.16	1.5
	108/80SW	**S**	268/44 (103)	13.89 (10)	13.79	2
	098/70SW	**D**			10.72	1.5
	098/79SW	**S**	094/6 (093)	9.88 (10)	4.06	1
	088/80SE	**D**			5.91	1
Means	104	S	099	10		
	094	D				
Rotated	098.9/89.9SW	S				
	101.9/88.2NE	S				
	089/87SE	D				
	103.8/89.7SW	**S**	273.7/44.2	13.89		
	093.8/80SW	**D**				
	093.9/89SW	**S**	089/5.9	9.88		
	084.1/89.9SE	**D**				
Dyke	094/80SW					
	100					
	098	D				
	112	**S**	102.5	19		
	093	**D**				
	122	**S**	104	36		
	086	**D**				
	105	**S**	097.5	15		
	090	**D**				
	120	**S c1**				1
	094	**D c2**	107	26		
	103	**D c2**	111.5	17		0.25
	096	**D c2**	108	24		2
	107/77SW	S			8.51	25
	107/77SW	S			8.51	9
	084/90	D			17.84	10
	093/80SW	D			7.20	5
	103/70SW	**S**	099/8 (096)	13.38 (14)	12.35	2
	089/72SE	**D**			14.65	
	122/75SW	**S**	112/5 (111)	21.43 (22)	22.65	
	100/77SW	**D**			5.00	
	086/90	**D c1**			16.08	
	113/74SW	**S c2**	104/31 (099.5)	31.08 (27)	15.01	4
	111/85SW	**S c2**	099/11 (098.5)	25.46 (25)	11.33	35
	115/80SW	**S**	101/18 (099)	33.37 (32)	14.95	3
	083/90	**D**			18.74	1.5
Means	112	S	102	20		
	092	D				
Rotated	096.8/84.9SW	S				
	096.8/84.9SW	S				
	073.9/82.3NW	D				
	083.1/87.9SE	D				
	092.9/78SW	**S**	087.9/7.8	13.38		
	079.4/79.9SE	**D**				
	111.4/82.4SW	**S**	101.2/6.6	21.43		
	090/85SW	**D**				
	75.9/82.2NW	**D c1**				
	102.6/81.8SW	**S c2**	089.2/31.2	31.08		
	101/87.1NE	**S c2**	087.5/10.8	25.46		
	104.8/87.7SW	**S**	088.4/18	33.37		
	072.8/82.4NW	**D**				
Dyke	100/82SW					

K134						
	106/88SW	D				25
	107/90	D				12
	108/86NE	D				20
	108	D				
	105	D				
	122/88NE	S			12.16	
	115/88SW	S			5.38	2
	115/83SW	S			8.60	1
	124/86NE	S			14.55	0.5
	126/88SW	S			16.12	
	121/90	S			11.00	
	120/90	S			10.00	5
	122/90	S			12.00	15
	101/85NE	D			10.29	10
	101/90	D			9.00	5
	102/82NE	D			11.30	1
	098/90	D			12.00	3
	106/86SW	D			5.65	20
	106/86SW	D			5.65	
	111/86SW	D			4.12	
	110/90	D			0.00	30
	112/89SW	D			2.24	20
	102/87SW	D			8.54	
	104/90	D			6.00	
	101/84SW	D			10.80	
	101/86SW	D			9.84	15
	105/90	D			5.00	5
	112/89NE	**S**	106/5 (106.5)	11.04 (11)	2.24	
	101/88NE	**D**			9.22	3
	118/90	**S**	109.5/0 (109.5)	17 (17)	8.00	
	101/90	**D**			9.00	
	119/89SW	**S**	112/0 (112)	14 (14)	9.05	
	105/89SW	**D**			5.10	
Means	119	S	111.5	15		
	104	D				
Rotated	102/88NE	S				
	095/88SW	S				
	095/83SW	S				
	104/86NE	S				
	106/88SW	S				
	101/90	S				
	100/90	S				
	102/90	S				
	081/85NW	D				
	081/90	D				
	082/82NW	D				
	078/90	D				
	086/86SE	D				
	086/86SE	D				
	091/86SW	D				
	090/90	D				
	092/89SW	D				
	082/87SE	D				
	084/90	D				
	081/84SE	D				
	081/86SE	D				
	085/90	D				
	092/89NE	**S**	086.4/5.3	11.04		
	081/88NW	**D**				
	098/90	**S**	090/0	17		
	081/90	**D**				
	099/89SW	**S**	092.5/0.1	14		
	085/89SE	**D**				
Dyke seg1	111/87NE					
Dyke seg2	108/86NE					
Dyke seg3	108/88SW					
Dyke seg4	111/88SW					
Dyke seg6	112/88SW					
Dyke seg7	110/88SW					
Average	110/90					
K137						
	100	S				
	099/86NE	S				7
	099/88NE	S				25
	100/88NE	S				6
	096/83NE	S				10

	104	S				3
	113	S				
	113	S				
	090	D				
	098	**S**	094	8		
	090	**D**				
	110	**S**	099.5	21		
	089	**D**				
	105	**S c1**				
	075	**D c2**	090	30		
	085	**D c2**	095	20		
	100/85NE	S			3.15	6
	108/86NE	S			10.97	2
	093/84NE	S			4.46	4
	099/86NE	S			2.00	3
	098/84NE	S			2.23	1
	099/87NE	S			2.23	5
	100/86NE	S			2.99	1.5
	104/90	S			8.06	8
	096/86NE	D			1.00	2
Means	103	S	095.5	15		
	088	D				
Rotated	093/89NE	S				
	101/89.9NE	S				
	086/88NW	S				
	092/90	S				
	091/88NE	S				
	092/89SW	S				
	093/90	S				
	097/86SW	S				
	089/90	D				
Dyke	097/86NE					
K147						
	115	S				2
	117	S				13
	115	S				
	109	*S*				5
	098	S				12
	101	S				3
	075	D				9
	086	D				5
	086	D				2
	083	D				3
	098	D				
	079	*D*				110
	089	D				22
	091	**S**	083	16		9
	075	**D**				1
	113	**S**	102.5	21		
	092	**D**				
	104	**S**	096	16		
	088	**D**				10
	093	***S***	085	16		3
	077	***D***				3
	097/87SW	S			5.09	2
	100/82SW	S			9.97	10
	103/86SW	S			11.16	3
	091/88SW	S			1.00	
	084/88SE	S			8.00	2
	082/83SE	D			11.15	6
	064/87SE	D			27.99	10
	086/89SE	D			6.08	
	068/86SE	D			24.05	8
	089/88SE	D			3.00	3
	089/88SE	D			3.00	
	087/81SE	D			8.59	35
	088/84SE	D			5.65	2.5
	094/84SW	**S**	084/5 (083.5)	21.01 (21)	4.47	5
	073/86SE	**D**			19.08	
	106/85SW	**S**	096/0 (096)	19.92 (20)	14.29	
	086/85SE	**D**			6.70	20
	109/90	**S**	277/20 (098)	23.34 (22)	17.11	10
	087/82SE	**D**			7.80	3
	110/87SW	**S**	093/2 (093)	33.98 (34)	18.01	
	076/88SE	**D**			15.99	
	094/86NE	**S**	263/26 (083.5)	23.23 (21)	6.32	3
	073/84SE	**D**			19.37	
	099/86SW	**S c1**			7.27	7

	085/87SE	**D c2**	092/4 (092)	14.01 (14)	7.06	15
	082/85SE	**D c2**	270/3 (090.5)	16.98 (17)	10.42	
	084/86SE	**D c2**	091/0 (091.5)	14.96 (15)	8.24	
	099/86SW	**S c3**	091/0 (091.5)	14.96 (15)	7.27	
	098/86SW	**S c3**	091/0 (091)	13.97 (14)	6.32	
	085/89NW	**D c1**			7.61	2
	097/86SW	**S c2**	092/23 (091)	12.99 (12)	5.38	2
	097/86SW	**S c2**	092/23 (091)	12.99 (12)	5.38	
Means	101	S	092			
	083	D				
Rotated	095/89SW	S				
	098/84SW	S				
	101/88SW	S				
	089/90	S				
	082/90	S				
	080/85SE	D				
	062/88.8SE	D				
	084/89NW	D				
	066/87.8SE	D				
	087/90	D				
	087/90	D				
	085/83SE	D				
	086/86SE	D				
	092/86SW	**S**	081.8/4.7	21.01		
	071/87.9SE	**D**				
	104/86.9SW	**S**	094/0.1	19.92		
	084/87SE	**D**				
	107/88.1NE	**S**	275.7/19.8	23.34		
	085/84SE	**D**				
	108/88.9SW	**S**	090.9/2	33.98		
	074/89.9SE	**D**				
	092/84NE	**S**	262/26.3	23.23		
	071.1/85.9SE	**D**				
	097/88SW	**S c1**				
	083/89SE	**D c2**	089.9/4	14.01		
	080/87SE	**D c2**	268.1/3.1	16.98		
	082/88SE	**D c2**	089/0	14.96		
	097/88SW	**S c3**	089/0	14.96		
	096/88SW	**S c3**	089/0	13.97		
	083/87NW	**D c1**				
	095/88SW	**S c2**	089.2/23	12.99		
	095/88SW	**S c2**	089.2/23	12.99		
Dyke	092/88SW					
K155b						
	086	S				
	089	**S**	085	8		
	081	**D**				
	093/90SW	S			10.76	
	083/87SE	D			1.00	
	084/86SE	D			1.00	
	087/86SE	**S**	081/16 (080)	14.55 (14)	3.99	
	073/90	**D**			10.76	
	086/80SE	**S**	089/45 (082.5)	9.86 (7)	6.70	
	079/87SE	**D**			4.12	
Means	088	S	084	8		
	080	D				
Rotated	100/86.1NE	S				
	090/89NE	D				
	091/90	D				
	094/90	**S**	086.9/15.8	14.55		
	080/86.1NW	**D**				
	093/84SW	**S**	092/45.3	9.86		
	086/89NW	**D**				
Dyke	083/86SE					
K164i						
	087/88SE	S			6.08	
	105/83NE	S			17.18	10
	086/89NW	D			3.60	
	059/90	D			29.25	15
	086/87SE	D			7.28	
	085/86SE	D			8.54	
	082/88NW	D			6.32	
	085/83SE	D			11.40	
	090/87SW	D			7.28	
	094/86SW	**S**	088/9 (087.5)	13.13 (13)	10.00	
	081/88SE	**D**			9.22	
Means	095	S	088.5	13		

	082	D				
Rotated	089/84SE	S				
	106.9/86.8NE	S				
	088/87SE	D				
	060.9/86.5SE	D				
	088/83SE	D				
	087/82SE	D				
	084/88SE	D				
	087/79SE	D				
	092/83SW	D				
	096/82SW	**S**	090.6/9	13.13		
	083/84SE	**D**				
Dyke	088/86NW					
K178						
	093	D				5
	093/90	D				220
	093/86SW	D				10
	093/86SW	D				110
	092/89SW	D				
	093	D				
	093/90	D				60
	093	D				160
	092/88NE	D				6
	092/90	D				6
	093/86NE	D				8
	092/87SW	D				10
	092/90	D				3
	090	D				100
	099	S				
	104	S				13
	102	S				
	098	S				
	101	S				10
	110	S				
	085	D				
	084	D				
	091	D				2
	083	D				40
	088	D				5
	099	**S**	095.5	7		45
	092	**D**				
	102	**S**	093	18		
	084	**D**				
	098	**S**	094	8		3
	090	**D**				3
	086	**D c1**				
	110	**S c2**	98	24		
	110	**S c2**	98	24		
	099/87NE	S			7.21	2
	110/82NE	S			19.19	
	102/88NE	S			9.49	
	108/90	S			15.03	
	083/88SE	D			10.05	
	086/90	D			7.07	
	090/90	D			3.16	
	088/88SE	D			5.10	
	089/89SE	D			4.00	
	072/89SE	D			21.00	6
	089/78SE	D			11.69	3
	086/77SE	D			13.86	1.5
	082/75SE	D			17.72	5
	087/90	D			6.08	
	094/88NE	D			3.16	6
	090/88NE	D			3.16	20
	084/88SE	D			9.05	5
	088/86SE	D			5.83	14
	079/88SE	D			14.03	15
	093/88SW	D			1.00	3
	084/88SE	D			9.05	4
	096/90	**S**	270/10 (090.5)	11.18 (11)	3.16	25
	085/88SE	**D**			8.06	180
	099/87NE	**S**	264/6 (084)	30.14 (30)	7.21	
	069/90	**D**			24.02	
	110/87NE	**S c1**			17.46	
	072/90	**D c2**	271/5 (091)	38.10 (38)	21.02	
	088/89NW	**D c2**	279/10 (099)	22.08 (22)	5.38	
	104/89NE	**S**	276/4 (096)	16.03 (16)	11.18	
	088/90	**D**			5.10	

	097/90	**S**	093.5/0 (093.5)	7 (7)	4.12	5
	090/90	**D**			3.16	5
	097/90	**S**	094.5/0 (094.5)	5 (5)	4.12	5
	092/90	**D**			1.41	5
	099/89SW	**S**	093/0 (093)	12 (12)	6.00	
	087/89SE	**D**			6.00	
Means	102	S	094	16		
	086	D				
Rotated	096/86NE	S				
	107/81NE	S				
	099/87NE	S				
	105/89NE	S				
	080/89SE	D				
	083/89NW	D				
	087/89NW	D				
	085/89SE	D				
	086/90	D				
	069/89.9SE	D				
	086/79SE	D				
	083/78SE	D				
	079/76SE	D				
	084/89NW	D				
	091/87NE	D				
	087/89SE	D				
	081/89SE	D				
	085/87SE	D				
	076/89SE	D				
	090/89SW	D				
	081/89SE	D				
	093/89NE	**S**	267.2/10.1	11.18		
	082/89SE	**D**				
	096/86NE	**S**	261.1/6.2	30.14		
	066/89.1NW	**D**				
	107/86NE	**S c1**				
	069/89.1NW	**D c2**	268.1/5	38.10		
	085/88NW	**D c2**	276.2/9.9	22.08		
	101/88NE	**S**	273.1/3.9	16.03		
	085/89NW	**D**				
	094/89NE	**S**	090.5/0	7		
	087/89NW	**D**				
	094/89NE	**S**	091.5/0	5		
	089/89NW	**D**				
	096/90	**S**	090/0	12		
	084/90	**D**				
Dyke	093/89SW					

Code for the Schmidt Plot thermal modelling (written in Visual Basic for Applications (VBA) in Microsoft Excel).

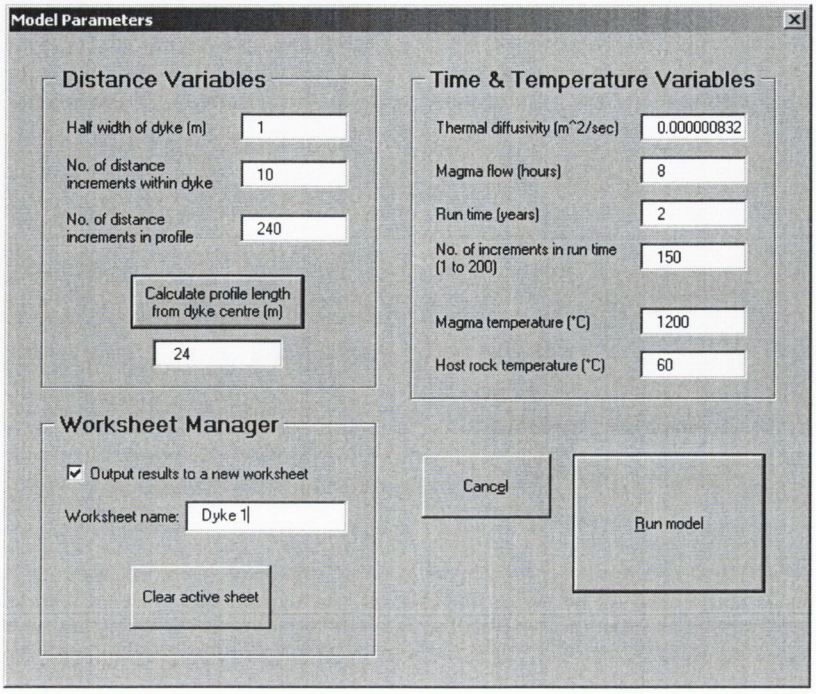

Forms

frmParameters

```
Private Sub cmdExit_Click()
        End
End Sub

**********************************************************************************************
**********************************************************************************************

Private Sub cmdClear_Click()

Clears the active sheet of its contents and formats, then reformats blank sheet into a usable state

With Worksheets(ActiveSheet.Name).Cells
        .ClearContents
        .ClearFormats
        .ColumnWidth = 12
        .HorizontalAlignment = xlLeft
        .VerticalAlignment = xlBottom
        .Font.Size = 9
        .Font.Name = geneva
        .Cells(1, 1).Select
End With

End Sub

**********************************************************************************************
**********************************************************************************************

Private Sub checkNewsheet_change()

txtSheetname.Enabled = CheckNewsheet.Value

End Sub
```

```
**********************************************************************************************
**********************************************************************************************

Private Sub cmdCalculate_Click()

Calculates profile length based on number of distance increments within dyke and whole profile.
Displays alerts if the input data is invalid

Dim DHWtxt As String
Dim Xtxt As String
Dim dykeXincrtxt As String
Dim totalXincrtxt As String
Dim check As Boolean
Dim check2(10)

DHWtxt = txtDHW
dykeXincrtxt = txtDykeXincr
totalXincrtxt = txtTotalXincr

check = IsNumeric(DHWtxt)
If check = False Then
        DHW = MsgBox("Enter a valid value for dyke half-width!", vbExclamation + vbOKOnly, "")
Exit Sub
End If
check = Val(DHWtxt) > 0
If check = False Then
        DHW = MsgBox("Enter a valid value for dyke half-width!", vbExclamation + vbOKOnly, "")
Exit Sub
End If

check = IsNumeric(dykeXincrtxt)
If check = False Then
        dykeXincr = MsgBox("Enter a valid value for no. of distance increments within dyke!", vbExclamation +
        vbOKOnly, "")
Exit Sub
End If
check = Val(dykeXincrtxt) > 0
If check = False Then
        dykeXincrtxt = MsgBox("Enter a valid value for no. of distance increments within dyke!", vbExclamation +
        vbOKOnly, "")
Exit Sub
End If
check = Val(dykeXincrtxt) < Val(totalXincrtxt)
If check = False Then
        dykeXincrtxt = MsgBox("No. of distance increments within dyke must be greater than that in profile!",
        vbExclamation + vbOKOnly, "")
Exit Sub
End If

totalXincrtxt = Replace(txtTotalXincr, ".", "dec_pt")
totalXincrtxt = Replace(txtTotalXincr, ",", "dec_pt")
check = IsNumeric(totalXincrtxt)
If check = False Then
        totalXincrtxt = MsgBox("Enter a valid integer value for no. of distance increments in profile!",
        vbExclamation + vbOKOnly, "")
Exit Sub
End If
totalXincrtxt = Replace(txtTotalXincr, ",", "dec_pt")
check = IsNumeric(totalXincrtxt)
If check = False Then
        totalXincrtxt = MsgBox("Enter a valid integer value for no. of distance increments in profile!",
        vbExclamation + vbOKOnly, "")
Exit Sub
End If

X = (Val(totalXincrtxt) * Val(DHWtxt)) / Val(dykeXincrtxt)
txtX.Text = Str(X)

cmdRun.Default = True

End Sub
```

```
**********************************************************************************************
**********************************************************************************************

Private Sub cmdRun_Click()

Runs model
Declares variables to validate input values

Dim DHWtxt As String
Dim Xtxt As String
Dim Tmtxt As String
Dim Thtxt As String
Dim diffusivtxt As String
Dim flowtxt As String
Dim runtimetxt As String
Dim columnstxt As String
Dim dykeXincrtxt As String
Dim totalXincrtxt As String
Dim check As Boolean
Dim message As Integer

Declares input variables

Dim DHW As Single
Dim X As Single
Dim Tm As Single
Dim Th As Single
Dim flow As Double
Dim diffusiv As Single
Dim runtime As Double
Dim columns As Integer
Dim totalXincr As Integer

Declares remaining variables

Dim T(), newT(), avT(), maxT()
Dim maxloop As Integer
Dim timesec As Double
Dim flowSec As Double
Dim dx, nd, dt
Dim c As Single
Dim newsheet As Boolean
Dim sheetname As String
Dim timestepcol As Single
Dim colincrement As Single
Dim colheadings As String
Dim timestring As Single
Dim iterations As Long
Dim outputstep As Long
Dim counter As Long, counter2 As Integer, ct As Long, ct2 As Long
Dim i As Integer, j As Long
Dim k As Double, g As Double
Dim outputstep2 As Long
Dim iterations2 As Long
Dim time As Double
Dim ctincrement As Boolean
Dim worksheetname As Excel.Worksheet

Assigns variables to input strings, then displays alerts if the input data is invalid

Tmtxt = txtTm
check = IsNumeric(Tmtxt)
If check = False Then
        Tmtxt = MsgBox("Enter a valid value for magma temperature!", vbExclamation + vbOKOnly, "")
Exit Sub
End If
check = Val(Tmtxt) > 800 And Val(Tmtxt) < 1500
If check = False Then
        Tmtxt = MsgBox("Enter a valid value for magma temperature!", vbExclamation + vbOKOnly, "")
Exit Sub
```

```
End If

Thtxt = txtTh
check = IsNumeric(Thtxt)
If check = False Then
        Thtxt = MsgBox("Enter a valid value for host-rock temperature!", vbExclamation + vbOKOnly, "")
Exit Sub
End If
check = Val(Thtxt) > 0 And Val(Thtxt) < 500
If check = False Then
        Thtxt = MsgBox("Enter a valid value for host-rock temperature!", vbExclamation + vbOKOnly, "")
Exit Sub
End If

runtimetxt = txtRuntime
check = IsNumeric(runtimetxt)
If check = False Then
        Thtxt = MsgBox("Enter a valid value for run time!", vbExclamation + vbOKOnly, "")
Exit Sub
End If
check = Val(runtimetxt) > 0
If check = False Then
        Thtxt = MsgBox("Enter a valid value for run time!", vbExclamation + vbOKOnly, "")
Exit Sub
End If

diffusivtxt = txtDiffusiv
check = IsNumeric(diffusivtxt)
If check = False Then
        Thtxt = MsgBox("Enter a valid value for thermal diffusivity!", vbExclamation + vbOKOnly, "")
Exit Sub
End If
check = Val(diffusivtxt) > 0 And Val(diffusivtxt) < 0.0001
If check = False Then
        Thtxt = MsgBox("Enter a valid value for thermal diffusivity!", vbExclamation + vbOKOnly, "")
Exit Sub
End If

flowtxt = txtFlow
check = IsNumeric(flowtxt)
If check = False Then
        Thtxt = MsgBox("Enter a valid value for magma flow!", vbExclamation + vbOKOnly, "")
Exit Sub
End If
check = Val(flowtxt) > 0
If check = False Then
        Thtxt = MsgBox("Enter a valid value for magma flow!", vbExclamation + vbOKOnly, "")
Exit Sub
End If

DHWtxt = txtDHW
check = IsNumeric(DHWtxt)
If check = False Then
        Thtxt = MsgBox("Enter a valid value for dyke half-width!", vbExclamation + vbOKOnly, "")
Exit Sub
End If
check = Val(DHWtxt) > 0
If check = False Then
        Thtxt = MsgBox("Enter a valid value for dyke half-width!", vbExclamation + vbOKOnly, "")
Exit Sub
End If

columnstxt = txtColumns
columnstxt = Replace(txtColumns, ".", "dec_pt")
columnstxt = Replace(txtColumns, ",", "dec_pt")
check = IsNumeric(columnstxt)
If check = False Then
        columnstxt = MsgBox("Enter a valid integer value for no. of time increments!", vbExclamation +
        vbOKOnly, "")
Exit Sub
End If
```

```
check = Val(columnstxt) > 0 And Val(columnstxt) <= 200
If check = False Then
        columnstxt = MsgBox("Enter a valid integer value for no. of time increments!", vbExclamation +
        vbOKOnly, "")
Exit Sub
End If

dykeXincrtxt = txtDykeXincr
check = IsNumeric(dykeXincrtxt)
If check = False Then
        dykeXincrtxt = MsgBox("Enter a valid value for no. of distance increments within dyke!", vbExclamation +
        vbOKOnly, "")
Exit Sub
End If

totalXincrtxt = txtTotalXincr
totalXincrtxt = Replace(txtTotalXincr, ".", "dec_pt")
totalXincrtxt = Replace(txtTotalXincr, ",", "dec_pt")
check = IsNumeric(totalXincrtxt)
If check = False Then
        totalXincrtxt = MsgBox("Enter a valid integer value for no. of distance increments in profile!",
        vbExclamation + vbOKOnly, "")
Exit Sub
End If
totalXincrtxt = Replace(txtTotalXincr, ",", "dec_pt")
check = IsNumeric(totalXincrtxt)
If check = False Then
        totalXincrtxt = MsgBox("Enter a valid integer value for no. of distance increments in profile!",
        vbExclamation + vbOKOnly, "")
Exit Sub
End If

Xtxt = txtX
If Xtxt = "" Then
        Xtxt = MsgBox("Calculate profile length!", vbExclamation + vbOKOnly, "")
Exit Sub
End If
check = ((CSng(Xtxt) = (CSng(totalXincrtxt) * CSng(DHWtxt)) / CSng(dykeXincrtxt)))
If check = False Then
        Xtxt = MsgBox("Recalculate profile length!", vbExclamation + vbOKOnly, "")
Exit Sub
End If

*****************************************************************************************

Converts input text box strings to respective numeric data types for calculation

DHW = CSng(DHWtxt)
X = CSng(Xtxt)
Tm = CSng(Tmtxt)
Th = CSng(Thtxt)
diffusiv = CDbl(diffusivtxt)
columns = CSng(columnstxt)
flow = CDbl(flowtxt)
runtime = CDbl(runtimetxt)
totalXincr = CInt(totalXincrtxt)
newsheet = CBool(CheckNewsheet)
sheetname = CStr(txtSheetname)

Alerts if about to overwrite an existing sheet

If (Not GetBottomRow = 0) And (newsheet = False) Then
        message = MsgBox("You are about to overwrite an existing sheet!  Do you want to do this?", vbExclamation
        + vbYesNo + vbDefaultButton2, "")
End If

If message = 7 Then
        message = MsgBox("Enter new worksheet name!", vbExclamation, "")
        txtSheetname.Enabled = True
        CheckNewsheet.Value = True
Exit Sub
```

```
End If

check = (txtSheetname.Enabled = True) And (sheetname = "")
If check = True Then
        message = MsgBox("Enter new worksheet name!", vbExclamation, "")
Exit Sub
End If

If txtSheetname.Enabled = True Then
        Set addnewsheet = Sheets.Add(Type:=xlWorksheet)
        ActiveSheet.Name = sheetname
End If

For i = 1 To columns + 4
        Range(Cells(1, i), Cells(2, i)).Select
        With Selection
                .Merge
                .HorizontalAlignment = xlCenter
                .VerticalAlignment = xlCenter
                .Font.Name = geneva
                .Font.Size = 9
                .Font.Bold = True
        End With
Next i

With Cells(1, 1)
        .ColumnWidth = 13
        .WrapText = True
End With

With Cells(1, 2)
        .ColumnWidth = 7
End With

With Cells(1, 3)
        .ColumnWidth = 12
End With

With Range(Cells(1, 4), Cells(1, columns + 4))
        .ColumnWidth = 14
End With

*****************************************************************************************

Defines the maximum no. of loops in the following calculations

maxloop = totalXincr + 3

Convert years to seconds

timesec = YearsToSec(runtime)
flowSec = HoursToSec(flow)

dx = X / (maxloop - 3)                  Assign distance increments
nd = Int((maxloop - 3) * DHW / X)       Assign dyke elements

*****************************************************************************************

Set "Distance" name for total element values in excel spreadsheet

Range("A1").Select
        ActiveCell.FormulaR1C1 = "Distance from dyke centre"
Range("A3").Select                      Sets initial value of Cell A2 to 0
        ActiveCell.FormulaR1C1 = 0

Populate cells with distance increments

c = 0  'Set initial distance at dyke origin

For i = 1 To maxloop – 3
        c = c + dx                      Increments distance to populate spreadsheet
        Cells(i + 3, "A").Value = c
Next i
```

Writes a record of the input parameters to bottom left of output spreadsheet

```
Cells(maxloop + 3, "A").Value = "INPUT PARAMETERS"
Cells(maxloop + 4, "A").Value = "Half width of dyke"
Cells(maxloop + 4, "B").Value = Str(DHW) + " m"
Cells(maxloop + 5, "A").Value = "No. of distance increments within dyke"
Cells(maxloop + 5, "B").Value = dykeXincrtxt
Cells(maxloop + 6, "A").Value = "No. of distance increments in profile"
Cells(maxloop + 6, "B").Value = totalXincrtxt
Cells(maxloop + 7, "A").Value = "Profile length from dyke centre"
Cells(maxloop + 7, "B").Value = Str(X) + " m"
Cells(maxloop + 8, "A").Value = "Thermal diffusivity"
Cells(maxloop + 8, "B").Value = Str(diffusiv) + " m^2/s"
Cells(maxloop + 9, "A").Value = "Magma flow"
If flow = 1 Then
        Cells(maxloop + 9, "B").Value = Str(flow) + " hour"
        Else: Cells(maxloop + 9, "B").Value = Str(flow) + " hours"
End If
Cells(maxloop + 10, "A").Value = "Run time"
If runtime = 1 Then
        Cells(maxloop + 10, "B").Value = Str(runtime) + " year"
        Else: Cells(maxloop + 10, "B").Value = Str(runtime) + " years"
End If
Cells(maxloop + 11, "A").Value = "No. of increments in run time"
Cells(maxloop + 11, "B").Value = Str(columns)
Cells(maxloop + 12, "A").Value = "Magma temperature"
Cells(maxloop + 12, "B").Value = Str(Tm) + " °C"
Cells(maxloop + 13, "A").Value = "Host rock temperature"
Cells(maxloop + 13, "B").Value = Str(Th) + " °C"

Range(Cells(maxloop + 3, "A"), Cells(maxloop + 13, "A")).Font.Bold = True
Range(Cells(maxloop + 3, "A"), Cells(maxloop + 13, "A")).Font.Italic = True
Range(Cells(maxloop + 3, "B"), Cells(maxloop + 13, "B")).Font.Bold = True
Range(Cells(maxloop + 3, "B"), Cells(maxloop + 13, "B")).Font.Italic = True

*******************************************************************************************
```

Defines size of dynamic arrays using variable, MaxLoop

```
ReDim T(maxloop + 1)
ReDim newT(maxloop + 1)
ReDim avT(maxloop + 1)
ReDim maxT(maxloop + 1)
```

Sets initial magma and host rock temperatures

```
For i = 3 To nd + 3
        T(i) = Tm                       Initial magma temp for dyke elements
        Cells(i, "B").Value = T(i)      Writes Tm to worksheet
Next i

For i = (nd + 4) To maxloop
        T(i) = Th                       Host rock temp
        Cells(i, "B").Value = T(i)      Writes intial Th to worksheet
Next i

Range("B1").Select                              Sets initial value of Cell B1 to 0
        ActiveCell.FormulaR1C1 = "T(initial)"

Range("C1").Select  'Writes "Tmax" to Cell C1
        ActiveCell.FormulaR1C1 = "T(max)"

For i = 0 To columns                    Sets up the loop for creating the correct amount of column Headings
        timestepcol = runtime / columns                 Calculates time increment of each column
        colincrement = colincrement + timestepcol       Increments time interval
        timestring = Format(colincrement, "0.0000")     Converts default number format to specified
                                                        format
        colheadings = "T after" + Str(timestring) + " Yr"       Creates column headings

        Cells(1, i + 4).Value = colheadings             Writes headings to spreadsheet
```

```
Next i

**********************************************************************************************

time = 0

dt = (dx ^ 2) / (2 * diffusiv):          Timestep calculation

iterations = CDbl(timesec) / dt          Calculates no. of computations

outputstep = iterations / columns        Increments for extracting data and writing to spreadsheet

Initialise counters

counter = 0          For extracting temperatures
k = 1                Ratio to increment excel column by 1
ct = 1
g = 0

outputstep2 = outputstep                 Outputstep2 is used for extracting time period of temperature to spreadsheet
k = k / outputstep                       Ratio to increment excel column by 1

iterations2 = iterations - (outputstep * 1)

**********************************************************************************************

For j = 0 To iterations                  No. of computations to perform
        ctincrement = True               Sets up a boolean expression for extracting the appropriate computation to
                                         spreadsheet

For i = 3 To maxloop
        If counter = Int(iterations) Then
                counter = MsgBox("Finished!", vbInformation + vbOKOnly, "")
                Cells(1, 1).Select
        End
        End If
Next i

For i = 3 To maxloop
        If newT(i) < Th Then newT(i) = Th
        If T(i + 1) = "" Then T(i + 1) = T(i)          Sets boundary condition for country rock temperature
        newT(i) = (T(i + 1) + T(i - 1)) / 2            Schmidt Plot
Next i

Smoothes plot

For i = 3 To maxloop
        avT(i) = (T(i) + T(i + 1)) / 2
Next i

counter = counter + 1
ct = ct + 1
g = g + k

ct2 = ((ct - outputstep2) + (g)) + 2          Variable used for writing T values to spreadsheet

If counter = outputstep2 Then ctincrement = False

For i = 3 To maxloop
        T(i) = newT(i)
        If ctincrement = False Then
                Cells(i, ct2).Value = avT(i)
        End If
Next i

Reset Maximum Temperature

For i = 3 To maxloop
        If avT(i) > maxT(i) Then maxT(i) = avT(i)
        If ctincrement = False Then
                Cells(i, "C").Value = maxT(i)
        End If
Next i
```

```
time = time + dt      Resets time

Holds half-dyke at initial Tm until magma flow complete

If time < flowSec Then
        For i = 3 To (nd + 4)
                T(i) = Tm
        Next i
End If

For i = 2 To maxloop
        If T(2) < T(4) Then T(2) = T(4)
Next i

T(2) = T(4)                    Dyke symmetry - boundary condition of dyke's initial temperature at each time slice

If ctincrement = False Then outputstep2 = outputstep2 + outputstep

Next j

End Sub
```

Modules

basMenus

```
Sub CreateCustomMenus()

Create custom menu on worksheets menu bar if not already present.  Use control's tag property to identify it

Dim cbcpop As CommandBarControl

Set cbcpop = Application.CommandBars("Worksheet menu bar").FindControl( _
Type:=msoControlPopup, Tag:="SchmidtPlotCustomMenu")

If Not cbcpop Is Nothing Then Exit Sub

Set cbcpop = Application.CommandBars("Worksheet menu bar").Controls.Add( _
Type:=msoControlPopup, Temporary:=True)
cbcpop.Caption = "&Schmidt Plot"

'Set tag property to find it later for deletion
cbcpop.Tag = "SchmidtPlotCustomMenu"

'Add menu item to popup menu
With cbcpop.Controls.Add(Type:=msoControlButton, Temporary:=True)
        .Caption = "&Set Parameters"
        .OnAction = "SchmidtPlot"
End With

End Sub

**********************************************************************************************
**********************************************************************************************

Sub DeleteCustomMenuItem()

Dim cbcpop As CommandBarControl
Set cbcpop = Application.CommandBars("Worksheet Menu Bar"). _
FindControl(Type:=msoControlPopup, Tag:="SchmidtPlotCustomMenu")
If Not cbcpop Is Nothing Then cbcpop.Delete
End Sub

Public Sub SchmidtPlot()
frmParameters.Show

End Sub
```

basSheetempty

```
Public Function GetBottomRow() As Long
On Error GoTo NoRow
Search the entire sheet for any data ("*" is a wildcard)
GetBottomRow = Cells.Find(what:="*", SearchOrder:=xlByRows, _
        SearchDirection:=xlPrevious).Row
Exit Function
NoRow:
        GetBottomRow = 0
End Function
```

basTime

```
Public Function YearsToSec(Value As Double) As Double
Const YearToSec As Double = 31557600
YearsToSec = Value * YearToSec
End Function
```

****

****

```
Public Function HoursToSec(Value As Double) As Double
Const HourToSec As Double = 3600
HoursToSec = Value * HourToSec
End Function
```

****

****

```
Public Function SecToYears(Value As Double) As Double
Const SecToYear As Double = 3.16880878140289E-08
SecToYears = Value * SecToYear
End Function
```

Schmidt Plot thermal modelling output data for the five dykes picked that describe the relationship between dyke width and the width of the dyke-associated fracture zone.

K12

Distance from dyke centre (m)	Maximun modelled temperature (°C)
0	1200
0.25	1200
0.5	630
0.75	437.10938
1	347.28699
1.25	292.80365
1.5	255.70433
1.75	228.83572
2	208.4814
2.25	192.5072
2.49	**180**
2.5	179.64005
2.75	169.05568
3	160.192
3.25	152.66168
3.35	**150**
3.5	146.18571
3.75	140.55585
4	135.61665
4.25	131.24875
4.33	**130**
4.5	127.35793
4.75	123.87015
5	120.72607
5.25	117.877
5.5	115.28333
5.75	112.9123
6	110.73628
6.09	**110**
6.25	108.73221
6.5	106.8805
6.75	105.16437
7	103.56947
7.25	102.0834
7.5	100.69537
7.75	99.395981
8	98.177032
8.25	97.031258
8.5	95.952248
8.75	94.934364
9	93.972534
9.25	93.062248
9.5	92.199463
9.75	91.380585
10	90.60231
10.20	**90**
10.25	89.861732
10.5	89.156143
10.75	88.483124
11	87.840492
11.25	87.226212
11.5	86.638466
11.75	86.075546
12	85.53595
12.25	85.018219
12.5	84.521049
12.75	84.043259
13	83.58374
13.25	83.141464
13.5	82.715485
13.75	82.304878
14	81.908867
14.25	81.526672
14.5	81.157578
14.75	80.800941
15	80.456108
15.25	80.12252
15.34	**80**
15.5	79.799652
15.75	79.486969
16	79.184021
16.25	78.890335
16.5	78.605515
16.75	78.32914
17	78.060883
17.25	77.800346
17.5	77.547211
17.75	77.301193
18	77.061981
18.25	76.829269
18.5	76.602837
18.75	76.382416
19	76.167755
19.25	75.958633
19.5	75.754868
19.75	75.556229
20	75.362526
20.25	75.173576

K32

0	1200
0.25	1200
0.5	1200
0.75	1200
1	1200
1.25	630
1.5	512.47552
1.75	448.50287
2	401.75568
2.25	365.42462
2.5	336.14087
2.75	312.00317
3	291.75775
3.25	274.53006
3.5	259.6893
3.75	246.77155
4	235.42444
4.25	225.37817
4.5	216.42072
4.75	208.38419
5	201.13338
5.25	194.5584
5.5	188.56892
5.75	183.09003
5.90	**180**
6	178.05913
6.25	173.42337
6.5	169.138
6.75	165.16467
7	161.4706
7.25	158.02721
7.5	154.80991
7.75	151.7971
7.91	**150**
8	148.96994
8.25	146.31168
8.5	143.80772
8.75	141.44492
9	139.21173
9.25	137.09772
9.5	135.09363
9.75	133.1911
10	131.3826
10.20	**130**
10.25	129.66135
10.5	128.02113
10.75	126.45637
11	124.96201
11.25	123.53337
11.5	122.16621
11.75	120.85666
12	119.60114
12.25	118.39639
12.5	117.23939
12.75	116.12735
13	115.05768
13.25	114.02802
13.5	113.03618
13.75	112.08009
14	111.15786
14.25	110.26773
14.33	**110**
14.5	109.40806
14.75	108.57729
15	107.77399
15.25	106.99683
15.5	106.24454
15.75	105.51598
16	104.81001
16.25	104.12561
16.5	103.46181
16.75	102.81766
17	102.19234
17.25	101.58501
17.5	100.99492
17.75	100.42134
18	99.863586
18.25	99.321045
18.5	98.793045
18.75	98.279037
19	97.778473
19.25	97.290848
19.5	96.81562
19.75	96.352379
20	95.900642
20.25	95.459984
20.5	95.030014
20.75	94.610352
21	94.20063
21.25	93.800484
21.5	93.409599
21.75	93.027649
22	92.654343
22.25	92.289375
22.5	91.932472
22.75	91.583389
23	91.241852
23.25	90.907608
23.5	90.580444
23.75	90.260132
23.96	**90**
24	89.946465
24.25	89.639214
24.5	89.338234
24.75	89.043266
25	88.754181
25.25	88.47081
25.5	88.192955
25.75	87.920471
26	87.653198
26.25	87.391006
26.5	87.133736
26.75	86.881241
27	86.633408
27.25	86.390114
27.5	86.151215
27.75	85.916595
28	85.686172
28.25	85.459778
28.5	85.237335
28.75	85.018753
29	84.803917
29.25	84.592758
29.5	84.385124
29.75	84.180984
30	83.980225
30.25	83.782753
30.5	83.588486
30.75	83.397369
31	83.209312
31.25	83.024208
31.5	82.842026
31.75	82.662689
32	82.486092
32.25	82.312218
32.5	82.140968
32.75	81.97229
33	81.806107
33.25	81.642372

33.5	81.481003	3.24	512.47552	35.100033	104.12561	68.580086	82.663368
33.75	81.321945	3.78	448.50287	35.640034	103.46181	69.120087	82.486938
34	81.165161	4.3200002	401.75568	36.180035	102.81766	69.660088	82.313248
34.25	81.010567	4.8600001	365.42462	36.720036	102.19234	70.200089	82.14222
34.5	80.858109	5.4000001	336.14087	37.260036	101.58501	70.740089	81.973793
34.75	80.707733	5.9400001	312.00317	37.800037	100.99492	71.28009	81.807899
35	80.559387	6.48	291.75775	38.340038	100.42134	71.820091	81.644485
35.25	80.413063	7.02	274.53006	38.880039	99.863586	72.360092	81.483521
35.5	80.268646	7.5599999	259.6893	39.42004	99.321045	72.900093	81.324905
35.75	80.126083	8.1000004	246.77155	39.960041	98.793045	73.440094	81.168625
35.97	**80**	8.6400003	235.42444	40.500042	98.279037	73.980095	81.014618
36	79.985413	9.1800003	225.37817	41.040043	97.778473	74.520096	80.862823
36.25	79.846481	9.7200003	216.42072	41.580044	97.290848	75.060097	80.713196
36.5	79.70929	10.26	208.38419	42.120045	96.81562	75.600098	80.565704
36.75	79.573776	10.8	201.13338	42.660046	96.352379	76.140099	80.420334
37	79.43988	11.34	194.5584	43.200047	95.900642	76.680099	80.276978
37.25	79.307541	11.88	188.56892	43.740047	95.459984	77.2201	80.135605
37.5	79.176743	12.42	183.09003	44.280048	95.030014	**77.75**	**80**
37.75	79.047424	**12.75**	**180**	44.820049	94.610352	77.760101	79.996231
38	78.919533	12.96	178.05913	45.36005	94.20063	78.300102	79.858749
38.25	78.793053	13.5	173.42337	45.900051	93.800484	78.840103	79.72316
38.5	78.667931	14.04	169.138	46.440052	93.409599	79.380104	79.589447
38.75	78.544113	14.58	165.16467	46.980053	93.027649	79.920105	79.457512
39	78.421555	15.12	161.4706	47.520054	92.654343	80.460106	79.327332
39.25	78.30024	15.66	158.02721	48.060055	92.289375	81.000107	79.198875
39.5	78.180115	16.200001	154.80991	48.600056	91.932472	81.540108	79.072098
39.75	78.061165	16.740002	151.7971	49.140057	91.583389	82.080109	78.946983
40	77.943314	**17.08**	**150**	49.680058	91.241852	82.62011	78.823502
40.25	77.826546	17.280003	148.96994	50.220058	90.907608	83.16011	78.701622
40.5	77.710846	17.820004	146.31168	50.760059	90.580444	83.700111	78.581291
40.75	77.596146	18.360004	143.80772	51.30006	90.260132	84.240112	78.462509
41	77.48243	18.900005	141.44492	**51.75**	**90**	84.780113	78.34523
41.25	77.369675	19.440006	139.21173	51.840061	89.946465	85.320114	78.229408
41.5	77.257835	19.980007	137.09772	52.380062	89.639214	85.860115	78.115044
41.75	77.146912	20.520008	135.09363	52.920063	89.338234	86.400116	78.002098
42	77.036842	21.060009	133.1911	53.460064	89.043266	86.940117	77.890541
42.25	76.927589	21.60001	131.3826	54.000065	88.754181	87.480118	77.780373
42.5	76.819138	**22.03**	**130**	54.540066	88.47081	88.020119	77.671562
42.75	76.711487	22.140011	129.66135	55.080067	88.192955	88.56012	77.564064
43	76.604599	22.680012	128.02113	55.620068	87.920471	89.100121	77.45784
43.25	76.498413	23.220013	126.45637	56.160069	87.653198	89.640121	77.352882
43.5	76.39296	23.760014	124.96201	56.700069	87.391006	90.180122	77.249245
43.75	76.28817	24.300014	123.53337	57.24007	87.133743	90.720123	77.146812
44	76.184044	24.840015	122.16621	57.780071	86.881248	91.260124	77.045586
44.25	76.080551	25.380016	120.85666	58.320072	86.633423	91.800125	76.945526
44.5	75.977684	25.920017	119.60114	58.860073	86.390121	92.340126	76.846672
44.75	75.875412	26.460018	118.39639	59.400074	86.15123	92.880127	76.748932
45	75.773697	27.000019	117.23939	59.940075	85.916618	93.420128	76.652359
45.25	75.672546	27.54002	116.12735	60.480076	85.686195	93.960129	76.556908
45.5	75.571938	28.080021	115.05768	61.020077	85.459801	94.50013	76.462509
45.75	75.47184	28.620022	114.02802	61.560078	85.237366	95.040131	76.369171
46	75.372253	29.160023	113.03618	62.100079	85.018784	95.580132	76.276863
46.25	75.273148	29.700024	112.08009	62.640079	84.803963	96.120132	76.185585
46.5	75.174515	30.240025	111.15786	63.18008	84.592812	96.660133	76.095306
46.75	75.076332	30.780025	110.26773	63.720081	84.385208	97.200134	76.00602
		30.95	**110**	64.260078	84.181091	97.740135	75.917694
K16		31.320026	109.40806	64.800079	83.98037	98.280136	75.830322
0	1200	31.860027	108.57729	65.34008	83.782944	98.820137	75.743881
0.54	1200	32.400028	107.77399	65.880081	83.58873	99.360138	75.658356
1.08	1200	32.940029	106.99683	66.420082	83.397659	99.900139	75.573746
1.6200001	1200	33.48003	106.24454	66.960083	83.209679	100.44014	75.490005
2.1600001	1200	34.020031	105.51598	67.500084	83.024658	100.98014	75.407143
2.7	630	34.560032	104.81001	68.040085	82.842583	101.52014	75.325127

102.06014	75.243965
102.60014	75.163605
103.14014	75.084061
103.68015	75.00531

K21

0	1200
0.9	1200
1.8	1200
2.6999998	1200
3.5999999	1200
4.5	630
5.4000001	512.47552
6.3000002	448.50287
7.2000003	401.75568
8.1000004	365.42462
9	336.14087
9.8999996	312.00317
10.799999	291.75775
11.699999	274.53006
12.599998	259.6893
13.499998	246.77155
14.399998	235.42444
15.299997	225.37817
16.199997	216.42072
17.099997	208.38419
17.999996	201.13338
18.899996	194.5584
19.799995	188.56892
20.699995	183.09003
21.25	**180**
21.599995	178.05913
22.499994	173.42337
23.399994	169.138
24.299994	165.16467
25.199993	161.4706
26.099993	158.02721
26.999992	154.80991
27.899992	151.7971
28.47	**150**
28.799992	148.96994
29.699991	146.31168
30.599991	143.80772
31.49999	141.44492
32.39999	139.21173
33.299992	137.09772
34.199993	135.09363
35.099995	133.1911
35.999996	131.3826
36.72	**130**
36.899998	129.66135
37.799999	128.02113
38.700001	126.45637
39.600002	124.96201
40.500004	123.53337
41.400005	122.16621
42.300007	120.85666
43.200008	119.60114
44.10001	118.39639
45.000011	117.23939
45.900013	116.12735
46.800014	115.05768
47.700016	114.02802
48.600018	113.03618
49.500019	112.08009
50.400021	111.15786
51.300022	110.26773
51.58	**110**
52.200024	109.40806
53.100025	108.57729
54.000027	107.77399
54.900028	106.99683
55.80003	106.24454
56.700031	105.51598
57.600033	104.81001
58.500034	104.12561
59.400036	103.46181
60.300037	102.81766
61.200039	102.19234
62.10004	101.58501
63.000042	100.99492
63.900043	100.42134
64.800041	99.863586
65.700043	99.321045
66.600044	98.793045
67.500046	98.279037
68.400047	97.778473
69.300049	97.290848
70.20005	96.81562
71.100052	96.352379
72.000053	95.900642
72.900055	95.459984
73.800056	95.030014
74.700058	94.610352
75.60006	94.20063
76.500061	93.800484
77.400063	93.409599
78.300064	93.027649
79.200066	92.654343
80.100067	92.289375
81.000069	91.932472
81.90007	91.583389
82.800072	91.241852
83.700073	90.907608
84.600075	90.580444
85.500076	90.260132
86.25	**90**
86.400078	89.946465
87.300079	89.639214
88.200081	89.338234
89.100082	89.043266
90.000084	88.754181
90.900085	88.47081
91.800087	88.192955
92.700089	87.920471
93.60009	87.653198
94.500092	87.391006
95.400093	87.133743
96.300095	86.881248
97.200096	86.633423
98.100098	86.390121
99.000099	86.15123
99.900101	85.916618
100.8001	85.686195
101.7001	85.459801
102.60011	85.237366
103.50011	85.018784
104.40011	84.803963
105.30011	84.592812
106.20011	84.385208
107.10011	84.181091
108.00011	83.98037
108.90012	83.782944
109.80012	83.58873
110.70012	83.397659
111.60012	83.209679
112.50012	83.024658
113.40012	82.842583
114.30013	82.663368
115.20013	82.486938
116.10013	82.313248
117.00013	82.14222
117.90013	81.973793
118.80013	81.807899
119.70013	81.644485
120.60014	81.483521
121.50014	81.324905
122.40014	81.168625
123.30014	81.014618
124.20014	80.862823
125.10014	80.713196
126.00014	80.565704
126.90015	80.420334
127.80015	80.276978
128.70015	80.135605
129.58	**80**
129.60014	79.996231
130.50014	79.858749
131.40013	79.72316
132.30013	79.589447
133.20012	79.457512
134.10011	79.327332
135.00011	79.198883
135.9001	79.072105
136.80009	78.946991
137.70009	78.823517
138.60008	78.70163
139.50008	78.581314
140.40007	78.462517
141.30006	78.345245
142.20006	78.229439
143.10005	78.115074
144.00005	78.002136
144.90004	77.890594
145.80003	77.780434
146.70003	77.671616
147.60002	77.564117
148.50002	77.457901
149.40001	77.352997
150.3	77.249359
151.2	77.146927
152.09999	77.045715
152.99998	76.945679
153.89998	76.846863
154.79997	76.749153
155.69997	76.652634
156.59996	76.557228
157.49995	76.462898
158.39995	76.369614
159.29994	76.277405
160.19994	76.186218
161.09993	76.096024
161.99992	76.006851
162.89992	75.91864
163.79991	75.83139
164.69991	75.745102
165.5999	75.659744
166.49989	75.57531
167.39989	75.491776
168.29988	75.409134
169.19987	75.32737
170.09987	75.246468
170.99986	75.166412
171.89986	75.087196
172.79985	75.008804

DK2

0	1200
2.5	1200
5	1200
7.5	1200
10	1200
12.5	630
15	512.47552
17.5	448.50287
20	401.75568
22.5	365.42462
25	336.14087
27.5	312.00317
30	291.75775
32.5	274.53006
35	259.6893
37.5	246.77155
40	235.42444
42.5	225.37817
45	216.42072
47.5	208.38419
50	201.13338
52.5	194.5584
55	188.56892
57.5	183.09003
59.04	**180**
60	178.05913
62.5	173.42337
65	169.138
67.5	165.16467
70	161.4706
72.5	158.02721
75	154.80991
77.5	151.7971
79.09	**150**
80	148.96994
82.5	146.31168
85	143.80772
87.5	141.44492
90	139.21173
92.5	137.09772
95	135.09363
97.5	133.1911
100	131.3826
102.01	**130**
102.5	129.66135

105	128.02113	257.5	87.920471	412.5	77.441116
107.5	126.45637	260	87.653198	415	77.334396
110	124.96201	262.5	87.391006	417.5	77.22879
112.5	123.53337	265	87.133743	420	77.124268
115	122.16621	267.5	86.881248	422.5	77.020782
117.5	120.85666	270	86.633423	425	76.918297
120	119.60114	272.5	86.390121	427.5	76.816856
122.5	118.39639	275	86.15123	430	76.71637
125	117.23939	277.5	85.916618	432.5	76.616829
127.5	116.12735	280	85.686195	435	76.518196
130	115.05768	282.5	85.459801	437.5	76.420456
132.5	114.02802	285	85.237366	440	76.323578
135	113.03618	287.5	85.018784	442.5	76.227539
137.5	112.08009	290	84.803963	445	76.132301
140	111.15786	292.5	84.592812	447.5	76.037842
142.5	110.26773	295	84.385208	450	75.944153
143.28	**110**	297.5	84.181091	452.5	75.851181
145	109.40806	300	83.98037	455	75.758934
147.5	108.57729	302.5	83.782944	457.5	75.667397
150	107.77399	305	83.588722	460	75.576515
152.5	106.99683	307.5	83.397652	462.5	75.486313
155	106.24454	310	83.209671	465	75.396729
157.5	105.51598	312.5	83.024651	467.5	75.30777
160	104.81001	315	82.842567	470	75.219406
162.5	104.12561	317.5	82.663353	472.5	75.131638
165	103.46181	320	82.486916	475	75.044434
167.5	102.81766	322.5	82.31321		
170	102.19234	325	82.142151		
172.5	101.58501	327.5	81.973709		
175	100.99492	330	81.807808		
177.5	100.42134	332.5	81.644379		
180	99.863586	335	81.483368		
182.5	99.321045	337.5	81.324722		
185	98.793045	340	81.168404		
187.5	98.279037	342.5	81.014343		
190	97.778473	345	80.862473		
192.5	97.290848	347.5	80.712784		
195	96.81562	350	80.565208		
197.5	96.352379	352.5	80.419724		
200	95.900642	355	80.276237		
202.5	95.459984	357.5	80.13472		
205	95.030014	**359.91**	**80**		
207.5	94.610352	360	79.995193		
210	94.20063	362.5	79.857529		
212.5	93.800484	365	79.721741		
215	93.409599	367.5	79.587784		
217.5	93.027649	370	79.455574		
220	92.654343	372.5	79.325073		
222.5	92.289375	375	79.196243		
225	91.932472	377.5	79.069077		
227.5	91.583389	380	78.943512		
230	91.241852	382.5	78.819511		
232.5	90.907608	385	78.697044		
235	90.580444	387.5	78.576065		
237.5	90.260132	390	78.456551		
239.57	**90**	392.5	78.33847		
240	89.946465	395	78.221764		
242.5	89.639214	397.5	78.106445		
245	89.338234	400	77.992424		
247.5	89.043266	402.5	77.879692		
250	88.754181	405	77.76825		
252.5	88.47081	407.5	77.65802		
255	88.192955	410	77.548996		

Appendix 18 Conjugate vein data from the dyke 'offset' in the Corvock granite

Data collected from the Corvock granite (south Co. Mayo), adjacent to the NNW-SSE fault.
Data is tabulated in blocks (separated by thick grey lines) corresponding to localities shown in Figure 4.4, moving southeast from the northwest end of the fault. Each block contains conjugate pairs (separated by dashed lines), for each of which the acute and obtuse angle bisecting lines correspond to the interpreted maximum (σ_1) and minimum (σ_3) compression directions respectively.

Orientation of conjugate pairs (strike/dip)	σ_1 (azimuth/plunge)	σ_3 (azimuth/plunge)
020/78SE 159/58SW	349/49	091/11
005/83SE 145/66SW	339/39	076/9
022/73SE 001/80NW	016/53	281/4
005/88SE 140/76NE	160/15	253/9
179/69NE 160/53SW	325/72	080/8
017/81SE 153/63SW	348/41	086/10
002/71SE 122/63SW	329/40	063/5
006/81SE 153/83SW	350/26	259/1
031/83SE 173/81SW	012/23	102/1

Orientation of conjugate pairs (strike/dip)	σ_1 (azimuth/plunge)	σ_3 (azimuth/plunge)
042/80SE 166/67SW	010/32	105/7
017/90 162/58SW	345/43	091/17
023/73SE 160/53NE	169/25	274/29
031/65SE 147/87SW	003/25	267/13
029/88NW 162/80NE	185/15	276/4
034/82SE 149/78NE	181/4	272/12
047/63NW 002/58NW	021/6	115/31
033/77NW 164/88SW	190/13	098/8
022/67NW 155/84NE	184/33	088/9

Orientation of conjugate pairs (strike/dip)	σ_1 (azimuth/plunge)	σ_3 (azimuth/plunge)
030/71NW 166/75SW	190/5	098/18
048/60SE 167/51NE	192/9	289/39
033/72SE 000/23SE	142/43	294/43
008/90 175/75NE	173/49	272/8
028/82SE 164/70NE	182/16	277/15
035/72SE 000/80SE	021/13	287/15
045/85SE 002/83SE	203/3	294/6
022/75SE 164/77SW	004/37	273/1

Appendix 19 Structural data from faulted dyke, K85, Downpatrick Head

Data from faulted dyke, K85, at Downpatrick Head west, north Co. Mayo (plotted in Figure 4.7).

Faults:

Sinistral, 024/86NW (pole, 114/4)
Dextral, 159/86SW (pole, 069/4)
Cooling joint accommodating flexural slip, 021/80SE (pole, 291/10)
Slip lineation pitch, 6NE
Slip vector, 022/5.9 (azimuth correction 1.05)

Note, 'Azimuth correction' is the value (in degrees) that is added to the strike of the slip plane in order to derive the azimuth of the slip vector. The following relationships are used to derive the slip vector:

$$Azimuthcorrection = \tan^{-1}[\tan\ pitch \times \cos dip]$$

$$Plunge = \sin^{-1}[\sin\ pitch \times \sin dip]$$

Palaeostress principal stress axes:

Maximum compressive stress (σ_1), 181.5/1
Minimum compressive stress (σ_3), 091.5/4.3

Common plane containing poles to fault planes and principal stress axes, 001.5/4.3SE

Slip plane data collected from St John's Point peninsula Co. Donegal.
The slip vectors are derived as described in Appendix 19. The palaeostress orientations σ_1, σ_2 and σ_3 (maximum, intermediate and minimum principal compressive stress directions respectively) are derived using the geometry described in Figure. 4.6.

Most of the fault displacements were measured either in the horizontal plane of the host rock platform, or in the vertical plane of the cliff section.

(n/d = not distinguishable.)

	Fault plane orientation	Fault displacment (m)	Pitch of slickenfibres	Azimuth/Plunge of slip vector	σ_1	σ_2	σ_3
Group A							
F1	078/60SE	1.5 (hor. plane)	25SW	245/21	028/5	125/52	294/38
F1a	046/60SE	~0.3	4NE	048/3	n/a	n/a	n/a
F1b	027/63SE	n/d	8NE	031/7	n/a	n/a	n/a
F1c	005/78SE	n/d	n/d	n/a	n/a	n/a	n/a
F1c	178/78NE	n/d	5NW	359/5	n/a	n/a	n/a
F1c	008/78SE	n/d	n/d	n/a	n/a	n/a	n/a
F2	099/52SW	n/d	21NW	266/16	052/14	157/47	310/40
Group B							
F3	085/74SE	~2 (hor. plane)	45SW	250/43	n/a	n/a	n/a
Minor fault - synthetic	134/65NE	0.21 (vert. plane)	n/d	n/a	antithetics below all use synthetic as conjugate		
Minor fault - antithetic	070/62SE	0.29 (vert. plane)	n/d	n/a	281/43	104/47	012/2
Minor fault - antithetic	075/55SE	0.24 (vert. plane)	n/d	n/a	279/49	111/40	016/6
Minor fault - antithetic	077/50SE	0.30 (vert. plane)	n/d	n/a	277/53	114/36	018/9
Minor fault	132/79NE	0.11 (vert. plane)	n/d	n/a	n/a	n/a	n/a
Minor fault	126/79NE	0.11 (vert. plane)	n/d	n/a	n/a	n/a	n/a

Slip plane data collected from Drogan, Doonan and Drumskew quarries, and from the A46 road cutting, Co. Fermanagh.

Column headings are mainly self-explanatory from the text. 'Azimuth correction' is the value (in degrees) that is added to, or subtracted from, the strike of the slip plane in order to derive the azimuth of the slip vector. The following relationships are used to derive the slip vector:

$$Azimuthcorrection = \tan^{-1}[\tan pitch \times \cos dip]; \quad Plunge = \sin^{-1}[\sin pitch \times \sin dip].$$

For 'slip-sense': S = sinistral; D = dextral; N = normal; R = reverse; ext. = extensional (fibres perpendicular to fracture plane); n/d = slip sense not distinguishable.

Face number	Slip plane (strike/dip)	Pitch of slickenfibres	Azimuth correction	Slip vector (azimuth/plunge)	Slip-sense
Drogan quarry					
1	067/88NW	11SW	0	247/11	SN
	078/70SE	12SW	4	254/11	SR
	049/72SE	8SW	2	227/8	SR
	070/75SE	3SW	1	249/3	SR
	068/72SE	10SW	3	245/10	SR
	064/87NW	12SW	1	245/12	SN
	078/87NW	4SW	0	258/4	SN
	052/70SE	9SW	3	229/8	SR
	077/89SE	22SW	0	257/22	SR
	063/76SE	22SW	6	237/21	SR
	053/76NW	12SW	3	236/12	SN
	057/72NW	17SW	5	242/16	SN
2	070/63SE	21SW	10	240/19	SR
	057/52SE	12SW	7	230/9	SR
	049/74SE	13SW	4	225/12	SR
	042/32SE	10SW	9	213/5	SR
	063/55SE	13SW	8	235/11	SR
	148/73NE	n/a	n/a	n/a	ext.
	147/77NE	n/a	n/a	n/a	ext.
	149/75NE	n/a	n/a	n/a	ext.
	040/85NW	14SW	1	221/14	SN
	044/90	10SW	0	224/10	nd
	036/53NW	15NE	9	027/12	SR
3	036/82SE	2NE	0	036/2	SN
	034/80SE	2SW	0	214/2	SR
	015/79SE	8NE	2	017/8	nd
	149/90	n/a	n/a	n/a	ext.
	052/84NW	14SW	1	233/14	SN
	048/85NW	5SW	0	228/5	SN
	042/85NW	2NE	0	042/2	SR
	136/80NE	8NW	1	317/8	DR
	040/80NW	46SW	10	230/45	SN
	140/87NE	9NW	0	320/9	nd
	053/85NW	5SW	0	233/5	nd
	050/78NW	11SW	2	232/11	SN
	059/87NW	30SW	2	241/30	nd
	157/83NE	3NW	0	337/3	nd
Doonan quarry					
1	046/58NW	3NE	2	044/3	SR
	056/88NW	7SW	0	236/7	SN
	043/79NW	8SW	2	225/8	SN
	166/82NE	2NW	0	346/2	SN
	158/82NE	7NW	1	339/7	DR
	155/82NE	5NW	1	336/5	DR
	062/88NW	15SW	1	243/15	nd
	055/87NW	11SW	1	236/11	SN
	049/86NW	5SW	0	229/5	SN
	060/85SE	2SW	0	240/2	SR
	148/83NE	37NW	5	333/37	DR
	143/75NE	38NW	11	334/36	DR
	146/80NE	58NW	16	342/57	DR
	065/83NW	25SW	3	248/25	SN
	145/80NE	67NW	22	347/65	DR
	052/74SE	9NE	2	054/9	SN
	043/85NW	7SW	1	224/7	SN
	047/77NW	6SW	1	228/6	SN
	055/90	10SW	0	235/10	SR
2	149/73NE	32NW	10	339/30	DR
	150/75NE	24NW	7	337/23	DR
	050/77SE	9SW	2	228/9	SR
	063/67SE	11SW	4	239/10	SR
	057/87SE	10SW	1	236/10	SR
	147/67NE	25NW	10	337/23	DR
	049/82NW	11SW	2	231/11	SN
	159/73NE	62NW	29	008/58	DR
	151/79NE	27NW	6	337/26	DR
	057/82SE	13SW	2	235/13	SR
	050/84NW	1NE	0	050/1	SR
	160/79NE	10NW	2	342/10	DR
	154/85NE	7NW	1	335/7	DR
	158/84NE	60NW	10	348/59	DR
	144/72NE	17NW	5	329/16	DR
	145/79NE	7NW	1	326/7	DR
	060/88SE	2SW	0	240/2	SR
	067/82SE	2SW	0	247/2	SR
	050/88SE	4SW	0	230/4	SR
	158/78NE	10NW	2	340/10	DR
	016/83SE	8NE	1	017/8	SN
	064/83NW	0	0	064/0	S
3	055/85SE	12SW	1	234/12	SR
	162/76NE	36NW	10	352/35	DR
	162/80NE	24NW	4	346/24	DR
	156/87NE	15NW	1	337/15	DR
	045/73SE	23SW	7	218/22	SR
	046/76SE	12SW	3	223/12	nd
5	050/82NW	6SW	1	231/6	SN
	055/82SE	16SW	2	233/16	SR
	047/80NW	2SW	0	227/2	SN
	053/90	7SW	0	233/7	SR
	053/71SE	22SW	7	226/21	SR
	053/60SE	8NE	4	057/7	SN
	044/65SE	14SW	6	218/13	SR
	045/57SE	21SW	12	213/17	SR
	048/58SE	10SW	5	223/8	SR
	050/58SE	14SW	8	222/12	SR
	049/78SE	3SW	1	228/3	SR
	041/78NW	1SW	0	221/1	SN
	050/60SE	10SW	5	225/9	SR
	071/49SE	40SW	29	222/29	SR
	153/83NE	10NW	1	334/10	DR
	031/80NW	8SW	1	212/8	SN
	048/65NW	10NE	4	044/9	SR
	045/73NW	8NE	2	043/8	SR
	036/72SE	15SW	5	211/14	SR
	046/87SE	2NE	0	046/2	SN
	047/77SE	3SW	1	226/3	SR
6	045/83SE	12SW	1	224/12	SR
	052/82NW	10SW	1	233/10	SN
	053/73SE	4SW	1	232/4	SR
	057/77SE	16SW	4	233/16	SR
	054/90	11SW	0	234/11	SR
	047/83SE	0	0	047/0	S
	050/78SE	2NE	0	050/2	SN
	150/82NE	11NW	2	332/11	nd
	049/65SE	9SW	4	225/8	SR
	044/80SE	5SW	1	223/5	SR
	034/80NW	0	0	034/0	S
	043/82SE	3SW	0	223/3	SR
	053/82NW	6SW	1	234/6	SN
	051/70NW	3SW	1	232/3	SN
	042/80NW	4SW	1	223/4	SN
	045/67NW	0	0	045/0	S
	049/70SE	5SW	2	227/5	SR
	056/85SE	7SW	1	235/7	SR
	047/90	5SW	0	227/5	SN
	049/90	6SW	0	229/6	SN
	046/77SE	3SW	1	225/3	SR
	160/82SW	8SE	1	161/8	DR
	054/86NW	7NE	0	054/7	SR
	043/85NW	7NE	1	042/7	DN
	045/75SE	7SW	2	223/7	SR
	136/75SW	3NW	1	315/3	DN
7	038/57SE	6SW	3	215/5	SR
	045/58SE	5SW	3	222/4	SR
	043/68SE	24SW	9	214/22	SR
	052/72NW	8SW	2	234/8	SN
	038/81SE	22SW	4	214/22	SR
	043/73NW	8SW	2	225/8	SN
	045/84SE	5SW	1	224/5	SR
8	112/87SW	17NW	1	291/17	DN
	111/84SW	6NW	1	290/6	DN
	049/80SE	0	0	049/0	S
	049/88SE	3NE	0	049/3	SN
	048/82SE	1SW	0	228/1	SR
	046/84SE	10SW	1	225/10	SR
9	052/79SE	4SW	1	231/4	SR
	051/67SE	4SW	2	229/4	SR
	043/75SE	5SW	1	222/5	SR
	043/70SE	4SW	1	222/4	SR
	124/85NE	13NW	1	305/13	DR
	145/82NE	40NW	7	332/40	DR
	130/83NE	15NW	2	312/15	DR
	132/75NE	8NW	2	314/8	DR
	053/82SE	4SW	1	232/4	SR
	135/80NE	30NW	6	321/29	DR
	148/85NE	12SE	1	147/12	DN
	047/63SE	4SW	2	225/4	SR
	052/69SE	5SW	2	230/5	SR
	051/64SE	4SW	2	229/4	SR
	150/86NE	6NW	0	330/6	DR
	051/82SE	4SW	1	230/4	SR
	153/85NE	10NW	1	334/10	DR
	146/82NE	12NW	2	328/12	DR
	052/68NW	5NE	2	050/5	SR
	157/85SW	4SE	0	157/4	DR
	044/73SE	11SW	3	221/11	SR
	041/74SE	2NE	1	042/2	SN
10	048/78NW	3NE	1	047/3	SR
	118/88NE	8NW	0	298/8	DR
11	042/85NW	7NE	1	041/7	SR
	052/74SE	4NE	1	053/4	SN
	037/62SE	9SW	4	213/8	SR
	032/40SE	2SW	2	210/1	SR
	045/85SE	12SW	1	224/12	SR
	054/88NW	0	0	054/0	S
	048/75NW	2NE	1	047/2	SR
	067/85SE	1NE	0	067/1	SN
	043/76SE	5NE	1	044/5	SN
	041/75NW	4NE	1	040/4	SR
	032/85NW	2SW	0	212/2	SN
	152/90	3NW	0	332/3	DR
	047/85NW	1NE	0	047/1	SR
	041/90	0	0	041/0	S
	123/90	5NW	0	303/5	DR
Drumskew quarry					
1	142/85NE	2NW	0	322/2	nd
	132/85SW	28NW	3	309/28	nd
	000/87W	12S	1	181/12	SN
	144/87SW	12SE	1	145/12	SN
	128/85SW	0	0	128/0	D
	117/85SW	10NW	1	296/10	DN
	002/85SE	5SW	0	182/5	SR
2	032/73NW	13SW	4	216/12	SN
	030/70NW	19SW	7	217/18	DR
	051/82NW	2NE	0	051/2	DN
	028/52NW	88NE	87	301/52	SR
	044/85NW	30NE	3	041/30	SR
	115/83SW	5NW	1	294/5	DN
	131/73NE	1SE	0	131/1	DN
	135/85NE	3SE	0	135/3	DN
A46 road cutting					
	042/78NW	5SW	1	223/5	SN

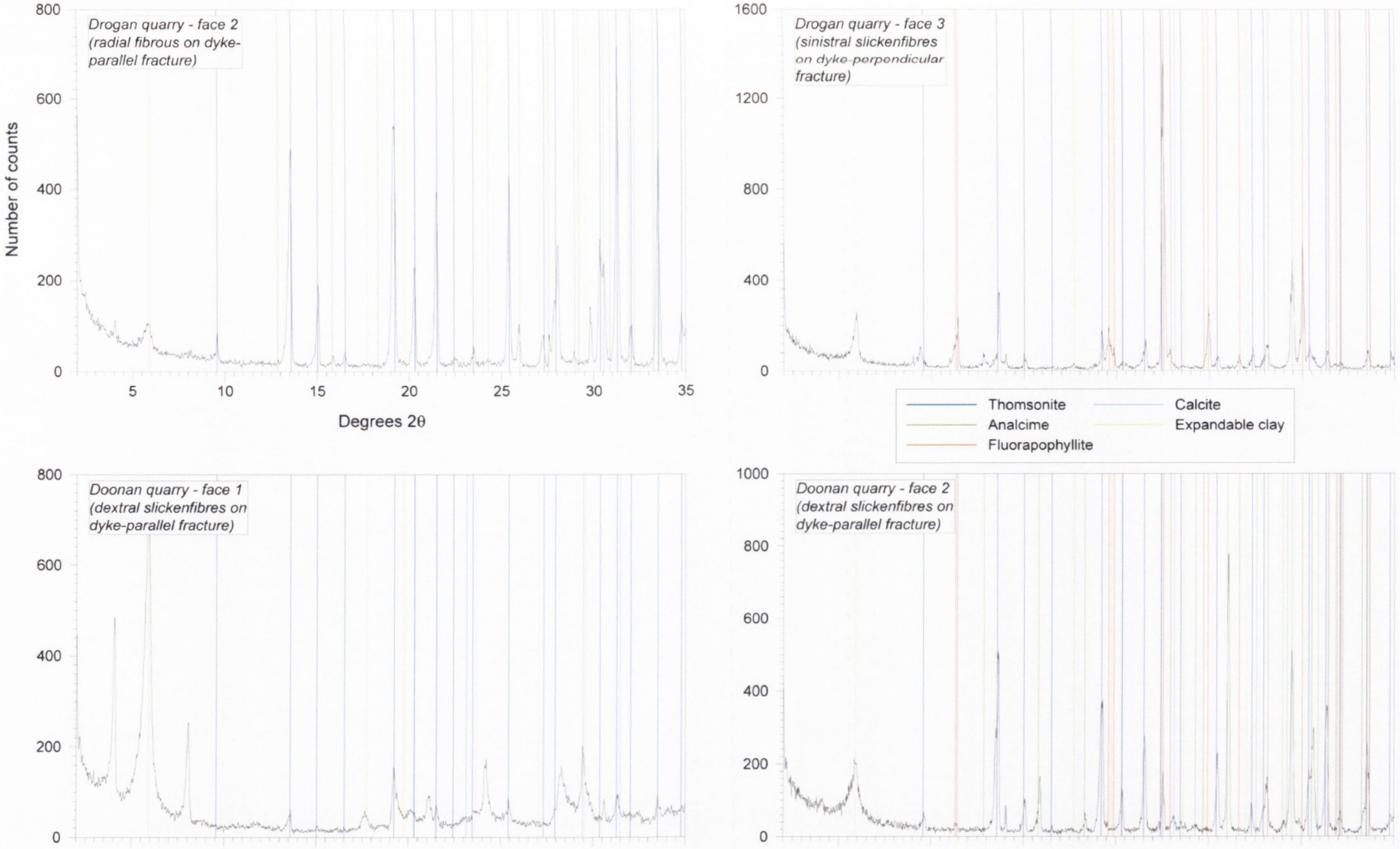
Drogan quarry - face 2
(radial fibrous on dyke-parallel fracture)
Drogan quarry - face 3
(sinistral slickenfibres on dyke-perpendicular fracture)
Doonan quarry - face 1
(dextral slickenfibres on dyke-parallel fracture)
Doonan quarry - face 2
(dextral slickenfibres on dyke-parallel fracture)
Number of counts
Degrees 2θ
Thomsonite
Analcime
Fluorapophyllite
Calcite
Expandable clay

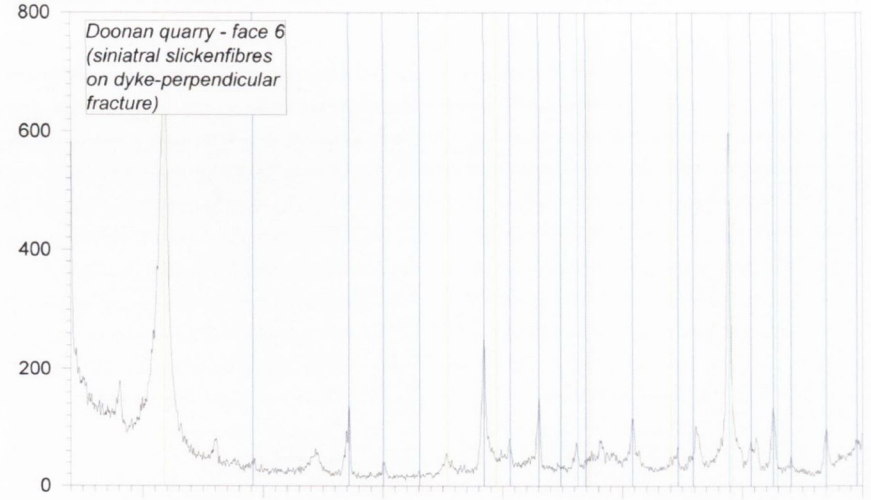
Doonan quarry - face 6
(siniatral slickenfibres
on dyke-perpendicular
fracture)
800
600
400
200
0

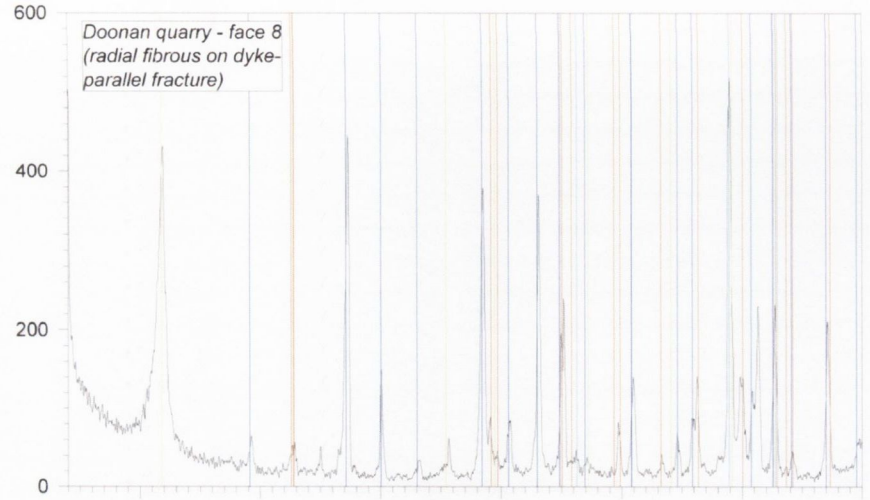
Doonan quarry - face 8
(radial fibrous on dyke-
parallel fracture)
600
400
200
0

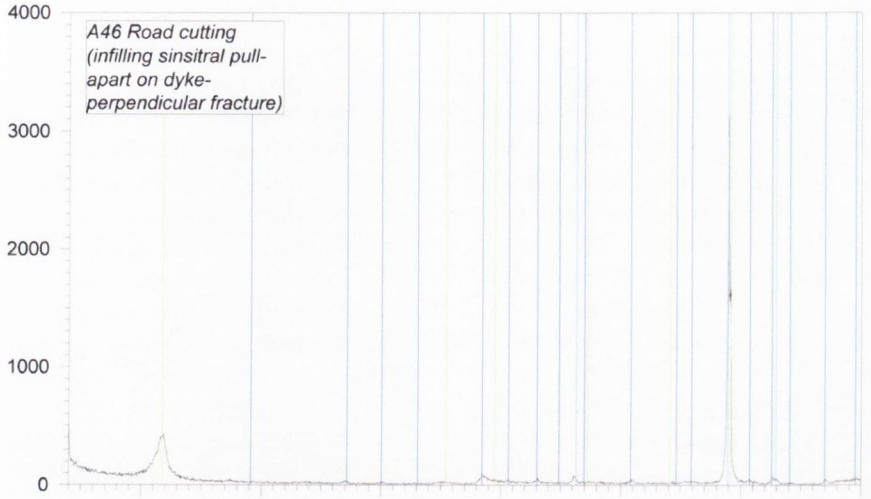
A46 Road cutting
(infilling sinsitral pull-
apart on dyke-
perpendicular fracture)
4000
3000
2000
1000
0

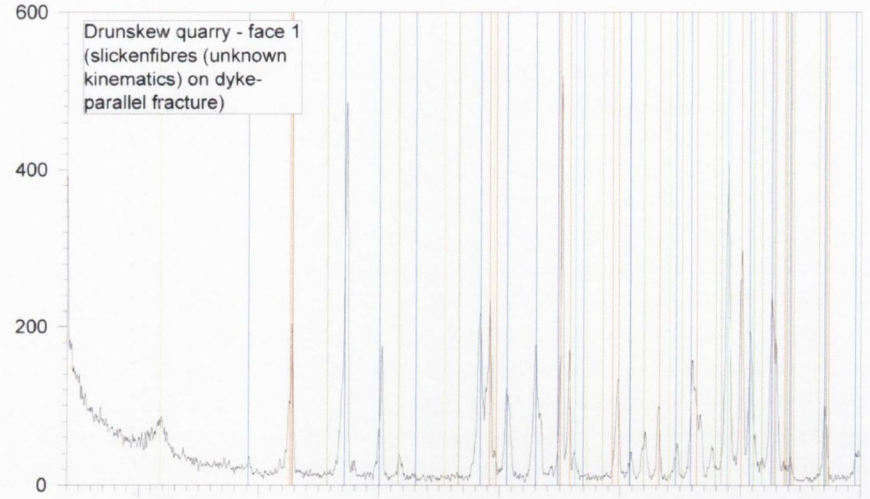
Drunskew quarry - face 1
(slickenfibres (unknown
kinematics) on dyke-
parallel fracture)
600
400
200
0

Slip plane data collected from Carn quarry, Co. Fermanagh.
The slip vectors are derived as described in Appendix 19.
For 'slip sense': S = sinistral; D = dextral; N = normal; R = reverse. n/d = not distinguishable.
The numbers in brackets (after the throw) refer to the calculated fault displacement, as described in Figure 4.28.

Reference (shear/fault no.)	Orientation of plane	Dyke width (m)	Pitch of slickenfibres	Azimuth/Plunge of slip vector	Slip sense	Throw on fault or across dyke (m)	Strike/dip of host rock strata	Type of structure
Figure 4.23								
	123/84NE	~3.1				n/d		Dyke (segment 2)
1	135/70NE	1.9	4NW	316/4	DR	n/d		Sheared margin of dyke segment 1
2	135/78NE		2SE	135/2	DN			Sheared margin of dyke segment 1
3	087/90		5NE	087/5	S			Shears in host rock
4	132/78NE		17SE	128/17	DN			Shears in host rock
5			35SE	124/34	n/d			Shears in host rock
6	132/78NE		30SE	125/29	n/d			Shears in host rock
7	142/77NE		64SE	117/61	DN			Shear facilitating opening of pull-apart
8	143/82NE		30SE	138/30	n/d			Shear facilitating opening of pull-apart
Figure 4.25								
	138/76NE	2.8	15			1.1 (6.5)	070/5SE	Dyke segment 2 (upper working level)
	128/82NE	4-5				1.5	083/8SE	Dyke segment 2 (quarry floor)
1	135/75NE		25SE	128/24	DN			Sheared margin of dyke segment 2
2	115/77NE		20SE	110/19	DN			Sheared host rock wall (dyke segment 3
			59SE	094/57	DN			margin) with rotation
3	002/86SE		21SW	180/21	DN			Shear in host rock
4	113/80SW		15SE	116/15	DR			Shear in dyke segment 2
5	116/37SW		56NW	246/30	n/d			Shear in dyke segment 2
6	120/77NE		6SE	119/6	DN			Sheared margin of dyke segment 2
7	136/78NE		15SE	133/15	DN			Shear in host rock
8	151/73NE		10NW	334/10	DR			Sheared reg./irreg. boundary in dyke segment 2
9	119/77NE		62NW	322/59	DR			Flower structure shear with rotation
			5SE	118/5	DN			Flower structure shear with rotation
10	94/65SW		85SE	172/65	DR			Flower structure shear with rotation
			64SE	135/55	DR			Flower structure shear with rotation
11	100/56SW		63SE	148/48	DR			Flower structure shears
12	120/62NE		72SE	065/57	SR			Flower structure shears
13	115/32SW		80SE	193/31	SN			Flower structure shears
14	115/77NE		45SE	102/44	DN	n/d		Sheared margin of dyke segment 3
15	123/82NE	~1.95	7SE	122/7	DN			Sheared margin of dyke segment 3
16	127/86NE	~2.1	5SE	127/5	DN		077/15SE	Sheared margin of dyke segment 3
17	123/82NE		5SE	122/5	DN			Sheared reg./irreg. boundary in dyke segment 3
	040/32SE		60SW	164/27	n/d			Shears in irregular part of dyke segment 3
	038/55SE		0	038/0	n/d			Shears in irregular part of dyke segment 3
	045/25SE		25SW	202/10	n/d			Shears in irregular part of dyke segment 3
	082/68NW		4NE	080/4	n/d			Shears in irregular part of dyke segment 3
	085/85NW		3NE	085/3	n/d			Shears in irregular part of dyke segment 3
	070/30NW		22NE	051/11	n/d			Shears in irregular part of dyke segment 3
	038/64NW		63SW	259/53	n/d			Shears in irregular part of dyke segment 3
	046/40SE		3NE	048/2	n/d			Shears in irregular part of dyke segment 3
Figure 4.28								
F1	144/76NE		38SE	133/37	DN	1.7 (3.91)		Fault
F2i	159/85NE		15SE	158/15	n/d	0.06 (0.68)		Fault
F2i	159/85NE		5SE	159/5	SR	0.01 (0.12)		Fault
F2ii	154/87NE		13SE	153/13	DN	0.27 (5.09)	078/10SE	Fault
F3i	166/85NE		12SE	165/12	n/d	0.115 (3.26)		Fault
F3ii	160/85NE		8SE	159/8	n/d	0.11 (-3.12)	075/10SE	Fault
F4i	162/84NE		12SE	161/12	DN	0.35 (9.93)	081/10SE	Fault
F4ii	163/85NE	0.35	18SE	161/18	n/d	0.65 (12.04)	076/15SE	Dyke emplaced along fault
F4iii	170/82NE	0.17	12SE	168/12	n/d	0.5 (-14.04)	086/14SE	Dyke emplaced along fault

Data from Allen *et al.* (2002) with modifications and addition of modelled palaeotemperatures.
Data origin: 1 – TULIP (Tertiary Uplift of Ireland Project, Department of Geology, Trinity College); 2 – previously Gleadow (unpublished); 3 - previously McCulloch (unpublished); 4 – Green *et al.* (2000); 5 – Keeley *et al.* (1993); 6 – McCulloch (1993); 7 – McCulloch (1994).
Fission track age types are given by: c=central age; p=pooled age; m=mean age. McCulloch (unpublished) and Gleadow (unpublished) age types are unknown but will be either pooled or mean.
Quoted age uncertainties are $\pm 1\sigma$ except those marked with * which are $\pm 2\sigma$. **McCulloch (unpublished) age uncertainties are unknown.
Quoted mean track length uncertainties are $\pm 1\sigma$.

Sample no.	Data origin	Grid reference		County	Stratigraphic age	Lithology	Elevation above sea level (m)	Fission Track Analysis			Thermal modelling			
											Laslett *et al.* (1987)		Gallagher	
		Easting	Northing					Fission track age (Ma)	Mean track length (µm)	Standard deviation (µm)	Temp. 65 Ma	Temp. 59 Ma	Temp. 65 Ma	Temp. 59 Ma
BS1	1	204527	369089	Donegal	Precambrian	Psammite	154	151.0±8.0 [c]	12.75±0.16	1.70	65.892	66.296	46.768	47.119
F1	1	202500	385400	Donegal	Devonian	Granite	100	189.0±7.0 [c]	12.84±0.14	1.77	42.496	43.042	43.068	44.475
MT1	1	184980	378454	Donegal	Carboniferous	Sandstone	70	191.0±8.0 [c]	12.35±0.20	2.33	64.006	61.470	50.439	48.574
F9	1	326850	326277	Down	Silurian	Quartzite	335	197.0±12.0 [c]	12.87±0.25	1.47	49.661	50.151	47.016	47.535
GG3	1	79610	242400	Galway	Devonian	Granite	10	197.0±10.0 [c]	12.98±0.11	1.49	55.276	55.651	47.544	46.194
GG9	1	82860	231453	Galway	Devonian	Granite	140	138.0±6.0 [c]	13.80±0.15	1.71	52.706	52.706	40.134	37.360
GG12	1	101740	228360	Galway	Devonian	Granite	164	141.0±4.0 [c]	13.11±0.10	1.37	59.560	50.399	53.344	53.647
GG13	1	109360	222060	Galway	Devonian	Granite	0	128.0±5.0 [c]	12.82±0.13	1.85	50.354	50.790	45.392	44.813
GG15	1	122590	225470	Galway	Devonian	Granite	70	152.0±7.0 [c]	13.09±0.17	2.00	55.624	56.207	41.464	42.469
IG1	1	56490	244670	Galway	Devonian	Granite	3	142.0±6.0 [c]	12.50±0.12	1.75	79.326	78.658	59.234	59.526
CL1	1	56890	257770	Galway	Devonian	Granite	20	146.0±5.0 [c]	12.98±0.11	1.57	50.550	51.094	43.423	42.377
LE	1	104900	267000	Mayo	Ordovician	Sandstone	248	275.0±28.0 [c]	12.79±0.58	2.64	59.097	59.328	42.092	42.741
GL	1	105900	270800	Mayo	Ordovician	Sandstone	225	200.0±23.0 [c]	12.60±0.30	1.91	56.392	56.719	41.783	42.152
CG1	1	85170	274020	Mayo	Devonian	Granite	388	172.0±8.0 [c]	13.23±0.19	1.51	57.110	57.372	44.901	45.141
OM1	1	164223	327635	Sligo	Dalradian	Paragneiss	60	159.0±7.0 [c]	12.79±0.11	1.40	62.205	62.471	43.038	43.488
OM2	1	123383	304852	Mayo	Silurian	Granite	11	159.0±7.0 [c]	13.27±0.11	1.31	60.179	60.412	48.865	49.176
LG2	1	321580	228571	Dublin	Devonian	Granite	25	165.0±4.0 [c]	12.43±0.15	2.11	51.136	51.487	42.668	43.177
LG3	1	325700	228000	Dublin	Devonian	Granite	2	138.0±4.0 [c]	12.91±0.16	1.97	54.006	54.351	46.988	47.492
LG5	1	326450	226040	Dublin	Devonian	Granite	90	142.0±5.0 [c]	12.85±0.12	1.72	52.540	53.313	37.687	38.077
LG6	1	326247	226304	Dublin	Devonian	Granite	115	133.0±5.0 [c]	12.42±0.15	2.09	52.725	53.180	42.659	43.171
LG7	1	325990	225550	Dublin	Devonian	Granite	150	127.0±4.0 [c]	12.85±0.15	1.87	49.873	50.328	43.464	43.419
LG8	1	327135	226371	Dublin	Devonian	Granite	2	131.0±4.0 [c]	12.60±0.15	2.14	51.727	52.207	39.203	39.717
LG10	1	324100	225459	Dublin	Devonian	Granite	40	151.0±6.0 [c]	12.53±0.27	2.20	75.572	63.539	55.940	51.578
LG11	1	318739	223458	Dublin	Devonian	Granite	240	166.0±4.0 [c]	12.55±0.12	1.73	54.148	54.618	46.328	47.284
LG12	1	317890	224230	Dublin	Devonian	Granite	250	169.0±4.0 [c]	12.24±0.12	1.71	59.330	58.545	46.336	46.908
LG13	1	317600	223400	Dublin	Devonian	Granite	450	181.0±5.0 [c]	12.28±0.13	1.85	68.121	65.818	54.885	54.117
LG14	1	315090	218000	Wicklow	Devonian	Granite	400	177.0±5.0 [c]	12.78±0.12	1.64	51.287	51.867	45.853	46.752
LG15	1	314290	215140	Wicklow	Devonian	Granite	470	178.0±5.0 [c]	12.72±0.12	1.60	54.244	54.612	45.715	46.324
LG16	1	312940	212200	Wicklow	Devonian	Granite	500	173.0±4.0 [c]	12.50±0.14	2.02	57.110	52.314	47.518	47.933
LG17	1	309480	205200	Wicklow	Devonian	Granite	570	170.0±5.0 [c]	12.22±0.17	1.78	60.253	60.712	40.576	41.063
LG18	1	309794	205293	Wicklow	Devonian	Granite	520	152.0±4.0 [c]	12.71±0.11	1.61	53.596	53.227	36.749	37.170
LG19	1	311310	203994	Wicklow	Devonian	Granite	380	147.0±4.0 [c]	12.93±0.15	1.54	62.620	52.584	48.619	47.679

LG22	1	306500	198500	Wicklow	Devonian	Granite	660	177.0±4.0 [c]	12.45±0.12	1.68	59.671	58.938	47.371	48.333
LG23	1	288770	185165	Wicklow	Devonian	Granite	117	169.0±5.0 [c]	12.38±0.13	1.88	58.560	59.004	43.248	43.825
LG26	1	293700	188250	Wicklow	Devonian	Granite	260	167.0±7.0 [c]	12.47±0.15	2.15	58.430	58.860	45.876	46.326
LG28	1	282743	152564	Carlow	Devonian	Granite	795	205.0±6.0 [c]	12.60±0.13	1.83	63.298	63.581	46.579	47.082
LG30	1	278140	153114	Carlow	Devonian	Granite	200	169.0±7.0 [c]	12.56±0.14	1.92	64.445	52.069	44.698	45.592
LG32	1	286582	173267	Carlow	Devonian	Granite	130	136.0±7.0 [c]	12.74±0.13	1.83	66.036	66.306	49.910	49.299
LG36	1	303180	191200	Wicklow	Devonian	Granite	740	174.0±7.0 [c]	12.57±0.12	1.50	72.176	72.397	53.460	53.645
SB1	1	223200	208250	Offaly	Carboniferous	Sandstone	150	240.0±9.0 [c]	12.52±0.13	1.62	53.565	54.077	49.205	49.383
SB2	1	229750	204450	Laois	Devonian	Sandstone	430	204.0±9.0 [c]	12.75±0.12	1.45	61.939	57.863	49.332	49.583
SB3	1	200163	196360	Tipperary	Carboniferous	Sandstone	98	228.0±13.0 [c]	12.84±0.15	1.47	57.042	57.289	43.775	43.934
GL1	2	182500	418000	Donegal	Devonian	Granite	40	188.1±3.6	12.25±0.22	2.15	78.952	75.295	52.647	53.631
GL2	2	183000	418000	Donegal	Devonian	Granite	60	195.0±7.0	12.05±0.19	1.93	72.152	72.982	50.256	47.402
GL3	2	180000	416000	Donegal	Devonian	Granite	72	197.1±6.8	11.88±0.22	2.15	78.411	78.593	60.390	59.964
GL4	2	182500	415800	Donegal	Devonian	Granite	55	200.9±7.1	12.23±0.20	2.04	73.569	73.776	55.198	52.214
GL5	2	179000	409900	Donegal	Devonian	Granite	30	194.1±8.0	12.22±0.23	2.42	75.466	66.399	20.000	20.000
GL6	2	180000	407300	Donegal	Devonian	Granite	28	179.9±8.8	12.34±0.23	2.27	66.676	53.012	42.136	34.228
GL7	2	173000	393000	Donegal	Devonian	Granite	20	175.5±9.3	12.39±0.18	1.88	72.841	73.115	50.909	44.993
GL8	2	86000	274000	Mayo	Devonian	Granite	175	124.1±5.1	12.26±0.24	2.36	78.446	77.302	63.938	56.662
GL9	2	57000	245500	Galway	Devonian	Granite	0	119.8±6.1	12.19±0.18	1.77	76.214	76.564	56.113	56.427
GL10	2	71000	239000	Galway	Devonian	Granite	8	149.7±6.4	12.44±0.21	2.10	68.912	67.549	48.744	51.066
GL11	2	73000	242000	Galway	Devonian	Granite	0	163.0±7.5	12.39±0.20	1.94	63.998	62.548	58.819	57.794
GL12	2	79000	232000	Galway	Devonian	Granite	7	182.7±5.3	11.93±0.22	2.17	59.017	59.975	60.215	51.040
GL13	2	301000	207500	Wicklow	Devonian	Granite	210	200.8±4.6	12.54±0.17	1.81	48.434	37.975	21.090	20.000
GL14	2	307000	201000	Wicklow	Devonian	Granite	470	208.2±6.4	12.20±0.23	2.30	57.178	57.885	56.203	56.379
Mc1	3	206200	427800	Donegal	Devonian	Granite	55	159.0±11.0**	12.41±0.21	1.65	69.753	70.165	54.772	55.056
Mc2	3	324300	426100	Antrim	Devonian	Sandstone	3	394.0±24.0**	12.37±0.20	1.59	47.096	39.290	44.846	45.266
Mc3	3	62000	245000	Galway	Devonian	Schist	8	154.0±9.0**	12.11±0.34	2.18	76.943	72.843	59.451	59.806
GC345-2	4	86000	77500	Kerry	Devonian	Sandstone	260	177.0±7.1 [p]	12.57±0.19	1.90	67.933	53.889	58.077	54.793
GC345-3	4	93400	85500	Kerry	Carboniferous	Sandstone	20	150.8±11.1 [c]	12.87±0.18	1.82	65.711	66.196	53.842	54.705
GC345-7	4	285155	281582	Cavan	Carboniferous	Sandstone	~80	78.5±6.9 [c]	12.12±0.27	2.72	93.195	93.544	73.739	68.136
GC458-1	4	171000	358000	Sligo	Carboniferous	Sandstone	0	164.0±10.0 [p]	11.76±0.24	2.38	80.959	79.765	64.184	55.925
GC458-2	4	165100	329600	Sligo	Carboniferous	Sandstone	50	164.2±21.6 [c]	13.31±0.30	1.49	56.725	57.023	37.719	38.292
GC458-5	4	202525	351773	Fermanagh	Carboniferous	Sandstone	205	148.1±13.6 [p]	11.95±0.30	2.40	77.062	71.378	52.279	53.239
GC543-63	4	340477	369575	Down	Ordovician?	Sandstone	40	318.9±25.3 [p]	12.33±0.17	1.77	64.937	65.166	34.426	35.191
GC543-64	4	342500	381400	Down	Carboniferous	Sandstone	10	321.7±18.7 [p]	12.62±1.18	1.76	41.569	30.246	26.219	26.843
GC543-65	4	347500	373100	Down	Triassic	Sandstone	30	72.9±5.6 [p]	13.21±0.23	1.51	67.587	68.187	51.117	51.810
GC543-72	4	324700	425000	Antrim	Devonian?	Alluvial sands	~0	312.9±29.2 [p]	11.89±0.19	1.96	44.338	41.328	39.485	32.229
GC543-73	4	325600	437000	Antrim	Precambrian	Dalradian	~0-150	291.9±43.5 [p]	12.51±0.28	1.50	60.704	61.463	49.154	46.669
659	5	275300	101420	Wexford	Devonian	Sandstone	0	226.1±11.1 [c]	12.38±0.15	1.58	68.486	68.653	46.371	47.479
660	5	271240	139420	Kilkenny	Devonian	Sandstone	110	130.3±7.3 [c]	12.38±0.19	1.67	73.163	73.467	54.556	54.974
664	5	221100	97380	Waterford	Devonian	Sandstone	100	154.5±13.9 [c]	12.56±0.31	1.55	66.326	66.591	52.067	52.350
665	5	199820	63880	Cork	Devonian	Sandstone	10	211.8±12.2 [c]	12.10±0.29	1.98	75.099	75.281	55.532	50.437
666	5	219760	76520	Waterford	Devonian	Sandstone	30	185.7±9.2 [c]	12.06±0.33	1.92	75.519	75.739	59.843	59.843
667	5	230060	121300	Waterford	Devonian	Sandstone	100	165.8±7.9 [c]	12.37±0.16	1.58	67.567	67.922	55.197	55.407
668	5	162420	40690	Cork	Devonian	Sandstone	50	154.2±5.6 [c]	12.65±0.15	1.44	65.897	66.136	53.494	53.211
671	5	184900	101700	Cork	Devonian	Sandstone	35	191.6±8.3 [c]	12.68±0.14	1.41	66.017	66.192	48.572	48.876
672	5	231240	89220	Waterford	Devonian	Sandstone	5	192.1±10.3 [c]	12.63±0.16	1.51	68.568	68.871	48.396	48.538
1	6	81000	274300	Mayo	Devonian	Granite	63	152.0±14.8 [p] *	12.89±0.19	2.00	50.960	51.325	47.817	48.029
4	6	89800	73000	Kerry	Devonian	Sandstone	70	156.3±26.8 [m] *	12.59±0.19	1.45	66.012	66.248	50.729	48.599
5	6	31600	96700	Kerry	Devonian	Sandstone	80	167.6±15.0 [p] *	11.80±0.24	2.07	72.835	71.379	62.216	62.400
7	6	93000	58300	Cork	Devonian	Sandstone	110	164.6±22.8 [p] *	12.61±0.26	1.88	70.162	70.639	52.280	52.686
8	6	73000	262900	Galway	Silurian	Sandstone	0	170.8±25.4 [p] *	13.27±0.23	2.15	42.981	43.718	20.000	20.216
9	6	113200	223000	Galway	Devonian	Granite	6	115.5±13.0 [p] *	12.24±0.23	2.13	71.297	71.789	56.023	56.433
11	6	145000	323700	Sligo	Devonian	Granite	190	168.7±15.6 [p] *	12.49±0.16	1.54	62.174	62.690	54.991	55.207
12	6	140200	314500	Sligo	Devonian	Granite	140	154.8±17.6 [p] *	12.55±0.16	1.53	68.254	68.601	50.813	51.315
14	6	108500	194800	Clare	Carboniferous	Sandstone	180	150.0±47.8 [m] *	12.15±0.43	2.30	79.016	79.498	62.794	63.008

16	6	72800	256000	Galway	Precambrian	Granite	270	156.4±17.2 [p] *	13.22±0.13	1.27	55.228	51.994	42.302	42.559
17	6	57400	256000	Galway	Devonian	Granite	0	135.2±15.0 [p] *	13.01±0.21	2.07	45.727	46.718	59.170	32.225
18	6	56900	245300	Galway	Devonian	Granite	0	129.1±11.8 [p] *	12.66±0.16	1.61	71.782	72.093	53.167	54.005
19	6	72300	240300	Galway	Devonian	Granite	16	127.3±14.8 [p] *	12.77±0.22	2.15	67.960	66.495	56.978	46.178
20	6	113200	222200	Galway	Devonian	Granite	0	115.9±10.2 [p] *	12.54±0.20	1.95	77.896	78.538	58.785	58.899
21	6	123400	222500	Galway	Devonian	Granite	0	119.1±11.0 [p] *	12.12±0.17	1.66	76.001	76.491	56.812	57.163
22	6	313100	179700	Wicklow	Devonian	Granite	70	181.9±16.6 [p] *	11.81±0.45	2.37	82.038	82.235	63.532	58.292
23	6	318300	185500	Wicklow	Devonian	Granite	130	184.2±24.2 [m] *	12.03±0.21	1.91	74.923	75.246	49.611	48.627
24	6	325100	188900	Wicklow	Devonian	Granite	55	217.2±19.8 [m] *	13.02±0.16	1.61	57.010	57.808	36.971	37.454
30	6	172500	393300	Donegal	Devonian	Granite	10	180.7±11.6 [p] *	12.50±0.16	1.56	66.813	67.100	52.381	52.564
31	6	95700	167500	Clare	Carboniferous	Sandstone	0	112.7±17.6 [p] *	13.20±0.26	1.45	55.252	55.861	44.145	44.640
32	6	171000	357900	Sligo	Carboniferous	Sandstone	5	165.7±15.0 [p] *	12.45±0.21	1.92	74.506	74.790	56.669	57.966
39	6	239700	354700	Fermanagh	Carboniferous	Sandstone	190	177.4±17.8 [p] *	11.48±0.20	1.67	77.432	77.603	59.553	59.707
43	6	148100	161600	Clare	Devonian	Sandstone	45	205.2±27.4 [m] *	12.52±0.18	1.70	70.443	70.653	52.968	53.679
45	6	225100	438000	Donegal	Devonian	Sandstone	1	300.8±25.4 [m] *	12.85±0.28	2.37	42.277	42.585	24.880	23.166
46	6	239500	209000	Laois	Devonian	Sandstone	55	179.4±16.4 [p] *	11.19±0.22	2.15	81.231	81.428	63.094	63.068
47	6	324400	427600	Antrim	Devonian	Andesite	0	267.2±26.2 [p] *	12.71±0.16	1.61	55.022	55.331	28.049	22.595
48	6	230200	341100	Fermanagh	Silurian	Sandstone	80	176.2±15.0 [p] *	12.28±0.20	2.07	76.783	77.002	56.639	55.823
51	6	266200	176700	Laois	Carboniferous	Sandstone	220	153.7±18.0 [p] *	12.14±0.34	2.18	82.060	82.298	34.039	34.039
54	6	107500	297300	Mayo	Devonian	Sandstone	25	186.5±15.2 [p] *	12.05±0.24	2.42	56.497	57.061	43.706	38.384
55	6	98100	249800	Galway	Precambrian	Schist	290	150.3±11.4 [p] *	12.66±0.20	1.94	77.237	73.800	60.177	56.685
56	6	88400	159800	Clare	Carboniferous	Sandstone	0	138.4±22.4 [m] *	12.54±0.23	1.36	64.302	64.546	54.979	55.223
57	6	93500	265700	Mayo	Ordovician	Sandstone	29	152.2±13.0 [p] *	12.62±0.18	1.81	75.047	72.433	52.808	32.489
60	6	111700	242600	Galway	Devonian	Granite	17	129.6±14.2 [p] *	12.37±0.25	1.91	66.006	66.408	49.725	50.686
64	6	340900	380700	Down	Carboniferous	Sandstone	0	273.8±26.8 [p] *	12.13±0.15	1.54	76.517	76.754	50.100	50.614
68	6	268300	382000	Tyrone	Ordovician	Tuff	160	225.2±21.4 [p] *	12.40±0.17	1.74	70.727	66.478	55.277	54.997
75	6	233600	94800	Waterford	Carboniferous	Sandstone	0	194.9±12.2 [p] *	12.94±0.17	1.67	67.194	61.029	45.537	38.318
76	6	228700	154200	Tipperary	Carboniferous	Sandstone	245	147.0±14.4 [p] *	12.03±0.26	1.92	78.673	78.914	61.857	59.438
77	6	87600	144900	Kerry	Carboniferous	Sandstone	52	133.9±28.4 [m] *	12.28±0.19	1.85	75.698	76.119	59.065	59.556
80	6	270800	143400	Kilkenny	Devonian	Granite	20	149.0±11.8 [p] *	12.35±0.13	1.76	75.853	76.525	56.891	57.214
82	6	84800	152400	Clare	Carboniferous	Sandstone	0	132.9±30.0 [m] *	11.77±0.26	2.58	87.511	83.939	66.142	59.782
83	6	69000	132100	Kerry	Devonian	Sandstone	75	154.3±26.0 [m] *	11.56±0.24	2.43	83.055	83.296	64.891	51.665
84	6	235200	300700	Cavan	Devonian	Granite	50	200.7±14.6 [p] *	12.13±0.18	1.76	67.080	67.464	53.294	53.692
86	6	310300	111400	Wexford	Ordovician	Tuff	19	219.8±19.4 [p] *	12.28±0.19	1.85	55.752	52.855	56.871	57.041
88	6	124700	152100	Limerick	Carboniferous	Sandstone	0	143.5±29.6 [m] *	12.40±0.21	2.24	80.016	80.292	55.371	56.353
90	6	154700	201300	Galway	Devonian	Sandstone	163	192.3±16.6 [p] *	12.88±0.18	1.71	69.055	69.436	48.833	44.311
2	7	316000	208600	Wicklow	Devonian	Granite	360	136.7±13.0 [p] *	12.27±0.17	1.71	72.453	72.749	59.996	58.006
3	7	319200	219300	Wicklow	Devonian	Granite	210	126.5±6.4 [p] *	12.27±0.16	1.62	73.596	73.866	58.889	59.204
4	7	317800	223200	Dublin	Devonian	Granite	440	161.9±33.4 [m] *	11.73±0.21	1.96	79.191	79.451	59.857	60.079
6	7	295500	279300	Meath	Ordovician	Tuff	110	212.1±31.6 [p] *	12.78±0.24	2.42	22.232	23.058	26.254	26.886
7	7	327800	344500	Down	Devonian	Granite	230	134.4±12.2 [p] *	11.74±0.15	1.46	74.360	74.592	56.216	56.440
8	7	327000	257700	Dublin	Carboniferous	Sandstone	25	70.2±30.4 [p] *	12.56±0.51	2.52	96.772	93.867	73.379	74.015
9	7	325300	260600	Dublin	Silurian	Sandstone	0	73.4±10.0 [p] *	12.20±0.50	2.45	88.369	89.197	71.305	71.085
11	7	321000	334800	Down	Devonian	Granite	90	58.3±7.4 [p] *	13.94±0.19	1.20	77.878	60.330	60.245	44.839
12	7	307200	302600	Louth	Silurian	Sandstone	0	64.5±14.2 [m] *	13.42±0.20	1.30	59.941	60.524	49.716	50.775
13	7	311500	293500	Louth	Silurian	Sandstone	0	46.0±15.6 [m] *	13.72±0.16	1.17	120.000	120.000	114.033	82.161
14	7	317100	284600	Louth	Silurian	Sandstone	0	50.8±6.4 [m] *	13.07±0.25	1.95	109.464	103.920	84.549	79.125
16	7	320300	264400	Dublin	Ordovician	Tuff	0	128.4±22.8 [p] *	13.54±0.38	2.41	45.452	37.650	20.000	20.000

A glossary of terms, followed by single grain fission track data for the margin and control samples from this study.

N_o	Number of each grain
N_s	Number of spontaneous fission tracks
N_i	Number of induced fission tracks
N_a	Number of area units counted in grain
RATIO	Ratio of N_s/N_i for each grain
U	Uranium concentration in each grain (ppm)
ρ_s	Density of spontaneous fission tracks (per cm^2)
ρ_i	Density of induced fission tracks (per cm^2)
F.T.AGE	Fission-track age for each grain (Ma)
χ^2	Chi Squared – a statistical test for determining whether grains derive from a single population
DEGREES OF FREEDOM	Number of crystals - 1
$P(\chi^2)$	Probability of less than 5% (a fail) indicates non-Poissonian distribution of grain ages and probable multiple grain populations
CORRELATION COEFFICIENT	A means to ascertain the goodness of fit of the data
VARIANCE OF SQR(N_S)	Statistical comparison of values of N_S for all grains
VARIANCE OF SQR(N_i)	Statistical comparison of values of N_i for all grains
SUMMED N_s/N_i	Ratio to derive Pooled Age (using summed N_s and summed N_i for all grains in the sample)
MEAN RATIO	Average value of (N_s/N_i) for grains
Pooled Age	Age calculated using SUMMED N_s/N_i (used when a sample has a single population of grains having passed the $P(\chi^2)$ test)
Mean Age	Age calculated using MEAN RATIO (for multiple populations within a sample showing non-Poissonian variation, having failed the $P(\chi^2)$ test)
Central Age	Weighted modal age that accounts for non-Poissonian variation (generally the preferred estimate)
R.E.%	Relative Error – a measure of age dispersion of individual grains relative to the central age (large values indicate high grain age variation)
ξ	Age of known standard with which to compare spontaneous and induced fission track density
ρ_d	Density of tracks in dosimeter used to monitor neutron fluence
N_d	Number of tracks in dosimeter used to monitor neutron fluence

M1

N_o	N_s	N_i	N_a	Ratio	U (ppm)	ρ_s	ρ_i (Ma)	F.T.Age
1	17	28	18	0.607	12.6	6.814E+05	1.122E+06	111.7±34.4
2	32	130	50	0.246	21.0	4.618E+05	1.876E+06	45.5±9.0
3	12	84	60	0.143	11.3	1.443E+05	1.010E+06	26.5±8.2
4	16	38	30	0.421	10.2	3.848E+05	9.139E+05	77.7±23.2
5	12	36	30	0.333	9.7	2.886E+05	8.658E+05	61.6±20.5
6	12	39	28	0.308	11.3	3.092E+05	1.005E+06	56.8±18.8
7	16	95	40	0.168	19.2	2.886E+05	1.714E+06	31.2±8.4
8	25	96	60	0.260	12.9	3.006E+05	1.154E+06	48.1±10.8
9	15	108	50	0.139	17.5	2.164E+05	1.558E+06	25.7±7.1
10	16	43	30	0.372	11.6	3.848E+05	1.034E+06	68.7±20.1
11	22	72	50	0.306	11.6	3.175E+05	1.039E+06	56.5±13.8
12	13	35	30	0.371	9.4	3.126E+05	8.418E+05	68.6±22.3
13	16	48	30	0.333	12.9	3.848E+05	1.154E+06	61.6±17.8
14	8	26	28	0.308	7.5	2.061E+05	6.700E+05	56.8±23.0
15	17	49	35	0.347	11.3	3.504E+05	1.010E+06	64.1±18.1
16	31	75	50	0.413	12.1	4.473E+05	1.082E+06	76.2±16.3
17	11	24	30	0.458	6.5	2.646E+05	5.772E+05	84.5±30.8
18	24	59	50	0.407	9.5	3.463E+05	8.514E+05	75.0±18.2
19	27	74	40	0.365	15.0	4.870E+05	1.335E+06	67.4±15.2
20	19	74	50	0.257	12.0	2.742E+05	1.068E+06	47.5±12.2
21	32	72	60	0.444	9.7	3.848E+05	8.658E+05	81.9±17.5
22	22	64	50	0.344	10.3	3.175E+05	9.235E+05	63.5±15.7
23	39	78	50	0.500	12.6	5.628E+05	1.126E+06	92.1±18.1
24	15	34	30	0.441	9.2	3.608E+05	8.177E+05	81.3±25.3
25	14	47	40	0.298	9.5	2.525E+05	8.478E+05	55.0±16.8
	483	1528			12.1	3.420E+05	1.082E+06	

Area of basic unit = 1.386E-06 cm^{-2}
χ^2 = 22.50295 (24 DEGREES OF FREEDOM)
$P(\chi^2)$ = 0.582 %
CORRELATION COEFFICIENT = 0.578
VARIANCE OF SQR(Ns) = 0.743262
VARIANCE OF SQR(Ni) = 3.094264
Ns/Ni = 0.316 ± 0.016
MEAN RATIO = 0.344 ± 0.022
Pooled Age = 58.4 ± 3.2 Ma
Mean Age = 63.4 ± 4.2 Ma
Central Age = 59.9 ± 4.3 Ma; R.E.% = 23.59
Ages calculated using ξ = 338 ± 4 for CN5 glass
ρ_d = 1.098E+06 cm^{-2}; N_d = 6089

M2

N_o	N_s	N_i	N_a	Ratio	U (ppm)	ρ_s	ρ_i (Ma)	F.T.Age
1	14	39	32	0.359	9.8	3.157E+05	8.793E+05	66.3±20.7
2	16	66	48	0.242	11.1	2.405E+05	9.921E+05	44.8±12.5
3	2	4	60	0.500	0.5	2.405E+04	4.810E+04	92.1±79.8
4	3	12	16	0.250	6.1	1.353E+05	5.411E+05	46.2±29.8
5	10	27	25	0.370	8.7	2.886E+05	7.792E+05	68.4±25.3
6	5	20	36	0.250	4.5	1.002E+05	4.008E+05	46.2±23.1
7	12	21	30	0.571	5.7	2.886E+05	5.050E+05	105.2±38.1
8	44	181	60	0.243	24.4	5.291E+05	2.177E+06	45.0±7.6
9	3	9	25	0.333	2.9	8.658E+04	2.597E+05	61.6±41.1
10	9	55	24	0.164	18.5	2.706E+05	1.653E+06	30.3±10.9
11	10	32	24	0.312	10.8	3.006E+05	9.620E+05	57.7±20.9
12	8	28	25	0.286	9.1	2.309E+05	8.081E+05	52.8±21.2
13	13	36	24	0.361	12.1	3.908E+05	1.082E+06	66.7±21.6
14	15	36	30	0.417	9.7	3.608E+05	8.658E+05	76.9±23.7
15	5	14	14	0.357	8.1	2.577E+05	7.215E+05	65.9±34.4
16	7	32	30	0.219	8.6	1.684E+05	7.696E+05	40.5±16.9
17	5	15	50	0.333	2.4	7.215E+04	2.164E+05	61.6±31.8
18	7	15	25	0.467	4.8	2.020E+05	4.329E+05	86.0±39.4
	188	642			9.0	2.347E+05	8.014E+05	

Area of basic unit = 1.386E-06 cm^{-2}
χ^2 = 6.446746 (17 DEGREES OF FREEDOM)
$P(\chi^2)$ = 74.3 %
CORRELATION COEFFICIENT = 0.960
VARIANCE OF SQR(Ns) = 1.405999
VARIANCE OF SQR(Ni) = 6.349193
Ns/Ni = 0.293 ± 0.024
MEAN RATIO = 0.335 ± 0.025
Pooled Age = 54.1 ± 4.6 Ma
Mean Age = 61.9 ± 4.7 Ma
Central Age = 54.3 ± 4.6 Ma; R.E.% = 3.84
Ages calculated using ξ = 338 ± 4 for CN5 glass
ρ_d = 1.098E+06 cm^{-2}; N_d = 6089

M3

N_o	N_s	N_i	N_a	Ratio	U (ppm)	ρ_s	ρ_i (Ma)	F.T.Age
1	72	190	30	0.379	51.2	1.732E+06	4.570E+06	69.9±9.8
2	53	148	20	0.358	59.8	1.912E+06	5.339E+06	66.1±10.6
3	27	72	60	0.375	9.7	3.247E+05	8.658E+05	69.2±15.7
4	43	127	20	0.339	51.3	1.551E+06	4.582E+06	62.5±11.1
5	39	130	40	0.300	26.3	7.035E+05	2.345E+06	55.4±10.2
6	19	84	20	0.226	33.9	6.854E+05	3.030E+06	41.8±10.7
7	52	155	40	0.335	31.3	9.380E+05	2.796E+06	62.0±10.0
8	11	46	10	0.239	37.2	7.936E+05	3.319E+06	44.2±14.9
9	24	69	20	0.348	27.9	8.658E+05	2.489E+06	64.2±15.3
10	24	65	42	0.369	12.5	4.123E+05	1.117E+06	68.2±16.3
11	50	153	15	0.327	82.4	2.405E+06	7.359E+06	60.4±9.9
12	61	162	30	0.377	43.6	1.467E+06	3.896E+06	69.5±10.5
13	48	150	20	0.320	60.6	1.732E+06	5.411E+06	59.1±9.9
14	42	106	18	0.396	47.6	1.684E+06	4.249E+06	73.1±13.4
15	35	142	40	0.246	28.7	6.313E+05	2.561E+06	45.6±8.6
16	23	59	30	0.390	15.9	5.532E+05	1.419E+06	71.9±17.7
	623	1858			33.0	9.879E+05	2.946E+06	

Area of basic unit = 1.386E-06 cm^{-2}
χ^2 = 4.907234 (15 DEGREES OF FREEDOM)
$P(\chi^2)$ = 83.1 %
CORRELATION COEFFICIENT = 0.943
VARIANCE OF SQR(Ns) = 1.963973
VARIANCE OF SQR(Ni) = 4.707341
Ns/Ni = 0.335 ± 0.016
MEAN RATIO = 0.333 ± 0.014
Pooled Age = 61.9 ± 3.1 Ma
Mean Age = 61.5 ± 2.7 Ma
Central Age = 61.9 ± 3.0 Ma; R.E.% = 0.03
Ages calculated using ξ = 338 ± 4 for CN5 glass
ρ_d = 1.098E+06 cm^{-2}; N_d = 6089

M4

N_o	N_s	N_i	N_a	Ratio	U (ppm)	ρ_s	ρ_i (Ma)	F.T.Age
1	34	106	100	0.321	8.6	2.453E+05	7.648E+05	59.2±11.7
2	43	158	50	0.272	25.5	6.205E+05	2.280E+06	50.3±8.7
3	40	106	60	0.377	14.3	4.810E+05	1.275E+06	69.6±13.0
4	38	128	60	0.297	17.2	4.570E+05	1.539E+06	54.9±10.2
5	9	62	49	0.145	10.2	1.325E+05	9.129E+05	26.9±9.6
6	36	105	70	0.343	12.1	3.711E+05	1.082E+06	63.3±12.3
7	34	95	60	0.358	12.8	4.088E+05	1.142E+06	66.1±13.3
8	39	127	50	0.307	20.5	5.628E+05	1.833E+06	56.7±10.4
9	36	109	50	0.330	17.6	5.195E+05	1.573E+06	61.0±11.8
10	43	128	50	0.336	20.7	6.205E+05	1.847E+06	62.0±11.0
11	83	220	100	0.377	17.8	5.988E+05	1.587E+06	69.6±9.1
12	94	270	100	0.348	21.8	6.782E+05	1.948E+06	64.3±7.8
13	22	65	30	0.338	17.5	5.291E+05	1.563E+06	62.5±15.5
14	13	57	50	0.228	9.2	1.876E+05	8.225E+05	42.2±13.0
15	41	116	30	0.353	31.3	9.861E+05	2.790E+06	65.3±11.9
16	56	168	80	0.333	17.0	5.050E+05	1.515E+06	61.6±9.6
17	9	22	50	0.409	3.6	1.299E+05	3.175E+05	75.5±29.9
18	27	86	30	0.314	23.2	6.494E+05	2.068E+06	58.0±12.8
19	29	92	36	0.315	20.7	5.812E+05	1.844E+06	58.2±12.4
20	9	45	24	0.200	15.2	2.706E+05	1.353E+06	37.0±13.5
	735	2265			16.2	4.697E+05	1.447E+06	

Area of basic unit = 1.386E-06 cm^{-2}
χ^2 = 6.637982 (19 DEGREES OF FREEDOM)
P(χ^2) = 82.4 %
CORRELATION COEFFICIENT = 0.979
VARIANCE OF SQR(Ns) = 3.22467
VARIANCE OF SQR(Ni) = 7.278821
Ns/Ni = 0.324 ± 0.014
MEAN RATIO = 0.315 ± 0.014
Pooled Age = 59.9 ± 2.8 Ma
Mean Age = 58.2 ± 2.8 Ma
Central Age = 59.9 ± 2.7 Ma; R.E.% = 0.02
Ages calculated using ξ = 338 ± 4 for CN5 glass
ρ_d = 1.098E+06 cm^{-2}; N_d = 6089

M5

N_o	N_s	N_i	N_a	Ratio	U (ppm)	ρ_s	ρ_i (Ma)	F.T.Age
1	7	27	24	0.259	9.1	2.104E+05	8.117E+05	47.9±20.3
2	12	40	28	0.300	11.5	3.092E+05	1.031E+06	55.4±18.3
3	17	39	24	0.436	13.1	5.111E+05	1.172E+06	80.4±23.4
4	19	77	42	0.247	14.8	3.264E+05	1.323E+06	45.6±11.7
5	64	208	50	0.308	33.6	9.235E+05	3.001E+06	56.8±8.2
6	1	4	48	0.250	0.7	1.503E+04	6.012E+04	46.2±51.7
7	41	131	18	0.313	58.8	1.643E+06	5.251E+06	57.8±10.4
8	17	37	35	0.459	8.5	3.504E+05	7.627E+05	84.7±24.9
9	15	62	40	0.242	12.5	2.706E+05	1.118E+06	44.7±12.9
10	6	20	30	0.300	5.4	1.443E+05	4.810E+05	55.4±25.8
11	10	44	24	0.227	14.8	3.006E+05	1.323E+06	42.0±14.7
12	11	43	50	0.256	7.0	1.587E+05	6.205E+05	47.3±16.0
13	2	2	20	1.000	0.8	7.215E+04	7.215E+04	182.9±183
14	48	137	30	0.350	36.9	1.154E+06	3.295E+06	64.7±10.9
15	5	34	15	0.147	18.3	2.405E+05	1.635E+06	27.2±13.1
16	7	24	25	0.292	7.8	2.020E+05	6.926E+05	53.9±23.2
17	6	20	24	0.300	6.7	1.804E+05	6.012E+05	55.4±25.8
18	18	43	30	0.419	11.6	4.329E+05	1.034E+06	77.2±21.7
19	44	126	20	0.349	50.9	1.587E+06	4.545E+06	64.5±11.3
20	1	6	21	0.167	2.3	3.436E+04	2.061E+05	30.9±33.3
	351	1124			15.2	4.235E+05	1.356E+06	

Area of basic unit = 1.386E-06 cm^{-2}
χ^2 = 6.318472 (19 DEGREES OF FREEDOM)
P(χ^2) = 85.7 %
CORRELATION COEFFICIENT = 0.981
VARIANCE OF SQR(Ns) = 3.879888
VARIANCE OF SQR(Ni) = 11.4947
Ns/Ni = 0.312 ± 0.019
MEAN RATIO = 0.331 ± 0.039
Pooled Age = 57.7 ± 3.7 Ma
Mean Age = 61.1 ± 7.4 Ma
Central Age = 57.7 ± 3.6 Ma; R.E.% = 0.01
Ages calculated using ξ = 338 ± 4 for CN5 glass
ρ_d = 1.098E+06 cm^{-2}; N_d = 6089

M7

N_o	N_s	N_i	N_a	Ratio	U (ppm)	ρ_s	ρ_i (Ma)	F.T.Age
1	13	51	30	0.255	12.1	3.127E+05	1.227E+06	54.2±16.9
2	31	87	50	0.356	12.4	4.473E+05	1.255E+06	75.7±15.9
3	39	171	50	0.228	24.4	5.628E+05	2.468E+06	48.5±8.7
4	45	172	80	0.262	15.3	4.058E+05	1.551E+06	55.6±9.4
5	36	146	80	0.247	13.0	3.247E+05	1.317E+06	52.5±9.8
6	28	103	40	0.272	18.4	5.051E+05	1.858E+06	57.8±12.4
7	58	199	40	0.291	35.5	1.046E+06	3.589E+06	62.0±9.3
8	20	79	40	0.253	14.1	3.608E+05	1.425E+06	53.9±13.5
9	69	165	30	0.418	39.2	1.660E+06	3.968E+06	88.7±12.8
10	14	50	40	0.28	8.9	2.525E+05	9.020E+05	59.5±18.0
11	32	81	50	0.395	11.6	4.618E+05	1.169E+06	83.8±17.6
12	25	130	40	0.192	23.2	4.509E+05	2.345E+06	40.9±9.0
13	10	55	35	0.182	11.2	2.061E+05	1.134E+06	38.7±13.3
14	43	142	50	0.303	20.3	6.205E+05	2.049E+06	64.4±11.3
15	61	229	50	0.266	32.7	8.802E+05	3.304E+06	56.7±8.2
16	83	315	50	0.263	45.0	1.198E+06	4.545E+06	56.0±7.0
17	57	229	30	0.249	54.5	1.371E+06	5.507E+06	53.0±7.9
18	24	96	30	0.25	22.8	5.772E+05	2.309E+06	53.2±12.2
19	48	164	30	0.293	39.0	1.154E+06	3.944E+06	62.2±10.3
20	46	168	100	0.274	12.0	3.319E+05	1.212E+06	58.2±9.7
	782	2832			21.4	5.971E+05	2.162E+06	

Area of basic unit = 1.386E-06 cm^{-2}
χ^2 = 10.253 (19 DEGREES OF FREEDOM)
P(χ^2) = 36.47 %
Ns/Ni = 0.276 ± 0.011
MEAN RATIO = 0.276 ± 0.013
Pooled Age = 58.7 ± 2.6 Ma
Mean Age = 58.8 ± 2.7 Ma
Central Age = 58.7 ± 2.5 Ma; R.E.% = 3.29
Ages calculated using ξ = 338.0 ± 4.0 for CN5 glass
ρ_d = 1.264E+06 cm^{-2}; N_d = 7010

M8

N_o	N_s	N_i	N_a	Ratio	U (ppm)	ρ_s	ρ_i (Ma)	F.T.Age
1	20	66	30	0.303	17.8	4.810E+05	1.587E+06	56.0±14.3
2	56	146	30	0.384	39.3	1.347E+06	3.511E+06	70.8±11.2
3	29	99	80	0.293	10.0	2.615E+05	8.929E+05	54.1±11.5
4	67	229	40	0.293	46.3	1.209E+06	4.131E+06	54.1±7.6
5	33	116	50	0.284	18.8	4.762E+05	1.674E+06	52.6±10.4
6	38	68	20	0.559	27.5	1.371E+06	2.453E+06	102.9±20.9
7	39	119	60	0.328	16.0	4.690E+05	1.431E+06	60.5±11.2
8	30	109	70	0.275	12.6	3.092E+05	1.123E+06	50.9±10.5
9	14	52	30	0.269	14.0	3.367E+05	1.251E+06	49.8±15.0
10	94	192	30	0.490	51.7	2.261E+06	4.618E+06	90.2±11.5
11	19	94	40	0.202	19.0	3.427E+05	1.696E+06	37.4±9.4
12	72	214	40	0.336	43.2	1.299E+06	3.860E+06	62.1±8.5
13	93	226	40	0.412	45.7	1.677E+06	4.076E+06	75.9±9.4
14	19	103	40	0.184	20.8	3.427E+05	1.858E+06	34.1±8.5
15	14	46	18	0.304	20.7	5.612E+05	1.844E+06	56.2±17.2
16	28	112	30	0.250	30.2	6.734E+05	2.694E+06	46.2±9.8
17	136	350	60	0.389	47.1	1.635E+06	4.209E+06	71.7±7.4
18	63	212	30	0.297	57.1	1.515E+06	5.099E+06	54.9±7.9
19	39	118	20	0.330	47.7	1.407E+06	4.257E+06	61.0±11.3
20	24	116	36	0.207	26.0	4.810E+05	2.325E+06	38.3±8.6
	927	2787			28.4	8.424E+05	2.533E+06	

Area of basic unit = 1.386E-06 cm^{-2}
χ^2 = 21.31726 (19 DEGREES OF FREEDOM)
$P(\chi^2)$ = 0.145 %
CORRELATION COEFFICIENT = 0.941
VARIANCE OF SQR(Ns) = 4.849773
VARIANCE OF SQR(Ni) = 9.288342
Ns/Ni = 0.333 ± 0.013
MEAN RATIO = 0.319 ± 0.021
Pooled Age = 61.4 ± 2.6 Ma
Mean Age = 59.0 ± 3.9 Ma
Central Age = 59.3 ± 3.6 Ma; R.E.% = 19.01
Ages calculated using ξ = 338 ± 4 for CN5 glass
ρ_d = 1.098E+06 cm^{-2}; N_d = 6089

M9

N_o	N_s	N_i	N_a	Ratio	U (ppm)	ρ_s	ρ_i (Ma)	F.T.Age
1	20	66	40	0.303	13.3	3.608E+05	1.190E+06	56.0±14.3
2	20	74	49	0.270	12.2	2.945E+05	1.090E+06	50.0±12.6
3	13	50	40	0.260	10.1	2.345E+05	9.019E+05	48.1±15.0
4	28	97	70	0.289	11.2	2.886E+05	9.998E+05	53.3±11.5
5	38	105	70	0.362	12.1	3.917E+05	1.082E+06	66.8±12.7
6	17	62	40	0.274	12.5	3.066E+05	1.118E+06	50.7±13.9
7	22	75	60	0.293	10.1	2.646E+05	9.019E+05	54.2±13.2
8	9	48	50	0.188	7.8	1.299E+05	6.926E+05	34.7±12.6
9	25	63	40	0.397	12.7	4.509E+05	1.136E+06	73.2±17.4
10	14	54	28	0.259	15.6	3.608E+05	1.391E+06	47.9±14.4
11	28	79	50	0.354	12.8	4.040E+05	1.140E+06	65.4±14.4
12	39	137	100	0.285	11.1	2.814E+05	9.885E+05	52.6±9.6
13	58	143	100	0.406	11.6	4.185E+05	1.032E+06	74.8±11.7
14	25	86	50	0.291	13.9	3.608E+05	1.241E+06	53.7±12.2
15	34	116	60	0.293	15.6	4.088E+05	1.395E+06	54.2±10.6
16	14	42	35	0.333	9.7	2.886E+05	8.658E+05	61.6±19.0
17	40	149	80	0.268	15.1	3.608E+05	1.344E+06	49.6±8.9
18	33	89	60	0.371	12.0	3.968E+05	1.070E+06	68.4±14.0
19	30	122	70	0.246	14.1	3.092E+05	1.257E+06	45.5±9.3
20	129	418	100	0.309	33.8	9.307E+05	3.016E+06	57.0±5.8
21	22	74	80	0.297	7.5	1.984E+05	6.674E+05	54.9±13.4
	658	2149			13.7	3.732E+05	1.219E+06	

Area of basic unit = 1.386E-06 cm^{-2}
χ^2 = 5.816639 (20 DEGREES OF FREEDOM)
$P(\chi^2)$ = 92.8 %
CORRELATION COEFFICIENT = 0.981
VARIANCE OF SQR(Ns) = 3.097104
VARIANCE OF SQR(Ni) = 8.897302
Ns/Ni = 0.306 ± 0.014
MEAN RATIO = 0.302 ± 0.011
Pooled Age = 56.6 ± 2.7 Ma
Mean Age = 55.8 ± 2.3 Ma
Central Age = 56.6 ± 2.6 Ma; R.E.% = 0.02
Ages calculated using ξ = 338 ± 4 for CN5 glass
ρ_d = 1.098E+06 cm^{-2}; N_d = 6089

M10

N_o	N_s	N_i	N_a	Ratio	U (ppm)	ρ_s	ρ_i (Ma)	F.T.Age
1	30	95	40	0.316	19.2	5.411E+05	1.714E+06	58.3±12.3
2	27	75	32	0.360	18.9	6.088E+05	1.691E+06	66.5±15.0
3	31	153	50	0.203	24.7	4.473E+05	2.208E+06	37.5±7.4
4	38	84	40	0.452	17.0	6.854E+05	1.515E+06	83.4±16.4
5	21	75	49	0.280	12.4	3.092E+05	1.104E+06	51.7±12.8
6	39	146	60	0.267	19.7	4.690E+05	1.756E+06	49.4±8.9
7	53	139	50	0.381	22.5	7.648E+05	2.006E+06	70.4±11.4
8	29	94	50	0.309	15.2	4.185E+05	1.356E+06	57.0±12.1
9	58	160	80	0.362	16.2	5.231E+05	1.443E+06	66.9±10.3
10	98	262	50	0.374	42.4	1.414E+06	3.781E+06	69.0±8.3
11	22	80	40	0.275	16.2	3.968E+05	1.443E+06	50.8±12.3
12	32	115	50	0.278	18.6	4.618E+05	1.659E+06	51.4±10.3
13	50	132	60	0.379	17.8	6.012E+05	1.587E+06	69.9±11.7
14	38	115	49	0.330	19.0	5.595E+05	1.693E+06	61.0±11.5
15	38	92	36	0.413	20.7	7.616E+05	1.844E+06	76.2±14.8
16	40	110	50	0.364	17.8	5.772E+05	1.587E+06	67.1±12.4
17	18	60	35	0.300	13.9	3.711E+05	1.237E+06	55.4±14.9
18	42	132	50	0.318	21.3	6.061E+05	1.905E+06	58.8±10.5
19	26	137	60	0.190	18.5	3.126E+05	1.647E+06	35.1±7.5
20	29	123	30	0.236	33.1	6.974E+05	2.958E+06	43.6±9.0
21	28	84	80	0.333	8.5	2.525E+05	7.576E+05	61.6±13.5
22	41	138	60	0.297	18.6	4.930E+05	1.659E+06	54.9±9.8
	828	2601			19.1	5.426E+05	1.704E+06	

Area of basic unit = 1.386E-06 cm^{-2}
χ^2 = 13.33103 (21 DEGREES OF FREEDOM)
$P(\chi^2)$ = 18.2 %
CORRELATION COEFFICIENT = 0.871
VARIANCE OF SQR(Ns) = 1.492493
VARIANCE OF SQR(Ni) = 3.395926
Ns/Ni = 0.318 ± 0.013
MEAN RATIO = 0.319 ± 0.014
Pooled Age = 58.8 ± 2.6 Ma
Mean Age = 58.9 ± 2.8 Ma
Central Age = 58.6 ± 2.8 Ma; R.E.% = 9.99
Ages calculated using ξ = 338 ± 4 for CN5 glass
ρ_d = 1.098E+06 cm^{-2}; N_d = 6089

M11

N_o	N_s	N_i	N_a	Ratio	U (ppm)	ρ_s	ρ_i	F.T.Age (Ma)
1	73	209	60	0.349	28.2	8.778E+05	2.513E+06	64.5±8.8
2	59	214	70	0.276	24.7	6.081E+05	2.206E+06	51.0±7.5
3	61	196	60	0.311	26.4	7.335E+05	2.357E+06	57.5±8.5
4	118	343	100	0.344	27.7	8.514E+05	2.475E+06	63.5±6.9
5	124	356	100	0.348	28.8	8.947E+05	2.569E+06	64.3±6.8
6	151	323	100	0.467	26.1	1.089E+06	2.330E+06	86.2±8.6
7	39	175	100	0.223	14.1	2.814E+05	1.263E+06	41.2±7.3
8	105	301	100	0.349	24.3	7.576E+05	2.172E+06	64.4±7.4
9	101	284	100	0.356	23.0	7.287E+05	2.049E+06	65.7±7.7
10	111	262	100	0.424	21.2	8.009E+05	1.890E+06	78.1±9.0
11	49	108	40	0.454	21.8	8.838E+05	1.948E+06	83.6±14.5
12	66	276	100	0.239	22.3	4.762E+05	1.991E+06	44.2±6.1
13	59	216	80	0.273	21.8	5.321E+05	1.948E+06	50.5±7.5
14	92	316	100	0.291	25.5	6.638E+05	2.280E+06	53.8±6.4
15	69	188	60	0.367	25.3	8.297E+05	2.261E+06	67.7±9.6
16	107	326	80	0.328	32.9	9.650E+05	2.940E+06	60.6±6.8
17	113	460	100	0.246	37.2	8.153E+05	3.319E+06	45.4±4.8
18	111	416	100	0.267	33.6	8.009E+05	3.001E+06	49.3±5.3
19	94	274	60	0.343	36.9	1.130E+06	3.295E+06	63.3±7.7
20	51	167	60	0.305	22.5	6.133E+05	2.008E+06	56.4±9.1
	1753	5410			26.2	7.574E+05	2.337E+06	

Area of basic unit = 1.386E-06 cm^{-2}
χ^2 = 25.0283 (19 DEGREES OF FREEDOM)
$P(\chi^2)$ = 0.013 %
CORRELATION COEFFICIENT = 0.805
VARIANCE OF SQR(Ns) = 2.732569
VARIANCE OF SQR(Ni) = 7.412341
Ns/Ni = 0.324 ± 0.009
MEAN RATIO = 0.328 ± 0.015
Pooled Age = 59.8 ± 1.9 Ma
Mean Age = 60.6 ± 3.0 Ma
Central Age = 59.9 ± 2.7 Ma; R.E.% = 14.85
Ages calculated using ξ = 338 ± 4 for CN5 glass
ρ_d = 1.098E+06 cm^{-2}; N_d = 6089

C2

N_o	N_s	N_i	N_a	Ratio	U (ppm)	ρ_s	ρ_i	F.T.Age (Ma)
1	111	164	60	0.677	19.2	1.335E+06	1.972E+06	143.0±17.7
2	65	51	60	1.275	6.0	7.816E+05	6.133E+05	266.7±50.1
3	63	43	100	1.465	3.0	4.545E+05	3.102E+05	305.6±60.7
4	158	200	100	0.790	14.0	1.140E+06	1.443E+06	166.6±18.0
5	99	120	80	0.825	10.5	8.929E+05	1.082E+06	173.9±23.8
6	128	143	60	0.895	16.7	1.539E+06	1.720E+06	188.4±23.1
7	182	171	100	1.064	12.0	1.313E+06	1.234E+06	223.4±24.1
8	205	179	100	1.145	12.6	1.479E+06	1.291E+06	240.1±24.9
9	139	140	100	0.993	9.8	1.003E+06	1.010E+06	208.7±25.2
10	148	187	100	0.791	13.1	1.068E+06	1.349E+06	166.9±18.6
11	144	130	100	1.108	9.1	1.039E+06	9.380E+05	232.4±28.4
12	99	113	100	0.876	7.9	7.143E+05	8.153E+05	184.5±25.6
13	117	132	100	0.886	9.3	8.442E+05	9.524E+05	186.6±23.9
14	82	103	100	0.796	7.2	5.916E+05	7.431E+05	167.9±25.0
15	210	183	100	1.148	12.8	1.515E+06	1.320E+06	240.6±24.7
16	73	79	100	0.924	5.5	5.267E+05	5.700E+05	194.4±31.7
17	190	177	100	1.073	12.4	1.371E+06	1.277E+06	225.3±23.8
18	162	142	100	1.141	10.0	1.169E+06	1.025E+06	239.2±27.8
19	77	90	70	0.856	9.0	7.936E+05	9.276E+05	180.2±28.1
20	109	94	100	1.160	6.6	7.864E+05	6.782E+05	243.1±34.5
	2561	2641			10.1	1.010E+06	1.041E+06	

Area of basic unit = 1.386E-06 cm^{-2}
χ^2 = 19.89549 (19 DEGREES OF FREEDOM)
$P(\chi^2)$ = 0.349 %
CORRELATION COEFFICIENT = 0.867
VARIANCE OF SQR(Ns) = 4.255615
VARIANCE OF SQR(Ni) = 4.576082
Ns/Ni = 0.970 ± 0.027
MEAN RATIO = 0.994 ± 0.044
Pooled Age = 203.9 ± 6.6 Ma
Mean Age = 209.0 ± 9.9 Ma
Central Age = 203.8 ± 8.4 Ma; R.E.% = 12.21
Ages calculated using ξ = 338 ± 4 for CN5 glass
ρ_d = 1.264E+06 cm^{-2}; N_d = 7010

C3

N_o	N_s	N_i	N_a	Ratio	U (ppm)	ρ_s	ρ_i	F.T.Age (Ma)
1	89	70	40	1.271	12.3	1.605E+06	1.263E+06	266.0±42.7
2	86	77	40	1.117	13.5	1.551E+06	1.389E+06	234.3±37.0
3	155	147	80	1.054	12.9	1.398E+06	1.326E+06	221.4±25.8
4	60	51	24	1.176	14.9	1.804E+06	1.533E+06	246.5±47.1
5	73	67	30	1.090	15.7	1.756E+06	1.611E+06	228.6±38.9
6	38	35	27	1.086	9.1	1.015E+06	9.353E+05	227.9±53.5
7	127	68	30	1.868	15.9	3.054E+06	1.635E+06	387.1±58.5
8	207	162	30	1.278	37.9	4.978E+06	3.896E+06	267.3±28.4
9	117	114	40	1.026	20.0	2.110E+06	2.056E+06	215.6±28.6
10	124	94	45	1.319	14.7	1.988E+06	1.507E+06	275.8±38.0
11	78	56	40	1.393	9.8	1.407E+06	1.010E+06	290.9±51.2
12	102	89	60	1.146	10.4	1.227E+06	1.070E+06	240.3±35.1
13	110	106	50	1.038	14.9	1.587E+06	1.530E+06	218.0±29.9
14	102	93	40	1.097	16.3	1.840E+06	1.677E+06	230.1±33.2
15	56	54	30	1.037	12.6	1.347E+06	1.299E+06	217.8±41.7
16	290	246	40	1.179	43.2	5.231E+06	4.437E+06	247.0±21.8
17	64	59	28	1.085	14.8	1.649E+06	1.520E+06	227.7±41.3
18	106	95	30	1.116	22.2	2.549E+06	2.285E+06	234.0±33.3
19	108	101	40	1.069	17.7	1.948E+06	1.822E+06	224.5±31.3
20	225	175	60	1.286	20.5	2.706E+06	2.104E+06	269.0±27.5
	2317	1959			17.1	2.079E+06	1.758E+06	

Area of basic unit = 1.386E-06 cm^{-2}
χ^2 = 8.835572 (19 DEGREES OF FREEDOM)
$P(\chi^2)$ = 54.4 %
CORRELATION COEFFICIENT = 0.969
VARIANCE OF SQR(Ns) = 7.062847
VARIANCE OF SQR(Ni) = 5.6381
Ns/Ni = 1.183 ± 0.036
MEAN RATIO = 1.187 ± 0.043
Pooled Age = 247.8 ± 8.7 Ma
Mean Age = 248.6 ± 9.9 Ma
Central Age = 247.8 ± 8.2 Ma; R.E.% = 1.14
Ages calculated using ξ = 338 ± 4 for CN5 glass
ρ_d = 1.264E+06 cm^{-2}; N_d = 7010

C4

N_o	N_s	N_i	N_a	Ratio	U (ppm)	ρ_s	ρ_i	F.T.Age (Ma)
1	237	226	100	1.049	15.9	1.710E+06	1.631E+06	220.2±20.8
2	256	216	100	1.185	15.2	1.847E+06	1.558E+06	248.3±23.3
3	91	66	40	1.379	11.6	1.641E+06	1.190E+06	288.0±46.8
4	133	111	50	1.198	15.6	1.919E+06	1.602E+06	251.0±32.5
5	108	79	40	1.367	13.9	1.948E+06	1.425E+06	285.6±42.6
6	59	71	40	0.831	12.5	1.064E+06	1.281E+06	175.1±31.0
7	213	165	100	1.291	11.6	1.537E+06	1.190E+06	270.0±28.4
8	124	123	60	1.008	14.4	1.491E+06	1.479E+06	211.8±27.2
9	125	88	60	1.420	10.3	1.503E+06	1.058E+06	296.5±41.6
10	264	207	100	1.275	14.5	1.905E+06	1.494E+06	266.8±25.2
11	146	123	60	1.187	14.4	1.756E+06	1.479E+06	248.7±30.7
12	69	55	70	1.255	5.5	7.112E+05	5.669E+05	262.6±47.7
13	77	53	28	1.453	13.3	1.984E+06	1.366E+06	303.1±54.3
14	48	29	35	1.655	5.8	9.895E+05	5.978E+05	344.2±81.2
15	69	55	30	1.255	12.9	1.659E+06	1.323E+06	262.6±47.7
16	251	224	100	1.121	15.7	1.811E+06	1.616E+06	235.0±22.0
17	128	116	60	1.103	13.6	1.539E+06	1.395E+06	231.5±29.9
18	250	199	60	1.256	23.3	3.006E+06	2.393E+06	262.9±25.4
19	114	101	50	1.129	14.2	1.645E+06	1.457E+06	236.7±32.6
20	132	84	40	1.571	14.7	2.381E+06	1.515E+06	327.2±46.0
	2894	2391			13.7	1.707E+06	1.411E+06	

Area of basic unit = 1.386E-06 cm^{-2}
χ^2 = 10.28802 (19 DEGREES OF FREEDOM)
P(χ^2) = 36.1 %
CORRELATION COEFFICIENT = 0.975
VARIANCE OF SQR(Ns) = 9.164872
VARIANCE OF SQR(Ni) = 8.620181
Ns/Ni = 1.210 ± 0.033
MEAN RATIO = 1.249 ± 0.043
Pooled Age = 253.5 ± 8.2 Ma
Mean Age = 261.5 ± 10.1 Ma
Central Age = 253.5 ± 7.7 Ma; R.E.% = 1.25
Ages calculated using ξ = 338 ± 4 for CN5 glass
ρ_d = 1.264E+06 cm^{-2}; N_d = 7010

C5

N_o	N_s	N_i	N_a	Ratio	U (ppm)	ρ_s	ρ_i	F.T.Age (Ma)
1	326	325	100	1.003	22.8	2.352E+06	2.345E+06	210.8±16.9
2	132	144	40	0.917	25.3	2.381E+06	2.597E+06	192.9±23.5
3	211	211	40	1.000	37.0	3.806E+06	3.806E+06	210.2±20.8
4	195	175	60	1.114	20.5	2.345E+06	2.104E+06	233.7±24.7
5	121	85	40	1.424	14.9	2.183E+06	1.533E+06	297.1±42.3
6	78	67	40	1.164	11.8	1.407E+06	1.209E+06	244.0±40.9
7	195	204	60	0.956	23.9	2.345E+06	2.453E+06	201.0±20.4
8	210	298	60	0.705	34.9	2.525E+06	3.583E+06	148.8±13.6
9	246	288	50	0.854	40.4	3.550E+06	4.156E+06	179.9±15.9
10	171	197	80	0.868	17.3	1.542E+06	1.777E+06	182.8±19.4
11	106	102	60	1.039	11.9	1.275E+06	1.227E+06	218.3±30.5
12	158	169	40	0.935	29.7	2.850E+06	3.048E+06	196.7±22.0
13	170	178	60	0.955	20.8	2.044E+06	2.140E+06	200.9±21.8
14	71	80	40	0.888	14.0	1.281E+06	1.443E+06	186.8±30.6
15	65	57	30	1.140	13.3	1.563E+06	1.371E+06	239.1±43.6
16	109	111	28	0.982	27.8	2.809E+06	2.860E+06	206.4±28.1
17	98	123	30	0.797	28.8	2.357E+06	2.958E+06	168.0±22.9
18	330	315	100	1.048	22.1	2.381E+06	2.273E+06	220.0±17.7
19	398	402	100	0.990	28.2	2.872E+06	2.900E+06	208.1±15.1
20	246	274	40	0.898	48.1	4.437E+06	4.942E+06	189.0±16.9
	3636	3805			24.3	2.389E+06	2.500E+06	

Area of basic unit = 1.386E-06 cm^{-2}
χ^2 = 15.95515 (19 DEGREES OF FREEDOM)
P(χ^2) = 3.2 %
CORRELATION COEFFICIENT = 0.965
VARIANCE OF SQR(Ns) = 11.25626
VARIANCE OF SQR(Ni) = 13.14984
Ns/Ni = 0.956 ± 0.022
MEAN RATIO = 0.984 ± 0.034
Pooled Age = 201.0 ± 5.8 Ma
Mean Age = 206.8 ± 8.0 Ma
Central Age = 201.7 ± 6.5 Ma; R.E.% = 7.94
Ages calculated using ξ = 338 ± 4 for CN5 glass
ρ_d = 1.264E+06 cm^{-2}; N_d = 7010

C6

N_o	N_s	N_i	N_a	Ratio	U (ppm)	ρ_s	ρ_i	F.T.Age (Ma)
1	98	75	80	1.307	6.6	8.838E+05	6.764E+05	273.2±42.2
2	110	101	80	1.089	8.9	9.921E+05	9.109E+05	228.6±31.7
3	103	115	100	0.896	8.1	7.431E+05	8.297E+05	188.5±25.8
4	164	99	100	1.657	7.0	1.183E+06	7.143E+05	344.5±44.2
5	141	99	80	1.424	8.7	1.272E+06	8.929E+05	297.3±39.3
6	92	65	60	1.415	7.6	1.106E+06	7.816E+05	295.5±48.1
7	140	133	100	1.053	9.3	1.010E+06	9.596E+05	221.0±27.0
8	113	112	100	1.009	7.9	8.153E+05	8.081E+05	212.0±28.5
9	132	109	80	1.211	9.6	1.190E+06	9.830E+05	253.6±33.1
10	149	122	100	1.221	8.6	1.075E+06	8.802E+05	255.8±31.5
11	101	74	80	1.365	6.5	9.109E+05	6.674E+05	285.2±43.9
12	105	102	80	1.029	9.0	9.470E+05	9.199E+05	216.2±30.3
13	147	146	100	1.007	10.2	1.061E+06	1.053E+06	211.6±25.0
14	180	129	100	1.395	9.1	1.299E+06	9.307E+05	291.4±34.0
15	139	127	80	1.094	11.1	1.254E+06	1.145E+06	229.7±28.5
16	87	58	50	1.500	8.1	1.255E+06	8.369E+05	312.7±53.3
17	70	68	60	1.029	8.0	8.418E+05	8.177E+05	216.2±37.0
18	117	101	100	1.158	7.1	8.442E+05	7.287E+05	242.8±33.2
19	133	116	100	1.147	8.1	9.596E+05	8.369E+05	240.4±30.8
20	110	109	100	1.009	7.7	7.936E+05	7.864E+05	212.0±28.9
	2431	2060			8.4	1.014E+06	8.591E+05	

Area of basic unit = 1.386E-06 cm^{-2}
χ^2 = 14.05639 (19 DEGREES OF FREEDOM)
P(χ^2) = 8.1 %
CORRELATION COEFFICIENT = 0.743
VARIANCE OF SQR(Ns) = 1.589625
VARIANCE OF SQR(Ni) = 1.539332
Ns/Ni = 1.180 ± 0.035
MEAN RATIO = 1.201 ± 0.045
Pooled Age = 247.3 ± 8.5 Ma
Mean Age = 251.5 ± 10.4 Ma
Central Age = 247.4 ± 9.4 Ma; R.E.% = 8.71
Ages calculated using ξ = 338 ± 4 for CN5 glass
ρ_d = 1.264E+06 cm^{-2}; N_d = 7010

C7

N_o	N_s	N_i	N_a	Ratio	U (ppm)	ρ_s	ρ_i (Ma)	F.T.Age
1	85	95	35	0.895	19.1	1.752E+06	1.958E+06	188.4±28.3
2	15	16	28	0.938	4.0	3.865E+05	4.123E+05	197.2±71.0
3	38	33	25	1.152	9.3	1.097E+06	9.524E+05	241.4±57.6
4	156	202	24	0.772	59.1	4.690E+06	6.073E+06	162.9±17.6
5	92	138	30	0.667	32.3	2.213E+06	3.319E+06	140.9±19.1
6	77	90	25	0.856	25.3	2.222E+06	2.597E+06	180.2±28.1
7	21	16	24	1.312	4.7	6.313E+05	4.810E+05	274.4±91.2
8	30	22	24	1.364	6.4	9.019E+05	6.614E+05	284.9±80.1
9	41	60	50	0.683	8.4	5.916E+05	8.658E+05	144.3±29.3
10	12	25	50	0.480	3.5	1.732E+05	3.608E+05	101.7±35.8
11	25	38	40	0.658	6.7	4.509E+05	6.854E+05	139.0±35.9
12	52	67	40	0.776	11.8	9.380E+05	1.209E+06	163.7±30.4
13	55	51	50	1.078	7.2	7.936E+05	7.359E+05	226.3±44.2
14	41	35	50	1.171	4.9	5.916E+05	5.050E+05	245.5±56.6
15	51	61	40	0.836	10.7	9.199E+05	1.100E+06	176.2±33.6
	791	949			12.5	1.067E+06	1.280E+06	

Area of basic unit = 1.386E-06 cm^{-2}
χ^2 = 9.505597 (14 DEGREES OF FREEDOM)
$P(\chi^2)$ = 16.5 %
CORRELATION COEFFICIENT = 0.974
VARIANCE OF SQR(Ns) = 5.772343
VARIANCE OF SQR(Ni) = 8.486681
Ns/Ni = 0.834 ± 0.040
MEAN RATIO = 0.909 ± 0.066
Pooled Age = 175.6 ± 9.0 Ma
Mean Age = 191.3 ±14.4 Ma
Central Age = 176.7 ± 9.4 Ma; R.E.% = 5.98
Ages calculated using ξ = 338 ± 4 for CN5 glass
ρ_d = 1.264E+06 cm^{-2}; N_d = 7010

C8

N_o	N_s	N_i	N_a	Ratio	U (ppm)	ρ_s	ρ_i (Ma)	F.T.Age
1	184	174	100	1.057	12.2	1.328E+06	1.255E+06	222.0±23.8
2	126	116	60	1.086	13.6	1.515E+06	1.395E+06	228.0±29.6
3	121	108	60	1.120	12.6	1.455E+06	1.299E+06	235.0±31.4
4	146	144	60	1.014	16.8	1.756E+06	1.732E+06	213.0±25.3
5	104	79	40	1.316	13.9	1.876E+06	1.425E+06	275.3±41.3
6	120	86	40	1.395	15.1	2.164E+06	1.551E+06	291.4±41.5
7	132	119	60	1.109	13.9	1.587E+06	1.431E+06	232.7±29.7
8	199	181	100	1.099	12.7	1.436E+06	1.306E+06	230.7±24.0
9	196	191	100	1.026	13.4	1.414E+06	1.378E+06	215.6±22.2
10	222	224	100	0.991	15.7	1.602E+06	1.616E+06	208.3±20.0
11	260	218	100	1.193	15.3	1.876E+06	1.573E+06	249.9±23.3
12	252	306	100	0.824	21.5	1.818E+06	2.208E+06	173.6±15.0
13	238	186	100	1.280	13.1	1.717E+06	1.342E+06	267.7±26.6
14	194	210	100	0.924	14.7	1.400E+06	1.515E+06	194.4±19.6
15	184	176	100	1.045	12.4	1.328E+06	1.270E+06	219.5±23.4
16	208	183	100	1.137	12.8	1.501E+06	1.320E+06	238.3±24.5
17	84	68	60	1.235	8.0	1.010E+06	8.177E+05	258.6±42.4
18	216	280	100	0.771	19.7	1.558E+06	2.020E+06	162.7±15.0
19	210	162	100	1.296	11.4	1.515E+06	1.169E+06	271.1±28.7
20	104	79	50	1.316	11.1	1.501E+06	1.140E+06	275.3±41.3
	3500	3290			14.2	1.549E+06	1.456E+06	

Area of basic unit = 1.386E-06 cm^{-2}
χ^2 = 21.43576 (19 DEGREES OF FREEDOM)
$P(\chi^2)$ = 0.135 %
CORRELATION COEFFICIENT = 0.901
VARIANCE OF SQR(Ns) = 4.375912
VARIANCE OF SQR(Ni) = 6.781905
Ns/Ni = 1.064 ± 0.026
MEAN RATIO = 1.112 ± 0.037
Pooled Age = 223.3 ± 6.6 Ma
Mean Age = 233.2 ± 8.7 Ma
Central Age = 226.9 ± 8.6 Ma; R.E.% = 11.49
Ages calculated using ξ = 338 ± 4 for CN5 glass
ρ_d = 1.264E+06 cm^{-2}; N_d = 7010

C9

N_o	N_s	N_i	N_a	Ratio	U (ppm)	ρ_s	ρ_i (Ma)	F.T.Age
1	93	78	40	1.192	13.7	1.677E+06	1.407E+06	249.8±38.6
2	114	86	36	1.326	16.8	2.285E+06	1.724E+06	277.1±39.9
3	121	139	50	0.870	19.5	1.746E+06	2.006E+06	183.3±23.0
4	146	156	40	0.936	27.4	2.633E+06	2.814E+06	196.9±22.9
5	104	132	32	0.788	29.0	2.345E+06	2.976E+06	166.1±22.0
6	88	103	50	0.854	14.5	1.270E+06	1.486E+06	180.0±26.3
7	189	175	40	1.080	30.7	3.409E+06	3.157E+06	226.7±24.1
8	154	126	40	1.222	22.1	2.778E+06	2.273E+06	255.9±31.0
9	114	127	30	0.898	29.7	2.742E+06	3.054E+06	189.0±24.6
10	153	138	50	1.109	19.4	2.208E+06	1.991E+06	232.6±27.6
11	244	224	40	1.089	39.3	4.401E+06	4.040E+06	228.6±21.5
12	194	194	40	1.000	34.1	3.499E+06	3.499E+06	210.2±21.6
13	84	74	40	1.135	13.0	1.515E+06	1.335E+06	238.0±38.2
14	133	110	40	1.209	19.3	2.399E+06	1.984E+06	253.2±32.9
15	221	240	40	0.921	42.1	3.986E+06	4.329E+06	193.8±18.4
16	88	108	40	0.815	19.0	1.587E+06	1.948E+06	171.7±24.8
17	264	206	60	1.282	24.1	3.175E+06	2.477E+06	268.1±25.3
18	418	416	100	1.005	29.2	3.016E+06	3.001E+06	211.1±15.0
19	229	182	80	1.258	16.0	2.065E+06	1.641E+06	263.3±26.5
20	261	233	60	1.120	27.3	3.139E+06	2.802E+06	235.0±21.5
	3412	3247			24.0	2.597E+06	2.471E+06	

Area of basic unit = 1.386E-06 cm^{-2}
χ^2 = 16.33503 (19 DEGREES OF FREEDOM)
$P(\chi^2)$ = 2.6 %
CORRELATION COEFFICIENT = 0.960
VARIANCE OF SQR(Ns) = 8.914821
VARIANCE OF SQR(Ni) = 7.90819
Ns/Ni = 1.051 ± 0.026
MEAN RATIO = 1.055 ± 0.037
Pooled Age = 220.7 ± 6.6 Ma
Mean Age = 221.6 ± 8.6 Ma
Central Age = 220.1 ± 7.5 Ma; R.E.% = 8.52
Ages calculated using ξ = 338 ± 4 for CN5 glass
ρ_d = 1.264E+06 cm^{-2}; N_d = 7010

Individual fission track lengths (in μm) listed for all samples.

M1

14.02763
14.19
454
13.46466
14.18663
14.3985
15.05162
12.92709
15.37781
15.87836
15.2827
16.33103
11.75712
13.3832
15.69364
14.93568
12.33438
15.45782
13.57045
13.72862
12.30708
14.41602
12.58641
14.13317
14.24187
14.93568
13.83239
14.25761
14.73534
14.47619
13.4125
13.80804
15.80757
14.97692
13.46258
15.13336
14.30473
13.46466
13.73066
15.01058
15.21651
14.59001
15.00124
17.05825
14.92629
14.49748
15.2386
16.13933
14.1292
14.64564
13.73066
11.72608
13.50625
14.58425
13.92934
13.26959
12.80724
13.66311
13.37063
13.25479
12.69289
13.80804
14.08548
15.57348
14.62073
14.49361
14.38487
13.83441
14.74486
15.51395
13.03294
15.01619
13.26959

M2

14.47851
15.52928
15.46
933
14.31719
14.37789
14.44438
12.36505
16.17401
16.30987
14.32935
15.52928
14.71719
13.27327
13.03267
14.15197
13.39087
13.63581
13.50315
14.25011
13.845
13.3322

M3

14.47491
15.83871
13.40606
13.66063
13.23363
13.91053
12.21844
13.4189
13.95998
13.37175
13.13564
13.72353
12.8952
15.7806
15.04101
13.36101
14.76359
13.41248
14.11338
13.17928
13.86713
13.50633
14.13777
13.93116
14.05835
14.9145
14.02359
14.11338
13.73398
13.29207
13.42959
13.63959
12.96847
13.44028
14.30131
12.50181
14.89717
14.13777
14.62487
15.58841
15.13425
15.30965
14.61702
15.01044
14.18845
14.042
13.44028
14.59933
14.62487
13.97
232
15.24011
12.3679
14.94527
14.53824
15.82421
14.80243
14.38139
13.4189
14.59933
14.82181
12.33536
14.74997
14.06448
14.94527
15.28338
14.97214
15.63622

M4

13.10789
15.63342
13.54407
14.39418
13.87273
13.25977
14.48087
14.09744
14.01037
14.69061
15.04415
13.73573
15.61028
15.56567
14.86563
13.71142
12.75519
14.27779
13.80239
14.02823
13.87273
13.40994
14.13685
14.36905
14.66977

M5

13.37216
14.41727
13.23087
15.26154
14.33805
14.88945
14.85883
13.14234
15.75723
15.35083
14.60174
14.97906
15.87604
15.81495
14.60174
12.16811
14.65235
13.69407
15.69386
13.9393
16.7471
15.46724
15.81495
14.39157
14.85883

M7

14.54199
15.1742
12.98733
14.2607
13.69366
14.54199
14.94615
15.30326
12.41178
14.83378
16.29
13.51022
15.38934
13.08416
14.00523
14.18641
14.19882
13.41428
13.90426
14.93043
14.92256
13.67435
15.65785
13.87679
14.75043
14.56418
14.06588
14.53997
14.49346
13.34627
13.99894
12.7524
14.36938
13.51674
14.78025
14.41222
13.96325
16.16337
14.78025
13.55577
11.72087
13.85985
14.30386
13.67435
16.08874
14.98734
13.06844
14.79812
12.47311
14.84565
14.78025
13.81318
15.2167
14.49346
14.84565
13.81318
13.34627
14.27099
13.58821
14.41222
15.29559
15.45595
14.48333
15.29559
15.01864
14.61046
14.12835
14.66661
14.76237
15.52418
15.63159
13.2203
15.86
088
16.87419
15.57515
13.40333
14.54603
14.06588
15.1742
13.96325
15.16452
14.07214
14.42851
13.55577
15.56949
14.19882
14.19882
15.38743
13.70651

M8

11.61168
12.81703
11.84362
13.31496
14.49865
14.44633
13.87803
14.22726
13.98071
14.40551
13.90024
14.16602
13.10052
13.25586
12.81703
13.45742
14.64682
14.54114
14.95002
14.60272
15.05284
14.77075
14.54114
13.03399
12.58743
13.99474
13.7481
14.91998
14.29804
15.50255
14.33721
14.25876
15.44456
14.70606
13.79494
13.03399
13.90831
14.77644
14.73082
15.05284
14.38603
14.9275
14.45409
12.9238
14.77075
15.9677

M9

14.27669
14.49236
13.64946
15.29605
14.7552
14.30167
13.75366
16.16011
12.97295
15.04267
13.74767
13.87291
13.98133
14.26515
14.03816
15.14453
13.60917
15.33907
12.49869
12.47451
14.4753
13.83327
14.82018
15.47272
12.49869
14.15696
13.75366

M10

14.25876
15.96594
15.67524
14.91246
15.04538
14.97813
13.60044
15.03979
15.35715
13.73177
13.50734
13.23045
14.75175
14.23514
13.57154
14.12439
13.45116
14.43662
14.97813
16.44187
15.15866
15.1457
16.35637
14.62191
15.43911
14.40745
15.63942
12.79075
12.73141
14.04474
13.50111
14.02876
14.38603
14.22725
16.65875
13.90831
14.69079
15.15125
13.99073
14.54114
12.88903
15.77511
15.67524
13.64778
13.85983
13.50734
15.44455
14.39967
15.65376
13.44074
15.67524
15.97999
14.33721
14.99684
15.34071
12.44628
14.52956
13.7807
16.40259
13.98071
13.99073
15.84075
14.24105
14.24892
14.83705
17.1318
13.31496
13.48032
16.07971
15.97297
14.95565
15.30594
14.53921
16.20998
14.33721
16.63854
14.62958
15.39363
14.42302
15.07146
14.02676
14.67933
14.98749
13.37171
13.7807
12.55396
13.99073
15.2472
13.90024
14.45409
15.45363
12.86725
15.30777
13.57154
15.50978
16.08319
15.07518
14.47736
16.8961
14.98

M11

13.69386
13.1994
15.16971
13.80043
12.76096
14.54392
14.02721
13.38801
14.27409
13.34586
13.64646
12.95161
14.02721
14.29382
14.54973
14.50318
13.72058
15.00163
14.76501
14.31351
14.0533
12.65454
14.09134
13.91024
13.30357
11.59011
15.37264
13.51577
13.19086
13.69386
14.13526
15.24012
13.49491
15.88283
14.78789
14.09134
14.09134
14.80502
13.53244
14.9546
14.99035
14.16711
14.29185
14.28199
13.10944
14.36852
15.61629
14.55747
13.48238
14.4155
13.62167
12.91458
14.34694
14.53229
15.08964
13.57816
14.60385
13.86764
13.1652
15.71162
13.26965
14.24643
13.37749
14.09134
15.55302
13.9325
13.48865
14.33122
14.95649
14.40182
15.07656
14.01315
14.40182
12.6144
15.44578
14.13326
14.80312
14.34104
15.61088
13.6382
15.65953
15.00163
12.838
14.06132
13.737
13.18445
13.69592
14.86579
15.3102
15.02227
13.53035
13.9325
13.03617
14.37048
13.72058

13.547
14.0051
12.66122
15.69009
13.72058

C2

10.15835
11.35233
11.21004
11.78106
13.04644
12.32565
14.1449
13.64988
14.76945
13.08374
12.42525
11.99326
13.61413
13.88721
13.78778
13.18631
13.5635
14.49519
12.98478
13.65617
12.24867
14.88544
13.48083
15.38542
15.13182
14.05341
12.23696
13.68134
12.44369
13.06401
13.22104
9.631109
14.01869
11.85141
15.29761
11.75427
14.15907
13.24487
11.88764
12.7711
12.77783
13.42757
14.31211
10.86991
13.22321
15.40218
12.36049
13.24487
10.63263
13.5635
15.73907
14.37406
10.06765
12.6629
13.3848
15.23753
13.22321
12.52864
9.313363
14.18335
12.41602
15.08438
13.46168
14.99098
15.09958
14.80047
13.02005
12.11691
15.35559
12.16413

13.93872
14.22573
15.14507
13.72318
13.29887
14.14895
13.70646
12.20882
13.10782
15.18288
10.82764
14.77721
14.80822
12.49886
11.41529
12.16413
14.32212
15.31821
14.39996
13.07059
13.24487
10.84087
16.59716
13.54447
13.1253
12.64478
12.86056
12.08611
12.95826
11.15108

C3

13.62141
11.32118
12.00043
15.60794
12.72045
14.52795
14.97507
13.99478
11.03256
11.64227
12.91817
13.45975
12.25925
12.62728
11.85555
12.05072
11.06385
15.17947
12.6819
12.98932
12.3155
12.23808
10.86685
12.51731
11.54039
14.719
13.05788
13.45119
12.32485
12.05072
15.15099
12.23808
12.29444
12.29912
10.86155
11.54538
12.77693
12.89139
14.19301
12.77693
14.65429
11.28296
13.13046
13.44048
13.68891

15.03649
14.20924
16.71811
14.2578
13.68049
15.11292
10.99072
14.36246
11.8992
13.20047
11.93786
14.2921
12.53801
11.93786
12.26629
12.92486
14.65822
13.15676
13.13046
12.05072
13.37173
11.43257
10.94608
13.79788
12.15306
11.54538
14.18286
12.19328
11.54039
12.57471
13.45975
11.59269
14.92884
13.54508
12.45503
15.54692
11.38461
11.29826
14.20113
16.24452
12.06983
14.11161
13.20702
12.72951
13.96388
14.45043
12.96046
11.79954
11.43257
13.79788
10.33152
14.20113
13.13046
11.85798
14.16051

C4

10.25
14.80173
12.32959
14.82694
11.45985
14.17698
13.18774
13.80105
13.66504
13.23994
12.70609
12.2454
8.593844
13.49575
12.3738
11.67598
12.72643
13.5616
13.4595
15.62897

13.19428
14.25581
15.52566
15.01377
15.44215
12.90135
12.9547
12.23601
13.58066
10.35044
13.94811
12.70835
13.50214
12.43404
11.4899
12.86566
15.32071
13.8903
11.61923
12.65169
14.07935
13.37812
14.41817
12.91026
11.15488
12.06573
13.58066
14.03642
12.85002
9.601479
13.31569
13.59758
12.70609
13.77396
15.54601
13.57007
11.98927
12.91026
13.9378
15.34507
14.38425
13.75726
9.075259
14.75701
10.81745
14.10178
12.9547
14.92161
14.66911
13.0012
11.26766
13.0012
11.86156
11.0201
11.98927
10.68111
12.24775
12.3226
12.76025
13.0012
13.57219
13.90064
13.72379
11.98927
12.76926
12.34124
13.26162
14.71801
14.38625
13.8903
14.14451
11.1523
13.29841
12.48708
11.39195
10.76686
12.74222

13.57219
12.87683
11.74714
13.66714
12.94582

C5

13.08321
11.66085
12.511
10.90938
10.97551
11.57115
11.19483
13.07436
12.83305
13.90679
12.86908
15.30956
10.89345
14.31699
14.95765
11.97434
12.02981
13.65476
14.30688
13.01223
12.77201
12.66277
11.40994
15.41506
13.3113
14.34324
14.91696
14.82353
13.52698
12.9565
12.26805
10.56981
15.20522
15.01173
15.27928
14.30688
12.08981
13.02112
12.35503
11.09093
12.29161
10.42367
12.10894
12.05864
12.13759
13.40878
13.12959
12.02981
11.12481
15.34543
12.511
13.25246
10.94382
10.71936
13.62718
11.84799
13.134
13.76664
13.1714
13.98772
10.75979
14.12158
13.14721
12.70384
12.46
8.674818
13.12738
15.24134
10.09931
13.50771

12.83305
11.23355
13.88179
15.18808
11.84799
13.59741
10.89345
12.47625
12.08981
14.09902
10.09931
15.01173
11.63849
9.890814
11.31058
11.09093
12.34566
15.05794
11.51347
13.68652
11.74987
12.697
13.30912
10.73016
11.16117
14.68425
10.67878
13.36338
10.67878
13.27428

C6

12.82922
13.11175
14.39047
12.87123
12.25623
15.50047
15.4362
10.58741
13.38195
10.34861
11.85327
11.83408
13.68836
12.45168
13.47081
12.58556
14.33509
12.83587
12.82922
14.97286
12.87123
14.55339
11.72557
12.57879
14.49863
12.59459
13.60301
14.34103
14.84903
15.26223
12.67104
11.73767
13.33516
15.22869
11.70131
12.37617
13.40104
13.77731
13.16364
13.15069
14.82605
11.67945
12.15382
12.3048
12.71356

12.15616
12.9614
12.69568
13.84313
13.00734
16.05501
14.08117
11.6307
14.08117
14.6332
12.89107
10.85502
12.15616
12.71356
13.8267
13.5528
14.81839
12.90209
13.40104
10.79203
15.09944
15.36056
10.67292
15.00129
14.28745
12.69568
13.10958
12.77597
11.96775
15.55901
13.82054
13.11175
13.58629
12.79153
10.73661
10.98767
9.827671
12.58782
10.23822
10.85502
11.62093
13.65096
13.68836
14.35291
12.31404
13.40104
13.31598
13.83697
9.919736
12.91969
12.97892
13.88411
14.07108
13.5528
14.2795
12.69344

C7

13.4441
13.31425
15.22952
10.89587
14.92027
13.36634
12.48829
13.36634
14.39277
13.46992
10.77562
12.16887
12.50683
14.08365
15.00735
15.95744
12.82912
15.14563
13.1038

10.35911
12.7635
13.66838
14.08365
13.776
13.31425
12.93701
16.31632
11.8139
14.56874
13.63232
11.79428
13.21602
16.00997
13.6832
11.55619
11.41247
12.50683
9.589814
12.66557
14.61834
14.92027
14.36256
15.19335
13.32294
13.90987
13.23791
13.02623
12.55536
12.17601
12.8989
13.48496
10.91446
11.64356
12.14028
13.95352
14.18404
12.62665
12.93701
10.33393
11.21798
7.077713
9.462147
15.64962
14.43897
14.18404
12.80879
15.00735
12.11163
11.9164
13.85146
12.66557
10.95946
12.87194
14.12471
14.88335
8.759773
13.58125
12.63352
15.37522
13.68955
14.00944
15.22001
13.78441
13.375
13.24447
11.09339
14.00323
13.07504
13.16553
14.00944
14.45701
12.48597
13.13691
12.97946
13.31207
12.7907

13.00398
12.09249
12.06132
13.19189

C8

12.47412
12.23179
13.89478
12.01782
9.563357
10.78772
13.42519
13.3592
12.49924
11.01783
12.32467
13.84339
12.799
13.17006
13.38052
14.33112
13.21113
12.15698
12.46498
13.24561
12.02494
13.26282
12.17807
13.6839
12.69163
11.88423
12.56748
14.61477
13.85162
12.24111
9.740581
14.63622
13.99088
12.17573
13.49509
10.72676
11.99883
13.74418
15.366
14.51887
15.55593
12.53113
14.35298
14.56592
13.97457
10.20093
14.3768
12.68938
13.55201
13.61287
14.09644
14.3132
11.94883
13.13538
14.71198
10.90077
11.9917
13.18521
13.03516
12.41685
11.46171
12.46498
15.56692
13.81865
13.42519
13.54359
12.49924
12.76554
14.85277
14.70617
12.01782

13.00231
13.70263
11.5262
12.49467
14.87579
10.50928
12.6759
13.40606
14.34504
12.17573
11.98932
13.70263
15.07379
14.71198
13.59192
14.76807
13.74626
14.05391
14.01531
14.19921
12.65564
14.69841
13.81865
12.21547
15.93436
15.19622
13.01108
11.22546
16.55045
14.21727
15.23931
13.44429
13.03516
13.49509

C9

12.22742
13.08799
14.07212
15.93955
12.63435
10.87117
13.56674
11.66691
14.14748
13.43689
14.16778
14.42511
11.90588
11.50816
11.70625
14.0966
14.03121
12.22507
13.3446
9.590137
13.91809
12.40478
14.06599
13.09677
10.20009
13.74145
12.43255
12.02597
13.83525
12.5155
14.24264
12.22507
11.53311
13.42619
14.58363
10.3428
12.20625
14.82793
11.52813
11.05209
12.48791

10.77024
13.49665
12.58648
9.664769
13.57097
12.18032
12.79484
10.32054
13.69955
9.652867
9.590137
12.77011
14.95147
14.72094
12.5155
12.70693
10.25068
13.83317
13.29281
11.10656
13.22127
14.67792
12.95556
12.28605
11.58036
12.43948
11.27096
12.54989
12.27435
13.68486
10.8553
11.58036
11.23009
15.70156
11.36745
13.19298
12.55219
14.11494
12.26498
12.04746
11.02084
10.55187
13.66805
12.32808
13.27333
11.86719
11.82837
11.08325
12.65253
14.24466
12.46948
14.72094
12.15434
11.98287
11.54805
13.83109
10.57364
13.95727
13.20386
13.57097

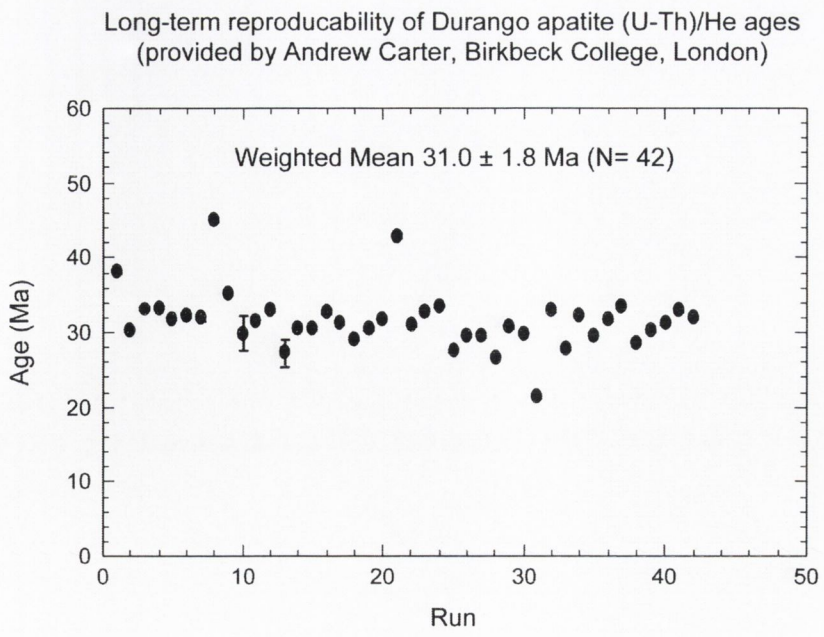

Appendix 28 Apatite microprobe analysis results

Microprobe analysis results for the control samples on northwest Co. Donegal.
Analyses were carried out by Andrew Carter, Birkbeck College, London. See text for details.

C3	O	F	Na	Si	P	S	Cl	Ca
Max.	39.78	2.18	0.82	0.72	18.69	0.6	-0.11	40.08
Min.	38.8	1.61	0.82	0.69	18.04	0.6	-0.11	39.02

C4	O	F	Na	Si	P	S	Cl	Ca
Long-	38.14	2.14		0.56	18.19		-0.01	38.82
Min.	33.99	1.8		0.56	17.66		-0.01	37.55

C5	O	F	Na	Si	P	S	Cl	Ca
Max.	35.96	2.4			17.82		-0.12	38.29
Min.	34.31	1.71			17.5		-0.12	37.14

C6	O	F	Na	Si	P	S	Cl	Ca
Max.	36.75	2.19			18.09		0.09	38.71
Min.	36.02	2.12			18.09		0	38.71

C7	O	F	Na	Si	P	S	Cl	Ca
Max.	36.43	2.45			17.94		0	38.55
Min.	34.75	1.87			17.38		0	37.67

C8	O	F	Na	Si	P	S	Cl	Ca
Max.	38.33	2.04		0.77	18.28		-0.01	39.26
Min.	36.36	1.9		0.77	17.75		-0.01	37.88

C9	O	F	Na	Si	P	S	Cl	Ca
Max.	38.28	2.31			18.19		-0.04	39.31
Min.	37.44	1.82			17.81		-0.04	38.55